Veterinary Comparative Hematopathology

VICTOR E. VALLI

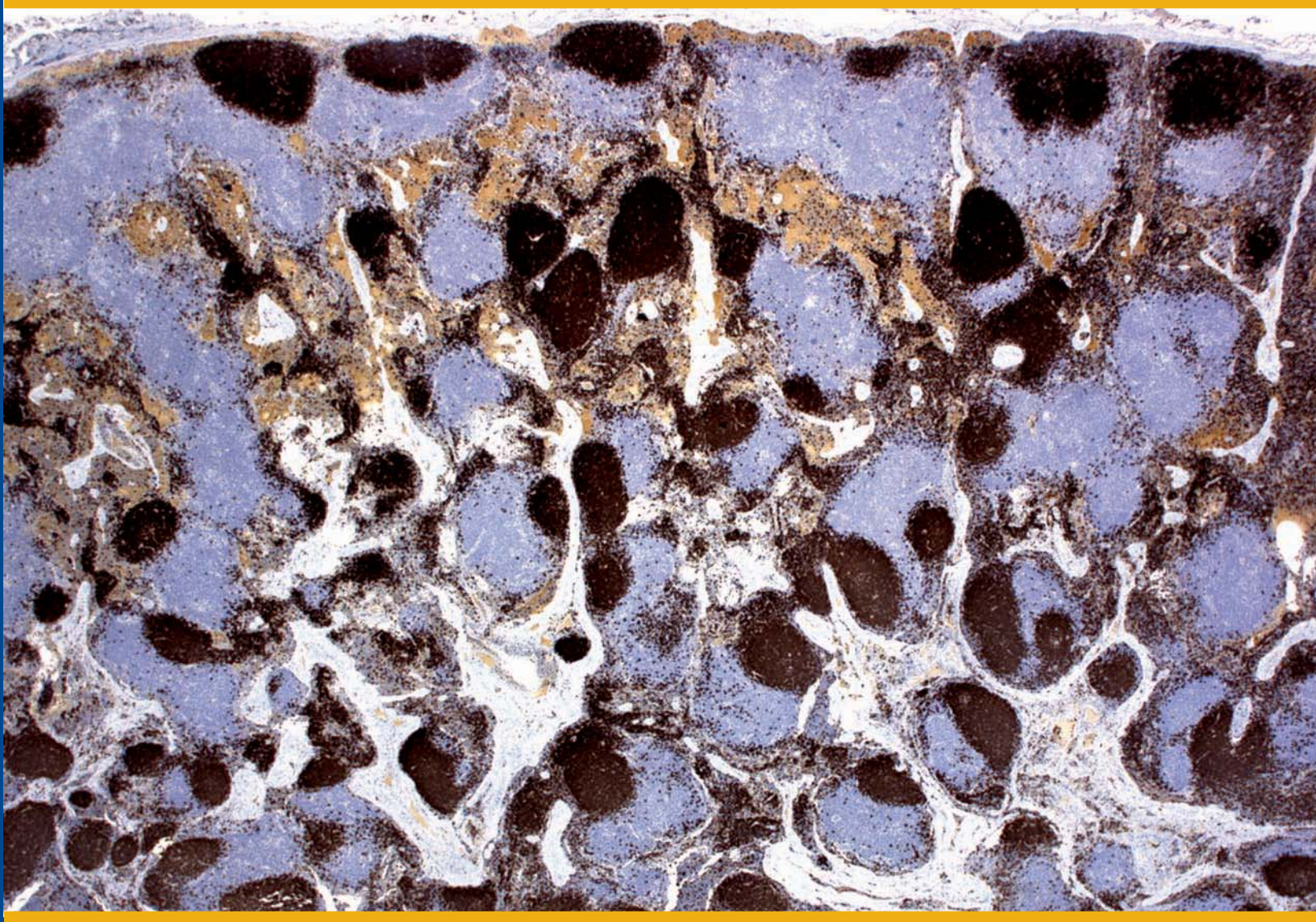

Blackwell Publishing

Veterinary Comparative Hematopathology

Veterinary Comparative Hematopathology

Victor E. Valli, DVM

Veterinary Comparative Hematopathology

VICTOR E. VALLI

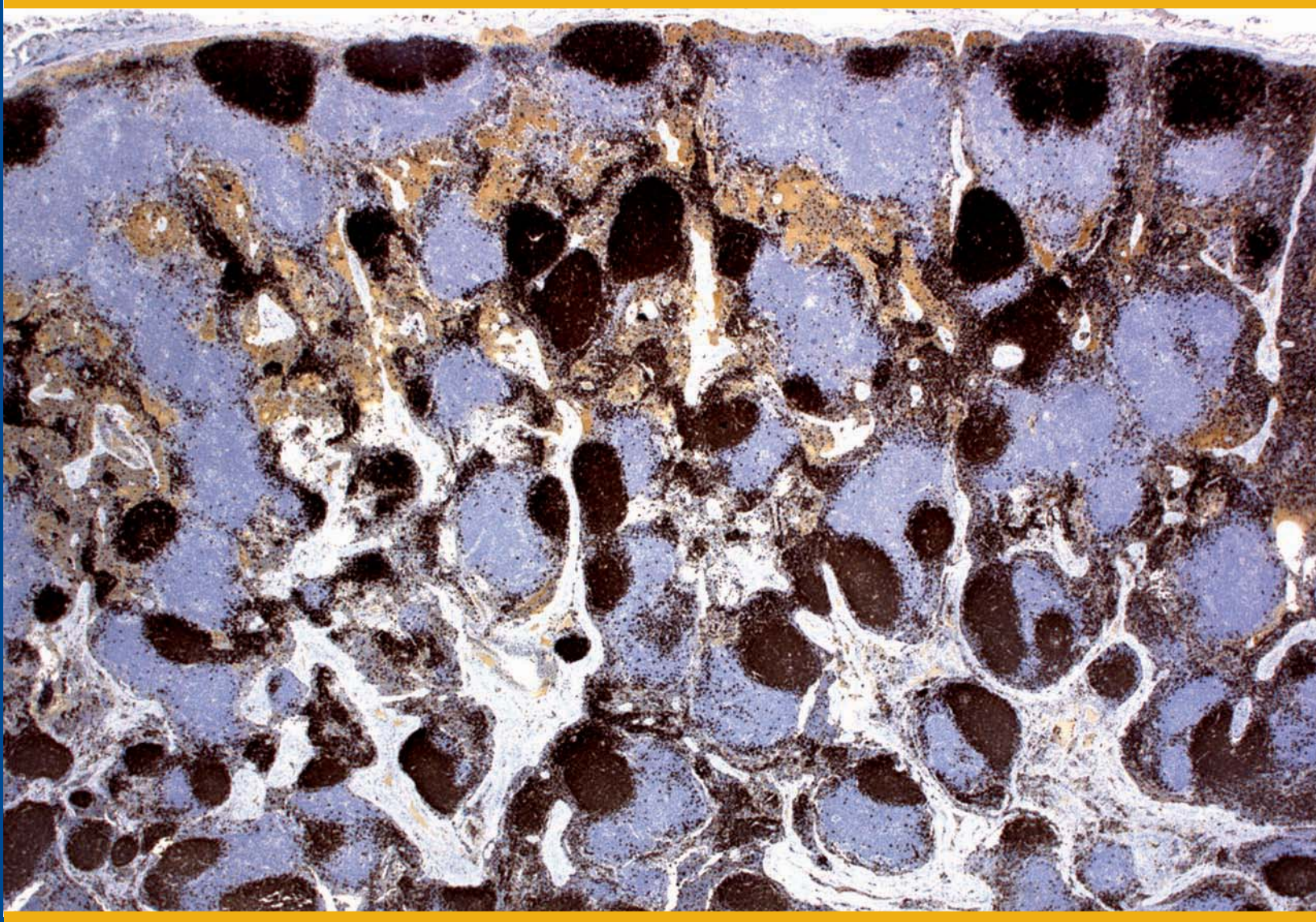

Blackwell Publishing

Blackwell Publishing Professional
2121 State Avenue, Ames, Iowa 50014, USA

Orders: 1-800-862-6657
Office: 1-515-292-0140
Fax: 1-515-292-3348
Web site: www.blackwellprofessional.com

Blackwell Publishing Ltd
9600 Garsington Road, Oxford OX4 2DQ, UK
Tel.: +44 (0)1865 776868

Blackwell Publishing Asia
550 Swanston Street, Carlton, Victoria 3053, Australia
Tel.: +61 (0)3 8359 1011

First edition, 2007

Library of Congress Cataloging-in-Publication Data

Valli, Victor E.
Veterinary comparative hematopathology /V.E. Valli.–1st ed.
p.; cm.
Includes bibliographical references and index.
ISBN-13: 978-0-8138-0924-3 (alk. paper)
ISBN-10: 0-8138-0924-X (alk. paper)
1. Veterinary hematology. I. Title.
[DNLM: 1. Hematologic Neoplasms–veterinary.
2. Leukemia–veterinary. 3. Bone Marrow Diseases–veterinary.
4. Lymphoma–veterinary. SF 910.L4 V188c 2007]
SF769.5.V35 2007
636.089′615–dc22
2006025003

The last digit is the print number: 9 8 7 6 5 4 3 2 1

Contents

Author vii
Chapter Reviewers vii
Preface xi
Acknowledgments xii

1 The Evolution of Classification Systems for Hematopoietic Neoplasms 3

2 Normal and Benign Reactive Hematopoietic Tissues 9
Lymph Nodes 9
Normal Form and Function 9
Developmental and Degenerative Diseases of Lymph Nodes 27
Hyperplastic and Dysplastic Changes 29
Metastatic Neoplasms 40
Spleen 47
Normal Form and Function 47
Developmental and Degenerative Diseases of the Spleen 62
Splenic Metastatic Neoplasms 76
Thymus 78
Normal Form and Function 78
Developmental Diseases of the Thymus 81
Degenerative Diseases of the Thymus Gland 84
Autoimmune Hyperplasia of the Thymus Gland 88
Bone Marrow 98
Normal Form and Function 98
Developmental and Degenerative Diseases 105
Degenerative Diseases of Bone Marrow 114
Technical Aspects of Marrow Biopsy and Preparation 117

3 B-Cell Neoplasms 119
Lymphoproliferative Diseases 119
Precursor B-Cell Neoplasms 124
Precursor B-Cell Lymphoma B Lymphoblastic Leukemia 124
Burkitt's Lymphoma 137
Atypical Burkitt's Lymphoma and Burkitt's-like Lymphoma 140
Mature (Peripheral) B-Cell Neoplasms 142
B-Cell Chronic Lymphocytic Leukemia/ Small Lymphocytic Lymphoma 142
B-Cell Prolymphocytic Leukemia/ Human Variant Hairy Cell Leukemia 161
Marginal Zone and MALT Lymphoma 168
Plasmacytoma and Multiple Myeloma 189
Lymphoplasmacytic Lymphoma 207
Follicular Lymphoma 215
Mantle Cell Lymphoma 227
Diffuse Large B-Cell Lymphoma 238
T-Cell Rich Large B-Cell Lymphoma/ Lymphomatoid Granulomatosis 260

4 T-Cell and NK-Cell Neoplasms 275
Precursor T-Cell Neoplasms 275
Precursor T-Cell Lymphoblastic Lymphoma and Lymphoblastic Leukemia 275
Mature (Peripheral) T-Cell and NK-Cell Neoplasms 287
Chronic Lymphocytic Leukemia 287
Mature (Peripheral) Nodal T-Cell (T-Zone) Lymphoma 294
T-Cell Prolymphocytic Leukemia 302
T-Cell Granular Lymphocytic Leukemia/Lymphoma 304
Aggressive NK-Cell Leukemia and Blastic NK-Cell Lymphoma 309
Mature Nodal and Extranodal T-Cell Lymphoma 312
Mycosis Fungoides and Sézary Syndrome 331
Anaplastic Large Cell Lymphoma 339
Adult T-Cell Lymphoma/Leukemia 346
Intravascular Large T-Cell Lymphoma 355
Peripheral T-Cell Lymphoma, NOS 360

5 Acute Myeloid Leukemias 367
Myeloproliferative Diseases 367

Myeloid AML 374
Minimally Differentiated M0 and Without Maturation M1 374
Acute Myeloblastic Leukemia with Maturation M2 382
Acute Promyelocytic Leukemia M3 389
Acute Myelomonocytic Leukemia M4 391
Acute Monoblastic Leukemia M5A and Acute Monocytic Leukemia M5B 395
Acute Erythroid Leukemia M6 401
Acute Megakaryoblastic Leukemia M7 412
Acute Panmyelosis with Myelofibrosis M8 417
Granulocytic Sarcoma 419

6 Chronic Myeloproliferative Diseases 425
Chronic Myeloid Leukemia 425
Human CML 425
Animal CML 429
Chronic Neutrophilic Leukemia 434
Chronic Eosinophilic Leukemia and Hypereosinophilic Syndrome 436
Polycythemia Vera 440
Blood 441
Essential Thrombocythemia 443
Chronic Idiopathic Myelofibrosis 449
Basophil Leukemia and Mast Cell Tumor 454
Mast Cell Tumors 456

7 Myeloproliferative/Myelodysplastic Diseases 461
Atypical Chronic Myeloid Leukemia 461
Chronic Myelomonocytic Leukemia 462
Juvenile Myelomonocytic Leukemia 467

8 Myelodysplastic Syndromes 473
Refractory Anemia 475
MDS of Refractory Anemia Without Ringed Sideroblasts 475
MDS of Refractory Anemia with Ringed Sideroblasts 477
Refractory Anemia with Excess Blasts 477
Refractory Cytopenia with Multilineage Dysplasia 481
Myelodysplastic Syndrome, Unclassified 483
MDS in Perspective: Differential Diagnosis of Myelodysplastic Syndromes 486
MDS: Prognosis 487
MDS: Management 488

9 Hodgkin's Lymphoma 491
Classification of Hodgkin's Lymphoma 491
The Morphology of the RS Cells 491
The Phenotypic Characteristics of the RS Cells 492
General Pathology of HL 492
Lymphocyte Predominance 492
Lymphocyte-Rich Classic HL 493
Nodular Sclerosis HL 494
Mixed Cellularity HL 496
Lymphocyte Depletion HL 497
Regional Pathology and Staging of HL 498
Hodgkin's-Like Lymphoma in Animals 499

10 Histiocytoses 505
Histiocytic and Dendritic Cell Proliferations 505
Variant Types of Histiocytic Neoplasms 506
Cutaneous Histiocytoma 506
Cutaneous Histiocytosis (Cutaneous Reactive Histiocytosis) 506
Systemic Histiocytosis (Systemic Reactive Histiocytosis) 506
Histiocytic Sarcoma 506
Hemophagocytic Histiocytic Sarcoma 506
Histiocytic Neoplasms 507
Cutaneous Histiocytoma 507
Cutaneous Histiocytosis (Cutaneous Reactive Histiocytosis) 510
Systemic Histiocytosis (Systemic Reactive Histiocytosis) 514
Histiocytic Sarcoma 515
Hemophagocytic Histiocytic Sarcoma 517
Human Lesions of Significance for Differential Diagnosis 521

Index 525

Author

Victor Edwin Valli, DVM, MSc, PhD, Diplomate ACVP
Dean Emeritus, Professor of Pathobiology
College of Veterinary Medicine
University of Illinois
2001 S. Lincoln Ave.
Urbana, IL 61802

Chapter Reviewers

William Vernau, BSc, BVMS, DVSc, PhD, Diplomate ACVP
Assistant Professor, Clinical Pathology
Department of Pathology, Microbiology & Immunology
School of Veterinary Medicine
University of California
1064 Haring Hall
Davis, CA 95616
Chapter 1

Robert M. Jacobs, DVM, PhD, Diplomate ACVP
Assistant Dean, Research and Graduate Affairs
Professor, Pathobiology
Ontario Veterinary College
University of Guelph
Guelph, Ontario
Canada N1G 2W1
Chapter 2

Amy L. MacNeill, DVM, PhD, Diplomate ACVP
Assistant Professor, Clinical Pathology
Department of Pathobiology
College of Veterinary Medicine
University of Illinois
2001 S. Lincoln Ave.
Urbana, IL 61802
Chapter 2

Jerrold M. Ward, DVM, PhD
Veterinary Pathologist
Chief, Infectious Disease Pathogenesis Section
Comparative Medicine Branch
NIAID, NIH & SoBran, Inc.
Twinbrook 3, Room 2W01A, MSC 8135
Bethesda, MD 20892-8135
Chapter 4

Dorothee Bienzle, DVM, MSc, PhD, Diplomate ACVP
Canada Research Chair, Veterinary Pathology
Associate Professor, Veterinary Pathology
University of Guelph
Guelph, Ontario
Canada N1G 2W1
Chapter 3

Rose E. Raskin, DVM, PhD, Diplomate ACVP
Professor of Clinical Pathology
Department of Veterinary Pathobiology
School of Veterinary Medicine
Purdue University
625 Harrison Street
West Lafayette, IN 47907
Chapters 5, 6

Joanne B. Messick, DVM, PhD, Diplomate ACVP
Associate Professor
Department of Veterinary Pathobiology
School of Veterinary Medicine
Purdue University
625 Harrison Street
West Lafayette, IN 47907
Chapter 7

Robert D. Cardiff, MD, PhD
Professor, Pathology
UCD Center for Comparative Medicine
University of California
County Road 98 and Hutchison Drive
Davis, CA 95616
Chapter 9

Peter F. Moore, BVSc, PhD, Diplomate ACVP
Professor of Pathology
Department of Pathology, Microbiology & Immunology
School of Veterinary Medicine
University of California–Davis
1126 Haring Hall
Davis, CA 95616
Chapter 10

Preface

Veterinary Comparative Hematopathology represents the clinical and research experiences gleaned, as well as the study of many of the cases collected, during 35 years of attempting to better understand and recognize hematopoietic neoplasia. It is appropriate to thank those many colleagues whose names appear in figure legends for their contributions. I did not intend to structure the text as a comparative review but came to this conclusion in response to comments from reviewers who wondered at the volume and level of comparative data contained herein.

This book does not trivialize the importance of hematopoietic neoplasia in animals by presenting them as models of human disease. Rather, this work draws heavily on the major and much more extensive current human literature for information on specific diseases not extant in veterinary publications. The major purpose of this book is to define hematopoietic neoplasms in animals, with comparison to those in humans where reasonable similarities exist to guide classification and understanding. In contrast, those neoplasms now defined in humans that lack a currently recognized animal counterpart are described in the human context and await the identification of a comparable animal neoplasm. This format provides veterinarians with a ready reference to help identify such diseases.

It is increasingly evident that diseases of mammals, particularly neoplasms, have a commonality, with those in humans best studied and understood. Genomic studies in humans and animals have demonstrated a remarkable level of conservation of genes and genetic traits extending across mammalian clades. How then can it be that there are more than 30 defined types of B- and T-cell neoplasms in humans that differ widely in biology and response to therapy, but all of those in dogs can be treated as one disease?

Despite the rapid progress that has occurred in oncology, many of us in diagnostic veterinary medicine have noted with concern that veterinary pathology has been slow to adapt to progress in the field. Veterinary oncologists will not be able to devise therapies for specific types of lymphoma unless and until veterinary pathologists provide them with a current level of diagnostic detail. The initiatives of the American College of Veterinary Pathologists in a variety of areas of animal oncology, including canine lymphomas, are timely and needed. This book provides both pathologists and oncologists with information to provide more specificity in both diagnosis and therapy of animal hematopoietic neoplasms.

The last revision of the WHO system of classifying human hematopoietic neoplasia, now in use for more than a decade, represents both a challenge and an opportunity for veterinary medicine. The major premise of the current WHO revision was that neoplasms were to be defined as diseases based on all available information rather than on cellular criteria. In the late 1990s, while updating the WHO Fascicle on histology of animal hematopoietic neoplasms, we found that the WHO system of hematopoietic disease classification in humans was readily applicable in animals. The utility of this system is immediately apparent. As new criteria define new entities they are added to the list of neoplasms based on characteristics that permit them to be reliably identified. This approach is readily applicable to any species and particularly to those domestic animals in which we most frequently encounter hematopoietic neoplasia. To that end, this first edition of *Veterinary Comparative Hematopathology* is based on the WHO classification framework on which future developments can logically be added. This textbook follows the philosophy of a noted fellow countryman, William Osler, who recognized that basic phenomena are common to diseases of all species; there is only one medicine.

V.E. Valli, DVM

Acknowledgments

In learning our disciplines we stand on the shoulders of those who have taught us and subsequently those who have sent us cases over the years that have shaped our perception and understanding of animal diseases. It is appropriate to recognize their invaluable assistance. More recently the principals at Blackwell Publishing deserve recognition for their guidance and diligent attention to the details of this book and to Nancy Albright for excellent copyediting. A book in preparation needs careful review and especially when written by a single author. I thank those colleagues recognized herein as chapter reviewers for their thoughtful and knowledgeable guidance. The scope of this subject and the comparative approach required that assistance was needed from many professionals in both human and veterinary medicine. Their names are gratefully credited in the descriptions of images. Their enthusiastic response to requests for use of images or slides of specific conditions was essential and much appreciated. This book is the result of many hours of concentrated effort at nights and on weekends over more than two years, always with encouragement and support from my beloved spouse Carroll.

V.E. Valli, DVM

Veterinary Comparative Hematopathology

Chapter 1

The Evolution of Classification Systems for Hematopoietic Neoplasms

Specific diseases are *named* to assist their correct recognition. These may be after the people who first described them as in Burkitt's lymphoma and the Reed-Sternberg cell of human Hodgkin's lymphoma. They are also named by the cause, as in the necrotizing laryngitis of diphtheria due to infection with *Corynebacterium diphtheriae*. Once identified as entities, specific diseases may then be *classified* as to cause if known, or on cell type(s) involved and observed rate of progression. Hematopathology has progressed through a series of systems for classifying diseases that were based mainly on cellular characteristics. These systems continued to evolve as it was recognized that cells with similar morphology on routine stains might have very different behavior in both normal and neoplastic states. The advantage of a classification system based on diseases is that the total entity is included in the context of a single disease.

The understanding of specific diseases evolved with steady progression in the recognition of subtle differences, such as in the subtypes of Hodgkin's lymphoma. In contrast, classifications based on cell types had many false starts as increased knowledge of cellular biology rendered early assumptions on lineage and activity to be in error. Many names for perceived cell types such as *reticulum cell* and *clasmatocyte* have happily been laid to rest as the discipline has advanced in understanding. The evolution in classification of lymphomas has not been without heated discussion, which has had interesting origins in both national preferences and geographic differences in incidence of neoplastic subtypes. But in review, the real reason that lymphoma classifications keep changing is that new understanding of cellular mechanisms drives cell and disease recognition into new categories.

The history of lymphoma classifications is described by Harris and Ferry in their chapter in the text, *Neoplastic Hematopathology*, edited by Daniel Knowles, in a manner that sets the stage for the current WHO system. Early descriptions of lymphoid neoplasms began in the 1800s with the recognition of a number of specific diseases. Virchow described and named leukemia in 1845 and lymphosarcoma as a distinct form of lymphoid tumor in 1863. Bilroth in 1871 suggested the term *malignant lymphoma*. The latter term may well have a rebirth in use to identify the clonal lymphoid neoplasms with aggressive behavior from those with an indolent but persistent habit of growth.

Harris and Ferry provide this chronology of the descriptions of lymphoid tumors:

- Hodgkin's disease: Hodgkin (1832), Wilkes (1865), Sternberg 1898), Reed (1902)
- Leukemia: Virchow (1845)
- Lymphosarcoma: Virchow (1863)
- Malignant Lymphoma: Bilroth (1871)
- Differentiation of Hodgkin's disease and lymphosarcoma: Kundrat (1893)
- Multiple myeloma: Bence Jones (1848), MacIntyre (1859), Wright (1933)
- Reticulum cell sarcoma: Ewing (1913), Roulet (1930)
- Follicular lymphoma: Brill (1925), Symmers (1927), Baehr (1932), Gall (1941)
- Burkitt's lymphoma: Burkitt (1958), O'Connor (1961)

As lymphoid neoplasms were described, attempts were made to put these together in early classifications with the main categories: lymphosarcoma, reticulum cell sarcoma, and Hodgkin's disease. It was recognized that the small cell lymphomas tended to be more slowly progressive than the large cell lymphomas, then known as *reticulum cell sarcomas*. In 1934, the American Registry of Pathology assembled a list of lymphoid neoplasms divided into lymphocytotic (small cell), lymphosarcoma (medium size cell), and reticulum cell (large cell) groups. The lymphocytotic group had a leukemic subdivision of chronic and acute types and an aleukemic group of diffuse and nodular types. In this system, the lymphosarcomas were divided into aleukemic (solid lymphoma) and leukemic forms. Of these, the large cell or reticulum cell tumors had leukemic reticulocytoma that included monocytic leukemia with an aleukemic form of the same cell types. Finally, reticulum cell sarcoma was retained for the solid large cell neoplasms. In England, Robb-Smith in 1938 devised a very complex list that included both benign and

malignant diseases based on the concept of the reticuloendothelial system. A legacy of that classification is the rather descriptive term *histiocytic medullary reticulosis*, a form of lymph node medullary sinus histiocytosis.

Gall and Mallory provided a shortened system in 1942 that was based on cell morphology but with distinctive clinical courses based on their 618 cases from Massachusetts General Hospital. Their system divided reticulum cell sarcoma into stem cell and clasmatocytic types and lymphoma into small cell, lymphoblastic, and follicular types followed by Hodgkin's lymphoma and sarcoma. This system came into wide use in the United States and was followed by a classification by Jackson and Parker, first in 1939 and updated in 1947. The latter system separated Hodgkin's disease into three categories and became widely used as well.

The next major change was initiated by Henry Rappaport, then at the University of Chicago, who studied some 300 cases of lymphoma in U.S. servicemen and concluded that regardless of cell type all lymphoid neoplasms, including Hodgkin's disease, had a better prognosis if accompanied by a nodular or follicular architectural pattern. The Rappaport classification removed the term *clasmatocytic* and also the follicular lymphoma of Gall and Mallory, which was replaced by four types of nodular lymphoma. The relationship of nodular lymphoma to follicular and to benign proliferation was not accepted. Although the process of lymphocyte "transformation" in culture was then described, the term *histiocytic* was retained for large cell lymphomas. In addition, the entity of aggressive small cell lymphoblastic lymphoma was lost in combination with diffuse poorly differentiated lymphocytic lymphoma. At this time, small lymphocytes were defined by the term *lymphocytic* and, as an extension, a slightly larger cell that today is likely to be called *lymphocytic intermediate* was called *poorly differentiated lymphocytic* (lymphoma). Thus, while the Rappaport system focused on the importance of architecture and nodularity, it lost the value of recognizing specific diseases such as lymphoblastic lymphoma. The Hodgkin's subtypes were not adequately categorized by nodularity alone and lost the recognition of the entities with lymphocyte depletion and Reed-Sternberg cell predominance. Although now considered a backward step in terms of biological understanding of lymphomas, the Rappaport system became the standard in the United States. This occurred because it required pattern recognition that separated indolent follicular lymphomas from the more aggressive diffuse lymphomas and 40% of adult lymphomas in the United States were of follicular type. On this basis, the Rappaport system could be shown to have "clinical relevance."

Although a major fraction of adult lymphomas were of follicular type, Hodgkin's lymphoma affected both the young and old, and in the United States it accounted for half of all human lymphoma cases. In 1966, Lukes and Butler described a new classification of Hodgkin's disease that separated the granuloma of Jackson and Parker into two subtypes of nodular sclerosis and mixed cellularity and showed that these two categories tended to affect a younger age group. At this time, the lymphocyte predominant types of Hodgkin's disease were shown to be highly radiosensitive and curable and great attention was attached to making the correct tumor categorization. The focus on Hodgkin's disease relegated other lymphomas to a new category of *non-Hodgkin's lymphoma*.

The growth in research in cell biology and immunology of the 1960s brought new information that had major implications for the understanding and interpretation of lymphoid neoplasms. First, the puzzle of how small lymphocytes, believed to be end-stage cells and unable to divide, could form tumorous masses was solved with the demonstration that they could enlarge and divide in response to mitogens and antigenic stimulation. Secondly, the thymus, long a mystery organ, became of major interest with the recognition that lymphocytes indistinguishable morphologically could be of several lineages based on functional activity. Further, in the 1970s, the antigen receptor capability of these lymphocyte subsets was identified as well as the means to their recognition in both normal and neoplastic populations. With the application of these technologies to the lymphomas, it became clear that a major new stratification was needed based on phenotype in addition to pattern recognition or determination of nodular and diffuse architecture.

The first classification system for lymphomas based on immunological principles was developed by Karl Lennert of Kiel, Germany, and was named the Kiel Classification of 1974. This was revised in 1988 and again in 1992. At this time, there was avid interest in how the cells observed in benign lymphoid proliferation were mimicked in neoplastic states and how the small and large "cleaved" lymphocytes fitted into the stream of lymphoid differentiation occurring in the germinal centers of lymph nodes. Lennert recognized that the lymphoid neoplasms were malignant counterparts of benign cells at various stages of differentiation and devised names accordingly. The small cells were named *centrocytes* and the large cells named *centroblasts* following the terminology of hematology, with the youngest form termed a *blast cell*. (Originally, the terms were *germinocyte* and *germinoblast,* but the possible confusion with cells of the developing ovarian follicle recommended the change.)

The Lennert publication was well described and well illustrated and rapidly became the standard in Europe, with a modified system used in the United Kingdom. In the United States, the Lukes and Collins classification of 1974 was also based on a B-/T-cell categorization similar

to the Kiel system. The latter system ignored pattern and assumed that cell type, of itself, was the determining factor in predicting clinical progression. The difficulties with this system were that while separation into B- and T-cell types was required, phenotyping was not generally practiced. Further, a single cell category—the follicular center cell lymphoma—contained most of the lymphomas seen. This classification is best remembered for a theoretical scheme of lymphocyte maturation in the normal germinal center from small lymphocyte through small- and large-cleaved cell categories to plasma cells and memory cells, all without phenotypic verification.

The Lukes-Collins system was not popular in the United States and, for that matter, neither was the Kiel classification. Oddly, there were fewer follicular lymphomas in Europe as compared to North America, and although the Kiel classification included pattern or architecture, the terminology was unfamiliar and the system did not seem to place the same emphasis on pattern as the older Rappaport system. In this climate, there arose a profusion of classification systems and it became difficult for pathologists as well as oncologists to communicate about cases of similar cell type.

To bridge this gap in communications, the American National Cancer Institute initiated a study of 1,200 cases of lymphoma from multiple institutions that were reviewed by six leading experts who had proposed classification systems and six other pathologists with expertise in lymphomas. Each pathologist was required to classify all cases by each of the six extant systems. A major determinant was the ability of each system to predict outcome, with the result that none proved superior. Other endpoints were both inter- and intraobserver reproducibility, and these were found to be disappointingly low. There was no consensus on a standard system, and as a result the derived system based on actuarial determined survival was called the *Working Formulation for Clinical Usage* (1982). A significant feature of the Working Formulation (WF) was that it divided the list of disease categories into three levels based on survival, which translated into rate of progression. There were difficulties in application of the WF system. The criteria for differentiating the large cell from the large immunoblastic cell lymphomas were not clearly defined. Also, there was overlap in separating the small non-cleaved cells of larger type from the large cell lymphomas of the smaller cell type. Finally, the term *small non-cleaved* described what the cell was not, but not the characteristics by which it could be recognized. Despite these deficiencies, the WF rapidly became the standard in North America and much of the world except for Europe, where the Kiel classification continued to dominate. Each category of the WF system was given a letter grade A–J that was rapidly adopted by oncologists who regarded them as identifying "treatment groups." In application, the WF system tended to delay recognition of emerging entities, such as MALT, marginal, and mantle cell lymphomas.

In the subsequent decades, new disease entities were described that were not included in the WF system and, in the meantime, immunophenotyping had become universally available and applied. In order to accommodate treatment trials, various study groups and large institutions devised their own modifications of the WF system, with the result that there again arose a problem in communication between institutions and pathologists and oncologists. To address the need for a new coherence in terminology, an international group of 19 hematopathologists from the United States, Europe, and Asia began meeting in 1991 and adopted new criteria for the inclusion of lymphoma categories, which included all the information required to define a distinct disease entity. Thus, the information might include for any category all or some of cellular morphology, phenotype, genotype, and clinical presentation.

The application of these criteria in system development resulted in the Revised European American Classification of Lymphoid Neoplasms (REAL, 1994) (Table 1.1). Subsequently the REAL system was largely adopted with minor changes to the revised Summary of the WHO classification of tumors of the hematopoietic and lymphoid tissues (2000). The REAL-WHO classification system has been criticized as being a list rather than a ranking of diseases in order of clinical progression but, in effect, it has that attribute as well. However, because each entity listed is accepted as a specific disease, it is feasible and most desirable that the management for each entity is specifically tailored to that entity rather than to a "therapeutic grouping."

In application, the REAL-WHO requires that morphology is the most basic criterion and sufficient for some types of lymphoma, particularly of follicular type where phenotyping and genotyping are not essential. A major advance in the application of the REAL-WHO system is that B-cell CLL (chronic lymphocytic leukemia) and SLL (small lymphocytic lymphoma) are accepted as different manifestations of the same disease, with the emphasis and designation placed on the tissue with the largest burden of tumor. Similarly, in the precursor cell neoplasms, lymphoblastic lymphoma and acute lymphoblastic leukemia are also manifestations of the same neoplasm. In animals where CLL of T-cell type predominates, the same continuity seems to apply for T-cell CLL and SLL and for T-cell ALL (acute lymphoblastic leukemia) and LBL (lymphoblastic lymphoma), at least in dogs.

In some cases, particularly in mediastinal large B-cell lymphoma, it is essential also to have the clinical presentation in order to arrive at a correct diagnosis. Further changes are the recognition that plasma cell myeloma and

Table 1.1. The revised European-American classification of lymphoid neoplasms (REAL) (1994).

B-cell neoplasms	
Precursor B-cell neoplasm: Precursor B-lymphoblastic leukemia/lymphoma	Provisional subtype: Nodal marginal zone lymphoma (±monocytoid B-cells)
Mature (peripheral) B-cell neoplasms	Provisional entity: Splenic marginal zone lymphoma (±villous lymphocytes)
B-cell chronic lymphocytic leukemia/prolymphocytic leukemia/small lymphocytic lymphoma	Hairy cell leukemia
Lymphoplasmacytoid lymphoma/Immunocytoma	Plasmacytoma/plasma cell myeloma
Mantle cell lymphoma	Diffuse large B-cell lymphoma[a]
Follicle center lymphoma, follicular	Subtype: Primary mediastinal (thymic) B-cell lymphoma
Provisional cytologic grades: 1 (small cell), II (mixed small and large cell), III (large cell)	Burkitt's lymphoma
Provisional subtype: diffuse, predominantly small cell type	Provisional entity: High-grade B-cell lymphoma, Burkitt's-like[a]
Marginal zone B-cell lymphoma, extranodal mucosa-associated lymphoid tissue type (±monocytoid B-cells)	
T-cell and putative natural killer-cell neoplasms	
Precursor T-cell neoplasm: Precursor T-lymphoblastic lymphoma/leukemia	Provisional subtypes
Mature (peripheral) T-cell and natural killer-cell neoplasms	Hepatosplenic γδ T-cell lymphoma
T-cell chronic lymphocytic leukemia/prolymphocytic leukemia	Subcutaneous panniculitic T-cell lymphoma
Large granular lymphocyte leukemia (LGL)	Angioimmunoblastic T-cell lymphoma
T-cell type	Angiocentric lymphoma
Natural killer-cell type	Intestinal T-cell lymphoma (±enteropathy-associated)
Mycosis fungoides/Sezáry syndrome	Adult T-cell lymphoma/leukemia
Peripheral T-cell lymphomas, unspecified[a]	Anaplastic large cell lymphoma, $CD30^+$, T- and null cell types
Provisional cytologic categories: medium-sized cell, mixed medium-sized and large cell, large cell, lymphoepithelioid cell	Provisional entity: anaplastic large cell lymphoma, Hodgkin's-like
Hodgkin's lymphoma	
Lymphocyte predominance	Mixed cellularity
Lymphocyte-rich (classical Hodgkin's lymphoma)	Lymphocyte depletion
Nodular sclerosis	

[a] Likely to include more than one disease

Hodgkin's disease are lymphoid neoplasms of B-cell lineage. Perhaps the most significant comment that may be made on the REAL-WHO system is that, in practical application in review of 1,403 cases of human lymphoma with all required data available in all cases, the review pathologists had an overall agreement rate of greater than 85%. Only 2.8% of the cases were felt to be unclassifiable, largely due to technical factors. Each review pathologist was required to reread 20% of the cases at each study site, as selected at random by the attending statisticians, which produced an agreement rate with their initial diagnosis also of 85% (82–89%). The strategy of case examination required each pathologist to render an initial diagnosis on only the hematoxylin-eosin–stained section. They were then provided with the phenotyping slides or flow data and required to make a second diagnosis. Finally, they were given the clinical history and presentation and then made a third and final diagnosis. This process demonstrated that phenotyping did not significantly increase the diagnostic accuracy for follicular lymphomas, marginal zone B-cell lymphoma of MALT type, and the small lymphocytic and lymphoplasmacytic lymphomas. On the other hand, detailed clinical data was helpful only in distinguishing primary mediastinal B-cell lymphoma from other large B-cell neoplasms. These results need to be verified in a veterinary setting, with each pathologist required to diagnose each case via the three-step system that was used in the human study on the application of the WHO system. Such a study has never been attempted in animal

pathology. It might be expected that with well-described entities there would be a reasonable level of reproducibility. Additionally, similar results might be obtained since the genotypic and cytogenetic information available for human hematopoietic neoplasms but lacking in the veterinary sphere is largely utilized for the classification of myeloid leukemias and not as critical for categorizing lymphomas.

REFERENCES

Armitage, J.O., and Weisenburger, D.D. (1998) New approach to classifying non-Hodgkin's lymphomas: Clinical features of the major histologic subtypes. *J Clin Oncol* 16:2780–2795.

Barcos, M., and Lukes, R.J. (1975) Malignant lymphoma of convoluted lymphocytes: A new entity of possible T-cell type. In Sinks, L., and Godden, J. (eds.), *Conflicts in Childhood Cancer: An Evaluation of Current Management*, vol. 4. Liss, New York, pp. 147–178.

Bence Jones, H. (1848) On a new substance occurring in the urine of a patient with millities and fragilitas ossium. *Philos Trans R Soc Lond* 55:673.

Brill, N., Baehr, G., and Rosenthal, N. (1925) Generalized giant lymph node follicle hyperplasia of the lymph nodes and spleen: A hitherto undescribed type. *JAMA* 84:668–671.

Burkitt, D.P. (1958/59) A sarcoma involving the jaws in African children. *Br J Surg* 46:218–223.

Cooper, M.D., Peterson, R.D.A., and Good, R.A. (1965) Delineation of the thymic and bursal lymphoid systems in the chicken. *Nature* 205:143–146.

Dorfman, R.F. (1994) Hematopathology: A crescendo of scholarly activity. *Mod Pathol* 7:226–241.

Gall, E.A., and Mallory, T.B. (1942) Malignant lymphoma: A clinicopathologic survey of 618 cases. *Am J Pathol* 18:381–395.

Gerard-Marchant, R., Hamlin, I., Lennert, K., et al. (1974) Classification of non-Hodgkin's lymphomas. *Lancet* ii:406–408.

Harris, N.L., and Ferry, J.A. (2002) Classification of non-Hodgkin's lymphomas. In Knowles, D.M., and Thompson, D.D. (eds.), *Neoplastic Hematopathology*, 2nd ed., Lippincott Williams & Wilkins, Philadelphia, pp. 691–745.

Harris, N.L., Jaffe, E.S., Stein, H., et al. (1994) A revised European-American classification of lymphoid neoplasms: A proposal from the International Lymphoma Study Group. *Blood* 84:1361–1392.

Jackson, H., Jr., and Parker, F., Jr. (1947) *Hodgkin's Disease and Allied Disorders*. Oxford University Press, New York.

Kundrat, H. (1893) Uber lymphosarkomatosis. *Wien klin Wochnschr* 6:211–213, 224–239.

Lukes, R., Butler, J., and Hicks, E. (1966) Natural history of Hodgkin's disease as related to its pathological picture. *Cancer* 19:317–344.

Lukes, R., and Collins, R. (1974) Immunologic characterization of human malignant lymphomas. *Cancer* 34:1488–1503.

Non-Hodgkin's Lymphoma Pathologic Classification Project. (1982) National Cancer Institute sponsored study of classifications of non-Hodgkin's lymphomas: Summary and description of a Working Formulation for clinical usage. *Cancer* 49:2112–2135.

Nowell, P.C. (1960) Phytohemagglutinin: An initiator of mitosis in cultures of normal human leukocytes. *Cancer Res* 20:462–466.

Rappaport, H., Winter, W., and Hicks, E. (1956) Follicular lymphoma: A re-evaluation of its position in the scheme of malignant lymphoma, based on a survey of 253 cases. *Cancer* 9:792–821.

Reed, D. (1902) On the pathological changes in Hodgkin's disease, with especial reference to its relation to tuberculosis. *Johns Hopkins Hosp Rep* 10:133–196.

Stansfeld, A., Diebold, J., Kapanci, Y., et al. (1988) Updated Kiel classification for lymphomas. *Lancet* i:292–293.

Symmers, D. (1927) Follicular lymphadenopathy with splenomegaly: A newly recognized disease of the lymphatic system. *Arch Pathol* 3:816–820.

Wilson, J.D., and Nossal, G.J.V. (1971) Identification of human T and B lymphocytes in normal peripheral blood and in chronic lymphocytic leukemia. *Lancet* II:788–791.

Wright, J.H. (1933) A case of multiple myeloma. *Bull Johns Hopkins Hosp* 52:156.

Chapter 2

Normal and Benign Reactive Hematopoietic Tissues

LYMPH NODES

Normal Form and Function

Embryology

The development of lymph nodes is part of an ancient and highly conserved phylogenetic process whereby mammals have a dual vascular network of blood and lymphatic vessels. In the early embryo, lymphatic vessels differentiate from blood vessels. The first stage of lymphatic development occurs in the cardinal vein of the early embryo as a subset of endothelial cells express the LYVE-1 and VEGFR-3 receptors that are present on normal adult lymphatic channels. As differentiation commences, these endothelial cells express different levels of the homeobox gene *Prox-1* and are induced to form buds from the vein that form the primordia of the lymphatic system. These first few lymphatic cells then express the secondary lymphoid chemokine (SLC) and increase expression of VEGFR-3 with both markers of mature lymphatic cells. As the embryo develops, the blood vessels deliver nutrients and later immune cells while the lymphatics collect extravasated leukocytes and fluid and return both to the blood vascular system. Failure of development of these two systems is characterized by congenital arteriovenous malformations resulting in edema and ascites. Knockout mice lacking the early lymphatic signaling genes develop arteriovenous shunts and embryonic hemorrhage.

Lymph node development begins as an anastomosis of adjacent lymphatic vessels with an aggregation of surrounding mesenchymal cells and small blood vessels. These associations form an eccentric folding of the vessels and surrounding mesenchyme that form the framework for the node with the capsule and afferent and efferent vessels. Studies conducted by injection of vessels with polymer followed by corrosion demonstrate that the hilar arterioles form many fine branches in the deep cortex that arborize in the outer cortex around the primordial germinal centers, which are themselves relatively avascular. The veins form in parallel with the arterial system and exit at the hilar pole with efferent lymphatics. All venules except those in the inner cortex have a low endothelial lining with fenestration of some medullary capillaries, but all others have a complete endothelial lining with basement membrane and pericytes.

Small and medium lymphocytes enter the area within 2 days after the initial formation at 18–19 days in the rabbit embryo. There is a slow increase in lymphocyte numbers with the early formation of nodular organization evident just prior to birth. In the dog, the organization of the lymph nodes follows that of the thymus and the spleen at 35–38 days and lymphocytic colonization is well advanced at 52–53 days. The ontogeny of immune competence varies widely with species, but generally well-developed germinal centers with antigen-related polarity are not present at birth unless there has been intrauterine infection as occurs in foals aborted at term with equine viral rhinopneumonitis (EVR) virus infection.

Structure

Lymph nodes having a dual vascular structure have cellular feed-in from both the lymphatic and the blood systems. Lymphatic drainage brings in antigenically charged cells from the tissues as well as antigen in various forms and, in some cases, neoplastic cells primarily from carcinomas. The vessels bring lymphocytes that are naive and recycled; these are able to enter the node cortex via the intercellular adhesion molecules (ICAMs) that permit cellular adhesion and transluminal migration across the postcapillary venules at specifically determined sites. These vascular structures of the blood and lymphatic channels form three endothelial-lined systems—intravascular, intralymphatic, and interstitial—by which the structure of nodes filter lymph, process antigen, and return lymphocytes from blood to tissue. The major anatomic regions of the lymph nodes are the containing capsule with afferent lymphatics (Fig. 2.1) and, progressing inward, the peripheral sinus, the outer and inner cortex, and the medulla containing the fixed cells of the cords surrounded by the sievelike structure of the sinuses that drain into the efferent lymphatics that surround the blood vessels at the hilar area of the node (Fig. 2.2). These

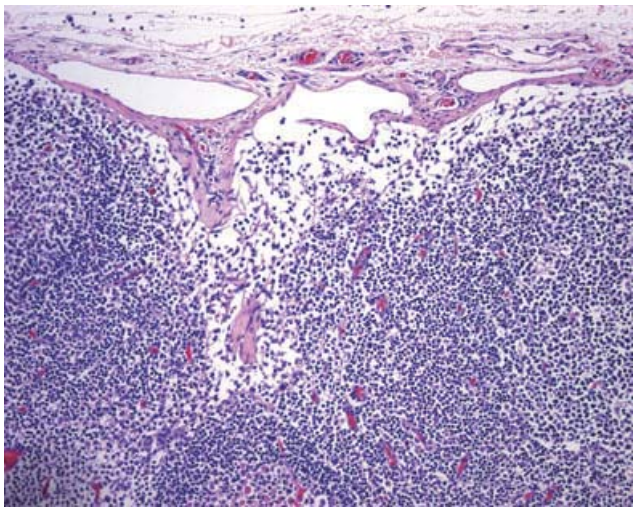

Figure 2.1. Dog: lymph node, afferent lymphatics. Peripheral capsule with several afferent lymphatic sinuses. Valves can be seen in the intercapsular sinus at upper right. There is a continuous pathway from the entering sinus (center) to the subcapsular sinus.

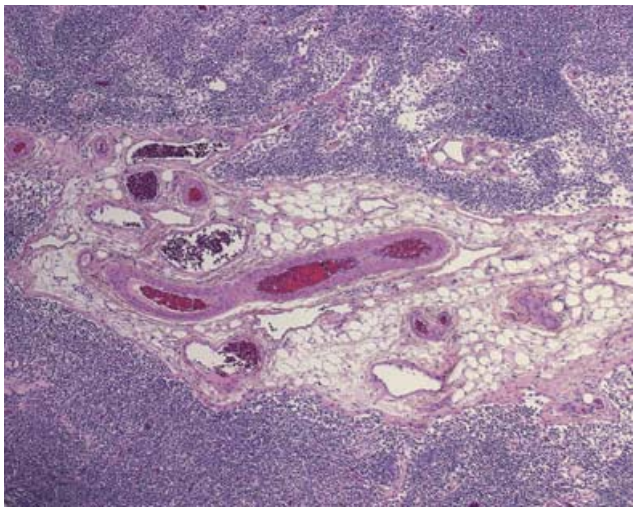

Figure 2.2. Dog: lymph node, efferent lymphatics. Hilar structures illustrating major arteries and veins surrounded by the efferent lymphatics.

relationships apply in domestic mammals except the pig, where the internal regions of the nodes are inverted with the afferent lymphatics entering in the center of the node surrounded by the cortex and germinal centers with the medullary structures in the periphery (Fig. 2.3). Like other animals, the recirculating lymphocytes enter the cortical area by migration through high endothelial venules (Fig. 2.4), but after residence in B- or T-cell architectural areas, they are returned to the blood by the venous system rather than by efferent lymphatics.

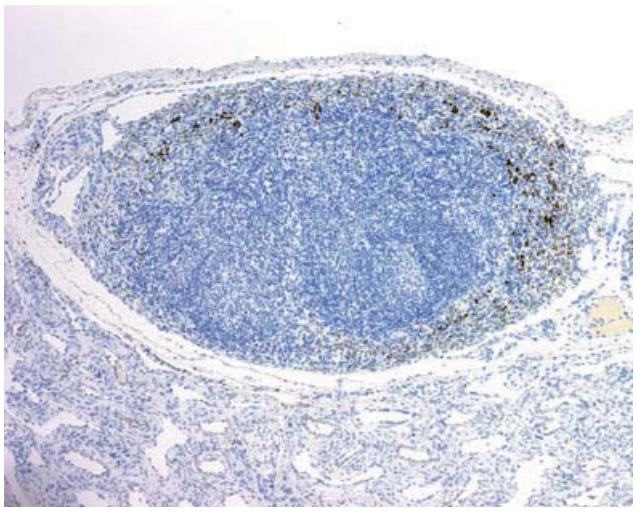

Figure 2.3. Pig: mesenteric lymph node. Inverted architecture with inner cortex and outer medullary regions containing hemosiderin-bearing macrophages.

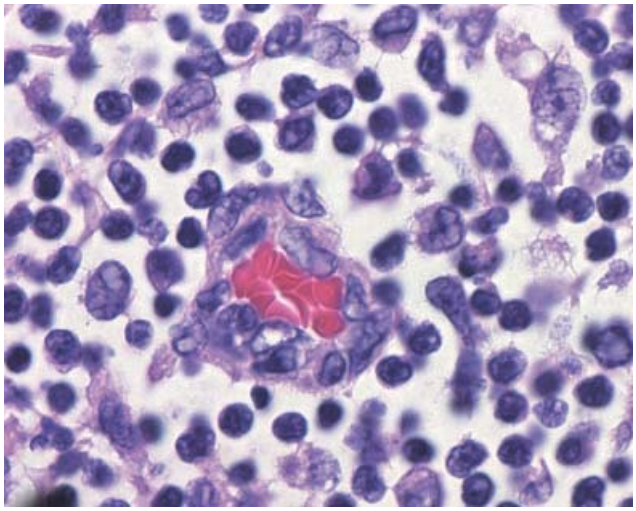

Figure 2.4. Dog: lymph node. Paracortex with high endothelial venule with several lymphocytes in transluminal exit through the vessel wall.

The supporting connective tissue superstructure of the node is of mature collagen that extends in fine supporting columns from the capsule to form larger aggregations in the medullary area that surrounds the hilar vessels (Fig. 2.5). In nodes that have increased rapidly in size, as occurs in lymphoma and lesser in acute inflammation, the node capsule is thinned and taut and compresses the peripheral sinus in formalin-fixed specimens (Fig. 2.6). In contrast, in atrophic states caused by chemotherapy or cachexia, the node capsule is thickened and wavy and the peripheral sinus may be wide and open (Fig. 2.7). In conjunction with these changes at the outer areas of the node, the

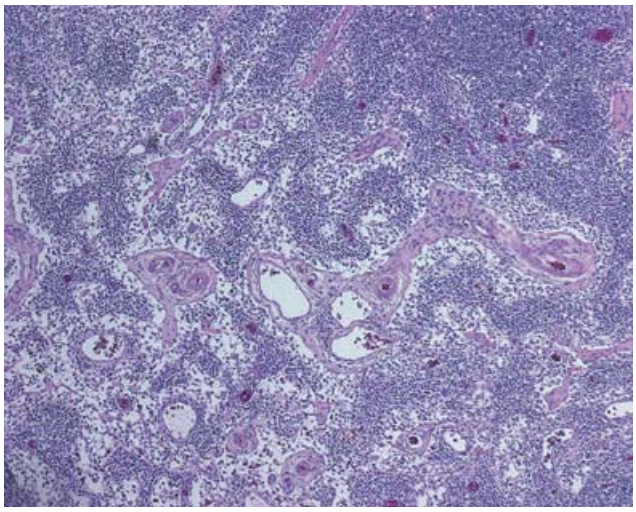

Figure 2.5. Dog: lymph node, medullary architecture. Hilar blood vessels sheathed in collagenous supporting structures surrounded by narrow medullary sinuses between the darker staining medullary cords.

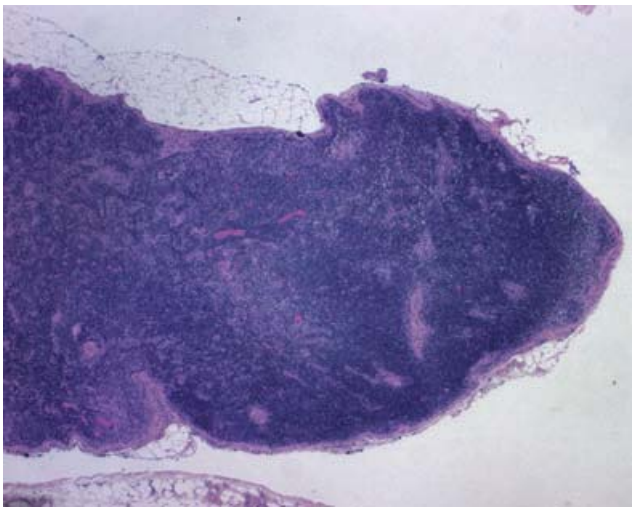

Figure 2.7. Cat: lymph node, lymphoid atrophy. The animal had recently completed a course of chemotherapy for an unrelated neoplasm. There is complete involution of germinal centers with dense cellularity of the paracortex in early cellular rebound. Note that the capsule is thickened and undulating with loss of node volume.

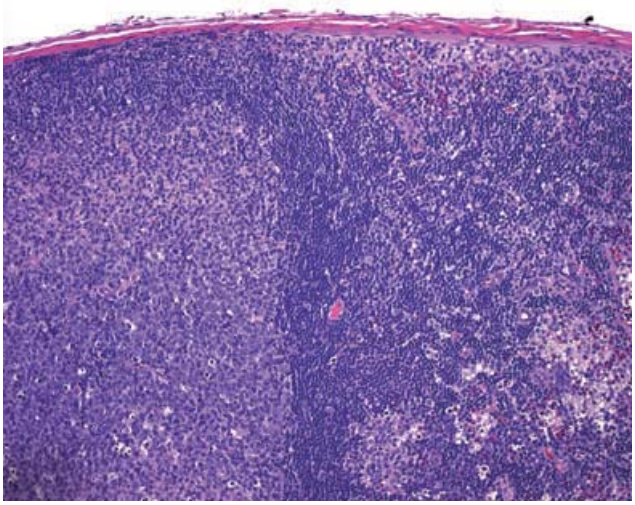

Figure 2.6. Cat: lymph node, capsule and peripheral sinus. Node cortex with follicular hyperplasia and a thinned, taut peripheral capsule and irregular compression of the peripheral or subcapsular sinus.

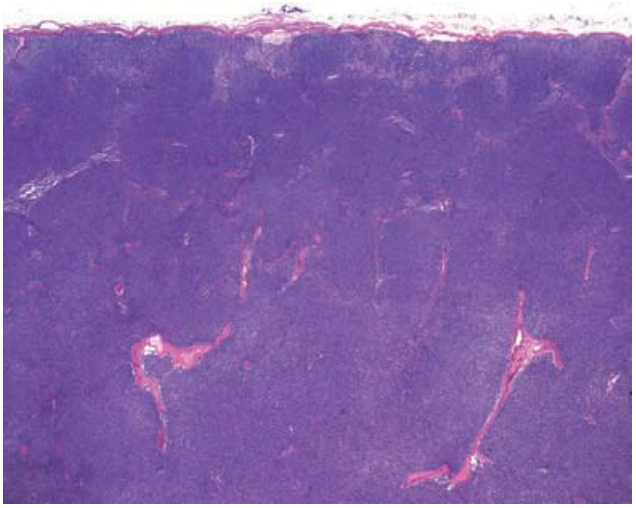

Figure 2.8. Dog: lymph node, lymphoid proliferation. Diffuse large cell lymphoma. In hyperplasia and lymphoma, the supporting collagenous structures become thinned and widely spaced as the parenchyma is increased in volume. These changes are similar to those seen in the spleen with thinning of the capsule and greater distance between the muscular trabeculae in a distended organ.

supporting raphe become thin and widely separated in hyperplastic nodes and in lymphoma (Fig. 2.8); in chronic inflammation they become greatly increased in volume and may dominate the medullary areas of the node (Fig. 2.9) Such changes are seen in submandibular lymph nodes of dogs with chronic periodontal disease and in the supramammary nodes of dairy cattle with chronic mastitis. The proliferation of connective tissue of chronic benign lymphadenopathy may be accompanied by follicular hyperplasia or lymphoma, but in either case, it is clear evidence of a long period of intense antigenic stimulation that preceded the current condition.

The cortex of the node contains the germinal centers with mantle, and in hyperplastic states, the outer rim of marginal zone cells (Fig. 2.10) The germinal centers are surrounded by the T-cell rich outer cortex (Fig. 2.11) that contains a mixture of cells, primarily small T-lymphocytes

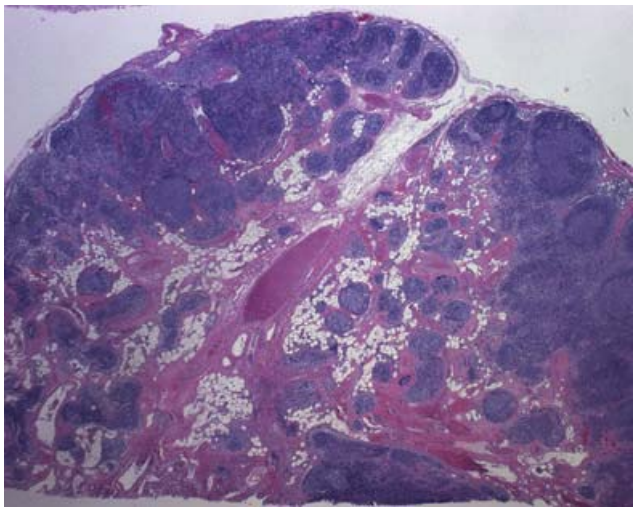

Figure 2.9. Cat: cervical lymph node, chronic hyperplasia and sclerosis. There is marked and irregular increase in medullary collagenous supporting structures with concurrent atrophy of the medullary cords and sinuses.

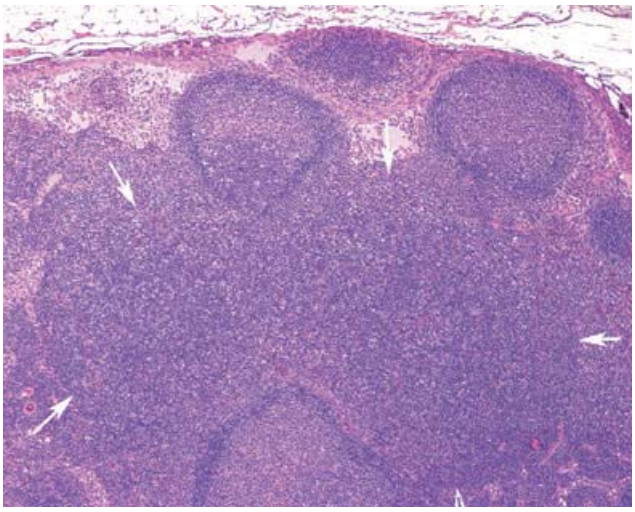

Figure 2.11. Cat: lymph node, focal paracortical nodular hyperplasia with two "deep cortical units" (arrows) flanked above and below by germinal centers.

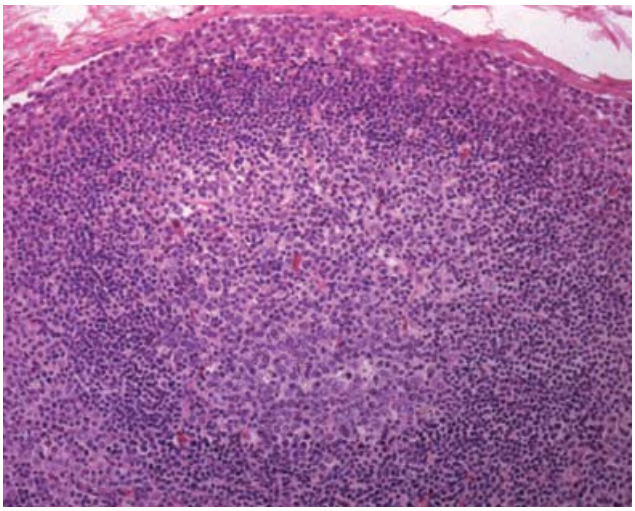

Figure 2.10. Dog: lymph node, follicular architecture. Follicular hyperplasia with irregularly defined germinal center surrounded by a more dense cuff of mantle cells with a peripheral rim (top) of larger marginal zone cells that have more vesicular nuclei and a larger volume of cytoplasm.

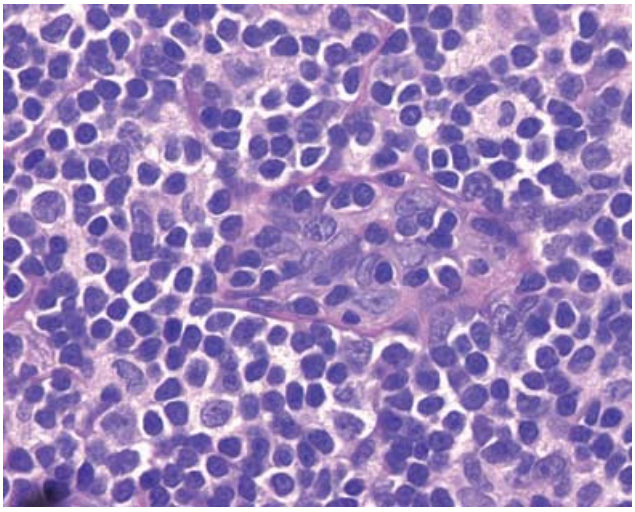

Figure 2.12. Detail of paracortex from Figure 2.11. The paracortex contains primarily small T-lymphocytes with a few lymphoblasts and larger dendritic cells with pale nuclei. High endothelial venule, center, has a high level of transmural cellular traffic.

with a few blasts and large pale nuclei of dendritic cells, a few macrophages, and the high endothelial postcapillary venules (Fig. 2.12) The node cortex may itself wax and wane in a focal manner with the medullary sinuses extending to the peripheral sinus in areas of cortical atrophy adjacent to large diffuse areas of cortical hyperplasia, termed *deep cortical units* (Fig. 2.13). Changes of this type are typical of the mesenteric nodes in mature rats. The reactivity of the node is segmental and related to the level and type of drainage from a particular efferent lymphatic. Experimentally, ligation of an efferent lymphatic results in atrophy of the underlying area of node cortex. Both antigenic stimulation and the presence of antigen-focusing cells are essential in the incoming lymph for the development and maintenance of the cortical and paracortical reactive units. In early stimulation of nodes, there is a regular sequence of cellular events that progresses over about 10–14 days from initiation to the appearance of well-formed germinal centers. In the early stages of reaction, the paracortex and cortex have a moth-

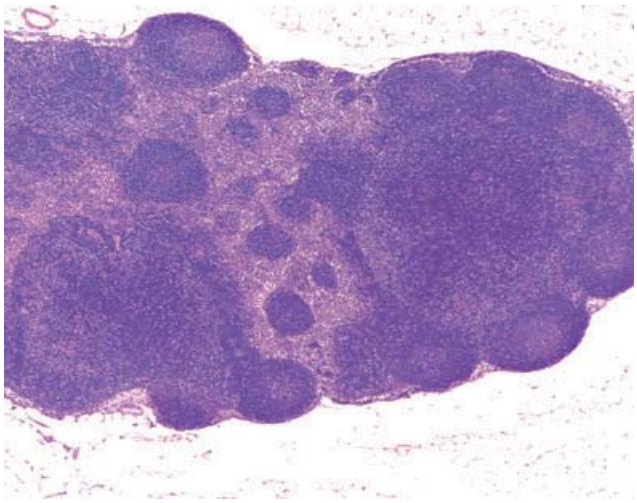

Figure 2.13. Mature Sprague-Dawley rat: mesenteric lymph node, focal paracortical nodular hyperplasia. Typical appearance with deep cortical units appearing as well-defined areas of the paracortex that have a mottled appearance due to the variation in cell types present. The deep cortical units are each related to and dependent upon the antigenic drainage from specific afferent lymphatics.

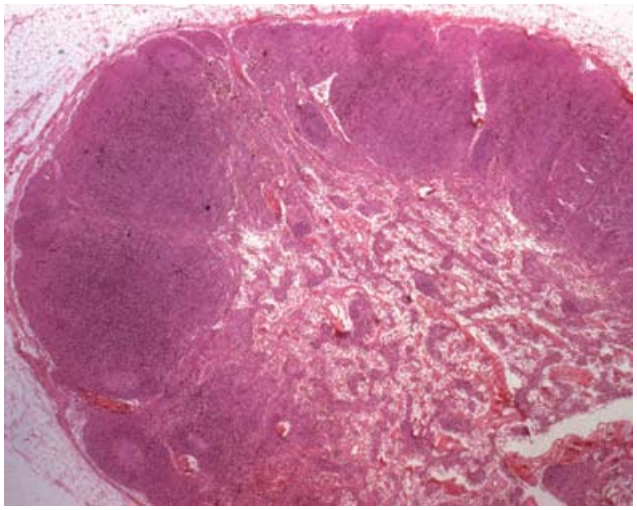

Figure 2.14. Dog: popliteal lymph node, diffuse paracortical hyperplasia. From a dog given vaccination in the ipsilateral foot pad 4 days earlier. There is ablation of previous germinal centers with diffuse paracortical hyperplasia.

eaten appearance at an architectural level of examination due to a very mixed small and large cell population with many large tingible body macrophages (Fig. 2.14). As antigen processing develops, a follicular pattern becomes dominant. The timing of these changes has been determined in detail in laboratory primates by serial removal of the axillary nodes after intrabrachial vaccination. That study was undertaken to assist in avoiding an erroneous diagnosis of lymphoma in children given routine immunization and then presented later with axillary lymphadenopathy but lacking the history of vaccination. The time to a follicular pattern in humans is closer to 2 weeks; in dogs given distemper hepatitis vaccination into the caudal footpad followed by serial removal of the popliteal node, the time to follicular development was nearer to 10 days.

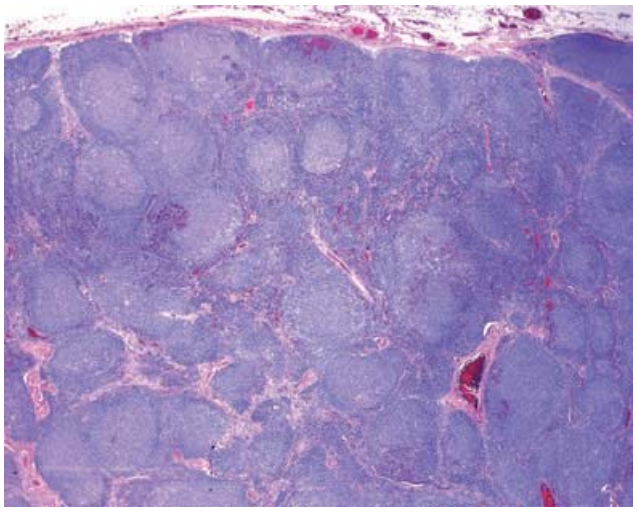

Figure 2.15. Dog: lymph node, follicular hyperplasia. Marked and chronic, with compression of medullary structures.

Germinal centers are confined to the outer cortex in nodes receiving moderate antigenic stimulation and may populate the inner or paracortex with strong and sustained stimulation. In conditions resulting in follicular hyperplasia, the germinal centers may impinge upon the medullary cords and sinuses that are then compressed into a small area in the center or hilar region of the node (Fig. 2.15). The germinal centers have a consistent architecture, with the interior cells having a superficial or light pole and a deep or dark pole that is always oriented with the light pole directed at the source of antigen (Fig. 2.16). Recognition of this polarity of germinal centers is an important observation in distinguishing follicular hyperplasia from follicular lymphoma. The superficial pole of the germinal centers is composed primarily of small lymphocytes, with a moderate amount of lightly stained cytoplasm giving that area a less dense appearance when observed at low magnification (Fig. 2.17). In contrast, the cells of the deep pole are primarily large lymphocytes with proportionately less cytoplasm that is very deeply amphophilic on hematoxylin and eosin staining, resulting in that area appearing much darker and more dense in comparison to the light zone (Fig. 2.18). In roughly the geographic center of the follicle, many large macrophages with ingested nuclear debris reside constituting the tingible or stainable body phages (Fig. 2.19). These phages are ingesting

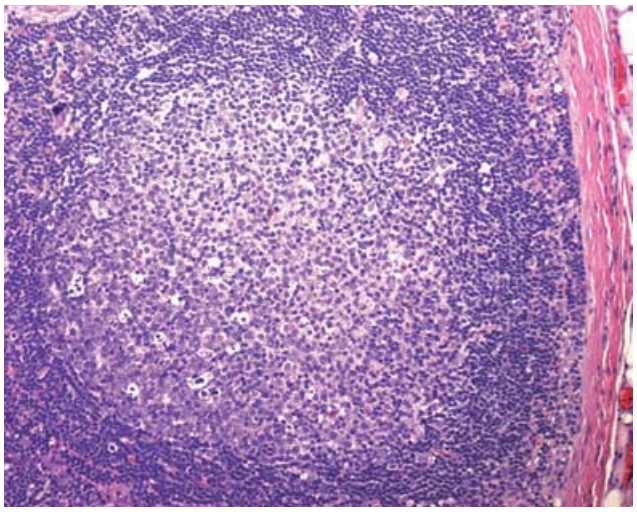

Figure 2.16. Cat: lymph node, follicular polarity. The deep or dark pole of the germinal center is to left. The superficial or lighter pole to the right is beneath the peripheral sinus of the lymph node.

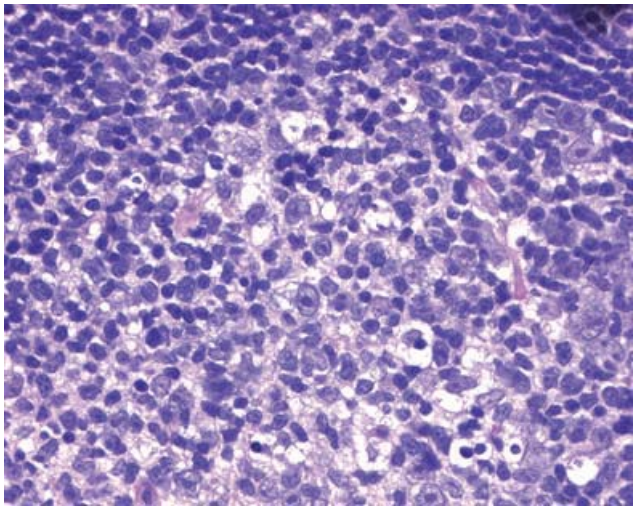

Figure 2.17. Cat: lymph node, follicular light pole. Cytologic detail of the light or superficial pole of the germinal center with a cuff of small mantle cells above the superficial pole cells, consisting primarily of small and medium-sized lymphocytes with relatively abundant pale staining cytoplasm.

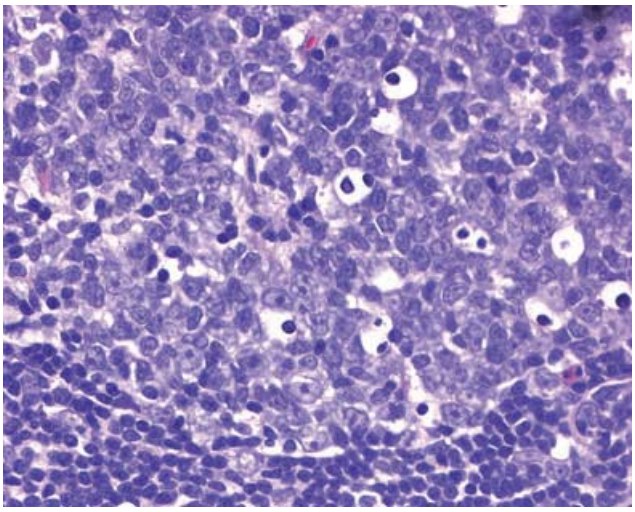

Figure 2.18. Cat: lymph node, follicular dark pole. Cytologic detail of the dark or deep pole of the germinal center with a cuff of small mantle cells below the deep pole cells, consisting primarily of large lymphocytes with vesicular nuclei, prominent (often peripheral) nucleoli, and a narrow rim of darkly stained cytoplasm.

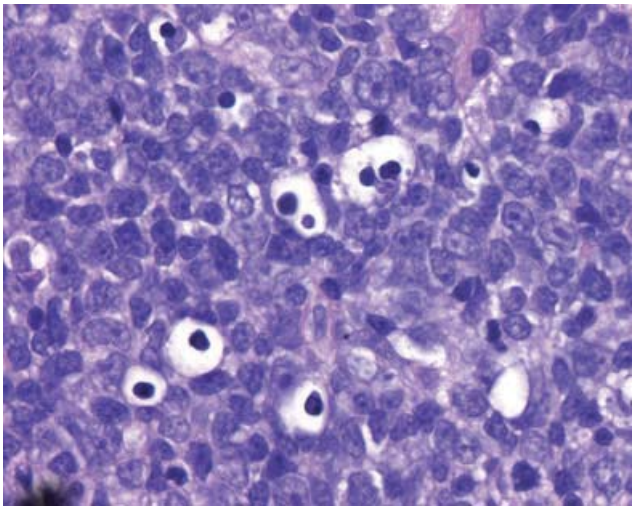

Figure 2.19. Cat: lymph node, follicular center. The central portion of the germinal center contains numerous large tingible body macrophages containing densely stained structures that are the nuclei of lymphocytes that have commenced apoptosis and are being removed by the surrounding phagocytic cells.

lymphocytes whose mutation of the variable portion of the immunoglobulin gene has produced an antibody felt to be of too high or too low avidity and which has not been "rescued" from apoptosis by the intrafollicular managerial T-cells in the process of immune cell selection. This anatomy of the germinal center can best be seen in the outer subcapsular area where the orientation of the polarity to the incoming antigen in the peripheral sinus is most apparent.

The mantle cell cuff surrounding the germinal centers tends to be elliptical and of greatest depth over the apical or light pole of the follicle. The mantle cells are a relatively homogeneous population of small lymphocytes that have round compact nuclei that lack nucleoli and have very little cytoplasm resembling those of the thymic cortex (Fig. 2.20). Although similar in appearance, the mantle cells are functionally heterogeneous and primarily

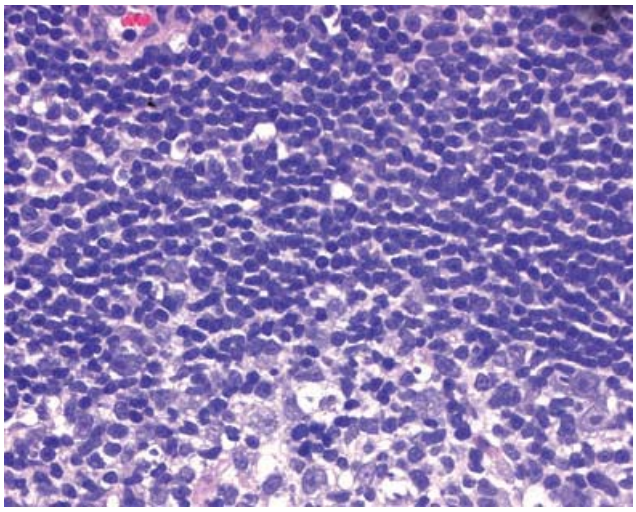

Figure 2.20. Cat: lymph node, superficial mantle cell cuff. Lying just beneath the peripheral sinus, the widest area of mantle cuff consists of small cleaved and intermediate-sized lymphocytes with compact chromatin without parachromatin clearing and small or inapparent nucleoli. The cytoplasm is minimal and lightly stained with the nuclei lying in close contact.

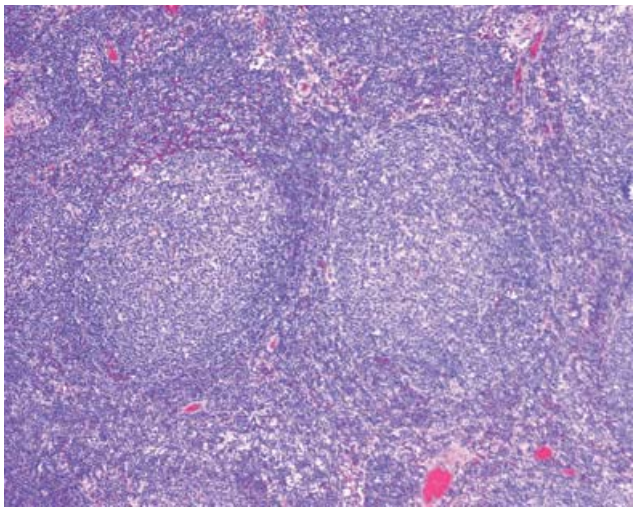

Figure 2.21. Dog: lymph node, follicular involution. Deep cortical germinal centers in a follicular reaction waning in intensity. The mantle cell cuffs are thinned and discontinuous and with reduced cell density of the germinal centers.

naive pregerminal center B-cells. About 10% of the mantle cells are similar-appearing small T-lymphocytes. The width and density of the mantle cell cuff are indications of the adequacy of host lymphocyte production kinetics. Animals mounting a robust humoral immune response have mantle cell cuffs that completely encircle the germinal center in wide and densely packed cellular columns. In contrast, with persistent stimulation and immune system depletion, the mantle cell cuffs become thinned, discontinuous, and with less dense cellular packing (Fig. 2.21). If follicular regression continues, the residual mantle cells collapse into the area occupied by the dendritic cells and appear histologically as clusters of small dark cells against the cortical background. As such they are referred to as "fading" or "inverted" follicles (Figs. 2.22, 2.23). Their recognition is important because if numerous, they indicate a history of follicular hyperplasia that has been superseded by atrophy or lymphoma. In addition, the residual mantle cells provide an orientation to lesions characterized by marginal zone hyperplasia or marginal zone lymphoma. In addition, follicular involution may be followed by cortical and paracortical proliferation of neoplastic small T-cells producing an architectural image remarkably similar to marginal zone lymphoma but having cytologic and lineage specificity.

Marginal zone cells are generally not prominent in normal nodes and, in follicular hyperplasias, may become large and tend to be most numerous over the light pole and sides of the germinal centers and mantle cells (Figs. 2.24, 2.25). The marginal zone cells are most often expanded in the dog and lesser in other domestic animals. Cytologically, the marginal zone cells have round nuclei about 1.5 red cells in diameter and have a fine dispersed chromatin pattern (Fig. 2.26). In contrast, in neoplastic proliferation, these cells have the chromatin peripheralized or marginated against the nuclear membrane. Their

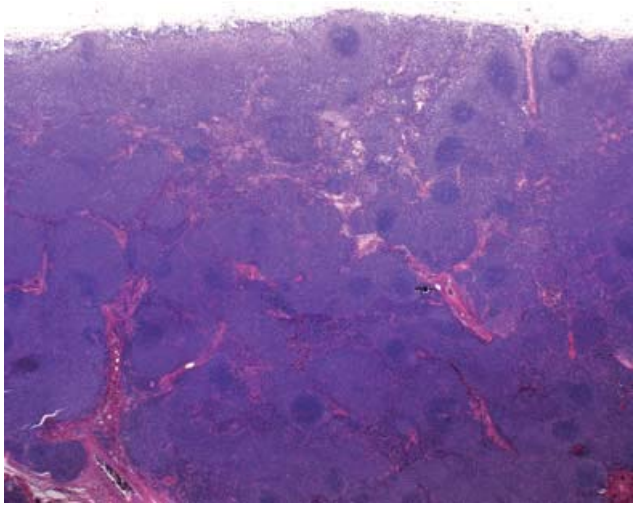

Figure 2.22. Dog: lymph node, T-zone lymphoma. With progressive involution of the germinal centers, the mantle cells collapse into the dendritic cell area forming a dense cluster of small deeply stained nuclei that indicate the area of an involuted germinal center and collectively, fading follicular hyperplasia. An occasional cluster of cells like that in the upper right has a pale center due to incomplete involution, making their origin in germinal centers more apparent.

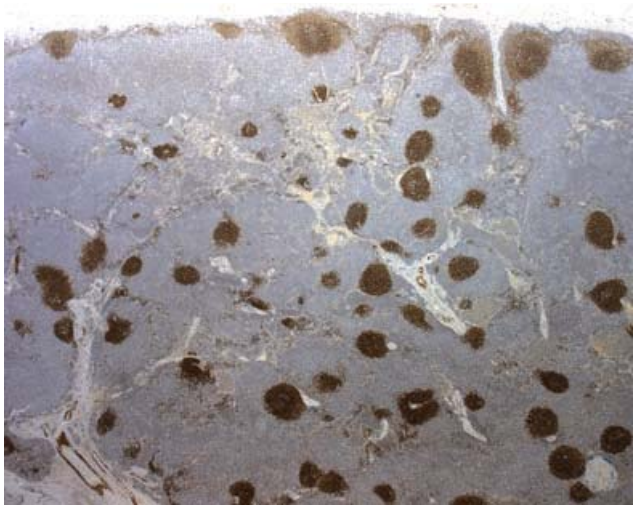

Figure 2.23. Detail of Figure 2.22 stained with CD-79, which sharply defines the focal clusters of mantle B-cells of involuted germinal centers.

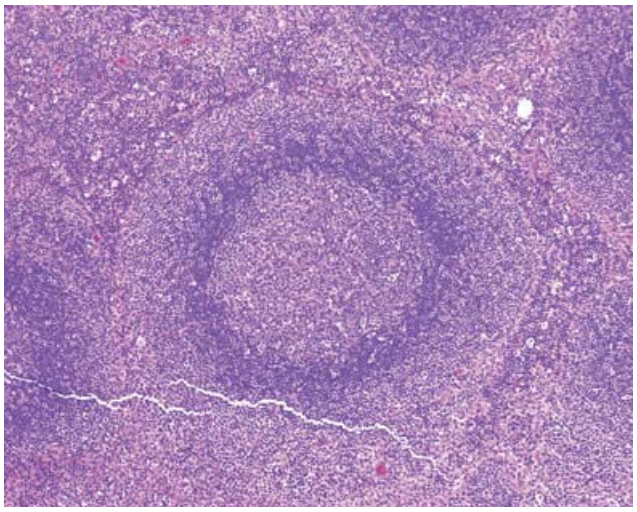

Figure 2.24. Dog: lymph node, marginal zone hyperplasia. In a vibrant benign reaction, a subcortical germinal center retains a dense and relatively uniform cuff of mantle cells that are surrounded by an unusually well-defined area of marginal zone hyperplasia.

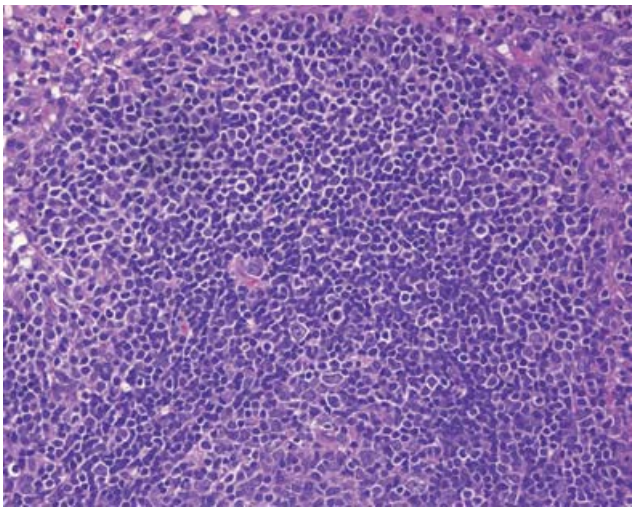

Figure 2.25. Detail of another follicle of the node depicted in Figure 2.24. The germinal center in the lower center has a narrow and ill-defined cuff of mantle cells surrounded by an adjoining proliferation of marginal zone cells that are well defined by a thin outer encapsulation. The "mixed" cellularity of marginal zone hyperplasia is characteristic of benign proliferation that assists in distinction from marginal zone lymphoma where the proliferating cells are more homogeneous.

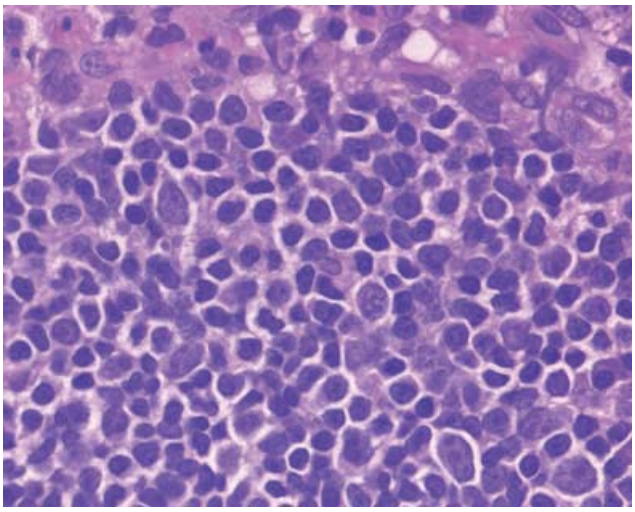

Figure 2.26. Detail of Figure 2.25. In marginal zone hyperplasia, the typical marginal zone cells have round nuclei with small central nucleoli and relatively abundant cytoplasm. The intermixing of lymphocytes with small cleaved nuclei is primarily of B-cell type and largely part of the mantle cell cuff.

most defining feature is a prominent single central nucleolus (Figs. 2.27, 2.28). The cytoplasm is relatively abundant and is lightly stained resulting in relatively low density of cellular packing that is most apparent at an architectural level of histologic examination (Fig. 2.29). In hyperplasia, the marginal zone cuffs tend to be cytologically heterogeneous with admixed cells of the paracortex. The marginal zone cells may be waxing, while the mantle cells are waning with a thin layer of mantle cells around the germinal center serving to identify the outer layer of cell proliferation as of marginal zone type. In marginal zone lymphoma, the perifollicular areas of cellular proliferation become cytologically homogeneous and may penetrate the fading germinal centers on the inside while coalescing with adjacent expanding areas on the outer side. A remarkable and important feature of the marginal zone cells is that in both hyperplastic and neo-

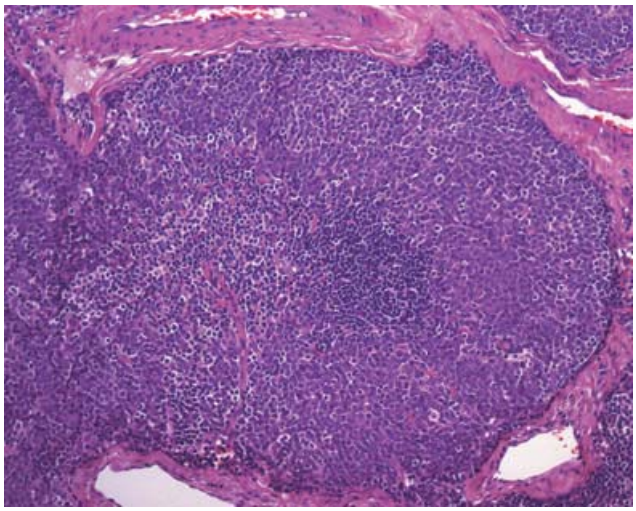

Figure 2.27. Dog: lymph node, marginal zone lymphoma. A previous area of germinal center formation is defined by the central cluster of dark-staining mantle cells and surrounded by a dense proliferation of more homogeneous-appearing cells.

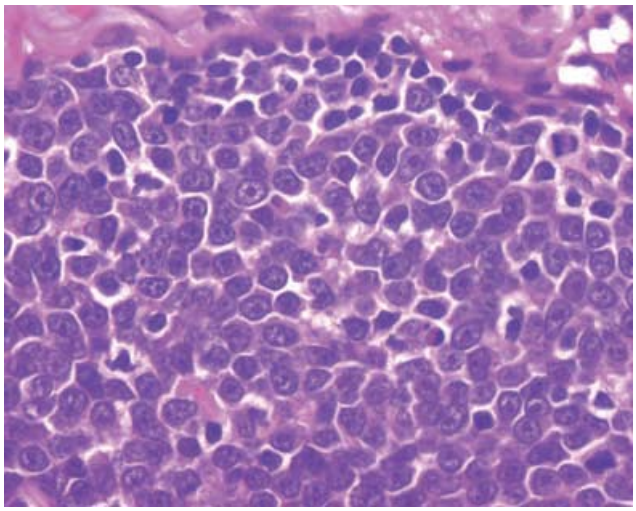

Figure 2.28. Detail of Figure 2.27. In marginal zone lymphoma, there is more uniform cell type with more nuclear atypia. The partial peripheralization of chromatin onto the nuclear membrane and irregular parachromatin clearing, makes the central nucleolus more apparent. Despite the relatively aggressive appearance of these nuclei, it is characteristic of this neoplasm that mitoses are not observed until the neoplasm has been present many months.

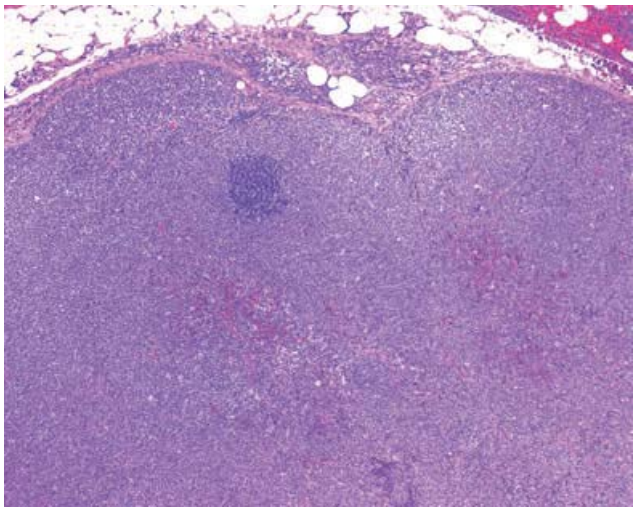

Figure 2.29. Dog: lymph node, marginal zone lymphoma. The architectural appearance of marginal zone lymphoma is similar to that of T-zone lymphoma with coalescing areas of cellular proliferation symmetrically surrounding mantle cells of involuted and collapsed germinal centers. Note the compression of the peripheral sinus with focal colonization of the capsule and perinodal fat.

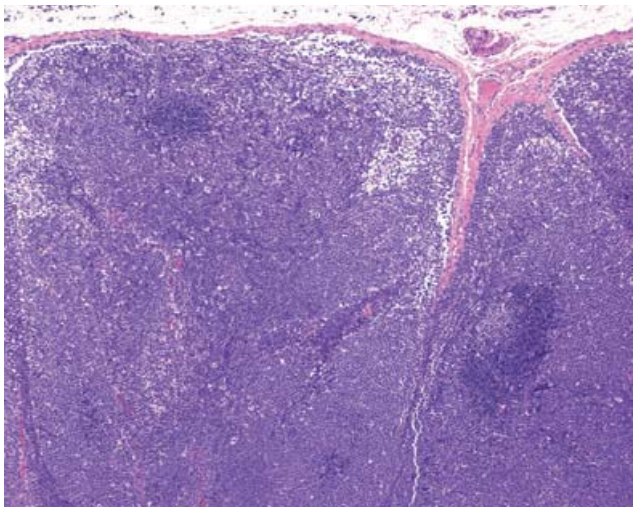

Figure 2.30. Dog: lymph node, late stage marginal zone lymphoma. After a period of indolent progression that may last 1–2 years the neoplasm becomes more aggressive with occasional mitoses and numerous tingible body macrophages that give the lesions a "moth-eaten" appearance like the starry sky pattern of high-grade lymphomas.

plastic states, they have a very low mitotic rate that seems out of character with the vesicular appearance of the nuclei and the prominent nucleoli. Typically, in hyperplasia and early marginal zone lymphoma, no cells in division will be seen on examination of several fields at 400× magnification (see Fig. 2.28). In late stage marginal zone lymphoma, 1–3 mitoses may be found in a field at the same magnification, and in addition, tingible body macrophages that are not seen in early lesions become numerous, with irregular dilation of the outer cortical sinuses with large areas of cellular laking and fragmentation of the node on sectioning (Figs. 2.30, 2.31).

The node medulla consists of cords and sinuses in about equal proportions in nodes at a moderate level of

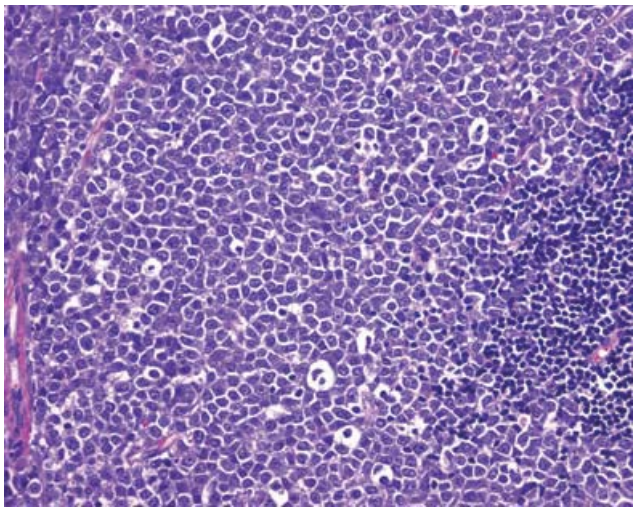

Figure 2.31. Detail of Figure 2.30. The cells of marginal zone lymphoma are much larger and have more cytoplasm than the residual small mantle cells of the involuted follicle at the right. The large macrophages contain nuclear debris of necrotic tumor cells.

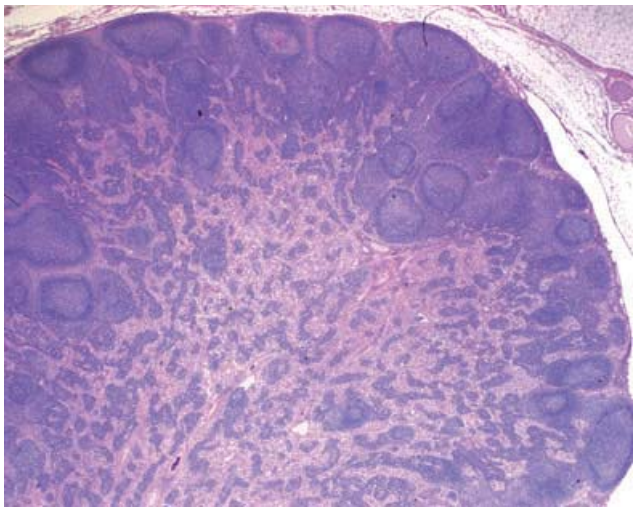

Figure 2.32. Cat: lymph node, benign follicular hyperplasia. In continuing follicular hyperplasias, the postgerminal center memory B-cells segregate in the medullary cords where they form serpiginous bands of cells that appear dark against the lighter staining areas of the medullary sinuses.

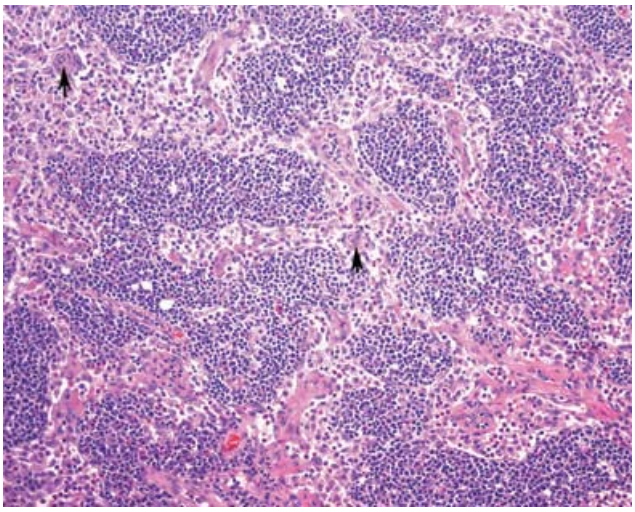

Figure 2.33. Detail of Figure 2.32, lymph node, medulla. The irregularly shaped areas of medullary cord plasma cell hyperplasia are sharply delineated against the less-cellular areas of the medullary sinuses. The arrows denote small medullary arterioles sheathed in a narrow band of pericytes containing a few lymphocytes and plasma cells.

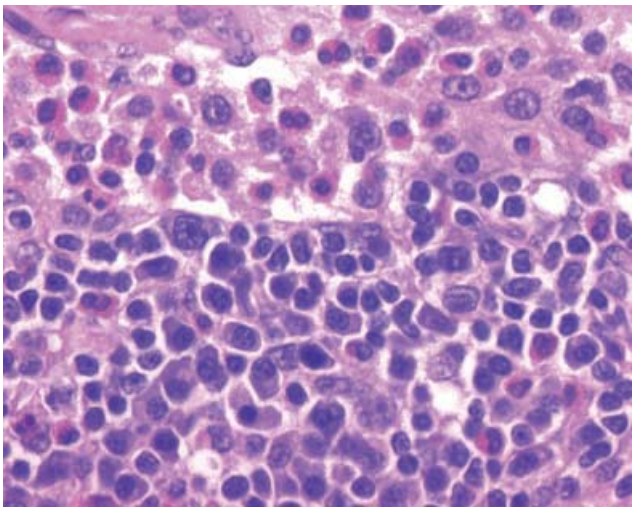

Figure 2.34. Detail of Figure 2.33, medullary cord plasma cell hyperplasia. The dark red appearance of the medullary area at an architectural level (Fig. 2.32) is found in nodes that have a high level of well differentiated plasma cells in the medullary cords. Lymphocytes may predominate, with the cords appearing more like the paracortex. This node contains an unusual level of eosinophils in medullary sinuses.

stimulation with the proportions of cortex to medulla and cord to sinus very plastic and varying widely in different conditions (Figs. 2.32, 2.33). The cords and sinuses are separated by delicate endothelial membranes with their boundaries not easily discernable when both areas are densely cellular. The medullary cords contain the progeny of the germinal centers, and the actual cell types present vary widely; plasma cells predominate in some cases of follicular hyperplasia, but in others there may be a mixture of lymphocytes of varying size and even macrophages (Figs. 2.34–2.36). In diseases characterized by phthisis of bone marrow but with adequate stem cells, there will be extramedullary hematopoiesis in the medullary cords, most easily recognized by the presence

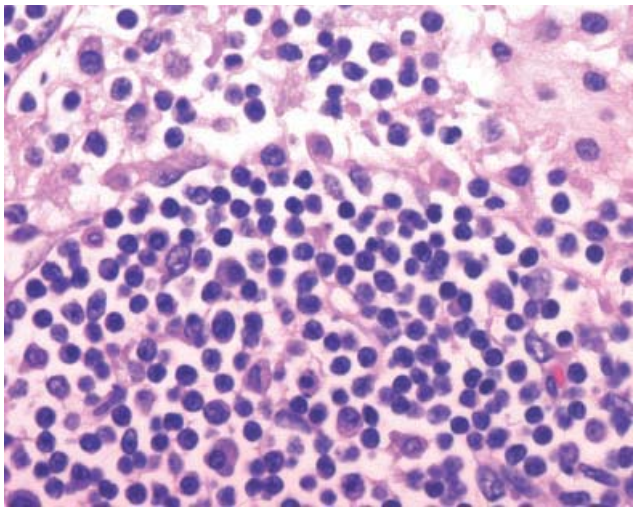

Figure 2.35. Calf: mesenteric lymph node, medullary cord early atrophy. The medullary cord contains loosely packed small lymphocytes with a few well-differentiated plasma cells with similar cells and macrophages in the sinus above. The tissue is from a neonatal animal that had mild serous atrophy of fat and is presumably on a declining level of lymphoid reactivity.

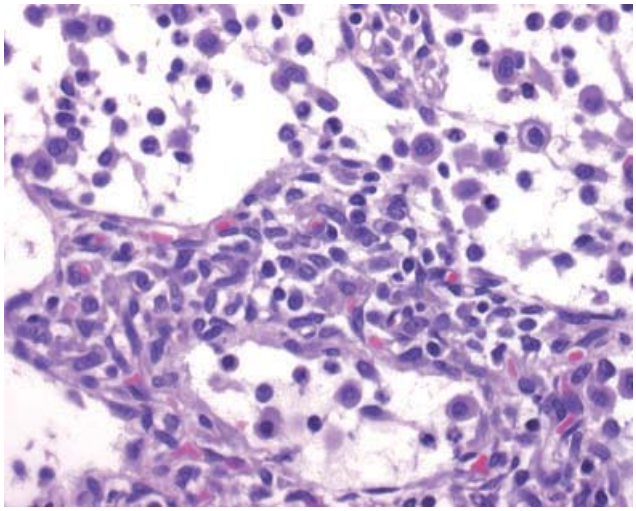

Figure 2.36. Harbor seal: lymph node, medullary cord atrophy. The animal had chronic bronchopneumonia and was in a declining state of health. The medullary cord consists primarily of stromal supporting cells with marked lymphoid depletion. The sinuses are also hypocellular.

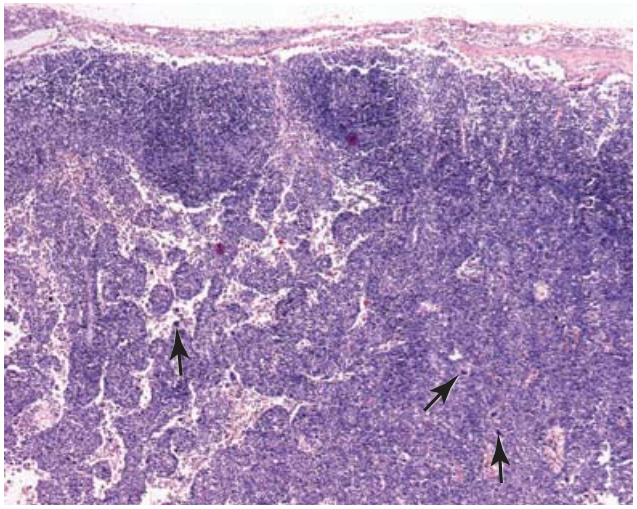

Figure 2.37. Cat: lymph node, acute myeloid leukemia. The node cortex is atrophic with widening of the peripheral sinus and focal colonization of the capsule. There is heavy colonization of the medullary cords' and irregular levels of cellularity in the medullary sinuses that extend irregularly to the subcapsular area. The large dark cells apparent at the architectural level in medullary sinuses (arrows) are extramedullary megakaryocytes.

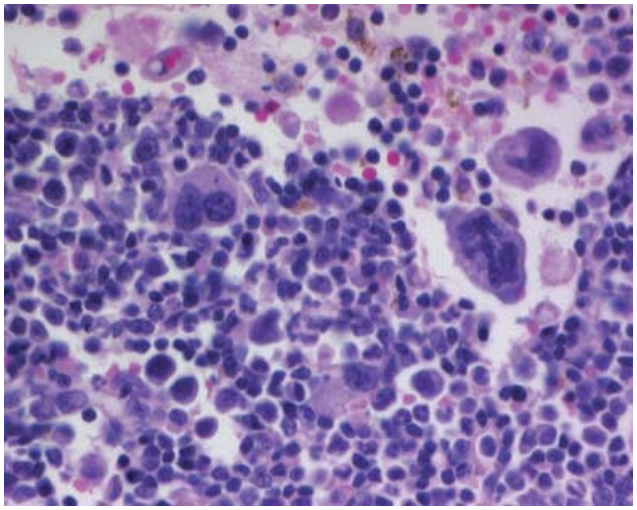

Figure 2.38. Detail of Figure 2.37. The medullary cords contain primitive blast cells of the myeloid tumor and early megakaryocytes identified with abundant cytoplasm and binucleation (upper left). More mature megakaryocytes now occupy the medullary sinuses. The maturing granulocytes in the medullary cord are likely the progeny of benign precursors that have been displaced by myelophthisis.

of megakaryocytes. In the myeloid leukemias, there will be benign hematopoiesis of all cell types in the medullary cords and, as the disease progresses, the neoplastic cells will displace the benign precursors and progeny that then are found in the sinuses (Figs. 2.37, 2.38). In general, the small cell lymphomas tend to fill the cords and compress the sinuses (Figs. 2.39, 2.40) and the large cell lymphomas fill the cortex and compress both cords and sinuses (Figs. 2.41, 2.42).

The sinuses have the distinction of containing the major blood vessels, with the veins and arteries sheathed in connective tissue that may be very thin and delicate or of

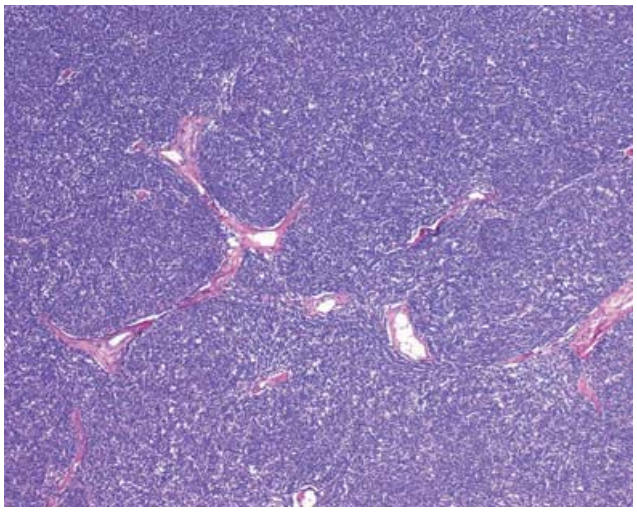

Figure 2.39. Dog: lymph node, small cell lymphocytic lymphoma. The entire cortical area is solidly occupied by small cell lymphoma that has colonized the medullary cords, now distended with neoplastic cells with complete compression of the surrounding medullary sinuses.

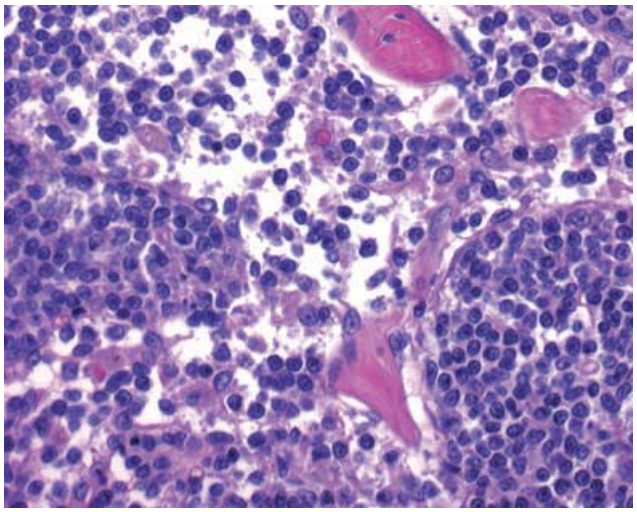

Figure 2.40. Detail of Figure 2.39. The medullary cords at left center and lower right are solidly cellular with residual plasma cells and small cell lymphocytic lymphoma. The medullary sinuses also contain the small neoplastic lymphocytes with few residual macrophages.

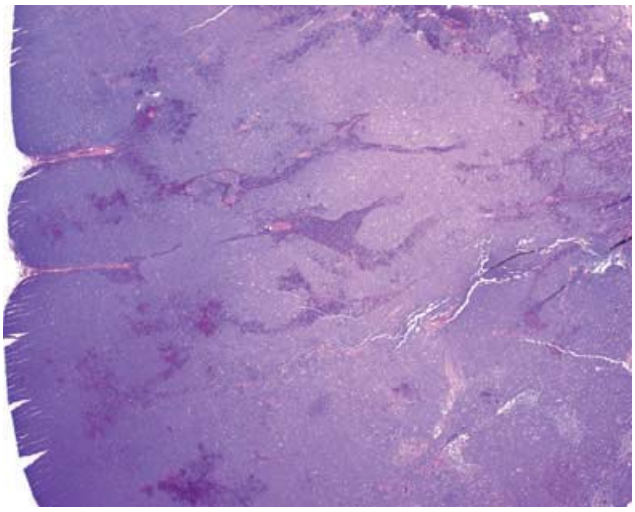

Figure 2.41. Dog: lymph node, diffuse large B-cell lymphoma. The neoplastic cells have preferentially colonized the outer cortex with marked thinning of the peripheral capsule and compression of the peripheral sinus. There is compression but minimal colonization of residual sinuses and medullary cords in the upper right.

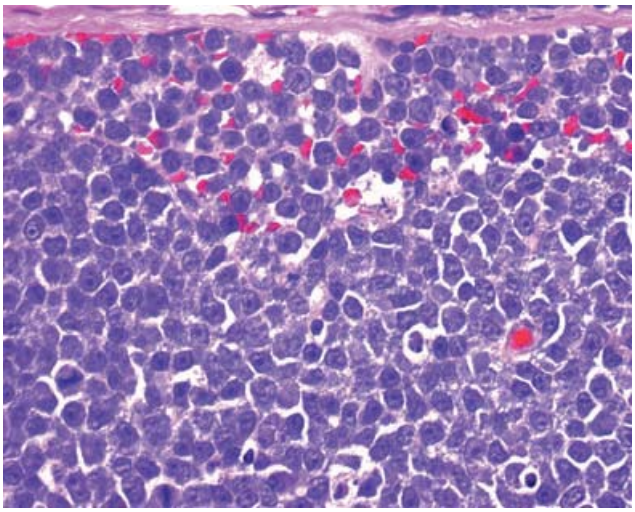

Figure 2.42. Detail of Figure 2.41, subcapsular region with thinned capsule and high cellularity of the peripheral sinus. The internal capsule of node cortex is greatly thinned and most visible in the upper left where it divides the more closely packed cells of the cortex from those in the peripheral sinus above. There are two cells in metaphase in the lower left and several tingible body macrophages identified by nuclear debris surrounded by a clear vacuole indicating a high death rate of the neoplastic cells.

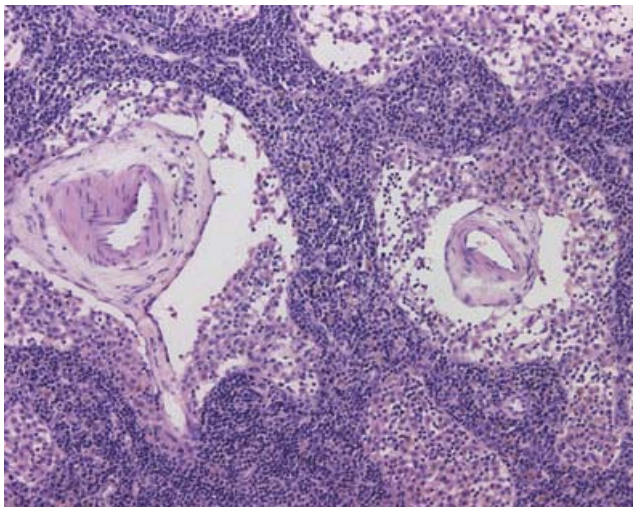

Figure 2.43. Dog: lymph node, hilar lymphatics, benign follicular hyperplasia. Hilus with major arteries and veins surrounded by efferent lymphatics, which are free of red blood cells.

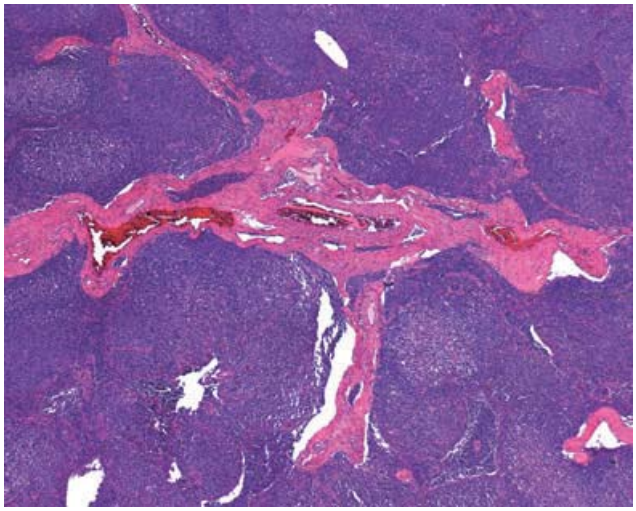

Figure 2.44. Dog: lymph node, medullary sclerosis, benign follicular hyperplasia. There is compression of the medullary sinuses by benign follicular hyperplasia with increased connective tissue surrounding the hilar vessels indicative of a long-standing benign reaction.

mature collagen if associated with one of the supporting bands of the node medulla (Figs. 2.43, 2.44). Although their anchoring is not obvious, the vessels of any size are always in the center of the sinus and surrounded by stellate macrophages and varying numbers of more polygonal forms of the same lineage (Fig. 2.45). There are gaps in the lining cells of both the outer peripheral and inner medullary sinuses that permit rapid passage of cells from the efferent lymph directly to the medullary areas without

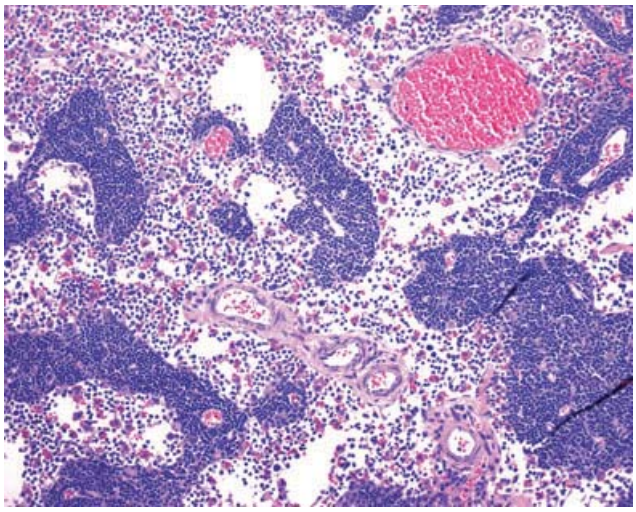

Figure 2.45. Dog: lymph node, hilar vessels, benign follicular hyperplasia. The larger arteries and veins in the medullary areas of lymph nodes remain centrally located within the sinuses with few apparent supporting structures. Smaller vessels, primarily veins, are located within the medullary cords. Knowledge of these relationships is important in interpreting cases where there is hypercellularity of the sinuses and/or medullary cords that obscures the boundaries between the sinuses and medullary cords.

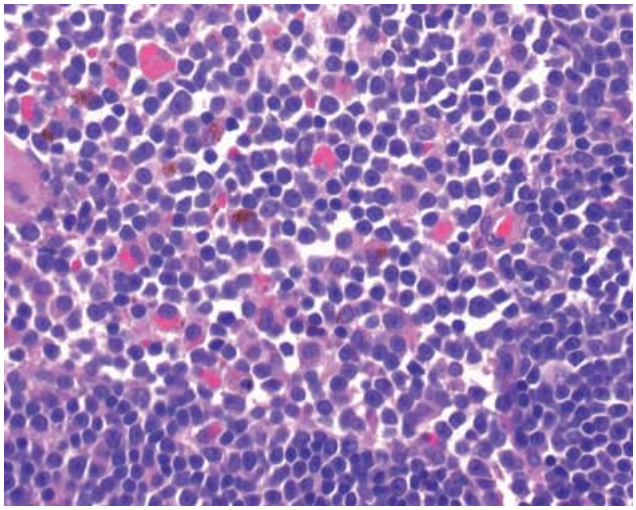

Figure 2.46. Dog: lymph node, medullary sinus, diffuse large B-cell lymphoma. The medullary cords below and at right contain closely packed cells with prominent central nucleoli. The medullary sinus has high cellularity with similar type cells as well as many macrophages that contain recently ingested red cells.

passage through the cortical filtering system. This ability is most evident in nodes removed for histological examination where the local hemorrhage is not well controlled and the node medullary sinuses contain abundant freshly shed red cells (Fig. 2.46).

REFERENCES

Belisle, C., and Sainte-Marie, G. (1990) Blood vascular network of the rat lymph node: Tridimensional studies by light and scanning electron microscopy. *Amer J Anat* 189:111–126.

Belz, G.T., and Heath, T.J. (1995) Pathways of blood flow to and through superficial lymph nodes in the dog. *J Anat* 187:413–421.

Jain, R.K., and Padera, T.P. (2003) Lymphatics make the break. *Science* 299:209–210.

Spaulding, H., and Heath, T. (1987) Pathways of lymph flow through superficial inguinal lymph nodes in the pig. *Anat Rec* 217:188–195.

Function

The cells constituting the adaptive immune system in the nodes include the naive B- and T-lymphocytes, the professional antigen presenting dendritic cells (APCs) and macrophages plus the very plastic but specifically organized system of supporting connective tissues, blood, and lymphatic channels. All the cells of hematopoietic origin are marrow derived either directly, as for the B-lymphocytes and monocyte/macrophages, or indirectly, for the T-lymphocytes via the thymus or the dendritic cells via the skin or other peripheral draining organ. The origin of the dendritic cells (DCs) is a fertile area of investigation with evidence that there is a great deal of variation in the generation of these cells both in lineage of origin and mature activity. Early work showed that monocytes could be induced to differentiate into DCs under the stimulation of GM-CSF and other factors. Later work has shown conclusively that DCs can be developed from either myeloid or lymphoid cells or from primitive marrow stem cells. Dendritic cells of CD8 alpha$^-$ type can be derived from myeloid precursors, and those of CD8 alpha$^+$ can be derived from thymic lymphoid precursors. The impact of organ-specific inductive cytokines may result in the same precursors producing different proportions of these subsets. Thus, in the thymus, DCs apparently derive about equally from lymphoid and myeloid progenitors, while other proportions exist in the spleen and nodes. In the thymus, the CD8 alpha$^+$ cells are believed to control T-cell development by determining negative selection and preventing self-reactive cells from maturing, and they appear to have the same function in the spleen and node paracortex. In contrast, DCs lacking CD8 alpha expression effect very strong stimulation on T-cells and may be important in recognition and production of immunity to foreign antigens.

Complex cocktails of stimulating cytokines (FKGm17) can induce marrow cells to differentiate into DCs along a lymphoid pathway; an altered mixture (FGKmT4) can induce stem cells and monocytes to differentiate into DCs along a myeloid pathway. A key factor on the developmental kinetics of the dendritic cell complement appears to arise in a zinc finger DNA-binding transcription factor Ikaros. Mice homozygous for the Ikaros null allele have deficient B- and NK-cells and a marked reduction in peripheral dendritic cells. Mice with this domain deleted have more severe lymphoid and DC defects. Blocking studies utilizing the dominant negative protein Ik7 have shown the molecular requirements for development of the different lines of DCs and provide strong evidence that there are intrinsic differences in the DC progenitors that provide distinct developmental pathways.

In the process of differentiation and maturation, the dendritic cells undergo a series of internal lysosomal developments. A unique aspect of dendritic lysosomes is that they do not result in complete degradation of ingested protein, thus preserving antigenic identity. Immature DCs are efficient in the capture and endocytosis of antigen but have limited ability to engage T-lymphocytes due to internal containment of MHC II molecules. In the immature DC, ingested antigen encounters newly synthesized MHC Class II in the lysosomal system that creates a union of the cleaved MHC II chain and partially digested antigen as a peptide-MHC II complex. On maturation, the DC can then present the internalized antigen hours or days later at the plasma membrane. Mature DCs don't have more proteolytic *enzyme* than immature cells, but they do have more *lytic activity,* apparently because less of it is in an inactive proenzyme form and because the pH of lysosomes in mature DCs is a full log lower than in the immature state. The enzymatic response patterns of mature DCs have been observed in oligonucleotide gene expression profiles following exposure to antigens from *Escherichia coli*, *Candida albicans,* and influenza virus. This exposure resulted in a remarkable variation in gene expression such that a basal level of the same genes was activated by all three infectious agents, but a very different or partially overlapping set of genes was ultimately engaged. Differences also occurred in the rate of cellular activation after exposure to these antigens with gene activation induced first by *E. coli* followed by *C. albicans* and lastly by influenza. These results indicate that DCs initiate a core response to most antigens but are also able to exert an antigen-specific activation and maturation.

The dendritic cells of the body surfaces, that is, the epidermal and dermal Langerhans cells and those of the lung and intestine, appear to have a patterned migration to the draining lymph nodes that is accelerated by inflammation occurring in the site. It appears that each site may have its own characteristics, with the skin providing a continuing flow of DCs after dermal injection of live virus while the lung produces a very large increase in DCs to bronchial nodes for the first day only after inflammatory challenge. These results may be influenced by the nature

of the studies and type of inflammatory reaction induced. Once charged with antigen and having migrated to the draining node, the DCs enter the node paracortex via the high endothelial venules (HEVs). In the node T-cell area, the DCs meet a variety of T-lymphocytes, including the CD4 T-helper cells of T_h1 and T_h2 types that have differing cytokine receptor profiles and functions. The T_h1 subset acts to protect against intracellular parasites like leishmania, and the T_h2 subset accelerates immunity to large extracellular invaders like nematodes. In the node cortex are B-cells that have also entered across the HEVs, and if in transport there is contact between a B-cell and a dendritic cell bearing a cognate or related antigen to that of the B-cell, there will be local retention and activation involving the appropriate T-helper cell, the B-cell, and the DC, with B-cell proliferation producing a *primary foci*. A fraction of these B-cells become short-lived plasma cells and produce IgM as a first response to the DC-borne antigen. Other B-cell progeny of this early reaction migrate into a primary follicular site where they initiate the formation of a germinal center.

In the germinal center, antigen-activated B-cells from the paracortex undergo rapid proliferation, usually about a week after the primary response. Germinal centers are formed by 3–10 naive B-cells and after about 10 generations contain 10,000–15,000 cells that fill the dendritic cell framework in about 3 days in animal studies. By 4–6 days, the architecture of the germinal center matures into a polar structure with a deep pole of Ig-negative B centroblasts with vesicular nuclei, peripheral nucleoli, and a narrow rim of deeply stained cytoplasm. In this process, the B blasts disable their production of BCL-2 protein and become able to undergo programmed cell death. In the opposite pole of the germinal center, the centrocytes that are the progeny of the centroblasts accumulate in a more dense area of dendritic cell background. In this process, the germinal center cells express a spectrum of surface antigens associated with interaction with T-cells, including CD23, CD71, CD40, CD86, and antigens permitting adhesion to dendritic cells CD11a and CD29. As well, cells of both the light and dark pole areas express BCL-6 protein, an essential promoter of germinal center formation. BCL-6 is not present in pre- (naive or mantle cell) or post-(immunoblast or plasma cell) germinal center cells. BCL-6 is rearranged in about a third of human diffuse large cell lymphomas (DLCL) and in a small proportion of follicular lymphomas, in which case its normal down regulation is blocked and results in continued proliferation of lymphoma rather than normal maturation of the germinal center progeny. Oddly, resting naive B-cells have high levels of mRNA but do not express the BCL-6 protein.

In the centroblasts, somatic mutation of the Ig gene variable regions begins and is followed by an isotype class switch from IgM to IgG or IgA characteristic of the late primary or *secondary immune response*. In early germinal center formation, there may be 5–10 clones of B-cells with early or minimal mutation of the variable region and with increasing V-region mutation and antibody affinity (as few as 3 clones in a mature reaction). In this transition, the centroblasts mature to the nondividing centrocytes of the light zone where they have more compact, irregularly shaped nuclei and absent or inconspicuous nucleoli. The centrocytes again express sIg that has the same VDJ rearrangement of the parent B-cell but may have had heavy chain class switch and much higher antibody avidity as a result of the hypermutation of the Ig gene V-region. In addition to the Ig gene, there is also mutation of the BCL-6 gene, with these changes serving as genetic markers of postgerminal center cells. The selection process for the centrocytes requires them to produce an antibody of sufficient avidity to bind to native unaltered antigen expressed in antigen-antibody complexes held by complement receptors on the dendritic cell processes. This binding by the centrocytes is then passed by the T-cells of the light zone that, by that contact, express CD40 ligand, which then can engage the CD40 antigen on the centrocyte. This centrocyte T-cell binding cleaves the CD40 antigen from the B-cell centrocyte and rescues the B-cell from apoptosis by activating the antiapoptosis gene. The centrocytes that fail this test of antibody specificity undergo programmed cell death and are phagocytosed by the tingible body macrophages of the germinal center light zone. Centroblasts that successfully undergo antigen receptor ligation and CD40 ligation also have the BCL-6 gene turned off, preventing mRNA transcription and protein production and thus permitting normal maturation and germinal center exit.

Follicular lymphomas arise from centrocytes that have undergone an inactivation that prevents down regulation of the antiapoptosis gene by chromosomal rearrangement in humans (t14;18) and unknown molecular changes in animals.

The mantle cell cuff described above consists of clonally diverse naive B-cells that have unmutated immunoglobulin genes as well as a surprising number of small T-cells that are not morphologically distinguishable from the more numerous B-type mantle cells. In humans and in animals neoplasms of the mantle cells tend to be indolent and of low grade with very few mitotic cells. Like the normal counterpart of naive resting B-cells that are in circulation, the mantle cell tumors may become leukemic and widespread but in animals are rarely recognized and appear as localized proliferations in the spleen or as chronic lymphocytic leukemia. Because the mantle cells may move into the germinal center and undergo centroblastic differentiation, it is logical that in declining benign reactions loss of the mantle cell cuff frequently occurs,

preceding involution of the germinal center as the kinetics of cellular supply fail to maintain a vibrant follicular hyperplasia.

In well-developed germinal centers, the postgerminal center B-cells leave the follicle and some colonize the area immediately outside the mantle cell cuff forming the marginal zone of cells. In animals, the marginal zone cells are inapparent in most lymph nodes with only mild immune stimulation and are present singly and in small clusters but do not form a complete cuff around the mantle cell layer unless there is prolonged and intense immune stimulation. In these conditions, the marginal zone cells are identified as larger than the mantle cells and have nuclei about 1.5 red cells in diameter, which are vesicular and not compact like the mantle cell nuclei and may have a prominent single central nucleolus plus relatively abundant cytoplasm that gives these cells specificity when seen as a cohesive cell layer. In benign states, the marginal zone cells are always seen in mixed company with a number of smaller lymphocytes. The counterpart neoplasm in humans has smaller nuclei, and most of the cells lack nucleoli. The architectural appearance is very similar as the areas of proliferation in both humans and animals appear lighter than the adjoining tissue due to the large volume of lightly stained cytoplasm; cytologically, these neoplasms in all species share a very low mitotic rate. Functionally, the marginal zone cells are felt to be memory cells, and on rechallenge with specific antigen, they reenter the germinal center and rapidly move to the paracortex as Ig-positive blast cells that mature to plasma cells.

REFERENCES

Galy, A., Christopherson, I., Ferlazzo, G., Liu, G., Spits, H., and Georgopoulos, K. (2000) Distinct signals control the hematopoiesis of lymphoid-related dendritic cells. *Blood* 95:128–137.

Hollowood, K., and Goodlad, J.R. (1998) Germinal centre cell kinetics. *J Pathol* 185:229–233.

Hommel, M., and Kyewski, B. (2003) Dynamic changes during the immune response in T-cell-antigen-presenting cell clusters isolated from lymph nodes. *J Exp Med* 197:269–280.

Huang, Q., Liu, D., Majewski, P., Schulte, L.C., Korn, J.M., Young, R.A., Lander, E.S., and Hacohen, N. (2001) The plasticity of dendritic cell responses to pathogens and their components. *Science* 294:870–875.

Legge, K.L., and Braciale, T.J. (2003) Accelerated migration of respiratory dendritic cells to the regional lymph nodes is limited to the early phase of pulmonary infection. *Immunity* 18:265–277.

Martin, P., Ruiz, S.R., del Hoyo, G.M., Anjuere, F., Vargas, H.H., Lopez-Bravo, M., and Ardavin, C. (2002) Dramatic increase in lymph node dendritic cell number during infection by the mouse mammary tumor virus occurs by a CD62L-dependent blood-borne DC recruitment. *Blood* 99:1282–1288.

Okada, T., Ngo, V.N., Ekland, E.H., Forster, R., Lipp, M., Littman, D.R., and Cyster, J.G. (2002) Chemokine requirements for B-cell entry to lymph nodes and Peyer's patches. *J Exp Med* 196:65–75.

Traver, D., Akashi, K., Manz, M., Merad, M., Miyamoto, T., Engleman, E.G., and Weissman, I.L. (2000) Development of CD8_-positive dendritic cells from a common myeloid progenitor. *Science* 290:2152–2154.

Trombetta, E.S., Ebersold, M., Garrett, W., Pypaert, M., and Mellman, I. (2003) Activation of lysosomal function during dendritic cell maturation. *Science* 299:1400–1403.

Vandenabelle, S., and Wu, L. (1999) Dendritic cell origins: Puzzles and paradoxes. *Immun Cell Biol* 77:411–419.

Wolf-Peeters, C.D., Tierens, A., and Achten, R. (2001) Normal histology and immunoarchitecture of the lymphohematopoietic system. In Knowles, D.M. (ed.), *Neoplastic Hematopathology,* 2nd ed. Lippincott Williams & Wilkins, Philadelphia, pp. 271–306.

Technical Considerations in Lymph Node Biopsy

Enlarged Node and Generalized Lymphadenopathy

There are three major areas where the biopsy of lymph nodes may lead to misdiagnosis. These are problems related to the surgery itself and choice of site, problems in the processing of the tissues, and problems associated with the interpretation of the lesions. The choice of node for biopsy is the first step in arriving at a clinically relevant diagnosis. If several nodes are enlarged, the largest is most likely to give evidence of the major problem to be addressed. If other considerations are not demanding, the popliteal node should be chosen only after other areas have been given careful consideration. Oddly, but reliably, the popliteal node of dogs and, to a lesser extent, cats is always hyperplastic with that background to be read against any other findings. In a study of the timing of follicular development after immunization into the caudal footpad of dogs (Carter and Valli, unpublished), we were surprised at the consistent high level of reactivity in the popliteal nodes of control animals. This experience is borne out in clinical practice. In general, the prescapular node of dogs and cats has less follicular activity, pigmentation, and medullary sclerosis than the popliteal node, and if both are enlarged, it is a better choice for diagnostic excisional biopsy. A prominent submandibular node is perhaps the most common presentation for dogs with a single node enlargement. On review of the last 100 cases of hematopoietic consultations for the cat and dog, the affected canine tissues received were

- submandibular node 18
- popliteal 9
- prescapular 2
- other node 24
- other tissues 47

For feline the submitted tissues were

- submandibular node 7
- popliteal 7
- prescapular 2
- other node 27
- other tissues 57

Clinicians recognize that enlargement of a submandibular node is reason to look in the mouth and doubly so if the enlargement is bilateral. With enlargement of a single submandibular node, a fine needle aspiration is helpful to rule out a metastatic oral or sinus carcinoma, but lymphoma remains a prime rule-out. It is possible to render a reliable diagnosis of lymphoma with tissue derived by Tru-cut biopsy but, as in human pathology, if the cost of therapy is considered, an excisional biopsy is greatly preferred. In an era when the diagnosis was "lymphosarcoma" or other, a diagnosis by fine needle aspiration was sufficient. However, with the advent of the WHO classification based on "clinically defined disease entities," it is not possible to make an adequate diagnosis based on cytology alone or on histology of tissue that is not sufficiently large to permit an architectural assessment. If a Tru-cut biopsy must suffice, then it needs to be a 2 mm needle to provide an adequate and preferably cohesive cylinder of tissue. It is abundantly apparent in assessing dog and cat nodes for lymphoma that neoplasia of the lymphoid system frequently follows a long period of benign hyperplasia. Thus, many of the lymphomas of submandibular and other nodes are superimposed on a background of cortical fading germinal centers and medullary sclerosis. The relatively infrequent recognition of follicular lymphoma in animals has permitted the development of a culture that they don't exist and, therefore, all lymphomas are of diffuse type with architectural assessment not required. The recent demonstration that the indolent lymphomas of dogs, at least, are not rare and moreover are most often derived from mantle cell or marginal zone areas of the germinal center emphasizes the need for nodal tissue for diagnostic purposes to be sufficiently large to enable an architectural evaluation. Thus, if there is not an excisional biopsy, there must at least be enough tissue to ensure that an architectural pattern based on fading germinal centers, if present, can be detected and interpreted.

Sample Processing

Once removed, the biopsy material should have imprints made with some wet-fixed and then placed in 10% neutral formalin fixative. If the cytologic preparations are not made on excision, the tissues should be placed on saline-moistened filter paper and not surgical gauze. Endoscopically, derived biopsies or thin needle Tru-cut biopsies that are placed on dry gauze may not be removed without tissue tearing and loss. Even wet gauze presents problems in tissue retrieval. Tissues not immediately placed in fixative will tend to have drying artifact at the edges even with prompt transport to the clinical laboratory. On nodal excision, the capsule should be opened longitudinally prior to placement in formalin. On trimming for embedding the node, the cut surface should then be squared up to the level of the capsule and a 2–3 mm thick area obtained by a second section parallel to the first exposed cut surface. This trimming can best be accomplished by use of a small support that permits the cut surface of the node to be held flat against a vertical member. Then the second cut is made evenly parallel to the first by cutting down through the node rather than with the cut face of the node on a horizontal surface where a parallel second cut is more difficult to achieve (Fig. 2.46A). The object of this approach is to get an evenly thick 2–3 mm width tissue from the long axis of node from the area that was first exposed to fixation. Lymphoid tissue will vary greatly in consistency depending on the type of reaction or lymphoma. Inflammation tends to produce a firm node that is cohesive and trims easily. Lymphomas characterized by T-cell proliferation will have fine vascular proliferation and fine sclerosis producing a tissue with no artifactual breaks. In contrast, a blastic lymphoma of B- or T-cell type will be very friable and tend to fragment on sectioning even if surrounded by capsule. Fixation of small tissues is optimal in 24 hours,

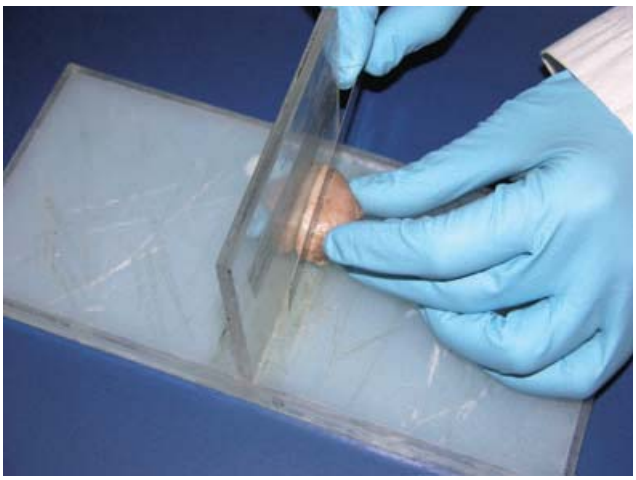

Figure 2.46A. Support device to assist gaining a uniformly smooth cut surface of a lymph node adjacent to an incision made in the fresh tissue to assist fixation. The frame is constructed of lucite plastic with the base filled with paraffin to reduce dulling of cutting instruments. The node is being trimmed with a disposable cryostat blade, with the tissue to be embedded clearly viewed by the prosector. *Photograph by S. H. Hsiao, DVM, and section by M. Chien, VM2.*

and longer duration in formalin tends to decrease the preservation of surface and cytoplasmic lineage-dependent antigens as detected in immunohistochemistry. Chromatin structure and internal nuclear detail are better preserved if 10 g of zinc chloride ($ZnCl.7H_20$) is added to each liter of buffered neutral formalin with no loss of immunoreactivity.

Tissue processing and even staining are now largely automated and of standard quality. Tissues are best preserved if the paraffin temperature is kept below 62°C, and the alcohols and xylene should be "forward shifted," with the most dilute member discarded and a fresh absolute station added in proportion to the number of tissues being processed. The freshness of cells on fixation, adequacy of fixation, and processing are the three areas of tissue fixing and paraffin infiltration in which irreparable damage to tissue may occur. If each of these three initial steps are optimally carried out, the final three—correct embedding, followed by thin sectioning (3–5 microns), and staining/cover-slipping—can be repeated if needed to achieve optimal histological preparations.

Diagnostic Cytopathology

Veterinary diagnostic cytopathology has largely become a process of making the most intuitive interpretation possible on air-dried preparations that are Wright's-stained or Diff-Quick–stained and often not cover-slipped. This is partly because the success of the services provided by academic and now private laboratories has resulted in such a large sample flow that only oversight stains can economically be employed. It should be kept in mind that cytology should always strive to show the continuity between exfoliated cells and the tissues from which they were derived, whether benign or malignant. To do this most effectively, cytologic specimens should be wet-fixed to permit the same character of chromatin condensation that occurs in formalin fixation to be viewed in cytologic specimens. This approach can be achieved by immediate immersion of fine needle aspirations or tissue imprints in absolute alcohol or by the preparation of air-dried mounts that later in the clinical laboratory can be placed in water for 3–5 minutes and *then* placed in absolute alcohol. The wetting process can occur with optimal results in minutes or months after the cells are mounted. One point of caution needs to be observed. If the preparations are to be air-dried initially, the cells must become fully dried or they will not remain adherent to the slide during the wetting/fixing/staining steps. Cells stained with hematoxylin and eosin or Schorr's or Papanicolaou after this late wet-fixation will have nuclear structures that permit direct comparison with histological preparations. Because cancer is primarily a nuclear change, it is essential to have cytologic techniques that permit cytoplasmic clearing and optical sectioning of large clusters of cells that are not interpretable with Wright's or other Romanovsky-type stain. A further strategy that we are employing is to collect cells into a transport media, as has been done for decades for human gynecologic cytology. These systems used weak alcohols to keep bacterial contamination from proliferating during transport while leaving the cells still soft enough to flatten and adhere to glass slides on reaching the laboratory. Today, many human CD (clusters of differentiation) antibody reagents will mark the counterpart antigens in animal tissues in cytologic preparations but not in paraffin-embedded or alcohol or formalin-fixed cytologic specimens. Instead, the most efficacious fixative for cytology to be followed by immunocytochemistry is absolute acetone. Part of the reason for this disparity seems to be that the alcohol and formalin fixatives harden the cell membranes to such an extent that cytoplasmic antigens are hidden while acetone perforates the cell membranes, permitting antibody binding. An appropriate transport media for cytologic purposes can be made by adding 2 ml saline containing 6% serum albumin to a 5 ml EDTA vacutainer tube. If the cells are to be in transport for more than a few hours, the 2 ml of saline should also contain 5% absolute acetone by volume. Cells collected in this media can be effectively stained with Wright's as well as immunostaining as long as 2–3 days later with the cells at ambient temperature. The addition of acetone to the cells prior to staining with Wright's results in the cytoplasm appearing more basophilic than with no fixative and with slightly less cytoplasmic volume due to less flattened cells. The major advantage to be gained by the use of transport media is that it permits the laboratory to make additional slides of the same aspiration after a first look at a Wright's stain on an air-dried preparation made prior to adding the rest of the aspiration to the transport media. The cells in the media can be efficiently deposited onto microscope slides in a cytocentrifuge for various immunostaining procedures. Because the cytocentrifuge permits the deposit of cells in two areas on each slide, it is possible to have cytologic control tissues made up in advance so that on staining there are control cells on the same slides as the patient positive and negative preparations. This approach gets around the main difficulty in clinical cytology in which typically only one or two slides are received on each submission, which eliminates the opportunity to carry out a battery of lineage-specific staining after determining the major tissue area being examined.

Intraoperative Procedures

It has been suggested that intraoperative microscopic examinations for lymph nodes do not have the same value as those where carcinoma is the main consideration and frozen sections the main strategy undertaken. Cytologic preparations taken intraoperatively can be very helpful in

ensuring that the area excised has diagnostic material by the relatively minor intervention of fine needle aspiration. With the area of lesion defined, imprints from Tru-cut samples or from a hemisectioned node can provide information that will not be available when the excised tissue is in fixative. A case of primitive "round cell tumor" that is suspected of being lymphoid but is later found to be negative for all lymphoid markers makes this point. The most reliable markers for early myeloid proliferation are Sudan Black-B, myeloperoxidase, and the esterases. The Sudan stain works on fresh tissue and will work to a lesser extent in fixed-frozen but not in tissue processed to paraffin. With small biopsies, often none is left unprocessed by the time it is realized that the lesion is not lymphoid. Myeloperoxidase fully active in animal tissues in paraffin is now being described, but the esterases are generally not active in processed tissue. Samples taken for cytology prior to tissue fixation would provide material on which all three of these reactions are active and by which the diagnosis could be efficiently and rapidly determined. The rapidly expanding use of ultrasound guided fine needle aspiration and Tru-cut biopsy are also areas where there is frequent failure to obtain diagnostic tissue and where an appropriate sample could be quickly verified by on-site intraoperative cytologic examination. It might be suggested that no tissue derived in this manner be processed for histological examination unless it had been established intraoperatively that diagnostic tissue had been obtained.

New Techniques of Examination

Biopsy of lymphoid tissue should be done with recognition of the impact of technologies now in development. Many laboratories now routinely do flow cytometry on lymphomas and leukemias. This is best done on fresh cells but can be done on disaggregated fixed tissues. In situ hybridization (FISH) is now being carried out on canine cells, and while it can best be done on fresh tissue, the need to establish the diagnosis prior to looking for molecular verification of subset type requires that initially most of the probing will be done on fixed tissue, where whole cells are again needed to avoid missing genes in partial cells present in thin sections. Because of the increased number of chromosomes in domestic animals as compared to humans and the need for cells in mitosis for cytogenetic studies, this modality will likely be surpassed as specific genes are identified with lymphoma subsets that can be identified in FISH and later in flow. Clonality is now being done on dog and cat lymphomas for B- and T-cell proliferation and has valid application for lesions felt to be atypical hyperplasias and in situ lymphomas. Fortunately the primers and probes for the T-cell receptor and immunoglobulin VDJ area can be applied in PCR analysis on paraffin-embedded tissue.

REFERENCES

Carter, R.F., and Valli, V.E.O. (1988) Advances in the cytologic diagnosis of canine lymphoma. *Sem Vet Med Surg* 3:167–175.

Carter, R.F., Valli, V.E.O., and Lumsden, J.H. (1986) The cytology, histology and prevalence of cell types in canine lymphoma classified according to the National Cancer Institute Working Formulation. *Can J Vet Res* 50:154–164.

Cowell, R.L., Dorsey, K.E., and Meinkoth, J.H. (2003) Lymph node cytology. *Vet Clin Small Anim* 33:47–67.

Eudy, G.E., Carlson, G.W., Murray, D.R., Waldrop, S.M., Lawson, D., and Cohen, C. (2003) Rapid immunohistochemistry of sentinel lymph nodes for metastatic melanoma. *Human Pathol* 34:797–802.

Langenbach, A., McManus, P.M., Hendrick, M.J., Shofer, F.S., and Sorenmo, K.U. (2001) Sensitivity and specificity of methods of assessing the regional lymph ndoes for evidence of metastasis in dogs and cats with solid tumors. *J Amer Vet Med Assoc* 218:1424–1428.

Nathanson, S.D. (2003) Insights into the mechanisms of lymph node metastasis. *Cancer* 98:413–423.

Smidt, M.L., Besseling, R., Wauters, C.A.P., and Strobbe, L.J.A. (2002) Intraoperative scrape cytology of the sentinel lymph node in patients with breast cancer. *Brit J Surg* 89:1290–1293.

Valli, V.E.O. (1988) Techniques in veterinary cytopathology. *Sem Vet Med Surg* 3:85–93.

Developmental and Degenerative Diseases of Lymph Nodes

Developmental Diseases

Animals born genetically immunodeficient have characteristic changes in the lymphoid tissues throughout the body. Mice deficient in a subset of lymphocytes $CD4^+$ and $CD3^-$ that produce lymphotoxin, interleukin 7a, and ligands for additional cells are unable to form lymph node framework or Peyer's patches. Thus, even before the absence of B- or T-lymphocytes becomes apparent, a cascade of cellular interactions is required for formation of the nodal architecture. The Arabian foals with combined immunodeficiency (CID) have lymph nodes that have normal capsular development and presumably normal afferent and efferent lymphatics, but the interior of the nodes consists of the reticular framework and the microvasculature to support the normal cortical areas of paracortex and germinal centers. Because these animals are very subject to infections, both bacterial and viral, their nodes contain macrophages and focal nodules that might be mistaken for early germinal centers but are foci of neutrophilic reaction around bacterial colonies. The immmunodeficient diseases may be combined or partial with primary B-cell deficiency and hypogammaglobulinemia. Horses with the latter disease, known as *common variable immunodeficiency,* live to maturity but have recurrent infections and generalized lymphadenopathy and presumably lack germinal centers.

In animals, the most studied examples of immunodeficiency are in the mouse where a range of deficient states has been described, including nude mice lacking a thymus and more severely deficient animals that have severe combined immunodeficiency (SCID) and must be maintained in isolator cages. Mice homozygous for the genes that depress T-lymphocyte formation (*nu*) and those that inhibit B-cell formation (*Xid*) have nodes with the deep cortical units as described in node cortex, but these are hypocellular and consist of large pale areas circumscribed by a narrow band that is densely cellular with small lymphocytes. Oddly, this band of cells is discontinuous over the outer area of the unit below the entry of the afferent lymphatic. The medullary area of the nodes was largely empty and consisted of very narrow cords with wide and empty sinuses. The cells in the outer cuff were marked with an anti-mouse IgM, and some nodes had medullary IgM positive plasma cells, but the main effect was the absence of germinal centers and lack of colonization of the cortical units by T-cells. All regions were negative for staining with anti-mouse IgG consistent with absence of germinal centers. The SCID mouse derived from a BALB/c strain has a genetic aberration at a higher level of cellular differentiation that renders it deficient in both B- and T-cells. Heterozygotes have normal levels of circulating lymphocytes and normal histology, but the mice homozygous for the SCID trait are lymphopenic and the nodes lack even the outline of the deep cortical units and are very small, consisting largely of condensed supporting stroma. Remarkably, these animals could be reconstituted with strain-specific bone marrow cells with some animals indistinguishable from wild-type mice in all hematopoietic tissues.

Others had mainly marrow in some nodes suggesting colonization by a single precursor of committed level of differentiation. One of the problems encountered with animals of this type is in distinguishing very small mediastinal nodes from remnants of thymus in presumably athymic animals. Histologically, even small nodes have a peripheral sinus evident in some areas, and nodes never have the epithelial Hassall's corpuscles characteristic of even atrophic thymus. When older wild-type mice were examined at 12 and 24 months of age, focal areas of atrophy closely resembled the nodes of young immunodeficient mice. In some cases, the nodes had a scalloped cortical surface due to atrophy of the paracortical areas between foci of germinal centers.

REFERENCES

Custer, R.P., Bosma, G.C., and Bosma, M.J. (1985) Severe combined immunodeficiency (SCID) in the mouse. *Amer J Pathol* 120:464–477.

Flaminio, M.J.B.F., LaCombe, V., Kohn, C.W., and Antezak, D.F. (2002) Common variable immunodeficiency in a horse. *J Amer Vet Med Assoc* 9:1296–1302.

Sainte-Marie, G., and Peng, F.-S. (1985) Lymph nodes of the N:NIH (S)II-nu/nu mouse. *Lab Invest* 52:631–637.

Sainte-Marie, G., and Peng, F.-S. (1987) Morphological anomalies associated with immunodeficiencies in the lymph node of aging mice. *Lab Invest* 56:598–610.

Somberg, R.L., Robinson, J.P., and Felsburg, P.J. (1994) T lymphocyte development and function in dogs with X-linked severe combined immunodeficiency. *J Immunol* 153:4006–4015.

Degenerative Diseases

Lymph nodes become impacted by a variety of vascular accidents that involve the inflow or outflow vessels of the blood or lymphatic channels. In general, obstruction of the arterial supply results in nodal atrophy or in infarction depending on the size of the gland and the integrity of lymph flow. Blockage of a single afferent lymphatic results in atrophy of the area of the gland fed by that source of antigen. Each lymphatic drives a semicircular deep cortical unit area of node cortex that consists of peripheral germinal centers and the surrounding area of paracortex with high endothelial venules and a peripheral vascular network that defines the boundary of the reaction area on the deeper surface (Fig. 2.47). Apparently, the integrity of these units is dependent not only on the antigen borne by the incoming lymph but also on the phagocytic cells that likely assist in antigen presentation. Though less defined, blockage of all incoming lymph would presumably result in generalized atrophy but not necrosis. A condition recognized in human nodes with

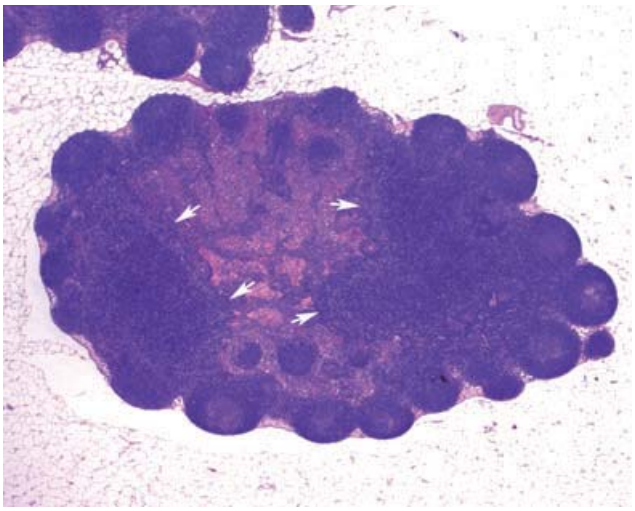

Figure 2.47. Sprague-Dawley rat: mesenteric lymph node, focal paracortical hyperplasia. The multifocal densely cellular areas of paracortex represent "deep cortical units" (arrows) and indicate highly antigenic drainage from a single afferent lymphatic.

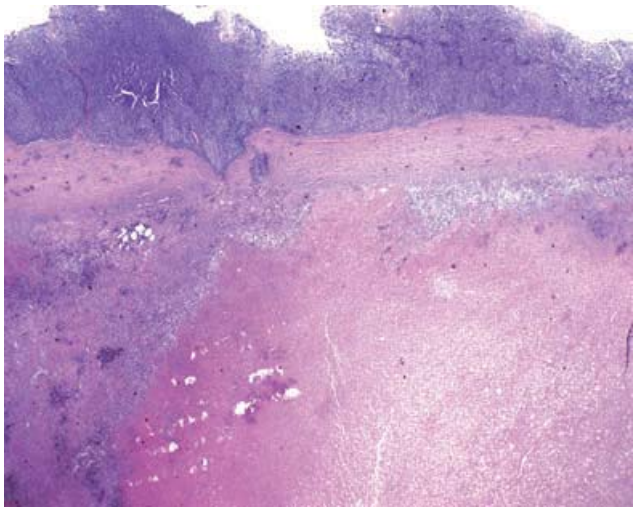

Figure 2.48. Dog: lymph node, diffuse large T-cell lymphoma. There is complete ischemic infarction of the interior of the node. The band of blue tissue at the top represents extranodal proliferation of lymphoma above the greatly thickened collagenous capsule. The pale area beneath the capsule is the residual area of peripheral sinus that lies above the pink-stained area of necrotic tumor.

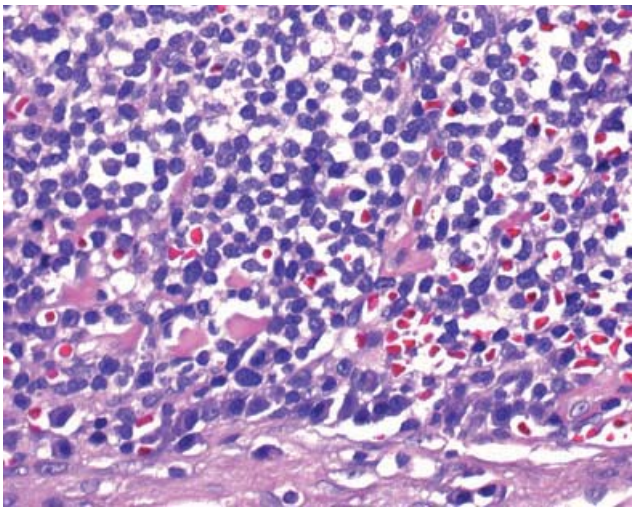

Figure 2.49. Detail of Figure 2.48. The residual peripheral capsule is at the bottom of the image with the proliferating neoplastic cells forming a thick band of perinodal colonization. Perinuclear clear areas are exaggerated by ischemic changes in the entire tissue.

blood-filled sinuses was termed *sinus vascular transformation* and in animal models was shown to be caused by blockage of the efferent veins. In this condition, the congested vascular channels open or develop anastomoses with the lymphatic sinuses that become dilated and lined by an endothelial lining with more prominent nuclei. The venous blood continues to exit the node by the efferent lymphatic system. Blockage of both the efferent venous and lymphatic drainage results in infarction of the node or progressive sclerosis with thickening of the capsule and sclerosis of the medullary sinuses with atrophy of the lymphoid compartments. When this sinus transformation occurs in a clinical context, the vascularization is so vibrant that in its initial description it was noted that the disorder needed to be distinguished from Kaposi sarcoma. In the dog, complete occlusion of the blood supply to the popliteal node results in revascularization of the node, provided that lymph flow is maintained. These demonstrations, although rarely mimicked in clinical practice, do provide a dynamic understanding of how the lymph node is able to respond and survive a variety of severe perturbations of the blood and lymphatic vascular systems. In my experience, unusual dilation of the medullary sinuses without alteration of vascular lining cells but with lymphoid atrophy is observed rarely, presumably of efferent lymphatic blockage.

Less rarely, node infarction may be encountered in association with large cell lymphoma. The node is usually partially infarcted with survival of the capsule and little reaction at the dead/viable interface (Figs. 2.48, 2.49). In human pathology, a totally infarcted node is occasionally the initial biopsy on a patient that on subsequent biopsy is found to have lymphoma. In a report of 16 cases presenting with infarction of a single node, 13 were subsequently diagnosed with lymphoma, and of these three cases, were of the small cleaved cell or relatively low grade type. In dogs where histiocytic diseases are relatively common, a partially infarcted node is likely to be a site of Langerhans cell histiocytosis where angiocentric and angioinvasive obstruction of small arterioles is part of the diagnostic picture (Figs. 2.50, 2.51). Sepsis appears much more likely to present as an active or inspissated abscess as in the corynebacterial adenitis of sheep rather than an ischemic infarct. In human pathology, a lesion called *inflammatory pseudotumor* is seen in the spleen and occasionally in lymph nodes with a variety of associated disease including local trauma, fever, autoimmune disease, and distant nonhematopoietic neoplasm. The nodes resemble cases of cat scratch fever in having greatly thickened capsules and being largely fibrotic but without abscessation and with a florid mixture of stromal proliferation with scattered plasma cells, lymphocytes, and granulation tissue of varying degrees of maturity.

Hyperplastic and Dysplastic Changes

Hyperplastic Changes

In general, the term *lymphadenopathy* is used to describe conditions characterized by regional or generalized lymph node enlargement of benign reactive origin. The inductive causes may be auto- or hyperimmune or may be due to infective agents. A condition originally described in

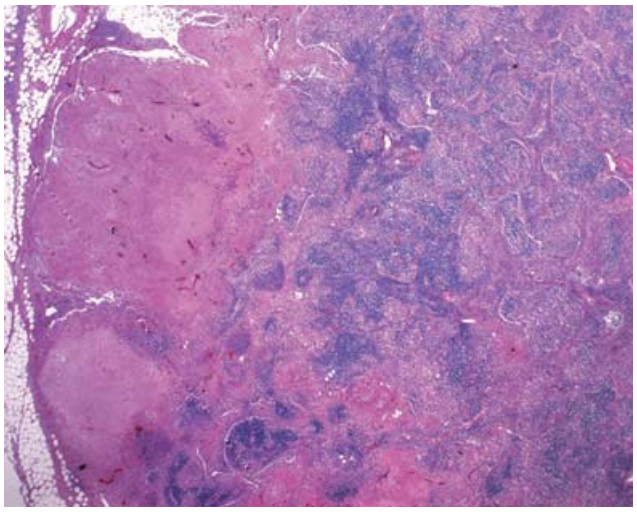

Figure 2.50. Dog: lymph node, disseminated histiocytic sarcoma. The homogeneously staining areas to the left of the image represent ischemic infarction of the outer node cortex. Histiocytic sarcoma tends to invade and obstruct small arterioles of the size supplying the outer cortical region of lymph nodes.

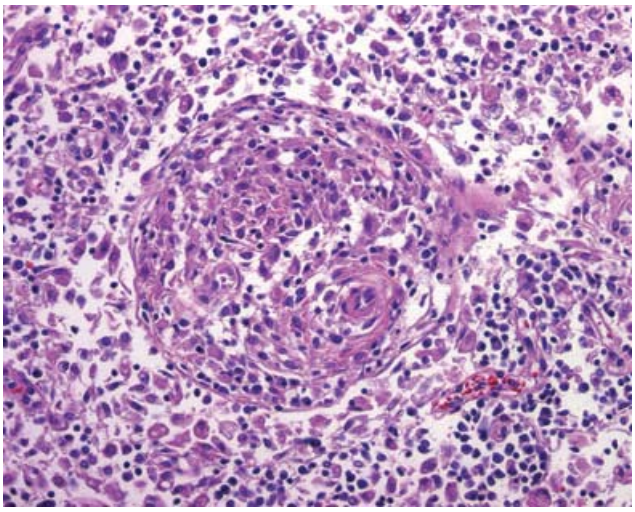

Figure 2.51. Detail of the interior of the lymph node depicted in Figure 2.50. Typical angiocentric proliferation of neoplastic Langerhans cells around small vessels. With CD-18 staining, neoplastic cells can be observed penetrating the adventitia, media, and intima of small arteries.

humans as *angioimmunoblastic lymphadenopathy with dysproteinemia (AILD)* has been found to be a subset of peripheral T-cell lymphoma, thus leaving the suffix adenopathy a designation for benign conditions. A benign condition of young mature cats has been described that has the mixed cellular reaction of a benign response but also the fine vascular prominence of AILD and may occur as a type of T-cell lymphoma as well. Some prefer to limit the use of the term *lymphadenopathy* to lesions of noninfective cause. However, since the etiology is not usually apparent in making a *clinical* assessment, the designation of lymphadenitis is more correctly reserved for pathological descriptions where the distinction may be made on the type of cellular reaction and any agents apparent. There is value in describing the *pathological* changes in lymph nodes in terms of general types of cellular reactions. Nodes that are enlarged because of increased numbers of lymphocytes have lymphoproliferative disease that may be hyperplastic (diffuse or follicular), atypical hyperplastic (undetermined benign or neoplastic), or frankly neoplastic. In contrast, lymphadenitis may present as a type of lymphoid atrophy as in cattle with virus diarrhea or enlarged with a septic (neutrophilic) granulomatous or necrotizing/sclerosing type of cellular reaction.

Diffuse Reactive Hyperplasia

Reactive nodes with high cellularity and a completely diffuse architecture are unusual and generally a transitional pattern preceding development of a follicular response to a very strong and usually local antigenic challenge. The opportunity to observe these reactions occurs when nodes are biopsied or animals succumb at a known time period after the antigenic challenge. Examples are nodes from the pelvic area generally of large animals, dead of genital trauma after dystocia, or a calf or foal injured at birth that dies within 10 days. In these cases, the node is at least moderately enlarged with a taut capsule and a compressed peripheral sinus. The entire node has a moth-eaten appearance due to a very mixed population of cells consisting of small, medium, and large lymphocytes plus dendritic cells with abundant pale cytoplasm and tingible body macrophages (Figs. 2.52, 2.53). The postcapillary venules are prominent and have a very high level of transmural lymphocytes. Because the antigenic stimulation generally arises from drainage from an area of sepsis, neutrophils are commonly found in the peripheral and medullary sinuses and sparsely in the intervening areas. The benign nature of the reaction is apparent from the history and the very uniformly mixed pattern of cellularity. A much more common type of diffuse pattern occurs in which a follicular component remains and there is expansion of the interfollicular areas with a bland, generally pale-staining mixed cellularity. This type of reaction is seen as a response to chronic dermatitis and some types of systemic drug reactions.

Follicular Hyperplasia

Follicular hyperplasia is the most common type of chronic reactive nodal architecture. The nodes most often involved are the mesenterics, where there is normally constant antigenic stimulation, and in the peripheral node draining areas with skin or mucosal inflammation, gen-

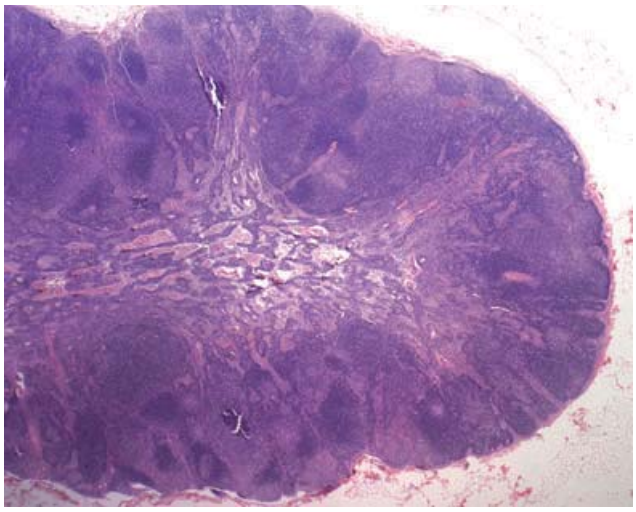

Figure 2.52. Dog: popliteal lymph node, diffuse hyperplasia 5 days following immunization into the ipsilateral foot pad. Previous germinal centers are obscured and surrounded by small areas of residual darker-stained areas of paracortex composed of a homogeneous population of small mature lymphocytes. The lighter areas of paracortex represent recent intense proliferation of mixed cellularity.

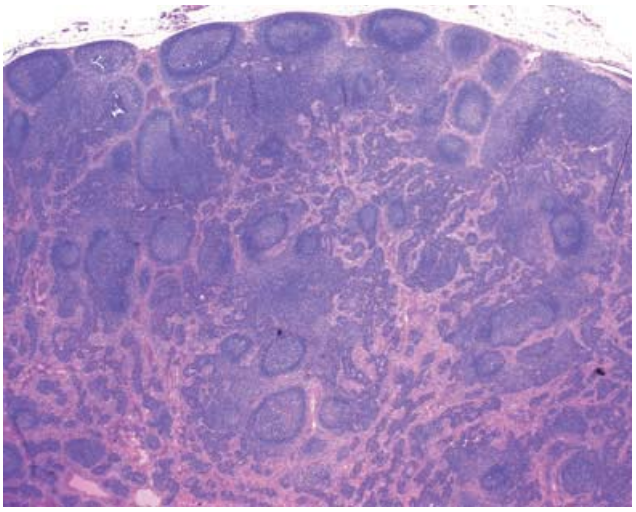

Figure 2.54. Cat: lymph node, moderate benign follicular hyperplasia. The germinal centers are widely separated and have high cellularity with well-defined mantle cell cuffs. The germinal centers are displacing a background of medullary cord and plasma cell hyperplasia that indicates that the reaction has persisted at this level for some time.

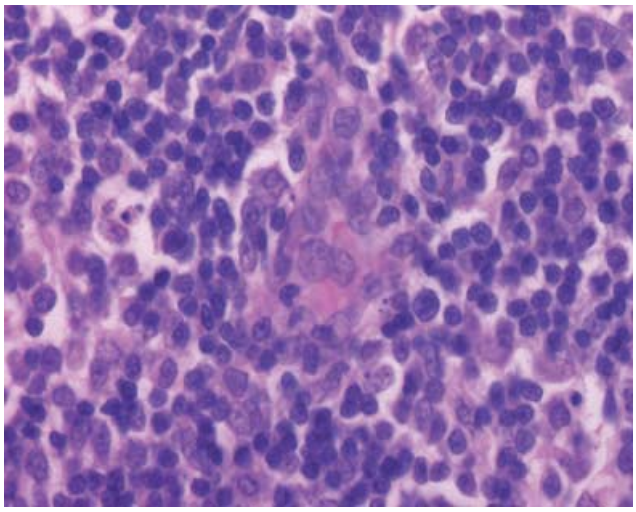

Figure 2.53. Detail of Figure 2.52, paracortex with high endothelial venule (center) with very vesicular endothelial nuclei. The surrounding cell population consists of small, medium, and large lymphocytes with occasional dendritic cells and tingible body macrophages characteristic of an early paracortical immunologic reaction.

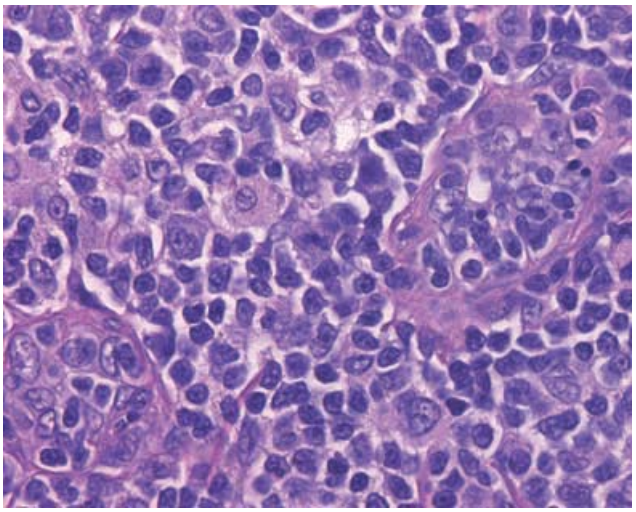

Figure 2.55. Detail of Figure 2.54, paracortical area with two high endothelial venules that have a high level of transmural cellular traffic and with the more homogeneous surrounding cellularity of a maturing immune response.

erally the submandibular and popliteal nodes. Follicular hyperplasia presents with both the outer and inner cortex occupied by closely packed germinal centers with impingement on the medullary cords and sinuses, with the former containing numerous mature plasma cells (Figs. 2.54, 2.55). As noted above, in vibrant reactions the mantle cell cuffs are broad and continuous and the germinal centers have high cellularity (Figs. 2.56, 2.57). Follicular hyperplasia may progress to a less florid reaction, with smaller and more widely separated germinal centers with less transmural traffic across the high endothelial venules (Figs. 2.58, 2.59), or to progression of the follicular reaction till the germinal centers coalesce and the mantle cell cuffs become depleted (Figs. 2.60–2.62). In diseases characterized by persistent high-level

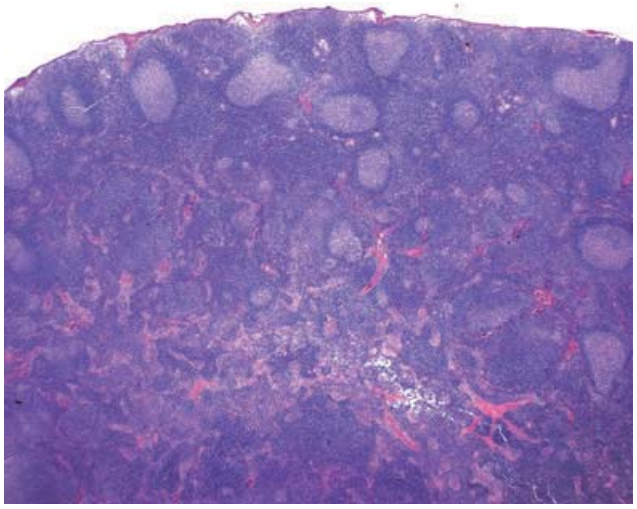

Figure 2.56. Cat: lymph node, benign follicular hyperplasia. Early follicular reaction with largely cortical germinal centers that have broad mantle cell cuffs. The surrounding paracortex is uniformly densely stained and there is high cellularity of medullary sinuses.

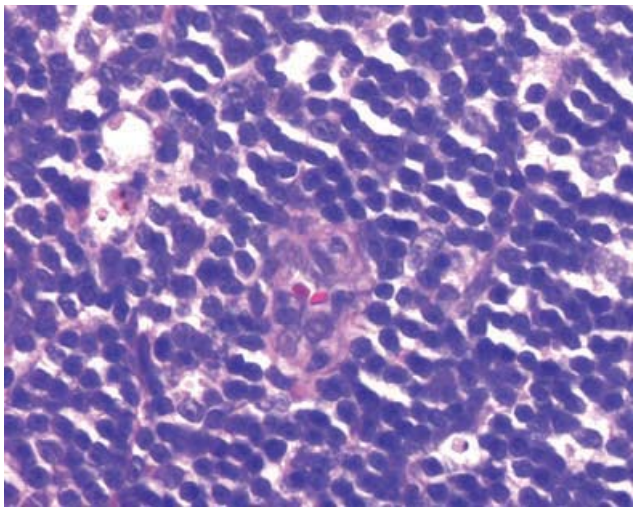

Figure 2.57. Detail of Figure 2.56, paracortical area with a background of mature small paracortical cells with numerous tingible body macrophages indicating high cell turnover. The high endothelial venule (center) has vesicular endothelial nuclei and a moderate number of cells in transmural migration.

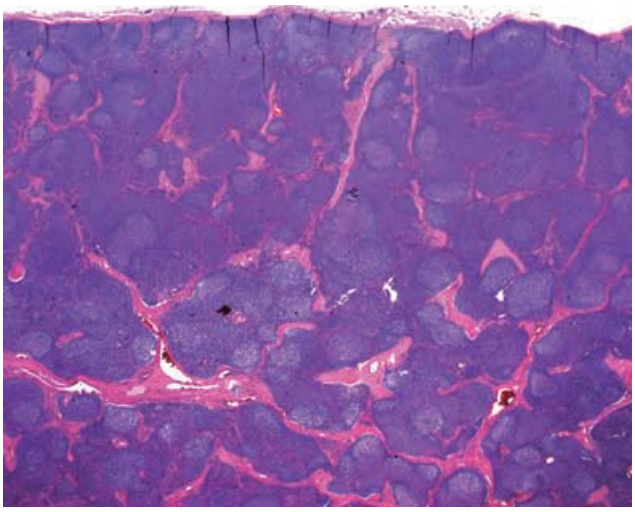

Figure 2.58. Dog: lymph node, fading follicular hyperplasia. The peripheral capsule is mildly thickened and there is proliferation of interstitial collagenous supporting structures. The follicles have been numerous and extend to the medullary area but are now reduced in size and cellular density, with narrow and discontinuous mantle cell cuffs.

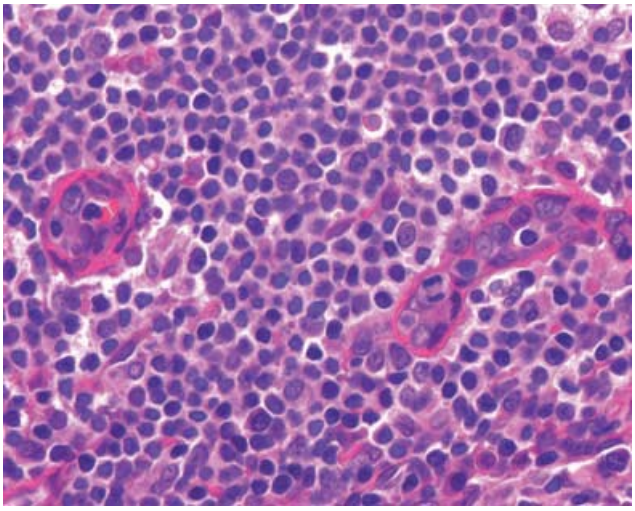

Figure 2.59. Detail of Figure 2.58, paracortex with reduced density of small mature lymphocytes and a high endothelial venule with low transmural cellular traffic indicative of a regressing immune response.

antigenemia, very reactive nodes may have lymphocytic colonization of the perinodal fat (see Fig. 2.60) and other supporting tissues, but there is not the sclerosis of perinodal structures with node fixation as may occur in septic adenitis and neoplastic diseases. Benign focal or multifocal perinodal lymphoid proliferation occurs in equine infectious anemia and in bovine trypanosomiasis. When follicular reactions wane, the mantle cell cuffs become depleted, the germinal centers become less densely populated with lymphocytes, and the dendritic cell background is more apparent as a pink-staining area with large, pale, vesicular nuclei. If there has been a more severe and toxigenic challenge, some germinal centers may contain large amorphous islands of persistent proteinaceous debris called *follicular hyalinosis* (Fig. 2.63). Chronic follicular hyperplasia may have a type of architectural development where diffuse follicular hyperplasia appears emphasized

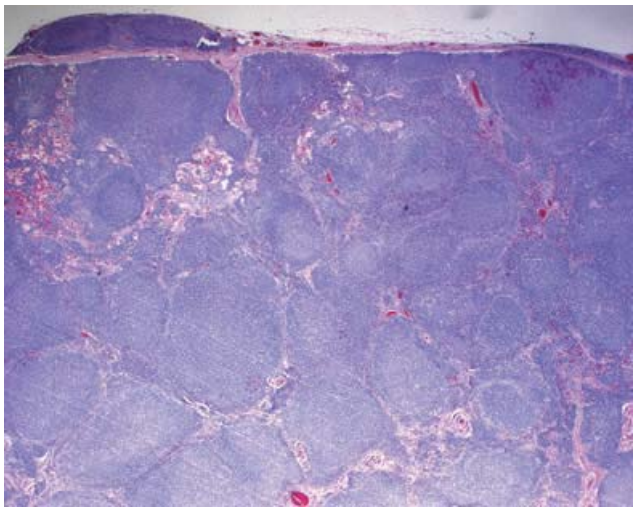

Figure 2.60. Dog: lymph node, atypical follicular hyperplasia. The peripheral capsule is distended with irregular colonization of perinodal tissues. There is macrofollicular hyperplasia with loss of well-defined mantle cell cuffs and irregular dilation of sinuses extending out to the peripheral capsule. On close examination, antigen-related polarity can still be determined in many of the germinal centers indicating a vibrant but benign response that is now in decline.

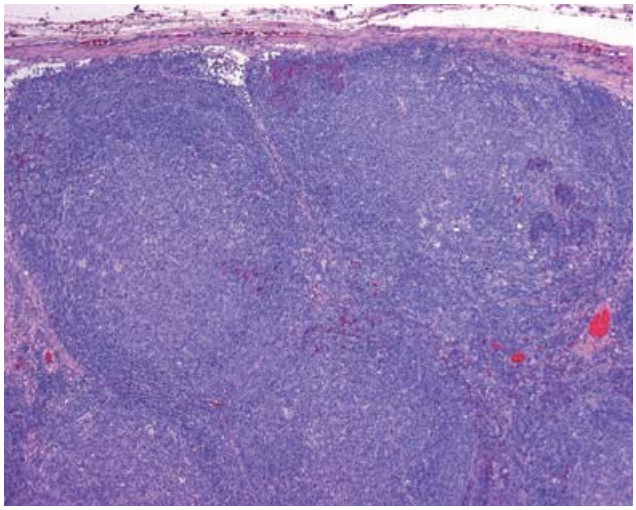

Figure 2.61. Detail of Figure 2.60. There is mild irregular colonization of the node capsule and superficial perinodal tissues. The peripheral sinus is irregularly open and compressed. The germinal centers have thinned discontinuous or absent mantle cell cuffs with antigen-related polarity inobvious. The small dark clusters of cells in the germinal center in the upper right represent infiltration of the germinal center by small lymphocytes in the process of progressive transformation of germinal centers.

by a dense rim of small lymphocytes without marginal zones and atrophy of the intervening paracortex. These lesions are termed *Castleman lymphadenopathy* or *Castleman disease* in human pathology and the changes can be local or systemic and multifocal. In animals, these

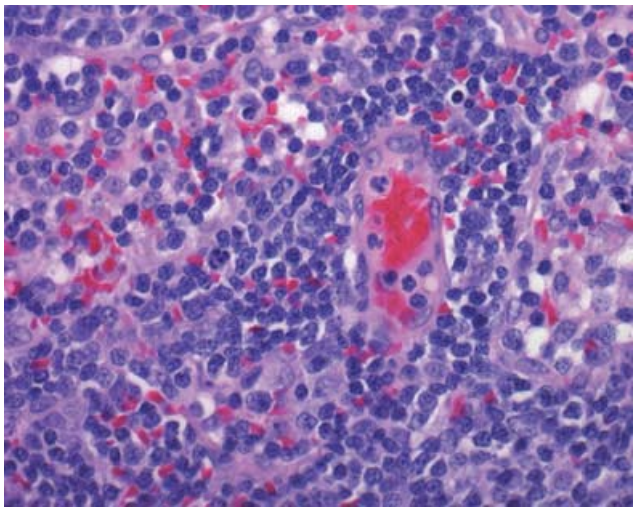

Figure 2.62. Detail of Figure 2.60, paracortical region with two high endothelial venules at the center and lower left with variable transmural cellular traffic surrounded by a very narrowed area of paracortex with abnormal sinus area to the right and left containing large macrophages and a mixture of cell types. These changes are consistent with a node undergoing continued immune stimulation with progressive depletion of the mantle cell cuffs indicative of declining immunologic capability.

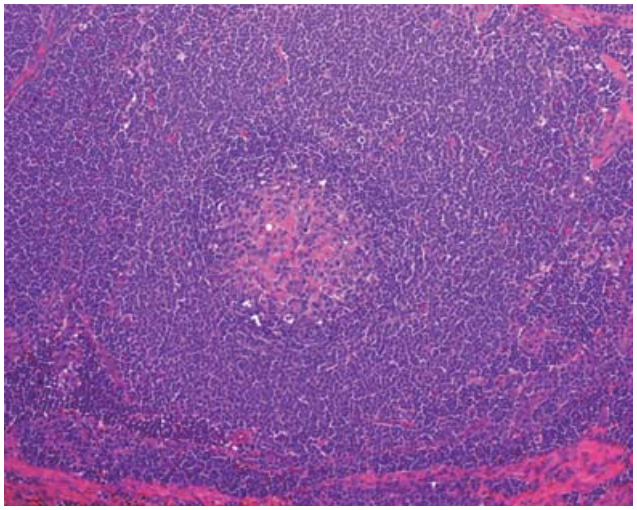

Figure 2.63. Dog: lymph node, atypical follicular hyperplasia. There is fading follicular reaction with hypocellular germinal centers occupied by a dense proteinaceous material known as *follicular hyalinosis*.

changes are seen in dogs and cats and in old sheep and goats (Fig. 2.64). In companion animals, the germinal centers tend to remain active and highly cellular, but in the small ruminants, they may become shrunken and hyalinized and characteristically are perforated by a prominent arteriole. When the vessels within the node, particularly those entering the follicle giving it a

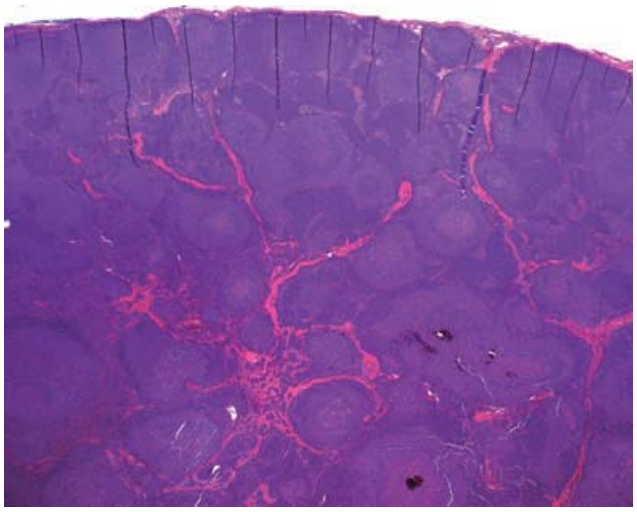

Figure 2.64. Architectural pattern of Figure 2.63. This node has features of Castlemanlike proliferation. The peripheral sinus is compressed and obliterated, with the interior of the node traversed by dense mature collagenous bands. The germinal centers have become hypocellular and are surrounded by concentric rings of small mantle cells with an absence of marginal zone areas. The interfollicular areas contain densely cellular masses usually with plasma cell type differentiation.

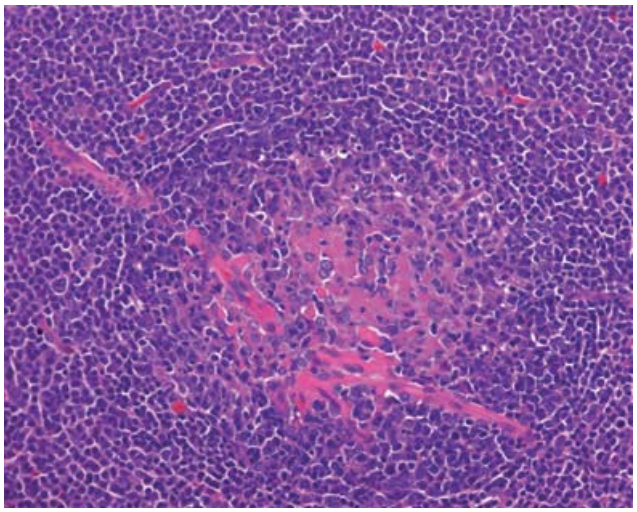

Figure 2.65. Detail of Figure 2.63. The hyalinized germinal center is surrounded by concentric rings of residual mantle cells, melding with a dense plasma cell population in the interfollicular areas. The germinal center is penetrated by radial blood vessels that may also have hyalinized walls and, if single, are termed a *lollipop vascular lesion*.

"lollipop" appearance (Fig. 2.65), have very prominent endothelium and are surrounded by prominent collagenous pericytes, the lesions are termed *Castleman lymphadenopathy of the hyaline-vascular type*. In sheep, the vascular hyalinization may be irregularly thickened and focally mineralized. The disease is not well understood in humans and is related to chronic immune phenomena but is not age limited. In sheep the hyaline-vascular type of lymphadenopathy has been seen with chronic parasitism. More often, chronic immune stimulation from areas of inflammation causes nodes to become very large and sclerotic, with the medullary areas largely occupied by thick mature collagenous bands that permeate the cortex and fuse with a greatly thickened capsule. Perhaps the most characteristic example of this type of reaction is seen in the supramammary glands of dairy cattle that have chronic mastitis where the nodes may be as much as 10 cm in diameter but with greatly reduced areas of responsive lymphoid tissue. In animals as in humans, persistent benign reactive nodal hyperplasia is a potent risk factor for lymphoma and for that reason the cause should always be sought and eliminated.

REFERENCES

Harris, N.L., McNeely, W.F., Shepard, J.O., Ebeling, S.H., Ellender, S.M., and Peters, C.C. (2002) Case records of the Massachusetts General Hospital. *New England J Med* 346:1989–1996.

Ioachim, N.L., and Petech, H. (2002) Castleman Lymphadenopathy (Chapter 43). In *Ioachim's Lymph Node Pathology*, 3rd ed. Lippincott Williams & Wilkins, Philadelphia, pp. 246–258.

Mooney, S.C., Patnaik, A.K., Hayes, A.A., and MacEwen, E.G. (1987) Generalized lymphadenopathy resembling lymphoma in cats: Six cases (1972–1976). *J Amer Vet Med Assoc* 190:897–900.

Yang, T.J., Mather, J.F., and Rabinovsky, E.D. (1988) Changes in subpopulation of lymphocytes in peripheral blood, and supramammary and prescapular lymph nodes of cows with mastitis and normal cows. *Vet Immunol Immunopathol* 18:279–285.

Lymphadenitis Due to Systemic Viral and Protozoal Infections

Lymphoid responses in a number of viral infections are characterized by early edema and swelling followed by widespread necrosis, particularly of the germinal center cells but involving the larger cells of both B- and T-cell types and likely based on cells that are mitotically active. Changes characteristic of this type of response are seen in bovine virus diarrhea (BVD) infection in lymph nodes but also in the Peyer's patches of the lower small intestine and in splenic follicles. In animals dying of acute infection with BVD virus, the lymph nodes are smaller than normal with the capsule undulating and thickened by condensation and contraction. The subcapsular sinus is dilated and contains few neutrophils and more numerous macrophages. There is complete follicular involution, and

the remaining cortex consists of a thin irregular band of small lymphocytes of the paracortex that lies above a dense infiltration of the medullary sinuses with large macrophages (Figs. 2.66, 2.67). With some variation in the timing and severity of lesions, similar changes occur in feline panleukopenia (Figs. 2.68–2.70) and canine parvoviral infection and in hog cholera and African swine fever.

In hog cholera, the virus has primary effects on microvascular endothelium with initial swelling of cells in small vessels that may occlude the lumen and accounts for the widespread petechial and ecchymotic hemorrhages. In nodes, the vascular infarction is primarily in the medulla; in swine it is peripheral, resulting in nodes with an outer ring of hemorrhage. In African swine fever the lesions are similar to hog cholera but more severe and with more extensive lympholysis. The pathogenesis of the severe hemorrhagic infarction is not a result of endothelial necrosis but of thrombocytopenia and a coagulopathy. In cattle with the acute form of malignant catarrhal fever (MCF), the lymph nodes have a short phase of lymphoid proliferation followed by locally extensive areas of hemorrhage and infarction as a result of widespread small vessel cuffing, vasculitis, and thrombosis. Rinderpest is like MCF with more severe lympholysis and more involvement of the intestinal tract. Animals that survive these diseases have varying degrees of recovery of follicular activity and generally medullary cord plasmacytosis

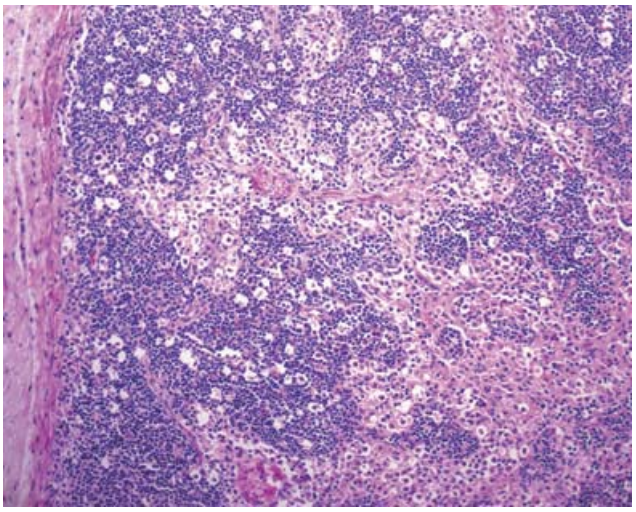

Figure 2.67. Detail of Figure 2.66. The node capsule lies to the left with the peripheral sinus having a high level of mixed cellularity. There is marked atrophy of cortical tissue with irregular islands of paracortex containing many tingible body macrophages. The cortex is regressing due to cell death and progressively invaded by passive expansion of the medullary sinuses containing large macrophages. These animals usually die with neutropenia and at this stage of the disease the long-lived and locally reproducing macrophages become the dominant reactive cell.

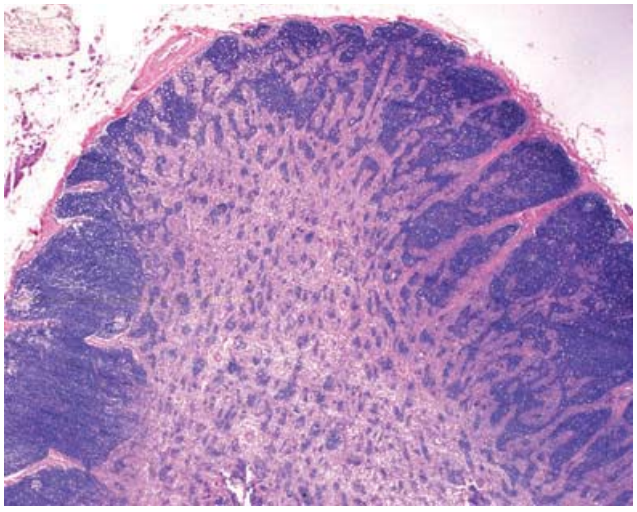

Figure 2.66. Cow: lymph node, bovine virus diarrhea. There is complete atrophy of the germinal centers with a small pale area (left center) likely representing a previous area of follicular development. Medullary cords have low cellularity and there is dilation and high cellularity of medullary sinuses with large activated macrophages. The residual areas of paracortex have a moth-eaten appearance due to the presence of many large macrophages.

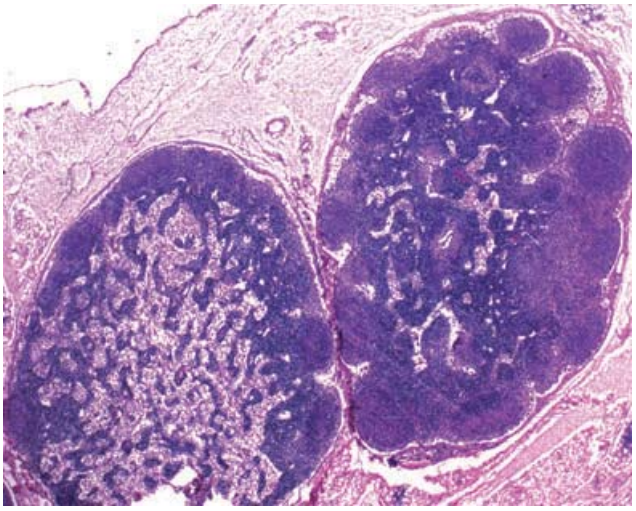

Figure 2.68. Cat: lymph node, panleukopenia virus infection. Cats with panleukopenia virus tend to die 7 to 9 days after first showing signs when early regeneration of bone marrow and lymph node tissues is just beginning. The lymph node to the left has complete lysis of germinal centers with passive enlargement of the medullary sinuses similar to that seen in the cow with bovine virus diarrhea. The cortical tissue has retracted slightly from the surrounding capsule in both nodes indicative of extensive cellular loss. The node on the right appears to be at an early stage of regeneration with the beginnings of diffuse paracortical hyperplasia.

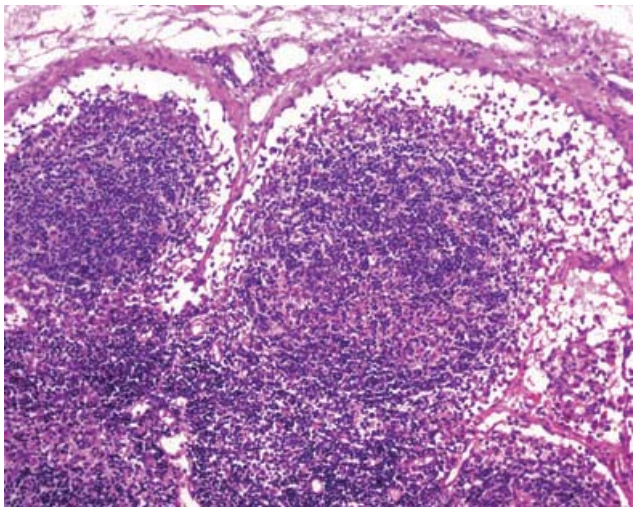

Figure 2.69. Detail of Figure 2.68, mixed cellular proliferation in the outer cortex. The lighter stained area of the nodule to the right likely represents the residual dendritic cells of a preexisting germinal center.

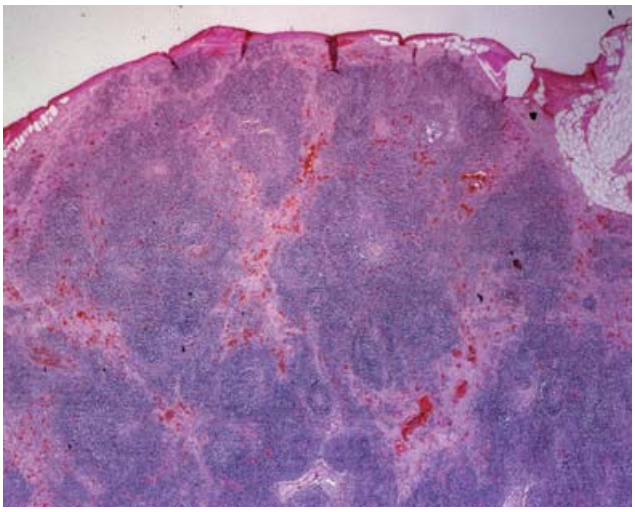

Figure 2.71. Calf: lymph node, salmonellosis. The node is swollen and edematous with high cellularity of the peripheral and internal sinuses. The germinal centers are small and poorly defined with hypocellular areas suggesting stress-related involution.

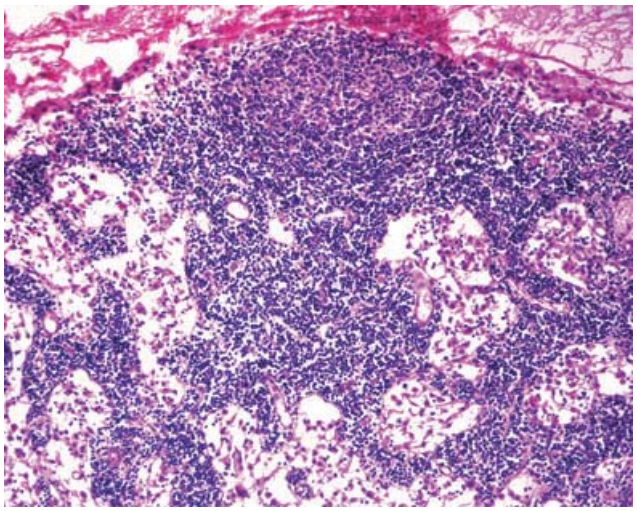

Figure 2.70. Detail from the lower-left area of Figure 2.68. An involuted germinal center that is becoming repopulated with small lymphocytes is present in the subcapsular region at the top of the image and surrounded by atrophic medullary cords with dilated hypocellular sinuses.

and generalized sclerosis. In cattle with theileriasis (East Coast Fever), the lymph node changes consist of an early proliferative response with diffuse lymphoid proliferation followed by lymphoid depletion with foci of necrosis and hemorrhage. In the very acute disease, the lymphocytes are parasitized by the large and diagnostic macroschizonts (Koch's Blue Bodies) that distend and block capillaries causing hemorrhage and infarction; in cases of longer duration, hemorrhage and necrosis of other causes occur in nodes depleted of lymphocytes. In toxoplasmosis, the nodes are variably involved but always in those draining affected organs. The nodes may be markedly enlarged and firm with focal areas of ischemic coagulation necrosis that are pale on gross examination. There is little cell reaction to the necrosis, and the diagnostic tachyzoites singly and in cysts are found adjacent to the areas of necrosis. There will be more severe lesions elsewhere in the brain, liver, intestine, and muscle. In dogs, *Neospora* must be distinguished from *Toxoplasma* organisms largely by immunohistochemical means and the fact that *Neospora* cysts occur only in the brain. In cattle, *Toxoplasma* is more easily distinguished from the much larger cysts of sarcosporidiosis. Oddly, in humans, *Toxoplasma* has such a characteristic clinical presentation of an enlarged posterior cervical node and histologic appearance with sinus histiocytosis that the diagnosis is usually made on history and oversight stains.

Lymphadenitis Due to Bacterial Infection

Disease characterized by septicemia, such as salmonellosis, results in swollen lymph nodes with edema and congestion. In early infections where the animal is responding strongly, there are neutrophils in the sinuses and these may form small foci around bacterial colonies. In cattle and calves where terminal septicemia is usually accompanied by neutropenia, there are few neutrophils in the nodes and a few eosinophils may be the last cells released from the marrow (Figs. 2.71, 2.72). In cases of anthrax the nodes have more severe changes with fibrin in the sinuses and severe congestion and hemorrhage

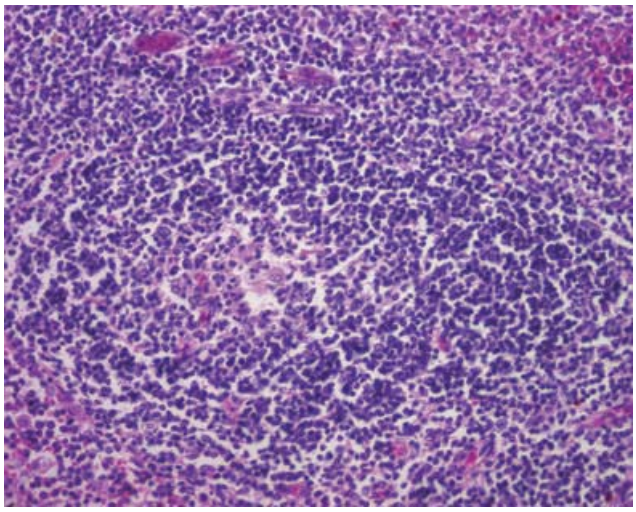

Figure 2.72. Detail of Figure 2.71, involuting hypocellular germinal center with collapse of the mantle cells into the central area of dendritic cells and macrophages. Few neutrophils are in evidence since these animals usually succumb with neutropenia.

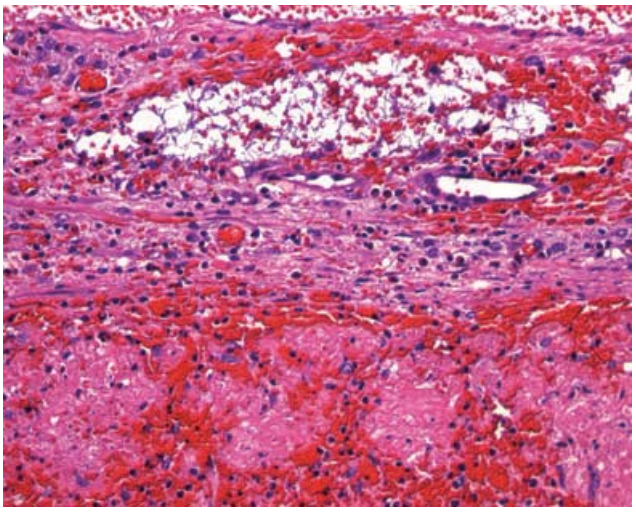

Figure 2.74. Detail of Figure 2.73. A dilated capsular vein contains hundreds of interweaving bacterial rods. There is hemorrhage, fibrin and degenerating cells present in the capsule and in the subcapsular sinus.

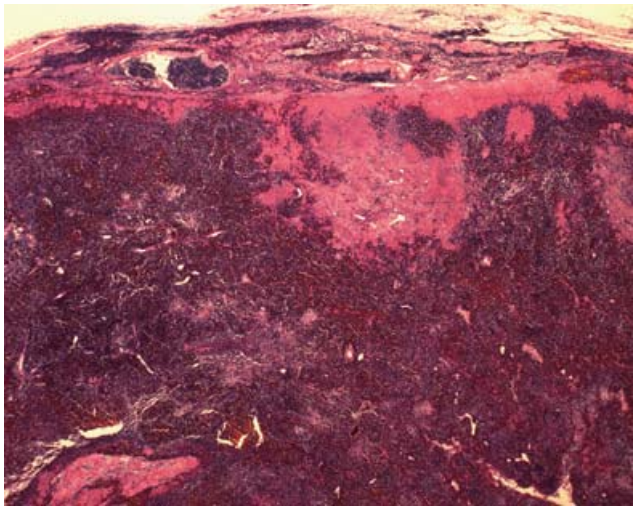

Figure 2.73. Cow: lymph node, anthrax. There is perinodal hemorrhage with fibrin in the capsular vessels. The lighter staining areas of the cortex consist of fibrinous exudation and necrosis with hemorrhagic infarction in the darker areas within the node.

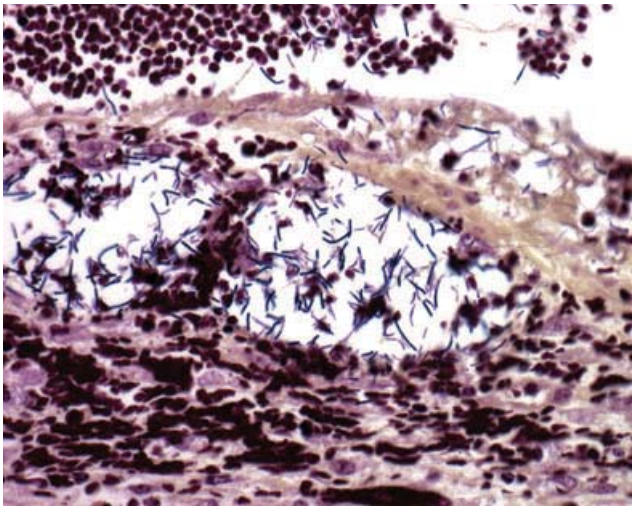

Figure 2.75. Detail of Figure 2.74 with Gram stain demonstrating a massive and overpowering septicemia.

(Figs. 2.73–2.75). Granulomatous lymphadenitis occurs in a number of animal diseases and most are characterized by gross enlargement with capsular and trabecular sclerosis with a predominant population of large epithelioid macrophages. In Johne's disease of cattle, the mucosa of the lower small intestine is always involved, as are the associated mesenteric nodes. The organisms are not seen on H&E staining but are present in large numbers on acid-fast staining and accompanied by a variable number of neutrophils and occasional eosinophils. In contrast to cattle, the lesions in sheep and goats may be more nodular with necrosis and focal mineralization that must be distinguished from tuberculosis (Figs. 2.76, 2.77). Tuberculosis in animals is usually of the bovine type that can infect many mammals but not domestic fowl, and mice and hamsters are resistant to infection with this species of organism. In contrast, the human type of TB infects nonhuman primates and occasionally dogs. In lymph nodes, the *M. bovis* in cattle causes a typical tubercle with a central area of epithelioid macrophages surrounded by circumferential layers of collagenous connective tissue of progressive maturity on the external surface. As these

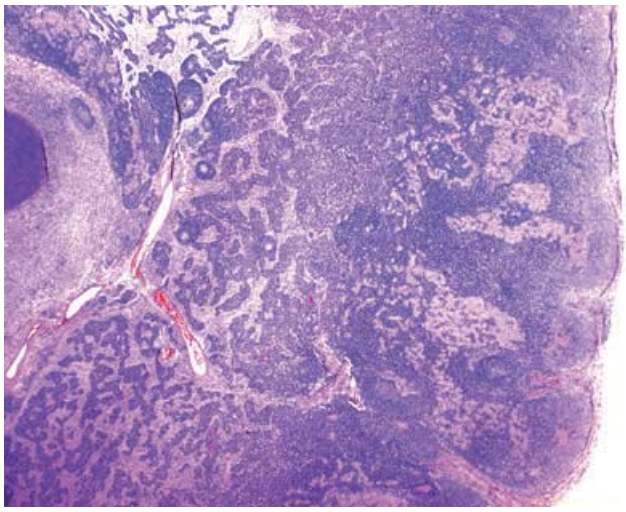

Figure 2.76. Goat: mesenteric node, Johne's disease. The node is enlarged with a thinned capsule and compressed sinus. The germinal centers are receding and the paracortex is irregularly permeated by pale areas consisting of islands of large macrophages. There is a focal area of necrosis in the medulla of the node (upper left) surrounded by a dense wall of connective tissue.

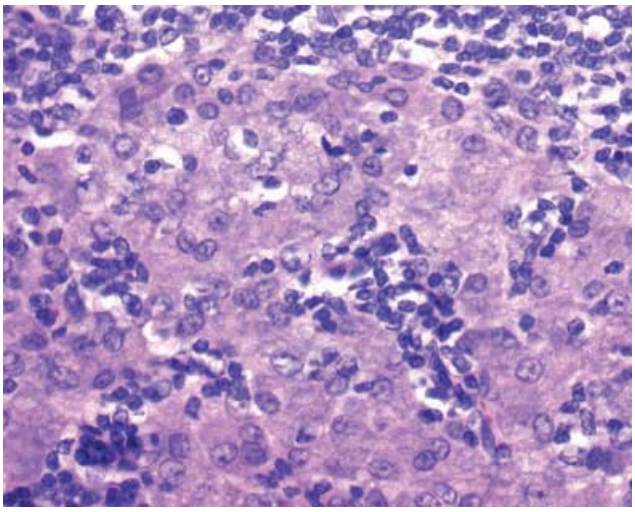

Figure 2.77. Detail of Figure 2.76, focus of macrophage proliferation with fine reticulated cytoplasm that provides faint negative staining of the acid-fast bacteria distending the phagocyte cytoplasm.

lesions enlarge, the center undergoes caseous necrosis and may calcify while giant-cells of Langerhans type with peripheral nuclei irregularly ring the outer epithelioid cells. In cattle, the gross lesion forms a smooth, round, shiny mass in nodes and other tissues (Pearl disease); in horses, the lesions are more diffuse and caseation and mineralization rarely occur. In sheep and goats, caseous lymphadenitis caused by *Corynebacterium pseudotuberculosis* has a characteristic appearance of onion skin ringing in masses of caseous necrosis, almost always in lymph nodes, particularly of the head region; but it may be deep seated as well. The caseous material is surrounded by a taut rim of epithelioid macrophages supported by the node capsule and with few lymphocytes remaining. The lesions usually remain confined to the nodes and even when they become very large they usually remain mobile.

Lymphadenitis Due to Fungal Infection

The dimorphic fungi causing systemic mycoses include *Blastomyces*, *Histoplasma*, *Coccidioides,* and *Cryptococcus* of the yeast family that are frequent invaders of domestic animals. Blastomycosis is most commonly encountered in the Ohio river basin and coccidioidomycosis is more confined to the drier areas of the southwest U.S. In infections with *Blastomyces* the organism can invade any tissue but is most commonly found in the lung and skin and the nodes that drain these sites. The characteristic reaction is granulomatous with a predominance of epithelioid macrophages, but caseation, necrosis, and abscesses may be present with prominent perilesional sclerosis. In surface lesions like those on the skin, blastomycotic lesions are more likely to be associated with a prominent neutrophil reaction as well as macrophages. The double-walled appearance on cytological or histological preparations and the broad-based budding are diagnostic features of this organism. The cellular reactions to these organisms are similar, but the overall appearance may be quite different, as in *Cryptococcus* infections where the broad capsule surrounding the yeast-like organism gives the gross lesion a very mucinous character; this makes the affected tissues difficult to grasp and histologically the lesions have a "soap-bubble" appearance due to the abundance of water clear-staining capsular material (Figs. 2.78–2.79). Coccidiodes spherules are typically very large and 10–70 microns in diameter and surrounded by an epithelioid macrophage reaction; *Histoplasma* organisms are very small intracellular parasites with the yeast bodies 2–4 microns in diameter and surrounded by a clear halo. They occur in clusters within a single macrophage and must be distinguished from leishmanial organisms, which have a small bar-shaped kinetoplast as well as the small dotlike nucleus. All of these mycotic agents can be stained with periodic Schiff stain (PAS) for the bound glycogen of the cell wall as well as by silver stains as for the deep-seated mycoses of Zygomycete type (Figs. 2.80, 2.81). Of these organisms, the *Coccidioides*, *Histoplasma,* and leishmanial organisms are not associated with necrosis but rather tend to be found in relatively solid areas of macrophage proliferation.

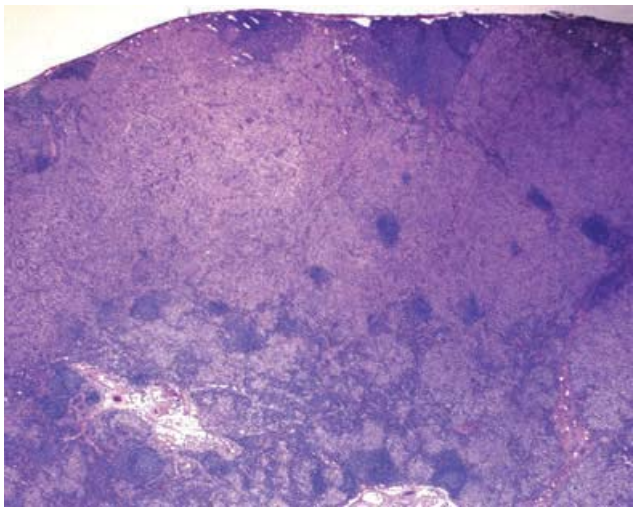

Figure 2.78. Cat: lymph node, cryptococcosis. The node is markedly enlarged with thinning of the capsule and compression of the peripheral sinus. Most of the node has become colonized by large macrophages occupying the lighter staining areas with residual areas of paracortex and medulla, darker staining with a few fading germinal centers.

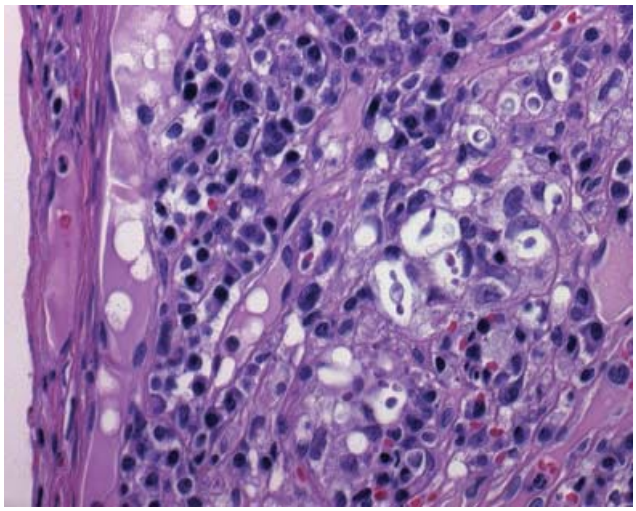

Figure 2.79. Detail of Figure 2.78. The node capsule and peripheral sinus are to the left with a residual area of paracortex above and the expanding area of granuloma formation below and to the right, with numerous budding organisms within the cytoplasm of large macrophages.

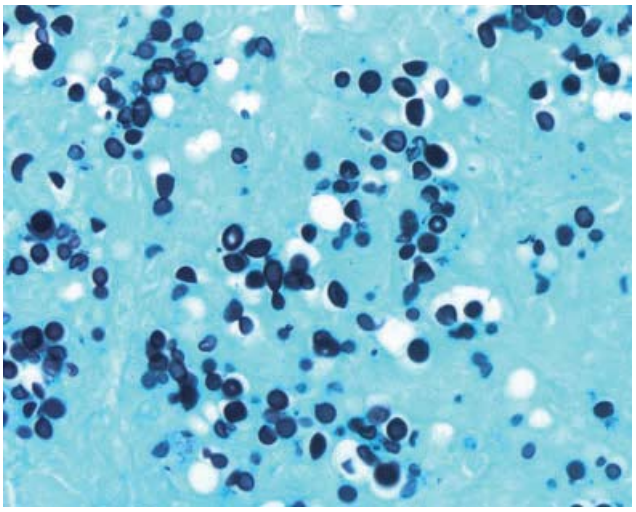

Figure 2.80. Detail of Figure 2.78, cryptococcosis, silver stain.

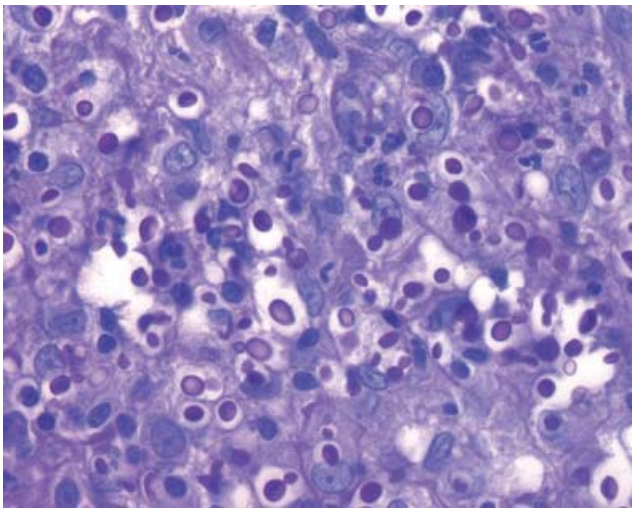

Figure 2.81. Detail of Figure 2.78, cryptococcosis, periodic acid-Schiff stain. The cell wall of the yeastlike structures marks with PAS staining, but the abundant capsular material is unmarked.

REFERENCES

Coggins, L. (1974) Progress in medical virology. *Progr Med Virol* 18:48–63.

Colgrove, G.S., Haelterman, E.O., and Coggins, L. (1969) Pathogenesis of African swine fever in young pigs. *Amer J Vet Res* 30:1343–1359.

Gray, G.F., Jr., Kimball, A.C., and Kean, B.H. (1972) The posterior cervical lymph node in toxoplasmosis. *Am J Pathol* 69:349–356.

Jones, T.C., Hunt, R.D., and King, N.W. (1988) Diseases caused by viruses (Chapter 8). In Jones, T.C., Hunt, R.D., and King, N.W. (eds.), *Veterinary Pathology,* 6th ed. Williams & Wilkins, Baltimore, pp. 197–370.

Jones, T.C., Hunt, R.D., and King, N.W. (1988) Diseases caused by bacteria (Chapter 10. In Jones, T.C., Hunt, R.D., and King, N.W. (eds.), *Veterinary Pathology,* 6th ed. Williams & Wilkins, Baltimore, pp. 413–504.

Jones, T.C., Hunt, R.D., and King, N.W. (1988) Diseases caused by fungi (Chapter 11). In Jones, T.C., Hunt, R.D., and King, N.W. (eds.), *Veterinary Pathology,* 6th ed. Williams & Wilkins, Baltimore, pp. 505–548.

Jones, T.C., Hunt, R.D., and King, N.W. (1988) Diseases due to protozoa (Chapter 12). In Jones, T.C., Hunt, R.D., and King, N.W. (eds.), *Veterinary Pathology,* 6th ed. Williams & Wilkins, Baltimore, pp. 549–600.

Kernkamp, H.C.H. (1939) The blood picture in hog cholera. *J Amer Vet Med Assoc* XCV:525–529.

Liebler, E.M., Kusters, C., and Pohlenz, J.F. (1995) Experimental mucosal disease in cattle: Changes of lymphocyte subpopulations in Peyer's patches and in lymphoid nodules of large intestine. *Vet Immunol Immunopathol* 48:233–248.

McAdaragh, J.P., Eustis, S.L., Nelson, D.T., Stotz, I., and Kenefick, K. (1982) Experimental infection of conventional dogs with canine parvovirus. *Amer J Vet Res* 43:693–696.

Palmer, M.V., Gosch, G., Lyon, R., Waters, W.R., and Whipple, D.L. (2002) Apoptosis in lymph node granulomas from white-tailed deer (*Odocoileus virginianus*) experimentally infected with *Mycobacterium bovis*. *J Comp Pathol* 127:7–13.

Reardon, M.J., and Pierce, K.R. (1981) Acute experimental canine ehrlichiosis. I. Sequential reaction of the hemic and lymphoreticular systems. *Vet Pathol* 18:48–61.

Tajima, M., and Ushijima, T. (1971) The pathogenesis of rinderpest in the lymph nodes of cattle. *Amer J Pathol* 62:221–228.

Thompson, K.G., Thomson, G.W., and Henry, J.N. (1981) Alimentary tract manifestations of bovine adenovirus infections. *Can Vet J* 22:68–71.

Metastatic Neoplasms

Mechanisms of Tumor Metastasis

In general, death from cancer in humans is due to dissemination of the primary tumor rather than growth of the primary itself. In animals with cancer, a primary tumor may reach a relatively larger size prior to initial detection, but the same dynamics seem to apply. Thus, a consideration of metastatic neoplasia has equal relevance in the context of animal oncology. In order for a neoplasm to become metastatic, a number of genetic, biophysical, and anatomic hurdles must be overcome. These include continuing growth of the primary with attendant neovascularization, invasion of benign supporting cells and blood or lymphatic vessels, survival in transport, extravasation, survival in a new organ or tissue, and continued angiogenesis to provide blood to the metastatic colony. It is unclear whether all neoplasms that have spread to distant sites initially had inherent capability for metastasis or whether this ability is gained in continued genetic mutations of the primary. Tumor mobility requires down regulation of the E-cadherin adhesion molecules in order that single or small clusters of malignant T-cells can detach from the primary site.

For malignant T-cells in transport to survive in a lymph node, they must first arrive via lymphatic drainage and then, as for lymphocyte homing, they must have molecules on the tumor cell plasma membrane that are complementary to the extracellular matrix of the node sinus cells. Integrin receptors áv â3 on a human melanoma cell line adhered to cryostat sections of human lymph node stroma by the vitronectin molecule more strongly than by fibronectin. Further, the invasion of the node by neoplastic cells up-regulates the synthesis of vitronectin, which suggests that local effects within the node may be active in assisting adhesion and colonization. It has been shown that the tumors do not have lymphatics within their interior but do produce a variety of vascular growth factors including VEGF-D that specifically stimulates the growth of benign lymphatic channels. It is by access to these vessels in adjacent benign tissue that neoplastic cells gain entry to the drainage system and ultimately to lymph nodes. The tendency for carcinomas to metastasize by lymphatics and end up in nodes, while sarcomas travel by the blood and tend to lodge in the lung, has been termed the *organ specificity of metastases*. This concept, while most often the rule, doesn't account for the fact that in humans colonic carcinoma may occasionally form metastases in the liver without colonizing the lymph nodes en route and can be cured by hepatic section. Similarly, breast carcinoma cells may colonize bone marrow but not the intervening nodes. Thus, it is occasionally possible for carcinoma to gain the blood system either initially or by passing through the sentinel node and exiting via the capillary system.

REFERENCES

Couzin, J. (2003). Tracing the steps of metastasis, cancer's menacing ballet. *Science* 299:1002.

Funaki, H., Nishimura, G., Harada, S-I., Ninomiya, I., Terada, I., Fushida, S., Tani, T., Fujimura, T., Kayahara, M., Shimizu, K., Ohta, T., and Miwa, K. (2003) Expression of vascular endothelial growth factor D is associated with lymph node metatasis in human colorectal carcinoma. *Oncol* 64:416–422.

Gershenwald, J.E., and Fidler, I.J. (2002) Targeting lymphatic metastasis. *Science* 296:1811–1886.

Gervasoni, J.E., Jr., Taneja, C., Chung, M.A., and Cady, B. (2000). Axillary dissection in the context of the biology of lymph node metastasis. *Amer J Surg* 180:278–283.

Nathanson, S.D. (2003) Insights into the mechanisms of lymph node metastasis. *Cancer* 98:413–423.

Metastatic Tumor in Lymph Nodes

As a filter for the lymph system, the nodes provide at least a temporary catchment for tumor metastases and thus provide a means of demonstrating not only malignant neoplasia but also a means of identifying the primary tissue of origin. Lymphatic-borne metastatic tumor cells will first accumulate in the peripheral sinus and then migrate to the medullary sinuses and then cortex and medulla (Figs. 2.82, 2.83). The tissue response in the node appears to be regulated by the immunomodulatory T-cells that determine whether no cellular reaction occurs or a

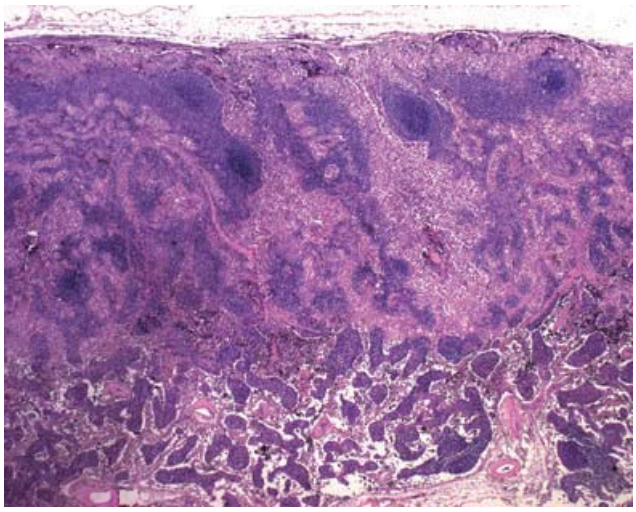

Figure 2.82. Dog: abdominal lymph node, gastric adenocarcinoma. The node is moderately enlarged with taut capsule and filling of the peripheral sinus. There is involution of germinal centers and atrophy of paracortex, with the lighter areas representing infiltration of neoplastic cells deeply into the cortex. There is waning medullary cord plasma cell hyperplasia and only moderate cellularity of the medullary sinuses.

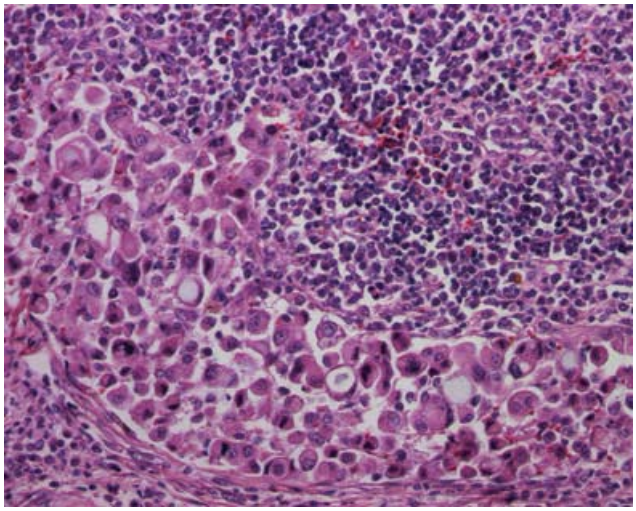

Figure 2.83. Detail of Figure 2.82, interface of residual paracortex (upper right) and dilated sinus largely containing neoplastic cells from the gastric lining, several of which have large secretion vacuoles forming signet ring configurations. Note the lack of cellular reaction to the neoplastic cells themselves.

vibrant desmoplastic proliferation with sinus histiocytosis. The only effective antitumor reaction is by NK-cells that can destroy the tumor cells by direct contact. The desmoplastic reaction, although a type of host defense, does not prevent survival of metastatic cells nor inhibit further growth but does insulate the tumor cells from potentially effective NK-cells. A particular type of metastasis-associated "fibrotic focus" is believed to result from intratumoral hypoxia and is an independent predictor of early distant recurrence, with histologic grade the only other parameter of equal implication. The current interest in microvessel density as a measure of tumor-produced VEGF induction has resulted in intensive morphometric examinations coupled with immunohistochemical detection of tumor secreted cytokines. The presence of the specific tumor-related fibrotic foci is highly associated with microvascular density, thus permitting a simple means of assessing VEGF induction. A further type of stromal response in nodes unassociated with metastatic tumor is termed *inflammatory pseudotumor of lymph nodes resembling focal fibroma* and is like the lesion of the same name in the spleen but with less inflammatory cell accompaniment. A similar condition occurs in animals but has not been given the dignity of a specific name.

REFERENCES

Arber, D.A., and Weiss, L.M. (2001) The presence of a fibrotic focus is an independent predictor of early metastasis in lymph node-negative breast cancer patients. *Am J Surg Pathol* 25:1557–1558.

Perrone, T., De Wolf-Peeters, C., and Frizzera, G. (1988) Inflammatory pseudotumor of lymph nodes. A distinctive pattern of nodal reaction. *Amer J Surg Pathol* 12:351–361.

Reis-Filho, J.S., Soares, R., and Schmitt, F.C. (2002) Angiogenesis in lymph node metastases. *Histopathol* 40:103–113.

Sentinel Node Detection of Metastatic Cancer

The sentinel node strategy is to define the field of lymph node drainage for a specific tumor bed, i.e., mammary, orofacial, colonic, gastric etc., by injection of a blue dye into the peritumoral area and then labeling nodes for excision that have received dye. Increased precision can be added by the concurrent injection of a radiolabeled colloid, usually technium^{99m}, which then facilitates the detection of labeled nodes that may be small and buried in fat by interoperative gamma scintillation scanning. Having mapped the area of lymph node drainage and removed key drainage areas the next issue is how extensive an examination is required of each node selected. There is a learning curve on the application of these techniques with a suggestion that at least 20 cases must have been attended to reduce the false negative rate to a minimal level. It appears that the sentinel node strategy when well applied has a high level of accuracy in detecting regional metastases but the nodes that are selected for examination require serial sectioning to ensure an accurate assessment. A novel method suggested to increase the efficiency of sentinel node identification utilizes a radiolabeled colloid that is taken up by the tumor cells themselves. The scanning is carried out following injection of

the colloid and after 90 and 180 minutes, at which time label is retained only in nodes that contain metastatic tumor; only these nodes are removed for histological examination.

REFERENCES

Blaheta, H-J., Paul, T., Sotlar, K., Maczey, E., Schittek, B., Paul, A., Moehrle, M., Breuninger, H., Bueltmann, B., Rassner, G., and Garbe, C. (2001) Detection of melanoma cells in sentine lymph nodes, bone marrow and peripheral blood by a reverse transcription-polymerase chain reaction assay in patients with primary cutaneous melanoma: Association with Breslow's tumour thickness. *Brit J Dermatol* 145: 195–202.

Cserni, G., Amendoeira, I., Apostolikas, N., Bellocq, J.P., Bianchi, S., Bussolati, G., Boecker, W., Borisch, B., Connolly, C.E., Decker, T, Dervan, P., Drijkoningen, M., Ellis, I.O., Elston, C.W., Eusebi, V., Faverly, D., Heikkila, P., Holland, R., Kerner, H., Kulka, J., Jacquemier, J., Lacerda, M., Martinez-Penuela, J., De Miguel, C., Peterse, J.L., Rank, F., Regitnig, P., Reiner, A., Sapino, A., Sigal-Zafrani, B., Tanous, A.M., Thorstenson, S., Zozaya, E., and Wells, C.A. (2003) Pathological work-up of sentinel lymph nodes in breast cancer. Review of current data to be considered for the formulation of guidelines. *European J Cancer* 39:1654–1667.

Ichikura, T., Ogawa, T., Chochi, K., Kawabata, T., Sugasawa, H., and Mochizuki, H. (2003) Minimum number of lymph nodes that should be examined for the International Union Against Cancer/American Joint Committee on Cancer TNM Classification of Gastric Carcinoma. *World J Surg* 27: 330–333.

Maffioii, L.S., Seregni, E., Chiesa, C., Nerini-Molteni, S., Gerali, A., Bombardieri, E., Greco, M., and Agresti, R. (2000) Detection of lymph node metastases by lymphoscintigraphy with a tumour-seeking tracer in breast patients. *Eur J Nucl Med* 27:744–749.

Tafra, L. (2001) The learning curve and sentinel node biopsy. *Amer J Surg* 182:347–350.

Torrenga, H., Rahusen, F.D., Meijer, S., Borgstein, P.J., and van Diest, P.J. (2001) Sentinel node investigation in breast cancer: Detailed analysis of the yield from strep sectioning and immunohistochemistry. *J Clin Pathol* 54:550–552.

Van der Ent, F.W.C., Kengen, R.A.M., van der Pol, A.G., Povel, J.A.C.M., Stroeken, H.J.G., and Hoofwijk, A.G.M. (2001) Halsted revisted: Internal mammary sentinel lymph node biopsy in breast cancer. *Ann Surg* 234:79–84.

Wawroschek, F., Wagner, T., Hamm, M., Weckermann, D., Vogt, H., Markl, B., Gordijn, R., and Harzmann, R. (2002) The influence of serial sections, immunohistochemistry, and extension of pelvic lymph node dissection on the lymph node status in clinically localized prostate cancer. *European Urol* 43:132–137.

Wiese, D.A., Saha, S., Badin, J., Ng, P.S.-T., Gauthier, J., Ahsan, A., and Yu, L. (2000) Pathologic evaluation of sentinel lymph nodes in colorectal carcinoma. *Arch Pathol Lab Med* 124:1759–1763.

Histopathology of Lymph Node Metastases

The examination of an excised node requires the determination of whether a neoplasm is present, whether it is primary or metastatic, and—if of metastatic type—what is the tissue and area of origin. Not infrequently a node may have been sampled by a number of means (fine needle aspiration, Tru-cut biopsy, or incisional or excisional biopsy) because it is enlarged and is found to contain metastatic tumor with no primary having been suspected. Occult tumor is most likely to be carcinoma or melanoma and in animal pathology most likely to be from skin or from a node draining the head and neck area. Adenocarcinomas of the sinonasal area, squamous carcinomas of the oropharynx, and thyroid cancer may present in this manner. Histiocytic sarcomas are frequently found in lymph nodes and usually are distinguishable from fibrous histiocytoma or plasmacytoma (Fig. 2.84). Ergthrophogocytic histiocytic sarcoma (EHS) and primitive myeloid neoplasms will colonize the medullary sinuses and mimic benign reaction, but in EHS the usual level of anaplasia and erythrophagocytosis are good markers. Because reliable indicators of acute myeloid leukemia, such as the esterase stains and Sudan Black-B, prefer or require fresh tissue, we still have difficulty identifying these types of tumors in paraffin-processed tissues. Since in paraffin-embedded tissues, lysozyme and myeloid/

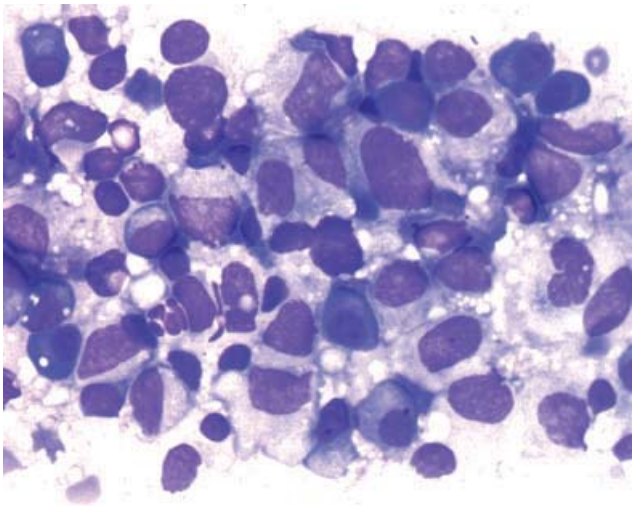

Figure 2.84. Dog: lymph node, fine needle aspiration, histiocytic sarcoma. The aspirate is dominated by large cells with a deeply stained, relatively uniform, chromatin pattern. The cells have small or inapparent nucleoli. The cytoplasm is abundant and lightly basophilic. Note that a number of the large cells have indented or kidney-shaped nuclei (upper left, upper and central right) similar to the counterpart cell seen in histology. The characteristic linear creases seen in Langerhans cell nuclei histologically are less apparent in cytologic preparations. The background contains well-matured plasma cells and a few small lymphocytes. *(Slide From R. M. Jacobs, DVM.)*

histiocyte reagents work weakly if at all, a new antibody reagent for myeloperoxidase active in histopathology is most welcome and needed. In general, lymphomas will distend the capsule of the node but occupy the node in a solid or regional manner. Carcinomas tend to occupy the peripheral sinus and may destroy it while leaving the capsule intact, and they tend to aggregate into nests or clusters often surrounded by reticulin fibers most readily demonstrated with a silver stain.

The era of immunohistochemistry has greatly improved our ability to identify metastatic tumor of epithelial type in lymph nodes with staining for cytokeratin. Melan A for melanoma, chromogranin and synaptophysin for neuroendocrine tumors, desmin and actins for stromal and smooth and striated muscle tumors, CD 31 for endothelium, and a growing list of CDs for the lymphoid tumors themselves are a small list of those most often used reagents. An additional list of antibodies help define specific infections formerly only identified on pattern recognition. For those areas, particularly of myeloid tumors, interoperative cytological imprints can provide cells for reactions that can be carried out on cytological preparations but not on formalin-fixed and paraffin-embedded tissue. Another major advantage of interoperative cytology is simply to ensure that the tissues selected for routine histological examination actually have cells present relating to the lesion being biopsied. Some cautions have been identified in the cross reactivity known to be present in immunohistochemical reactions. Plasma cells are not reactive with cytokeratins but may be with epithelial membrane antigen (EMA) and may be mistaken for scattered metastatic epithelial cells. In cases with chronic ascites or pleural effusion, there is hyperplasia of the mesothelial cells lining the serous cavities. These large reactive-appearing mesothelial cells are commonly seen in cytologic preparations and histological buttons of cavity fluid. Less well recognized is that these mesothelial cells can gain entry into lymphatics draining the cavities and appear in the sinuses of the draining nodes where, in human cases, they stained positively with the AE1–AE3 anticytokeratin cocktail as well as with smooth muscle actin, vimentin, desmin, and tissue polypeptide antigen. These cells were felt to be the deeper basal cells of the mesothelial surfaces while the more superficial cells in the cavity lining marked only with the high molecular weight anticytokeratin. With cavity cells to compare to and a history of fluid accumulation, these cells in nodes were recognized to be benign and reactive, but in an isolated node from such a case, a diagnosis of metastatic carcinoma might be considered.

Finally, all is not resolved on the significance of micrometastatic disease in sentinel nodes. The references following include two papers with discordant results on the significance of size of primary tumor and the presence of axillary node metastasis in human breast cancer as a predictor of locoregional recurrence. In one report, additional recuts of axillary nodes from breast cancer patients were stained with cytokeratin and in 13% of 477 cases, originally felt to be node negative, metastatic disease was found, but there was no difference in survival in the node positive and node negative groups (Figs. 2.85–2.87). Survival was found to be related to histological grade and

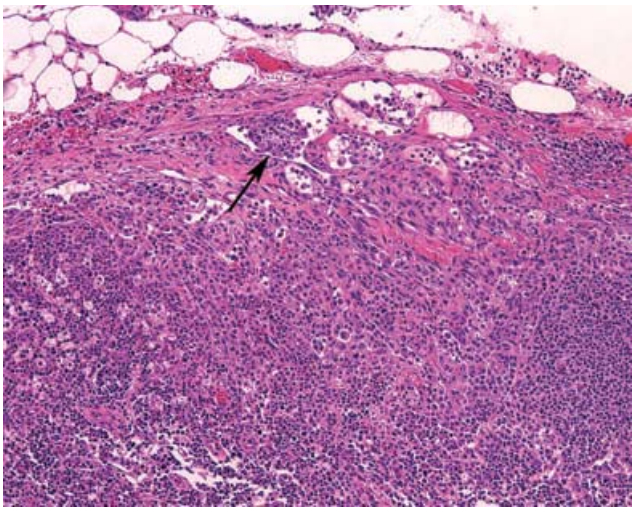

Figure 2.85. Dog: lymph node, pulmonary adenocarcinoma. Mediastinal node with a thickened capsule, compressed peripheral sinus with follicular atrophy, and small areas of residual paracortex characterized by focal clear areas occupied by tingible body macrophages. There is a small cluster of cells within an afferent lymphatic (arrow), in the node capsule.

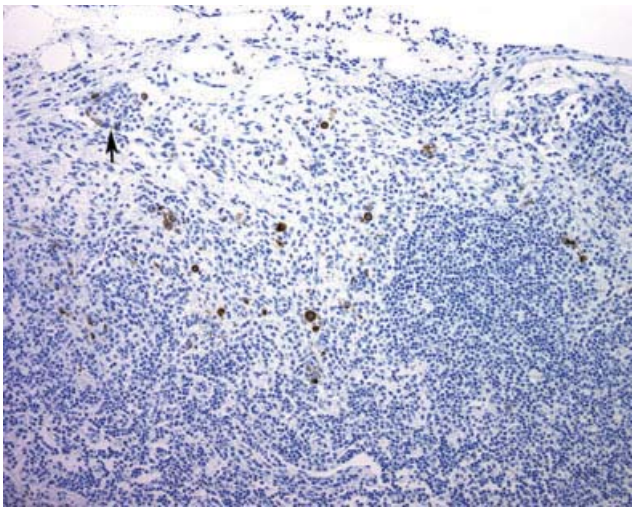

Figure 2.86. Detail of Figure 2.85, immunohistochemistry for cytokeratin. The arrow denotes the lymphatic metastasis evident in Figure 2.85. This preparation demonstrates the value of immunohistochemical staining when the level of cell invasion is beneath easy detection with oversite stains.

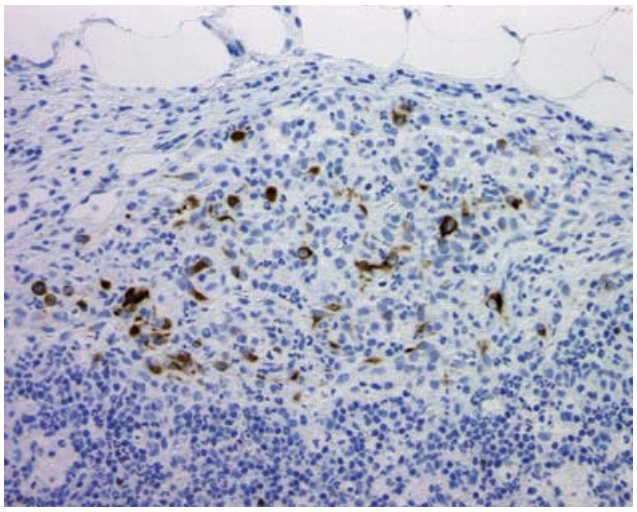

Figure 2.87. Detail of Figure 2.86, medullary area of the node stained for cytokeratin. The neoplastic cells are contained within an area of granuloma formation consisting of loosely arranged connective tissue with lymphocytes, neutrophils, and macrophages.

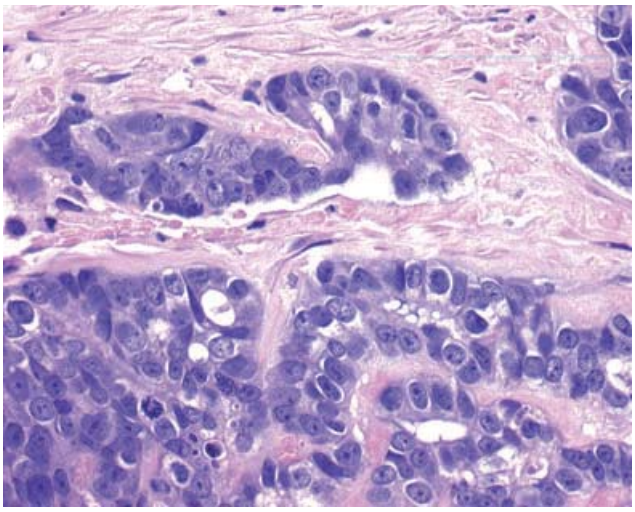

Figure 2.89. Detail of Figure 2.88. The top half of the image consists of the node capsule with metastatic tumor in a lymphatic indicated by the arrow in Figure 2.88. Note the almost complete lack of cellular reaction to the infiltrating adenocarcinoma.

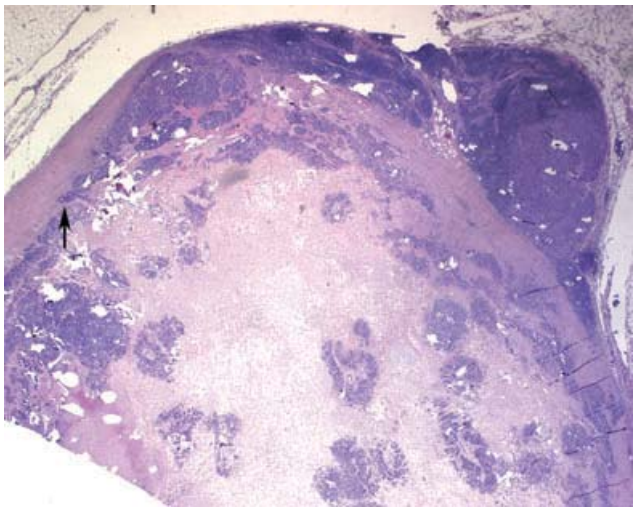

Figure 2.88. Cat: axillary lymph node, mammary adenocarcinoma. The node is heavily invaded by metastatic carcinoma with ischemic infarction of almost the entire center of the gland. Viable tumor survives in collar lesions around residual vessels. The peripheral capsule is irregularly and markedly thickened as in the upper left and thinned and penetrated by tumor as in the lower right. The arrow indicates a capsular vessel containing metastatic tumor.

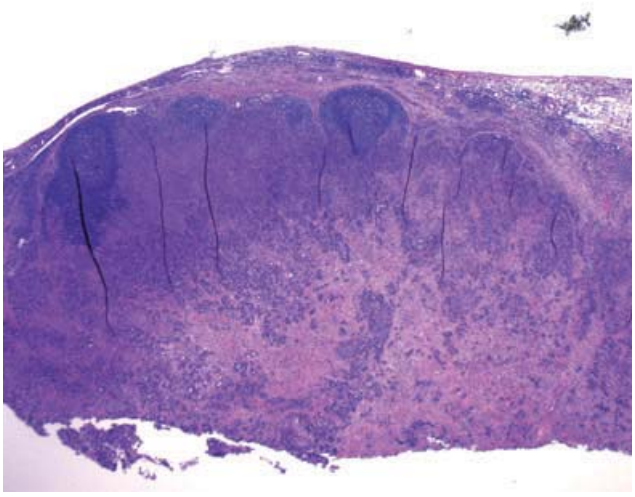

Figure 2.90. Cat: mesenteric lymph node, intestinal adenocarcinoma. An incisional biopsy of an enlarged mesenteric node from a cat with a mass obstructing the ileocecal junction. The node capsule is thickened with irregular lymphoid colonization in reaction to infiltrating tumor. There is fading follicular hyperplasia with very extensive involvement of the node cortex and medulla by infiltrating tumor. The pale areas in the medullary region consist of solid collagenous connective tissue proliferation in a desmoplastic reaction against infiltrating carcinoma.

tumor size. The second report found no value in postmastectomy radiation in node negative invasive breast cancer and concluded that axillary node status and not tumor size was the best predictor of tumor recurrence. It is well recognized that some tumors in humans and animals can reach large size but remain localized in the primary site. In contrast, very small tumors may metastasize, and in the final analysis, finding and correctly interpreting those metastases needs to be the objective of the examination of nodes for metastatic disease. In late disease, no special stains are required to demonstrate metastatic colonization (Figs. 2.88, 2.89), and in other cases a cytokeratin stain may demonstrate many more sites of nodal infiltration than was suspected on oversight staining (Figs. 2.90–94). Not all nodal colonization by

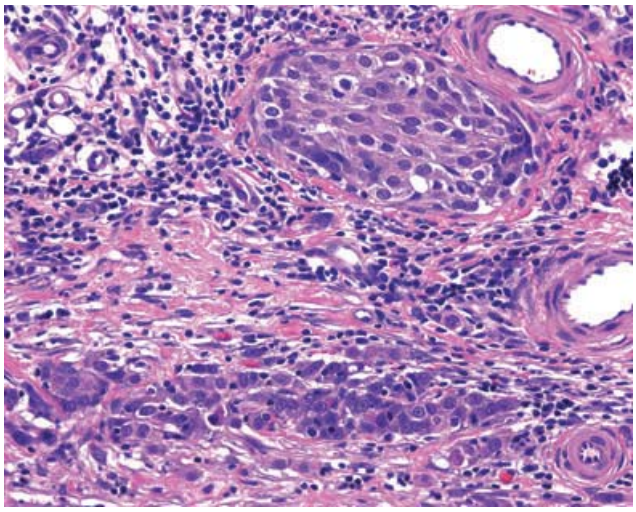

Figure 2.91. Detail of Figure 2.90, node capsule with vessels, likely lymphatics, irregularly invaded and distended by infiltrating carcinoma. There is mild lymphocytic infiltration into areas of neoplastic cells but the reaction appears to be primarily one of connective tissue proliferation.

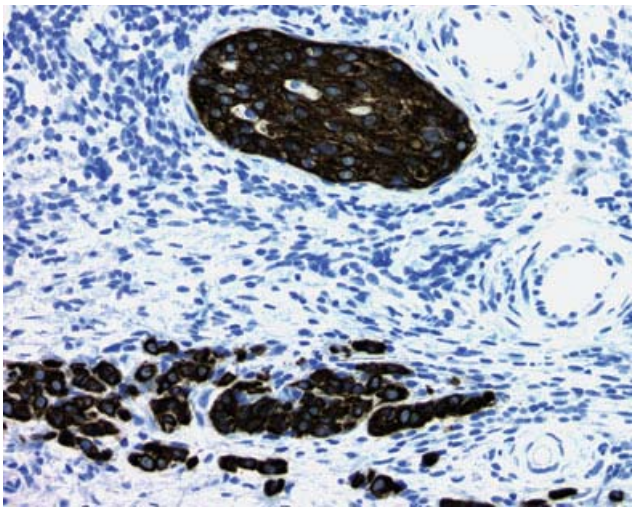

Figure 2.93. Detail of Figure 2.90 with immunohistochemical stain for cytokeratin to demonstrate metastatic carcinoma in peripheral node vessels.

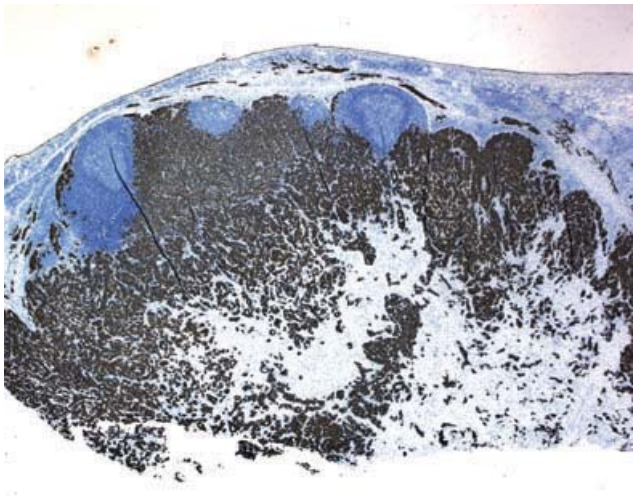

Figure 2.92. Detail of Figure 2.90 with immunohistochemical stain for cytokeratin. The extent of neoplastic infiltration into the node can best be determined with specific staining for the neoplastic cells. Note frequent areas of tumor colonization of vessels in the capsule that may represent ongoing lymphatic drainage from the primary tumor. The medullary area that largely consists of mature collagen remains unmarked.

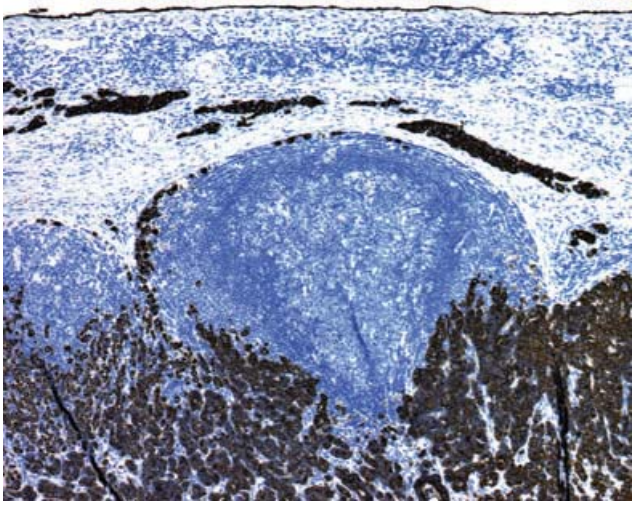

Figure 2.94. Detail of Figure 2.90 with immunohistochemical reaction against cytokeratin. Note the pattern of involvement of tumor cells extending in serpigenous columns from deeper areas of the node to encircle the germinal centers. The mesothelial lining of the node capsule is strongly marked with this immunohistochemical preparation.

epithelial type cells are an indication of metastatic neoplasia. In some circumstances of chronic pleural effusion, there may be mesothelial cells in clusters within the peripheral node sinus and even in deeper areas involving the medullary sinuses (Figs. 2.95–2.97). The extent of this type of benign infiltration may not be suspected or perceived on routine staining but is made evident on specific immunohistochemical staining (Fig. 2.98).

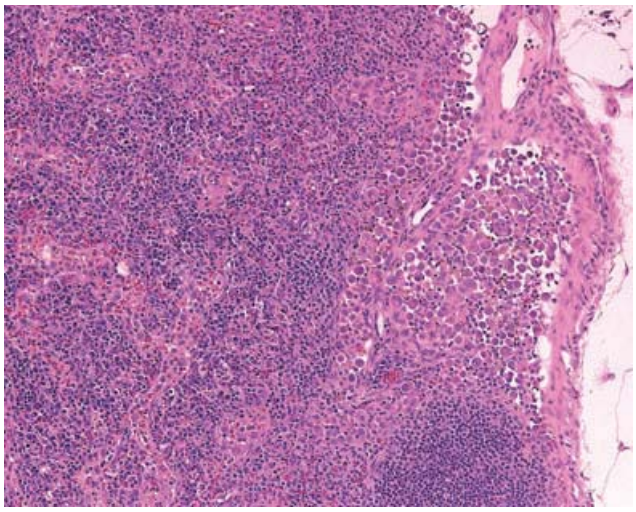

Figure 2.95. Five-year-old Labrador male: sternal node, chest injury resulting in hemorrhagic pleural effusion. A focal area of subcapsular sinus contains exfoliated mesothelial cells. *Slide from Moira Kerr, DVM.*

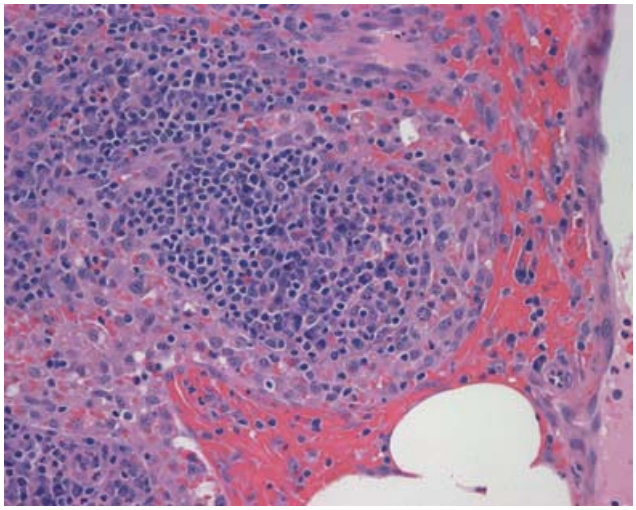

Figure 2.96. Detail of Figure 2.95, node, medulla. A medullary cord (center) is expanded by a laminar layer of macrophages, many of which contain ingested red cells. The surrounding medullary sinus is dilated primarily with red cells and contains free lipid globules (lower right) with the wall of a large medullary vein at right.

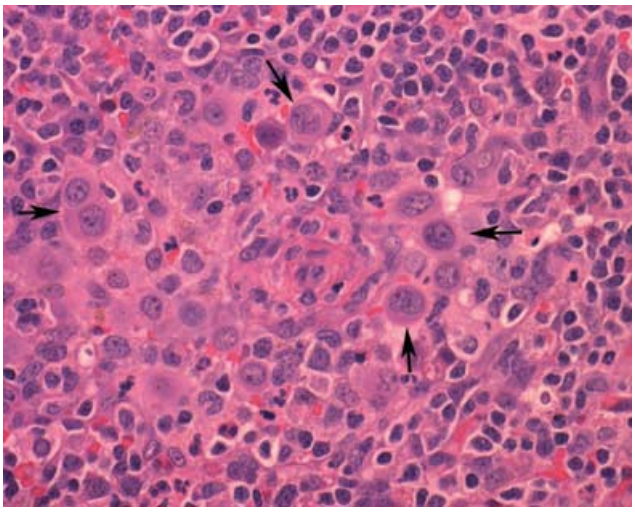

Figure 2.97. Detail of Figure 2.95, node, outer cortex. A poorly delineated cortical sinus surrounding a small arteriole center is distended with mesothelial cells (arrows) that are occasionally binucleated with abundant cytoplasm and have the characteristic cytoplasmic fringe with thin projections. These mesothelial cells are intermixed with macrophages that have smaller nuclei, often indented and with more granular-appearing cytoplasm.

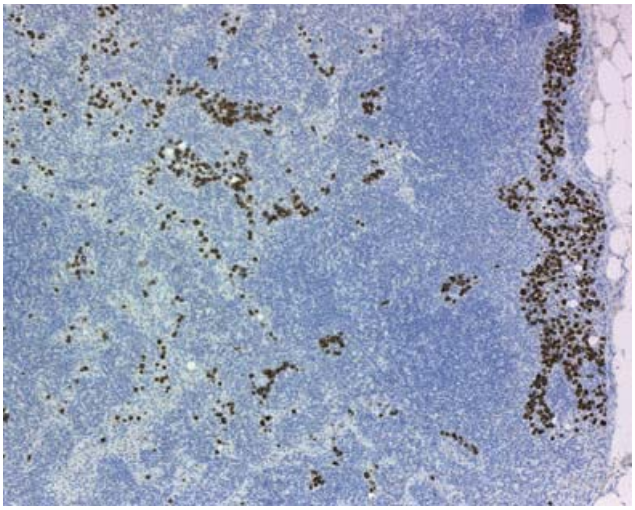

Figure 2.98. Detail of Figure 2.95 stained with cytokeratin. There is a laminar accumulation of positively staining mesothelial cells in the subcapsular sinus, irregularly within the node cortex, and more frequently in the medullary sinuses. The cluster of positive cells to the right of center in the outer cortex are typical of those depicted in Figure 2.97.

REFERENCES

Beenken, S.W., Urist, M.M., Zhang, Y., Desmond, R., Krontrias, H., Medina, H., and Bland, K.I. (2003) Axillary lymph node status, but not tumor size, predicts locoregional recurrence and overall survival after mastectomy for breast cancer. *Ann Surg* 237:732–739.

Chiu, A., Hoda, S.A., Yao, D.X., and Rosen, P.P. (2001) A potential source of false-positive sentinel nodes. Immunostain misadventure. *Arch Pathol Lab Med* 125:1497–1499.

Ioachim, H.L., and Ratech, H. (2002) Part X: Metastatic tumors in lymph nodes. In *Ioachim's Lymph Node Pathology,* 3rd ed. Lippincott Williams & Wilkins, Philadelphia, pp. 539–547.

Langenbach, A., McMnus, P.M., Hendrick, M.J., Shofer, F.S., and Sorenmo, K.U. (2001) Sensitivity and specificity of methods of assessing the regional lymph nodes for evidence of metastasis in dogs and cats with solid tumors. *J Amer Vet Med Assoc* 218:1424–1428.

MacKenzie, D.N., McCormick, C.S.F., and Morris, R.J. (2003) Lymph node metastasis from a primary skin carcinoid tumour. *Brit Assoc Plastic Surgeons* 56:718–721.

Millis, R.R., Springall, R., Lee, A.H.S., Ryder, K., Rytina, E.R.C., and Fentiman, I.S. (2002) Occult axillary lymph node metastases are of no prognostic significance in breast cancer. *Brit J Cancer* 86:396–401.

Nascimbeni, R., Burgart, L.J., Nivatvongs, S., and Larson, D.R. (2002) Risk of lymph node metastasis in T1 carcinoma of the colon and rectum. *Dis Colon Rectum* 45.

Sauer, T., Engh, V., Holck, A.M., Sorpebol, G., Heim, M., Furu, I., and Schlichting, E. (2003) Imprint cytology of sentinel lymph nodes in breast cancer. *Acta Cytologica* 47:768–773.

Vilela, D.S., and Garcia, F.M.I. (1998) Embolization of mesothelial cells in lymphatics: The route to mesothelial inclusions in lymph nodes? *Histopathol* 33:570–575.

SPLEEN

Normal Form and Function

Embryology

The spleen is a hematopoietic organ that filters the blood through a system of sinusoids in contrast to the lymph nodes that filter lymph through a sinusoidal system. Thus the spleen, which lacks an afferent or incoming lymphatic system, deals with antigen or foreign material being carried in the blood stream. The immune functions of the spleen are accomplished by small sprigs of vessels that permeate the dendritic cell beds of the germinal centers, allowing these cells to react to blood-borne antigen. The mechanical filtering function of the spleen is carried out after the blood leaves the arteriolar lymphoid sheaths and germinal centers and enters the meshlike sinusoidal system where macrophages line the narrow vascular spaces. In contrast, the filtered media processed by the nodes is the lymph itself, which is low in cellularity compared to the blood but contains foreign material and antigen-laden cells that arise in the second or lymphatic vascular system of the tissue being drained. Lymph nodes have a nutritive blood vascular system that enters the hilar area of the node and parallels the efferent or exiting lymph that has passed through the germinal centers of the cortex and macrophages of the medullary sinuses.

In phylogenetic terms, the spleen appears in primitive vertebrates as a spiral fold in the midgut, with lymphoid sheaths encircling arterioles in cartilaginous fishes, and becomes a retroperitoneal structure in bony fishes. Sharks have a spleen much like mammals and also a thymus. In mammals, the spleen begins as a thickening of the dorsal mesogastrium containing a loose supporting stroma, which in mouse embryos becomes occupied by primitive mononuclear cells by 2 weeks of gestation and with erythroid and lymphocytic differentiation evident by day 16.

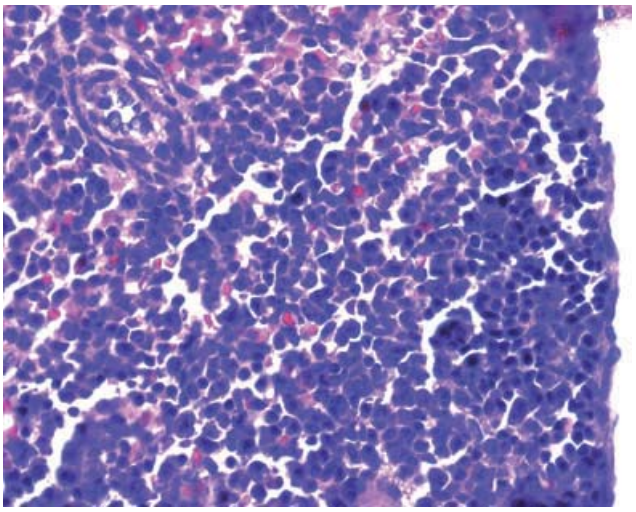

Figure 2.99. Neonatal mouse: spleen. The capsule is delicate and internal muscular elements are inapparent. The arterioles lack a lymphoid cuff, and sinus areas are highly hematopoietic and consist primarily of erythroid cells.

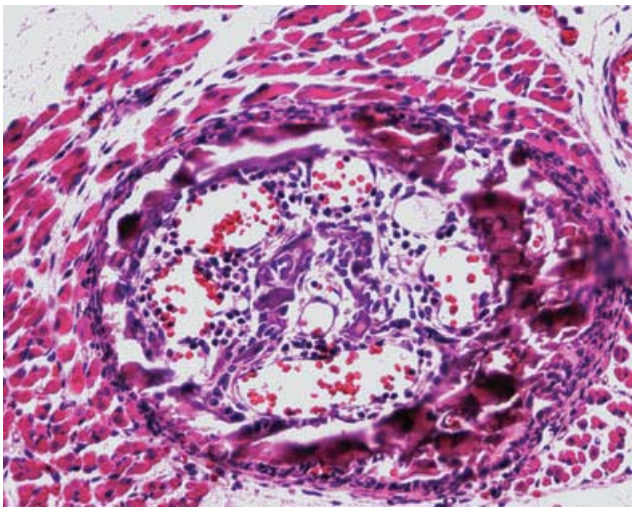

Figure 2.100. Neonatal mouse: marrow. The marrow cavity is still in the process of remodeling from the cartilage model, with very large sinuses and interstitial areas of low cellular density with hematopoietic cells that are largely erythroid.

In rats and mice, there is active hematopoiesis in the spleen in the latter part of gestation. This organ becomes a major source of blood cells as hematopoiesis declines in the liver and before the fetal bones develop a medullary cavity (Figs. 2.99, 2.100). In larger mammals like domestic animals and humans, the fetal spleen does not contribute to myelopoiesis as in rodents. In the latter species, the liver is much more involved in hematopoiesis during fetal development. This is especially apparent in the pig where neonatal animals are frequently seen in pathology examinations due to various diseases causing death in

sucklings. Piglets up to about 1 week of age have scattered foci of erythropoiesis in liver that must be recognized as a normal finding.

In health, there is a constant relationship between splenic mass and body weight, as there is for the liver and kidney. In beagles, the average weights of the spleen of 95 male and female pups at birth was 0.8 g, rising to 3.4 g at 1 month, 10.6 g at 2 months, 46 g at 6 months, and 45 g at 1 year.

REFERENCES

Calhoun, D.A., Li, Y., Braylan, R.C., and Christensen, R.D. (1996) Assessment of the contribution of the spleen to granulocytopoiesis and erythropoiesis of the mid-gestation human fetus. *Early Human Develop* 46:217–227.

Namikawa, R., Mizuno, T., Matsuoka, H., Fukami, H., Ueda, R., Itoh, G., Matsuyama, M., and Takahashi, T. (1986) Ontogenic development of T and B cells and non-lymphoid cells in the white pulp of human spleen. *Immunol* 57:61–69.

Quesada, J., Villena, M.I., and Navarro, V. (1994) Ontogeny of the Sea Bass spleen (*Dicentrarchus labrax*): A light and electron microscopic study. *J Morphol* 221:161–176.

Sasaki, K., and Matsumura, G. (1988) Spleen lymphocytes and haemopoiesis in the mouse embryo. *J Anat* 160:27–37.

Vascular Structure

The vascular system of the spleen has remained an active area of study since the development of the light and electron microscopes and is now extended by descriptions of splenic immunological compartmentalization. The spleen has a complex arterial and venous system but only an efferent lymphatic system. Thus, all antigen enters the spleen via the arterial system and must be captured in an appropriate rheological and cellular environment. The arborization of the arterial system ends in a series of capillaries that have been described as penicillary, where a series of small vessels all terminate in a fanlike projection reminiscent of a fungal fruiting body. These small vessel terminations, referred to as *ellipsoids* and *sheathed capillaries*, terminate with the endothelium encircled by a series of concentric cells now recognized to be largely macrophages. The "open" and "closed" concept of splenic circulation is based on these terminations occurring into germinal centers and splenic sinus interstitium (open mode) or directly into large bore veins with relatively direct return to the systemic circulation (closed mode). There are differences in the circulation through the spleens of mammals with those described as *sinusal* (including the dog) having relatively direct connections between the sheathed capillaries and the larger splenic sinuses. In contrast, the cat spleen has no direct connections between the sheathed capillaries and veins and is termed *nonsinusal* type. These determinations were made by utilizing erosion casts of dilated and contracted spleens injected with polymer prior to fixation to avoid normal vascular contraction from obscuring vascular channels. Despite these differences, the blood return to the systemic circulation in the cat is as rapid as in the dog, apparently because the distance of sojourn in the interstitial areas in the cat are very short. In all mammals, including human, the venule walls are constructed with the endothelial cells elongated in the long axis of the vessel. Endothelial cells are not joined laterally but are held in place by very thin reticulin fibers that periodically encircle the vessels like hoops around barrel staves. This architecture permits red cells to permeate between the membranes of adjacent endothelial cells; phagocytic cells remain able to pinch off intracellular Heinz or Howell-Jolly bodies from erythrocytes. This allows unwanted remnants of RBCs to remain in the interstitial area to be phagocytosed.

In the dog, there are 3–4 major branches of the hilar arterial system that make partial splenectomy possible should there be a need to do so (Figs. 2.101, 2.102). The splenectomized dog is highly susceptible to red cell parasitisms and may re-present with anemia due to *Mycoplasma haemocanis* with a high level of red cells infected.

Hemal nodes are found in ruminants and a like structure is present in rats. Hemal nodes have a fibromuscular capsule with the smooth muscle component more apparent than in lymph nodes. The vascular system of hemal nodes includes both efferent and afferent sides of the blood vascular and lymphatic systems, with the efferent lymph vessels less frequent than in lymph nodes. The hemal node vascular system is like that of the lymph

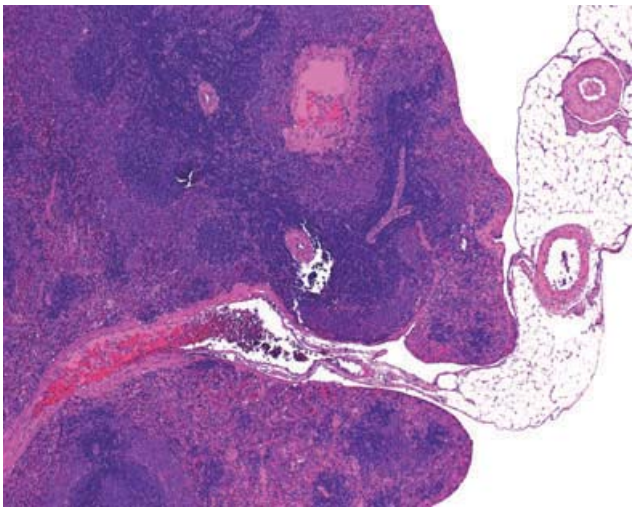

Figure 2.101. Adult rat: spleen. The splenic artery in cross section (top) enters the spleen at the junction of the proximal (head) and middle thirds and bifurcates into 3–4 major branches that extend though the central areas of the spleen to each end.

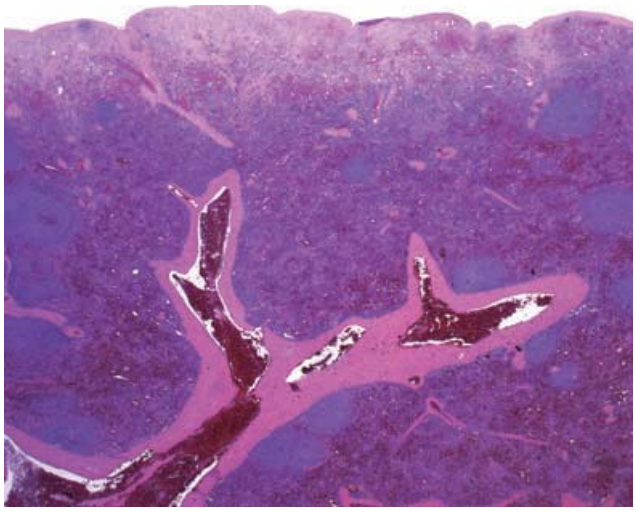

Figure 2.102. Dog: spleen. Branches of the major splenic artery near the area of entry at the splenic hilus.

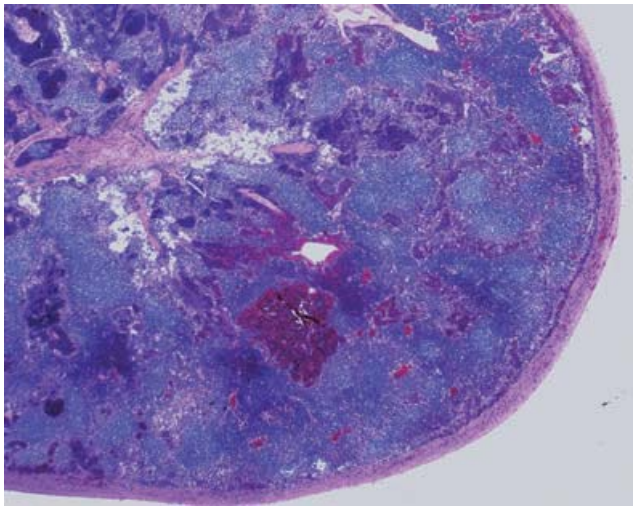

Figure 2.103. Bovine: hemal node. The node is enclosed in a smooth muscle capsule and has parenchymal areas with lymphoid follicles that are bordered by blood-filled sinuses.

nodes with the major vessels entering via the hilus and branching to the periphery. There is a wide and irregular peripheral sinus that is blood filled. The interior of the node contains peripheral germinal centers with minimal paracortical areas that are surrounded by sinuses. Sinuses are either of lymphatic or blood systems and are separated by an attenuated blood filtering system like that of the spleen (Figs. 2.103, 2.104). In conditions of immune hyperplasia, as in bovine trypanosomiasis, the hemal nodes in the abdominal cavity become large and spherical (reaching 1–2 cm in diameter) and are grossly deep red. Hemal nodes in subcutaneous areas remain discoid and mobile beneath the skin.

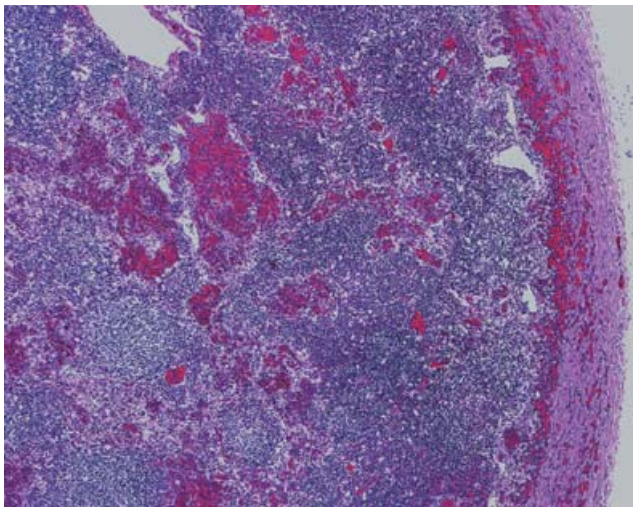

Figure 2.104. Detail of Figure 2.103. There is a very narrow peripheral blood-filled sinus that may be artifactually reduced by capsular contraction in fixation. The follicular structures are poorly defined without apparent mantle cell cuffs. The sinus areas devoid of red cells may be lymphatic rather than blood vascular.

REFERENCES

Chen, L-T., and Weiss, L. (1973) The role of the sinus wall in the passage of erythrocytes through the spleen. *Blood* 41:529–537.

Elfvin, L-G., Johansson, J., Hoijer, A-S., and Aldskogius, H. (1994) The innervation of the splenic capsule in the guinea pig: An immunohistochemical and ultrastructural study. *J Anat* 185:267–278.

Folse, D.S., Beathard, G.A., Marshall, R.B., Fish, J.C., Sarles, H.E., Remmers, A.R., and Ritzmann, S.E. (1971) Characterization of the bovine hemal node. *J Reticuloendothel Soc* 10:461–481.

Kasai, K., Nakayama, A., Ohbayashi, M., Nakagawa, A., Ito, M., Saga, S., and Asai, J. (1995) Immunohistochemical characteristics of chicken spleen ellipsoids using newly established monoclonal antibodies. *Cell Tissue Res* 281:135–141.

Liu, D.L., Xia, S., Xu, W., Ye, Q., Gao, Y., and Qian, J. (1996) Anatomy of vasculature of 850 spleen specimens and its application in partial splenectomy. *Surgery* 119:27–33.

McClusky, D.A., Skandalakis, L.J., Colborn, G.L., and Skandalakis, J.E. (1999) Tribute to a triad: History of splenic anatomy, physiology, and surgery. Part I. *World J Surg* 23:311–325.

McClusky, D.A., Skandalakis, L.J., Colborn, G.L., and Skandalakis, J.E. (1999) Tribute to a triad: History of splenic anatomy, physiology, and surgery. Part II. *World J Surg* 23:514–526.

Nopajaroonsri, C., Luk, S.C., and Simon, G.T. (1974) The structure of the hemolymph node—A light, transmission and scanning electron microscopic study. *J Ultrastructure Res* 48:325–341.

Sasou, S., and Sugai, T. (1992) Periarterial lymphoid sheath in the rat spleen: A light, transmission and scanning electron microscopic study. *Anat Rec* 232:15–24.

Schmidt, E.E., MacDonald, I.C., and Groom, A.C. (1983) Circulatory pathways in the sinusal spleen of the dog, studied by scanning electron microscopy of microcorrosion casts. *J Morphol* 178:111–123.

Schmidt, E.E., MacDonald, I.C., and Groom, A.C. (1983) The intermediate circulation in the nonsinusal spleen of the cat, studied by scanning electron microscopy of microcorrosion casts. *J Morphol* 178:125–138.

Tanaka, Y., and Hirahara, Y. (1995) Spleen of the snake (*Elaphe climacophora*) and intrasplenic vascular architecture. *J Morphol* 226:223–2325.

Yang, T.J., and Gawlak, S.L. (1989) Lymphoid organ weights and organ:body weight ratios of growing beagles. *Lab Anim* 23:143–146.

Zidan, M., Kassem, A., Dougbag, A., El Ghazzawi, E., El Aziz, M.A., and Pabst, R. (2000) The spleen of the one humped camel (*Camelus dromedarius*) has a unique histologic structure. *J Anat* 196:425–432.

Lymphoid Structure

The lymphoid structure of the spleen is similar in most mammals, but the rat and mouse have a definite structural containment of the germinal center that is not present in many domestic species or in humans (Figs. 2.105, 2.106). Cats have a peripheral sinus that separates the mantle and marginal zone lymphoid compartments, is not present in dogs, and is not apparent histologically. In the rat and mouse the germinal center and, to a lesser extent, the periarteriolar lymphoid sheath have a stromal encapsulation, but the marginal zone cells lie directly on these capsules and the peripheral sinus lies outside the marginal zone cells regardless of the depth of this cuff. In the calf, cat, dog, and rodents, the peripheral sinus forms a band surrounding the germinal center outside the mantle cells and current level of marginal zone cells and appears as a layer with more red cells and fewer nucleated cells than the adjacent splenic sinus area. It appears that this peripheral sinus may have a counterpart in other species but may be less well defined both anatomically and histologically.

The major difference between human and animal spleens is that, in humans, the thymic-dependent T-cell cuff around the central arterioles is discontinuous and does not enter regions of germinal centers. In the rat and mouse, the marginal zone cells may surround the periarteriolar lymphoid sheaths, but it does not in domestic animals or in human spleens. In animals there is some degree of T-cell cuffing around all small arterioles in contrast to the human spleen. Small radicles that branch from the larger arterioles at right angles form the source of antigen for the lymphocytes and dendritic cells of the germinal centers. In most sections, the arteriole is seen eccentric to the germinal center with the initiating small arterial branch seldom in the plane of section (Fig. 2.107). The arteriole is surrounded by the "periarteriolar lymphoid sheath" (PALS).

An apparent continuation of this sheath extends around the periphery of the germinal center (Fig. 2.108). The germinal center is surrounded by a narrow cuff of mantle cells that are morphologically small lymphocytes

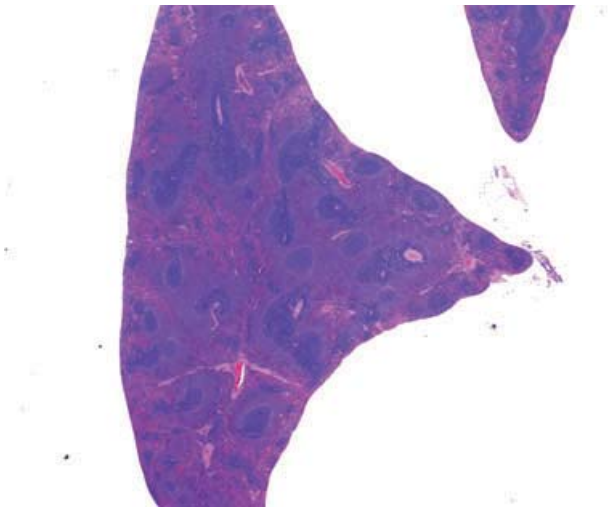

Figure 2.105. Adult rat: spleen. Periarteriolar sheath areas are darkly stained, with a very narrow lightly stained border containing the sheath capsule that separates the intracapsular lymphoid tissue from the lighter-stained marginal zone area encircling these structures.

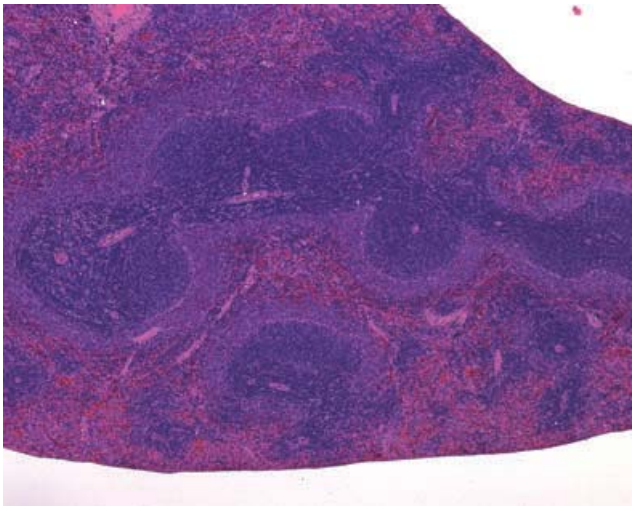

Figure 2.106. Detail of Figure 2.105. The largely thymic-dependent periarteriolar lymphoid sheath areas are surrounded by a discontinuous encapsulation that separates the sheath and mantle cells from the lighter-staining outer layer of marginal zone cells.

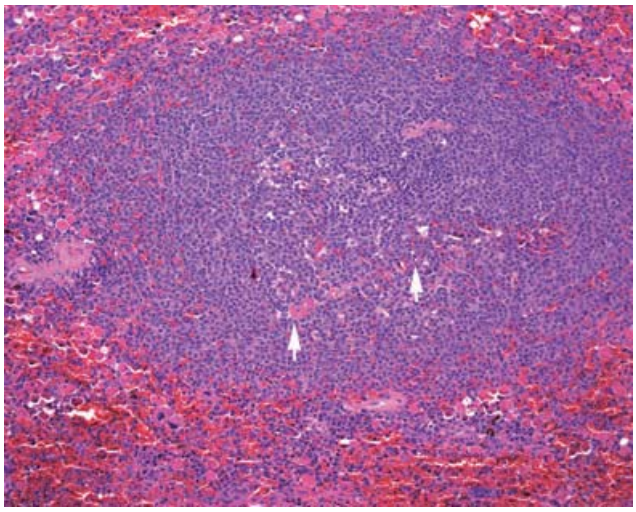

Figure 2.107. Dog: spleen. There is atrophy of arteriolar lymphoid sheath cells surrounding the arteriole (arrows), delineating segments of the small branch vessel supplying the follicle center.

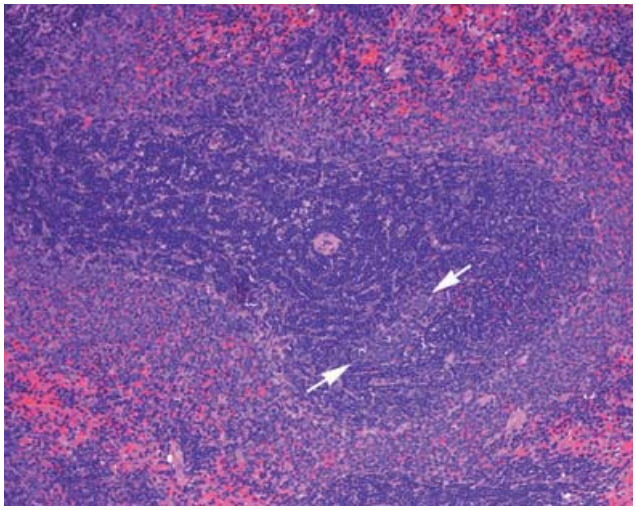

Figure 2.108. Rat: spleen. Germinal centers in the rat are poorly defined, with the oval follicle center consisting of much larger cells (indicated by arrows).

with round or minimally indented nuclei with minimal cytoplasm and immunologically are naive B-cells (Figs. 2.109, 2.110). The marginal zone cells are comprised of postgerminal center memory B-cells that lie outside the mantle cell cuff. Marginal zones are of variable thickness depending on the activity of the spleen (Figs. 2.111–2.113). In humans, but not in most domestic animals except the cat, the division between the mantle cell and marginal zone layers is a potential space (the perifollicular zone) that is rich in sheathed capillaries and corresponds to the region in rats rich in metallophilic macrophages (Fig. 2.114).

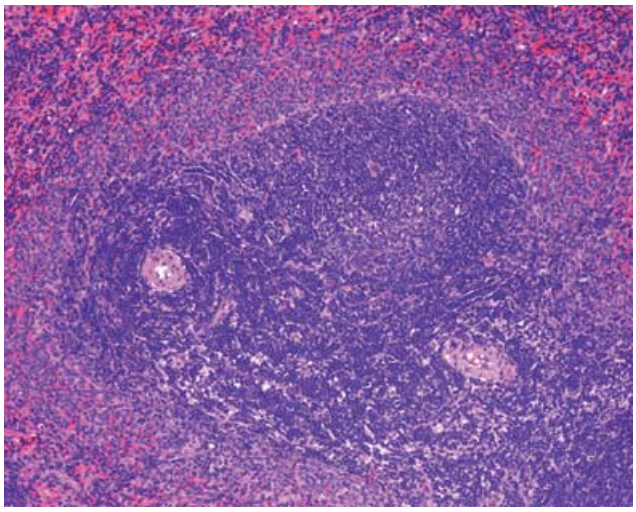

Figure 2.109. Rat: spleen. The arterioles are surrounded by the small densely stained lymphocytes of the thymic-dependent periarteriolar lymphoid sheath (PALS). The germinal center is eccentric to the arterioles, consisting of larger, lighter-stained cells that are surrounded by small cells of the B-dependent mantle cell cuff. These B-cells are morphologically similar to those of the thymus-dependent PALS. The marginal zone is of lighter-staining cells that surround the entire structure outside of the encapsulating sheath.

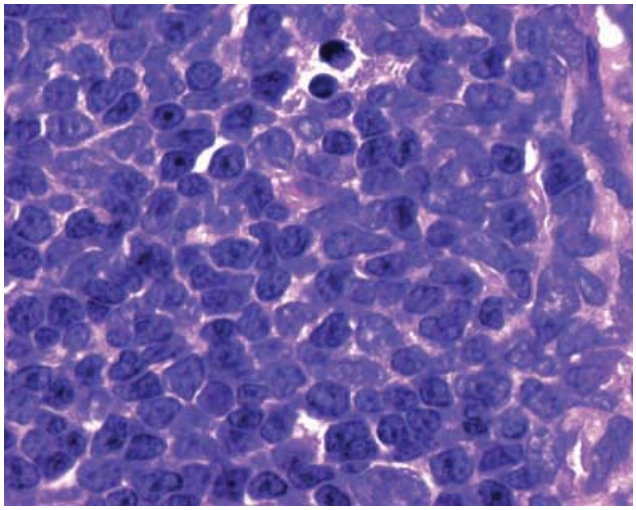

Figure 2.110. Detail of Figure 2.109. Lymphocytes of the mantle cell cuff lying beneath the sheath capsule right. The mantle cells have small round to irregular-shaped nuclei only slightly larger than red cells. They are densely stained with little internal nuclear detail and are closely packed with very narrow cytoplasmic boundaries.

There are many T-cells within the largely B-cell mantle cell cuff of humans and domestic animals. These T-cells are small and morphologically not distinguishable from B-cells of the mantle cell area. In follicular involution, these T-cells persist and identify former areas of germinal

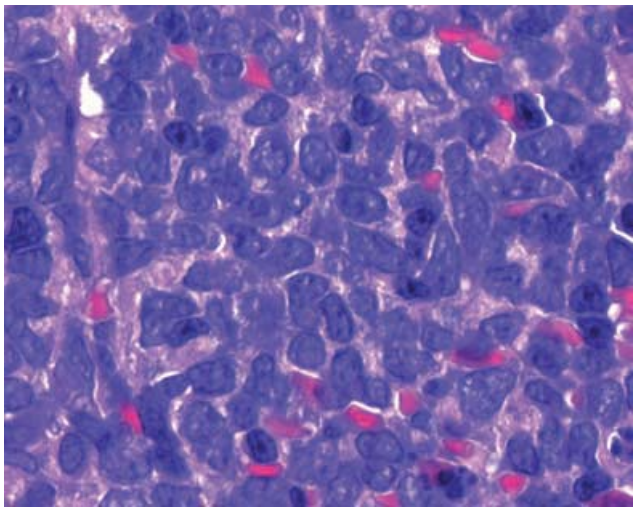

Figure 2.111. Detail of Figure 2.109. Lymphocytes of the marginal zone area lie outside of the sheath encapsulation (left) and have irregularly shaped nuclei 2 to 3 red cells in length, with greater internal nuclear detail and greater cytoplasmic volume. These cells appear less densely packed than those of the mantle cells.

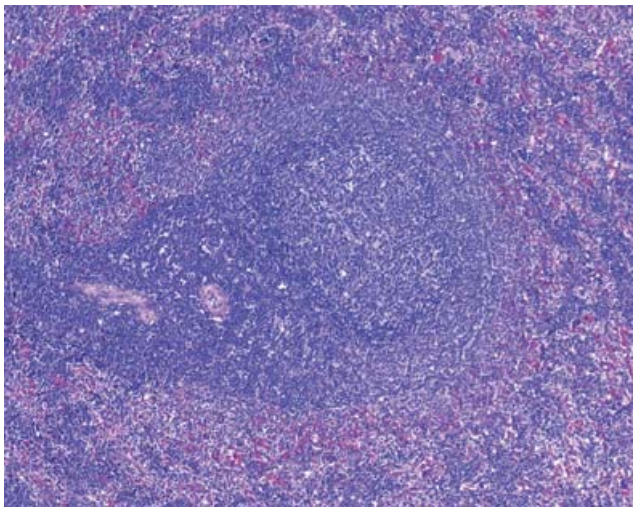

Figure 2.112. Dog: spleen, arteriole (center left) surrounded by the periarteriolar lymphoid sheath with germinal center eccentric to the artery and surrounded by a prominent outer marginal zone layer. In contrast to rodents, germinal centers in most domestic animals are more well defined, with the small dark cells of the mantle cell cuff forming a continuous band around the germinal center and separating it from the lighter-stained marginal zone cells that interface with the marginal sinus.

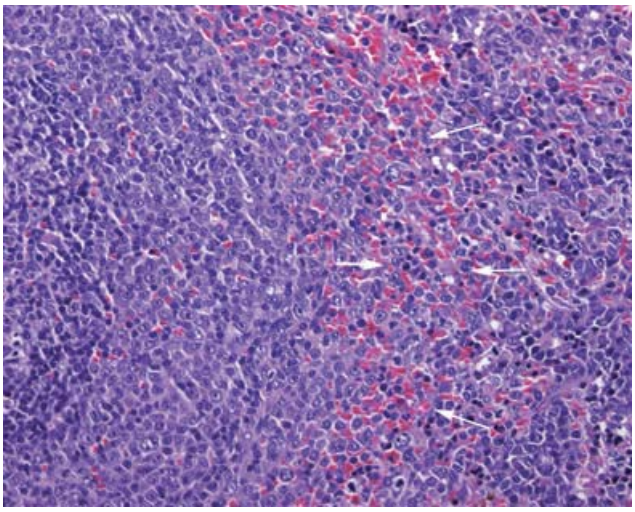

Figure 2.113. Detail of Figure 2.112. The cells of the germinal center (left) are surrounded by a narrow cuff of small darkly stained mantle cells, with a wider layer of lighter-stained marginal zone cells that are separated from the hematopoietic areas of the splenic sinuses (right) by the peripheral sinus (center), which has a high proportion of red cells (arrows).

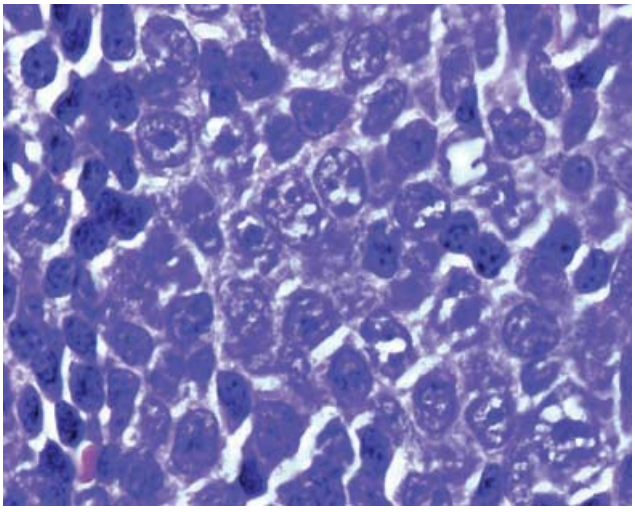

Figure 2.114. Detail of Figure 2.113. Marginal zone cells of the dog are larger than the mantle cells (left) and larger than the marginal zone cells in humans and rodents. Canine marginal zone cells have round to oval nuclei 1.5 red cells in diameter with more dispersed chromatin and prominent nucleoli. Cells in this region become more homogenous with prolonged hyperplasia. Neoplastic marginal zone cells have a more vesicular appearance.

center activity in tissues stained with CD3. In dogs and humans, and less so in cats, the marginal zone cells tend to be closely associated with splenic follicles and don't extend along the periarteriolar lymphoid sheaths. In the dog, marginal zone hyperplasia of the spleen is commonly seen in association with both follicular and PALS atrophy. This process appears as cohesive clusters of large lymphocytes with prominent nucleoli adjacent to small arterioles and often hyalinized germinal centers. In splenic marginal zone lymphoma in the dog, the area of neoplastic proliferation is usually multicentric in a single region.

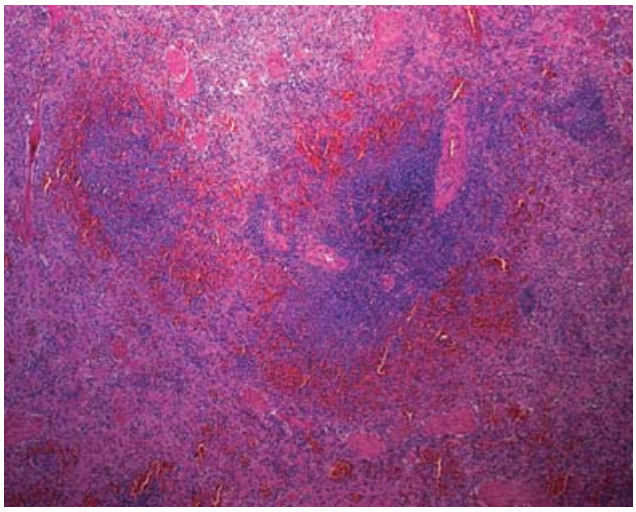

Figure 2.115. Dog: spleen, congestion due to barbiturate anesthesia. Periarteriolar lymphoid sheath areas irregularly delineated by a higher proportion of red cells in the surrounding peripheral sinuses distribute blood coming through arterioles into the surrounding sinus filtering structures.

The region or perifollicular zone between the mantle cell cuff and the marginal zone cells is the area where the sheathed capillaries open for filtering of the arterial blood through the meshwork of the marginal zone cells. These marginal zone cells colonize stroma of very specific phenotype that express smooth muscle actin and myosin and specific adhesion molecules in humans. There are numerous T-cells in this area, which suggests this as a T-cell area in quiescent spleens with little marginal zone cell proliferation. In inflammatory states, the area outside the perifollicular and marginal zone cells may appear reddened at an architectural level of histologic examination because this is the area where the cells exiting the sheathed capillaries into an "open" circulation accumulate as they are filtered back into the splenic red pulp sinuses (Fig. 2.115). In animals like the cat and dog, which mount a strong neutrophilia in response to infectious and inflammatory diseases, this area will contain many mature neutrophils. In contrast, cattle tend to develop neutropenia during acute inflammation, so mature neutrophils may be absent from the perifollicular and marginal zones, but band and metamyelocyte neutrophils may be detected. The splenic lymphatics are largely unrecognized and are located near the small arterioles where they may appear as slitlike structures with a thin lining membrane and an empty lumen.

REFERENCES

Alferink, J., Lieberam, I., Reindl, W., Behrens, A., Weib, S., Huser, N., Gerauer, K., Ross, R., Reske-Kunz, A-B., Ahmad-Nejad, P., Wagner, H., and Forster, I. (2003) Compartmentalized production of CCL17 *in vivo*: Strong inducibility in peripheral dendritic cells contrasts selective absence from the spleen. *J Exp Med* 197:585–599.

Kotani, M., Matsuno, K., Miyakawa, K., Ezaki, T., Hayama, T., and Ekino, S. (1985) Migration of macrophages from the marginal zone to germinal centers in the spleen of mice. *Anat Rec* 212:172–178.

Steiniger, B., Ruttinger, L., and Barth, P.J. (2003) The three-dimensional structure of human splenic white pulp compartments. *J Histochem Cytochem* 51:655–663.

Van Krieken, J.H.J.M., and te Velde, J. (1992) Spleen. In Sternberg, S.S. (ed), *Histology for Pathologists*. Raven Press Ltd., New York, pp. 253–260.

Sinus Structure

The dendritic cell population of the spleen has been extensively studied in the mouse and rat where it is found that all splenic dendritic cells are of relatively direct lymphoid or myeloid origin. This is in contrast to the other lymphoid tissues where some dendritic cells are derived first from myeloid cells that then form a secondary progeny of Langerhans cells. The phagocytic cells of the spleen are found primarily in the sinus or red pulp areas but are also prominent in the perifollicular areas. Following intravenous injection of mice with India ink, the perifollicular zone was heavily laden with carbon-bearing phages within an hour, suggesting that many of these had arrived from the blood and entered the area via the sheathed capillaries. Some of the labeled cells migrated into the adjacent germinal centers where they persisted for at least 6 months. Similarly, dendritic cells resident in the sinus or perifollicular areas migrate into the germinal centers following systemic immunization.

The spleen modulates the febrile response to various antigens. Splenectomized guinea pigs given lipopolysaccharide intravenously mounted a 1.2–1.8°C increase in temperature that did not occur in sham-operated intact controls. It has been suggested that the spleen effects control over systemic blood pressure in response to sympathetic nervous control of renal rennin release determined by injection of donors or inhibitors of NO release into the splenic arterial system and by selective denervation of both organs. In the latter species the liver is much more involved in hematopoiesis during fetal development. This is especially apparent in the pig where neonatal animals are frequently seen in pathology examinations due to various diseases causing death in sucklings. Piglets up to about a week of age have scattered foci of erythropoiesis in liver that must be recognized as a normal finding. The sinus areas of the spleen are areas of recognition and removal of senescent blood cells by the combined effects of the latticelike endothelial cells of the sinus veins and the extravascular phagocytic macrophages. The littoral or lining cells of the splenic

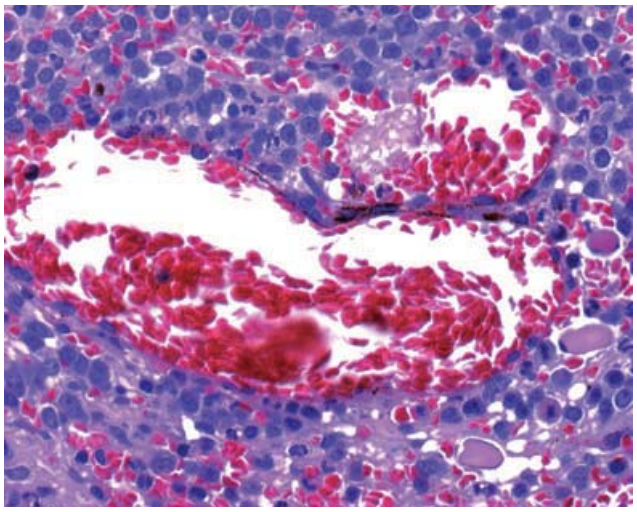

Figure 2.116. Dog: spleen, dilated sinus lined by littoral cells with cytoplasm containing ingested debris, most apparent on the upper sinus wall.

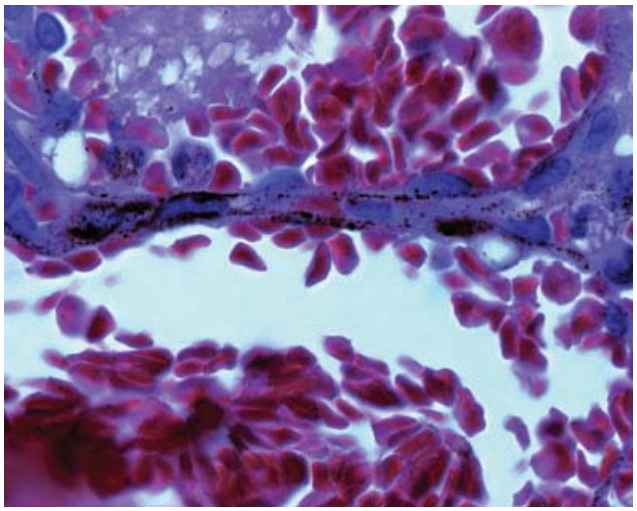

Figure 2.117. Detail of Figure 2.116. Brown granular material, likely hemosiderin, lies within the cytoplasm of (littoral) sinus lining cells.

sinuses are themselves phagocytic as can be visualized microscopically by the presence of hemosiderin in the cytoplasm of otherwise flattened lining cells (Figs. 2.116, 2.117). Anatomically, the littoral cells share function and staining characteristics of both endothelial cells ($CD31^+$) and of phagocytes ($lysozyme^+$). Aging red cells contain altered hemoglobin in small focal areas of the cytoplasm. These areas are pinched off as they squeeze between the endothelial cells to reenter the systemic circulation. These vesiclelike structures are approximately 0.3 microns in diameter and can be seen in older red cells of normal individuals. It is estimated that 20% of hemoglobin is lost from aging red cells in this manner. In asplenic individuals, these vesicles remain within the red cells in the absence of the "pitting" function of the spleen.

REFERENCES

Balogh, P., Aydar, Y., Tew, J.G., and Szakal, A.K. (2001) Ontogeny of the follicular dendritic cell phenotype and function in the postnatal murine spleen. *Cell Immunol* 214:45–53.

Deng, Y., and Kaufman, S. (2001) Splenorenal reflex regulation of arterial pressure. *Hypertension* 38:348–352.Feleder, C., Li, Z., Perlik, V., Evans, A., and Blatteis, C.M. (2003) The spleen modulates the febrile response of guinea pigs to LPS. *Am J Physiol Regul Integr Comp Physiol* 284:466–476.

McIlroy, D., Troadec, C., Grassi, F., Samri, A., Barrou, B., Autran, B., Debre, P., Feuillard, J., and Hosmalin, A. (2001) Investigation of human spleen dendritic cell phenotype and distribution reveals evidence of *in vivo* activation in a subset of organ donors. *Blood* 97:3470–3477.

Randolph, D.A., Huang, G., Carruthers, C.J.L., Bromley, L.E., and Chaplin, D.D. (1999) The role of CCR7 in TH1 and TH2 cell localization and delivery of B cell help *in vivo*. *Science* 286:2159–2162.

Romanovsky, A.A., and Peterson, S.R. (2003) The spleen: Another mystery about its function. *Am J Physiol Regul Integr Comp Physiol* 284:378–379.

Willekens, F.L.A., Roerdinkholder-Stoelwinder, B., Groenen-Dopp, Y.A.M., Bos, H.J., Bosman, G.J.C.G.M., van den Bos, A.G., Verkeij, A.J., and Were, J.M. (2003) Hemoglobin loss from erythrocytes *in vivo* results from spleen-facilitated vesiculation. *Blood* 101:747–751.

Function

Splenic function is defined more on the consequences of hypofunction, splenic disease, and splenectomy than on normal physiology. The major functions of the spleen include antibody production, hematopoiesis, and removal of aged blood cells and microorganisms. The first of these two can be entirely managed by other areas of the body in asplenic animals. However, the loss of the blood filtering capacity leaves the asplenic individual much more susceptible to coccal bacteremia and red cell parasitism. The amount of antibody production and hematopoiesis that occurs in the spleen varies between species, but the extent of splenic involvement for clearance of infectious agents is very similar in all species. For example, mice have splenic trilineage hematopoiesis throughout life, which should be differentiated from myeloproliferative disease during histopathologic examination. Rodents do not have well-defined splenic germinal centers (which are found in domestic animals), and there are minor differences in the anatomy of the vascular sinus interface in species as noted above.

It is felt that in most normal mammals the spleen functions largely as a "closed" organ in that most of the blood

is directly returned to the systemic circulation. About 3% of arterial blood enters the sinus filtering system with each passage through that organ. The rate of flow through the spleen is sufficient that the total blood volume is filtered through the sinus system at least once each day. In terms of function, as determined from examination of peripheral blood, there is a marked difference in the function of the spleen in animals such as the dog and horse with very muscular spleens and ruminants with more collagenous and less contractile splenic capsules. The spleen of the dog is extremely efficient in removing senescent cells and nuclear fragments such as Howell-Jolly bodies from young red cells. If Howell-Jolly bodies are present in the blood of a dog without other clinical signs (such as regenerative anemia), some occult lesion in the spleen should be expected and defined. Typical lesions include focal areas of peliosis or focal nodular lymphoid hyperplasia flanked by abnormal areas of sinus dilation that defeats the efficiency of the sinus filter. More serious causes include hemangiosarcoma or other diffuse splenic neoplasms. Similarly the splenic filter may become overloaded by a very high leukocyte count that presents the sinuses with many aging leukocytes. This allows some aging cells to circulate with nuclear hypersegmentation or pyknotic nuclei. An example of this situation is seen in dogs with a high neutrophilia caused by pyometra or pyelonephritis. If there is very brisk red cell destruction, as occurs in aggressive immune-mediated hemolytic anemia, the overload of sensitized red cells will result in the presence of peripheral blood Howell-Jolly bodies and senescent leukocytes of all types (Fig. 2.118). Leukemias will also result in splenic hypofunction; this is due partially to an increased burden of removing the effete neoplastic leukocytes but also because the spleen itself may be primarily involved with tumor that has resulted in altered patterns of flow. Proper function of the spleen requires that the organ is free of focal lesions that can distort vascular flow patterns. Thus a mass lesion as small as 1–2 cm in diameter may in itself be no hazard to the major function of cellular and microbial clearance, but it may create flanking areas of sinus dilation that permits pooling of platelets and clinically evident thrombocytopenia (Figs. 2.119, 2.120). The cat seems less often

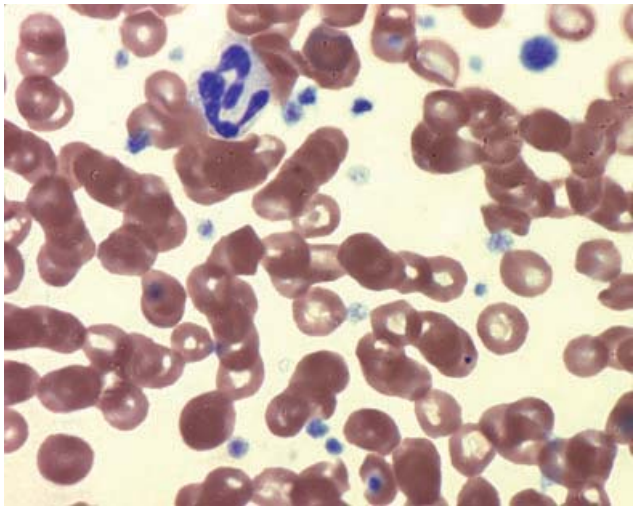

Figure 2.118. Dog: blood, postsplenectomy 1 year. The neutrophil in the upper left has nuclear hypersegmentation likely due to prolonged sojourn in the blood, and there is a red cell in the lower right with a Howell-Jolly body.

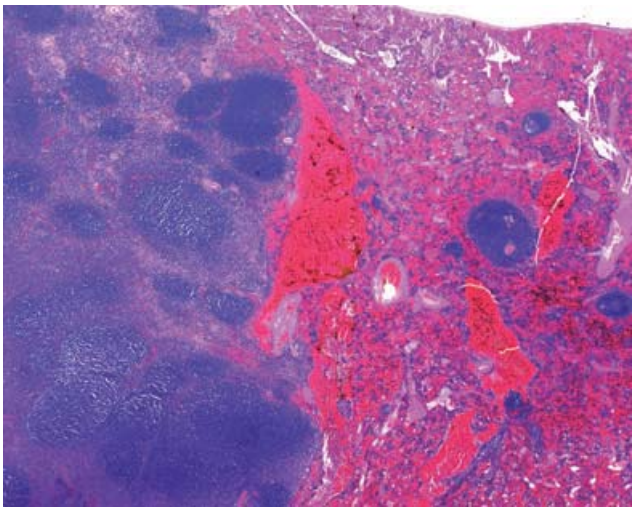

Figure 2.119. Dog: spleen. Mantle cell lymphoma (left) has irregular dilated sinuses in the adjacent areas of spleen free of neoplasm (center). These areas of sinus ectasia have resulted in foci of platelet sequestration and clinical thrombocytopenia despite the physical mass of the lymphoma being less than 2 cm in diameter.

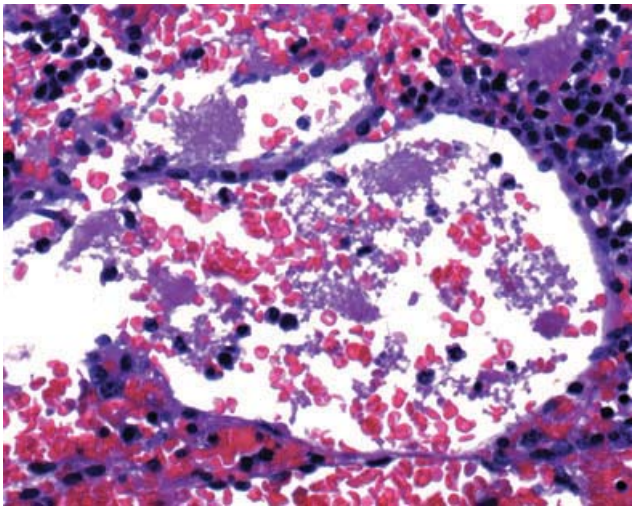

Figure 2.120. Detail of Figure 2.119. Dilated sinus filled with clusters of platelets undergoing activation and cohesion.

affected in this manner, and lymphoid hyperplasia is more likely to be diffuse than focal as in the dog.

The horse, like the dog, has a very efficient system of controlling the age of cells in circulation and the horse does not release reticulocytes into the peripheral blood stream. Responsive anemias in the horse can be measured in terms of upward shift in the mean cell volume (MCV) that will be maximal within a week of significant blood loss of any cause. Horses made anemic by bleeding had a mean upward shift in MCV of only 4 fl and those made anemic by intravascular hemolysis had a mean upward MCV shift of 12 fl, with none of these animals having reticulocytosis. Foals with isoimmune hemolytic anemia will have a rare late stage rubricyte in the peripheral blood but no reticulocytes. Horses have fewer causes of focal splenic dysfunction than dogs but rarely permit aged leukocytes to circulate in non-neoplastic diseases.

Ruminants, principally sheep and cattle, are much less reactive hematologically than horses or carnivores and have spleens that are much less capable of volume change over a short time span. The differences in splenic architecture with species are evident in the proportions of smooth muscle to collagen, but how this translates into splenic function is less clear. Perhaps a reduced ability of ruminant spleens to contract permits larger sinus diameter and less efficient filtering in some disease states. In any case the latter animals are characterized by frequent neutropenia in acute septic diseases and more variability in the character of cells in circulation during wide fluctuations in levels of blood cells.

The filtering actions of the spleen have been described in the vascular and sinus areas above. The phagocytic cells of the spleen include the macrophages (Figs. 2.121, 2.122) and littoral cells of the sinuses. Both cell types are capable of ingesting injured and senescent cells, as evidenced by their frequent hemosiderin granulation (Fig. 2.123). The splenic macrophages are primarily derived from the marrow via the blood, but under demand there is undoubtedly local proliferation. Labeling studies indicate a local proliferative fraction of 3–5% for tissue macrophages. Oddly, the kinetics of the phagocytic cells have been determined for a variety of sites, but not the spleen. From donor and labeling studies in mice, it is estimated that the turnover time for Kupffer cells of the liver is 21 days, and for the alveolar macrophages of the lung it is 27 days. The rate for the spleen is likely in the same time frame. Blood flow through the sinus areas of the spleen is slow, with compression of blood cells by leakage of plasma into the efferent lymphatics facilitating sorting of blood cells by the macrophages and littoral cells. The red cell membranes become less flexible as the cells age, and their decreased ability to deform to pass between endothelial membranes makes them more easily recognized by the phagocytic complement. The storage function of the spleen is likely overstated but the surface charge of red cells causes them to adhere to splenic membranes when they are very young and again when senescent. The pooling of young red cells in the spleen may be a form of storage in the delivery of immature cells. The spleen may also contain a large number of platelets. Interestingly, there are likely more platelets sequestered in the normal lung than in the spleen as demonstrated by epinephrine-mediated release.

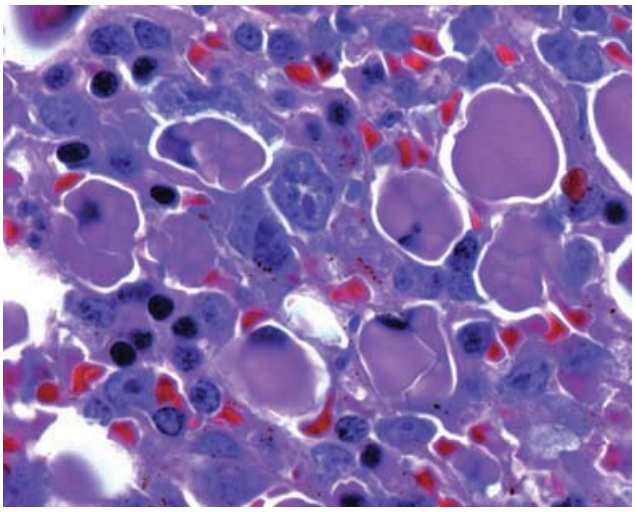

Figure 2.121. Dog: spleen, sinus area containing macrophages with fine granular inclusions (likely hemosiderin). The sinus is surrounded by numerous Mott-type plasma cells containing large homogeneous globulin inclusions or Russell bodies that might resemble erythrophagocytosis.

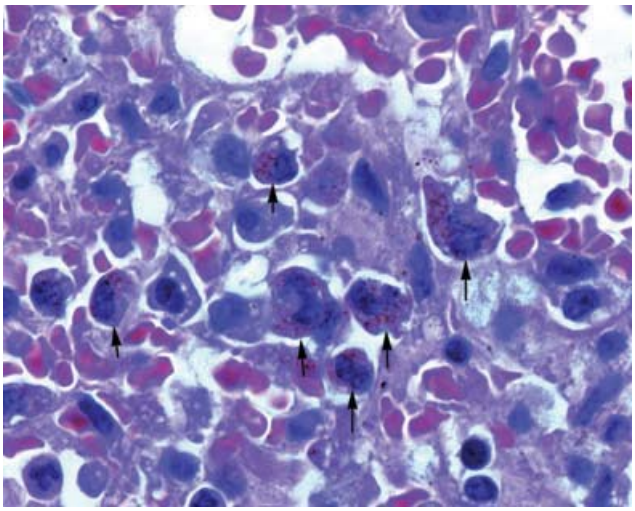

Figure 2.122. Dog: spleen, macrophages with fine hemosiderin granules, indicated by arrows, represent previous episodes of erythrophagocytosis.

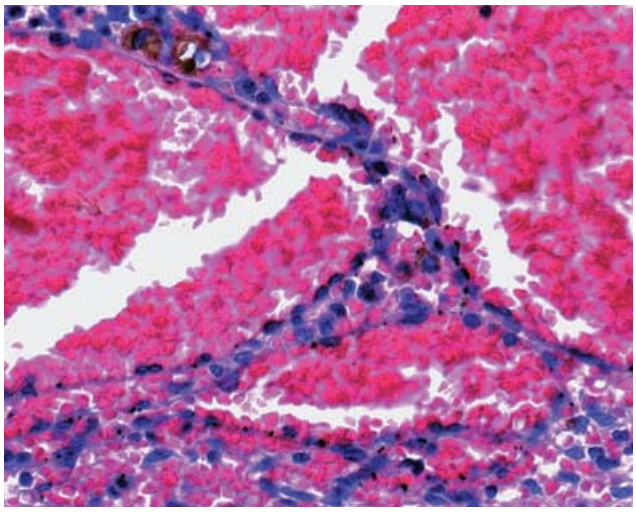

Figure 2.123. Dog: spleen. Littoral (lining) cell type of endothelium lining dilated splenic sinuses bearing cytoplasmic hemosiderin granules.

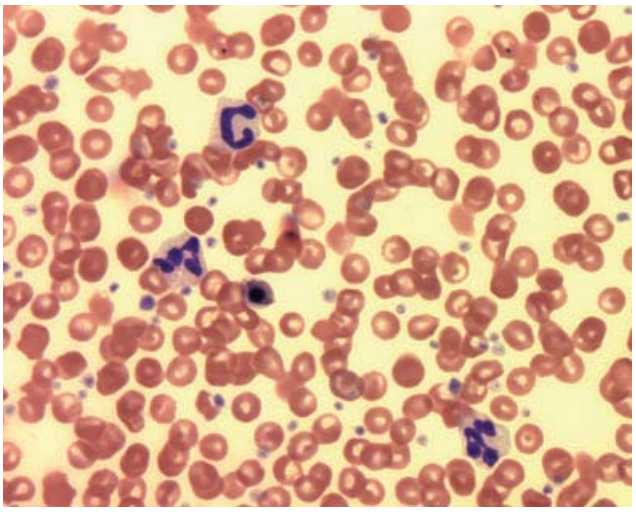

Figure 2.124. Dog: blood, postsplenectomy, same case as Figure 2.118. There are multiple changes in the peripheral blood of an asplenic dog in the homeostatic state. The neutrophils are at normal levels in the blood, but older forms with hypersegmentation are present. There is a polychromatic rubricyte in the center in a nonanemic animal as well as Howell-Jolly bodies in red cells in the upper and right left and a persistent thrombocytosis with some platelets as large as red cells (not shown).

REFERENCES

Chadburn, A. (2000) The spleen: Anatomy and anatomical function. *Semin Hematol* 37:13–21.

Iversen, P.O., and Benestad, H.B. (1994) Role of the spleen in leucocytosis after exercise: Reply. *Clin Sci* 87:369–370.

Kaufman, S., and Deng, Y. (1993) Splenic control of intravascular volume in the rat. *J Physiol (Lond)* 468:557–565.

Mazzeo, R.S. (2000) Aging, immune function, and exercise: Hormonal regulation. *Int J Sports Med* 21:S10–S13.

Pabst, R., and Westermann, J. (1993) The functional anatomy of the spleen. *Chir Gastroenterol* 9:86–90.

Powers, L.V. (2000) The avian spleen: Anatomy, physiology, and diagnostics. *Compend Contin Educ Pract Vet* 22:838–843.

Romanovsky, A.A., and Petersen, S.R. (2003) The spleen: Another mystery about its function. *Am J Physiol Regul Integr Comp Physiol* 284:R1378–R1379.

Tichelli, A. (1993) Hematological and immunological aspects of spleen loss. *Chir Gastroenterol* 9:103–107.

Technical Considerations in Splenic Biopsy

Clinical Presentation

The animal presenting with a splenic lesion is most often a mature dog. Formerly dogs with splenic hemangiosarcoma presented in some degree of collapse and on examination were found to have pale mucus membranes and some degree of abdominal distension. Usually, the diagnosis was made on the basis of anemia with acanthocytes in the peripheral blood and free blood in the peritoneal cavity. If surgery was not carried out at that point, a very characteristic rebound in the PCV occurred, with the hemoglobin level rising more rapidly than could be accredited to new cell production by reperfusion of the blood cells in the abdominal cavity back into the circulation. In regaining the peripheral circulation, the red cells look effete, with abnormal shapes due to premature aging in the low glucose and abnormal pH environment of the abdominal cavity. Currently, it is much more likely that a well dog that presents for routine examination is noted to have a mass on palpation of the anterior abdomen. On ultrasound examination, focal lesions are identified in the spleen. The issue then becomes whether to undertake a directed fine needle aspiration of a splenic mass or to biopsy by laparotomy or laparoscopic biopsy (Fig. 2.124).

Splenic Biopsy

By current technology an ultrasound examination of a splenic mass lesion can provide a great deal of information on the character of the lesion and on more solid areas likely to yield cells of diagnostic value. The most likely presentation is a mass several centimeters in diameter and easily accessible through the anterior abdominal wall. Primary differentials for these lesions include lymphoid proliferation or a vascular tumor. Focal lesions are less likely to be myelolipoma or metastatic tumor. If the mass is lymphoid it is most likely what is known in current terminology as a *fibrohistiocytic nodule* (Figs. 2.125, 2.126). These lesions are in fact, an assembly of lymphoid and stromal proliferations that include nodular hyperplasia

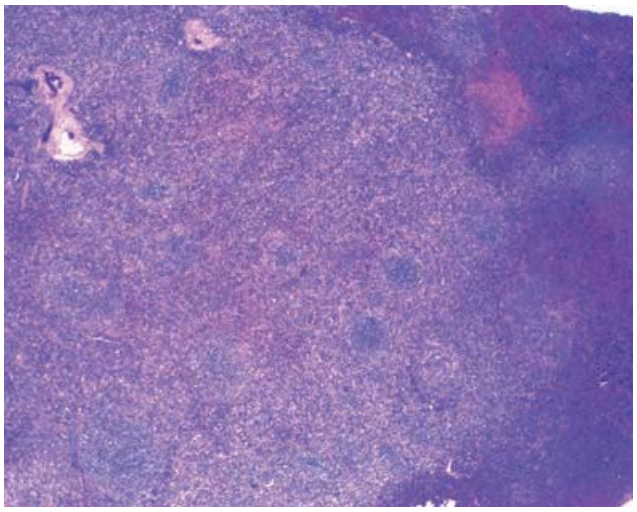

Figure 2.125. Dog: spleen, fibrohistiocytic nodule. Residual small lymphoid nodules are present in adjacent sinus areas (right) and undergoing atrophy in a solid stromal proliferative area (center).

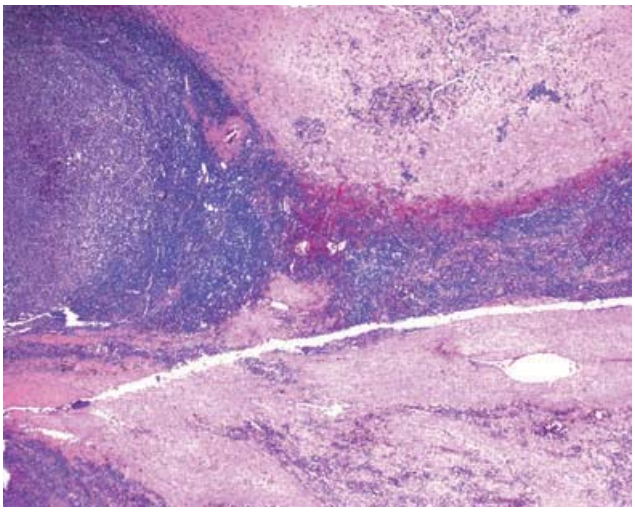

Figure 2.127. Dog: spleen, multilobular focal splenic lesion containing large atypical areas of lymphoid proliferation (left) and ischemic infarction (right).

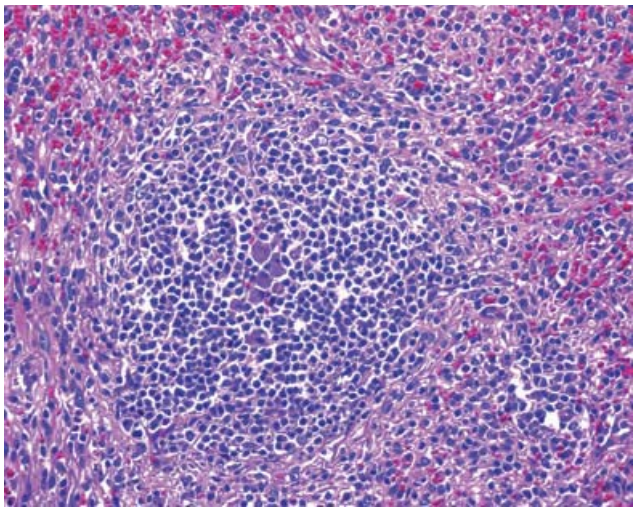

Figure 2.126. Detail of Figure 2.125. Residual lymphoid nodule of mantle-type cells, with central large phagocytic cells with granular debris. There is marked peripheral stromal proliferation, likely condensation, and thickening of the periarteriolar sheath capsule.

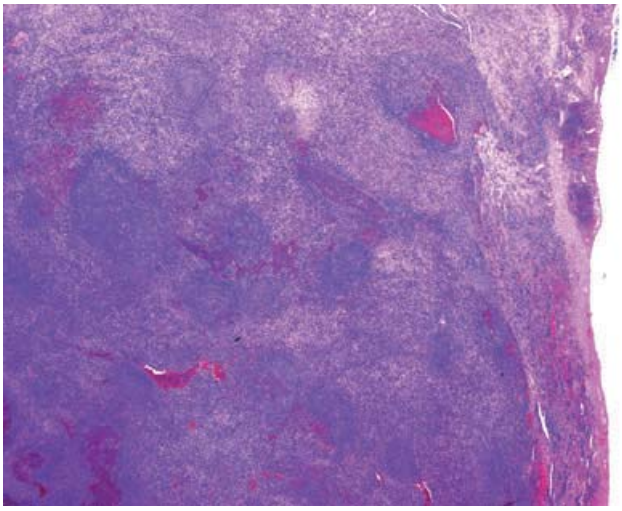

Figure 2.128. Dog: spleen, fibrohistiocytic nodule with focal areas of mantle cell proliferation that may be hyperplasia or lymphoma. In mantle cell lymphoma, some of the proliferative areas will be coalescing.

(Fig. 2.127), mantle cell lymphoma (Figs. 2.128, 2.129), marginal zone lymphoma (Figs. 2.130, 2.131), and nodular pseudotumor, or plasmacytoma (Figs. 2.132, 2.133). Oddly, all of these lesions tend to be surrounded by maturing collagenous tissue heavily infiltrated with plasma cells and foci of extramedullary hematopoiesis (Fig. 2.134). There are also frequently adjacent areas of atypical sinus ectasia (Fig. 2.135). If the lesion is a mantle cell lymphoma (MCL) composed of small mature-appearing lymphocytes it is likely to be interpreted as benign; biologically, that is not much in error, because, even if clonal, they are indolent. If the lesion is a marginal zone lymphoma (MZL) that is composed of a homogeneous population of larger (but not large) lymphocytes with a single prominent central nucleolus, it will likely be correctly recognized as lymphoma on cytologic examination. With both MCL and MZL, the surrounding areas of plasma cell and hematopoietic foci are usually associated with areas of stromal proliferation that would decrease the yield of free cells that tend to dilute the malignant population.

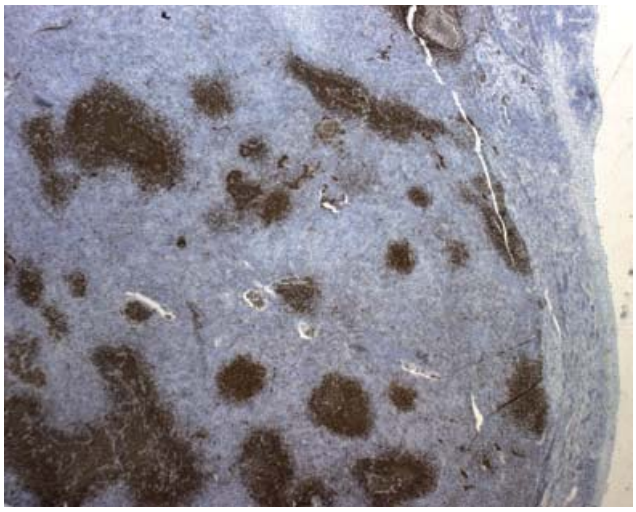

Figure 2.129. Detail of Figure 2.128. CD79 staining that demonstrates large irregular areas of B-lymphocyte proliferation within a mass lesion of nodular proliferation. The nodule is surrounded by an narrow band of uninvolved spleen (right).

Figure 2.131. Detail of Figure 2.130. CD79 staining delineates coalescing areas of marginal zone proliferation.

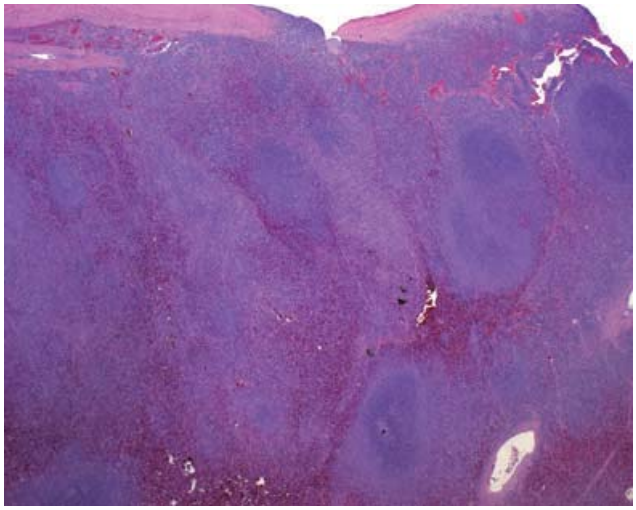

Figure 2.130. Dog: spleen, marginal zone lymphoma centered on darkly stained areas of mantle cells surrounding splenic arterioles. The marginal zone layers are of lighter-stained cells of irregular width with focal areas of coalescence.

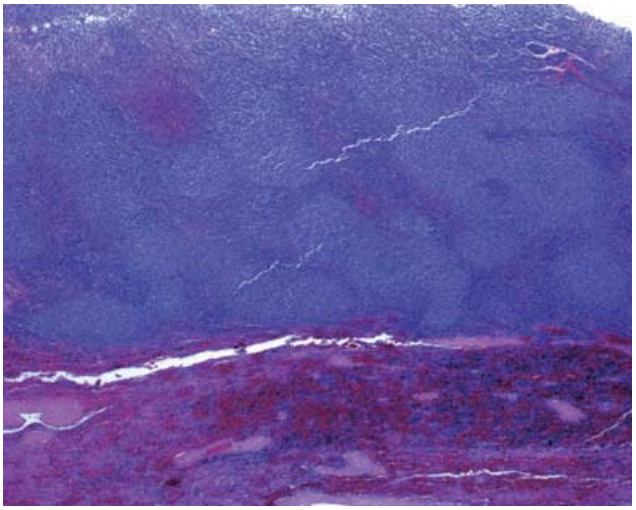

Figure 2.132. Dog: spleen, multiple coalescing areas of lymphoid proliferation (top), forming a cohesive mass of cellular proliferation.

Lesions that consist of small clusters of dilated sinuses, such as littoral cell ectasia or angioma, are unlikely to give an altered echo on ultrasound examination. They may however, yield endothelium with features of phagocytic activity in stellate or bipolar cells that are not recognized as endothelial (Figs. 2.136–2.138). If the lesion is a vascular dilation, as seen in hemangioma or hemangiosarcoma, the chances of getting more endothelium than frank blood are very slender. Despite all of these hazards, a fine needle aspiration of a splenic mass is likely to provide an answer that will permit a management decision in the case. If open abdominal surgery is elected, it is almost always the case that the entire spleen is removed and either the surgeon or a pathology prosector decides which areas of the spleen to fix and which to discard.

Sample Processing

Samples obtained by fine needle aspiration of splenic lesions, if voluminous, should be immediately put into an EDTA vial of appropriate size. Alternatively, the whole sample could be hemolyzed with 1–2% acetic acid and then centrifuged to concentrate the nucleated cells present. After the sediment is obtained, the lysate should

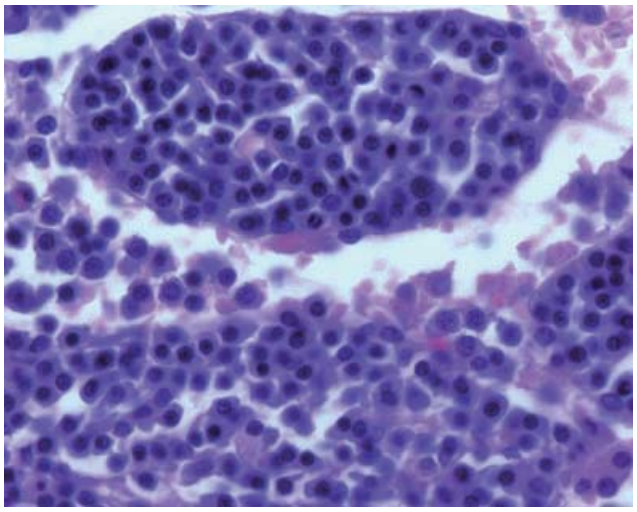

Figure 2.133. Detail of Figure 2.132. The proliferating cells have round, densely stained nuclei with abundant eccentrically distributed cytoplasm that is highly amphophilic, characteristic of plasma cells. Binucleated cells are present (center).

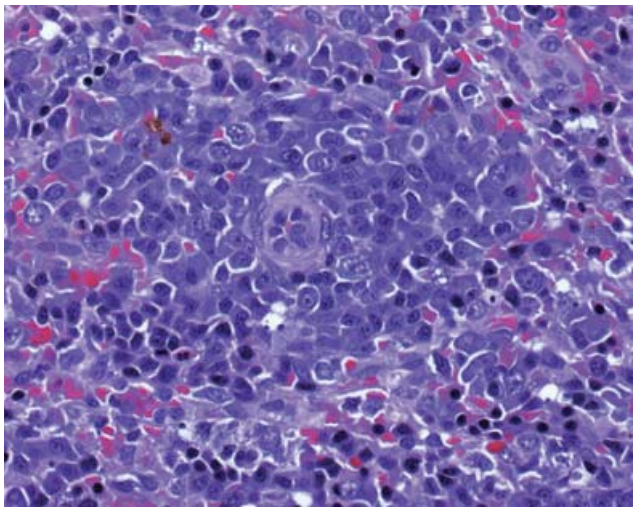

Figure 2.134. Dog: spleen, focal nodular lymphoid hyperplasia. There is marked atrophy of the periarteriolar lymphoid sheath. The artery is surrounded by plasma cells and hematopoietic blast cells with focal and diffuse areas of erythropoiesis.

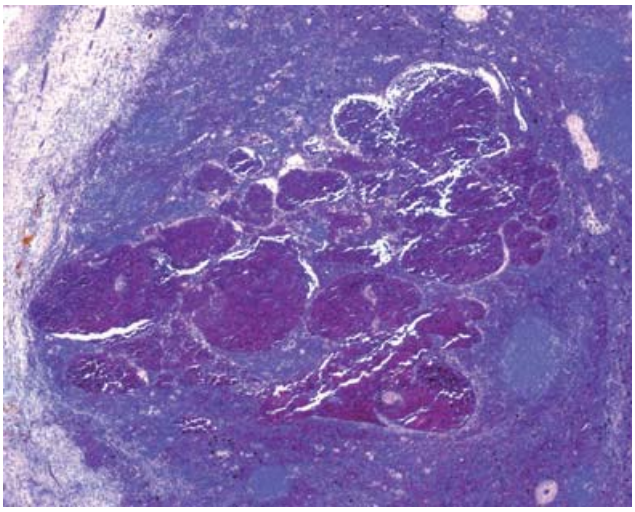

Figure 2.135. Dog: spleen, myelolipoma. Area of ischemic infarction (left) that is adjacent to clustered foci of sinus ectasia.

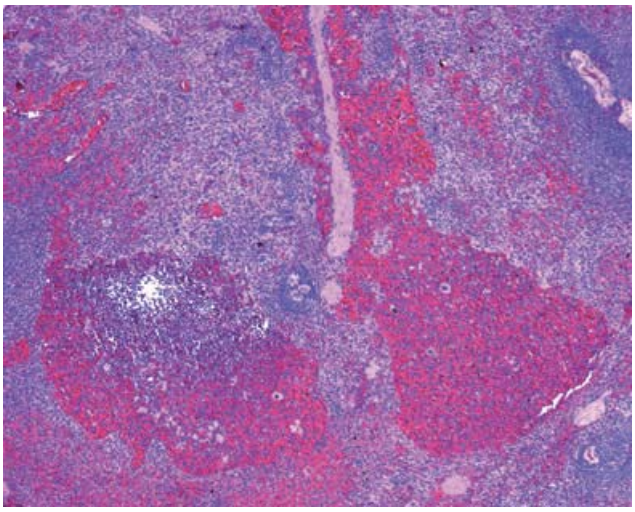

Figure 2.136. Dog: spleen. Splenectomy was performed for a nodular lesion with focal areas of sinus ectasia. Note papillary areas of sinus wall.

be poured off. Serum may be added to resuspend the cells in an isotonic environment for making cellular spreads. Staining should be done with both hematoxylin-eosin as well as a Wright's stain because it is likely there will be diagnostic material that is in clusters too dense to properly interpret with a Romanovsky-type blood stain. Depending on the cell yield, the sediment could be left unsuspended and fixed in situ with formalin for sectioning, providing a cell button with excellent cellular concentration and cytologic detail. Multiple slides should be prepared from whatever method is used in order to provide the capability to utilize additional stains to identify specific hematopoietic, vascular, or stromal cells.

If splenectomy has been carried out, it is preferable to sample multiple areas of tissue that are not more than 2 cm in any dimension, because formalin perfusion into clotted blood is slow and fixation will be delayed. If most of what is received fresh appears to be dilated areas of thrombosis, an imprint from several areas should assist in choosing tissue with viable cells present. Gentle agitation of the tissues during fixation is always desirable. In trimming tissues from splenic vascular lesions, the outer rim of tissue from an area infarction is most likely to provide

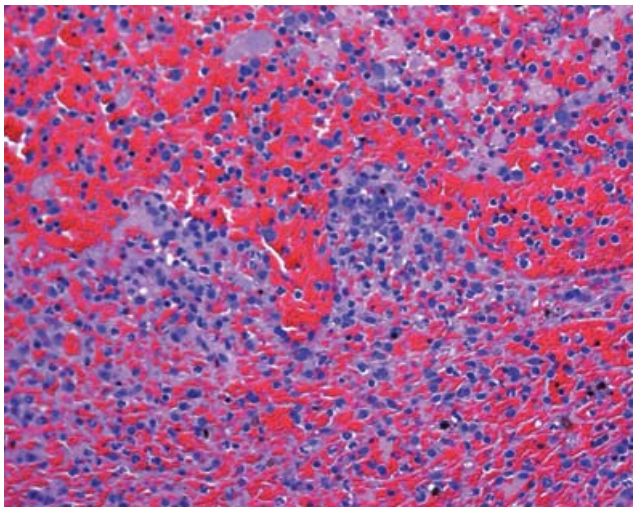

Figure 2.137. Detail of Figure 2.136. Sinus wall has papillary foci of endothelial proliferation typical of littoral cell angioma.

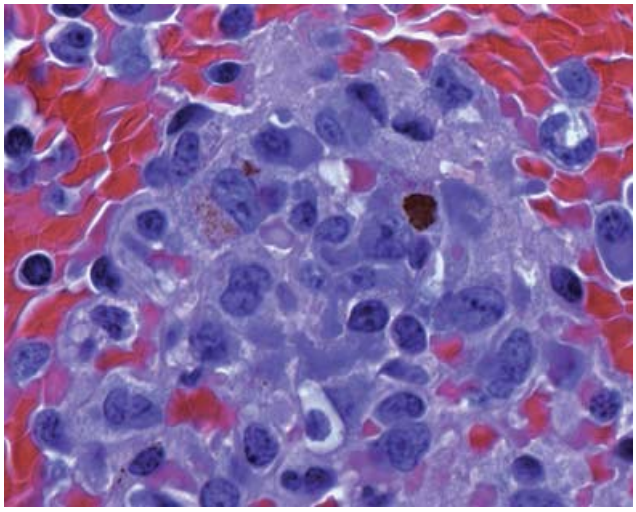

Figure 2.138. Detail of Figure 2.137. Lining cells have abundant cytoplasm with focal areas of cytoplasmic granules, likely hemosiderin, that are characteristic of littoral lining cells.

viable diagnostic material. These decisions are critical to obtaining a conclusive and correct pathologic interpretation. The largest lesion may be the most recent to thrombose and infarct but not necessarily the one with diagnostic tissue. The usual strategy is to fix a lot of tissue and make sections of six or more areas to obtain diagnostic tissue. Even then the decision may rest on a few strands of endothelial cells with large atypical nuclei and nucleoli coursing through a large mass of clotted blood. In many areas of these lesions there are foci of robust benign stromal proliferation organizing areas of previous hemorrhagic infarction, and these must be distinguished from endothelial cells as aided by immunohistochemical staining for Factor VIII or the more helpful CD31. In addition to the well-recognized vascular neoplasms of hemangioma and hemangiosarcoma, there is now evidence that dogs have a second type of lesion that arises in the sinus lining or littoral cells. Those from the more common sinus lining cells may form a very dense cohesive neoplasm called a *capillary* type of angioma that may be benign or malignant. These neoplasms may be mistaken for an area of sclerosis, and careful examination is required to detect red cells in very narrow vascular slits. They are readily identified as vascular by CD31 staining. The early lesions involving the littoral type of endothelium appear as multiple clusters of cyanotic areas formed by 20 or more sinus areas dilated to up to a millimeter in diameter and solidly congested with blood (see Figs. 2.135–2.138). These lesions stand out against the normal areas of splenic parenchyma that are not congested, and in that manner are differentiated from generalized splenic congestion. Cytologically, they have the distinction of being obvious sinus lining cells, but they are also phagocytic with hemosiderin and other debris in their cytoplasm, which remains low and flattened.

If the splenic lesion is of a more solid cellular type, on gross examination of fixed tissue the lymphoid areas will appear white against the dark areas of congestion. It is always desirable to fix and trim those areas of the spleen that are felt to be more normal, as well as solid focal lesions. Atrophy of the follicular and thymic-dependent areas of lymphoid tissue in more normal areas of spleen are important indicators of the effects on normal cellular kinetics of the main tumor mass. In mantle cell and marginal zone lymphomas the surrounding areas of intact spleen will have atrophy of normal cells and foci of hypertrophy of the population making up the clonal neoplastic mass.

REFERENCES

Al-Omishy, H., Lockett, C., Rees, J.A., and Davidson, B.R. (1997) Splenomegaly. *Postgrad Med J* 73:125–126.

Arber, D.A., Strickler, J.G., and Weiss, L.M. (1997) Splenic mesothelial cysts mimicking lymphangiomas. *Am J Surg Pathol* 21:334–338.

Burke, J.S. (1993) Splenic lymphoid hyperplasias *versus* lymphomas/leukemias: A diagnostic guide. *Am J Clin Pathol* 99:486–493.

Christopher, M.M. (2003) Cytology of the spleen. *Vet Clin North Am Small Anim Pract* 33:135–152.

Day, M.J., Lucke, V.M., and Pearson, H. (1995) A review of pathological diagnoses made from 87 canine splenic biopsies. *J Small Anim Pract* 36:426–433.

Falk, S., Krishnan, J., and Meis, J.M. (1993) Primary angiosarcoma of the spleen: A clinicopathologic study of 40 cases. *Am J Surg Pathol* 17:959–970.

Ha, H.K., Kim, H.H., Kim, B.K., Han, J.K., and Choi, B.I. (1994) Primary angiosarcoma of the spleen. CT and MR imaging. *Acta Radiol* 35:455–458.

Hardie, E.M., Vaden, S.L., Spaulding, K., and Malarkey, D.E. (1995) Splenic infarction in 16 dogs: A retrospective study. *J Vet Intern Med* 9:141–148.

Horny, H.P., Ruck, M.T., and Kaiserling, E. (1992) Spleen findings in generalized mastocytosis—A clinicopathologic study. *Cancer* 70:459–468.

Hurwitz, N., and Sauter, G. (1993) Pathology of the spleen in malignant systemic diseases. *Chir Gastroenterol* 9:91–96.

Kumar, P.V. (1995) Splenic hamartoma: A diagnostic problem on fine needle aspiration cytology. *Acta Cytol* 39:391–395.

McAneny, D., LaMorte, W.W., Scott, T.E., Weintraub, L.R., and Beazley, R.M. (1998) Is splenectomy more dangerous for massive spleens? *Am J Surg* 175:102–107.

Piscaglia, F., Donati, G., Cecilioni, L., Celli, N., Stagni, B., Pini, P., Gaiani, S., Gherlinzoni, F., and Bolondi, L. (2002) Influence of the spleen on portal haemodynamics: A non-invasive study with Doppler ultrasound in chronic liver disease and haematological disorders. *Scand J Gastroenterol* 37:1220–1227.

Zeppa, P., Vetrani, A., Luciano, L., Fulciniti, F., Troncone, G., Rotoli, B., and Palombini, L. (1994) Fine needle aspiration biopsy of the spleen: A useful procedure in the diagnosis of splenomegaly. *Acta Cytol* 38:299–309.

Developmental and Degenerative Diseases of the Spleen

Developmental Diseases of the Spleen

Congenital anomalies of the spleen include complete absence or asplenia, as well as polysplenia or fusions during embryonic development with other organs including the kidney and gonads. Asplenia occurs in a strain of inbred mice and rarely in humans. Calves may present with chronic skin disease in a syndrome with splenic maldevelopment. Human asplenia is associated with other malformations of the heart and great vessels. Nude mice have spleens that lack the thymic-dependent periarteriolar inner sheath lymphoid areas. A condition of hyposplenia occurs in humans in which the spleen may weigh less than a gram and has deficient development of the lymphoid areas, although thymus and nodes are not affected. An accessory spleen occurs in many species and consists of an additional small splenic mass (or masses) in the region of the hilar vessels, but it may occur in other organs including the pancreas and omentum. Accessory spleen has also been applied to a condition more correctly termed *splenosis*, where there are multiple splenic implants throughout the abdomen. This is usually as an acquired condition following splenic trauma (Figs. 2.139–2.141). The latter condition is typically asymptomatic, but occasionally the explants that have a smooth muscle capsule may rupture and result in serious hemorrhage. In the event that splenectomy is performed for splenic hyperfunction, is it important to review the likely areas for accessory spleen to ensure that they are also removed if present.

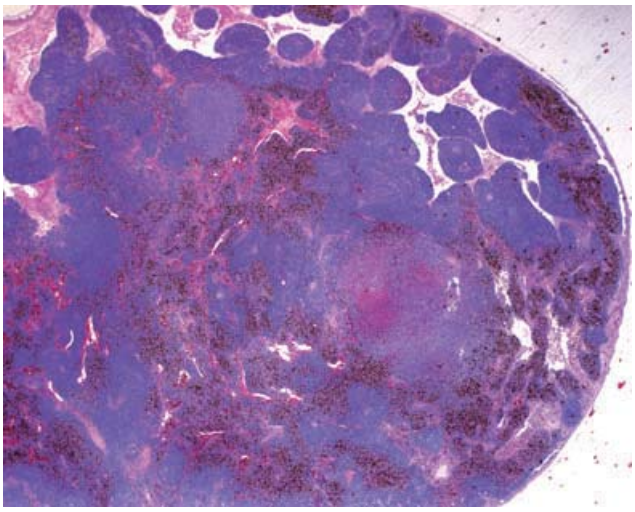

Figure 2.139. Dog: splenosis. One of multiple abdominal explants developed following prior splenic trauma. A thin, smooth muscle capsule surrounds multifocal areas of lymphoid proliferation separated by apparent blood-filled sinuses. The foci of dark staining consist of hemosiderin-laden macrophages.

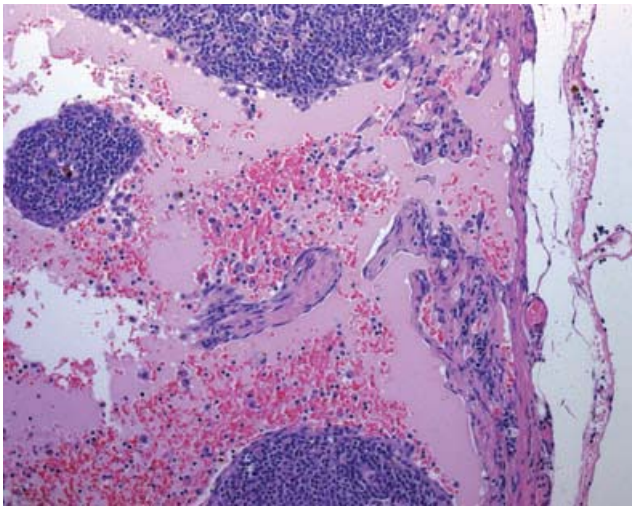

Figure 2.140. Detail of Figure 2.139. Margin of splenic explant with thin smooth muscle capsule and internal smooth muscle trabeculae (mid-center) form a sinus area surrounding foci of lymphoid proliferation resembling a hemal node.

REFERENCES

Budke, H.L., Breitfeld, P.P., and Neiman, R.S. (1995) Functional hyposplenism due to a primary epithelioid hemangioendothelioma of the spleen. *Arch Pathol Lab Med* 119:755–757.

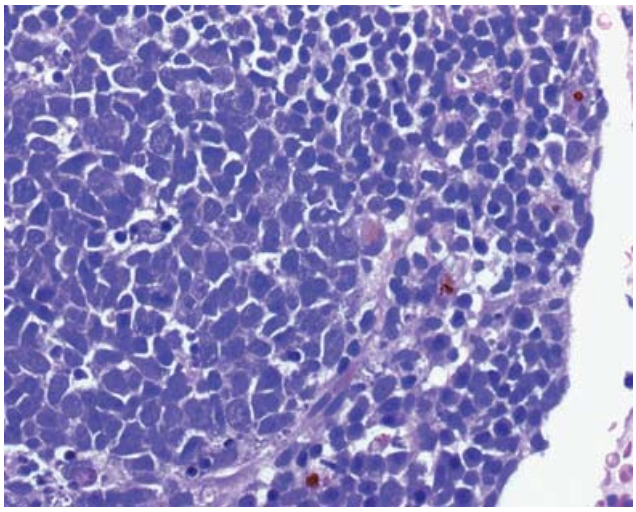

Figure 2.141. Detail of Figure 2.139. Large cells forming a germinal center (left) are surrounded by smaller cells resembling a mantle cell cuff and limited by an endothelial-lined boundary demonstrating physiologic and structural integrity of splenic explant.

Carr, N.J., and Turk, E.P. (1992) The histological features of splenosis. *Histopathol* 21:549–553.

Christopher, M.M. (2003) Cytology of the spleen. *Vet Clin North Am Small Anim Pract* 33:135–152.

Cowles, R.A., and Yahanda, A.M. (2000) Epidermoid cyst of the spleen. *Am J Surg* 180:227.

Cui, H.M., Jing, F., and Xi, P. (2003) Pathology of the thymus, spleen and bursa of Fabricius in zinc-deficient ducklings. *Avian Pathol* 32:259–264.

Day, M.J., Lucke, V.M., and Pearson, H. (1995) A review of pathological diagnoses made from 87 canine splenic biopsies. *J Small Anim Pract* 36:426–433.

Engel, P., Tjalve, E., and Horn, T. (1993) Peliosis of the spleen associated with a paraganglioma. Case report. *Acta Radiol* 34:148–149.

Hale, T.W., Rais-Bahrami, K., Montgomery, D.L., Harkey, C., and Habersang, R.W. (1995) Vitamin E toxicity in neonatal piglets. *J Toxicol Clin Toxicol* 33:123–130.

Hardie, E.M., Vaden, S.L., Spaulding, K., and Malarkey, D.E. (1995) Splenic infarction in 16 dogs: A retrospective study. *J Vet Intern Med* 9:141–148.

Hurwitz, N., and Sauter, G. (1993) Pathology of the spleen in malignant systemic diseases. *Chir Gastroenterol* 9:91–96.

Körner, M., and Gebbers, J.O. (2002) Peliosis of the spleen and haemolytic anaemia. *Histopathol* 41:179–180.

Kumar, P.V. (1995) Splenic hamartoma: A diagnostic problem on fine needle aspiration cytology. *Acta Cytol* 39:391–395.

Lecavalier, P., Chu, I., Yagminas, A., Villeneuve, D.C., Poon, R., Feeley, M., Håkansson, H., Ahlborg, U.G., Valli, V.E., Bergman, Å., Seegal, R.F., and Kennedy, S.W. (1997) Subchronic toxicity of 2,2′,3,3′,4,4′-hexachlorobiphenyl in rats. *J Toxicol Environ Health* 51:265–277.

Ohno, H., Ogawa, M., Nishikawa, S., Hayashi, S., and Kunisada, T. (1993) Conditions required for myelopoiesis in murine spleen. *Immunol Lett* 35:197–204.

Wien, T.N., Sorby, R., Espenes, A., Gunnes, G., Nordstoga, K., Landsverk, T., and Husby, G. (2003) Splenic ellipsoids: An early target for deposition of AA amyloid induced in mink. *Amyloid-J Protein Fold Disord* 10:240–249.

Degenerative Diseases of the Spleen

Age-associated atrophy occurs in the spleen as in other lymphoid organs in animals like dogs and horses that live to full maturity. Atrophy of the lymphoid areas of the spleen occurs in autoimmune diseases treated by immunosuppression. The most marked atrophy is seen in animals that have had several courses of combination chemotherapy, in which case destruction of cells is added to the atrophy usually associated with severe and chronic disease (Figs. 2.142–2.144). Acute lympholysis consisting of generalized apoptosis of germinal center cells may occur as a result of an endogenous steroid in acute stressing diseases (Fig. 2.145). This change is seen in foals aborted at term due to equine herpesvirus type 1. In animals that survive this initial reaction, there is complete removal, within 24 hours, of the apoptotic debris, and the germinal centers then appear hypocellular and consist of the dendritic cell bed and a few macrophages. The presence but not the absence of the apoptotic debris can be used to estimate the onset of the disease prior to death. Hyalinized germinal centers with associated vascular changes occasionally occur in old sheep, goats, and dogs (Fig. 2.146). When encircled by concentric rings of small lymphocytes the lesion is referred to as *Castleman's disease*. In animals this change is seen most often as a type of fading follicular hyperplasia representing a reaction

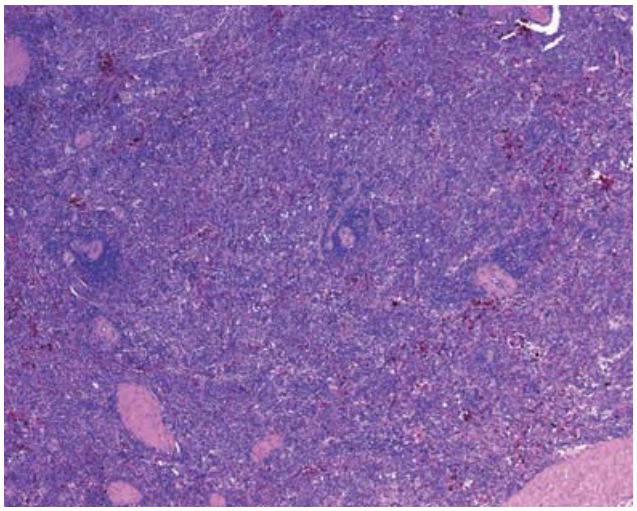

Figure 2.142. Dog: spleen, histiocytic sarcoma. Cachexia of cancer and likely therapy with marked atrophy of periarteriolar lymphoid sheaths, only small cuffs of thymic-dependent lymphocytes surrounding splenic arterioles (center).

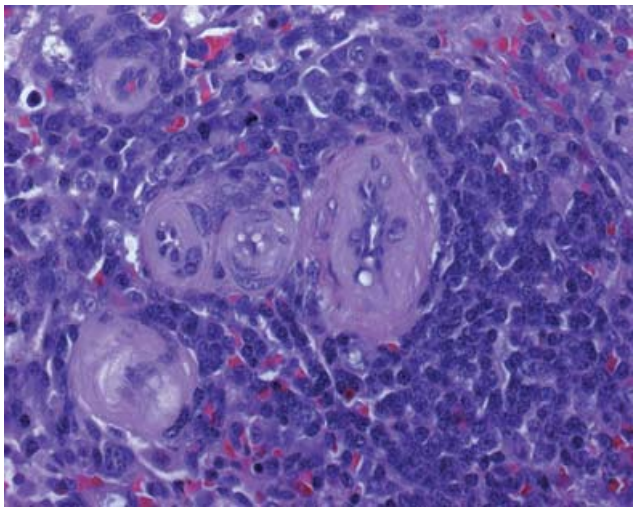

Figure 2.143. Detail of Figure 2.142. Splenic arterioles surrounded by a narrow cuff of small lymphocytes with many of the remaining cells plasmacytic, likely of B-cell rather than T-cell phenotype.

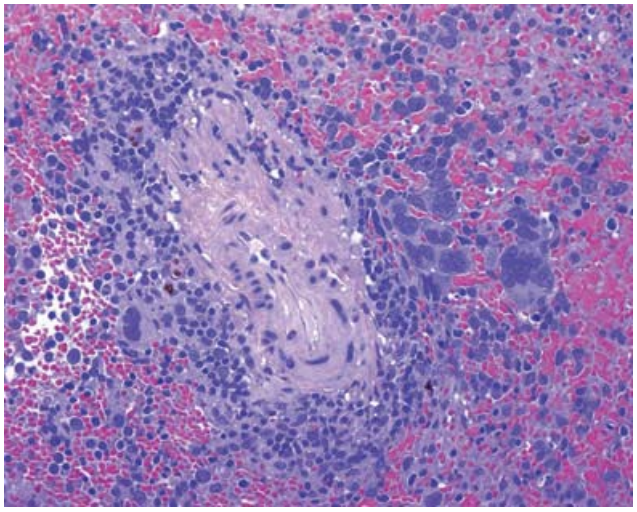

Figure 2.144. Dog: spleen, chronic idiopathic thrombocytopenic purpura. There is severe atrophy of periarteriolar lymphoid sheaths after prolonged steroid therapy. There is accompanying low sinus cellularity and megakaryocytic hyperplasia.

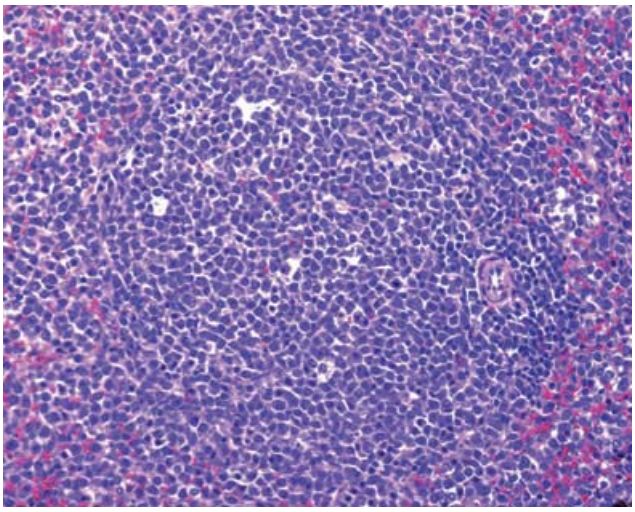

Figure 2.145. Dog: spleen, chronic dermatitis. There is marked atrophy of the periarteriolar lymphoid sheath (PALS, right), reduced cell density of the germinal center (center), with numerous cells undergoing apoptosis. There is a complete absence of a mantle cell cuff. This finding with the PALS atrophy is indicative of incipient B- and T-cell depletion.

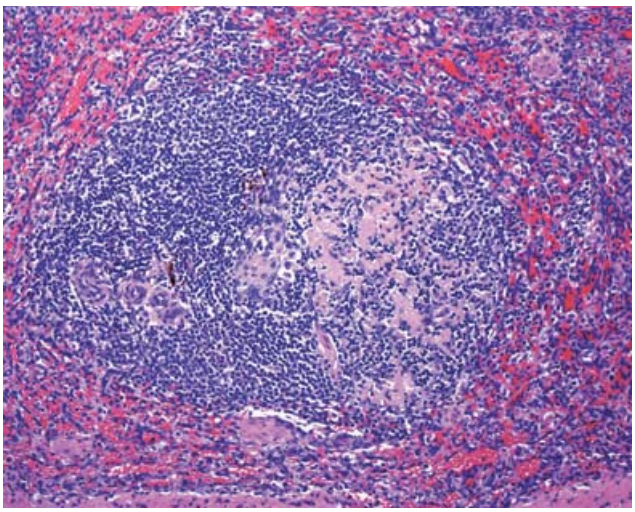

Figure 2.146. Macaque: spleen, follicular hyalinosis and involuting germinal center occupied by amorphous hyalin debris.

that is in decline, but rarely lymphoid hyperplasias in the dog lymph node may closely resemble the human reaction.

The spleen as a major lymphoid organ and a site of macrophage accumulation reflects systemic changes involving these cell systems. In systemic amyloidosis, the spleen is always involved, usually not to a major degree, with only the germinal centers affected and the sinuses are usually spared (Fig. 2.147). Even in advanced involvement of the lymphoid follicles producing waxy nodules (*sago-spleen*) on the cut surface, the organ is not enlarged and hyperfunction is not present. The lysosomal storage diseases of animals like the gangliosidoses and globoid cell leukodystrophy have major effects in the nervous system with minor involvement of the liver and spleen. In contrast, the glucosylceramidase deficiency (Gaucher's disease) is termed a *neurovisceral* storage disease with major involvement of the liver and spleen. This rare disease has been reported in Sydney silky terrier dogs and in sheep.

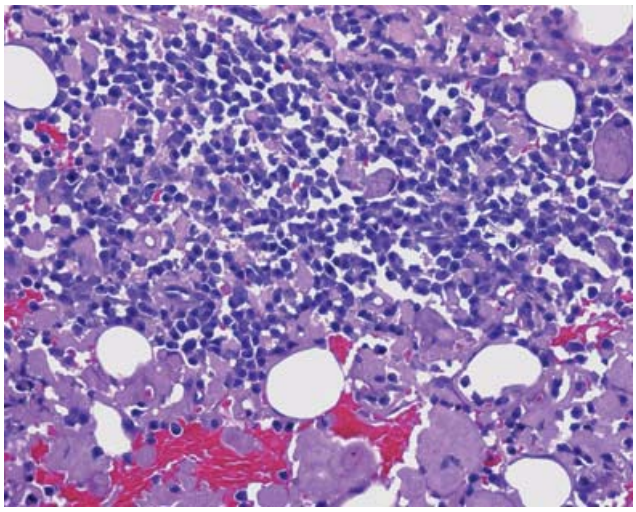

Figure 2.147. Dog: spleen, myelolipoma with plasmacytoid lymphoma and amyloidosis. Clear areas are fat cells irregularly surrounded by plasmacytoid cells with nucleoli. There are multiple lakes of amorphous pink staining material that is strongly green and birefringent on polarized light.

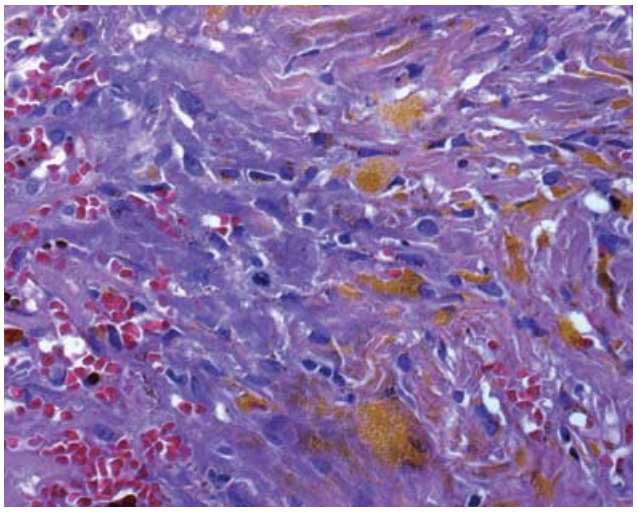

Figure 2.148. Dog: spleen, hemosiderosis with iron staining of smooth muscle fibers and focal areas of yellow ceroid pigment due to extensive local red cell destruction, likely as a result of focal interstitial hemorrhage.

The most common pigment accumulation in the spleen consists of iron and calcium-protein complexes of various types that produce black to brown or yellow nodules in the capsular margins called *siderotic nodules* or *Gamna-Gandy bodies*. These elements deposit in fibrous and elastic tissues, are blue-black with hematoxylin, and in fibrillar form may be mistaken for fungal hyphae. These changes often occur in association with areas of yellow ceroid pigment and suggest a genesis in focal areas of hemorrhage (Fig. 2.148). Hemosiderin is present in sinus macrophages of mature animals in some degree and may be very extensive, but it is only significant if it is accompanied by fibrosis. This level of hemosiderin accumulation is rarely seen, but when present indicates chronic hemolytic anemia usually associated with congenital red cell deficiencies. This is likely the basis of the hemosiderosis of marrow and spleen seen in the marrow failure syndrome of the black rhinocerus (Fig. 2.149).

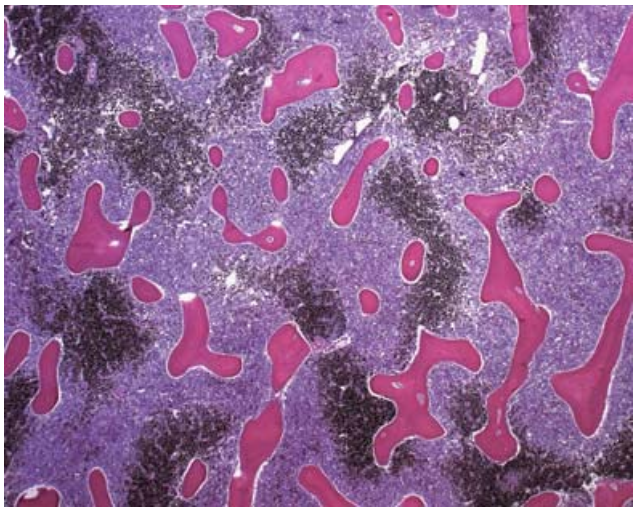

Figure 2.149. Black rhinoceros: marrow, chronic anemia and hemosiderosis. The marrow has solid cellularity, lacks fat cells, and has multifocal areas of interstitial large darkly stained, hemosiderin-laden macrophages.

The type of iron deposition is indicative of the rate of iron turnover. Hemosiderin iron is relatively inert and unavailable for short-term utilization in response to hemorrhage even if present in abundance. Hemosiderin accumulation occurs in anemias of chronic disease where there is enzymatic scavenging of iron from transport proteins to deny iron use by bacterial pathogens. In these conditions splenic macrophages contain large deeply stained aggregates of hemosiderin and very little fine diffuse iron on specific staining (Fig. 2.150). In contrast, in hemolytic anemias where there is very rapid recycling of iron, the macrophages contain iron in very fine aggregates. These are smaller complexes more rapidly digested for iron release with iron present in combination with ferritin and some hemosiderin.

Splenic infarction is a rare occurence in animals as compared to humans. In humans hypertension and vascular accidents are more common as well as thrombotic lesions associated with sickle cell anemia, all of which can lead to infarcts. Dogs with myeloma may have splenomegally and these may be associated with focal septic infarction due to the hyperviscosity of hyperglobulinemia causing impaired splenic circulation. Animals presenting with

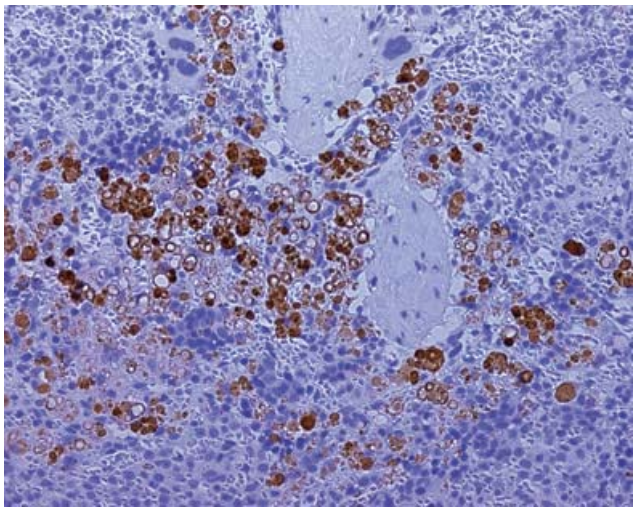

Figure 2.150. Dog: spleen, marginal zone lymphoma. Hematoxylin counter stain on a slide with no cytoplasmic stain, demonstrates clusters of macrophages heavily laden with hemosiderin surrounding smooth muscle trabeculae.

these signs (serum protein above 10 g) are highly vulnerable to hypotensive shock even with minor sedation, as required for marrow or splenic aspiration.

Splenic Trauma and Splenic Torsion

Most frequently, trauma to the spleen occurs as a result of crushing injury or puncture wounds. These events result from a variety of causes that often involve falls, contact with moving vehicles, and gunshot wounds. Often, massive abdominal hemorrhage is the net result. Extensive bleeding from many small vessels is compatible with life as bleeding slows and hypotensive shock approaches, and over a period of hours autoperfusion likely provides some protection. If the animal survives to have the lesion identified later (as often occurs), the spleen may be completely bisected or appear twisted and with deep linear creases in areas of capsular rupture. These changes may be accompanied by several areas of extra splenic explants or splenosis consisting of red round masses 1–2 cm in diameter resembling hemal nodes and usually attached to areas of omentum or mesentery. Trauma sufficient to cause rupture of the splenic capsule will often also result in hepatic laceration. Hepatic involvement is evident at the time by increase in hepatic enzymes and later as hepatic capsular scarring. The essential functions of the spleen are not altered by previous trauma, and signs of splenic hypofunction with aged cells or Howell-Jolly bodies in peripheral blood cells have not been associated with healed trauma.

An enlarged spleen of any cause is much more susceptible to tearing of the capsule with fatal hemorrhage resulting. Splenic rupture is one of the most common causes of death in juvenile infectious mononucleosis. Splenic rupture without apparent trauma is seen in dairy cattle with the adult type of bovine lymphoma. In these cases the spleen is massively enlarged and the capsule is greatly thinned. Similar events are rare in the dog or horse but do occur occasionally in the mouse and rat, likely associated with capture and restraint.

Torsion of the spleen occurs rarely in large-breed dogs and in humans. The broad attachment of the spleen to the rumen makes torsion impossible in cattle, sheep, and goats. Torsion occurs rarely in sows. In other species it is largely unrecorded. In the dog, torsion of the spleen is surprisingly compatible with life. Animals present with a distended anterior abdomen that contains a completely infarcted spleen, which may weigh 5–10 lbs. After torsion has occurred, the peripheral blood picture appears similar to postsplenectomy cases with hypersegmented neutrophils, Howell-Jolly bodies in red cells, and a severe moderately responsive anemia. If the infarction occurred several days earlier, the plasma will be brown from blood pigments leaching from the splenic capsule and the urine will be dark brown. Torsion is usually of 180 degrees with complete occlusion of the veins but not the arteries, permitting slow distension of the spleen with ultimate blockage, thrombosis, and infarction. Less often the spleen may be rotated on its long axis with congestion and infarction of the tail area. Splenectomy in humans has the risk of pneumococcal sepsis within the first year after surgery with prevention by vaccination. Dogs, even in research settings, are subject to severe anemia due to *Mycoplasma hemocanis* (hemobartonella) following splenectomy. The frequency of this occurrence might suggest that many dogs are occult carriers prior to splenectomy.

REFERENCES

Anderson, D.M., Stidworthy, M., James, R., and White, R.A.S. (2000) Traumatic subcutaneous translocation of the spleen in an Old English sheepdog. *J Small Anim Pract* 41:515–518.

Carr, N.J., and Turk, E.P. (1992) The histological features of splenosis. *Histopathol* 21:549–553.

Day, M.J., Lucke, V.M., and Pearson, H. (1995) A review of pathological diagnoses made from 87 canine splenic biopsies. *J Small Anim Pract* 36:426–433.

Engel, P., Tjalve, E., and Horn, T. (1993) Peliosis of the spleen associated with a paraganglioma. Case report. *Acta Radiol* 34:148–149.

Hardie, E.M., Vaden, S.L., Spaulding, K., and Malarkey, D.E. (1995) Splenic infarction in 16 dogs: A retrospective study. *J Vet Intern Med* 9:141–148.

Keramidas, D.C., and Soutis, M. (2003) The function of the spleen in adults after ligation of the splenic artery of the traumatized spleen in childhood. *Surgery* 133:583–585.

Körner, M., and Gebbers, J.O. (2002) Peliosis of the spleen and haemolytic anaemia. *Histopathol* 41:179–180.
Mason, K.D., and Juneja, S.K. (2003) Spontaneous rupture of the spleen as the presenting feature of the blastoid variant of mantle cell lymphoma. *Clin Lab Haematol* 25:263–265.
Oinonen, R., Franssila, K., and Elonen, E. (1997) Spontaneous splenic rupture in two patients with a blastoid variant of mantle cell lymphoma. *Ann Hematol* 74:33–35.
Pabst, R., and Westermann, J. (1992) Regeneration of the spleen and splenic autotransplantation. *Br J Surg* 79:91.
Sandler, S.G. (2000) The spleen and splenectomy in immune (idiopathic) thrombocytopenic purpura. *Semin Hematol* 37:10–12.
Taylor, A.J., Dodds, W.J., Erickson, S.J., and Stewart, E.T. (1991) CT of acquired abnormalities of the spleen. *Am J Roentgenol* 157:1213–1219.
Treutner, K.H., Klosterhalfen, B., Winkeltau, G., Moench, S., and Schumpelick, V. (1993) Vascular anatomy of the spleen: The basis for organ-preserving surgery. *Clin Anat* 6:1–8.
Wisner, D.H., and Blaisdell, F.W. (1992) When to save the ruptured spleen. *Surgery* 111:121–122.

Hyperplastic and Dysplastic Changes of the Spleen

Splenic Hyperplasia

Hyperplasia of the spleen may involve the white pulp and lymphoid proliferation or may be primarily of sinus areas. These do not usually occur together and follicular hyperplasia is usually accompanied by compression of the sinuses; sinus distension or sinus hyperplasia is usually seen with follicular and even thymic-dependent atrophy (Figs. 2.151–2.153). Hypersplenism is a condition of increased blood destruction by the spleen accompanied by marrow hyperplasia and cytopenia of one or more elements of the blood. Splenomegaly may not be observed. Hyperfunction of the sinus areas of the spleen may occur in a spleen of normal size with histologic evidence of increased numbers of macrophages; often, hemosiderosis

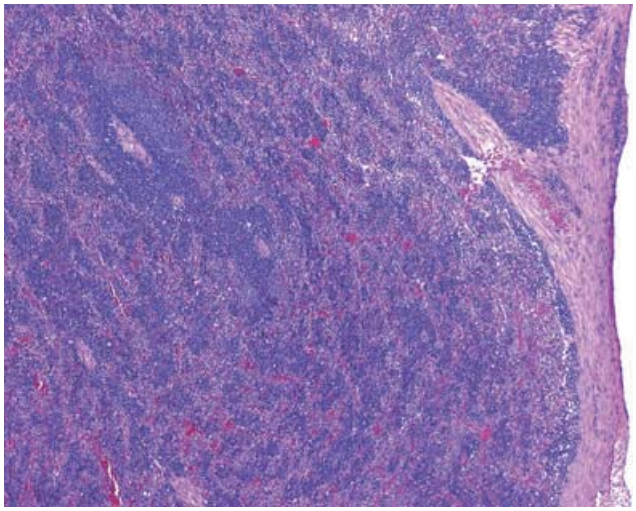

Figure 2.151. Dog: spleen. There is atrophy of periarteriolar lymphoid sheath (upper left) and marked multifocal areas of sinus hematopoiesis primarily of erythroid type. Changes are compatible with chronic hemolysis or blood loss.

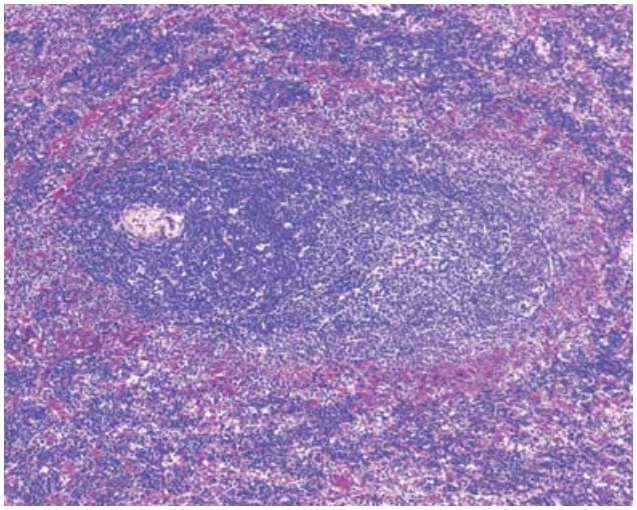

Figure 2.152. Dog: spleen. Prominent periarteriolar lymphoid sheath and germinal center with atrophy of the mantle cell cuff. There is mild marginal zone hyperplasia with an increased level of reactivity evident in the uniform dilation of the peripheral sinus made prominent by the greater proportion of red cells.

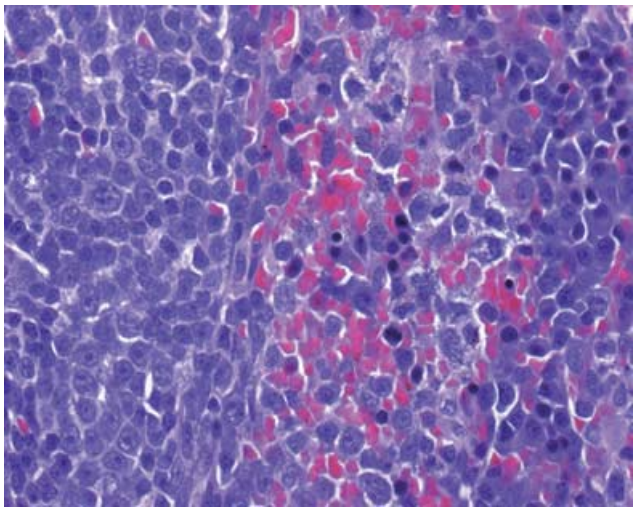

Figure 2.153. Detail of Figure 2.152. Lymphocytes with small densely stained nuclei (left) are remnants of the fading mantle cell cuff with marginal zone cells lying adjacent and appearing irregularly within the sheath of the lymphoid follicle. The central area is the expanded peripheral sinus with pigment-bearing macrophages on the outer surface of the sinus. Extramedullary hematopoiesis and plasma cells are seen at the right of the image.

and sinuses may have irregular distension that is not perceived as peliosis. Hypersplenism may be accompanied by immune sensitization of any one of the cellular elements but may be entirely mechanical. An enlarged spleen of any cause results in slower passage of cells through the sinus areas that in itself is a hazard to cell survival. The environment of the sinus plasma is of lowered pH, cholesterol, and glucose as compared to the peripheral circulation. Under these circumstances red cells especially are prematurely aged in a process known as *conditioning* (Figs. 2.154–2.156).

Extramedullary hematopoiesis (EMH) is one of the most common types of sinus hyperplasia that occurs in all species and occurs normally in mice at all ages. EMH is usually of trilineage type, but any one cell line may predominate depending on the condition and the ability of the marrow to respond. In the dog with immune-mediated hemolytic anemia, the EMH is largely erythroid but other cells are always present to some degree. If there is concurrent thrombocytopenia, megakaryocytes may be prominent as well, particularly near the muscular trabeculae. In the dog with immune-mediated anemia it may not be possible to determine if the spleen is producing more cells than it is destroying without resorting to tracking isotopically labeled red cells.

Myelolipoma is a benign proliferation of fatty tissue with varying amounts of trilineage hematopoiesis that occurs in as a focal mass in spleen and liver (Fig. 2.157). In spleen, the fatty tissue contrasts sharply with the surrounding sinus areas that delineate the areas involved (Figs. 2.158, 2.159). They are primarily important only to recognize they are not neoplastic.

Myeloid metaplasia is characterized by marked EMH with myeloid predominance and is dealt with under dysplastic changes. In acute septicemia (as occurs in calves with Salmonellosis and rarely in canine pyometra), the

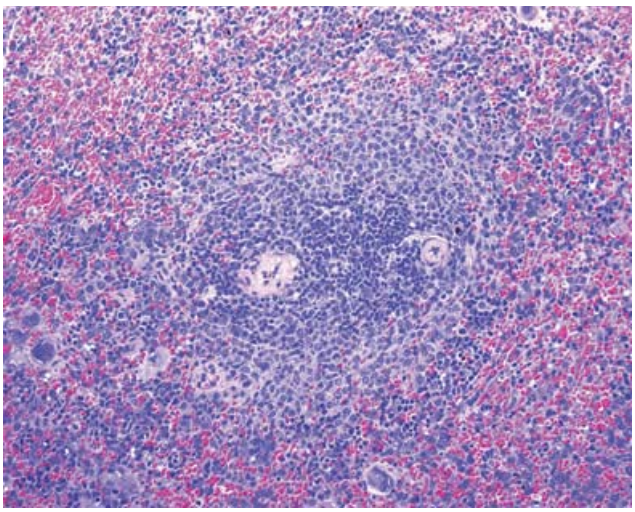

Figure 2.155. Detail of Figure 2.154. The periarteriolar lymphoid sheath has marked reduction in lymphoid area and is surrounded by a lighter staining zone of marginal cell hyperplasia. The sinus areas have dilation of vascular spaces with a mild increase in phagocytic cells. An increase in extramedullary hematopoiesis with numerous megakaryocytes is also seen.

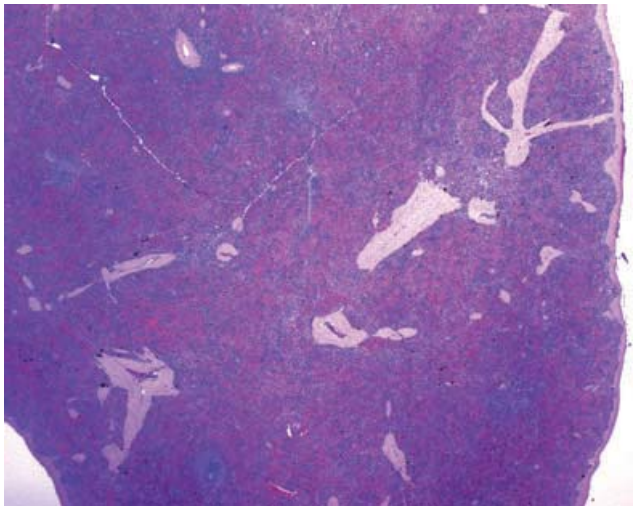

Figure 2.154. Dog: spleen, immune thrombocytopenic purpura. The spleen is enlarged as can be deduced from the thinned capsule and quite widely separated smooth muscle trabeculae. There is atrophy of periarteriolar lymphoid sheaths and a complete absence of germinal centers, likely due to immunosuppressive therapy. There is quite marked expansion of sinus areas.

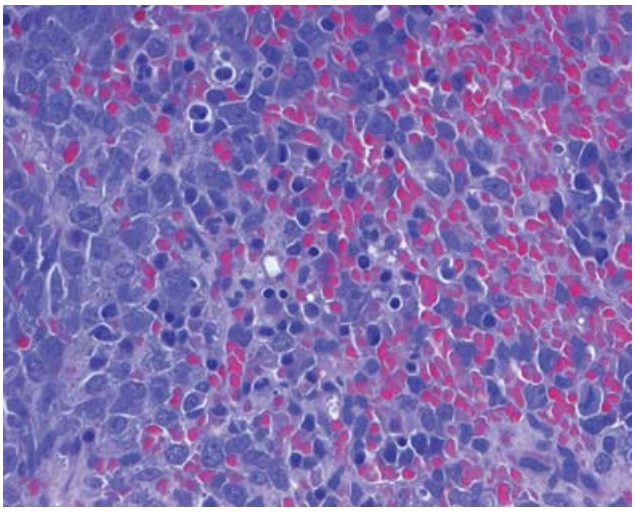

Figure 2.156. Detail of Figure 2.155. The curved encapsulation of the periarteriolar lymphoid sheath is at the left of the image, with a narrow irregular zone of marginal cell hyperplasia adjacent. The sinus areas are dilated with relatively low cellularity and scattered hematopoiesis.

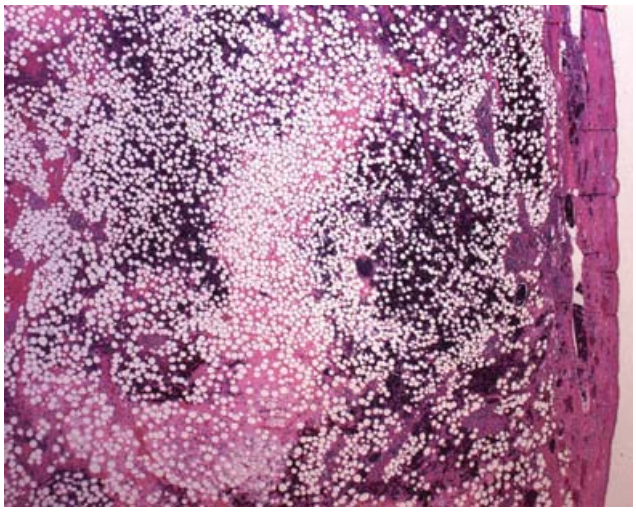

Figure 2.157. Dog: spleen. A large myelolipoma contains a central area of ischemic infarction. Clear cells represent clusters of normal-appearing adipocytes.

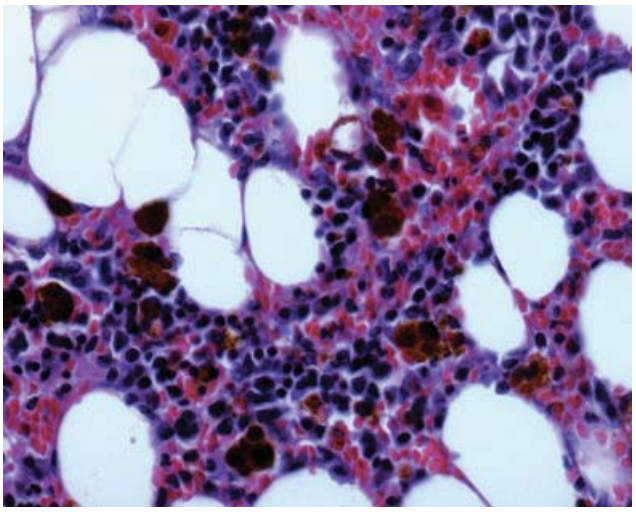

Figure 2.159. Detail of Figure 2.158. Normal fat cells surrounded by trilineage hematopoiesis with erythroid predominance and numerous large macrophages heavily laden with coarse hemosiderin granules.

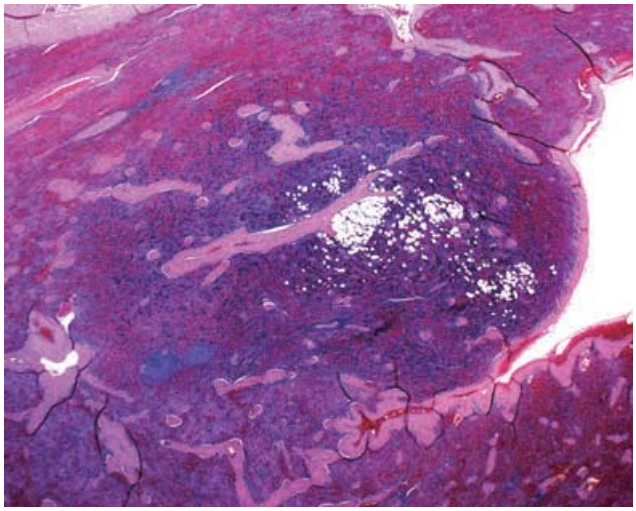

Figure 2.158. Dog: spleen. Focal myelolipoma with small clusters of fat cells is surrounded by deeper staining areas of splenic sinus due to presence of dense trilineage extramedullary hematopoiesis.

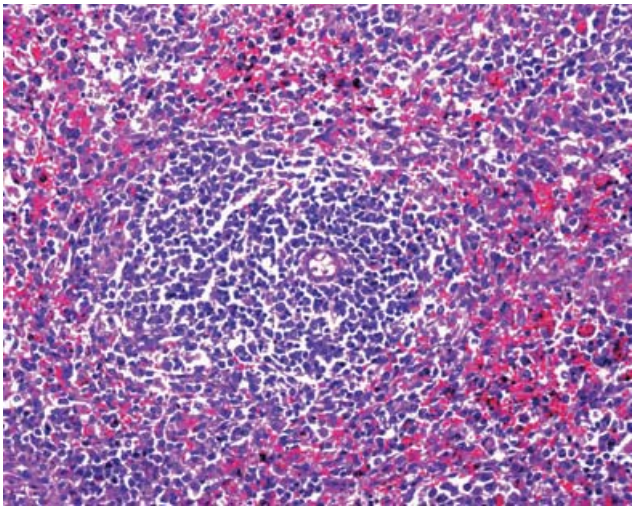

Figure 2.160. Dog: spleen, septic shock. Arteriole with involuting periarteriolar lymphoid sheath, with reduced cell density due to apoptosis and with dilation of peripheral sinuses.

germinal centers are outlined by a reddened ring consisting of a dilated peripheral sinus (Figs. 2.160–2.163). The perifollicular sinus area contains the cells that are most predominant in the peripheral blood circulation; dogs will have many mature neutrophils present, whereas calves will have few mature neutrophils with immaturity to myelocytes (Figs. 2.164, 2.165). These changes are very dynamic and the animal either succumbs to disease at this stage or contains the infection. If the animal survives, the splenic reaction becomes more of a general sinus hyperplasia with a follicular reaction following in several days.

Hyperplasia of the white pulp or lymphoid areas of the spleen is seen in chronic systemic infections as occurs in bovine trypanosomiasis, equine infectious anemia, feline leukemia virus, or pseudorabies virus infection of swine. A very vibrant follicular hyperplasia will have large well-defined germinal centers that have complete cuffs of mantle cells and may have some marginal zone cells in eccentric layers outside the mantle cell

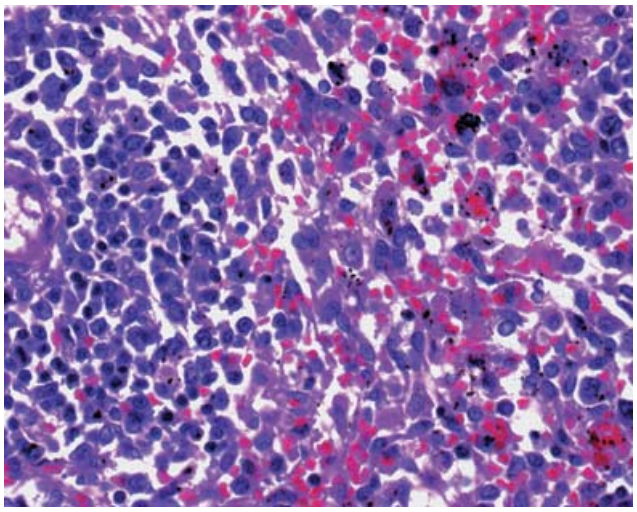

Figure 2.161. Detail of Figure 2.160. Atypical response in a dog with marrow failure and neutropenia permits septicemia and toxemia. The peripheral sinus has low cellularity with only very immature granulocytes present.

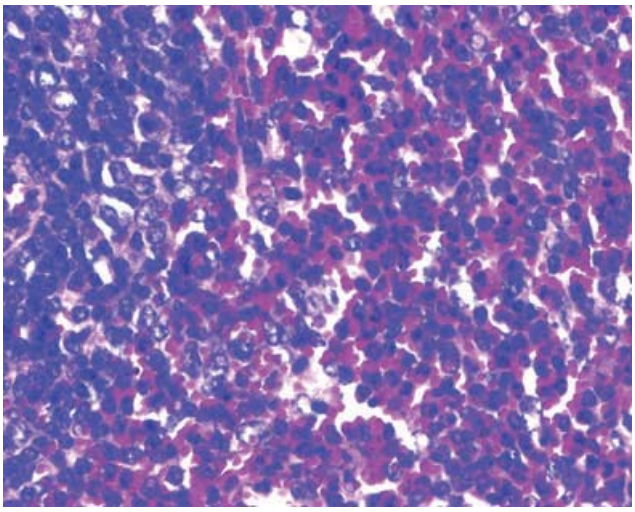

Figure 2.163. Detail of Figure 2.162. The arteriole and surrounding lymphoid sheath (left), with the peripheral sinus above that contains a high level of mature granulocytes, which is an atypically strong response for the calf.

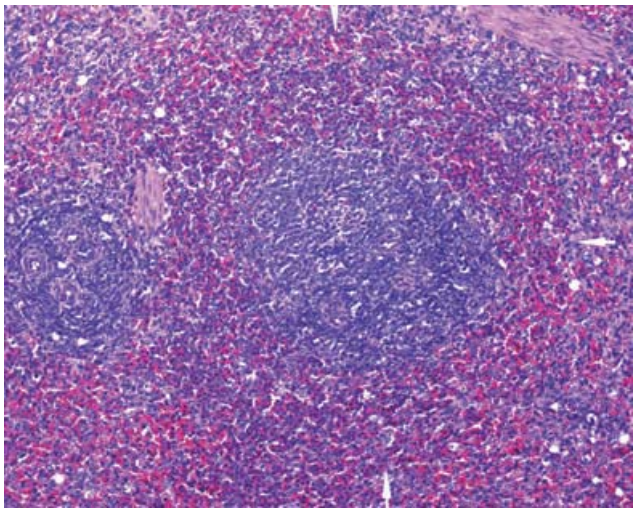

Figure 2.162. Calf: spleen, salmonella septicemia. Periarteriolar lymphoid structure is sharply delineated with marked dilation of the peripheral sinus (arrows), which has high cellularity.

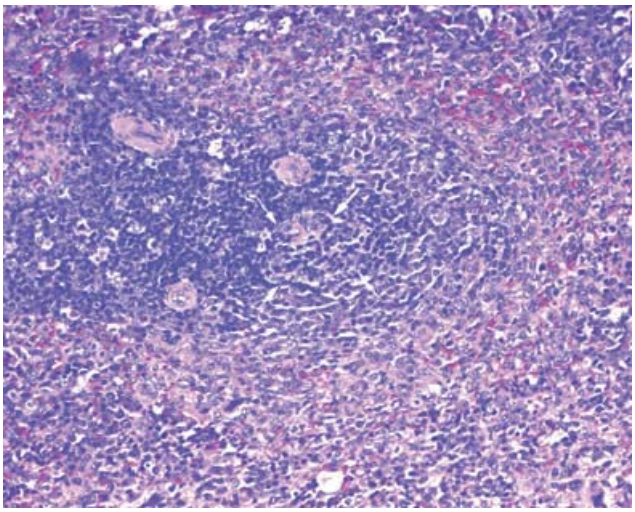

Figure 2.164. Dog: spleen, pyometra. There is atrophy of the periarteriolar lymphoid sheath with a hypocellular germinal center with follicular hyalinosis (arrows, center) surrounded by a narrow band of darkly stained mantle cells. A broad band of marginal zone hyperplasia lies between the mantle cells and a dilated peripheral sinus with very high cellularity.

cuffs (Fig. 2.166). Marginal zone hyperplasia does not usually occur with complete mantle cell cuffs and more often is seen with follicular involution of some degree (Fig. 2.167). Frequently there is also atrophy of the thymic-dependent periarteriolar lymphoid sheaths (PALS, Figs. 2.168, 2.169). Because so-called nodular hyperplasia or fibrohistiocytic nodule (Figs. 2.170, 2.171) is so often associated with other lesions, including inflammatory pseudotumor, plasmacytoma, fibrous dysplasia, and mantle cell or marginal zone lymphoma, these changes are considered as dysplastic lesions.

Splenic Dysplastic Changes

Nodular lesions of the spleen that project above the normal contour of the splenic capsule may have a variety of causes, most often due to types of lymphoid hyperplasia or angiomatous dilations of sinuses. Abscesses of the spleen are uncommon and may be miliary or large multifocal and due to pyogenic bacteria. Splenic cysts due to *Cyticercus* sp. or hydatid cestodes have occurred but are

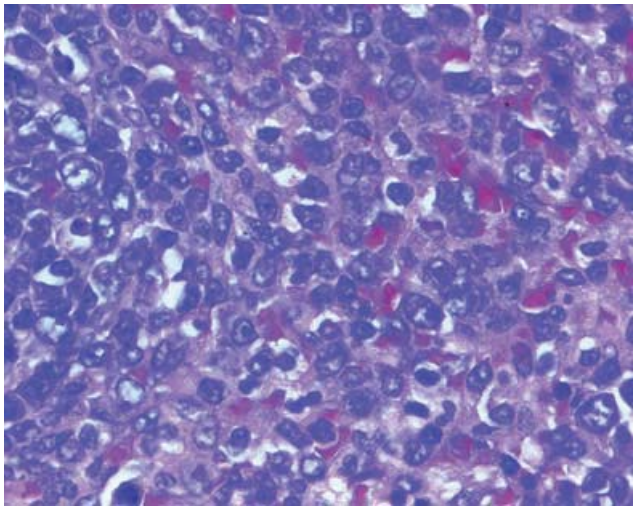

Figure 2.165. Detail of Figure 2.164. Dilated peripheral sinus contains a high level of mature segmented neutrophils and large lymphocytes, typical of increased granulopoiesis in the face of localized sepsis.

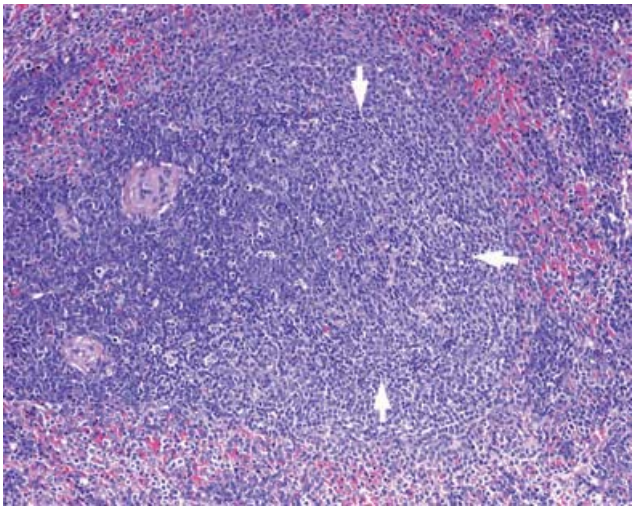

Figure 2.167. Dog: spleen, chronic immune stimulation. Periarteriolar lymphoid sheaths are reduced in volume (left), with the germinal center poorly outlined by a fading and incomplete mantle cell cuff (arrows). A continuous layer of marginal zone hyperplasia lies outside of the mantle cell cuff area.

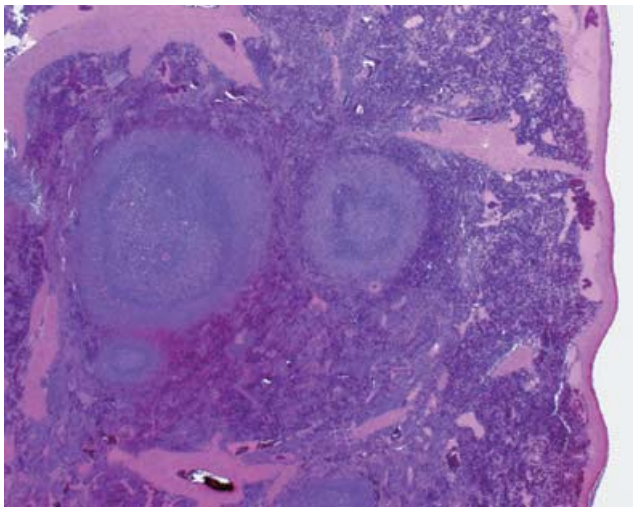

Figure 2.166. Dog: spleen, atypical follicular hyperplasia with marked variation in size of germinal centers have irregular atrophy of the mantle cell cuffs and prominent peripheral bands of marginal zone hyperplasia.

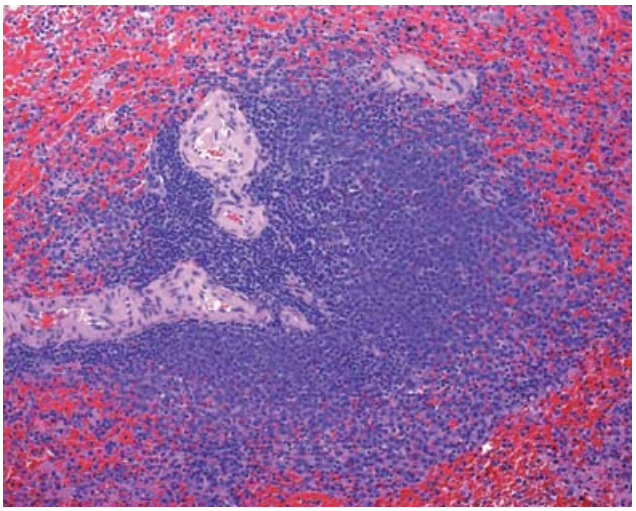

Figure 2.168. Dog: spleen. The animal presented with a markedly enlarged spleen due to widespread hemorrhagic infarction within an area of myelolipoma. There is marked atrophy of the small lymphocytes of the periarteriolar lymphoid sheath, with a surrounding area of marginal zone hyperplasia and a dilated peripheral sinus. A germinal center is likely present in an adjacent plane of section.

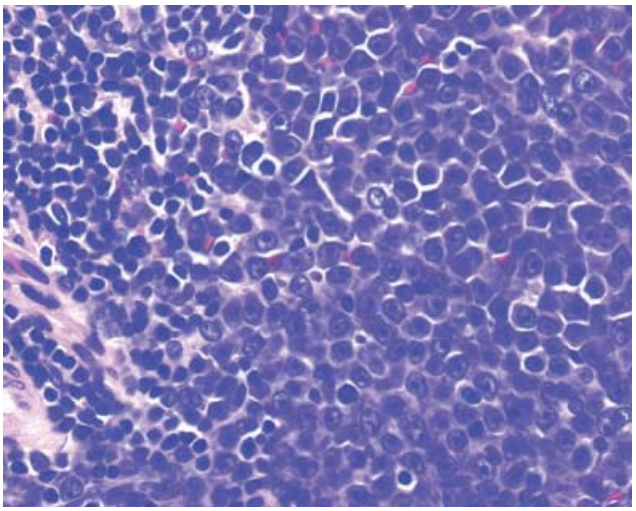

Figure 2.169. Detail of Figure 2.168. Arteriole with residual small lymphocytes at the bottom left, surrounded by a broad zone of lymphocytes with intermediate-sized nuclei that have prominent single central nucleoli and quite abundant cytoplasm, typical of marginal zone cells.

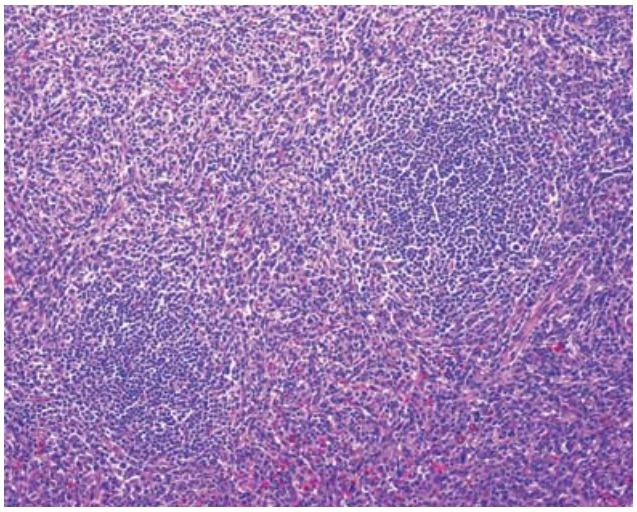

Figure 2.170. Dog: spleen, fibrohistiocytic nodule with involuting areas of lymphoid proliferation surrounded by connective tissue and mixed cellularity.

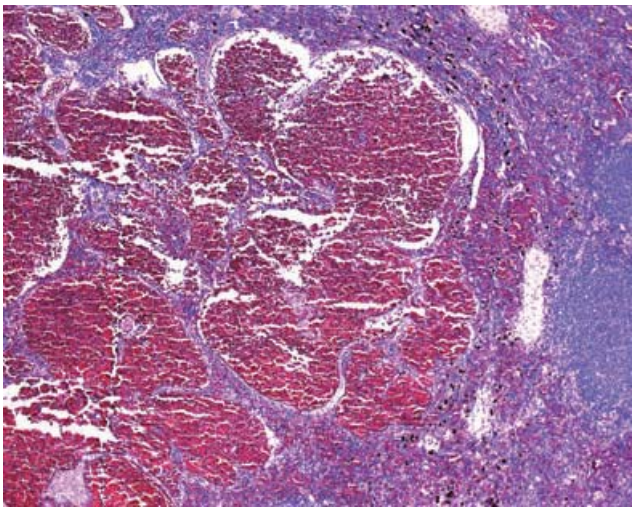

Figure 2.172. Dog: spleen, myelolipomas and littoral cell sinus ectasia. There are closely aggregated clusters of sinus dilation lined by endothelial partitions of varying width.

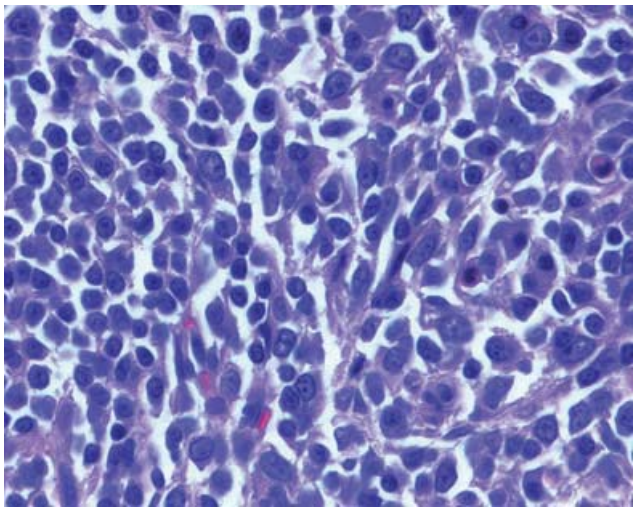

Figure 2.171. Detail of Figure 2.170. A fading area of lymphoid proliferation is at the left, surrounded by cells with oval nuclei of the stromal background plus small to large lymphocytes, plasma cells, and several eosinophils.

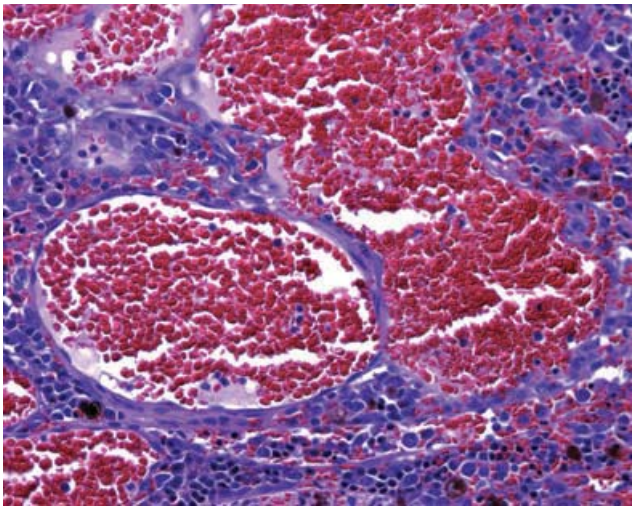

Figure 2.173. Detail of Figure 2.172. Benign but atypical areas of sinus dilation, limited by flattened benign endothelial cells.

not seen under current management systems. Focal clusters of sinuses may become widely dilated forming multiple histological foci of 15–20 cross sections of dilated sinuses, each from about 0.5–1.0 mm in diameter (Figs. 2.172, 2.173). These structures are lined by littoral cells that have low, flat nuclei and narrow flattened layers of cytoplasm that contains fine basophilic granular debris and hemosiderin (Fig. 2.174). In foci of this type with closely clustered small areas of venous ectasia, the endothelial lining cells react positively for CD31 and focally for lysozyme (Figs. 2.175, 2.176). Sinus cystic foci of this small type are seen with large cystic hematomas 2–5 cm in diameter, which undergo pathologic examination because of removal for suspected hemangiosarcoma, which is often present. Cysts of this small clustered type are found in human splenic lesions, are known as littoral cell angiomas, and may become metastatic. In the dog, the biological intent and importance of these lesions are largely unknown. Their association with hemangiosarcoma suggests that they be looked on as a precursor lesion as they become better recognized and studied. It would be logical to consider these lesions as dysplastic changes of sinus lining cells that focally may dedifferentiate to a benign or malignant vascular neoplasm.

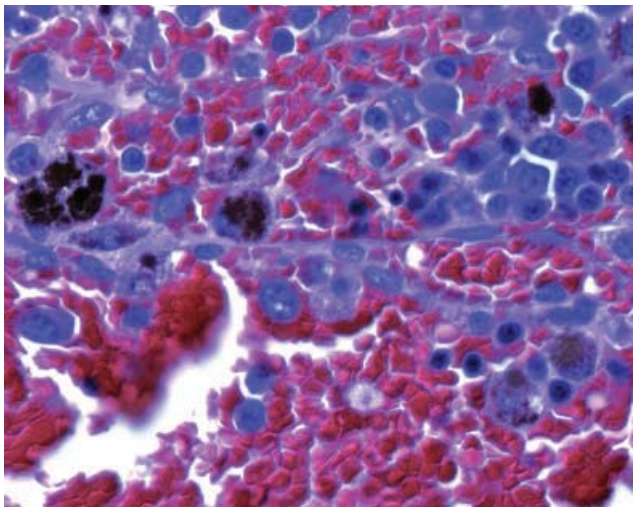

Figure 2.174. Detail of Figure 2.173. Littoral sinus lining cells irregularly project into the vascular spaces with abundant cytoplasm and ingested debris, likely hemosiderin. The large cells with black pigment are hemosiderin-laden sinus macrophages.

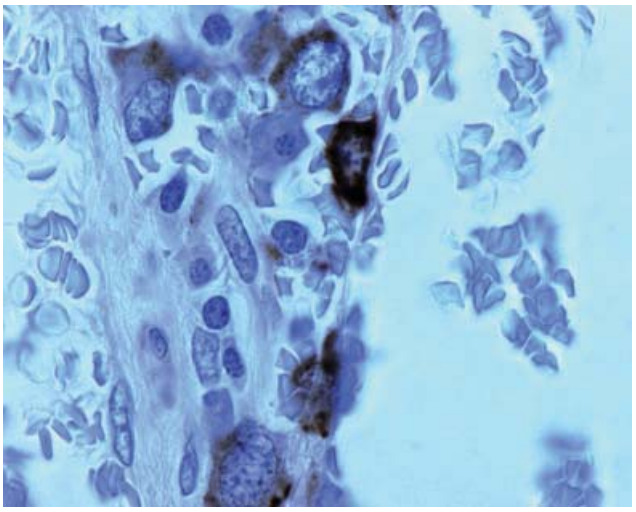

Figure 2.176. Detail of Figure 2.174, stained for lysozyme. The same area as Figure 2.175. Sinus lining cells react irregularly and strongly for cells with phagocytic characteristics.

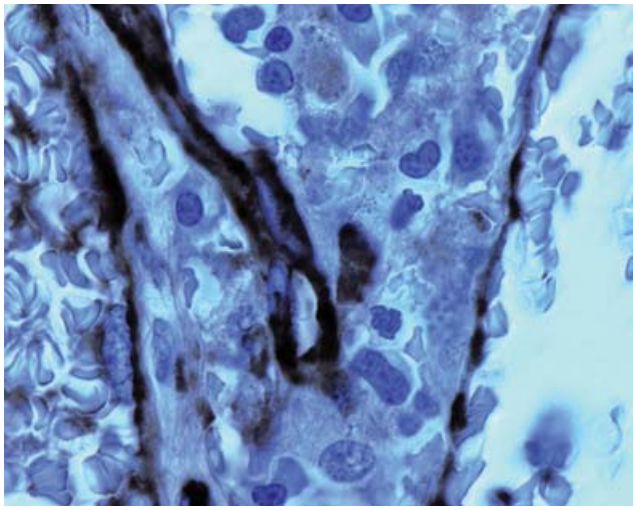

Figure 2.175. Detail of Figure 2.174, CD31 stained to identify endothelial cells. Venous sinuses are lined by a continuous layer of vascular endothelium.

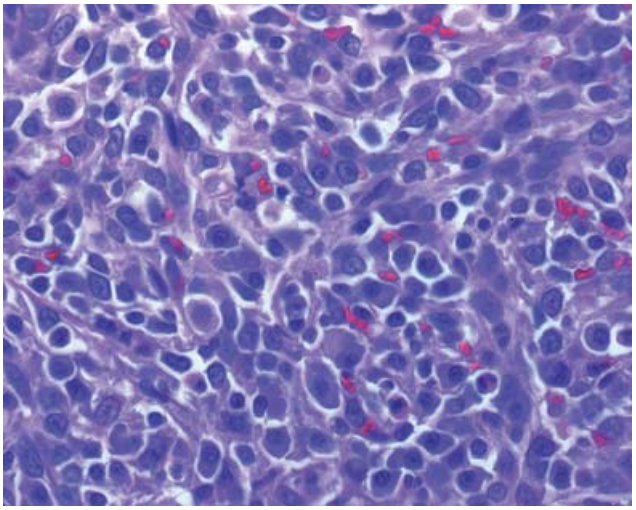

Figure 2.177. Dog: spleen. Focal sclerotic lesion resembles human inflammatory pseudotumor, accompanied by sclerotic background, numerous plasma cells, and hemosiderin-bearing macrophages.

The focal nodular proliferations of the canine spleen commonly referred to as *nodular hyperplasia* or *fibrohistiocytic nodules*, deserve further definition. Occasionally nodular lesions appear in canine spleen that are largely fibrotic and have irregular infiltration with plasma cells, small and medium lymphocytes, and large hemosiderin-bearing macrophages (Fig. 2.177). These lesions resemble what is referred to in the human spleen as *inflammatory pseudotumor* and are differentiated from a similar lesion of spleen and other soft tissues known as *inflammatory myofibroblastic tumor* by being negative for the ALK tyrosine kinase that is found in anaplastic large cell lymphoma of T-cell type. Little is known of these lesions in animals, but it is likely that most lesions with this general type of histology are called *malignant fibrous histiocytoma*. Also part of this complex of lesions are lesions characterized by focal proliferation of lymphocytes and usually large foci of ischemic or hemorrhagic infarction (Fig. 2.178).

If the lesions are solid lymphoid proliferation and 1–2 cm in diameter, they are likely a large cell lymphoma or what has been interpreted to be benign nodular lymphoid hyperplasia. Some of these lesions contain fading

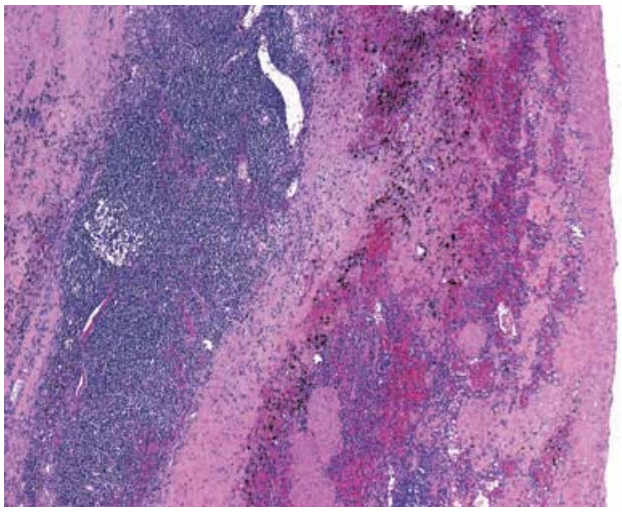

Figure 2.178. Dog: spleen, nodular lymphoid proliferation. Irregular areas of sclerosis and lymphoid proliferation are accompanied by focal areas of ischemic necrosis.

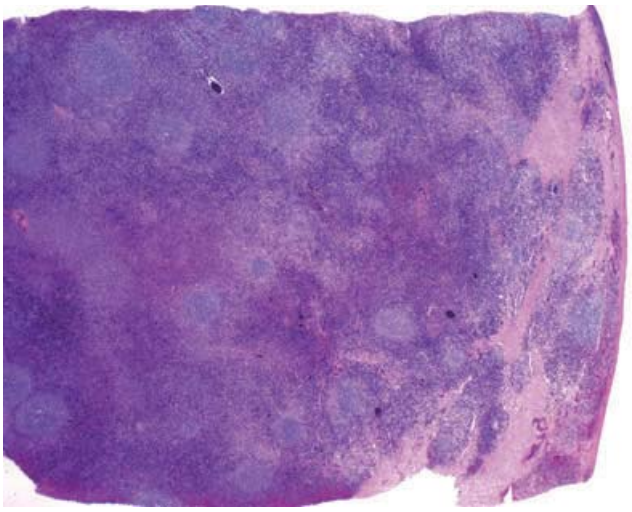

Figure 2.179. Dog: spleen, foci of nodular proliferation, interpreted to be a fibrohistiocytic nodule with multiple small foci of lymphoid proliferation. The irregularly thinned splenic capsule is at the right.

germinal centers surrounded by concentric rings of small lymphocytes like a human Castleman's lymphoma. When multifocal, it can usually be deduced that the areas of proliferation have the periodicity of end arterioles with some centered on hypocellular or hyalinized germinal centers and are MCLs. It is likely that all the focal lymphoid proliferations are centered on involuted germinal centers that are not present in the plane of section.

Early lesions often associated with nodular splenic proliferations are smaller, and they don't appear to be associated with arterioles but are surrounded by a stromal encapsulation and consist of typical mantle cells with small regular round nuclei and occasional nucleoli but without mitoses (Figs. 2.179, 2.180). These lesions are likely hyperplastic and dysplastic and should be identified as mantle cell hyperplasia (MCH). These foci of lymphoid proliferation are surrounded by quite dense connective tissue, which is irregularly infiltrated with plasma cells that have the atypia and binucleation of plasmacytomas.

A further lesion found in splenic hyperplastic nodules are also centered on end arterioles and germinal centers. These lesions are more obvious because residual foci of mantle cell cuffs makes it apparent that the proliferating cells are arising outside of the mantle cells and are therefore of marginal zone type and likely hyperplastic (Fig. 2.181). Marginal zone hyperplasia (MZH) cells have typical cytomorphology characterized by round nuclei 1.5 red cells in diameter that have chromatin peripheralization onto the nuclear membrane to a variable degree, making a single large central nucleolus appear very prominent (Fig. 2.182). In hyperplasias the marginal zone cuff has a heterogeneous cell population

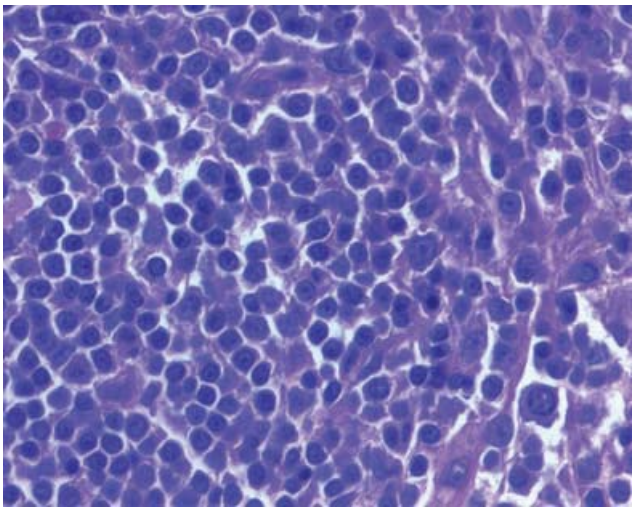

Figure 2.180. Detail of Figure 2.179. The focal areas of lymphoid proliferation consist of a homogenous population of cells with small, round, densely stained nuclei with small or inapparent nucleoli and a narrow rim of quite densely stained cytoplasm. These cells are strongly positive for B-lymphocyte markers and likely constitute focal mantle cell hyperplasia.

with intermixed small mantle cells and others of larger size with less prominent nucleoli. Cells of malignant MZL have a more vesicular appearance and are more homogeneous in cell type. Both the mantle cell and the marginal zone proliferations are characterized by very low mitotic rate, with most fields at 400× having no mitoses at all. All these lesions have hyperplastic and neoplastic variations with the gray area between them still requiring better

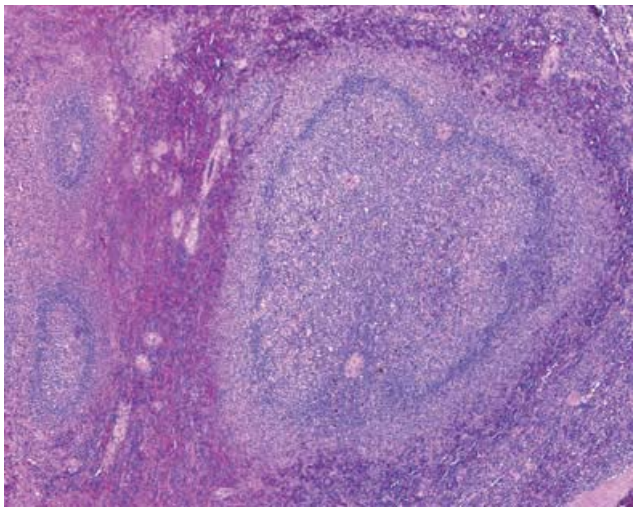

Figure 2.181. Dog: spleen, marginal zone hyperplasia. Germinal centers of varying size with a narrow residual cuff of deeply stained mantle cells identify the outer lighter-stained area of cellular proliferation as marginal zone hyperplasia. Note that the large germinal center surrounds the arterioles rather than being eccentric to them as an indication of atypical hyperplasia.

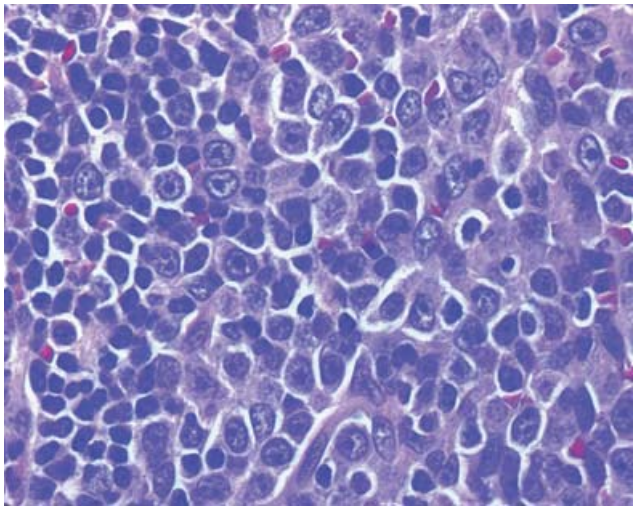

Figure 2.182. Detail of Figure 2.181. Narrow mantle cell cuff is at the left with marginal zone cells above having typical prominent single central nucleoli. The intermixing with other cells in the marginal zone layer is typical of marginal zone hyperplasia and unlike marginal zone lymphoma. Note the lack of mitotic figures.

definition. This uncertainty justifies their study by clonal analysis to provide molecular definition of the hyperplastic and neoplastic boundary for better definition on microscopic examination. These conditions are included here as dysplasias that with persistence have the propensity to become malignant.

REFERENCES

Al-Omishy, H., Lockett, C., Rees, J.A., and Davidson, B.R. (1997) Splenomegaly. *Postgrad Med J* 73:125–126.

Anadol, A.Z., Oguz, M., Bayramoglu, H., and Edali, M.N. (1998) Cystic lymphangioma of the spleen mimicking hydatid disease. *J Clin Gastroenterol* 26:309–311.

Arber, D.A., Strickler, J.G., and Weiss, L.M. (1997) Splenic mesothelial cysts mimicking lymphangiomas. *Am J Surg Pathol* 21:334–338.

Bach, J.-M., Hurtrel, M., Chakrabarti, L., Ganiere, J.-P., Montagnier, L., and Hurtrel, B. (1994) Early stages of feline immunodeficiency virus infection in lymph nodes and spleen. *AIDS Res Hum Retroviruses* 10:1731–1738.

Bonilla, F., Provencio, M., Fernandez, E., and España, P. (1994) Malignant fibrous histiocytoma of the spleen and chronic myelogenous leukemia. A case report. *Oncol* 51:465–466.

Burchard, G.D., Reimold-Jehle, U., Bürkle, V., Kretschmer, H., Vierbuchen, M., Racz, P., and Lo, Y. (1996) Splenectomy for suspected malignant lymphoma in two patients with loiasis. *Clin Infect Dis* 23:979–982.

Burke, J.S. (1993) Splenic lymphoid hyperplasias versus lymphomas/leukemias: A diagnostic guide. *Am J Clin Pathol* 99:486–493.

Chotivanich, K., Udomsangpetch, R., McGready, R., Proux, S., Newton, P., Pukrittayakamee, S., Looareesuwan, S., and White, N.J. (2002) Central role of the spleen in malaria parasite clearance. *J Infect Dis* 185:1538–1541.

Colovic, M., Jankovic, G., Perisic-Savic, M., and Colovic, R. (1993) Splenic lymphoma with circulating villous lymphocytes and huge pseudocyst of the spleen. *J R Soc Med* 86:361.

Cowles, R.A., and Yahanda, A.M. (2000) Epidermoid cyst of the spleen. *Am J Surg* 180:227.

Dalal, B.I., Greenberg, H., Quinonez, G.E., and Gough, J.C. (1991) Inflammatory pseudotumor of the spleen—Morphological, radiological, immunophenotypic, and ultrastructural features. *Arch Pathol Lab Med* 115:1062–1064.

Engel, P., Tjalve, E., and Horn, T. (1993) Peliosis of the spleen associated with a paraganglioma. Case report. *Acta Radiol* 34:148–149.

Estrella, M., and Cosgrove, S.E. (2002) Images of Osler—Cases from the Osler Medical Service at Johns Hopkins University—Bartonella henselae infection of the liver and spleen. *Am J Med* 113:344–346.

Gärtner, F., Santos, M., Gillette, D., and Schmitt, F. (2002) Inflammatory pseudotumour of the spleen in a dog. *Vet Rec* 150:697–698.

Kraus, M.D., and Dehner, L.P. (1999) Benign vascular neoplasms of the spleen with myoid and angioendotheliomatous features. *Histopathol* 35:328–336.

Kraus, M.D., Fleming, M.D., and Vonderheide, R.H. (2001) The spleen as a diagnostic specimen—A review of 10 years' experience at two tertiary care institutions. *Cancer* 91: 2001–2009.

Kutok, J.L., Pinkus, G.S., Dorfman, D.M., and Fletcher, C.D.M. (2001) Inflammatory pseudotumor of lymph node and spleen: An entity biologically distinct from inflammatory myofibroblastic tumor. *Hum Pathol* 32:1382–1387.

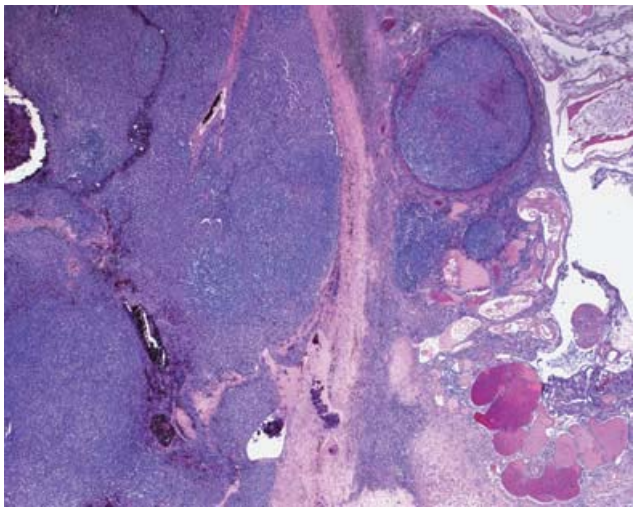

Figure 2.183. Dog: spleen, metastatic histiocytic sarcoma. There is extensive colonization of splenic serosal vessels, and solid areas of cellular proliferation are compressing narrow bands of residual splenic sinus.

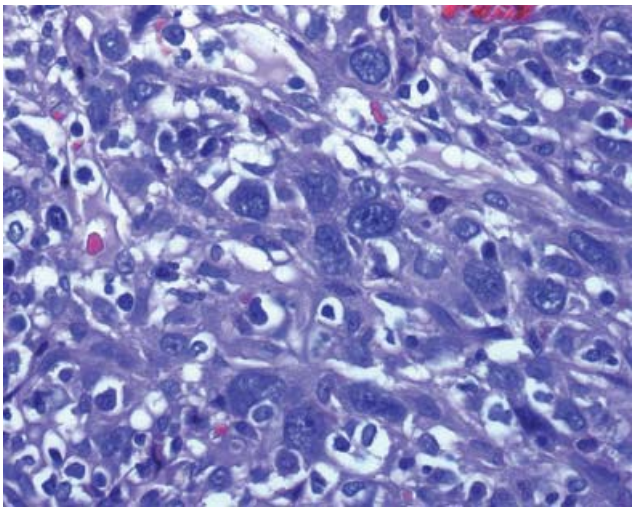

Figure 2.184. Detail of Figure 2.183. Neoplastic cells with abundant cytoplasm, marked anisokaryosis, and numerous mitoses. The cells mark positively with CD18.

Lamb, P.M., Lund, A., Kanagasabay, R.R., Martin, A., Webb, J.A.W., and Reznek, R.H. (2002) Spleen size: How well do linear ultrasound measurements correlate with three-dimensional CT volume assessments? *Br J Radiol* 75:573–577.

Özen, S., Ferhanoglu, B., Senocak, M., and Tüzüner, N. (1997) Idiopathic myelofibrosis (agnogenic myeloid metaplasia): Clinicopathological analysis of 32 patients. *Leuk Res* 21: 125–131.

Puli, S.R., Presti, M.E., and Alpert, M.A. (2003) Splenic granulomas in Crohn disease. *Am J Med Sci* 326:141–144.

Sandler, S.G. (2000) The spleen and splenectomy in immune (idiopathic) thrombocytopenic purpura. *Semin Hematol* 37:10–12.

Spangler, W.L., and Kass, P.H. (1998) Pathologic and prognostic characteristics of splenomegaly in dogs due to fibrohistiocytic nodules: 98 cases. *Vet Pathol* 35:488–498.

Spangler, W.L., and Kass, P.H. (1999) Splenic myeloid metaplasia, histiocytosis, and hypersplenism in the dog: 65 cases. *Vet Pathol* 36:583–593.

Taylor, A.J., Dodds, W.J., Erickson, S.J., and Stewart, E.T. (1991) CT of acquired abnormalities of the spleen. Am J *Roentgenol* 157:1213–1219.

Treutner, K.H., Klosterhalfen, B., Winkeltau, G., Moench, S., and Schumpelick, V. (1993) Vascular anatomy of the spleen: The basis for organ-preserving surgery. *Clin Anat* 6:1–8.

Weston, J., Balfour, B.M., Tsohas, W., English, N., Farrant, J., and Webster, A.D.B. (1993) Splenic lesions in hypogammaglobulinaemia. *Adv Exp Med Biol* 329:437–441.

Wisner, D.H., and Blaisdell, F.W. (1992) When to save the ruptured spleen. *Surgery* 111:121–122.

Zingman, B.S., and Viner, B.L. (1993) Splenic complications in malaria: Case report and review. *Clin Infect Dis* 16:223–232.

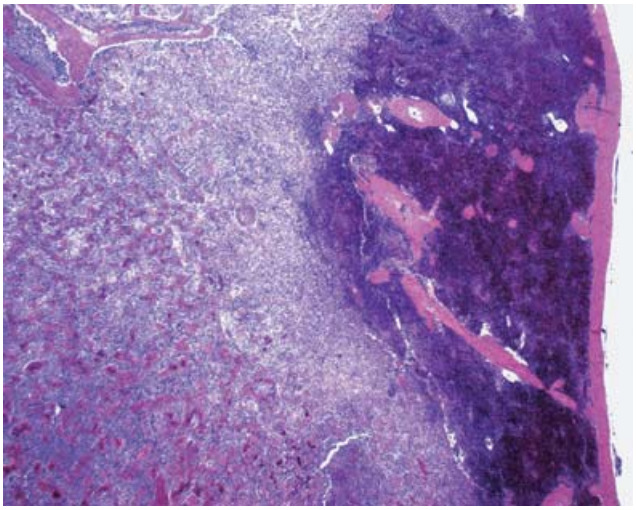

Figure 2.185. Dog: spleen, metastatic osteosarcoma. Intact but congested splenic sinus at the top lies above a large area of neoplastic proliferation that consists of interlacing bands of osteoid.

Splenic Metastatic Neoplasms

The spleen is often involved in metastatic neoplastic disease. Nonhematopoietic sarcomas that originate in the spleen include hemangiosarcoma, leiomyomas, leiomyosarcomas, and fibrosarcomas. In humans, when the spleen is involved in metastatic carcinoma there typically are already widespread areas of tumor in other tissues. In animals, the spleen is most often involved in metastatic sarcoma rather than carcinoma (Figs. 2.183–2.188). The reason generally expressed for the low

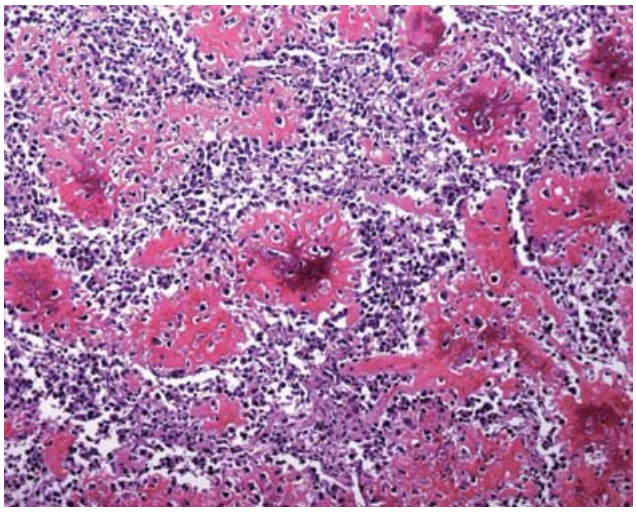

Figure 2.186. Detail of Figure 2.185. Irregular foci of osteoid matrix (enclosing the progenitor cells) are surrounded by a densely cellular background of neoplastic osteoblasts.

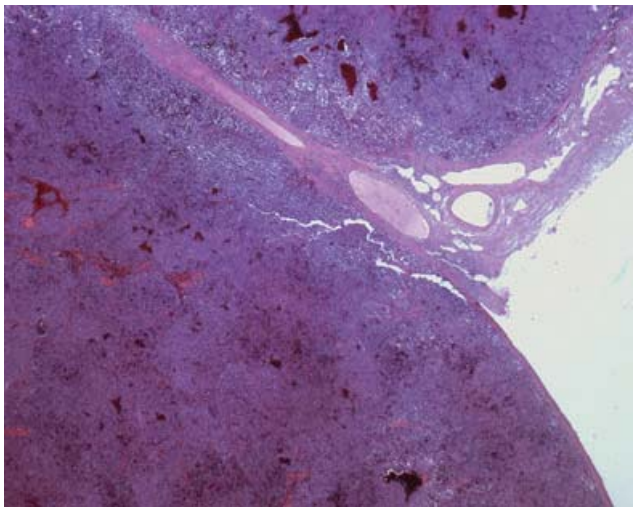

Figure 2.187. Cat: spleen, metastatic mast cell tumor. The spleen is markedly enlarged with thinning of the capsule and displacement of the smooth muscle trabeculae with obliteration of normal sinus structure.

incidence of metastatic carcinoma in spleen is not that the spleen is not unexposed, but the sinus system is relatively efficient in preventing colonization. Even the cat with more carcinomas of the oral cavity and mammary gland than the dog, has few metastatic carcinomas in the spleen as compared to lung and regional nodes.

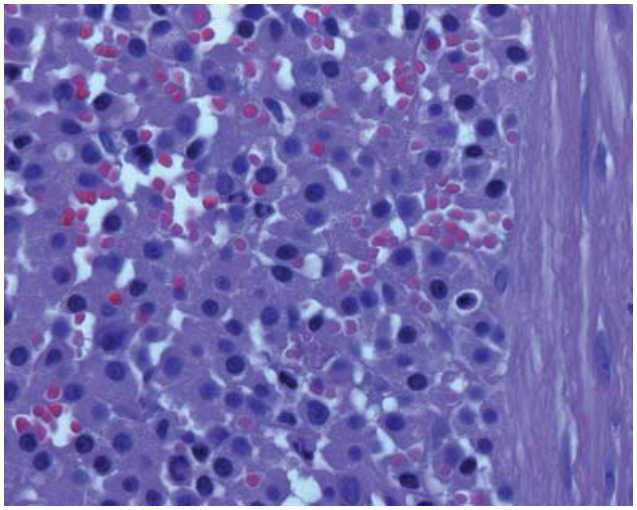

Figure 2.188. Detail of Figure 2.187. The splenic capsule (right), contains sinus areas filled with neoplastic mast cells. Note that the mast cell cytoplasmic membranes appear to form walls of venous sinuses without inducing clotting.

REFERENCES

Arber, D.A., Strickler, J.G., and Weiss, L.M. (1997) Splenic mesothelial cysts mimicking lymphangiomas. *Am J Surg Pathol* 21:334–338.

Cowles, R.A., and Yahanda, A.M. (2000) Epidermoid cyst of the spleen. *Am J Surg* 180:227.

Du, M.Q., Peng, H.Z., Dogan, A., Diss, T.C., Liu, H.Q., Pan, L.X., Moseley, R.P., Briskin, M.J., Chan, J.K.C., and Isaacson, P.G. (1997) Preferential dissemination of B-cell gastric mucosa-associated lymphoid tissue (MALT) lymphoma to the splenic marginal zone. *Blood* 90:4071–4077.

Horny, H.P., Ruck, M.T., and Kaiserling, E. (1992) Spleen findings in generalized mastocytosis—A clinicopathologic study. *Cancer* 70:459–468.

Hosotani, R., Momoi, H., Uchida, H., Okabe, Y., Kudo, M., Todo, A., and Ishikawa, T. (1992) Multiple hemangiopericytomas of the spleen. *Am J Gastroenterol* 87:1863–1865.

Hurwitz, N., and Sauter, G. (1993) Pathology of the spleen in malignant systemic diseases. *Chir Gastroenterol* 9:91–96.

Isaacson, P.G. (1998) Pathology of the spleen: Report on the workshop of the VIIIth meeting of the European Association for Haematopathology, Paris 1996. *Histopathol* 32:172–179.

Kraus, M.D., Fleming, M.D., and Vonderheide, R.H. (2001) The spleen as a diagnostic specimen—A review of 10 years' experience at two tertiary care institutions. *Cancer* 91: 2001–2009.

Weh, H.-J., and Arps, H. (1993) Involvement of the spleen and the indication for splenectomy in malignant and benign hematological diseases. *Chir Gastroenterol* 9:98–102.

Westra, W.H., Anderson, B.O., and Klimstra, D.S. (1994) Carcinosarcoma of the spleen: An extragenital malignant mixed müllerian tumor. *Am J Surg Pathol* 18:309–315.

THYMUS

Normal Form and Function

Embryology

The thymus is unique in the lymphoid organs in having tissues derived from both epithelial and mesenchymal origins. The epithelial component is derived from the foregut endoderm of the third pharyngeal pouch as paired migrations that meet on the midline and migrate caudally from the neck to the mediastinal area. The migrations from the upper area of the pharyngeal pouch form the thymic ducts and the concentric epithelial clusters known as *Hassall's corpuscles* in the fully formed organ. Migrations from the lower pouch, also thought to arise from the ectoderm of the branchial clefts, invade the mediastinal interstitial tissues forming solid nodules that then dilate into slender reticular epithelial cells that form the faceting thymic lobules. This reticular epithelium surrounds the invading vessels in narrow cuffs of pericytes that persist in maturity and are obvious following atrophy. This early structure is colonized by primitive lymphocytes from the liver and spleen at 8–10 weeks of gestation in large mammals, including humans, and much earlier in laboratory rodents.

Much of current understanding of thymic development has been learned from studies of cellular migration patterns from the yolk sac in mouse and chick embryos. Lymphoid colonization of the thymic anlagen follows the penetration of blood vessels and occurs at 7–8 days in the chick embryo and at 11 days of gestation in the mouse. At these times the only sources of lymphocytes are the yolk sac and the liver, with the former considered the major source. The vascular pattern in the thymus is formed by vessels entering each lobule via the medulla, with radiating vessels sheathed by reticular epithelial cells penetrating the cortical tissue. Some lymphocytes leave the thymus by draining lymphatics, but apparently most leave by veins, as established by cannulation of thymic arteries and veins that demonstrated a higher level of lymphocytes in the draining veins than in the arteries. The vascular patterns in embryonic development are of importance in interpreting changes in the adult organ. Thus, thymic hyperplasia may result in large irregular lobulations, but the vascular system remains inapparent. In contrast, in thymoma there are areas where the interlobular stroma becomes loosely aggregated and the vessels in these areas will have an "onion ring" type of loose encirclement by stellate cells that look stromal but mark positively with cytokeratin and are a recapitulation of the embryonic architecture.

In the caudal or ventral migration down the neck, some islands of tissue are occasionally left behind in isolation and may become hyperplastic or cystic as a cervical mass in a neonate or more likely as an acquired mass in an adult. Evidence of fetal migration of the thymus is apparent in the infrequent occurrence of small areas of normal-appearing thymic tissue embedded within the thyroid gland (Figs. 2.189, 2.190).

Thymic growth has a characteristic pattern in that growth is most rapid in postnatal and juvenile life and reaches a maximum at puberty, followed by a slow involution with some tissue remaining functional throughout life. Various events may influence this pattern. Young

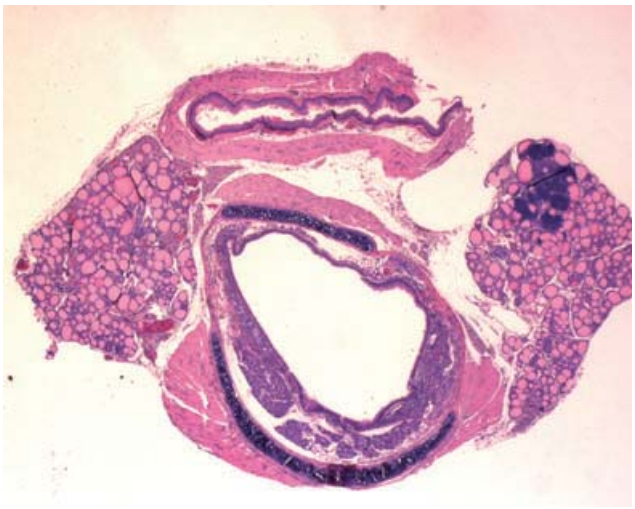

Figure 2.189. Adult wild-type mouse: trachea at the level of the thyroid gland, with a focal thymic remnant in one thyroid lobe.

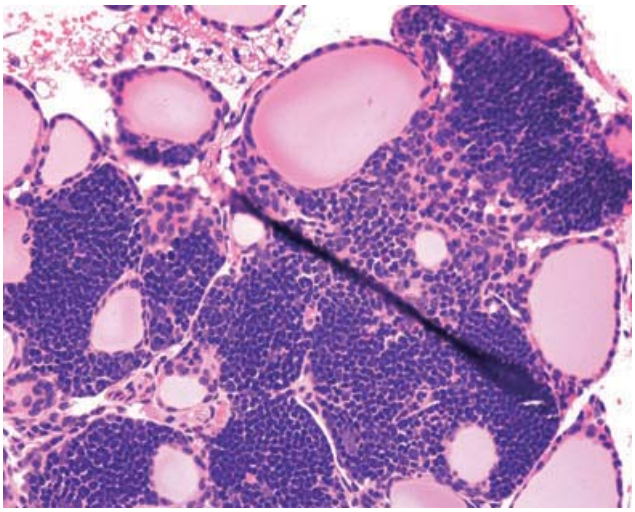

Figure 2.190. Mouse: thyroid. Detail of Figure 2.189. The thymic tissue is complete even to having epithelium and a few eosinophils and must be distinguished from an inflammatory reaction.

calves given repeated immunizations with endotoxin have massive hypertrophy by 6–9 months of age with normal-appearing thymic tissue extending in solid columns from the rami of the mandibles down each side of the neck to the major mass in the anterior mediastinum.

Physiologically, the naive marrow-derived T-cells enter the thymus near the outer capsule, and in this area there are more large lymphocytes compatible with increased mitosis in the incoming cells. In the cortex the naive cells come in contact with large saclike epithelial cells, which provide the opportunity for elimination of lymphocytes that react with self antigens. Naive T-cells rearrange their cell receptor genes (TCR) forming heterodimers, most of alpha/beta ($\alpha\beta$) configuration and fewer of $\gamma\delta$ type. They are initially negative for both CD4 and CD8, and as they gain TCR rearrangement, those with the $\alpha\beta$ heterodimer become positive for CD4 and CD8. TCRs are coexpressed with CD3 on the cell surface. Those T-cells with TCRs that recognize antigen with Class II MHC become more positive for CD4 and lose all of CD8; those that recognize antigen in a Class I MHC context remain as CD8 positive cells. The much smaller population of cells, with the $\gamma\delta$ heterodimer, mature as cytotoxic T-cells. The cortex contains many cells undergoing apoptosis in the negative selection process and as a consequence there are many macrophages also in this area. The nuclei of the endothelial cells and the macrophages are larger and less densely stained than those of the surrounding lymphocytes and have much more cytoplasm. They can be distinguished by immunohistochemistry, but with oversight stains the macrophages frequently have the signature of cytoplasmic nuclear debris. The maturing lymphocytes leave the thymus via the medullary vessels, having gained "homing" intercellular adhesion molecules (ICAMs) that direct them to specific areas of the peripheral lymphoid system.

The thymic medulla is histologically distinct in having less dense cellularity and more variation in nuclear size and cytoplasmic volume. The thymic medulla contains the Hassall's corpuscles as well as a variety of cell types not or rarely found in the cortex, including Langerhans cells, eosinophils, and mast cells. Most specifically the medulla contains neuroendocrine cells and autonomic nerve fibers that are largely unrecognized but credited with the very real neuroendocrine effects on immune function and stress-related immune deficiency. The medulla also contains myoid cells that are common in birds and reptiles but identified with difficulty in mammals. The myoid cells have striations like skeletal muscle and share antigens with the motor end plates that appear to be operative in myasthenia gravis. B-cells may be found in a normal thymus and even germinal centers that in disease are associated with autoimmune phenomena. The explanation for this is the concept of the thymus as having intraparenchymal (inside the epithelial blood–thymus barrier) and extraparenchymal compartments. Most B-cells are in the medullary area, and those that are between the vessels and the epithelial barrier are felt to be immunologically outside of the thymus and resemble B-cells in other parts of the body (Figs. 2.191, 2.192). Some B-cells are "intracompartmental" and have a distinct phenotype that is characterized by pan B-cell antigens but, like most T-cells, are also CD2 and CD40 positive.

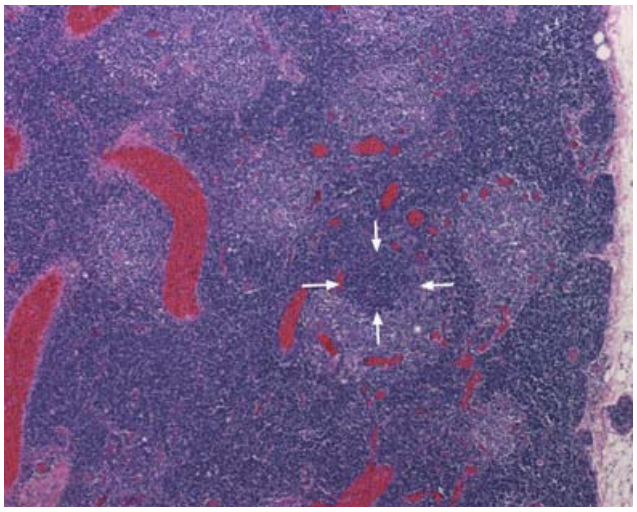

Figure 2.191. Dog: thymic B-cell nodule. An outwardly normal mature dog has a focal solid proliferation of B-lymphocytes (arrows) likely sharing an epithelial barrier with a vessel and immunologically outside of the thymus.

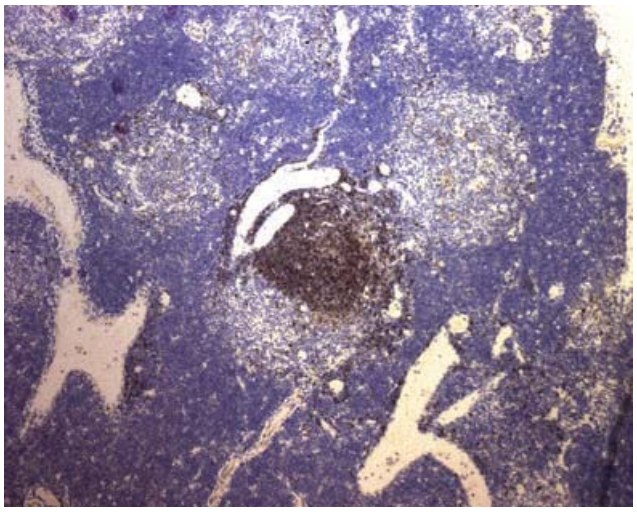

Figure 2.192. Dog: same area as in Figure 2.191 with CD79 stain to demonstrate B-cell lineage of the lymphoid nodule.

REFERENCES

Bleul, C.C., and Boehm, T. (2000) Chemokines define distinct microenvironments in the developing thymus. *Eur J Immunol* 30:3371–3379.

Bockman, D.E. (1997) Development of the thymus. *Microsc Res Tech* 38:209–215.

Douagi, I., André, I., Ferraz, J.C., and Cumano, A. (2000) Characterization of T cell precursor activity in the murine fetal thymus: Evidence for an input of T cell precursors between days 12 and 14 of gestation. *Eur J Immunol* 30: 2201–2210.

Fernandez, J.G., Sanchez, A.J., Melcon, C., Chamorro, C.A., Garcia, C., and Paz, P. (1994) Development of the chick thymus microenvironment: A study by lectin histochemistry. *J Anat* 184:137–145.

Galy, A., Verma, S., Bárcena, A., and Spits, H. (1993) Precursors of $CD3^+CD4^+CD8^+$ cells in the human thymus are defined by expression of CD34. Delineation of early events in human thymic development. *J Exp Med* 178:391–401.

Hayday, A. (1993) T-cell development: Not in the thymus. *Curr Biol* 3:525–528.

Haynes, B.F., and Heinly, C.S. (1995) Early human T cell development: Analysis of the human thymus at the time of initial entry of hematopoietic stem cells into the fetal thymic microenvironment. *J Exp Med* 181:1445–1458.

Howie, D., Spencer, J., DeLord, D., Pitzalis, C., Wathen, N.C., Dogan, A., Akbar, A., and MacDonald, T.T. (1998) Extrathymic T cell differentiation in the human intestine early in life. *J Immunol* 161:5862–5872.

Janeway, C.A., Jr. (1999) The discovery of T cell help for B cell antibody formation: A perspective from the 30th anniversary of this discovery. *Immunol Cell Biol* 77:177–179.

Johnson, C.M., Papadi, G.P., Tompkins, W.A., Sellon, R.K., Orandle, M.S., Bellah, J.R., and Bubenik, L.J. (1998) Biphasic thymus response by kittens inoculated with feline immunodeficiency virus during fetal development. *Vet Pathol* 35:191–201.

Kacker, A., April, M., Markentel, C.B., and Breuer, F. (1999) Ectopic thymus presenting as a solid submandibular neck mass in an infant: Case report and review of literature. *Int J Pediatr Otorhinolaryngol* 49:241–245.

Kato, S. (1997) Thymic microvascular system. *Microsc Res Tech* 38:287–299

Lam, S.H., Chua, H.L., Gong, Z., Wen, Z., Lam, T.J., and Sin, Y.M. (2002) Morphologic transformation of the thymus in developing zebrafish. *Dev Dyn* 225:87–94.

Luer, C.A., Walsh, C.J., Bodine, A.B., Wyffels, J.T., and Scott, T.R. (1995) The elasmobranch thymus: Anatomical, histological, and preliminary functional characterization. *J Exp Zool* 273:342–354.

Lundeen, B.E., and Sty, J.R. (1994) Ectopic cervical thymus: A rare neck mass in an infant. *JCU J Clin Ultrasound* 22:412–415.

Scott, K.J., Schroeder, A.A., and Greinwald, J.H., Jr. (2002) Ectopic cervical thymus—An uncommon diagnosis in the evaluation of pediatric neck masses. *Arch Otolaryngol Head Neck Surg* 128:714–717.

Snyder, P.W., Kazacos, E.A., and Felsburg, P.J. (1993) Histologic characterization of the thymus in canine X-linked severe combined immunodeficiency. *Clin Immunol Immunopathol* 67:55–67.

Tanegashima, A., Ushiyama, I., Kikui, Y., and Yamamoto, H. (2001) Intrathymic lymph nodes in humans. *J Anat* 198:491–495.

Wu, S.L., Gupta, D., and Connelly, J. (2001) Adult ectopic thymus adjacent to thyroid and parathyroid. *Arch Pathol Lab Med* 125:842–843.

Normal Function of the Thymus Gland

The major functions of the thymus have been discussed in other sections, and newer concepts will be considered here. The major selection for self-reacting lymphocytes occurs in the thymic context with negative selection and apoptosis removing the overreacting and self-reacting cells. One problem is that not all of the body proteins are expressed by the cortical epithelial cells and some extrathymic induction of tolerance to self is required. One support system includes a medullary transcription factor termed *autoimmune regulator* that acts to upregulate the epithelial cells to express an additional array of antigens. This pathway came to light in the investigation of a human autoimmune disorder called *autoimmune polyendocrinopathy*, characterized by immune destruction of endocrine glands and persistent yeast infections. Because the disease is inherited, the same gene was tracked and deleted in mice, permitting determination of the mechanism of the defect.

The process of antigen recognition known as *MHC restriction* consists of antigen presenting cells (APCs) that have contacted a pathogen expressing proteins of that organism on their surface in combination with their host MHC proteins. In order for the immune system to react to the invading organism, a T-cell must recognize the presented pathogen protein as foreign. However, in order for the pathogen protein to bind to a host MHC, there must be sufficient MHC polymorphism to permit binding, and in this context broad host variability in MHC genes would infer greater protection in permitting antigen recognition. The corollary is that the T-cells then must also recognize this level of MHC diversity. Thus, greater MHC polymorphism requires a broader selection of T-cells. The process of selection of thymocytes (naive T-cells) has been proposed to be dependent on the number of binding sites involved and antigen avidity that determines whether the selection is positive (survival and differentiation) or negative (apoptosis). More recent work proposes that the cells may be able to read the residence time of antigen binding (kinetic proofreading) as the critical factor in T-cell differentiation. By this system, thymocytes double positive (DP) for CD4 and CD8 recognize antigen on APCs, and if there is a high affinity ligand that

might result in autoimmune disease in the peripheral body, apoptosis results. With low affinity ligand, the DP cells recognizing antigen linked to MHC Class I are "rescued" from apoptosis and become CD8 cytotoxic T-cells. Those DP cells recognizing antigen linked to MHC Class II at low ligand binding mature to CD4 helper T-cells.

The process is repeated in the periphery with different outcomes, where ligand binding at low affinity within the appropriate MHC restriction causes CD8 cells to continue to survive as memory cells and high affinity ligand binding results in proliferation. A similar process occurs for CD4 cells, and ligand antigen recognized in association with MHC Class II. Thus, with any given T-cell receptor, the TCR/CD3 complex is able to deliver a series of signals through a single tyrosine kinase signaling system (ERK) that can result in a number of contrary responses, including differentiation, cell proliferation, cycle arrest, or senescence and apoptosis.

It has been suggested that some T-cell maturation may occur in the intestine independent of the thymus. However, it is certain that those intestinal lymphocytes resident in the epithelial layers are of thymic-dependent type and that the thymus is required for both the development of the IEL and for their maturation. Logic would suggest that the pattern understood for the intestine is likely also operative for the lung and skin.

REFERENCES

Anderson, M.S., Venanzi, E.S., Klein, L., Chen, Z., Berzins, S.P., Turley, S.J., von Boehmer, H., Bronson, R., Dierich, A., Benoist, C., and Mathis, D. (2002) Projection of an immunological self shadow within the thymus by the aire protein. *Science* 298:1395–1401.

Kim, S.V., and Flavell, R.A. (2004) CD8αα and T cell memory. *Science* 304:529–530.

Lefrancois, L., and Puddington, L. (1996) The role of the thymus in intestinal intraepithelial T-cell development. *Ann NY Acad Sci* 778:36–46.

Madakamutil, L.T., Christen, U., Lena, C.J., Wang-Zhu, Y., Attinger, A., Sundarrajan, M., Ellmeier, W., von Herrath, M.G., Jensen, P., Littman, D.R., and Cheroutre, H. (2004) CD8αα-mediated survival and differentiation of CD8 memory T cell precursors. *Science* 304:590–593.

Messaoudi, I., Guevara Patino, J.A., Dyall, R., LeMaoult, J., and Nikolich-Zugich, J. (2002) Direct link between *mhc* polymorphism, T cell avidity, and diversity in immune defense. *Science* 298:1797–1800.

Ohashi, P.S. (2002) Exposing thy self. *Science* 298: 1348–1349.

Werlen, G., Hausmann, B., Naeher, D., and Palmer, E. (2003) Signaling Life and Death in the Thymus: Timing is Everything. *Science* 299:1859–1863.

Developmental Diseases of the Thymus

Abnormalities of migration are evident in thymic "rests" or remnants appearing in the cervical area or alternately within an otherwise normal thyroid gland, and alternatively a normal parathyroid gland may appear in an otherwise normal thymus. The thymic remnants that appear in the cervical area have a tendency to become cystic in adult life and may be mistaken for a lymph node with obstructed drainage if the epithelial components are not recognized (Figs. 2.193–2.196). These changes are more of interest in their correct recognition than in their impact on animal health.

In contrast, congenital abnormalities resulting in immune deficiencies are of great importance because they are either lethal or life threatening. Nearly 100 types of immune deficiencies have been identified in humans and are now classified by the molecular or genetic abnormality rather than by an eponym of the first author to report the condition. In humans, the incidence of one of these types of deficiencies is estimated to be 1 of every 10,000 live births. In general, defects in the B-cell system increase the likelihood of recurrent pyogenic infections, and deficiencies in the T-cell system predispose to opportunistic infections of the adenovirus, Candida, and Pneumocystis type. The most life-threatening deficiencies are of the severe combined immunodeficiency (SCID) type, which have X-linked or autosomal recessive types of inheritance. Both types occur in animals and of these, SCID in the inbred mouse has had the greatest impact on medical sciences. The autosomal recessive type of SCID disease can occur with low or absent B- or T-cells and with (nude) or

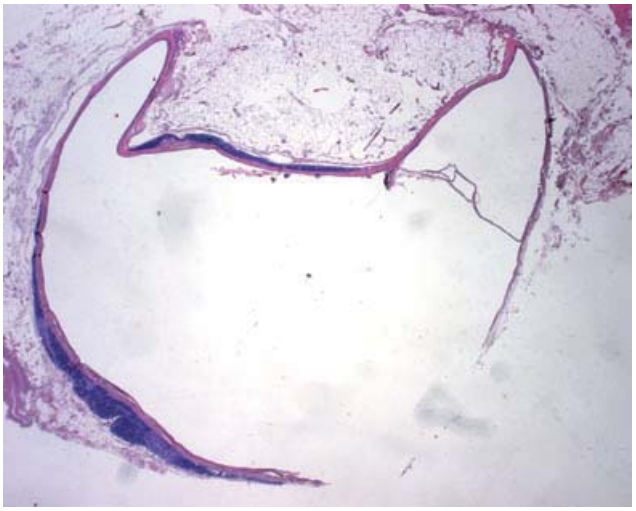

Figure 2.193. Cat: subcutaneous cervical cyst. The cystic structure is derived from thymic remnant rising in the subcutaneous area and consisting primarily of a thin-walled cyst containing epithelial debris lost in sectioning.

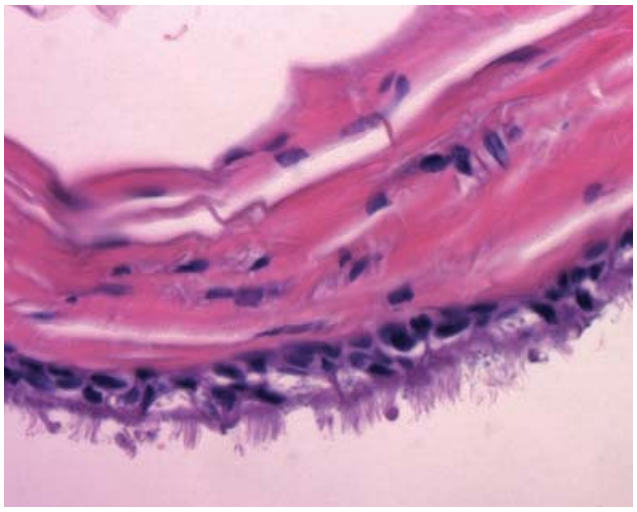

Figure 2.194. Cat: cervical cyst. Detail of cyst wall from Figure 2.193. The ciliated epithelium identifies this structure as likely of thymic origin rather than an epithelial inclusion cyst derived from a hair follicle.

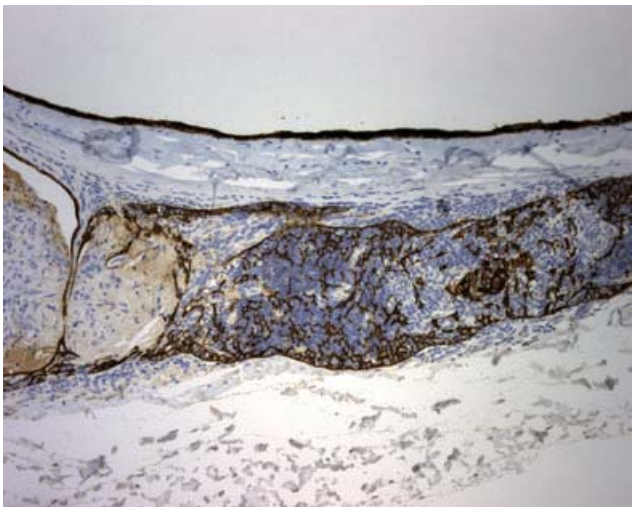

Figure 2.196. Same area as in Figure 2.195 with cytokeratin stain. The inner lining of the cyst is strongly marked, indicating an epithelial-lined cystic structure. The peripheral areas of lymphoid and epithelial proliferation represent residual small areas of thymic cortex and medulla in an aberrant location.

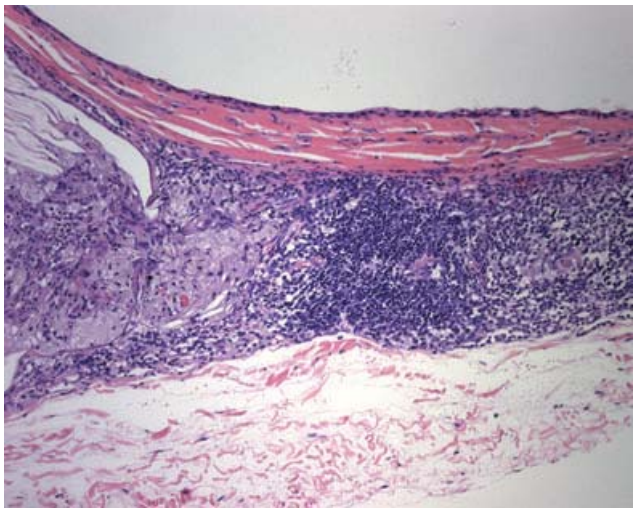

Figure 2.195. Further detail of Figure 2.193. Area of cyst wall, with lymphoid proliferation of irregular density that includes focal pink areas representing foci of large epithelial cells.

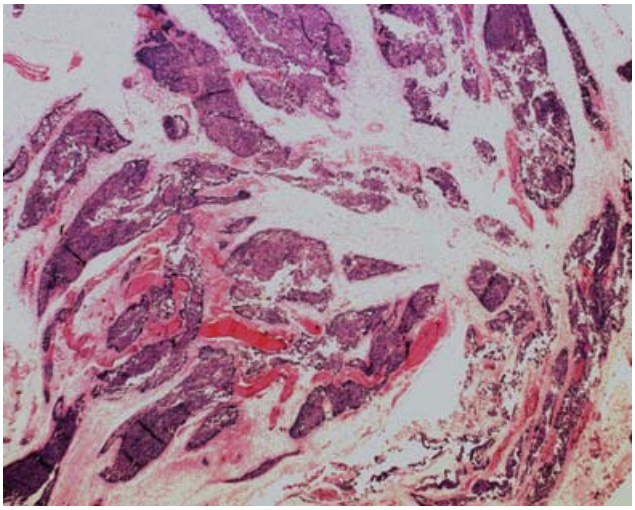

Figure 2.197. Dog: thymus, marked hypoplasia. A 2-month-old dog presented with diffuse necrotizing skin disease, generalized lymphadenopathy and sepsis. The thymus is hypoplastic with an almost complete absence of cortex that is largely limited to a single row of cells beneath the capsule. There is extensive interlobular edema.

without (beige) NK-cells. The SCID genotype occurs in mice, horses, and dogs as well as in humans. The relation of hypotrichosis to the athymic condition has led to the identification of the trait as well as provided a model for the study of a huge array of immune interventions with many involving tissue xenografts of benign and malignant cells. The SCID condition in domestic animals and in human infants is recognized by very low circulating lymphocytes levels at birth and by recurrent and persistent infections as passive antibody wanes (Figs. 2.197–2.200). In human infants with SCID, hematopoietic stem cell transplantation has provided a near 95% chance of survival. The general classification of congenital immune deficiencies can be considered as follows:

1. Deficiencies of B-cell or T-cell receptors, characterized by deficiencies of one or more of the types of immunoglobulin
2. Deficiencies of cytokine receptor chains, including X-linked and autosomal types of SCID

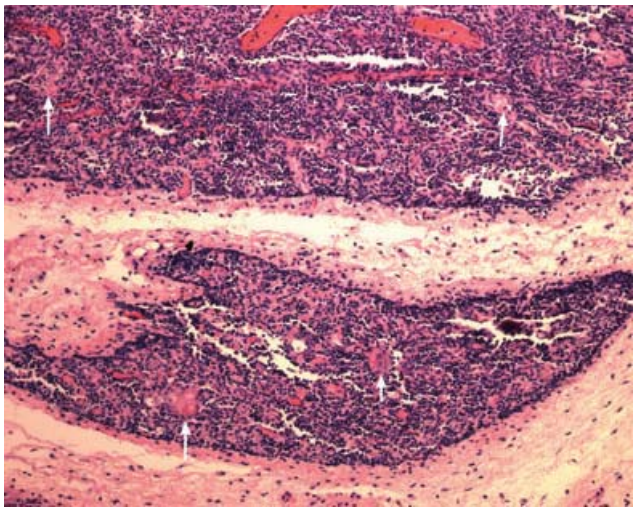

Figure 2.198. Detail of Figure 2.197. The residual thymic tissues consist of a loose primitive stroma separating thickened cortical capsules that contain areas of low lymphoid cellularity, but with normal epithelial development and frequent Hassall's corpuscles {arrows}. The syndrome is known as *puppy strangles*.

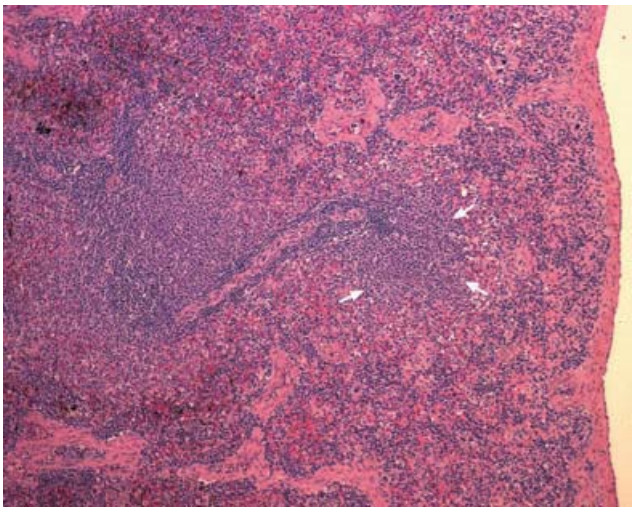

Figure 2.200. Dog: spleen, marked atrophy of lymphoid sheaths and follicle (arrows), same case as Figures 2.197–2.199. The periarteriolar lymphoid sheaths are only a few cells thick with a small foci of B-cell proliferation (arrows).

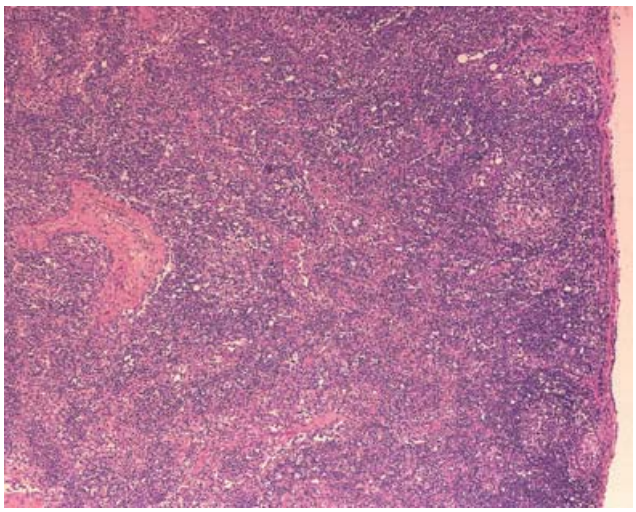

Figure 2.199. Dog: lymph node, marked follicular hypoplasia, same animal as in Figures 2.197–2.198. There is cortical expansion with mixed cellular proliferation. The subcapsular pale areas represent hypocellular germinal centers that lack a mantle cell cuff and colonization by B-cells undergoing immunoglobulin gene hypermutation.

3. Deficiencies of one member of a ligand pair, as in the X-linked hyper IgM syndrome with IgG and IgA deficiency
4. Deficiencies of signaling molecules, including various types of SCID and MHC Class I and II deficiencies, immunodeficiency with thrombocytopenia and eczema, and SCID with cerebellar ataxia5. Metabolic defects, deficiency of adenosine deaminase.

The recognition of defects of immune function in animals in the current era of molecular characterization has great potential value to comparative medicine in providing opportunities to define the mechanisms of these diseases.

REFERENCES

Bell, S.C., Savidge, C., Taylor, P., Knottenbelt, D.C., and Carter, S.D. (2001) An immunodeficiency in Fell ponies: A preliminary study into cellular responses. *Equine Vet J* 33(7):687–692.

Buckley, R.H. (2000) Primary immunodeficiency diseases due to defects in lymphocytes. *New Eng J Med* 343(18):1313–1324.

Casal, M.L., Straumann, U., Sigg, C., Arnold, S., and Rusch, P. (1994) Congenital hypotrichosis with thymic aplasia in nine Birman kittens. *J Amer Anim Hosp Assoc* 30:600–602.

Chang, H., Leeder, S., Cook, V.A., Patterson, B., Dosch, M., Minden, M.D., and Messner, H.A. (1992) Growth of human lymphoma cells in SCID mice. *Leuk and Lymph* 8:129–136.

DeMartini, J.C. (1974) Thymic hypoplasia and lymphopenia in a Siberian tiger. *JAVMA* 165(9):824–826.

Greenwood, J.D., and Croy, B.A. (1993) A study on the engraftment and trafficking of bovine peripheral blood leukocytes in severe combined immunodeficient mice. *Vet Immunol Immunopathol* 38:21–44.

Hutchison, J.M., Garry, F.B., Johnson, L.W., Quackenbush, S.L., Getzy, D.M., Jensen, W.A., and Hoover, E.A. (1992) Immunodeficiency syndrome associated with wasting and opportunistic infection in juvenile llamas: 12 cases (1988–1990). *JAVMA* 201(7):1070–1076.

Perryman, L.E. (2004) Animal models: Molecular pathology of severe combined immunodeficiency in mice, horses, and dogs. *Vet Pathol* 41:95–100.

Snyder, P.W., Kazacos, E.A., and Felsburg, P.J. (1993) Histologic characterization of the thymus in canine X-linked severe combined immunodeficiency. *Clin Immunol and Immunopathol* 67(1):55–67.

Splitter, G.A., Incefy, G., Iwata, T., and McGuire, C. (1979) Evaluation of funtional thymic hormones in Arabian horses with severe combined immunodeficiency. *Clin Exp Immunol* 38:37–44.

Degenerative Diseases of the Thymus Gland

The impact of diet on the development of the immune system and responsiveness in aging humans and animals is recognized to be a major factor in longevity. The lifespan of inbred mice subject to autoimmune disease can be doubled and in some cases tripled by caloric restriction. The general concept is that a very high level of nutrition in juveniles promotes early development of the immune and endocrine systems and early decline and atrophy. Animals on 2-year carcinogenicity studies have fewer spontaneous neoplasms of pituitary and mammary gland type if fed caloric-restricted diets. This increase in longevity permits a greater number of animals to survive a 2-year test period essential to detect late onset lesions like treatment-related tumors. Recently it has been noted that humans who have maintained a caloric intake of about 2,000 per day for several (6) years have virtually no vascular plaque formation, blood pressure characteristic of juveniles, and low overall cholesterol levels. In addition, high caloric intake is especially deleterious when accompanied by a high intake of animal fat, particularly in regard to spontaneous carcinogenicity. Thymic involution can be due to specific dietary deficiency of zinc with restoration of delayed or cellular immunity on provision of supplementary ion.

Many environmental contaminants result in thymic involution, and of these the chlorinated hydrocarbons of the PCB and PBB type are most toxic and still irregularly prevalent. Some of the confusion regarding these compounds is that much of the testing has been done on a cocktail or mixture of isomers that vary by several orders of magnitude in overall toxicity. Thus the 126 isomer of PCB is extremely toxic to lymphoid tissue, including the thymus; the other congeners with the same level of chlorine can be relatively nontoxic, leading to misleading generalizations on overall risk of exposure. The rat has a predictable response to thymic toxicity caused by dioxin and other cyclic chlorinated hydrocarbons. Mild toxicity may cause an increase in the medullary areas in proportion to cortical volume (Figs. 2.201, 2.202). More sustained or higher levels of the same compound then cause reduced cortical volume, and severe atrophy is characterized by a symmetrical reduction in both regions (Fig. 2.203).

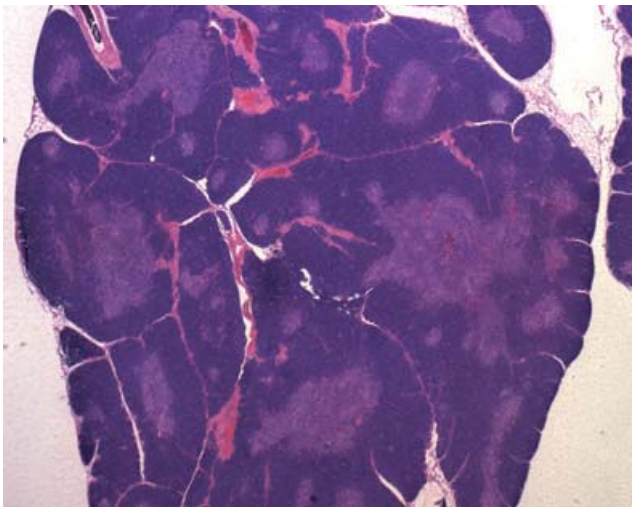

Figure 2.201. Sprague-Dawley rat: thymus, normal. The tissues are densely cellular with well-defined cortico-medullary junctions. Normally, the medulla makes up roughly 1/3 of a lobular diameter. The glandular capsule is thin and inapparent and the lobules are closely faceted.

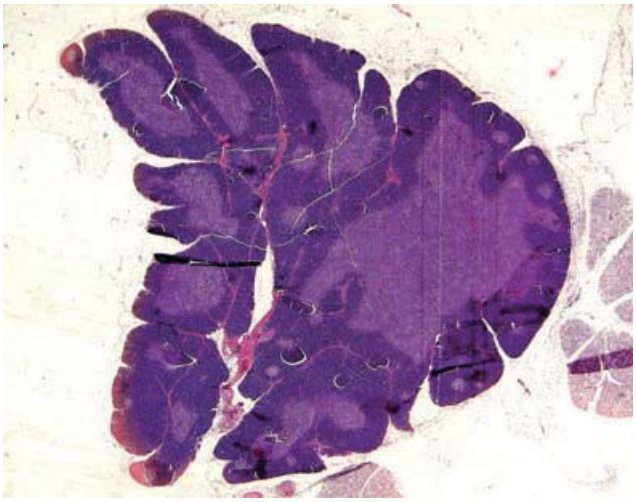

Figure 2.202. Sprague-Dawley rat: thymus, moderate toxic response to chlorinated hydrocarbon. Low-level exposure to polychlorinated biphenyls has resulted in mild cortical atrophy and medullary hyperplasia.

An unusual form of thymic hemorrhage occurs in young dogs in the first year of life. The cause of the hemorrhage is not known and the disease is usually fatal. Young animals have been in transport prior to onset of bleeding, and both natural and stress-related involution have been proposed as inciting causes. Pathologically there is hemorrhagic infarction of the thymus that usually involves all lobes, and the lesions are microbiologically sterile (Figs. 2.204, 2.205). Unusual sequelae of animals surviving less severe hemorrhage have been the appear-

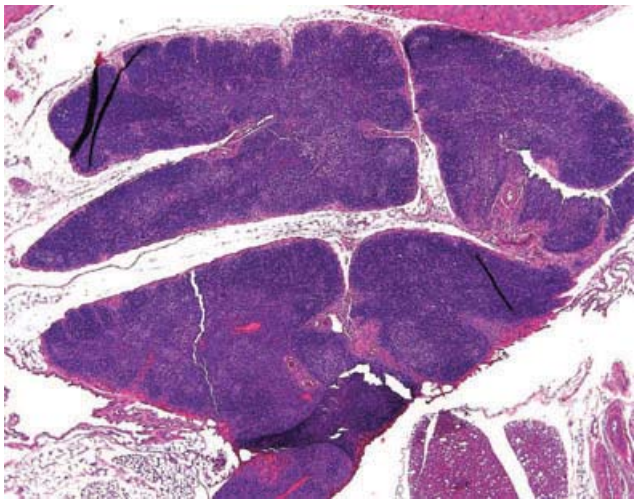

Figure 2.203. Sprague-Dawley rat: thymus, marked toxic induced atrophy. Involution due to high levels of dichloroacetonitrile, in drinking water. There is marked atrophy of both thymic medulla and cortex and thickening of the capsule due to condensation. There is loss of cortical medullary distinction with edematous separation of thymic lobules. The large pale epithelial cells of the thymus persist and their increased proportion results in the tissue losing staining density.

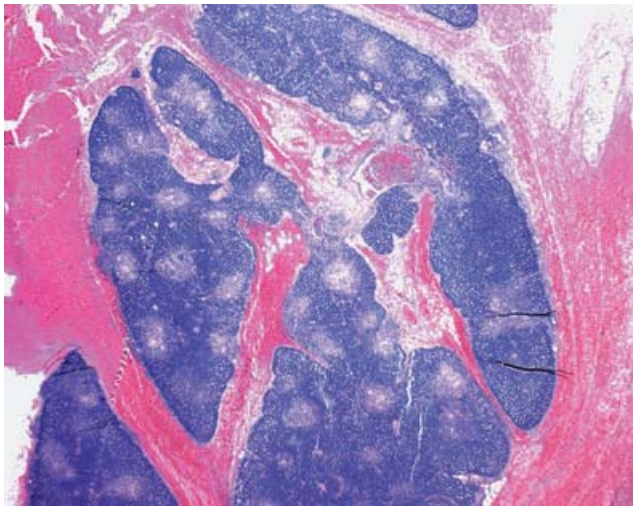

Figure 2.204. Dog: thymus, idiopathic hemorrhagic infarction, weaned pup, stress induced. Focal surviving lobules and complete necrosis in the areas of hemorrhage. The thymic lobules are dissected by diffuse hemorrhage with the cortical cells undergoing massive apoptosis. *Slide from S. D. Fitzgerald, DVM, Midwest Pathologist's meeting, 2002.*

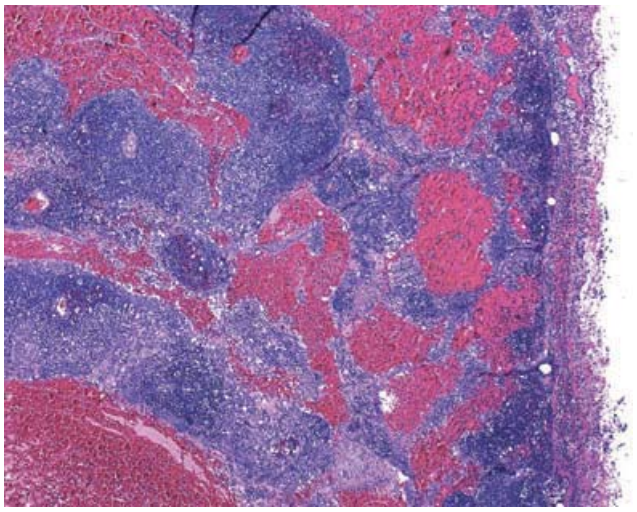

Figure 2.205. Detail of Figure 2.204. There is diffuse interstitial hemorrhage with islands of tissues surviving around small vessels. The necrosis extends through to the mediastinal area with most of the hemorrhage contained within the thymic tissues.

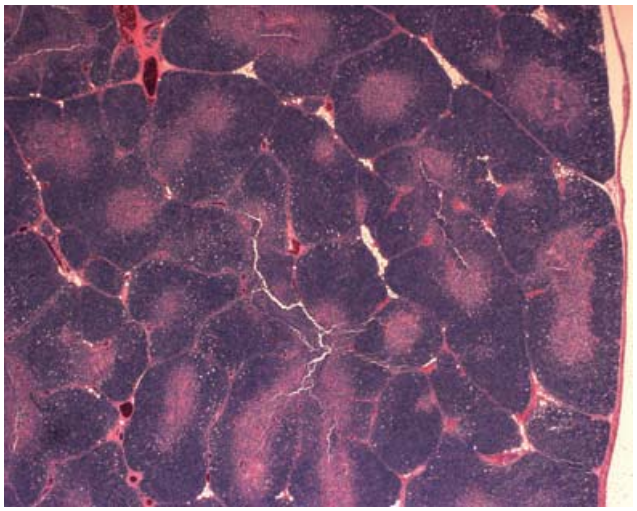

Figure 2.206. Calf: thymus, bovine viral diarrhea (BVD) infection induced atrophy. The thymic lobules are small with symmetrical reduction in both medulla and cortical areas. The widespread fine vacuolation of cortical areas is due to the presence of many large tingible body macrophages removing apoptotic lymphocytes.

ance of exfoliated mesothelial cells from the visceral pleura in the peripheral sinuses of the sternal lymph nodes that resembles metastatic disease.

Steroid therapy and endogenous steroid production during acute stressing conditions results in widespread apoptosis of thymic cortical lymphocytes (Figs. 2.206, 2.207). Changes of this type are seen in animals that have died of trauma, particularly if there have been therapeutic attempts to sustain them. Acute thymic involution is seen in foals born dead at term due to infection with equine herpesvirus, where there is marked lympholysis and inclusion bodies may be found in the epithelial cells (Figs. 2.208–2.210). The spleens of these animals have follicular hyperplasia indicating fetal infection, and the

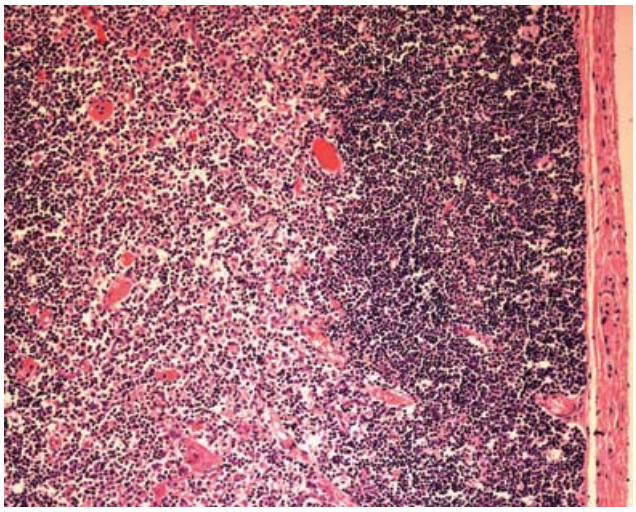

Figure 2.207. Detail of Figure 2.206. There is mild capsular thickening due to condensation with reduction in size of the thymic tissue. Both cortex and medulla are reduced in size and have reduced cellular density due to massive apoptosis. Since the BVD virus primarily affects B-lymphocytes, the attrition in the thymus is likely primarily due to endogenous steroid.

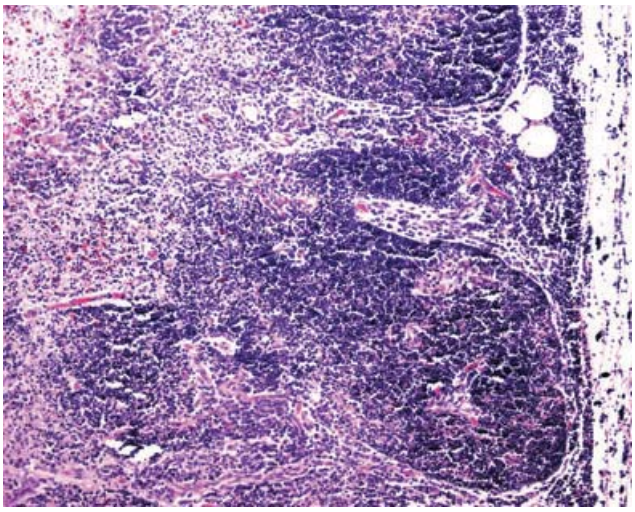

Figure 2.209. Detail of Figure 2.208. There is massive cortical collapse with reduced cellular density and interstitial edema.

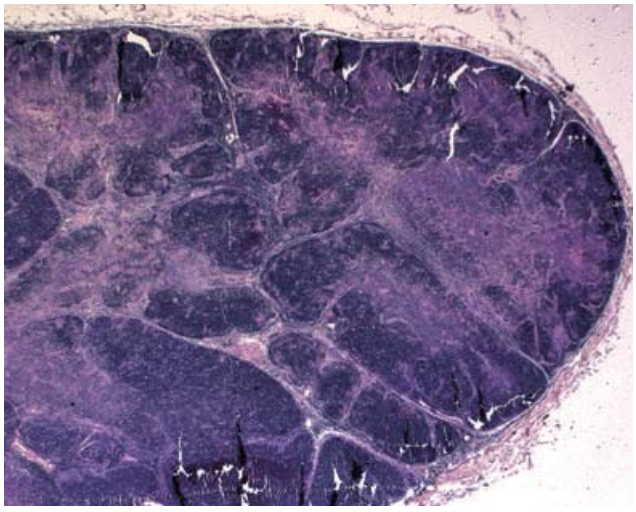

Figure 2.208. Foal: thymus, EHV-induced involution, abortion at term. There is quite marked reduction in overall size with lobular collapse, loss of lobular definition, and irregular definition of cortical medullary junctions.

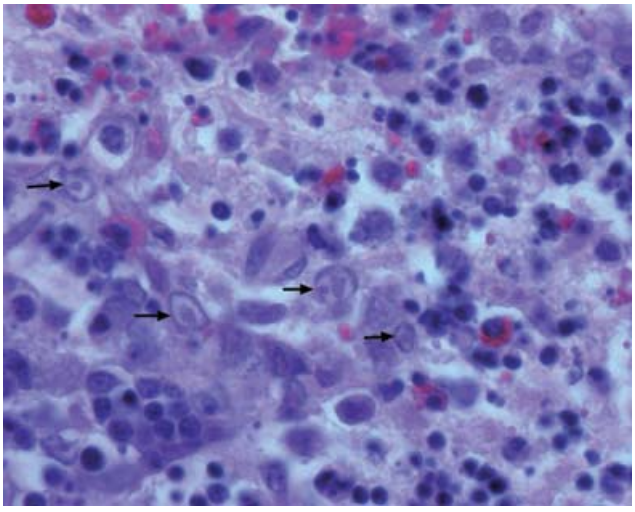

Figure 2.210. Detail of Figures 2.208 and 2.209. In medullary areas, there are numerous herpes-type intranuclear inclusions (arrows) within epithelial cells. The surrounding cellular debris is indicative of very recent massive necrosis of lymphoid cells.

germinal centers are also centers of massive apoptosis (Fig. 2.211). A second naturally occurring viral-induced thymic involution is seen in cats dying of feline panleukopenia virus, where the organ is markedly reduced in size with condensation and folding of the capsule and interlobular septa widely separating residual areas of thymic parenchyma (Figs. 2.212, 2.213).

Aging changes in the thymus result in marked reductions in overall size but not necessarily a cessation of function. There is current interest in thymic function in aging animals and humans with specific regard to resistance to infectious, neoplastic, and autoimmune diseases.

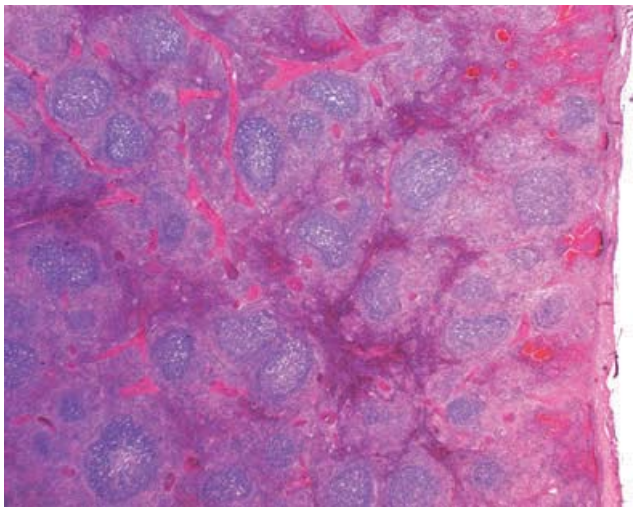

Figure 2.211. Foal: spleen, EVR-induced intrauterine follicular hyperplasia, abortion at term. There is prominent diffuse follicular hyperplasia indicative of antigenemia in the fetus following the development of immune competence. Germinal centers are hypocellular as a result of lympholysis as has occurred within the thymus. Normal neonatal mammals are born without the development of secondary lymphoid follicles.

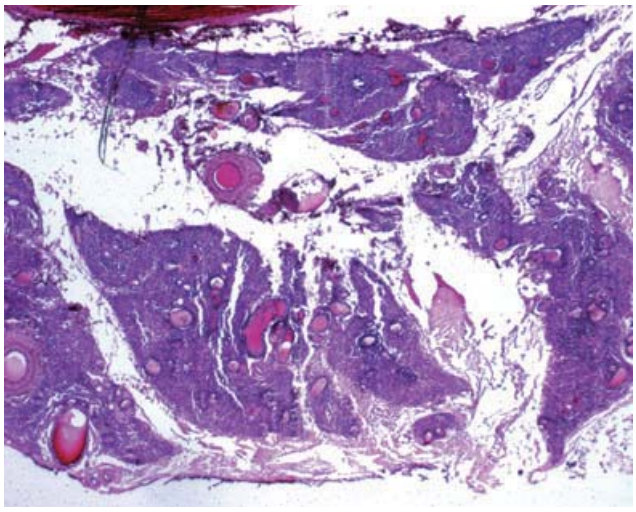

Figure 2.212. Cat: thymus atrophy due to panleukopenia viral infection. There is massive collapse of thymic tissue with complete loss of cortical medullary distinction and marked interlobular edema. The density of large vessels gives indication of the volume of tissue that has been lost.

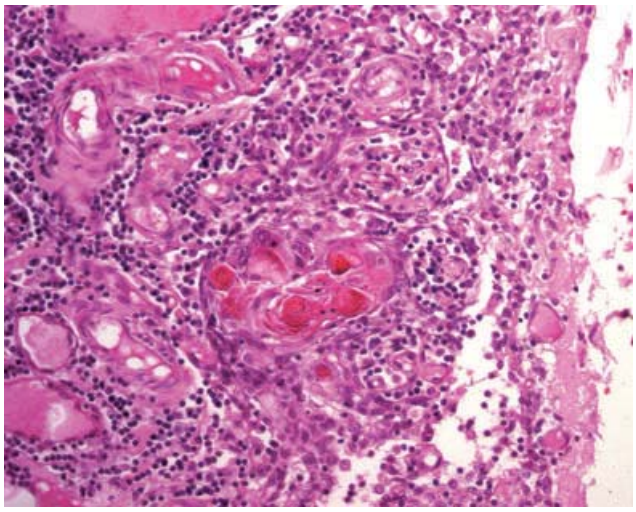

Figure 2.213. Detail of Figure 2.212. Hassall's corpuscles lying in subcapsular areas indicate complete cortical destruction and collapse.

REFERENCES

Abou-Rabia, N., and Kendall, M.D. (1994) Involution of the rat thymus in experimentally induced hypothyroidism. *Cell Tissue Res* 277:447–455.

Bar-Dayan, Y., Afek, A., Goldberg, I., and Kopolovic, J. (1999) Proliferation, apoptosis and thymic involution. *Tissue Cell* 31:391–396.

Bertho, J.M., Demarquay, C., Moulian, N., Van der Meeren, A., Berrih-Aknin, S., and Gourmelon, P. (1997) Phenotypic and immunohistological analyses of the human adult thymus: Evidence for an active thymus during adult life. *Cell Immunol* 179:30–40.

Ciriaco, E., Píñera, P.P., Díaz-Esnal, B., and Laurà, R. (2003) Age-related changes in the avian primary lymphoid organs (thymus and bursa of Fabricius). *Microsc Res Tech* 62: 482–487.

Coolman, B.R., Brewer, W.G., D'Andrea, G.H., and Lenz, S.D. (1994) Severe idiopathic thymic hemorrhage in two littermate dogs. *J Am Vet Med Assoc* 205:1152–1153.

Cui, H.M., Jing, F., and Xi, P. (2003) Pathology of the thymus, spleen and bursa of Fabricius in zinc-deficient ducklings. *Avian Pathol* 32:259–264.

Cunningham, C.P., Kimpton, W.G., Holder, J.E., and Cahill, R.N.P. (2001) Thymic export in aged sheep: A continuous role for the thymus throughout pre- and postnatal life. *Eur J Immunol* 31:802–811.

Godfrey, D.I., Purton, J.F., Boyd, R.L., Purton, J.F., and Cole, T.J. (2001) Glucocorticoids and the thymus: the view from the middle of the road. *Immunol Today* 22:243.

Hale, L.P., Braun, R.D., Gwinn, W.M., Greer, P.K., and Dewhirst, M.W. (2002) Hypoxia in the thymus: Role of oxygen tension in thymocyte survival. *Am J Physiol Heart Circ Physiol* 282:H1467–H1477.

Hannestad, J., Monjil, D.F., Díaz-Esnal, B., Cobo, J., and Vega, J.A. (2004) Age-dependent changes in the nervous and endocrine control of the thymus. *Microsc Res Tech* 63:94–101.

Hartwig, M., and Steinmann, G. (1994) On a causal mechanism of chronic thymic involution in man. *Mech Aging Dev* 75:151–156.

Haynes, B.F., Sempowski, G.D., Wells, A.F., and Hale, L.P. (2000) The human thymus during aging. *Immunol Res* 22:253–261.

Hirokawa, K., Utsuyama, M., Kasai, M., Kurashima, C., Ishijima, S., and Zeng, Y-X. (1994) Understanding the mechanism of the age-change of thymic function to promote T cell differentiation. *Immunol Lett* 40:269–277.

Kaiser, H.E., Krenn, M., Bodey, B., Jr., and Bodey, B. (2000) Involution and neoplasms of the thymus. *In Vivo* 14:189–198.

Krenn, V., Müller, J., Mosgöller, W., Czub, S., Schindler, C., Stahl-Hennig, C., Coulibaly, C., Hunsmann, G., and Müller-Hermelink, H.K. (1993) Simian immunodeficiency virus (SIV) induced alterations of thymus IDCs. *Adv Exp Med Biol* 329:527–531.

Lecavalier, P., Chu, I., Yagminas, A., Villeneuve, D.C., Poon, R., Feeley, M., Håkansson, H., Ahlborg, U.G., Valli, V.E., Bergman, Å., Seegal, R.F., and Kennedy, S.W. (1997) Subchronic toxicity of 2,2′,3,3′,4,4′-hexachlorobiphenyl in rats. *J Toxicol Environ Health* 51:265–277.

Mazzeo, R.S. (2000) Aging, immune function, and exercise: Hormonal regulation. *Int J Sports Med*21:S10–S13.

Nezelof, C. (1992) Thymic pathology in primary and secondary immunodeficiencies. *Histopathol* 21:499–511.

Orandle, M.S., Papadi, G.P., Bubenik, L.J., Dailey, C.I., and Johnson, C.M. (1997) Selective thymocyte depletion and immunoglobulin coating in the thymus of cats infected with feline immunodeficiency. *AIDS Res Hum Retroviruses* 13:611–620.

Poon, R., Chu, I., LeBel, G., Yagminas, A., and Valli, V.E. (2003) Effects of dibromoacetonitrile on rats following 13-week drinking water exposure 1. *Food Chem Toxicol* 41: 1051–1061.

Prentice, A.M. (1999) The thymus: A barometer of malnutrition—Invited commentary. *Br J Nutr* 81:345–347.

Rodewald, H.R. (1998) Immunology—The thymus in the age of retirement. *Nature* 396:630–631.

Torroba, M., and Zapata, A.G. (2003) Aging of the vertebrate immune system. *Microsc Res Tech* 62:477–481.

Woo, J.C., Dean, G.A., Pedersen, N.C., and Moore, P.F. (1997) Immunopathologic changes in the thymus during the acute stage of experimentally induced feline immunodeficiency virus infection in juvenile cats. *J Virol* 71:8632–8641.

Autoimmune Hyperplasia of the Thymus Gland

Asymptomatic hyperplasia of the thymus gland occurs in juvenile animals and may be exacerbated by various immunizations. In these conditions the lobules are all of similar size and there is a symmetrical increase in both thymic lobes. In mature and aging mice, hyperplasia is occasionally seen with asymmetrical lobulation and with varying proportions of thymic cortex to medulla (Fig. 2.214). These changes do not appear to foretell a more serious change, and normal mice tend to have more variation in thymic lobulation and cortico-medullary proportions than the rat or other species.

In contrast, autoimmune hyperplasia of the thymus causes histological changes that distort normal architecture often associated with germinal center formation, which also may be present in the absence of any apparent disease. The pathogenesis for several of these changes has been determined but not the initial events that must occur while the thymus still has apparently normal structure. In myasthenia gravis (MG), a disease primarily of dogs and humans, the myoid cells of the thymic medulla share antigens with striated muscle, which results in antibodies against the acetylcholine receptors of the motor end plates in the peripheral musculature. The initiating events that cause this to occur remain unknown, but variations in interleukin levels may be involved and genetic tendencies are also likely. In this form of MG, where the antibody causing the symptoms of disease arises in germinal centers located in the thymus itself, simple thymectomy is most likely to be therapeutically effective. In contrast, in the form of MG that occurs in association with cortical thymoma, genetics do not appear to be involved and there is no intratumoral antibody or abnormal T-cell activation. Instead the neoplastic epithelial cells express an antigen called *titan* that is shared with normal skeletal muscle. It appears that the neoplastic cells continue to direct the maturation of thymocytes and may cause them to become sensitized to the normal self antigen of titan epitope. Oddly, those thymomas involving the medullary region do not result in MG by this mechanism. The most common morphologic alteration in MG is of thymitis with follicular lymphoid hyperplasia (Figs. 2.215–2.219). In these cases the B-cell proliferation occurs in the perivascular spaces between the vessel wall and the epithelial pericytes, with eventual rupture of the basal lamina and fusion of the two areas (Figs. 2.220, 2.221). The myoid cells continue to occur only in the medullary areas and outside of the germinal centers.

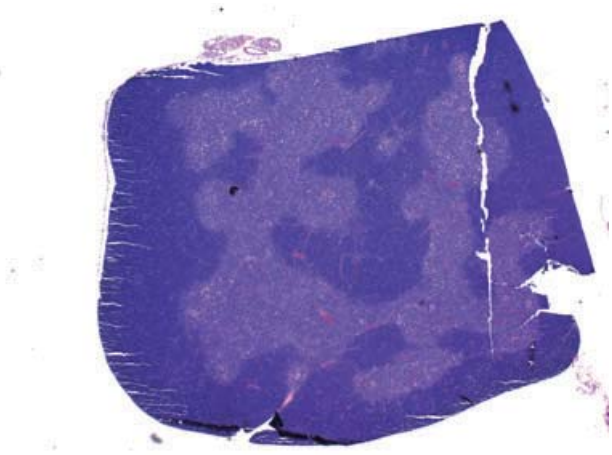

Figure 2.214. Mouse: adult murine thymus, atypical hyperplasia. Mouse with knockout of gene, controlling cell proliferation. There is sharp cortico-medullary distinction with increased volume of both areas and exaggeration of the murine irregular lobular pattern.

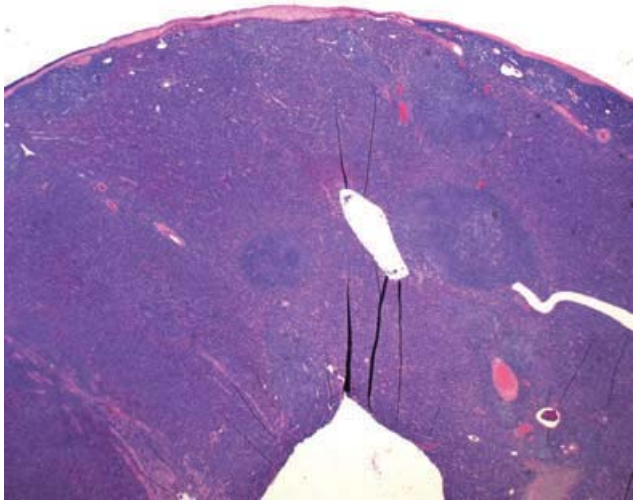

Figure 2.215. Dog: thymoma, intrathymic follicular formation. The dog presented with esophageal dilation and caudal paresis typical of myasthenia gravis. Germinal centers occurring within contact of thymic epithelium are considered indicative of autoimmune reaction.

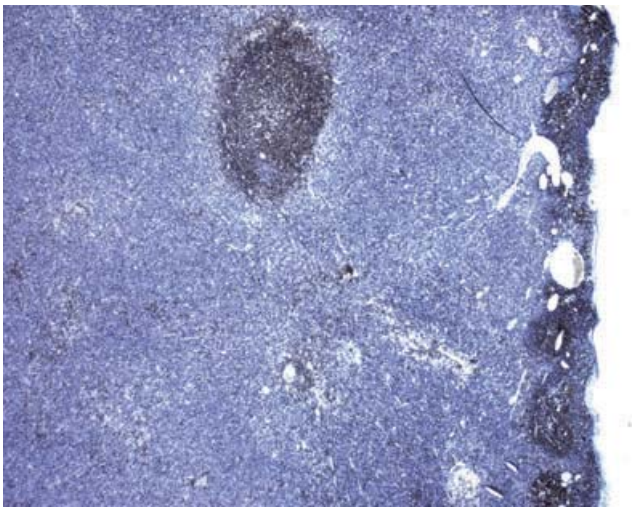

Figure 2.217. Area of Figure 2.216 with CD3 stain for T-lymphocytes. There is widely scattered marking in the area of thymoma with much more dense labeling of cells within the focal area of lymphoid proliferation and in the subcapsular areas of residual benign thymus.

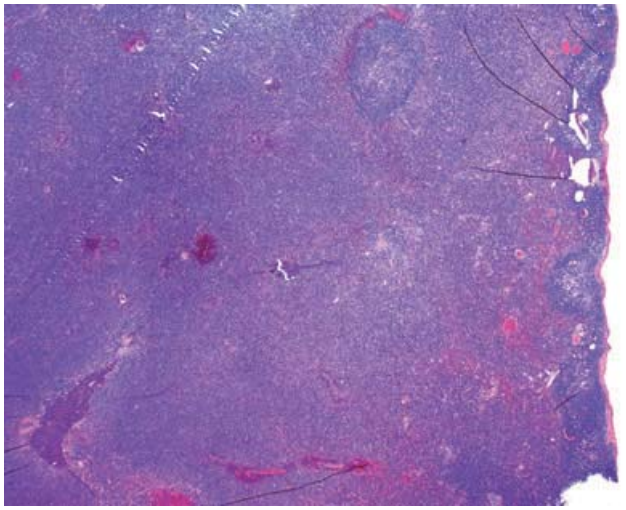

Figure 2.216. Detail of Figure 2.215. Poorly defined areas of follicular hyperplasia are present within the area of neoplastic epithelium and thymoma formation. A thin irregular area of residual benign thymic tissue is compressed beneath the remaining capsule.

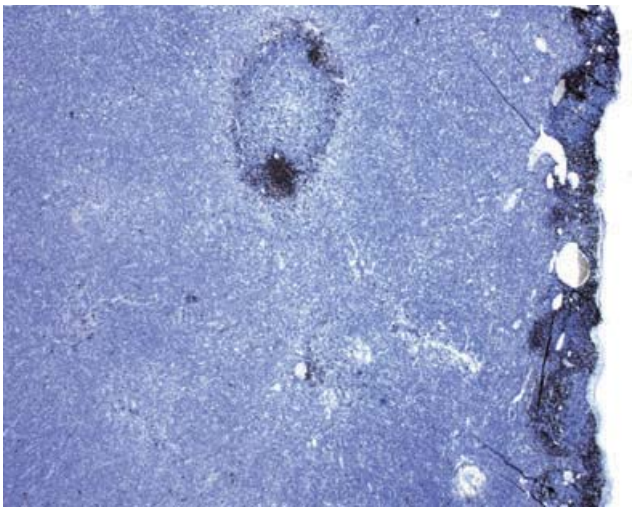

Figure 2.218. Area of Figure 2.216 with CD20 stain for B-lymphocytes. The area of thymoma is almost completely negative, and there is focal and peripheral staining of the area of lymphoid proliferation and mild irregular staining of residual areas of subcapsular cortex.

Other types of MG may have a diffuse B-cell proliferation that may be an early stage of the follicular lesion. Some cases of the diffuse type of B-cell proliferation are seronegative, with few B-cells in the thymus, and have T-cell expansion outside the perivascular spaces. MG may occur with thymic atrophy, which appears to run a shorter course than those types characterized by intrathymic cellular proliferation. In a study of 120 healthy young dogs (6–23 months) of both sexes, germinal centers were found always located in the medullary areas in 70% of animals. The phenotype of the cells was verified by immunohistochemistry, but cytokeratin staining was not carried out to define the centers as occurring within perivascular areas and therefore outside the thymic area of immune control. It was noted that Hassall's corpuscles seen in medullary areas were not found within the germinal centers or B-cell foci.

In autoimmune diseases it has generally been felt that the offending antibody was produced in germinal centers

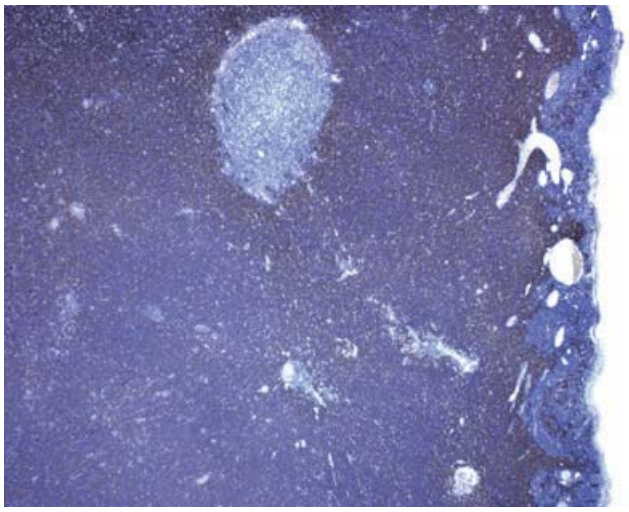

Figure 2.219. Area of Figure 2.216 stained with cytokeratin. There is extremely dense marking of the area of thymoma indicating that the bulk of that tissue is composed of epithelial cells. Note there are scattered epithelial cells within the periphery of the area of lymphoid follicle formation and irregularly in the subcapsular area of residual thymus.

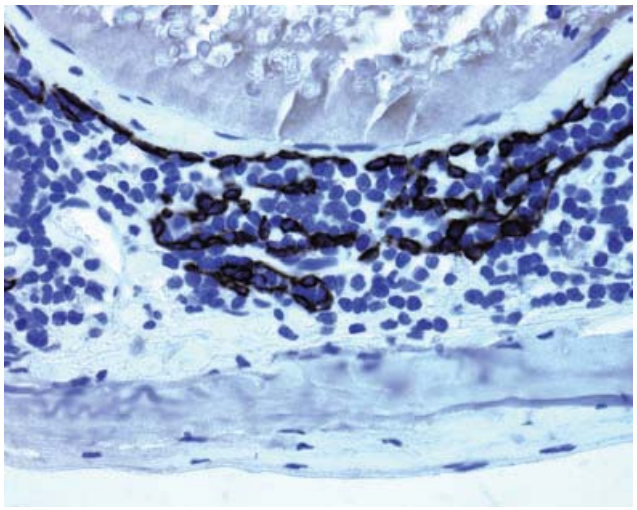

Figure 2.220. Detail of area of Figure 2.216, cytokeratin stain. Image taken at the edge of a vein, in the residual benign area of subcapsular thymus. Note that the venous endothelium is complete and distinctly separate from an outer sheath of epithelial cells that maintain a barrier between the immunologically competent areas of the thymus gland and the vascular system.

either in the thymus or elsewhere in the body. In studies on the MRL.Fas strain of a mouse that develops lupus erythematosus, it was found that B-cells producing the offending antibody developed in the spleen on the outer surface of the periarteriolar lymphoid sheaths. More surprising is the fact that these cells, once committed to the self antigen, do not then enter the germinal center but

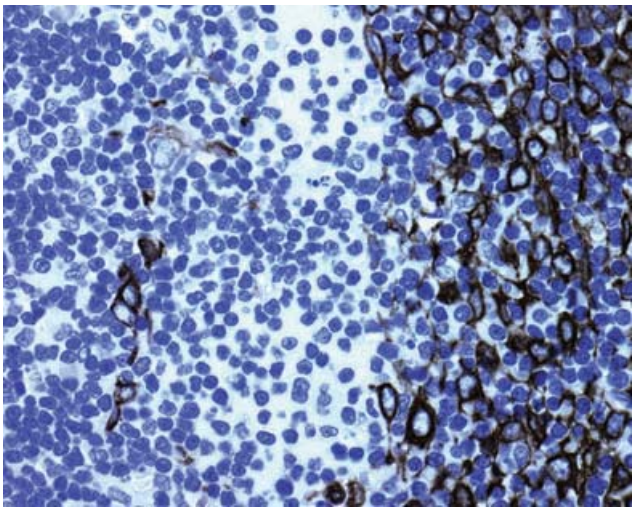

Figure 2.221. Detail of area of Figure 2.216 edge of inner germinal center with cytokeratin stain. A dense network of epithelial cells in the bordering area of thymoma (right) surrounds the germinal center. The lack of an epithelial sheath enclosing the germinal center within a vascular structure means it is in an immunologically competent area and is indicative of autoimmune lymphoid proliferation within the thymus.

remain in the periphery of these B-cell areas. Further it has been shown that these cells undergo hypermutation of the variable portion of the immunoglobulin gene in the area of splenic interface between the lymphoid and sinus areas, a role felt confined to the germinal centers. By this means the B-cells escape the normal control mechanisms of the germinal center by which apoptosis would have been induced in an autoreactive B-cell mutation.

Myasthenia gravis occurs in dogs and has been found to be familial and congenital in smooth fox terriers, Jack Russell terriers, and springer spaniels. In the smooth fox terriers the disease is inherited in an autosomal recessive manner and affects both males and females. The inherited form of MG appears to result from a defect in the acetylcholine receptor as a postsynaptic defect in the absence of any abnormal circulating antibody. The disease is slowly progressive, and affected animals could not be raised to sexual maturity. The acquired form of MG usually affects large-breed dogs and may present with a more chronic form characterized by weakness that is partially alleviated by rest and characterized by shortened gait, facial drooping, and difficulty in closing the mouth and swallowing. The most life threatening of these appears to be partial paralysis of the esophagus with dilation followed by regurgitation after eating, resulting in aspiration pneumonia. Affected dogs have normal nerve conduction velocity, and most appear to have serum antibody directed against acetylcholine receptors. Immunosuppressive therapy has been effective in some cases.

REFERENCES

Beeson, D., Bond, A.P., Corlett, L., Curnow, S.J., Hill, M.E., Jacobson, L.W., Maclennan, C., Meager, A., Moody, A.M., Moss, P., Nagvekar, N., Newsom-Davis, J., Pantic, N., Roxanis, I., Spack, E.G., Vincent, A., and Willcox, N. (1998) Thymus, thymoma, and specific T cells in myasthenia gravis. *Ann NY Acad Sci* 841:371–387.

Boehm, T., Scheu, S., Pfeffer, K., and Bleul, C.C. (2003) Thymic medullary epithelial cell differentiation thymocyte emigration, and the control of autoimmunity require lymphoepithelial cross talk via LTβR. *J Exp Med* 198:757–769.

Durelli, L., Maggi, G., Casadio, C., Ferri, R., Ferrero, B., Poccardi, G., Dutto, A., and Bergamini, L. (1993) Searching for prognostic factors at the time of thymectomy for myasthenia gravis. Correlation between outcome after long-term follow-up and immunophenotype of thymic and peripheral blood lymphocytes. *Ann NY Acad Sci* 681:556–560.

Levinson, A.I., and Wheatley, L.M. (1996) The thymus and the pathogenesis of myasthenia gravis. *Clin Immunol Immunopathol* 78:1–5.

Linegar, A.G., Odell, J.A., Pitt Fennell, W.M., Close, P.M., De Groot, M.K., Casserly, D.R., and Perold, J.I. (1993) Massive thymic hyperplasia. *Ann Thorac Surg* 55:1197–1201.

Marx, A., Wilisch, A., Schultz, A., Gattenlöhner, S., Nenninger, R., and Müller-Hermelink, H.K. (1997) Pathogenesis of myasthenia gravis. *Virchows Arch Int J Pathol* 430:355–364.

Nagane, Y., Utsugisawa, K., Obara, D., Yamagata, M., and Tohgi, H. (2003) Dendritic cells in hyperplastic thymuses from patients with myasthenia gravis. *Muscle Nerve* 27:582–589.

Pompeo, E., Cristino, B., Mauriello, A., and Mineo, T.C. (1999) Recurrent massive hyperplasia of the thymus. *Scand Cardiovasc J* 33:306–308.

Rice, H.E., Flake, A.W., Hori, T., Galy, A., and Verhoogen, R.H. (1994) Massive thymic hyperplasia: Characterization of a rare mediastinal mass. *J Pediatr Surg* 29:1561–1564.

Wong, K.F., Chau, K.F., Chan, J.K.C., Chu, Y.C., and Li, C.S. (1995) Pure red cell aplasia associated with thymic lymphoid hyperplasia and secondary erythropoietin resistance. *Am J Clin Pathol* 103:346–347.

Inflammation of the Thymus Gland Due to Infectious Agents

The feline immunodeficiency virus (FIV) has been shown to cause involution in the thymus of cats most marked in neonates. Although the thymus is reduced in overall size, this change is not as remarkable as the internal histology that consists of follicular hyperplasia with multiple foci of B-cell proliferation. By immunohistochemical staining it has been shown that there are no epithelial cells in the areas occupied by the germinal centers. This indicates that they are located in the perivascular spaces between the endothelium and the surrounding stellate epithelium and are therefore physiologically outside the thymus in terms of the immunological barrier cells. The presence of epithelial cells within a thymic germinal center indicates that it is not sheathed within a tube of epithelium surrounding a vascular structure and is exposed to the immune-processing environment of the thymus. Marked changes occur in the proportion of CD4 cells that are specifically targeted and reduced and the CD8 cells, which remain largely unaffected or slightly reduced in overall numbers. Treatment of FIV-infected cats with the antiviral drug Zidovudine reduces the viral load in circulating lymphocytes, but it does not restore the levels of CD4-positive cells. Cats previously infected with the lion or puma lentivirus have an asymptomatic infection and show no outward signs of illness. When the animals are then superinfected with virulent FIV, they have the FIV viral infection, but the disease is greatly suppressed with less reduction in CD4 cell levels and reduced viral load in plasma and peripheral blood mononuclear cells.

The immunodeficiency viruses that have specificity for the mouse and nonhuman primates cause a variety of responses that have many parallels with HIV infection and the AIDS symptomatology. Early infection is characterized by lymphoproliferation that, in the mouse with the murine leukemia virus (MuLV), results in massive splenomegaly (Figs. 2.222–2.224) and lymphadenopathy (Figs. 2.225, 2.226) that is associated with gradual loss of thymic volume (Fig. 2.227) but with very marked loss of immune reactivity.

The simian immunodeficiency virus (SIV) had very different effects in different species from a largely asymptomatic infection in Suity Mangabeys and causing progressive disease and death in macaques. Early effects

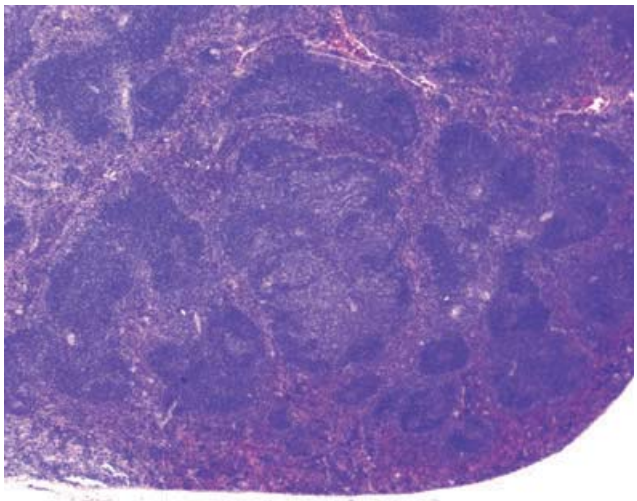

Figure 2.222. Mouse: spleen, murine leukemia virus (MuLV) induced lymphoid hyperplasia. Marked splenomegaly is due to hyperplasia of lymphoid tissue surrounding the small arterioles. In the center, there is a poorly defined germinal center consisting of lighter-stained cells that are peripheralizing the surrounding cuff of small lymphocytes. *Slide from J. M. Ward, DVM.*

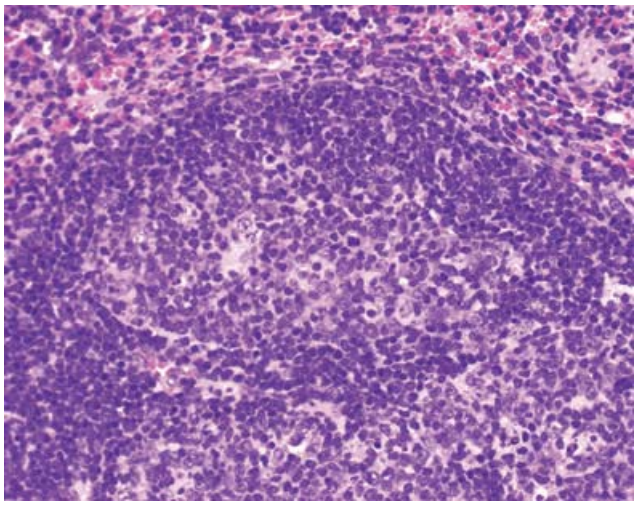

Figure 2.223. Detail of Figure 2.222. There are coalescing germinal centers with a smaller center partially separated from a much larger germinal center to the lower right. This level of proliferation is indicative of chronic antigenic stimulation.

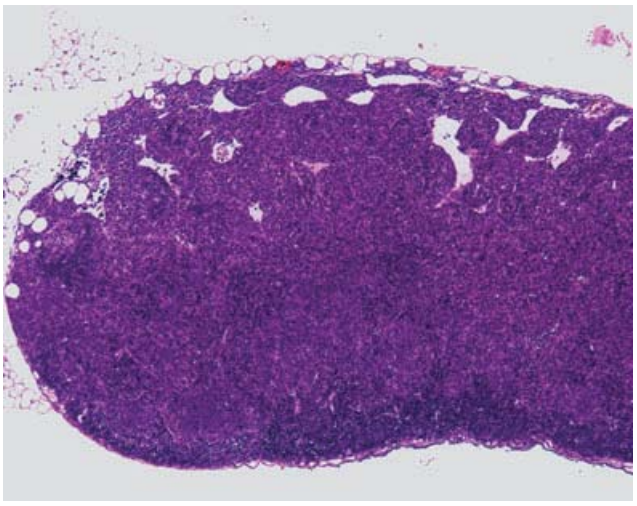

Figure 2.225. Mouse: mesenteric lymph node, hyperplasia of MuLV infection. There is diffuse lymphoid hyperplasia with an absence of germinal centers. A small area of relatively normal paracortex at the (bottom) is more darkly stained, with the node filled with a heterogeneous population of lymphocytes and macrophages. There is filling and distention of the medullary cords (left) with the sinuses almost devoid of cells. *Slide from J. M. Ward, DVM.*

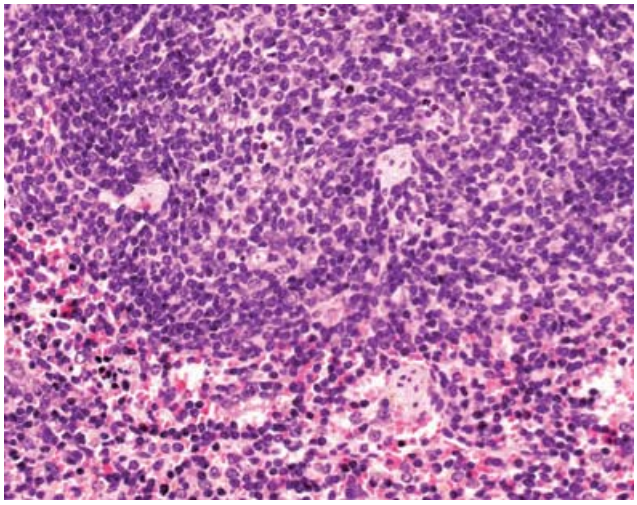

Figure 2.224. Mouse: spleen, MuLV infection, later stage of hyperplasia. With chronicity, the follicles persist but are reduced in size and there is virtually complete atrophy of these small cell thymic-dependent lymphoid cuffs normally present around the small arterioles (lower right). *Slide from J. M. Ward, DVM.*

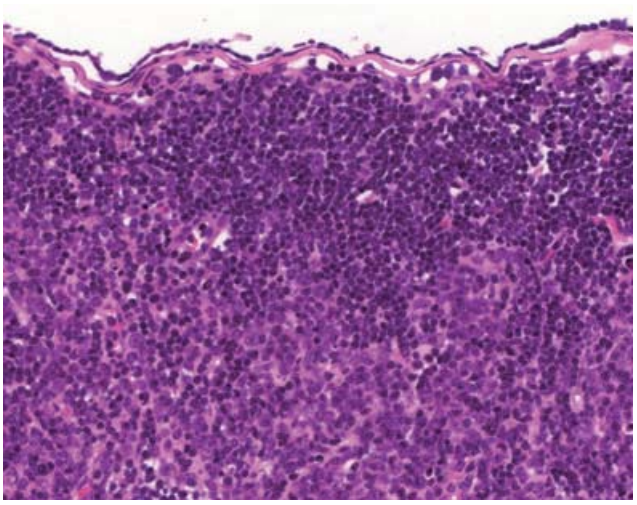

Figure 2.226. Detail of Figure 2.225. The capsule is very thin with the peripheral sinus intact with low cellularity. The normal paracortex is markedly thinned (above) with the interior of the node distended by a mixed population of cellular proliferation (bottom).

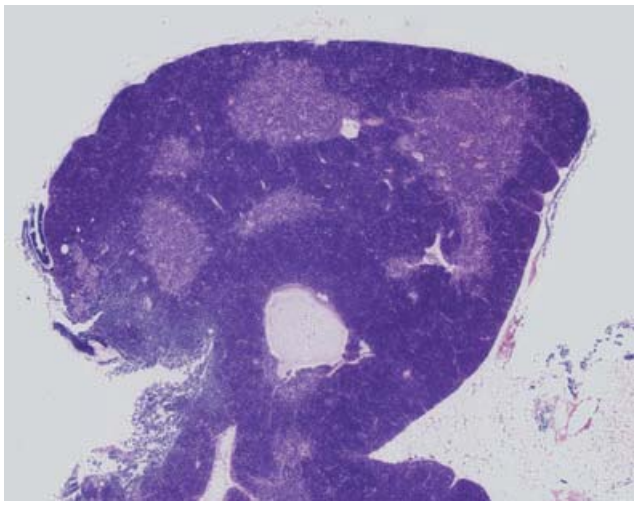

Figure 2.227. Mouse: thymus atrophy, MuLV infected mouse at the stage of involution with the thymus decreased in size with reduction in area of both cortex and medulla. *Slide from J. M. Ward, DVM.*

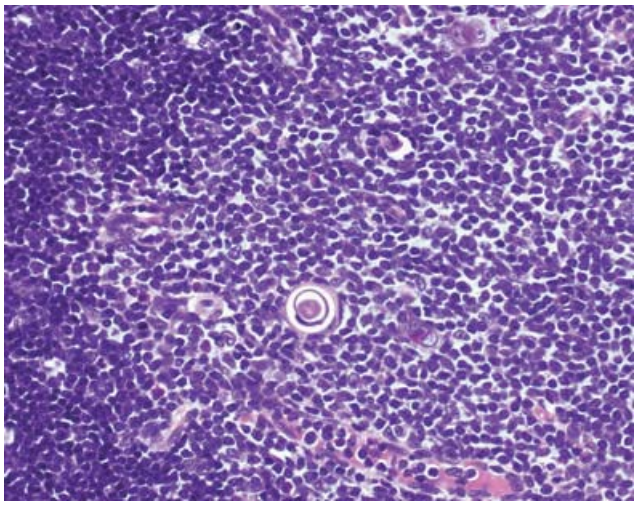

Figure 2.229. Detail of Figure 2.228. Thymus at cortico-medullary junction with normal density of cortex and medulla and prominent central Hassall's corpuscle.

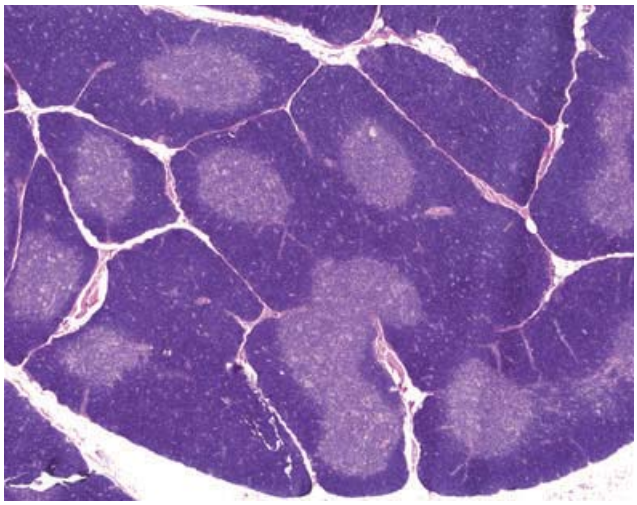

Figure 2.228. Macaque: thymus, 3-year-old with simian immunodeficiency virus (SIV) infection. The initial response in the thymus is involution followed by hyperplasia and general recovery of lobular size with normal proportions of cortex and medulla and normal cell density. *Slide from R. P. Tarara, DVM.*

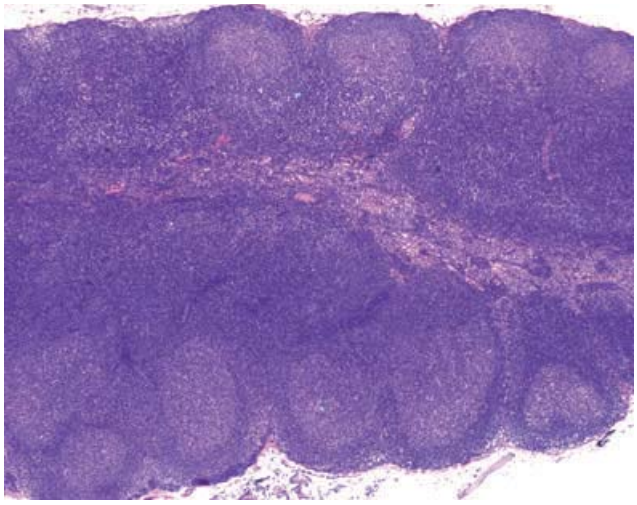

Figure 2.230. Same animal as Figure 2.228, mesenteric lymph node, follicular hyperplasia. In the early period of infection, there is widespread follicular hyperplasia with thinned mantle cell cuffs and mild marginal zone hyperplasia.

of SIV in macaques include a marked increase in apoptosis in the thymic cortex, which is followed by proliferation and recovery (Figs. 2.228, 2.229). In other organs there is an atypical hyperplasia in nodes and spleen with increased size of these organs (Figs. 2.230–2.232). Late in the disease process there is progressive loss in the CD4 positive T-cell subset associated loss of immune reactivity and atrophy of lymphoid tissues (Figs. 2.233–2.240) and presence of lymphoid reaction in marrow (Fig. 2.241) and unusual tissues like brain (Fig. 2.242). In SIV-infected macaques, as in humans infected with HIV, there is increased susceptibility to various infectious agents.

Infection with hog cholera is usually of peracute or acute type, with rapid death due to generalized microvasculitis with hemorrhage and necrosis and widespread lympholysis. Much less often, a pig will survive the acute disease and develop chronic infection with continual shedding of virus, gradual loss of weight, and eventual death. Pathologically, animals that live 2 months or more have atrophic germinal centers in the node, spleen, and

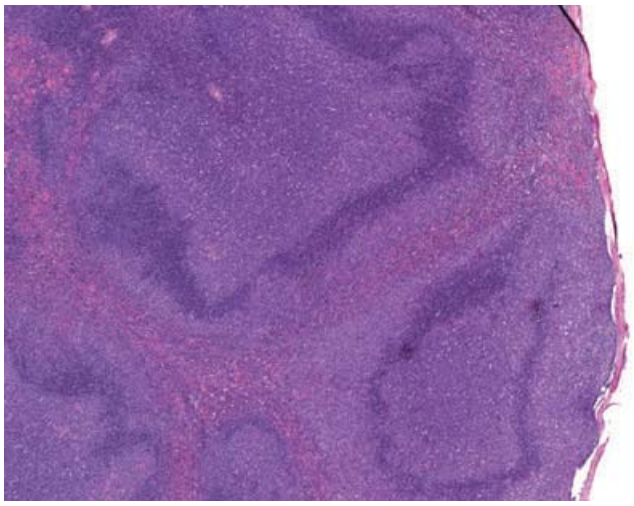

Figure 2.231. Same animal as Figure 2.228, spleen, follicular hyperplasia. Spleen is uniformly enlarged with coalescing areas of lymphoid proliferation consisting of germinal centers of large and irregular size and shape, with thinned mantle cell cuffs surrounded by a lighter-staining sheath of marginal zone hyperplasia. Note the marked thinning of the capsule and complete absence of internal smooth muscle trabeculae in this area. These spleens are subject to hemorrhage with minor trauma somewhat similar to the situation with mononucleosis in human juveniles.

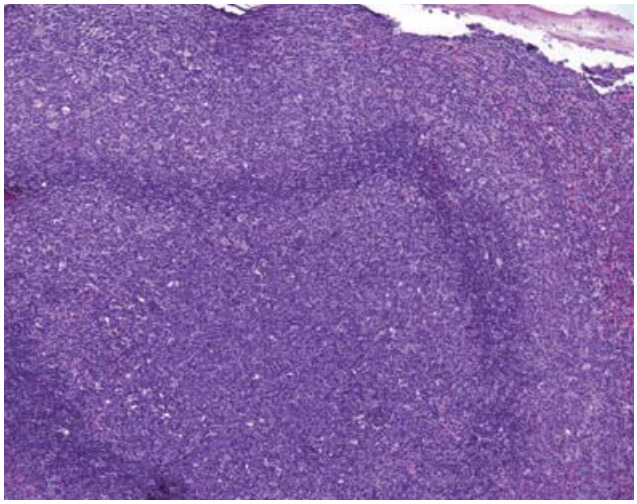

Figure 2.232. Detail of Figure 2.231. Typical splenic follicular hyperplasia with irregular-shaped germinal center and prominent marginal zone hyperplasia.

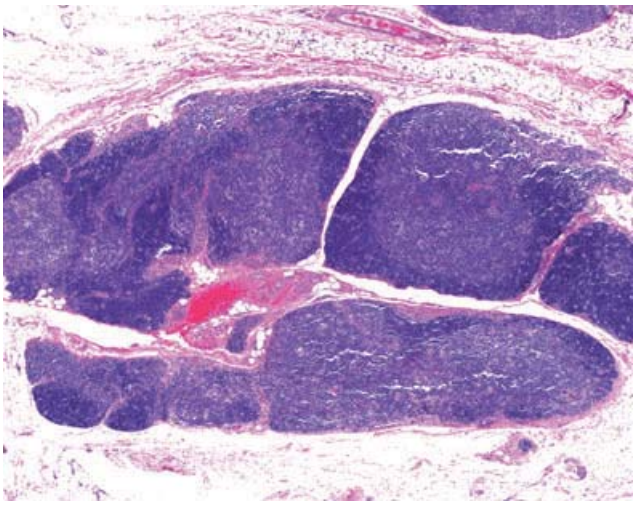

Figure 2.233. Macaque: thymus, 8-year-old female, SIV infected, marked cortical atrophy. The gland is markedly reduced in size and surrounded by a thick layer of edematous adventitia. There is marked and irregular loss of cortical tissue with condensation and thickening of the thymic capsule and irregular separation of lobules. *Slide from R. P. Tarara, DVM.*

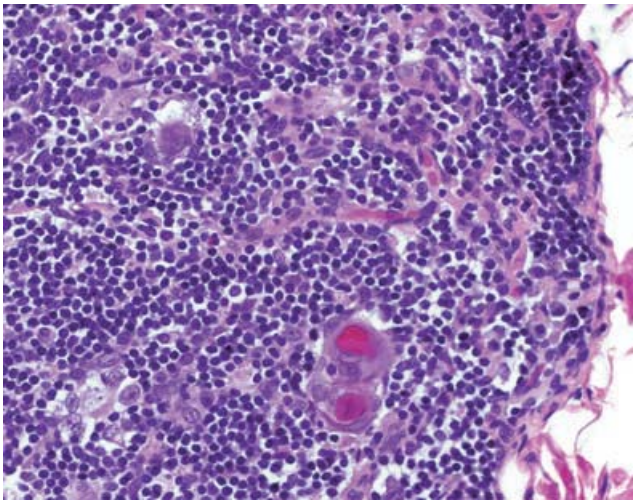

Figure 2.234. Detail of Figure 2.233. Area of thymus with complete cortical atrophy, with only a small area of subcapsular cortical thymocytes remaining (right). The proximity of medullary Hassall's corpuscles to the lobular capsule is indicative of complete loss of cortical tissue.

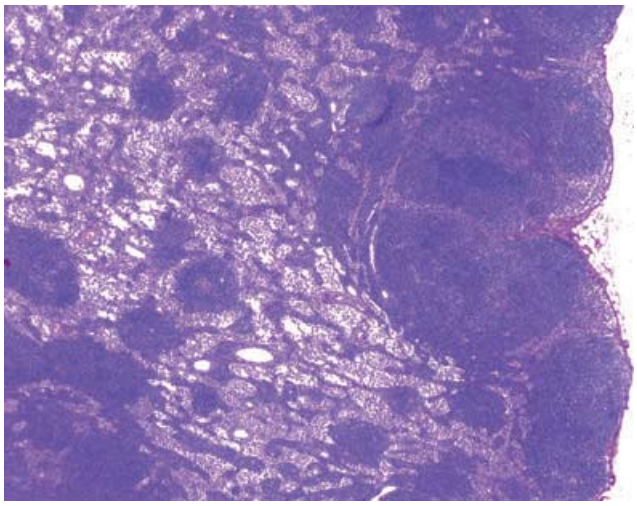

Figure 2.235. Macaque: lymph node atrophy, 8-year-old female, SIV infected. Note capsule is thinned and taut, suggesting previous enlargement with hyperplasia. There is now cortical atrophy with expansion of the medullary sinuses filled with macrophages and cords thinned and relatively poorly cellular. There is involution of cortical germinal centers with the dark area at the right of center due to small densely stained lymphocytes invading the involuting germinal center. *Slide from R. P. Tarara, DVM.*

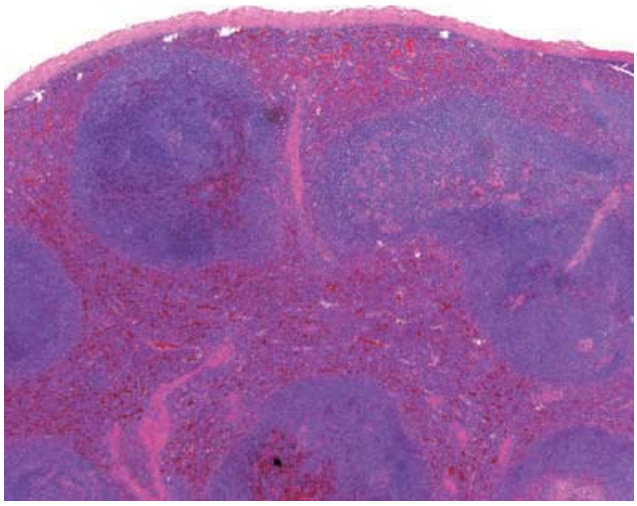

Figure 2.236. Macaque: spleen, 8-year-old female, SIV infected. There is irregular hyperplasia of the periarteriolar lymphoid sheaths, with the germinal centers undergoing involution with the invasion by small lymphocytes and irregular congestion.

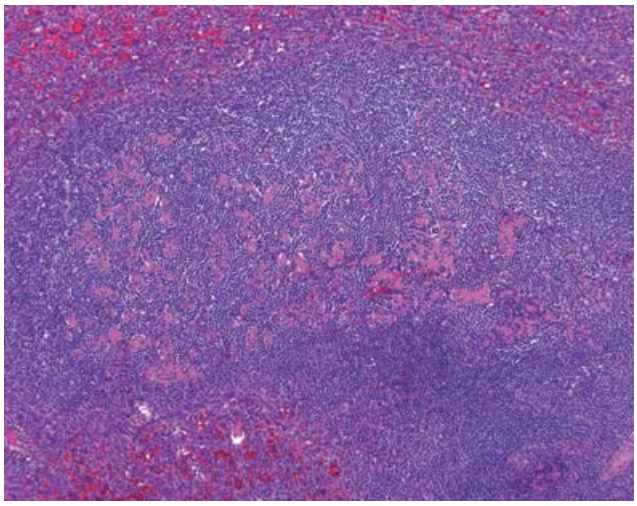

Figure 2.237. Detail of Figure 2.236. Fading splenic germinal center with "bare" dendritic cells in an area normally hypercellular with B-lymphocyte differentiation.

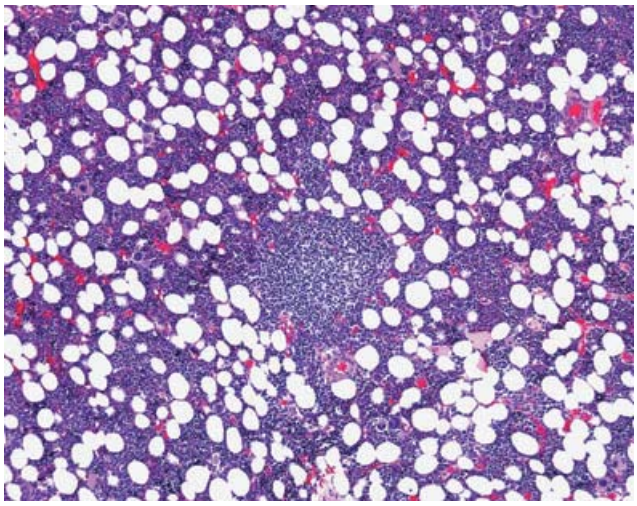

Figure 2.238. Macaque: bone marrow, 8-year-old female, SIV infected. The marrow is moderately hypercellular with multiple foci of involuting lymphoid follicles now lacking a germinal center.

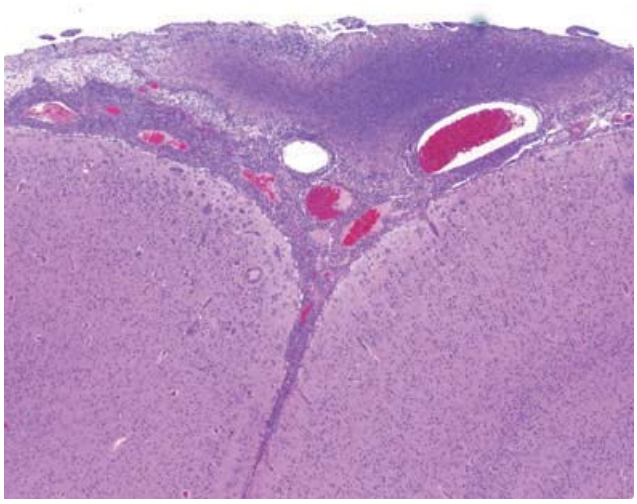

Figure 2.239. Macaque: cerebral cortex, 8-year-old female, SIV infected. There is intense meningeal reaction with heavy inflammatory cell infiltration and early sclerosis.

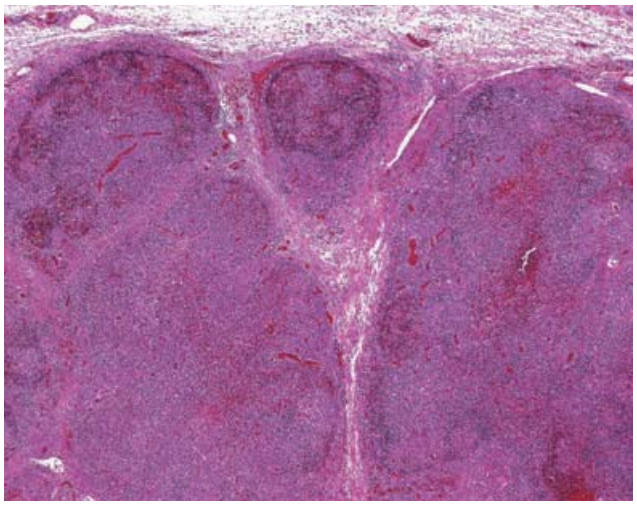

Figure 2.240. Bovine: term fetus, thymus, epizootic bovine abortion (EBA). The tissue is congested with hypercellularity and loss of distinction of cortico-medullary junctions, with focal hemorrhagic necrosis. *Slide from P. C. Kennedy, DVM.*

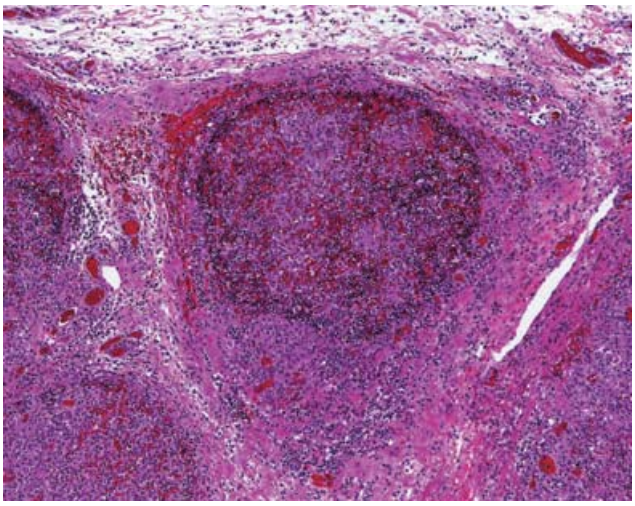

Figure 2.241. Detail of Figure 2.240. There is marked thickening of the thymic lobular encapsulation that greatly separates the underlying lymphoid structures. The lower area of the thymic lobule is undergoing hemorrhagic necrosis, with the cortical area reduced to a thinned layer of small darkly stained lymphocytes 2–3 cells thick immediately beneath the lobular capsule.

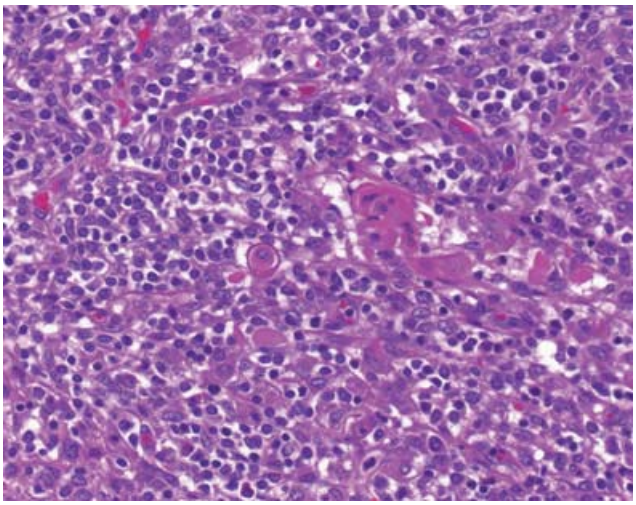

Figure 2.242. Detail of Figure 2.240. Medullary areas of thymus have a marked increase in connective tissue with a mixture of inflammatory cells and loss of normal medullary lymphocytic density.

tonsil and atrophy of the thymus to the extent that it cannot be positively identified on gross examination.

Cattle in areas of California where the vector tick *Ornithodorus coriaceous* is endemic have been subject to infection with the agent of epizootic bovine abortion (EBA), which characteristically causes late abortion or dead calves at term. The disease characteristically affects first calf heifers that survive the infection and remain fertile on subsequent matings. Lesions in the aborted calves consist of thymic involution (see Figs. 2.240–2.242) and pyogranulomas in the lymph nodes and spleen (Figs. 2.243–2.246). The pathogenesis of the infection appears to be the result of immune competence in the fetus mounting an ineffective response, with immune complex injury becoming prominent as the animals develop complement in the face of circulating antibody and persistent antigenemia. Epidemiologically, the disease incidence has declined, with areas originally populated by the tick vector becoming flooded in the formation of water reservoirs.

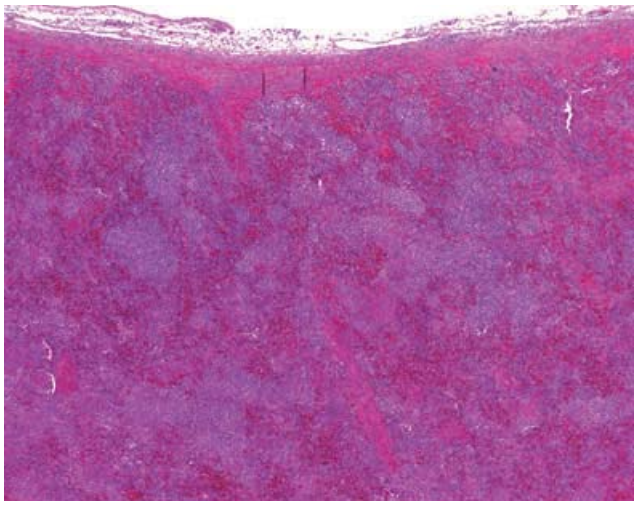

Figure 2.243. Bovine: term fetus, spleen, epizootic bovine abortion. There is marked congestion. The lighter pink areas represent irregular foci of hemorrhagic necrosis, with marked increase in sinus cellularity and atrophy of periarteriolar lymphoid sheaths. *Slide from P. C. Kennedy, DVM.*

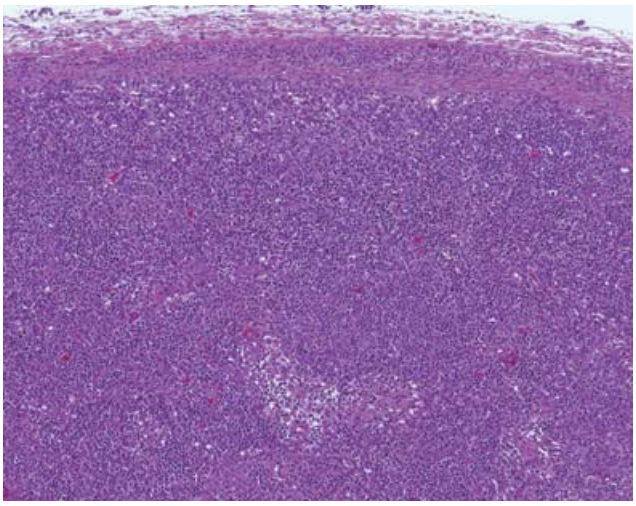

Figure 2.245. Bovine: term fetus, lymph node, epizootic bovine abortion. The node has a thickened capsule that is heavily infiltrated with mixed inflammatory cells and there is compression of the peripheral sinuses and early germinal center formation at bottom center. *Slide from P. C. Kennedy, DVM.*

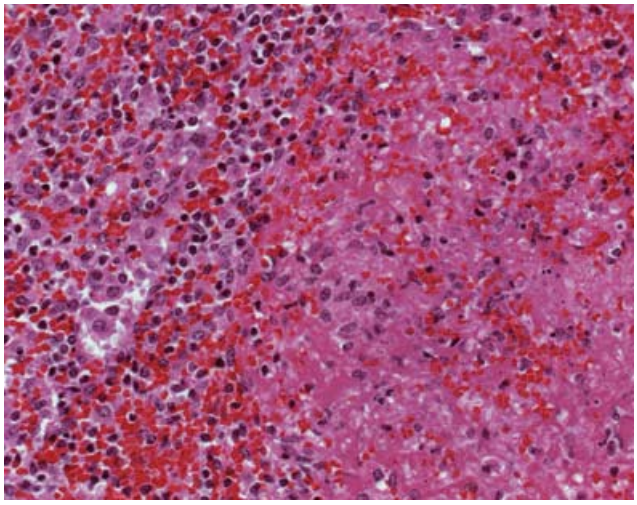

Figure 2.244. Detail of Figure 2.243. Focal splenic necrosis with fibrin and scattered inflammatory cells (right) and congestion and mixed cellular sinus cells (left).

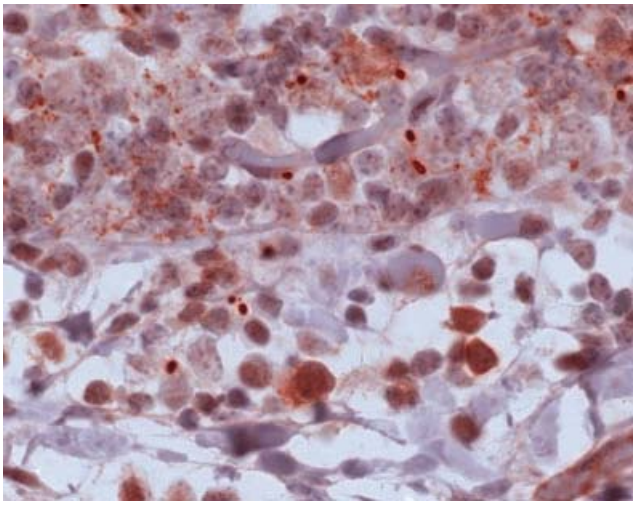

Figure 2.246. Detail of Figure 2.245. Immunohistochemical staining, with antibody specific for the agent of EBA. The agent is present within the cytoplasm of both lymphocytes and macrophages. *Slide from P. C. Kennedy, DVM.*

Although not seen since the general application of vaccinations, canine distemper virus causes generalized lymphoid destruction with thymic atrophy.

REFERENCES

Cheville, N.F., and Mengeling, W.L. (1969) The pathogenesis of chronic hog cholera (swine fever). *Lab Invest* 20(3):261–274.

Iwatsuki, K., Okita, M., Ochikubo, F., Gemma, T., Shin, Y.-S., Miyashita, N., Mikami, T., and Kai, C. (1995) Immunohistochemical analysis of the lymphoid organs of dogs naturally infected with canine distemper virus. *J Comp Path* 113:185–190.

Johnson, C.M., Papadi, G.P., Tompkins, W.A., Sellon, R.K., Orandle, M.S., Bellah, J.R., and Bubenik, L.J. (1998) Biphasic thymus response by kittens inoculated with feline immunodeficiency virus during fetal development. *Vet Pathol* 35:191–201.

Kennedy, P.C., Casaro, A.P., Kimsey, P.B., BonDurant, R.H., Bushnell, R.B., and Mitchell, G.M. (1983) Epizootic bovine

abortion: Histogenesis of the fetal lesions. *Am J Vet Res* 44(6):1040–1048.

Kimsey, P.B., Kennedy, P.C., Bushnell, R.B., Casaro, A.P., BonDurant, R.H., Oliver, M.N., and Kendrick, J.W. (1993) Studies on the pathogenesis of epzootic bovine abortion. *Am J Vet Res* 44(7):1266–1271.

Morse, H.C., Chattopadhyay, S.K., Makino, M., Fredrickson, T.N., Hügin, A.W., and Hartley, J.W. (1992) Retrovirus-induced immunodeficiency in the mouse: MAIDS as a model for AIDS. *AIDS* 6:607–621.

Müller, J.G., Krenn, V., Czub, S., Stahl-Hennig, C., Coulibaly, C., Hunsmann, G., and Müller-Hermelink, H.K. (1993) The thymic epithelial reticulum and interdigitating cells in SIV-induced thymus atrophy and its comparison with other forms of thymus involution. *Res Virol* 144:93–98.

Orandle, M.S., Papadi, G.P., Bubenik, L.J., Dailey, C.I., and Johnson, C.M. (1997) Selective thymocyte depletion and immunoglobulin coating in the thymus of cats infected with feline immunodeficiency virus. *AIDS Res and Human Retrov* 13(7):611–620.

Rovid, A.H., Carpenter, S., Miller, L.D., Flaming, K.P., Long, M.J., Van der Maaten, M.J., Frank, D.E., and Roth, J.A. (1996) An atypical T-cell lymphosarcoma in a calf with bovine immunodeficiency-like virus infection. *Vet Pathol* 33:457–459.

Wykrzykowska, J.J., Rosenzweig, M., Veazey, R.S., Simon, M.A., Halvorsen, K., Desrosiers, R.C., Johnson, R.P., and Lackner, A.A. (1998) Early regeneration of thymic progenitors in rhesus macaques infected with simian immunodeficiency virus. *J Exp Med* 187(11):1767–1778.

BONE MARROW

Normal Form and Function

Embryology

The bone marrow cavities are formed when the cartilage model for bone is first invaded by blood vessels with provisional calcification of the cartilage followed by osteoblastic cells that form a hollow cavity within the cartilage framework. Cartilage resorption begins at 8–9 days in the chick embryo, followed by dilation of small veins and colonization of vessels with stem cells with high cytoplasmic basophilia (Fig. 2.247). The first hematopoietic cells at 11–12 days are erythroid and intravascular in the chick embryo. Myelopoiesis (which occurs in the extravascular space) begins soon after erythropoiesis in the chick embryo.

In the mouse, the long bones at 15 days of gestation are very largely cartilaginous with a cuff of mineralizing mesenchyme that begins in midshaft and extends inward and longitudinally to remodel the cartilage framework. A marrow cavity is formed by 17 days, and a day later granulocytic colonization begins followed by extravascular myelopoiesis, whereas erythropoiesis is confined to liver and spleen till after birth (Figs. 2.248, 2.249). The coccygeal vertebrae are the last to become calcified, with marrow cavities developing at 1 week of age. The rat is similar, with medullary erythropoiesis beginning after birth, and in the human fetus medullary myelopoiesis begins at 75 days of gestation.

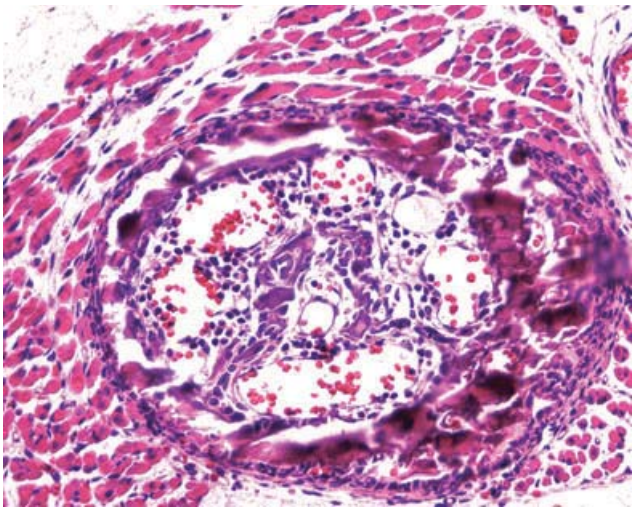

Figure 2.247. Mouse pup: rib, neonatal marrow with high vascularity and low cellularity. Bone fragments in the central area indicate early stage of bone remodeling.

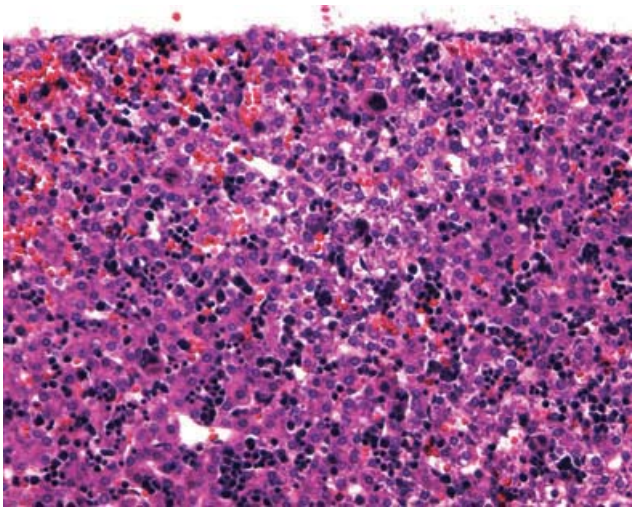

Figure 2.248. Mouse pup: neonatal liver with high level of extramedullary hematopoiesis. These small dark cells are largely erythroid and accommodate the need for increasing red cell mass with a very rapidly increasing body weight.

Early attempts to define the origin of the hematopoietic stem cells involved in vitro culture of embryonic cartilaginous bone. These explants degenerated in culture if not accompanied by surrounding mesenchymal cells that were essential for the penetration, vascularization, and remodeling of the cartilage model. It was thus logical to

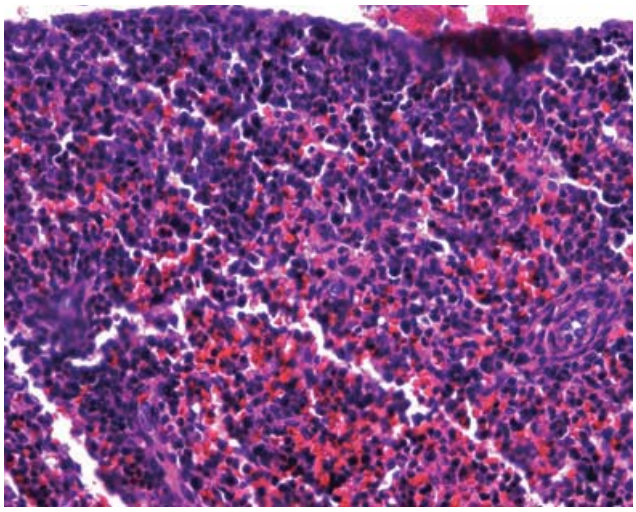

Figure 2.249. Mouse pup: neonatal spleen. At this stage, there is little lymphoid colonization, and the small arterioles (left) have a very narrow cuff of pericytes and mononuclear cells. The sinus areas have high cellularity due to trilineage hematopoiesis with erythroid predominance.

suppose that the hematopoietic stem cells also arose from these same mesenchymal progenitors. This proposal was disproved by forming parabiotic pairs of chick embryos of opposite sexes that demonstrated full chimerism of the marrow cells by sex chromatin analysis, proving that the hematopoietic cells originated from circulating precursors and were not derived from local osteoprogenitors. Subsequently, the blood islands of the yolk sac in the chick embryo were found to be the source of the primordial hematopoietic stem cells and these precursors are likely segregating in the primitive streak stage of development. Similar structures occur in mammals, and the logic of yolk sac origin for hematopoiesis for both birds and mammals is that it isolates the primitive precursors from the multiplicity of inductive forces present in the early embryo as the tissue layers and organs develop. The concept was further enhanced by the demonstration of pluripotency of the primitive yolk sac cells in being able to differentiate into all subsequent types of bloods cells. This was accomplished by irradiation of the blood island cells to produce viable progeny, with characteristic and identifiable chromosomal changes that could be identified in all cell lines resulting from differentiation of a single precursor cell.

Stem cell biology is now of major interest in medicine because of the possibility of using these cells to repair various organs injured by abnormal genetics and development or disease in adult life. Stem cells have a hierarchical system of development that protects against the short and long-term needs of postnatal survival. The most primitive of the hematopoietic stem cells (HSC) is the long term (LT) cells that are largely inactive and not cycling and are capable of sustaining the individual throughout life. The LT-HSCs are totipotential and have the ability to differentiate into any and all of the myeloid, erythroid, monocytic, megakaryocytic, and lymphoid lineages. The progeny of the LT cells are the less capable short term (ST) HSCs that can produce lineage-specific or lineage committed progenitor (LCP) cells. These latter LCP cells are produced in direct relation to the immediate needs of the body, with each progenitor capable of differentiating into 10 mature cells as seen in the peripheral blood. This amplification is achieved through three homomorphogenic divisions that, for the myeloid series, are the myeloblast, promyelocyte, and myelocyte in which the progeny of each division are indistinguishable. This is followed by three heteromorphogenic stages of maturation in which each succeeding cell type is readily recognizable as the metamyelocyte, band, and segmented neutrophil. The HSCs circulate in the blood at low levels, but they are numerous in cord blood and are banked for future use by the donor with proper matching for allogeneic transplantation. This aspect of HSC biology has been utilized in treating lymphoma by "half-body irradiation." In this strategy, sufficient exposure is given to the upper and lower halves of the body in order to eliminate neoplastic cells that are fixed in situ, while giving the migratory HSCs the opportunity to seed out the treated areas that can produce marrow cells before the effects of irradiation cause fatal cytopenia from the most recently treated portion. More recently it has been found that some allogeneic marrow transplants given for tumor ablation have been most successful if the MHC match differs in a manner that does not cause graft versus host disease but does result in effective antitumor T-cells. The process requires that the donor cells are matched for only one HLA haplotype and are mismatched for the unshared haplotype (haploidentical stem cell transplant). This strategy requires complete T-cell depletion of the donor cells to avoid graft versus host disease. The mismatch promotes NK-cell activation and effective antitumor control. The beneficial effects are most apparent against acute myeloid leukemia (AML) and less effective for treating acute lymphoid leukemia (ALL).

In terms of gross anatomy, the bone marrow functions as an organ that in total volume is approximately equal to that of the liver. Not all bones contribute in the same manner, and in most species the long bones, vertebrae, flat bones of the ribs, pelvis, jaws, and calvarium contain most of the hematopoietic marrow tissue. It is apparent that the system functions as an organ because red marrow from any site will have the same cellularity and cellular distribution, with the exceptions being focal infectious agents or focal metastatic disease. In rodents, the whole femur is involved in hematopoiesis throughout life. It has

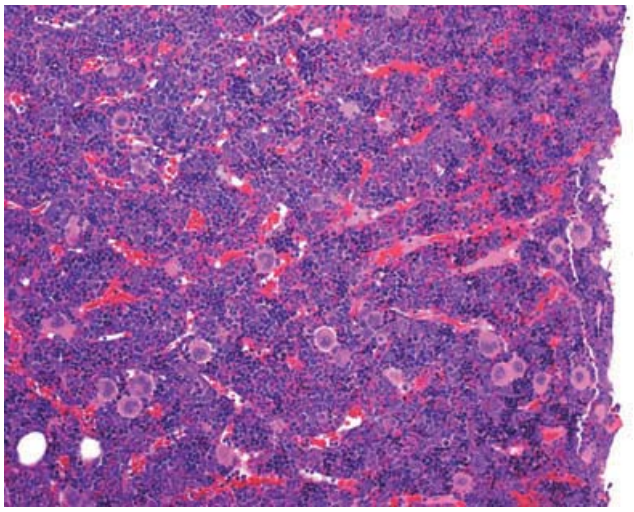

Figure 2.250. Rat: normal mature male Sprague-Dawley, femoral marrow with high cellularity. Note the vascular pattern with sinusoids lining columns of marrow that are of fairly consistent width. Erythropoiesis occurs in clusters of small round, deeply stained nuclei that represent the progeny of a blast-forming unit. This area has the typical myeloid erythroid ratio of a normal animal with the megakaryocytes frequently more prominent in subendosteal areas.

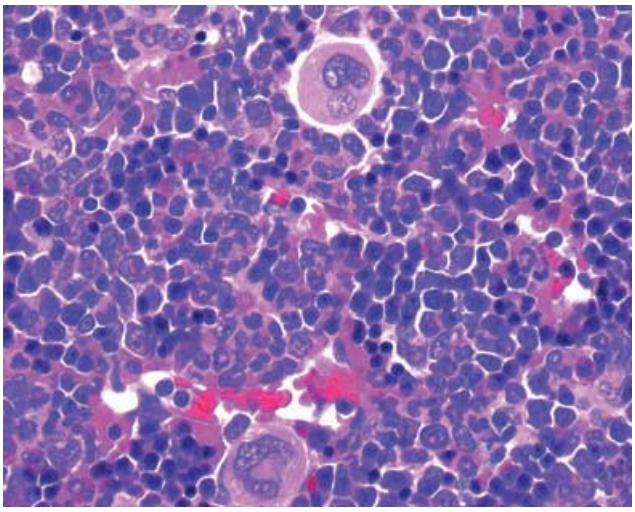

Figure 2.251. Detail of Figure 2.250. The proximity of nonmotile cells like platelets and red cells to an endothelial surface is apparent in several areas in this image.

been estimated that in the mouse some 6% of total marrow is present in the femoral cavity. In humans and domestic animals, the central femoral cavity becomes occupied by fat in early life, and in calves, this occurs within the first 2 months of life. In mature animals, red marrow must be obtained from an area of cancellous bone, and in dogs, this is always present in the femoral neck. Red marrow can be obtained from the vertebral spines or sternum of mature cattle but not from the tuber coxae. In horses, the sternum at the level of the elbow in the standing animal is always the best site for obtaining a marrow core or aspirate.

In terms of microanatomy, the bone marrow has vessels lined by flattened endothelium with fenestrations and a discontinuous supporting basement membrane that permits rapid cell traffic (Fig. 2.250). Nonmotile cells such as platelets and erythroid cells develop in juxtasinusoidal parenchyma that permits egress from the marrow to the blood by passage directly through an adjacent endothelial membrane (Fig. 2.251). Motile cells like the granulocytes develop further back but migrate with maturity. In mammals, all hematopoiesis is extravascular, and in birds, the myeloid lineage cells are extravascular and erythropoiesis takes place within the sinusoids. Also in birds, hematopoiesis tends to be dependent on nutrition with rapid cycling between production and cessation in birds deprived of food.

The stromal cells of bone marrow are essential to normal hematopoiesis and provide the critical hematopoietic microenvironment required for full cellular maturation. Evidence for the inductive effects of marrow stromal cells were demonstrated by the finding that marrow cells in culture rapidly differentiated and died without stem cell input, but they could be maintained in long-term (a month) culture if grown over a subculture of marrow stroma (Dexter culture). Marrow stromal cells constituitively produce a variety of molecules stimulatory to differentiating marrow cells. Production of these growth factors requires homologous serum but not inflammation, suggesting that they function in a manner to maintain a basal level of hematopoiesis under conditions of homeostasis. Typical production is of granulocyte macrophage-colony stimulating factor (GM-CSF) and IL-6, but not the more restricted granulocyte factor (G-CSF) or IL-3. The anatomic relationship of marrow cells can be related to the distribution of these growth factors that are active over only very short distances so that the pattern of factor diffusion is part of the mechanism of regulation of cell production. The fat cells or adipocytes of the marrow are felt to have a reciprocal relationship with the marrow stromal cells but it is not clear that there is direct ability for differentiation between fibroblasts, osteoblasts, and fat cells.

It has been estimated that in the normal adult mammal, red marrow takes place within 200 microns of bone. Thus red marrow is found in the metaphyses of long bones where the cancellous scaffolding supports the weight bearing of the thinner cortical bone (Fig. 2.252). Further, the bone has a portal-type venous drainage system in which the blood from the cortical bone arborizes on the endosteal surfaces and then becomes nutritive to the red

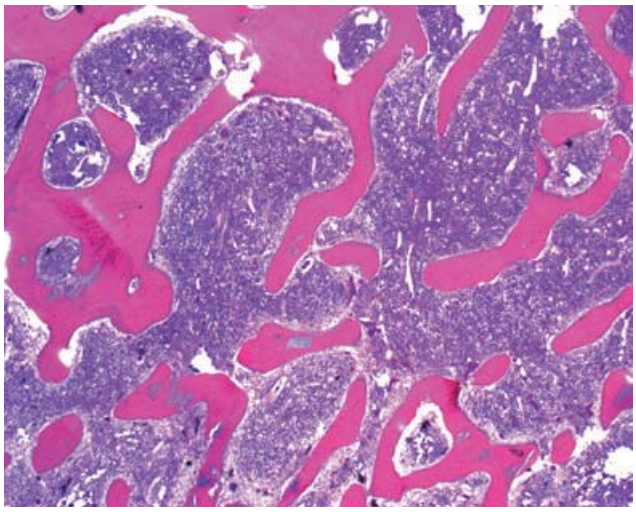

Figure 2.252. Macaque: young male, subphyseal area of proximal femur. Focal areas of intratrabecular cartilage (bottom) indicate ongoing remodeling. Vascularization of these areas is followed by solid infiltration with trilineage hematopoiesis.

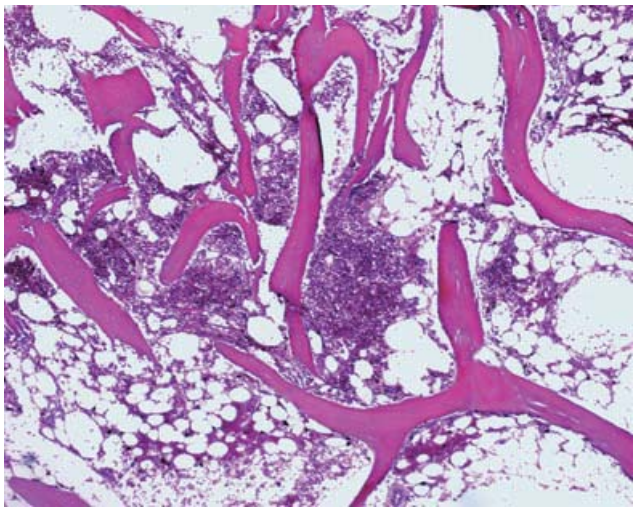

Figure 2.253. Dog: adult male, bone marrow, aplastic pancytopenia. There is marked marrow hypocellularity with the space occupied by fat cells and dilated sinusoids.

marrow. Those areas immediately adjacent to the endosteum have the highest inductive capacity for blood stem cells that are in greatest concentration in those areas. This relationship is seen in regenerative marrows where the early conversion of fatty to red marrow occurs in an endosteal cuff in diaphyseal areas that increases in width in a centripetal manner if the stimulus is maintained.

This relationship has relevance in the type and impact of neoplastic cell implantation in marrow with progression of the leukemias. In acute myeloid leukemia, the malignant precursors compete with the benign stem cells for space in the subendosteal areas. As benign precursors are driven centripetally, they undergo differentiation but not self renewal, thus leading to early marrow failure with peripheral cytopenia of benign cells. In contrast, in acute or chronic lymphoid leukemia the neoplastic cells colonize the marrow in a random fashion that is often in fatty areas, and marrow failure is much later when half or more of the marrow is occupied by tumor. Marrow failure may result from loss or depression of stem cells resulting in aplastic pancytopenia or in selective loss of one of the marrow cellular lineages (Figs. 2.253, 2.254). In infectious panleukopenia of cats, the marrow becomes devoid of mature cells of all lineages and in rebound the advancing "front" of new cell production resembles the early asynchrony and atypia of acute myeloid leukemia (Figs. 2.255, 2.256).

The development of the spleen colony technique was a major step ahead in the understanding of stem cell biology because it was the first method of actually quantitating the stem cells themselves. By this technique mice were

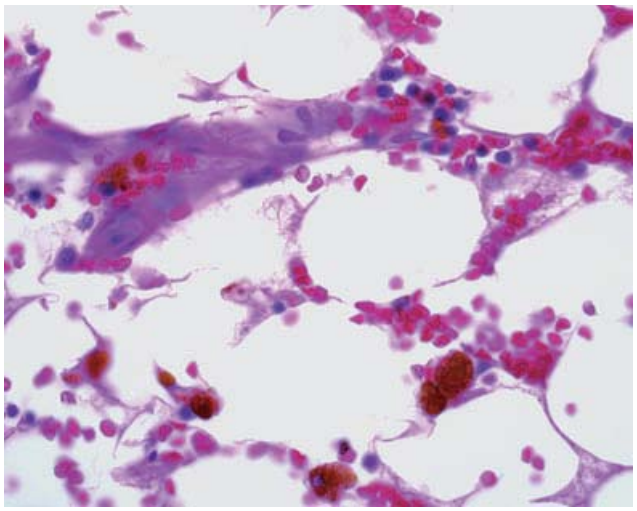

Figure 2.254. Detail of Figure 2.253. Hemosiderin-bearing macrophages at the interstices of fat cells is indicative of areas of bone marrow that were once hematopoietic and have undergone atrophy of specialized cells. Since aplastic pancytopenia may be a slowly developing disease, there is time for fatty replacement of hematopoietic areas and the marrow is not as red grossly or histologically as it is in cases of rapidly developing aplasia.

radiated to render their bone marrow aplastic, and then they were given an intravenous injection of marrow cells from a congenic donor. The stem cells in the donor marrow "seeded" the marrow and spleen of the recipient mouse, with those colonies in the spleen forming grossly visible nodules that could be counted with each a clonal colony from a single stem cell "committed" to a single hematopoietic lineage. Histologically the colonies could

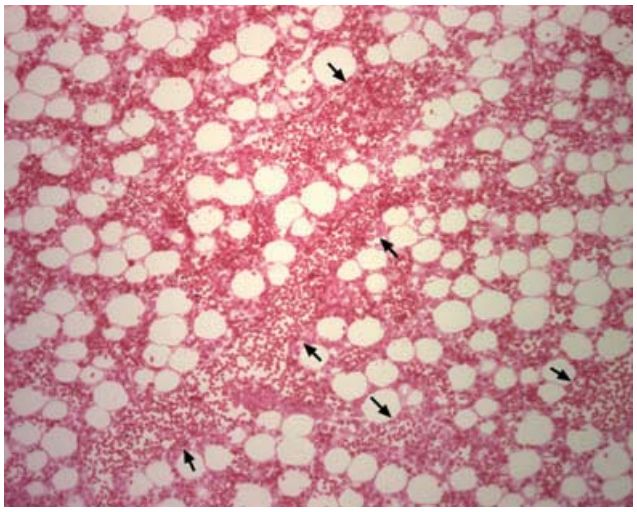

Figure 2.255. Cat: bone marrow with acute aplasia due to infection with feline panleukopenia virus. With loss of specialized cells from the marrow, the intercavitary space is filled by dilation of sinusoids (arrows) that give the tissue a very red appearance on gross examination that may be misleading and interpreted as active hematopoiesis.

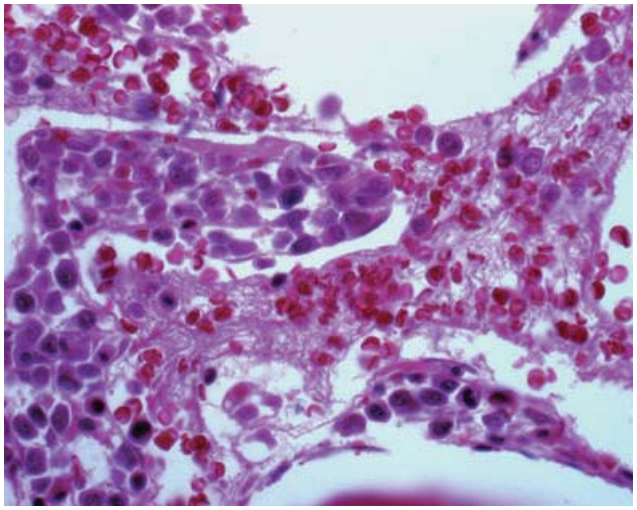

Figure 2.256. Detail of Figure 2.255. Focal area of early marrow rebound with all cells appearing primitive and resembling acute leukemia.

be determined to be of erythroid, myeloid, or megakaryocytic type (Figs. 2.257, 2.258).

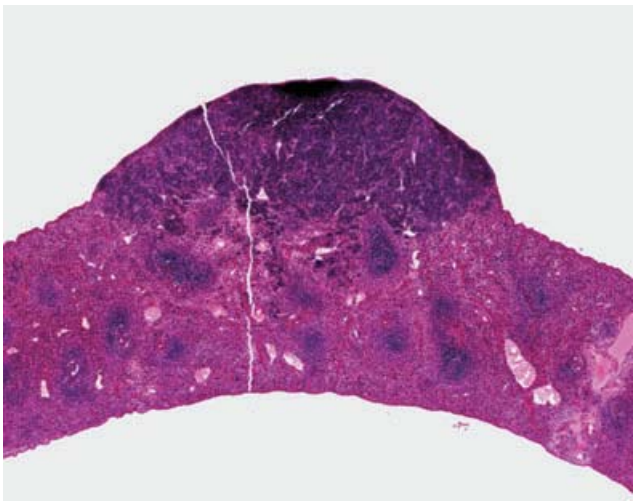

Figure 2.257. Mouse: spleen colony technique. Mouse irradiated to hematopoietic incompetence was given an intravenous injection of marrow from a congenic donor that contains hematopoietic stem cells forming benign clonal proliferation in the spleen.

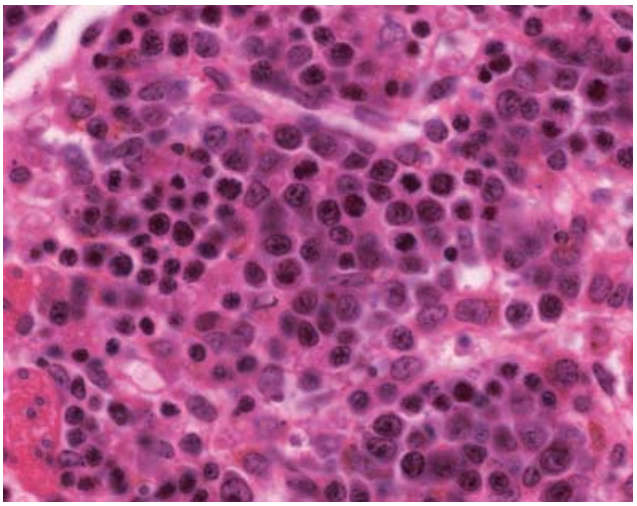

Figure 2.258. Detail of Figure 2.257. This spleen colony is entirely of erythroid type, with the cells all having round nuclei that are densely stained but vary in diameter with degrees of maturation.

REFERENCES

Bondurant, M.C., and Koury, M.J. (2004) Origin and development of blood cells (Chapter 6). In Greer, J.P., Foerster, J., Lukens, J.N., Rodgers, G.M., Paraskevas, F., and Glader, B. (eds.), *Wintrobe's Clinical Hematology*, Eleventh Edition, Volume 1. Lippincott Williams & Wilkins, Philadelphia.

Chen, C.-Z., Li, L., Lodish, H.F., and Bartel, D.P. (2004) MicroRNAs modulate hematopoietic lineage differentiation. *Science* 303:83–86.

Cohen, Y., and Nagler, A. (2003) Hematopoietic stem-cell transplantation using umbilical-cord blood. *Leuk & Lymph* 44(8):1287–1299.

Dührsen, U., and Hossfeld, D.K. (1996) Stromal abnormalities in neoplastic bone marrow diseases. *Ann Hematol* 73:53–70.

Ferkowicz, M.J., Starr, M., Xie, X., Li, W., Johnson, S.A., Shelley, W.C., Morrison, P.R., and Yoder, M.C. (2003) CD41

expression defines the onset of primitive and definitive hematopoiesis in the murine embryo. *Development*, pp. 4393–4403.
Gimble, J.M., Robinson, C.E., Wu, X., and Kelly, K.A. (1996) The function of adipocytes in the bone marrow stroma: An update. *Bone* 19(5):421–428.
Guba, S.C., Sartor, C.I., Gottschalk, L.R., Ye-Hu, J., Mulligan, T., and Emerson, S.G. (1992) Bone marrow stromal fibroblasts secrete interleukin-6 and granulocyte-macrophage colony-stimulating factor in the absence of inflammatory stimulation: Demonstration by serum-free bioassay, enzyme-linked immunosorbent assay, and reverse transcriptase polymerase chain reaction. *Blood* 80(5):1190–1198.
Mayani, H., Guilbert, L.J., and Janowska-Wieczorek, A. (1992) Biology of the hemopoietic microenvironment. *Eur J Haematol* 49:225–233.
Metcalf, D., and Moore, M.A.S. (1971) *Haemopoietic Cells*. American Elsevier Publishing Company, New York, p. 21.
Riddell, S.R., Berger, C., Murata, M., Randolph, S., and Warren, E.H. (2003) The graft versus leukemia response after allogeneic hematopoietic stem cell transplantation. *Blood Reviews* 17:153–162.
Wright, D.E., Wagers, A.J., Gulati, A.P., Johnson, F.L., and Weissman, I.L. (2001) Physiological migration of hematopoietic stem and progenitor cells. *Science* 294:1933–1936.

Normal Function

By a series of feedback mechanisms the marrow maintains a volume of hematopoietic tissue appropriate to the individual, much like the liver in terms of its overall size relative to the body as a whole. Each marrow cell lineage has specific chains of inductive factors that act to induce stem cell differentiation and maturation of progeny. Before identification of the interleukins, hematologists described the function of the marrow as replacing each peripheral cell that was lost by another. In fact the body responds differently to loss of blood cells by different means. Anemias that result from blood destroyed within the body are much more responsive than those due to hemorrhage (Figs. 2.259, 2.260). This is apparently because of retained access to iron and cellular proteins. A similar phenomenon occurs in the myeloid system where diseases that result in neutrophils being destroyed within the body are much more likely to have a neutrophilic leukocytosis than those where the spent cells are lost entirely to the exterior (Figs. 2.261, 2.262). Thus, inflammations characterized by localized infections, particularly with abscess formation, will usually be associated with neutrophilia; those like enteritis, mastitis, and metritis, where the cells are lost from the body, are likely to accompany neutropenia, particularly in the cow.

In interpretations of the myeloid system, it has been a lingering concept that the bone marrow contains many more (hundreds of times as many) neutrophils in the marrow granulocyte reserves (MGR) than are present in the circulating granulocyte pool (CGP). However, in quantitative studies done in the calf and the dog, the MGR of the calf was determined by leukopheresis to be twice the size of the CGP and totaled 2 billion granulocytes per kg. This same relationship was present in the dog. Leukopheresis (LAP) was accomplished by systemic heparinization and passing blood through a siliconized glass wool column in an extracorporeal circuit that passed the red cells, lymphocytes, and most of the platelets but retained the neutrophils in a nontoxic but quantitative sequestration. In the calf, following marrow depletion by

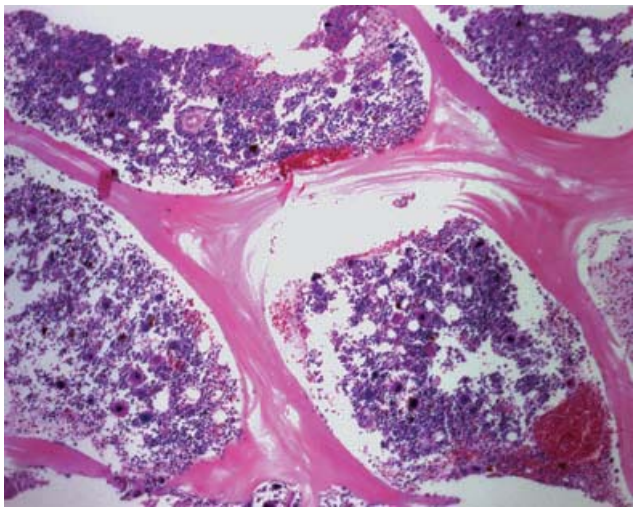

Figure 2.259. Dog: bone marrow with erythroid hyperplasia due to immune mediated hemolytic anemia.

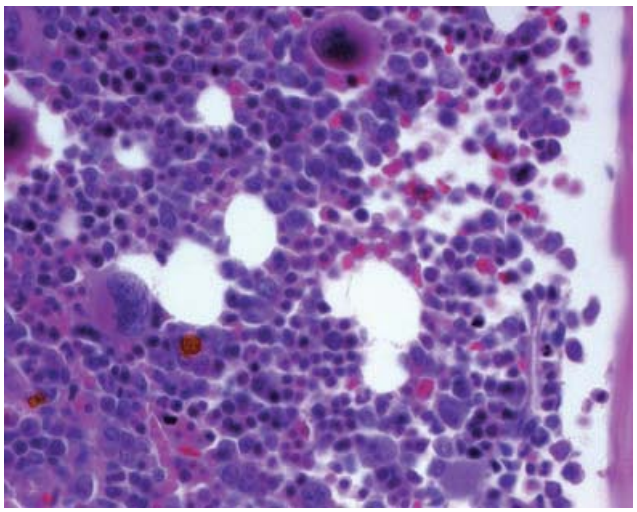

Figure 2.260. Detail of Figure 2.258. The subendosteal marrow has marked erythroid and megakaryocytic hyperplasia and reduced proportion of fat cells. Normal response to hemolytic anemia permitted by reutilization of breakdown products of destroyed cells. Note prominent coarse hemosiderin pattern.

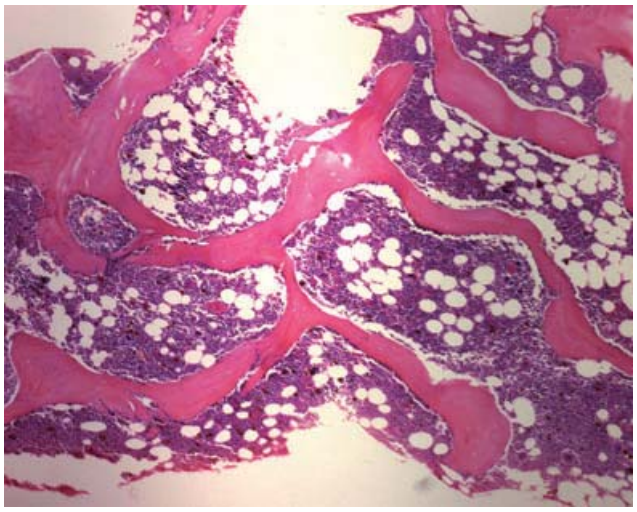

Figure 2.261. Dog: marrow myeloid hyperplasia associated with pyometra.

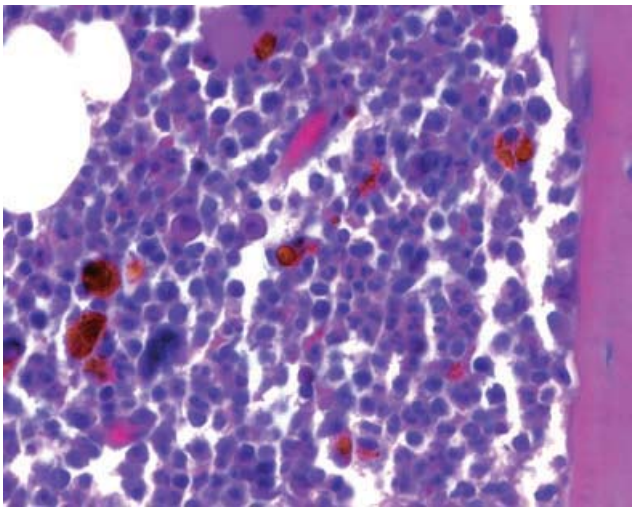

Figure 2.262. Detail of Figure 2.261. The subendosteal marrow has marked myeloid hyperplasia, increased marrow granulocyte reserves, many myeloid cells in the postmitotic phase of the metamyelocyte band, and segmented neutrophils. Accelerated myelopoiesis is accompanied by a coarse hemosiderin pattern of anemia of chronic disease.

leukopheresis the peripheral blood granulocytes remained low for a week, increased to above normal for a few hours, and then maintained a normal level. This brief neutrophil rebound at 1 week after LAP corresponded exactly to the production time of the neutrophil as determined by tritiated thymidine labeling. In contrast, in the dog, though marrow depletion was reached, as determined by concurrent marrow aspirations, the rebound was characterized by a steady rise in the CGP after cell removal, peaking in 3–4 days with significant immaturity. This work showed that the marked hematologic responsiveness of the dog was primarily due to much faster mobilization of the stem cell pool rather than a shorter production time for granulocytes. This interpretation is borne out by the 12–14–day cycle time of neutropenia in dogs with cyclic hematopoiesis. Presumably, about half of that period is due to the time required for the generation of a pool of committed stem cells, with the rest of the time related to the production time of the neutrophils at about a week, with the same production time for the calf and a bit longer for humans.

In a prescient observation, Oscar Schalm noted that the level of leukocyte reactivity of various domestic species in infectious diseases was related to the neutrophil/lymphocyte (N:L) level in the peripheral blood of normal animals. By this criteria, the dog with an N:L ratio of 2.4 is the most reactive of domestic animals, and the cow with an N:L of 0.5 is the least reactive. I have extended this observation by noting that if the N:L in homoestasis of each species is multiplied by 50, that number is the approximate peak level of neutrophilia likely to be encountered in an animal responding well to an infectious process. By this interpretation the maximum neutrophilia expected for the dog is 120,000/ul and for the cow, 25,000/ul.

With homeostatic hematopoiesis, there is a very constant 1:4 relationship between the proliferating cell pool of the marrow and their progeny in the maturation pool of cells. This relationship relates the sequence of dividing cells to the total cell production. Thus, for a single myeloblast there are 2 promyelocytes and 4 myelocytes, totaling 7 dividing level cells. In the maturation pool, the 4 myelocytes each divide to produce 8 nondividing metamyelocytes plus their further sequence of 8 band cells and 8 segmented neutrophils. There are thus 3 maturation phase cells in each of the 8 sets of progeny for a total of 24 maturing cells. These 24 are augmented by a small number of additional divisions, likely in the myelocyte pool, that adds about 6 mature neutrophils to the output of each single myeloblast, which totals 30 maturing cells in the marrow granulocyte reserve pool. These calculations are validated by differential counts on marrow cytological preparations showing that for each 7 dividing cells in the myeloid lineage there are 30 maturing cells for a proportionate ratio that is very close to 1:4. A similar relationship exists for the erythroid series, and these estimates are valid for males, females, and pregnant females in Sprague-Dawley rats. This information is very important in the evaluation of marrow proliferation in disease states, particularly when there is a hyperplastic marrow, but peripheral cytopenia and myelodysplasia is a likely differential. In the various types of myelodysplasia, early asynchrony is a constant feature; with the recognition of

dysplastic changes in each of the marrow lineages, the proportion of proliferating to maturing cells assists in the recognition of dysplastic states in which there is early asynchrony but not to exceed a level that would make a diagnosis of acute leukemia.

In the evaluation of bone marrow where there are about 25 morphologically distinct cell types present, it is useful to have guidelines to assist the evaluation of marrow biopsies. The first criterion is to determine whether all the cells essential for trilineage hematopoiesis are present and in the correct proportion. The next step is to determine whether, in addition to the normal complement, there are cells present not normally seen in the bone marrow.

REFERENCES

Lumsden, J.H., Valli, V.E.O., McSherry, B.J., and Willoughby, R.A. (1974) The Piromen Test as an assay of bone marrow granulocyte reserves in the calf, I. Studies on bone marrow and peripheral blood leukocytes. *Canadian J Comp Med* 38(1):56–64.

Valli, V.E., McSherry, J., Robinson, G.A., and Willoughby, R.A. (1969) Leukopheresis in calves and dogs by extracorporeal circulation of blood through siliconized glass wool. *Res Vet Sci* 10:267–278.

Valli, V.E., Villeneuve, D.C., Reed, B., Barsoum, N., and Smith, G. (1990) Evaluation of blood and bone marrow, rat. In Jones, T.C., Ward, J.M., Mohr, U., and Hunt, R.D. (eds.), *Hemopoietic System*. Springer-Verlag, Berlin, pp. 9–26.

Valli, V.E.O., McSherry, B.J., Hulland, T.J., Robinson, G.A., and Gilman, J.P.W. (1971) The kinetics of haematopoiesis in the calf, II. An autoradiographical study of erythropoiesis in normal, anaemic and endotoxin treated calves. *Res Vet Sci* 12(6):551–564.

Valli, V.E.O., McSherry, B.J., Hulland, T.J., Robinson, G.A., and Gilman, J.P.W. (1971) The kinetics of haematopoiesis in the calf, I. An autoradiographical study of erythropoiesis in normal, anaemic and endotoxin treated calves. *Res Vet Sci* 12(6):535–550.

Developmental and Degenerative Diseases

Congenital Diseases of Bone Marrow

Congenitally Defective Stem Cells

Congenital diseases that are primary disorders of the bone marrow are rarely recognized in animals and are likely of relatively rare occurrence. Because most of the known diseases are heritable or have heritable tendencies that would be culled from animal populations, there is a strong negative bias against these diseases being propagated. Reticular Dysgenesis is a rare disease of human infants that is characterized by congenital agranulocytosis and severe combined immunodeficiency. The cases present with enteritis or pneumonia and are recognized as abnormal by very low blood leukocyte counts. Treatment is by hematopoietic stem cell transplantation; otherwise, the disease is fatal within weeks of birth. Despite the deficient cellular status, complete myeloablation is a prerequisite for what is usually successful transplantation. The primary defect is unknown or undefined, and the condition is felt to be inherited as an autosomal recessive because both males and females are known to be carriers and cases have resulted from parental consanguinity.

Other diseases of this type include the Diamond Blackfan anemia, which is a congenital disorder of red cells believed to be carried as an autosomal recessive trait and affecting 5–7 infants per million live human births. The characteristics that define the disease are a normochromic macrocytic anemia with reticulocytopenia, with normal leukocyte and platelet counts. There is severe marrow erythroid hypoplasia and very low erythroid colony-forming units indicating an intrinsic defect in erythroid differentiation. Some patients respond to steroid therapy and survivors have a high incidence of myelodysplastic disease in later life.

An intriguing disease of the black rhinoceros is a congenital anemia with survival to maturity and reproduction. The cases terminate in marrow failure with chronic nonhealing ulcers. The marrow at that time has myelophthisic fibrosis with severe hemosiderosis (Figs. 2.263–2.265). The disease resembles a congenital hemolytic anemia as seen in humans with erythroid dysplasia. There are three types of human congenital dyserythropoietic anemia, all characterized by moderate anemia that may not be noticed until maturity. They all have marked marrow erythroid hyperplasia with reticulocy-

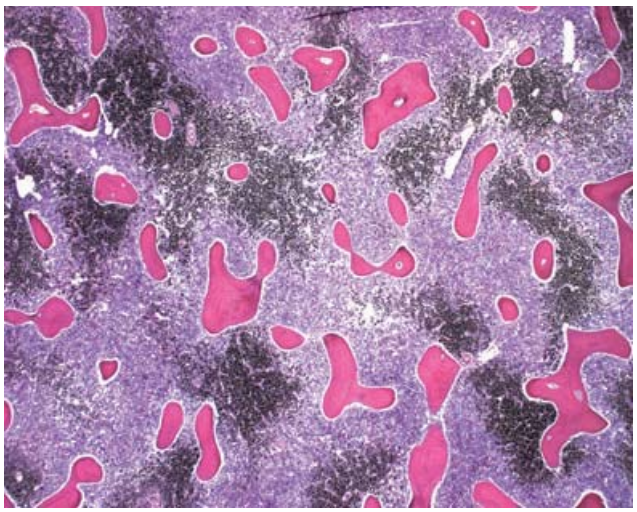

Figure 2.263. Black rhinoceros: bone marrow with marked hyperplasia and massive hemosiderosis due to congenital hemolytic anemia.

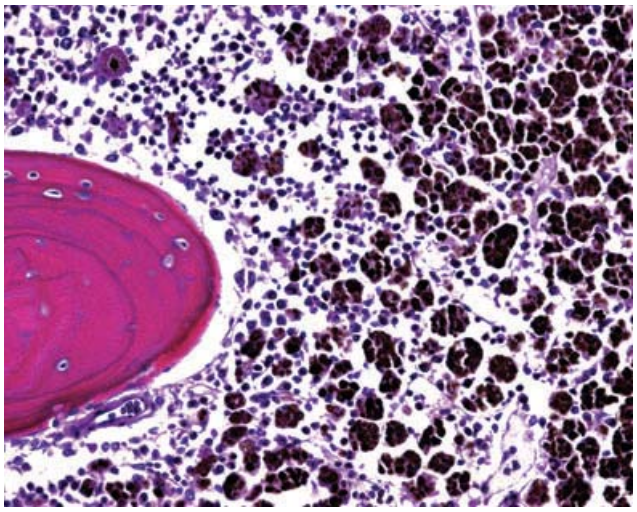

Figure 2.264. Detail of Figure 2.263. Interface of a solid area of hemosiderosis with more normal but hyperplastic bone marrow. Large macrophages contain multiple large aggregates of hemosiderin accumulation.

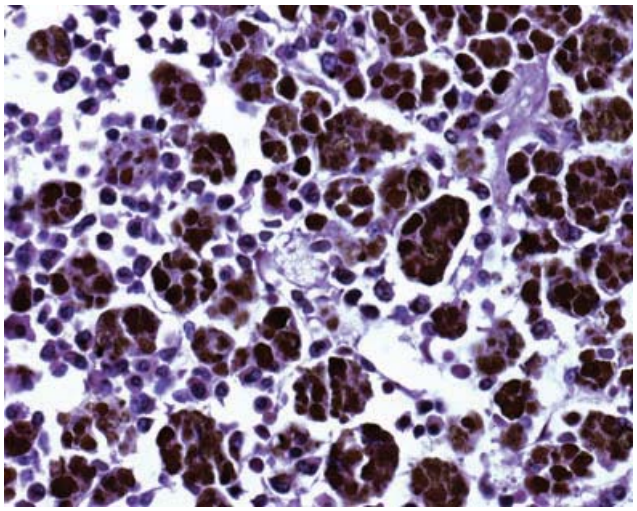

Figure 2.265. Detail of Figure 2.263. There is accumulation of large hemosiderin-bearing macrophages with phthisis of most hematopoietic precursors. This level of hemosiderin accumulation results in thickening of the marrow stroma and ultimately reticulin sclerosis. Marrow iron patterns are indicative of rate of marrow iron turnover. Coarse hemosiderin is indicative of nonutilization, and fine granules are more characteristic of responsive hemolytic anemias.

topenia, and kinetically there is ineffective erythropoiesis. There is a marked increase in serum iron turnover, but poor utilization and hemochromatosis is common. Type II congenital dyserythropoietic anemia is most common and may be similar in the black rhinoceros because it appears to share the morphological defects of rubricyte multinuclearity. This multinuclearity appears in the culture of marrow from affected humans, and therefore the defect is intrinsic to the erythroid lineage and is not due to a microenvironmental defect. The peripheral red cells are unusually sensitive to acid hemolysis (Ham test), and diagnosis includes a positive acidified serum test known by the acronym *HEMPAS* for hereditary erythroblast multinuclearity with positive acidified serum. This type of marrow multinuclearity may be mimicked by heavy metal poisonings of arsenic or lesser lead where the nervous signs should be prominent.

Other rare human forms of congenital marrow disease include severe congenital neutropenia with maturation arrest at the promyelocyte stage and high likelihood of progression to acute myeloid leukemia (AML) or myelodysplastic syndrome (MDS). Fanconi anemia is an autosomal recessive disease associated with multiple congenital malformations. Most cases are not recognized as such, with the malformations supervening until blood examination is carried out. I know of no animal counterpart.

REFERENCES

Abrams-Ogg, A.C.G., Kruth, S.A., Carter, R.F., Dick, J.E., Valli, V.E.O., Kamel-Reid, S., and Dubé, I.D. (1993) Clinical and pathological findings in dogs following supralethal total body irradiation with and without infusion of autologous long-term marrow culture cells. *Can J Vet Res* 57:79–88.

Bertrand, Y., Müller, S.M., Casanova, J.L., Morgan, G., Fischer, A., and Friedrich, W. (2002) Reticular dysgenesis: HLA non-identical bone marrow transplants in a series of 10 patients. *PaperBone Marrow Transplantation* 29:759–762.

De La Calle-Martín, O., Badell, I., García, A., Gelpí, C., Casamitjana, N., Estella, J., and Rodríguez-Sánchez, J.L. (1997) B cells and monocytes are not developmentally affected in a case of reticular dysgensis. *Clin Exp Immunol* 110:392–396.

Gazda, H. (1999) Congenital bone marrow failure. *Int J Pediatric Hematol/Oncol* 6(2):131–145.

Walker, J.M., Valli, V.E.O., Lumsden, J.H. (1974) Colony formation in culture by bovine granulopoietic progenitor cells. *Can J Comp Med* 38(2):145–152.

Watts, R. (2004) Neutropenia (Chapter 63). In Greer, J.P., Foerster, J., Lukens, J.N., Rodgers, G.M., Paraskevas, F., and Glader, B. (eds.), *Wintrobe's Clinical Hematology*, Eleventh Edition, Volume 1. Lippincott Williams & Wilkins, Philadelphia.

Cyclic Hematopoiesis

Cyclic hematopoiesis is an autosomal recessive disease of grey collie dogs and a dominant recessive disorder in humans. The disease is remarkably similar in humans and dogs and was originally known as *cyclic neutropenia* before it was recognized that there was cycling of other cell lineages as well. The average cycle time for

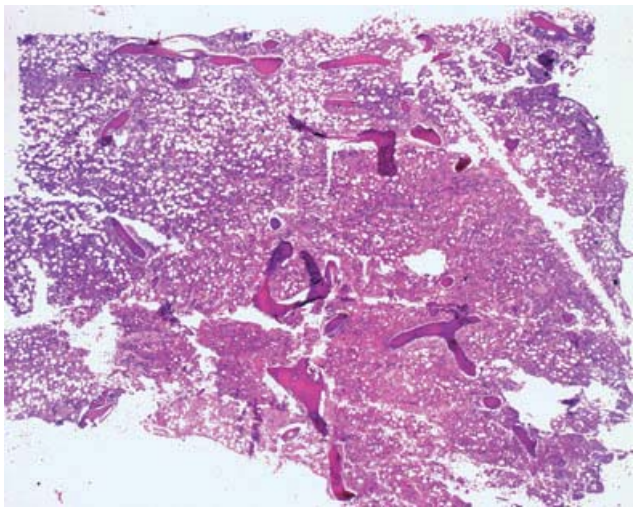

Figure 2.266. Dog: bone marrow, gray collie syndrome with reduced proportion of fat cells and marked congestion due to cyclic evacuation in cyclic neutropenia.

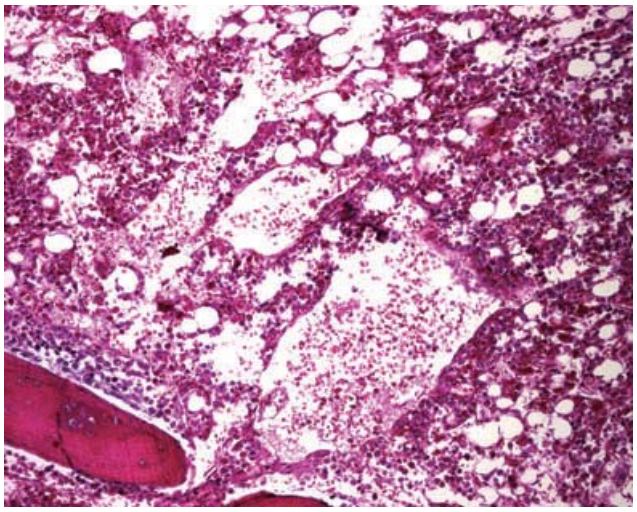

Figure 2.267. Detail of Figure 2.266. Note marked dilation of sinusoids with low cell density of interstitial areas.

neutrophils in humans is 21 ± 3 days for most cases, with some as short as 12 days and others as long as 36 days; in the dog, the cycle time is always 12–14 days. The defect appears to lie in a cyclic lack of response of marrow precursors to growth factors G-CSF or GM-CSF. The defect is not due to levels of intrinsic growth factors, and CFUs (colony forming units) representing marrow stem cells share the timing defect in culture, indicating that the defect is cellular and likely due to genetic control of cell receptors rather than microenvironmental. The disease is characterized by repeated bouts of febrile disease associated with mucositis and skin infections and often septic arthritis. Dogs have monocytosis, presumably because these cells are longer lived than neutrophils and have a shorter production time. Cycling of platelets and reticulocytes occurs in dogs, but it is not of clinical significance in comparison to the susceptibility of the animals to infection during periods of neutropenia. The bone marrow is highly variable, depending on the stage of cycle, and in rebound may resemble acute myeloid leukemia, with many blast cells and promyelocytes with maturation appearing to arrest at that stage (Figs. 2.266–2.268). In dogs, the disease is aided by lithium administration, which appears to set the level of stem cell differentiation slightly higher. In humans and dogs, the disease can be transmitted by marrow transplantation, as occurred in a human sibling given marrow for therapy of acute myeloid leukemia. The disease can also be cured in both species by marrow transplant, firmly indicating the defect is at the level of pluripotential stem cell.

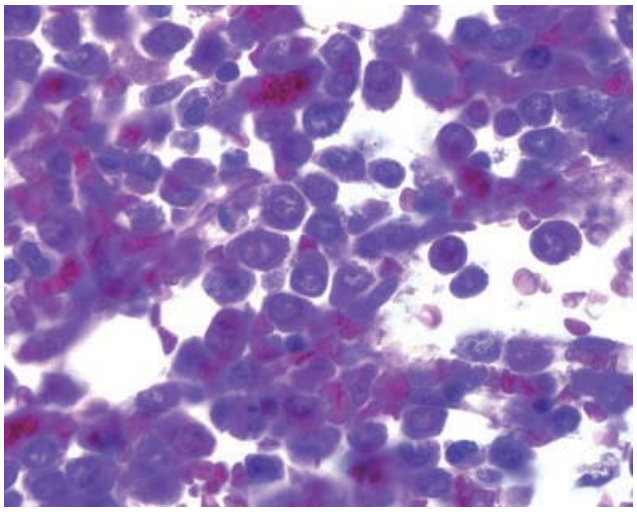

Figure 2.268. Detail of Figure 2.266. Early rebound, with the marrow primarily composed of blasts of promyelocytes and myelocytes presenting an appearance of marked early immaturity similar to that seen in acute leukemia.

REFERENCES

Dunn, C.D.R., Jones, J.B., Lange, R.D., and Quesenberry, P.J. (1983) Cyclic hematopoiesis: Stem cell disorders, human diseases, animal models, mathematical models. In Heim, L.R. (ed.), *Immunol & Hematol Res Monograph* 1:1–57.

Hammond, W.P., and Dale, D.C. (1982) Cyclic hematopoiesis: Effects of lithium on colony-forming cells and colony-stimulating activity in grey collie dogs. *Blood* 59(1):179–184.

Lothrop, C.D., Warren, D.J., Souza, L.M., Jones, J.B., and Moore, M.A.S. (1988) Correction of canine cyclic

hematopoiesis with recombinant human granulocyte colony-stimulating factor. *Blood* 72(4):1324–1328.
Shull, R.M., and Powell, D. (1979) Acquired hyposegmentation of granulocytes (pseudo-Pelger-Huët anomaly) in a dog. *Cornell Vet* 69(3):241–247.
Tvedten, H. (1983) Pelger-Huët anomaly, hereditary hyposegmentation of granulocytes. *Comparative Pathology Bulletin*. Registry of Comparative Pathology, Armed Forces Institute of Pathology, Washington D.C. 15(2):3–4.
Watts, R. (2004) Neutropenia (Chapter 63). In Greer, J.P., Foerster, J., Lukens, J.N., Rodgers, G.M., Paraskevas, F., and Glader, B. (eds.), *Wintrobe's Clinical Hematology*, Eleventh Edition, Volume 1. Lippincott Williams & Wilkins, Philadelphia.

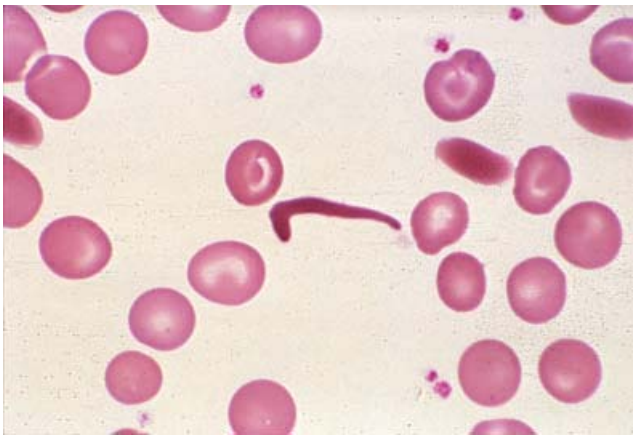

Figure 2.269. Human: blood, sickle cell anemia. In low oxygen states, the hemoglobin S variant loses its normal tertiary molecular structure and converts to linear arrays and becomes dense and inflexible. Multiple abnormally shaped red cells may result in small vessel thrombosis.

Hemoglobinopathies and Hereditary Anemias

Inherited defects in red cells may involve the synthesis of heme, the globin chains, or the cell membrane or deficiencies in the enzyme systems that protect these structural elements of the red cell. There are more than 600 types of human hemogloblinopathy of which the sickle cell trait and sickle cell anemia are most prevalent and best known. These diseases are largely due to substitution of a single amino acid, usually in the beta globin chain. The other chains may be involved at lesser frequency, particularly of the alpha globin chain, because these are duplicated and even homozygotes with variants in alpha chains tend to be protected from abnormal hemoglobin production. In sickle cell trait, valine replaces glutamic acid in the 6th position from the N-terminal of the beta globin chain. Those with homozygous substitutions at the same site have anemia and the clinical syndrome.

The discovery of sickle cell disease and its molecular basis (Hb S) represents a landmark advance in medicine (Fig. 2.269). The initial report of a patient with "sickle shaped red cells" was made by J. B. Herrick in 1910. This was followed by the observation by V. E. Emmel in 1917 that normal biconcave cells from affected people would alter to the sickle form in vitro and in asymptomatic carriers, thus establishing both the anemic condition and the carrier trait. In 1940 I. J. Sherman noted that the cells in sickle cell disease were birefringent and mentioned this to Linus Pauling who wondered whether the phenomenon was due to abnormal configuration of the hemoglobin molecule and showed an abnormal migration pattern by Hb S. The various alterations of the globin chains are classified by the type of change including single or double amino acid substitutions as well as deletions, insertions, and fusion between chains. Subsequent descriptions name the conditions after the city of the author.

Clinically, the disease is not manifest in infants and does not occur until the fetal hemoglobin level drops below a critical level at which the Hb S dilution is insufficient to prevent sickling on loss of oxygenation. In infants homozygous (Hb SS) for the trait, there is mild anemia by 3–4 months, splenomegaly after 6 months, and about half of cases will have a vascular occlusive episode in the first year, with most before 6 years of age. These vascular blockages account for more of the clinical syndrome of Hb SS carriers than of the anemia. The inciting causes for the sickling-based thrombi include low oxygen levels as in high-altitude flying, infections, acidosis, fever, and dehydration. The symptoms are painful foci that can appear in any part of the body, most often in an extremity but also in bone marrow. Mice bearing the variant human beta globin genes have the trait but produce enough normal globin to prevent sickle cell disease. The sickle cell trait and disease have been produced in mice in which both copies of both the beta and alpha genes have been deleted. When these mice are mated to others bearing the variant human genes for Hb SS or alpha or beta thalassemia, full-blown disease results in the progeny. Further, a means of treating sickle cell anemia was tested by generating Hb SS erythroid precursors from cord blood of infant patients that were exposed to a transsplicing ribozyme derived from *Tertrahymena thermophila*, which resulted in RNA repair and production of antisickling beta globin. Since as much as 10% of normal hemoglobin greatly reduces the severity of the disease, the approach may have clinical application. These developments are examples of the application of molecular medicine to disease resulting from a genetic germ line mutation.

Later studies identified thalassemia as a separate condition with characteristic Mediterranean background (Fig. 2.270). In thalassemia there is deficient production of one of the hemoglobin chains ($\alpha\beta$), and the normal

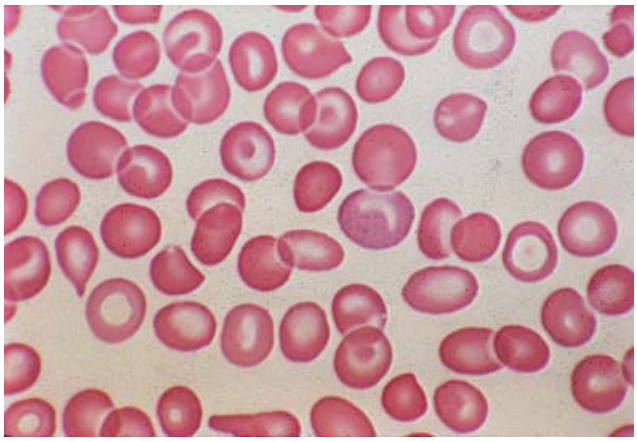

Figure 2.270. Human: blood, beta thalassemia minor. Mild hypochromasia with some cells much more affected than others. Abnormal shapes include leptocytes, elliptocytes, and teardrop-shaped cells. These changes in red cell morphology result from genetic errors in hemoglobin synthesis.

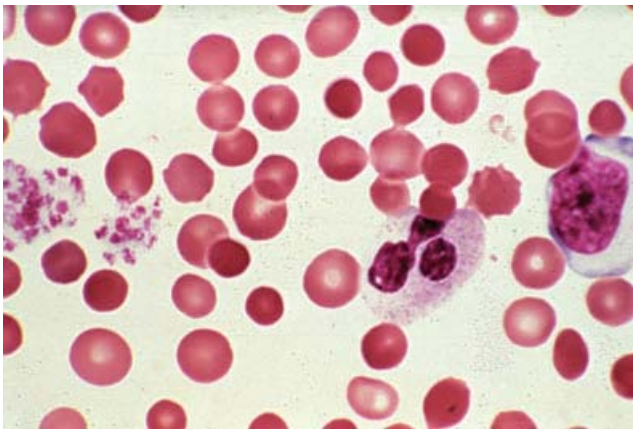

Figure 2.272. Human: blood, hereditary spherocytosis. Genetically abnormal red cells have increased rigidity and lack the ability to deform shape on passing through small vessels. They are recognized as abnormal by splenic macrophages resulting in a constant high-level intracellular hemolysis.

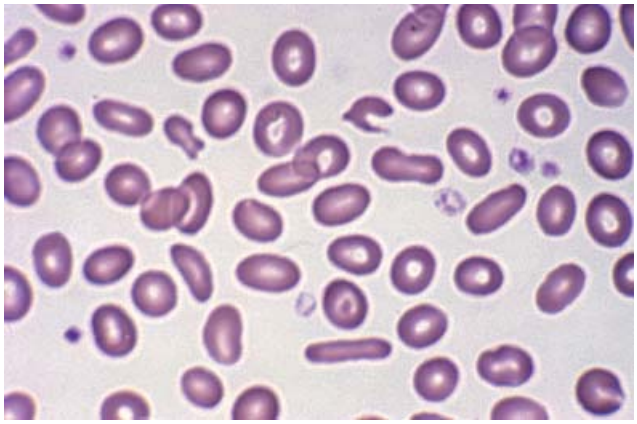

Figure 2.271. Human: blood, beta thalassemia and elliptocytosis. Anemia is due to deficient cells and deficient hemoglobin. The irregularly shaped cells represent minor peripheral fragmentation, and the oval-shaped cells are due to genetic abnormalities in the red cell framework. A minor degree of elliptocytosis in genetically normal humans and animals with cytopenias is an indication of early marrow myelofibrosis.

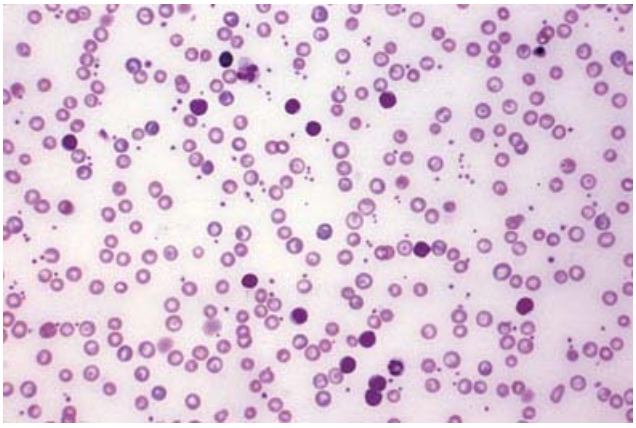

Figure 2.273. Dog: blood, pyruvate kinase deficiency in young male basenji dog. There is moderate anemia with macrocytosis and prominent red cell basophilia indicating new red cell production. There are several target cells present with lymphocytosis and thrombocytosis. *Image from G. P. Searcy, DVM.*

chains are synthesized in excess resulting in ineffective erythropoiesis. Any one of the chains may be involved, but the alpha and beta chains are most often those inherited with amino acid substitutions. More than one defect may be present in the same individual, with thalassemia and elliptocytosis (Fig. 2.271) occurring together. Inherited defects in the red cell membrane occur as hereditary spherocytosis (Fig. 2.272), which results in chronic hemolytic anemia and jaundice that is responsive to splenectomy. There are similar diseases in animals for some of these human conditions with the identification of pyruvate kinase deficiency in a strain of basenji dogs (Figs. 2.273, 2.274). More commonly, unusual bricklike condensations are seen in dogs and cats due to the presence of hemoglobin "C" in sufficient quantity to result in crystalline collapse (Fig. 2.275). The finding is more of interest in terms of pathogenetic mechanisms than clinical importance.

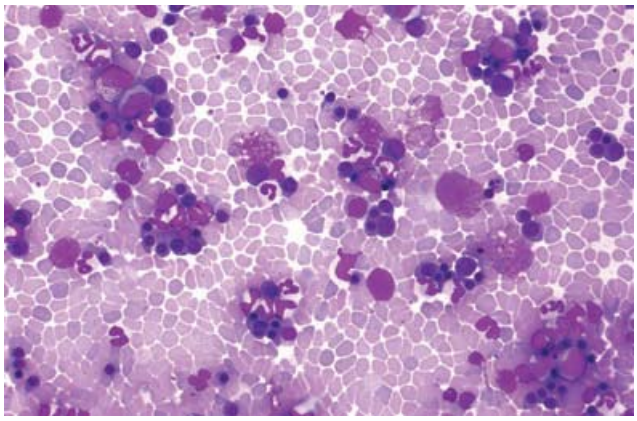

Figure 2.274. Dog: bone marrow aspirate, pyruvate kinase deficiency. There is a mild to moderate erythroid hyperplasia and a marked increase in polychromatophilic red cells that would stain as reticulocytes with supervital staining. *Image from K. W. Prasse, DVM.*

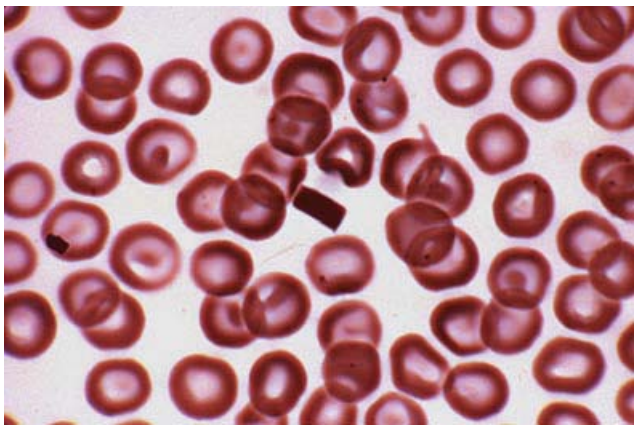

Figure 2.275. Dog: blood, hemoglobin "C." Hemoglobin of this variant tends to form linear arrays of globin chains in the peripheral blood. The finding is of little importance other than to understand the genesis of the change. Their presence of these changes in the globin chains may be increased by the stresses on the erythron. Note that there are numerous Howell-Jolly bodies in the surrounding normal-appearing red cells.

REFERENCES

Lan, N., Howrey, R.P., Lee, S.-W., Smith, C.A., and Sullenger, B.A. (1998) Ribozyme-mediated repair of sickle β-globin mRNAs in erythrocyte precursors. *Science* 280:1593–1596.

Lukens, J.N. (2004) Abnormal Hemoglobins: General Principles (Chapter 39). In Greer, J.P., Foerster, J., Lukens, J.N., Rodgers, G.M., Paraskevas, F., and Glader, B. (eds.), *Wintrobe's Clinical Hematology*, Eleventh Edition, Volume 1. Lippincott Williams & Wilkins, Philadelphia.

Pászty, C., Brion, C.M., Manci, E., Witkowska, H.E., Stevens, M.E., Mohandas, N., and Rubin, E.M. (1997) Transgenic knockout mice with exclusively human sickle hemoglobin and sickle cell disease. *Science* 278:876–878.

Ryan, T.M., Ciavatta, D.J., and Townes, T.M. (1997) Knockout-transgenic mouse model of sickle cell disease. Science 278:873–875.

Pelger-Huët Anomaly

The Pelger-Huët anomaly is a benign form of granulocyte hyposegmentation that affects humans, dogs, and rabbits. In humans and rabbits the condition is an autosomal dominant trait that has been reproduced in the homozygous state in the rabbit, where it was associated with limb deformities and short survival and all leukocytes had round nuclei. In the dog the condition is not associated with increased incidence of infectious disease, and tests of leukocyte migrations have given normal results. The condition appears less common in dogs than humans, and it is notable only to recognize the condition as not requiring therapy.

REFERENCES

Berrier, H.H., Robinson, F.R., Reed, T.H., and Gray, C.W. (1975) The white-tiger enigma. *Vet Med/Small An Clin* 70(4):467–472.

Burns, G.L., Meyers, K.M., and Prieur, D.J. (1984) Secondary amyloidosis in a bull with Chédiak-Higashi syndrome. *Can J Comp Med* 48:113–114.

Fagerland, J.A., Hagemoser, W.A., and Ireland, W.P. (1987) Ultrastructure and stereology of leukocytes and platelets of normal foxes and a fox with a Chédiak-Higashi–like syndrome. *Vet Pathol* 24:164–169.

Kramer, J.W., Davis, W.C., and Prieur, D.J. (1977) The Chédiak-Higashi syndrome of cats. *Lab Invest* 36(5):554–562.

Ménard, M., and Meyers, K.M. (1988) Storage pool deficiency in cattle with Chédiak-Higashi syndrome results from an absence of dense granule precursors in their megakaryocytes. *Blood* 72(5):1726–1734.

Oliver, C., and Essner, E. (1975) Formation of anomalous lysosomes in monocytes neutrophils, and eosinophils from bone marrow of mice with Chédiak-Higashi syndrome. *Lab Invest* 32(1):17–26.

Renshaw, H.W., Davis, W.C., Fudenberg, H.H., and Padgett, G.A. (1974) Leukocyte dysfunction in the bovine homologue of the Chédiak-Higashi syndrome of Humans. *Infect Immun* 10(4):928–937.

Skubitz, K.M. (2004) Qualitative disorders of leukocytes (Chapter 64). In Greer, J.P., Foerster, J., Lukens, J.N., Rodgers, G.M., Paraskevas, F., and Glader, B. (eds.), *Wintrobe's Clinical Hematology*, Eleventh Edition, Volume 1. Lippincott Williams & Wilkins, Philadelphia.

Chédiak Higashi Anomaly

The Chédiak Higashi anomaly is an autosomal recessive disorder characterized by the presence of giant lysosomal organelles in most granule-containing leukocytes. The

condition occurs in humans, Aleutian mink, Hereford cattle (Fig. 2.276), Persian cats (Fig. 2.277), beige mice (Fig. 2.278), rats, foxes, and a killer whale. The condition is associated with partial ocular and cutaneous albinism with a tendency to increased pyogenic infections. The clinical manifestations of the anomaly are felt to be related to the larger and fewer than normal leukocyte granules that are less than normally effective in phagocytosis and lysis. It appears that primary granule formation occurs, but it is followed by fusion rather than by formation of secondary granules (Figs. 2.279, 2.280). There may as well be defective fusion and release of enzyme in phagocytic vacuoles although the respiratory burst and peroxide production is normal. Abnormal migration of neutrophils occurs in skin window preparations in affected humans, mink, and mice. The defect in

Figure 2.276. Twin calves: 1 year of age. The white calf has the Chédiak-Higashi anomaly and is visibly smaller. *Image from D. J. Prieur, DVM.*

Figure 2.277. Persian cats: The cat with less depth of pigmentation in hair has the Chédiak-Higashi trait. Note that animal is squinting in the level of ambient light due to lack of iris pigmentation. *Image from D. J. Prieur, DVM.*

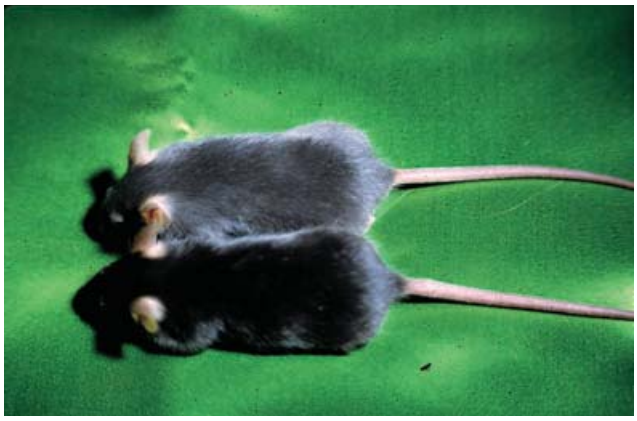

Figure 2.278. Black and beige mice: The mouse with color dilution is beige and has the Chédiak-Higashi genotype. *Image from D. J. Prieur, DVM.*

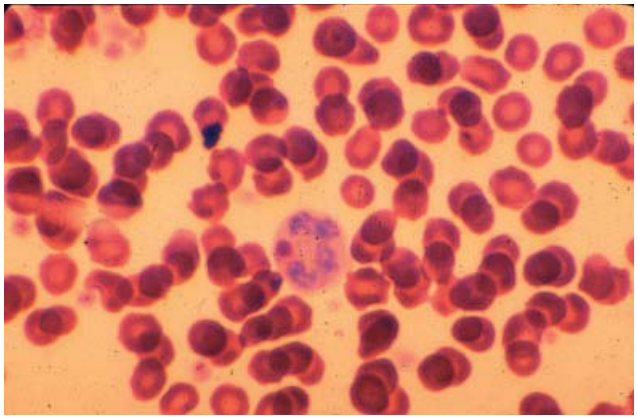

Figure 2.279. Blood from a cat with the Chédiak-Higashi trait. The neutrophil has normal nuclear segmentation but reduced cytoplasmic volume that is pale and of even density with only a single very large cytoplasmic granule. *Image from D. J. Prieur, DVM.*

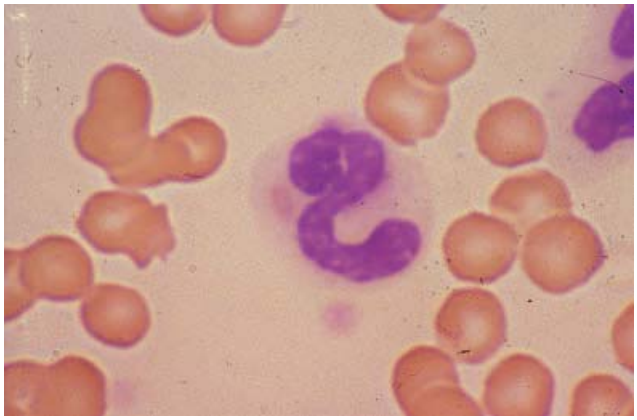

Figure 2.280. Blood from a cat with the Chédiak-Higashi trait. A mature peripheral blood neutrophil has very low cytoplasmic density that is only slightly more densely stained than the surrounding background of serum proteins. There is a single large cytoplasmic granule of low-staining density left of the nucleus. *Image from D. J. Prieur, DVM.*

migration is due to impaired microtubular assembly as occurs in normal cells treated with colchicine. Some restoration of function is achieved by administration of ascorbic acid and cholinergic agonists. Large granules are also found in vascular endothelium, Schwann cells, fibroblasts, melanosomes, and hair shafts. In cattle a bleeding tendency in affected animals was found to be due to lack of granule formation in megakaryocytes and subsequently in platelets. Long-term survivors have a tendency to develop amyloidosis. Aleutian mink are abnormally susceptible to a retrovirus and develop plasmacytosis and hyperglobulinemia and generally don't survive longer than a year.

REFERENCES

Berrier, H.H., Robinson, F.R., Reed, T.H., and Gray, C.W. (1975) The white-tiger enigma. *Vet Med/Small An Clin* 467–472.

Burns, G.L., Meyers, K.M., and Prieur, D.J. (1984) Secondary amyloidosis in a bull with Chédiak-Higashi syndrome. *Can J Comp Med* 48:113–114.

Fagerland, J.A., Hagemoser, W.A., and Ireland, W.P. (1987) Ultrastructure and stereology of leukocytes and platelets of normal foxes and a fox with a Chédiak-Higashi–like syndrome. *Vet Pathol* 24:164–169.

Kramer, J.W., Davis, W.C., and Prieur, D.J. (1997) The Chédiak-Higashi Syndrome of Cats. *Lab Invest* 36(5):554–562.

Ménard, M., and Meyers, K.M. (1988) Storage pool deficiency in cattle with Chédiak-Higashi syndrome results from an absence of dense granule precursors in their megakaryocytes. *Blood* 72(5):1726–1734.

Oliver, C., and Essner, E. (1975) Formation of anomalous lysosomes in monocytes, neutrophils, and eosinophils from bone marrow of mice with Chédiak-Higashi syndrome. *Lab Invest* 32(1):17–26.

Renshaw, H.W., Davis, W.C., Fudenberg, H.H., and Padgett, G.A. (1974) Leukocyte dysfunction in the bovine homologue of the Chédiak-Higashi syndrome of humans. *Infect Immun* 10(4):928–937.

Skubitz, K.M. (2004) Qualitative disorders of leukocytes (Chapter 64). In Greer, J.P., Foerster, J., Lukens, J.N., Rodgers, G.M., Paraskevas, F., and Glader, B. (eds.), *Wintrobe's Clinical Hematology*, Eleventh Edition, Volume 1. Lippincott Williams & Wilkins, Philadelphia.

Leukocyte Adhesion Deficiency

Leukocyte adhesion (CD11, CD18) deficiency (LAD) is a rare disease of humans, Irish setter dogs, and Holstein cattle. Two forms of the LAD disease occur in humans with the LAD-1 type similar to the animal diseases; the LAD-2 type is characterized by normal phagocytosis and expression of surface CD18, but deficient motility and aggregation and associated with severe mental retardation. The CD11 and CD18 family consists of three heterodimeric proteins, each composed of non-covalently associated alpha and beta chains. The alpha chain has three isomers (alpha L, alpha M, alpha X). The dimeric chains must complete assembly prior to translocation to the cellular surface. Mutations arise in the beta 2 chain, which prevents dimeric assembly and loss of the beta 2 integrin on the cell surface. In tests of neutrophil function, these cells roll normally along the endothelium but don't migrate in response to chemotactic or inflammatory stimulation. The human form of LAD-1 has two syndromes, including those with less than 0.3% of CD11a/CD18 glycoproteins on the cell surface and those with 2.5–31% of normal levels. The animal cases have not been categorized to this level, but it appears from flow cytometric studies that the cases described have the severe form of deficiency. In function testing the neutrophils fail to migrate in skin window tests, and in vitro there are defects in motility, phagocytosis, granule secretion, and respiratory burst activity. In the human cases the humoral and cellular arms of the lymphocytic system and the complement system function normally. The clinical presentation in humans is of an infant or young child with frequent bacterial and occasionally viral infections and persistently high neutrophil counts. Infections usually involve the skin and subcutaneous tissues, middle ear, and oropharynx.

Calves heterozygous for the LAD have nearly normal levels of peripheral blood neutrophils and normal levels of CD11 and CD18 in contrast to calves homozygous for the trait that have about 10–15% of the level of cell surface integrins, as measured in flow cytometry. The carrier and control animals were very similar in their levels of phagocytosis and killing of yeast cells in in vitro studies, whereas the homozygous animals had markedly decreased ability in both areas but had much higher levels of respiratory burst activity. The greater production of peroxide by the neutrophils of homozygous calves was felt more likely to be due to constant priming of the cells rather than greater immaturity. The mononuclear cells of LAD-affected calves share the deficiency of surface CD18 in both lymphocytes and monocytes, but the lymphocytes have strong responses in blastogenic assays and affected calves have higher levels of IgG. The monocytes have markedly reduced adherence and diminished chemotaxis and phagocytosis. The calves homozygous for LAD have to be maintained on antibiotics for survival.

Pathologically, animals had multiple subcutaneous abscesses associated with ear tagging and were cachectic, often with ventral edema and extensive inflammation of the respiratory and enteric tracts. These changes had progressed to pseudomembranous rhinitis, necrotic laryngitis, and catarrhal bronchopneumonia involving most of the lung capacity. Enteric inflammation included severe gingivitis and periodontitis with tooth loss, catarrhal to pseudomembranous enteritis, and wide-

spread lymphadenopathy. The bone marrow was solidly hematopoietic.

The incidence of the LAD disease in dogs (initially called *canine granulocytopathy syndrome*) is apparently less than observed in Holstein calves, possibly because of the impact of artifical insemination in cattle permits wide dissemination of recessive genes that may have become associated with high production. Affected dogs have mild to moderate anemia, often with marked neutrophilic leukocytosis and varying levels of lymphocytosis and monocytosis and mild polyclonal gammmopathy. In function testing, the neutrophils have reduced adherence and motility to chemotaxis but increased respiratory burst function. In a single dog, the tendency for repeated infections accompanied by leukocytosis was noted at 2 months of age, and at 18 months the animal was presented with deep skin wound infections, pododermatitis, pyoderma, gingivitis, pneumonia, thrombophlebitis, and focal hindlimb osteomyelitis. Diagnosis is likely to be related to poor survival within a litter, particularly on repeat matings and early and recurrent skin infections.

REFERENCES

Giger, U., Boxer, L.A., Simpson, P.J., Lucchesi, B.R., and Todd, R.F. (1987) Deficiency of leukocyte surface glycoproteins Mo1, LFA-1, and Leu M5 in a dog with recurrent bacterial infections: An animal model. *Blood* 69(6):1622–1630.

Kehrli, M.E., Schmalstieg, F.C., Anderson, D.C., Van Der Maaten, M.J., Hughes, B.J., Ackermann, M.R., Wilhelmsen, C.L., Brown, G.B., Stevens, M.G., and Whetstone, C.A. (1990) Molecular definition of the bovine granulocytopathy syndrome: Identification of deficiency of the Mac-1 (CD11b/CD18) glycoprotein. *Am J Vet Res* 51(11):1826–1836.

Nagahata, H., Nochi, H., Sanada, Y., Tamoto, K., Noda, H., and Kociba, G.J. (1994) Analysis of mononuclear cell functions in Holstein cattle with leukocyte adhesion deficiency. *Am J Vet Res* 55(8):1101–1106.

Renshaw, H.W., and Davis, W.C. (1979) Canine granulocytopathy syndrome: An inherited disorder of leukocyte function. *Am J Pathol* 95(3):731–741.

Sipes, K.M., Edens, H.A., Kehrli, M.E., Miettinen, H.M., Cutler, J.E., Jutila, M.A., Quinn, M.T. (1999) Analysis of surface antigen expression and host defense function in leukocytes from calves heterozygous or homozygous for bovine leukocyte adhesion deficiency. *Am J Vet Res* 60(10):1255–1261.

Skubitz, K.M. (2004) Qualitative disorders of leukocytes (Chapter 64). In Greer, J.P., Foerster, J., Lukens, J.N., Rodgers, G.M., Paraskevas, F., and Glader, B. (eds.), *Wintrobe's Clinical Hematology*, Eleventh Edition, Volume 1. Lippincott Williams & Wilkins, Philadelphia.

Trowald-Wigh, G., Håkansson, L., Johannisson, A., Norrgren, L., Hård af Segerstad, C. (1992) Leucocyte adhesion protein deficiency in Irish setter dogs. *Vet Immunol and Immunopathol* 32:261–280.

van Garderen, E., Müller, K.E., Wentink, G.H., and van den Ingh, T.S.G.A.M. (1994) Post-mortem findings in calves suffering from bovine leukocyte adhesion deficiency (BLAD). *Vet Quarterly* 16(1):24–26.

Lysosomal Storage Diseases

Lysosomal storage diseases are the result of an abnormal aggregation of cytoplasmic structures or metabolites in secondary lysosomes. These structures are formed by the fusion of primary lysosomes and autosomal vacuoles. In the normal process of metabolizing cellular effluent, the containing vacuoles fuse with the primary lysosomes that contain the necessary lytic enzymes. If the appropriate enzyme is absent or nonfunctional, the metabolite or target material accumulates in membrane-bound vesicles that enlarge until cell function is irreparably impaired. Most storage diseases, excluding hemosiderosis, result from genetically defective synthesis of a particular enzyme that may result in a complete absence of the specific product or a product of abnormal stability or structure or of abnormal transport. There are four general categories of genetic errors classified as lysosomal storage diseases, including:

- Sphingolipidoses
- Mucopolysaccharidoses
- Mucolipidoses
- Glycogen storage diseases

The list includes diseases not recognized in animals, such as the sphingolipidosis known as *Tay-Sachs disease* characterized by GM2 ganglioside accumulation in ganglion cells resulting in neonatal death. The mucopolysaccharidoses (MPS) involve the glycosaminoglycans that form the ground substance for connective tissues. The diseases in this category include MPS type I and VI, and Fabry's disease (caused by a deficiency of alpha galactosidase). MPS types I and VI have been reported in the cat. There are a number of mucolipidoses caused by a deficiency of phosphotransferase, which results in severe retardation of ossification and the glycogen storage diseases that occur in dogs. For the purposes of this area of interest in bone marrow, the diseases are usually more narrowly defined as those resulting from abnormalities of the monocyte macrophage system. These diseases include Fabry's disease, Gaucher's disease (caused by the deposition of glucocerebroside in cells of the monocyte/macrophage system), and Nieman-Pick disease (due to a deficiency of acid sphingomyelinase).

REFERENCES

Bundza, A., Lowden, J.A., and Charlton, K.M. (1979) Niemann-Pick disease in a poodle dog. *Vet Pathol* 16:530–538.

Haskins, M.E., Aguirre, G.D., Jezyk, P.F., et al. (1983) The pathology of the feline model of mucopolysaccharidosis I. *Am J Pathol* 112:27–36.

Hochachka, P.W., Liggins, G.C., Qvist, J., Schneider, R., Snider, M.Y., Wonders, T.R., and Zapol, W.M. (1977) Mucopolysaccharidosis in a cat with arylsulfatase B deficiency: A model of Maroteaux-Lamy Syndrome. *Science* 198:834–833.

McGovern, M.M., and Desnick, R.J. (2004) Abnormalities of the Monocyte-Macrophage System: Lysosomal Storage Diseases (Chapter 65). In Greer, J.P., Foerster, J., Lukens, J.N., Rodgers, G.M., Paraskevas, F., and Glader, B. (eds.), *Wintrobe's Clinical Hematology*, Eleventh Edition, Volume 1. Lippincott Williams & Wilkins, Philadelphia.

The Mucopolysaccharidoses

A domestic short-haired cat had the MPS type I form of Hurler Scheie disease, which is characterized by hepatosplenomegaly, thickened mitral valve leaflets and chordae tendinae, and radiographically left atrial enlargement. On a lateral view of the head there was moderate facial dysmorphia with frontal bossing or prominence. Microscopically, the neurons in several areas of the brain were swollen with cytoplasmic vacuolations, and on electron microscopy the typical membrane-bound inclusions were present with parallel laminations referred to as "zebra bodies." The MPS type VI form of the disease (known as *Maroteaux-Lamy Syndrome*) has been found in Siamese cats that have more prominent frontal bossing with a depressed nasal bridge, small ears, and bilaterally clouded corneas. The presence of increased levels of polymeric glycosaminoglycans composed primarily of dermatan sulfate constitutes a diagnostic test for the condition that appears identical to the human form of the disease.

Niemann-Pick Disease

Niemann-Pick disease (NPD) results from an autosomal recessive mutation that prevents synthesis of the enzyme sphingomyelinase. The absence of this enzyme results in the accumulation of sphingomyelin and cholesterol in the macrophages of the central nervous system as well as in liver, kidney, and lungs. The subtypes of the disease include A and B, in which sphingomyelin is the major lipid accumulation. In types C and D the defect involves the transport of cholesterol with a slower progression of disease. The D type is largely traceable to a common ancestry in Yarmouth county of Nova Scotia. Human infants appear normal at birth often with prolonged jaundice. Hepatosplenomegaly, lymphadenopathy, and psychomotor retardation are evident by 6 months of age. Diagnosis is made in infants less than a year of age that fail to thrive and have splenomegaly. Splenomegaly usually prompts a bone marrow aspiration in which the characteristic foamy laden macrophages typical of Niemann-Pick disease are present.

A case of NPD in a miniature poodle dog was the result of a mother-son mating. The animal was presented at 5 months of age with ataxia, hypermetria, continuous head shaking, and loss of balance. The dog's attitude and appetite were unaffected and its head was radiographically normal. The animal was not responsive to medicinal treatment. Cerebrospinal fluid analysis reported 187 cells/ul with some well-preserved, large, foamy macrophages. The dog was then euthanized for further examination. The dog was in good body condition, but the lungs were firm and gray with confluent white nodules 1–2 mm in diameter on the pleural surfaces. The liver and spleen were enlarged but no other gross changes were found. On microscopic examination, almost all neurons in the brain and spinal cord were vacuolated, most particularly those of the medulla, brain stem, and Purkinje cells of the cerebellum. Similar types of foamy macrophages were present in the alveolar septa, liver, intestinal lamina propria, medullary cords of lymph nodes, splenic arteriolar sheaths, and sinuses. The intracytoplasmic material was autofluorescent on ultraviolet light.

Degenerative Diseases of Bone Marrow

Nutritional Diseases of Bone Marrow

The most common nutritional disease of marrow is starvation, generally of the marasmus type with deficient protein and caloric intake. Changes of this type are most likely to be seen in old sheep or goats with loss of teeth or severe dental attrition and complicated by mismanagement or neglect. The animals are cachectic with sharp bony prominences that may be less obvious in sheep if they have missed a shearing. There is loss of body fat and atrophic muscle that is dark and contrasts sharply with the tendinous sheaths. There may be edematous separation of muscle layers in dependent areas, and long bones are osteoporotic with thin cortices and loss of trabecular bone in the diaphyses. On gross examination, the marrow on the cut surface is translucent and rapidly recedes below the cortical margins on exposure to air with subsequent drying. Generally, the marrow is devoid of fat in the central long bone cavities, with most of the marrow cavity occupied by serous atrophy with the few sinuses functional and visible within the surface tissue. On histological examination, the atrophic fat stains a pale pink with previous areas of hematopoietic activity evident in isolated hemosiderin containing macrophages (Figs. 2.281, 2.282). The few remaining developing blood cells are widely separated and the supporting stroma is delicate and inapparent. Most remaining cells are primitive with loss of the marrow granulocyte reserves or mature granulocytes. Most of the mature cells of the leukocyte series are eosinophils and small lymphocytes. Erythropoiesis is

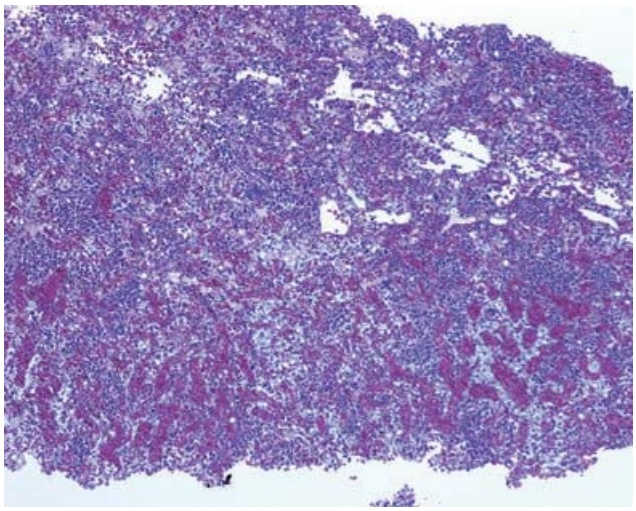

Figure 2.281. Bone marrow section from an aged macaque that was presented with signs of chronic inanition or starvation. The bone marrow has dilated sinuses and pale areas in the interstitium that are acellular and represent foci of serous atrophy of fat.

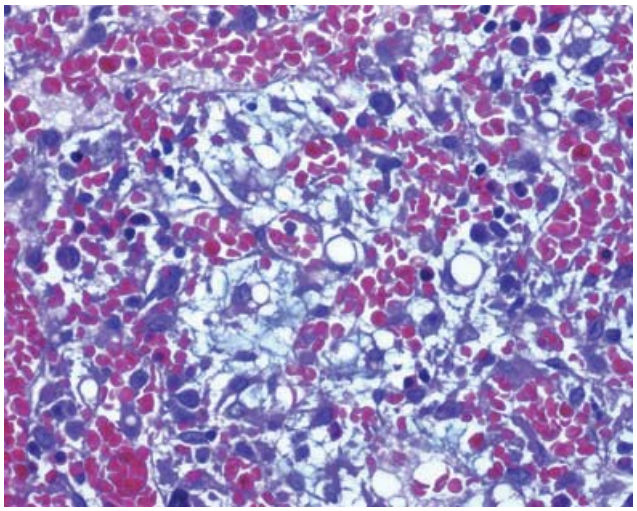

Figure 2.282. Detail of Figure 2.281. There is dilation and congestion of the marrow sinusoids with very low cellularity of the interstitial areas. There are small residual fatty vacuoles surrounded by interstitial areas of atrophy that stain with a faint basophilic background.

more volatile than the myeloid series and in chronic decline may be nearly absent.

If the decline has been more acute, the marrow will appear uniformly red on gross examination, with the volume of cells now depleted from all cell lineages replaced in the closed cavity of the bone marrow by dilation of the sinuses. This type of reaction is seen in horses that have succumbed after repeated acute phases of equine infectious anemia (EIA). The red appearance of the marrow may be misinterpreted as active hematopoiesis rather than general congestion with parenchymal atrophy. In chronic EIA, hemosiderosis in areas of previous erythroid activity is much more marked, with large coarse granules of hemosiderin.

In neonates with marasmus or kwashiorkor types of malnutrition, anemia may be quite prominent and is worsened by provision of an adequate diet. The mechanism is related to the body placing the most emphasis on maintaining the levels of serum proteins. Thus as nutrition improves, the level of serum protein rises and increases the osmotic tension of the plasma, which draws in water and expands the plasma volume and further dilutes the low red cell mass. This dilution occurs more rapidly than the marrow in increasing red cell production. This phenomenon is occasionally seen in lambs, and awareness of it is important in interpreting the response to therapy of animals with this condition.

Toxic and Drug-Induced Changes in Bone Marrow

Toxic effects on bone marrow may occur through accidental exposure or by intended studies of treatment effects of new compounds undergoing safety testing. Heavy metals like lead and mercury cause mild myelodysplastic changes that are less important than the changes in kidney and nervous tissue. Arsenic causes a remarkable multinuclearity of the erythroid system that might cause concern for erythremic myelosis. The changes are reversible on cessation of exposure if the initial exposure is not fatal due to asphyxia of convulsions or other causes.

A variety of changes are induced in marrow by cyclic hydrocarbons bearing varying amounts and locations of chlorine. In general low doses of those congeners with toxic effects tend to cause myeloid hyperplasia with only mild effects on the erythroid system. Higher doses result in dysmyelopoietic changes, including giant metamyelocytes and an "early asynchrony" with an increase in the pool of dividing myeloid precursors in relation to the maturation pool of cells. Prolonged exposure at high levels may result in focal areas of myelofibrosis in at least some of the exposed animals. Dysplastic changes in the erythroid system are evident in nuclear changes that consist of increased numbers of nuclear fragments in maturing rubricytes (incipient Howell-Jolly bodies) as well as binucleated late stage cells and others with budding nuclear projections. Dysplastic changes in the megakaryocytic system also occur with some exposures to chlorinated hydrocarbons and consist of delayed nuclear fusion and asynchronous maturation between the nucleus and cytoplasm. Toxic dyspoiesis is evident as pyknotic nuclei in megakaryocytes that still have a full complement of cytoplasm. Attention to these cells may be drawn by

retraction of their cytoplasm from surrounding cells, which is often associated with increased depth of cytoplasmic staining.

Direct cytotoxic agents, such as the alkylating agents used in cancer chemotherapy, result in marrow hypoplasia and produce radiomimetic effects like parvoviral infection with temporary loss of the committed stem cell pool. Mycotoxins can cause aplastic pancytopenia in both man and animals that ingest grain improperly stored and allowed to become damp. Pancytopenia caused by ingestion of feed contaminated by the fungus *Stachybotrys alternans* occurs in horses and cattle in Eastern Europe. More commonly, aplastic pancytopenia, may be caused in animals grazing in pastures containing Bracken fern, by which cattle, horses, sheep, and pigs may be affected. The toxic substance is a thiaminase, and poisoning is cumulative with repeated exposure required to produce the disease. Cattle respond by developing marrow failure characterized by bacteremia and thrombocytopenic purpura. Other species are more likely to have nervous signs and polioencephalomalacia.

In interpreting myelotoxicity it is important to keep the "pipeline" process of marrow cellular proliferation and maturation in mind. If there has been a complete cessation of hematopoiesis, as occurs in parvoviral infection, the recovery will have the appearance of maturation arrest with many primitive cells and no progeny mimicking acute leukemia. In general, the cells of the marrow move through three proliferation stages (blast, promyelocyte/prorubricyte, myelocyte/basophilic rubricyte) and three maturation stages (metamyelocyte, band and segmented neutrophil or polychromatic, normochromic and metarubricyte). The intercompartment transit time is 1 day for each stage for the myeloid system and a 4-day total production time for the platelets, with the erythroid system production intermediate between those two. Thus, a marrow with maturation to the myelocyte stage may have some immature cells in the peripheral blood but will not have mature neutrophils for a further 3 days.

Agents that delay nuclear maturation, such as vitamin B12 deficiency, result in a hyperplastic marrow with a preponderance of primitive cells and a picture of "early asynchrony." In contrast, agents that delay cytoplasmic maturation, such as iron deficiency, result in a hyperplastic marrow with a preponderance of late stage cells and a picture of "late asynchrony." These changes are apparent on examination of marrow in cytologic or histologic preparations and can be quantified for statistical comparison by differential counts of proliferating and maturing cells in each lineage. There are now reagents that can identify marrow cells into lineage and staining for ploidy that can be used to evaluate the relative numbers of proliferating and maturing cells. Methods such as these provide additional data, which aids in diagnosis of bone marrow abnormalities.

REFERENCES

Criswell, K.A., Bleavins, M.R., Zielinzki, D., and Zandee, J. (1998) Comparison of flow cytometric and manual bone marrow differentials in Wistar rats. *Cytometry* 32: 9–17.

Dacie, J.V., and Lewis, S.M. (1991) Blood cell morphology in health and disease. In *Practical Hematology*, 7th ed., Churchill Livingstone, New York, pp. 87–114.

Huff, J., Waalkes, M., Nyska, A., and Chan, P.O. (1999) Apoptosis and growth inhibition in malignant lymphocytes after treatment with arsenic trioxide at clinically achievable concentrations. *J Natl Cancer Inst* 91:1690.

Kim, Y., Park, J., and Moon, Y. (1999) Hematopoietic and reproductive toxicity of 2-bromopropane, a recently introduced substitute for chlorofluorocarbons. *Toxicol Lett* 108:309–313.

Lung, J.E., and Brown, P.K. (1997) Hypersegmented megakaryocytes and megakaryocytes with multiple separate nuclei in dogs treated with PNU-100592, an oxazolidinone antibiotic. *Toxicol Pathol* 25(4):339–343.

Pallardy, M., Kerdine, S., and Lebrec, H. (1998) Testing strategies in immunotoxicology. *Toxicol Lett* 102–103:257–260.

Peraica, M., Radic, B., Lucic, A., and Pavlovic, M. (1999) Toxic effects of mycotoxins in humans. *Bull WHO* 77: 754–766.

Phillips, B. (1999) Severe, prolonged bone marrow hypoplasia secondary to the use of carboplatin in an azotemic dog. *J Am Vet Med* 215(9):1250–1253.

Pisciotta, A.V. (1990) Drug induced agranulocytosis: Peripheral destruction of polymorphonuclear leukocytes and their marrow precursors. *Blood Rev* 4:226–237.

Rinkardt, N.E., and Kruth, S.A. (1996) Azathioprine-induced bone marrow toxicity in four dogs. *Can Vet J* 37:612–613.

Valli, V.E., McGrath, J.P., and Chu, I. (2002) Hematopoietic System (Chapter 40). In Haschek, W., Rousseaux, C.G., and Wallig, M. (eds.), *Handbook of Toxicologic Pathology, Second Edition, Volume 2*. Academic Press, St. Louis, pp. 647–679.

Valli, V.E., Villeneuve, D.C., Reed, B., Barsoum, N., and Smith, G. (1990) Evaluation of blood and bone marrow, rat. In Jones, T.C., Ward, J.M., Mohr, U., and Hunt, R.D. (eds.), *Hemopoietic System*. Springer-Verlag, Berlin, pp. 9–26.

Valli, V.E.O., and McGrath, J.P. (1997) Comparative leukocyte biology and toxicology (4.12). In Bloom, J.C. (ed.), *Comprehensive Toxicology: Volume 4, Toxicology of the Hematopoietic System*. Eli Lilly and Company, Indianapolis, pp. 201–205.

Weiss, D.J., Blauvelt, M., Sykes, J., and McClenahan, D. (2000) Flow cytometric evaluation of canine bone marrow differential cell counts. *Vet Clin Pathol* 29:97–104.

Technical Aspects of Marrow Biopsy and Preparation

The examination of bone marrow begins with getting a sample suitable for diagnostic purposes. In dogs, the femoral neck is always hematopoietic and the tip of the ischium is easily palpated and always yields red marrow. The wing of the ileum is less reliable than the former two sites. Mature cats are more likely to have red marrow in the ileum than the dog. If marrow is to be taken, a Jamshidi needle should be used to provide first an aspirate and then a core of marrow. In cattle and horses, the sternum at the level of the point of the elbow in the standing animal is the best site and is most safely and easily accessed if the animal can be restrained on its side in a rotating squeeze. In the cow or calf, the vertebral processes always have red marrow, with L1 the most appropriate because it is the only one that is vertical with those anterior pointing back and those posterior pointing ahead. The ileal crest is always fatty in cattle and becomes so in young calves over 1 month of age. Small ruminants are similar to cattle, as are camelids.

In preparation for marrow biopsy, slides should be set out ready for preparation of marrow spreads. The most reliable technique requires wetting of the barrel of the syringe with 1% EDTA in saline and also the biopsy trocar and sound. The skin is prepared as for surgery and skin and the periosteum should be infiltrated with local anesthetic. A small incision with the tip of a scalpel permits the tip of the trocar to be inserted without contamination by the skin surface. The trocar is tapped with a hammer with attention to the resulting sound that is sharp while engaging cortical bone and changes to a much softer impact on entering the marrow cavity. The marrow is richly innervated and if the needle is correctly placed, a conscious animal may flinch on withdrawing the sound or stilette. The syringe with a small volume of anticoagulant is attached and strong vacuum applied. The animal may show pain at this time and the aspirate should stop when 2–3 ml of blood and marrow are obtained. If no blood appears in the syringe it should be detached and the stilette replaced and the needle redirected without withdrawing it from the skin. When marrow is obtained, use the Dacie technique to prepare the marrow films, which provides a "marrow granule trail" at the tip of the slide. The syringe with the marrow aspirate is detached with the plunger and the stilette replaced, with full attention to the preparation of slides. The syringe is rotated with the plunger retracted slightly to permit mixing of the anticoagulant, and then a sample of the aspirate of about 0.2 ml is discharged onto a slide. The slide is then tipped toward a gauze sponge held to one side to draw off the excess blood and a portion of the marrow granules and blood are picked up by drawing the tip of another slide completely across part of the marrow sample; slides are made in the manner of a blood film. The slides must be immediately waved dry by assistants as additional slides are made. If the technique is done correctly, each slide will have a series of granules at the tip of the preparation with each leading a trail of marrow cells. The slides should be waved with the tip of the spread upward so that if excess blood is present it will not spread over the thin area of the preparation. Slides made in this manner have the advantage over the "crush method" in that the marrow and blood cells are not intermingled, and problems of high blood lymphocytes can be separated into marrow and peripheral blood components. In addition, if marrow counts are to be made, the "marrow granule trail" following each granule can reliably be considered to be of marrow origin.

After the slides of marrow are made, a second aspirate might be considered of lesser volume and without anticoagulant and allowed to clot and then fixed for histological examination. Most preferably, the marrow instrument is then advanced further into the marrow cavity with the sound or stilette removed to gain a core of marrow that is then discharged into fixative. Although many fixatives like Zenkers or B5 have been shown to give excellent or superior cytologic detail, formalin is currently preferred because it permits optimal use of immunohistochemical procedures should these be needed. A heavy yield of marrow will have too many nuclei for optimal staining by automated systems designed for blood samples, and staining the slides twice may be needed for best results. Marrow slides that have been dried properly following preparation may be stored unstained and unfixed indefinitely if they are maintained at low humidity.

REFERENCES

Carter, R.F., and Valli, V.E.O. (1990) Taking a biopsy. *Vet Clin North Am: Small An Pract* 20(4):939–968.

Dacie, J.V., and Lewis, S.M. (1975) Bone marrow biopsy (Chapter 6). In *Practical Haematology, Fifth Edition*. Churchill Livingstone, New York, pp. 150–170.

Hoff, B., Lumsden, J.H., and Valli, V.E.O. (1985) An appraisal of bone marrow biopsy in assessment of sick dogs. *Can J Comp Med* 49:34–42.

Pasquale, D., and Chikkappa, G. (1986) Comparative evaluation of bone marrow aspirate particle smears, biopsy imprints, and biopsy sections. *Am J Hematol* 22:381–389.

Relford, R.L. (1991) The steps in performing a bone marrow aspiration and core biopsy. *Vet Med* 86:670–688.

Valli, V.E., McSherry, B.J., and Hulland, T.J. (1969) A review of bone marrow handling techniques and description of a new method. *Can J Comp Med* 33(1):68–71.

Weiss, D.J. (1987) A review of the techniques for preparation of histopathologic sections of bone marrow. *Vet Clin Pathol* 16(4):90–94.

Chapter 3

B-Cell Neoplasms

LYMPHOPROLIFERATIVE DISEASES

The definition of lymphoproliferative diseases has gone through a series of changes in concert with greater understanding of the underlying processes. As recently as a decade ago, lymphoid proliferations were described as a subset of conditions affecting the reticuloendothelial system (RES). That concept of multifunctionality of individual cells of the blood vascular system has now been replaced because of the ability to identify individual cell types by surface and molecular markers and to ascribe separate and specific functions. The most significant steps in the evolution of understanding was the demonstration of B-cell Ig gene rearrangement by Southern blot analysis, followed by demonstration of the T-cell receptor. Prior to these developments, B-cell lineage could be demonstrated only by surface or cytoplasmic Ig. As a consequence, most acute leukemias of childhood were known as "common" or "non-B, non-T" type. The ability to detect Ig gene rearrangement in gels permitted the recognition of clonality in B-cell neoplasms. Thus, lymphoid proliferation could then be determined to be malignant or benign, and the definition of lymphoproliferation became much more precise. Gray areas still exist, with the indefinite area now referred to as *atypical lymphoproliferative disorders* (ALPDs), which lie between the better-defined benign lymphoid hyperplasias and the frankly malignant neoplasms. Even these disorders now have specific descriptions and include angioimmunoblastic lymphadenopathy, which appears to occur in cats; post-transplantation lymphoproliferative disorders; Multicentric Castleman's Disease: IL-6 Syndrome; and finally conditions associated with overproduction of IL-6 due to infection with human herpesvirus-8 infection.

A difficult descriptive and diagnostic distinction between leukemia and lymphoma was largely resolved by the REAL/WHO classification system. Pragmatically, this distinction is now based on linking the nomenclature to the tissue with the greatest volume of tumor. According to this system, if most of the neoplasm is in the marrow it is termed *leukemia*, and if most is in peripheral tissues it is termed *lymphoma*. Equally important is the recognition that neoplasms of a similar cell type may occur as either leukemia or lymphoma and in that context are different manifestations of the same disease.

Further, in lymphomas there are always neoplastic cells in circulation, and the likelihood of distant dissemination is a function of the intercellular cytoplasmic adhesion molecules (ICAMs) that determine where lymphocytes may adhere, and exit, the vessel wall. By this understanding, the acute leukemias lack most adhesion sites and tend to remain in circulation. At the other end of the adhesion spectrum, the MALT-type lymphomas may remain so tightly adhered to a single location that they may be curable by surgical excision. A valid general distinction is that *malignancy in a largely undifferentiated lymphocyte is likely to occur in the marrow of a young individual and present as leukemia,* and *malignancy in a mature lymphocyte will likely occur in the peripheral tissues of a mature individual and present as lymphoma*. As usual, exceptions to the more common presentations occur, as seen in the γδ T-cell lymphomas of humans, dogs, and cats that arise in the intestine, involve the spleen, and present with leukemia but without overt involvement of the marrow. Thus, our definition of leukemia needs to be broadened to include a prominent level of circulating neoplastic lymphocytes that arise in the periphery. The distinction of whether marrow is involved when neoplastic cells are in circulation is always an important determination for purposes of clinical management. When bone marrow is involved with hematopoietic neoplasms, there will always be some degree of marrow failure when 50% or greater of the marrow is involved with tumor. Further, in some cases there may be clinically relevant cytopenias with much less than 50% of marrow involved, as can occur with some peripheral T-cell lymphomas. Marrow failure will be manifest as anemia, thrombocytopenia, or neutropenia, singly or in combination. Cytopenias occur earlier in course of the disease with myeloid neoplasms because these compete directly with benign stem cells for preferred space in subendosteal areas. In contrast, neoplastic lymphocytes colonize the

marrow in a random fashion and may displace normal fat without causing a reduction in output of normal stem cells until very late in the disease process.

The classification of cell types in the peripheral blood was defined in the French-American-British (FAB) system, which preceded universal immunophenotypic analysis. Use of the FAB system has declined in use in human pathology, and it has not been applied extensively in animals. The FAB system is practical and, though based on morphology that does not infer phenotype, the classification does fit the leukemias seen in animals and is a useful method of initial definition by oversight stains. By these criteria the L1 form consists of small cells with round nuclei 1.5× the diameter of a red cell with coarsely cribriform densely stained chromatin, small or absent nucleoli, and a narrow rim of lightly basophilic cytoplasm (Fig. 3.1). The L1 form of acute lymphoblastic leukemia (ALL) comprised 85% of childhood "common" type cases, and virtually all of these were of B-cell type (Figs. 3.2, 3.3). L1 can be confused with normal small lymphocytes in overstained preparations because of the narrow incomplete rim of cytoplasm and nucleoli that are inapparent.

The L2 type of ALL have round or sharply indented nuclei 2× the diameter of a red cell with hyperchromatic fine uniform chromatin, 1–2 distinct nucleoli, more abundant cytoplasm, generally with a complete rim, slightly eccentric, and with perinuclear clearing and more basophilic at the cell margins (Figs. 3.4, 3.5). L2 cells resemble the poorly differentiated myeloid blasts of FAB M0 or M1, which may be one of the reasons why acute myelogenous leukemia (AML) is underdiagnosed in animal pathology. Most human adult ALL is of the L2 type and most L2 are of B-cell type.

L3 ALL is the most characteristic of the human ALL types and likely most resembles the predominant type of

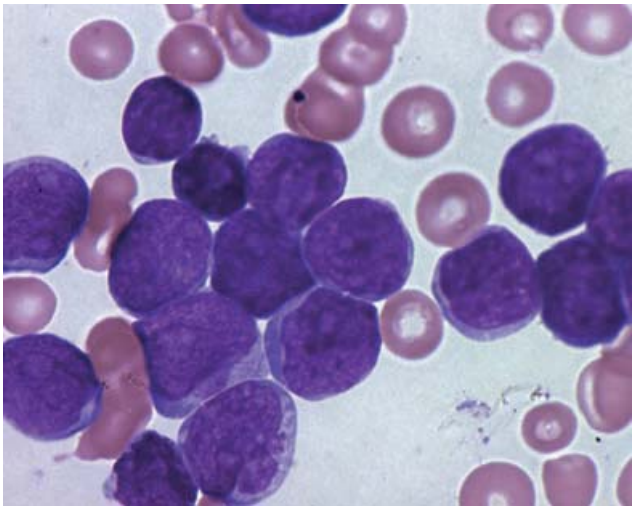

Figure 3.2. Human: blood, acute lymphoblastic leukemia, L1 type. The nuclei are generally round, with the chromatin pattern largely dispersed with small chromocenters and poorly defined nucleoli in a number of cells. The small lymphocyte at the lower right and lower center are benign with much more densely aggregated chromatin. The neoplastic cells have an ellipse of cytoplasm generally not visible throughout the circumference of the cell. *Slide from Cornell Tutorial.*

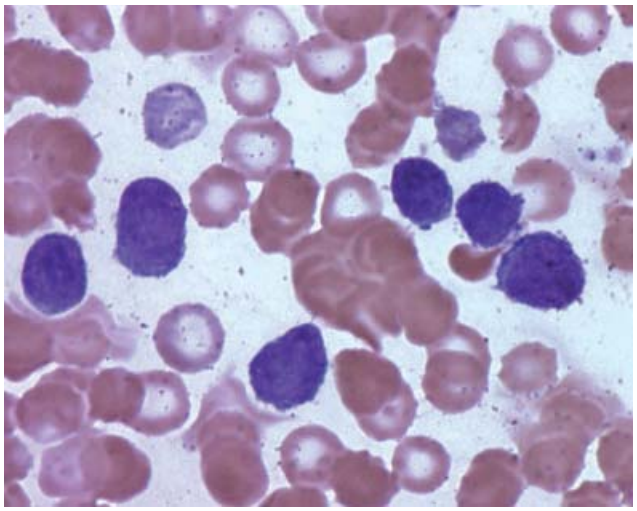

Figure 3.1. Dog: blood, acute lymphocytic leukemia, L1 type. The neoplastic cells have nuclei about 1.5 times the diameter of red cells with deeply stained chromatin and small or inapparent nucleoli. There is a narrow rim of cytoplasm visible at one pole of the nucleus, with perinuclear clearing and peripheral basophilia.

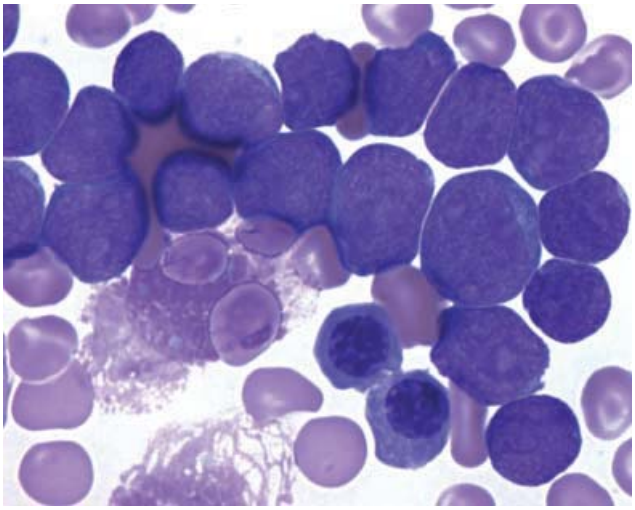

Figure 3.3. Human: bone marrow, ALL-L1, same case as Figure 3.2. The marrow is largely occupied by cells similar to those in the blood with phthisis of normal cells. Two polychromatic rubricytes are present center right. *Slide from Cornell Tutorial.*

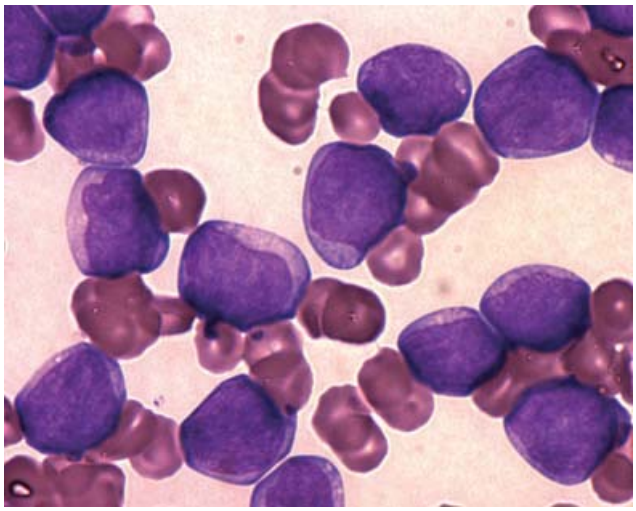

Figure 3.4. Dog: blood, ALL L2 type. The L2 nuclei are more variable in shape and often indented or lobulated and generally 2 red cells in diameter. The cytoplasm is more abundant and generally visible throughout the circumference of the cells not in contact. The lymphoid tendency for perinuclear clear areas with peripheral increase in basophilia is retained. The chromatin is dispersed without large chromocenters, and nucleoli are irregularly discernible.

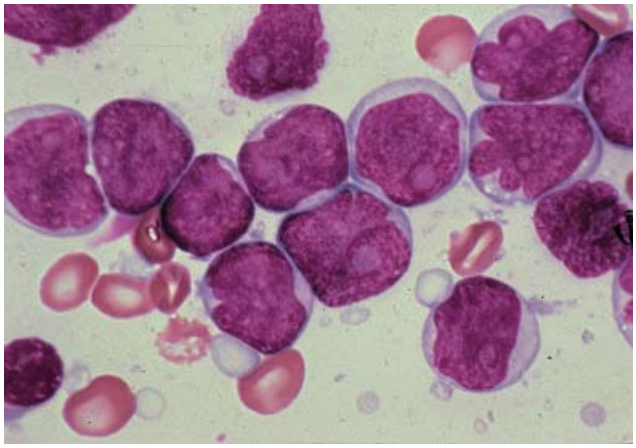

Figure 3.5. Human: marrow aspirate, ALL L2 type. The nuclei are generally 2 red cells in diameter with moderate irregular, clearly sharp shallow indentations, and focal lobulations. The chromatin pattern is dispersed with fine chromocenters, and nucleoli are apparent. There is a greater volume of cytoplasm visible throughout the circumference of most cells, with lighter perinuclear staining and peripheral increased basophilia. *Image courtesy R. D. Brunning, MD.*

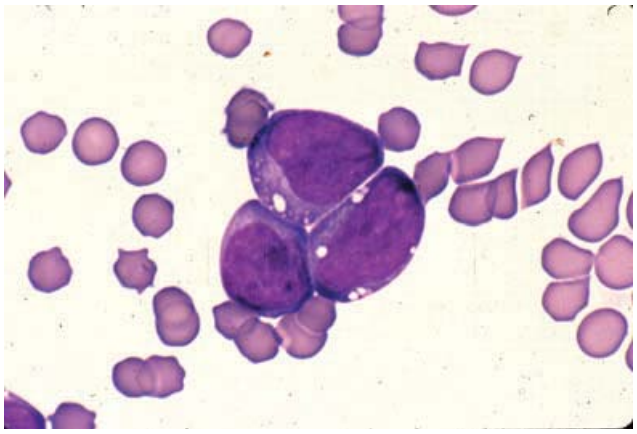

Figure 3.6. Cat: blood, ALL L3 type. The nuclei are large and round or oval without sharp indentations and 2.5–3 red cells in diameter. The chromatin pattern is fine and densely stained with an irregular appearance of a fine cribriform pattern with a very small round lightly stained and irregular gridlike pattern. The nucleoli are generally more apparent in these cells but the abundant cytoplasm and quite high basophilia and small peripheral vacuoles are characteristic.

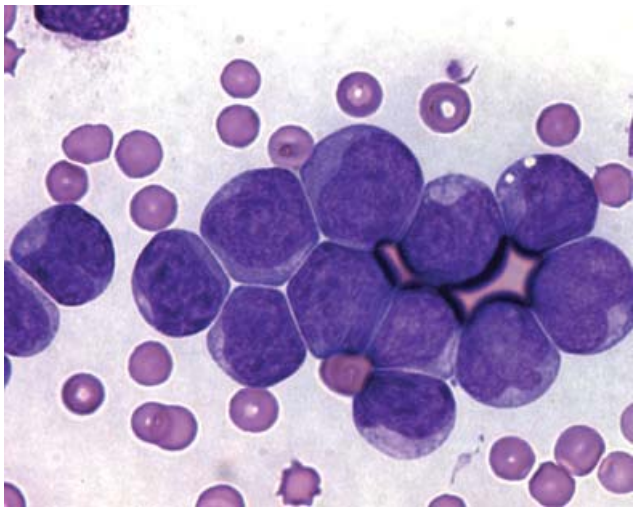

Figure 3.7. Cat: blood, ALL L3 type. The typical appearance of L3 blasts, with large relatively round nuclei, fine chromatin pattern, and often multiple large nucleoli. The cytoplasm is highly basophilic with frequent small vacuoles that tend to mark positively with fat stains.

ALL of animals. L3 cells have round nuclei that are 3× the diameter of a red cell with hyperchromatic fine cribriform chromatin, multiple prominent nucleoli, and relatively abundant highly basophilic cytoplasm, which frequently has fine vacuoles (Figs. 3.6–3.9). L3 resembles the Burkitt's type of lymphoma and most are of B-cell type (Fig. 3.10). Most cases of L1-2 do well with aggressive chemotherapy and by immunologic classification there does not appear to be a prognostic difference between L1 and 2. In contrast the L3 cases do poorly, even with special therapy. Response to therapy in human lymphoblastic leukemia is limited by the toxic side effects of myeloablative therapy. Patterns of gene expression within subtypes of ALL may indicate better tolerance of certain

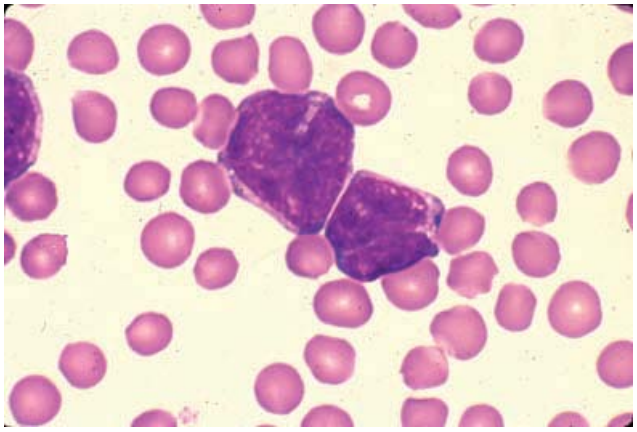

Figure 3.8. Bovine: blood, ALL L3 type. Blood from a mature cow, which presented with a leukemic blood picture. The nuclei are large and tend to be round with a few larger chromocenters and multiple relatively apparent nucleoli. The cytoplasm is apparent throughout the circumference of the cell, with small cytoplasmic vacuoles often present. The lower cell is either binucleated or more likely deeply cleft.

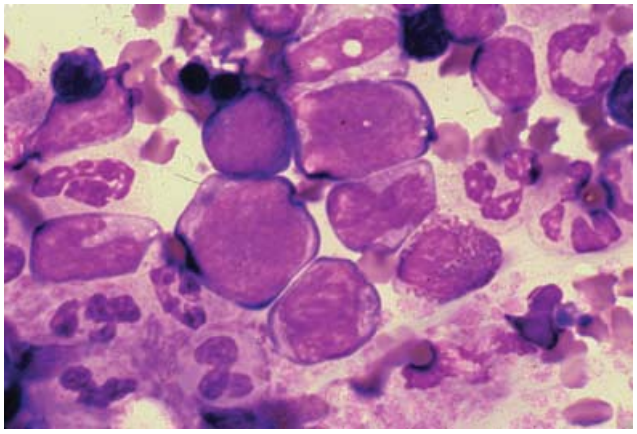

Figure 3.9. Bovine: marrow aspirate, ALL L3 type, same case as Figure 3.8. Large atypical cells are frequently present with early phthisis of normal marrow elements. The nuclei are typically rounded with a fine chromatin pattern, relatively abundant, and cytoplasm occasionally with small vacuoles.

chemotherapeutic agents and thus in certain individuals improved responses may be attained.

Each case of lymphoproliferative disease presents a diagnostic challenge that involves consideration of cellular features in cytological preparations and architecture in histology. To assist in the orderly deduction of benign or malignant disease and subtype of neoplasm, the algorithms in Tables 3.1 and 3.2 have been prepared to provide a series of branching decision points that can designate a lesion as primarily of blood or tissue, and nodal or extranodal. Then, cytologically, tumors will be designated as homogeneous or mixed cellularity and

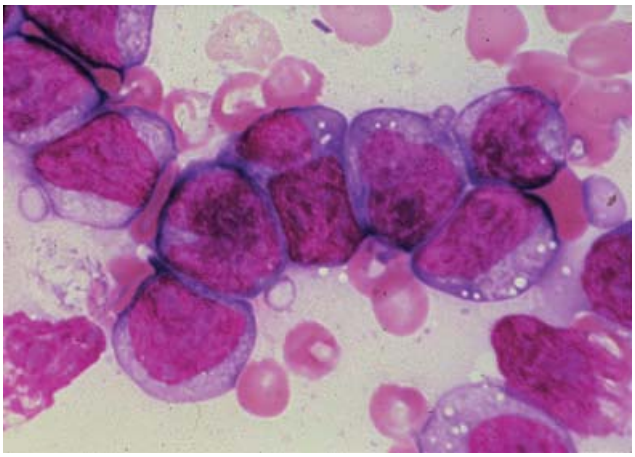

Figure 3.10. Human: marrow aspirate, ALL L3 type. The nuclei are large, 2.5 red cells in diameter, round to irregular, in outline with a fine chromatin pattern with a few large chromocenters and apparent, often multiple nucleoli. The cytoplasm is relatively abundant and moderately basophilic with frequent small vacuolations. *Image from R. D. Brunning, MD.*

Table 3.1. Algorithm for classification of lymphoproliferations.

Blood	**Nodes**		
Lymphocytosis ↔ Normal	Enlarged ↔ Normal		
↓	↓		
Predominant topography of proliferation			
↓			
Marrow	**Node**		
↓	↓		
Reactive ↔ Leukemia	Reactive ↔ Lymphoma		
Phenotype	Node Lymphoma Algorithm		
Mixed = reactive			
Clonal = neoplastic			
Ephemeral = reactive			
Persistent = neoplastic			
Mitoses – = reactive or CLL			
Mitoses + = ALL			
	Nuclear Size		
	Small	Medium	Large
	CLL or L1	L2	L3
Nuclear shape	Round = CLL Indented = L1	± Indented	Round
Cyto volume	Variable CLL	Moderate	Abundant + Fine peripheral vacuoles
Nucleoli	None or small CLL	1–2 small	1–3 large

Table 3.2. Algorithm for lymphoma classification lymphoproliferation in lymph node tumor architecture.

Follicular	Diffuse		
	Nuclear Size ↓		
Grade according to number of large cells per high power field → I 0–5 (FSCCL) II 6–15 (FMCL) III 16+ (FLCL)	↓ **Small** (nuclear diameter = 1.5–2 rbc)	↓ **Mixed Large and Small** T-cell rich large B-cell lymphoma (DMCL)	↓ **Large** (nuclear diameter = 2–3 rbc)
→ **Floral variant***—large irregular follicles with their mantle cell bands invading follicles	**Mitotic Rate**		→ **Large B-Cell Neoplasms**
	High	**Low**	
→ **Large cell transformation**—fading germinal centers with diffuse proliferation of large cells	→ **Leukemic** ALL (B) ALL (T)	**Leukemic** ← CLL (B) Hairy cell (B)* CLL (T)	B-cell large cell lymphoma (BLCL) Diffuse large-cleaved cell (DLCL) Multilobulated-BL Immunoblastic (IBL) Mediastinal-B-cell Lymphomas Anaplastic large Cell Myeloma
→ **Mantle cell lymphoma**—small nuclei, no nucleoli, scant cytoplasm, mantle cell architecture, occurring in lymph nodes, mucosal areas, marrow, and spleen	→ **Nonleukemic** Precursor B (B-LB) Precursor T (T-LB) High-grade B or Burkitt's-like (SNCCL)	**Nonleukemic** ← SLL (B) (DSLL) Plasmacytoid (DSLPL) Plasmacytoma SLL (T) (DSLL) T Prolymphocytic (PLL)	→ **Large T-Cell Neoplasm** → **Leukemic** Large granular lymphocytic leukemia (LGL): T-LGL NK-LGL → **Nonleukemic Extranodal** Peripheral T-cell lymphoma Nodal Angioimmunoblastic T-lymphoma **Nodal or extranodal** Anaplastic large CD30+ Cell Angiocentric Cutaneous lymphomas: Mycosis fungoides Sézary syndrome
→ **Mantle cell lymphoma blastoid variant**—vesicular nuclei with nucleoli, scant cytoplasm, and mantle cell architecture, occurring in above sites			
→ **Marginal zone lymphoma**—medium-sized nuclei, + nucleoli, abundant cytoplasm, and marginal zone architecture, occurring in lymph nodes (synonymous with monocytoid B-cell lymphoma) In extranodal sites of mucosal origin = MALT In spleen ± villous lymphocytes			

ALL Acute Lymphocytic Leukemia*
CLL Chronic Lymphocytic Leukemia
DLCL Diffuse Large Cell Lymphoma
DLCCL Diffuse Large-Cleaved Cell Lymphoma
DMCL Diffuse Mixed Cell Lymphoma
DSLL Diffuse Small Lymphocytic Lymphoma
DSLPL DSL Plasmacytoid Lymphoma
FMCL Follicular Mixed Cell Lymphoma
FLCL Follicular Large Cell Lymphoma
FSCCL Follicular Small Cleaved Cell Lymphoma
IBL Immunoblastic Lymphoma
LBL Lymphoblastic Lymphoma
LGL Large Granular Lymphocytic Leukemia
MALT Mucosa-Associated Lymphoid Tumor
PLL Prolymphocytic Leukemia
SLL Small Lymphocytic Lymphoma
SNCCL Small Noncleaved Cell Lymphoma

* Rarely recognized in animals

according to predominant cell size. Finally, and most importantly, they are designated according to low or high proliferative rate based on observed mitotic figures. These steps should be followed, in the order presented in Table 3.1, to make the decision of a benign or malignant proliferation and of topographical localization, and then by the steps in Table 3.2 for disease subtype based on cytological interpretations.

REFERENCES

Admirand, J.H., Rassidakis, G.Z., Abruzzo, L.V., Valbuena, J.R., Jones, D., and Medeiros, L.J. (2004) Immunohistochemical detection of ZAP-70 in 341 cases of non-Hodgkin and Hodgkin lymphoma. *Modern Pathol* 17:954–961.

Canoz, O., Rassidakis, G.Z., Admirand, J.H., and Medeiros, L.J. (2004) Immunohistochemical detection of BCL-3 in lymphoid neoplasms: A survey of 353 cases. *Modern Pathol* 17:911–917.

Dobson, J.M., Blackwood, L.B., McInnes, E.F., Bostock, D.E., Nicholls, P., Hoather, T.M., and Tom, B.D.M. (2001) Prognostic variables in canine multicentric lymphosarcoma. *J Sm An Prac* 42:377–384.

Greenlee, P.G., Filippa, D.A., Quimby, F.W., Patnaik, A.K., Calvano, S.E., Matus, R.E., Kimmel, M., Hurvitz, A.I., and Lieberman, P.H. (1990) Prognostic variables in canine multicentric lymphomas in dogs: A morphologic, immunologic, and clinical study. *Cancer* 66:480–490.

Harris, N.L., Jaffe, E.S., Stein, H., Banks, P.M., Chan, J.K.C., Cleary, M.L., Delsol, G., De Wolf-Peeters, C., Falini, B., Gatter, K.C., Grogan, T.M., Isaacson, P.G., Knowles, D.M., Mason, D.Y., Muller-Hermelink, H.-K., Pileri, S.A., Piris, M.A., Ralfkiaer, E., and Warnke, R.A. (1994) A revised European-American classification of lymphoid neoplasms: A proposal from the International Lymphoma Study Group. *Blood* 84(5):1361–1392.

Kiupel, M., Teske, E., and Bostock, D. (1999) Prognostic factors for treated canine malignant lymphoma. *Vet Pathol* 636:292–300.

Kiyokawa, N., Sekino, T., Matsui, T., Takenouchi, H., Mimori, K., Tang, W., Matsui, J., Taguchi, T., Katagiri, Y.U., Okita, H., Matsuo, Y., Karasuyama, H., and Fujimoto, J. (2004) Diagnostic importance of CD179a/b as markers of precursor B-cell lymphoblastic lymphoma. *Modern Pathol* 17:423–429.

Küppers, R., Klein, U., Hansmann, M.-L., and Rajewsky, K. (2003) Cellular origin of human B-cell lymphomas. *New Engl J Med* 197:1213–1219.

NHL Classification Project. (1997) ISLG Classification for NHL. *Blood* 89:3909–3918.

Ponce, F., Magnol, J.-P., Ledieu, D., Marchal, T., Turinelli, V., Chalvet-Monfray, K., and Fournel-Fleury, C. (2003) Prognostic significance of morphological subtypes in canine malignant lymphomas during chemotherapy. *Vet J* 167:158–166.

Ponce, F., Magnol, J.-P., Marchal, T., Chabanne, L., Ledieu, D., Bonnefont, C., Felman, P., Fournel-Fleury, C. (2003) High-grade canine T-cell lymphoma/leukemia with plasmacytoid morphology: A clinical pathological study of nine cases. *J Vet Diagn Invest* 15:330–337.

PRECURSOR B-CELL NEOPLASMS

Precursor B-Cell Lymphoma B Lymphoblastic Leukemia

Definition

Acute lymphoblastic leukemia (B-ALL) is a malignant neoplasm of bone marrow occurring most frequently in young animals, which is rapidly progressive and characterized cytologically by small intermediate to large cells that have fine chromatin with nucleoli and have cytoplasm marking positively with CD79 and/or CD20.

B-cell lymphoblastic lymphoma is a disease of mature dogs that present in good health and condition with, typically, a single enlarged peripheral node that rapidly becomes generalized lymphadenopathy. Initially, the animals are not leukemic and are not anemic or thrombocytopenic. The cell type is indistinguishable from that of B-ALL.

Epidemiology and Incidence

B-cell lymphoblastic neoplasms (B-ALL) are rapidly progressive diseases that may occur in marrow or peripheral tissues or both. B-cell lymphoblastic neoplasms occur in all species; in animals they occur most frequently in dogs, cats, and calves. They are often diseases of the young, in cats all ages, dogs bimodal, less than 5 years, and in old dogs and in calves less than 6 months. Rarely, the disease may be congenital and cause dystocia due to massive hepatosplenomegaly. With the advent of vaccination for FeLV the incidence of acute leukemia has decreased in cats, and there may be a shift in the predominant phenotype of those cases now seen. In the calf, acute lymphoid leukemia is not associated with infection with the bovine leukemia virus. The immunophenotype of acute leukemia in the dog has not been adequately studied, but it appears that acute myeloid leukemia of poorly differentiated cells likely constitutes over half of cases. Those cases of the lymphoid acute leukemias that are phenotypically defined are more than half of T-ALL type, followed by B-ALL, with about 1 in 10 cases undifferentiated by current methodology. Recent screening of infant blood with PCR techniques for specific breakpoint and fusion sequences suggests that human ALL may have a prenatal origin characterized by a long latent period until the disease is apparent.

Clinical Presentation and Features

Animals with B-cell lymphoblastic leukemia generally present in good body condition with a shiny hair coat and with apparent illness of less than a week (Fig. 3.11).

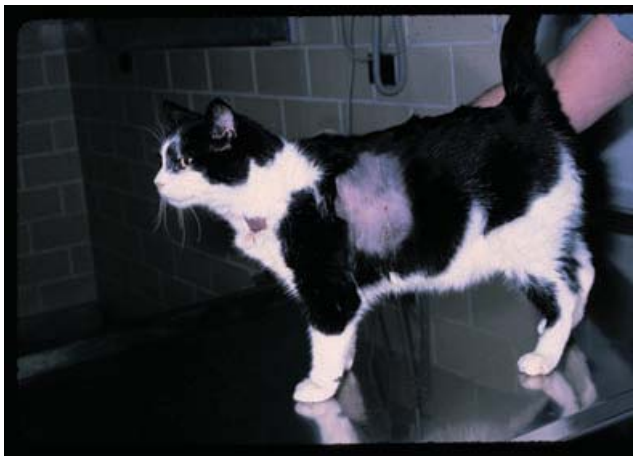

Figure 3.11. A young mature cat that presented in good condition with mild dyspnea was found to have pleural effusion and a thymic mass. The normal body condition without weight loss and the normal glossy hair coat are indicative of acute onset.

Figure 3.13. A mature Holstein bull with blood sample taken on routine examination that had a total leukocyte count of 105,000 per microliter, mainly lymphocytes. The animal was in full service and felt to be normal.

Figure 3.12. A 6-year-old cow in good body condition was presented because of a rapid drop in milk production. The cow presented with a leukemic blood picture without involvement of peripheral lymph nodes. Note good body condition and shiny hair coat.

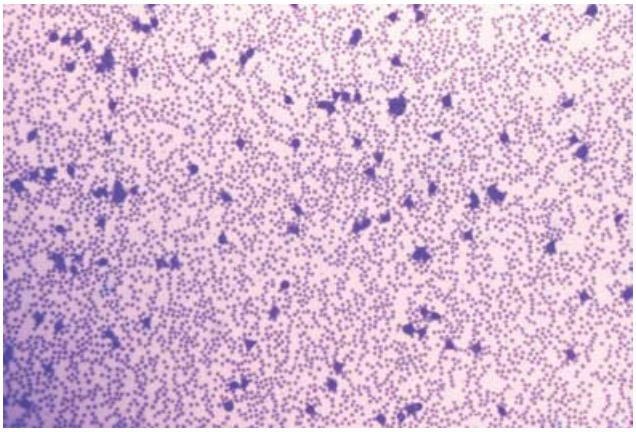

Figure 3.14. Bovine: blood, ALL L3 type. Blood from the case of Figure 3.13. The animal subsequently declined rapidly in health and on examination was found to have widespread marrow involvement including enteric nodes.

Those with leukemia usually have some degree of anemia with accompanying mucosal pallor. Epistaxis due to myelophthisic thrombocytopenia may be seen but is not common. In contrast to lymphoma, dairy cows with ALL may be in excellent condition and high production (Fig. 3.12). This is similar with bulls maintained in excellent body condition for regular semen collection (Fig. 3.13). These animals may be identified for unusual reasons, such as hoof trimming with blood taken as a routine examination, and the diagnosis of ALL may be initially discredited as laboratory error in animal identification (Fig. 3.14). In contrast to almost all other animals, young calves that present with ALL are cachectic with a rough hair coat, and in those that present at 2–4 months of age there is poor body condition with skin tightly applied over bony prominences (Figs. 3.15–3.18). Calves with ALL have generalized lymphadenopathy and are usually recumbent due to the bone pain of multiple areas of infarcted marrow (Fig. 3.19). All peripheral nodes are enlarged to 10 cm or more and the diagnosis is not obscure on the physical examination. B-ALL is rare in horses and may be seen in animals in excellent condition that have been racing or performing and are presented for sudden onset of poor performance (Figs. 3.20–3.24). Dogs presenting with B-LBL are usually felt to have normal attitude and characteristically have an enlarged submandibular or popliteal node recently noticed to be

Figure 3.15. A 4-month-old Holstein heifer calf was presented because of declining appetite and condition and was found to have generalized lymphadenopathy.

Figure 3.16. Calf: ALL L3, same case as Figure 3.15. When viewed from above, the loss of body condition with poor hair coat and scaly skin is apparent. The submandibular and parotid nodes are markedly enlarged and apparent just anterior to the ears, with the prescapular nodes very large and apparent ahead of each shoulder.

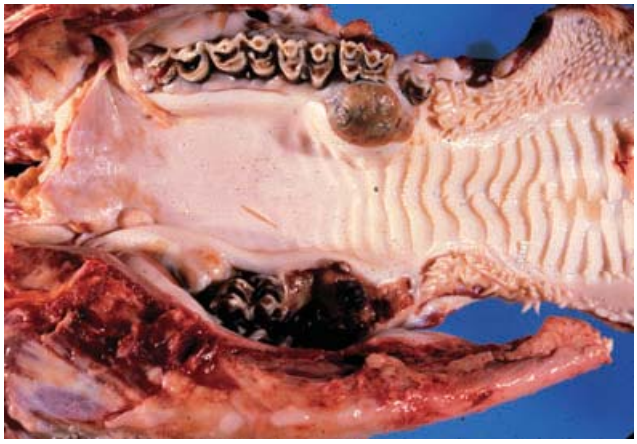

Figure 3.17. Bovine calf: lymphoma, ALL L3, hard palate and maxilla, same case as Figure 3.15. The anterior area (right) with bilateral ulceration around the dental arcade causing massive disruption and loss of teeth (bottom) and similar infiltration with less progression (above). The involvement of the dental arcade with high-grade lymphoma is reminiscent of the Burkitt's-type lymphoma of African children that frequently presents with maxillary involvement. Localization is felt due to induction by areas of rapid cell proliferation in the development of permanent teeth.

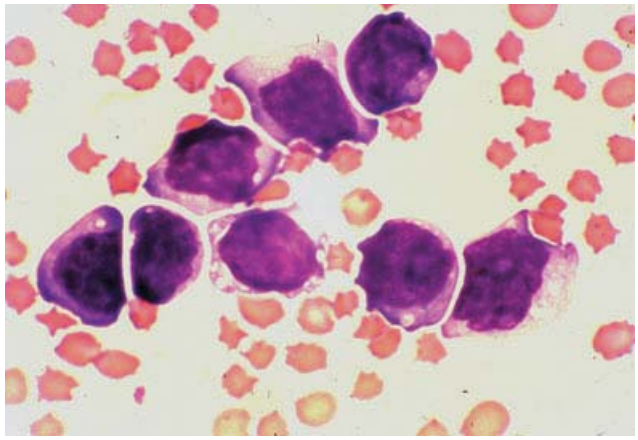

Figure 3.18. Bovine: blood, ALL L3, same case as Figure 3.15. Peripheral blood is dominated by large lymphocytes with large relatively round nuclei and densely stained chromatin with a few large chromocenters, with several having evident large nucleoli. The cytoplasm is abundant, is moderately basophilic, and has focal small vacuolations.

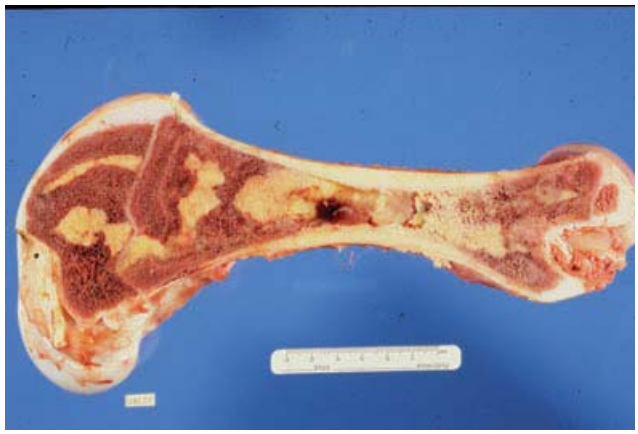

Figure 3.19. Bovine: hemisection of femur, ALL L3. The yellow areas represent ischemic infarction typical of acute leukemia in the calf-type bovine lymphoma.

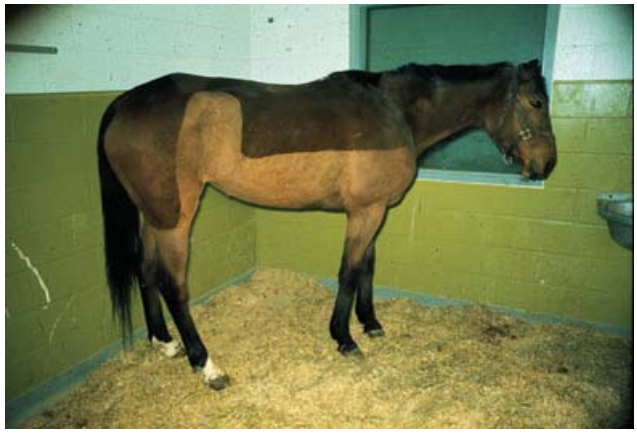

Figure 3.20. A thoroughbred mare was returned from the racetrack due to loss of stamina and was found to be in good body condition with anemia and normal peripheral lymph nodes. The color pattern is due to a trainer's strategy of clipping hair.

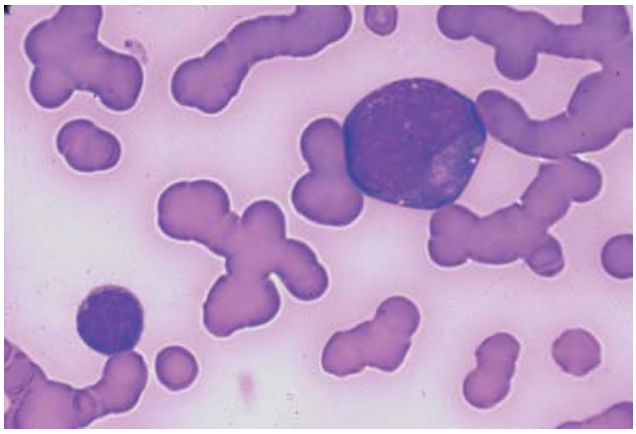

Figure 3.21. Equine: blood, ALL L3, same case as Figure 3.20. The horse had a hemoglobin level of 8.4g per dl and a total leukocyte count of 3,500 per ul of which 92% were lymphocytes. The anemia is normochromic, normocytic, and nonresponsive, with thrombocytopenia and the presence in the blood of medium and large lymphocytes, with the upper cell typical of the predominant population and with mild irregularity, in nuclear shape, multiple nucleoli, and relatively abundant cytoplasm with fine vacuolations. The lymphocyte in the lower left is a small benign type.

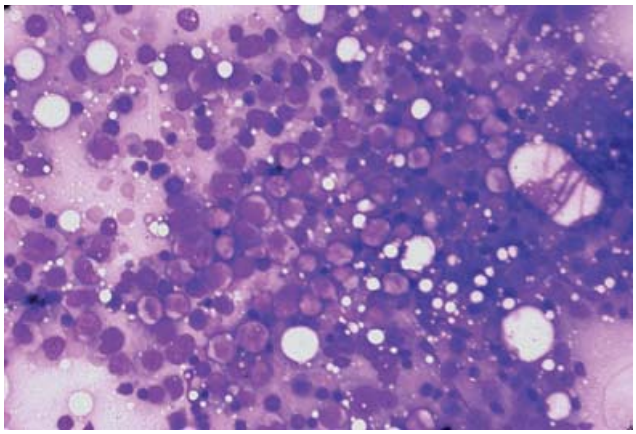

Figure 3.22. Equine: bone marrow imprint, ALL L3, same case as Figure 3.20. The marrow is heavily infiltrated by the mononuclear cells, surrounded by an irregular envelope of lightly stained cytoplasm. The case is unusual in that there appears to be depression of myelopoiesis with almost no neutrophils present, but some maturing rubricytes remain.

enlarged. In a group of 100 dogs with B-cell lymphoma, 6 had B-LBL, and of these 4 had enlarged submandibular nodes and one each of popliteal and prescapular nodes. Their ages ranged from 4–12 years with a mean of 8.3 years and included 4 females spayed and 1 each of male and male neutered. All but one was of large breed type.

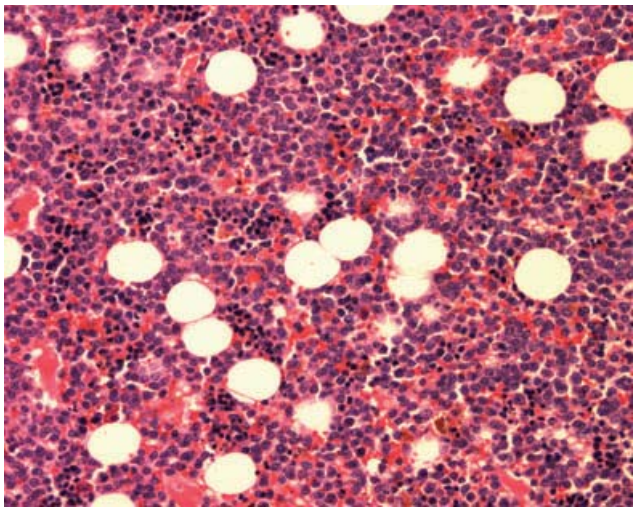

Figure 3.23. Equine: bone marrow histology, same case as Figure 3.20. There is a marked increase in cellularity, with about 80% of marrow occupied by nonfat tissue. The focal clusters of small round deeply stained nuclei represent colonies of erythropoiesis, with most of the marrow occupied by an intermediate-sized cell of monomorphic type. Note complete absence of megakaryocytes.

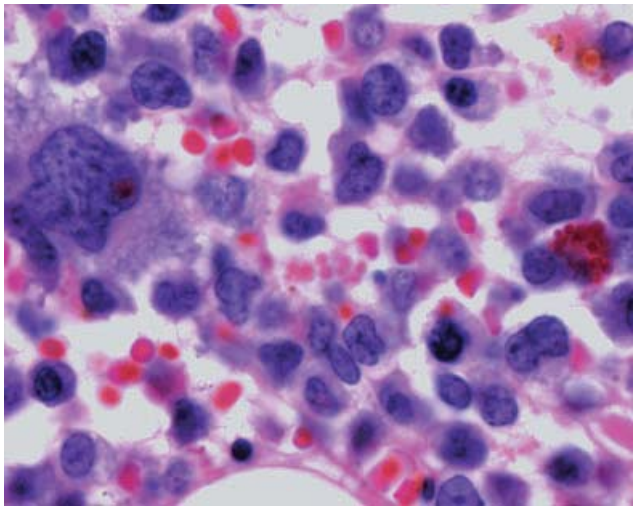

Figure 3.24. Equine: marrow. Detail of Figure 3.20. The bone marrow is dominated by medium and large cells with irregularly shaped nuclei and relatively abundant pale staining cytoplasm. The cells have a fine dispersed chromatin pattern and multiple, quite prominent nucleoli. There is a maturing megakaryocyte at the left with decreased cytoplasmic volume, and the cell below is likely a basophilic rubricyte. There is an eosinophil with prominent pink granules at right with a complete absence of neutrophils in any recognizable stage of maturation corresponding to the peripheral pancytopenia. There is abundant coarse hemosiderin in the marrow with a single small aggregate in the cytoplasm of the cell in the upper right.

Pathologic Features

Blood

In general, the blood in B-ALL is almost always diagnostic with total counts above 50×10^9/L with moderate anemia and thrombocytopenia, but petechial hemorrhage is much less common in ALL than in AML. In fact, presentation with epistaxis should ensure that careful examination of blood is carried out to eliminate myeloblastic leukemia. Dogs may present with ALL of the L1 type (Figs. 3.25, 3.26) and, rarely, horses (Figs. 3.27, 3.28). In human ALL, the L1 and L2 types (Fig. 3.29) may be of either B- or T-cell type and tend to be more effectively treated than L3 type, which is usually of B-cell type. Most animals with ALL present with a blood picture of larger lymphocytes of L3 type, including adult cattle (Fig. 3.30, see also 3.8), dogs (Fig. 3.31), and cats (Fig. 3.32). A syndrome in human adolescents that present with acute T-cell leukemia and mediastinal mass (Figs. 3.33–3.35) also occurs in young dogs at 1–2 years of age with both of L1 type (Fig. 3.36). The disease begins in the thymus but very rapidly peripheralizes to the marrow with presentation

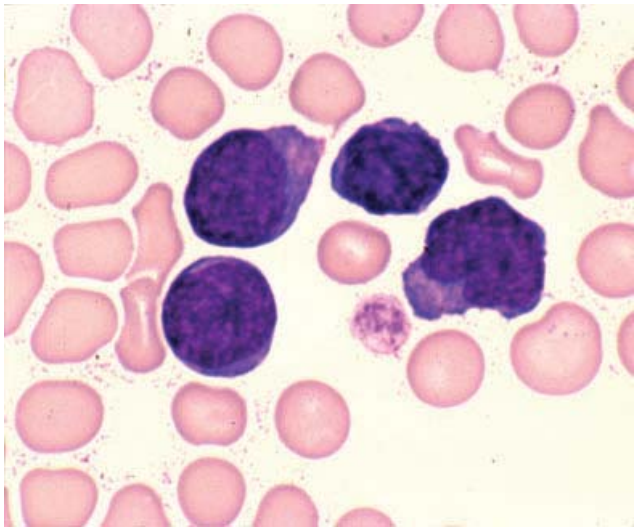

Figure 3.25. Dog: blood, ALL L1. The leukemic lymphoblasts have relatively round nuclei that vary moderately in diameter but have very similar chromatin patterns with a dense reticulated pattern and irregularly apparent multiple small nucleoli. The cytoplasm is minimal and characteristically slightly eccentric. Note there is only one platelet in the field (center) that is small and poorly granulated.

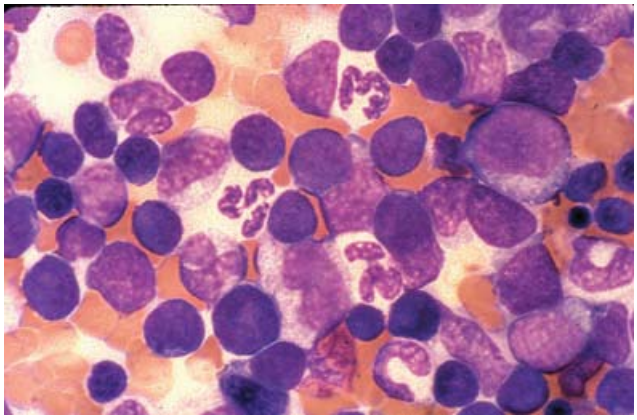

Figure 3.26. Dog: marrow aspirate, ALL L1. Half or more bone marrow cells consist of the lymphoid blasts. Typically, there is residual myelopoiesis but very little erythropoiesis typical of bone marrow undergoing myelophthisis.

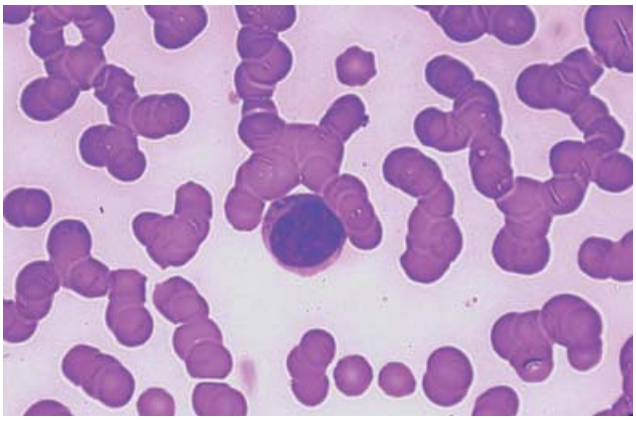

Figure 3.27. Equine: blood, ALL type with pancytopenia. A 5-year-old female event horse in excellent condition was presented because of a sharp drop in performance and appetite. The animal had mucosal petechiation and, on examination of blood, there is mild anemia resulting from marked thrombocytopenia as well as pancytopenia with only a few lymphocytes present and the bone marrow packed with cells similar to that in the blood.

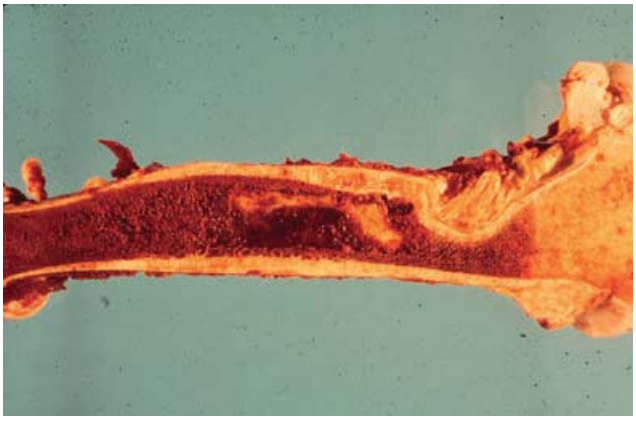

Figure 3.28. Equine: hemisection of femur, ALL L1, same case as Figure 3.27. The marrow in central marrow cavity has been almost completely converted from fatty marrow with the progressive invasion of the lymphoid tumor. There is a small triangular yellow area of residual fatty marrow in the center of the image.

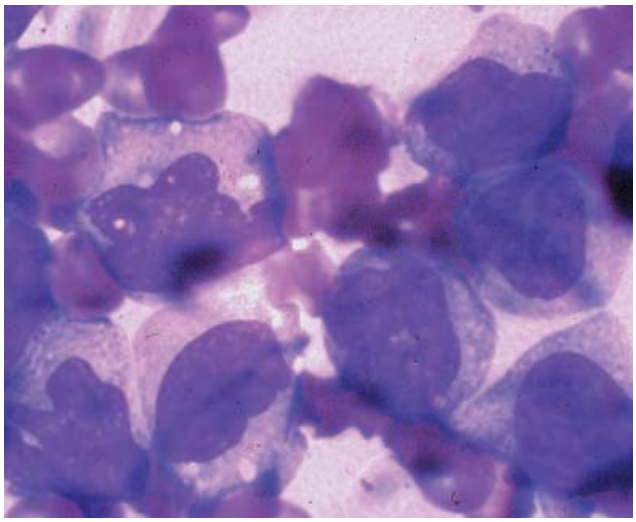

Figure 3.29. Human: marrow aspirate, ALL L2 type. The nuclei are large, 2.5 red cells in diameter, round to irregular, in outline with a fine chromatin pattern with a few large chromocenters and apparent often multiple nucleoli. The cytoplasm is relatively abundant and moderately basophilic, with frequent small vacuolations. *Image from R.D. Brunning, MD.*

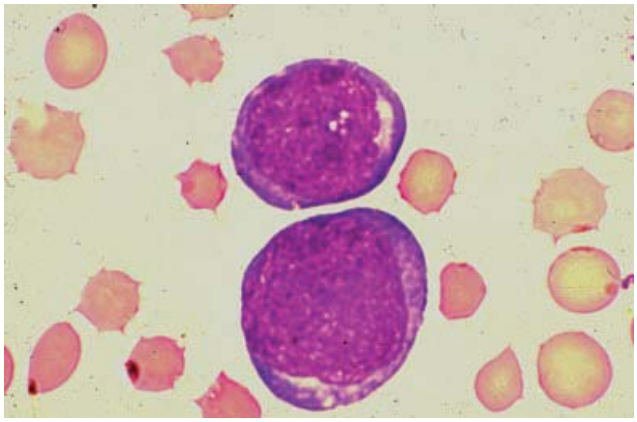

Figure 3.30. Bovine: blood, lymphoma/leukemia. The peripheral blood contains cells with large round and lightly indented nuclei that have a cribriform chromatin pattern with a few larger chromocenters in smaller cells and multiple relatively inapparent nucleoli. The cytoplasm is generally minimal and moderate with light perinuclear clearing and occasional cytoplasmic vacuoles.

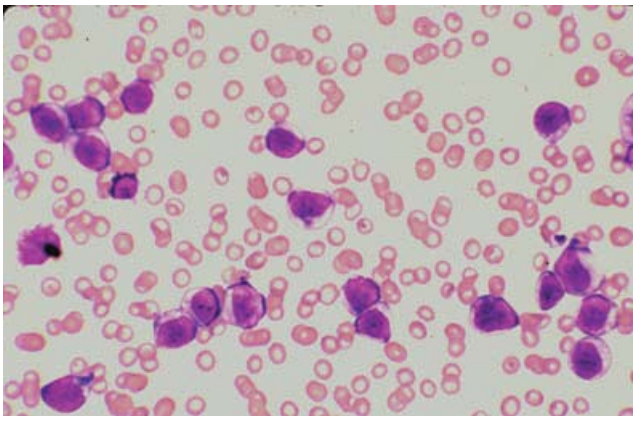

Figure 3.31. Dog: blood, ALL L3. A dog was presented with mucous membranes that were pale with petechiation. On examination of blood, there was a total leukocyte count of 120,000 per ul, with very few neutrophils and no platelets found.

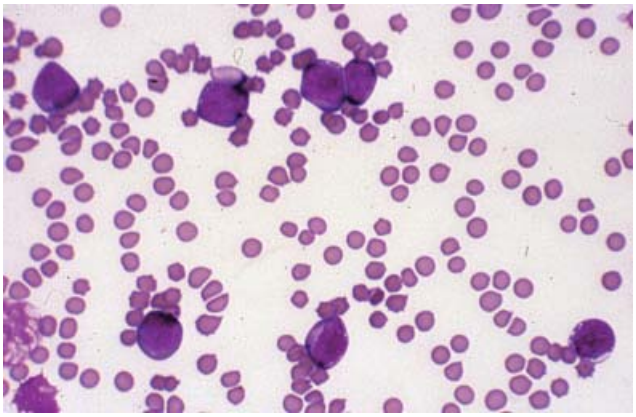

Figure 3.32. Cat: blood, ALL L3. The cat presented with a hemoglobin level of 7.2 g per dl, with marked neutropenia and thrombocytopenia with the leukocytes largely primitive lymphocytes. The nuclei are 2.5–3 red cells in diameter and round to irregularly indented, with 1–2 nucleoli. The cytoplasm is moderate in volume and staining density, with fine peripheral vacuolations.

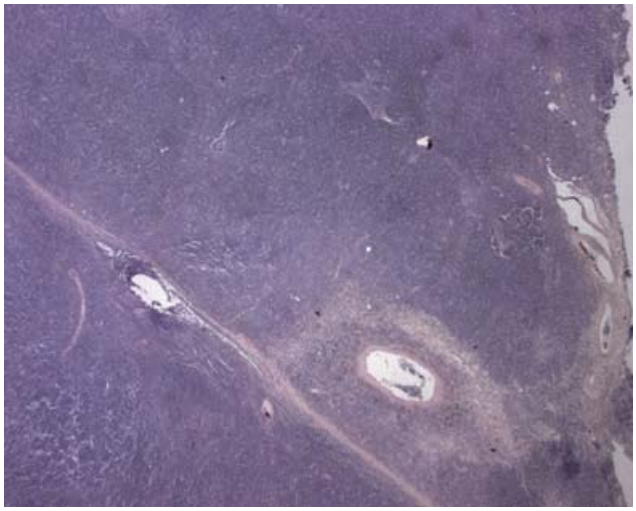

Figure 3.33. Human: mediastinal mass, T-lymphoblastic lymphoma. There is complete destruction of the thymic lobulation with a diffuse lymphoid proliferation. *Slide from Cornell Tutorial.*

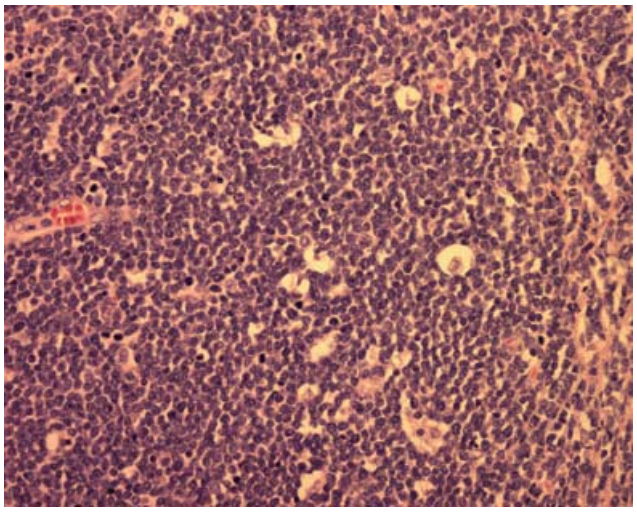

Figure 3.34. Human: mediastinal mass. Detail of Figure 3.33. The lighter area at the right is a heavily invaded lobular capsule. Note the starry sky effect due to many large tingible body macrophages with the small darkly stained nuclei, apoptotic figures, and some mitoses.

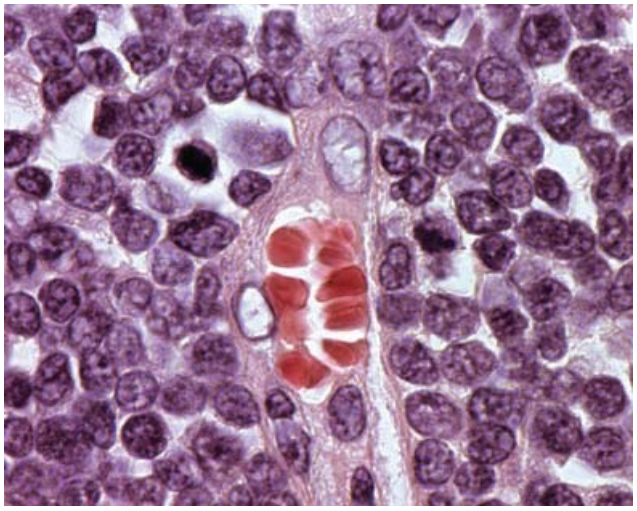

Figure 3.35. Human: mediastinal mass. Detail of Figure 3.33. Cytologically, the T-lymphoblastic nuclei are only slightly larger than the red cells, with the chromatin relatively dispersed and nucleoli small and obscured. Note the similarity between the metaphase just right of the central vessel and the nucleus within a tingible body macrophage just left of the vessel.

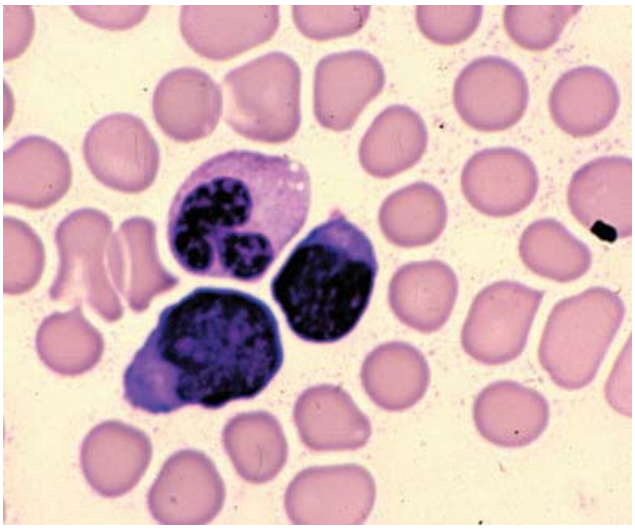

Figure 3.36. Dog: blood, ALL L1. A young dog was presented with a recent onset of malaise and found to have a total leukocyte count of 110,000 per ul with cells of typical L1 type and heavy marrow involvement.

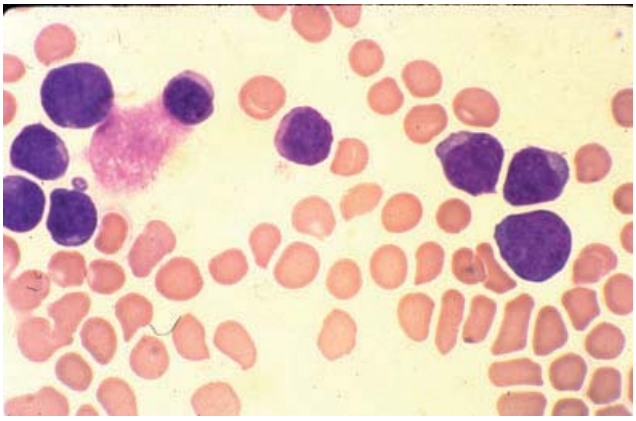

Figure 3.37. Cat: blood. Chronic lymphocytic leukemia, likely in accelerated phase. The smaller lymphocytes are typical of a small cell CLL, and the larger cells, with less cytoplasm and multiple small nucleoli, represent an increasing population of proliferative phase cells.

like ALL L1 of B-cell type, with the thymic mass often not recognized as a key observation in the identification of the specific neoplasm. Adult dogs that present with a leukemic blood picture and a symmetrically enlarged spleen are likely to have T-cell leukemia; dogs with peripheral lymphadenopathy and a leukemic blood picture are more likely to have B-cell ALL (see Fig. 3.1). Dogs of 10 or more years of age that present with a lymphocytosis over 100×10^9/L and that have a predominantly small or intermediate-sized lymphocyte with 10% large blastic cells likely have CLL in blastic or accelerated phase (Fig. 3.37).

Bone Marrow

Aspirated marrow in B-cell ALL is always hypercellular with trilineage phthisis (Fig. 3.38). There is usually a high proportion of bare nuclei and cytoplasmic debris. If thrombocytopenia has been a prominent symptom with epistaxis, there is usually focal hemorrhagic necrosis in

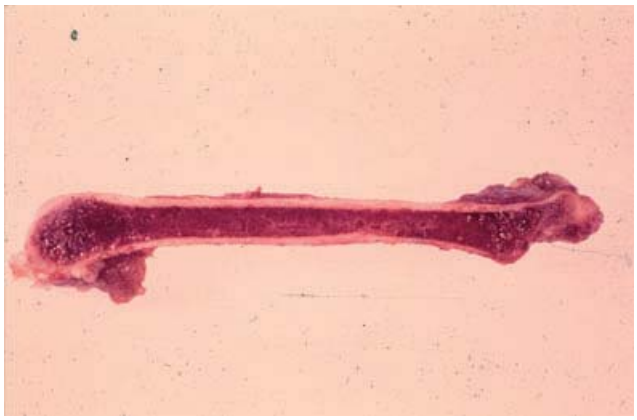

Figure 3.38. Cat: femur, ALL L3. Nearly all of the central marrow cavity has been converted to red marrow with advancing lymphoid keukemic.

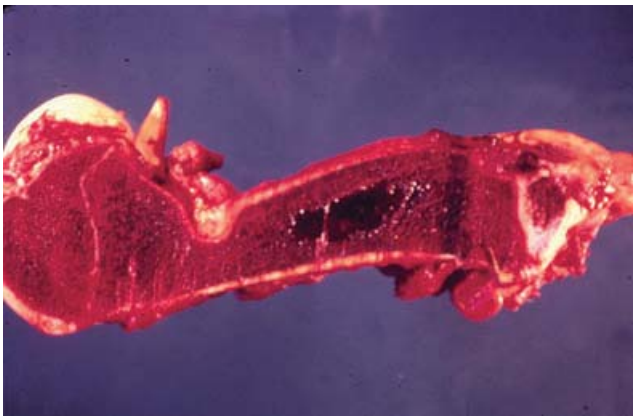

Figure 3.40. Bovine: lymphoma, femur. Femur from a young animal with the enzootic type of BLV-associated lymphoma and very extensive conversion of the metaphyses and marrow cavity to hemopoietic areas with loss of fat.

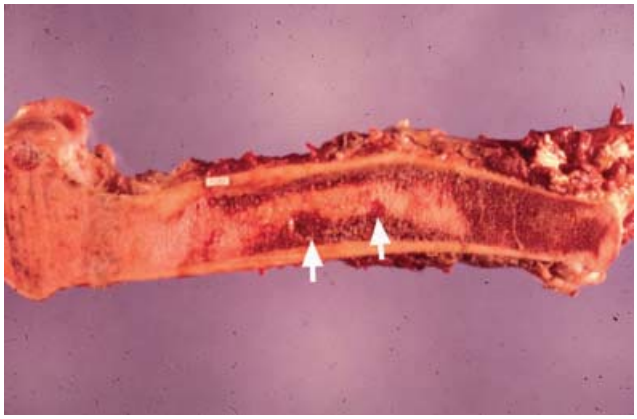

Figure 3.39. Equine: femur, ALL. A mature horse had presented with leukemic blood picture with thrombocytopenia. The femoral cavity has laminar subendosteal marrow activation and conversion from fatty marrow, with the arrows indicating two areas of hemorrhagic infarction due to phthisis of megakaryocytes and thrombocytopenia.

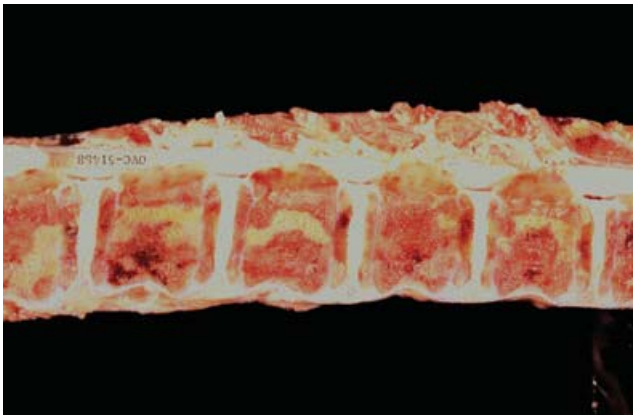

Figure 3.41. Bovine: hemisection of spinal column, acute Lymphoid leukemia. Multifocal marrow ischemic infarction, which is typical of calf type of sporadic lymphoma with acute lymphocytic leukemia. The irregularly shaped yellow areas within the spinal bodies represent foci of ischemic infarction that are irregularly outlined by areas of hyperemia. The focal areas of reddening near the left represent areas of hemorrhage.

the marrow that is dark and cyanotic on gross examination of the marrow cavity (Figs. 3.39–3.41, see also 3.28). Histologically, at an architectural level of marrow examination there is very high cellularity, generally over 90%, with few fat cells remaining, generally near the large vessels of the marrow central cavity (Fig. 3.42). The involvement of the marrow may be patchy with focal areas of residual hematopoiesis and adjacent foci with solid lymphoid proliferation (Figs. 3.43–3.45). The changes are generally of an acute nature in dogs, cats, horses, and cattle; in calves with ALL, there will be frank areas of ischemic necrosis, primarily in the epiphyseal and metaphyseal areas of cancellous bone. These infarcted areas appear grossly yellow and have a narrow hemorrhagic border (Fig. 3.46).

Lymph Node

At the time of diagnosis, the node selected for biopsy has diffuse architecture with a thinned and taut capsule and compression of the peripheral sinus. There is usually focal bridging of the capsule and colonization of perinodal fat (Fig. 3.47). There is evidence of benign hyperplasia with fading clusters of mantle cells in cortical areas, but there is not the level of medullary sclerosis seen in the more indolent lymphomas of marginal zone type. There is diffuse involvement of the paracortex and filling of the

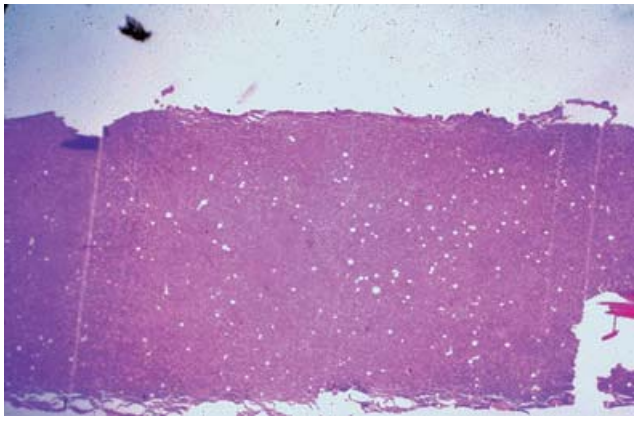

Figure 3.42. Cat: bone marrow histology, ALL. The femoral marrow is a solid cylinder of hematopoietic tissue with almost complete loss of fat cells and phthisis of normal marrow precursors and progeny.

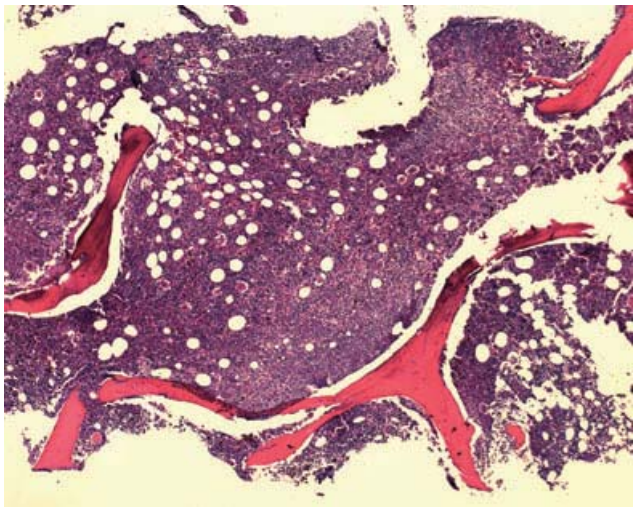

Figure 3.43. Dog: marrow core, same case as Figure 3.1. The marrow is hypercellular with residual hematopoiesis in the areas of most numerous fat cells and solid tumor in the areas with fat cells excluded (center).

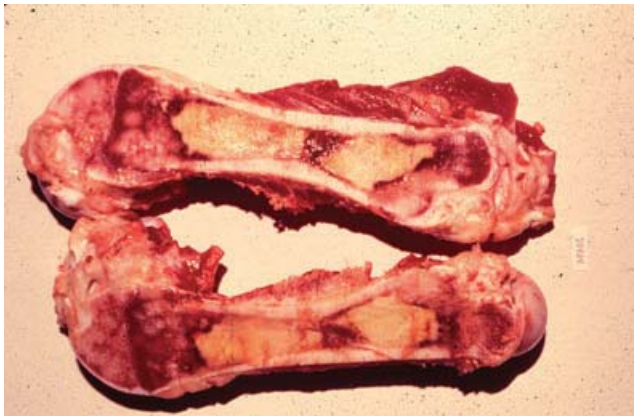

Figure 3.46. Calf: femur, ALL L1. Femoral cavity from an animal with the calf type of acute lymphoblastic leukemia, with extensive marrow infarction. The yellow areas in the central marrow cavity surrounded by a hyperemic reddish border have undergone ischemic infarction due to blockage of the microvasculature by the rapidly growing neoplastic cells.

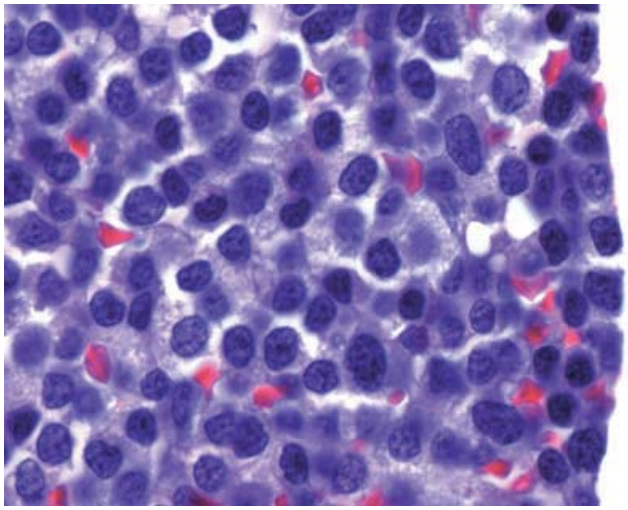

Figure 3.44. Dog: marrow, histology. Detail of Figure 3.43. The L1 cells are of relatively uniform size, with largely dispersed chromatin and nucleoli inapparent in most cells. The cytoplasm appears more abundant than in peripheral blood.

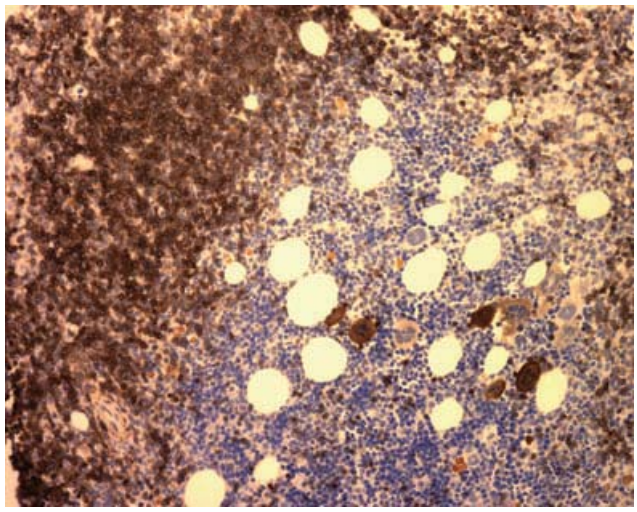

Figure 3.45. Dog: marrow core. Detail of Figure 3.43. Stained with CD79 for lymphocytes of B lineage. Note the relationship of fat cells to residual hematopoiesis, with solid tumor areas having excluded most fat cells. The maturing megakaryocytic cytoplasm marks with this reagent.

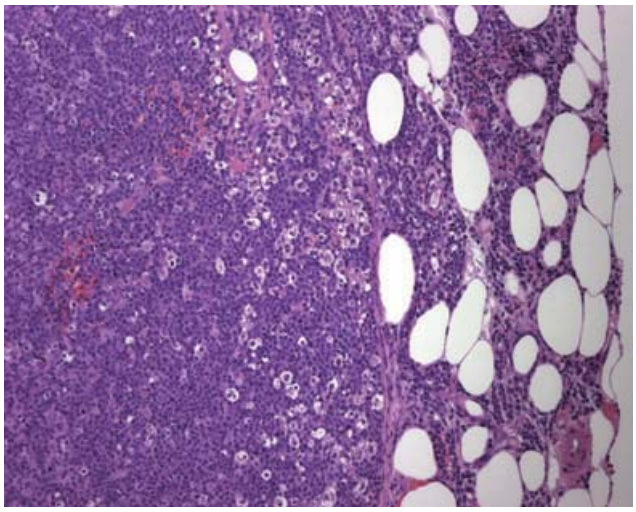

Figure 3.47. Dog: node, B-type lymphoblastic lymphoma. The rapidly advancing neoplasm has bridged the peripheral sinus and the nodal capsule and is infiltrating the perinodal fat.

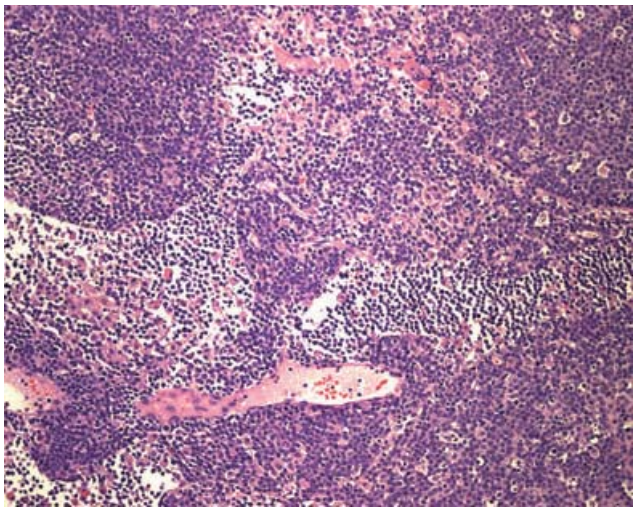

Figure 3.48. Dog: node medulla, B-LBL, same case as Figure 3.47. There is solid filling and distension of the medullary cords and irregular compression of the medullary sinuses.

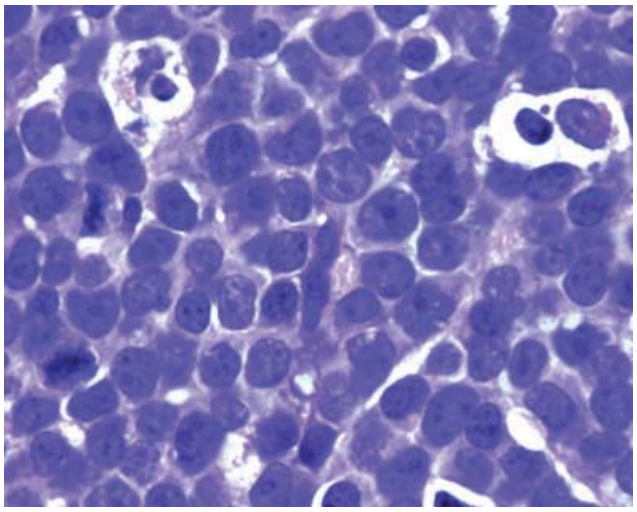

Figure 3.49. Dog: node, B-LBL. Detail of the case in Figure 3.47. The nuclei are generally round with the largest being 1.5 red cells in diameter. The chromatin is hyperchromatic, fine, and dispersed with multiple small nucleoli that may be confused with more dense aggregations of chromatin. The prominent tingible body macrophages in the top are typical of lymphomas with a high mitotic and death rate.

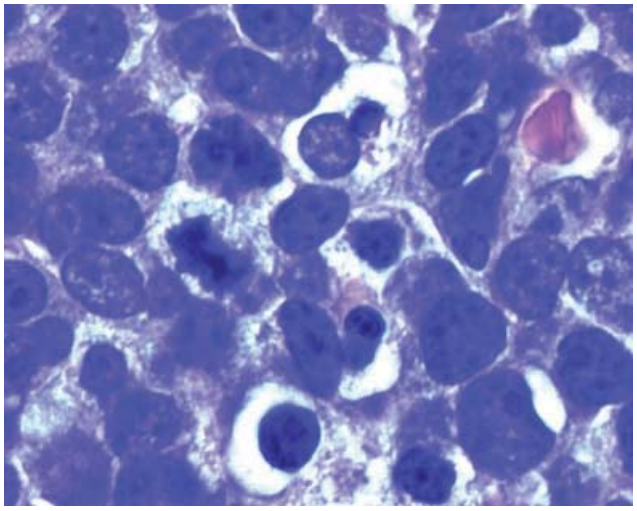

Figure 3.50. Dog: node, B-LBL. Detail of Figure 3.49. The red cell in the upper right provides an index of size for the lymphoblastic nuclei. There are 2 mitoses left center that characteristically lack the sharp outlines of lymphocytes in metaphase.

medullary cords with compression and obliteration of the medullary sinuses (Fig. 3.48). The key to the diagnosis of B-cell lymphoblastic lymphoma (B-LBL) is the recognition of the high mitotic rate in a relatively small cell neoplasm. Cytologically the neoplastic cells have round to oval nuclei, occasionally with sharp shallow indentations of the lymphoblastic convoluted cell type. The nuclei are 1.5–2.0 red cells in diameter with a fine hyperchromatic uniform chromatin pattern without any tendency to parachromatin clearing that distinguishes this neoplasm from the Burkitt's-like lymphoma. There are single small, centrally located nucleoli that are obscured by the density of the chromatin and are not seen unless looked for (Fig. 3.49). Oddly, the mitoses themselves are less obvious than in other lymphomas because the metaphases have a "smoky" indefinite outline unlike the sharp delineation of chromosomes characteristic of other lymphoid neoplasms (Fig. 3.50). The diagnosis of LBL of B- or T-cell type requires optimal handling of the specimen at each step of

the tissue removal and processing. If the node biopsy is excisional, it is likely that the penetration of fixative into the inner areas of the node has been too slow for optimal preservation of chromatin structure. Therefore, it is essential in making the initial examination to note any change in character of nuclei in the outer cortex and inner areas and confine the interpretation to the periphery. With the LBL neoplasms, if formalin fixation is delayed, the chromatin collapses on the nuclear membrane and the uniform character of the LB cells is lost. The diagnosis of the LBL type of neoplasms is one of the most misinterpreted aspects of veterinary hematopathology. There is a general and persistent failure to distinguish between the older veterinary literature where *lymphoblastic* in the hematologic sense means a large cell neoplasm while in the histologic nomenclature this cell type, as defined by Henry Rappaport, is small or intermediate-sized. The B-cell LBL (Fig. 3.51) is like the B-ALL, a highly aggressive neoplasm that requires aggressive therapy. In terms of prevalence, B-cell ALL is much more common than B-LBL in humans, but in animals it appears that the opposite is the case. This opinion may be derived from the fact that specific terminology is even less commonly used in veterinary hematology than in histology. Therefore, accurate estimates of the incidence of neoplasms that present as B-ALL, have the cytomorphology of L1 or L2, and have the histological appearance of dispersed chromatin and small nucleoli are virtually an unknown entity.

Spleen

Lymphomas tend to involve the spleen in a focal or multifocal manner that results in irregular masses that distend the capsule and may be pale, suggesting underlying lymphoid tissue, or dark and hemorrhagic (Fig. 3.52). Architecturally, the areas of proliferation arise from components of the arteriolar lymphoid sheath (PALS), whether of B- or T-cell type. In contrast, in the leukemias the spleen is more likely to have diffuse sinus involvement with symmetrical splenomegaly and generalized atrophy of the PALS system. Most lymphoid neoplasms, if malignant, will result in subendothelial colonization of the large muscular venous sinuses, and this may be subtle compared to the level of involvement of the rest of the spleen. In general, if there is colonization of the lining of the larger splenic veins, there will also be at least focal involvement of the liver.

Liver

In ALL, there is usually sinus involvement of the liver that varies in intensity with the degree of leukemia (Fig. 3.53). This is not, however, always consistent, and in some cases there will be periportal and perivenus colonization without heavy involvement of the hepatic cords. Significantly though, if ALL is present, there will be sufficient involvement of the hepatic parenchyma in a diffuse manner that will provide a positive sample on a blind fine needle aspiration of the liver. ALL may involve any tissue in the body, but in some cases—likely as a function of the immunosuppression that accompanies advanced cancer—there may be severe atrophy of the thymus gland (Fig. 3.54).

Immunologic Features

The phenotypic characterization of ALL in animals is still a work in progress. Currently most cases in animals are

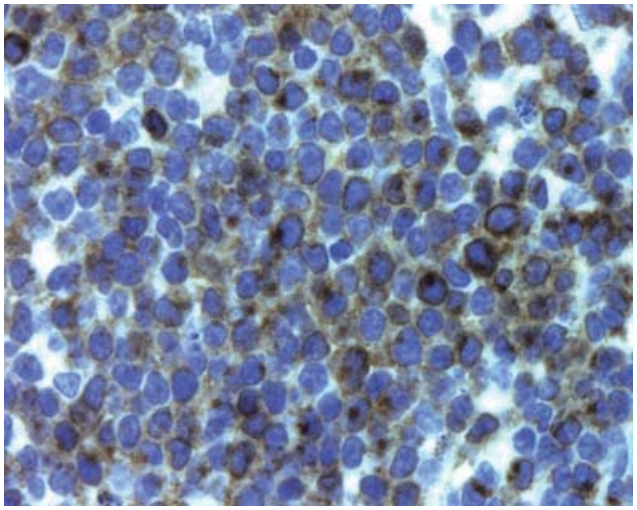

Figure 3.51. Dog: node, B-LBL. Phenotype of case 3.47. With immunohistochemical staining for B-cells with CD79 alpha, the neoplastic cells are strongly and uniformly labeled.

Figure 3.52. Equine: ALL L3 splenomegaly. At necropsy, the animal was mildly icteric and the spleen was markedly enlarged and weighed 29 pounds. The combination of small or only slightly enlarged nodes with a solid involvement of bone marrow and splenomegaly is highly supportive of the diagnosis of primary leukemia despite the fact that the peripheral blood changes were of a relative pancytopenia with a mild lymphocytosis of atypical type.

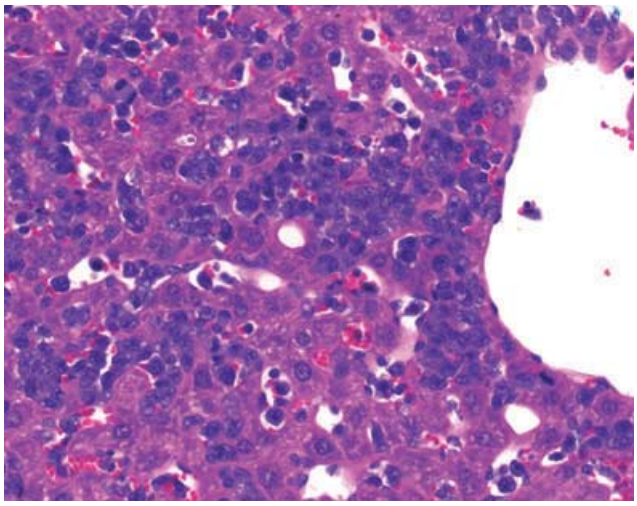

Figure 3.53. Mouse: liver, ALL. In acute lymphoid leukemias, the marrow involvement is more characteristically one of irregular sinus infiltration rather than of solid areas of neoplastic cells that tend to surround vascular structures in the lymphomas. *Slide from J. M. Ward, DVM.*

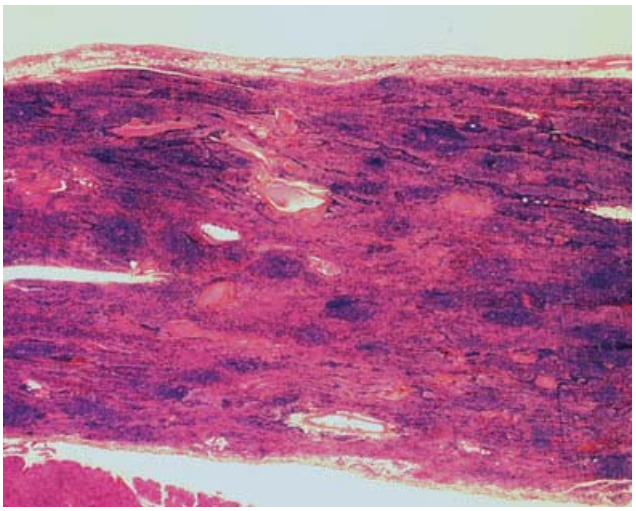

Figure 3.54. Equine: thymic atrophy, ALL L3. The thymus is markedly atrophic and reduced to a thin fibrous raphe anterior to the heart. The capsule is intact on both sides of the organ with the entire width of the thymus included in this low-power micrograph. The cortical areas are reduced to small linear areas of dark-staining cells, with the more bland areas in between bare oval-shaped epithelial cells that were likely part of the normal anatomy and appear increased due to marked lymphoid depletion. The change is compatible with the immunosuppression frequently coexistent with cancer.

diagnosed as a form of acute leukemia on Romanovsky-type stains on blood and marrow, with few receiving immunocytochemical verification of phenotype. Flow cytometry is being increasingly employed, with an array of phenotyping reagents active on fresh unfixed cells. Most cases proceed to histology where the range of reagents active on paraffin-embedded tissues is much reduced. The development of molecular detection methods utilizing fluorescent in situ hybridization (FISH and ISH) and chip array systems for detecting gene amplification are providing the tags to identify the acute leukemias with much greater precision. Although the great majority of human ALL is in children and most of these are of B-cell type, there is apparently more heterogeneity of phenotype in animals. On the basis of very few animals studied, about 60% of canine ALL is of B-cell type, as determined by cytoplasmic IgH or by marking of cytoplasm by CD79 alpha. In dogs with proven heavy T-cell neoplastic involvement of bone marrow, less than half of these have neoplastic cells detectable in the blood by experienced observers. It appears that the proportion of ALL that is of B-cell type is less in cats than in dogs, and in both species lymphoma is far more common than acute leukemia. In contrast, in ALL of cattle those that are positive for bovine leukemia virus (BLV) have a peripheral picture that is predominantly of B-cell type. Rarely, the sporadic form of lymphoma that presents in 2-year-old cattle with a multifocal skin disease of Mycosis Fungoides type will become leukemic in a type of Sézary syndrome and these will be T-type ALL. In contrast, the calf type of lymphoma leukemia that is also sporadic or non-BLV associated is about 90% of B-cell type by immunophenotypic staining of histological tissues with CD79 alpha and with BLA36 that marks B-cells in most domestic animals (but also marks T-cells to the extent that it is not a reliable reagent). ALL in horses is rarely encountered, and few of these have been phenotyped, but on subsequent staining of histological tissues these seem to be predominantly of B-cell type. Even more rarely, horses may present with a disease like Mycosis Fungoides with large nodes and brick red mucosa but no apparent skin disease, and these progress to a leukemic phase like Sézary syndrome with the neoplastic cells in blood with convoluted nuclei, and these are presumably also of T-cell type.

Cell of Origin

Both B-cell ALL and LBL are presumed to be a variant of a normal pre–B-cell precursor. In human practice, ALL is very heterogeneous, and the heavy chain rearrangement that is present in virtually all cases of B-cell ALL also occurs in some cases of T-cell ALL. Therefore, for diagnostic purposes, rearrangement of the light chain gene is considered more specific for B-cell differentiation. At the stage of rearranged heavy chain gene the cells lack surface immunoglobulin (sIg) and are termed precursor B-cells or pre–pre-B-cells. The next step in differentiation is the

production of cytoplasmic mu heavy chain protein, but no light chain and no sIg. Both the pre–pre-B- and pre–B-cells are lymphoblasts by definition and by morphology as they have dispersed chromatin and small inapparent nucleoli. It has been suggested that the normal counterpart of B-cell ALL is present in such low numbers that it has not yet been characterized on an anatomic as well as molecular basis. In terms of cyto-histo correlations, the L1 and L2 types of ALL are indistinguishable from lymphoblastic lymphoma, and ALL of the L3 type is like Burkitt's or Burkitt's-like lymphoma. The latter type of neoplasm is of the cell type that was termed *small noncleaved cell* by the Working Formulation.

Diagnostic Criteria

B-cell ALL must be distinguished from T-cell ALL and from AML. ALL does not present with preleukemic symptoms, and therefore the blood and marrow are typical of a frank neoplasm. If there are no primary peripheral lesions, heavy (greater than 20% of marrow cells) marrow infiltration of intermediate-sized cells with blastic conformation, and positive cytoplasmic staining with CD20 and or CD79 alpha, the diagnosis is confirmed. B-cell LBL must be distinguished from T-cell LBL on results of phenotypic staining. The critical diagnostic features of B-LBL are the high and easily overlooked mitotic rate in a lymphoma of intermediate cell size with dispersed chromatin and small obscured nucleoli.

Differential Diagnosis

AML of the M0-M1 stage of differentiation is the most likely neoplasm to be confused with ALL. Because a reliable staining reaction for myeloperoxidase that is active in paraffin-embedded tissues has only recently become available, the true proportions of acute lymphoid and myeloid leukemias are yet to be determined. For numerous technical and other reasons, a negative reaction for B- and T-cell differentiation in immunohistochemistry cannot be considered a presumptive diagnosis of AML. In human medicine, Rhabdomyosarcoma is considered the small round cell tumor most likely to be misdiagnosed as ALL. B-cell LBL must be distinguished from T-cell LBL on the basis of phenotype. In addition, B-LBL must be distinguished from intermediate cell lymphoma on the basis of dispersed chromatin and much higher mitotic rate in the lymphoblastic population.

Staging

The most important features of B-cell ALL that might dictate a favorable response to therapy are a relatively low leukocyte count (WBC <50,000/ul) and the absence of thrombocytopenia or severe anemia. The clinical features of progression are adenopathy, organomegaly, mediastinal mass (T-cell ALL), and involvement of the central nervous system. In human ALL, adults do not respond as well to treatment as children do, and it is not known whether this applies in animals because most treated animals are given a palliative rather than curative level of therapy. As with other neoplasms, a good initial response to therapy is a good indicator of overall survival. B-LBL is a very aggressive neoplasm, and it is not known whether the LBL of B-cell type is any more easily brought into remission than the T-cell type. It appears likely that the poor response of the LBL lymphomas to combination chemotherapy is not in the lack of initial debulking but in the rapid recovery of the neoplastic population.

Transformation and Progression

Because the disease is already of blastic nature, no further parameters of aggression are helpful other than a rising WBC level and an increase in mitotic rate.

Evaluation of the Treated Animal

The most useful criterion of therapeutic efficacy is an examination of bone marrow 2–4 weeks after initiation of therapy to determine the level of blast cells remaining. With normal marrow having about 1% of blasts of all cell types, the level of blast cells remaining can be used to direct subsequent therapy. In human practice, the following criteria are used. A reduction of blasts to a level of 5% or less is considered a good response, and these cases may then be given an "intensification or consolidation" level of treatment. Cases with 5–25% of blasts present are given a second course of induction therapy, and those with more than 25% marrow blasts are considered to have failed the induction therapy and have to be considered for unproven or experimental strategies. Currently sensitive techniques utilizing heteroduplex PCR techniques permit the detection of "minimal residual disease" in animals that have a previous diagnosis of a clonal neoplasm. Using identical techniques, the specificity of repeat banding in gel-separated PCR product derived from a posttherapy sample has a high likelihood of detecting cured cases or early recurrence of tumor.

Treatment and Survival

Little is known of these features in animal ALL because the disease is heterogeneous and a molecular level of subtyping will be required to know that cases have a similar biology and response to therapy. Secondly, it is not feasible to treat animal ALL with a curative level of therapy because this would require continued hospitalization that in most cases is, in itself, cost prohibitive.

REFERENCES

Downing, J.R. (2004) TGF-β signaling, tumor suppression, and acute lymphoblastic leukemia. *N Engl J Med* 351(6):528–530.

Dunphy, C.H., van Deventer, H.W., Carder, K.J., Rao, K.W., and Dent, G.A. (2004) Mature B-cell acute lymphoblastic leukemia with associated translocations (14;18) (q32;q21) and (8;9) (q24;p13): A Burkitt varient? (2003) *Arch Pathol Lab Med* 127:610–613.

Faderi, S., Jeha, S., and Kantarjian, H,M, (2003) The biology and therapy of adult acute lymphoblastic leukemia. *Am Canc Soc* 1337–1354.

Germano, G., Songia, S., Biondi, A., and Basso, G. (2001) Rapid detection of clonality in patients with acute lymphoblastic leukemia. *Haematologica* 86(4):382–385.

Gleiner, B., Rieder, H., Thiel, E., Fonatsch, C., Janssen, L.A.J., Heinze, B., Janssen, J.W.G., Schoch, C., Goekbuget, N., Maurer, J., Hoelzer, D., and Bartram, C.R. (2001) Prospective BCR-ABL analysis by polymerase chain reaction (RT-PCR) in adult acute B-lineage lymphoblastic leukemia: Reliability of RT-nested-PCR and comparison to cytogenetic data. *Leukemia* 15:1834–1840.

Harbo, S.J., Barrington, G.M., Allen, A.J., Sample, G.L., Parish, S.M., Hamilton, M.J., and Davis, W.C. (2004) Characterization of lymphocyte populations by flow cytometry in a calf with sporadic juvenile lymphoma. *Vet Clin Path* 33(3): 1663–1667.

Hollerman, A., Cheok, M.H., den Boer, M.L., Yang, W., Veerman, A.J.P., Kazemier, K.M., Pei, D., Cheng, C., Pui, C.-H., Relling, M.V., Janka-Schaub, G.E., Pieters, R., and Evans, W.E. (2004) Gene-expression patterns in drug-resistant acute lymphoblastic leukemia cells and response to treatment. *N Engl J Med* 351(6):533–542.

Huh, Y.O., and Ibrahim, S. (2000) Immunophenotypes in adult acute lymphocytic leukemia. *Hematol/Oncol Clin North Amer* 14(6):1251–1265.

Keller, R.L., Avery, A.C., Burnett, R.C., Walton, J.A., and Oliver, C.S. (2004) Detection of neoplastic lymphocytes in peripheral blood of dogs with lymphoma by polymerase chain reaction for antigen receptor gene rearrangement. *Vet Clin Pathol* 33(3):145–149.

Li, S., and Lew, G. (2003) Is B-lineage acute lymphoblastic leukemia with a mature phenotype and L1 morphology a precursor B-lymphoblastic leukemia/lymphoma or Burkitt leukemia/lymphoma? *Arch Pathol Lab Med* 127:1340–1344.

Pérez-Losada, J., Gutiérrez-Cianca, N., and Sánchez-García, I. (2001) Philadelphia-positive B-cell acute lymphoblastic leukemia is initiated in an uncommitted progenitor cell. *Leuk Lymph* 42(4):569–576.

Pui, C.-H., Relling, M.V., Downing, J.R. (2004) Mechanisms of disease: Acute lymphoblastic leukemia. *N Engl J Med* 350:1535–48.

Steinherz, P.G., Gaynon, P.S., Breneman, J.C., Cherlow, J.M., Grossman, N.J., Kersey, H.J., Johnstone, H.S., Sather, H.N., Trigg, M.E., Chappell, R., Hammond, D., and Bleyer, W.A. (1996) Cytoreduction and prognosis in acute lymphoblastic leukemia—The importance of early marrow response: Report from the children's cancer group. *J Clin Oncol* 14(2):389–398.

Stock, W., and Estrov, Z. (2000) Studies of minimal residual disease in acute lymphocytic leukemia. *Hematol/Oncol Clin North Amer* 14(6):1289–1305.

Taub, J.W. (2004) The prenatal origin of childhood acute lymphoblastic leukemia. *Leuk & Lymph* 45(1):19–25.

van der Burg, M., Poulsen, T.S., Hunger, S.P., Beverloo, H.B., Smit, E.M.E., Vang-Nielsen, K., Langerak, A.W., and van Dongen, J.J.M. (2004) Split-signal FISH for detection of chromosome aberrations in acute lymphoblastic leukemia. *Leukemia* 18:895–908.

Velders, M.P., ter Horst, S.A.J., and Kast, W.M. (2001) Prospects for immunotherapy of acute lymphoblastic leukemia. *Leukemia* 15:701–706.

Vialle-Castellano, A., Laduron, S., De Plaen, E., Jost, E., Dupont, S., Ameye, G., Michaux, L., Coulie, P., Olive, D., Boon, T., and van Baren, N. (2004) A gene expressed exclusively in acute B lymphoblastic leukemias. *Genomics* 83:85–94.

Winick, N.J., Carroll, W.L., and Hunger, S.P. (2004) Childhood leukemia—New advances and challenges. *N Engl J Med* 351(6):601–603.

Wolfraim, L.A., Fernandez, T.M., Mamura, M., Fuller, W.L., Kumar, R., Cole, D.E., Byfield, S., Felici, A., Flanders, K.C., Walz, T.M., Roberts, A.B., Aplan, P.D., Balis, F.M., and Letterio, J.J. (2004) Loss of Smad3 in acute T-cell lymphoblastic leukemia. *N Engl J Med* 351(6):552–559.

Workman, H.C., and Vernau, W. (2003) Chronic lymphocytic leukemia in dogs and cats: The veterinary perspective. *Vet Clin Small An* 33:1379–1399.

Burkitt's Lymphoma

Definition

Burkitt's lymphoma is a high-grade, often extranodal B-cell lymphoma characterized by diffuse architecture, tingible body starry sky appearance at low magnification, monotonous appearance of cells with vesicular nuclei of intermediate size, multiple nucleoli, moderate volume of cytoplasm usually with small lipid vacuoles, and very high mitotic rate.

The recognition of the disease that became known as Burkitt's lymphoma (BKL) has been characterized by a series of very important discoveries relating to human oncology. Burkitt's lymphoma was the first tumor shown to be curable by chemotherapy and the first shown to be associated with a virus that became known as the Epstein-Barr virus or EBV. Burkitt's was also one of the first solid tumors to be shown to be associated with a recurring nonrandom chromosomal translocation and the first in which that change was recognized to involve the deregulation of an oncogene, c-myc. Further, in recognition of the multifactorial causation of most human cancers, it was recognized that the distribution of Burkitt's-type lymphoma in Africa had the same geographic distribution as holoendemic malaria and of the mosquito vector. Although much more complex than a dual infection with malaria and EBV, the constant antigenic stimulation of malaria provides a sustained high background population of naive B-cells in immunoglobulin gene rearrangement that are more susceptible to chromosomal injury by the EBV-type herpesvirus. In the western world, only 10–20% of cases

are associated with EBV, but these cases still have the c-myc gene rearrangement. Human BKL is found in association with immunodeficiency virus infection, but oddly in Africa, where HIV infection has become well established, there has not been an increased incidence of this type of lymphoma.

Clinical Presentation and Features

The clinical presentation of human Burkitt's lymphoma has many aspects that appear similar in animal oncology. In equatorial Africa, which is the domain of the anopheles mosquito, 50–70% of patients present with lymphoma involving the jaw or orbital area, and these are age associated and in children 3 years of age with emergent teeth. Less than 25% of cases older than 16 years have jaw tumors and, in sporadic BKL outside of the area of endemic malaria, the proportion of jaw tumors is less than 10% of cases. Breast involvement with BKL occurs without geographic limitation but always in prepubertal girls or lactating women, emphasizing the relationship between cell proliferation of mammary epithelium or periodontal membrane and tumor induction. From 50–90% of patients worldwide that present with BKL have abdominal involvement, and this may have relevance to the relatively frequent occurrence of intestinal lymphoma in dogs that are of high-grade type and generally poor prognosis. Because most of these cases in animals are categorized on a topographical but not disease type of classification, it is not known if these tumors in the dog have a BKL type of morphology and phenotype. In humans with abdominal BKL, there is frequent involvement of adjacent mesenteric tissue and nodes and foci in the kidneys and pancreas, but there is involvement less often in the liver and spleen. There is usually ascites and often pleural effusion, both of which contain the Burkitt's lymphoma cells. Many of these characteristics are seen in the dog with intestinal lymphoma, including perforation and peritonitis. Bone marrow involvement is becoming more frequently recognized in human BKL of sporadic type and is found in about 20% of cases, indicating the need to differentiate the BKL from the precursor type of LBL and ALL. Human BKL may occasionally present with apparent leukemia and lymphadenopathy but without extranodal disease other than hepatosplenomegaly. Thus there is a need to identify the cell type on molecular grounds to differentiate BKL that is a post-germinal center B-cell from the pre–B-cell precursor type neoplasms because the topographical distributions overlap in some cases. Finally, human BKL may occur in the central nervous system as an extranodal high-grade lymphoma. The disease may present as facial palsy with neoplastic cells in the cerebrospinal fluid, and these cases are more frequent in the endemic areas in Africa than in the sporadic cases. Cranial nerves are involved, and of these the facial and ophthalmic nerves are most often involved and patients may present with blindness. The latter symptomatology and topographical involvement are seen in both dogs and cats.

Pathologic Features

Lymph Node

Human Burkitt's lymphoma of the classical type includes the endemic cases of equatorial Africa and many of the sporadic cases, as well as cases with acquired immunodeficiency syndrome–related lymphoma. The architecture is diffuse and characteristically with a "moth-eaten" appearance at low magnification due to the presence of many large tingible body macrophages that reflect the high apoptotic rate and high proliferative rate of BKL (Figs. 3.55–3.58). The cells are described as medium size with cell size about the same size as the nucleus of the tingible body macrophages (see Fig. 3.57). In the dog and cat, the nuclei are of similar size and like cells described as having nuclei of intermediate size more precisely defined as equivalent to 1.5 red cells in diameter. An important feature of these nuclei and cells is that they are all very similar in size and shape and have been described like "peas in a pod"; this description is also appropriate for the animal cases that are given this designation (Figs. 3.59, 3.60). With relatively abundant cytoplasmic volume and with centrally placed nuclei, the artifactual contraction associated with formalin and particularly the mercury-based B5 fixative, the tissue contraction results in the cells having distinct cellular margins. With good fixation and the proper field, the cells are hexagonal with

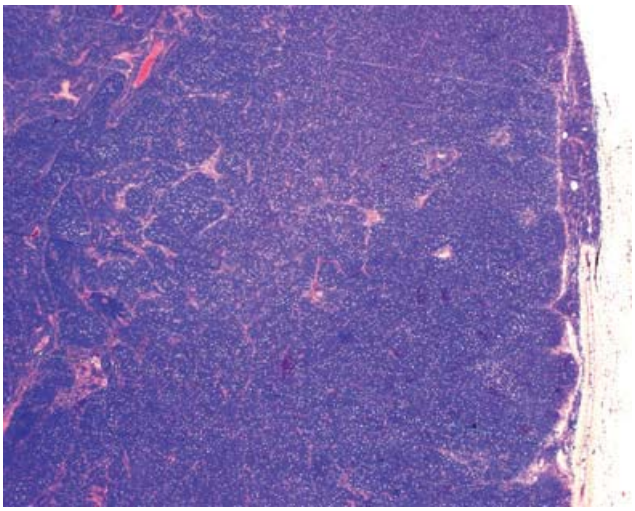

Figure 3.55. Human: mesenteric node, Burkitt's-type lymphoma. The rapid cellular proliferation has distended the node capsule that is focally bridged with colonization of perinodal tissues. *Slide from Cornell Tutorial.*

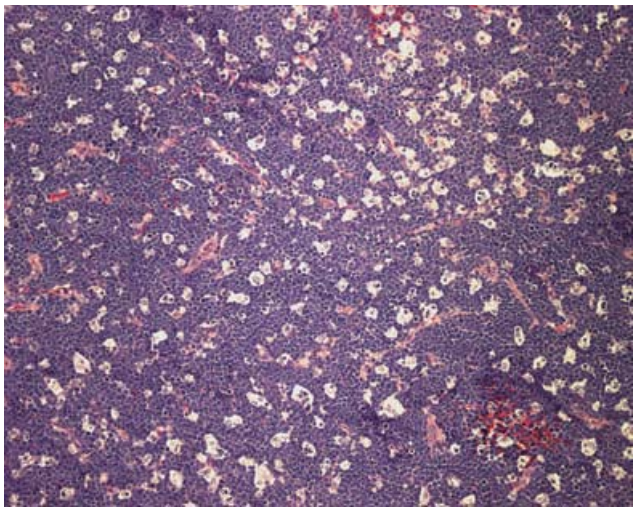

Figure 3.56. Human: mesenteric node. Detail of Figure 3.55. At an intermediate level of magnification the starry sky appearance due to a high level of tingible body macrophages is very apparent.

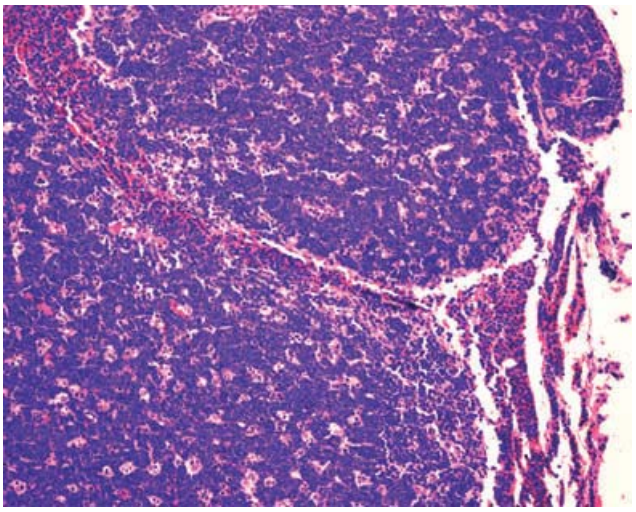

Figure 3.58. Human: breast biopsy, Burkitt's lymphoma. Note the similarity of the lymphoid tissue from this unusual site to that from the nodal area in the abdomen of Figure 3.56.

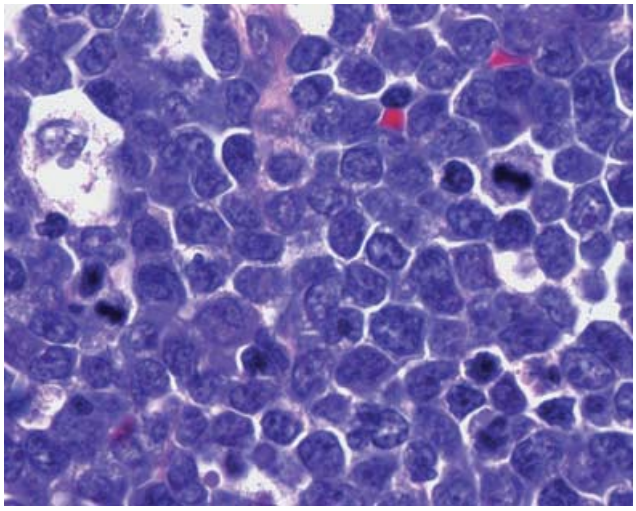

Figure 3.57. Human: mesenteric node. Detail of Figure 3.55. At a cytologic level of examination the neoplastic nuclei appear regularly of similar size and shape with hyperchromatic chromatin with irregular distribution and focal parachromatin clearing. There are multiple small nucleoli and mitoses at the left and right. There are tingible body macrophages at the upper left and right center. The cytoplasmic borders are narrow and can be seen to have angular interfacing between cells in the upper center typical of the "squaring-off" appearance.

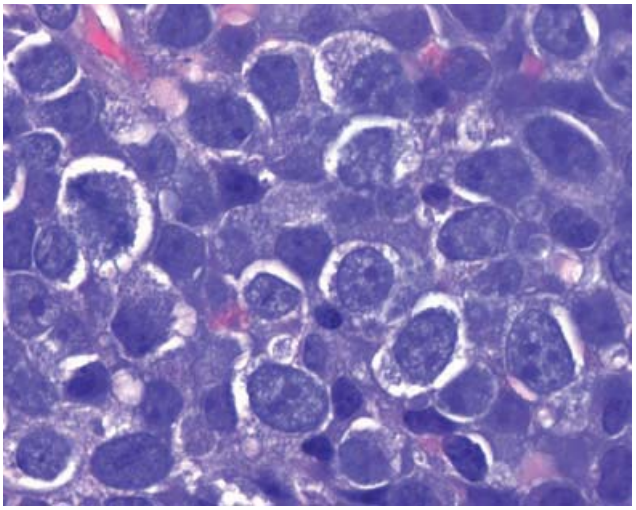

Figure 3.59. Dog: node, Burkitt's-type lymphoma. The nuclei are round and regular with the smaller cells of benign and pyknotic origin. The chromatin is finely reticular, and multiple small nucleoli are readily apparent. The red cells indicate that the nuclear size is about 1.5 red cells in diameter and cytoplasm is irregularly apparent. There is a cell in metaphase in the left center. Numerous macrophages are adjacent.

flat cytoplasmic boundaries referred to as a "squaring-off" appearance. In humans and animals, the chromatin is irregularly aggregated in large chromocenters with surrounding parachromatin clearing giving the nuclei a vesicular appearance of greater size. This chromatin configuration is important to recognize in order to distinguish Burkitt's lymphoma from lymphoblastic lymphoma, which is of the same nuclear size and also has a very high mitotic rate. Nucleoli are always present, small, numbering 2–5, and tend to be centrally located. The cytoplasm frequently contains small lipid vacuoles like the L3 form of ALL, with this feature relatively inconspicuous in histological preparations and quite prominent in cytologic

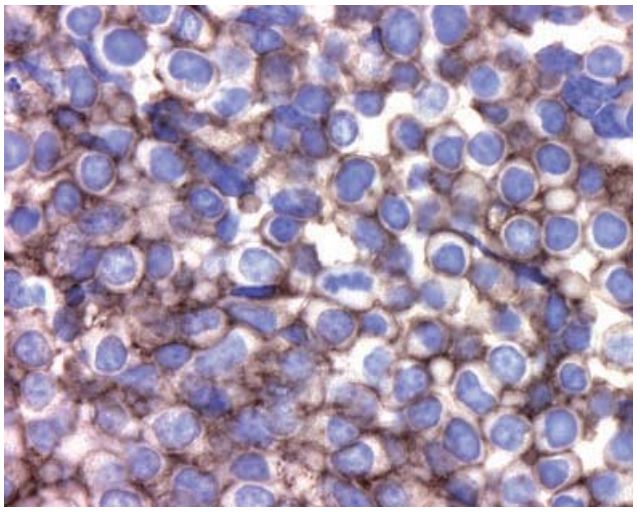

Figure 3.60. Dog: node, Burkitt's lymphoma. Phenotype of Figure 3.59. With CD20 staining, the neoplastic cells have uniformly strong membrane labeling consistent with a B-cell lineage.

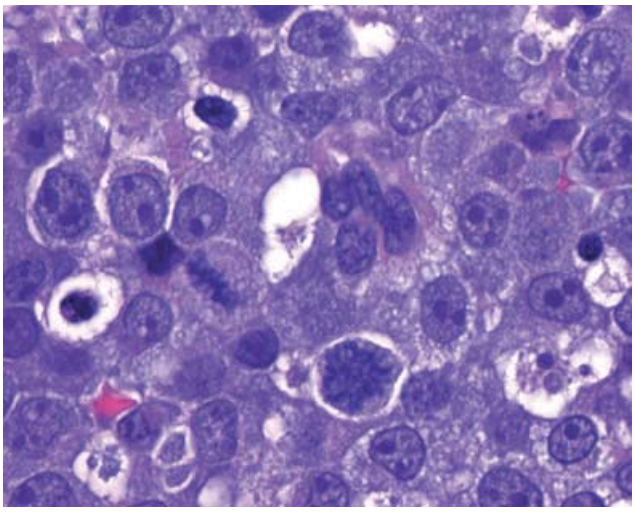

Figure 3.61. Dog: node, Burkitt's-like lymphoma. In comparison to the cells in Figure 3.59 of classic Burkitt's lymphoma, these have moderate anisokaryosis and vary more in shape. The folded nucleus in the upper center with eosinophilic cytoplasm is of structural supporting tissue. The chromatin pattern is like that of classic Burkitt's lymphoma with apparent nucleoli, and the variant form also shares a high mitotic rate and numerous tingible body macrophages indicative of a high apoptotic rate.

imprints. Multinucleation and, by definition, anisokarosis are not found.

Atypical Burkitt's Lymphoma and Burkitt's-like Lymphoma

In human pathology, but not in animals, a diagnosis of atypical Burkitt's lymphoma is given in cases that have a very high proliferative fraction approaching 100%, as determined by Ki-67 or MIB-1 staining and proven or presumed evidence of MYC translocation. These cases are presumed to be classical BKL type, but for technical reasons in processing or accepted tumor variation, have minor morphological changes. These criteria are not fulfilled in animal cases and the terminology is therefore not used. *Burkitt's-like* lymphoma is the diagnostic term given by the WHO classification for that quite large group of lymphoid neoplasms that are in the same size range as classical Burkitt's lymphoma but have more variation in nuclear size and, at the upper boundary, are indistinguishable from diffuse large cell lymphoma on morphological grounds. In the Working Formulation, this category of neoplasms were grouped as the *small noncleaved cell* lymphomas that on morphometric determinations were not distinguishable from diffuse large cell lymphoma in animals or humans. Currently in both human and animal diagnostic usage, the term *Burkitt's-like lymphoma* is used to identify those neoplasms of intermediate size, B-cell phenotype, and high mitotic rate that appear to lie between classical BKL and diffuse large B-cell lymphoma. Human Burkitt's-like lymphoma differs from classical BKL in having variable staining for CD10 and Bcl-6, which are strongly positive in both classical Burkitt's lymphoma and in the variant type of atypical BKL, and tend to be positive for Bcl-2, which is not expressed in the classical and atypical types. The Burkitt's-like lymphoma is more common in adults than in children, but it occurs worldwide.

Pathologic Features

Lymph Node

The Burkitt's-like lymphomas have diffuse architecture and have a high mitotic rate, and a starry sky pattern may be present. Rarely, some cells with centroblastic nuclei are present, which blurs the distinction from diffuse large B-cell lymphoma. The most consistent characteristic is a mild anisokaryosis of nuclei with cells that have smooth nuclear contours without nuclear indentations (i.e., small noncleaved). The chromatin and nucleolar patterns are like those of the classic BKL and with similar topographical distribution (Fig. 3.61). They are strongly positive with CD20 and CD79 alpha with these criteria, the current diagnostic features of Burkitt's-like lymphoma in animals (Fig. 3.62). In a review of lymphomas in cats where immunophenotyping was not carried out, 13% or 79 of 602 cases were felt to be of small noncleaved cell type, with cases with this morphology on oversight or H&E staining found in most locations, including the mediastinum, but less common in the intestine than other cell types. The Burkitt's-type lymphoma is rare in cattle, but the Burkitt's-like type was found in 17% of 1,072

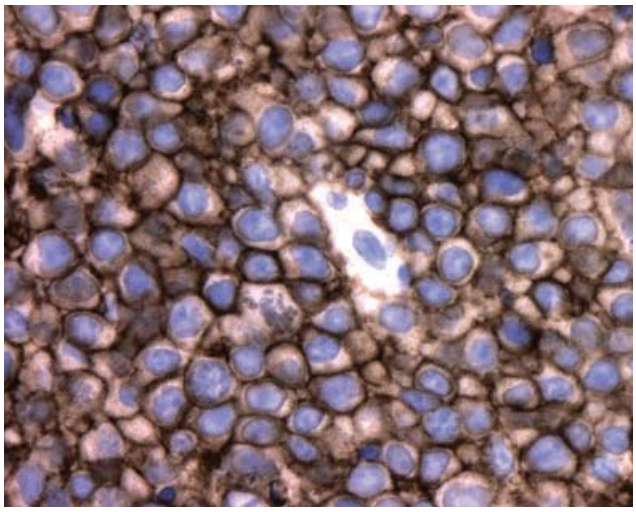

Figure 3.62. Dog: node, Burkitt's-like lymphoma. Phenotype of Figure 3.61. With CD20 staining the neoplastic cells are strongly and uniformly labeled in keeping with the B-cell phenotype of variant Burkitt's lymphoma.

cattle felt to have the enzootic type of lymphoma associated with BLV infection. In current work, few authors specifically mention Burkitt's or Burkitt's-like lymphoma in association with phenotypic identification, and the incidence is low—generally in the range of 1%. In one report on morphological subtypes and response to therapy in dogs, all of the Burkitt's-type lymphomas were of enteric type, in advanced stage on diagnosis, and responded for very short periods only.

Differential Diagnosis

Burkitt's lymphoma and Burkitt's-like lymphoma must be distinguished from acute lymphoblastic leukemia (ALL) and acute lymphoblastic lymphoma (LBL) on the basis of the aggregated chromatin with parachromatin clearing and prominent small nucleoli, which differs from the uniformly dispersed chromatin and obscured nucleoli of ALL and LBL. Burkitt's lymphoma is distinguished from Burkitt-like lymphoma on the basis of very uniform cell type in BKL and mild anisokaryosis in Burkitt's-like lymphoma. In addition, Burkitt's lymphoma and Burkitt's-like lymphoma are both strongly positive with CD20 and CD79 and must be distinguished from LBL of T-cell type and from peripheral T-cell lymphoma not otherwise specified (NOS) of similar nuclear type but with cytoplasm positive for CD3.

REFERENCES

Anonymous. (1982) National Cancer Institute sponsored study of classifications of non-Hodgkin's lymphomas: Summary and description of a Working Formulation for clinical usage. The Non-Hodgkin's Lymphoma Pathologic Classification Project. *Cancer*, 49:2112–2135.

Aquino, S.M., Hamor, R.E., Valli, V.E., Kitchell, B.E., Tunev, S.S., Bailey, K.L., and Ehrhart, E.J. (2000) Progression of an orbital T-cell rich B-cell lymphoma to a B-cell lymphoma in a dog. *Vet Pathol* 37:465–469.

Braziel, R.M., Arber, D.A., Slovak, M.L., et al. (2001) The Burkitt-like lymphomas: A Southwest Oncology Group study delineating phenotypic, genotypic, and clinical features. *Blood* 97:3713–3720.

Burkitt, D. (1958) A sarcoma involving the jaws in African children. *Br J Surg* 46:218–223.

Burkitt, D. (1962) Determining the climatic limitations of a children's cancer common in Africa. *BMJ* 2:1019–1026.

Chapman, C.J., Mockridge, C.I., Rowe, M., et al. (1995) Analysis of VH genes used by neoplastic B cells in endemic Burkitt's lymphoma shows somatic hypermutation and intraclonal heterogeneity. *Blood* 85:2176–2181.

Dalldorf, G., Linsell, C.A., Marnhart, F.E., et al. (1964) An epidemiological approach to the lymphomas of African American children and Burkitt's sarcoma of the jaws. *Perspect Biol Med* 7:435–449.

Epstein, M.A., Achong, B.G., Barr, Y.M. (1964) Viral particles in cultured lymphoblasts from Burkitt's lymphoma. *Lancet* 1:702–703.

Fournel-Fleury, C., Magnol, J.P., Bricaire, P., Marchal, T., Chabanne, L., Delverdier, A., Bryon, P.A., and Felman, P. (1997) Cytohistological and immunological classification of canine malignant lymphomas: Comparison with human non-Hodgkin's lymphomas. *J Comp Path* 117:35–59.

Gabor, L.J., Canfield, P.J., and Malik, R. (1999) Immunophenotypic and histological characterization of 109 cases of feline lymphosarcoma. *Aust Vet J* 77:436–441.

Gaulard, P., Delsol, G., Callat, M.P., et al. (2002) Cytogenetic and clinicopathologic features of B-cell lymphomas associated with the Burkitt translocation t(8;14)(q24;q32) or its variants. *Ann Oncol* 13[Suppl 2]:33.

Grogan, T.M., Warnke, R.A., and Kaplan, H.S. (1982) A comparative study of Burkitt's and non-Burkitt's "undifferentiated" malignant lymphoma: Immunologic, cytochemical, ultrastructural, cytologic, histopathologic, clinical and cell culture features. *Cancer* 49:1817–1828.

Harris, N.L., Jaffe, E.S., Diebold, J., et al. (1999) World Health Organization classification of neoplastic diseases of the hematopoietic and lymphoid tissues: Report of the Clinical Advisory Committee meeting-Airlie House, Virginia, November 1997. *J Clin Oncol* 17:3835–3849.

Harris, N.L., Jaffe, E.S., Stein, H., et al. (1994) A revised European-American classification of lymphoid neoplasms: A proposal from the International Lymphoma Study Group. *Blood* 84:1361–1392.

Hutchison, R.E., Finch, C., Kepner, J., et al. (2000) Burkitt lymphoma is immunophenotypically different from Burkitt-like lymphoma in young persons. *Ann Oncol* 11[Suppl 1]:35–38.

Jaffe, E.S., Harris, N.L., Stein, H., and Vardiman, J.W. *World Health Organization Classification of Tumours, Pathology & Genetics: Tumours of Haematopoietic and Lymphoid Tissues*. IARC Press, Lyon, France.

Klein, U., Klein, G., Ehlin-Henriksson, B., et al. (1995) Burkitt's lymphoma is a malignancy of mature B cells expressing somatically mutated V region genes. *Mol Med* 1:495–505.

Lefborn, B.K., and Parker, G.A. (1995) Ataxia associated with lymphosarcoma in a dog. *JAVMA* 207(7):922–923.

Macpherson, N., Lesack, D., Klasa, R., et al. (1999) Small noncleaved, non-Burkitt's (Burkitt-like) lymphoma: Cytogenetics predict outcome and reflect clinical presentation. *J Clin Oncol* 17:1558–1567.

Magrath, I.T., Venkatesh, H., and Gascoyne, R.D. (2004) Burkitt's lymphoma. In Mauch, P.M., Armitage, J.O., Coiffier, B., Dalla-Favera, R., and Harris, N.L. (eds.), *Non-Hodgkin's Lymphomas*. Lippincott Williams & Wilkins 2004, Philadelphia, pp. 477–501.

Mann, R.B., Jaffe, E.S., Braylan, R.C., et al. (1976) Nonendemic Burkitt's lymphoma. A B-cell tumor related to germinal centers. *N Engl J Med* 295:685–691.

O'Conor, G.T., and Davies, J.N.P. (1960) Malignant tumors in African children with special reference to malignant lymphomas. *J Pediat* 56:526–535.

Ponce, F., Magnol, J.P., Ledieu, D., Marchal, T., Turinelli, V., Chalvet-Monfray, K., and Fournel-Fleury, C. (2004) Prognostic significance of morphological subtypes in canine malignant lymphomas during chemotherapy. *Vet J* 2004, 167:158–166.

Valli, V.E., Jacobs, R.M., Norris, A., Couto, C.G., Morrison, W.B., McCaw, D., Cotter, S., Ogilvie, G., and Moore, A. (2000) The histologic classification of 602 cases of feline lymphoproliferative disease using the National Cancer Institute Working Formulation. *J Vet Diagn Invest* 12:295–306.

Vernau, W., Valli, V.E.O., Dukes, T.W., Jacobs, R.M., Shoukri, M., and Heeney, J.L. (1992) Classification of 1,198 cases of bovine lymphoma using the National Cancer Institute Working Formulation for human non-Hodgkin's lymphomas. *Vet Path* 29:183–195.

Warnke, R.A., Weiss, L.M., Chan, J.K.C., et al. (1994) *Tumors of the Lymph Nodes and Spleen,* 3rd ed. Armed Forces Institute Of Pathology, Washington, D.C.

Yano, T., van Krieken, J.H., Magrath, I.T., et al. (1992) Histogenetic correlations between subcategories of small noncleaved cell lymphomas. *Blood* 79:1282–1290.

MATURE (PERIPHERAL) B-CELL NEOPLASMS

B-Cell Chronic Lymphocytic Leukemia/ Small Lymphocytic Lymphoma

Definition

Chronic lymphocytic leukemia (B-cell) is a clonal lymphoproliferative disease primarily involving the bone marrow and characterized by the accumulation of relatively uniform, immunologically competent, small lymphocytes with low rates of proliferation and apoptosis.

Small lymphocytic lymphoma (B-cell SLL) is a low-grade clonal neoplasm primarily involving the lymph nodes, spleen, and parenchymal organs and characterized morphologically by accumulation of small mature lymphocytes.

Epidemiology and Incidence

Clonal neoplasms of small mature lymphocytes are slowly progressive diseases that may be primarily in marrow or peripheral tissues or both. B-cell mature lymphocytic neoplasms occur rarely in all domestic animals, most frequently in cats and less often in dogs, and seldom in cattle or horses. It is a disease of mature animals and occurs most often in cats 5–10 years of age and in dogs of 10–15 years. The disease occasionally occurs in younger animals, but seldom in those under 3 years of age. There does not appear to be any gender predominance in animals or humans. The small lymphocytic neoplasms are found in all breeds of both dogs and cats and in cattle, most often in dairy breeds, probably because they are more likely to be examined frequently. In horses, the small lymphocytic neoplasms are found most often in hot-blood breeds, but most likely again a matter of prevalence of the breeds and likelihood of coming to clinical or laboratory examination. In humans, these diseases are rare under 50 years of age and usually present with advanced disease. Animals, like humans, are often diagnosed on routine examination when no specific abnormality is anticipated, particularly with B-CLL where palpable nodes are normal or actually atrophied.

Clinical Presentation and Features

In all domestic animals, the most consistent history on presentation with CLL is weight loss. In dairy cattle a drop in production is noted in lactating animals along with reduced feed consumption. In dogs and cats, lethargy and anorexia are noted along with weight loss. In contrast to acute leukemia (ALL), those with CLL are occasionally described as thin, but some, as in humans, are diagnosed on routine examination prior to immunization on elevated blood lymphocyte counts. An almost consistent finding is hepatosplenomegaly. The spleen is always enlarged and the liver usually is, but this seems less consistent in animals diagnosed prior to the era of ultrasound examination. Like the presentation in humans, dogs and cats are most often presented with advanced disease. However, in contrast to humans, where the lymph nodes are usually enlarged, in animals they may be normal, irregularly enlarged, or even atrophic. Animals with CLL occasionally present with epistaxis in animals that are in an accelerated phase of an advanced disease. Less commonly, vomiting and diarrhea may be the presenting complaints.

Animals with small lymphocytic lymphoma (SLL) may be recognized on routine examination of blood because they have become leukemic. In contrast to older systems of classification, it is now recognized that CLL and SLL

are different presentations of the same cell type and there is not a clear-cut distinction between the solid forms primarily involving lymph nodes and the leukemic forms that likely originate in bone marrow. It is now accepted that neoplastic cells are in circulation in all lymphomas and that the tissues that become involved with neoplasm relate to the level and type of cellular adhesion molecules that determines sites at which the cells in blood can marginate and invade tissue. Since SLL is by definition a disease primarily of accumulation and not of proliferation, these cases tend to be indolent and slowly progressive. For this reason, these diseases tend not to result in organ failure as an early event, providing time for the neoplastic cells to spread widely in the body by the time of clinical presentation. SLL may involve any or all nodes but tends to do so in an irregular manner. For this reason animals may present with a single or regional nodes involved; most have involvement of the spleen and liver and, in decreasing order, the bone marrow and intestine and irregularly other tissues, including the heart, nervous system, eye, tonsil, and adrenal glands.

Pathologic Features

Blood

With CLL the blood is always diagnostic with marrow usually heavily involved at time of diagnosis (Figs. 3.63–3.65). There is inadequate distinction between the presenting signs of animals with CLL of B- and T-cell type. In contrast to CLL in humans, 75% of CLL in dogs is of T-cell lineage. Where phenotype has been determined, B-cell CLL is not morphologically distinctive (Figs. 3.66–3.68). In fact, there are virtually no reliable morphologic differences between the cell types found in B-cell CLL and the various subtypes of non-LGL, T-cell CLL including the NK-cell neoplasms when identified by multiparameter flow cytometry. The general blood presentation is of a very high cell count generally in excess of

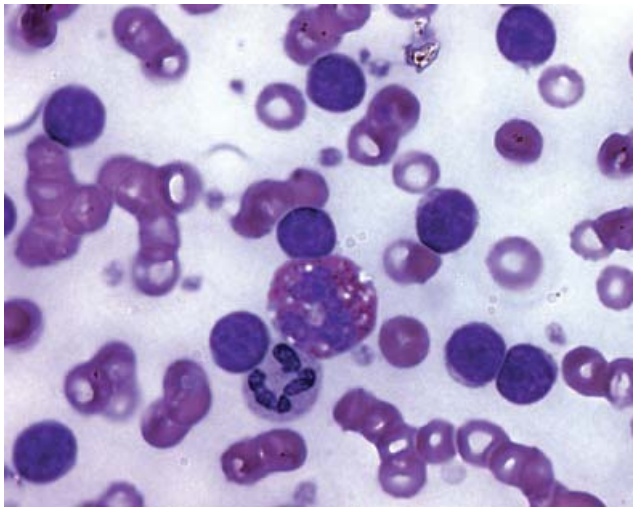

Figure 3.63. Dog: blood, CLL. A mature large-breed dog in good condition was presented because of recent onset of reduced appetite. A blood sample was taken, with the leukocyte count near 200,000 per ul composed almost entirely of small lymphocytes. These cells including the cytoplasm are only slightly larger than red cells with compact chromatin composed of large chromocenters, with little internal nuclear detail and no nucleoli. There is only a very narrow rim of cytoplasm visible at one pole at each cell. *Slide from R. M. Jacobs, DVM.*

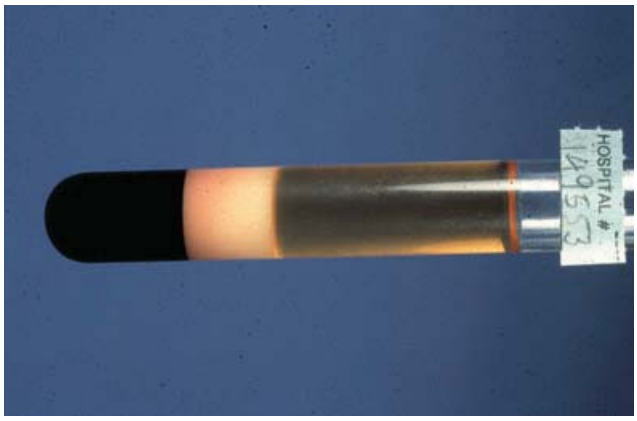

Figure 3.64. Dog: blood, CLL. The animal had an extremely high white count that has produced a remarkably thick buffy coat. Note the very pale plasma due to the low production and destruction of red cells and a relatively short red cell column that appears to indicate a packed cell volume of about 25%.

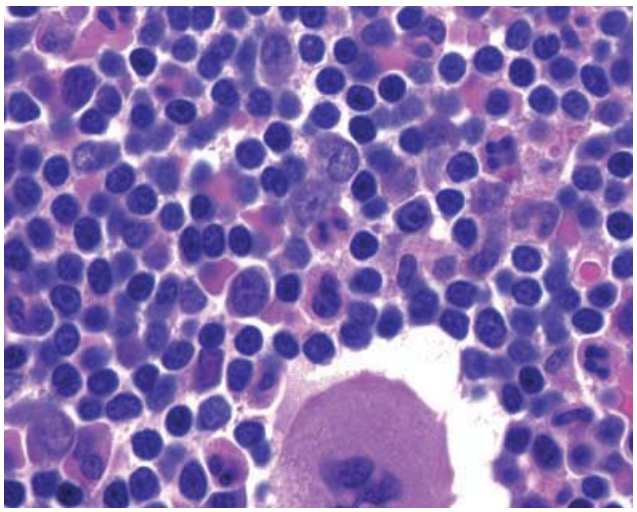

Figure 3.65. Dog: marrow core, same case as Figure 3.64. The neoplastic cells have small, round, densely stained nuclei, with most cells lacking nucleoli with a prominent central dark chromocenter; the larger cells (center) have a single small nucleolus. There is almost complete phthisis of normal marrow cells with a few residual granulocytes and megakaryocyte at bottom. *Slide from R. M. Jacobs, DVM.*

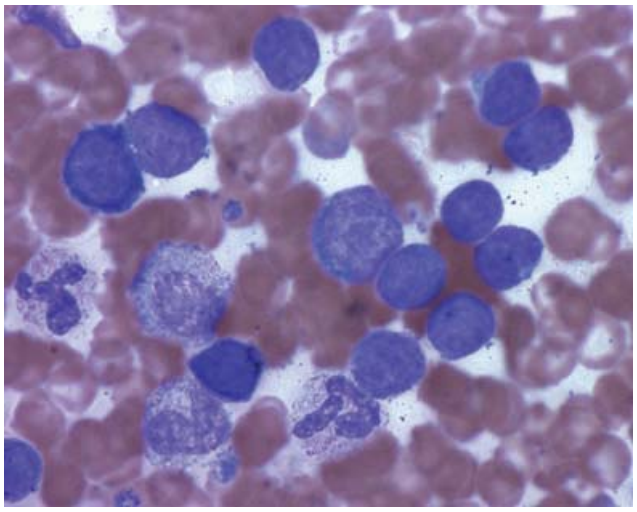

Figure 3.66. Dog: marrow aspirate, chronic lymphocytic leukemia. A 5-year-old dog presented with a leukemic blood picture, with the marrow aspirate containing a high level of small lymphocytes with nuclei slightly larger than homologous red cells. The larger cell in the center represents the dividing part of the neoplastic population with the cell at left a myelocyte and a band and segmented cell below, and 2 early rubricytes with markedly basophilic cytoplasm above and below the myelocyte.

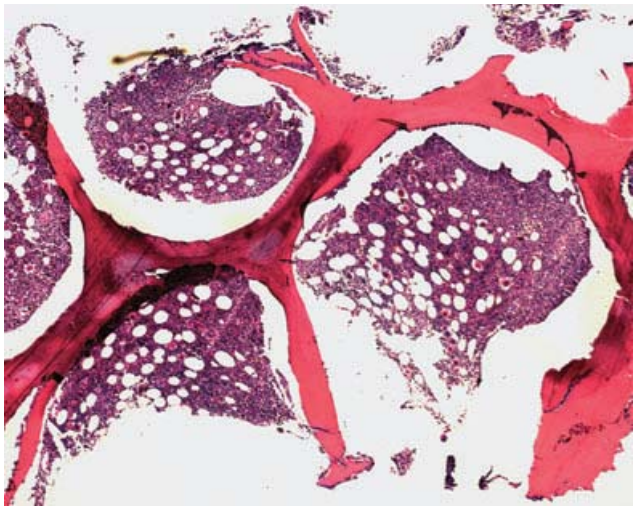

Figure 3.67. Dog: marrow core, CLL, same case as Figure 3.64. The cancellous areas of marrow are irregularly hypercellular, with the areas devoid of fat cells and focal areas of subendosteal tumor formation.

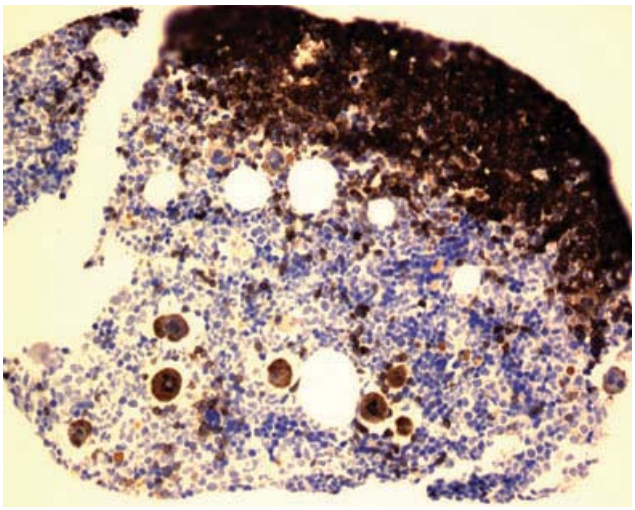

Figure 3.68. Dog: marrow core, CLL CD79 stain, same case as Figure 3.66. The heavily marked area in the upper left identifies a region almost completely occupied by neoplastic lymphocytes of B lineage. The adjacent areas with some residual fat cells represent residual areas of largely benign marrow. The megakaryocytes when mature, are marked with CD79.

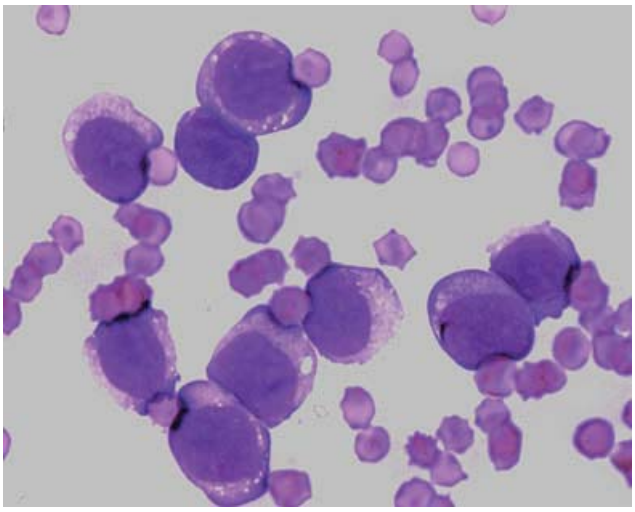

Figure 3.69. Cat: blood, CLL. A 9-year-old male Siamese weighing 10 pounds was presented for examination because of recent onset of lethargy. On blood examination, there were 660,000 leukocytes per ul with hemoglobin of 6.7 g per dl and platelets 10,000 per ul. The smallest cell in the upper left is more typical of this disease, with the larger cells, many of which have nucleoli, likely representing the terminal transformation of the tumor into a more aggressive neoplasm.

100,000/ul and as high as 500,000–600,000/ul (Figs. 3.69, 3.70). In cats, the cell type is usually of the small round cell type with nuclei 1–1.5 red cells in diameter and a very narrow rim of moderately stained cytoplasm (Fig. 3.71). In the dog, most cases are of that type, but some have slightly larger nuclei that vary in shape from round to oval or lightly indented and with relatively abundant, lightly stained cytoplasm; many of these are of LGL type (Fig. 3.72). Both of these cell types have barely discernible areas of perinuclear clearing with more basophilia near the outer membrane. Nucleoli are absent or small and indistinct but may be multiple. The chromatin is quite

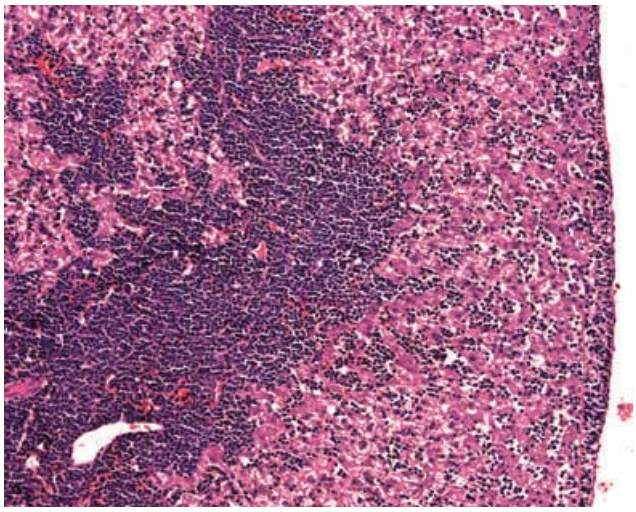

Figure 3.70. Cat: liver, CLL, same case as Figure 3.69. There is marked and irregular colonization of hepatic tissue surrounding vessels but in addition, quite marked dilation of sinusoids that contain many cells, most of which are likely in circulation.

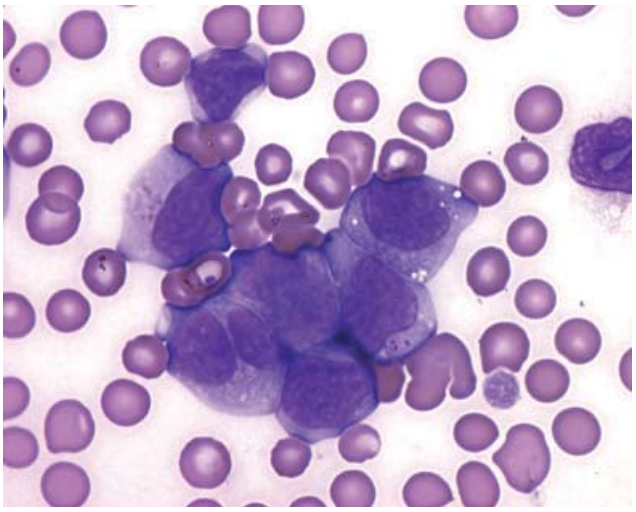

Figure 3.72. Dog: blood, CLL LGL type. lymphocytic leukemia in the dog of the chronic LGL type is characterized by high leukocyte counts without phthisis of normal cells, with the cases tending to run a chronic course. Note the few azurophilic granules in the cells at the left and right areas.

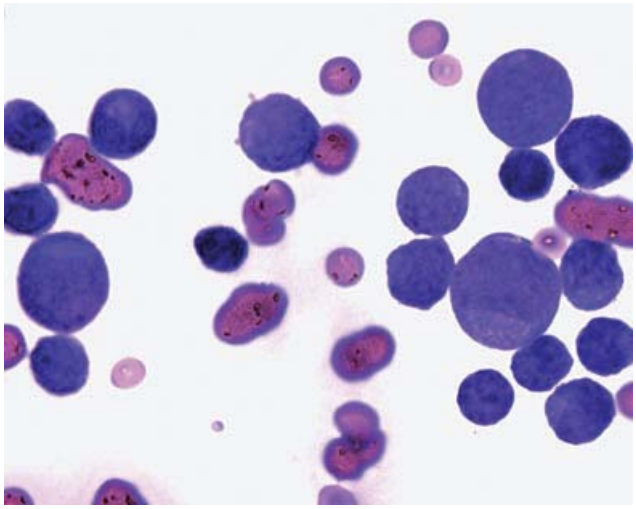

Figure 3.71. Cat: blood, CLL. The case is likely in transition to an acceleration phase. The small cells represent the predominant population throughout most of the clinical phase, with the larger cells likely of the neoplastic clone but representing an increasing level of the dividing cell population.

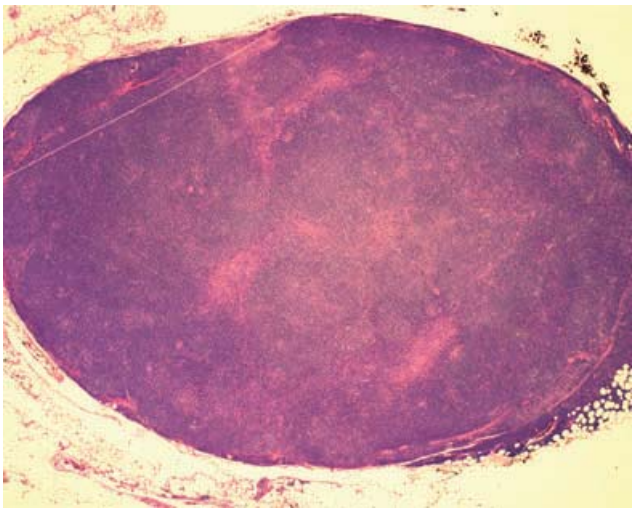

Figure 3.73. Dog: lymph node, small cell lymphocytic lymphoma (SLL). The capsule is thin and taut and irregularly encompassed with involvement of perinodal fat. There is complete effacement of internal architecture with loss of cortico-medullary distinction.

dense with some large chromocenters compatible with a population of cells with low proliferative rate. In any population, there will be a rare larger cell with more prominent nucleoli and may have the nuclear morphology of prolymphocytes with multiple large chromocenters separated by much less densely stained areas. These cells represent the dividing population.

SLL is poorly characterized from the standpoint of blood changes both because the disease is relatively rare and because the small compact nature of the neoplastic cells makes them likely to be considered reactive if the peripheral lymphocyte count is not much above normal levels. Logic would suggest that biologically neoplastic cells are in circulation in animals with SLL; however, unless their numbers draw attention, these cases would be undiagnosed or ultimately recognized as having small cell lymphoma (Figs. 3.73, 3.74). At this point the blood picture of animals with SLL is a category to be defined

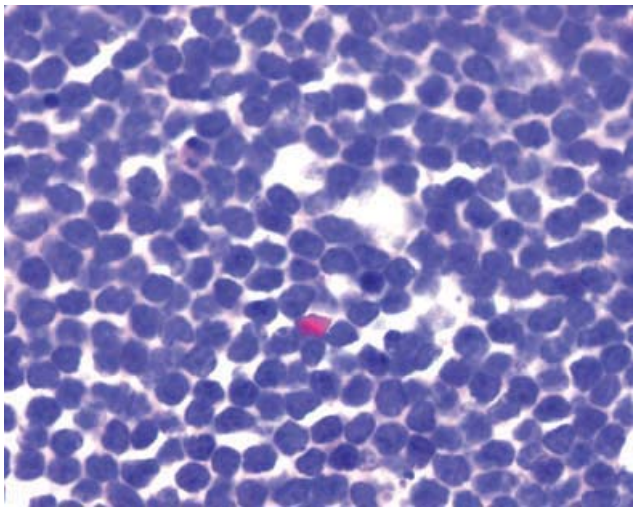

Figure 3.74. Dog: node, SLL. Detail of Figure 3.73. The tissue is occupied by sheets of lymphocytes with very small nuclei only slightly larger than red cells with a very narrow inapparent rim of cytoplasm. Mitoses are rare, with an occasional cell undergoing apoptosis (upper left).

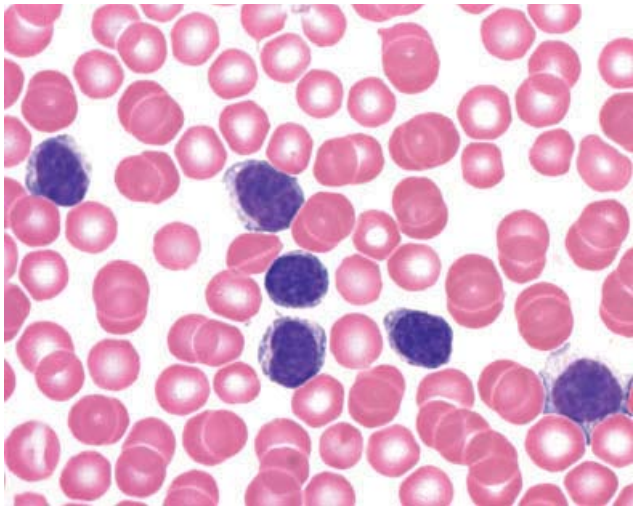

Figure 3.75. Dog: blood, small lymphocytic lymphoma. Blood is typical of CLL, but the bone marrow appears almost completely normal. There is lymphadenopathy with proliferation of cells of this type that have likely entered the blood from the spleen and nodes with leukemic phase of SLL.

(Figs. 3.75–3.78). In contrast, the small cell lymphomas of intermediate differentiation (ILL, Figs. 3.79, 3.80) are included with SLL and are similar morphologically to the small cell variant of mantle cell lymphoma (MCL, Figs. 3.81, 3.82). The "blastoid" variant of human MCL is known to become leukemic, and a similar lymphoma appears to invade the blood in cows, cats and dogs (Figs. 3.83–3.85) although these diseases have not yet been

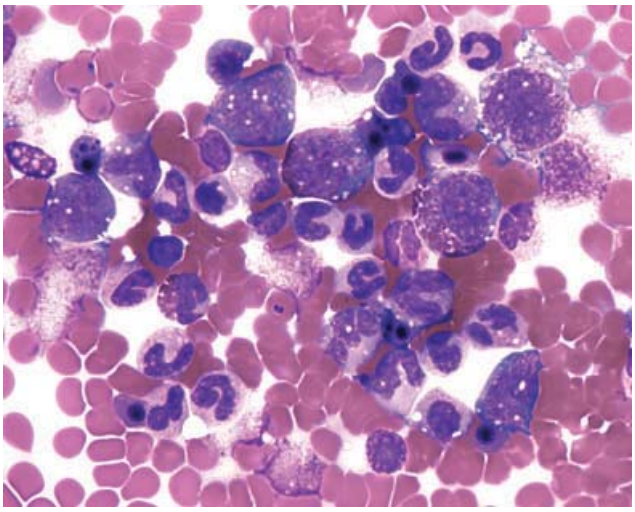

Figure 3.76. Dog: marrow aspirate, SLL, same case as Figure 3.75. The bone marrow has normal cellularity, mild myeloid predominance, and all normal cell lines are represented without evidence of excess of small lymphocytes. The large cell with orange granules at the right center is an eosinophil myelocyte surrounded by maturing myeloid cells of neutrophil lineage. There are maturing rubricytes on the upper and lower borders with the binucleated cell at the left likely a megakaryoblast.

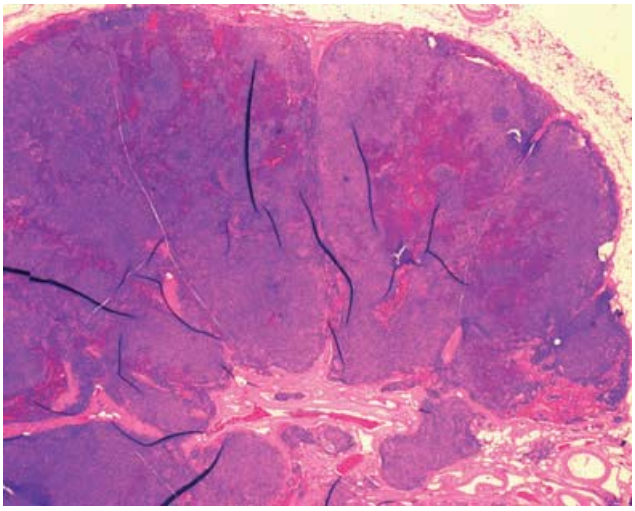

Figure 3.77. Dog: node, small cell lymphocytic lymphoma. The capsule is thin and taut with the peripheral sinus compressed but intact. The node has diffuse architecture with patchy irregular cortical congestion and a complete absence of follicular development. There is filling of the medullary cords and compression of the medullary sinuses. The prominent fibrovascular structures in the medullary area are indicative of a prolonged period of benign hyperplasia.

given the distinction of a separate category in animal neoplasms. Animals that fit these categories are not described as such in animal pathology but are included in descriptions of papers on leukemia as a group or as lymphomas

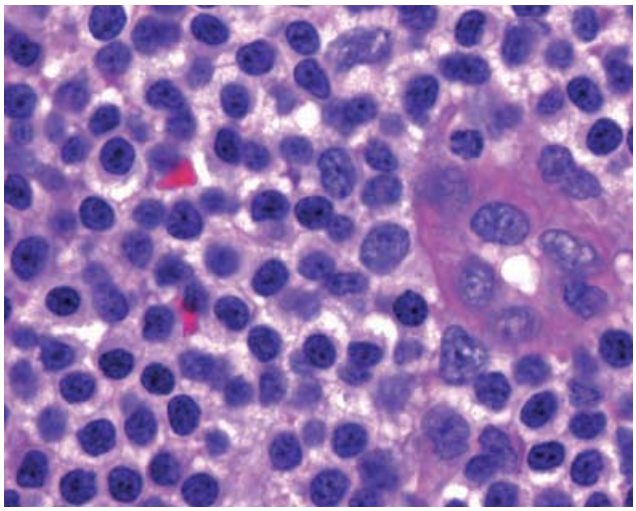

Figure 3.78. Dog: node, SLL. Detail of Figure 3.76. A postcapillary venule devoid of transluminal cellular traffic is at the right. Lymphocytes resemble those of T-zone lymphoma that have round or oval nuclei, densely stained and only slightly larger than red cells. The cytoplasmic volume is greater than in adjacent areas to enhance nuclear detail.

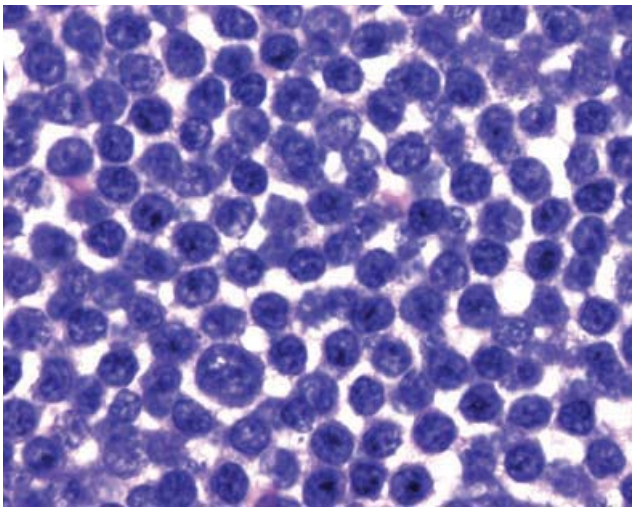

Figure 3.80. Dog: node, DSLI. Detail of Figure 3.79. The nuclei are 1.5–2.0 red cells in diameter and round, with the major difference from SLL in having greater internal nuclear detail. The chromatin is distributed in large dense chromocenters with irregular parachromatin clearing. Cytoplasm is minimal and tends to surround the nuclei evenly.

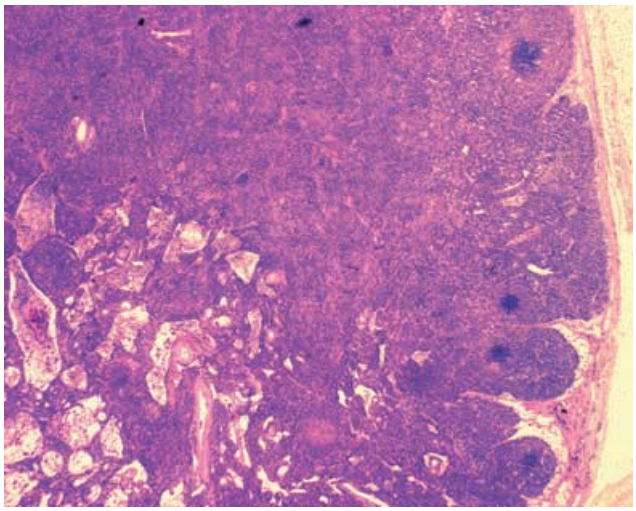

Figure 3.79. Dog: node, diffuse small cell lymphoma intermediate type (DSLI). At the architectural level the capsule and peripheral sinus are intact and the small dark foci of cells represent the collapsed mantle cells of fading germinal centers. The architecture of the cortex is diffuse and there is filling of the medullary cords with the sinuses poorly cellular.

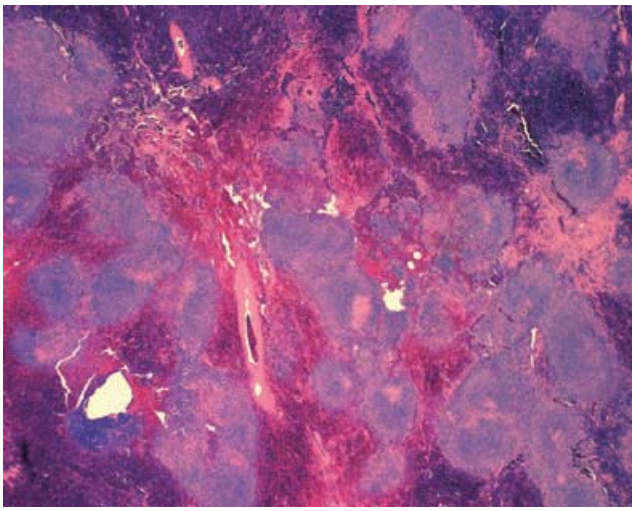

Figure 3.81. Dog: spleen, mantle cell lymphoma. The architecture of the affected area consists of multinodular areas of lymphoid proliferation about the size of large germinal centers that arise on end arterioles. The frequent pale areas (center) represent the bare dendritic cells of former germinal centers.

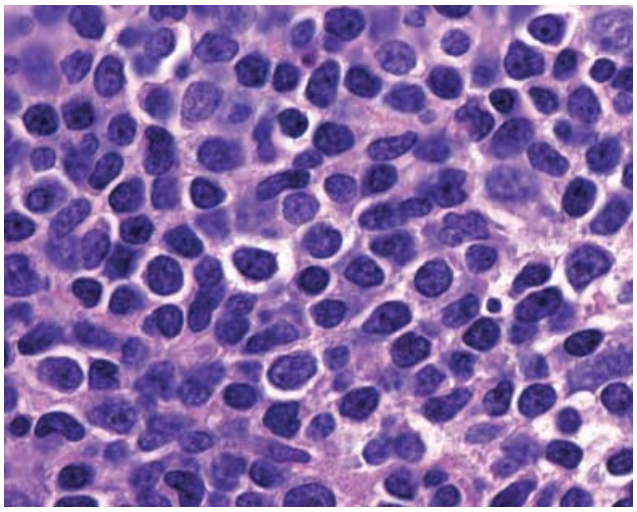

Figure 3.82. Dog: spleen, mantle cell lymphoma. Detail of Figure 3.81. The nuclei are the small cell variant of mantle cell lymphoma and are of intermediate size very similar to those of lymphocytic lymphoma of intermediate type (Fig. 3.80). The nuclei are round to oval and slightly larger than red cells, with densely stained nuclei that have occasional small nucleoli with a moderate volume of lightly stained cytoplasm. Mitoses are very rare in this cell population.

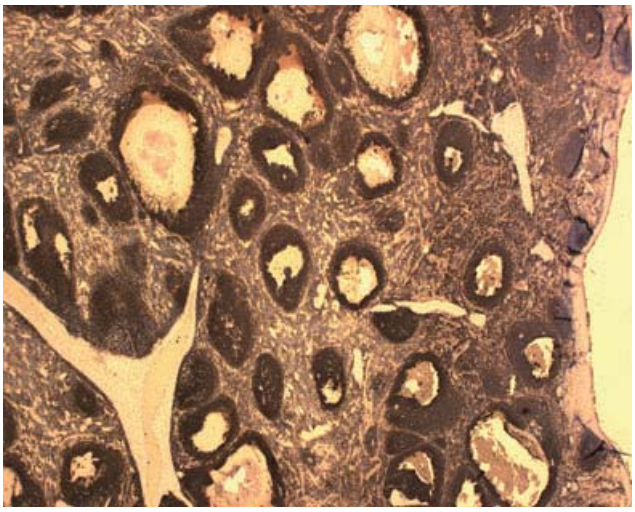

Figure 3.84. Dog: spleen, mantle cell lymphoma with CD20, marking B-lymphocytes in the same areas as Figure 3.83. There is very dense marking of the areas of lymphoid proliferation as well as the intervening cells in sinus areas characteristic of very strong B-cell marking with this neoplasm.

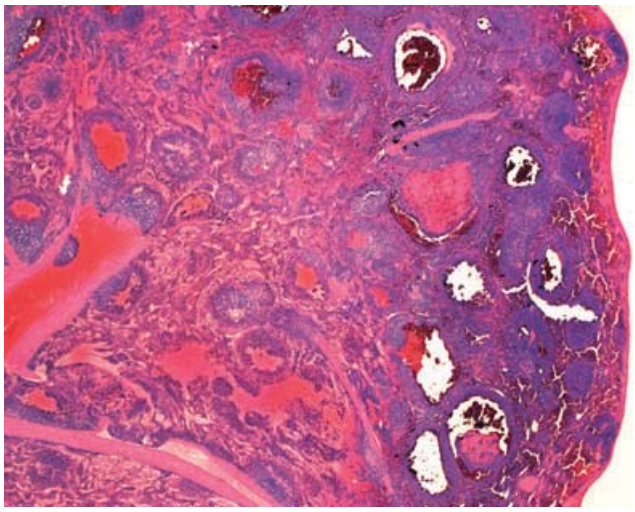

Figure 3.83. Dog: spleen, mantle cell lymphoma, blastoid type. This type of lymphoma has an unusual architecture, with multiple foci of lymphoid proliferation that have blood-filled centers. The pathogenesis of this lesion can be seen in the large homogenous pink area in the upper right of center where the central portion of focal lymphoid proliferation has undergone ischemic coagulative necrosis. A similar change is ongoing at the lower right in a later stage where remnants of the dying cells remain with the cavity becoming filled with blood.

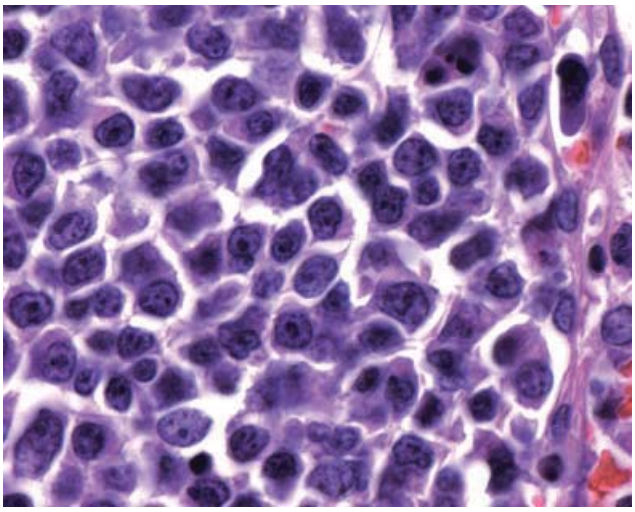

Figure 3.85. Dog: spleen, mantle cell lymphoma. Detail of Figure 3.83. The edge of a focal area of lymphoid proliferation is at the right with a very thin layer of endothelial encapsulation. The lymphocytes are of intermediate type with round to oval nuclei 1.5–2 red cells in diameter. They have a diffuse hyperchromatic chromatin pattern with 1–3 small nucleoli and a moderate amount of quite highly basophilic cytoplasm. Unlike the small cell variant, mitoses are present in this cell population as well as numerous tingible body macrophages.

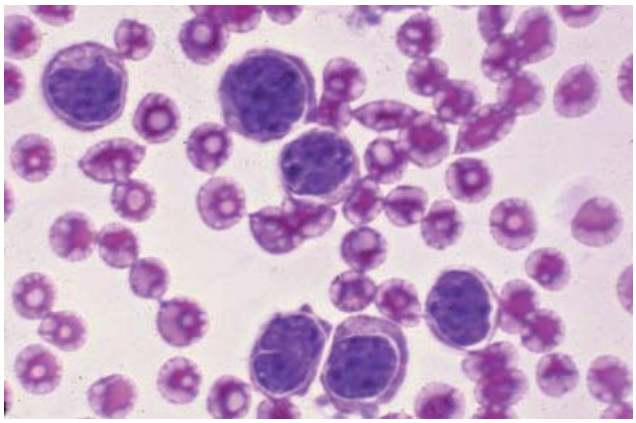

Figure 3.86. Cow: blood, leukemic phase of small lymphocytic lymphoma. The cells and blood are surprisingly large with some irregularity of nuclear shape and some deeply cleft (lower center). Wet fixed preparation with H&E stain.

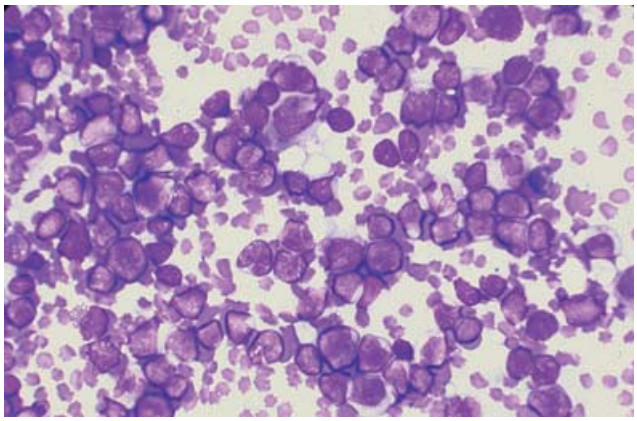

Figure 3.87. Bovine: node imprint, small cell lymphocytic lymphoma. On imprint of a fresh surface of the affected lymph node, there is quite marked variation in size of nuclei, with the smallest 1.5–2 red cells in diameter and the largest nearly twice that size. The chromatin pattern is fine dispersed, typical of a rapidly dividing population.

with the changes in peripheral blood not adequately described. There may be more large cells in the peripheral blood than in the marrow or nodes, and these same changes appear to occur in all animals as well as in humans (Figs. 3.86–3.88).

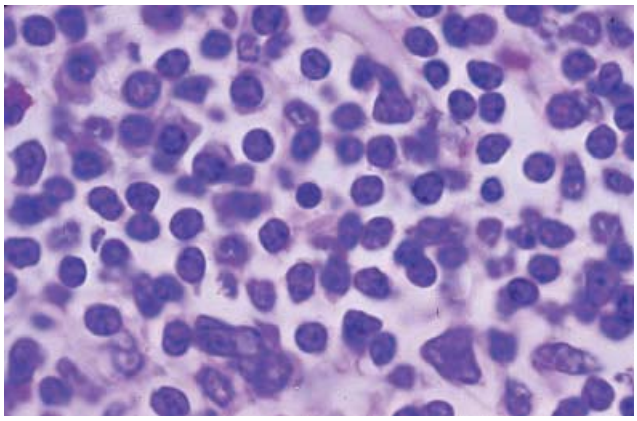

Figure 3.88. Cow: node, small lymphocytic lymphoma, same case as Figure 3.86. Note the much more uniform size of nuclei in histologic preparations as compared to cytologic imprints and peripheral blood. There is a red cell out of focus in the upper right that is indicative of the size of nuclei of the predominant cell population. This image is taken at the same magnification as that of the peripheral blood (Fig. 3.86). Since the animal apparently did not have bone marrow involvement, it would suggest that those cells that are released into the circulation are much more variable in size as compared to cells seen in histological preparations.

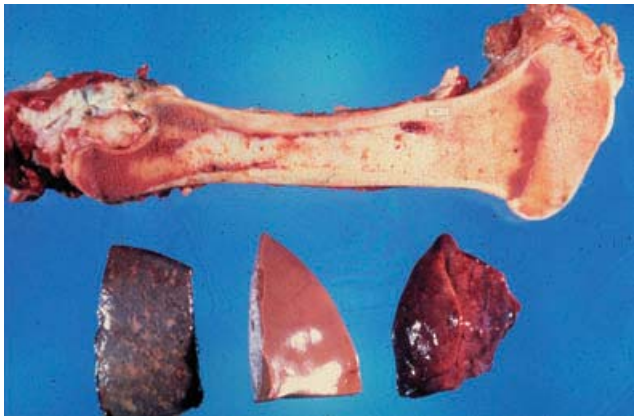

Figure 3.89. Cow: femur, SLL. Hemisection of a femur from a cow with multicentric lymphoma. Cross sections of spleen, liver, and lung below. The marrow is largely unaffected, with the reddened areas within cancellous bone likely sites of increased myelopoiesis as well as the subendosteal areas of the femoral shaft. The small irregular areas within the central marrow cavity are more likely foci of lymphoid colonization with little impact on the general marrow economy.

Bone Marrow

Lymphoid neoplasms do not home to subendosteal areas of bone marrow like myeloid neoplasms but tend to involve the marrow in a more random fashion. This type of invasion is not limited to the red or hematopoietic areas of the marrow, but they may involve fatty areas where the presence of tumor foci has little impact on the production of normal benign cells (Figs. 3.89–3.92). Due to this important feature, the lymphoid leukemias tend to cause much later marrow failure than the myeloid leukemias that compete directly with the benign cells for the most fertile space in subendosteal areas. Because animals, like humans, with CLL tend to come to clinical attention late in the progression of the disease, the marrow may be solidly involved with tumor at the time of diagnosis (Figs.

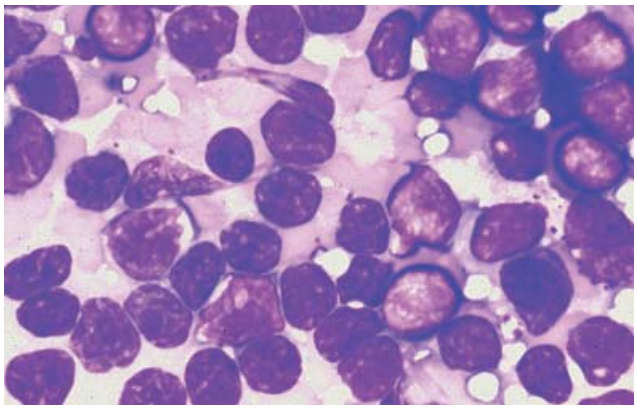

Figure 3.90. Bovine: lymph node imprint, SLL, same case as Figure 3.89. Most of the nuclei are round and approximately 1.5 red cells in diameter. The chromatin pattern is irregularly condensed into large chromocenters with 1–2 small nucleoli per cell. There is very little cytoplasm and some nuclei are bare.

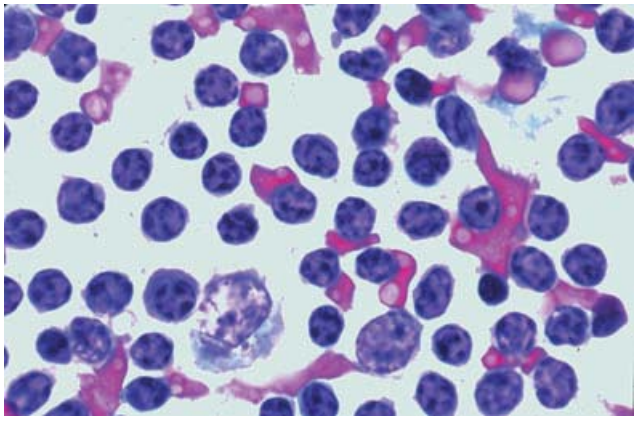

Figure 3.91. Cow: node imprint, same case as Figure 3.89. Fresh specimen wet-fixed and stained with Papanicolaou method. This method preserves nuclear and cytoplasmic integrity, with wet fixation providing the same chromatin pattern as are seen in histology.

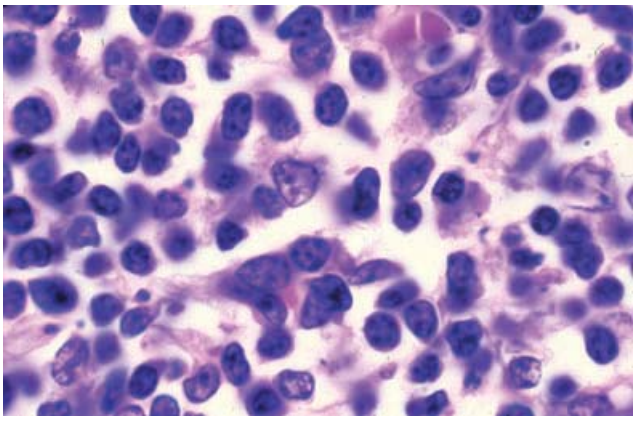

Figure 3.92. Cow: node, SLL, same case as Figure 3.89 and same magnification as Figure 3.91. Histological preparations of the cells are only slightly smaller than they appear in wet-fixed preparations. The proportions of small to large cells are very comparable with the two methods. The red cell (upper right) gives indication of the relatively small nuclear size.

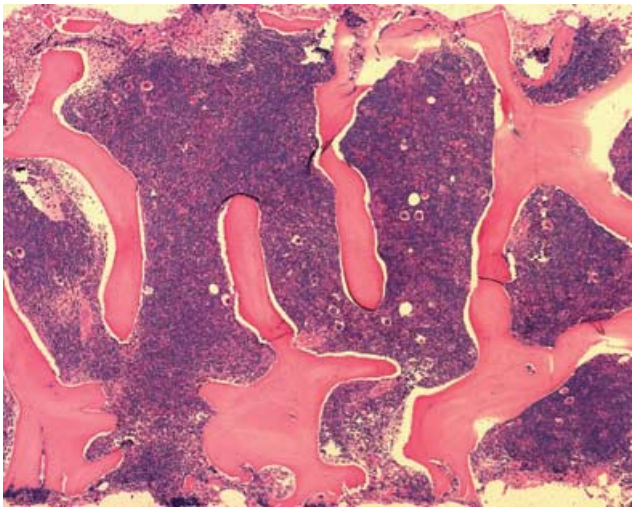

Figure 3.93. Dog: marrow core, CLL, same case as Figure 3.63. Histologically, the bone marrow in cancellous areas of bone is very hypercellular, with almost complete loss of fat cells due to a very heavy infiltration of small lymphocytes. A few large cells apparent by surrounding clear area are residual benign megakaryocytes. *Slide from R. M. Jacobs, DVM.*

3.93–3.96). In CLL, the marrow is always diagnostic and always heavily involved and may present a solid sheet of small cells on histologic section with only an occasional residual megakaryocyte to identify the tissue of origin (Fig. 3.97). The pattern of marrow involvement in less severely colonized areas may be focal and paratrabecular or interstitial and surrounded by fat or hematopoietic areas. The marrow may contain a number of fading germinal centers that likely indicate a long period of benign lymphoid hyperplasia prior to neoplastic transformation (Fig. 3.98). These benign follicles must be distinguished from pale areas of about the same size that are histologically poorly defined and are composed of larger cells that have nucleoli and more numerous mitoses. These latter areas are referred to as *proliferation centers* in human pathology and are considered part of the diagnostic criteria for CLL (Fig. 3.99). They do not appear to be as prominent in animals as in humans or have been missed in description.

In SLL the marrow is usually largely or totally intact, and if focal tumor is present there is no indication of peripheral deficit in neutrophils or platelets, but anemia of some degree is always present and poorly responsive.

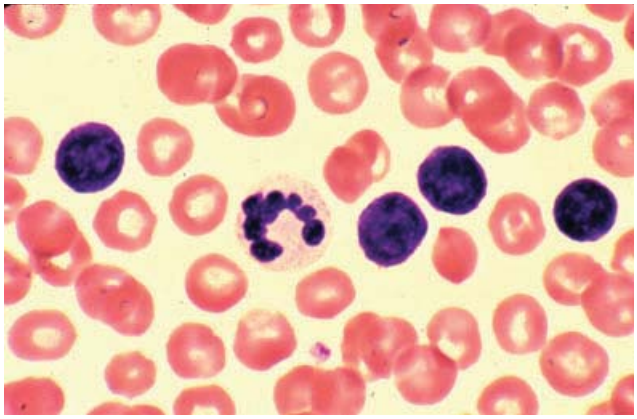

Figure 3.94. Dog: blood, CLL, different case from Figure 3.93. The neoplastic cells have round nuclei only slightly larger than red cells, with compact densely stained chromatin and barely visible cytoplasmic margins. Note that the few platelets have low basophilia and the neutrophil has reduced cytoplasmic granulation with a tendency to nuclear hypersegmentation likely due to splenic overload.

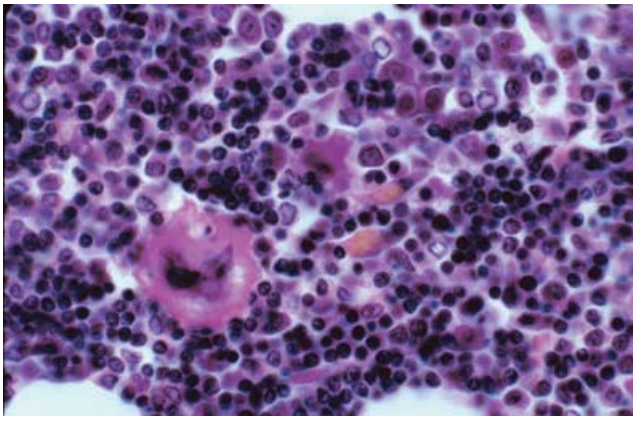

Figure 3.96. Dog: marrow, CLL, same case as Figure 3.94. There is almost complete phthisis of normal marrow cells, with a megakaryocyte remaining and a few larger nuclei in the upper right that are likely of myeloid lineage. The hemosiderin bearing macrophages (center) are indicative of low iron utilization of chronic disease.

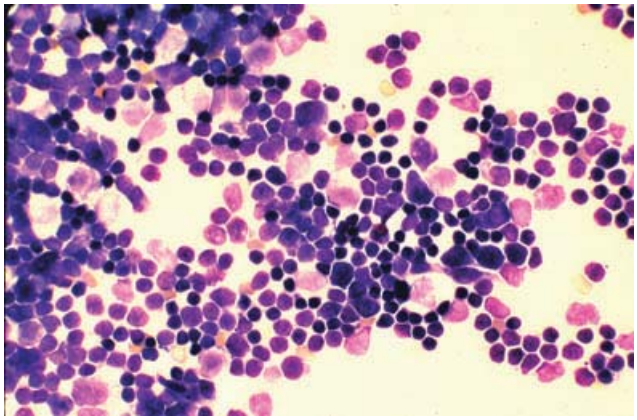

Figure 3.95. Dog: marrow imprint, CLL, same case as Figure 3.94. There is almost complete phthisis of normal marrow elements. The cells with small round nuclei that are deeply stained are all small lymphocytes, with the slightly larger and lighter-staining nuclei of similar type with injured cellular and nuclear membranes.

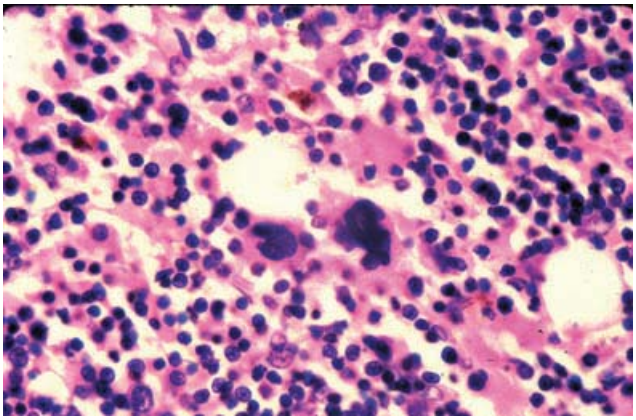

Figure 3.97. Cat: bone marrow, CLL. The bone marrow has high cellularity with few fat cells but reduced cell density with a high level of small lymphocytes. There is a complete loss of marrow granulocyte reserves with 2 residual megakaryocytes and early serous atrophy. The coarse hemosiderin granules are indicative of chronic nonresponsive anemia.

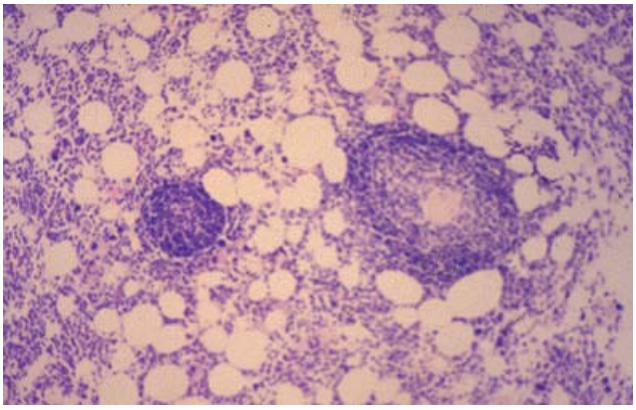

Figure 3.98. Cat: bone marrow, anemia of chronic disease. Two lymphoid follicles are present in the bone marrow, which has a normal proportion of fat but with hematopoietic marrow volume increased with hematopoiesis in the midfemoral shaft. These findings are much more common in older animals that had survived a variety of inflammatory conditions.

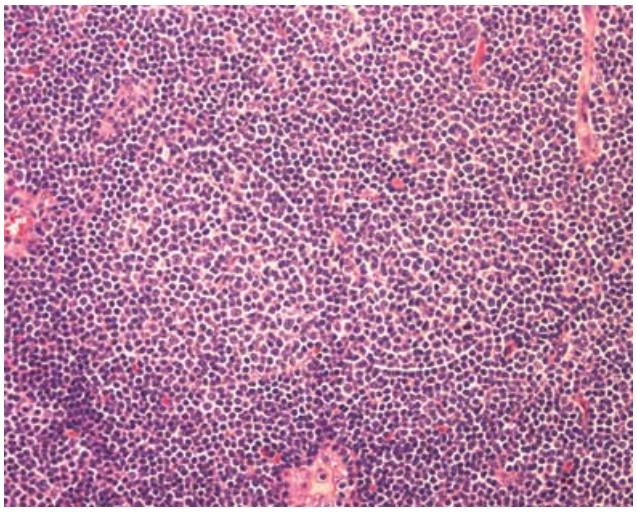

Figure 3.99. Human: lymph node, CLL. Relatively circumscribed areas of less dense cellularity (center) are occupied by slightly larger cells of typical "reaction centers" and have foci of cell proliferation within a general population of very low mitotic rate. *Slide from Cornell Tutorial.*

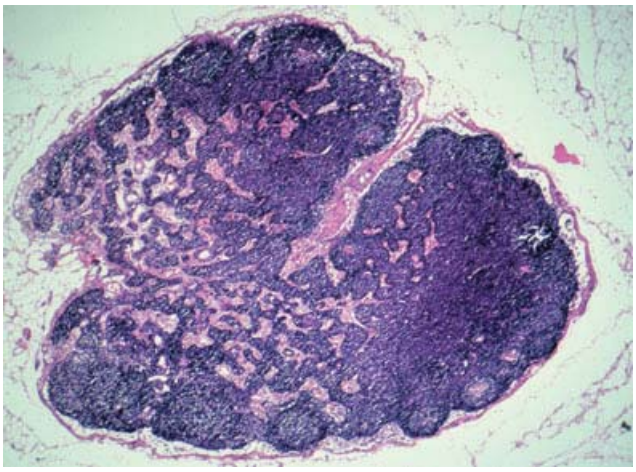

Figure 3.100. Cat: lymph node, CLL. The node is small and about 5 mm in overall diameter. The capsule is thin, and the peripheral sinus is irregularly widened due to loss of nodal volume. The outer cortex is occupied by a row of fading germinal centers that are identified by a narrow rim of mantle cells, with the central areas lighter-staining due to hypocellularity. The inner cortex is atrophic with expansion of the sinuses in some areas coming very near to the peripheral sinus. The medullary cords are occupied by small lymphocytes and plasma cells, and the sinuses have a mild sinus histiocytosis.

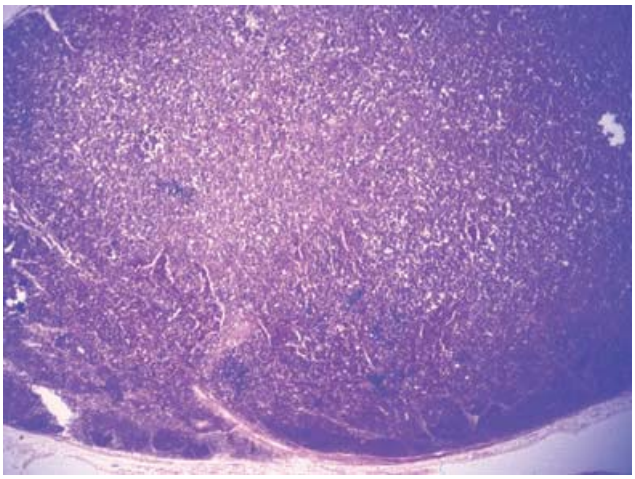

Figure 3.101. Rabbit: lymph node, SLL. The capsule is thin and taut with the peripheral sinus compressed or invaded with a diffuse architecture. There is a complete loss of germinal centers and solid filling of the cortex and medullary areas typical of small cell lymphocytic lymphoma.

Lymph Node

CLL is perhaps best understood in cats where the disease is most common. In cats with very high peripheral blood counts, the nodes are almost never markedly enlarged, and most are actually small and somewhat atrophic (Fig. 3.100). The latter changes are likely a representation of the depletion of the normal stem cell pool of benign B-cells that are displaced from the marrow by phthisis of the neoplastic population. In SLL, the nodes are at least moderately enlarged and the capsule is thinned and taut (Fig. 3.101) around a densely aggregated population of small lymphocytes with round nuclei about the same diameter as a red cell and with very little cytoplasm (Fig. 3.102). These cells individually resemble the cells of the normal thymic cortex, but collectively they don't have the interposition of epithelial cells and apoptotic cells of the thymus that gives the node in SLL a distinctive solid appearance. A further possibly unique characteristic of nodes in SLL is the presence of widely dilated lymphatics that contain lymphocytes like those of the solid areas of paracortex (Fig. 3.103) without red cells that would suggest an ectatic vein. The postcapillary venules are not obvious and have low transluminal cellular traffic (Fig. 3.104). The medullary cords are solidly distended with neoplastic lymphocytes and the medullary sinuses are obliterated (Fig. 3.105).

Spleen

In a review of 600 lymphoid neoplasms in cats, only 23 cases were felt to be of CLL or SLL type, with these related entities split about evenly at 10 and 13, respectively. With both neoplasms having the same cell type, there are architectural differences in the manner in which leukemias and lymphomas involve the spleen. These differences are in the manner of involvement of the spleen evident in all species of animals. Lymphomas, in general, result in solid areas of neoplasm that may be focal (Figs.

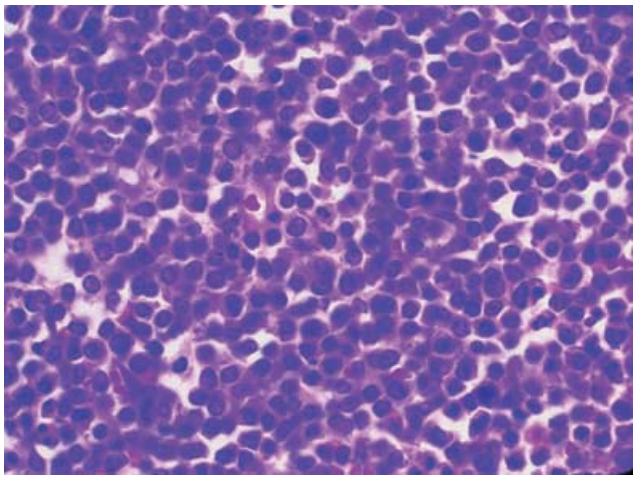

Figure 3.102. Rabbit: lymph node, SLL. Detail of Figure 3.101. A single red cell within a vessel in the center provides an index of size of surrounding lymphocytes that tend to be small to intermediate with a moderate volume of densely stained cytoplasm.

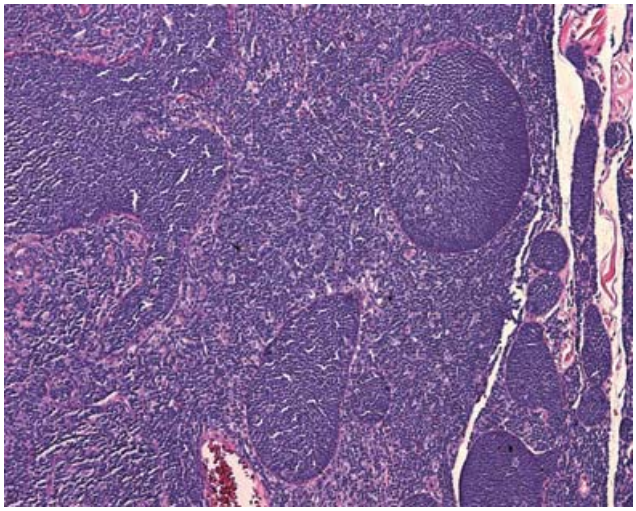

Figure 3.103. Dog: lymph node, SLL. Thin-walled lymphatic sinuses near the medullary area of the node are markedly distended, with small cells similar to those occupying the tissue areas.

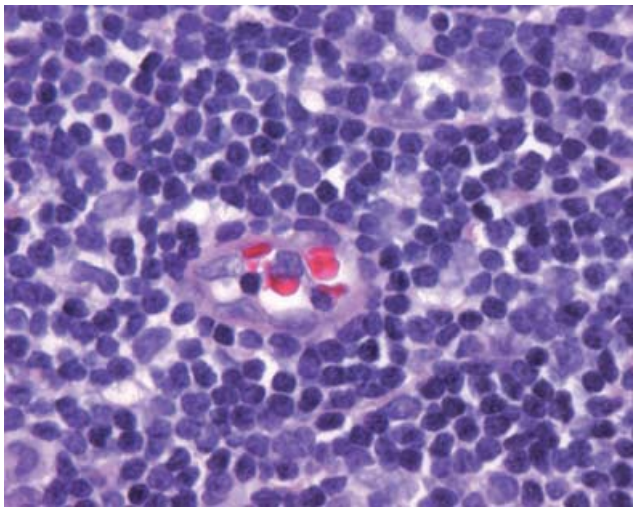

Figure 3.104. Dog: node, SLL, same case as Figure 3.103. Post-capillary venule that retains quite high and vesicular endothelial nuclei but has no lymphocytes in apparent transmural cellular migration.

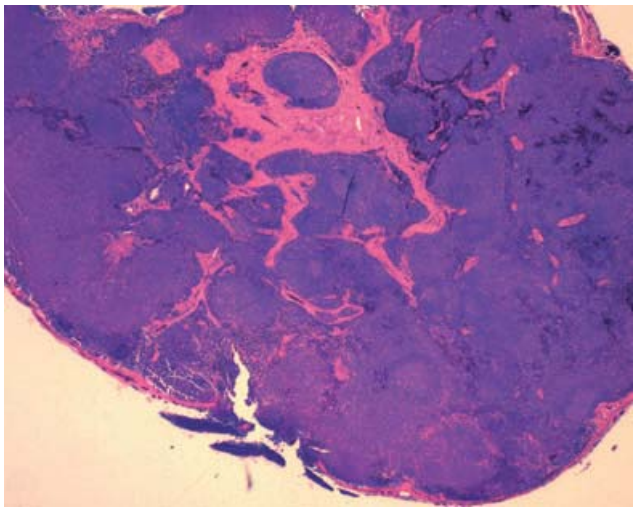

Figure 3.105. Dog: node, SLL. The cortex has a diffuse filling with fading germinal centers and mild medullary sclerosis. The proliferating cells have completely filled the medullary cords that have irregular perimeters of compressed sinuses (upper right) and contain increased numbers of red cells.

3.106–3.108) or diffuse (Figs. 3.109, 3.110). SLL tends to be multifocal and arising in relation to the arterial system, though not obviously centered on small arterioles. In contrast, in CLL there are usually many well-defined, small, involuting germinal centers that may have hyalinized centers, and a diffuse sinus filling (Figs. 3.111, 3.112). The nature of this filling is unique in that, while dense, it is never solid like lymphoma and the neoplastic cells remain surrounded by a variable number of red cells (see Figs. 3.110, 3.111). Lymphoid neoplasms of both small cell indolent and large cell type frequently colonize the large muscular veins. This type of involvement may be more related to the stage of tumor growth than cell type, and if present usually corresponds to a significant level of involvement of the liver (Figs. 3.113, 3.114). It appears that in the lymphoid leukemias of larger cell type, there will be early colonization of the subendothelial areas of the large veins; in small cell lymphoma, these are more likely to be late stage developments.

If there is involvement of the marrow to the extent of phthisis of benign cells, there may be many large blastic

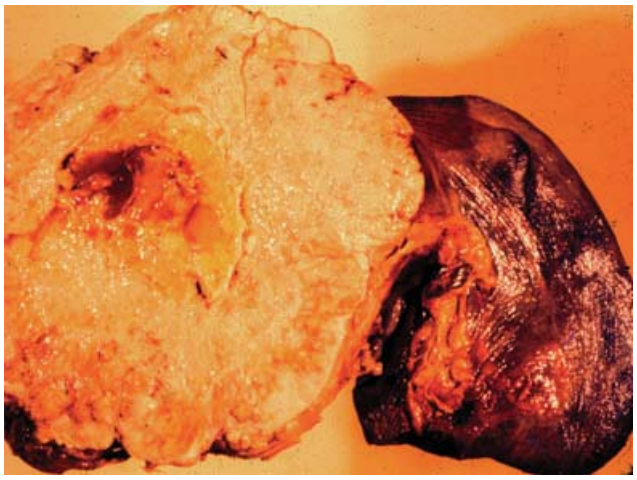

Figure 3.106. Horse: spleen, SLL. A rare but recurring form of lymphoma in the horse involves only the spleen, with a huge mass that may weigh 25–30 pounds. The lesions are not palpable per rectum but are evident on ultrasound with the animal presenting usually with anemia and hypersplenism.

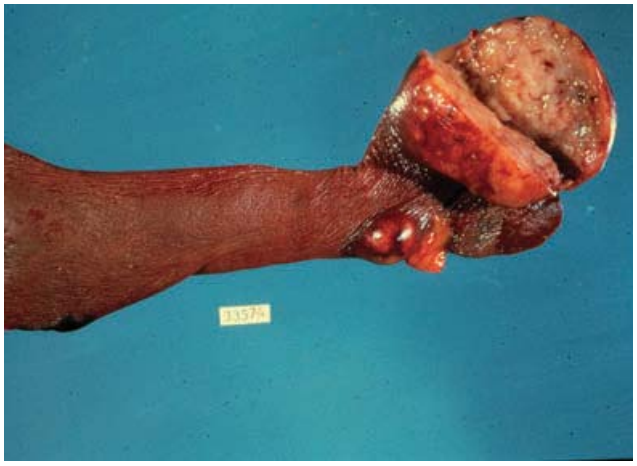

Figure 3.107. Dog: spleen, SLL. The head and body of the spleen are of normal size, with solid lymphoid proliferation markedly distending with the capsule in the tail of the spleen. Because of their indolent nature, these lesions have largely been referred to as *nodular hyperplasia*.

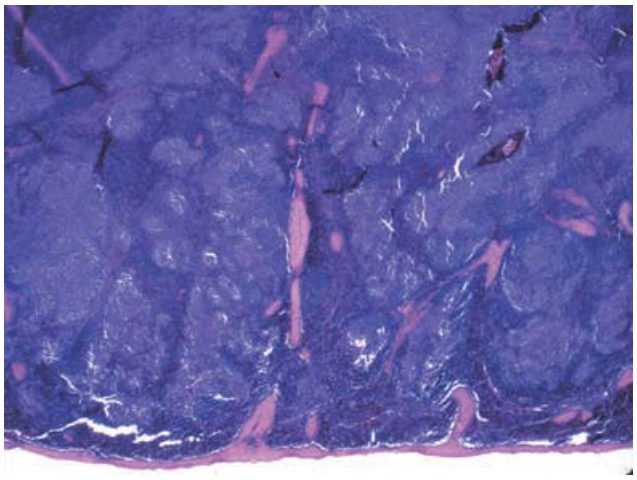

Figure 3.110. Dog: spleen, CLL. There is capsular thinning and the muscular trabeculae are widely separated, indicative of splenomegaly. There is no evidence of follicular activity with complete sinus filling characteristic of leukemia. The darker areas represent residual areas of sinus with mixed cellularity and numerous red cells.

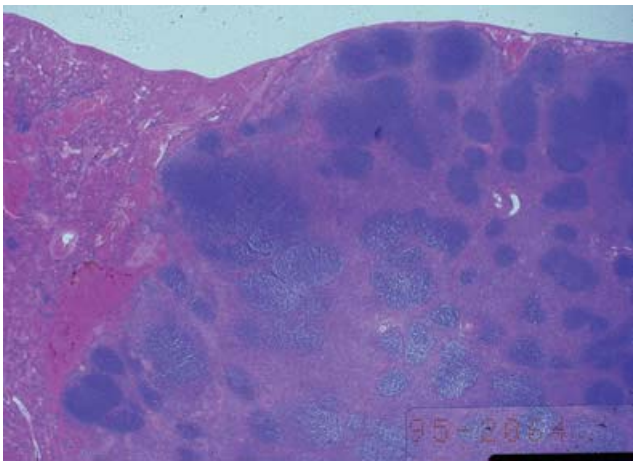

Figure 3.108. Dog: spleen, SLL. Focal splenic lymphoma of small cell type typical of mantle cell lymphoma with the periodicity of tumor foci related to the vascular architecture of the spleen.

Figure 3.109. Cow: spleen, CLL. A mature Holstein cow in good milk production was suddenly found recumbent due to abdominal hemorrhage. The animal had not been noted to be ill but had massive diffuse involvement of the spleen that resulted in multiple areas of rupture of the splenic capsule with fatal hemorrhage.

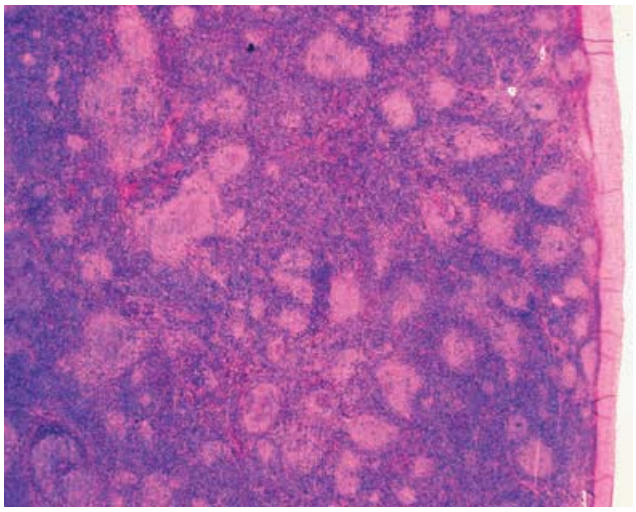

Figure 3.111. Human: spleen, prolymphocytic leukemia (PLL). The pale areas represent foci of neoplastic cell proliferation, with the darker areas in the background less involved areas of sinus with numerous red cells. *Slide from Cornell Tutorial.*

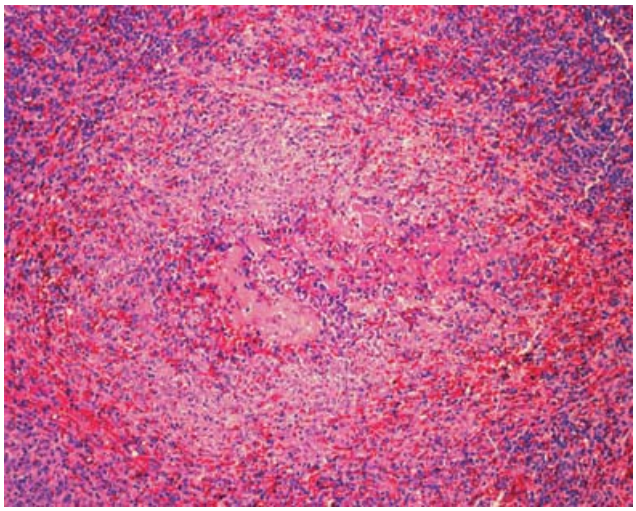

Figure 3.112. Human: spleen, PLL. Detail of Figure 3.111. Many of the foci of neoplastic colonization are centered on former germinal centers, some of which are identified by central foci of amorphous proteinaceous deposition characteristic of follicular hyalinosis.

cells of myeloid origin along the splenic smooth muscle trabeculae. They are at wide variance in size with the tumor cell population, and their lineage can be deduced by their proximity to an occasional megakaryocyte and differentiation to the level of metamyelocytes and mid-stage rubricytes.

Other Organs

CLL tends to involve the tissues with a fine fibrovascular net like the choroid plexus of the brain, adrenal gland,

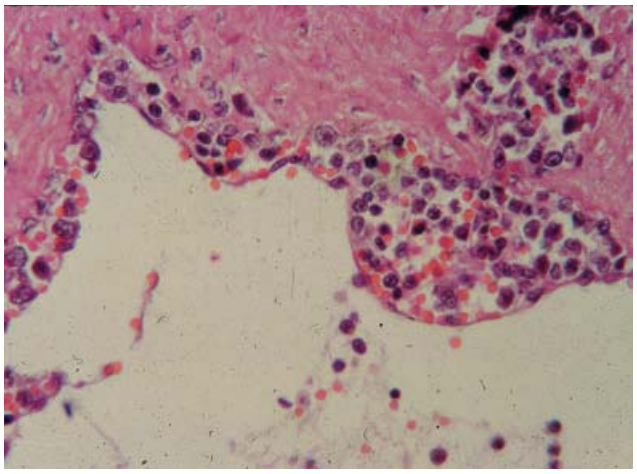

Figure 3.113. Dog: spleen, SLL. Subendothelial colonization of a large muscular vein in a case with extensive splenic involvement.

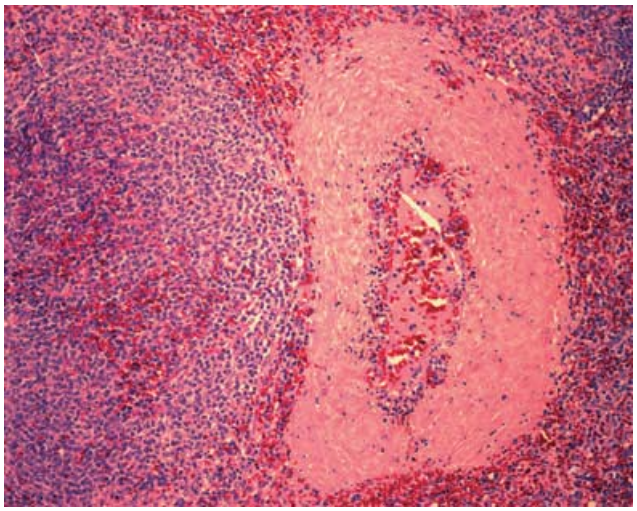

Figure 3.114. Human: spleen, prolymphocytic leukemia. The left area of the image is occupied by a focal nodule of neoplastic cell colonization, with a large venous sinus at right with extensive subendothelial colonization and vascularization by the neoplastic lymphocytes. *Slide from Cornell Tutorial.*

and pancreas; SLL colonizes the fat around mesenteric nodes; and both invade the liver and kidney. It is difficult to gauge the level of leukemic leukocytosis on hepatic histology, but in general, there are fewer neoplastic cells in the hepatic sinusoids with SLL (Figs. 3.115–3.117) than with CLL (Fig. 3.118, see also Fig. 3.117) and both will have perivascular colonization most prominent abound the portal tracts.

Immunologic Features

Until very recently most reports on CLL and SLL in animals were morphologic in nature without determina-

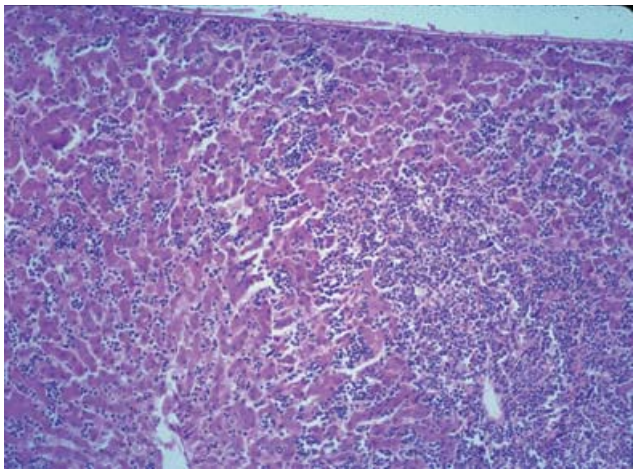

Figure 3.115. Cat: liver, ALL L1. There is quite extensive periportal involvement surrounding the vessel at the right while the central vein area at the bottom left has only sinus involvement. There is irregular dilation of hepatic cords with quite large numbers of cells, many of which are presumably in circulation.

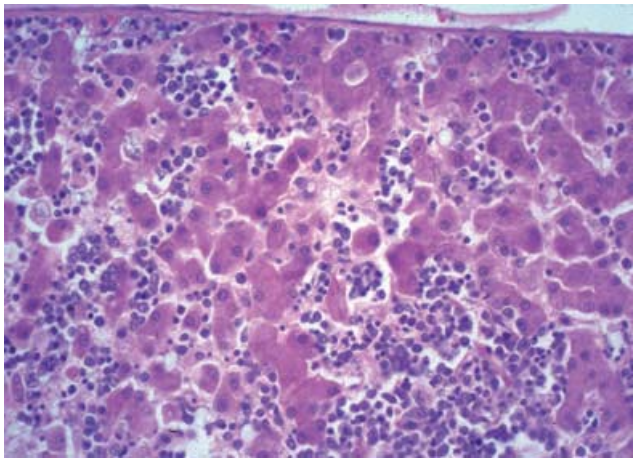

Figure 3.116. Cat: liver, ALL L1. Detail of Figure 3.115. Note the mild to moderate atrophy of hepatocytes most apparent near the left with sinus dilation and the presence of leukemic lymphocytes that appear more numerous than red cells.

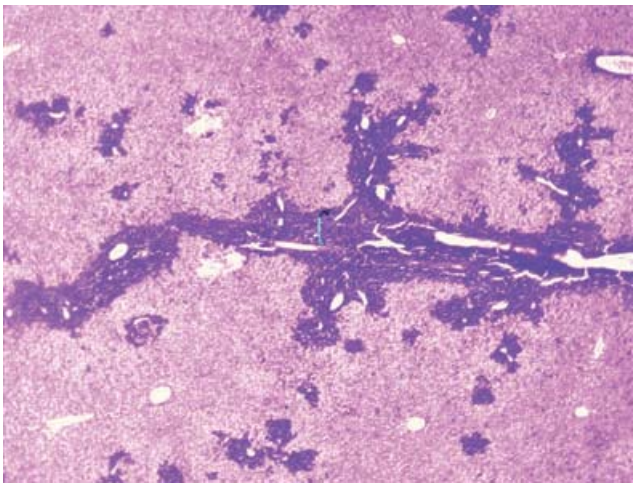

Figure 3.117. Cat: liver, CLL. The pattern of colonization at the architectural level appears primarily periportal and is indistinguishable from lymphoma.

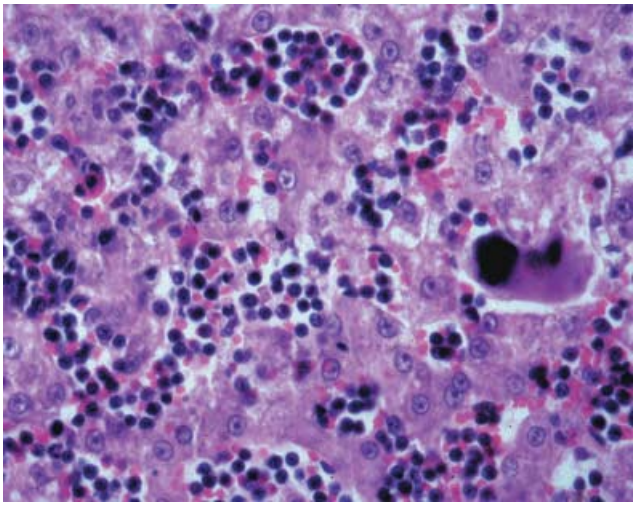

Figure 3.118. Cat: liver, CLL. Detail of Figure 3.117. The cat had a total leukocyte count of over 600,000 per ul with the sinus pattern more apparent at higher magnification. The megakaryocyte at the right is indicative of myelophthisis and extramedullary hematopoiesis.

tion of immunologic features. In the dog, and less well defined in other species, the well-differentiated leukemias and lymphomas are predominantly of T-cell type. Those B-cell neoplasms of CLL type studied are CD79 and CD21 positive and lack T-cell antigens. Unlike Human B-cell CLL, they are CD5 negative, but most express CD1c, and 3/4 of the latter population are also positive for CD1a. CD1c is always more strongly expressed than CD1a. Occasionally, animals with small cell leukemia will have a gammopathy like that of Waldenstom's macroglobulinemia, which may be signaled in a wide albumin globulin ratio that must be verified on serum electrophoresis or the demonstration of strong IgM heavy chain cytoplasmic staining. Because the finding of immunoglobulin production indicates a more mature cell of postgerminal center origin, the neoplasm is then likely not a true CLL but a prolymphocytic leukemia (PLL) or plasmacytoid type of lymphoma.

Cytogenetic and Molecular Features

Molecular changes specific to CLL and SLL in animals are currently largely undefined. However, the primers and

immunoglobulin gene VDJ regions developed for probing clonality in the B-cell neoplasms of the dog and cat regularly identify small cell lymphomas of CLL/SLL and mantle cell types. In the human counterpart neoplasms, there is rearrangement of both the light and heavy Ig genes in almost all cases. In addition in human SLL about 8% of patients also have rearrangement of the beta chain of the T-cell receptor gene locus. This finding is paralleled in the dog, where about 10% of B-cell lymphomas of indolent type were found to have rearrangement of the T-cell receptor gene. This is a most important point to emphasize because it indicates that lineage cannot reliably be determined by tests of clonality for either the immunoglobulin gene or the T-cell receptor gene. Thus, the advent of clonal determination has not obviated the need for determination of phenotype on the basis of predominant marking of neoplastic cells in immunocytological or immunohistochemical preparations. The low mitotic rate of these neoplasms made cytogenetic studies technically difficult to carry out because of the challenge in obtaining cells in metaphase for chromosomal analysis. The advent of in situ hybridization, which can be carried out on interphase cells, and development of molecular probes has resulted in much higher estimates of genetic changes than were found by classic cytogenetics. Like most other lymphomas in humans most cases of CLL/SLL have chromosomal abnormalities, but unlike other lymphomas none of these are characteristic of these diseases, though changes are most common in chromosomes 12 and 14.

Cell of Origin

In contrast to most other B-cell lymphomas of more aggressive type, there is not hypermutation of the variable portion of the Ig gene in human SLL or CLL that is taken as evidence of origin from a population of naive pregerminal center B-cells. Because the precursor cells of this type are likely rare and a very low population of cells in transport from marrow to peripheral tissues, the benign counterpart of CLL/SLL is relatively unknown.

Diagnostic Criteria

The diagnosis of B-cell CLL is made on finding a leukemic blood picture, often with very high total leukocyte counts of small mature-appearing cells with round, densely stained nuclei and very few mitoses. There is not a defined lower limit of blood lymphocyte numbers as in the human levels of $5–10 \times 10^3$/ul, but a sustained lymphocyte level in an animal above 10,000/ul should suggest the need for marrow examination. The diagnosis is confirmed by bone marrow aspirate or core biopsy, with a replacement of almost all fat and normal hematopoietic cells by neoplastic cells morphologically like those in the peripheral blood and phenotypically of B-cell type.

The diagnosis of SLL is on irregular enlargement of nodes with hepatosplenomegaly and a population of small mature-appearing lymphocytes with densely stained nuclei usually lacking nucleoli and with a very narrow rim of cytoplasm. The diagnosis is confirmed by a relatively normal blood leukocyte picture, mild to moderate anemia, very few mitoses in aspirated cells of liver and spleen, and phenotypic staining for B-cell type.

Differential Diagnosis

The most important differential in the diagnosis of B-cell SLL and CLL is of benign reactive hyperplasia. Because the cells are not discernibly neoplastic, the degree of change in cell numbers and the homogeneity of cell type are the most important criteria in making the interpretation of neoplasia. The second most important differential is the phenotypic demonstration of B-cell lineage. Because the evolution of CLL is to a larger cell type with nucleoli generally referred to as *prolymphocytic leukemia (PLL)* the proportion of cells present of PLL type is an important distinction.

Staging

Staging has not been routinely carried out in animals because of the infrequency with which the diagnosis of CLL is made. In human medicine, there are two systems in use that have been shown to have clinical relevancy. They are the Rai and Binet systems, of which the latter is the most easily applied. For the Binet system there are three categories of disease progression known as A–C, and they are based on changes in the blood and on the involvement of anatomic lymphoid areas in groups consisting of cervical, axillary, and inguinal areas, plus the spleen and liver. The criteria for each of these stages are

A. No anemia or thrombocytopenia and involvement of fewer than 3 lymphoid areas
B. No anemia or thrombocytopenia and involvement of 3 or more lymphoid areas
C. Anemia of less than 10 g/dL or thrombocytopenia of less than 100×10^3/u

The Binet system would seem to be readily applied to animals where it is likely that most would be at stage C at the time of diagnosis. To provide a frame of reference in terms of survival with an indolent lymphoid neoplasm, the average survival for humans with the lowest stage of tumor involvement (Rai stage O) is 120–180 months, while the survival with the highest stage of tumor progression (Rai stage IV) is 18–60 months.

Transformation and Progression

It is known that CLL in animals progresses to an accelerated phase, as in humans. As yet we have not categorized these stages of progression in morphologically

defined steps. In humans the most common form of progression is to PLL or prolymphocytic leukemia (Figs. 3.119–3.123). There are five categories of progression recognized in human CLL:

- PLL
- Richter's syndrome (large cell lymphoma)
- Blastic transformation (Fig. 3.124)
- Plasmacytoid transformation (Figs. 3.125, 3.126)
- Immunoblastic transformation Figs. 3.127, 3.128)

Diagnostic features suggested to relate to prognosis in human CLL are the following:

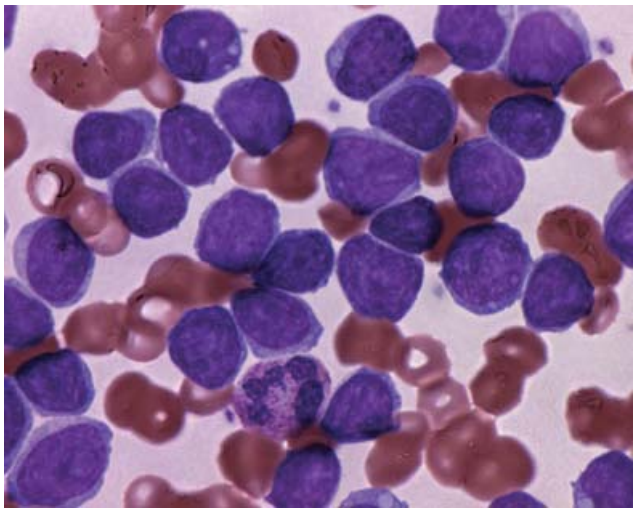

Figure 3.119. Human: blood, PLL. There is a very high level of leukemia, with the predominant cells having nuclei about 1.5 red cells in diameter. The nuclei retain some large chromocenters that are irregularly linked by coarse chromatin bands. The cells frequently have nucleoli and more abundant cytoplasm than in the small cell type of CLL. *Slide from Cornell Tutorial.*

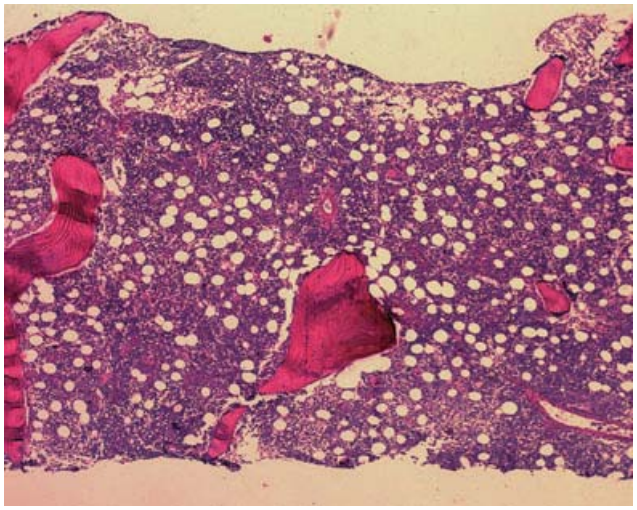

Figure 3.120. Human: bone marrow core, PLL. The marrow is hypercellular with less than the normal level of fat cells and has a higher level of cellular homogeneity than would be found in normal marrow. There are several megakaryocytes present at lower center that make their absence more conspicuous in other areas. *Slide from Cornell Tutorial.*

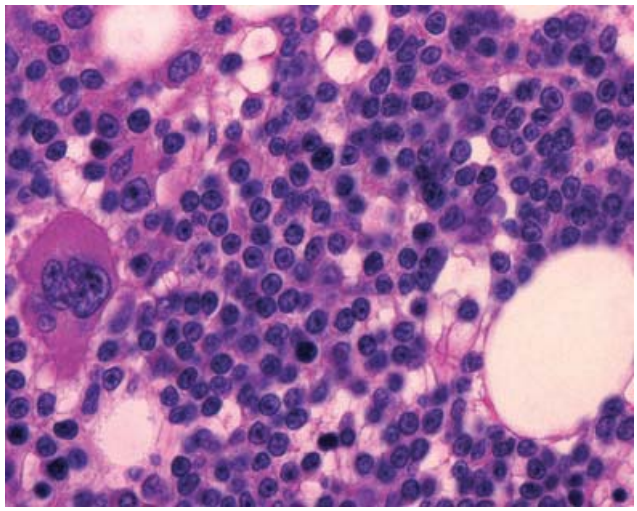

Figure 3.121. Human: marrow core, PLL. Detail of Figure 3.120. The megakaryocyte is likely the only benign cell in the field. There is a complete loss of marrow granulocyte reserves and of cells of erythroid lineage. In histologic preparations, most cells of the PLL type have nucleoli with the chromatin more coarsely granular than apparent at this magnification. The cytoplasm appears more abundant than in cytologic preparations. *Slide from Cornell Tutorial.*

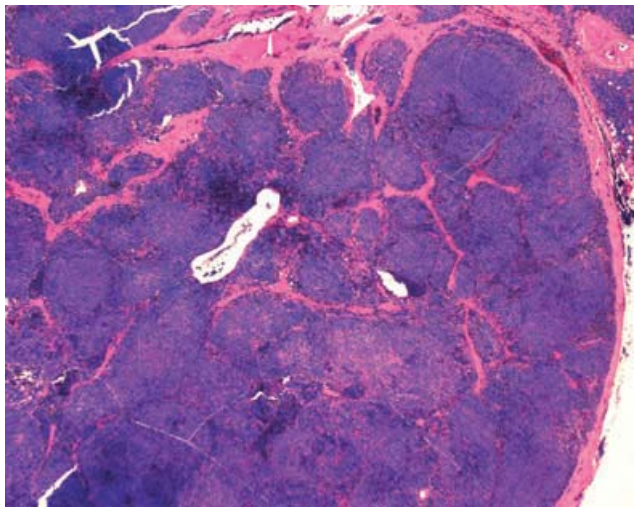

Figure 3.122. Human: lymph node, PLL. Architectural view of prolymphocytic leukemia in lymph node. There is a complete absence of fading germinal centers and irregular filling of paracortex and medullary cords, with proliferating cells typical of smaller cell lymphomas. *Slide from Cornell Tutorial.*

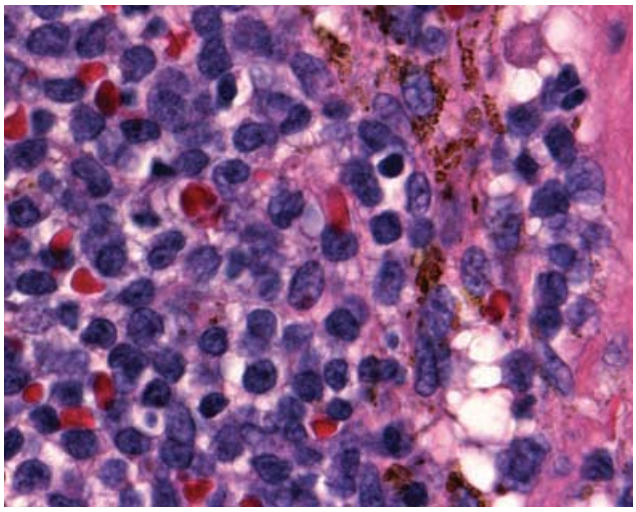

Figure 3.123. Human: lymph node, PLL. Detail of Figure 3.122. Medullary cords have very narrow regions of compressed sinus at the right with numerous hemosiderin-bearing macrophages. The infiltrating lymphocytes have more variation in size and nuclear shape than was apparent on the blood film. There is a coarse chromatin pattern and frequent nucleoli and relatively abundant cytoplasm. *Slide from Cornell Tutorial*. Comparable changes occurring in the spleen in different cases with PLL are present in Figures 3.111 and 3.112.

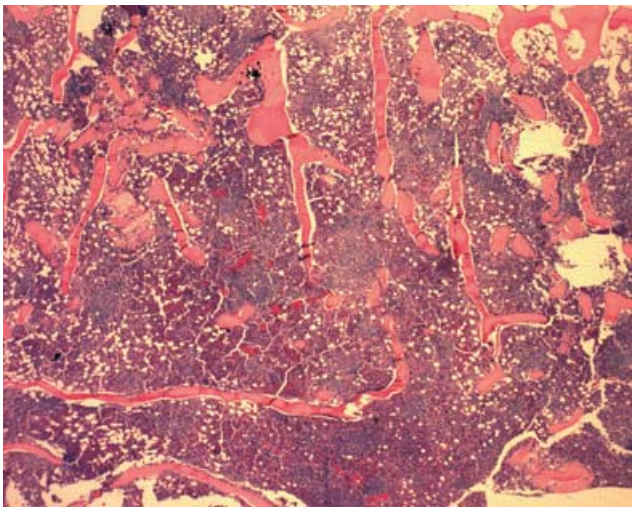

Figure 3.125. Human: bone marrow, B-cell chronic CLL with plasmacytic conversion. The irregular lighter-stained areas in the center of the image with reduced fat cells represent foci of diffuse leukemic infiltration.

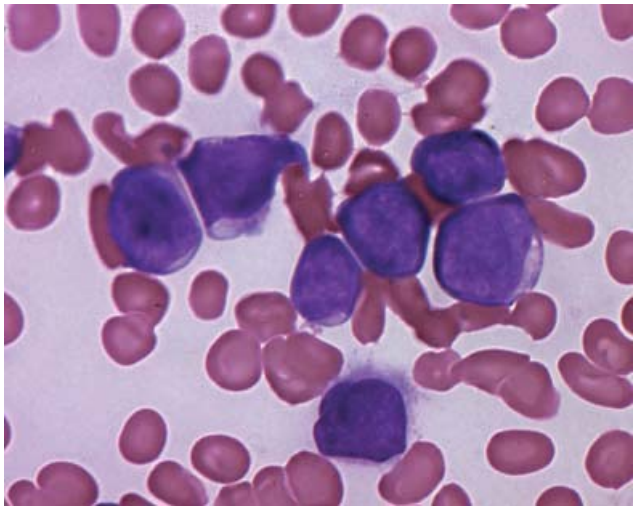

Figure 3.124. Human: blood, variant-type B-cell CLL. This form of CLL also occurs in dogs where the cells have larger nuclei and more abundant cytoplasm with the nuclei occasionally appearing cleft. In this patient, the larger cells have nucleoli suggesting that the disease is entering an accelerated phase. *Slide from Cornell Tutorial*.

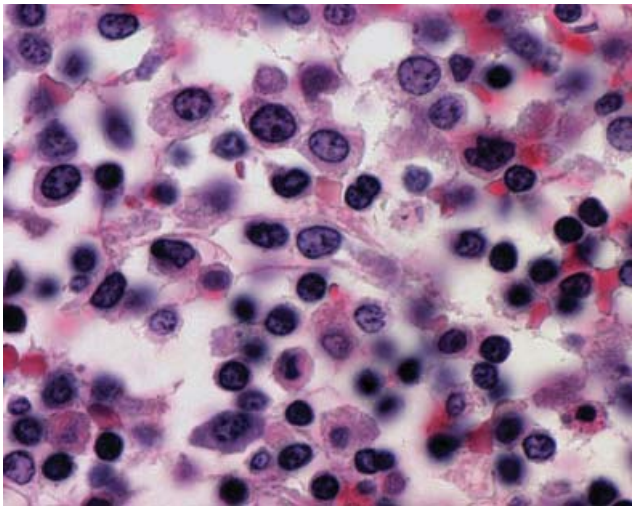

Figure 3.126. Human: marrow, B-cell CLL. Detail of Figure 3.125. The marrow is becoming occupied by cells with large nuclei and abundant cytoplasm often eccentrically located and with irregular often high levels of basophilia with perinuclear Golgi areas (lower center). The patient had IgM gammopathy. *Slide from Cornell Tutorial*.

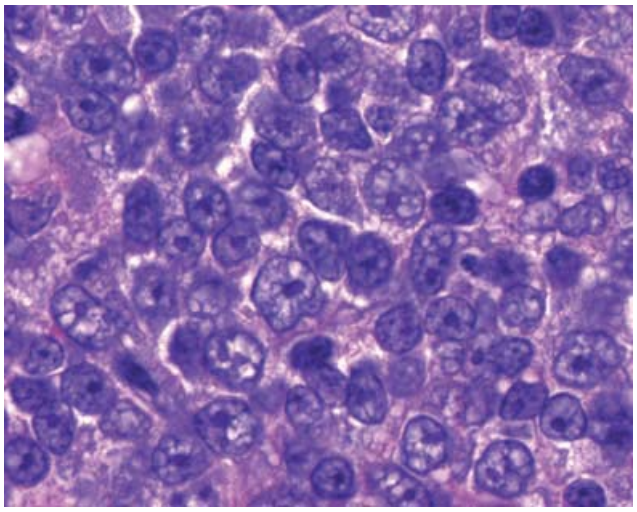

Figure 3.127. Dog: lymph node, immunoblastic lymphoma. The dog presented with lymphadenopathy and it is not clear that there was a previous history of low-grade lymphoma. The cells are large and very large with a branched chromatin pattern and characteristically a single prominent central nucleolus. The cytoplasm is quite abundant and highly amphophilic with cell boundaries irregularly distinct.

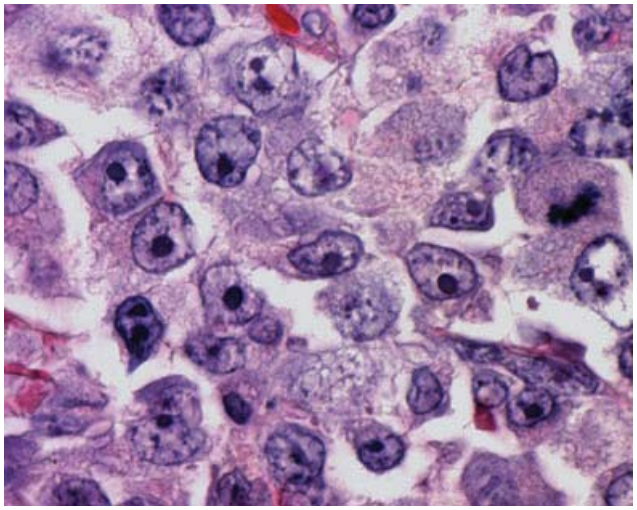

Figure 3.128. Human: lymph node, immunoblastic lymphoma. The presentation was of an enlarged spleen with a leukemic pattern without history of evolution from a small cell lymphoma. The nuclei are large and vesicular, with a branched chromatin pattern with quite marked parachromatin clearing and generally a prominent single central nucleolus. The cytoplasm is relatively abundant and variably stained with cell boundaries irregularly distinct. *Slide from Cornell Tutorial.*

- Clinical stage (RAI, Binet)
- Lymphocyte count and doubling time
- Pattern of marrow involvement
- Cytogenetic abnormalities
- Atypical immunophenotype

Evaluation of the Treated Animal

In cases previously diagnosed as CLL, the follow-up examinations may be limited to determination of the peripheral blood picture to determine if the leukocyte count is stable or to determine the rate of rise in the lymphoid count and progression of cytopenias of other cell types. Once chemotherapeutic treatment has been initiated, the cell type will change, usually to a cell with a smaller nucleus with more variability in chromatin patterns and cytoplasmic volume and staining density. Binucleated cells may become more numerous, but anemia is seldom a major problem unless there is thrombocytopenic bleeding. Animals with less than 1,000 neutrophils/ul may have ulceration of the oral cavity or skin that are persistent and slow healing.

SLL may progress to a large cell lymphoma or prolymphocytic or blastic transformation with or without leukemic accompaniment (see Figs. 3.119–128). Often the increase in the size of the spleen and liver results in systemic signs that precede elective termination.

Treatment and Survival

The survival of animals with CLL is likely potentially better than observed, because most are electively terminated on the basis of having a neoplastic disease with a slow but progressive disease and because "leukemia" is generally viewed as less treatable than solid tumors. Because most cases are not recognized until the disease is advanced, it may have been present for 1–2 years at the time of diagnosis. If the animal enters an accelerated phase, the variant clone may be more susceptible to combination chemotherapy than the initial small cell neoplasm with low mitotic rate. In contrast, in SLL in humans the 2-year survival varies from 60–70% and the 5-year survival is between 50 and 70%. The comparable times in animals are not known because of the cost of irradiation and chemotherapy and the option of elective termination.

REFERENCES

Asplund, S.L., McKenna, R.W., Howard, M.S., and Kroft, S.H. (2002) Immunophenotype does not correlate with lymph node histology in chronic lymphocytic leukemia/small lymphocytic lymphoma. *Am J Surg Pathol* 26(5):624–629.

Bonato, M., Pittaluga, S., Tierens, A., Criel, A., Verhoef, G., Wlodarska, I., Vanutysel, L., Michaux, L., Vandekerckhove, P., Van den Berghe, H., and De Wolf-Peeters, C. (1998) Lymph node histology in typical and atypical chronic lymphocytic leukemia. *Am J Surg Pathol* 22(1):49–56.

Dürig, J., Nückel, H., Cremer, M., Führer, A., Halfmeyer, K., Fandrey, J., Möröy, T., Klein-Hitpass, L., and Dührsen, U.

(2003) ZAP-70 expression is a prognostic factor in chronic lymphocytic leukemia. *Leukemia* 17:2426–2434.

Hainsworth, J.D., Litchy, S., Barton, J.H., Houston, G.A., Hermann, R.C., Bradof, J.E., and Greco, F.A. (2003) Single-agent Rituximab as first-line and maintenance treatment for patients with chronic lymphocytic leukemia or small lymphocytic lymphoma: A Phase II trial of the Minnie Pearl Cancer Research Network. *J Clin Oncol* 21(9): 1746–1751.

Hamblin, T.J., and Oscier, D.G. (1997) Chronic lymphocytic leukaemia: The nature of the leukaemic cell. *Blood Rev* 11:119–128.

Hammarsund, M., Corcoran, M.M., Wilson, W., Zhu, C., Einhorn, S., Sangfelt, O., and Grandér, D. (2004) Characterization of a novel B-CLL candidate gene—*DLEU7*—located in the 13q14 tumor suppressor locus. *FEBS Letters* 556:75–80.

Huh, Y.O., Keating, M.J., Saffer, H.L., Jilani, I., Lerner, S., and Albitar, M. (2001) Higher levels of surface CD20 expression on circulating lymphocytes compared with bone marrow and lymph nodes in B-cell chronic lymphocytic leukemia. *Am J Clin Path* 116(3):437–443.

Montserrat, E., Villamor, N., Reverter, J.-C., Brugués, R.-M., Tàssies, D., Bosch, F., Aguilar, J.-L., Vives-Corrons, J.-L., Rozman, M., and Rozma, C. (1996) Bone marrow assessment in B-cell chronic lymphocytic leukaemia: Aspirate or biopsy? *Brit J Hematol* 93:111–116.

Novak, U., Tobler, A., and Fey, M.F. (2004) Allelotyping in B-cell chronic lymphocytic leukemia (B-CLL). *Leuk & Lymph* 45(5):887–896.

Oppezzo, P., Vuillier, F., Vasconcelos, Y., Dumas, G., Magnac, C., Payelle-Brogard, B., Pritsch, O., and Dighiero, G. (2003) Chronic lymphocytic leukemia B cells expressing AID display dissociation between class switch recombination and somatic hypermutation. *Blood* 101(10):4029–4032.

Parker, D., Alison, D.L., Barnard, D.L., Child, J.A., Dovey, G., Farish, J., Norfolk, D.R., O'Brien, C.J., Parapia, L.A., Sharp, J., and Simmons, A.V. (1994) Prognosis in low grade non-Hodgkin's lymphoma: Relevance of the number of sites involved, absolute lymphocyte count and serum immunoglobulin level. *Hematol Oncol* 12:15–27.

Pritsch, O., Maloum, K., and Dighiero, G. (1997) Basic biology of autoimmune phenomena in chronic lymphocytic leukemia. *Sem Oncol* 25(1):34–41.

Raskin, R.E., and Krehbiel, J.D. (1988) Histopathology of canine bone marrow in malignant lymphoproliferative disorders. *Vet Pathol* 25:83–88.

Rice, T.W., and Milstone, A.P. (2004) Chylothorax as a result of chronic lymphocytic leukemia: Case report and review of the literature. *South Med J* 97(3):291–294.

Robertson, T.I., and Byth, K. (1993) Sequential changes in the bone marrow trephine biopsy in B-cell chronic lymphocytic leukaemia. *Aust NZ J Med* 23:470–476.

Schmid, C., and Isaacson, P.G. (1994) Proliferation centres in B-cell malignant lymphoma, lymphocytic (B-CLL): An immunophenotypic study. *Histopath* 24:445–451.

Shanafelt, T.D., and Call, T.G. (2004) Current approach to diagnosis and management of chronic lymphocytic leukemia. *Mayo Clin Proc* 79:388–398.

Sthoeger, Z.M., Sthoeger, D., Shtalrid, M., Sigler, E., Geltner, D., and Berrebi, A. (1993) Mechanism of Autoimmune hemolytic anemia in chronic lymphocytic leukemia. *Am J Hematol* 43:259–264.

Su, Y.-C., Wu, W.-M., Wu, M.-F., and Chiang, B.-L. (2001) A model of chronic lymphocytic leukemia with Richter's transformation in severe combined immunodeficiency mice. *Exp Hematol* 29:1218–1225.

Troussard, X., and Flandrin, G. (1996) Chronic B-cell lymphocytosis with binucleated lymphocytes (LWBL): A review of 38 Cases. *Leuk & Lymph* 20:275–279.

Valli, V.E., Jacobs, R.M., Norris, A., Couto, C.G., Morrison, W.B., McCaw, D., Cotter, S., Ogilvie, G., and Moore, A. (2000) The histologic classification of 602 cases of feline lymphoproliferative disease using the National Cancer Institute Working Formulation. *J Vet Diagn Invest* 12:295–306.

Vernau, W., and Moore, P.F. (1999) An immunophenotypic study of canine leukemias and preliminary assessment of clonality by polymerase chain reaction. *Vet Immunol and Immunopathol* 69:145–164.

Xu, Y., McKenna, R.W., Asplund, S.L., and Kroft, S.H. (2002) Comparison of immunophenotypes of small B-cell neoplasms in primary lymph node and concurrent blood or marrow samples. *Am J Clin Pathol* 118:758–764.

Zwiebel, J.A., and Cheson, B.D. (1998) Chronic lymphocytic leukemia: Staging and prognostic factors. *Sem Oncol* 25(1):42–59.

B-Cell Prolymphocytic Leukemia/Human Variant Hairy Cell Leukemia

Definition

Prolymphocytic leukemia (PLL) of B- or T-cell type is a clonal neoplasm involving the marrow and characterized by high levels of leukemic leukocytosis at presentation and by splenomegaly.

Prolymphocytic leukemia in animals is recognized as a cell type, but not as a disease entity.

Epidemiology and Incidence

Prolymphocytic leukemia occurs in cattle and rarely in small ruminants. It is seen most frequently in dogs and cats and is usually considered to be chronic lymphocytic leukemia in an accelerated phase. In humans this disease occurs with male predominance and in the elderly.

Clinical Presentation and Features

Leukemias in animals with characteristic cytology of prolymphocytic leukemia are described but are given generic terminology. Most cases occur in older animals that are cachectic or have very marked weight loss and muscle atrophy. The spleen is enlarged and may be congested and mesenteric more often than peripheral lymph nodes are enlarged. The liver is typically not enlarged but is involved histologically.

Pathologic Features

Blood

Like chronic lymphocytic leukemia (CLL), the blood in PLL is always diagnostic and the cell type is characteristic. The level of leukemia is high, generally in excess of 50×10^3/ul and often around 100×10^3/ul. The nuclei of neoplastic PLL cells have a characteristic chromatin pattern that is typical of their stage of differentiation regardless of T- or B-cell origin. The nuclei are round and 2.0 red cells in diameter with relatively abundant pale basophilic cytoplasm. The nuclei contain large densely stained chromocenters that are evenly distributed and joined by thin chromatin bands with parachromatin clearing between the bands (Figs. 3.129, 3.130). The chromatin is of moderate staining density, and most cells lack nucleoli. One percent or less of the leukemic cells have slightly larger nuclei with a finer chromatin distribution, less prominent chromocenters, and a single nucleolus of moderate size. These latter cells are considered the dividing population, and an increase in their frequency is taken as indication of a more aggressive phase of the disease.

Bone Marrow

The bone marrow in PLL has not been adequately described in animals and the diagnosis is usually made on blood with marrow changes not specifically recognized. It appears that early cases have nodular interstitial involvement of marrow, and with progression the lesions become diffuse and involve paratrabecular regions (Fig. 3.131).

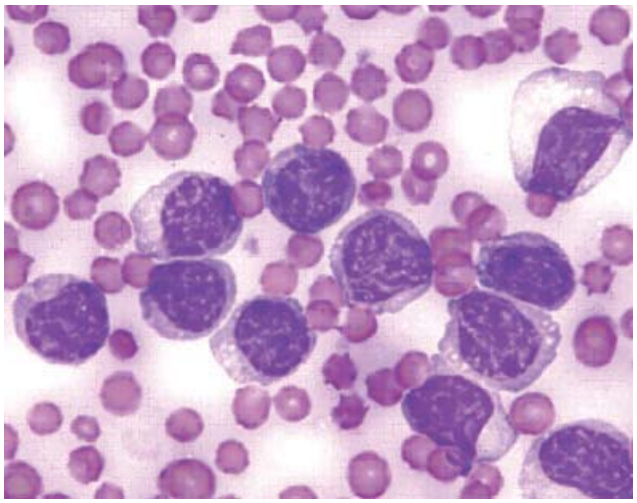

Figure 3.129. Bovine: blood, prolymphocytic leukemia. Blood was drawn from a mature Holstein cow that had a total leukocyte count of 112,000 per ul. The nuclear morphology is typical of PLL, with large chromocenters separated by sharply defined chromatin bands with narrow areas of parachromatin clearing. An occasional larger cell has a nucleolus and the cytoplasm is quite abundant, lightly basophilic, and finely vacuolated.

On histologic examination, most cells have nucleoli and the PLL cells differ from benign cells of the erythroid and lymphoid systems by the characteristic chromatin pattern, small but obvious nucleoli, and more abundant pale-staining cytoplasm (Fig. 3.132).

Lymph Nodes

PLL is similar to CLL in the spleen, and nodes are frequently involved. Nodal changes are irregular and may be

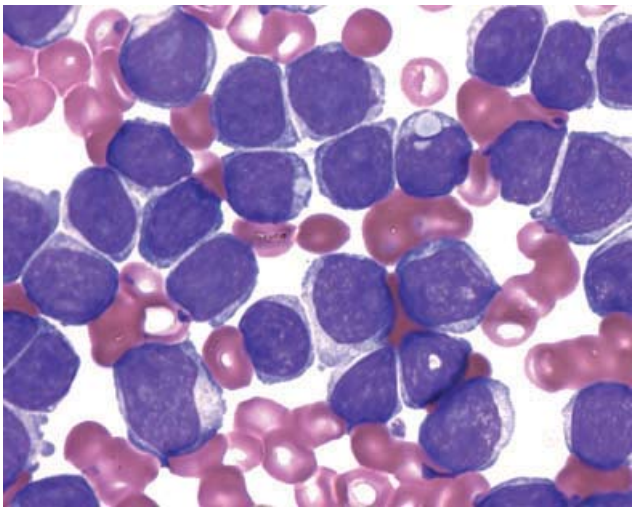

Figure 3.130. Human: blood, PLL, B-type prolymphocytic leukemia. The chromatin patterns are not quite as clear as in the case of Figure 3.129. Note the basic pattern of dense chromocenters with small areas of parachromatin clearing. The human cells have quite prominent nucleoli. *Slide from Cornell Tutorial.*

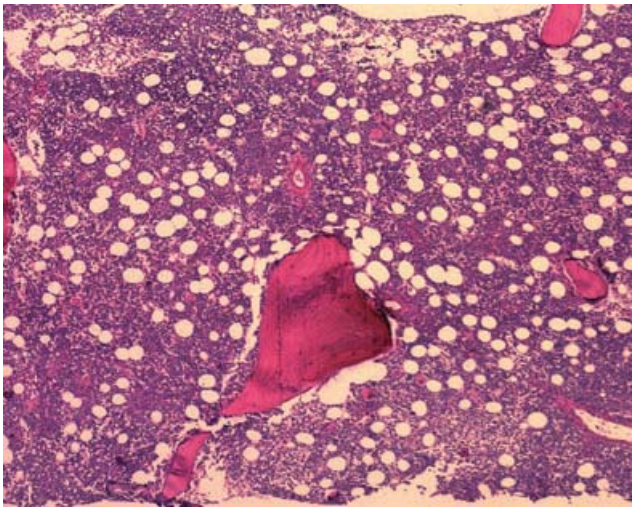

Figure 3.131. Human: marrow, PLL. At the architectural level, the marrow is hypercellular with reduced area occupied by fat and with a homogenous appearance due to very diffuse colonization. *Slide from Cornell Tutorial.*

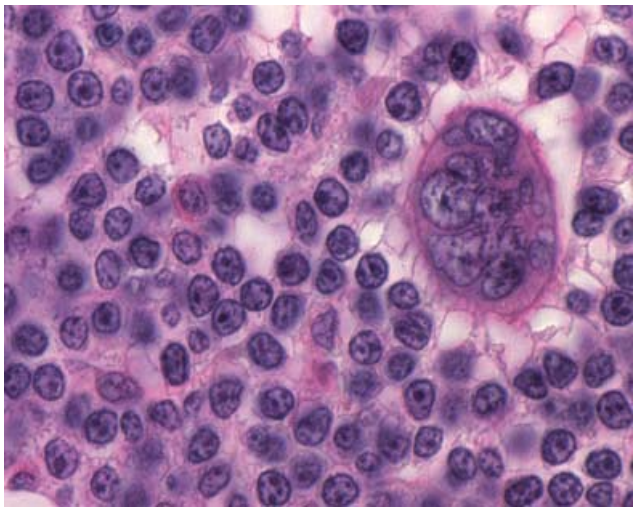

Figure 3.132. Human: marrow, PLL. Detail of Figure 3.131. The marrow is very heavily infiltrated with the neoplastic lymphocytes. There is a young megakaryocyte at the right and an eosinophil myelocyte in the left center. Neoplastic cells are of uniform size and shape with peripheralized chromatin and 1–2 prominent nucleoli. There are occasional binucleated forms and a moderate volume of lightly stained cytoplasm.

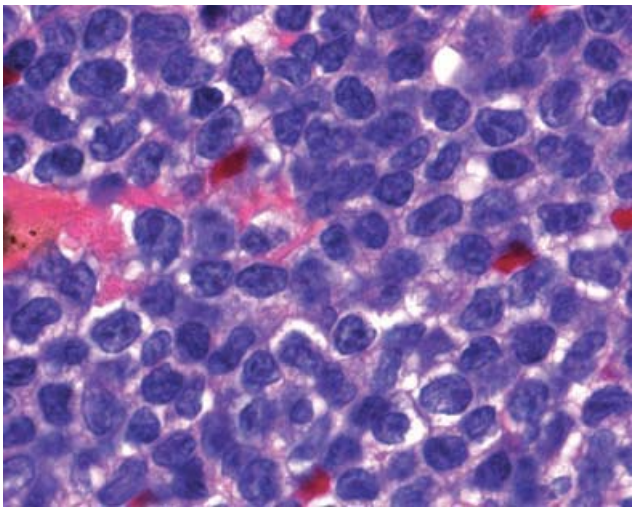

Figure 3.134. Human: lymph node, PLL. Detail of Figure 3.133. A cortical foci of follicular hyalinosis (left) indicates an area of previous germinal center. The nuclei are of intermediate size with more irregularity of nuclear shape than evident in blood but retaining the large chromocenters with irregular parachromatin clearing and many with prominent nucleoli. The cytoplasm is moderate in volume and staining density with cell boundaries irregularly distinct.

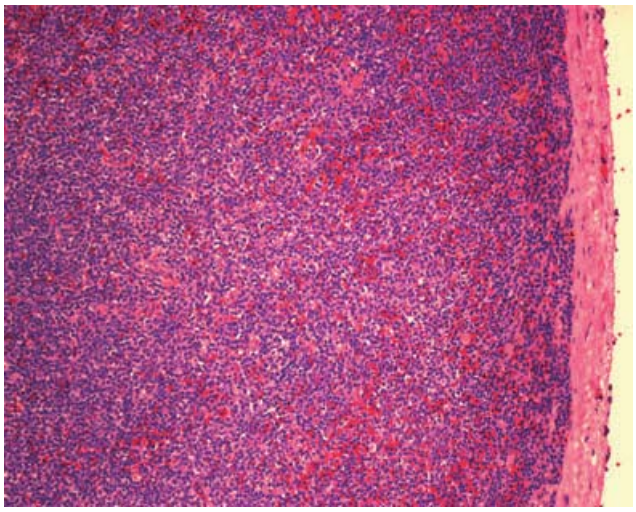

Figure 3.133. Human: lymph node, PLL. The node has diffuse architecture with distention but not thinning of the capsule and apparent colonization and destruction of the peripheral sinus. *Slide from Cornell Tutorial.*

single or regional, and involvement may be focal or diffuse. Early PLL may begin around fading germinal centers and resemble mantle cell lymphoma on architectural examination (Fig. 3.133). Cytologically, the presence of the large distinct chromocenters and small nucleoli imparts much more internal nuclear detail than is present in mantle cells, and is also distinct from the peripheralization of chromatin and large nucleoli in marginal zone cells. Mitoses are more frequent than in either of the latter two diseases, and generally several are present in each field at 400× (Fig. 3.134).

Spleen

Splenic involvement is diffuse with uniform organ enlargement, but it is primarily related to the arteriolar system and presents a fine multifocal nodular proliferation. The homing pattern of the neoplastic cells is like that of the nodes with fading germinal centers, whereby a central cluster of small darkly stained benign mantle cells is surrounded by a lighter-stained encirclement of PLL cells (Fig. 3.135). The distinction from marginal zone cells is again on the chromatin pattern, smaller nucleoli, and more frequent mitoses (Fig. 3.136).

Other Organs

Animals with high levels of PLL cells in blood have a sinusoidal pattern in the liver like that of CLL, but despite early splenic involvement the liver is usually not a major site of colonization.

Immunologic Features

PLL is not well characterized by immunological or other methods. In contrast to B-cell CLL, the PLL cells in blood tend to express surface immunoglobulin consistently. B-cell PLL cells express CD79 alpha and lack CD3.

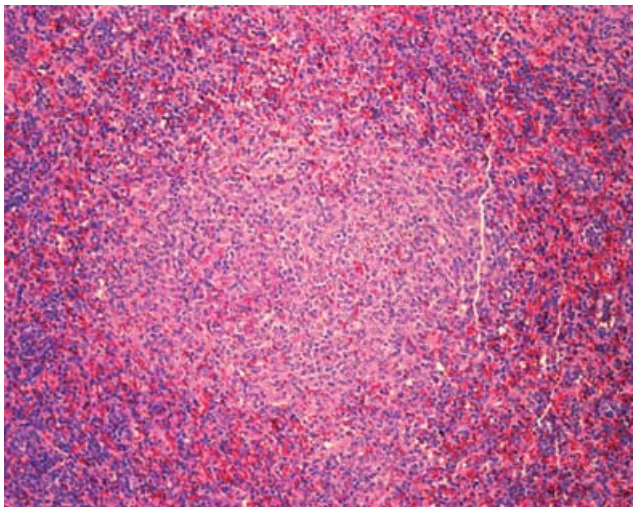

Figure 3.135. Human: spleen, PLL. Architecturally, the tissue is dominated by foci of compact cellular proliferation with periodicity of end arterioles (Fig. 3.111). These are surrounded by a rim of tissue with increased density of red cells typical of perifollicular sinus. *Slide from Cornell Tutorial.*

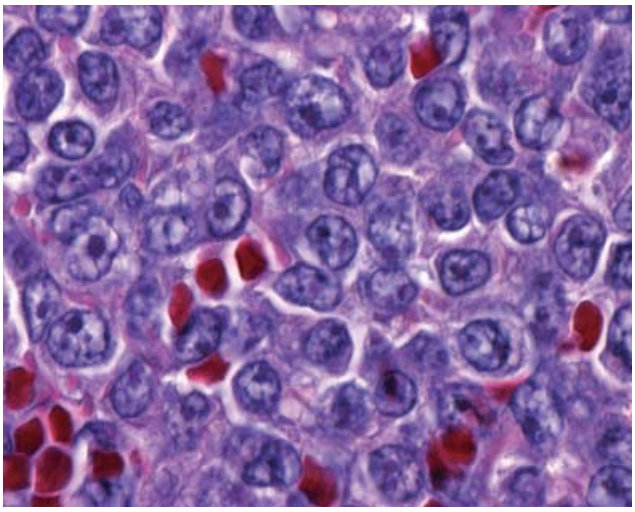

Figure 3.136. Human: spleen, PLL. Detail of Figure 3.135. In the area of the follicular center, there are a few larger cells (left) with most of the nuclei of intermediate size. There is a branched chromatin pattern and prominent parachromatin clearing. There are prominent nucleoli with moderate cytoplasmic volume and staining density and with cell boundaries generally distinct.

Cytogenetic and Molecular Features

B-cell PLL cells have clonal rearrangement of the Immunoglobulin gene.

Cell of Origin

Because the morphologic entity of PLL occurs in both B- and T-cell lineage it is logical that the PLL cell is related to a normal progenitor at a relatively mature stage of lymphoid proliferation. As such, it is most likely that the benign counterpart of PLL is a transition stage that is present for only very short periods of time because there is no natural tissue architectural or blood reactive picture in which lymphocytes with the characteristic PLL nuclear chromatin pattern predominate.

Diagnostic Criteria

PLL cells must predominate in the blood for the diagnosis to be made. They have nuclei that are round to oval and may have smooth, occasionally deep, but not sharp shallow indentations, and they are 1.5 red cells in diameter. The cytoplasm is moderate in volume, with most cells about 2.0 red cells in diameter, but some have relatively abundant cytoplasm that is always lightly basophilic and moderately eccentric so that there is not a complete rim of cytoplasm evident on most cells. The chromatin pattern is characteristic, and it must be examined with a 100× objective to be fully recognized. There are multiple (10–15), irregularly shaped, densely stained areas of chromatin that are joined by irregular chromatin bands delineated by small areas of parachromatin clearing (see Figs. 3.129, 3.130). Most cells lack nucleoli, and in the body of the blood film where the cells are less flattened, there is at least mild anisokaryosis with the larger cells having relatively inapparent nucleoli and representing the dividing cell population. As the disease progresses, the proportion of these large cells increases with increasing levels of leukemic cells. Mitotic cells are rarely encountered in the blood.

Differential Diagnosis

PLL must be differentiated from CLL of B- or T-cell type and from lymphoplasmacytoid lymphoma cells if in leukemic phase. In human conditions, PLL must be differentiated from *hairy cell leukemia* (Figs. 3.137–3.143) and from the leukemic phase of mantle cell lymphoma (Figs. 3.144, 3.145). Neither of these categories is recognized in animal oncology, but the cells of splenic marginal zone lymphoma gain polar cytoplasmic extrusions in the blood and have nuclei and cytoplasmic volume of similar dimensions to PLL. Because marginal zone lymphoma is relatively common in dogs, there may be conditions not described where these cells enter the circulation and constitute a lymphoid leukemia of "intermediate cells" not unlike PLL in size, but with very dissimilar nuclear characteristics with the large single central nucleolus of MZL cells (Figs. 3.146–3.148).

Staging

There is insufficient characterization of B-PLL for helpful comment. It appears that most cases are identified late in

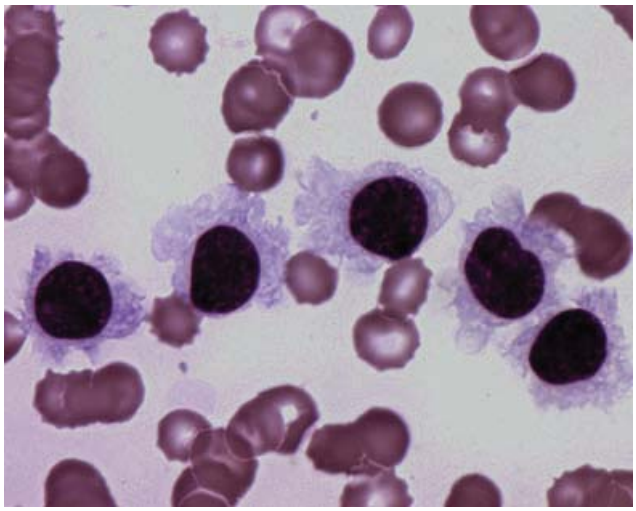

Figure 3.137. Human: blood, hairy cell leukemia. Hairy cell leukemia has not been recognized as a diagnostic entity in domestic animals. The cytoplasmic boundaries are visibly irregular and in wet mount under dark field or phase contrast staining; there are fine, wispy fibrillar-type projections that are much finer than seen in this air-dried preparation. The nuclei are quite uniformly densely stained and lack the internal nuclear detail of prolymphocytic leukemia. *Slide from Cornell Tutorial.*

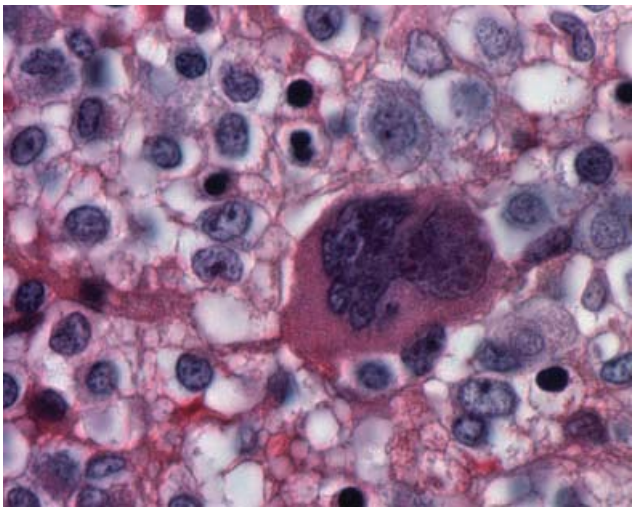

Figure 3.139. Human: bone marrow, hairy cell leukemia. The histologic appearance of hairy cell leukemia is typical in most tissues due to the quite uniform round regular nuclei with abundant cytoplasm and well-defined cell margins. A residual megakaryocyte is present with the much darker and smaller nuclei representative of late-stage rubricytes. *Slide from Cornell Tutorial.*

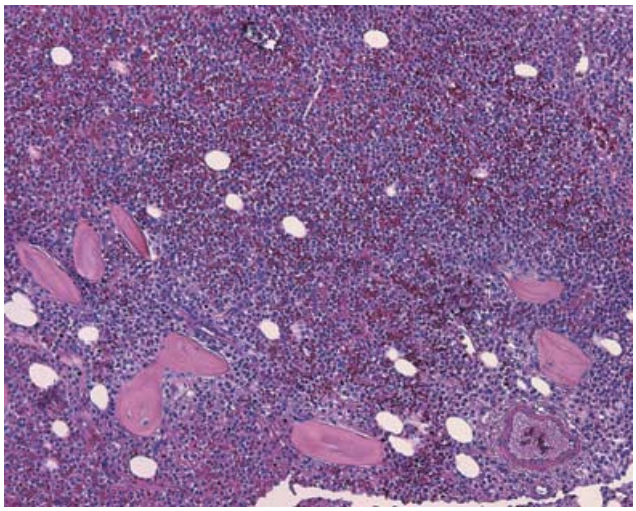

Figure 3.138. Human: bone marrow, hairy cell leukemia. An advanced case with heavy marrow involvement with a marked reduction in fat cells but presenting a homogenous pattern with almost complete phthisis of normal marrow cells. *Slide from Cornell Tutorial.*

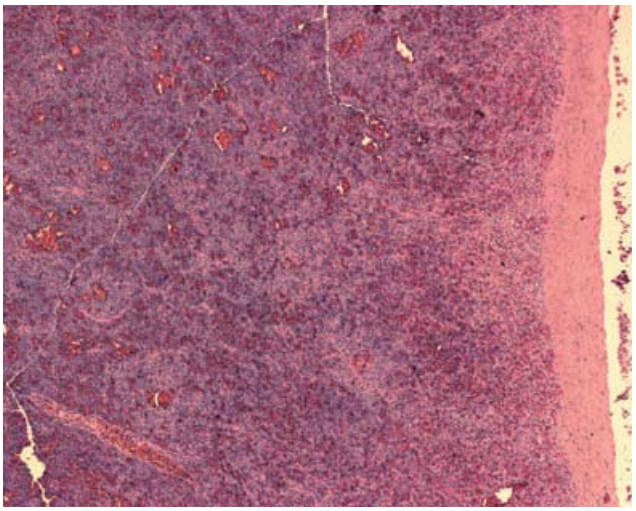

Figure 3.140. Human: spleen, hairy cell leukemia. Splenic involvement with hairy cell leukemia presents a characteristic image with very diffuse sinus involvement with round regular cells with quite abundant cytoplasm. Architecturally, there is atrophy of thymic-dependent areas, and the lesion resembles that of splenic mast cell tumor or plasmacytoma in the cat. *Slide from Cornell Tutorial.*

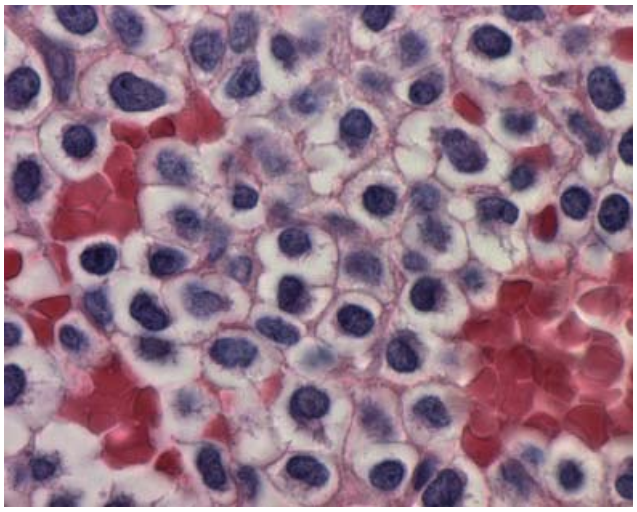

Figure 3.141. Human: spleen, hairy cell leukemia. Detail of Figure 3.140. There is marked thickening of the sinus cords with the splenic sinus vascular areas (lower right) less apparent. The hairy cells appear in sheets of closely aggregated cells with abundant water-clear cytoplasm with relatively round uniform nuclei with relatively few mitoses.

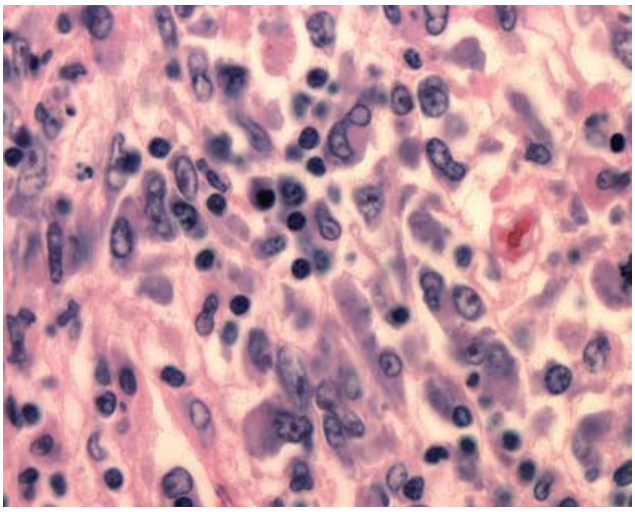

Figure 3.143. Human: lymph node, hairy cell leukemia. The tissue has relatively low cellularity with phthisis of the benign cells represented by small dark residual mantle cells, with the neoplastic cells having abundant cytoplasm relatively deeply stained but not uniformly surrounding the nucleus as in the spleen. *Slide from Cornell Tutorial.*

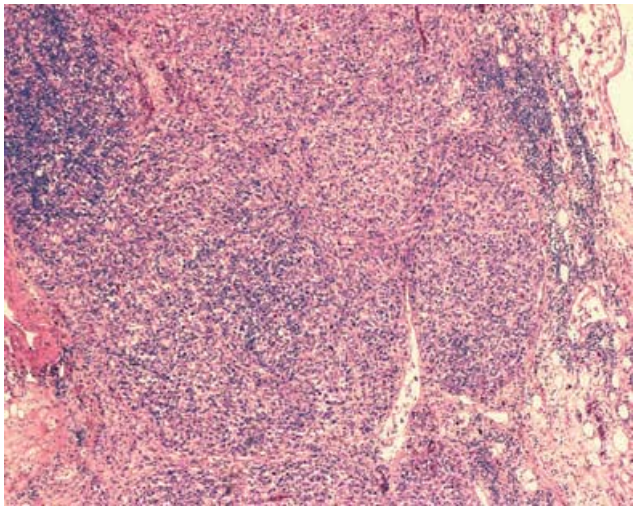

Figure 3.142. Human: lymph node, hairy cell leukemia. The more darkly stained areas represent residual benign small lymphocytes that stand out against a background of neoplastic infiltration by cells with abundant cytoplasm that give a less dense appearance on architectural examination. The peripheral capsule is compressed and irregularly compromised. *Slide from Cornell Tutorial.*

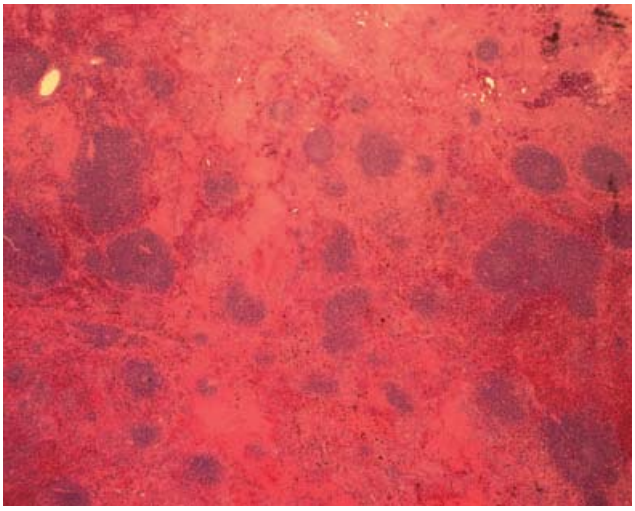

Figure 3.144. Dog: spleen, mantle cell lymphoma. At the architectural level, the blastoid type of mantle cell lymphoma resembles the small cell variant but is more often associated with focal areas of venous ectasia and hemorrhagic infarction.

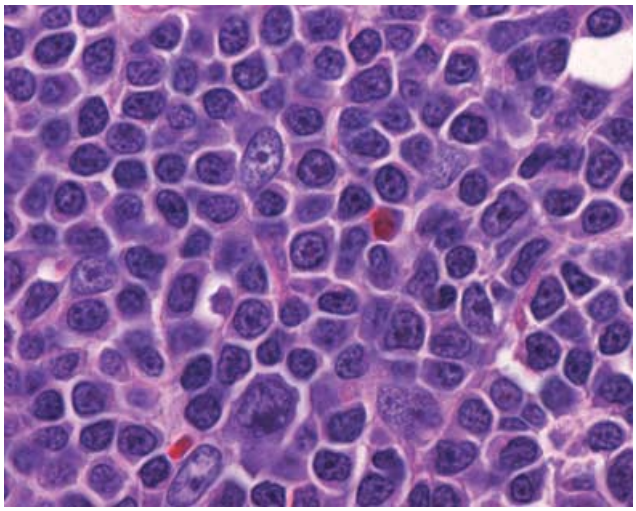

Figure 3.145. Dog: spleen, mantle cell lymphoma. Detail of Figure 3.144. The nuclei are larger than those of the small cell variant with greater internal nuclear detail and most cells 1–2 small but quite prominent nucleoli. The chromatin pattern is coarse granular and the cytoplasm is reasonably abundant and deeply stained. These diseases are known to become leukemic in humans, and cells in the blood from this type of tumor have not been identified in animals.

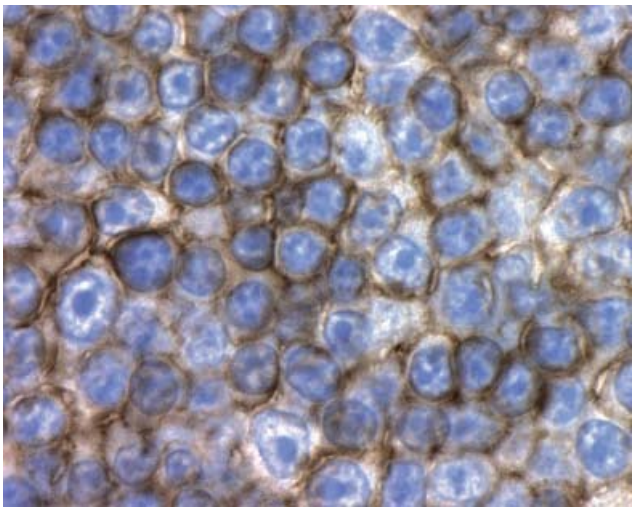

Figure 3.147. Dog: lymph node, MZL. Detail of Figure 3.146. The tissue is stained with CD20 for B-lymphocytes with the intercellular membranes strongly labeled. There is a characteristic pattern of a prominent single central nucleolus that, with a background of chromocenters separated by areas of parachromatin clearing with a relatively abundant cytoplasm, would make these cells a differential diagnosis to distinguish from prolymphocytic leukemia.

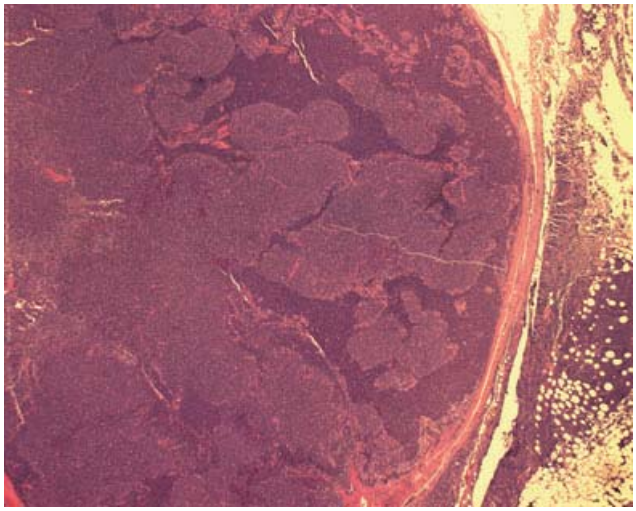

Figure 3.146. Dog: node, marginal zone lymphoma (MZL). Late stage of MZL with typical focal perinodal colonization, irregular thinning of the capsule, and marked and irregular dilation of peripheral sinuses that appear as darker areas colonized by free tumor cells and red cells. There is complete loss of fading germinal centers and the nodular areas of proliferation are now coalescing.

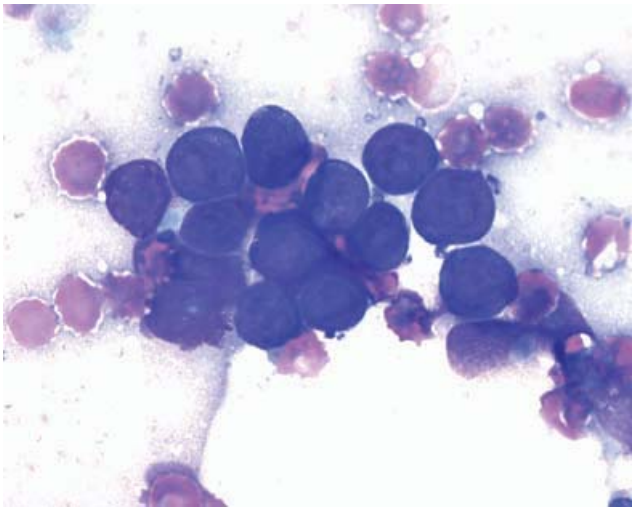

Figure 3.148. Dog: lymph node, marginal zone lymphoma. Cytologic imprint from Figure 3.147. The cells can be seen to be of intermediate size with nuclei approximately 1.5 red cells in diameter. There is a deeply stained cribriform chromatin pattern with a prominent central nucleoli visible. The cytoplasm is relatively abundant but very highly basophilic unlike the level seen in prolymphocytic leukemia.

the disease with extensive marrow involvement and are electively terminated.

Transformation and Progression
The progression of PLL is by increasing levels of circulating neoplastic cells with slightly larger nuclei and by a greater proportion of cells bearing prominent nucleoli.

Evaluation of the Treated Animal
No information on this aspect.

Treatment and Survival
Treatment and response of PLL have not been specifically identified. It is likely that the disease responds like CLL in accelerated phase.

REFERENCES

Álvaro, N.T., Matutes, E., Jaén, M.J., Font, F.L., Domingo, A., Bosch, P.R., and Salvadó, U.T. (2002) Prolymphocytic leukaemia and Hodgkin's lymphoma. *Eur J Haematol* 69:182–184.

Gribben, J.G., Harris, N.L., and Dalla-Favera, R. (2004) Small B-cell lymphocytic lymphoma/chronic lymphocytic leukemia and prolymphocytic leukemia. In Mauch, P.M., Armitage, J.O., Coiffier, B., Dalla-Favera, R., and Harris, N.L. (eds.), *Non-Hodgkin's Lymphomas*. Lippincott Williams & Wilkins, Philadelphia, p. 243.

Hercher, C., Robain, M., Davi, F., Garand, R., Flandrin, G., Valensi, F., Vandeputte, H., Albert, A., Maynadie, M., Troussard, X., Simon, G.H., Lespinasse, J., Portefaix, G., and Merle-Beral, H. (2001) A multicentric study of 41 cases of B-prolymphocytic leukemia: Two evolutive forms. *Leuk and Lymph* 42(5):981–987.

Merchant, S., Schlette, E., Sanger, W., Lai, R., and Medeiros, J. (2003) Mature B-cell leukemias with more than 55% prolymphocytes. *Arch Pathol Lab Med* 127:305–309.

Valentine, B.A., and McDonough, S.P. (2003) B-cell leukemia in a sheep. *Vet Pathol* 40:117–119.

Marginal Zone and MALT Lymphoma

Definition
Marginal zone lymphoma (MZL) is a clonal proliferation of so-called "monocytoid B-cells," due to their abundant pale staining cytoplasm. The latter designation is not used in veterinary literature but needs to be mentioned because of the confusion of terms used for this neoplasm in human pathology. MZL is a B-cell lymphoma of distinctive architecture and cytologic type that arises as an encircling cuff of proliferation outside of the mantle cell layer of germinal centers. In human pathology, MZL is recognized as three related diseases arising most often in extranodal sites as a MALT (mucosal associated lymphoid tissue lymphoma) type lymphoma in mucosal areas and as nodal and splenic types.

Epidemiology and Incidence
MZL is recognized most frequently in mature dogs and cats and likely occurs in all domestic animals. In dogs, MZL is the most common lymphoma related to germinal center proliferation. In collected reviews of canine lymphoma, the indolent types constitute 20–25%, and of these MZL is the largest segment. In one study of recurrent B-cell lymphoma, 24 of 88 (27%) cases were of low-grade type, and of these 13/88 (15%) were MZL. In a second review of canine lymphomas by Dr. William Kisseberth utilizing immunohistochemistry by tissue array, 17.4% of 380 (66/380) cases initially submitted for diagnosis to Dr. Gary Kociba of Ohio were of MZL type. For comparison, in humans the extranodal MALT type of MZL constitutes about 8% of all cases of non-Hodgkin's lymphoma (NHL). The nodal type of MZL is about 1.8% of NHL and the splenic type about 1% of human NHL. In animals, the MALT type of lymphoma is rarely recognized, which needs to be distinguished from rarely occurring. This is partly because the criteria for diagnosing MALT lymphoma are seldom applied in those mucosal surfaces like intestine where lymphoma frequently occurs (Figs. 3.149–3.152). In humans, splenic MZL is a diffuse disease, whereas in the dog, splenic MZL is neither rare nor diffuse and occurs as a focal splenic mass often identified in asymptomatic dogs presented for other reasons (Figs. 3.153–3.157). In other domestic animals, many of

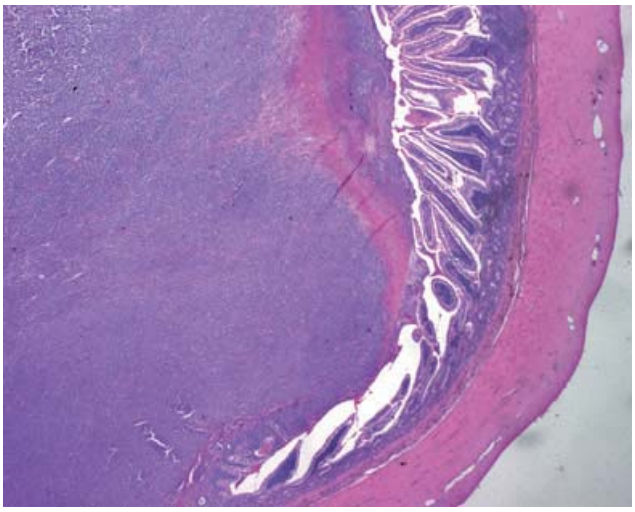

Figure 3.149. Cat: ileum, lymphoma. This image is of an enteric mass 2.2 × 2.8 cm localized to the small intestine with penetration of the muscularis deep to the lower area of the picture with a residual slitlike lumen of small intestine without physiologic obstruction. Note the partial destruction of glands in the lower center area.

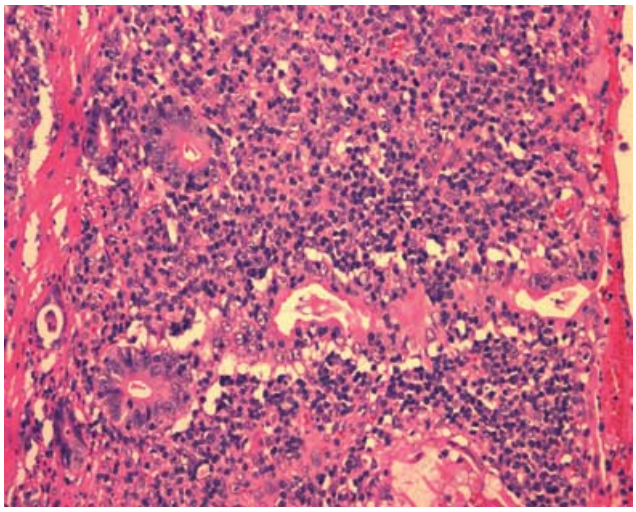

Figure 3.150. Cat: ileum. Detail of Figure 3.149. The enteric surface is at the right with the muscularis mucosa at the left. Several glandular structures are partially or almost completely invaded by the lymphoid proliferation forming the "lymphoepithelial lesion."

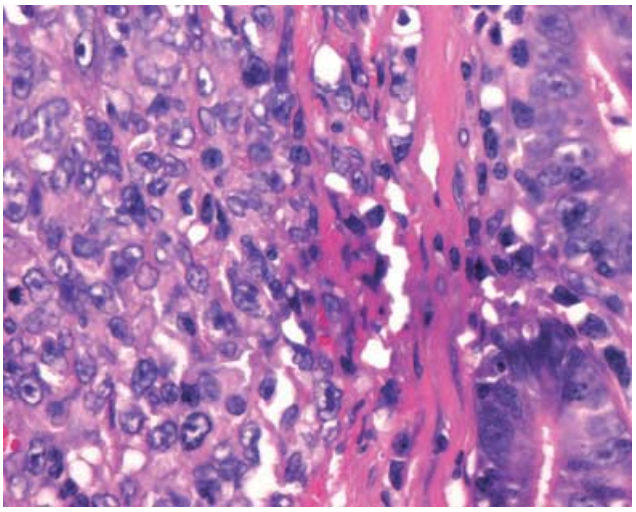

Figure 3.152. Cat: ileum. Detail of Figure 3.151. There are 2 compressed and invaded residual glands above the muscularis mucosa at the right, and the mass of lymphoma cells to the left can be seen to have quite variable nuclear size and shape with vesiculation and prominent nucleoli. Despite the aggressive appearance of the neoplastic lymphocytes, the mitotic rate is surprisingly low, and the tumor has characteristically remained localized to the area while increasing in size over a number of months.

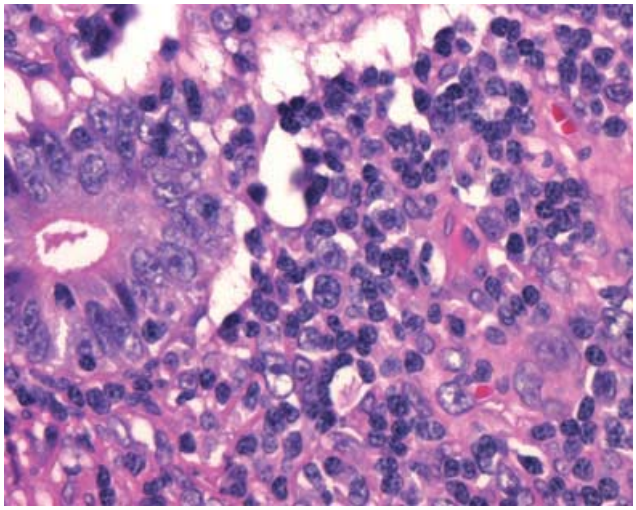

Figure 3.151. Cat: ileum. Detail of Figure 3.149. An intestinal gland at the left has infiltration of small- or medium-sized lymphocytes while larger more vesicular nuclei in the lower right invade a gland that is now almost completely destroyed. The small dark-staining lymphocytes are likely residual benign cells of the intestinal mucosa; cells with larger nuclei that appear vesicular with prominent central nucleoli are typical of the tumor population.

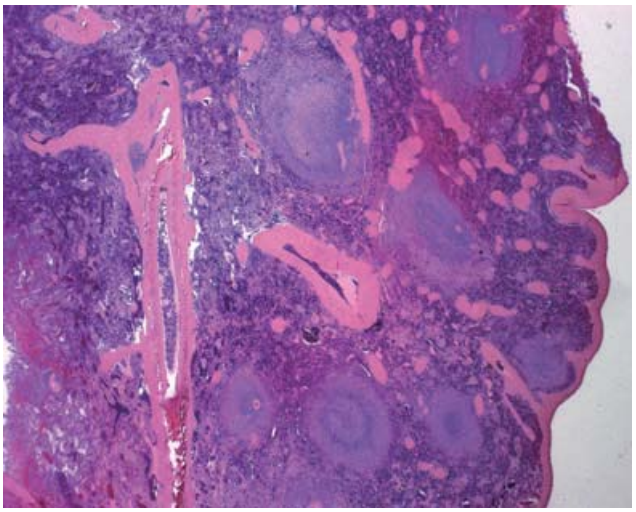

Figure 3.153. Dog: spleen, MZL. An early stage of tumor progression that has fading germinal centers and beginning coalescence of adjacent follicular structures.

the larger reviews were reported in the era of lymphoma classification by the NCI Working Formulation, which recognized follicular lymphoma but not mantle cell or marginal zone lymphomas.

Clinical Presentation and Features

The most characteristic presentation of MZL is in a mature large breed dog that presents with a single enlarged lymph node, often submandibular. The animals invariably feel well and have normal appetite and activity. The nodes are always mobile and there is seldom any local pericapsular spread. Cases with splenic involvement

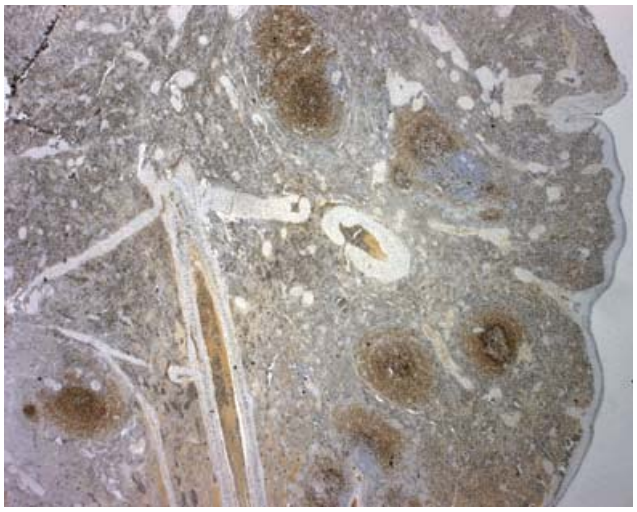

Figure 3.154. Dog: spleen, MZL. Phenotype of Figure 3.153. With CD79 stain the follicular areas stand out against background sinus areas with both the follicular centers and peripheral marginal zone all uniformly marked.

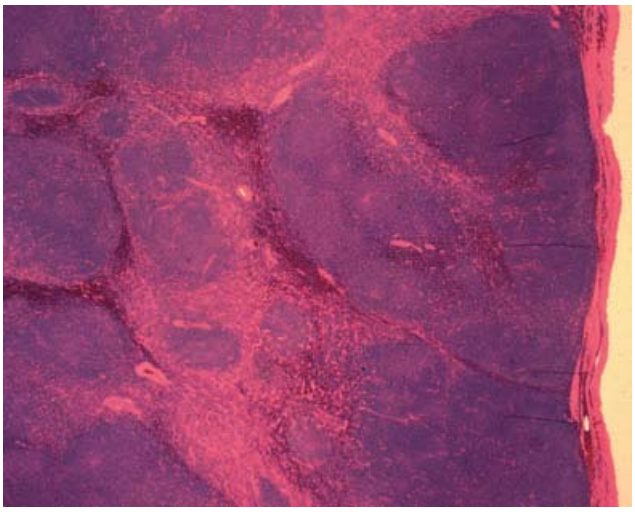

Figure 3.156. Dog: spleen, MZL. Late-stage marginal zone lymphoma with irregular coalescence of follicular areas; the fading germinal centers have now been obliterated and appear irregularly as small pale areas. There is major distortion to the sinus blood flow that frequently results in hemorrhagic infarction.

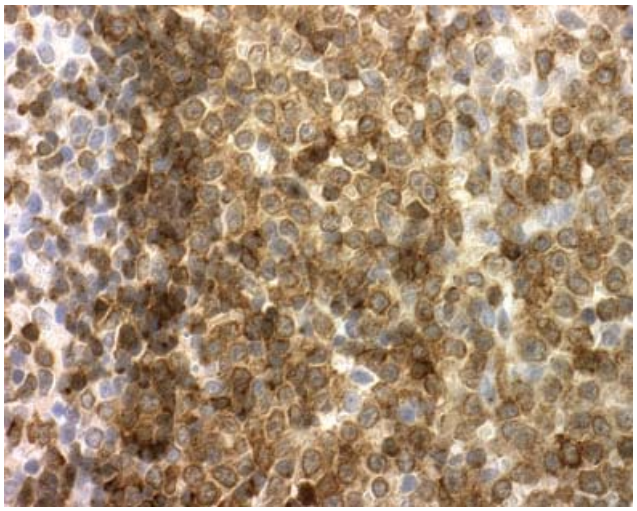

Figure 3.155. Dog: spleen, MZL. Detail of Figure 3.154. The germinal center is at the left, with the narrow band of darker cells the residual mantle cells that lie adjacent to the outer expanding layer of marginal zone cells. The homogeneity of cell type with prominent central nucleoli is characteristic of marginal zone lymphoma at an early stage of development.

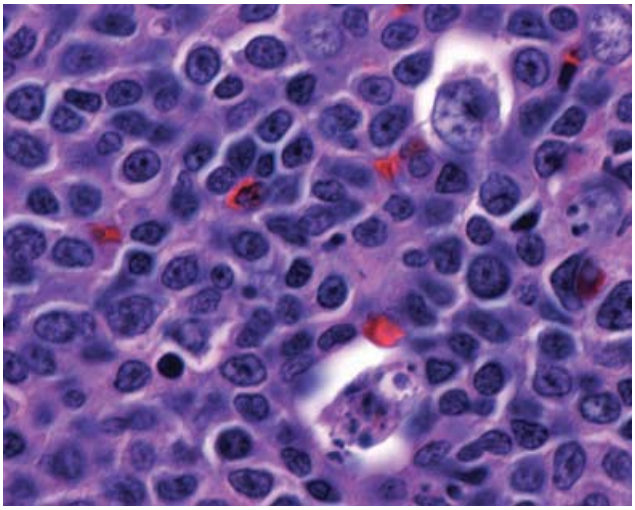

Figure 3.157. Dog: spleen, MZL. Detail of Figure 3.156. The early stages of MZL lack mitoses and tingible body macrophages. After a year or more of progression, mitoses are seen as well as tingible body macrophages, seen at the right and lower center.

usually present with no evidence of lymphoma in other tissues and, in the dog, as in humans, MZL is the type of lymphoma most likely to be primary in the spleen. Spread from the spleen is slow and likely to go to the hilar nodes and thus removed in routine splenectomy. Both the nodal and splenic MZL progress slowly, but only the nodal type tends to become generalized, after 18 months to 2 years of initial lymphadenopathy. Dogs with late stage MZL still tend to feel well even with bulky adenopathy.

Pathologic Features

Blood

MZL has not been noticed to induce leukemia in animals. In most cases the only blood manifestations of MZL are in animals with splenic MZL that may present with thrombocytopenia due to sequestration of platelets in

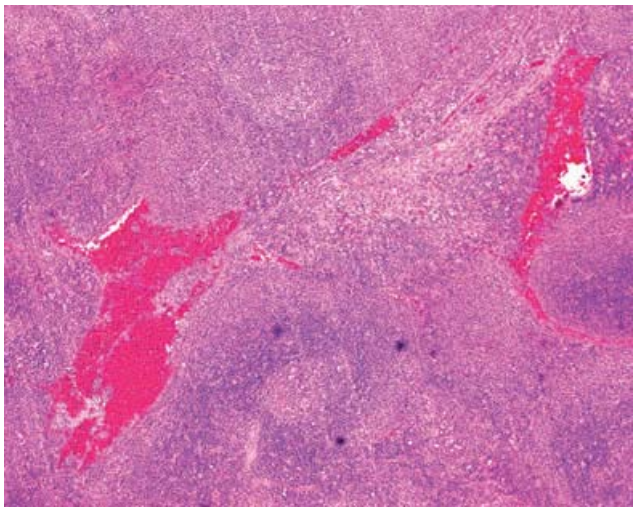

Figure 3.158. Dog: spleen, MZL. Irregular areas of sinus dilation are frequent occurrences both within areas of tumor and in areas of uninvolved spleen adjacent to a large bulging mass of focal tumor. There is stagnant blood flow in these areas, which tends to trap platelets and can result in clinically apparent thrombocytopenia.

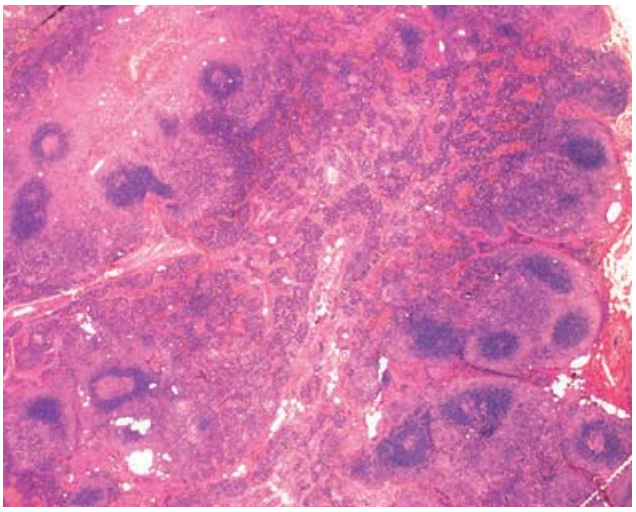

Figure 3.159. Dog: lymph node, MZL. A 13-year-old dog presented with a footpad lesion and an enlarged popliteal node. The architectural presentation is typical of early marginal zone lymphoma, with multiple fading germinal centers represented by clusters of mantle cells, some of which retain a follicular center and some of which are collapsed nodules. There is coalescing marginal zone proliferation around these structures that would be unusual in marginal zone hyperplasia. The center of the image is composed of medullary cord plasma cell hyperplasia and sinus histiocytosis from chronic antigenic stimulation.

stagnant areas of sinus dilatation surrounding and within focal areas of tumor (Fig. 3.158). In human MZL some of the splenic cases become leukemic and of these a particular subset known as *hairy cell leukemia,* which is a type of B-cell CLL, is a consideration for differential diagnosis (see Fig. 3.137). Human cases of splenic MZL that become leukemic tend to have "polar villi" in the peripheral blood and may appear as a unipolar hairy cell. There does not appear to be an animal counterpart for this type of cell; however, the report years ago of leukemic reticuloendotheliosis in cats had the sinus pattern of colonization of spleen and liver like that of the human HCL. That disease appears to have disappeared or has been eliminated by the advent of vaccination or testing for feline leukemia virus infection.

Bone Marrow

Bone marrow is seldom found to be involved in any of the three presentations of nodal, splenic, or MALT types of MZL unless the disease is at an advanced stage as judged by nodal changes of increased mitotic rate, sinus dilation, and presence of tingible body macrophages (Fig. 3.159). Blood is rarely noted to be involved with MZL (Fig. 3.160).

Lymph Node

Nodal MZL is the most common presentation in the dog. In almost all cases the node is at least twice normal diameter and the capsule is taut and irregularly thinned. Involvement of perinodal fat is unusual and the peripheral sinus is intact and not breached by the cell proliferation. There is, invariably, fading follicular hyperplasia (FFH), with germinal centers extending into the medullary areas and usually some degree of sclerosis of the medulla supporting collagenous raphe (Fig. 3.159). In early stages, the subcapsular germinal centers may still be active and have antigen-related polarity. However, with progression, the follicular center cells atrophy and the residual mantle cells collapse into the hypocellular dendritic cell bed. The characteristic lesion is then formed, with the lighter-staining MZL cells forming a broad cuff around small foci of darkly stained residual benign mantle cells (Fig. 3.161). In hyperplasias, the marginal zone cells are of mixed cell type and the cuff may be discontinuous (Figs. 3.162, 3.163). In MZL, the cell type is homogenously composed of lymphocytes with round to oval nuclei 2 red cells in diameter, a prominent single central nucleolus with peripheralization of chromatin onto the nuclear membrane, and some degree of parachromatin clearing (Fig. 3.164). The cytoplasm is abundant and pale staining, which gives the nuclei an even type of spacing, though cell boundaries are not always distinct. Despite the aggressive appearance of the MZL cells with prominent nucleoli (see Fig. 3.159), there will be an almost complete lack of mitotic activity within the areas of neoplastic proliferation. Progression of nodal MZL is by coalescence of the adjacent areas of proliferation and almost complete loss of paracortical areas and compression of medullary

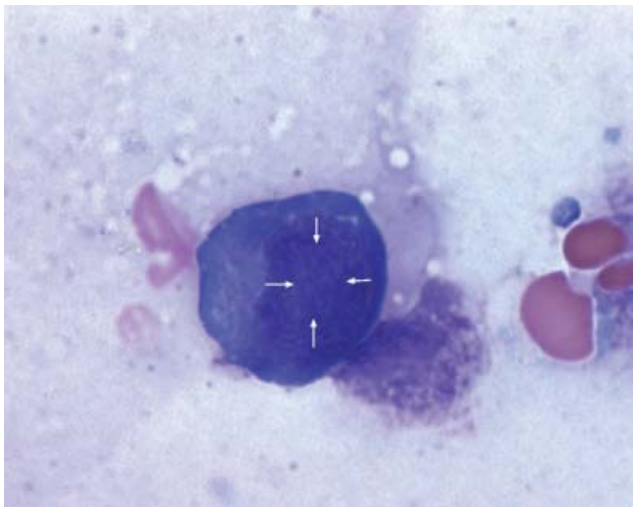

Figure 3.160. Dog: bone marrow, marginal zone lymphoma. The dog did not have lymphocytosis, but atypical cells were occasionally in blood, and in the bone marrow there are cells of intermediate size with dense chromatin and abundant cytoplasm with huge nucleoli that occupy at least a central 1/3 of the nucleus (arrows). In the flattened state of cytological preparations, the nucleoli of marginal zone lymphoma appear even more prominent than in histological preparations.

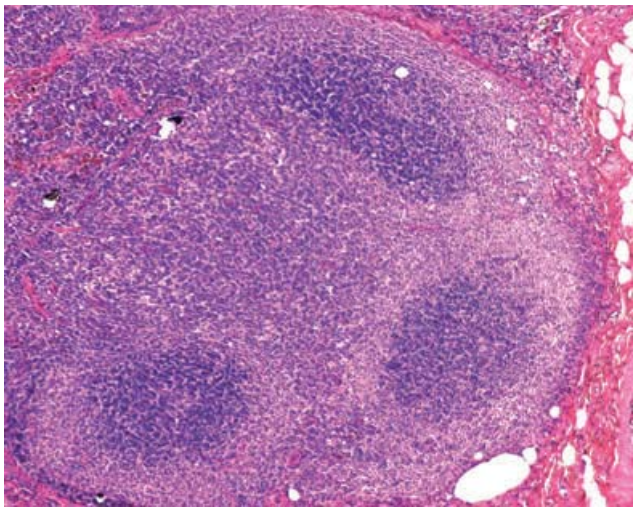

Figure 3.161. Dog: lymph node. Detail of Figure 3.160. With the progression of marginal zone lymphoma, there is involution of the germinal centers with collapse of the mantle cells into the dendritic cell bed. Some centers will retain a slight central pale area (lower left) that indicates their origin from germinal centers.

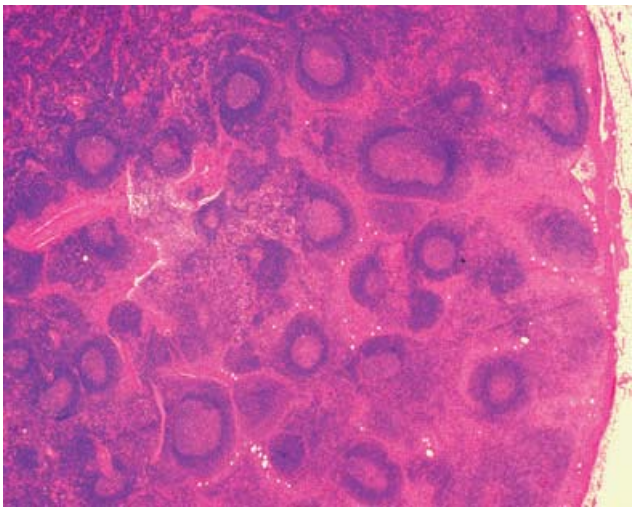

Figure 3.162. Dog: node, marginal zone hyperplasia. The germinal centers retain broad and active central areas with complete encirclement by the mantle cell cuffs. The expanding areas of marginal zone proliferation that are the darker-stained areas outside of the thin mantle cell cuffs are rarely in contact between adjacent follicles.

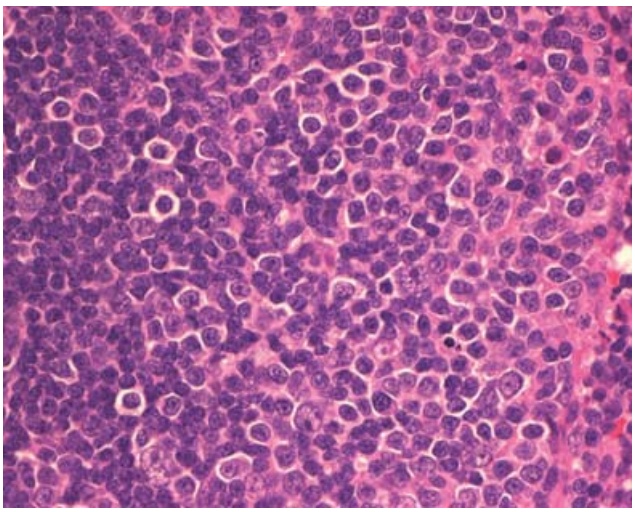

Figure 3.163. Dog: lymph node, marginal zone hyperplasia. Detail of Figure 3.162. The area at the left of the image is at the junction of the mantle cell cuff and the germinal center; the right side of the image is just at the outer limit of marginal zone hyperplasia. The upper region has a heterogeneous makeup, with the marginal zone cells most uniform at the outer margin and irregularly mixed with mantle cells in the mid and inner areas.

cords and sinuses (Fig. 3.165). The changes as described appear to take about a year to develop. In nodes affected for 18–24 months with MZL, there is a progressive and irregular dilatation of the lymphatic sinuses in the outer cortex that contain cells like those of MZL type and are made apparent by an equal number of red cells (Fig. 3.166). These areas may be solidly packed with free cells and be mistaken for solid tissue that is congested (Fig. 3.167). These areas of sinus distension often extend to the subcapsular sinus and may result in the node capsule tearing on sectioning, resulting in a tissue that consists of a fragmented node. The other characteristic change that

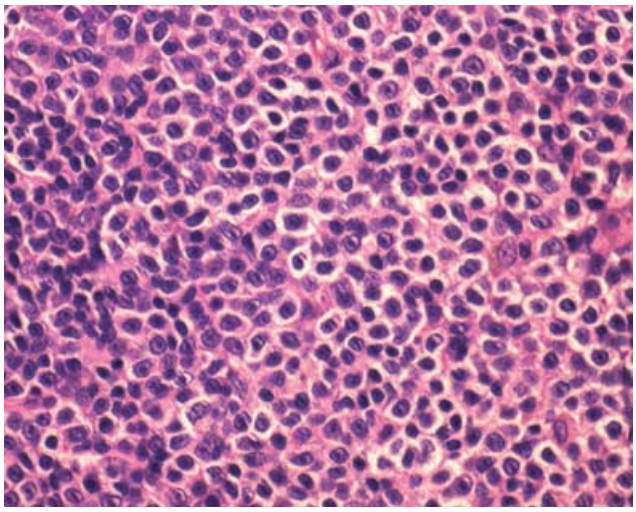

Figure 3.164. Dog: node, MZL. Detail of Figure 3.161. Note that although the architectural differences between the hyperplastic and neoplastic conditions are easily misinterpreted, the cytologic changes are very consistent and specific. In contrast to the relatively mixed cell population of the marginal zone area in the node with hyperplasia (Fig. 3.163) in this image of early marginal zone lymphoma, the homogeneity of cell type in the marginal zone area is readily apparent, with most cells having a prominent single central nucleolus.

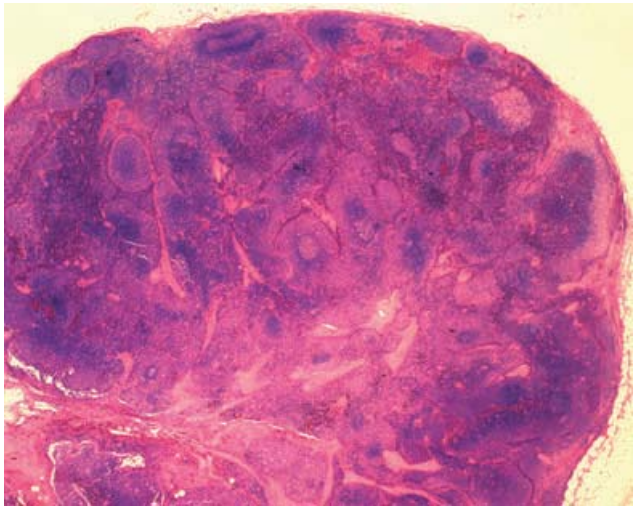

Figure 3.165. Dog: lymph node, marginal zone lymphoma, late stage. The capsule is thinned and taut but there is no involvement of perinodal tissues. The benign residual germinal centers are completely effaced or compressed against the capsule (right upper). The darkly stained foci are areas of germinal centers within the inner cortex that are now obliterated by coalescing marginal zone proliferations.

occurs with time and progression is an increase in the mitotic rate of the MZL cells to 3–5/400× field with an accompanying presence of tingible body macrophages (Fig. 3.168).

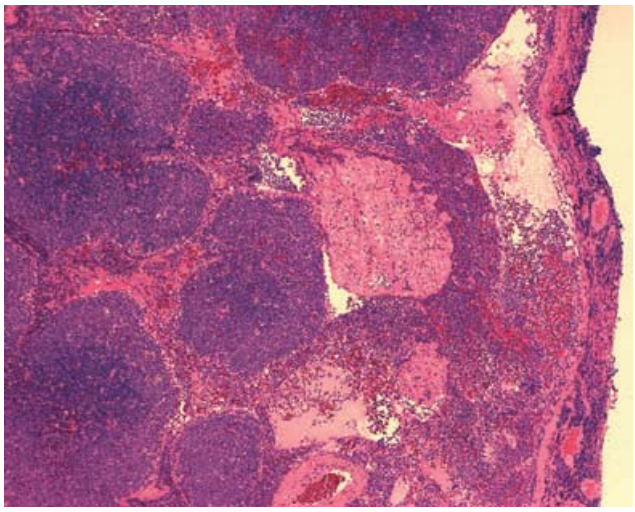

Figure 3.166. Dog: lymph node, marginal zone lymphoma, late stage. Detail of Figure 3.165. There is irregular cavitation beneath the node capsule with broad areas of open sinuses irregularly filled with red cells and neoplastic lymphocytes. These areas increase in size with time and if there is thinning of the node capsule, the tissue may fragment on sectioning.

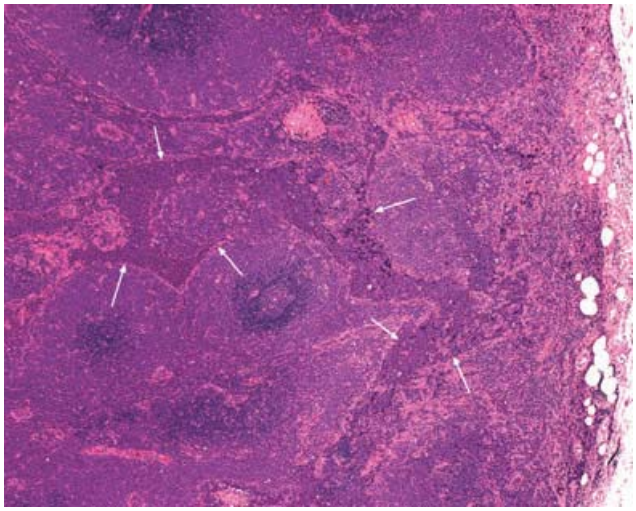

Figure 3.167. Dog: node, marginal zone lymphoma, late stage. There is thinning of the capsule and irregular dilatation of subcapsular sinuses in the outer cortex that are solidly filled with lymphocytes and red cells (arrows) and may be mistaken for solid tissue on architectural examination.

Spleen

Splenic MZL occurs regularly in both cats and dogs, and benign marginal zone hyperplasia is, as might be expected, even more common (Figs. 3.169, 3.170). In currently reactive spleens and many hyperplasias, the splenic perifollicular sinus is more prominent and appears as a reddened border around the mantle cell cuff (Fig. 3.171).

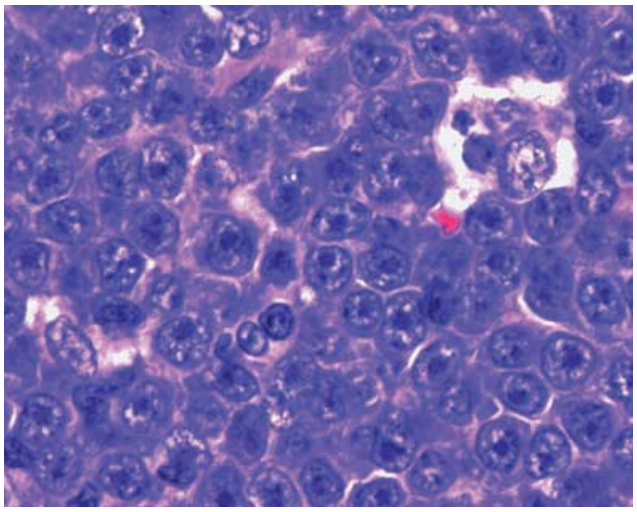

Figure 3.168. Dog: lymph node, marginal zone lymphoma, late stage. Detail of Figure 3.167. There are on average 1–2 tingible body macrophages per 400× field that would not be seen in MZL before mitoses are apparent but with many fewer macrophages than would be seen with a high-grade lymphoma with typical starry sky appearance at architectural examination.

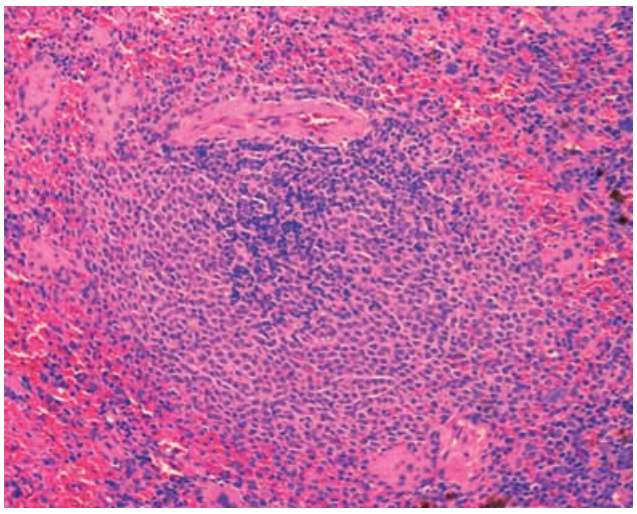

Figure 3.169. Dog: spleen, marginal zone hyperplasia. There is marked atrophy of the periarteriolar lymphoid sheath with very few small lymphocytes remaining adjacent to the vessel. The small deeply stained cells in the center are small benign mantle cells that have collapsed into the center of a fading germinal center. The surrounding larger cells are a relatively homogenous population of larger cells typical of marginal zone areas.

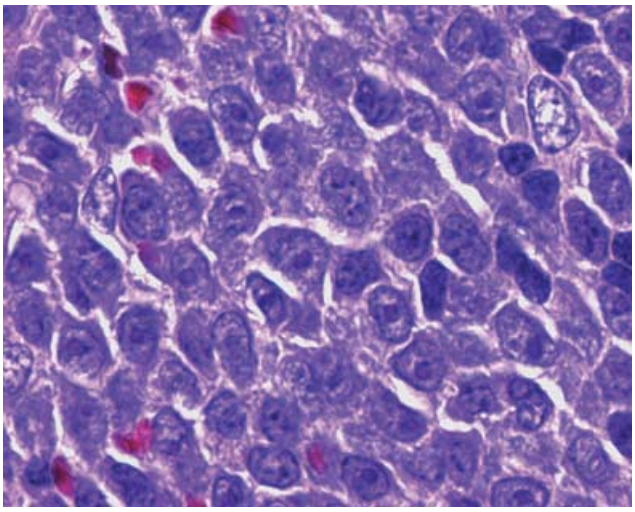

Figure 3.170. Dog: spleen, marginal zone hyperplasia. Detail of Figure 3.169. The small darkly stained nuclei near the right are the mantle cells from the fading follicle. The cells of marginal zone hyperplasia are somewhat heterogenous with variation in size and nucleolar number, likely due to admixed cells of other types.

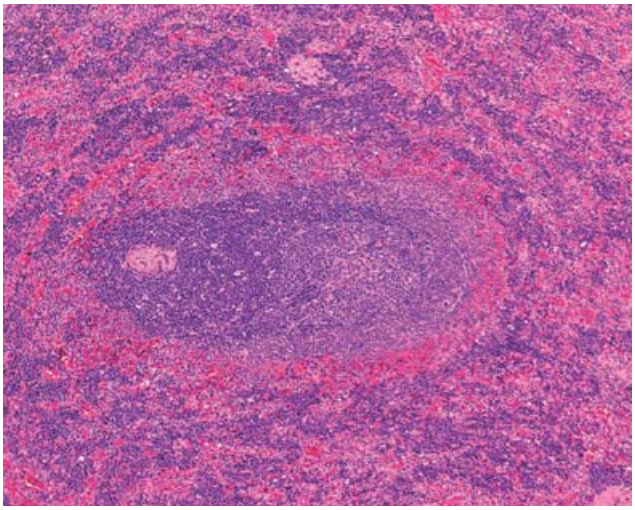

Figure 3.171. Dog: spleen, benign reactive. The sinus areas have marked trilineage hematopoiesis, with the follicular structures highlighted by increased numbers of red cells in the perifollicular sinus.

Splenic marginal zone hyperplasia (MZH) is found with follicular hyperplasia but more often with follicular atrophy. In hyperplastic follicles there is a layer of lighter-staining nucleated cells lying outside the small darkly stained cells of the mantle cell cuff (Figs. 3.172, 3.173); in follicular atrophy the marginal zone cells surround the residual mantle cells and end arteriole (Figs. 3.174, 3.175). Cytologically, in benign proliferations, the MZH cells are of mixed type, including lymphocytes of variable size along with those of MZH type that are distinctive, because of the broad rim, of lightly stained cytoplasm (Figs. 3.176, 3.177). In contrast, in MZL the rim of proliferation is equal to the diameter of the germinal center, making the overall diameter about three times normal size (Figs. 3.178, 3.179). There is less coalescence of the proliferative areas of splenic MZL because the origin of the

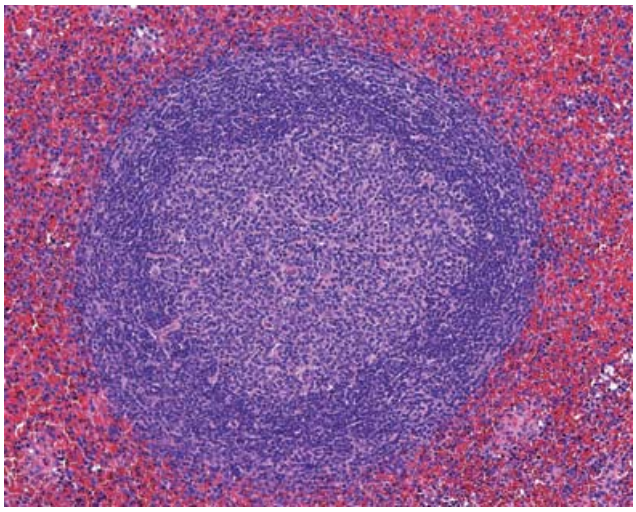

Figure 3.172. Cat: spleen, immune hemolytic anemia. The follicles are reactive with a broad pale area of the germinal center surrounded by dark-staining mantle cells, with the narrow area of lighter-staining cells at the periphery representative of marginal zone hyperplasia.

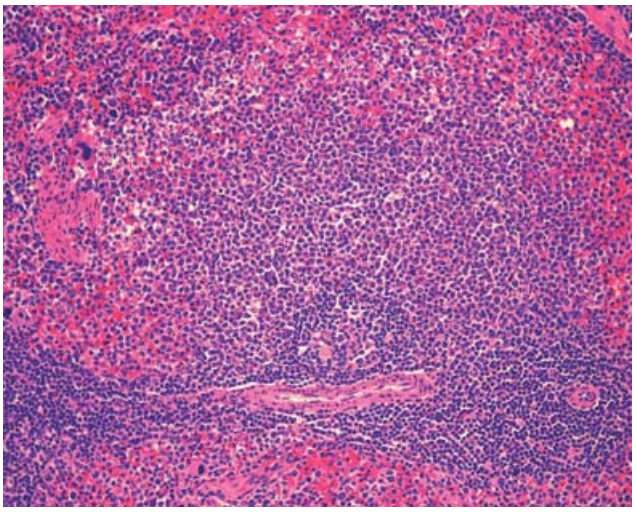

Figure 3.174. Dog: spleen, fading follicular hyperplasia with marginal zone hyperplasia. Spleen from a 2-month-old dog that had severe diffuse dermatitis, with Demodex infestation. The periarteriolar sheaths are small but not atrophic; the germinal centers are in decline with only a very small pale area (lower center adjacent to the arteriole) remaining of this follicle. The lighter-stained area is surrounded by a narrow rim of darkly stained mantle cells cuffed with a broad area of lighter-staining cells of marginal zone hyperplasia.

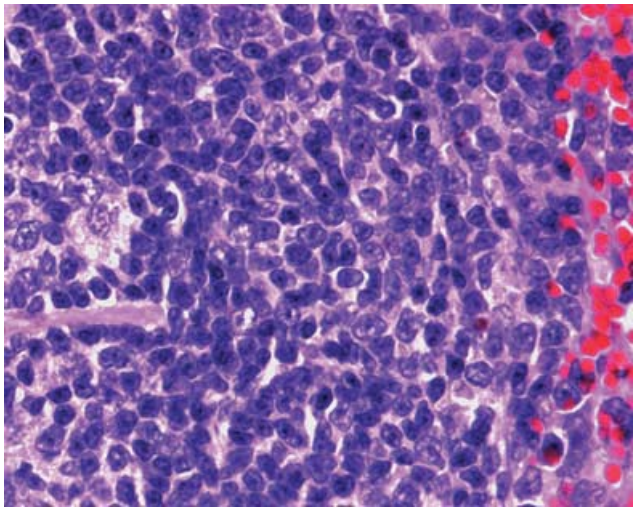

Figure 3.173. Cat: spleen, benign reactive. Detail of Figure 3.172. The sinus area is at the right of the image; the benign marginal zone cells are those in the adjacent area with vesicular nuclei and apparent nucleoli. The darkly stained smaller cells are the mantle cells that end quite abruptly near the left at the edge of the germinal center. The heterogeneity of the outer cell layer helps distinguish marginal zone hyperplasia from early marginal zone lymphoma.

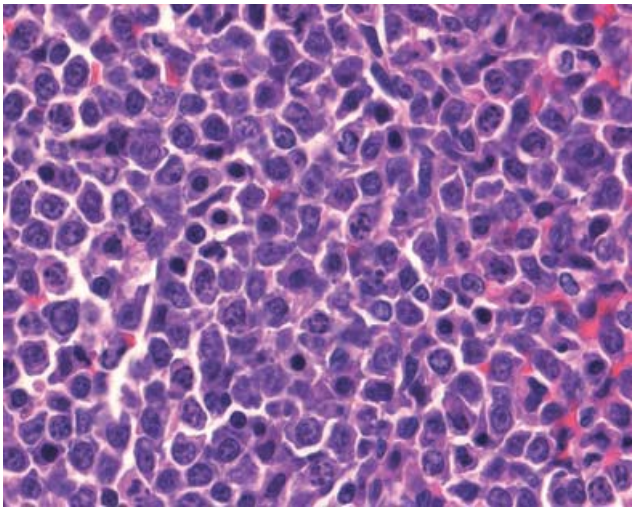

Figure 3.175. Dog: spleen, benign reactive. Detail of Figure 3.174. The interface between the foci of marginal zone hyperplasia with the sinus areas is at the right with increased numbers of red cells. The marginal zone cells have vesicular nuclei with an irregular nucleolar pattern and relatively abundant, highly amphophilic cytoplasm. The admixture of other cell types and absence of peripheralized chromatin aids in distinguishing marginal zone hyperplasia from lymphoma.

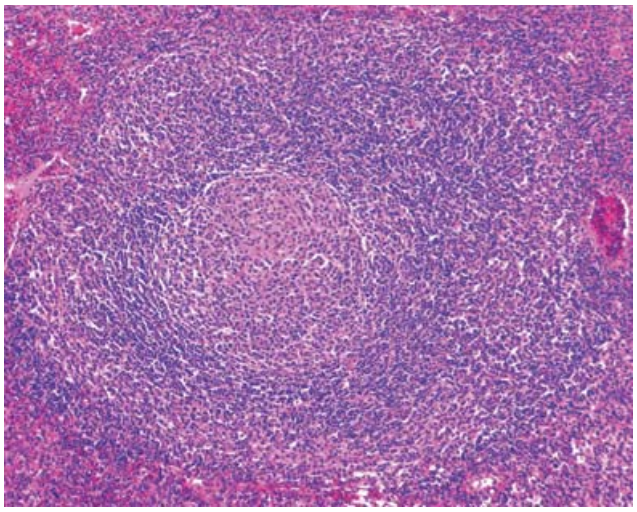

Figure 3.176. Dog: spleen, marginal zone hyperplasia. In benign but vibrant splenic immune reactions, the germinal centers have normal cellular density with the mantle cell rim diluted by infiltration from a broad outer layer of marginal zone hyperplasia.

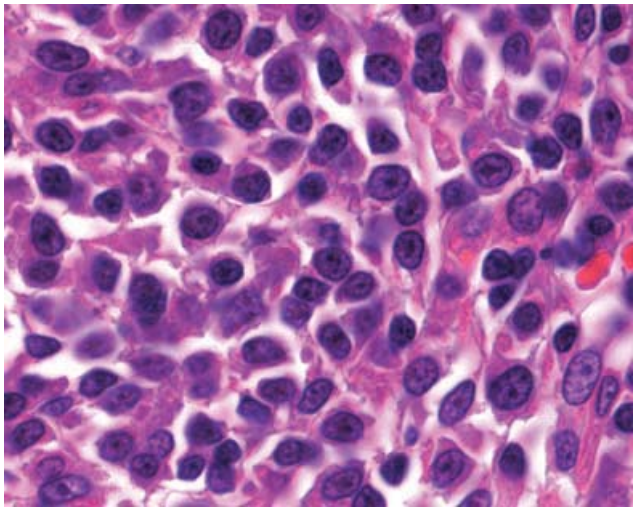

Figure 3.177. Dog: spleen, marginal zone hyperplasia. Detail of Figure 3.176. The outer edge of the marginal zone layer is at the right. Note that the nuclei of cells with prominent central nucleoli are 1.5–2.0 times the diameter of the red cells. The chromatin pattern is largely dispersed, with some increased prominence of nuclear membranes of benign marginal zone cells within an irregular admixture of smaller lymphocytes with compact nuclei and small or absent nucleoli. The abundance of cytoplasm and relative spacing of nuclei is characteristic.

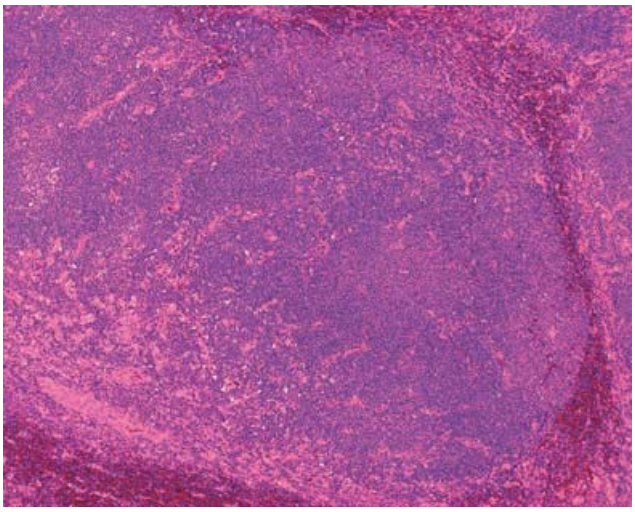

Figure 3.178. Dog: spleen, marginal zone lymphoma. A late-stage marginal zone lymphoma in which the germinal center is now obscured by neoplastic cellular colonization. The area depicted is at least twice the size of a benign reactive germinal center with marginal zone hyperplasia.

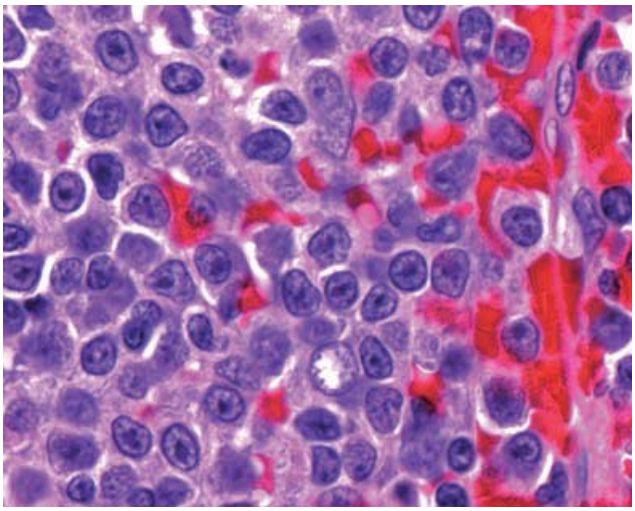

Figure 3.179. Dog: spleen, marginal zone lymphoma. Detail of Figure 3.178. The edge of the marginal zone region is at the right of the image. Malignant proliferations of the marginal zone cells have greater homogeneity and fewer other cell types present. The nucleoli tend to appear more prominent because there is peripheralization of chromatin with more generalized parachromatin clearing. Although the area is small, it is important to note that there are, characteristically, no mitotic figures.

germinal centers on end arterioles insures their separation in a more even pattern than in nodal MZL. In the cat, MZL is more like the human form with a uniform involvement of all follicular areas (Fig. 3.180), while in the dog, MZL appears invariably to be a focal and locally extensive disease. It may be that in the cat, a splenic lesion with three cellular layers in the germinal centers (follicular center cells, mantle cells, and marginal zone cells, Fig. 3.181) in a bulls-eye configuration is already a malignant neoplasm. In humans, splenic MZL is always a diffuse disease involving all areas of the spleen, and a three-laminar lesion in one area of a diffusely enlarged spleen

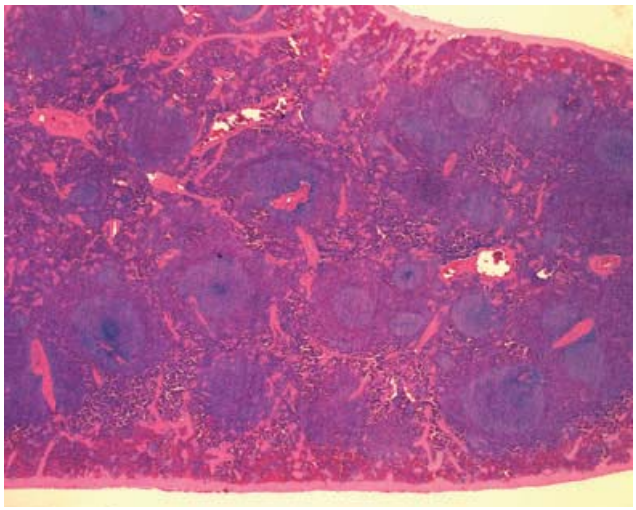

Figure 3.180. Cat: spleen, marginal zone lymphoma. In the cat, splenic lesions are more often diffuse than in the dog. Although the follicular structures are sectioned at different levels, it is apparent that the same process is occurring at all end arterioles throughout the spleen. The changes consist of atrophy of periarteriolar lymphoid sheaths with follicular atrophy and proliferation of a broad corona of marginal zone cells around former follicles.

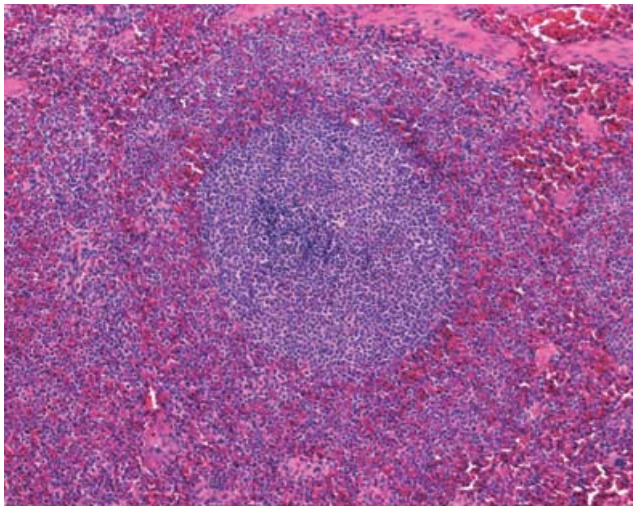

Figure 3.181. Cat: spleen, marginal zone lymphoma. Detail of Figure 3.180. Many follicles in this tissue retain a vestige of the germinal center that has declined to the stage of a collapsed cluster of darkly stained mantle cells present in the center of this image. The central dense cluster of neoplastic marginal zone cells is outlined by the slightly reddened peripheral sinus within an outer corona of less densely stained cells that are also of marginal zone type.

is considered diagnostic of MZL. The cat may be different from the dog in that involvement of the spleen, plus other tissues, may be more common but the cell type is very similar (Figs. 3.182, 3.183).

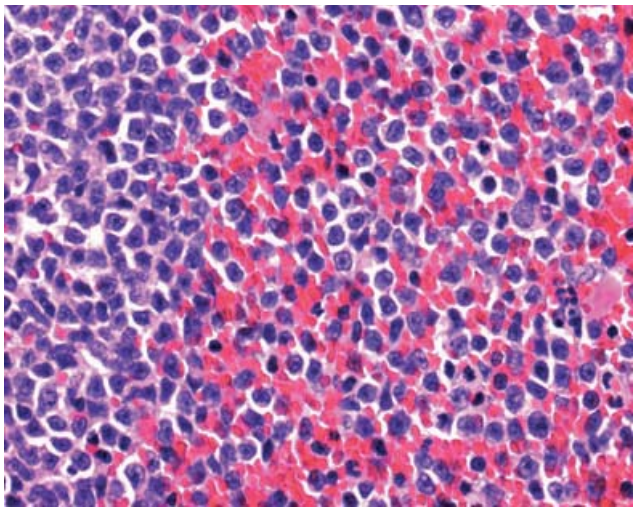

Figure 3.182. Cat: spleen, marginal zone lymphoma. Detail of Figure 3.181. The edge of the outer rim is at the right of the image. The outer ring of cells is mixed with a small number of smaller lymphocytes and the inner solid area is of more uniform cell type.

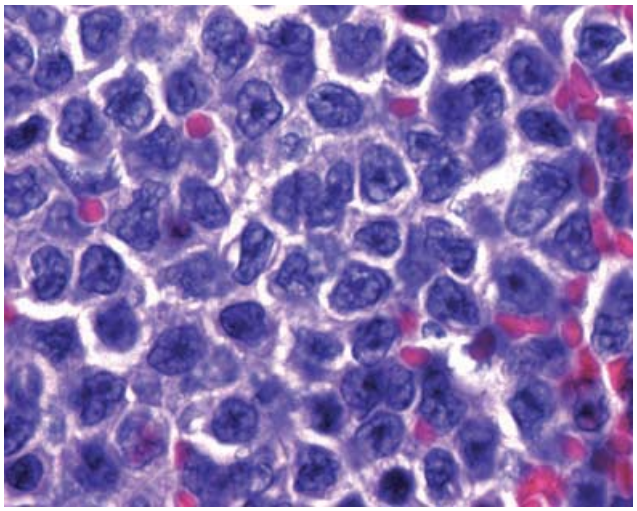

Figure 3.183. Cat: spleen, marginal zone lymphoma. Detail of Figure 3.181. Marginal zone cells in the cat are similar in size to those of the dog, with a more coarsely branched chromatin pattern with a prominent central nucleolus attached by broad chromatin bands to the nuclear membrane. The cytoplasm is abundant with moderate amphophilia and characteristic uniform separation of nuclei. The irregular shape is partially due to delay in fixation.

Other Organs

In the dog, MZL is rarely seen in tissues other than node and spleen, but the MALT variant does occur in dogs as an unusual lesion in the salivary gland of animals with MZL in adjacent submandibular nodes (Figs. 3.184–3.187). A dog with splenosis, likely of very long standing, that developed MZL had tumor in both a

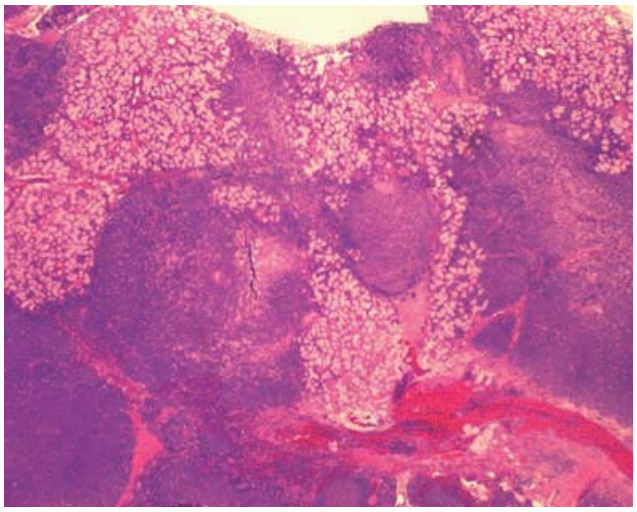

Figure 3.184. Dog: salivary gland, MALT-type lymphoma. The body of the gland is destroyed by a relatively diffuse infiltration of lymphoid tissue displacing and destroying the acini of the sublingual salivary gland.

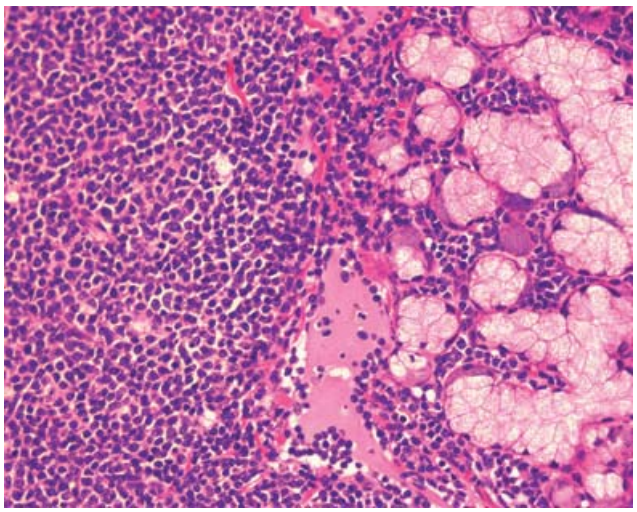

Figure 3.185. Dog: salivary gland, MALT lymphoma. Detail of Figure 3.184. Interface of the lymphoid proliferation and glandular structures. In this image, lymphoma is infiltrating the gland in a tentacular manner advancing along interstitial lines between glandular acini.

primary splenic mass and several mesenteric explants (Figs. 3.188–3.193). In cats, MZL appears to be much less common than in dogs, with 1 case recognized in 50 cases accessed since the disease became recognized in the early 1990s. However, in cases accessed earlier, where spleen was one of the tissues included, MZL has been recognized in retrospect in animals that had involvement of nodes and intestine (Figs. 3.194–3.196).

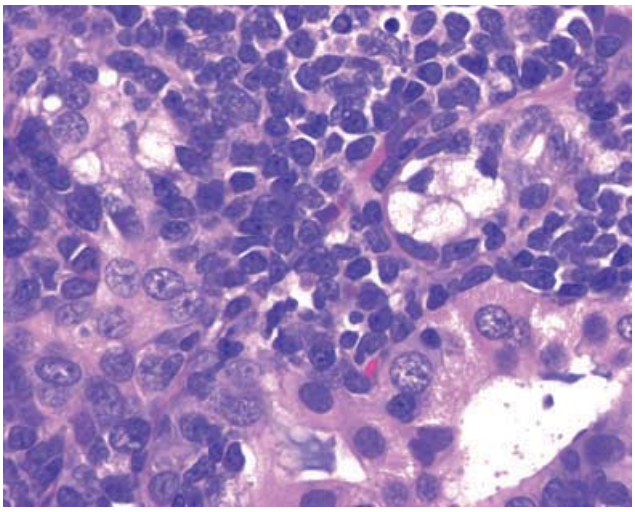

Figure 3.186. Dog: salivary gland, MALT lymphoma. Detail of Figure 3.185. An example of the characteristic "lymphoepithelial lesion" of MALT lymphoma. The upper-left mucus acinus has lymphocytes penetrating the basement membrane and displacing the nuclei. Below, there are series of epithelial cells infiltrated at the borders with lymphocytes. In the upper right is a lesion similar to that below and in the right, a striated duct with irregular penetration of the basement membrane and infiltration of the epithelium.

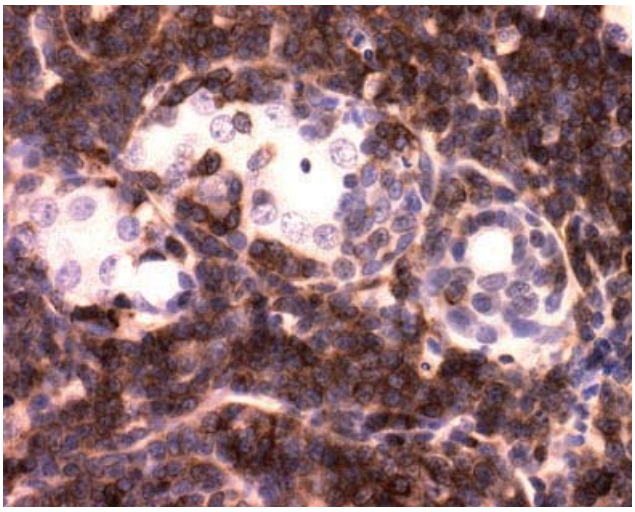

Figure 3.187. Dog: salivary gland, MALT lymphoma. An area similar to that of Figure 3.186 stained with CD79 alpha for B-lymphocytes demonstrating the lymphoepithelial lesion with lymphocytes penetrating the basement membrane and infiltrating between the epithelial cells.

Immunologic Features

Marginal zone lymphomas in animals and in all organ sites are strongly positive with CD79 alpha and CD20 antibodies, and are negative with T-cell markers. Oddly, it appears that some MZL cases stain more strongly in late stages of the disease than early cases, but it is not

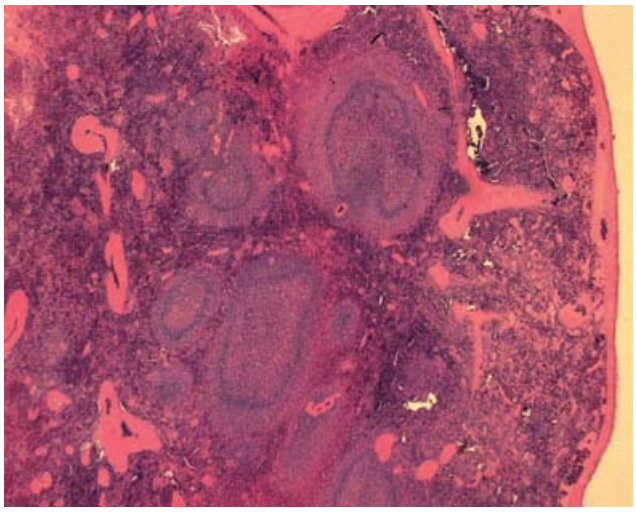

Figure 3.188. Dog: spleen, marginal zone lymphoma. A relatively early stage of marginal zone lymphoma with more advanced areas in outer parts of the spleen. The lesion was clonal on PCR amplification of the immunoglobulin gene.

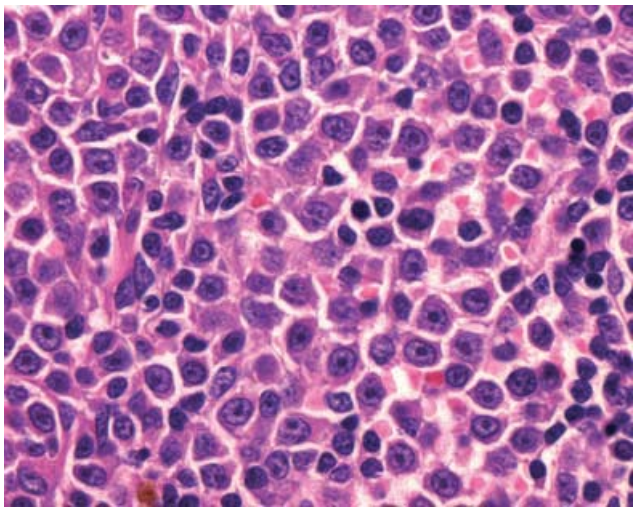

Figure 3.189. Dog: spleen, marginal zone lymphoma. Detail of Figure 3.188. The edge of the mantle cell cuff is at the right. The cells typical of marginal zone lymphoma form a double rim outside a thin linear mantle cell encapsulation visible near the left of the image. There is a relatively mixed population of cells present; however, the peripheralization of chromatin and very distinct nucleoli is characteristic of lymphoma rather than hyperplasia.

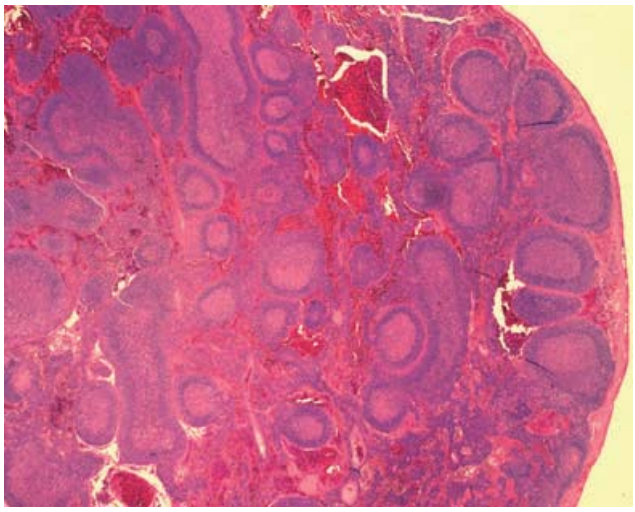

Figure 3.190. Dog: splenic mesenteric explant in splenosis. Image of a 1.7 cm round structure enclosed by smooth muscle and having blood-filled sinuses with lymphoid areas similar to splenic architecture.

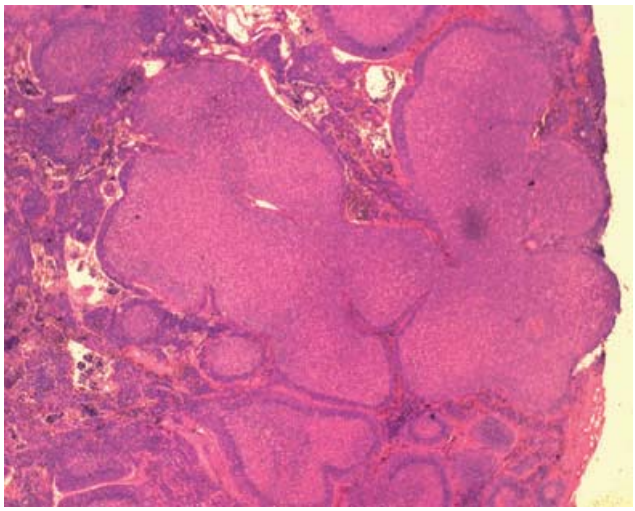

Figure 3.191. Dog: splenosis with marginal zone lymphoma. Detail of Figure 3.190. In another area of the same tissue, there is an abnormal melding of follicular structures.

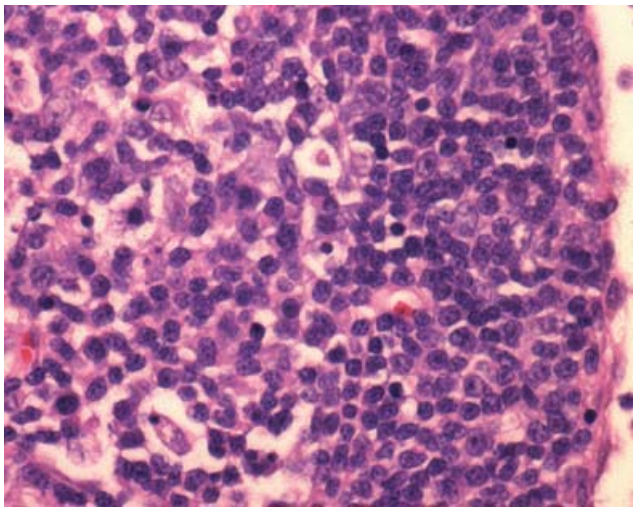

Figure 3.192. Dog: splenosis and marginal zone lymphoma. Detail of the edge of atypical nodular proliferation. Residual mantle and marginal zone cells are thinned into a narrow cuff around an internal area of proliferation that resembles follicular lymphoma.

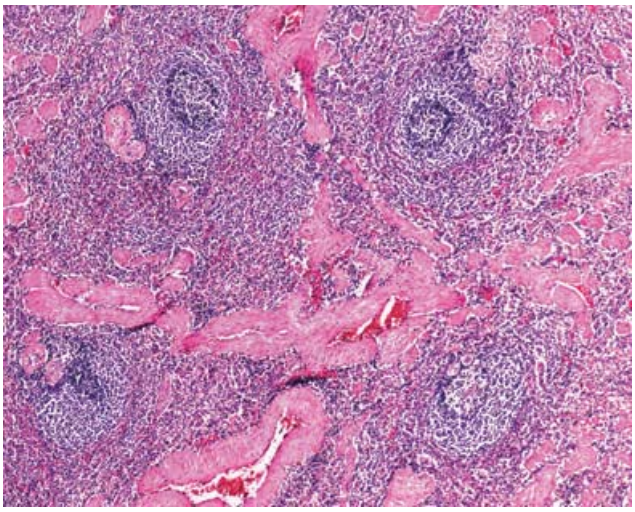

Figure 3.194. Cat: spleen, marginal zone lymphoma. The spleen is contracted with loss of sinus area with thickened smooth muscle trabeculae. The germinal centers are small and fading with broad cuffs of marginal zone proliferation.

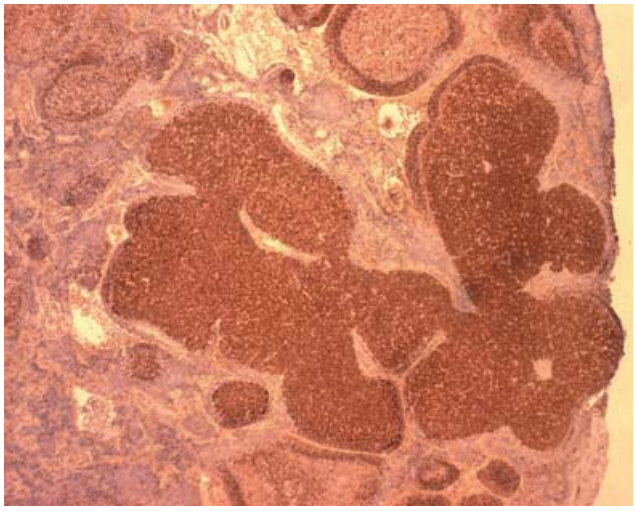

Figure 3.193. Dog: splenosis, marginal zone lymphoma. Detail of Figure 3.191. With CD79 alpha staining for B-lymphocytes, the areas of proliferation are sharply and strongly delineated. Characteristically, the cells of the marginal zone cuff stain more densely for B-cells than for the cells of the germinal center.

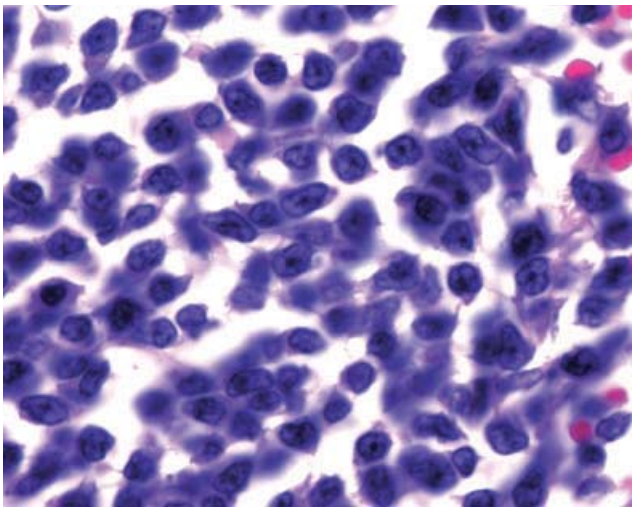

Figure 3.195. Cat: spleen, marginal zone lymphoma. Detail of Figure 3.194. The edge of the marginal zone proliferation is at the right with a few red cells representing interface with splenic sinus. The cells are of intermediate size with characteristic peripheralization of chromatin and a single prominent central nucleolus.

clear that the same case may mark with a different intensity with disease progression (Figs. 3.197–3.199). In human MZL, the nodal form is usually identical to the MALT type and positive for surface IgM and IgG and variable for cytoplasmic immunoglobulin (Figs. 3.200–3.202). These human cases are positive for CD19, 20, and 25 and negative for CD10 and 23 and cyclinD-1. The splenic form of human MZL is very similar to the nodal type. Rarely, cases of MZL have been associated with a macroglobulinemia of Waldenstrom type.

Cytogenetic and Molecular Features

The most consistent cytogenetic changes in human MZL are in the splenic form in which trisomy 3 and trisomy X and the deletion del (10) (q22q24) were found to be recurrent in a small group of patients. In the MALT type of human MZL, the translocation t(11;18) (q21;q21) is seen

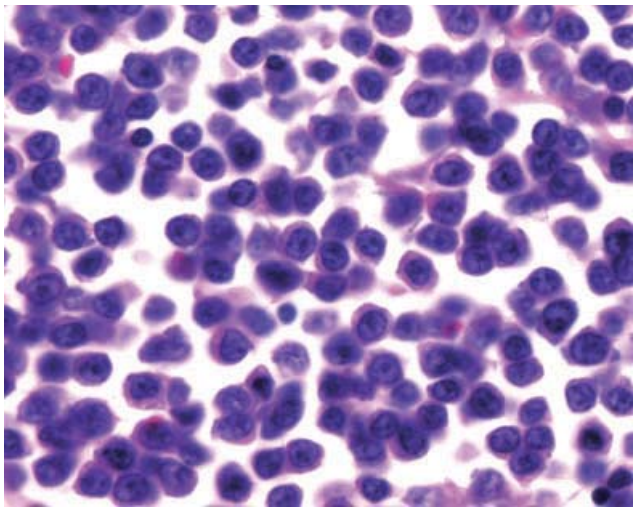

Figure 3.196. Cat: small intestine, intermediate-type lymphoma, same animal as in Figure 3.195. The cells are of the same size category as those in the splenic marginal zone areas and are likely of the same phenotype. Note the prominent single central nucleoli with quite abundant moderately amphophilic cytoplasm with relatively low mitotic rate.

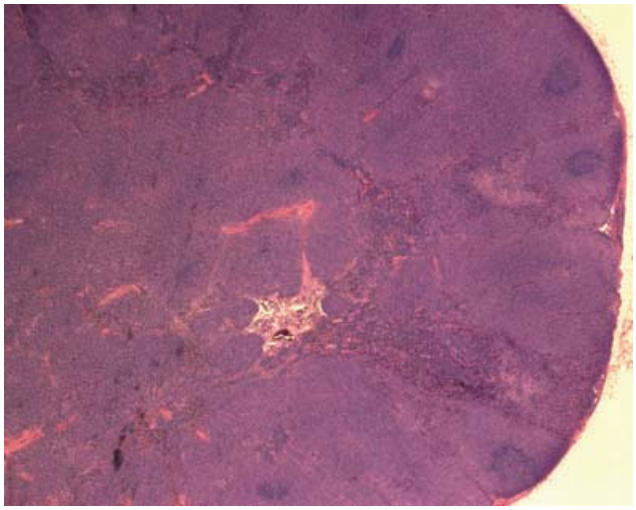

Figure 3.197. Dog: lymph node, MZL, late stage. There is coalescence of the cortical areas of proliferation with 3 subcapsular fading germinal centers still apparent. The slightly darker areas represent residual areas of paracortex and sinus areas occupied by a variety of smaller cells with less cytoplasm that have a greater density on architectural examination.

in 20–40% of gastric cases, but is seen at lower levels in MZL in other mucosal sites. The cases of nodal MZL appear to have less consistent recurring chromosomal changes. A recently described differentiation antigen IRTA1 (immune receptor translocation associated-1) appears to be specific for nodal MZL in a variety of sites.

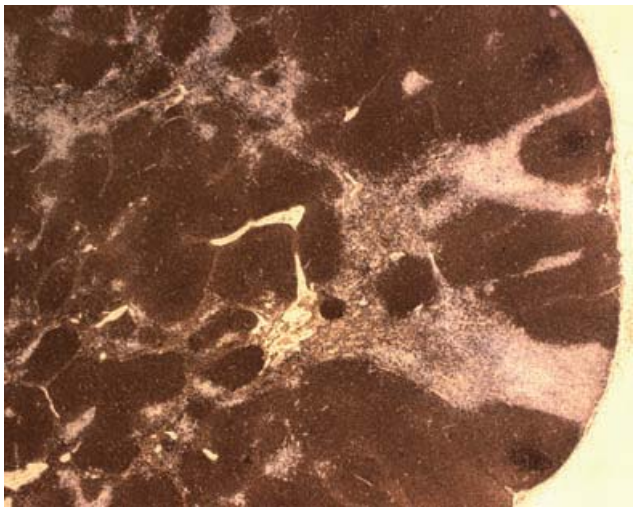

Figure 3.198. Dog: lymph node, marginal zone lymphoma, late stage. Phenotype of Figure 3.197. The cortical area is irregularly colonized by marginal zone cells that mark strongly with CD20 for B-cells. The residual areas of paracortex and irregular areas of sinus dilation have only scattered positivity.

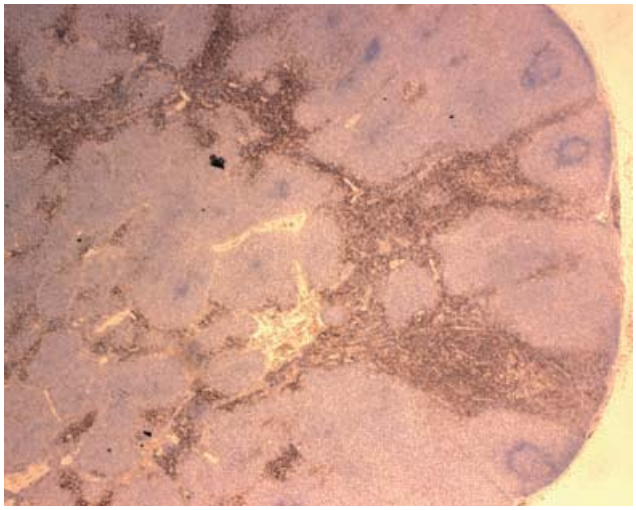

Figure 3.199. Dog: lymph node, MZL, late stage. Detail of Figure 3.197. With staining for CD3, areas of fading germinal centers and surrounding marginal zone areas are negative, with the sinus areas having a mixed population of cells that mark strongly with CD3 for T-lymphocytes.

There is no information on specific genetic changes in MZL of animals.

Cell of Origin

The Ig gene rearrangement status has been determined in a small number of human nodal MZL, with somatic changes in the heavy chain gene found in most cases. The situation is less clear in the spleen where most cases are

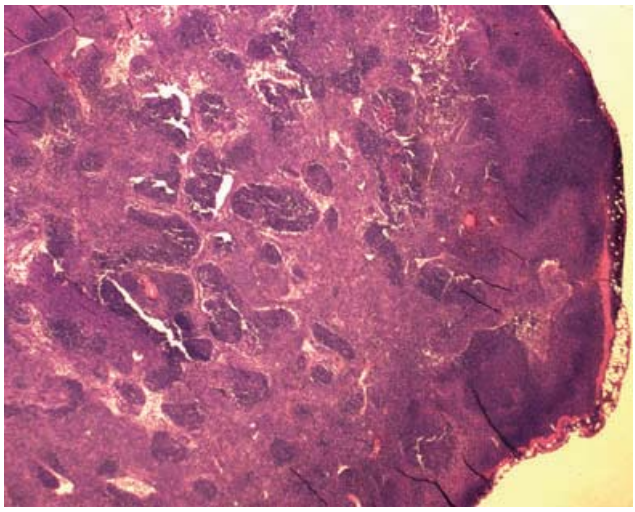

Figure 3.200. Human: node, marginal zone lymphoma. The capsule is thin and taut and there is focal colonization of perinodal tissues. The peripheral sinus is destroyed over much of the node surface with the focal darker areas representing fading germinal centers. There is complete coalescence of cell proliferation around follicles with the paracortical and medullary area completely occupied by neoplastic cell proliferation. *Slide from Cornell Tutorial.*

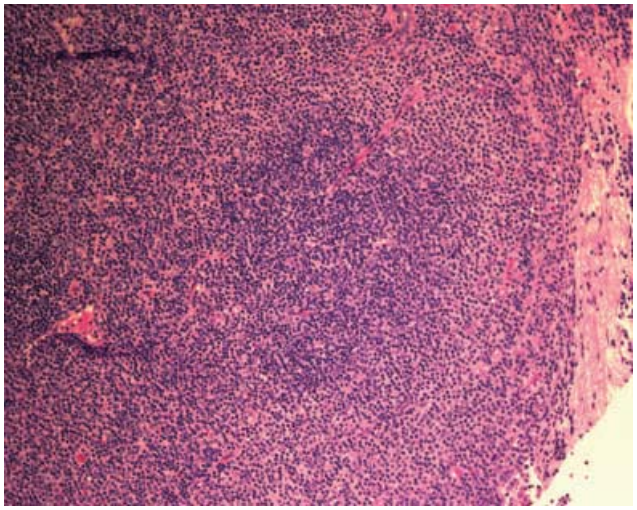

Figure 3.201. Human: lymph node, MZL. Detail of Figure 3.197. The peripheral sinus is encompassed by proliferating cells that are focally infiltrating the capsule (right). The center of the image is occupied by deeply stained small lymphocytes of the mantle cell cuff that have now collapsed into the area of the germinal center. Architecturally, the lesion is similar to that seen in animals, with the proliferating cells symmetrically surrounding the fading germinal centers.

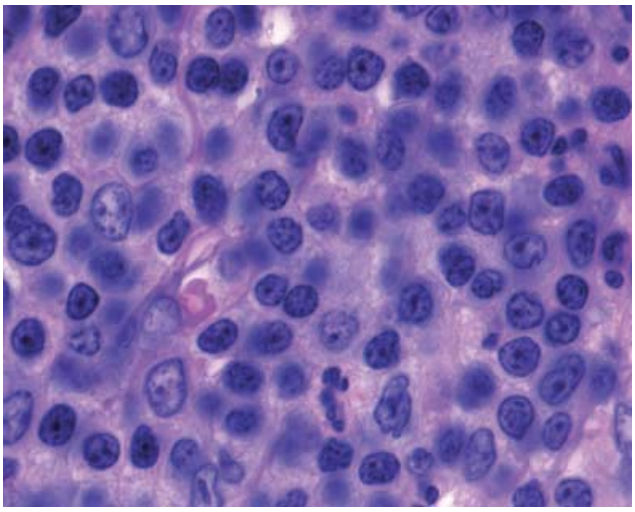

Figure 3.202. Human: lymph node, MZL. Detail of Figure 3.197. The margin of the original peripheral sinus is at the right. The nuclei are generally smaller than in the dog and cat with more variability in shapes that tend to have a similar chromatin pattern with a prominent central nucleolus. The cytoplasmic volume is typically abundant and lightly stained giving the nuclei an evenly spaced character. The red cell in the left center gives an index of relative cell size. The similarity to the monocytoid B-cells of MALT lymphoma are apparent.

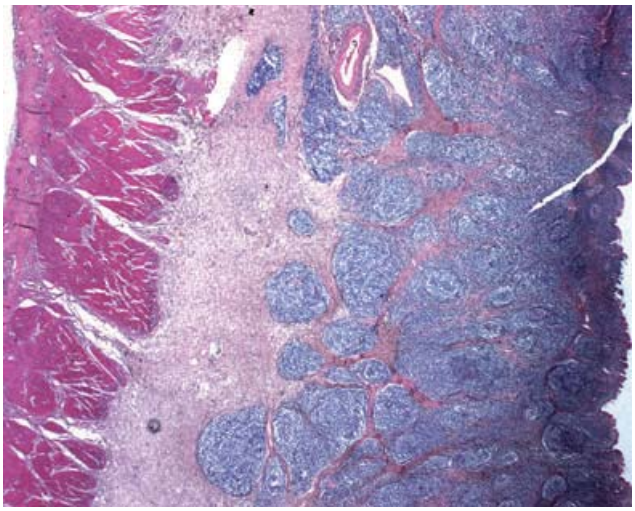

Figure 3.203. Human: gastric MALT lymphoma. The mucosa is completely destroyed by a multinodular lymphoid proliferation with sclerosis of the deep mucosa and with the tunica muscularis relatively uninvolved. *Slide from Cornell Tutorial.*

positive for IgD but more than half of cases are negative for somatic mutation in the IgVH genes. In MALT cases, the constant association with chronic immune stimulation, as in *Helicobacter* spp. gastritis, is felt to suggest strongly an origin from a postgerminal center marginal zone B-cell (Figs. 3.203–205). No information is present in animals, but some cases have been shown to express either kappa or lambda light chains, which would be consistent with clonal B-cell origin but does not indicate a heritage in germinal centers.

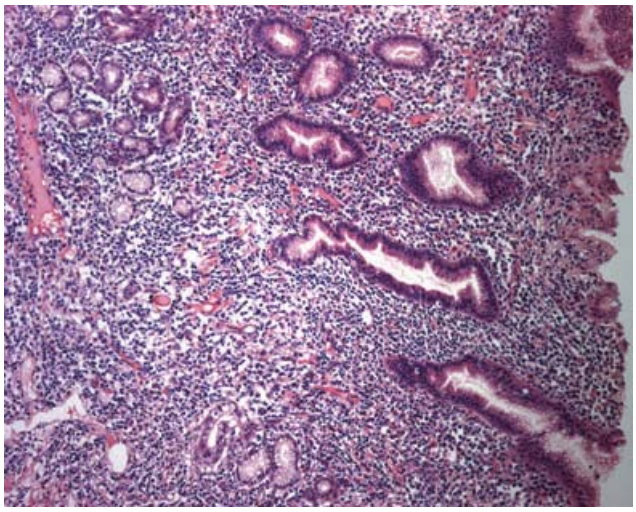

Figure 3.204. Human: gastric MALT lymphoma. Detail of Figure 3.203. The infiltration has destroyed the surface mucosa and much of the deeper glands. The infiltration tends to be monomorphic with little surface cellular reaction in response to ulceration.

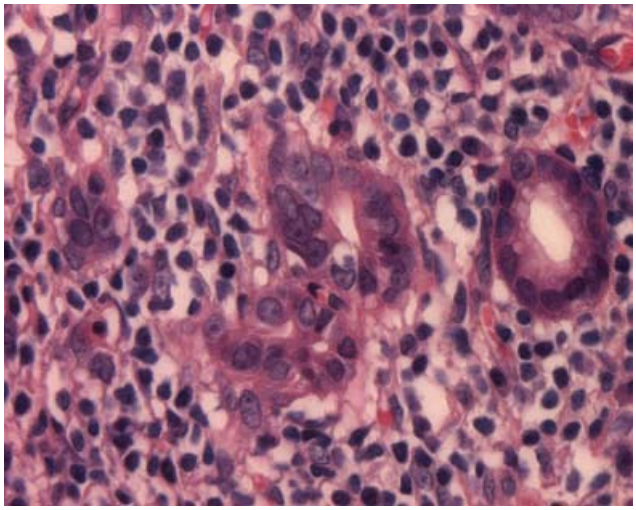

Figure 3.205. Human: gastric MALT lymphoma. Detail of Figure 3.203. The deeper mucosa has glands in various stages of infiltration by MALT lymphoma in the process of forming the changes known as the "lymphoepithelial lesion." The nuclei are generally compact with little internal nuclear detail, and mitoses are rarely encountered.

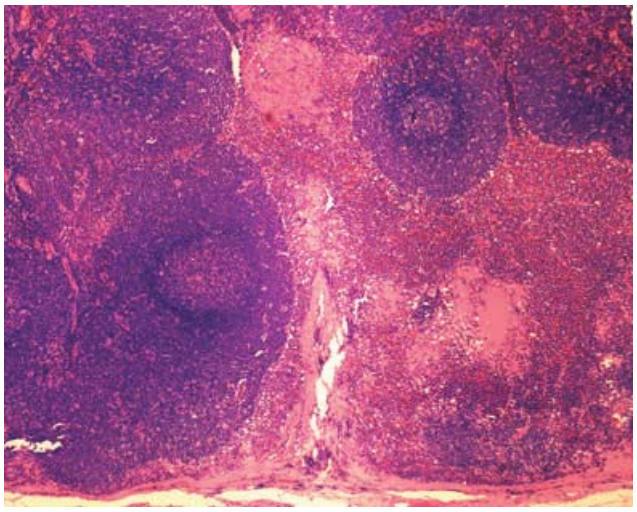

Figure 3.206. Dog: lymph node, MZL, late stage. The capsule is typically thinned and underlined by a darkly stained focal area of marked sinus dilation (right). Two fading germinal centers have thinned or incomplete mantle cell cuffs and are surrounded by broad lighter-stained homogenous zones of marginal zone proliferation.

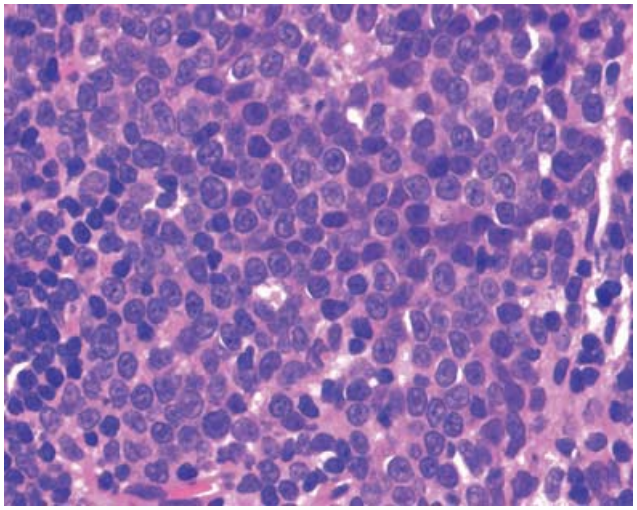

Figure 3.207. Dog: lymph node, MZL, late stage. Detail of Figure 3.206. The endothelial margin at the right is the boundary of the dilated subcapsular sinus. The increased density of small darkly stained nuclei at the left represents the fading mantle cell cuff. The homogenous encirclement of marginal zone cells have typical round to oval nuclei with a mild irregular parachromatin clearing and prominent central nucleoli. The cytoplasm is typically abundant and atypically darkly stained. The absence of mitoses is typical, and an occasional tingible body macrophage is consistent with the late stage of the neoplasm in this node.

Diagnostic Criteria

In all sites, MZL is associated with fading germinal centers. In both nodal and splenic sites, the key to diagnosis rests with the recognition of cellular proliferation arising outside a mantle cell layer. The mantle cells may survive in some areas as a thin cuff around a hypocellular germinal center (Figs. 3.206, 3.207), but most will consist of a focus of small cells with deeply stained nuclei that form a dense cluster in the area of the dendritic cell bed of an involuted germinal center (Figs. 3.208, 3.209). The diagnosis rests on the architecture that defines the homing area of the neoplasm to the marginal zone layer

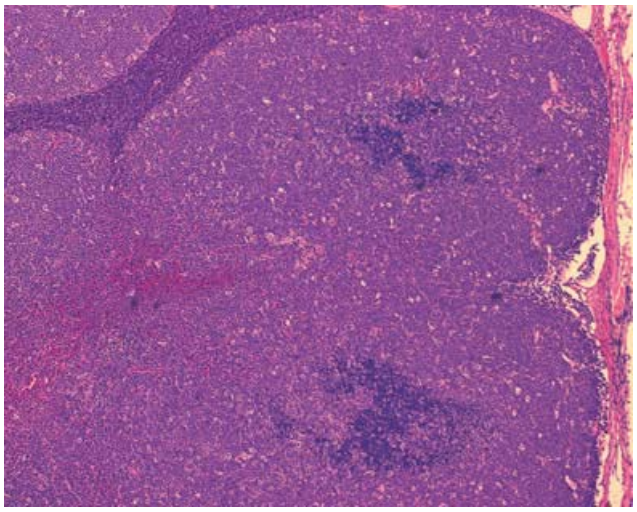

Figure 3.208. Dog: lymph node, marginal zone lymphoma, late stage. The capsule is typically thinned and taut with the peripheral sinus still intact. The fading germinal centers have retreated to irregular clusters of small darkly stained benign cells surrounded by broad homogenous cuffs of marginal zone proliferation. The irregular dilation of the subcapsular sinus at the upper left is typical.

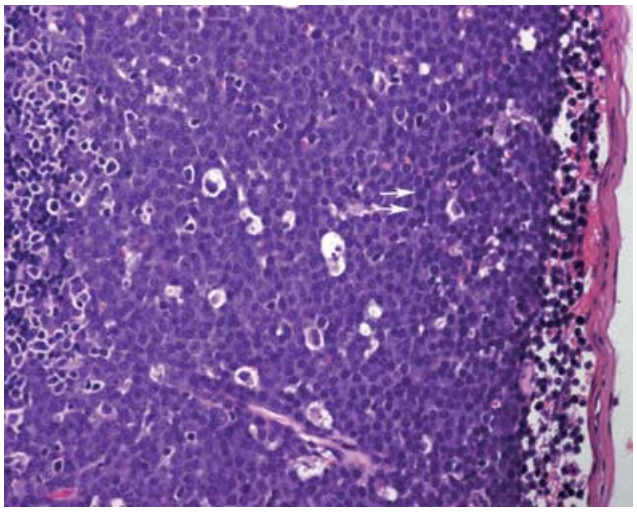

Figure 3.209. Dog: lymph node, MZL, late stage. Detail of Figure 3.207. The marginal zone cells form a homogenous band between the subcapsular sinus (right) and the fading mantle cells (left). The tingible body macrophages represented by large vacuoles with stainable nuclear debris and 2 metaphases indicated by arrows are typical changes of marginal zone lymphoma in the late stage.

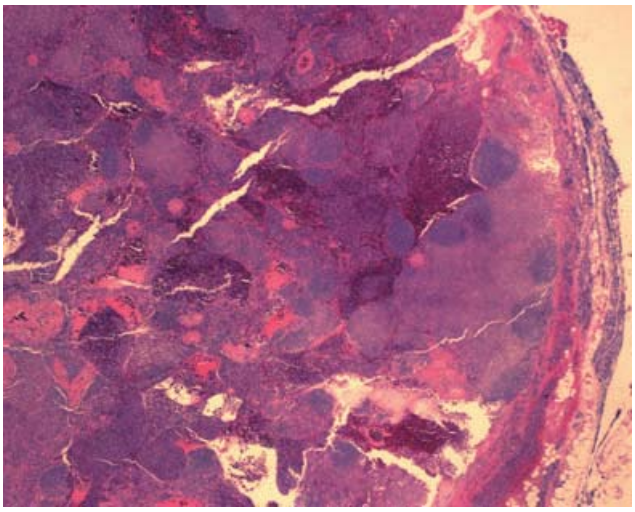

Figure 3.210. Dog: lymph node, T-zone lymphoma, late stage. The capsule is thinned and irregularly invaded with multiple large areas of subcapsular sinus ectasia partially filled with blood. Note that the subcapsular fading germinal centers are compressed tightly against the peripheral sinus rather than being surrounded by the proliferating cells as a marginal zone lymphoma. The deeper areas of fading follicles are present as foci of small dark cells are compressed against trabecular margins by proliferating paracortical expansion.

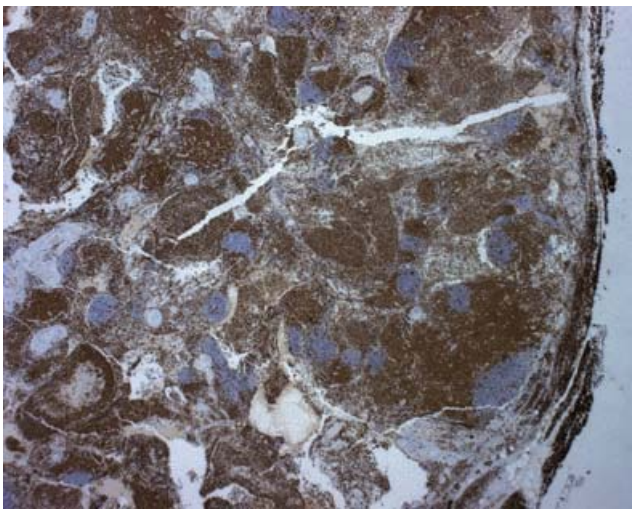

Figure 3.211. Dog: lymph node, T-zone lymphoma, late stage. Phenotype of Figure 3.210. With staining for CD3, which marks T-lymphocytes, the fading areas of B-cell proliferation can be seen to be marginalized at the edges of expanding paracortical cell population.

and to the unique cytomorphology of the MZL cells with very prominent nucleoli but with a very low mitotic rate.

Differential Diagnosis

In nodal MZL, the major differential is T-zone lymphoma (TZL) (Figs. 3.210–3.213, see also 3.209), which is of much smaller cells with inapparent nucleoli but also of very low mitotic rate. In phenotypic staining of MZL, the architecture is clearly of nodular proliferation of B-lymphocytes with prominent nucleoli that *surround* the fading areas of germinal centers. On staining of nodal MZL with CD3 only irregular foci of paracortex remain. In contrast with TZL, the proliferation is of the paracortex, with the fading germinal centers *eccentric* to the area

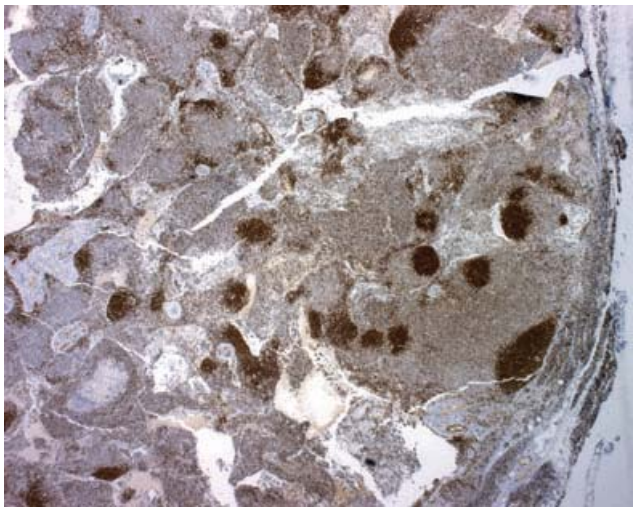

Figure 3.212. Dog: lymph node, T-zone lymphoma, late stage. Phenotype of Figure 3.210. With staining for CD79 alpha, which marks B-cells, there is a remarkable pattern of fading germinal centers throughout the interior of the node, surrounded by irregular areas of sinus dilation with the residual B-cells compressed against the subcapsular sinus at the right, irregular sinus margins in the center, and fibrous trabecula at left.

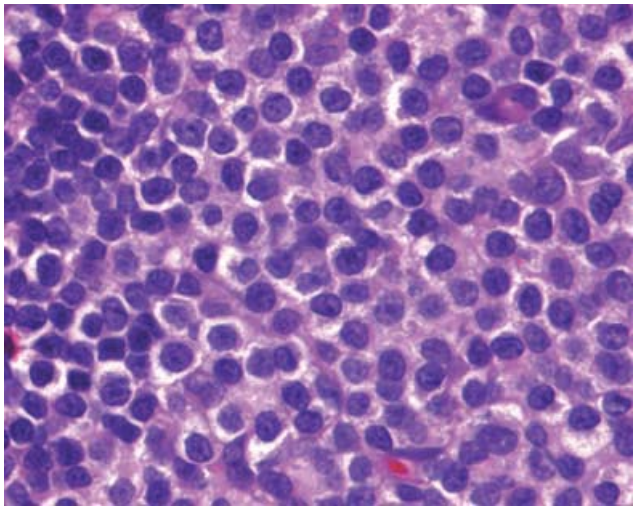

Figure 3.213. Dog: lymph node, T-zone lymphoma. Detail of Figure 3.210. A fading germinal center is at the left with the small deeply stained cells of the residual benign mantle cell cuff. The neoplastic T-cells of paracortical type are of the same size as the benign mantle cells, with outwardly round to oval nuclei that have sharp shallow indentations on close inspection. The cytoplasm is relatively abundant and lightly stained, providing even nuclear separation similar to that seen with marginal zone lymphoma. The chromatin pattern is compact, and, unlike MZL, most cells lack nucleoli, but the lesion is similar in having a very low mitotic rate.

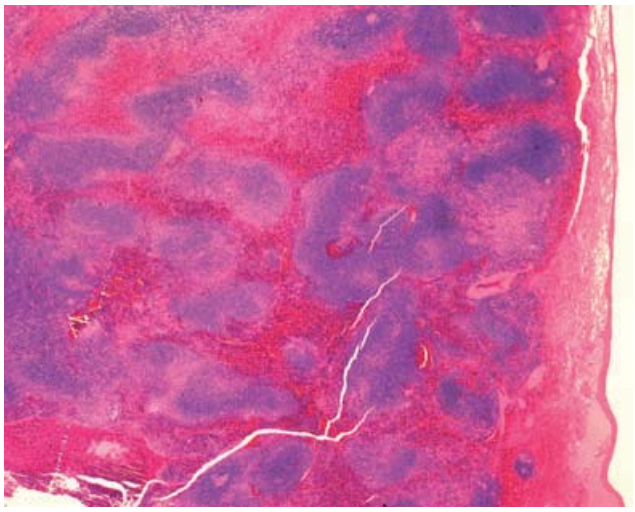

Figure 3.214. Dog: spleen, mantle cell lymphoma. There are coalescing clusters of small deeply stained lymphocytes arising on or adjacent to small arterioles. There are small central foci of lightly stained cells that represent residual areas of hypocellular dendritic cells with most of the areas of uniform density.

of expansion and not surrounded by them (see Figs. 3.210–3.213). In the spleen, the major differential is mantle cell lymphoma (MCL) that has a regular periodicity of focal proliferation like MZL because both arise on the splenic arterioles (Fig. 3.214). In MCL, previous areas of germinal center formation are difficult to identify because the mantle cells fill those areas for most tumor nodules and these then present a relatively solid area of small cell proliferation (Fig. 3.215). The cell type in MCL has a much smaller nucleus than that of MZL (Fig. 3.216). In contrast, in splenic MZL some germinal centers will remain to provide orientation to the cellular layer that is in excess (Figs. 3.217, 3.218), and the cell type with vesicular nuclei and prominent nucleoli identifies the proliferative cells as of MZL type (Fig. 3.219). MALT lymphomas of animals have not been well described, but the cell type is much more variable than in nodal or splenic MZL and is more lymphoplasmacytic, but the neoplastic cells that invade the epithelium in the characteristic "lymphoepithelial lesion" have a moderate volume of lightly stained cytoplasm (Fig. 3.220).

Staging

Most splenic cases of MZL appear to be identified relatively early in the disease and splenectomy is usually curative. Because the splenic form tends to involve the hilar nodes first and these are usually removed with the spleen, spread from this area is unusual. It is likely that many cases of canine nodular masses contain areas of MZL or MCL that is unrecognized as part of "fibrohistiocytic

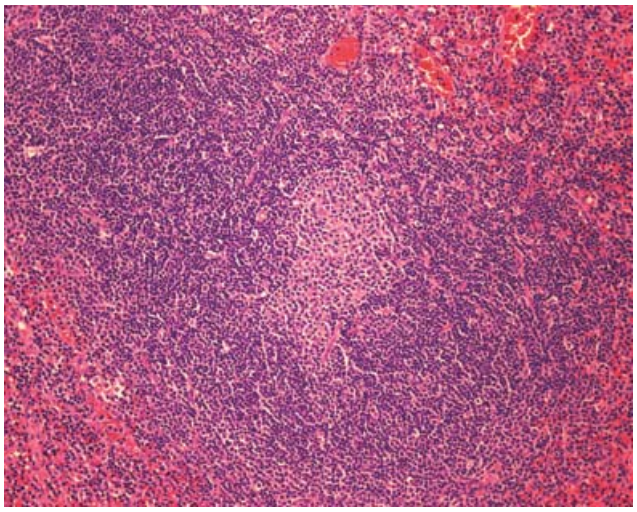

Figure 3.215. Dog: spleen, mantle cell lymphoma. Detail of Figure 3.214. A focus of mantle cell proliferation sectioned through the center in which the neoplastic cells have not yet completely obscured the central dendritic cell bed of the former germinal center. The identification of a very few pale nodules of this type serves to identify the surrounding solidly cellular population as mantle cells arising on germinal centers.

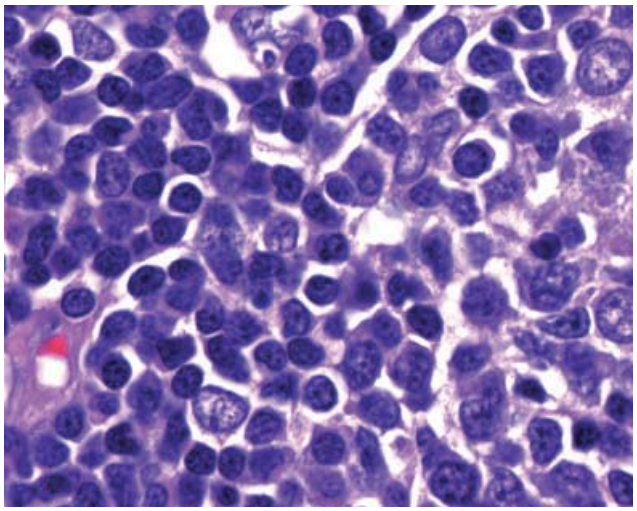

Figure 3.216. Dog: spleen, MCL. Detail of Figure 3.214. Residual large dendritic cells of a fading germinal center are at the right with the typical small round slightly indented deeply stained nuclei of the mantle cell region in center. Note the size of the red cell in the lower left in comparison to the nuclear diameters.

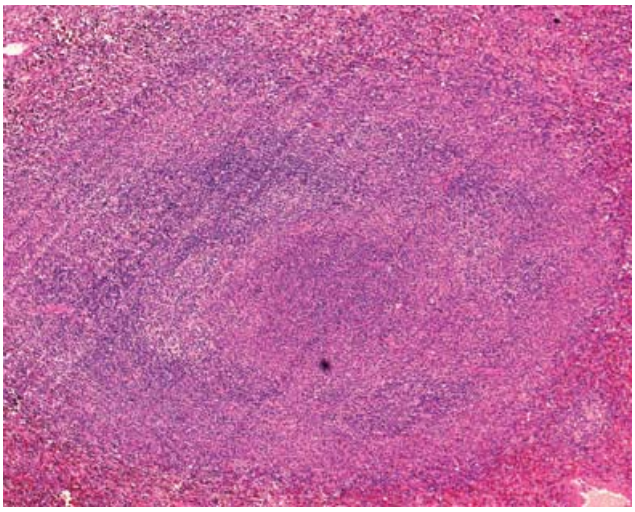

Figure 3.217. Dog: spleen, marginal zone lymphoma, early lesion. The large but involuting germinal center, a lightly stained oval structure in the center, is surrounded by a discontinuous mantle cell cuff of smaller darkly stained cells, with the proliferation clearly extending outside the mantle cell layer identifying this as marginal zone rather than mantle cell proliferation.

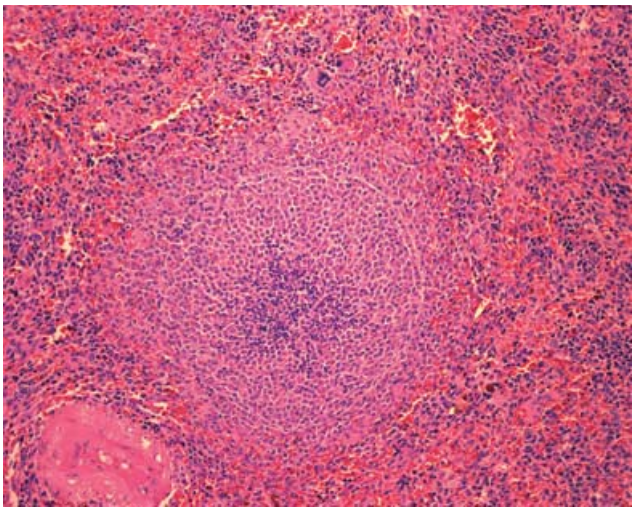

Figure 3.218. Dog: spleen, marginal zone lymphoma, late stage. The fading germinal center characterized by the cluster of darkly stained cells in the center of the cellular mass resembles that seen in the outer cortex of lymph nodes with marginal zone lymphoma. The abnormal proliferation surrounding the fading germinal center identifies this and other lesions that may be more advanced as having the architecture of marginal zone proliferation.

nodules" (Figs. 3.221–3.223). The nodal cases tend to be diagnosed in more advanced cases, generally in stage IIa and IIIa. These animals tend to feel well even in advanced disease; that may be one of the reasons they may be allowed to progress prior to diagnosis. Most cases tend to involve peripheral nodes, but internal nodes may at times be affected. Histologically, within an individual tissue early cases have minimal coalescence of adjoining areas of proliferation, and late stage cases have almost complete coalescence so that only with immunophenotyping is the outline of the nodular origins apparent.

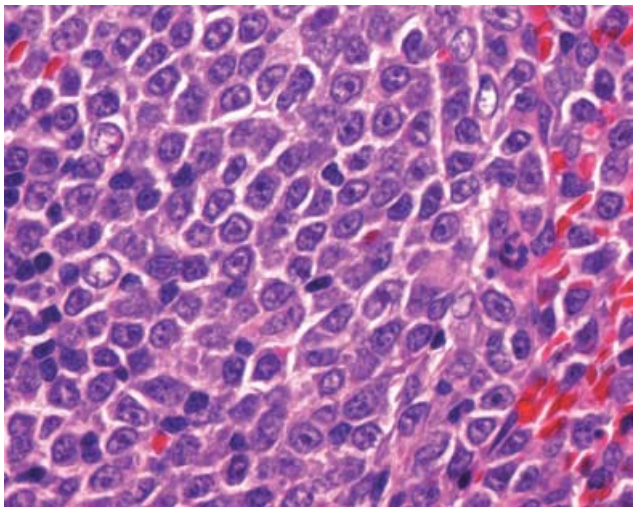

Figure 3.219. Dog: spleen, marginal zone lymphoma, late stage. Detail of Figure 3.218. The interface of expanding marginal zone proliferation and splenic sinus is at the right, with the small dark cells at the left on the edge of the fading germinal center. The homogeneity of cell type with peripheralized chromatin, mild parachromatin clearing, and prominent nucleoli in medium-sized nuclei with relatively abundant cytoplasm provides the cytologic identity of lymphoma to the architectural image, which together indicate marginal zone proliferation.

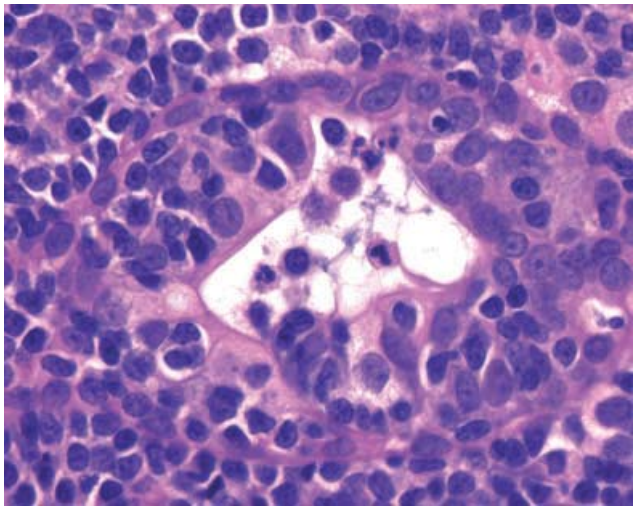

Figure 3.220. Dog: mandibular salivary gland, MALT lymphoma. Lymphocytes with small nuclei, occasionally with sharp shallow indentations and compact chromatin, are invading ductular epithelium. The cells have small nucleoli that are relatively inconspicuous, and the lymphocytes in this region are smaller than in surrounding areas.

Transformation and Progression

As noted above under diagnostic criteria, early stages of MZL have a very low mitotic rate, with none found in most areas at 400× magnification. As the disease progresses over about 2 years, the late stage MZL has a low but evident level of mitoses accompanied by tingible body macrophages and the irregular dilatation of cortical sinuses. The cell type does not change in size or nuclear characteristics.

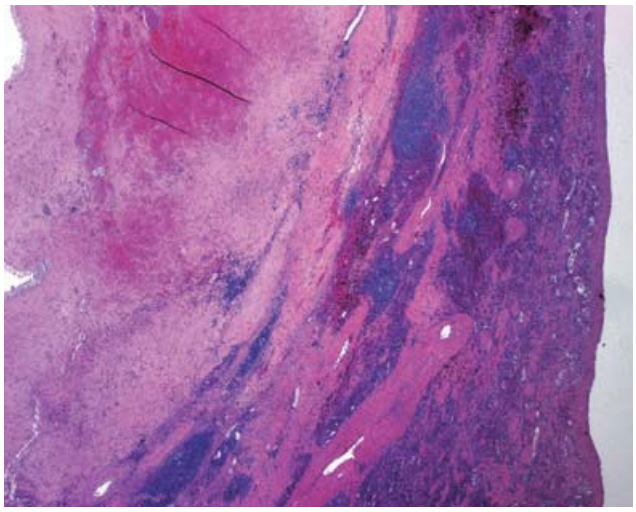

Figure 3.221. Dog: spleen, fibrohistiocytic nodule. A focal splenic area of stromal proliferation often associated with hemorrhagic infarction is generally known as a *fibrohistiocytic nodule*. These nodules often contain other types of lesions, including plasmacytoma and both mantle and marginal zone lymphomas.

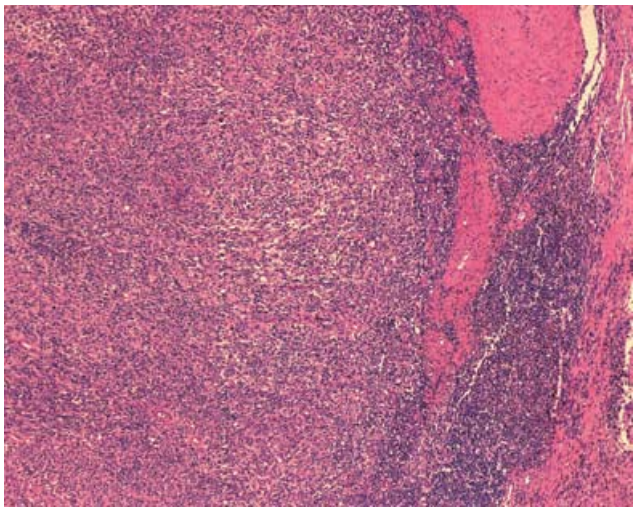

Figure 3.222. Dog: spleen, fibrohistiocytic nodule. Detail of Figure 3.221. The nodule is bordered by smooth muscle trabeculae and fibrous scarring, with the large central area of mixed cellularity containing a variety of lymphocytes interspersed between heavy stromal proliferation forming a homogeneous background.

Evaluation of the Treated Animal

Animals with a prior diagnosis of MZL tend not to have systemic signs and remain in stage IIIa or IVa, and most

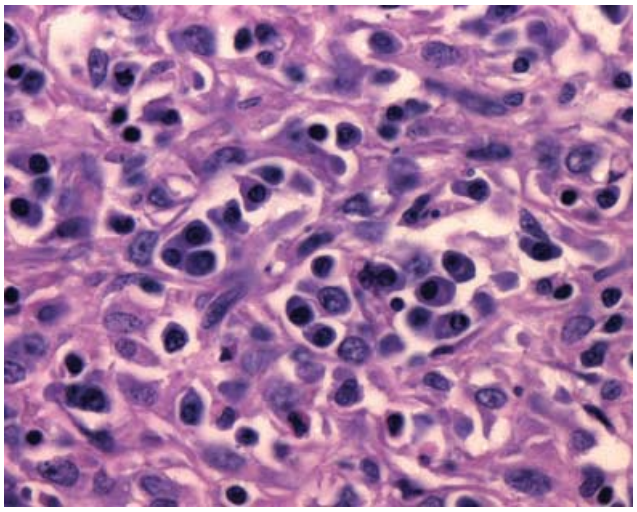

Figure 3.223. Dog: spleen, fibrohistiocytic nodule. Detail of Figure 3.221. Detail of the fibrous area with lymphocytes and plasma cells resting within a dense fibrovascular network.

don't become leukemic. Most affected nodes seem to give the same answer, and peripheral nodes can be relied on to predict changes in internal nodes. In an animal that presents with generalized lymphadenopathy, a fine needle aspiration may be interpreted as a high-grade lymphoma due to the fine chromatin and large nucleoli. In all the lymphomas with a follicular heritage, including follicular (FL), MCL, and MZL, an excisional biopsy may be required to reach the correct diagnosis because the architecture is a major factor in recognizing the nodular character of the proliferating cells. An incisional biopsy is preferred to a Tru-cut and, if the latter technique is to be used, it should be with a 2 mm diameter instrument.

Treatment and Survival

Remarkably, some animals with nodal MZL continue to respond to the same treatment protocol with a full remission, even with repeated courses over a period of 1–2 years. In follow-up of three cases of primary splenic lymphoma, none of them died of lymphoma when treated only by splenectomy. In one case of nodal MZL first diagnosed in stage IIIa, the animal lived for 43 months and died of renal failure. Canine MZL is a malignant disease that can be shown to be clonal by PCR promotion of the immunoglobulin gene and is of indolent type characterized by long survival. Dogs with this diagnosis have undergone multiple, relatively complete remissions on repeat therapy using the same drugs. In human MZL, the 5-year survival of the nodal form is near 60% and for the nongastric type of MALT lymphoma is near 90%. With the splenic form, the 5-year survival is 65% after splenectomy and 78% for those splenic lymphomas with villous lymphocytes in the peripheral blood.

REFERENCES

Berger, F., Traverse-Glehen, A., and Salles, G. (2004) Nodal marginal zone B-cell lymphoma. In Mauch, P.M., Armitage, J.O., Coiffier, B.C., Dalla-Favera, R., and Harris, N.L. (eds.), *Non-Hodgkin's Lymphomas*. Lippincott Williams & Wilkins, Philadelphia, p. 361.

Boonstra, R., Bosga-Bouwer, A., van Imhoff, G., Krause, V., Palmer, M., Coupland, R., Dabbagh, L., van den Berg, E., van den Berg, A., and Poppema, S. (2003) Splenic marginal zone lymphomas presenting with splenomegaly and typical immunophenotype are characterized by allelic loss in 7q31–32. *Modern Pathol* 16(12):1210–1217.

Dargent, J.L., Delville, J.P., Kornreich, A., Pradier, O., Cochaux, P., Velu, T., Capel, P., Feremans, W., and Neve, P. (1997) Morphologic and phenotypic changes of the leukemic cells in a case of marginal zone B-cell lymphoma. *Ann Hematol* 74:149–153.

Day, M.J., Lucke, V.M., and Pearson, H. (1995) A review of pathological diagnoses made from 87 canine splenic biopsies. *J Sm An Pract* 36:426–433.

Fisher, R., Dahlberg, S., Nathwani, B., Banks, P., Miller, T., and Grogan, T. (1995) A clinical analysis of two indolent lymphoma entities: Mantle cell lymphoma and marginal zone lymphoma (including the mucosa-associated lymphoid tissue and monocytoid B-cell subcategories): A Southwest Oncology Group Study. *Blood* 85(4):1075–1082.

Fournel, C., Magnol, J.P., Marchal, T., Chabanne, L., Bryon, P.A., and Felman, P. (1995) An original perifollicular zone cell in the canine reactive lymph node: A morphological, phenotypical and aetiological study. *J Comp Path* 113:217–231.

Jaffe, E., Raffeld, M., and Medeiros, J. (1993) Histopathologic subtypes of indolent lymphomas: Caricatures of the mature B-cell system. *Sem in Oncol* 20:3–30.

Kolbjornsen, O., Press, C.M., Moore, P.F., and Landsverk, T. (1994) Lymphoid follicles in the gastric mucosa of dogs. Distribution and lymphocyte phenotypes. *Vet Immunol and Immunopathol* 40:299–312.

Kruschinski, C., Zidan, M., Debertin, A., Von Horsten, S., and Pabst, R. (2004) Age-dependent development of the splenic marginal zone in human infants is associated with different causes of death. *Human Pathol* 35:113–121.

Lee, J., Hughes, C., Fine, R., and Page, R. (1996) P-Glycoprotein expression in canine lymphoma: A relevant, intermediate model of multidrug resistance. *Cancer* 77:1892–1898.

Meda, B., Frost, M., Newell, J., Bohling, S., Huebner-Chan, D., Perkins, S., Lim, M., Medeiros, L., and Elenitoba-Johnson, K. (2003) BCL-2 is consistently expressed in hyperplastic marginal zones of the spleen, abdominal lymph nodes, and ileal lymphoid tissue. *Am J Surg Pathol* 27(7):888–894.

Muller-Hermelink, H.K. (2003) Genetic and molecular genetic studies in the diagnosis of B-cell lymphomas: Marginal zone lymphomas. *Human Pathol* 34:336–340.

Murakami, H., Irisawa, H., Saitoh, T., Matsushima, T., Tamura, J., Sawamura, M., Karasawa, M., Hosomura, Y., and Kojima, M. (1997) Immunological abnormalities in splenic marginal zone cell lymphoma. *Am J Hematol* 56:173–178.

Oscier, D., Owen, R., and Johnson, S. (2005) Splenic marginal zone lymphoma. *Blood Rev* 19:35–51.

Piris, M., Mollejo, M., Chacon, I., Garcia, J., Camacho, F., and Cruz, M. (2004) Splenic marginal zone lymphoma. In Mauch, P.M., Armitage, J.O., Coiffier, B.C., Dalla-Favera, R., and Harris, N.L. (eds.), *Non-Hodgkin's Lymphomas*. Lippincott Williams & Wilkins, Philadelphia, p. 275.

Rosso, R., Castello, A., Colosini, G., Astori, C., Lazzarino, M., and Magrini, U. (1996) Splenic marginal zone cell lymphoma involving liver and bone marrow. Report of a case with protracted follow-up, showing progressive disappearance of the lymphoma after splenectomy. *Haematologica* 81:44–46.

Skacel, M., Ross, C.W., and His, E.D. (2000) A reassessment of primary thyroid lymphoma: High-grade MALT-type lymphoma as a distinct subtype of diffuse large B-cell lymphoma. *Histopathol* 37:10–18.

Spangler, W.L., and Kass, P.H. (1998) Pathologic and prognostic characteristics of splenomegaly in dogs due to fibrohistiocytic nodules: 98 cases. *Vet Pathol* 35:488–498.

Stein, K., Hummel, M., Korbjuhn, P., Foss, H., Anagnostopoulos, I., Marafioti, T., and Stein, H. (1999) Monocytoid B cells are distinct from splenic marginal zone cells and commonly derive from unmutated naïve B cells and less frequently from postgerminal center B cells by polyclonal transformation. *Blood* 94(8):2800–2808.

Troussard, X., Valensi, F., Duchayne, E., Garand, R., Felman, P., Tulliez, M., Henry-Amar, M., Bryon, P.A., and Flandrin, G. (1996) Splenic lymphoma with villous lymphocytes: Clinical presentation, biology and prognostic factors in a series of 100 patients. *Brit J Haematol* 93:731–736.

Valdez, R., Finn, W., Ross, C., Singleton, T., Tworek, J., and Schnitzer, B. (2001) Waldenstrom macroglobulinemia caused by extranodal marginal zone B-cell lymphoma. *Am J Clin Pathol* 116:683–690.

Wolvius, E.B., van der Valk, P., van der Wal, J.E., van Diest, P.J., Huijgens, P.C., van der Waal, I., and Snow, G.B. (1996) Primary non-Hodgkin's lymphoma of the salivary glands. An analysis of 22 cases. *J Oral Pathol Med* 25:177–181.

Yahalom, J., Isaacson, P., and Zucca, E. (2004) Extranodal marginal zone B-cell lymphoma mucosa-associated lymphoid tissue. In Mauch, P.M., Armitage, J.O., Coiffier, B.C., Dalla-Favera, R., and Harris, N.L. (eds.), *Non-Hodgkin's Lymphomas*. Lippincott Williams & Wilkins, Philadelphia, p. 345.

Plasmacytoma and Multiple Myeloma

Definition

Plasmacytoma and myeloma are considered together in the WHO classification system for human hematopoietic neoplasms because the human form of plasmacytoma, unlike the case in animals, is primarily a malignant disease. Plasmacytoma in animals is predominantly a benign polyclonal proliferation of cells, with morphologic features of plasma cell hyperplasia but occurring in a focal proliferation in soft tissue, and known as *extramedullary plasmacytoma*, or in bone, and known as *solitary osseous plasmacytoma*. Plasmacytomas have dysplastic features that distinguish them from plasma cell hyperplasia, as might occur in a site of chronic antigenemia (Fig. 3.224) that may include some or all of larger nuclei with hyperchromicity, anisokaryosis and nucleoli, binucleation, and even multinucleation while maintaining abundant cytoplasmic volume and staining density (Figs. 3.225–3.227).

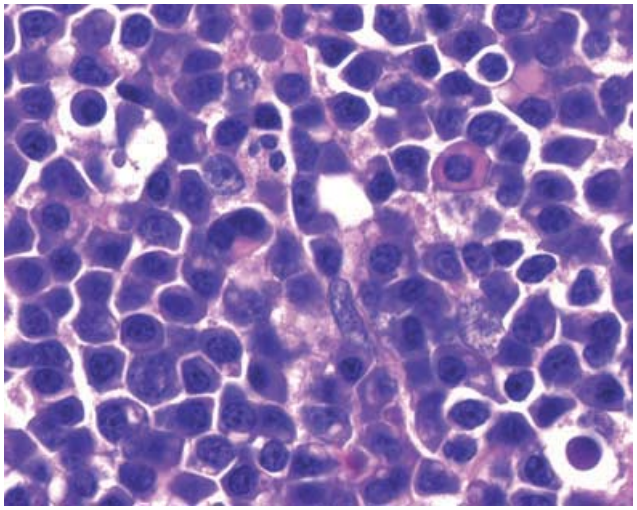

Figure 3.224. Dog: lymph node, benign medullary cord plasma cell hyperplasia. Vibrant reactive plasmacytosis, of the type that occurs, for example, in nodes draining chronic periodontal disease or chronic dermatitis. The cells are of generally uniform size, with deep cytoplasmic amphophilia, prominent Golgi zones, and compact chromatin with most cells lacking nucleoli. There are 2 Mott or "flame" cells in the upper right with distended cytoplasmic vacuoles containing immunoglobulin.

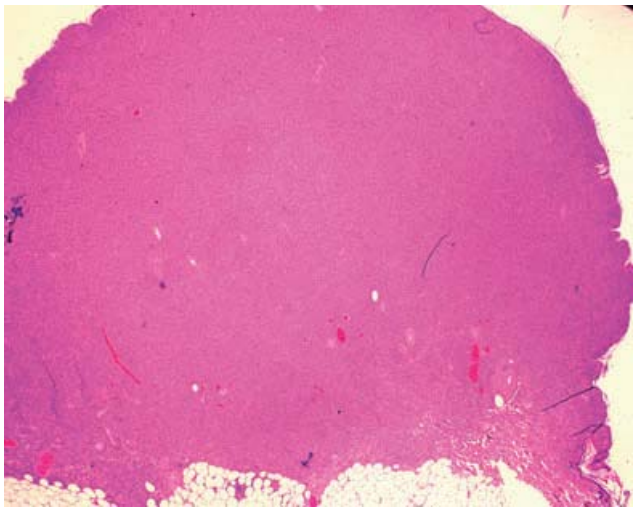

Figure 3.225. Dog: skin, plasmacytoma. A focal lesion flanked by normal-haired skin extends from the dermal/epidermal junction down to the depths of the dermis, with wide separation of the dermal collagen bundles. The lesion presents a smooth interface with the panniculus and has been removed in its entirety.

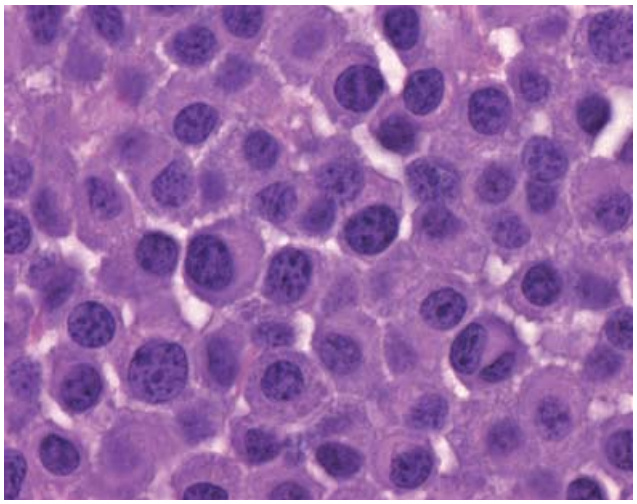

Figure 3.226. Dog: skin, plasmacytoma. Detail of Figure 3.225. Cytologically, the cells have round to oval nuclei, 1.5–3 red cells in diameter with a hyperchromatic chromatin pattern characterized by large dense chromocenters surrounded by lighter-stained dispersed chromatin with larger cells having prominent nucleoli. Binucleation is frequent, and anisokaryosis is prominent. The cytoplasm is eccentrically placed, highly amphophilic, and with frequent apparent Golgi zones. Cell boundaries are generally distinct near the margins of the tumor. Mitoses are present but not in every field at 400× magnification.

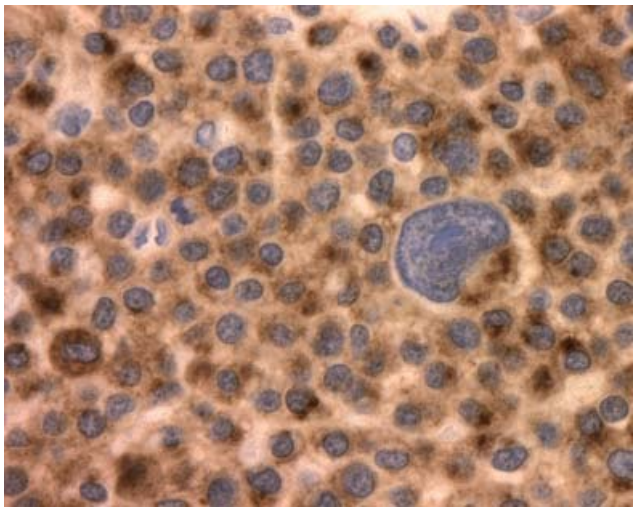

Figure 3.227. Dog: skin, plasmacytoma. Phenotype of Figure 3.224. On staining with CD79, two patterns are found, with some tumors marking strongly and some irregularly. In this field, there is a remarkably large nucleus in the center right and in left center is a cell in metaphase. In this neoplasm, there is relatively uniform marking of all cells.

In the context of human pathology, plasmacytoma is a clonal proliferation that is treated as a malignant neoplasm and, unlike with animals, may be accompanied by gammopathy.

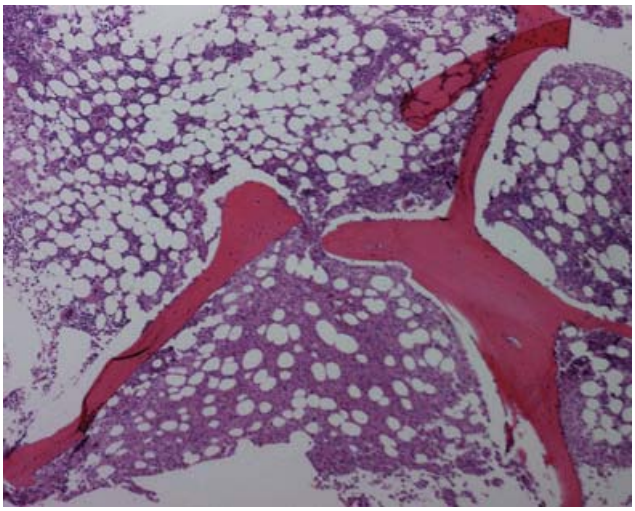

Figure 3.228. Dog: bone marrow core biopsy, myeloma. There is relatively normal marrow in the upper and lower-left areas of the image; the area enclosed by trabecula in the lower center area is almost entirely myeloma with the exception of the remaining fat cells.

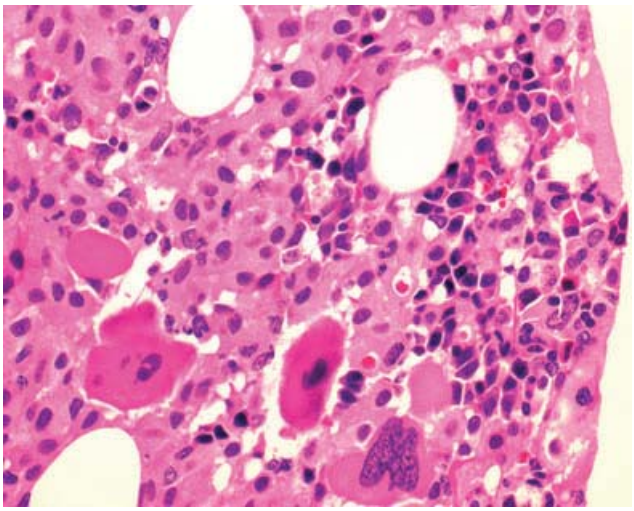

Figure 3.229. Dog: marrow core, myeloma. Detail of Figure 3.228. Interface of tumor and focal areas of residual hematopoiesis. There is phthisis of normal marrow elements with the megakaryocyte with prominent cytoplasmic eosinophilia likely undergoing degeneration.

Myeloma is a medullary clonal neoplasm characterized by low mitotic rate and nuclear cytoplasmic ratio, pale staining cytoplasm, and usually a gammopathy of the IgM type (Figs. 3.228, 3.229). Most myelomas are multifocal and are termed *multiple myeloma* (Fig. 3.230, see also Figs 3.228 and 3.229). The etiology of myeloma is unknown; however, the history of chronic inflammation and plasma cell hyperplasia are considered risk factors for clonal plasmacytoma and myeloma. An intriguing association has been found between infection with human

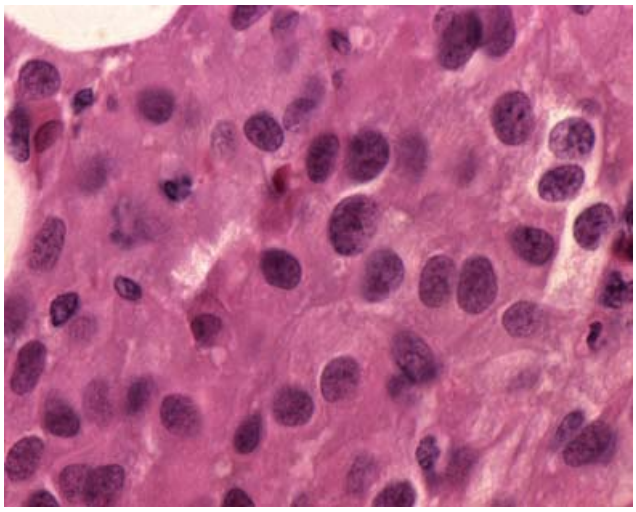

Figure 3.230. Dog: marrow core, myeloma. Detail of Figure 3.228. The myeloma cells have bland-appearing nuclei, with finely granular hyperchromatic nuclei with abundant highly amphophilic cytoplasm and with cell boundaries indistinct. The abundant cytoplasm is typical, as is the low mitotic rate that makes this tumor particularly difficult to treat since its proliferative rate is less than that of normal marrow.

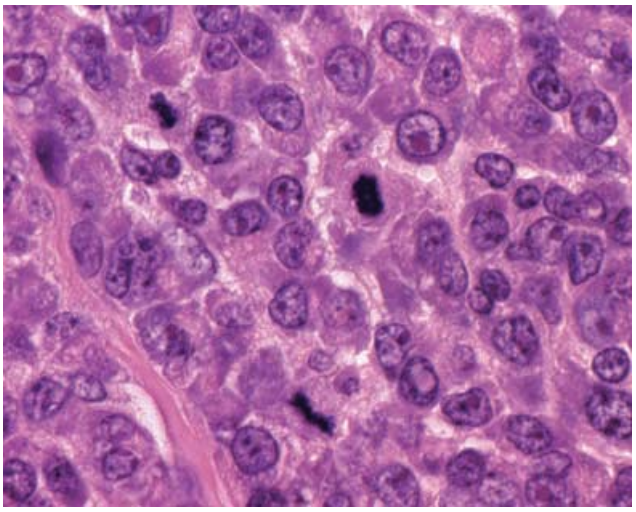

Figure 3.232. Human: bone marrow, myeloma. Detail of Figure 3.231. The nuclei are round to oval, about 1.5 red cells in diameter and appear vesicular with irregular peripheralization of chromatin and nucleoli that vary from very prominent and single to small and multiple. The cytoplasm is abundant with cell boundaries irregularly distinct. It is very unusual to find 3 mitoses in the same field at this magnification and it is not common in this neoplasm.

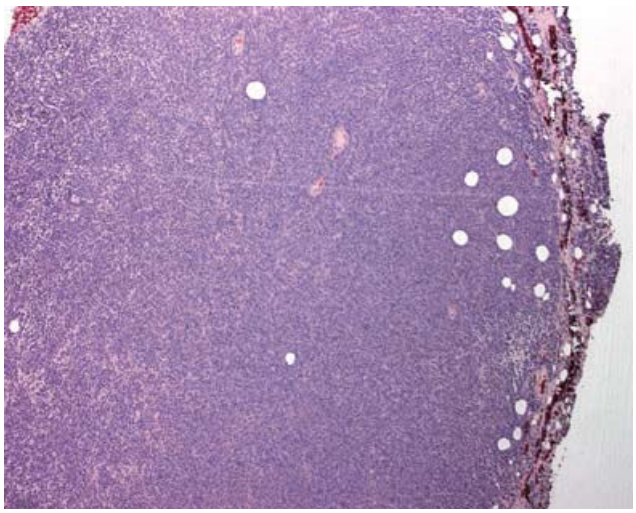

Figure 3.231. Human: bone marrow, myeloma. Marrow architecture of a very advanced neoplasm. The residual fat cells are the only evidence that the tissue is of marrow origin. There is a diffuse infiltration of neoplastic cells with complete phthisis of normal marrow elements. *Slide from Cornell Tutorial.*

herpesvirus 8, the accepted cause of Kaposi sarcoma, and human multiple myeloma (Figs. 3.231, 3.232). The proposed pathogenetic mechanism is that dendritic cells infected with herpesvirus 8 in marrow and other sites secrete high levels of IL-6, which is a growth factor for plasma cells and for myeloma cells. Thus chronic infection with the specific herpesvirus results in a prolonged but ineffective immune response and is suggested to be a likely cause of a syndrome of monoclonal gammopathy of undetermined significance (MGUS), which is not uncommon and a small number of which may ultimately develop myeloma.

Epidemiology and Incidence Plasmacytoma

Solitary extramedullary plasmacytomas are found most frequently in the dog and less commonly in cats and are uncommon or undescribed in other domestic species. Most cases in the dog occur in the skin as focal cutaneous masses that involve the dermis and superficial panniculus and are almost invariably benign. Plasmacytomas also occur in the upper and lower digestive tract in dogs, and in these locations the lesions are more likely to be malignant. In dogs, plasmacytomas are lesions of older animals, unusual in dogs under 5 years and more common in dogs 10 years and older. In cats, the same age-related incidence is found, but the lesions may be found in internal organs with the most typical involvement a diffuse infiltration of the splenic sinuses.

Solitary osseus plasmacytoma is rare in both cats and dogs, but more diffuse plasma cell hyperplasia is regularly found in diseases characterized by chronic antigenemia. In both dogs and cats, osseus plasmacytic proliferations are likely to be multifocal and malignant. Myeloma is estimated to represent less than 1% of all malignant neoplasms of animals and is a disease of mature animals, with

occurrence under 5 years unusual in the dog and most cats. There is a slight male predominance for human and dog plasmacytomas, but a strong—about 2:1—male predominance in the cat.

Clinical Presentation and Features

The majority of canine nonosseous plasmacytomas are found in the upper respiratory and digestive systems, with the remainder largely in the skin. In the cat, the disease may occur as a diffuse infiltration of the splenic red pulp areas completely filling the sinus areas. Most plasmacytomas are noticed on grooming or clinical examination and rarely cause clinical signs. Those in the oral cavity may be noticed due to difficulties in swallowing or noisy respiration (Figs. 3.233–3.235), and a smaller number found in the stomach (Figs. 3.236–3.240) and in the colorectal area (Figs. 3.241–3.244) present with problems of digestion and defecation with none of the signs incurred specific for plasmacytoma. The lesions may be ulcerated, and those in the skin and on mucus membranes tend to be smooth swellings generally less than 3 cm in diameter (Figs. 3.245–3.247). Extramedullary plasmacytomas are uncommon in cats, and those that are seen may, as in the dog, have primary involvement of the spleen (Figs. 3.248–3.250) and, rarely, skin. Oddly, plasmacytoma is generally not seen in lymph nodes as a primary site in any species (Fig. 3.251). As molecular determinations of clonality become more common, it appears that even plasmacytomas of small size that are malignant have similar clinical behavior to those found to be benign if surgery is accomplished with clean margins. Plasmacytomas may be accompanied by amyloid deposition (Figs. 3.252, 3.253), often with focal mineralization, and in cutaneous areas these lesions are prone to ulceration.

In contrast to plasmacytoma, dogs with myeloma generally present with clinical signs that are most often related to changes in gait. A common history in the diagnosis of myeloma is of a dog presented because of hindlimb lameness. On radiographic examination, one or

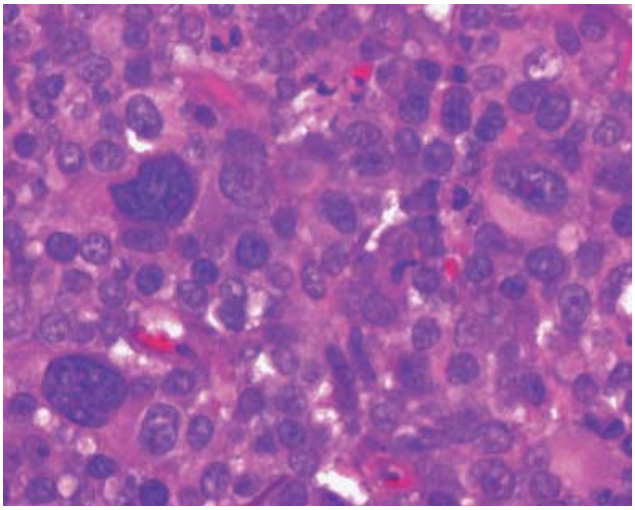

Figure 3.234. Dog: oral cavity, plasmacytoma. Detail of Figure 3.231. There is marked anisokaryosis more prominent than that observed in plasmacytoma located elsewhere in the skin. The mitotic rate is not noticeably higher, but the risk of recurrence in this area is greater.

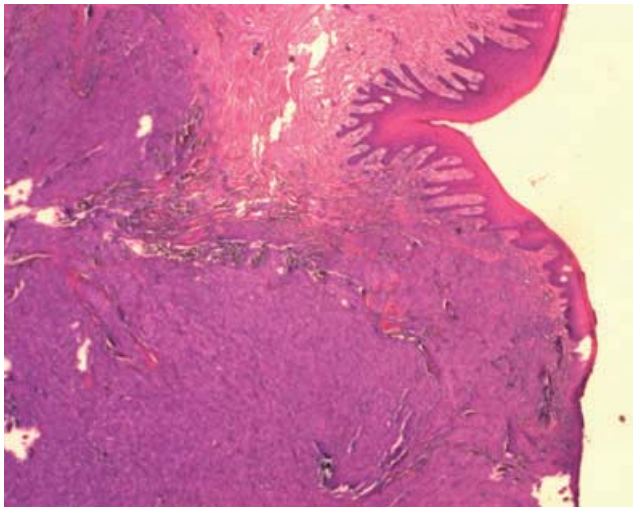

Figure 3.233. Dog: oral cavity, plasmacytoma. A mass 2.5 × 1.0 cm was removed from the lower-left lip margin. There is focal hyperplasia of the oral epithelium with adjacent ulceration (right) and a dense cellular infiltration extending focally from the basement membrane down to the skeletal muscle.

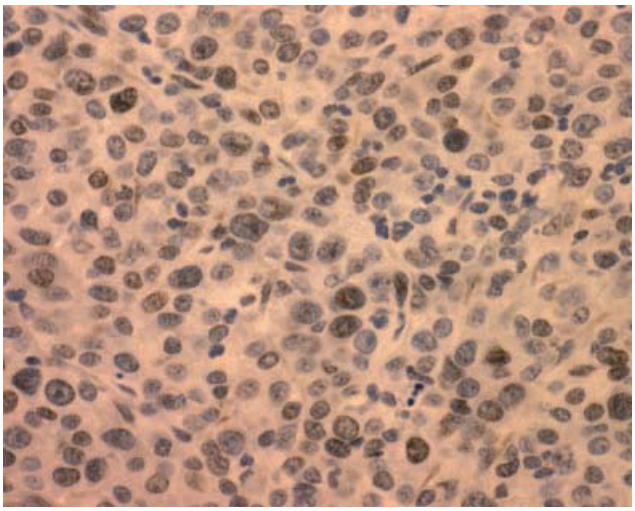

Figure 3.235. Dog: oral plasmacytoma. Phenotype of Figure 3.230. On staining with CD79, there is spurious marking of nuclei but cytoplasm is largely unlabeled. This is a typical response in as many as half of the more anaplastic-appearing canine plasmacytomas.

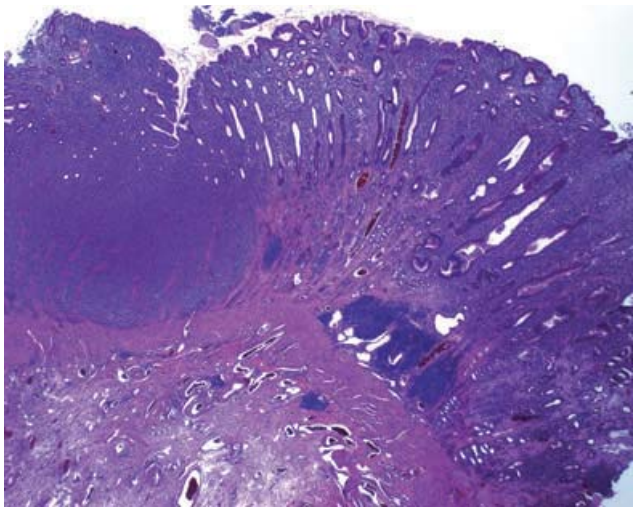

Figure 3.236. Dog: gastric plasmacytoma. The gastric mucosa has severe lymphoplasmacytic infiltration in the upper area of the image with progressive destruction of glands and solid cellular infiltration in the upper-left area.

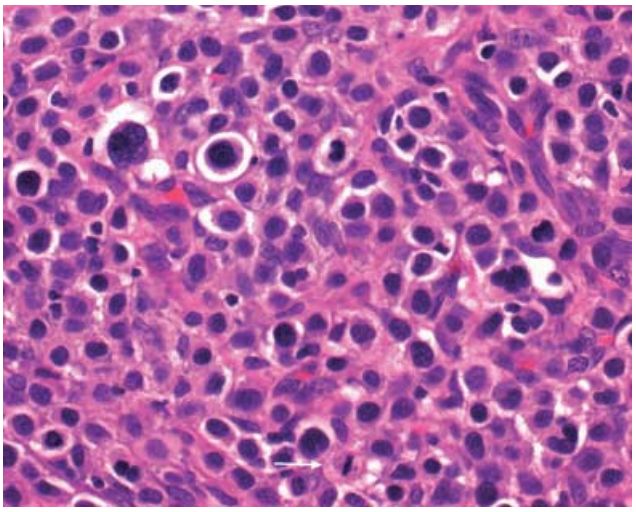

Figure 3.238. Dog: gastric plasmacytoma. Detail of Figure 3.236. At this magnification marked anisokaryosis is apparent with a trinucleated cell in the upper left and the right center. A cell in mitosis at the bottom is indicated by an arrow. The nuclei are deeply stained with nucleoli that are obscured. The cytoplasm is abundant, deeply stained with cell boundaries irregularly apparent.

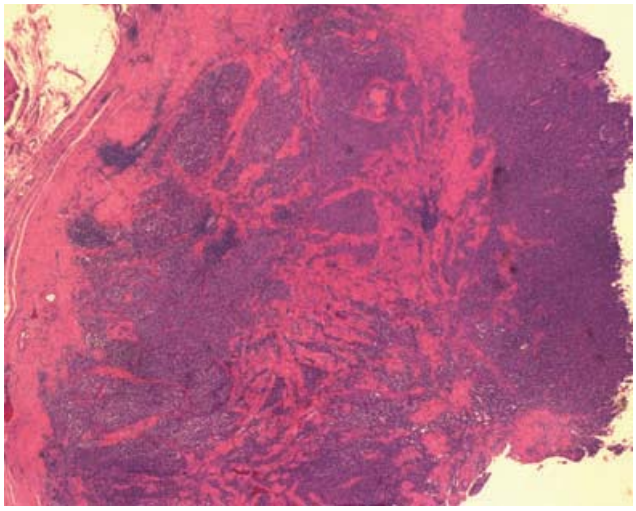

Figure 3.237. Dog: gastric plasmacytoma. Detail of Figure 3.236. In this area, there is complete ulceration of the surface mucosa with irregular infiltration of the submucosa with complete destruction of glands and sclerosis of surrounding supporting tissues.

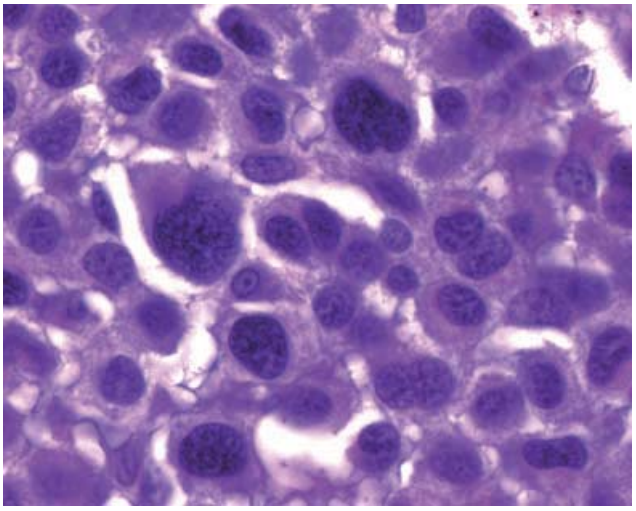

Figure 3.239. Dog: gastric plasmacytoma. Detail of Figure 3.236. The degree of anaplasia including anisokaryosis, hyperchromicity, and binucleation is strongly suggestive of malignant neoplasia. Some of the membrane separations and vacuolations are artifactual.

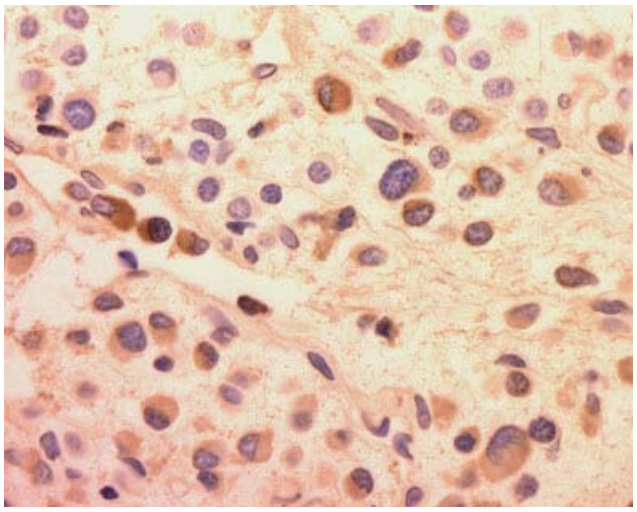

Figure 3.240. Dog: gastric plasmacytoma. Phenotype of Figure 3.236. On staining for IgM, there is irregular marking with focal strong positive cytoplasmic staining of very atypical cell types.

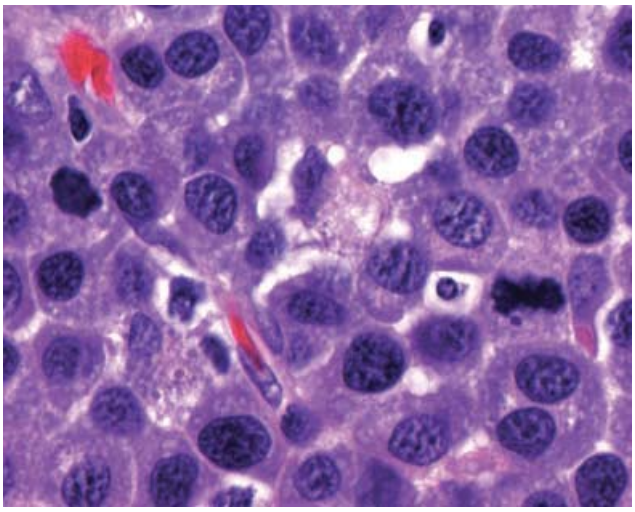

Figure 3.242. Dog: pararectal plasmacytoma. Detail of Figure 3.241. The mass, despite being encapsulated, is moderately anaplastic with 2 multinucleated cells within this field (lower left and upper right) and 2 mitoses (top center and lower left of center). There is moderate anisokaryosis with hyperchromatic nuclei and multiple small nucleoli. The cytoplasm is characteristically abundant, highly amphophilic with cell boundaries generally distinct.

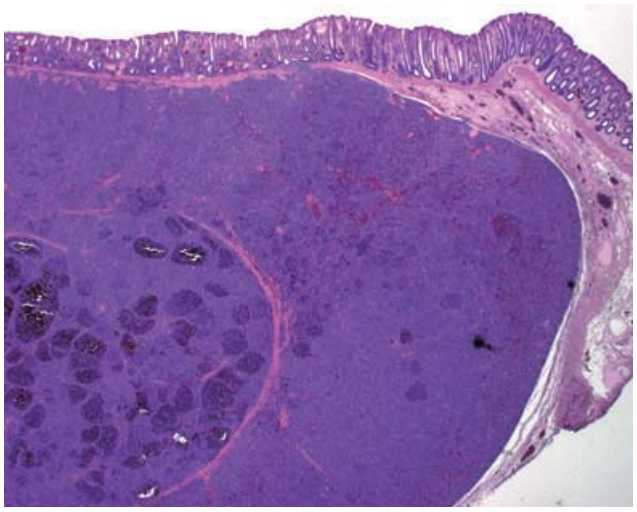

Figure 3.241. Dog: pararectal plasmacytoma. A submucosal mass 2 × 1 cm was removed intact. The lesion is lightly encapsulated and appears to have been removed in its entirety. Architecturally, the mucosa was intact with the mass lying between the muscularis mucosa and tunica muscularis. The lesion is solidly cellular with multifocal areas of venous ectasia.

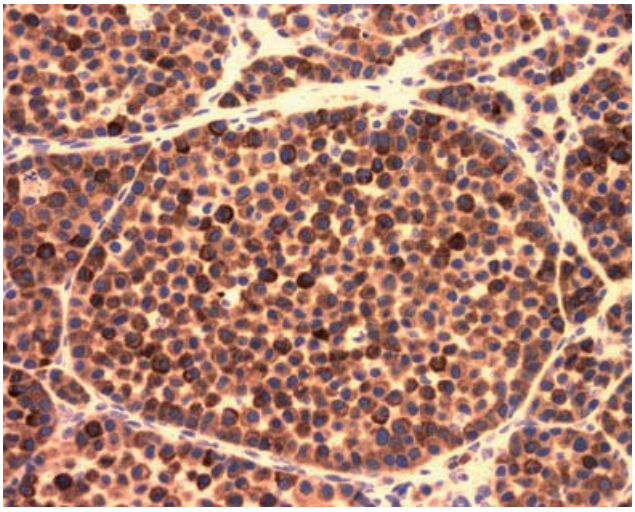

Figure 3.243. Dog: pararectal plasmacytoma. Phenotype of Figure 3.241. On staining with CD79 alpha, the infiltrating plasma cells are strongly and solidly labeled in all areas of the mass.

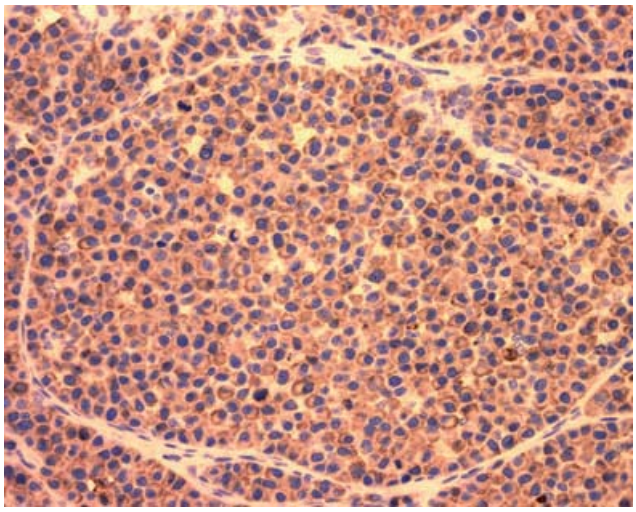

Figure 3.244. Dog: pararectal plasmacytoma. Phenotype of Figure 3.241. On staining for the lambda light chain, the cells are uniformly and strongly labeled, with the staining for the kappa light chain completely negative, strongly suggesting that the plasma cell population is clonal and malignant.

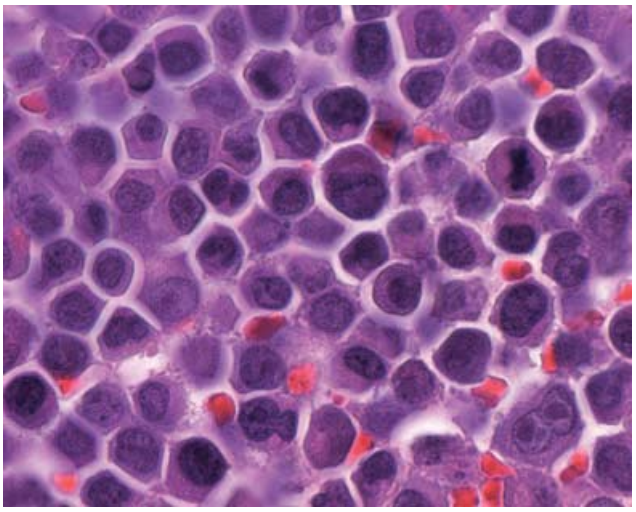

Figure 3.246. Cat: skin, plasmacytoma. Detail of Figure 3.245. There is an unusual level of cytologic anaplasia. A number of the cells have very large nucleoli and several binucleated cells are present in this field as well as a cell in mitosis (upper right).

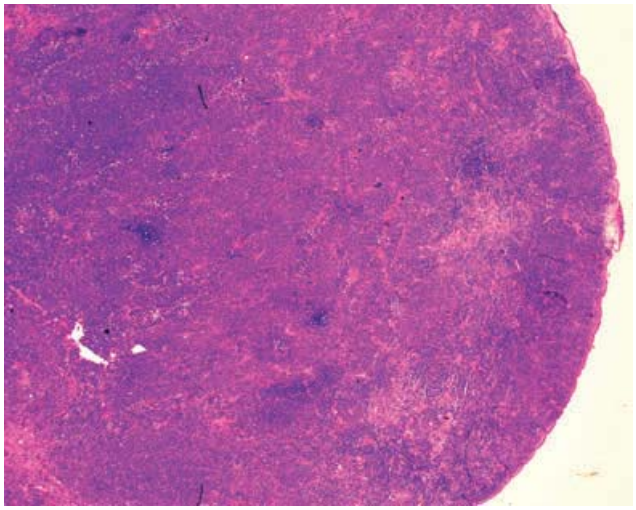

Figure 3.245. Cat: skin, plasmacytoma. A 10-year-old spayed female domestic shorthair cat presented with a 1.5 cm mass over the left shoulder felt to be of recent development. The mass was raised, conical, and with the skin markedly thinned and focally ulcerated.

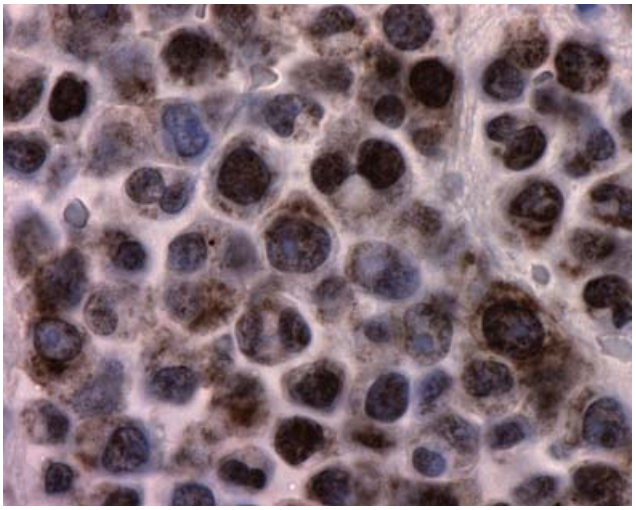

Figure 3.247. Cat: skin, plasmacytoma. Phenotype of Figure 3.245. CD79 stain gives variable results with artifactual nuclear marking and irregular staining of cytoplasm.

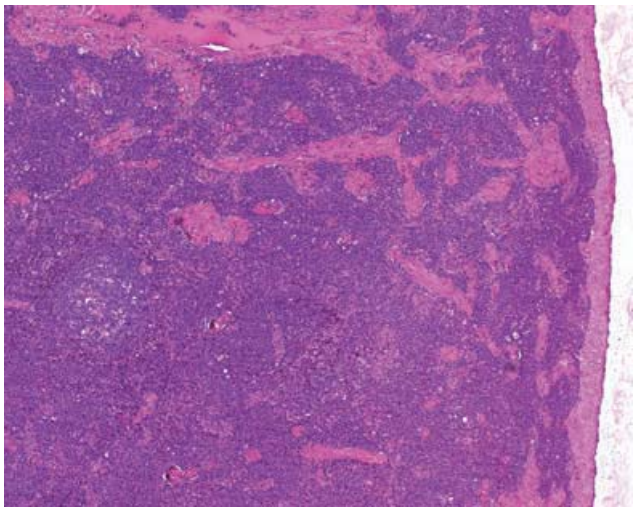

Figure 3.248. Cat: spleen, plasmacytoma. There is a fading lymphoid nodule in the left center eccentric to a small arteriole on the right upper surface. There is complete sinus filling with diffuse sheets of plasma cells. The depth of redness is typical of plasmacytomas with abundant highly amphophilic cytoplasm.

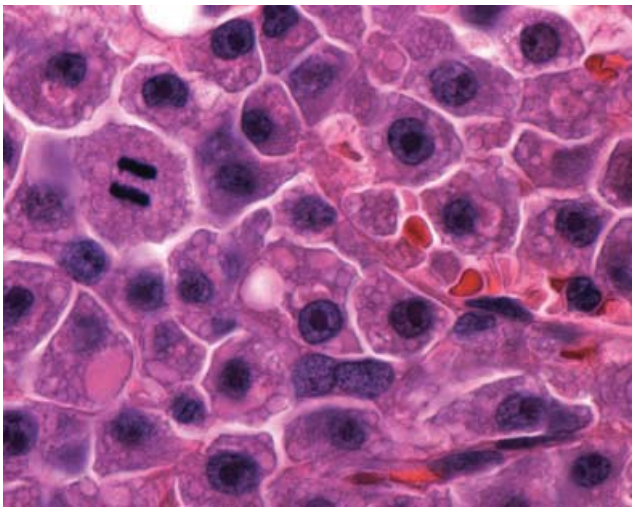

Figure 3.250. Dog: spleen, plasmacytoma. Cytologically, the constituent cells are quite anaplastic with hyperchromatic dispersed chromatin and very large prominent central nucleoli more typical of immunoblastic-type lymphoma. The cytoplasm is abundant, highly amphophilic and irregularly eccentrically placed, with most cells having irregular cytoplasmic vacuoles containing pink proteinaceous material presumably immunoglobulin. Note that even those cells that appear sufficiently differentiated to have immunoglobulin vacuolation of cytoplasm are capable of undergoing mitosis (upper left).

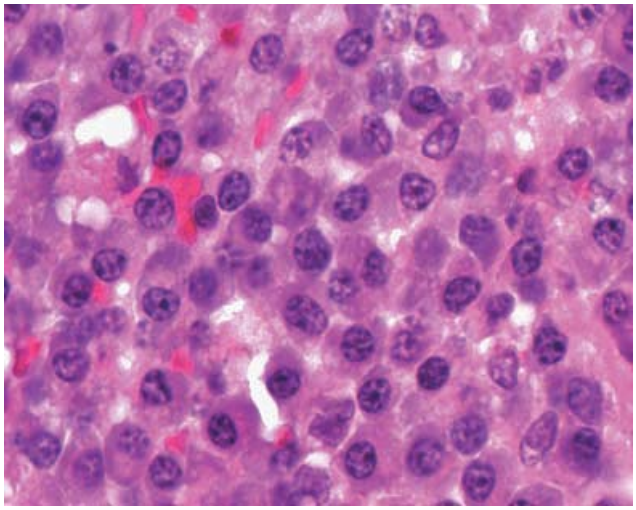

Figure 3.249. Cat: spleen, plasmacytoma. Detail of Figure 3.248. The nuclei are round to oval and 1.5 red cells in diameter with larger densely stained chromocenters and irregular parachromatin clearing. At low-power examination, the cells look relatively similar and might be mistaken for benign proliferation except for their abundance and homogeneity. Mitoses are rarely found. About half of the cells have a small relatively inapparent nucleolus. The cytoplasm is abundant and deeply stained with many cells having a perinuclear lighter-stained area or Golgi zone.

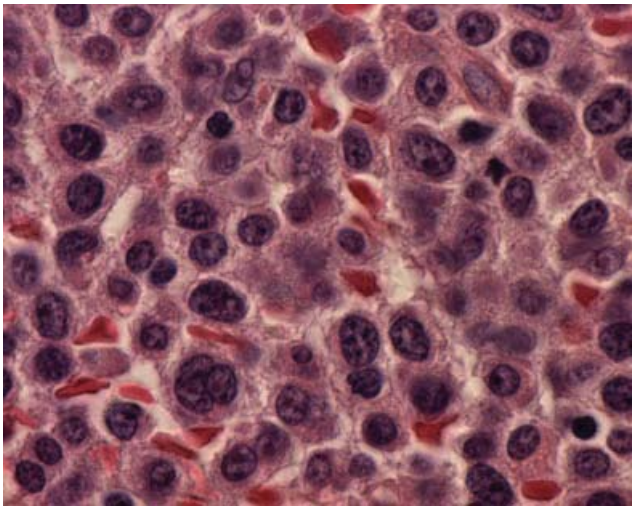

Figure 3.251. Human: lymph node, plasmacytoma. The node was diffusely involved with cells of this type. There is diffuse proliferation of cells with moderate anisokaryosis, and deeply stained nuclei. Nucleoli are present as well as binucleation but mitoses are rare. The cytoplasm is deeply stained and cell boundaries typically distinct. *Slide from Cornell Tutorial.*

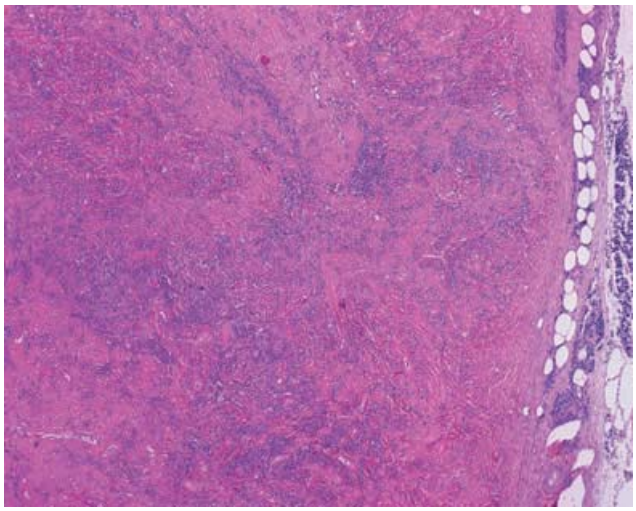

Figure 3.252. Dog: node, plasmacytoma with amyloid. There is complete loss of normal architecture, with the interior of the node dominated by amorphous proteinaceous deposition.

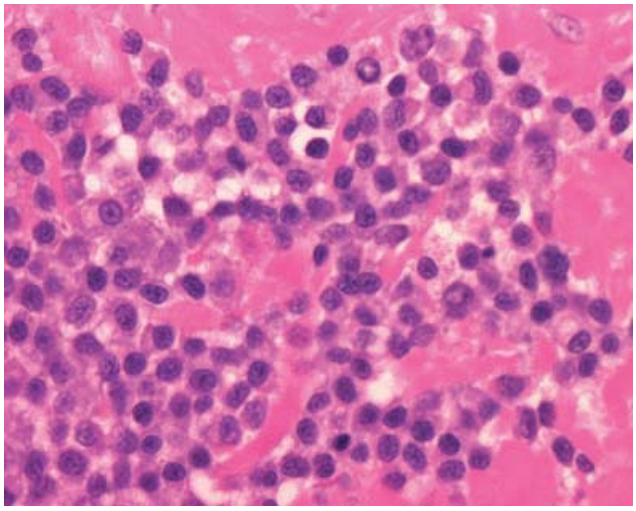

Figure 3.253. Dog: node, plasmacytoma with amyloid. Detail of Figure 3.252. Only scattered islands of neoplastic cells remain in the tissue that is now poorly vascularized and occupied by scattered connective tissue and residual plasma cells.

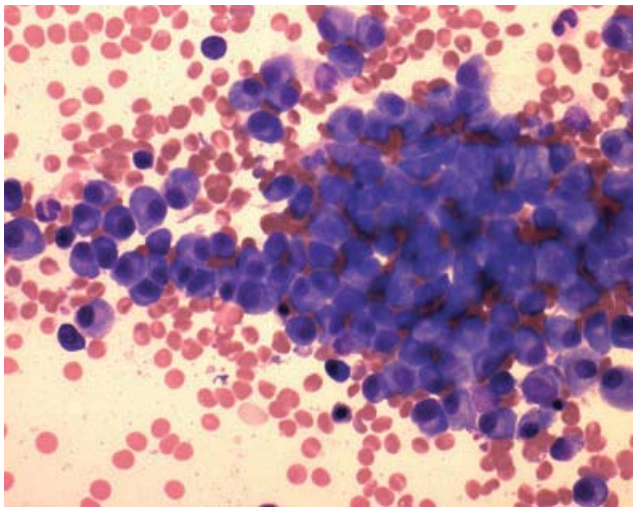

Figure 3.254. Dog: marrow aspirate, myeloma. There is complete phthisis of normal marrow cells, with a uniform population of plasmacytic-appearing cells with very basophilic cytoplasm and prominent Golgi zones. *Slide from R. M. Jacobs, DVM.*

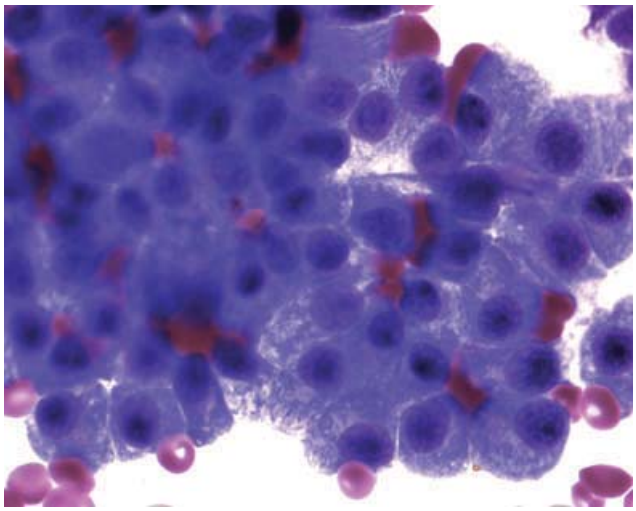

Figure 3.255. Dog: marrow aspirate, myeloma. Detail of Figure 3.254. Cytologically, there is little anisokaryosis, and cytoplasmic volume is abundant and uniform in volume and staining characteristics. The cells have small central nucleoli that are obscured by the cytoplasm. Binucleation and mitotic figures both are present in other fields but not frequently encountered.

more foci of bone lysis are noted, and on aspiration (Figs. 3.254, 3.255) or core biopsy (Figs. 3.256, 3.257) of specific sites, the diagnosis is made. Confirmation is generally made on the identification of hyperglobulinemia and gammopathy. Nonsecretory myelomas are uncommon, but the presence of lytic bone lesions and a focal population of atypical cells is strong evidence of malignant neoplasm, and the cells can usually be identified as of lymphoid origin by immunohistochemistry. The serum protein level may exceed 10 g/dl, and there is a marked increase is serum viscosity because of the excess of high molecular weight proteins. This protein level does not by itself appear to cause clinical signs; however, dogs with hyperglobulinemia may develop hypotensive shock under even light anesthesia for bone marrow biopsy. The presence of the light chain of the atypical globulin may appear in the urine of dogs and can be of either type, but it is predominantly of the lambda light chain type in plasmacytomas where that determination is a useful estimation

of clonality. Both cats and dogs with myeloma may have elevations in serum creatinine and urea and there is usually hypercalcemia of bone resorption and nonregenerative anemia and often thrombocytopenia. The latter effect on platelets is likely due to adherence of the high molecular weight proteins to the platelet membranes, resulting in venous sequestration.

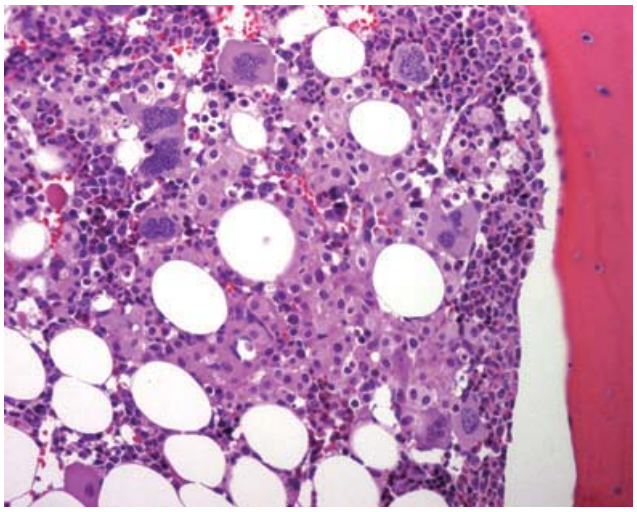

Figure 3.256. Dog: bone marrow core, myeloma. There is juxtacortical myelopoiesis (right) with the large pale myeloma cells immediately adjacent infiltrating and displacing bone marrow and fat.

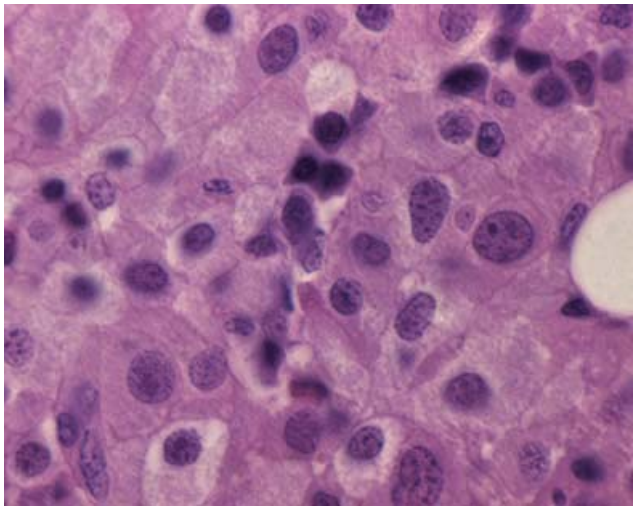

Figure 3.257. Dog: marrow, myeloma. Detail of Figure 3.256. An area dominated by myeloma cells with a few residual benign cells, likely late-stage rubricytes. The neoplastic cells have fine granular and dispersed chromatin with small nucleoli and abundant cytoplasm that is highly amphophilic, and cell boundaries are generally distinct.

Pathologic Features

Blood

There are no consistent changes in the blood with plasmacytoma unless the neoplasm happens to be secretory, as has been reported in the horse and appears to occur in about 1% of canine cases. These findings are in contrast to plasmacytoma in humans, where 25% of the extramedullary forms are accompanied by monoclonal gammopathy and plasmacytoma and myeloma are considered together because even focal osseus lesions have a high risk of dissemination.

In contrast, myeloma in the dog is most often secretory and accompanied by hyperglobulinemia of monoclonal type. The presenting blood picture is of an animal with mild anemia, with globulin levels in excess of 6.0 g/dl and albumin less than 2.0 g/dl, and moderate hypercalcemia. In dogs the gammopathy is about evenly split between IgG and IgA with all having a lambda light chain. Cats appear to be similar in these regards. Thrombocytopenia does not appear to be present in most cases at diagnosis, but the presence of hyperglobulinemia may be suspected on examination of the stained blood film because of the presence of the "lunar" or elliptical contraction artifacts, present in the background plasma, that occur as the preparation is drying (Fig. 3.258). Plasma cell neoplasms are only rarely leukemic and always at low levels (Fig. 3.259).

Bone Marrow

Myeloma or multiple myeloma, as it most often occurs, is a medullary lesion occurring in the axial skeleton and

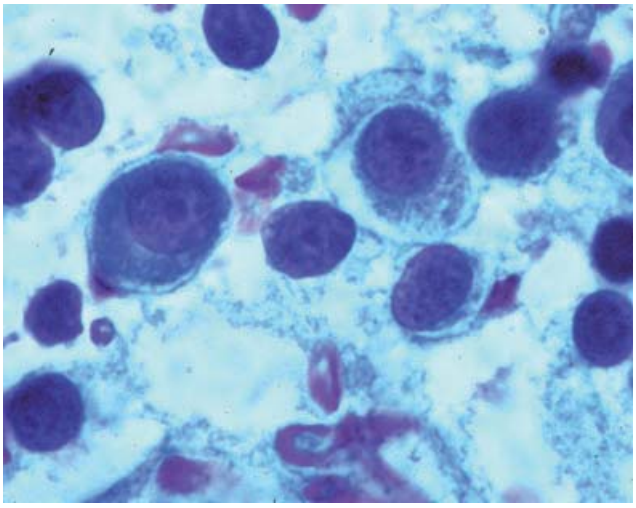

Figure 3.258. Dog: marrow aspirate, myeloma. The tumor is of secretory type, and the marrow aspirate was stained with the Papanicolaou method that accentuates the irregular chromatin distribution. There is a heavy proteinaceous background that has irregular dense aggregations accentuated by wet fixation.

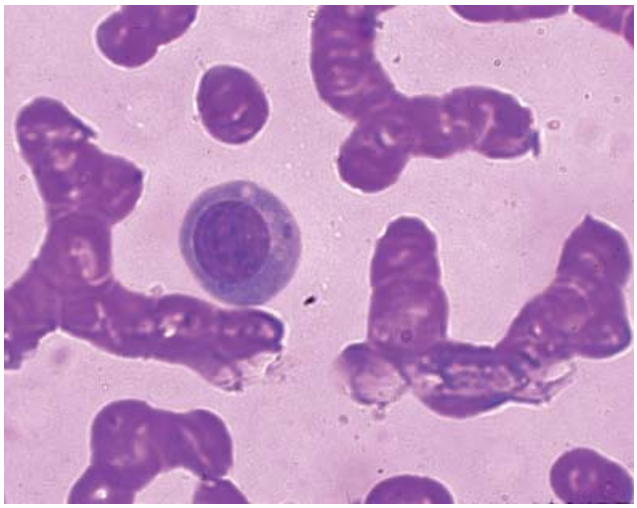

Figure 3.259. Dog: blood, myeloma. There is hyperproteinemia that contributes to the density of the background and prominent rouleau formation. The finding of neoplastic cells in the blood is a rare event that may be encouraged by manipulation and marrow biopsy.

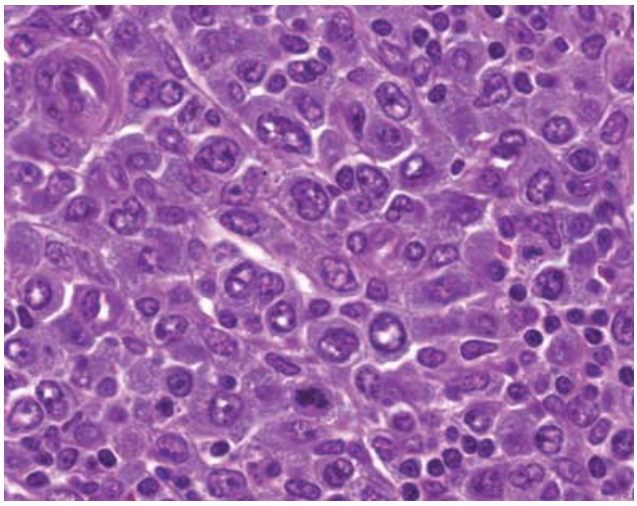

Figure 3.260. Mouse: spleen, anaplastic plasmacytoma. There is quite marked anisokaryosis and variation in nuclear shape with irregular chromatin patterns and marked parachromatin clearing. The nucleoli are prominent when in the plane of section and often multiple. The cytoplasm is abundant and highly amphophilic with cell boundaries generally distinct. *Slide from J. M. Ward, DVM.*

less often in proximal long bones and ribs. In bone, the lesions may be termed *monostotic* if single or *polyostotic* if multiple. Imaging directed aspiration or core biopsy of focal lytic regions of bone regularly results in a positive diagnosis if the bony lysis is caused by myeloma. Most myelomas are histologically and cytologically distinct, with nuclei regularly round and very uniform, 2 red cells in diameter, and occasionally binucleated (see Fig. 3.230). The chromatin is always densely stained and is arranged in very coarse large chromocenters, with small foci of parachromatin clearing in more mature neoplasms that have small or inapparent nucleoli (see Figs. 3.255, 3.257, 3.258). Rarely, amyloid may occur in cases of myeloma and in bone marrow. In the few cases described, the neoplasm is of a well-differentiated type that suggests the amyloid is of primary or lymphoid type and that both lesions likely arose as a consequence of chronic benign antigenemia and plasma cell hyperplasia. The myelomas with more clinically aggressive biology have a chromatin pattern that is much finer and often cribriform and have 1–2 prominent centrally located nucleoli (see Fig. 3.251). The cytoplasm also varies with the type of neoplasm and tends to be abundant, mildly eccentric, and highly amphophilic in more indolent cases and more closely resembles that of high-grade B-cell lymphoma in the most poorly differentiated tumors (Fig. 3.260). The mitotic rate varies, with the apparent nuclear and cytoplasmic maturation being almost absent in the most differentiated neoplasms and relatively frequent in those that border on plasmablastic lymphoma in the poorly differentiated types.

Because benign conditions may result in even diffuse marrow plasmacytosis, the diagnosis of myeloma generally rests on the presence of two or more of the classical findings, which include lytic bone lesions, focal atypical plasmacytosis, monoclonal gammopathy, and light chain or Bence-Jones proteinuria. Because the cytologic and histologic findings are very typical, particularly when associated with focal phthisis of normal marrow cells, and hyperproteinemia is easily measured, these two steps usually are taken as confirmation of the diagnosis. Not all myelomas are secretory and marked plasmacytosis may be present without gammopathy, which would in itself be an indication of malignancy since benign plasmacytosis like that associated with Leishmaniasis is characterized by marked gammopathy of polyclonal type. The presence of light chain proteinuria is not consistent in dogs, even in cases of secretory myeloma, and is not always looked for.

Lymph Node

Plasmacytoma is less frequent in the lymph nodes of both the dog and cat than in the skin or oral-digestive mucosa. Architecturally, nodal plasmacytoma tends to be a medullary lesion that progresses by peripheral expansion irregularly compressing the medullary sinuses and residual cortical areas with fading germinal centers beneath the outer sinus (Fig. 3.261). Cytologically, the disease in nodal areas is identical to that described below for the skin. Myeloma may be found in the nodes in advanced cases of that disease with cytomorphology like that of the more aggressive myeloma of marrow (Fig. 3.262).

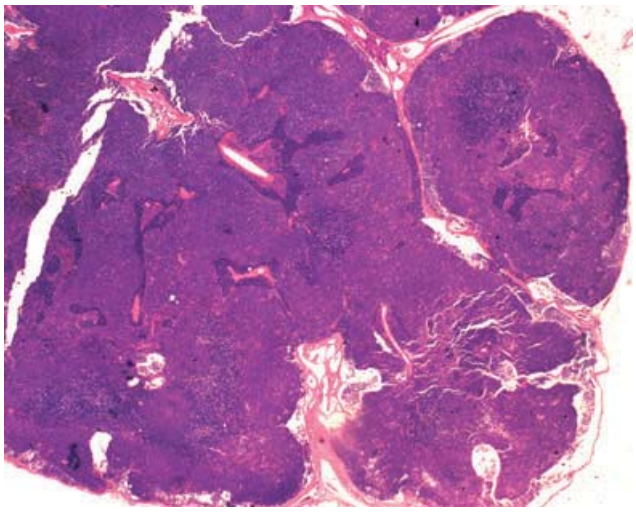

Figure 3.261. Dog: lymph node, plasmacytoma. The node is moderately enlarged without colonization of perinodal tissue. The peripheral sinuses are compressed but intact and the deep more basophilic stained areas represent fading areas of benign paracortex. The sinus areas are deeply stained and stellate, often compressed against the supporting vascular structures.

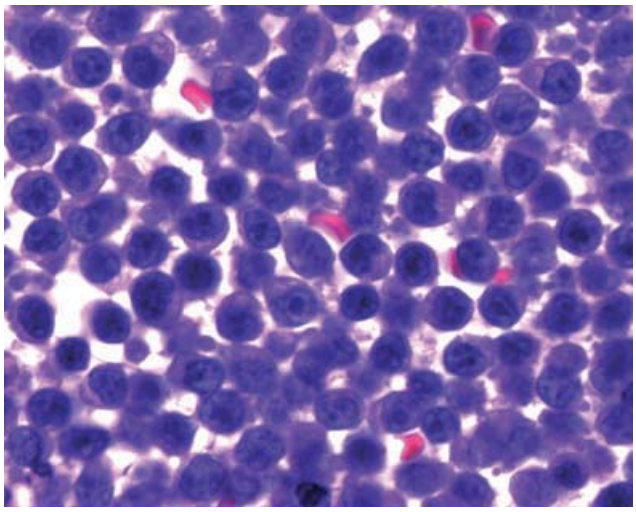

Figure 3.262. Dog: node, plasmacytoma. Detail of Figure 3.261. Image from a sinus area to better demonstrate cytoplasmic volume. The nuclei are generally round but occasionally indented, with densely stained dispersed chromatin with a few large dense chromocenters and prominent, often multiple, nucleoli. The cytoplasm is moderate in volume and highly amphophilic with irregular perinuclear clearing or Golgi areas. The mitotic rate is too low for plasmablastic lymphoma, which the lesion closely resembles.

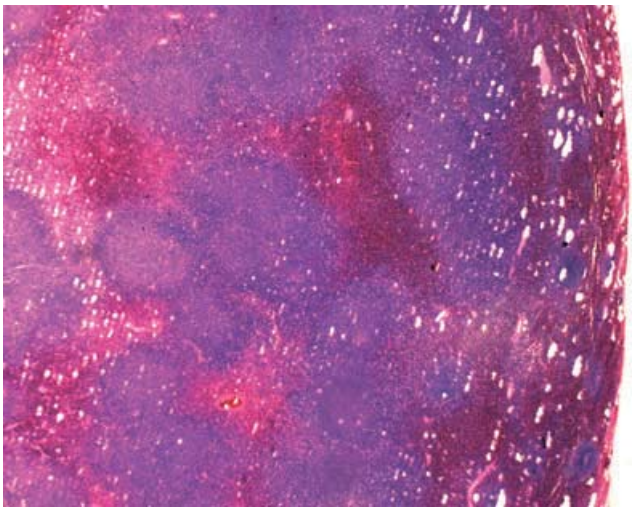

Figure 3.263. Dog: spleen, plasmacytoma. The lesion is a protruding area of spleen with a greatly thinned capsule that has multifocal areas of cellular proliferation, architecturally suggesting mantle cell lymphoma.

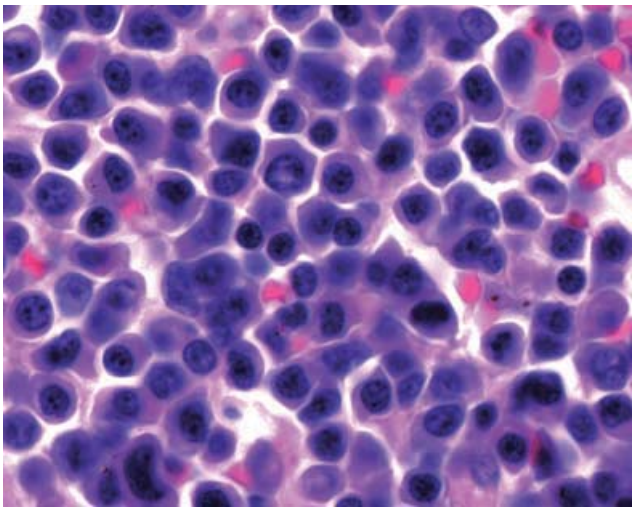

Figure 3.264. Dog: spleen, plasmacytoma. Detail of Figure 3.263. The proliferating cells have intermediate-sized nuclei that are hyperchromatic with a coarse chromatin structure and relatively prominent nucleoli. The cytoplasm is abundant and highly amphophilic with irregular Golgi zones and eccentric placement. The nuclei are larger and with greater atypia than seen in mantle cell lymphoma and with a higher mitotic rate with a mitotic figure (lower right).

Spleen

Plasmacytoma occurs frequently as a focal lesion in the spleen of the dog and less commonly in the cat where it is characteristically completely uniform and diffuse. In dogs, splenic plasmacytoma is usually part of a focal lesion that projects from the splenic surface and is usually considered part of a "fibrohistiocytic nodule"(Figs. 3.263, 3.264). Much less commonly in dogs, sheets of relatively normal-appearing plasma cells may be present between multiple foci of mantle cell lymphoma and may themselves be a precursor of the MCL neoplasm (Figs. 3.265, 3.266). In contrast in the cat plasmacytoma may be found

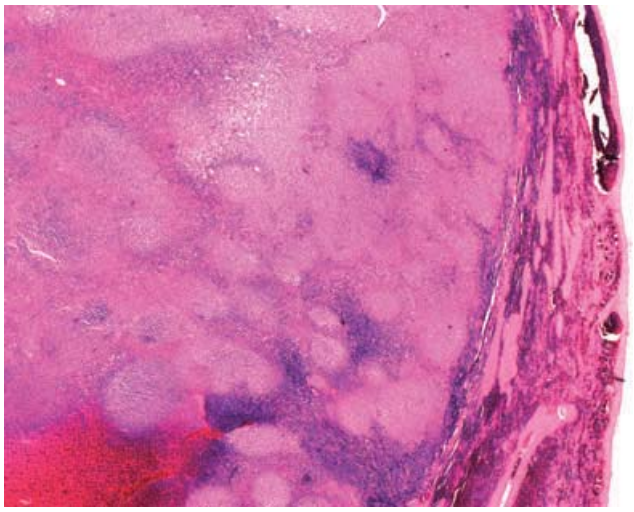

Figure 3.265. Dog: spleen, mantle cell lymphoma and plasmacytoma. Architecturally, the spleen contains a round nodular proliferation several centimeters in diameter that is compressing residual benign areas of spleen (right) and has focal interstitial areas of hemorrhagic infarction (lower left).

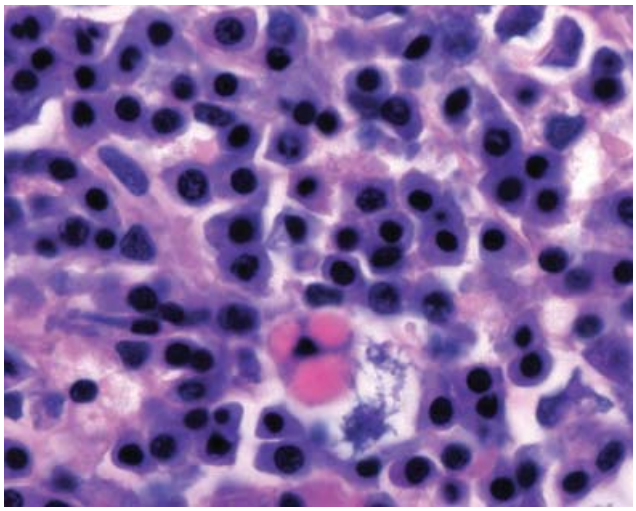

Figure 3.266. Dog: spleen, mantle cell lymphoma and plasmacytoma. Detail of Figure 3.265. Internodular area of mantle cell lymphoma with plasmacytosis. There is an accumulation of plasmacytoid like cells that have more than the usual anisokaryosis and nuclear hyperchromicity but with typical cytoplasmic volume and staining characteristics. The common association of these two lesions is suggestive that the plasmacytoma with a very low mitotic rate may be the initial lesion, with the mantle cell lymphoma arising as a second neoplasm.

as a diffuse sinus proliferation without major change in splenic size but with complete atrophy of both the follicular and thymic-dependent periarteriolar lymphoid sheaths. In the cat, the cells have minimal atypia and appear as diffuse sheets of well-differentiated plasma cells and without gammopathy (see Figs. 3.248, 3.249).

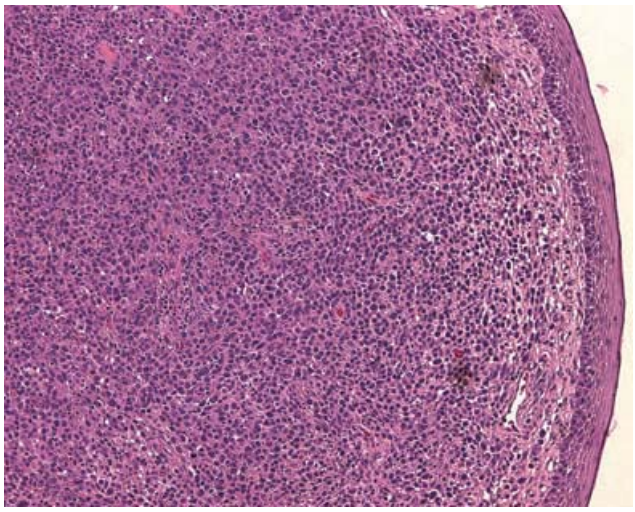

Figure 3.267. Cat: oral cavity, plasmacytoma. There is intact oral epithelium over a bulging maxillary mass. There is a narrow Grenz zone beneath the basement membrane of normal superficial dermis with dense cellular infiltrate extending to the depths of the biopsy.

Other Organs

Plasmacytoma in its usual presentation as a skin or aero-digestive lesion consists of a focal proliferation of atypical plasma cells that generally extend from a narrow Grenz zone to the depth of the dermal layer (Fig. 3.267). Architecturally, there is a solid mass of cells in central regions with a very fine fibrovascular supporting network and usually some indication of encapsulation that may be largely by compression of surrounding stroma by broad front expansion. The nuclei are round and regular, larger than normal plasma cells, and 2–2.5 red cells in diameter, and mitoses are rarely encountered (Fig. 3.268). The chromatin is uniformly distributed and hyperchromatic with nucleoli generally not present. Plasmacytomas have mild anisokaryosis in the more common cases and a few quite markedly enlarged nuclei in the atypical and likely clonal lesions. In addition, the other characteristic nuclear change is binucleation, which increases in frequency in more atypical cases. The cytoplasm is abundant and eccentrically placed and highly amphophilic, with Golgi zones present in many, but not all, cells. There are very few other cells present; ischemic necrosis with attendant reactive cell infiltration is not seen, but focal areas of amyloid deposition may be present. There is no clear distinction in histologic features between benign and clonal plasmacytomas, and even those that appear malignant are usually curable by wide excision. Most cases are diagnosed without phenotypic confirmation and while all are positive for vimentin, many are negative for CD79 alpha and CD20 but are often positive for lambda light chain (Fig. 3.269).

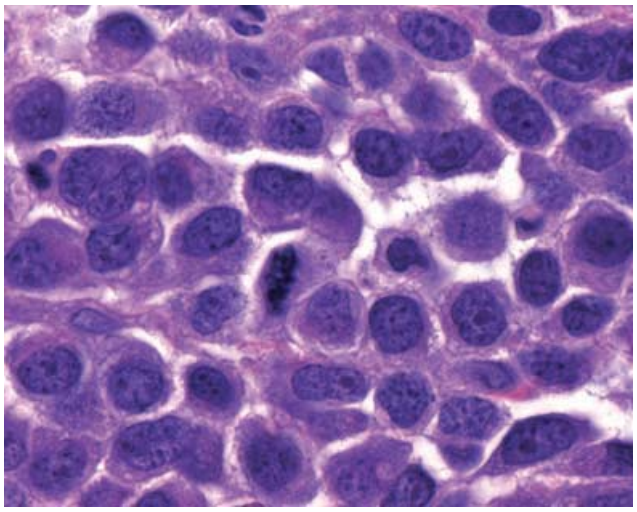

Figure 3.268. Cat: oral cavity, plasmacytoma. Detail of Figure 3.267. This lesion has extensive atypia with both mitosis and binucleation in this field as well as cells with quite large nuclei and 1–2 prominent nucleoli. The cytoplasm is abundant and highly amphophilic with mild irregular eccentric placement and Golgi zones and cell boundaries generally distinct.

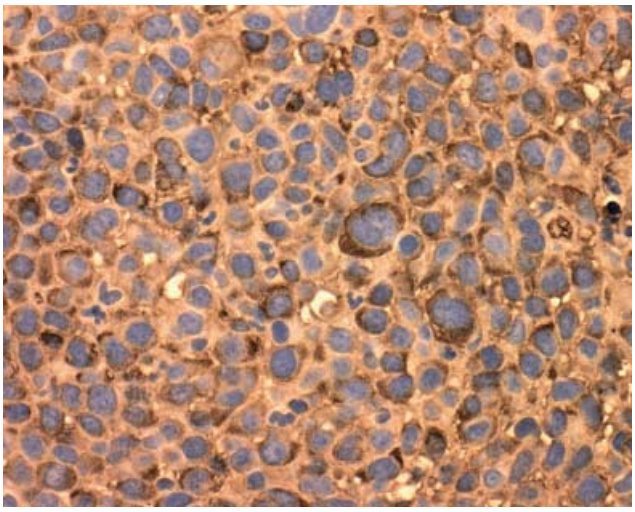

Figure 3.269. Cat: oral plasmacytoma. Phenotype of Figure 3.267. On staining with CD79, there was artifactual labeling of nuclei but no cytoplasmic marking. In contrast, on staining for the kappa light chain, the tissue was completely negative; for the lambda light chain (illustrated), there was uniform marking of cytoplasm and membranes with an unusually strong marking of large binucleated cells (center right). The uniform labeling with light chain strongly suggests clonality and the morphologic atypia supports the findings that those lesions located in the digestive tract are more likely to be biologically aggressive.

Immunologic Features

Plasmacytomas are consistently marked by vimentin and label irregularly with CD79 alpha in the dog, but they may be more consistently marked in the cat. Plasmacytomas in all animals are negative with CD3 and are less likely to mark with CD20 than for CD79. In limited personal experience, if staining for immunoglobulin is carried out there is occasionally marking for both IgM and IgG but most cases are negative for both. In contrast staining plasmacytomas in both the dog and cat with antibodies against the light chains for kappa and lambda are usually irregularly positive for both in benign cases and likely to be positive for lambda only in the more atypical lesions with nucleoli and evident mitotic activity. The latter strategy is a useful test for clonality and should be verified against molecular probes for immunoglobulin gene clonality by molecular means.

In contrast to plasmacytomas, the myelomas of the dog and cat mark consistently with CD79 alpha and are more likely to mark with reagents to identify IgG or IgA. In the few cases of myeloma recognized in other domestic animals, the same staining properties appear to apply. In cases with monoclonal gammopathy, the protein appearing in urine will reflect the genetic makeup of the clonal serum protein. In one case with the clonal serum protein identified as IgA with only alpha heavy chain and without kappa or lambda light chain, only alpha heavy chain appeared in the urine. The passage of this protein is not without impact on the kidney itself with a glomerulopathy resulting known as *myeloma kidney*.

Cytogenetic and Molecular Features

The only constant that can be stated for the plasma cell derived neoplasm is that they all are of B-cell origin and have rearrangement of the immunoglobulin gene that may be transcribed to a greater or lesser extent, depending on the stage of differentiation of the individual neoplasm.

Cell of Origin

Myeloma derives from a postgerminal center B-cell that has undergone isotype class switch and is likely a memory B-cell that becomes neoplastic late in B-cell ontogeny. In human myeloma, studies of the variable region of the immunoglobulin gene confirm a postgerminal center origin for these neoplasms. This evidence fits a pathogenetic origin in a plasma cell compartment and chronic immune stimulation with a high plasma cell population as a likely risk factor for oncogenic change. The rare concurrence of amyloidosis in plasma cell dyscrasias is compatible with a history of chronic benign lymphoid hyperplasia with ultimate neoplastic dysregulation.

Diagnostic Criteria

Architecturally, plasmacytomas are solidly cohesive cellular masses. Those near mucus membranes tend to be completely surrounded by a narrow encapsulation; those in skin present a solid front beneath the epidermis and on

the deeper surface but tend to have some irregular boundaries on the end interfaces with adjacent dermis. Cytologically, the cells are round and discrete with very well-defined cellular margins. The cells tend to be large and overall in the same size range as mast cells because of the cytoplasmic volume. They have more cytoplasm than most lymphomas plus binucleation that is characteristically most frequent in deeper areas of the tumor mass. The nuclei are round to oval 1.5–2.0 red cells in diameter with densely stained chromatin that varies in distribution with the degree of anaplasia. Plasmacytomas with a minimum of anisokaryosis and binucleation tend to have relatively densely stained chromatin that appears uniform at low magnifications and has large chromocenters on detailed examination but no parachromatin clearing between the most dense regions. The most characteristic appearance, inappropriately called "clock face," in benign cells has a very coarse cribriform pattern with chromatin densely stained with a "ropy" or woven pattern, with parachromatin clearing in a relatively regular pattern throughout the nucleus and with multiple nucleoli. The most anaplastic forms have a coarsely branched chromatin pattern with peripheralization onto the nuclear membrane and marked parachromatin clearing around prominent nucleoli. All of these have abundant cytoplasm that is highly amphophilic, and some in each population will have some degree of Golgi zone formation. Anaplastic plasmacytomas may have very irregular nuclei with bizarre anisokaryosis and may have occasional nuclei 6–10 red cells in diameter and lightly lobulated. The most typical forms in terms of uniform cell type are seen in the skin, and the most anaplastic forms are seen in those tumors arising in the stomach and rectum. The supporting fibrovascular stroma is delicate and relatively inapparent, and necrosis is not a feature. The mitotic rate is low in all forms.

Myelomas as they arise in bone are focal accumulations of neoplastic cells that are identified on architectural examination of marrow by complete phthisis of all marrow elements and including fat cells. The exclusion of fat cells from a dense focus of cellularity in an interstitial or paratrabecular area is typical, and the homogeneity of cell type found on cytologic examination is unlike myeloproliferation and indicative of neoplasm. Myelomas like plasmacytomas can be divided into three morphologic types that have been suggested to correspond to a tumor grading system. The most common type of myeloma as seen in dogs has round regular nuclei about 2 red cells in diameter with coarse cribriform chromatin pattern and multifocal small areas of parachromatin clearing. Most cells have one central nucleolus of moderate size and abundant, uniformly stained cytoplasm. The nuclei are centrally placed, with the cell size almost 3 times the nuclear diameter. The cell boundaries are closely faceted without intercellular spaces, but cell boundaries are distinct. Binucleation is present in most fields at 400× and mitoses are not found. The mitotic rate on this form of myeloma has been estimated at 1/20,000 neoplastic cells, whereas the mitotic rate for normal marrow cells is 1/8,000 indicating why cytoreductive therapy is ineffective on this tumor.

The next "grade" of myeloma has nuclei like the midgrade of plasmacytoma, with slightly larger nuclei about 2.5 red cells in diameter that are round and have a coarsely branched or coarsely granular chromatin pattern with parachromatin clearing and a prominent single central nucleolus. The cytoplasm is abundant but eccentrically or irregularly placed and cell boundaries are distinct with narrow cell separation. The architectural pattern is like the most differentiated form, and mitoses are not seen.

The most anaplastic-appearing myeloma has nuclear anisokaryosis that varies from 1.5 to 3.0 red cells in diameter. This size variation is coupled with much more variability in shape from round to oval or pear shaped, and occasionally with sharp nuclear indentations. The chromatin pattern is irregular coarse granular with very marked parachromatin clearing and 1–2 prominent nucleoli that are ringed by large dense chromocenters. The cytoplasm is moderate in volume and much more irregular in size and distribution than in the differentiated and moderately anaplastic types. Cell boundaries are distinct and the cytoplasmic staining is more irregular and less amphophilic than the more regular types. Mitoses are present and may reach 5–10/400× field with some apoptotic bodies but few tingible body macrophages.

The ultimate diagnosis of myeloma relies with the identification of neoplastic cells of plasmacytic lineage. This may be efficiently accomplished by marrow aspiration if the disease is well established and of typical homogeneous morphology of cells with very abundant deeply staining cytoplasm. However, if the cells are more representative of normal plasma cells and gammopathy is not identified or not present, the distinction between neoplasm and plasma cell dyscrasia may not be possible. To ensure that sufficient material is present to carry out additional studies, a marrow core is always a preferred addition to marrow aspiration permitting staining for B-cell lineage and followed, if needed, by light chain clonality.

Most cases of canine myeloma are of the secretory type and hyperglobulinemia of IgA or IgG type is found first as increased globulin of 6–10 g/dl on routine serum profile with monoclonal spike present if electrophoresis is carried out. If the latter procedure is done, it is preferable to run urine in parallel with the serum electrophoresis so the migration patterns of the protein peaks can be compared. The principal criteria for the diagnosis of myeloma are atypical marrow plasmacytosis associated with focal lytic

bone lesions and serum hyperglobulinemia. If focal lytic bone lesions are not found, but there is diffuse plasmacytosis and progressive increase in serum globulins, electrophoresis is indicated and myeloma confirmed if a monoclonal spike is present. Myeloma may be diagnosed in the absence of hyperglobulinemia if there is focal bone lysis associated with neoplastic-appearing plasma cells of myeloma cell type. In advanced cases, other signs may include hypercalcemia with uremia and thrombocytopenia and or coagulopathy and bleeding.

Differential Diagnosis

Plasmacytoma needs to be differentiated from plasmablastic lymphoma and melanoma or mast cell tumor with minimal cytoplasmic granulation. Plasmablastic lymphoma is rare and has a high mitotic rate, has multiple prominent nucleoli, and regularly marks with CD20 and less often with CD79 (Figs. 3.270–3.273). Plasmacytoma has a very low or absent mitotic rate and marks poorly with B-cell markers but is usually positive for staining with lambda light chain. The latter reaction distinguishes plasmacytoma from amelanotic melanoma, as does staining with Melan A. Mast cell tumors don't mark with staining for immunoglobulin or lambda light chain and are usually accompanied with numerous eosinophils not seen in plasmacytoma (Figs. 3.274–3.276).

Myeloma must be differentiated from causes of benign marrow plasmacytosis that may reach 50% in Leishmaniasis and is accompanied by hyperglobulinemia that is always polyclonal. In conditions of benign plasmacytosis, the cells are not atypical, the inciting agent may be intralesional in marrow or elsewhere, and focal bone lysis is not present.

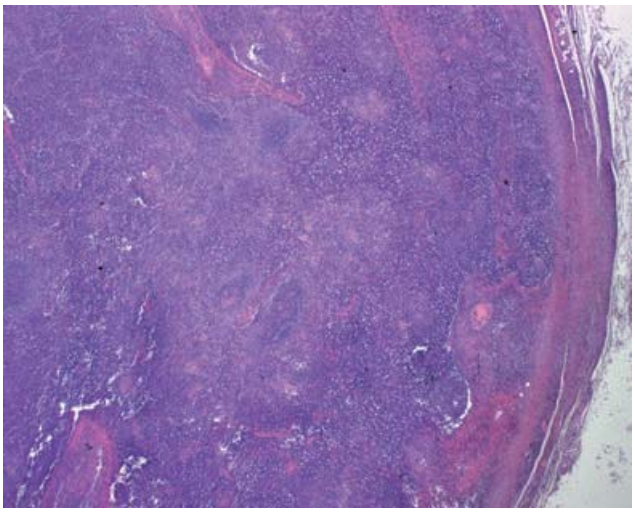

Figure 3.270. Horse: lymph node, plasmablastic lymphoma. There is marked thickening of the nodal capsule with destruction of the peripheral sinus. Small dark areas represent fading germinal centers with the nodal architecture largely completely destroyed. The sheets of cells with deeply stained cytoplasm are accompanied by a starry sky infiltration of tingible body macrophages. *Slide from J. Morrison, DVM, and S. P. McDonough, DVM.*

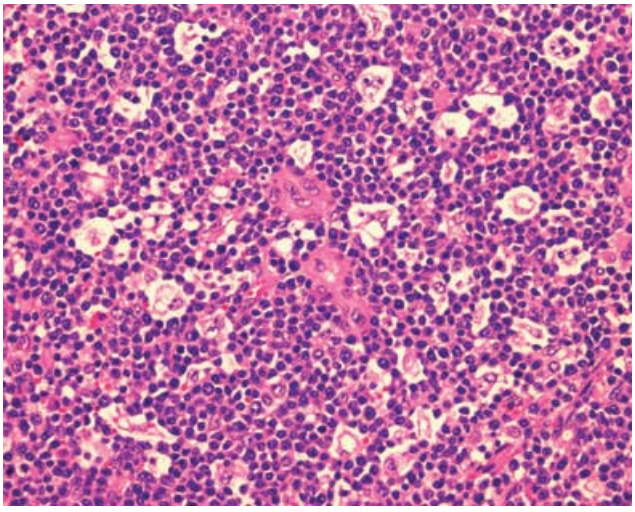

Figure 3.271. Horse: lymph node, plasmablastic lymphoma. Detail of Figure 3.170. On medium power, the diffuse areas of involvement resemble an abnormally large accumulation of plasma cells except for the presence of many tingible body macrophages typical of lesions with a high rate of proliferation and cell death.

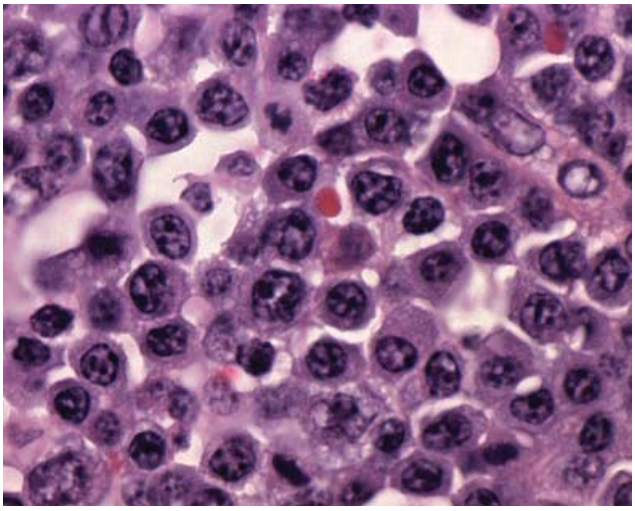

Figure 3.272. Horse: lymph node, plasmablastic lymphoma. Detail of Figure 3.270. Cytologically, the nuclei are hyperchromatic with irregular chromatin distribution, prominent parachromatin clearing, and multiple large nucleoli. There are 3 mitoses in this field at upper center and lower right and center. The high proliferative rate might be expected with the presence of the large number of tingible body macrophages. The nuclei are caricatures of benign germinal center centroblastic cells with multiple nucleoli impinging on the nuclear membranes. The cytoplasm is abundant and highly amphophilic with cell boundaries generally distinct.

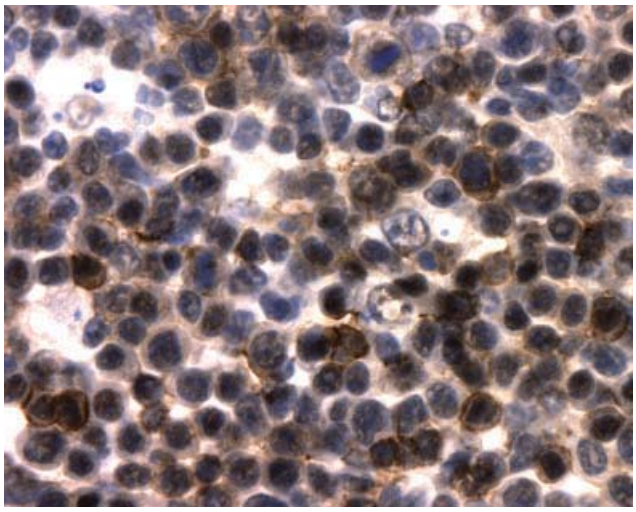

Figure 3.273. Horse: node, plasmablastic lymphoma. Phenotype of Figure 3.270. On staining with CD79, the tissues are largely negative. In contrast, on staining with CD20, the neoplastic cells are strongly and somewhat irregularly labeled. The positive marking with CD20 is indicative of these cells being of a more primitive type than is usual in plasmacytomas.

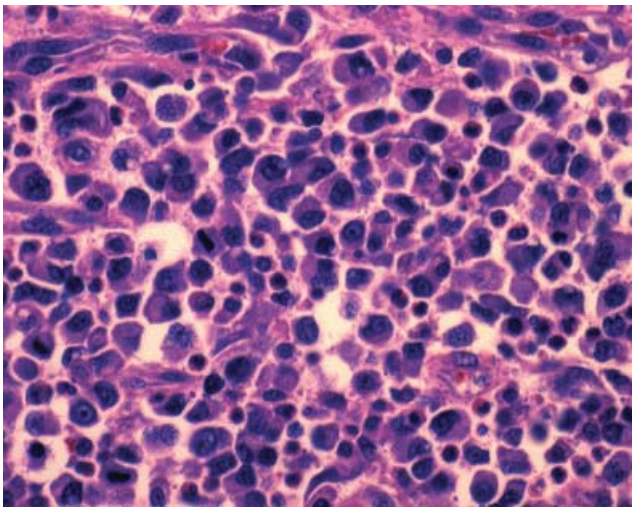

Figure 3.275. Dog: skin, mast cell tumor. Detail of Figure 3.274. The neoplastic cells have abundant cytoplasm frequently eccentrically placed and occasionally with perinuclear clear areas resembling Golgi zones. The cytoplasm is relatively agranular and eosinophils are not prominent.

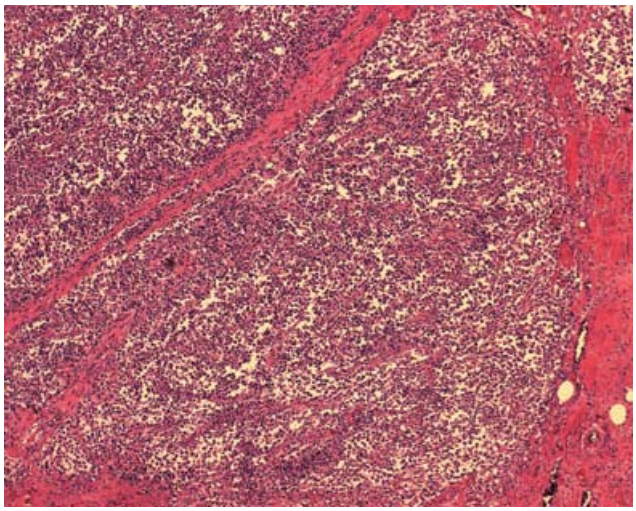

Figure 3.274. Dog: skin, mast cell tumor. A large-breed dog with recurrent mast cell tumor presented with a firm subcutaneous nodule interlaced with heavy collagen bands.

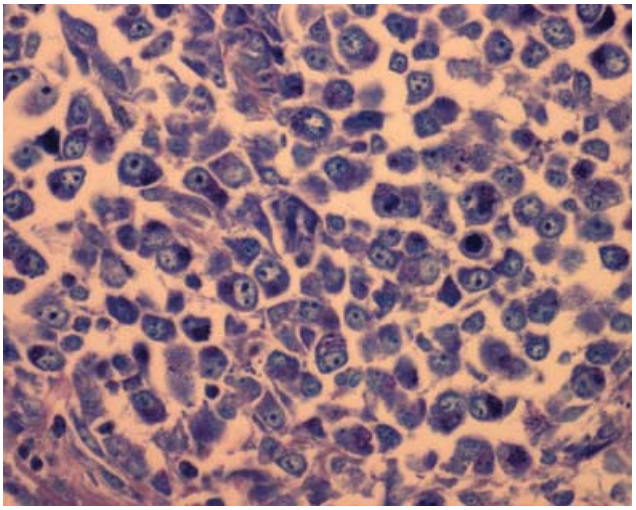

Figure 3.276. Dog: skin, mast cell tumor, Giemsa stain. Despite the apparent lack of granulation on routine staining, there are prominent aggregations of metachromatic material in the cytoplasm of most of the neoplastic cells.

Staging

Most plasmacytomas are single lesions and, unless in the aerodigestive tract and malignant in appearance with evidence of secretory activity, no staging is required. In contrast with myeloma, the major parameters applied in human medicine are logically applicable to the dog, though these seem not to be generally followed. A universal feature of myeloma is that tumor mass closely relates to stage of tumor progression. Because the mitotic rate is characteristic of the grade of myeloma, the rate of increase in the level of serum globulin is proportional to the mass of the neoplasm. Thus, screening radiographs for areas of bone lysis and levels of serum monoclonal globulin are the two most directly measurable parameters of staging. In addition, in human medicine and with logic for animals, the level of depression of albumin has prognostic value as does the appearance and increase in levels of serum beta$_2$-microglobulin. This latter serum factor

appears to closely correlate with both tumor mass and renal function, and hence survival.

Transformation and Progression

Focal plasmacytomas may be indolent and benign or aggressive and malignant at the time of first recognition. The outcome is then determined by the likelihood of complete surgical excision.

Myeloma appears not to change in cell type with progression but in cell numbers. The problem with myeloma is not in the proliferative rate of the neoplasm but in the death rate of tumor cells. Myeloma cells have a very low apoptotic rate and in early stages apoptosis of tumor cells may be initiated by administration of dexamethasone that in humans is felt likely related to reduced levels of BCL-2 expression. In myeloma, progression of the disease appears more related to increase in tumor cell mass and tumor-produced protein. These in combination result in pathologic fracture of affected bones and organ dysfunction due to gammopathy most apparent in decline of renal clearance.

Evaluation of the Treated Animal

The evaluation of a previously diagnosed case of myeloma in a dog most often is related to the rate of rise in serum globulin and difficulties in ambulation as a result of focal bone lysis. Because the neoplasm is unlikely to have changed, there is little to be gained by further bone biopsy, and renal function is closely related to survival and a good indicator of response to therapy. Like chronic myelogenous leukemia myeloma may rarely undergo "phenotypic escape" and convert to a high-grade lymphoblastic lymphoma with involvement of nodes, liver, and blood. This transition is less apparent in the dog, likely because canine myeloma is less often a spontaneous death but a judicious decision based on the stage of the disease.

Treatment and Survival

Initial therapy of myeloma is directed at reducing bone pain and tumor burden. Melphalan is the initial treatment of choice with cyclophosphamide and chlorambucil used as alternative alkylating agents. In dogs that have relapsed under therapy for myeloma, vincristine and doxorubicin have been used in combination with dexamethasone. Most treated dogs survive longer than a year with mean survival of 1.5 years reported. Cats appear to do less well and seldom survive to 5–6 months.

Newer targets of therapy in myeloma and other hematologic malignancies include the proteasome, a nuclear protease structure involved in cell cycle regulation, cell adhesion, inflammation and protein kinetics. Agents to inhibit proteasome activity are in trial and appear to have activity alone and in combination with more currently used agents.

REFERENCES FOR PLASMACYTOMA

Chaffin, K., Cross, A., Allen, S., Mahaffey, E., and Watson, S. (1998) Extramedullary plasmacytoma in the trachea of a dog. *JAVMA* 212(10):1579–1581.

Clark, G., Berg, J., Engler, S., and Bronson, R. (1992) Extramedullary Plasmacytoma in dogs: Results of surgical excision in 131 cases. *J Am An Hosp Assoc* 28:105–111.

Hamilton, T., and Carpenter, J. (1994) Esophageal plasmacytoma in a dog. *JAVMA* 204(8):1210–1211.

McConkey, S., Lopez, A., and Pringle, J. (2000) Extramedullary plasmacytoma in a horse with ptyalism and dysphagia. *J Vet Diagn Invest* 12:282–284.

Platz, S., Breuer, W., Pfleghaar, S., Minkus, G., and Hermanns, W. (1999) Prognostic value of histopathological grading in canine extramedullary plasmacytomas. *Vet Pathol* 36:23–27.

Ramos-Vara, J., Miller, M., Pace, L., Linke, R., Common, R., and Watson, G. (1998) Intestinal multinodular A-amyloid deposition associated with extramedullary plasmacytoma in three dogs: Clinicopathological and immunohistochemical studies. *J Comp Path* 119:239–249.

Rowland, P., Valentine, B., Stebbins, K., and Smith, C. (1991) Cutaneous plasmacytomas with amyloid in six dogs. *Vet Pathol* 28:125–130.

REFERENCES FOR MYELOMA

Bienzle, D., Silverstein, D., and Chaffin, K. (2000) Multiple myeloma in cats: Variable presentation with different immunoglobulin isotypes in two cats. *Vet Pathol* 37:364–369.

Burnett, R., Blake, M., Thompson, L., Avery, P., and Avery, A. (2004) Evolution of a B-cell lymphoma to multiple myeloma after chemotherapy. *J Vet Intern Med* 18:768–771.

Durie, B., and Salmon, S. (1975) Cellular kinetics, staging, and immunoglobulin synthesis in multiple myeloma. *Ann Rev Med* 283–288.

Kim, D., Taylor, H., Eades, S., and Cho, D. (2005) Systemic AL amyloidosis associated with multiple myeloma in a horse. *Vet Pathol* 42:81–84.

Lautzenhiser, S., Walker, M., and Goring, R. (2003) Unusual IgM-secreting multiple myeloma in a dog. *JAVMA* 223(5): 645–648.

MacEwen, E., Patnaik, A., Hurvitz, A., Bradley, R., Claypoole, T., Withrow, S., Erlandson, R., and Lieberman, P. (1984) Nonsecretory multiple myeloma in two dogs. *JAVMA* 144(10):1283–1286.

Rettig, M., Ma, H., Vescio, R., Pold, M., Schiller, G., Belson, D., Savage, A., Nishikubo, C., Wu, C., Fraser, J., Said, J., and Berenson, J. (1997) Kaposi's sarcoma–associated herpesvirus infection of bone marrow dendritic cells from multiple myeloma patients. *Science* 276:1851–1854.

Richardson, P., Hideshima, T., Mitsiades, C., and Anderson, K. (2004) Proteasome inhibition in hematologic malignancies. *Ann Med* 36:304–314.

Sheafor, S., Gamblin, R., and Couto, C. (1996) Hypercalcemia in two cats with multiple myeloma. *J Am An Hosp Assoc* 32:503–508.

Sukpanichnant, S., Cousar, J., Leelasiri, A., Graber, S., Greer, J., and Collins, R. (1994) Diagnostic criteria and histologic grading in multiple myeloma: Histologic and immunohistologic analysis of 176 cases with clinical correlation. *Human Pathol* 25(3):308–318.

Weber, N., and Tebeau, C. (1998) An unusual presentation of multiple myeloma in two cats. *J Am An Hosp Assoc* 34:477–483.

Lymphoplasmacytic Lymphoma

Definition

Lymphoplasmacytic lymphoma (LPL) is a clonal neoplasm of intermediate-sized cells that have nuclei 1–1.5 red cells in diameter, with relatively broad and eccentrically located cytoplasm that is highly amphophilic. The chromatin pattern is coarsely granular, with most cells lacking nucleoli, and the mitotic rate is very low, usually less than 1.0 per 400× field.

Epidemiology and Incidence

Lymphoplasmacytic lymphoma occurs in all domestic animals and is seen most frequently in the horse and cat, less common in other species. LPL was found in 37 of 751 cases of feline lymphoproliferative disease (4.9%) and in 17 of 503 cases of canine lymphomas (3.4%). LPL occurs over a wide age range in the dog and cat, but is mainly seen in mature animals in the cow and horse. In 36 cases of LPL in the cat, the age ranged from 1–18 years with a mean of 9.0 years. In dogs, the age ranged from 2.5–14 years with a mean of 3.4 years. In cattle, LPL appears to be a disease of mature animals and has a similar age distribution in the horse. In cats, the gender ratio including neutered was M = 21 and F = 15, and in dogs the ratio was M = 11 and F = 7. In cattle, the disease is diagnosed most often in dairy animals, which results in a wide apparent predominance in females. In horses, the gender ratio is about 1:1. LPL is rare in humans and constitutes less than 2% of all non-Hodgkin's lymphomas, and it may be seen with the gammopathy of the Waldenstrom IgM type (Figs. 3.277, 3.278).

Clinical Presentation and Features

In cats, the presentation of animals with LPL was multicentric in 14/37, gastrointestinal in 14/37, mediastinal in 6, and renal in 2. In dogs, the presentation was primarily nodal and in cattle and horses primarily gastrointestinal. Cats and dogs generally present in good condition and retaining a normal appetite. In contrast, in cattle there may be melena of recent onset with declining production and activity for some time, often with recurrent diarrhea. Horses tend to present with recurrent colic and mild to moderate weight loss.

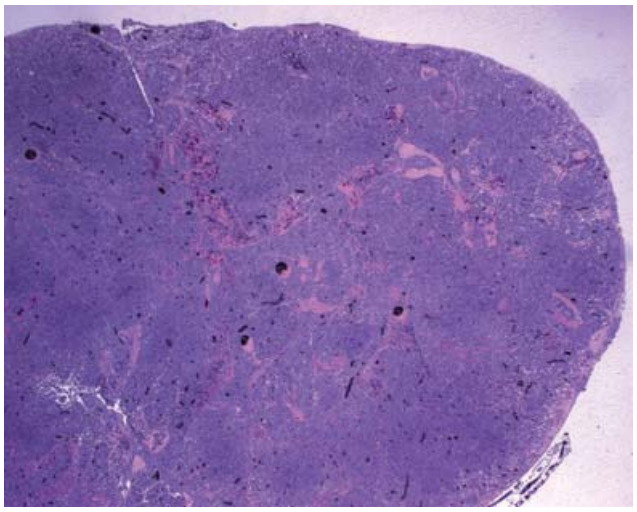

Figure 3.277. Human: lymph node, lymphoplasmacytic lymphoma. The capsule is thinned and taut without involvement of perinodal tissue and with the peripheral sinus compressed and a complete loss of normal follicular and medullary architecture. *Slide from Cornell Tutorial.*

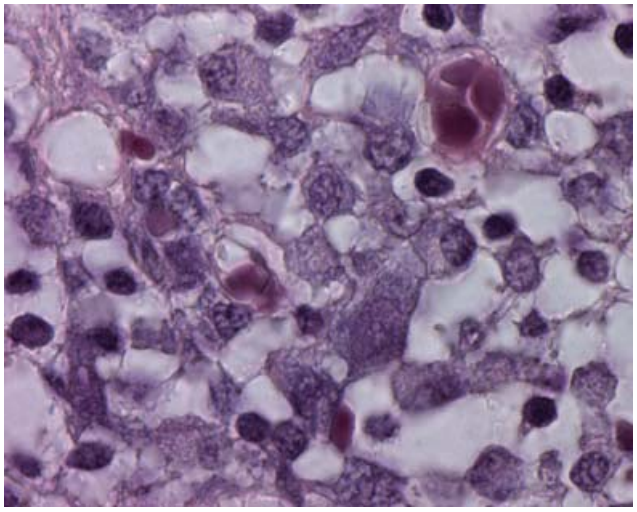

Figure 3.278. Human: node, lymphoplasmacytic lymphoma. Detail of Figure 3.277. The nuclei appear vesicular but are quite small compared to the size of red cells (upper right). The cytoplasm is relatively abundant with moderate basophilia and fine vacuolations. The patient had Mu heavy chain disease.

Pathologic Features

Blood

In animals, LPL does not generally present with specific changes in the blood, and mild to moderate anemia of chronic disease is the most frequent abnormality. Rarely, horses will have a gammopathy that is associated with a laminar infiltration of plasmacytoid cells in the small intestine extending several feet and usually with focal

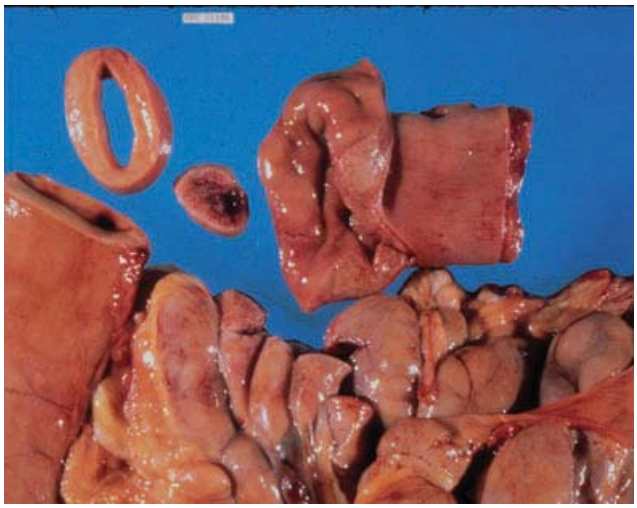

Figure 3.279. Equine: small intestine, lymphoplasmacytic lymphoma. There is laminar infiltration of the small intestine over an extended region of the upper small intestine that is limited to the pancreas and adjacent mesenteric nodes.

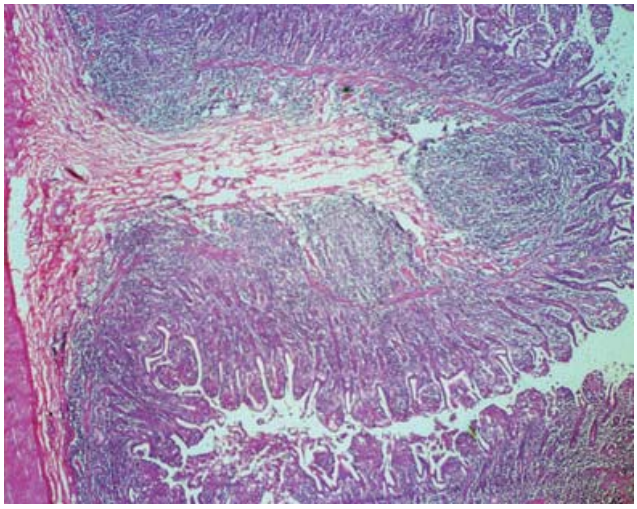

Figure 3.280. Horse: small intestine, lymphoplasmacytic lymphoma. Histology of the case in Figure 3.279. There is massive infiltration into the lamina propria and irregularly into the villi with relative sparing of the submucosa and tunica muscularis. The increased mucosal volume has caused the intestinal mucosa to form deep linear folds.

involvement of the pancreas (Figs. 3.279–3.281). These cases are remarkably similar to the macroglobulinemia of Waldenstrom type seen in about 1/3 of humans with LPL. In the human form of LPL hyperviscosity of blood resulting from the paraproteinemia may be the only symptom causing examination because of dizziness or recurrent nasal or oral bleeding.

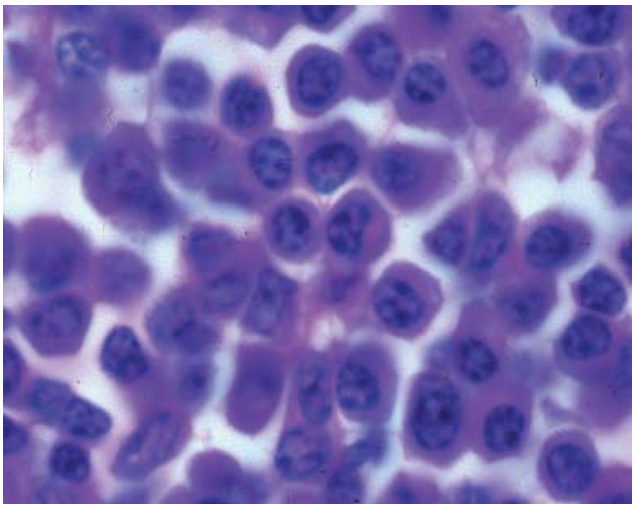

Figure 3.281. Horse: small intestine, lymphoplasmacytic lymphoma. Detail of Figure 3.279. The nuclei are of intermediate size, with mild anisokaryosis and large deeply stained chromocenters with marked irregular parachromatin clearing. The cytoplasm is relatively abundant and highly amphophilic.

Bone Marrow

Marrow has not been examined with sufficient frequency in LPL of animals to comment with any confidence. Most papers on small cell lymphomas of animals have not recognized LPL as a neoplasm separate from CLL or SLL. In humans, LPL usually presents as a disseminated disease and tends to have a poor prognosis. Because the disease in animals is usually diagnosed on node biopsy and treated as a small cell lymphoma with low proliferative rate, the marrow tends not to be examined. Further, on aspiration, focal tumor may not be recognized because the small cells of LPL are easily missed if they do not predominate. In cases where marrow has been examined, there is very high cellularity of about 80–90%, with fat cells largely remaining in the central cavity. The marrow is uniformly infiltrated with LPL cells, with the tissue having a more pink appearance histologically because of the number of LPL cells with pink cytoplasm (Fig. 3.282). There is an apparent reduction in marrow granulocyte reserves that gives the tissue an appearance of cellular uniformity. The LPL cell nuclei are similar in diameter to those of polychromatic rubricytes, but they have more cytoplasmic volume and are much more eosinophilic than the red cell precursors at that stage of development (Fig. 3.283). Megakaryocytes persist as the lone cell type that stands out. Without immunohistochemistry, it is impossible to realize the number of neoplastic cells present.

Lymph Node

Nodal histology in LPL is relatively consistent with a thinned and intact capsule usually without involvement of

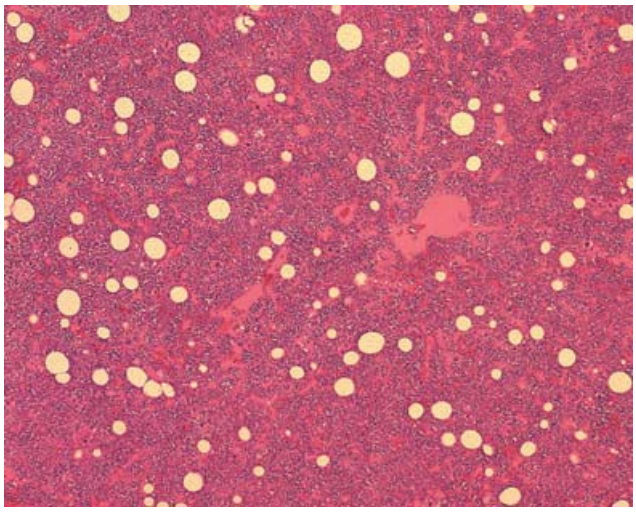

Figure 3.282. Cat: bone marrow, lymphoplasmacytic lymphoma. The marrow is almost solidly infiltrated with atypical cells with relative phthisis of normal cell types.

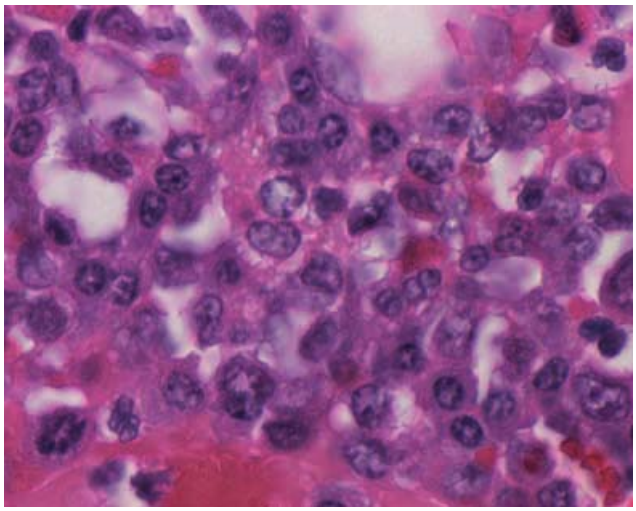

Figure 3.283. Cat: marrow, lymphoplasmacytic lymphoma. Detail of Figure 3.282. The neoplastic cells irregularly infiltrate the marrow and are identified as those with small round to oval nuclei that have relatively abundant highly amphophilic cytoplasm. The cells are present in small clusters at upper center and lower right and lower center.

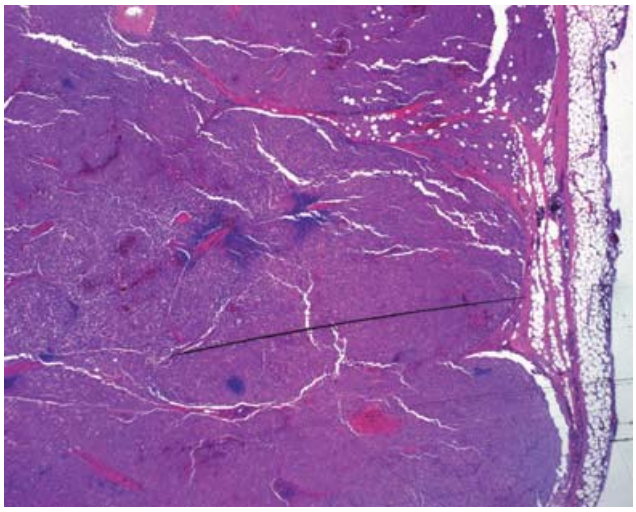

Figure 3.284. Dog: lymph node, lymphoplasmacytic lymphoma. The capsule is thinned but there is no involvement of perinodal tissues. The cellular proliferation is irregularly compressing the peripheral sinus and there is loss of normal cortical architecture. The small dark-staining areas represent residual foci of small benign lymphocytes.

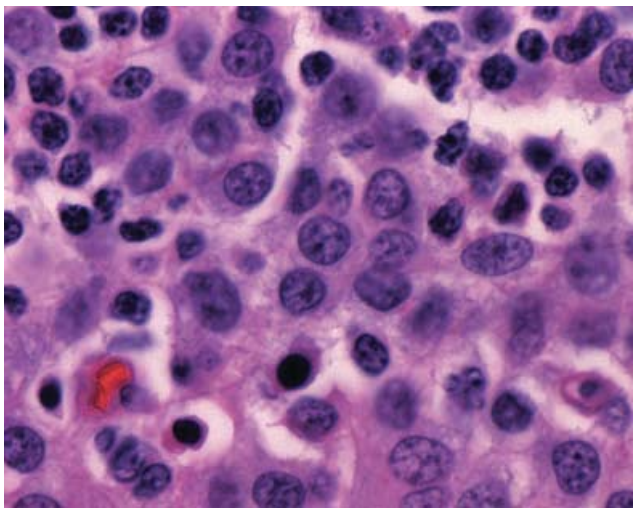

Figure 3.285. Dog: lymph node, lymphoplasmacytic lymphoma. Detail of Figure 3.284. Image taken adjacent to (upper) foci of fading mantle cells, for size comparison. The neoplastic cells have round to oval nuclei that are without indentation and have a fine granular chromatin pattern with nucleoli generally indistinct. The cytoplasm is relatively abundant and highly amphophilic with cell boundaries generally indistinct.

perinodal structures. The peripheral sinus may be compressed but is intact, and the medullary stroma is limited to the larger vascular structures. Architecturally, the node has a bland diffuse appearance with multiple small foci of small darkly staining cells of fading mantle cell areas. There is a general appearance of greater "redness" than the blue usually associated with small nuclei (Figs. 3.284, 3.285). There is complete filling of the medullary cords and sinuses with residual fine sinus boundaries defining the areas of cellular proliferation (Figs. 3.286, 3.287). Oddly, there may be focal dilation of small veins without general congestion of the node parenchyma (Fig. 3.288). In some cases, there is also marked dilation of thin-walled medullary sinuses by highly proteinaceous fluid that may result from products of the neoplastic cells causing

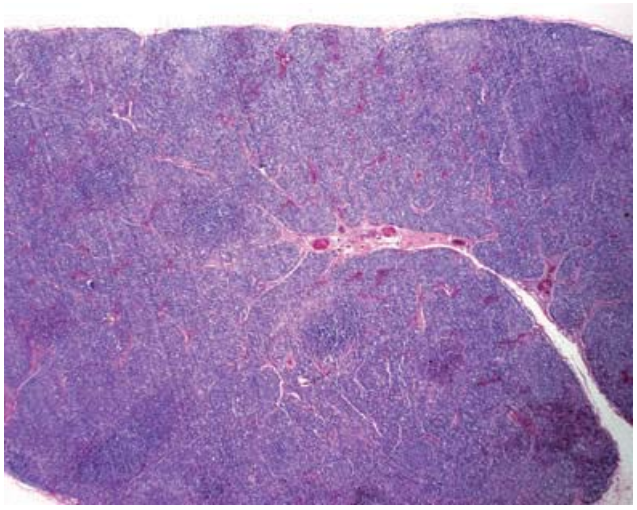

Figure 3.286. Cat: lymph node, lymphoplasmacytic lymphoma. The capsule is thinned without involvement of perinodal tissues and with complete effacement of normal node architecture. There is filling of the medullary cords and complete compression of medullary sinuses, all of which are tightly applied to the central larger vessels and supporting structures.

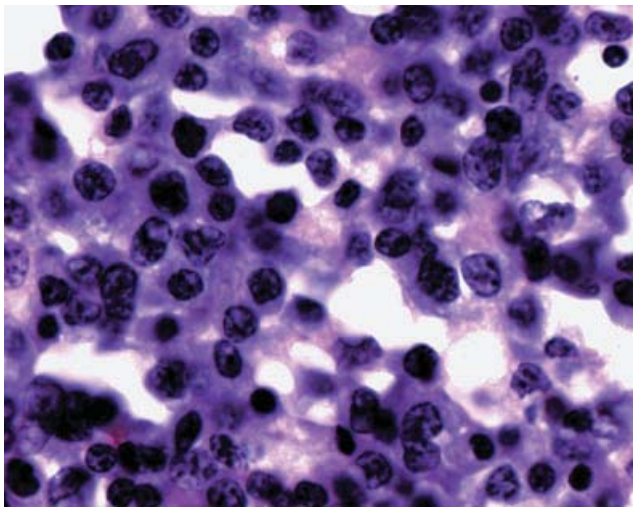

Figure 3.287. Cat: node, lymphoplasmacytic lymphoma. Detail of Figure 3.286. The lesion is characterized by quite widespread apoptosis with the small more densely stained nuclei, part of the neoplastic population that is being engulfed by tingible body macrophages accounting for the wide irregular spaces. The nuclei are round to oval and generally 1.5 red cells in diameter, with a hyperchromatic coarse chromatin distribution with mild irregular parachromatin clearing and relatively abundant highly amphophilic cytoplasm.

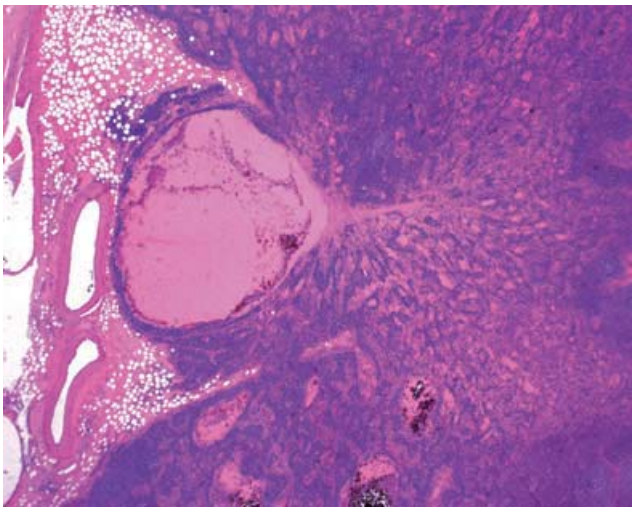

Figure 3.288. Cat: lymph node, lymphoplasmacytic lymphoma. There is quite prominent medullary venous ectasia involving dilated and thin walled veins in the hilar area of the node.

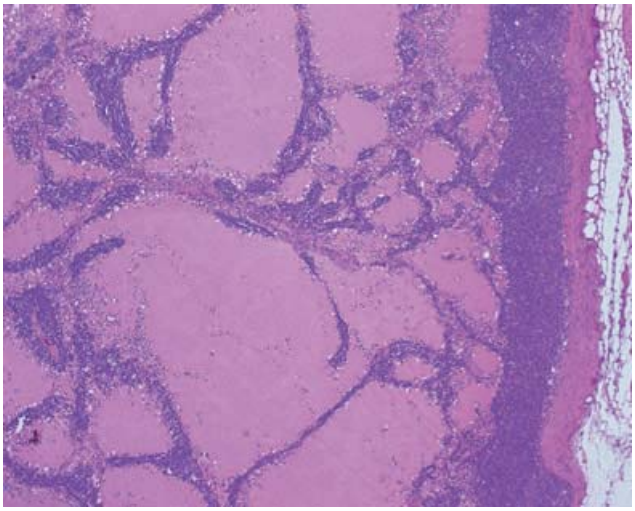

Figure 3.289. Cat: lymph node, lymphoplasmacytic lymphoma, same case as Figure 3.288. In this node, there is marked distention of medullary sinuses by a thick proteinaceous fluid that is very largely cell free. The compartments are each lined by very delicate membrane with no indication of inflammatory or other change. It is not known whether the animal had a gammopathy associated with the neoplastic proliferation.

increased viscosity in local lymphatic and venous drainage (Fig. 3.289). Cytologically, the LPL cells with adequate fixation have round entire nuclei with large chromocenters and variable parachromatin clearing, and many have small but prominent nucleoli that may be multiple in some cases. The mitotic rate varies from rare to 1–2/400× field, but most have numerous apoptotic nuclei and a moderate number of tingible body macrophages. The nuclei appear dense at low magnification but have a surprising level of vesiculation when seen at high magnification. The cytoplasm is characteristic and not abundant, forming a relatively complete envelope around most nuclei that is deep

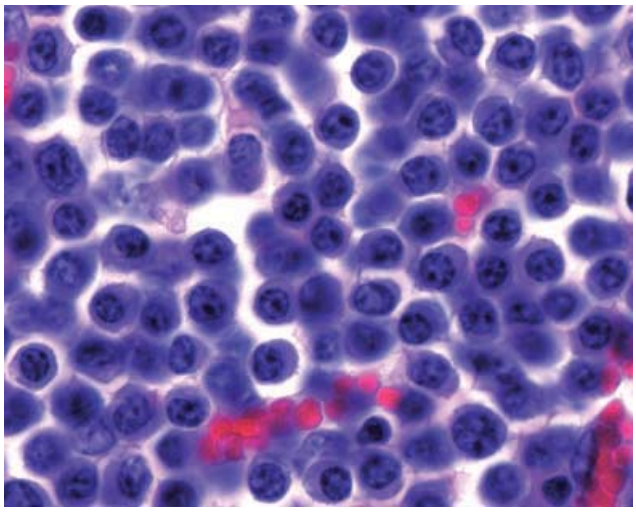

Figure 3.290. Horse: lymph node, lymphoplasmacytic lymphoma. This tissue is typical of most equine necropsy specimens, with considerable delay between death and tissue collection and fixation that results in more pronounced variations in chromatin distribution. This image accurately depicts nuclear size, shape, and size variation with a distinct ellipse of finely amphophilic cytoplasm. There is a very coarse chromatin pattern with irregular and incomplete parachromatin clearing and most cells lacking nucleoli.

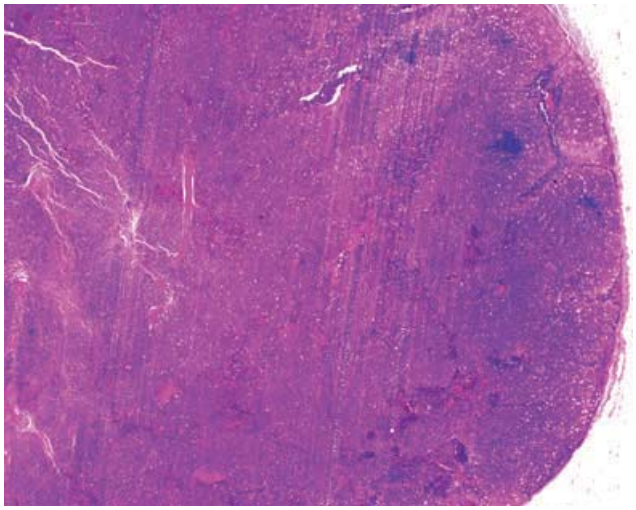

Figure 3.291. Dog: lymph node, lymphoplasmacytic lymphoma. The degree of redness is typical of the small cell lymphomas with lymphoplasmacytoid level of cytoplasmic development. The fading clusters of dark cells represent residual subcapsular germinal centers.

red on most hematoxylin and eosin preparations (Figs. 3.290–3.292). Unlike most small cell lymphomas, the cell boundaries are distinct. The LPL of animals much more closely fits the description of cells of "lymphoplasmacytoid" type with minimal cytoplasm rather than the "lymphoplasmacytic" used to designate cells with greater cytoplasmic volume and more typical eccentric placement.

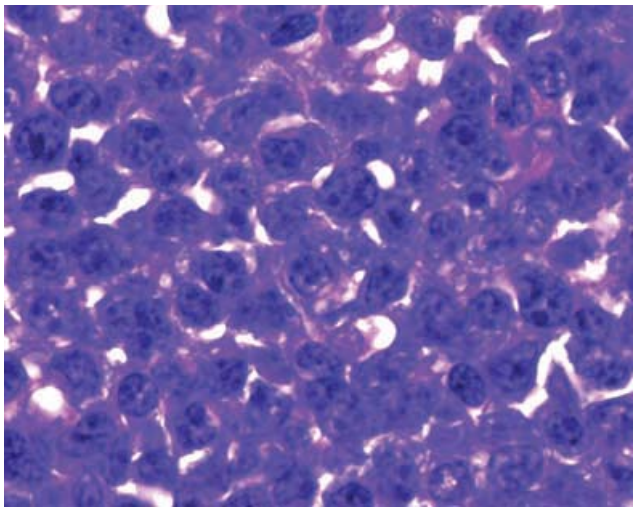

Figure 3.292. Dog: lymph node, lymphoplasmacytoid lymphoma. Detail of Figure 3.291. The nuclei are round to oval and vary moderately in diameter with a coarse chromatin pattern and irregular parachromatin clearing. There are 1–2 quite prominent nucleoli with most nuclei having a relatively complete encirclement of cytoplasm that is highly amphophilic.

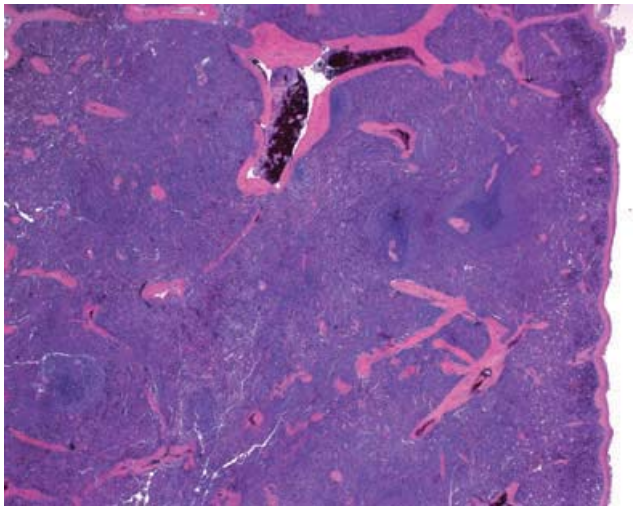

Figure 3.293. Dog: spleen, lymphoplasmacytoid lymphoma. The round pale areas represent a cuff of benign marginal zone cells around the collapsed cuff of mantle cells of fading germinal centers. The sinus areas are solidly filled with plasmacytoid cells of the same type as in nodes imparting a reddish appearance at the architectural level. Note the complete absence of periarteriolar lymphoid sheaths that have undergone atrophy along with the B-cell system.

Spleen

Splenic changes in LPL tend to be diffuse, with the organ not enlarged and with muscular trabeculae prominent and closely linked and the whole tissue having an overall "redness" due to the uniformity of the packed cells of the sinus areas (Figs. 3.293, 3.294). In advanced cases, there

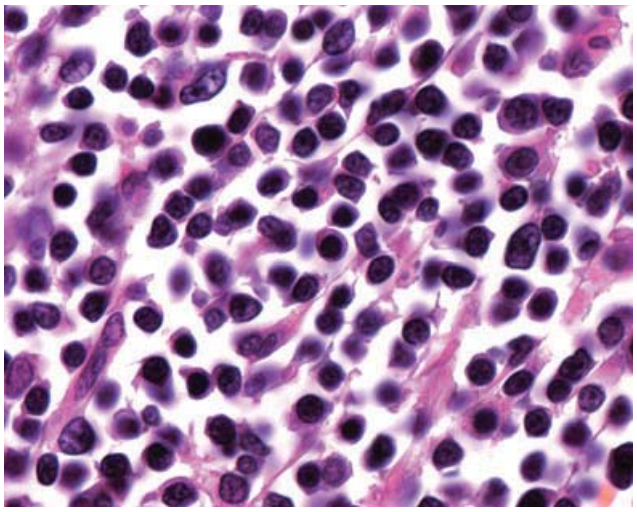

Figure 3.294. Dog: spleen, lymphoplasmacytoid lymphoma. Detail of Figure 3.293. The nuclei tend to roundness and regularity with large chromocenters resembling those of plasma cells but differing in that nucleoli are present and there is more irregularity in parachromatin clearing. The cytoplasm tends to form a complete but narrow envelope around each nucleus and is highly amphophilic with cell boundaries distinct, which assists differentiation from plasmacytoma.

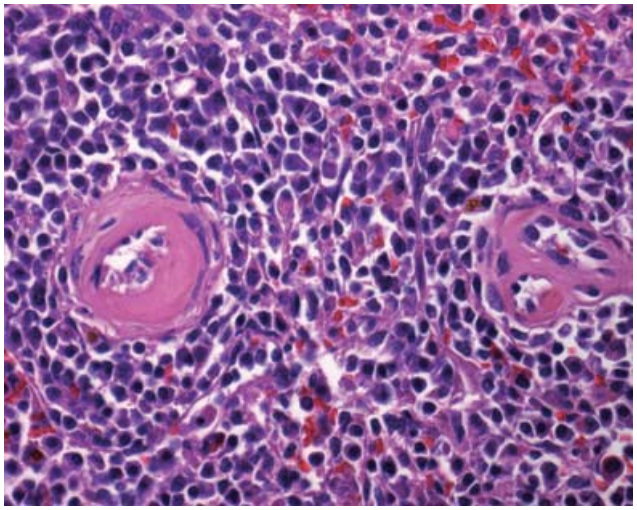

Figure 3.295. Dog: spleen, lymphoplasmacytoid lymphoma. Detail of Figure 3.293. Splenic arterioles with an almost complete absence of residual small lymphocytes and a narrow cuff of atypical plasmacytoid cells.

is complete atrophy of thymic-dependent cuffs with small lymphocytes limited to a layer of only 1–2 cells thick and an apparent cuff of atypical plasmacytoid cells (Fig. 3.295). The germinal centers are atrophic and tend to persist as a collapsed mantle cuff (Fig. 3.296). The sinus

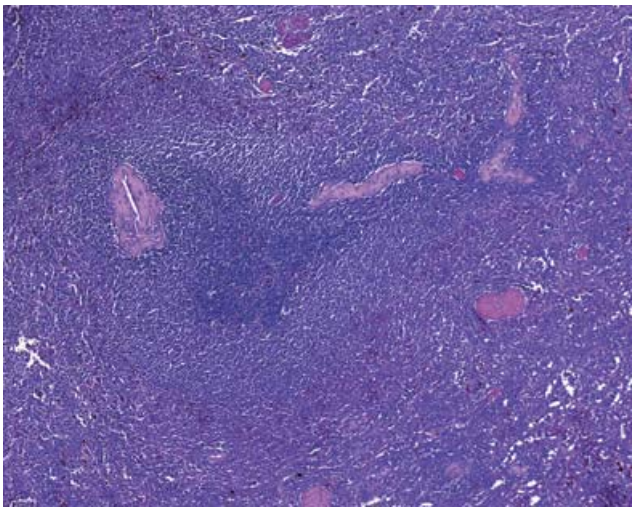

Figure 3.296. Dog: spleen, lymphoplasmacytoid lymphoma. Detail of Figure 3.293. The dark cluster of cells in the center are mantle cells collapsed into the area of the germinal center. The lighter-staining corona is of benign cells of marginal zone type.

areas are solid with cells that more closely resemble plasma cells than the LPL cells in other areas. Mitoses are again almost absent and there is complete absence of extramedullary hematopoiesis.

Other Organs

The central nervous system, kidney, and lung are usually spared, but all tissues may have focal LPL cell invasion. The liver typically has only fine small foci of infiltration even in advanced involvement of the spleen. Typically, the LPL cells form narrow cuffs of only 1–2 cells deep around vascular structures and small clusters of 10–50 cells in mid zone areas (Fig. 3.297). Small foci may appear in other organs, including kidney (Figs. 3.298, 3.299). In the absence of frank neoplasm in other tissues, the cells in the liver might be mistaken for benign reactive lymphocytes or plasma cells.

Immunologic Features

Most of the cases accessed to date were in the era before immunohistochemical staining. LPL cells have surface and usually cytoplasmic IgM but not IgG and stain with CD79 alpha and CD20. It is likely that there are peripheral and nodal T-cell lymphomas that have similar cytoplasmic appearance on oversight stains and are not distinguishable from the B-cell LPL without special stains. In the human form of LPL, the cells are $CD5^{-}$, and the presence of strong Ig staining is used to differentiate them from B-cell CLL.

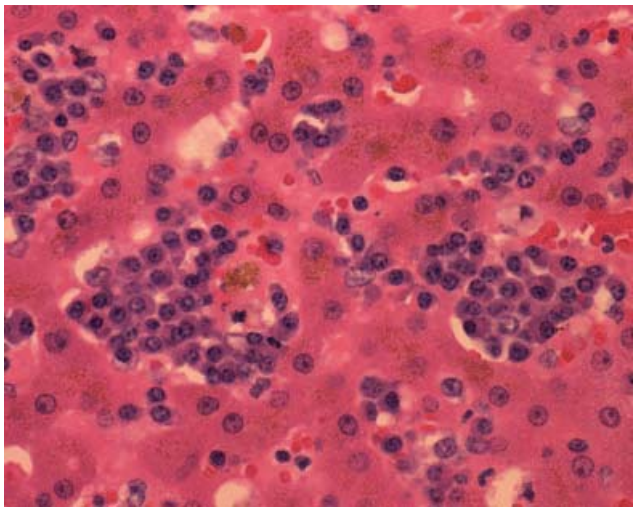

Figure 3.297. Cat: liver, lymphoplasmacytoid lymphoma. There are irregular clusters of plasmacytic-appearing cells irregularly in mid-zone areas of hepatic parenchyma. In some areas, the cytoplasmic boundaries are less distinct, and occasional cells have nucleoli that more closely relates them to the lesions in other organs.

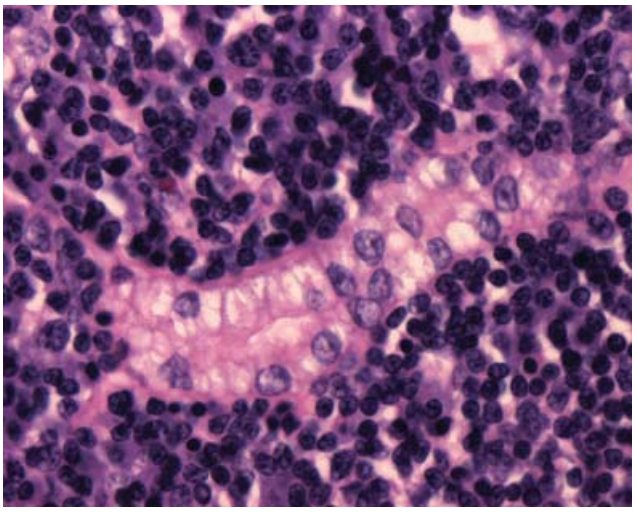

Figure 3.299. Cat: kidney, lymphoplasmacytoid lymphoma. Detail of Figure 3.298. The nuclei retain the tendency to roundness with irregularly aggregated chromatin and relatively abundant deeply stained cytoplasm. These small cells with densely stained nuclei are undergoing apoptosis with the accompaniment of tingible body macrophages (upper right).

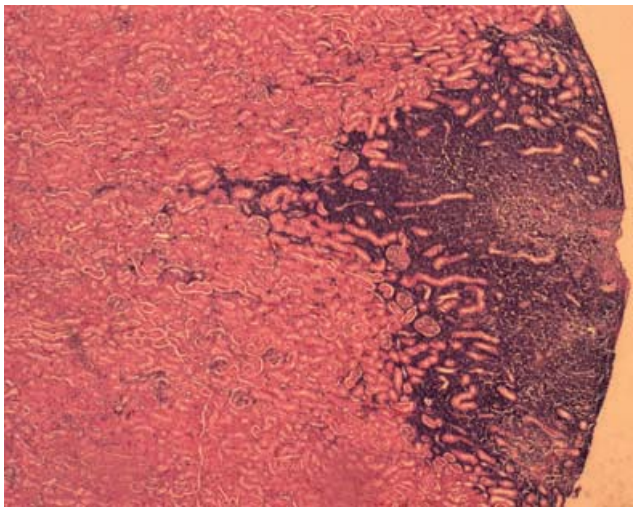

Figure 3.298. Cat: kidney, lymphoplasmacytoid lymphoma. Focal subcortical foci of neoplastic cells are permeating the outer cortex, apparently from interstitial implantations.

Cytogenetic and Molecular Features

The LPL cell of animals has not been characterized by chromosomal or molecular changes. The LPL cells of humans have the heavy and light chains rearranged, and there are variable region gene mutations suggesting that these neoplasms arise from postgerminal center development and have an antigen-driven selection in their heritage. Translocation of t(9;14) (p13;q32) type involving rearrangement of the *PAX5* gene occurs in 50% of cases. The PAX5 gene encodes a factor called BASP that is needed for B-cell lineage commitment and is found in all B-cells but is down-regulated in the process of early plasmacytic differentiation. In the human translocation the PAX5 gene is constitutively expressed with Ig transcriptional factors and is not down-regulated as in the normal differentiation of plasma cells. This change is felt to force proliferation instead of further differentiation. The activity of the PAX5 gene appears to act in this manner even in cases that lack the translocation.

Cell of Origin

The postulated cell of origin of human LPL is a peripheral B-cell stimulated to plasmacytic differentiation from a primary immune response to antigen or a postgerminal center cell that has undergone somatic mutation but not heavy chain class switch.

Diagnostic Criteria

The diagnosis of lymphoplasmacytic lymphoma (LPL) is made on the recognition of nodal, splenic, and marrow proliferation by a nonleukemic population of lymphoid cells with nuclei of intermediate size with coarse irregular chromatin distribution, occasional nucleoli, very low mitotic rate, and a complete rim of highly amphophilic cytoplasm with distinct cell boundaries. Serum paraprotein of high molecular weight may

occasionally be present. The cellular proliferation must be of B-cell type.

Differential Diagnosis

LPL must be distinguished from T-cell lymphomas of similar morphology and from small lymphocytic lymphoma on the basis of an increased volume of deeply stained cytoplasm. LPL is distinguished from plasmacytoma that has similar nuclei with less chromatin irregularities but no nucleoli and more clearly eccentric cytoplasm with distinct cell boundaries and at least some cells having apparent Golgi zones. The nuclei of LPL cells are similar in size to those of the "blastoid" type of mantle cell lymphoma, but the cells of MCL have little cytoplasm that is very lightly stained and cell boundaries are indistinct. In addition LPL is a diffuse disease, and MCL tends to be multifocal even in late stages of that disease. LPL must be differentiated from mast cell tumor of poorly granulated type that closely resembles LPL in the spleen of cats. Cases of LPL with gammopathy need to be distinguished from myeloma that has larger nuclei, has much more cytoplasm, and is usually causing focal bone lysis.

Staging

Routine staging procedures for lymphoma are in order with blood examination including total protein and electrophoresis for monoclonal gammopathy if elevated. Nodal biopsy with immunohistochemistry is required to prove B-cell lineage and the extent of spread to splenic, hepatic, and marrow areas as well as to other nodes. Renal function is generally not an issue unless due to gammopathy.

Transformation and Progression

Nothing is known in this area for animals and there are few studies in humans, with those completed suggesting that the treatment of LPL provides results like that for human CLL and SLL. LPL does not appear to go into blastic crisis in advanced cases.

Evaluation of the Treated Animal

No reports appear to have been made on treatment of this specific disease in animals. In humans, the level and rebound of macroglobulinemia is a major factor in evaluating risk of recurrence after treatment. Anemia and advanced age appear to be major indicators of short survival.

Treatment and Survival

A variety of therapies are used in human LPL, including alkylating agents, purine analogs (Fludarabine and Cladaribine), anti-CD20 (Rituximab), plus marrow allografts. The most valuable prognostic factors in the evaluation of human cases are age and albumin level at presentation and degree of cytopenia. Using these criteria, those graded in the most favorable category had 92% survival at 5 years with 27% survival in the third and least favorable group. No information on progression of this disease in animals is available.

REFERENCES

Greenlee, P.G., Filippa, D.A., Quimby, F.W., Patnaik, A.K., Calvano, S.E., Matus, R.E., Kimmel, M., Hurvitz, A.I., and Lieberman, P.H. (1990) Lymphomas in dogs: A morphologic, immunologic, and clinical study. *Cancer* 66(3):480–490.

Kiupel, M., Teske, E., and Bostock, D. (1999) Prognostic factors for treated canine malignant lymphoma. *Vet Pathol* 36:292–300.

Mahony, O.M., Moore, A.S., Cotter, S.M., Engler, S.J., Brown, D., and Penninck, D.G. (1995) Alimentary lymphoma in cats: 28 cases (1988–1993). *JAVMA* 207(12):1593–1598.

Ponce, F., Magnol, J.-P., Ledieu, D., Marchal, T., Turinelli, V., Chalvet-Monfray, K., and Fournel-Fleury, C. (2004) Prognostic significance of morphological subtypes in canine malignant lymphomas during chemotherapy. *Vet J* 167:158–166.

Ponce, F., Magnol, J.P., Marchal, T., Chabanne, L., Ledieu, D., Bonnefont, C., Felman, P., and Fournel-Fleury, C. (2003) High-grade canine T-cell lymphoma/leukemia with plasmacytoid morphology: A clinical pathological study of nine cases. *J Vet Diagn Invest* 15:330–337.

Ramos-Vara, J.A., Miller, M.A., Pace, L.W., Linke, R.P., Common, R.S., and Watson, G.L. (1998) Intestinal multinodular Aλ-amyloid deposition associated with extramedullary plasmacytoma in three dogs: Clinicopathological and immunohistochemical studies. *J Comp Path* 119:239–249.

Richter, K.P. (2003) Feline gastrointestinal lymphoma. *Vet Clin Small Anim* 33:1083–1098.

Rohatiner, A.Z., Harris, N.L., Dalla-Favera, R., and Lister, T.A. (2004) Lymphoplasmacytic lymphoma and Waldenström's Macroglobulinemia. In Mauch, P.M., Armitage, J.O., Coiffier, B., Dalla-Favera, R., and Harris, N.L. (eds.), *Non-Hodgkin's Lymphomas*. Lippincott Williams & Wilkins, Philadelphia, p. 263.

Teske, E., van Heerde, P., Rutteman, G.R., Kurzman, I.D., Moore, P.F., and MacEwen, G. (1994) Prognostic factors for treatment of malignant lymphoma in dogs. *JAVMA* 205(12):1722–1728.

Trevor, P.B., Saunders, G.K., Waldron, D.R., and Leib, M.S. (1993) Metastatic extramedullary plasmacytoma of the colon and rectum in a dog. *JAVMA* 203(3):406–409.

Valli, V.E., Jacobs, R.M., Norris, A., Couto, C.G., Morrison, W.B., McCaw, D., Cotter, S., Ogilvie, G., and Moore, A. (2000) The histologic classification of 602 cases of feline lymphoproliferative disease using the National Cancer Institute Working Formulation. *J Vet Diagn Invest* 12:295–306.

Vernau, W., Valli, V.E.O., Dukes, T.W., Jacobs, R.M., Shoukri, M., and Heeney, J.L. (1992) Classification of 1,198 cases of bovine lymphoma using the National Cancer Institute Working Formulation for human non-Hodgkin's lymphoma. *Vet Pathol* 29:183–195.

Follicular Lymphoma

Definition

Follicular lymphoma (FL) is defined as a neoplasm of follicle center B-cells composed of centrocytes and centroblasts that has at least a partially follicular pattern on architectural examination.

Epidemiology and Incidence

Remarkably, follicular lymphoma in animals is an uncommon, if not rare, diagnosis. In a personal collection of 502 canine lymphomas collected over 20 years that are primarily consultations, there are 13 cases of follicular lymphoma and 15 cases of benign and atypical follicular hyperplasia. Because most of these cases were collected before the advent of immunohistochemistry this is likely an underestimate, but even if half of the cases believed to be benign were actually FL, that would total only 4.0% of the collection. In a review of canine lymphoma from the New York City area consisting of 176 cases in which phenotyping was carried out, there were 8 cases of "nodular histiocytic" lymphoma roughly corresponding to FL III, 2 cases of "nodular mixed" roughly corresponding to FL II, and no cases of "nodular lymphocytic" corresponding to FL I for a total incidence of 10 cases or 5.7%. In a histological review limited to H&E stained tissues of 602 cases of feline lymphoma derived from multiple institutions in the U.S. and Canada, there were 6 cases of FL or 1% of cases. In a review of 1,198 cases of bovine lymphoma detected by inspectors at Canadian slaughter plants, there were 4 cases of follicular lymphoma (0.3%), again done only with oversight stains. In a personal collection of 89 cases of equine lymphoma, no cases of follicular lymphoma were recorded, and none were recorded in a recent study of 31 equine cases done with immunophenotyping. These results might reflect both changing interpretations of follicular lesions and lack of assistance in detecting faintly nodular lesions by immunohistochemistry. However, in a recent review of 238 cases of canine lymphoma from Ohio, in which phenotyping was done on tissues derived by necropsy only, one case of follicular lymphoma was found. It should be recognized that the diagnosis of follicular lymphoma is based on architectural features and in that context, biopsies taken by Tru-cut needle or cases phenotyped by tissue array might easily miss the nodular or follicular characteristics. In terms of signalment, of the 13 cases of canine follicular lymphoma noted above, 11 cases were 10 years of age or older and 2 cases were 2 years of age, with 7 males, 5 females, and 1 unknown. It is equally instructive that neither of two current major texts on small animal oncology even mention follicular lymphoma. It is hoped that this description will assist the recognition of this unusual, but indolent and deserving, disease.

Clinical Presentation and Features

Animals with follicular lymphoma tend to present with multiple sites involved and usually include both peripheral and internal nodes, but none of these masses are large. FL may present in any of the peripheral nodes but those in the head, neck, prescapular, and popliteal areas are likely to be involved, as well as mediastinal and sublumbar nodes internally but not usually mesenteric. The nodes are always nonpainful and not fixed to the deeper tissues. FL is often noticed on incidental examination as for dental care because the animals are normally active and have normal appetites. There may be focal involvement of liver and multifocal involvement of spleen or bone marrow, but this may not be apparent in examination of blood unless cells of centrocytic type are suspected and carefully looked for (Figs. 3.300–3.304). It appears that, as in the human, as more tissues are involved the grade of FL is likely to be higher.

Pathologic Features

Blood

This area has had little attention in animal pathology because marrow is not routinely examined in cases with nodal enlargement (Figs. 3.305–3.307). Thus without having found the neoplastic follicles in marrow, the centrocytic cells of malignant type would not likely be recognized in the peripheral blood examination. Because marrow is the tissue most often involved outside of nodal FL it is likely that neoplastic cells are in the blood; in humans, this occurs in about 30% of cases. The key factors in recognition of the centrocytic cells in the blood

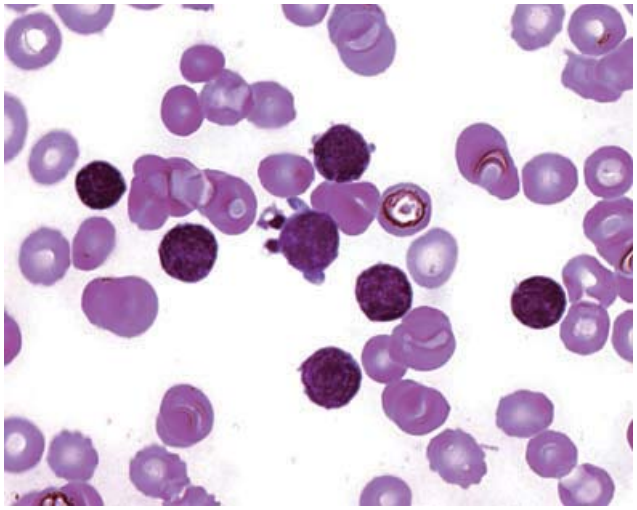

Figure 3.300. Human: blood, follicular lymphoma, Grade I. The centrocytic-type cells are rare in the peripheral blood and identified by very sharp shallow nuclear indentations not seen in other blood cells. *Slide from Cornell Tutorial.*

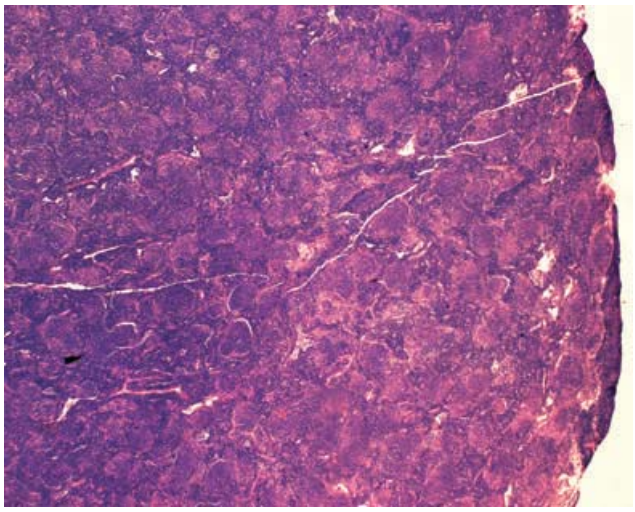

Figure 3.301. Human: lymph node, follicular lymphoma, Grade I same case as Figure 3.300. The node is a large tissue several centimeters in diameter, with the entire area occupied by small closely faceted nodules of lymphoid proliferation that lack a mantle cell cuff but are compressing residual benign cells.

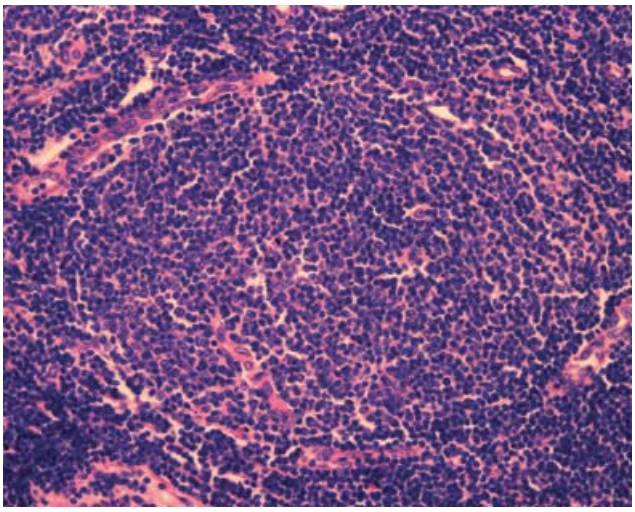

Figure 3.303. Human: lymph node, follicular lymphoma, Grade I. Detail of Figure 3.301. The single follicle seen in isolation demonstrates an important diagnostic point that the postcapillary venules are never within the follicles but always compressed into the internodular areas.

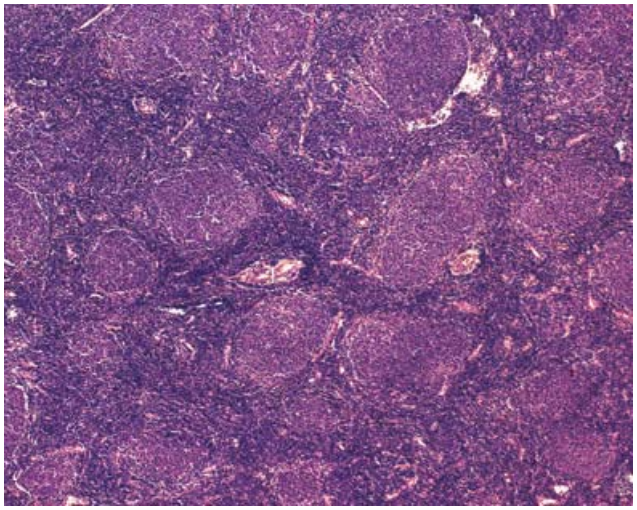

Figure 3.302. Human: lymph node, follicular lymphoma, Grade I. Detail of Figure 3.301. The nodules vary in size and are poorly demarcated. The diagnosis becomes evident because of the continuity of the same reaction throughout the entire node tissue.

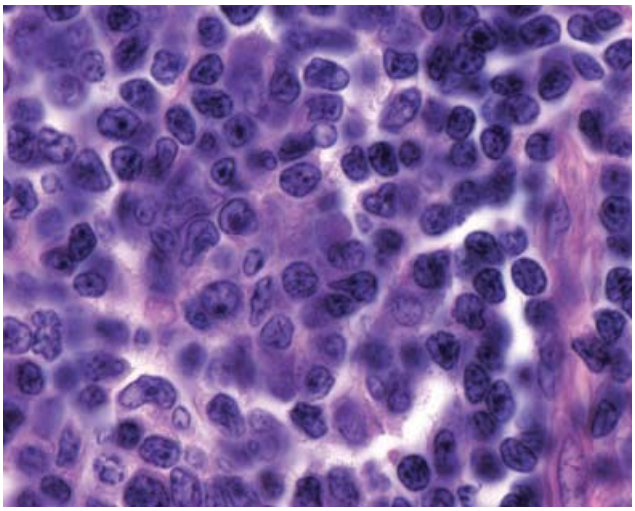

Figure 3.304. Human: lymph node, follicular lymphoma, Grade I. Detail of Figure 3.301. The centrocytes are characteristically small lymphocytes with irregularly and sharply indented nuclei that have densely stained nuclei when viewed at low magnification and mild vesiculation at the cytologic level with most cells lacking nucleoli; when nuclei are present, they are small and inapparent. The cytoplasm is moderate in volume and lightly stained and mitoses are typically confined to the larger cells. The vessel at the right is a postcapillary venule present in Figure 3.303.

are the deep nuclear clefts of the centrocytes (Fig. 3.308) that are absent in cells of chronic lymphocytic leukemia, are unusual in the blood in small lymphocytes, but may be seen in large lymphocytes in the blood of cattle with inflammatory diseases.

Bone Marrow

Marrow, like blood, tends to be relatively normal, usually with the nonspecific changes of cancer, including a higher proportion of coarse hemosiderin and often some degree of plasmacytosis (Fig. 3.309). The marrow is involved in advanced cases of FL, and the follicular pattern is maintained and often near trabecular bone. The absence of a mantle cell cuff and lack of polarity and tingible body

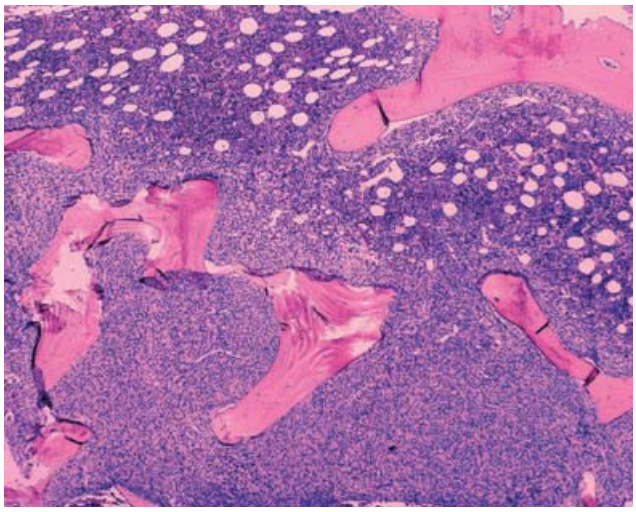

Figure 3.305. Human: bone marrow, follicular lymphoma, Grade I. The marrow core has focal lymphoma occupying the solidly cellular area below with residual fat cells and a more mixed pattern of normal marrow apparent above. *Slide from Cornell Tutorial.*

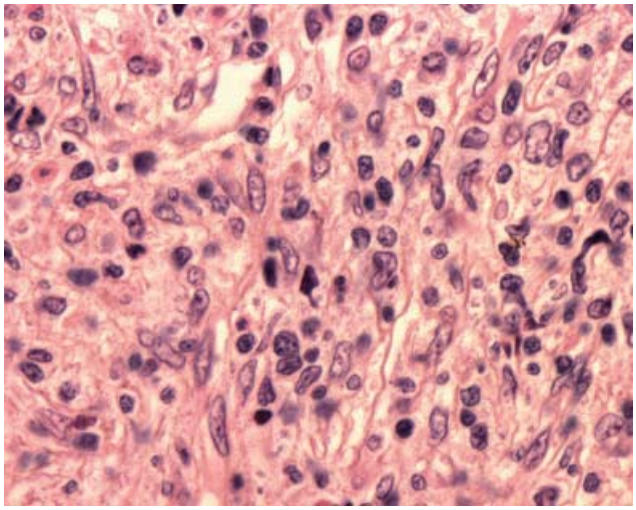

Figure 3.306. Human: marrow, follicular lymphoma. Detail of Figure 3.305. An area of tumor involvement that has a fine but dense reticular background with complete phthisis of normal marrow cells and a predominant population of centrocytes. The elongated pale nuclei in the upper left and lower right are of benign fibrous marrow stromal origin.

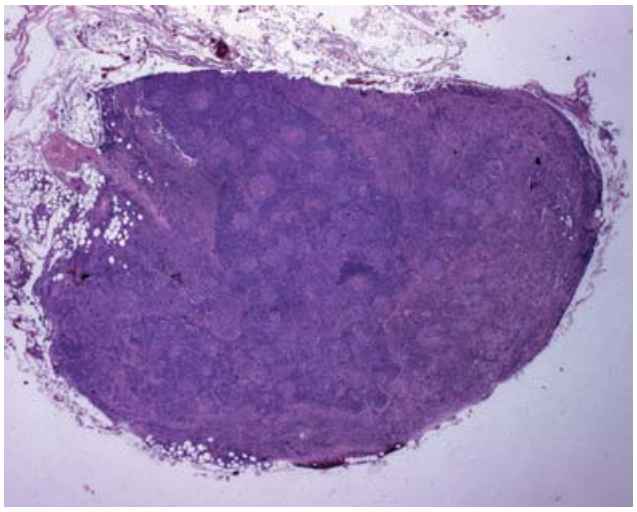

Figure 3.307. Human: lymph node, follicular lymphoma, Grade I, same case as the bone marrow in Figure 3.306. The follicular pattern is more apparent in the central area of the node with left and right areas with less well-defined follicular pattern. The node is just over 0.5 cm in length, and this histological pattern in a node that small would likely be dismissed in an animal if there were not other signs of lymphoma.

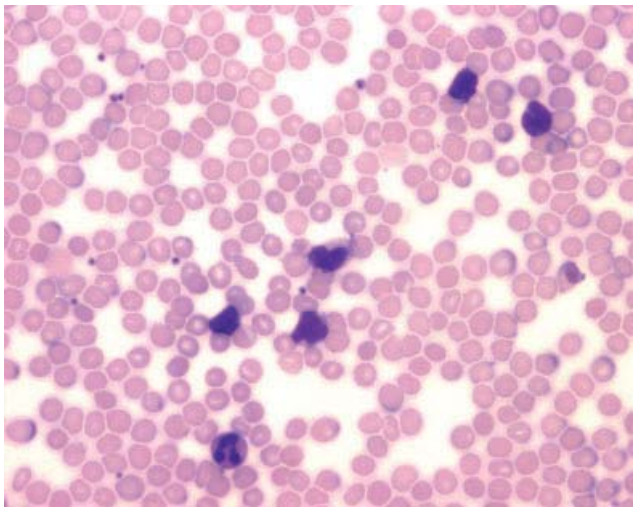

Figure 3.308. Human: blood, follicular lymphoma, Grade I. Deeply cleft cells more typical of the usual centrocyte-type cells seen in the leukemic phase of FL I in blood.

macrophages assists in relating the marrow lesions to follicular proliferation elsewhere. In human FL, the marrow is the most common other site besides nodal involvement, but this may not be the case in animals and will not be known until topographic staging has been described on a number of cases at differing histologic grades.

Lymph Node

The classical characteristics of follicular lymphoma are seen in lymph nodes (Figs. 3.310–3.312). There may be encircling involvement of perinodal tissues in advanced cases, but this is usually not the case (Fig. 3.313). The peripheral capsule is thinned and taut, and the peripheral sinus is compressed and will be destroyed in regions of perinodal colonization. In most cases, the general pattern

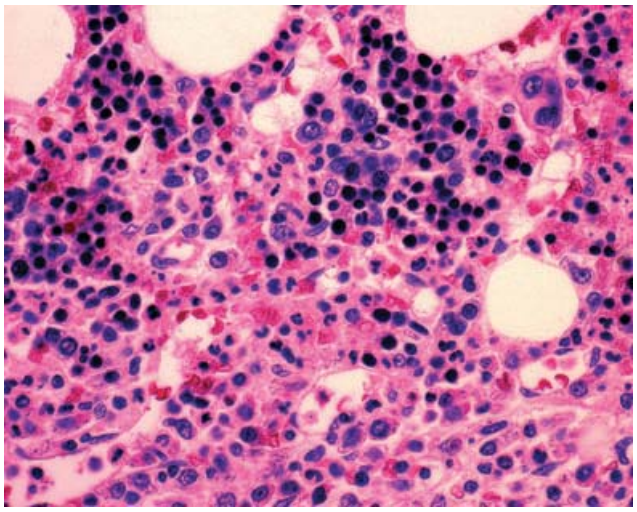

Figure 3.309. Human: bone marrow, follicular lymphoma, Grade I, same tissue as Figure 3.305. The junction of normal marrow is above and advancing FL-1 is below. The transition is rather abrupt with residual areas of marrow relatively undisturbed.

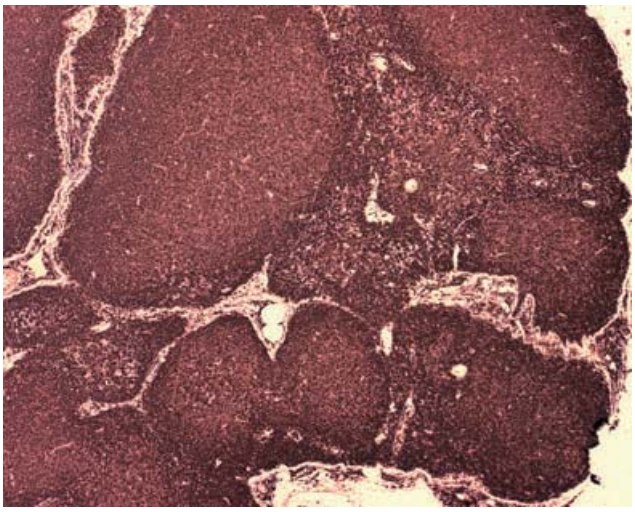

Figure 3.311. Dog: node, follicular lymphoma, Grade I. Phenotype of Figure 3.310. With CD79 alpha staining, the proliferating tissue cells, as well as the perifollicular tissues, are strongly and uniformly labeled.

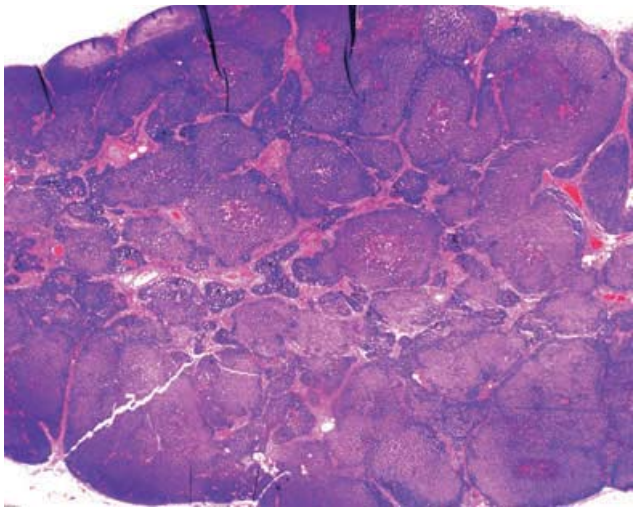

Figure 3.310. Dog: lymph node, follicular lymphoma, Grade I. The follicular proliferations in animals tend to be larger and more variable in size than in humans. Expanding areas of neoplastic follicles are lightly rimmed by residual small lymphocytes forming the discontinuous cuffs more evident at top. The increased prominence of medullary connective tissues suggests a previous history of chronic benign hyperplasia.

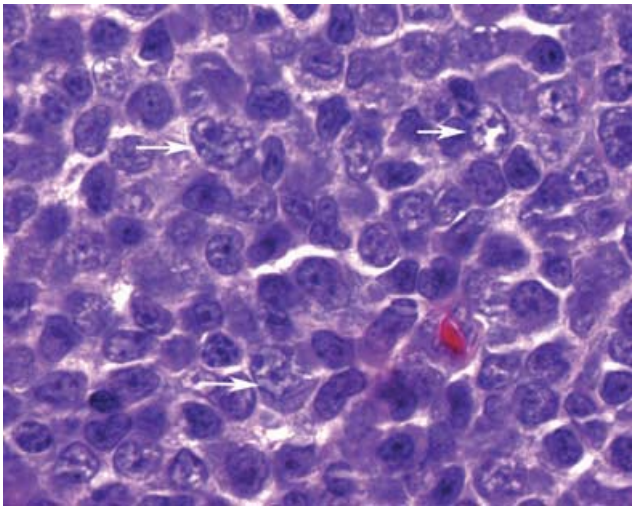

Figure 3.312. Dog: node, follicular lymphoma, Grade I. Detail of Figure 3.310. The follicular center cells are of intermediate size with irregularly indented nuclei. The chromatin pattern is coarse granular with most cells having a small or inapparent nucleolus. The cytoplasm is moderate in volume and staining density, and cell boundaries are generally indistinct. The larger nuclei with peripheralized chromatin and nucleoli (arrows) are centroblasts.

seen on oversight staining is of a solidly diffuse lymphoid proliferation without fading germinal centers and with only vestiges of small cell proliferation, which may not suggest a nodular or follicular architecture (Fig. 3.314). Careful examination, at low magnification, suggests multinodular filling of the entire cortex and inner areas of the node with compression and low cellularity of any areas of medulla in the plane of section. It may be perceived that some of the nodular areas are about the size of large germinal centers and are separated by bands of tissue that are slightly more darkly stained and of uniform width wherever apparent. Cytologically, the increased density of the internodular areas is because they contain a mixed cell population, with many small cells with densely stained

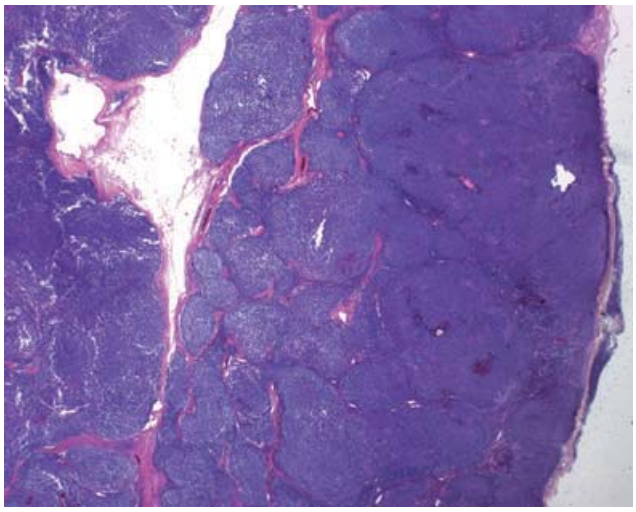

Figure 3.313. Dog: lymph node, follicular lymphoma, Grade II. The peripheral capsule is thinned and taut with the peripheral sinus compressed. The node measured 2.8 × 1.8 cm, and the small area of perinodal colonization at the right was the only area of extracapsular involvement despite the apparent size and time of involvement of this node.

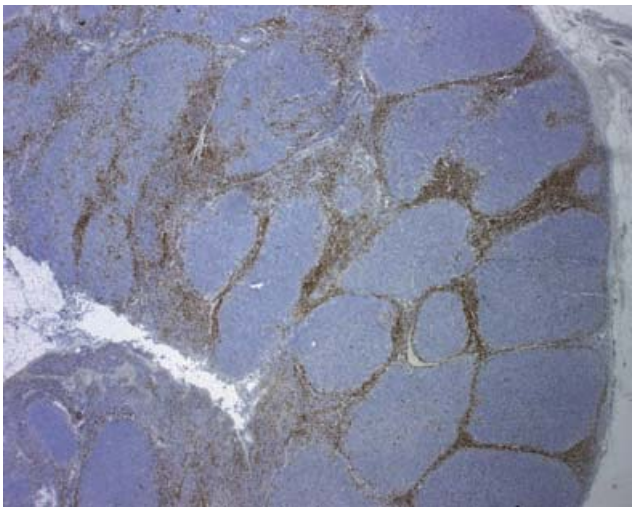

Figure 3.315. Dog: node, follicular lymphoma, Grade II. Phenotype of Figure 3.314. With CD3 staining, the interfollicular areas are sharply and distinctly defined, indicating that these cells are primarily of T-cell type and a residue of paracortex rather than of mantle cell origin.

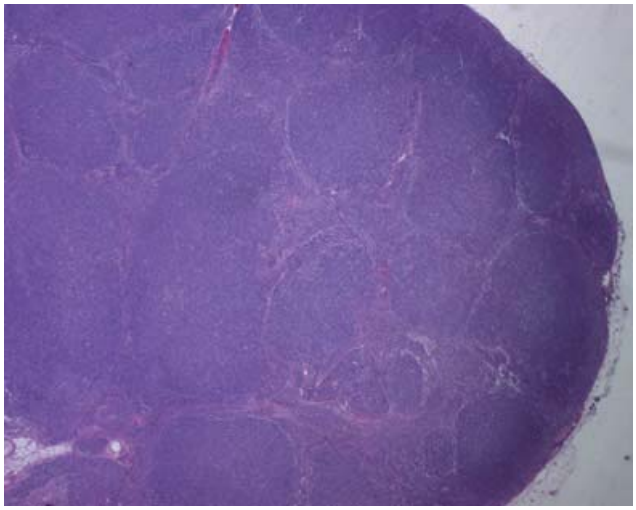

Figure 3.314. Dog: lymph node, follicular lymphoma, Grade II. There is marked thinning of the capsule but without involvement of perinodal tissues and with complete effacement of normal node architecture. There is a faint but definite multinodular filling of the entire interior of the node. There is a complete absence of fading germinal centers and of mantle cell cuffs that might more directly suggest follicular heritage.

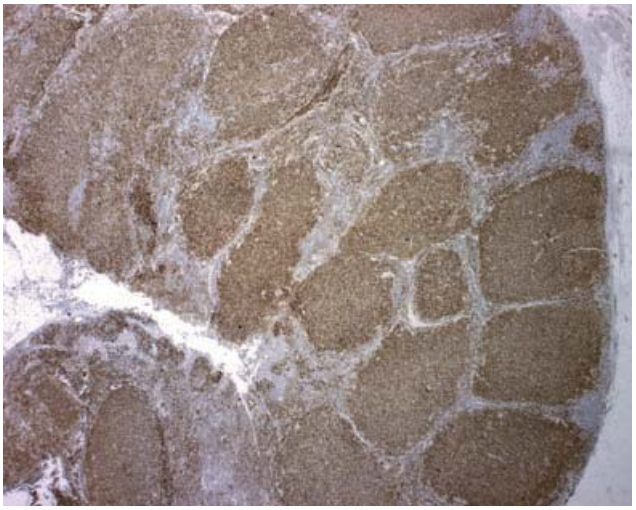

Figure 3.316. Dog: node, follicular lymphoma, Grade II. Phenotype of Figure 3.314. CD79 stain distinctly marks the areas of proliferation in a uniform manner with the interfollicular areas very largely unmarked. The impact of phenotyping on recognition of follicular lymphoma is readily apparent, particularly in nodes without a well-defined nodular pattern.

nuclei and minimal cytoplasm including some residual mantle cells. In follicular lymphoma, the internodal areas differ from mantle cell cuffs in not being related to either adjoining follicle but rather a separate interfollicular area of residual paracortex (Figs. 3.315, 3.316). An additional important feature of the internodular areas is that they always contain the postcapillary venules that are never in the areas of follicular proliferation (Figs. 3.317, 3.318, see also 3.303). These features of the internodular septa are constant regardless of the cellular makeup and grade of the follicles themselves.

The process of grading follicular lymphoma is based on the proportion of large centroblasts to the smaller

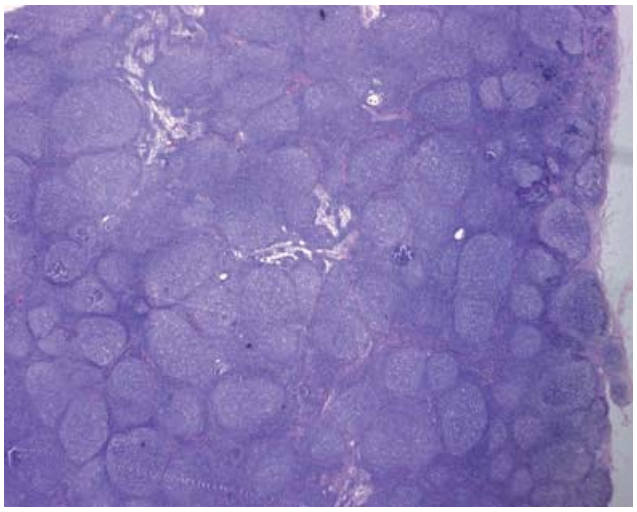

Figure 3.317. Dog: lymph node, follicular lymphoma, Grade II. This case more closely resembles human forms of this disease with multiple small follicles of more similar diameter. There is typically a complete loss of mantle cell cuffs with some follicles beginning to coalesce.

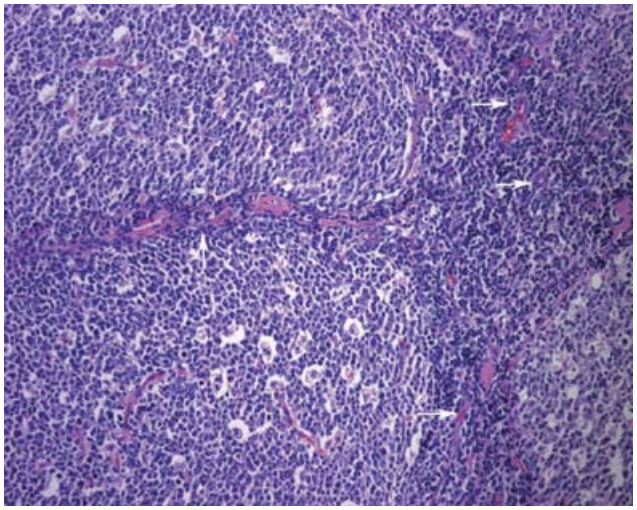

Figure 3.318. Dog: node, follicular lymphoma. Detail of Figure 3.317. The postcapillary venules (arrows) are compressed between the expanding follicles and they are never within the areas of lymphoid proliferation.

centrocytes, with the former being the dividing population. These neoplastic cells of FL are morphologically not different from their counterpart cell types in benign reactive follicles. The centrocytes are small "cleaved" lymphocytes with nuclei 1.5–2.0 red cells in diameter. The nuclear irregularities are relatively shallow, and the chromatin is of large dense chromocenters with mild parachromatin clearing. Small and generally inapparent nucleoli are present, and the cytoplasm is minimal and

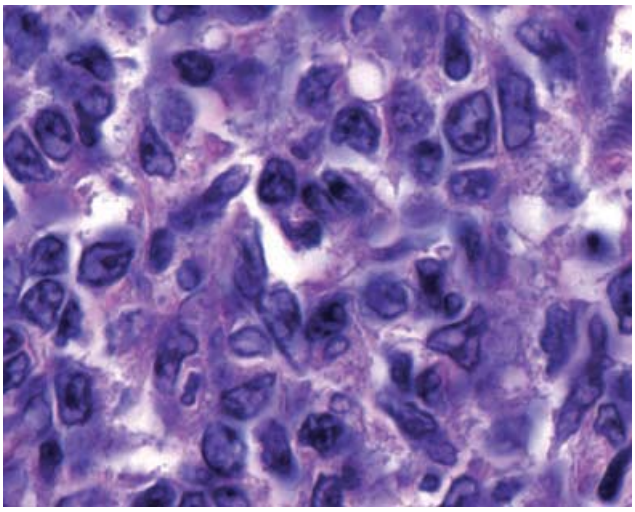

Figure 3.319. Human: lymph node, follicular lymphoma, Grade I. Detail of follicular center cells with centrocytes having markedly variable nuclear shapes with peripheralized chromatin and small nucleoli. *Slide from Cornell Tutorial.*

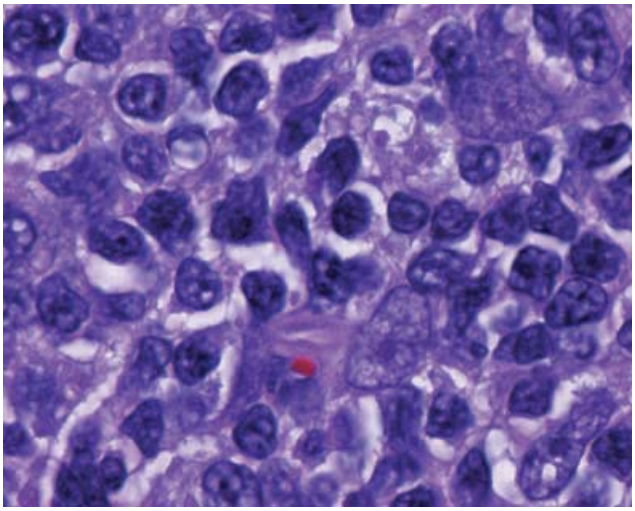

Figure 3.320. Cat: lymph node, follicular lymphoma, Grade I. The centrocytes in animals are remarkably similar to those in humans with irregularly shaped nuclei and densely stained chromatin. There is mild irregular parachromatin clearing, and many cells have small and inapparent nucleoli. The cytoplasm is moderate in volume and staining density with cell boundaries indistinct. The 3 large pale nuclei to the right with prominent nucleoli and finely branched chromatin are of dendritic cells.

lightly stained (Figs. 3.319, 3.320). These cells are not found in mitosis. The centroblasts have round or oval nuclei that may be deeply cleft and 2.0–2.5 red cells in diameter. The chromatin is fine and dispersed and usually peripheralized on the nuclear membrane with marked areas of parachromatin clearing. There are 1–3 nucleoli

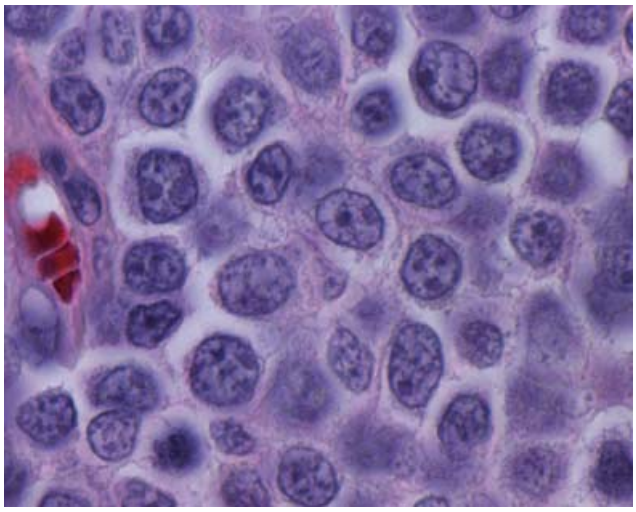

Figure 3.321. Human: lymph node, follicular lymphoma, Grade III. The field is dominated by large cells with vesicular nuclei and multiple nucleoli, often peripherally placed with parachromatin clearing and a relatively narrow cytoplasmic envelope that may be quite highly basophilic (upper left). *Slide from Cornell Tutorial.*

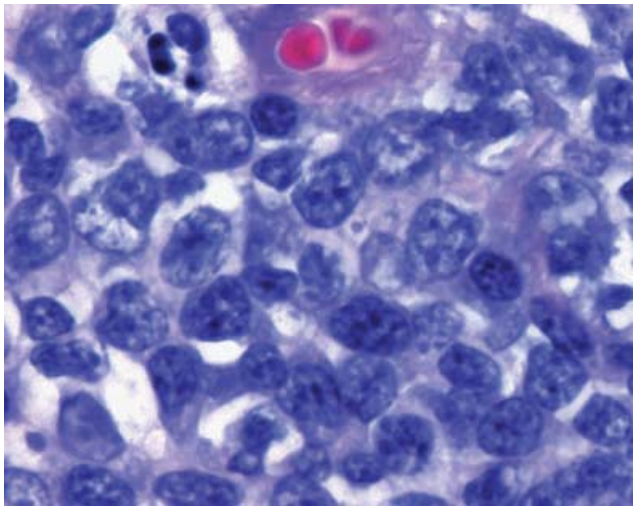

Figure 3.322. Dog: lymph node, follicular lymphoma, Grade III. The centroblasts greatly predominate, with branched chromatin pattern and multiple nucleoli that frequently are impinging on the nuclear membranes. The cytoplasm is moderate in volume and staining density and cell boundaries are indistinct. Mitoses and apoptosis may be present but not tingible body macrophages.

present in each cell and these are characteristically impinging on the nuclear membrane. The cytoplasm is minimal and highly amphophilic (Figs. 3.321, 3.322). These cells are seen in mitosis, but the tingible body macrophages of benign follicles are not present in human FL. This finding also seems to be the case in animals, and cases where tingible body macrophages appear within follicles should be carefully evaluated to rule out follicular hyperplasia. The other major feature to be noted is that the cellularity of the follicles in FL is uniform throughout and the polarity of reactive hyperplasia is lost along with the mantle cell cuffs (Fig. 3.323).

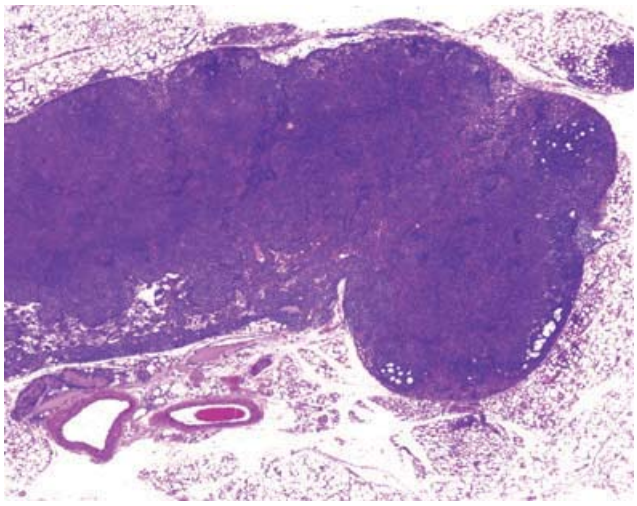

Figure 3.323. Mouse: lymph node, follicular lymphoma. There is faint nodularity, most evident adjoining the medullary area to the right. There is almost complete loss of the mantle cell cuffs and there is focal coalescence of follicles. *Slide from J. M. Ward, DVM.*

The WHO classification system of grading is for 0–5 centroblasts per high power field (hpf or 400×) as grade 1, 6–15/hpf as grade 2, and more than 15 centroblasts/hpf as grade 3. In general, individual pathologists tend to have good correlation with outcome based on this grading system, but the overall application gives poor results. The application of this system in human pathology is to treat grades 1–2 as low-grade or indolent lymphomas and grade 3 as an aggressive neoplasm. The principle behind this grading scheme is in contrast to grading on cell type, as in the NIH Working Formulation with FL (small cleaved cell, now grade 1), FL (mixed cellularity, now grade 2) and FL (large cell, now grade 3), the latter known as *histiocytic* in older literature. The change is based on the current understanding that all FL progresses from grades 1 to 3 over a period of years and grading is, in effect, a staging evaluation. Although the designation of FL type tends to vary with the observer, the major distinctions between FL 1–II and the aggressive type FLIII that are important distinctions for management show that the REAL/WHO system is much superior to previous systems of histologic classification.

Unlike the marginal and T-zone lymphomas that tend to have fading follicles and sclerosis of the medullary perivascular raphe, the sclerosis in FL tends to be of reticulin fibers rather than apparent collagen bands. This feature was utilized before immunohistochemistry by

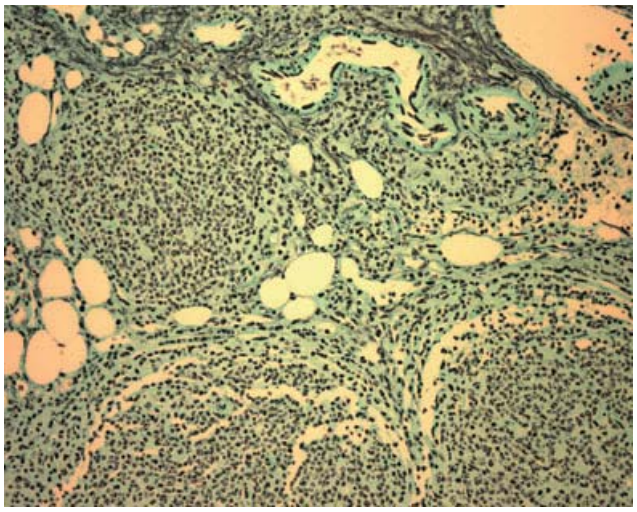

Figure 3.324. Cat: lymph node, follicular lymphoma, Grade III. Silver stain, for demonstration of reticulin fibers. The compression of normal node-supporting structures into branching internodular columns is made apparent with this staining method. The changes are due to rearrangement of existing fibers rather than of proliferation, and collagen is never formed.

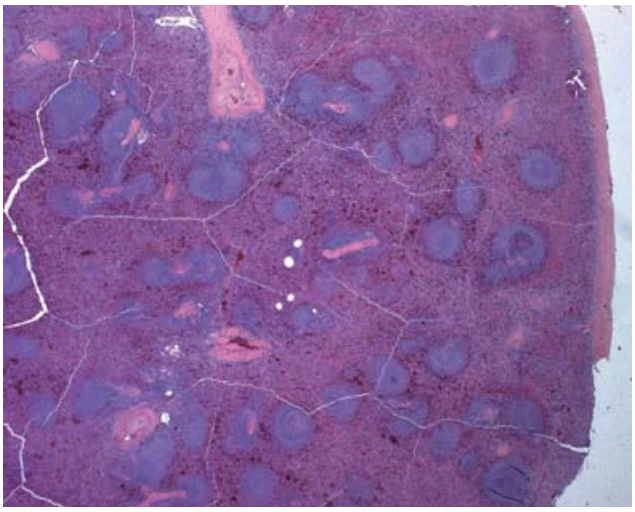

Figure 3.325. Human: spleen, follicular lymphoma, Grade I. The lesion is characterized by multiple nodules of lymphoid proliferation arising on end arterioles similar to that of marginal zone lymphoma. The architectural pattern is one of proliferation arising outside the mantle cell layer and would seem to resemble more closely marginal zone lymphoma. *Slide from Cornell Tutorial.*

silver staining for reticulin fibers that are compressed into the interfollicular tissue areas (Fig. 3.324). FL may be focal in a given node, with areas remaining of follicles with clearly defined antigen-related polarity and remnants of mantle cell cuffs. As well, some cases of FL may have nodes with diffuse areas that are made up of cells identical in type to those of the neoplastic follicles. This occurrence does not appear to indicate a more aggressive form of FL, but the current recommendation of the WHO classification is to quantify regions of diffuse proliferation in the event their presence is later determined to be of significance.

Spleen

Follicular lymphoma of the spleen has not been adequately described in animals, and it is likely that in those cases observed the multinodular pattern was described and even the relation of the nodules to the arteriolar system, but the lesion and specific disease was not identified by the nodular pattern. It is unclear whether FL in the spleen in animals tends to involve the entire organ, like human FL and MZL, or is more like MZL and MCL in the dog, which appears always to be multifocal within a locally extensive area (Figs. 3.325–3.328). Architecturally, FL in the spleen of mouse, cat, and humans is associated with at least moderate enlargement, with the capsule thinned and the smooth muscle trabeculae thin and widely separated. The distribution of FL in the spleen is characteristic with diffuse involvement in terms of all

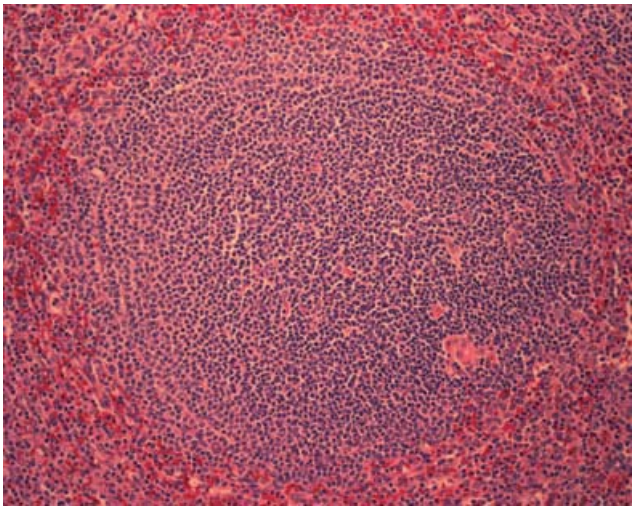

Figure 3.326. Human: spleen, follicular lymphoma. Detail of Figure 3.325. There is a uniform proliferation of small lymphocytes eccentric to the arteriole, with an outer cuff of cells with slightly larger round nuclei representing residual marginal zone hyperplasia.

regions involved, but the sinus areas are spared and the focal proliferations are sharply defined. To provide a concept of the density of the lesions, there may be 50 or more neoplastic follicles in a typical cross section of feline spleen. The follicular proliferations are generally larger than germinal centers, with about half located adjacent to an arteriole or partially enclosing one and the rest having no apparent arteriolar association. However, the perio-

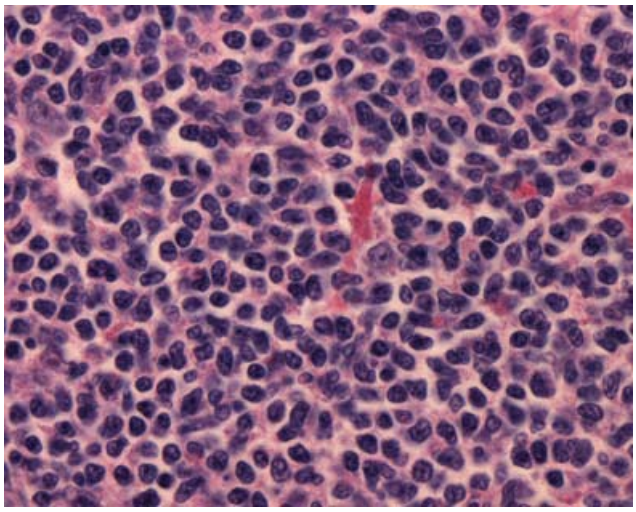

Figure 3.327. Human: spleen, follicular lymphoma, Grade I. Detail of Figure 3.325. The follicular center cells are the typical centrocyte type that lends validity to the interpretation of follicular lymphoma.

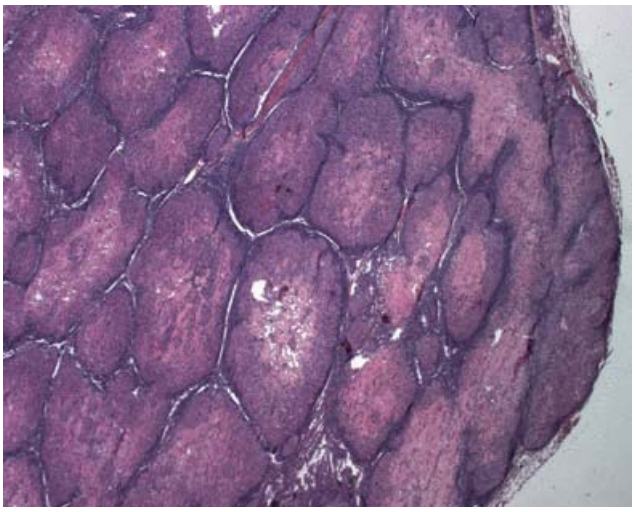

Figure 3.329. Human: node, follicular lymphoma, Grade II. Follicular hyalinosis involving large areas of most follicles. Large areas of the central lymph nodules are replaced by amorphous proteinaceous residue. *Slide from Cornell Tutorial.*

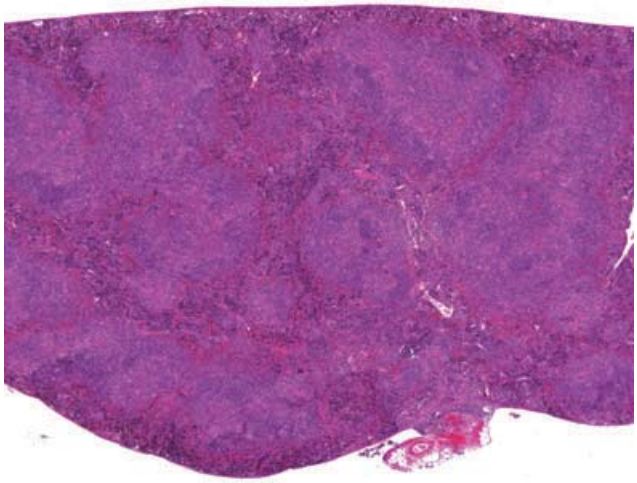

Figure 3.328. Mouse: spleen, follicular lymphoma. There is irregular proliferation of cells surrounding the arterioles, with peripheralization of residual mantle cells with marked enlargement of the organ and thinning of the capsule and muscular trabeculae with reduced areas of sinus still bearing trilineage hematopoiesis. *Slide from J. M. Ward, DVM.*

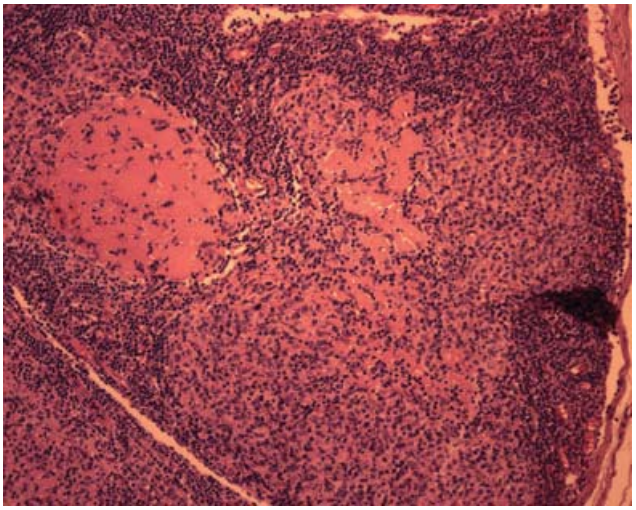

Figure 3.330. Human: node, follicular lymphoma, Grade II. Detail of Figure 3.329. Amorphous protein deposits similar to amyloid regularly displace follicular center cells.

dicity of the lesions throughout the spleen is indicative of involvement of the B-cell areas of the periarteriolar lymphoid sheaths (PALS). Although the proliferative areas are of B-cell lineage, there is complete atrophy of the T-cell–derived and thymic-dependent cuffs of small lymphocytes. In addition, the follicular heritage of the B-cell foci can also be deduced from frequent occurrence of pink areas of amorphous protein in the center of the follicles, which is the residue of "follicular hyalinosis" (Figs. 3.329, 3.330). These foci are likely indicative of a long and vibrant period of follicular hyperplasia preceding neoplastic transformation.

Cytologically the follicles are completely devoid of mantle cell cuffs, but many follicles appear to be partially encapsulated by 1–2 cell layers of stromal-appearing cells that may be related to the benign marginal sinus. The follicular cells will have exactly the same cellular composition as neoplastic follicles elsewhere in the body. The sinus areas may be mildly congested and have little extramedullary hematopoiesis and relatively low nucleated cellularity. The sinus cells present consist mainly of

small lymphocytes and plasma cells, with the vascular ellipsoids more conspicuous due to the absence of other cells. In advanced cases the splenic foci may come into contact with each other and may coalesce, as in the proliferative areas of marginal zone lymphoma.

Other Organs

The other organ most consistently involved is the liver. Hepatic colonization in FL is related to the vascular structures, with the sharply defined focal structures tending to surround biliary ducts and portal arterioles and to be adjacent to portal and central veins. Oddly, any extramedullary hematopoiesis is completely excluded from the areas of lymphoid proliferation and may be seen as isolated foci in midhepatic zonal areas. As in other areas, the cell type in the liver is the same as in the nodal neoplasm and the same grade. Like the liver, marrow may be involved in multifocal to coalescing involvement with relatively normal marrow adjacent (Figs. 3.331, 3.332).

Immunologic Features

All follicular lymphomas mark with B-cell markers CD 79 alpha and CD20 and are negative for CD3. Most cases of FL have surface immunoglobulin (sIg^+), can be concluded to be clonal by positivity with lambda light chain, and are negative with kappa light chain. In the human counterparts, most cases (about 60%) are positive for IgM and the remainder for IgG, with rare cases marking for IgA. When human Fl involves extranodal sites, the follicular dendritic cells continue to be present. Presumably, this is a prerequisite for true follicle formation and would also be the case for animal cases of FL.

Cytogenetic and Molecular Features

Because Fl is so seldom identified in animal pathology, the molecular characteristics of these lesions are virtually unknown. It is firmly established that human Fl is the result of neoplastic change in a postgerminal center cell. In human FL, the Ig heavy and light chain genes are rearranged and in those cases studied, the Ig variable regions are rearranged and have extensive somatic mutations. More particularly, there is extensive intraclonal diversity indicating that mutations are ongoing similar to benign germinal centers. One might expect that as FL progresses from grade 1 to 3 there will be considerable drift in Ig gene arrangement. No specific genetic alterations have been noted in dogs, but no doubt these will be identified as a sequel to the animal types of FL being identified by routine pathology procedures of histology and immunohistochemistry. In human FL, the characteristic genetic alterations are the chromosomal breaks at 18q21 and rearrangements of the BCL-2 gene present in 80–90% of cases. By this translocation, the BCL-2 gene in chromosome 18 is juxtaposed to the Ig heavy-chain region of chromosome 14 that results in the bcl-2/IgH rearrangement, and since the Ig heavy-chain region is in active transcription, there is up-regulation of the BCL-2 gene. As a result of this translocation, the affected cells have constitutively high levels of the bcl-2 protein. The normal bcl-2 gene encodes a protein present in the mitochondria, the endoplasmic reticulum, and the nuclear membrane. The aberrant bcl-2 product has no impact on cell proliferation but regulates the apoptotic initiation and prevents pro-

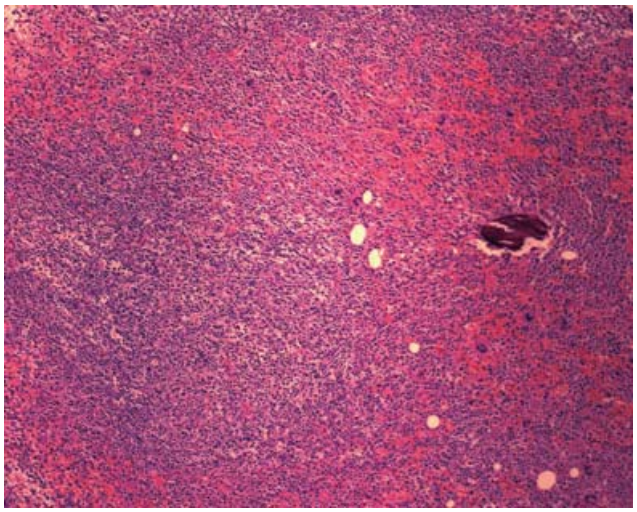

Figure 3.331. Cat: bone marrow, follicular lymphoma, Grade II. There is a focal area of marrow involvement at the lower-left center with the upper area of marrow relatively normal.

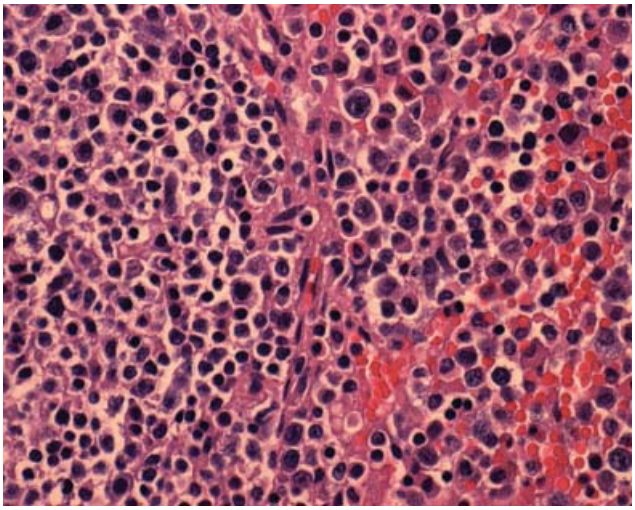

Figure 3.332. Cat: bone marrow, follicular lymphoma, Grade II. Detail of Figure 3.331. The left half of the image is of an expanding lymphoid nodule with the right area a mixture of normal bone marrow cells and a few neoplastic lymphocytes. All involvement appears to remain focal but may progress to coalescing lesions.

grammed cell death. In benign nodal reactions, the bcl-2 expression is limited to germinal centers and is credited with permitting B-cells that have passed through the nodal T-cell selection process to become long-lived memory B-cells. Because many benign cells have the apoptotic mechanism down-regulated and cells bearing the t(14;18) translocation are present in normal individuals, this suggests that this change alone is insufficient to result in the neoplastic transformation of FL. Mice transgenic for BCL-2 develop polyclonal B-cell hyperplasia but not lymphoma. However, chronic antigen stimulation appears to synergize with down-regulation of apoptosis and this combination may mimic the normal pathogenesis of neoplastic transformation in FL.

Cell of Origin

Follicular lymphoma is a neoplasm of germinal center B-cells in which the constituent centrocytes are unable to undergo apoptosis due to a chromosomal rearrangement that prevents the normal process of turning off the anti-apoptosis gene bcl-2.

Diagnostic Criteria

Follicular lymphoma is recognized as a neoplasm that results in architecture like that of benign follicular hyperplasia. The neoplastic pattern may be entirely follicular or partially follicular with diffuse areas. The neoplastic follicles are recognized as having the same cellular components across the face of the nodule with an absence of antigen-related cellular polarity. Malignant follicles usually lack mantle cell cuffs and, while apoptosis may be found in neoplastic follicles, the tingible body macrophages commonly found in benign follicles are not present. If FL is suspected in the examination of nodal lymphoma, cells of similar type should be looked for in liver and marrow aspirates.

Differential Diagnosis

The major differential diagnosis to be considered with follicular lymphoma is benign follicular hyperplasia. Criteria of malignancy include major tissue areas or diffuse nodal involvement with closely packed follicles with minimal internodal area and loss of mantle cell cuffs. Any diffuse area of nodal proliferation should be closely examined for cells of germinal center type. The larger centroblastic cells may occupy the internodal regions, but the typical centrocytes of the germinal center are not found outside of the follicles in benign hyperplasia. In advanced FL, there may be concentric layers of follicular formation outside of the normal node capsule with intervening bands of connective tissue representing progressive perinodal extension. In hyperplasias, there may be reactive cells, including lymphocytes and plasma cells in the perinodal fat, but very rarely actual germinal centers. Sclerosis of diffuse areas of nodal expansion is mentioned as a feature of lymphoma in human FL. This finding would need to be distinguished from the heavy and mature collagenous proliferations seen in animal nodes in medullary areas in most cases of chronic benign hyperplasia, and those remaining in nodes with lymphoma particularly of the indolent B- and T-cell types. Finally, invasion of the walls of veins by centrocytic and larger-type cells with progressive narrowing of the lumen is seen in lymphomas in animals and is highly supportive of a diagnosis of lymphoma. Finally, it appears that the centrocytic cells of follicular lymphoma in animals have cytologic identity, as is found in human neoplasms and with greater experience, recognition of this cell type will aid in identifying early and advanced FL in animals.

Staging

In terms of topographic extension, animals with Fl usually present after the neoplasm has spread to many areas, because the progression is slow and associated morbidity that would promote clinical examination is very low. Animals with follicular lymphoma of grades 1–2 should be considered to have indolent lymphoma and treated appropriately. In contrast, animals with grade 3 FL should be considered to have aggressive large B-cell lymphoma and treated as for diffuse large B-cell lymphoma.

Transformation and Progression

A small proportion of human cases of follicular lymphoma will progress to large cell lymphoma of diffuse type. More uncommonly, human patients with FL that have received extensive alkylating agent therapy may develop acute myeloid leukemia, usually as a risk of treatment-related changes. Rarely, some patients with FL may develop acute lymphoid leukemia, which is likely due to blast transformation of the original B-cell neoplasm. At this point, the risk of these events in animals is unknown because most are electively terminated when their disease prevents them from remaining an effective animal companion, or for compassionate reasons or cost of therapy.

Evaluation of the Treated Animal

Nothing is known about the risk factors for survival of animals with follicular lymphoma. In human patients, the categories to be determined in evaluating progression in follicular lymphoma are age and age since diagnosis, presence of nodes larger than 3 cm in diameter, and number of extranodal sites involved. Other negative factors that have been evaluated and suggested to be related to survival are the presence of "B" symptoms (night sweats), elevations of lactate dehydrogenase, male sex, and elevations above 30 mm/hr in the erythrocyte sedimentation rate. In evaluating animals with FL that have had their disease for some time, the most logical approach would

be to determine the overall quality of life of the animal in terms of activity and normal habits and an evaluation of the extent of the disease. In terms of histological progression the proportion of large cells appears to relate to progression as well as changes in the histology to a diffuse lymphoid proliferation and signs of marrow failure. All of these are evaluated as standard practice by veterinary oncologists.

Treatment and Survival

Radiation therapy is the main treatment for human patients with clinical stage I or II disease that appears capable of providing cures as measured by relapse-free survival for more than 10 years. As an alternative, alkylating agents including chlorambucil and cyclophosphamide provide remission rates of 30–60% of previously untreated human patients. A number of strategies are employed for patients who fail these treatments or who present in a more advanced stage of the disease. These include the purine analog agents, interferon, and newer anti–B-cell antibodies. Currently, the median survival of human patients with follicular lymphoma is about 9 years, and the survival after relapse is about 4.5 years. It is likely that dogs and cats diagnosed with follicular lymphoma have had the disease for 1–2 years prior to diagnosis and have the likelihood of living 2–3 years after diagnosis if FL proves to be clinically similar to other indolent lymphomas of animals.

REFERENCES

Ashley, P.F., and Bowman, L.A. (1999) Symmetric cutaneous necrosis of the hind feet and multicentric follicular lymphoma in a cat. *JAVMA* 214(2):211–214.

Bechter, O.E., Eisterer, W., Dirnhofer, S., Pall, G., Kuhr, T., Stauder, R., and Thaler, J. (1999) Expression of LFA-1 identifies different prognostic subgroups in patients with advanced follicle center lymphoma (FCL). *Leuk Res* 23:483–488.

Carter, R.F., Valli, V.E.O., and Lumsden, J.H. (1986) The cytology, histology and prevalence of cell types in canine lymphoma classified according to the National Cancer Institute Working Formulation. *Can J Vet Res* 50:154–164.

Cook, J.R., Craig, F.E., and Swerdlow, S.H. (2003) bcl-2 expression by multicolor flow cytometric analysis assists in the diagnosis of follicular lymphoma in lymph node and bone marrow. *Am J Clin Pathol* 119:145–151.

Federico, M., Vitolo, U., Zinzani, P., Chisesi, T., Clo, V., Bellesi, G., Magagnoli, M., Liberati, M., Boccomini, C., Niscola, P., Pavone, V., Cuneo, A., Santini, G., Brugiatelli, M., Baldini, L., Rigacci, L., and Resegotti, L. (2000) Prognosis of follicular lymphoma: A predictive model based on a retrospective analysis of 987 cases. *Blood* 95(3):783–789.

Freedman, A.S., Friedberg, J.W., Mauch, P.M., Dalla-Favera, R., and Harris, N.L. (2004) Follicular lymphoma. In Mauch, P.M., Armitage, J.O., Coiffier, B., Dalla-Favera, R., and Harris, N.L. (eds.), *Non-Hodgkin's Lymphomas*. Lippincott Williams & Wilkins, Philadelphia, pp. 367–388.

Greenlee, P.G., Filippa, D.A., Quimby, F.W., Patnaik, A.K., Calvano, S.E., Matus, R.E., Kimmel, M., Hurvitz, A.I., and Lieberman, P.H. (1990) Lymphomas in dogs: A morphologic, immunologic, and clinical study. *Cancer* 66:480–490.

Harris, N.L., and Ferry, J.A. (2001) Follicular lymphoma. In Knowles, D.M. (ed.), *Neoplastic Hematopathology*. 2nd ed. Lippincott Williams & Wilkins, Philadelphia, pp. 823–853.

Jager, U., Bocskor, S., Le, T., Mitterbauer, G., Bolz, I., Chott, A., Kneba, M., Mannhalter, C., and Nadel, B. (2000) Follicular lymphomas' BLC-2/IgH junctions contain templated nucleotide insertions: Novel insights into the mechanism of t(14;18) translocation. *Blood* 95(11):3520–3529.

Kelley, L.C., and Mahaffey, E.A. (1998) Equine malignant lymphomas: Morphologic and immunohistochemical classification. *Vet Pathol* 35:241–252.

Nathwani, B.N., Anderson, J.R., Armitage, J.O., Cavalli, F., Diebold, J., Drachenberg, M.R., Harris, N.L., Maclennan, K.A., Muller-Hermelink, H.K., Ullrich, F.A., and Weisenburger, D.D. (1999) Clinical significance of follicular lymphoma with monocytoid B cells. *Human Pathol* 30(3):263–268.

Renard, N., Valladeau, J., Barthelemy, C., Ribeiro, P., Berger, F., Saeland, S., and Salles, G. (1999) Characterization of germinal center dendritic cells in follicular lymphoma. *Exp Hematol* 27:1768–1775.

Robetorye, R.S., Bohling, S.D., Medeiros, L.J., and Elenitoba-Johnson, K.S.J. (2000) Follicular lymphoma with monocytoid B-cell proliferation: Molecular assessment of the clonal relationship between the follicular and monocytoid B-cell components. *Lab Invest* 80(10):1593–1599.

Skinnider, B.F., Horsman, D.E., Dupuis, B., and Gascoyne, R.D. (1999) Bcl-6 and Bcl-2 protein expression in diffuse large B-cell lymphoma and follicular lymphoma: Correlation with 3q27 and 18q21 chromosomal abnormalities. *Human Pathol* 30(7):803–808.

Soubeyran, P., Debled, M., Tchen, N., Richaud, P., Monnereau, A., Bonichon, F., and Eghbali, H. (2000) Follicular lymphomas—A review of treatment modalities. *Crit Rev in Oncol/Hematol* 35:13–32.

Teske, E., van Heerde, P., Rutteman, G.R., Kurzman, I.D., Moore, P.F., and MacEwen, E.G. (1994) Prognostic factors for treatment of malignant lymphoma in dogs. *JAVMA* 205(12):1722–1728.

Vail D.M., and MacEwen. E.G. (2001) Feline lymphoma and leukemias. In Withrow, S.J., and MacEwen, E.G., *Small Animal Clinical Oncology,* 3rd ed., Chapter 28, Hematopoietic tumors. Saunders Elsevier, Philadelphia, pp. 590–611.

Vail, D.M., MacEwen, E.G., and Young, K.M. (2002) Canine lymphoma and lymphoid leukemias. In Withrow, S.J., and MacEwen, E.G., *Small Animal Clinical Oncology,* 3rd ed., Chapter 28, Hematopoietic tumors. Saunders Elsevier, Philadelphia, pp. 558–590.

Valli, V.E., Jacobs, R.M., Norris, A., Couto, C.G., Morrison, W.B., McCaw, D., Cotter, S., Ogilvie, G., and Moore, A. (2000) The histologic classification of 602 cases of feline lymphoproliferative disease using the National Cancer Institute Working Formulation. *J Vet Diagn Invest* 12:295–306.

Vernau, W., Valli, V.E.O., Dukes, T.W., Jacobs, R.M., Shoukri, M., and Heeney, J.L. (1992) Classification of 1,198 cases of bovine lymphoma using the National Cancer Institute Working Formulation for human non-Hodgkin's lymphomas. *Vet Pathol* 29:183–195.

Vonderhaar, M.A., and Morrison, W.B. (2002) Lymphosarcoma. In Morrison, W.B., *Cancer in Dogs and Cats—Medical And Surgical Management*. Teton New Media, Jackson, Wyoming, pp. 641–670.

Wood, L.A., Coupland, R.W., North, S.A., and Palmer, M.C. (1999) Outcome of advanced stage low grade follicular lymphomas in a population-based retrospective cohort. *Cancer* 85(6):1361–1368.

Mantle Cell Lymphoma

Definition

Mantle cell lymphoma (MCL) is a distinct neoplastic disease of humans and animals characterized architecturally by multifocal origin around fading germinal centers and composed of small round to lightly cleaved B-cells that lack nucleoli and mitoses and are characterized biologically by an indolent course.

MCL is of recent recognition in human pathology and had been termed as *centrocytic lymphoma* in Europe and *lymphoma of intermediate cell type* in the U.S. It was then called *mantle zone lymphoma*, and finally *MCL,* and identified as a distinct identity arising from the presence of a specific translocation t(11;14) and characterized by the overexpression of the cyclin D1 protein.

Epidemiology and Incidence

Mantle cell lymphoma constitutes about 5% of human lymphoma cases in North America and about twice that level in Europe. There is a 3:1 male predominance in humans, and the disease is seen in elderly patients with a median age of 65–75 years. Mantle cell lymphoma became recognized in the 1980s and fully characterized in the early 1990s. With the further definition of marginal and mantle type lymphomas, the adjunct term of *zone* has been reserved for the marginal layer of perifollicular lymphoma, with the mantle layer lymphomas identified as mantle cell type. My first use of this diagnosis was in a dog in 1992 under the rubric of "mantle zone lymphoma." Since that case was received, 11 cases of canine MCL have been diagnosed out of 461 total cases for an incidence in the dog of about 2%. The gender was known in 8 of the 11 cases of MCL, and of these 5 were male and 3 female. The ages on 10 of these dogs ranged from 1.5 to 15 years with a mean of just under 8.0 years. In the comparable period, 150 cases of cat lymphoma have been diagnosed, with only 1 case of MCL. No cases of MCL have been recognized in the horse, with one in each of a pig and spectacled bear.

Clinical Presentation and Features

One of the more remarkable features of MCL is that in the dog, 7 of the 11 cases were found only in the spleen. Like marginal zone lymphoma, and unlike follicular lymphoma, MCL in the spleen presents as a locally extensive mass and not as a diffuse involvement. Like splenic marginal zone lymphoma, MCL may be associated with other lesions, including plasmacytoma, myelolipoma, fibrosis, and focal hemorrhagic infarction (Figs. 3.333–3.336). In

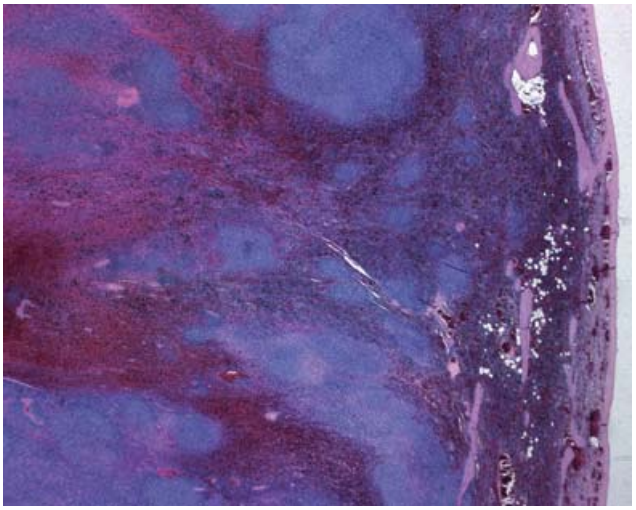

Figure 3.333. Dog: spleen, mantle cell lymphoma. This lesion illustrates the likelihood that splenic lymphoma in the dog would be associated with a number of other lesions. The vacuolar areas beneath the splenic capsule are fat cells associated with an area of myelolipoma. The irregular areas of lymphoid proliferation are largely foci of mantle cell lymphoma.

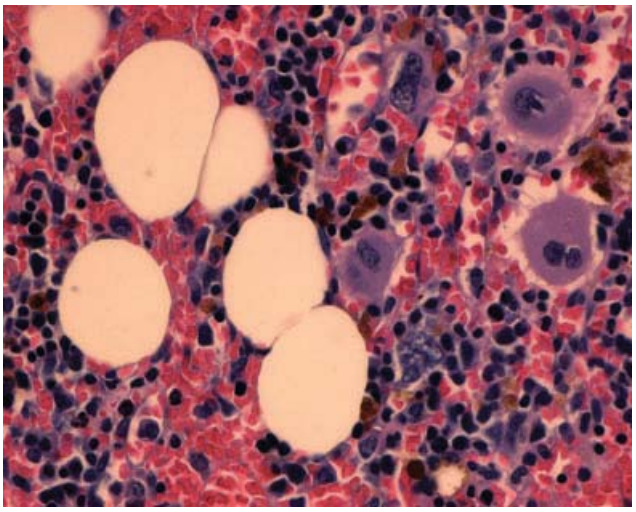

Figure 3.334. Dog: spleen, mantle cell lymphoma. Detail of Figure 3.333. Area of myelolipoma with fat cells, megakaryocytes, scattered erythropoiesis, and numerous hemosiderin-bearing macrophages.

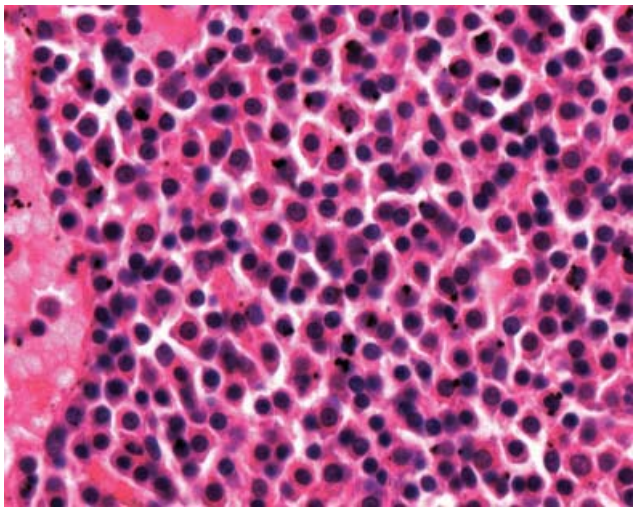

Figure 3.335. Dog: spleen, mantle cell lymphoma. Detail of Figure 3.333. A solid area of plasmacytoma, adjacent to an area of ischemic necrosis. There are many binucleated cells as well as frequent small nucleoli that indicate this is an autonomous area of cell proliferation rather than a benign reactive process.

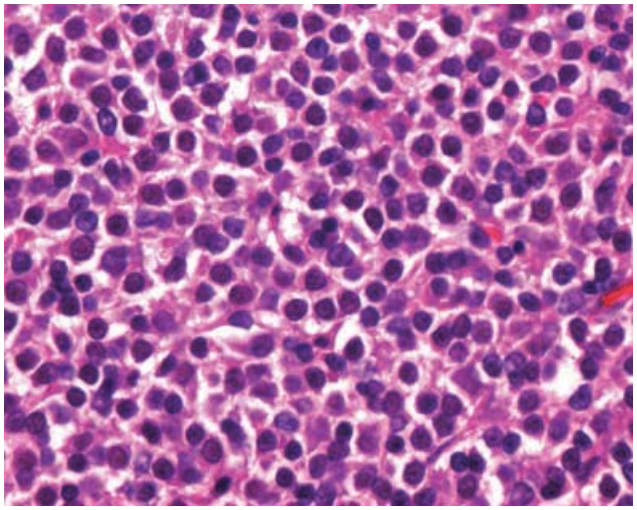

Figure 3.336. Dog: spleen, mantle cell lymphoma. Detail of Figure 3.333. Mantle cell lymphoma from a relatively well-fixed area. The size of the cells is typical but the cell separation is exaggerated by edematous changes associated with widespread hemorrhagic infarction. The nuclei are round to oval and slightly larger than red cells, with relatively compact chromatin and a narrow rim of quite highly amphophilic cytoplasm. Some of the cells have quite prominent central nucleoli with the mitotic rate typically very low. The case illustrates the variety of lesions occurring within splenic lymphoproliferation that are easily overlooked, especially when complicated by hemorrhagic infarction.

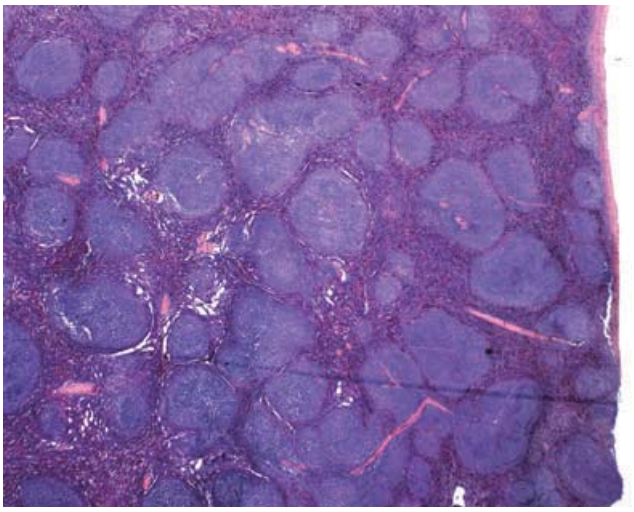

Figure 3.337. Human: spleen, mantle cell lymphoma. The organ is uniformly enlarged with multifocal areas of small lymphoid proliferation arising on end arterioles. *Slide from Cornell Tutorial.*

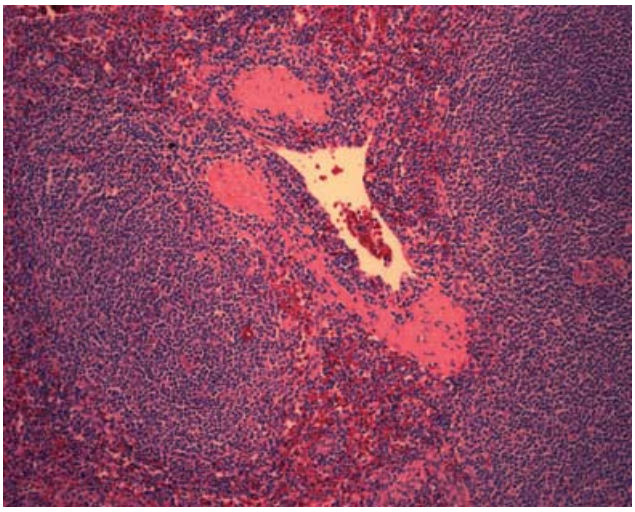

Figure 3.338. Human: spleen, mantle cell lymphoma. Detail of Figure 3.337. A typical large area of proliferation surrounds a small arteriole (top) with a muscular sinus (center) that has extensive subendothelial colonization by neoplastic cells. The smaller focus of mantle cell proliferation is at the left, likely the edge of a larger nodule.

human cases of MCL, most are advanced at diagnosis with generalized lymphadenopathy with splenomegaly in about half of cases and extra nodal involvement usually including bone marrow in most cases (Figs. 3.337–3.341). Other areas frequently involved include lymphomatous polyposis of the intestine (Figs. 3.342, 3.343) and, less commonly, the skin, lung, breast, and other soft tissues. The central nervous system is involved in 5–20% of relapsed cases. The extent of involvement on both

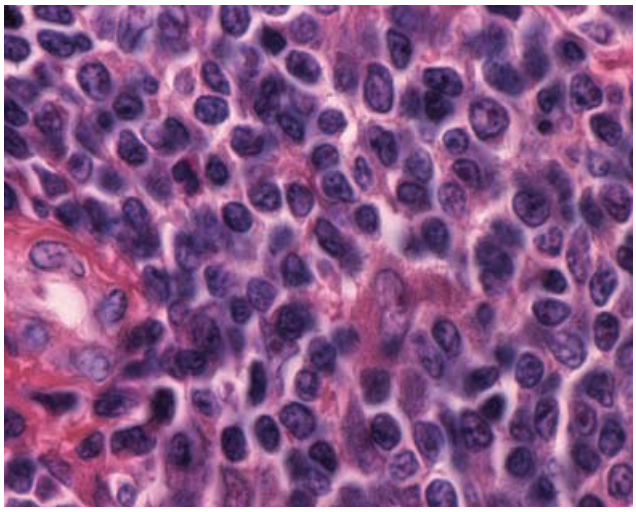

Figure 3.339. Human: spleen, mantle cell lymphoma. Detail of Figure 3.337. The mantle cell cuff is replaced by population of lymphocytes of intermediate size, with round to oval, and lightly indented nuclei. The chromatin pattern is quite dense, with some parachromatin clearing and about 1/3 of the cells having a relatively prominent nucleolus. The cytoplasm is minimal in volume and staining density and mitoses are rare. The large pale cell in the center may be a residual dendritic cell, and there is a single eosinophil above the artery.

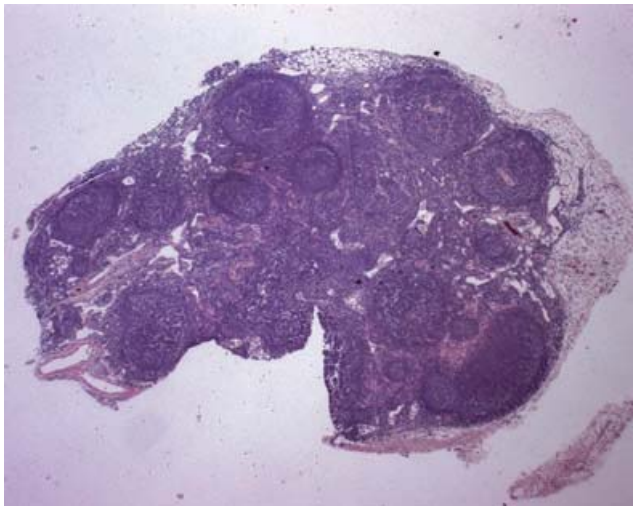

Figure 3.340. Human: lymph node, mantle cell lymphoma. There are multiple nodules without polarity of normal germinal centers. There is mild irregular involvement of perinodal fat. *Slide from Cornell Tutorial.*

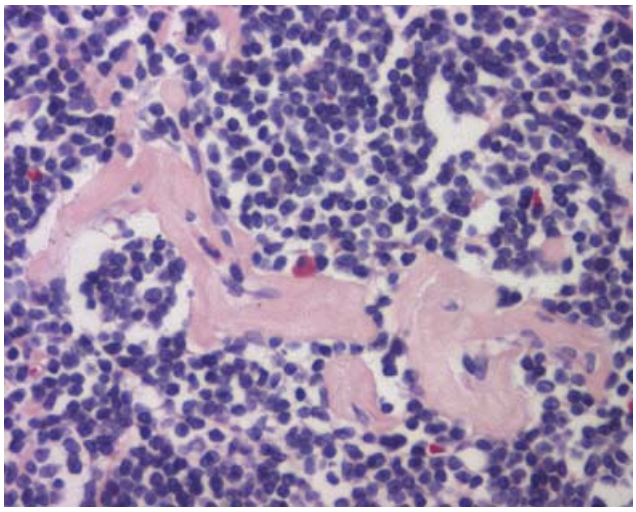

Figure 3.341. Human: node, mantle cell lymphoma. Detail of Figure 3.340. The pale areas at the center of some of the nodules are hyalinized vessels. The infiltrating cells are round to oval with nuclei slightly larger than red cells, with shallow indentations and minimal cytoplasm.

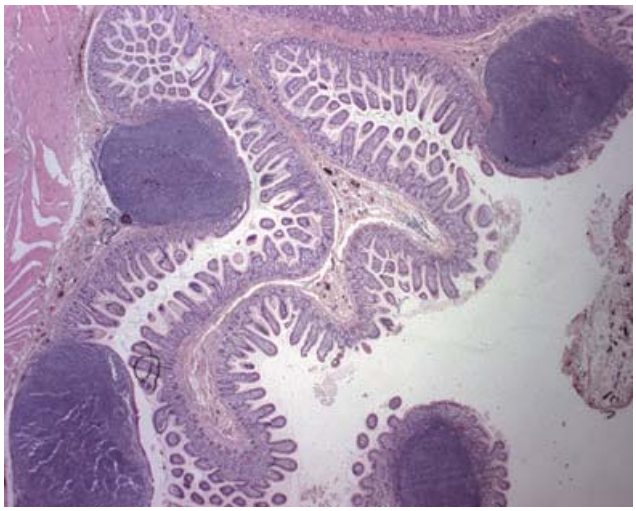

Figure 3.342. Human: colon, mantle cell lymphoma. Lymphomatous polyposis occurs in about 25% of human cases of mantle cell lymphoma, particularly in advanced cases. The colonic involvement is by multifocal areas of discrete nodular lymphoid proliferation. *Slide from Cornell Tutorial.*

humans and animals appears to depend largely on the extent of the staging procedures. In all of the cases in the dog where there was peripheral node lymphadenopathy, the submandibular node was involved, and 3 of the 4 cases that presented with nodal involvement had generalized lymphadenopathy. The extent of extrasplenic spread in the cases that came to clinical attention because of a focal splenic mass is not known, but many of these cases were examined in oncology practices and presumably were staged as splenic only.

In human pathology a "blastoid variant" of MCL has been identified that has slightly larger nuclei and nucleoli and tends to become leukemic and have extensive marrow involvement. Remarkably, this variant type is also seen in

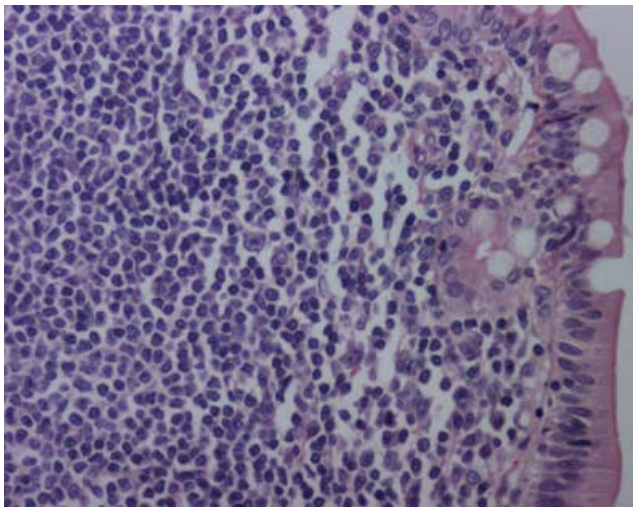

Figure 3.343. Human: colon, mantle cell lymphoma. Detail of Figure 3.342. The lesion consists of uniform infiltration of typical small lymphocytes with focally distended mucosa (preparation too thick for higher magnification).

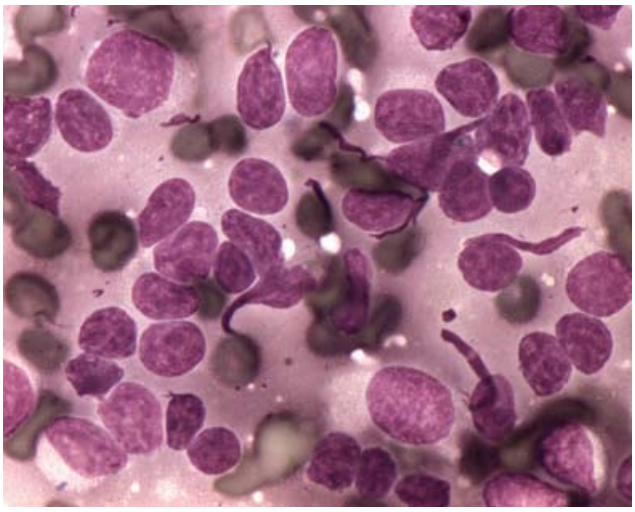

Figure 3.344. Dog: submandibular node and salivary gland mass, imprint, mantle cell lymphoma. The cells are of intermediate size and slightly larger than red cells, with densely stained chromatin that is largely dispersed with large chromocenters and without parachromatin clearing. The nucleoli are small and frequently inapparent and mitoses are very infrequent. The cytoplasm is minimal and with moderate staining density.

the dog, with a characteristic splenic lesion consisting of tumor foci that surround blood-filled cavities.

Pathologic Features

Blood

On the basis of one case of canine MCL that presented with splenic involvement there was a gammopathy with moderate anemia that reversed on splenectomy. Some cases at least may present with little or no change in normal blood parameters. Oddly, the blastoid variant that characteristically becomes leukemic in humans has not proven to be the case in dogs on the strength of only three cases that were managed by competent clinicians. In human cases, the neoplastic cells in blood are characterized by sharp shallow indentations in cells that otherwise closely resemble chronic lymphocytic leukemia (CLL). These characteristics can only be inferred for the dog because a leukemic case of MCL has yet to be described.

Bone Marrow

Bone marrow tissue has not been described in animals with mantle cell lymphoma. In humans, a wide variation in pattern is seen with focal neoplastic colonization in a paratrabecular or even diffuse pattern. It is stated that the cells in the blood and marrow do generally resemble those seen in lymph nodes.

Lymph Nodes

Nodal MCL appears to be rarely encountered, and as a consequence also rarely recognized. Nodes with this type of lymphoma are usually recognized in a late stage of involvement and in an animal that has more than one site involved. Typically there is no, or minimal, involvement of perinodal tissues, and nodal fixation is not found. The capsule is thinned and taut and the peripheral sinus is compressed and at least focally invaded with minor capsular infiltration. The node has a diffuse architecture and there is complete loss of germinal centers and filling of the medullary cords and compression of the medullary sinuses. There is a lack of the medullary sclerosis seen with marginal zone and T-zone lymphoma (TZL), with the medullary areas retaining a fine sinus and cord outline with the proliferative cells of similar type throughout the node. On phenotypic staining, former areas of germinal centers may be identified by the presence of a few larger cells and T-lymphocytes plus tingible body macrophages.

Cytologically, the cells of MCL are like those of T-zone lymphoma and have nuclei that are round and about the same size as a red cell, with dense chromatin with little intranuclear detail and lack of nucleoli. The cytoplasm is relatively abundant and lightly stained with cell boundaries indistinct, but with the nuclei having very uniform spacing. Mitoses are rarely encountered and apoptotic cells and macrophages are not present (Figs. 3.344, 3.345). Some cases may have fine, sharp, shallow nuclear membrane indentations—again like TZL. Focal necrosis is not a feature of MCL, nor is the irregular sinus dilation of cortical areas seen in late stage MZL and TZL. The nodal MCL cells as described are like the typical presentation of MCL in the spleen but are smaller and unlike

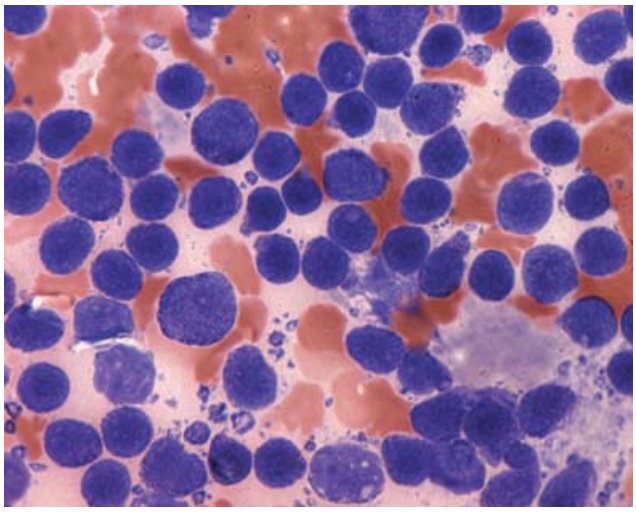

Figure 3.345. Dog: spleen, mantle cell lymphoma, fine needle aspirate. The nuclei tend to be round with an occasional shallow nuclear indentation (top center) obscured by the depth of cytoplasmic staining. Small nucleoli are present, with the larger cells likely the dividing population. Cytologically, these lesions resemble small cell hyperplasia if nucleoli are not recognized.

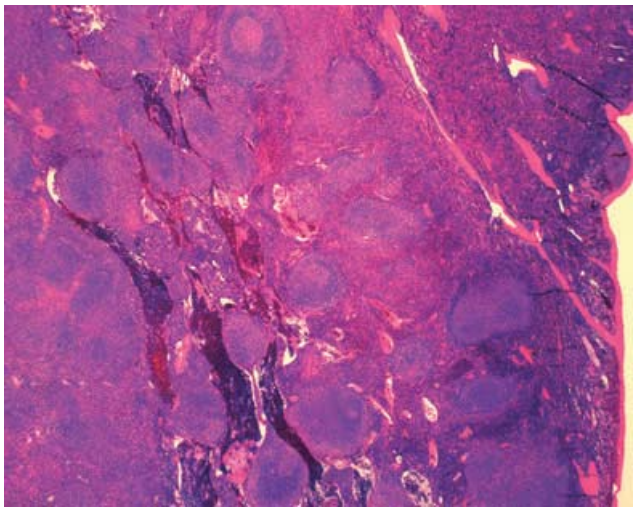

Figure 3.346. Dog: spleen, mantle cell lymphoma. A large focal mass that locally projects from the splenic contour has a small area of uninvolved tissue in the upper right. The mass is composed of a peripheral area of individual nodules centered on end arterioles and a large central mass of solid neoplastic proliferation (lower left). A few of the peripheral nodules have a central pale area of dendritic cell bed that identifies the proliferation as of mantle cell type. On needle aspiration the cell population would likely be considered benign.

those of the "blastoid" type of MCL recognized in the spleen and presumably present in other tissues.

Spleen

In both the dog and cat, MCL is likely to be encountered in a splenic mass that is multifocal and locally extensive and not diffuse as in the more aggressive types of lymphoma. When primary in the spleen, MCL is subsequently found in many other tissues. Two forms of splenic MCL occur, with the most common type still a rare finding and characterized by multifocal areas of round solid foci of lymphoid proliferation that can occasionally be found associated with an end arteriole. These foci are larger than germinal centers and may be sharply defined against a background of intense congestion or hemorrhagic necrosis that has brought the lesion to clinical attention (Figs. 3.346–3.349). Like MZL, the internodular areas may have diffuse sheets of plasma cells. There may be coalescing areas of lymphoid proliferation (Fig. 3.350) and the splenic capsule may be focally thinned or invaded (Fig. 3.351). The only indication of germinal centers associated with these foci is an occasional pale area in the center of a nodular proliferation that is the residue of the larger dendritic cells or of an area of follicular hyalinosis. There is a complete absence of the residual normal mantle cells and none of the fading clusters of small benign cells seen at the center of splenic MZL (see Fig. 3.347).

The second form of splenic MCL is of the blastic or blastoid type, which has a unique architecture and genesis. A major difference of the blastoid MCL as seen

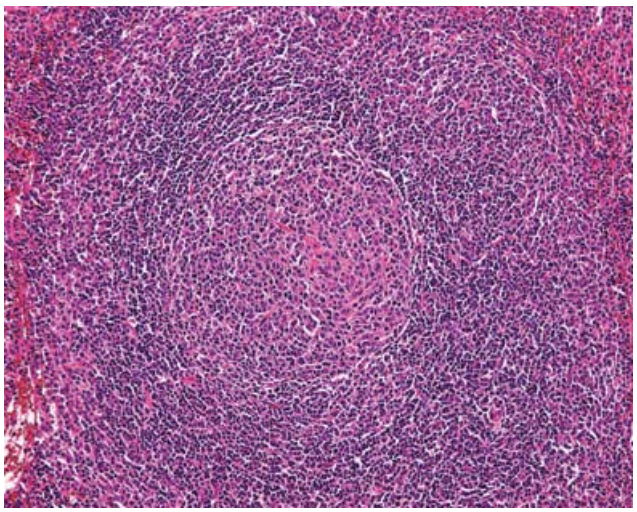

Figure 3.347. Dog: spleen, mantle cell lymphoma. Detail of Figure 3.346. The mantle cell signature is a fading germinal center with a hypocellular dendritic cell bed (center) surrounded by a proliferating cuff of small lymphocytes. The lesion is the inverse of marginal zone lymphoma where the mantle cells have collapsed into the dendritic cell bed and they are surrounded by the larger cells of marginal zone type.

in the dog is that the lesion is now diffuse with multifocal nodules of lymphoid tumor throughout a more uniformly enlarged organ. The lymphoid nodules are roughly twice the size of germinal centers, and in the well-

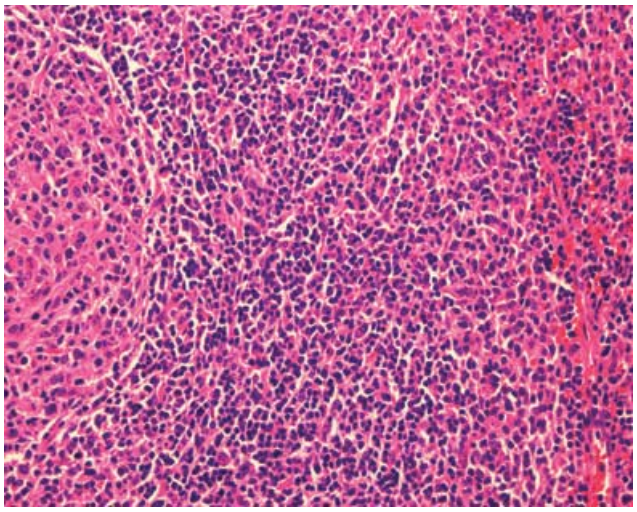

Figure 3.348. Dog: spleen, mantle cell lymphoma. Detail of Figure 3.347. The hypocellular germinal center area is at the left surrounded by a broad cuff of small cells of uniform size throughout without an outer cuff of larger marginal zone cells.

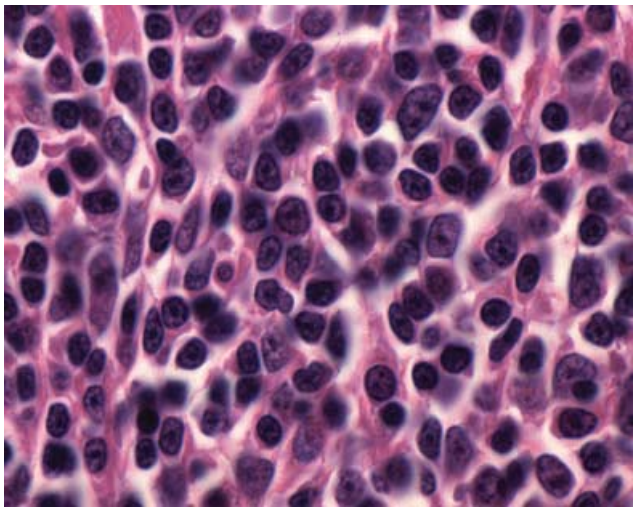

Figure 3.349. Dog: spleen, mantle cell lymphoma. Detail of Figure 3.348. The nuclei are round to oval and occasionally irregular in shape and vary from slightly larger to 1.5 times a red cell in diameter. The chromatin is dispersed and deeply stained with small, generally inapparent central nucleoli in about 1/2 of the cells. The cytoplasm is limited to a narrow ellipse of moderate staining density. Mitoses are typically absent. The tissue was clonal on PCR probe of the immunoglobulin gene.

advanced neoplasm many or most of these will appear as a narrow rim of lymphoid tissue surrounding a central lake of red blood cells (Fig. 3.352). In viewing multiple areas and neoplastic foci the progression of lesions can be deduced to arise as proliferative nodules, apparently overgrow their blood supply, and undergo central ischemic necrosis. These necrotic cells rapidly disappear and the

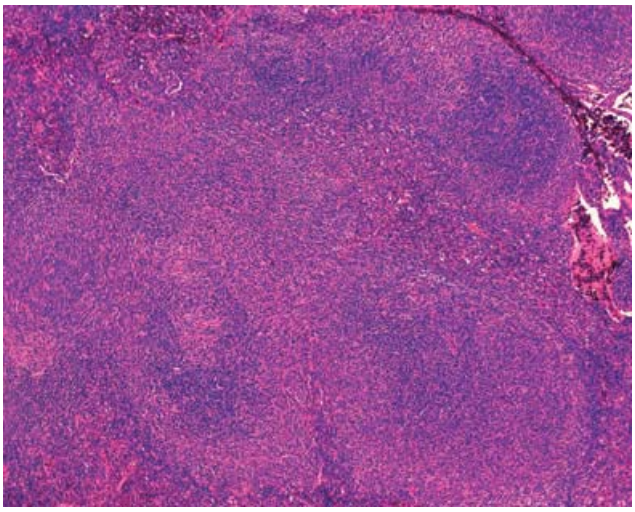

Figure 3.350. Dog: spleen, mantle cell lymphoma, same case as Figure 3.346. Interior of a splenic mass with coalescing nodules of mantle cell proliferation.

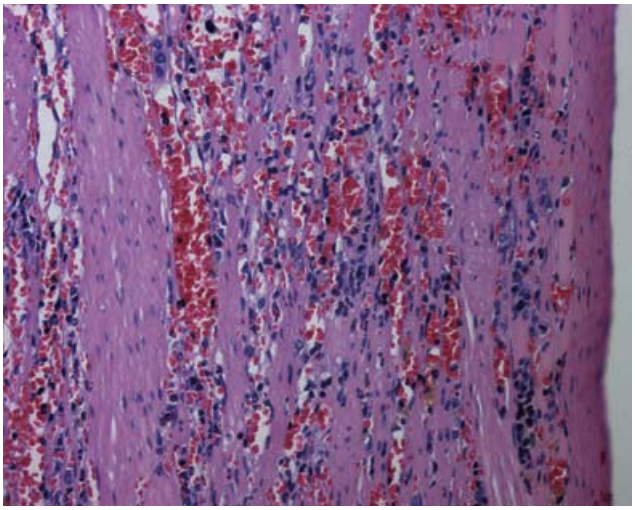

Figure 3.351. Dog: spleen, mantle cell lymphoma. The splenic capsule is invaded by small vessels that are irregularly lined and surrounded by cells of the same type as the inner nodular proliferation.

central area of the nodule becomes filled with blood, presumably as a result of having arisen on an end arteriole (Figs. 3.353, 3.354). Animals with this form of MCL often have recurrent febrile episodes and a gammopathy, both of which might arise as a result of the continuing areas of tumor necrosis. Both of these changes regress or disappear following splenectomy, which suggests that the gammopathy is not a constituitive product of the tumor cells but of host response to the tumor and tissue necrosis.

Cytologically, the cells of the blastoid type of MCL have nuclei that are 1.5 red cells in diameter and may be

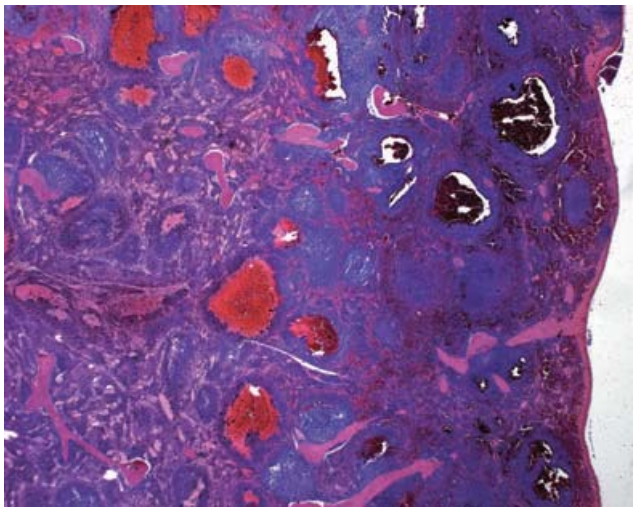

Figure 3.352. Dog: spleen, blastoid-type mantle cell lymphoma. Architecturally, the spleen is uniformly enlarged with thinning of the capsule and widely spaced muscular trabeculae. In contrast to the focal lesions of the more common small cell type of mantle cell lymphoma, the blastoid neoplasm diffusely involves the entire spleen with multifocal areas of lymphoid proliferation, with a periodicity that indicates relation to the end arterioles of the splenic circulation. Unlike other neoplasms, the blastoid type is characterized by lymphoid structures represented by a thinned rim of lymphoid tissue surrounding a central area of virtual hemorrhage and a nonendothelial-lined cavity. Because of the size of the organ, fixation was delayed and a darker area at the right represents inadequate fixation.

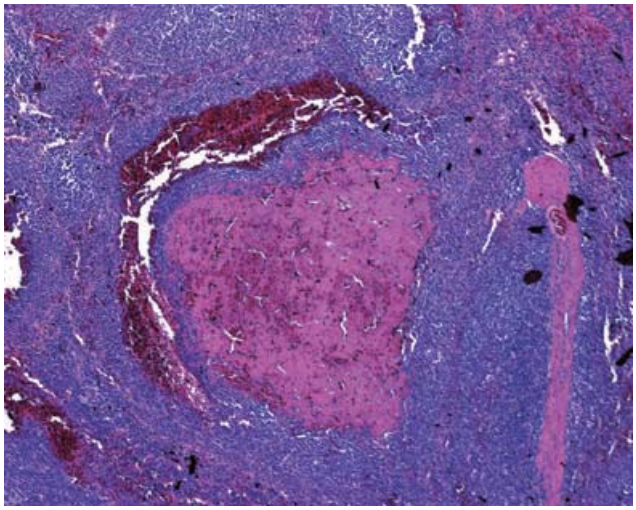

Figure 3.353. Dog: spleen, blastoid-type mantle cell lymphoma. The pathogenesis of the lesion begins with a lymphoid follicle that has overgrown and compressed the small radical supplying an initial germinal center. The center of the lymphoid mass undergoes ischemic coagulative necrosis, and with collapse of the cellular proliferation there is apparent dilation of the vascular supply leading to flooding of the central cavity.

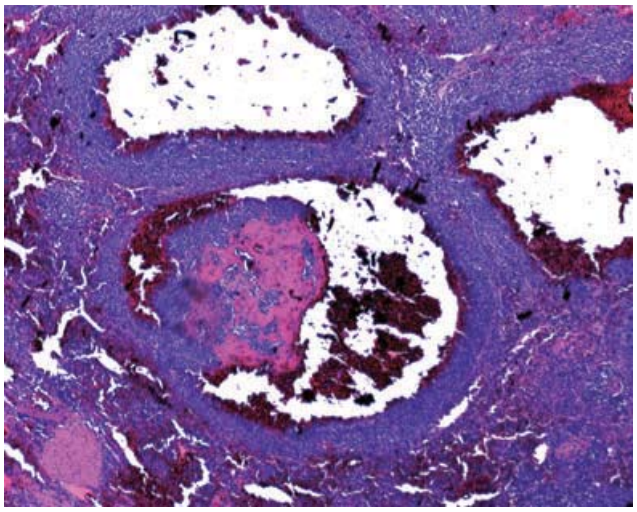

Figure 3.354. Dog: spleen, blastoid-type mantle cell lymphoma. Detail of same case as Figure 3.352. The center structure is an area of lymphoid proliferation at a further stage of coagulative necrosis and vascular flooding as in Figure 3.353.

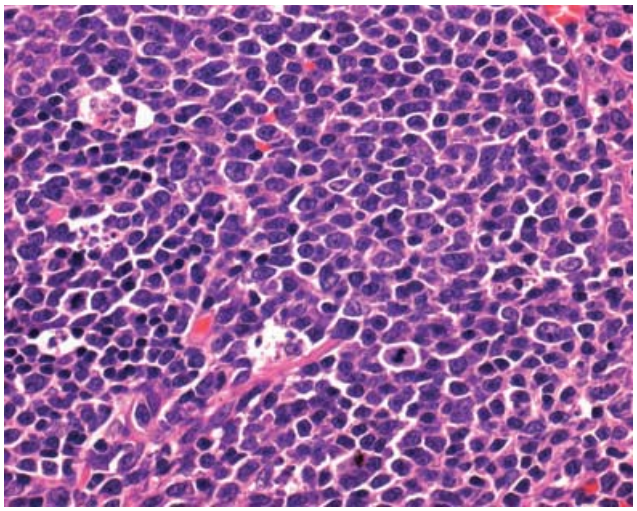

Figure 3.355. Dog: spleen, blastoid-type mantle cell lymphoma, same case as Figure 3.352. At the right is at the outer rim of an area of lymphoid proliferation, and the inner area (left) is at the edge of a hemorrhagic cavity. Note the small dark nuclei at the lower center that represent residual benign mantle cells from the original reaction center. The presence of tingible body macrophages and mitotic figures gives indication to the higher proliferative activity of the blastoid type of mantle cell tumor.

round, oval, or triangular and have shallow nuclear indentations (Figs. 3.355, 3.356). The chromatin pattern is coarse granular with a regular deposition highlighting the nuclear membrane and mild parachromatin clearing. There are 1–2 small but prominent nucleoli and 4–6 mitoses/400× field. Within the individual neoplastic foci

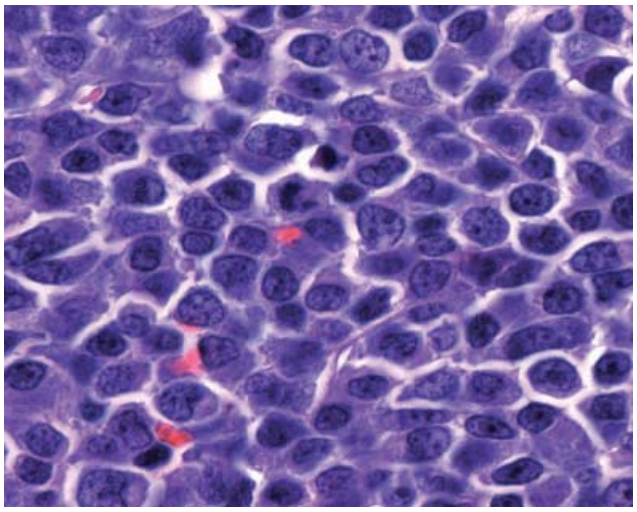

Figure 3.356. Dog: spleen, blastoid-type mantle cell lymphoma. Detail of Figure 3.352. The larger cell type of mantle cell lymphoma has nuclei 1.5–2 red cells in diameter, largely round to oval, with frequent fine sharp shallow indentations. The chromatin pattern is hyperchromatic fine granular with 1–3 moderately prominent nucleoli and relatively abundant, highly amphophilic cytoplasm.

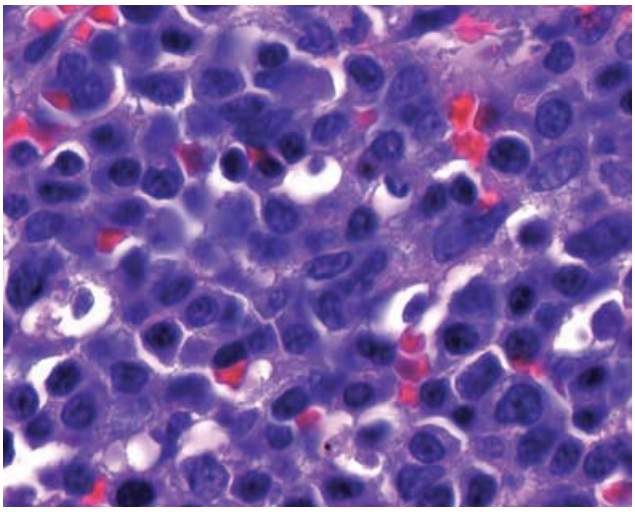

Figure 3.357. Dog: spleen, blastoid-type mantle cell lymphoma. The residual areas of splenic sinus contained solid clusters of atypical-appearing plasma cells that retain nucleoli with deeply amphophilic and eccentric cytoplasm and frequent binucleation.

there may a fading dendritic area or a central area of smaller benign mantle cells with round and densely stained nuclei. (see Fig. 3.356). Most of the foci have numerous tingible body macrophages and a number of apoptotic nuclei. Due to the presence of surrounding congestion and focal areas of necrosis it is essential to evaluate cells in areas where they are vibrant and well fixed without autolytic change. The surrounding areas of sinus have a mixture of lymphocytes and atypical plasmacytoid cells (Fig. 3.357), and the muscular veins have endothelial colonization by the same cells as the blastoid follicles (Fig. 3.358). The architectural pattern of blastoid MCL is not specific to the diagnosis but to the nature of the canine splenic circulation and may occur in other types of neoplasms including plasmacytoma and mast cell tumor.

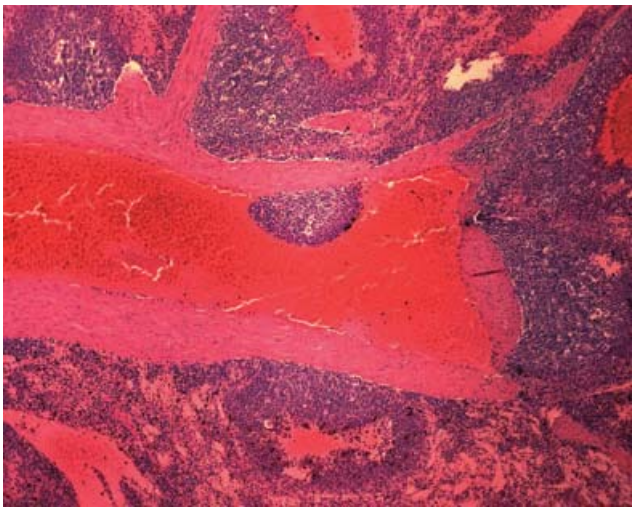

Figure 3.358. Dog: spleen, blastoid-type mantle cell lymphoma. Indication of the neoplastic nature of the proliferation is present in foci of subendothelial colonization of large muscular sinuses (center).

Other Organs

Because the diagnosis of MCL is usually made late in the development of the neoplasm, there is disseminated disease and involvement of nodes, spleen, and marrow; the liver is the additional organ most often invaded (Figs. 3.359–3.362). The pattern of involvement of the liver is by irregular but concentric foci in portal areas and smaller foci that are typically eccentric to the central veins. These foci tend to be entire and cohesive and impact the hepatic cords with a broad front type of expansion (see Fig. 3.361) Cytologically, the invading cells within the liver share the morphology of the MCL cells in other tissues but tend to retain the characteristic uniform separation of nuclei with cell boundaries generally distinct (see Fig. 3.362).

Immunologic Features

Mantle cell lymphoma is strongly and uniformly positive with CD79 alpha and CD20 (Figs. 3.363, 3.364) and negative with CD3. In human cases of MCL in frozen sections there is surface IgM and, often, surface IgD, with about 20% of cases expressing surface IgG. Oddly there is a kappa lambda ratio reversal in human MCL with

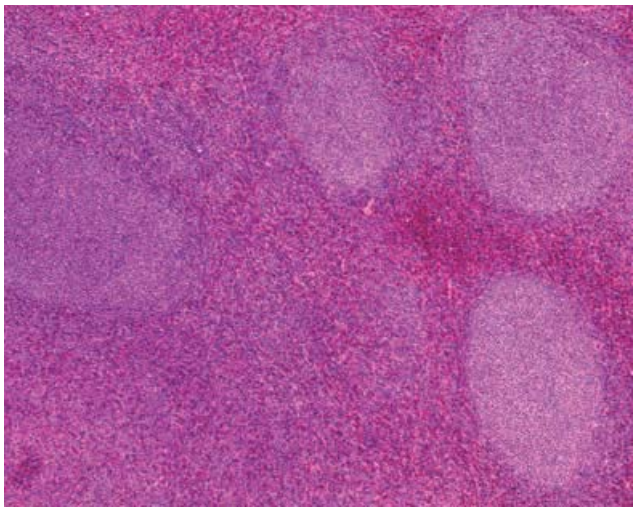

Figure 3.359. Cat: spleen, mantle cell lymphoma. At the architectural level, there is the usual periodicity of solid-appearing areas of lymphoid proliferation about the size of germinal centers.

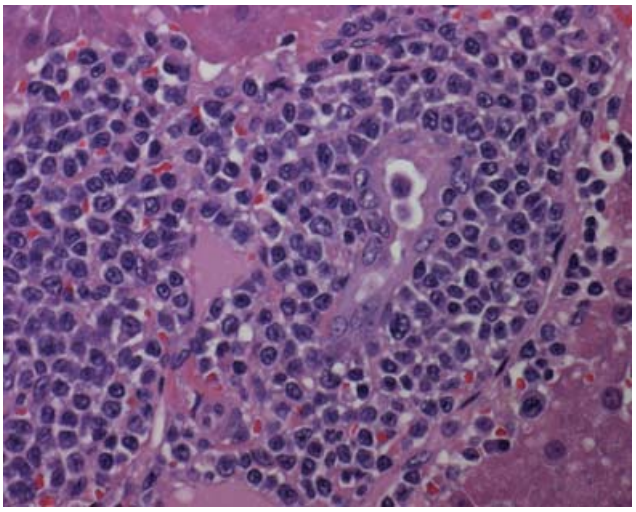

Figure 3.361. Cat: liver, mantle cell lymphoma. Detail of Figure 3.360. The atypical lymphocytes of MCL type form a tight cuff around the portal vessels with mild focal colonization outside of the periportal connective tissue (upper right).

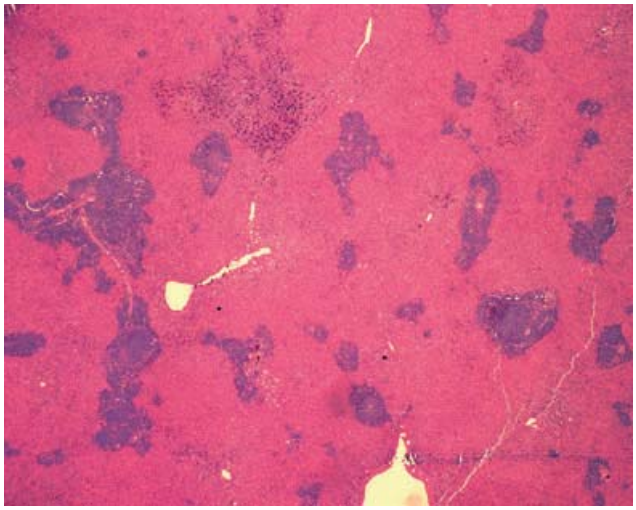

Figure 3.360. Cat: liver, mantle cell lymphoma, same case as Figure 3.359. There are relatively sharply defined multiple foci of lymphoid colonization—virtually all related to the portal tracts.

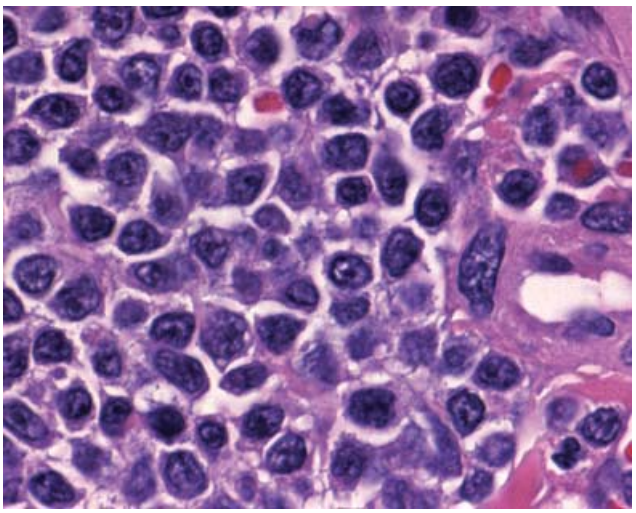

Figure 3.362. Cat: liver, mantle cell lymphoma. Detail of Figure 3.360. Note the size of the neoplastic cells compared to red cells. The portal artery is at the center right. The cells are outwardly round to oval but have sharp, shallow indentations as seen in the dog. The chromatin is hyperchromatic with a coarsely granular and occasionally branched pattern, with some parachromatin clearing and most cells having a central small prominent nucleolus. The cytoplasm is moderate in volume and staining density.

about 60% of cases positive for the lambda light chain. In a very few cases where the cells have been tested, MCL in animals is kappa negative and lightly but uniformly positive for lambda light chain. Animal and human MCL are negative for T-cell markers.

Cytogenetic and Molecular Features

Nothing is known about genetic changes that are recurring and characteristic of MCL in animals. In human MCL the t(11;14) (q13;q32) translocation is seen in most cases and is considered presumptive of MCL but not confirmative, because the same translocation occurs rarely in CLL and myeloma requiring morphologic and immunologic correlation to confirm the diagnosis of MCL. The oncogene believed to be dysregulated by the t(11;14) has been termed *CCND1* and encodes for the cyclin D1 that is overexpressed in nearly all cases of MCL. Antibodies

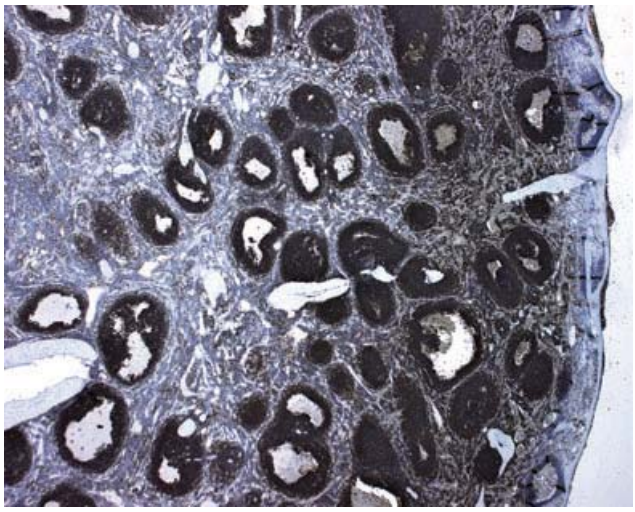

Figure 3.363. Dog: spleen, blastoid-type mantle cell lymphoma. Phenotype of Figure 3.352. With CD20 the areas of lymphoid proliferation are strongly and uniformly labeled, but the interfollicular areas of atypical-appearing plasma cells are unlabeled.

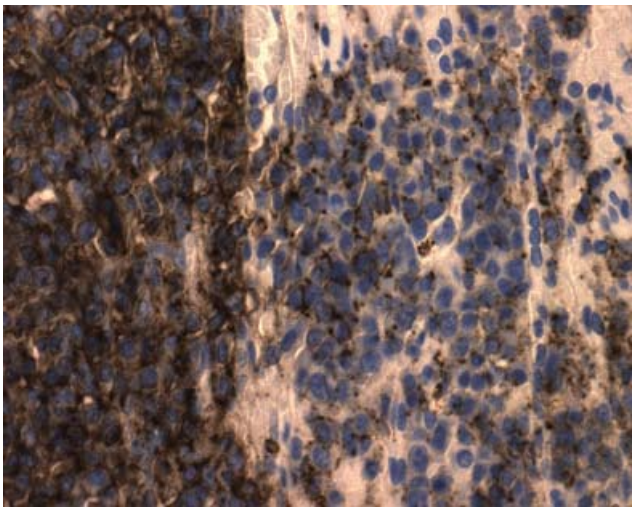

Figure 3.364. Dog: spleen, blastoid-type mantle cell lymphoma. Detail and phenotype of Figures 3.352 and 3.363. On staining with CD20 an area of mantle cell lymphoma (left) is strongly and uniformly labeled; a focus of atypical plasmacytoma cells (center) are only lightly and irregularly labeled. In contrast, CD79 marks the plasmacytoid cells very strongly as well as the neoplastic mantle cells.

to the protein product of the cyclin D1 gene are active in paraffin embedded tissue, and this reaction is a highly sensitive and specific marker for MCL. The cyclin D1 immunohistochemical reaction is not easily performed and is a difficult determination even in skilled hands. It has not been positive in limited trials on canine tissues of suspected MCL.

Cell of Origin

Mantle cell lymphoma is felt to be derived from a subset of naive bone marrow B-cells that are pregerminal center cells located in primary follicles or in the mantle cell region of secondary follicles. The progeny of these cells are capable of proliferation in a follicular or diffuse pattern or a combination of both.

Diagnostic Criteria

Mantle cell lymphoma is a lymphoid neoplasm with a nodular or follicular growth pattern in the spleen and liver and in nodes is follicular and coalescing in later development. The periodicity of the neoplastic foci in the spleen is characteristic and representative of origin around end arterioles. The origin from germinal centers in lymphoid organs is evidenced by the presence of fading germinal centers in some foci, the residue of follicular hyalinosis in others, and the presence of small mature cells of the benign fading mantle cell cuff in the center of others. The most common small cell type of MCL is identified by nodular proliferations composed of cells with small, round, densely stained nuclei and absent nucleoli. The mitotic rate is very low or absent in the standard type of MCL and low but present in the blastoid type.

Differential Diagnosis

MCL must be differentiated from follicular lymphoma of grade 1 where the centrocytes lack the sharp shallow nuclear indentations of the MCL cells. The centrocytes of FL I have more internal nuclear detail than the small type MCL and are more similar to the blastoid type of MCL but again lack the nuclear indentations. In lymph nodes in early MCL, the very wide mantle cell cuffs are unlike those o the larger cells of MZL and unlike the narrower cuffs of follicular hyperplasia. In differentiation from diffuse small cell proliferation, MCL needs to be differentiated from CLL, where again the indented nuclei of MCL is an important distinction not present in CLL. The angiofollicular type of hyaline vascular lymphoid hyperplasia is rare in animals and presents as follicles with small lymphocytes surrounding fading germinal centers in uniform concentric circles of small cells. Cytologically, MCL is similar to the cells of cutaneous T-cell lymphoma (CTCL) and to those of T-zone lymphoma (TZL Figs. 3.365, 3.366), both of which have small nuclei with sharp, shallow indentations and a low mitotic rate; both are also characterized by diffuse rather than nodular proliferations and are not primary in the spleen.

Staging

Most cases of MCL in humans and animals present in advanced disease, usually at stage III–IV. The staging process requires recognizing the tendency for MCL to dis-

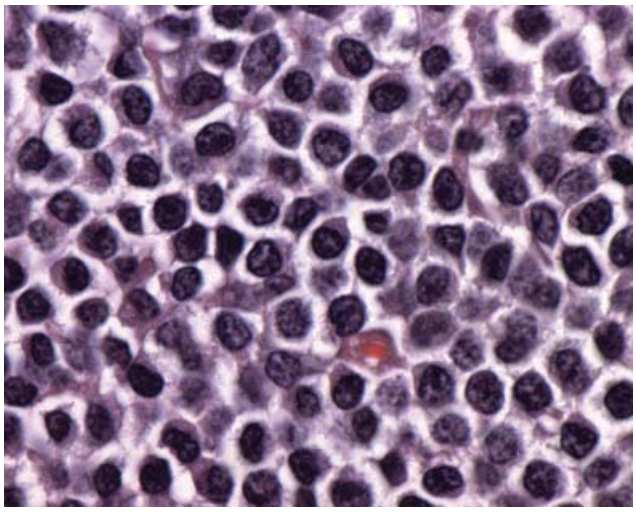

Figure 3.365. Dog: lymph node, T-zone lymphoma. The cell proliferation is of small cells with small nuclei and fine sharp, shallow nuclear indentations apparent in the nucleus to the left above the red cell. The cytoplasm is minimal, and nuclear spacing is characteristic.

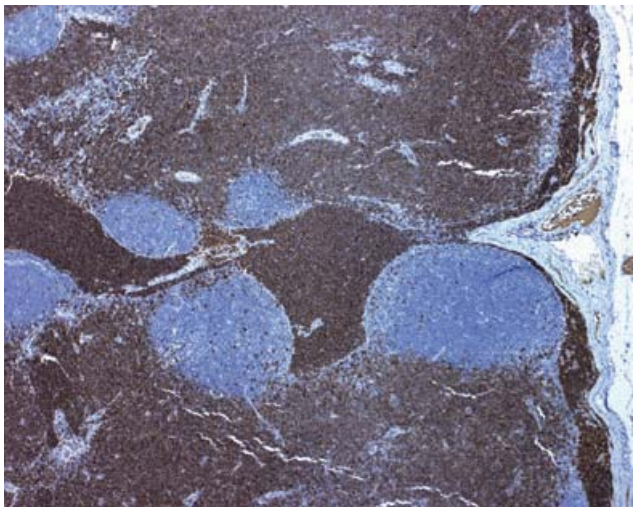

Figure 3.366. Dog: lymph node, T-zone lymphoma. Phenotype of Figure 3.365. With CD3 staining, the fading areas of B-cells are peripheralized near connective tissue boundaries, with the proliferating T-cells occupying paracortical areas.

seminate, and imaging is necessary to identify involvement of both internal and peripheral nodes as well as hepatosplenomegaly. Examination of marrow and blood is essential. Because the involvement of both the spleen and liver is multifocal, it is likely that neoplastic cells would be obtained on an undirected aspirate of liver and of spleen if uniformly enlarged. If there is focal enlargement of the spleen it can be expected to yield a variety of cell types, and the cleft nature of the MCL cells must be kept in mind from cells of all areas including the blood and marrow.

Transformation and Progression

There does not appear to be any change is cell type in MCL with progression of the disease. In humans, MCL is not a curable disease and there is relentless progression despite various therapies. The rate of progression of MCL in animals is largely unknown. In human MCL the most significant prognostic factor is a short time to treatment failure. Other important factors are (increasing) age, poor performance status at inception of treatment, advanced stage of disease, high serum lactate dehydrogenase, splenomegaly, and anemia. The so-called "B-symptoms" of fever, night sweats, and weight loss are important factors in humans as well as leukemic spread. In multivariate analysis, the only independently significant prognostic factors are age, poor performance status, leukemia, and splenomegaly. Information specifically on animals must be determined by follow-up of cases with reliable initial diagnostic workup and treatment history.

Evaluation of the Treated Animal

Virtually nothing is known about the progression of MCL in animals. Because marrow has not been routinely examined in animals with lymphoma, examination of that tissue in the face of anemia or other cytopenia would be in order in an animal with a splenic neoplasm. As noted above, a fine needle aspiration of node liver and spleen would likely yield neoplastic cells if the diagnosis were already known. In the absence of a specific diagnosis, the presence of a poorly responsive small cell lymphoma of B-cell type with lightly cleft nuclei should raise suspicion of advanced MCL.

Treatment and Survival

In the absence of any data for animals, the median survival of human patients with MCL is 3 years with no long-term survivors. In human studies, the blastoid variant is associated with a poorer survival than that of the classical small cell form of MCL. The overall median survival for patients with the blastoid variant of MCL was 14.5 months, with 53 months for the more common small cell form. Growth pattern has been suggested to favor cases with nodular over diffuse architecture, but other studies have found no difference in either growth pattern or cytology. Despite a variety of treatments, MCL has the poorest overall survival of all human lymphoma subtypes. Splenectomy is recommended only in patients with significant splenic-induced cytopenias. The overall response rate for human MCL is about 70–80% with complete remissions achieved in 20–50% of cases.

Chemotherapeutic agents used include the anthracycline regimens and those with purine analogs. Interferon has been tried as well as the newer anti-CD20 B-cell antibodies. The only potential curative treatment used so far is allogeneic marrow transplantation with the development of graft versus lymphoma effect. A drug that acts by inhibition of cyclin D1 may be of assistance in combination therapy, and a proteasome inhibitor is in trial that suppresses the necrosis factor kB that is an essential factor in up-regulating the antiapoptotic genes.

REFERENCES

Belaud-Rotureau, M.A., Parrens, M., Dubus, P., Garroste, J.C., Mascarel, A., and Merlio, J.P. (2002) A comparative analysis of FISH, RT-PCR, and immunohistochemistry for the diagnosis of mantle cell lymphomas. *Mod Pathol* 15(5):517–525.

Bjorck, E., Landgren, O., Schoumans, J., Christensson, B., Bjorkholm, M., Macdonald, A.P., and Nordenskjold, M. (2003) Molecular cytogenetic approach to the diagnosis of splenic lymphoma: A case report of blastoid mantle cell lymphoma. *Leuk and Lymph* 44(7):1229–1234.

Bosch, F., Lopez-Guillermo, A., Campo, E., Ribera, J., Conde, E., Piris, M.A., Vallespi, T., Woessner, S., and Montserrat, E. (1998) Mantle cell lymphoma: Presenting features, response to therapy, and prognostic factors. *Cancer* 82(3):567–575.

Carbone, A., Gloghini, A., Volpe, R., Attadia, V., Gattei, V., Zagonel, V., and Pinto, A. (1992) Follicular lymphoma of compartmentalized small cleaved center cells and mantle zone lymphocytes: Evidence for a common derivation. *Am J Clin Pathol* 98(4):437–448.

Decaudin, D., Bosq, J., Munck, J.N., Bayle, C., Koscielny, S., Boudjemaa, S., Bennaceur, A., Venuat, A.M., Naccache, P., Bendahmane, B., Ribrag, V., Carde, P., Pico, J.L., and Hayat, M. (1996) Mantle cell lymphomas: Characteristics, natural history and prognostic factors of 45 cases. *Leuk and Lymph* 26:539–550.

Gu, J., Huh, Y.O., Jiang, F., Caraway, N.P., Romaguera, J.E., Zaidi, T.M., Fernandez, R.L., Zhang, H., Khouri, I.F., and Katz, R.L. (2004) Evaluation of peripheral blood involvement of mantle cell lymphoma by fluorescence in situ hybridization in comparison with immunophenotypic and morphologic findings. *Mod Pathol* 17:553–560.

Hiddemann, W., Lenz, G., Weisenburger, D.D., and Dreyling, M.H. (2004) Mantle cell lymphoma. In Mauch, P.M., Armitage, J.O., Coiffier, B.C., Dalla-Favera, R., and Harris, N.L. (eds.), *Non-Hodgkin's Lymphomas*. Lippincott Williams & Wilkins, Philadelphia, pp. 461–476.

Korz, C., Pscherer, A., Benner, A., Mertens, D., Schaffner, C., Leupolt, E., Dohner, H., Stilgenbauer, S., and Lichter, P. (2002) Evidence for distinct pathomechanisms in B-cell chronic lymphocytic leukemia and mantle cell lymphoma by quantitative expression analysis of cell cycle and apoptosis-associated genes. *Blood* 99(12):4554–4561.

Medeiros, L.J., Hai, S., Thomazy, V.A., Estalilla, O.C., Romaguera, J., and Luthra, R. (2002) Real-time RT-PCR assay for quantifying cyclin D1 MRNA in B-cell non-Hodgkin's lymphomas. *Mod Pathol* 15(5):556–564.

Moynihan, M.J., Bast, M.A., Chan, W.C., Delabie, J., Wickert, R.S., Wu, G., and Weisenburger, D.D. (1996) Lymphomatous polyposis: A neoplasm of either follicular mantle or germinal center cell origin. *Am J Surg Pathol* 20(4):442–452.

Nelson, B.P., Variakojis, D., and Peterson, L.C. (2002) Leukemic phase of B-cell lymphomas mimicking chronic lymphocytic leukemia and variants at presentation. *Mod Pathol* 15(11): 1111–1120.

Ott, M.M., Helbing, A., Ott, G., Bartek, J., Fischer, L., Durr, A., Kreipe, H., and Muller-Hermelink, H.K. (1996) bcl-1 Rearrangement and Cyclin D1 Protein Expression in Mantle Cell Lymphoma. *J Pathol* 179:238–242.

Pittaluga, S., Wlodarska, I., Stul, M.S., Thomas, J., Verhoef, G., Cassiman, J.J., Van Den Berghe, H., and De Wolf-Peeters, C. (1995) Mantle cell lymphoma: A clinicopathological study of 55 cases. *Histopathol* 26:17–24.

Schlette, E., Fu, K., and Medeiros, L.J. (2003) CD23 expression in mantle cell lymphoma: Clinicopathologic features of 18 cases. *Am J Clin Pathol* 120:760–766.

Singleton, T.P., Anderson, M.M., Ross, C.W., and Schnitzer, B. (1999) Leukemic phase of mantle cell lymphoma, blastoid variant. *Am J Clin Pathol* 111:495–500.

Valdez, R., Kroft, S.H., Ross, C.W., Schnitzer, B., Singleton, T.P., Peterson, L.C., and Finn, W.G. (2002) Cerebrospinal fluid involvement in mantle cell lymphoma. *Mod Pathol* 15(10): 1073–1079.

Weisenburger, D.D., and Armitage, J.O. (1996) Mantle cell lymphoma—An entity comes of age. *Blood* 87(11):4483–4494.

Diffuse Large B-Cell Lymphoma

Definition

Diffuse large B-cell lymphoma (DLBCL) is a neoplasm of large transformed B-lymphocytes. Topographically, large B-cell lymphoma may arise in nodal or extranodal sites and may be found in mucosal areas like the MALT lymphomas. Architecturally, the lymphomas of this type always obliterate the normal architecture of the invaded tissue with sheets of large neoplastic cells. Cytologically, DLBCL can be of predominantly centroblastic, immunoblastic, anaplastic, or multilobated cellular types. It is likely that as more molecular means of classification are developed, DLBCL will be subdivided into several new entities that have unique biological features and response to therapy.

Epidemiology and Incidence

Diffuse large B-cell lymphoma occurs in all domestic animals and birds and is the most common lymphoid neoplasm in most species, including human. In cats and cattle, lymphoma is associated with retroviral infection, but lymphoma occurs in the absence of viral infection in cats and rarely in adult cattle that are not of sporadic type and are BLV negative. In dogs, a retroviral infection has

been found in animals with a cutaneous form of lymphoma of T-cell type, but there is no specific viral association with large B-cell lymphoma. It is likely that chronic benign lymphoid hyperplasia, as occurs in association with chronic periodontal and skin diseases, may be a risk factor for malignant transformation of immune cells.

In cattle in a study not accompanied by immunophenotypic identification in which nodal large cell lymphoma (DL) was assumed to be of B-cell type, of 1,198 cases 366 were of diffuse large cell type and 424 were of large cleaved cell type (DLC), for 66% of total cases. Breed and sex were not known, but they were from cattle sent for slaughter and most were assumed to be female of dairy breeding. In 136 cases of lymphoma in swine, 81, or 60%, were of large cell type. In a collection of 502 cases of canine lymphoma and leukemia, there were 69 cases of large cell lymphoma, including 19 cases of large cleaved cell type for a proportion of 69/502 or 14% of total cases. Of these 69, the gender was known in 41 cases—19 female and 22 male dogs. The age of the dogs was known in 47 cases, with a mean age of 6.1 years. In a review of hematopoietic neoplasms in 751 domestic cats, there were 54 cases of large cell lymphoma, 76 cases of large cleaved cell lymphoma, and 184 cases of immunoblastic large cell lymphoma that included 13 cases of immunoblastic polymorphous type. These cases totaled 314 of 751 or 42% of all cases. On an overall basis including other types of lymphoma, 58% of cats were male or male neutered and 425 were female or female neutered. Their ages ranged from 1 to 22 years, with 244 cats less than 6 years and 326 cats greater than 6 years at time of death or biopsy. In a collection of 89 horses with lymphoid neoplasms, there were 19 cases of diffuse large cell type and 2 cases of large cleaved cell. There was a slight majority of female cases, and most cases were over 10 years old.

Clinical Presentation and Features

The topographical presentation in 50 cases of diffuse large cell lymphoma in the dog included generalized lymphadenopathy in 18, enteric or abdominal in 9, one enlarged node in 7, multicentric and skin in 4 each, tonsil in 3, mediastinum and spleen in 2 each, and central nervous system in 1. In the group of 314 cats with a type of DLBCL there were 85 cases with gastrointestinal involvement, 68 multicentric, 56 mediastinal, 35 in small intestine, 21 primary renal, 20 with one or two nodes only involved, 7 in nasal cavity, 6 as a subcutaneous mass, 3 in skin, 3 in heart, 2 in urinary bladder, and 1 primary in liver. These totals include the tissues examined on which the diagnosis was made and, because in many cases more than one tissue was involved, the presentation—e.g., abdominal—might involve several tissues. In terms of the actual tissues on which DLBCL tumor was found, these included internal lymph node, 54; thymus, 51; peripheral node, 46; small intestine, 35; kidney, 24; liver, 15; large intestine, 12; oral cavity, 12; subcutaneous mass, 11; nasal cavity, 9; central nervous system, 6; spleen, 4; bone marrow, 3; and 1 each for lung, heart, and pancreas. In a collection of 118 cases of equine hematopoietic neoplasia, there were 25 cases of diffuse large cell lymphoma with 20 cases of DL, 4 of IB, and 1 of DLC. The presentation was unknown on most of these, but 1 had generalized lymphadenopathy, 1 splenic only, and 4 had enteric involvement. There is little information that specifically relates to the clinical signs associated with animals with any form of DBLCL. About one-third of human patients with a form of DLBCL present with symptoms that may include recurrent fever and weight loss, and in animals the symptoms can be expected to be little or none in skin types of disease or related to the organ system affected.

Pathologic Features

Blood

It is now accepted that in lymphoid neoplasia there are always neoplastic cells in the blood with the "homing" tendencies of the cells related to their intercellular adhesion molecules (ICAMs), which determines where the tumor will develop and how it will spread. Traditionally, about 20% of dogs and 15% of cats with lymphoma have been felt to be frankly leukemic. These numbers are likely still a thumb rule that can be applied to the results obtained from a cell counter, but the examination of a stained blood film by an experienced pathologist will detect cells in blood like those in tissue, where both are examined in a higher proportion of cases. As the sophistication of our flow cytometric counting systems increases and the number of reagents active in animal tissue also increases, this number and proportion will continue to rise. There is little prognostic value in identifying lymphocytes of neoplastic type in the blood of an animal with an established diagnosis of lymphoma, which lacks cytopenia. However, the examination of blood and marrow is an important and ultimately essential step in the staging of animals' intended to be treated for lymphoma, and it becomes essential in determining the response to therapy. Of all of the types of lymphoma, DLBCL is one of the easiest to recognize in the blood because of the prevalence of nucleoli in large nuclei with finely distributed chromatin. It has often been noted, however, that the cytological characteristics of neoplastic cells in the blood and those in marrow and other tissues may differ for reasons not understood but likely related to features of cellular maturation and adhesion.

Bone Marrow

It is likely that the bone marrow is always involved in most types of DLBCL if the disease is allowed to progress without therapy, and likely despite therapy in advanced

cases of lymphoma. There may be information in the pattern of marrow involvement with a variety of types identified, including diffuse, paratrabecular, and multifocal interstitial. In all types, there is usually complete exclusion of fat cells from foci of neoplastic infiltration that, with the homogeneity of cell type, draws attention to areas of tumor on architectural examination. Cytologically, the detection of neoplastic cells when there is minor and diffuse infiltration is demanding and is best assisted by immunocytochemistry (Fig. 3.367).

Lymph Node

A number of morphologic variants of DLBCL are recognized and identified in the REAL and WHO classifications. These include the centroblastic and immunoblastic types distinguished in the Working Formulation (WF) that have been found not to have any different survival characteristics and as a consequence have subsequently been considered together and are treated together here. The anaplastic variant is more typically identified as a T-cell lymphoma in both humans and animals and was known as the Ki-1 or CD30 positive neoplasm characterized by quite marked irregularity of nuclear shapes. The so-called kidney-shaped or, more rarely, the horseshoe-shaped nuclei termed the *hallmark cells* are not frequent in the B-cell variant of anaplastic large cell lymphoma (ALCL) that is diagnostic of the T-cell variant of ALCL. In human oncology, the B-cell ALCL has not been found to behave differently in clinical course from other large cell B-cell lymphomas and is included with them. Other more unusual variants are the plasmablastic type and intravascular large B-cell lymphomas that are included here. The T-cell rich large B-cell lymphoma (TCRLBCL) and the lymphomatoid granulomatosis (LYG) variants are given a separate category in this publication because in animals the TCRLBCL variants are not uncommon and have a distinctly more indolent progression.

In general, in nodes the large B-cell lymphomas present with diffuse architecture and frequent bridging of the node capsule and colonization of the perinodal fat (Fig. 3.368). The most common types are the centroblastic (CB, Figs. 3.369, 3.370) and immunoblastic (IB, Figs. 3.371, 3.372) that are similar architecturally and differ only in typical placement of the nucleoli. Both types compress the node medullary structures and tend to have less medullary sclerosis (Fig. 3.373) than the more indolent B-cell lymphomas that arise in a background of chronic follicular hyperplasia (Fig. 3.374). Both CB and IB cell types have round to oval nuclei 2–2.5 red cells in diameter and course granular or branched chromatin patterns with mild parachromatin clearing. The CB variant has 2–4 quite prominent nucleoli that are typically impinging on the inner nuclear membranes and are the neoplastic counterpart of the normal dividing cell of the reactive germinal center (Fig. 3.375). In contrast, the IB variant has a single prominent central nucleolus, and both can have quite high mitotic rates with 5–10 mitoses/400× field. The cytoplasm is moderate in volume and staining density, and cell boundaries are irregularly distinct. There are usually about the same number of apoptotic nuclei as mitoses per high power field but not a lot of tingible body macrophages (Figs. 3.376–3.380).

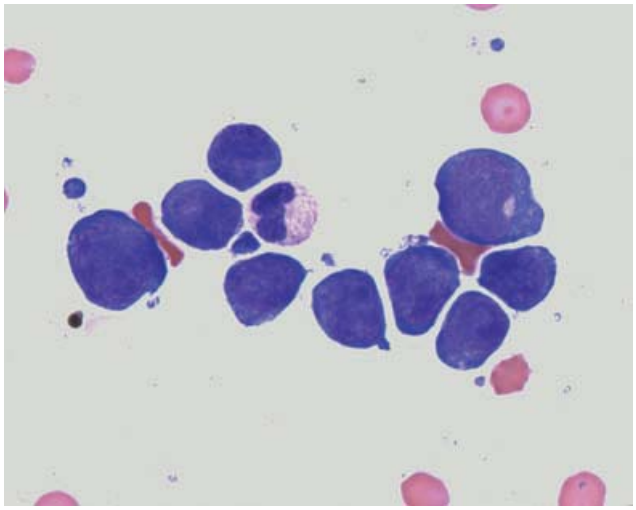

Figure 3.367. Dog: bone marrow aspirate, large cell lymphoma. In the marrow, the neoplastic cells are of intermediate to large size with round entire nuclei and a moderate volume with highly basophilic cytoplasm. The chromatin pattern is obscured with generally a fine granular type with multiple prominent nucleoli.

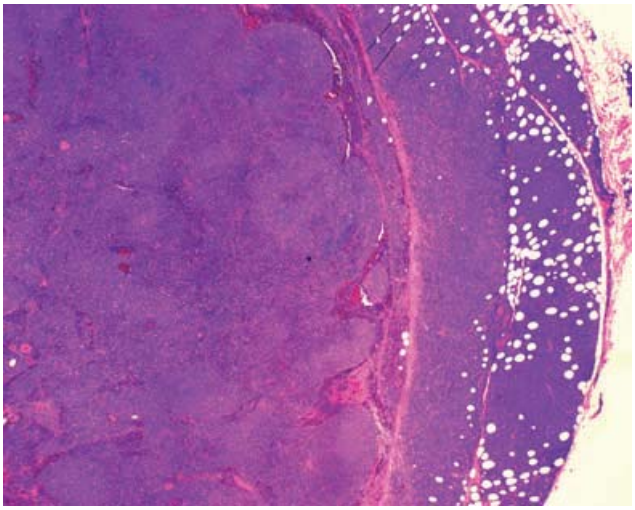

Figure 3.368. Dog: lymph node, diffuse large B-cell lymphoma. There are numerous "tide marks" representing successive waves of proliferation that have expanded beyond the initial node capsule with advancement of the tumor into the surrounding panniculus.

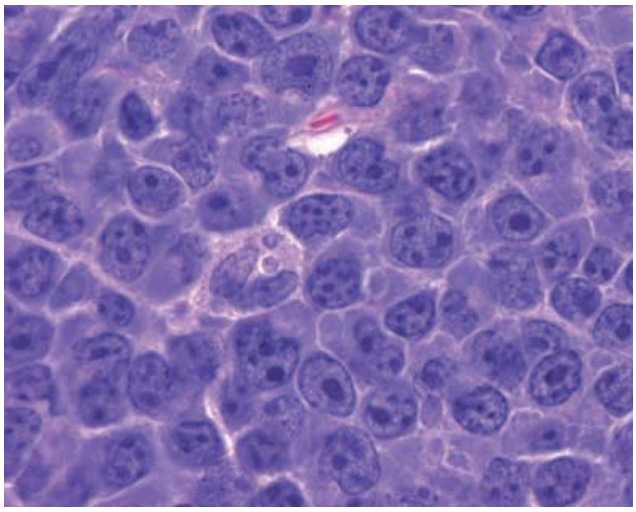

Figure 3.369. Dog: lymph node, diffuse large B-cell lymphoma, centroblastic type. The size of the nuclei can be deduced from the size of the single red cell. There is usually a mixture of nucleolar configurations with this most typical of the centroblastic type with multiple nucleoli that frequently impinge on the nuclear membranes. There is abundant cytoplasm that is highly amphophilic and cell boundaries are well defined. There is a single tingible body macrophage in mid-center.

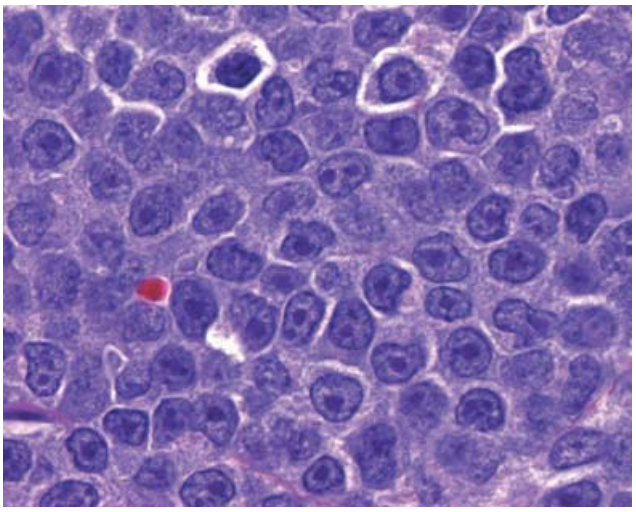

Figure 3.371. Dog: node, diffuse large B-cell lymphoma, immunoblastic type. The immunoblastic type of large cell lymphoma is characterized by a single, very prominent central nucleolus. The chromatin pattern is typically fine with some peripheralization on the nuclear membrane, and cytoplasmic volume may be variable and usually quite highly amphophilic with cell boundaries irregularly distinct.

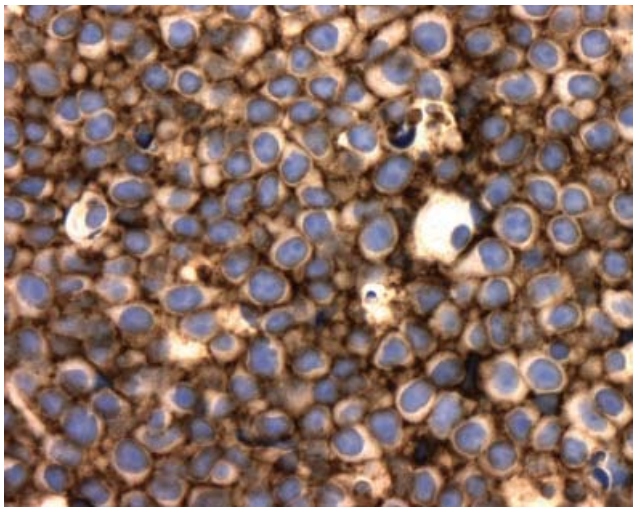

Figure 3.370. Dog: node, large B-cell lymphoma. Phenotype of Figure 3.369. On staining with CD20, there is very strong and uniform labeling of cell membranes with the nuclear patterns still apparent.

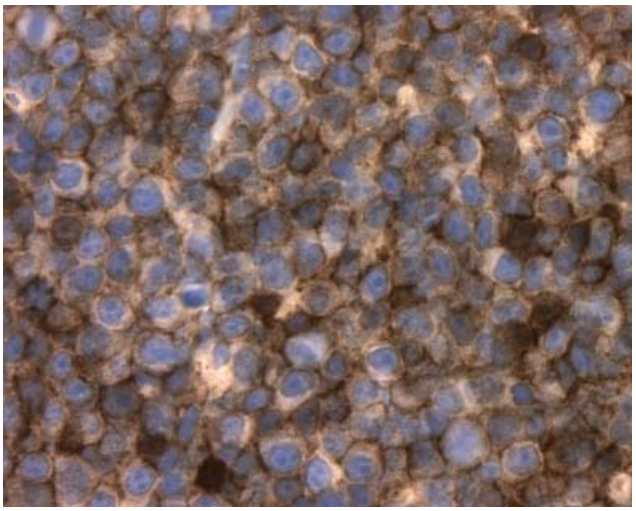

Figure 3.372. Dog: lymph node, large cell lymphoma. Phenotype of Figure 3.371. On staining with CD20, there is strong and relatively uniform marking of cell membranes with a lighter-stained area selected to show nucleolar conformation.

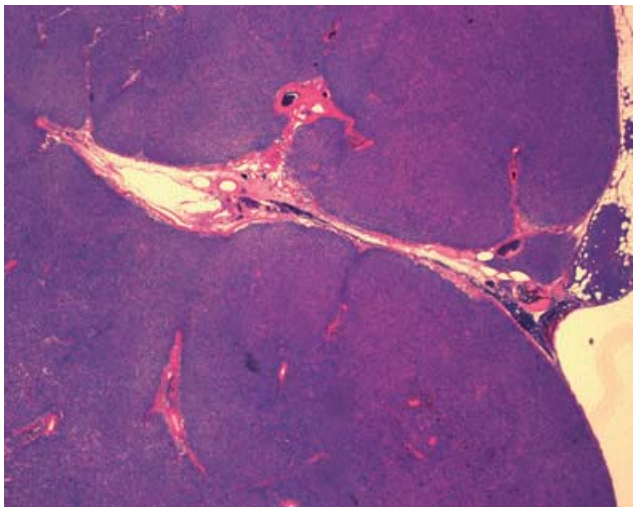

Figure 3.373. Dog: node, diffuse large B-cell lymphoma. Large B-cell lymphomas tend to fill and compress the medulla rapidly, obliterating initial sinus and cord architecture.

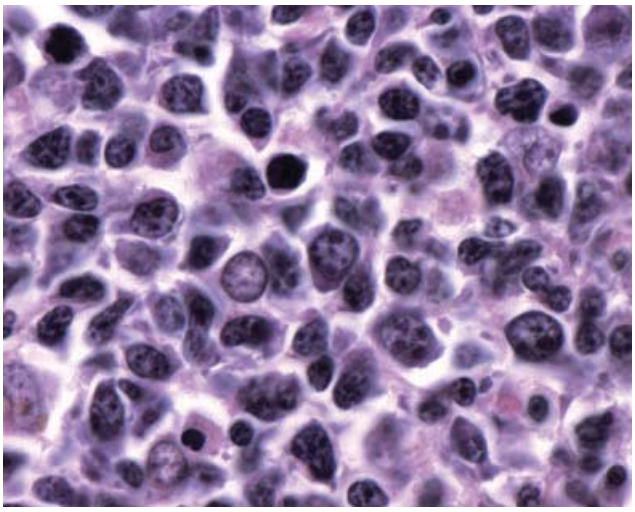

Figure 3.375. Dog: lymph node, benign follicular hyperplasia. Image from the deep pole of a germinal center, with the large benign centroblasts (center) having multiple peripheralized nucleoli typically impinging on the nuclear membrane.

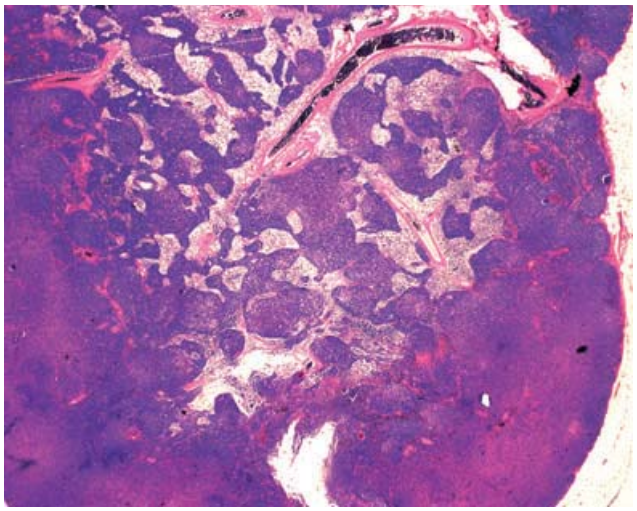

Figure 3.374. Dog: lymph node, follicular lymphoma, Grade III. In comparison to Figure 3.373, this indolent type of lymphoma, even at a late stage, retains the architecture of expanded medullary sinus and cords that has developed without the node having marked medullary sclerosis of chronic benign hyperplasia.

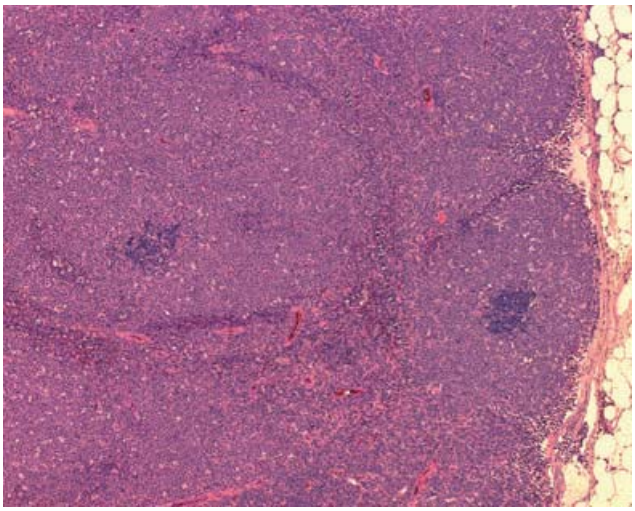

Figure 3.376. Dog: lymph node, diffuse large B-cell lymphoma. There is fading follicular hyperplasia with proliferation of neoplastic cells around involuting clusters of benign deeply stained mantle cells resembling the architecture of late marginal zone lymphoma.

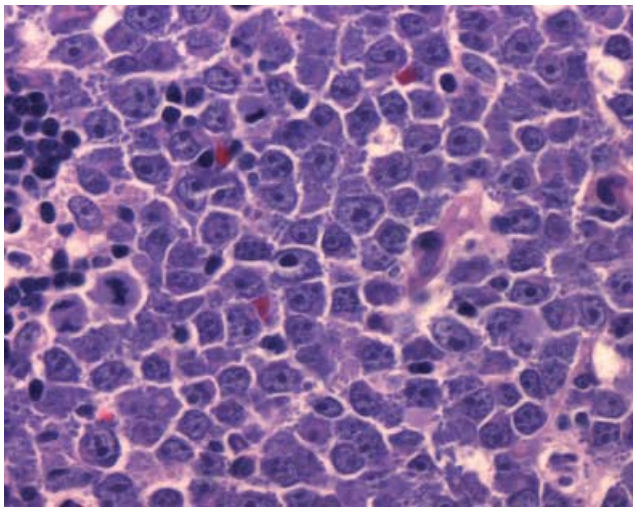

Figure 3.377. Dog: node, diffuse large B-cell lymphoma. Detail of Figure 3.376. An image near the edge of a benign mantle cell cluster (left). The very high mitotic rate as well as numerous apoptoses and presence of tingible body macrophages would be incompatible with an interpretation of marginal zone lymphoma and indicates this is high-grade large B-cell lymphoma. This level of proliferative activity is less common in diffuse large B-cell lymphoma.

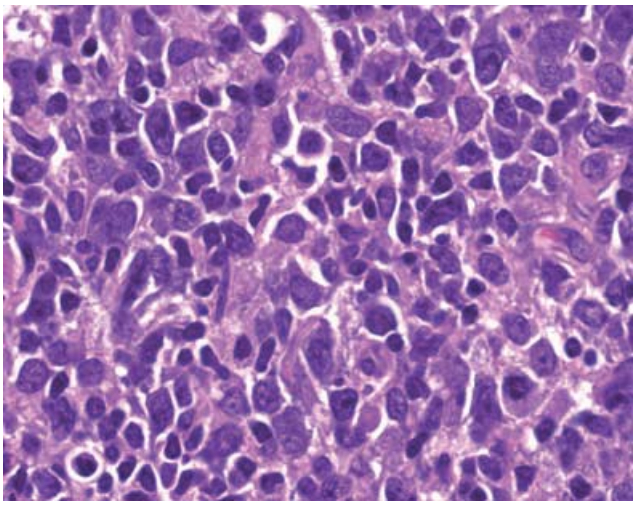

Figure 3.379. Mouse: lymph node, diffuse large B-cell lymphoma. There is more variation of nuclear type with the small more densely stained nuclei, likely benign. The neoplastic cells have large round or oval nuclei with fine granular chromatin and frequently prominent nucleoli. There are frequent apoptotic bodies and a moderate proliferative rate. *Slide from J. M. Ward, DVM.*

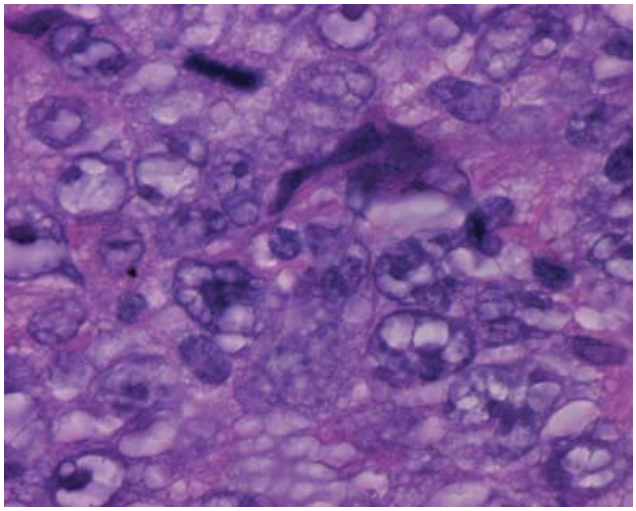

Figure 3.378. Human: lymph node, diffuse large B-cell lymphoma. The neoplastic cells have very vesicular nuclei with coarsely branched chromatin and marked parachromatin clearing. There are prominent, frequently multiple, nucleoli and relatively abundant cytoplasm that is lightly stained. There is a cell in mitosis in the upper left with a contracted nucleus in the center with more eosinophilic cytoplasm and neoplastic cells undergoing cell death, likely of non-apoptotic type. *Slide from Cornell Tutorial.*

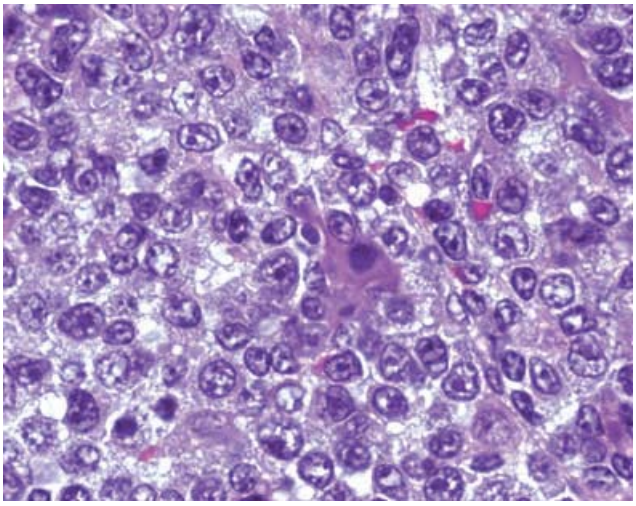

Figure 3.380. Rhesus macaque: adrenal gland, diffuse large cell lymphoma. The nuclei are round to oval, vesicular, with branched chromatin pattern and a mixture of centroblastic and immunoblastic nucleolar configurations. The cytoplasm is abundant and lightly stained with cell boundaries generally indistinct. There is a moderate proliferative and apoptotic rate with the cell in the center, with eosinophilic cytoplasm undergoing nonprogrammed cell death. *Slide from R. P. Tarara, DVM.*

The *plasmablastic variant* of DLBCL had not been identified as a specific subtype prior to its identification as a recognized entity in the REAL/WHO classifications. The disease occurs in dogs (Figs. 3.381, 3.382), cats, horses (Figs. 3.383, 3.384), mice (Figs. 3.385, 3.386), and likely other species. The distribution of this type of tumor can vary widely and involve the lung (Figs. 3.387–3.390). The staining is not uniform with B-cell markers and, in

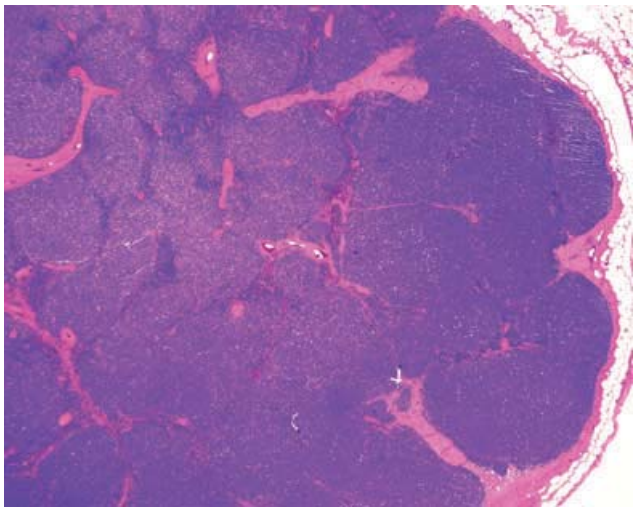

Figure 3.381. Dog: lymph node, plasmablastic-type large cell lymphoma. The capsule is undulating around a multinodular proliferation without involvement of perinodal tissues. The architecture is solidly cellular with the darker areas representing residual benign cells. The deeply stained cytoplasm imparts redness on observation at an architectural level that is typical of plasmablastic cytoplasmic differentiation.

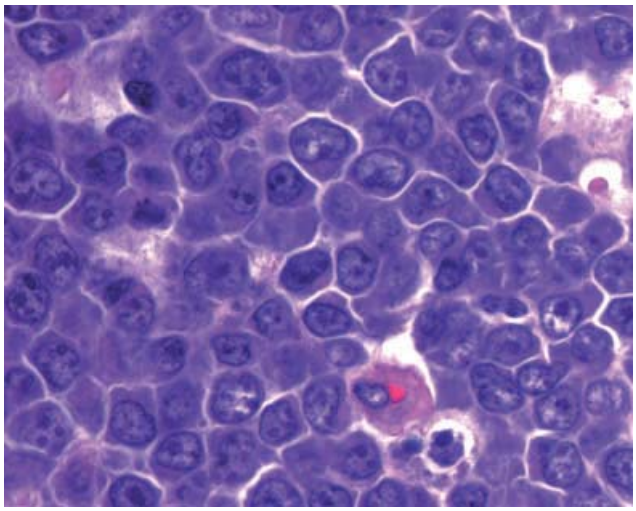

Figure 3.382. Dog: node, plasmablastic lymphoma. Detail of Figure 3.381. The nuclei are large and vesiculated, with hyperchromatic chromatin of coarse granular distribution and marked and irregular parachromatin clearing. There are multiple, often very large, nucleoli with abundant highly amphophilic cytoplasm that is eccentrically placed and, significantly, cell boundaries are generally distinct. There is an anaphase in the upper left, partially in the plane of section, and a tingible body macrophage in the lower center; an adjacent vessel and red cell provide an indication of cell size.

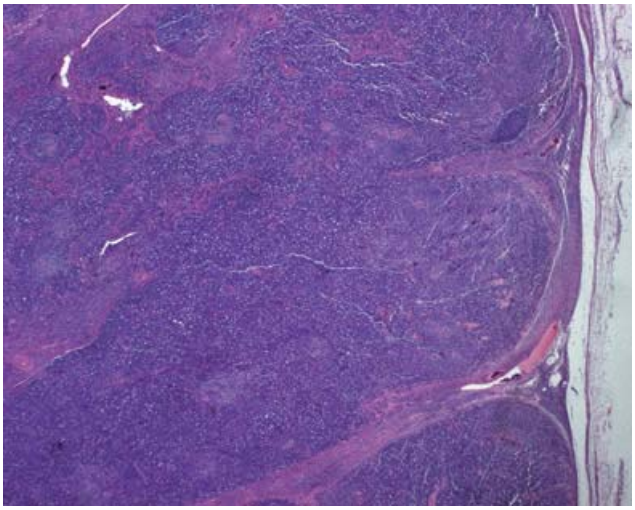

Figure 3.383. Horse: lymph node, plasmablastic lymphoma. The capsule has a thickened inner layer that is irregularly and heavily infiltrated with neoplastic cells, with the node having a diffuse architecture and the tinctorial depth of deeply stained cytoplasm. There is a prominent starry sky tingible body macrophage presence that is most apparent centrally. *Slide from J. Morrison, DVM, and S. P. McDonough, DVM.*

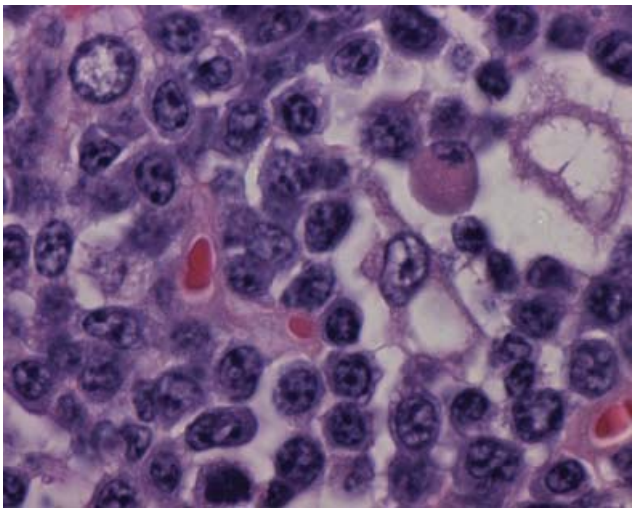

Figure 3.384. Horse: lymph node, plasmablastic lymphoma. Detail of Figure 3.383. The nuclei are round to oval and are of moderate size with large hyperchromatic chromocenters joined by coarse chromatin bands that are caricatures of normal plasma cells. The cytoplasm is moderate in volume but highly amphophilic and occasionally eccentrically placed with cell boundaries, again unusually distinct. A degenerating cell in the upper right with eosinophilic cytoplasm appears to be a Mott cell suggesting that some of the cells may be producing immunoglobulin. The horse had chronic diffuse skin disease diagnosed as erythema multiforme.

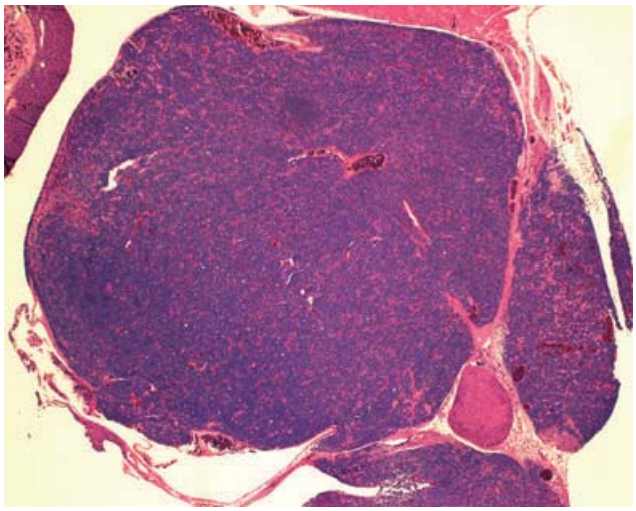

Figure 3.385. Mouse: lymph node, plasmablastic lymphoma. Hepatic hilar area, with extensive abdominal involvement. There is diffuse architecture with tinctorial properties of deep cytoplasmic staining. *Slide from J. M. Ward, DVM.*

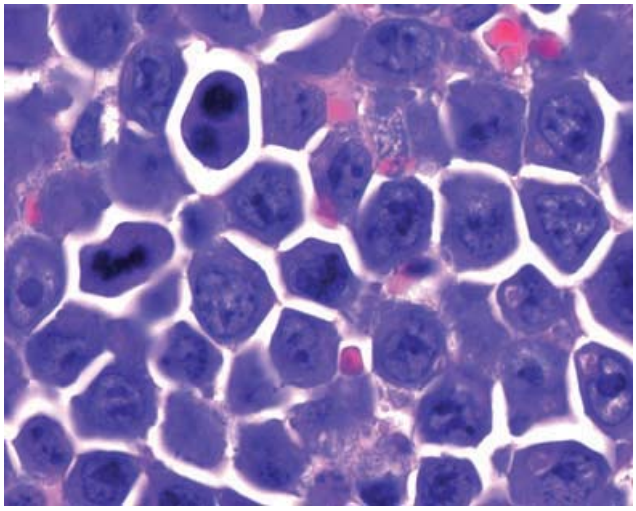

Figure 3.386. Mouse: node, plasmablastic lymphoma. Detail of Figure 3.385. The neoplastic cells have round to oval nuclei, occasionally with sharp, shallow indentations. The chromatin pattern is coarsely granular with irregular parachromatin clearing and peripheralization on the nuclear membranes. The nucleolar pattern is variable from 3–4 small nucleoli to one centrally located and very large. The cytoplasm is relatively abundant, highly amphophilic, and cell boundaries are characteristically distinct. The cell in the left center is in metaphase and a binucleated cell is partially in focus in the upper left. This neoplasm was spontaneous in this mouse, but the neoplastic cells strongly resemble those of a transplantable murine plasmacytic tumor of MOPC-315 type.

general, CD20 marks a greater proportion of the neoplastic cells of plasmablastic type while providing better nuclear detail than CD79 in tissues regularly invaded (Figs. 3.391, 3.392), as well as in tissues less often

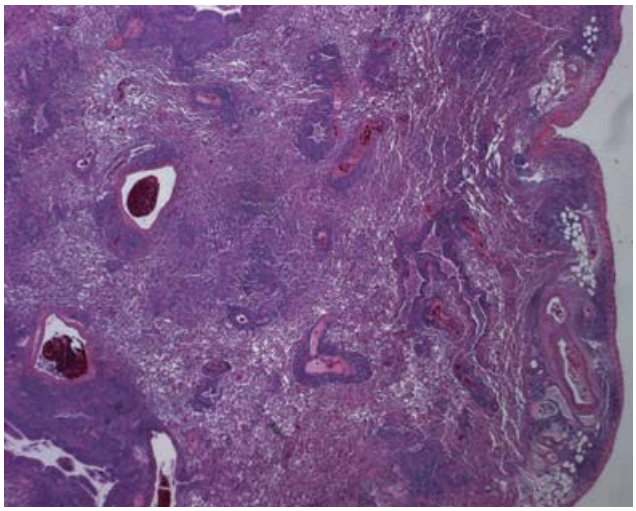

Figure 3.387. Horse: lung, plasmablastic lymphoma. The lung is collapsed with thickening of the visceral pleura, and there is extensive and irregular cuffing of vessels in airways with multifocal increased density of lung due to infiltration of neoplastic and reactive cells. *Slide from J. Morrison, DVM, and S. P. McDonough, DVM.*

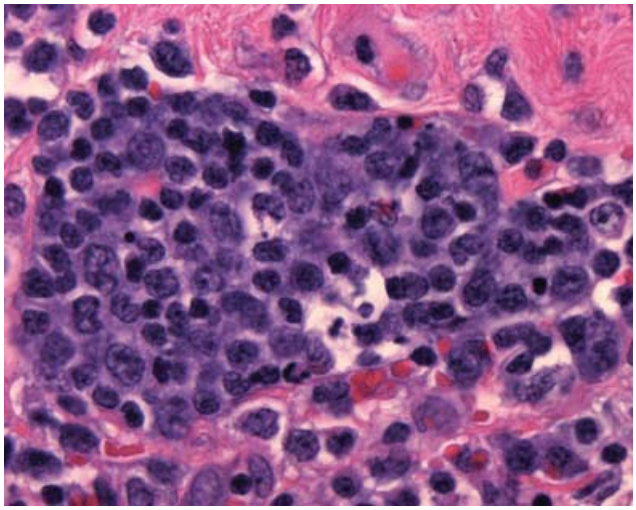

Figure 3.388. Horse: lung, plasmablastic lymphoma. Detail of Figure 3.387. A pleural lymphatic has a dense cluster of atypical cells with morphology similar to those in the node (Fig. 3.384) and other involved tissues.

involved in lymphoma (Fig. 3.393). In nodes, the neoplastic cells form solid clusters and sheets in the inner cortex and may be mistaken for benign plasmacytic expansion of medullary cords. Cytologically, the nuclei are uniformly round and 2.5 red cells in diameter with hyperchromatic staining of chromatin that is arranged in coarsely branched bands that surround and highlight multiple prominent nucleoli. The cytoplasm is relatively

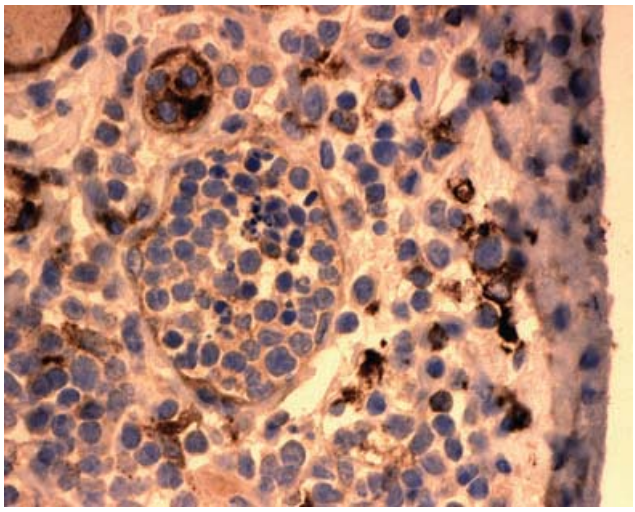

Figure 3.389. Horse: lung, plasmablastic lymphoma. Phenotype of Figure 3.387. The pleural lymphatic in the center field is comparable to that in Figure 3.388. The neoplastic cells are only lightly and irregularly marked with CD79 alpha, in contrast to staining with CD20, in Figure 3.390. *Tissue from J. Morrison, DVM, and S. P. McDonough, DVM.*

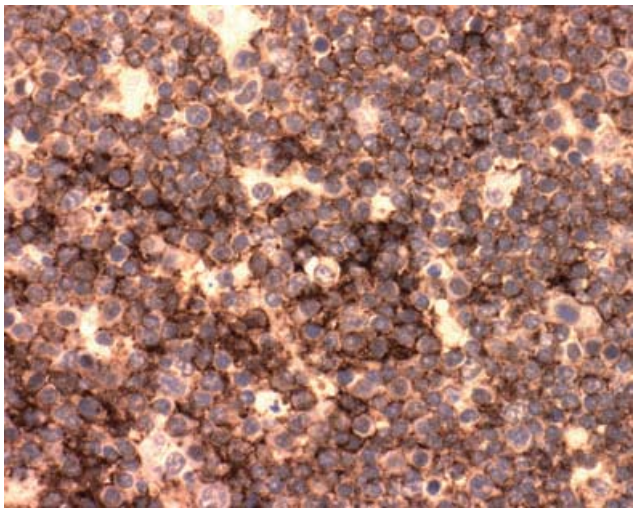

Figure 3.390. Equine: lymph node, plasmablastic lymphoma. Phenotype of Figure 3.384. In contrast to the light and irregular staining of the neoplastic cells in the lung by CD79, those in the node are more strongly and uniformly labeled with CD20. This may indicate that the neoplastic cells are of a more primitive type than their morphology might suggest.

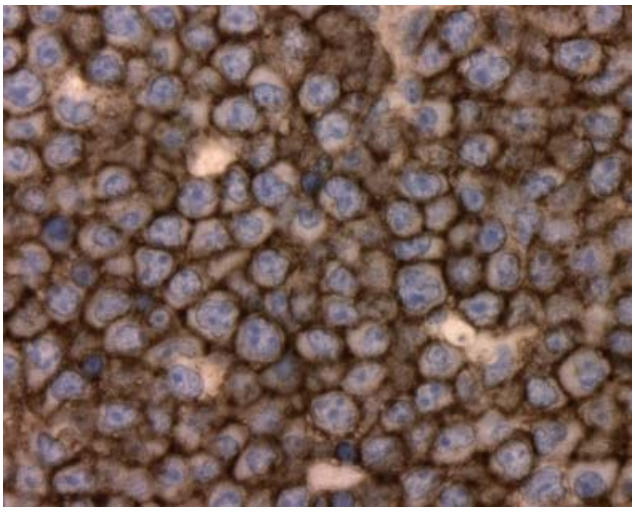

Figure 3.391. Dog: node, plasmablastic lymphoma. Phenotype of Figure 3.381. On staining with CD20, canine plasmablastic lymphoma has strong and uniform marking that is primarily membranous.

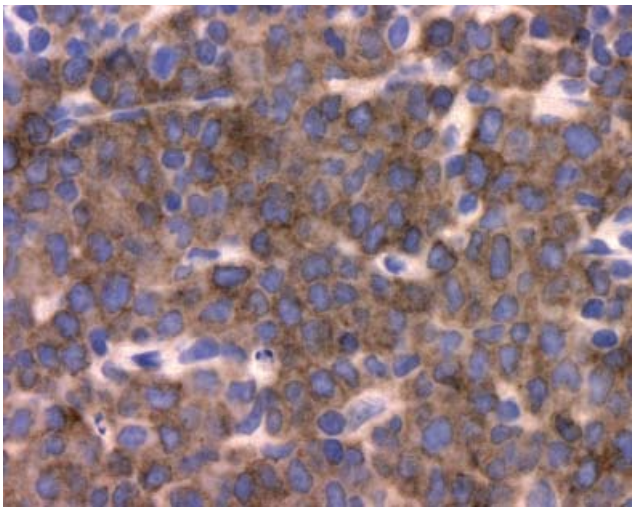

Figure 3.392. Dog: node, plasmablastic lymphoma. Phenotype of Figure 3.381. On staining with CD79, the neoplastic cells are strongly and uniformly labeled, with the reaction more cytoplasmic than membranous and with the nuclei less clearly defined.

abundant and may be irregularly eccentrically placed, but it is very highly amphophilic on HE staining (see Fig. 3.384). Significantly, mitoses are frequent and 4–8/400×, often without a full field of neoplastic cells. The presence of nucleoli in cells of plasmacytic type and staining along with the presence of mitotic figures distinguishes this tumor from benign plasmacytosis. Plasmablastic lymphoma is convincingly if not uniformly positive for B-cell markers (see Figs. 3.391, 3.392).

The *intravascular variant* of large B-cell lymphoma is rare and may be found in any tissue, but with an outwardly similar tumor of T-cell type both may be found as primary neoplasms in the central nervous system. The disease is seen most often in the dog and cat and may be rare in other animals. Animals with this form of lymphoma are presented in good condition, with rapid onset of nervous signs that may be caudal paresis, if the spinal

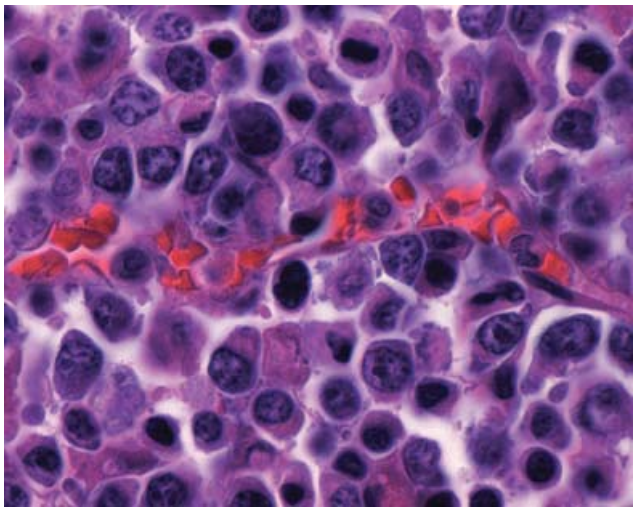

Figure 3.393. Dog: brain, plasmablastic lymphoma. A 10-year-old collie presented with nervous signs and died with a 2 cm mass found in the medulla of the brain, with only aging changes in other areas. The neoplasm has multifocal areas of ischemic necrosis and is composed of cells with large round to oval nuclei with hyperchromatic coarse granular chromatin patterns and 1–3 large nucleoli. The cytoplasm is abundant, often eccentrically placed and highly amphophilic.

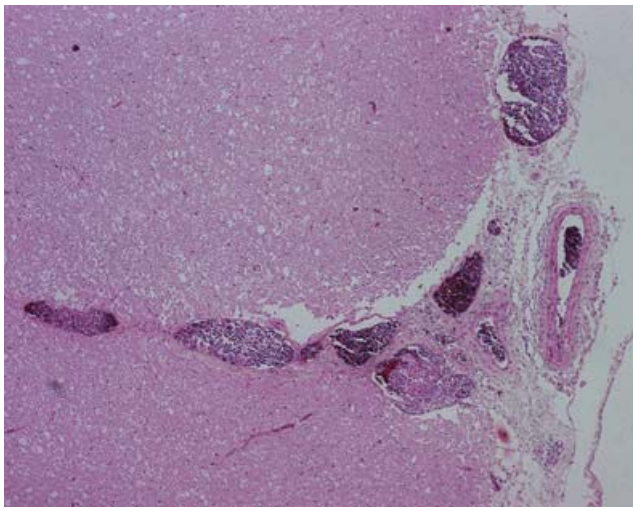

Figure 3.394. Dog: spinal cord, intravascular large B-cell lymphoma. The animal was presented in collapse and shortly died of respiratory failure. Lesions were found only in the central nervous system, with irregular dilation of meningeal vessels in both the brain and spinal cord with some having developed fibrinous thrombi (lower right). *Slide from R. M. Jacobs, DVM.*

cord is the major site of involvement. The changes in the surrounding tissue are minimal because the disease tends to proceed to convulsions and collapse within hours. Histologically, there is dilation of veins in the cerebral meninges and in the subdural vessels in the spinal cord.

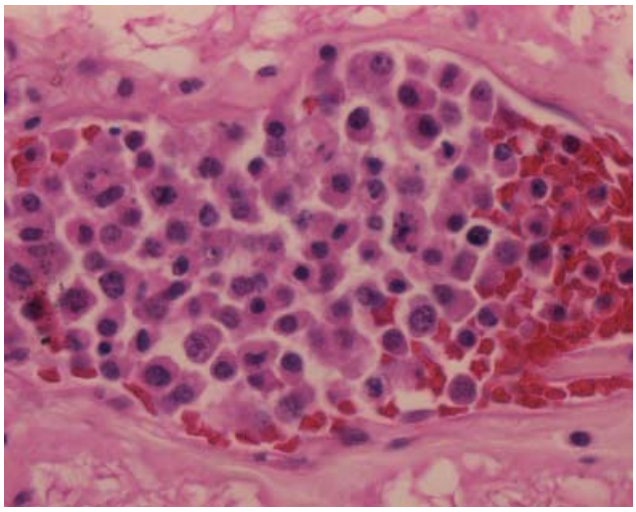

Figure 3.395. Dog: spinal cord, intravascular B-cell lymphoma. Detail of Figure 3.394. The neoplastic cells do not appear fixed in the vessels but had not been noted in the peripheral blood. There is moderate autolysis with the cells having round to oval nuclei with a coarse chromatin pattern and abundant, quite deeply stained cytoplasm.

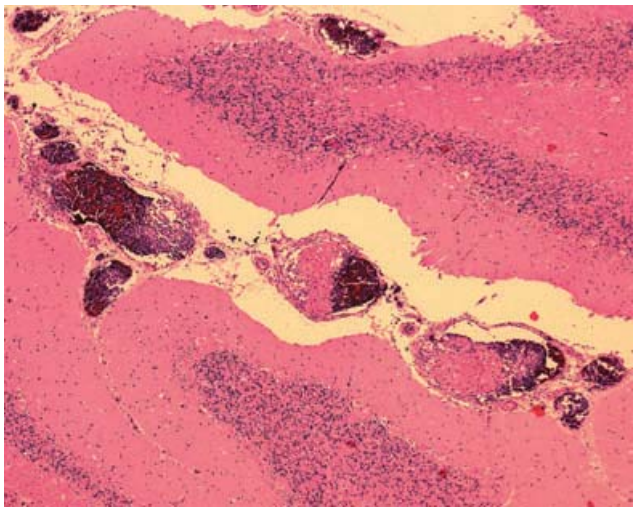

Figure 3.396. Dog: brain, intravascular B-cell lymphoma, same case as Figure 3.395. There is quite marked dilation of meningeal vessels with the pink areas representing fibrin thrombi that are in early stages of organization. *Slide from R. M. Jacobs, DVM.*

The cells appear in clusters that distend the vessels but do not appear to be attached to the vessel walls (Figs. 3.394, 3.395). Cytologically, there is quite marked anisokaryosis with round nuclei 2–4 red cells in diameter and occasionally binucleated and even multinucleated. The nuclei are vesicular with peripheralized and branched chromatin patterns and prominent nucleoli. The cytoplasm is moderate in volume and staining density and cell boundaries are distinct (Figs. 3.396, 3.397).

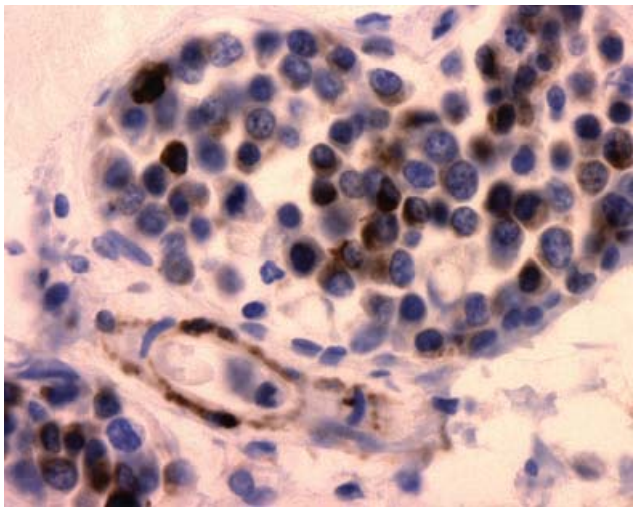

Figure 3.397. Dog: brain, intravascular B-cell lymphoma. Phenotype of Figure 3.396. With CD79 staining, the cells are irregularly but strongly labeled.

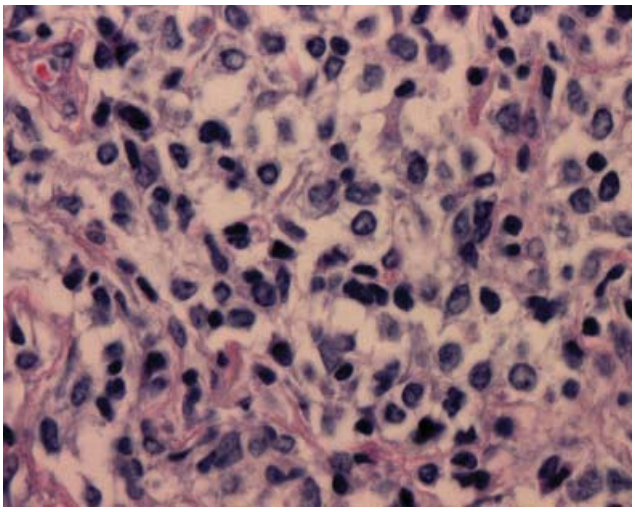

Figure 3.399. Human: mediastinal large B-cell lymphoma. Detail of Figure 3.398. The neoplastic cells are quite variable with round to oval, and occasionally indented or lobated, nuclei with relatively abundant lightly stained cytoplasm; cell boundaries are indistinct.

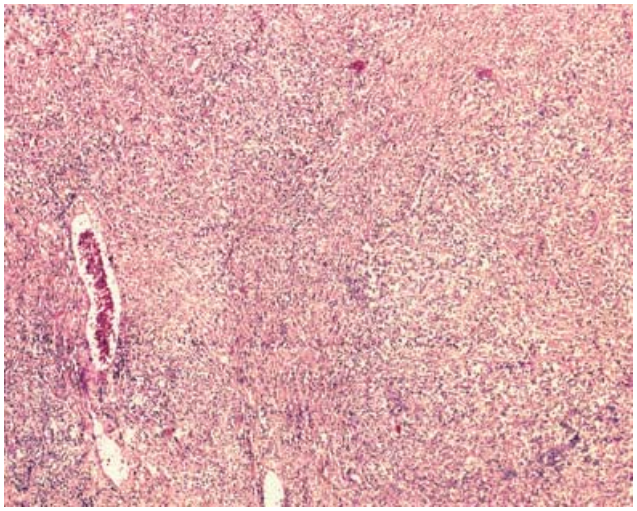

Figure 3.398. Human: mediastinum, large B-cell lymphoma. The tissue is a cohesive mass with abundant fine fibrillar supporting tissues infiltrated with neoplastic cells. *Slide from Cornell Tutorial.*

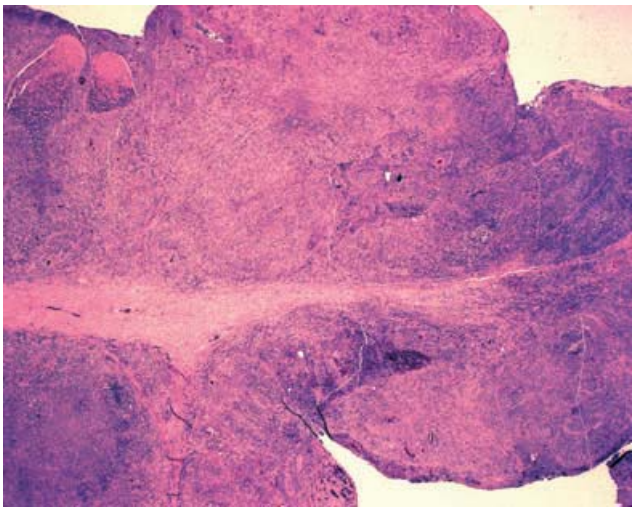

Figure 3.400. Human: mediastinal mass, large B-cell lymphoma. An incisional biopsy consists of an irregularly shaped mass of tissue that is highly cohesive with focal areas of sclerosis and quite dense cellularity. *Slide from Cornell Tutorial.*

The cells are not seen in mass involvement in adjacent tissues so there is never a field of tumor cells at 400× magnification, but mitoses are found within the intravascular clusters.

The *mediastinal large B-cell variant* of large B-cell lymphomas is also rarely encountered or recognized. The disease is described in humans (Figs. 3.398–3.401) and has been found in the dog (Figs. 3.402–3.405) and cat and may have a wider distribution. In the dog, a tumor of similar type is rarely encountered as a subcutaneous mass that may have arisen in a node. The cell type was formerly known as the multilobated B-cell with the cells described as occurring in human nodal lymphoma. With the development of phenotyping, the lobated type of cell that was formerly considered to be of T-cell type was recognized to occur in both B- and T-cell neoplasms. It became apparent that a neoplasm of this cell type existed as a recurring entity in the mediastinal area in humans, and the counterpart neoplasm was found in the dog and recognized by the presence of surface Ig to be of B-cell type (R. F. Carter, DVM, unpublished). In humans, the disease occurs in young adults and in women three times

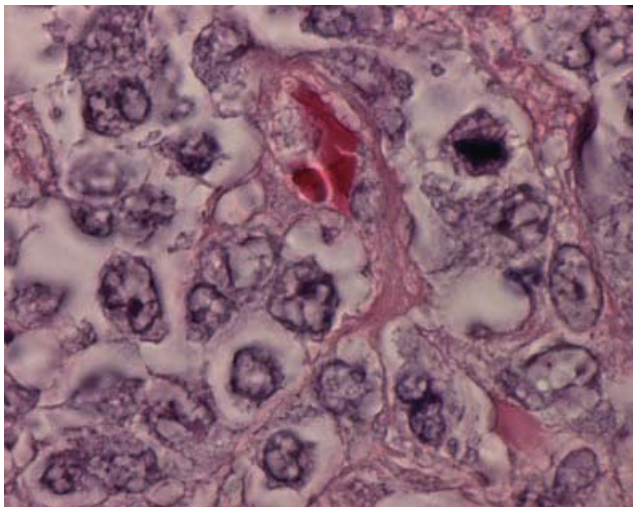

Figure 3.401. Human: mediastinal large B-cell lymphoma. Detail of Figure 3.400. The cells are large with round to cleft and irregularly shaped nuclei with branched chromatin and irregularly prominent nucleoli. The cytoplasm is abundant and lightly stained with cell boundaries indistinct. The tissues are supported by a quite dense fibrovascular network enclosing groups of 10–50 cells. The cell in the upper right is in mitosis.

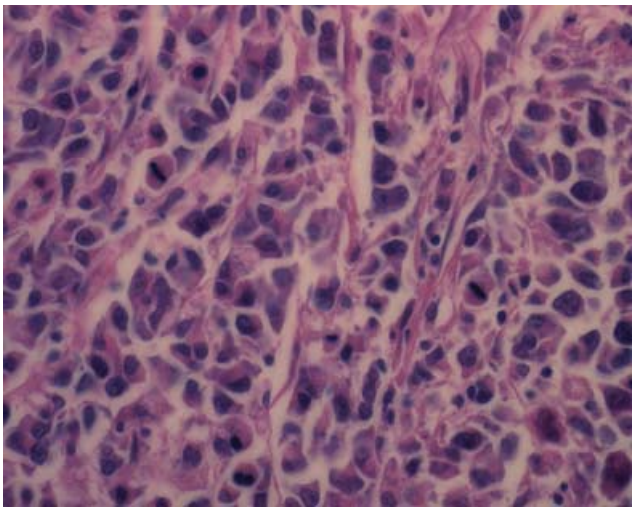

Figure 3.403. Dog: mediastinal mass, large B-cell lymphoma. Detail of Figure 3.402. Somewhat similar to the human cases, the lesion is characterized by a very dense fine fibrovascular network that divides the cells into small groups. The nuclei are round, oval, and indented, and occasionally binucleated with relatively abundant cytoplasm of moderate density. There are numerous mitotic and apoptotic cells.

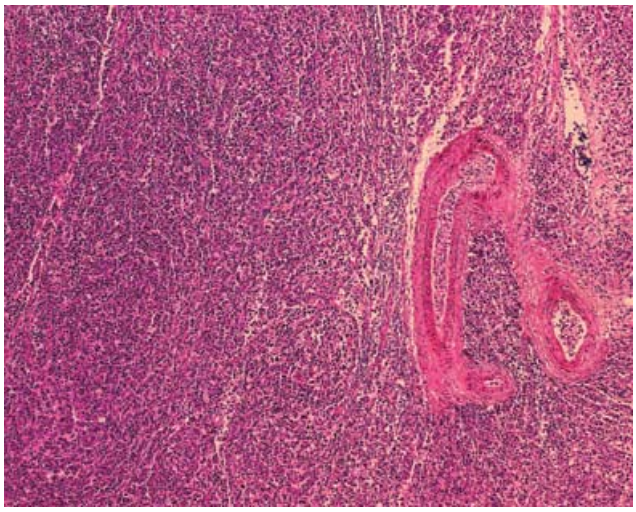

Figure 3.402. Dog: mediastinal mass, diffuse large B-cell lymphoma. A mature dog presented with an anterior mediastinal mass with incisional biopsy performed. The mass has diffuse architecture and is cohesive with a mixed cellular appearance.

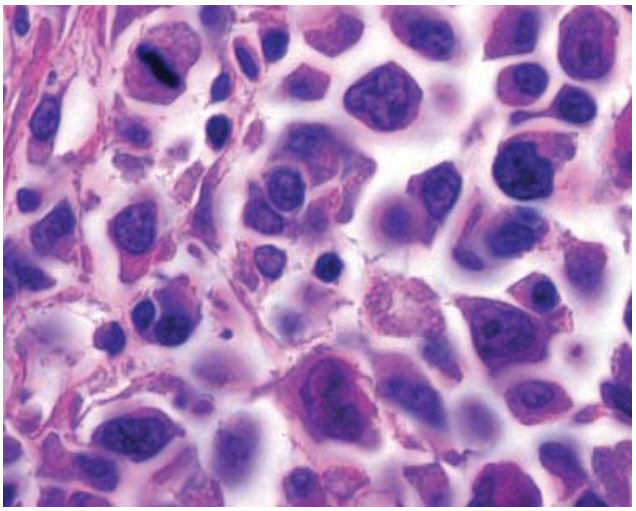

Figure 3.404. Dog: mediastinal mass, large B-cell lymphoma. Detail of Figure 3.402. The nuclei are remarkably variable in size and shape with varying levels of lobulation. The cytoplasm is relatively abundant with moderate staining depth and there are numerous mitoses.

more often than in men. Unlike lymphoma that can become large without invasion of adjacent organs, the large B-cell lymphoma of the mediastinum is a rapidly progressive mass that invades widely. The presenting symptoms in the dog are not available, but they can be expected to be similar to that in humans with rapidly progressive cough and chest pain and dyspnea. The disease is usually identified by fine needle aspiration and occasionally Tru-cut biopsy. Architecturally, the lesion is diffuse with a relatively dense fine fibrovascular network (see Figs. 3.398, 3.403) and occasional foci of ischemic necrosis. Cytologically, the cells have large round nuclei with a fine hyperchromatic chromatin pattern and multi-

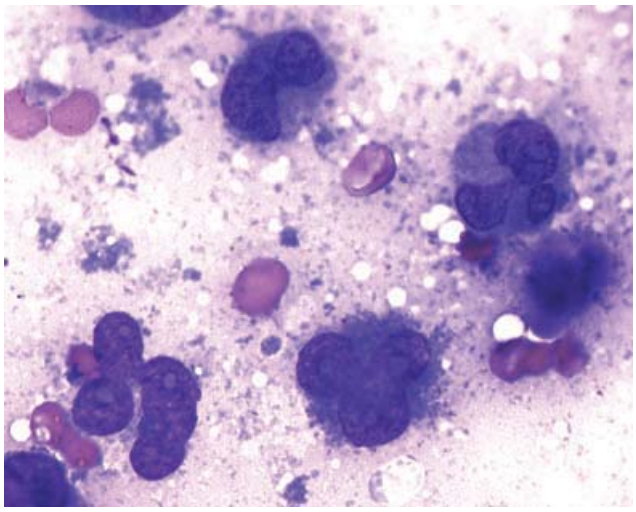

Figure 3.405. Dog: mediastinal mass, large B-cell lymphoma. Cytologic imprint of the tissue from Figure 3.402. With loss of some cytoplasm, the remarkably abnormal nuclear shapes provide evidence for the earlier name of *multilobated large B-cell lymphoma*.

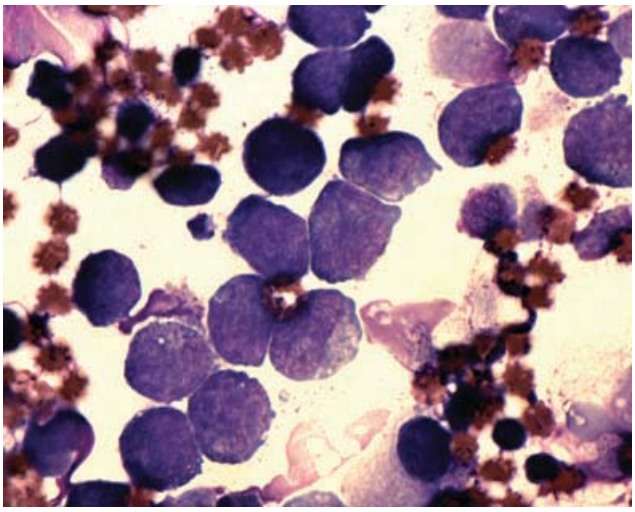

Figure 3.406. Dog: cerebrospinal fluid, "Effusion lymphoma." CSF was taken from a large-breed dog that presented with progressive deterioration in gait. The fluid had a very high cell count that included small, medium, and large lymphocytes. It is likely that the large cells are most representative of the primary neoplasm, with the cells decreasing in size with prolonged sojourn in the spinal fluid. *Slide from R. M. Jacobs, DVM.*

ple small but prominent nucleoli. Some cases have more anisokaryosis than multilobation, with some nuclei double the size of the predominant population and occasionally large atypical cells that are bilobed or binucleated or both. The cases in the dog are CD79 positive and likely CD 20 positive and CD3 negative. Human cases have been found to be CD30 positive, which also marks the T-type of anaplastic large cell lymphoma and lymphomatoid papulosis and the Reed-Sternberg cells of human Hodgkin's lymphoma. In the dog, the mediastinal large B-cell lymphoma needs to be distinguished from histiocytic sarcoma, which is CD18 positive, and from both T-cell rich large B-cell lymphoma and lymphomatoid granulomatosis on the basis of a more uniform large cell type and relative absence of T-cells. Despite its aggressive nature if left untreated, the human disease responds to both chemotherapy and radiation.

The final subtype of diffuse large B-cell lymphoma is the *primary effusion lymphoma* variant. This form of lymphoma is exceedingly rare in humans and has not been recognized as an entity in animals. The disease is defined as an effusion of fluid containing neoplastic large B-cells into the serous cavities, including pleura, pericardium, and peritoneum. In humans, the disease is seen most frequently in immunosuppressed and posttransplant patients, but it also is seen in individuals with an intact immune system. The most common presentation of this type of neoplasm in animals is the rare spinal fluid tap in an animal with nervous signs that is found to contain abundant, usually large neoplastic lymphocytes of a primary lymphoma involving the meninges (Figs. 3.406, 3.407). In addition, an occasional cow with lymphoma will present with cardiac tamponade as a result of pericardial involvement with the enzootic or BLV-associated form of bovine lymphoma. As well, lymphoma may be first recognized as a pleural aspirate in cats, with mediastinal lymphoma or with erosion of the thoracic duct in

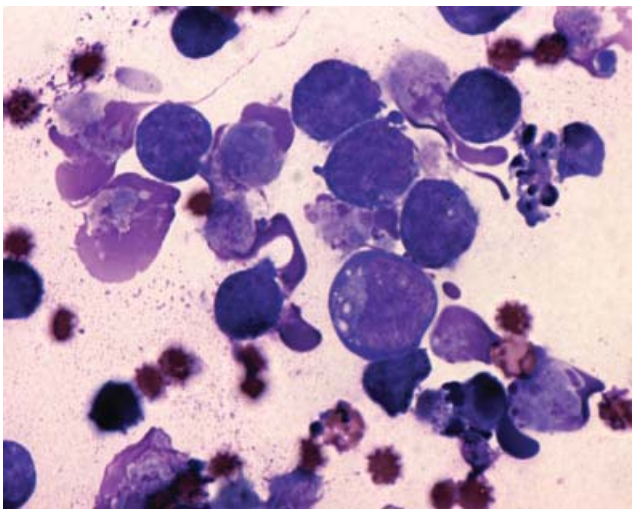

Figure 3.407. Dog: cerebrospinal fluid, Effusion lymphoma, same case as Figure 3.406. This image has a more distinct array of cell sizes accompanied by cells with karyolytic nuclei indicating that they are degenerating in a compartment with relatively few or inadequate phagocytic cells.

cats with lymphoma above or below the diaphragm. These are more appropriately expressions of lymphoma of solid tissue that has progressed to invade a serous cavity but not a true effusion lymphoma in which the neoplasm is primary in the serous lining itself. The entity remains to be defined in animals.

Spleen

In most species, the involvement of the spleen by DLBCL is initially multifocal and becomes coalescing. The overall involvement of the spleen may be diffuse, but in the horse, cow, dog, pig, and cat it may be large multifocal and a solid diffuse mass at the time of diagnosis (Figs. 3.408–3.412). In all of these species, there is patchy to large focal areas of necrosis in advanced involvement of the spleen (Figs. 3.413, 3.414). The initial involvement

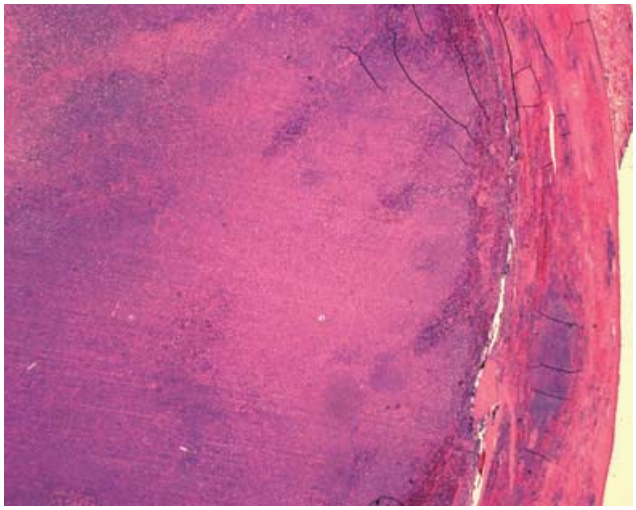

Figure 3.408. Dog: spleen, focal large B-cell lymphoma. There is a solid focal mass of tumor in the head of the spleen approximately 7 cm in diameter. The surrounding splenic tissue has atrophy of the lymphoid structures and compression of the sinuses.

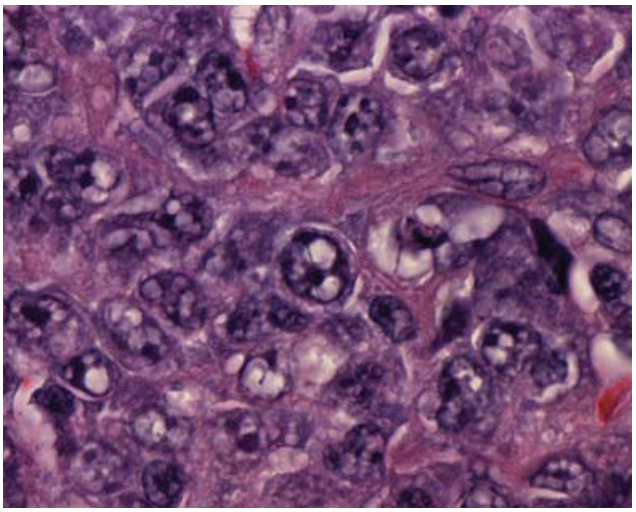

Figure 3.410. Dog: spleen, large B-cell lymphoma. Detail of Figure 3.408. The nuclei are large, round to oval, with a coarsely branched chromatin pattern, with marked parachromatin clearing and a pattern that is predominantly of peripheralized nucleoli with some retaining prominent central placement. The cell with the wedge-shaped nucleus in the upper right of center is likely benign and of supporting connective tissue.

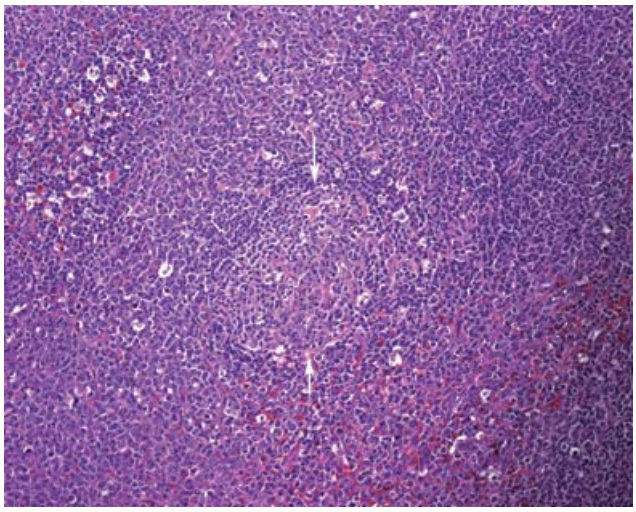

Figure 3.409. Dog: spleen, diffuse large B-cell lymphoma. Detail of Figure 3.408. A residual dendritic cell area from an atrophic germinal center is indicated by the arrows. There is almost complete loss of the mantle cell cuff with small cell remnants above and to the right.

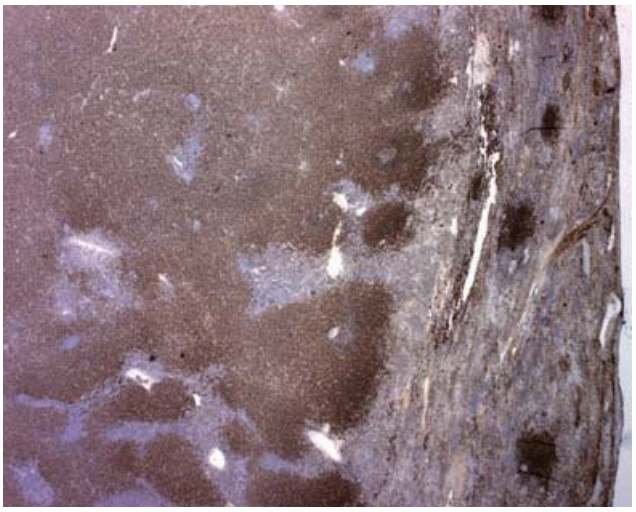

Figure 3.411. Dog: spleen, large B-cell lymphoma. Phenotype of Figure 3.408. On staining with CD79, the residual areas of B-cell in the collapsed spleen (right) are strongly marked as well as the diffuse areas of lymphoid proliferation with focal diffuse areas unlabeled, presumably residual benign T-cells (lower right).

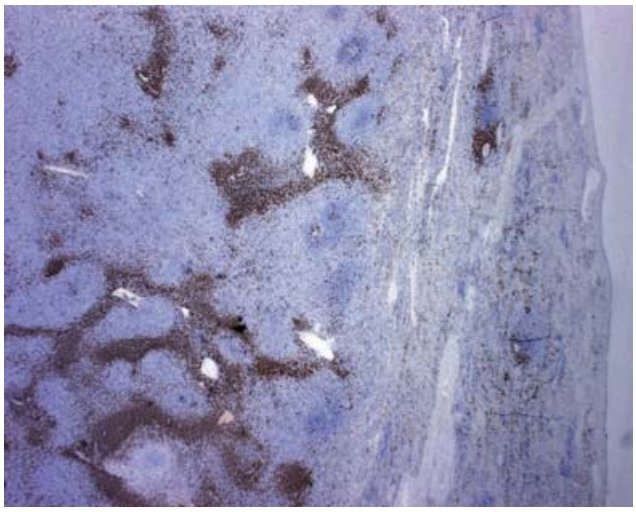

Figure 3.412. Dog: spleen, diffuse large B-Cell lymphoma. Phenotype of Figure 3.408. On staining with CD3, the focal areas unmarked by CD79 are clearly reactive areas of T-cell proliferation. There are large areas of ischemic infarction within the mass that are negative with both reagents.

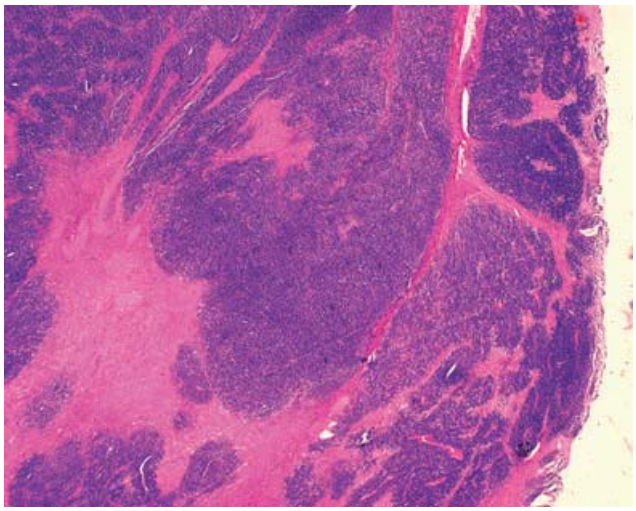

Figure 3.413. Horse: spleen, large cell lymphoma. A 4-year-old pony gelding weighing 650 pounds was treated for progressive anemia, with the animal finally euthanized and necropsy carried out that demonstrated a spleen that weighed 85 pounds. There were no lesions in other tissues other than bone marrow erythroid hyperplasia. The spleen consisted of solid lymphoid proliferation traversed by fibrous septa of varying diameter and with multiple irregular areas of ischemic necrosis.

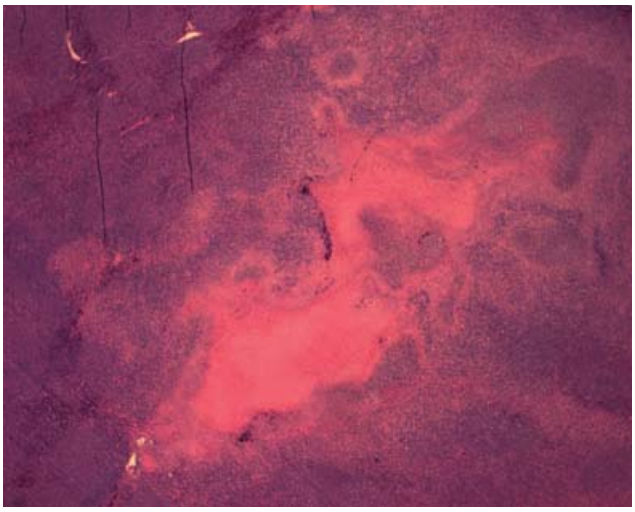

Figure 3.414. Dog: spleen, diffuse large B-cell lymphoma. Large serpiginous area of ischemic infarction near center of mass.

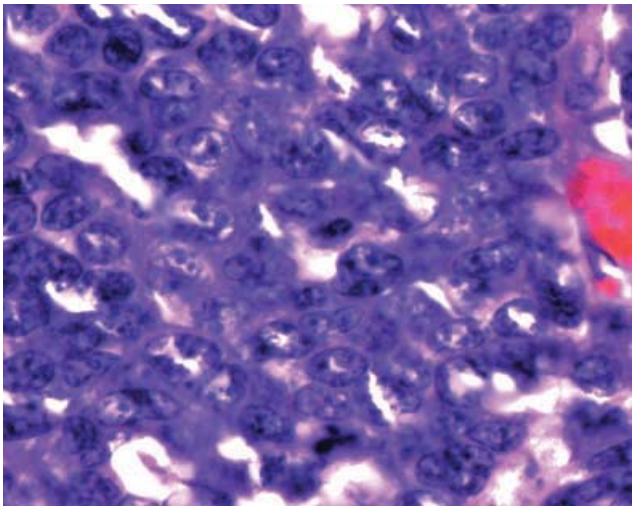

Figure 3.415. Horse: spleen, diffuse large cell lymphoma. Detail of Figure 3.414. The nuclei are round to oval with irregular shallow indentations and 2.5–3 red cells in diameter. The chromatin is hyperchromatic with large chromocenters and irregular parachromatin clearing. There are multiple nucleoli of moderate size, and the cytoplasm is moderate in volume and quite deeply amphophilic with cell boundaries indistinct. There is a moderate mitotic rate and a very high rate of cell death with many large tingible body macrophages.

may be deduced to be multifocal and related to the arterial architecture and of B-cell type by the presence of focal areas of follicular hyalinosis in the centers of the proliferating masses. In addition, as the disease progresses, the normal T-cell complement is reduced to thin cuffs of small lymphocytes surrounding the larger arterioles, which identifies the proliferating masses as large cell but not necessarily B-cell. In the horse with the focal type of splenic involvement, the tumor masses may be large and several centimeters in diameter and separated by a large area of hemorrhage and connective tissue proliferation and focal clusters of hemosiderin-bearing macrophages (Figs. 3.415, 3.416, see also 3.411–413). Cytologically, the cell type is as seen in nodes and other tissues. Oddly, in the

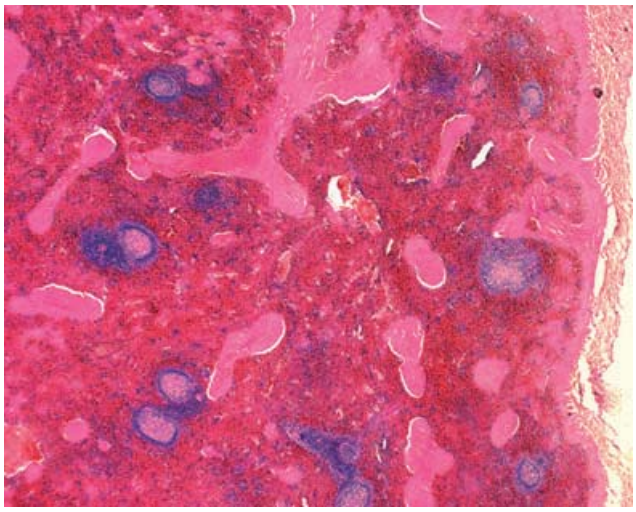

Figure 3.416. Horse: spleen, uninvolved area from the same tissue as Figure 3.414. The horse had not been given steroids, but there is massive atrophy of periarteriolar lymphoid sheaths with prominent lymphoid follicles with very narrow mantle cell cuffs. The normal area of spleen is contracted with broad smooth muscle trabeculae, and the sinus areas are congested with sinus histiocytosis and very heavy hemosiderosis. The latter indicative of accelerated hemolysis due to irregular flow patterns through functional areas of splenic sinus.

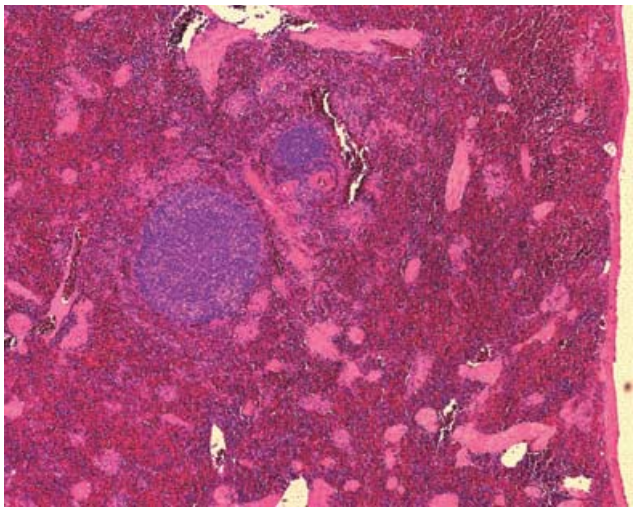

Figure 3.417. Cat: spleen, diffuse large B-cell lymphoma. The cat had massive enlargement of mesenteric nodes with splenic involvement consisting of atrophy of periarteriolar lymphoid sheaths (mid-left) and solid infiltration of residual follicles.

cat there may be extensive splenic involvement with large cell lymphoma and renal involvement to the extent of renal failure but almost no neoplastic cells in the liver (Figs. 3.417–3.420). Cytologically, large B-cell lymphoma in the human spleen is similar to the same neoplasm in nodes (Figs. 3.421, 3.422).

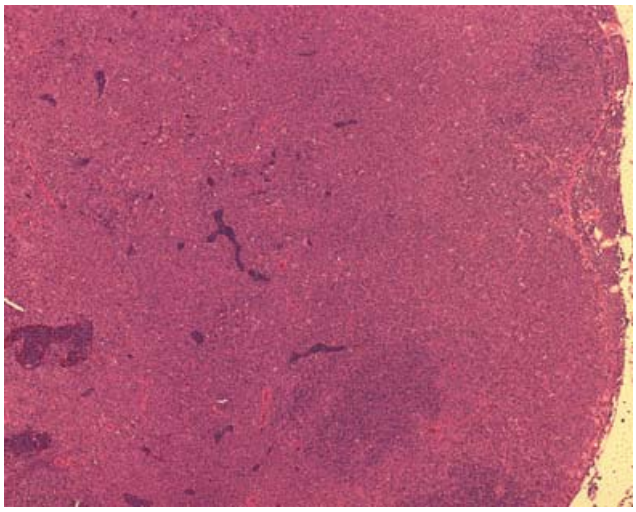

Figure 3.418. Cat: lymph node, diffuse large cleaved cell lymphoma, same case as Figure 3.417. There is diffuse architecture with complete loss of normal node structure and almost complete destruction of the peripheral capsule (top). The dark areas represent lymphatics dilated with lymphocytes with nuclei similar to those in node cortex with less cytoplasm.

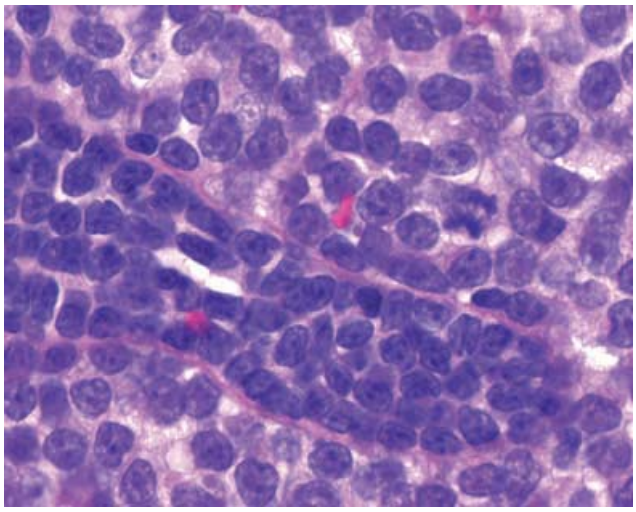

Figure 3.419. Cat: lymph node, diffuse large cleaved cell lymphoma, same case as spleen, Figure 3.417 and detail of Figure 3.418. The neoplastic cells have nuclei, round to oval, 2 red cells in diameter with irregular sharp and often deep nuclear indentations. The chromatin pattern is coarsely branched with 1–2 prominent nucleoli. There is a single mitotic cell right center. The sinus cells likely represent the portion of the neoplastic population in circulation.

Other Organs

The other organs likely to be involved are the liver (Figs. 3.423, 3.424) and kidney (Figs. 3.425, 3.426), but almost any tissue in the body may be affected, including the uterus, skeletal muscle, heart, bone, and tonsil (Figs.

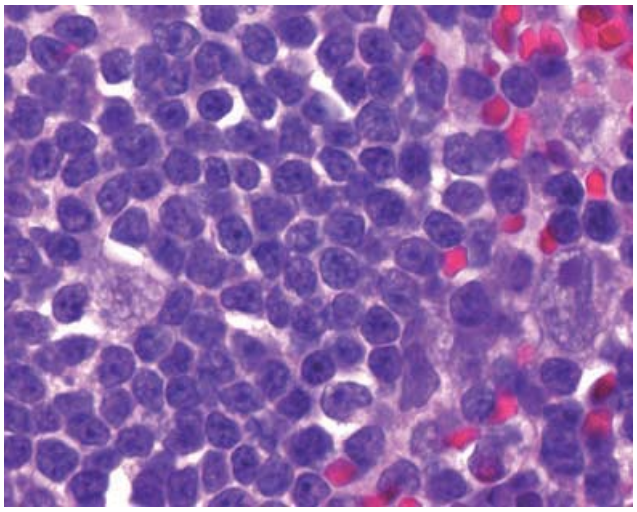

Figure 3.420. Cat: spleen. Detail of Figure 3.417. The neoplastic lymphocytes are loosely infiltrating the sinus areas (right) and solidly infiltrating the area of the follicular center. The nuclei have densely stained chromatin with prominent nucleoli and irregular nuclear indentations and strongly resemble those in the node sinuses. The splenic lesion represents an example of multifocal involvement of spleen with diffuse lymphoma elsewhere in nodes.

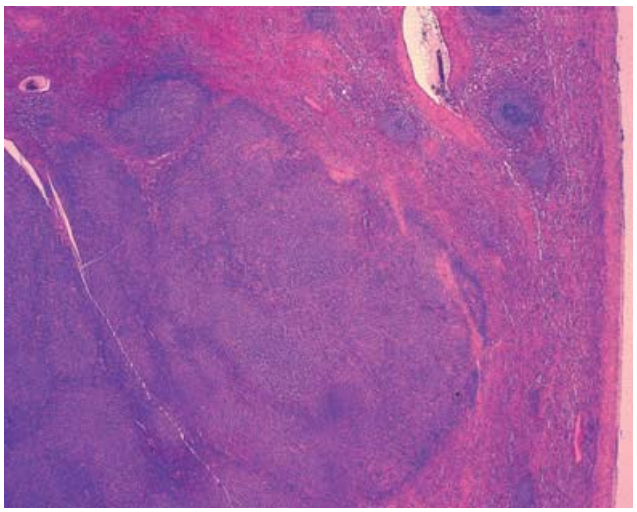

Figure 3.421. Human: spleen, diffuse large B-cell lymphoma. Note the fading germinal centers in the upper right with a narrow cuff of marginal zone hyperplasia. The neoplasm has formed several large masses within the spleen enlarging on a broad front basis with a narrow rim of residual small darkly stained cells. *Slide from Cornell Tutorial.*

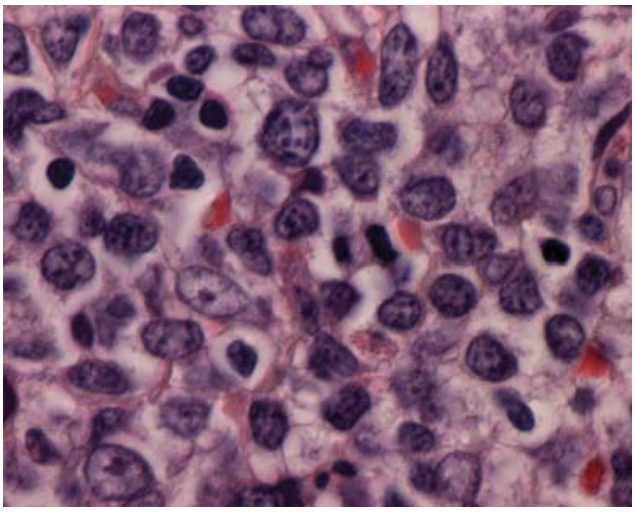

Figure 3.422. Human: spleen, diffuse large B-cell lymphoma. Detail of Figure 3.421. The nuclei are round to oval, 2–2.5 red cells in diameter with hyperchromatic coarse, granular chromatin pattern and moderate irregular parachromatin clearing. There are multiple small nucleoli and the cytoplasm is relatively abundant and lightly stained. There is a cell in anaphase in the center and a number of lymphocytes with small dense nuclei are likely benign. The large pale oval nucleus (left center) with prominent nucleolus is likely part of benign stroma.

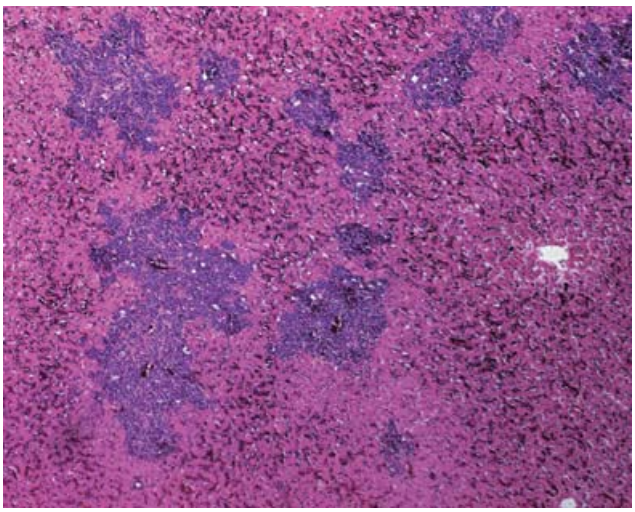

Figure 3.423. Cat: liver, large cell lymphoma. There is multifocal involvement of vascular structures involving both veins and portal areas.

3.427–3.429). The involvement in the liver is characteristically perivascular in lymphoma and sinusal in leukemia, but both types of involvement occur in DLBCL, which may reflect progression to leukemia in advanced cases. In the cat and in the cow, there may be laminar involvement of the space beneath the hepatic capsule without major infiltration of the hepatic parenchyma.

Immunologic Features

The diffuse large B-Cell lymphomas of domestic animals mark positively with CD79 and CD20 and are negative with CD3. Most canine large B-cell lymphomas will mark

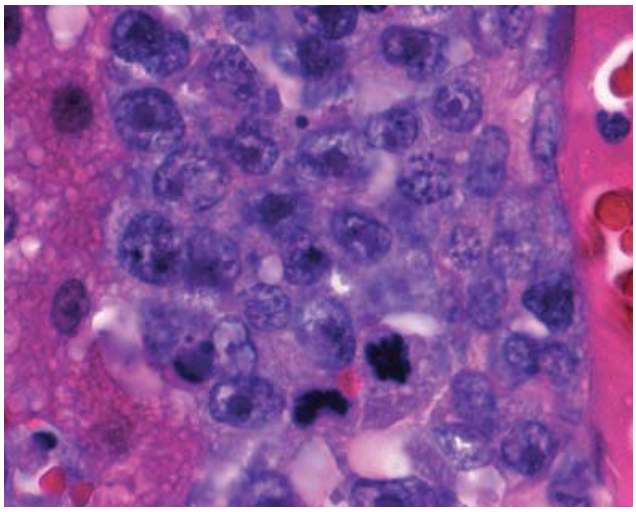

Figure 3.424. Cat: liver, large cell lymphoma. A mantle of neoplastic lymphocytes lines a thin walled vein (right) and is compressing hepatocytes, with nuclei becoming pyknotic at the left. There are 2 cells in mitoses at lower center.

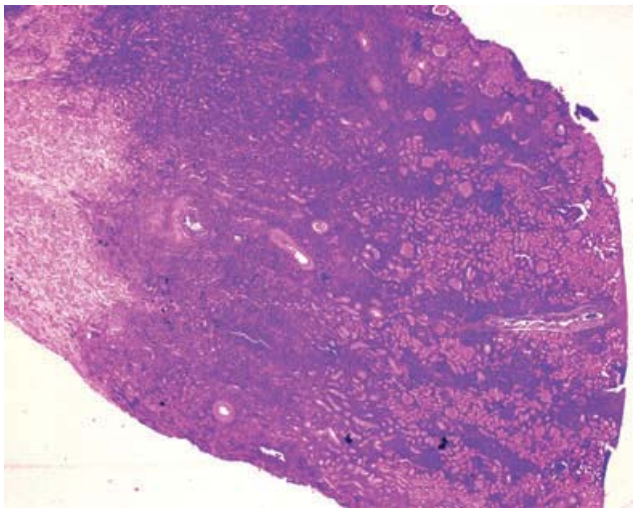

Figure 3.425. Cat: kidney, large cell lymphoma. There is dense and irregular infiltration of the tubular arrays in the outer cortex with solid infiltration of the inner cortex and cortico-medullary junction.

for surface or cytoplasmic Ig and most are clonal for the lambda light chain.

Cytogenetic and Molecular Features

Although studies are underway, there is not currently genetic information on the molecular changes occurring in DLBCL of the dog. In DLBCL of humans, there are frequent chromosomal alterations involving the 3q27 band, usually as a translocation involving regions of other chromosomes at sites of the Ig genes, including 14q32 (IgH) and 2p11 (Ig kappa) and 22q11 (Ig lambda).

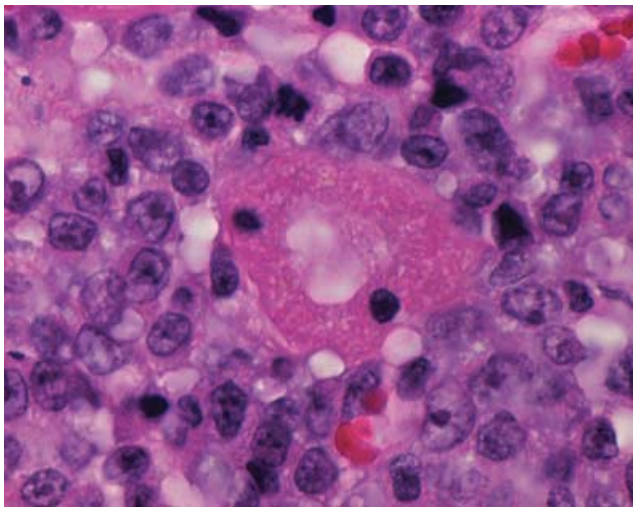

Figure 3.426. Cat: kidney, large cell lymphoma. Detail of Figure 3.425. A distal tubule in the center is undergoing phthisis by surrounding infiltration of neoplastic lymphocytes with round to oval nuclei with branched chromatin pattern and prominent central nucleoli. The lymphocyte cytoplasm is moderate in volume and staining density with cell boundaries indistinct. There is a cell in mitosis the upper center.

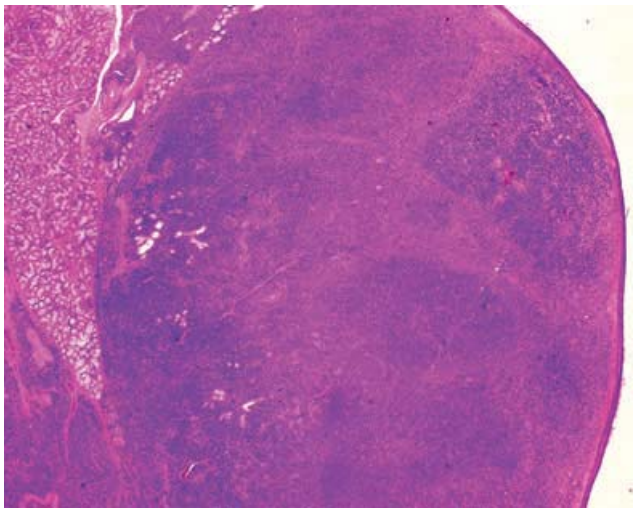

Figure 3.427. Dog: tonsil, diffuse large cell lymphoma. The oral epithelium is greatly thinned with a diffuse proliferation of lymphoid tissue that has replaced follicular structures and is compressing glandular tissues below.

Cell of Origin

In human DLBCL, there is usually hypermutation of the V_H region gene compatible with an origin from a post-germinal center cell. The same origin is likely to be the case in animal large B-cell, and clonality determined by PCR amplification of the VDJ region in dogs and cats is now routinely carried out in several institutions.

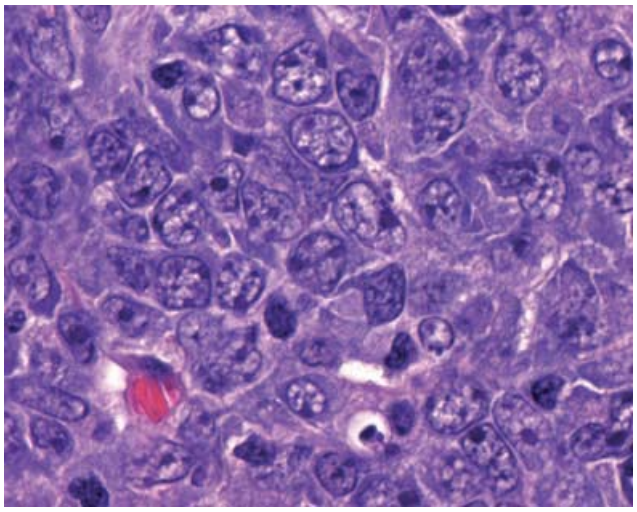

Figure 3.428. Dog: tonsil, large cell lymphoma. Detail of Figure 3.427. The nuclei are round to oval and frequently irregular in outline, 2 red cells in diameter, with a coarse granular chromatin pattern and irregular parachromatin clearing. There are multiple relatively prominent nucleoli frequently impinging on the nuclear membrane. The cytoplasm is moderate in volume and staining density with cell boundaries generally distinct.

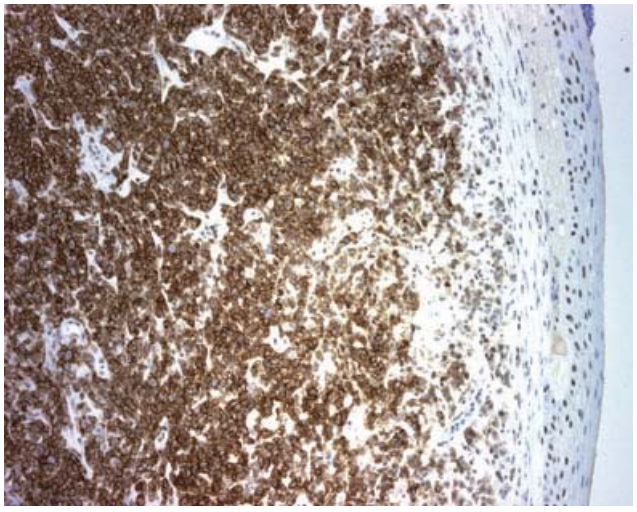

Figure 3.429. Dog: tonsil, diffuse large B-cell lymphoma. Phenotype of Figure 3.427. With CD20 staining, the neoplastic cells are strongly and uniformly labeled. The negative cells in the subcapsular area represent residual benign T-lymphocytes and stromal cells.

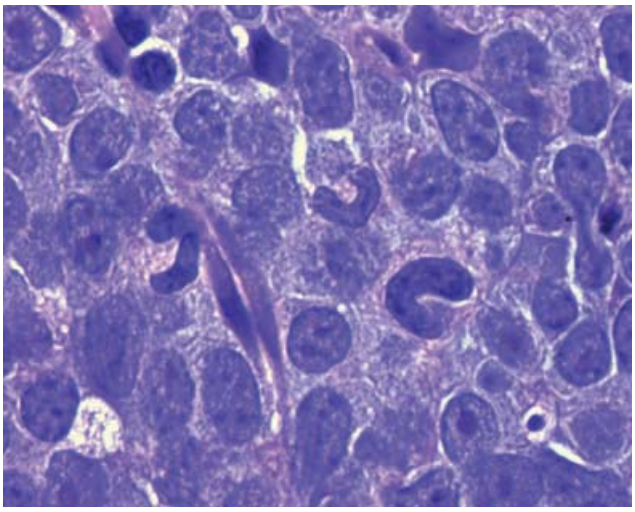

Figure 3.430. Dog: lymph node, anaplastic large cell lymphoma. The 3 horseshoe-shaped nuclei are the hallmark cells that characterize ALCL (see T-cell ALCL). Most lesions of this type in both humans and animals are of T-cell type but this lesion marked strongly with CD20 for B-cells.

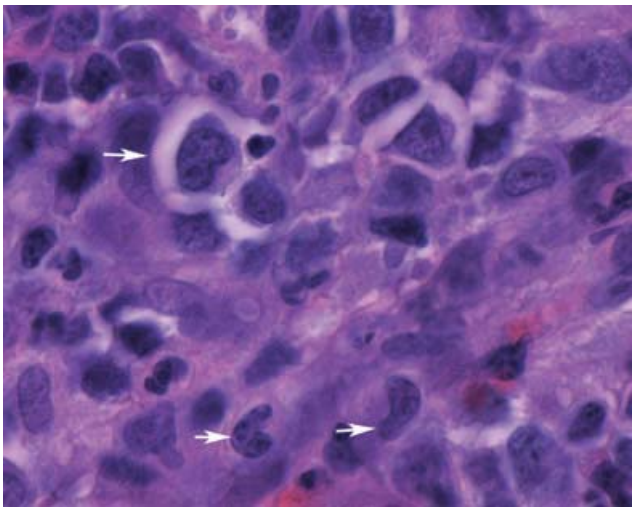

Figure 3.431. Cat: lymph node, anaplastic large cell lymphoma. This large cell lymphoma has nuclei with reniform or kidney-shaped nuclei, like that in the upper left, often with cells like those in lower center right that have more definite horseshoe-shaped nuclei and likelihood of neoplasm of ALCL type.

Diagnostic Criteria

Diffuse large B-cell lymphoma is recognized at the architectural level by complete tissue involvement that destroys the normal structural relations in node and other tissues. Cytologically, DLBCL is not single entity, and the cell type varies from a relatively uniform population of neoplastic cells in the centroblastic (CB, see Fig. 3.369) and immunoblastic (IB, see Fig. 3.371) variants to one of quite marked cellular variability in the anaplastic large cell lymphoma (ALCL-B) variant (Figs. 3.430–433). All types are characterized by large nuclei 2.0–3.0 red cells in diameter with a vesicular appearance and usually some degree of parachromatin clearing and most specifically numerous mitotic figures.

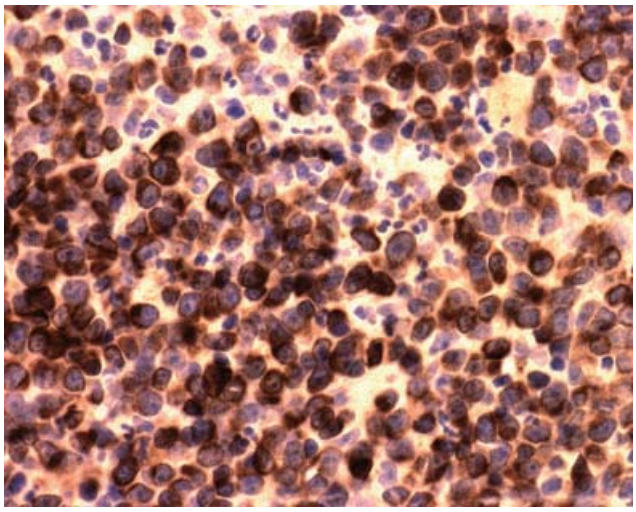

Figure 3.432. Cat: node, anaplastic large cell lymphoma. Phenotype of Figure 3.431. With CD79 alpha staining, the large atypical cells are strongly and uniformly positive.

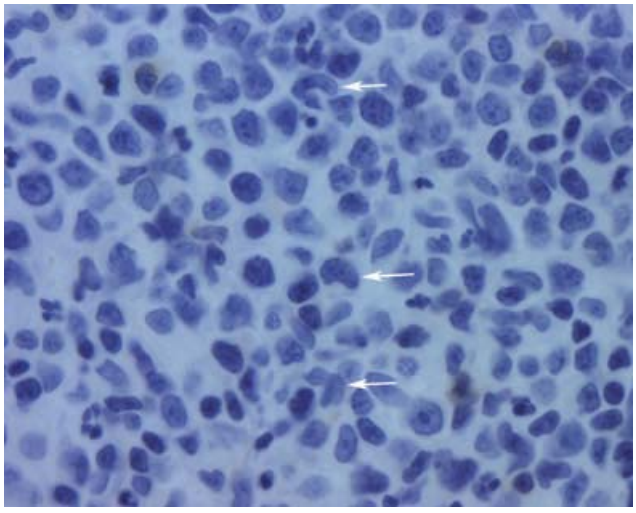

Figure 3.433. Cat: node, anaplastic large cell lymphoma. Phenotype of Figure 3.431. With CD3 staining, the atypical cells are completely negative; however, the lack of cytoplasmic stain renders the abnormally shaped nuclei more apparent (arrow).

Differential Diagnosis

DLBCL must be distinguished from indolent lymphoma of intermediate cell type like marginal zone lymphoma, which, like the immunoblastic variant of DLBCL, also has a prominent single central nucleolus. For this distinction, the virtual absence of mitoses in MZL in early stages along with the architectural arrangement around fading germinal centers are reliable features. In late stage MZL, the distinction is less clear but there are nearly always some fading follicles still present, and the irregular dilation of sinuses is not seen in diffuse large cell lymphoma.

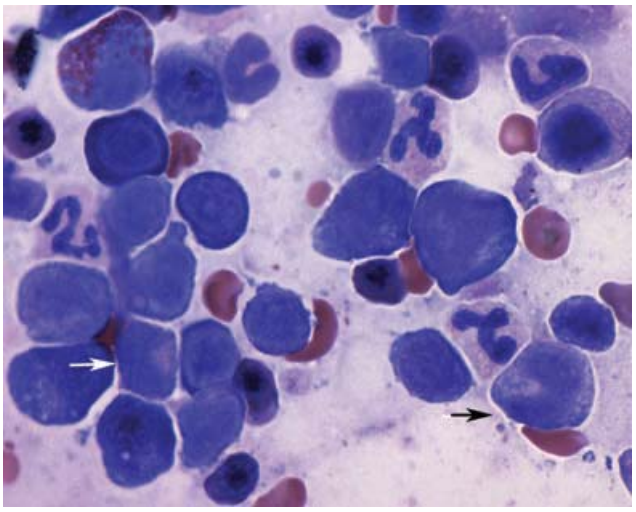

Figure 3.434. Dog: bone marrow, likely anaplastic large cell lymphoma. With marrow, there is need to distinguish the cells with reniform or horseshoe-shaped nuclei from metamyelocytes (upper left) and monocytic cells. The lack of granularity and cytoplasmic vacuolation accompanied with other large lymphocytes is more suggestive of lymphoid type (the large cells indicated by arrows).

The ALCL of B-cell type must have immunohistochemical differentiation from the T-cell ALCL as well as the more frequent hallmark kidney-shaped nuclei in the T-type neoplasm and relative paucity in B type ALCL. The DLBCL of CB type mimics the large cells of the reactive germinal center. For this reason, the later stages of follicular lymphoma (FL III) will cytologically look like large cell DL-IB in the central follicular areas and the remaining heterogeneity of cell type in the interfollicular areas must be recognized in the follicular lymphoma. In addition there may be some tingible body macrophages in the centers of FL III but these are not usually present in DL and never confined to nodular areas. In bone marrow, there is need to differentiate the large cells with reniform nuclei from metamyelocytes and monocytic precursors on oversight stains (Fig. 3.434).

Diffuse large B-cell lymphoma is staged in the conventional manner based on the number of tissues involved, including bone marrow and the presence or absence of clinical signs. The most common site of extranodal extension is in the abdominal cavity and involves the intestine, which may be primary, and the liver, spleen, kidney, and pancreas.

Transformation and Progression

The progression of large cell lymphoma largely proceeds with no morphologic change in cell type. Changes at the molecular level that may correlate with progression have been studied in human DLBCL with a remarkable finding that appears to relate the degree of somatic

hypermutation to the variability seen in lymphomas of large cell type. Whereas in benign B-cells the somatic hypermutation permits antibody diversity in large cell lymphoma dysfunction of this process drives the disease progression. These changes in the Ig genes affect both nontranslated as well as coding regions leading to changes in amino acid sequence and to malignant transformation. Because the process of hypermutation itself is highly variable, the dysfunction of this process is felt to be the basis for the biologic and clinical variability within the diffuse large B-cell lymphomas.

Evaluation of the Treated Animal

Treated animals need to be restaged for subsequent treatment planning. In human studies doxorubicin-based therapies are used followed by radiation therapy. Even disseminated stage large cell lymphoma in human patients has been followed by apparent cures using combination chemotherapy, with CHOP being the most common initial regimen. Advancing age is considered an important negative factor in the treatment of human patients with large cell lymphoma, and more frequent treatments of less toxic regimens seems to benefit older patients in some trials. Early results of gene activation profiles suggests that human patients who have gene expression that mimics cells of reactive germinal centers have a better survival than those whose gene profile reflects that pattern of activated peripheral blood lymphocytes. This might be another way of stating that the cells like those of the normal germinal center are a more differentiated and mature cell type than those of the blood that might be expected to be more naive B-cells recently released from the bone marrow.

Treatment and Survival

Many factors have been considered in the prognosis of human large cell lymphoma. About a third of human patients have "B" symptoms (night sweats, irregular fever, and weight loss) at the time of diagnosis. About half of human patients present at stage I/II and the other half with stage III/IV disease. An International Prognostic Index (IPI) developed for large cell lymphoma places 35% of cases at stage 0–1, 45% at 2–3, and 20% at 4–5. The survival at 5 years using the IPI system was 73% of 2,000 patients with the low risk group, and the 5-year survival with the highest risk group was 26%. An almost equivalent level of survival was predicted by measuring only the levels of serum lactate dehydrogenase and beta 2 microglobulin. The rapidity of achieving a complete response on first cycles of treatment is prognostically favorable in humans and apparently in animals as well. The determination of the proliferative rate of tumor cells predicts poor survival with high proliferative rate and retention of normal immune responses predicts a longer survival. Molecular studies of diffuse large cell lymphoma have shown that in human patients the overexpression of bcl-2 protein, but not the presence of BCL-2 gene rearrangement, is associated with more frequent relapse. More recently, gene activation profiling has shown patterns of expression in human large cell lymphoma that correlates with survival but are not related to a normal cellular counterpart

REFERENCES

Abou-Elella, A.A., Weisenburger, D.D., Vose, J.M., Kollath, J.P., Lynch, J.C., Bast, M.A., Bierman, P.J., Greiner, T.C., Chan, W.C., and Armitage, J.O. (1999) Primary mediastinal large B-cell lymphoma: A clinicopathologic study of 43 patients from the Nebraska Lymphoma Study Group. *J Clin Oncol* 17(3):784–790.

Aisenberg, A.C. (1993) Primary large-cell lymphoma of the mediastinum. *J Clin Oncol* 11(12):2291–2294.

Akasaka, T., Ueda, C., Kurata, M., Akasaka, H., Yamabe, H., Uchiyama, T., and Ohno, H. (2000) Nonimmunoglobulin (non-*Ig)/BCL6* gene fusion in diffuse large B-cell lymphoma results in worse prognosis than *Ig/BCL6*. *Blood* 96(8): 2907–2909.

Alizadeh, A.A., Eisen, M.B., Davis, R.E., Ma, C., Lossos, I.S., Rosenwald, A., Boldrick, J.C., Sabet, H., Tran, T., Yu, X., Powell, J.I., Yang, L., Marti, G.E., Moore, T., Hudson, Jr., J., Lu, L., Lewis, D.B., Tibshirani, R., Sherlock, G., Chan, W.C., Greiner, T.C., Weisenburger, D.D., Armitage, J.O., Warnke, R., Levy, R., Wilson, W., Grever, M.R., Byrd, J.C., Botstein, D., Brown, P.O., and Staudt, L.M. (2000) Distinct types of diffuse large B-cell lymphoma identified by gene expression profiling. *Nature* 403:503–511.

Armitage, J.O., Mauch, P.M., Harris, N.L., Dalla-Favera, R., and Bierman, P.J. (2004) Diffuse large B-cell lymphoma. In Mauch, P.M., Armitage, J.O., Coiffier, B.C., Dalla-Favera, R., and Harris, N.L. (eds.), *Non-Hodgkin's Lymphomas*. Lippincott Williams & Wilkins, Philadelphia, pp. 427–453.

Canoz, O., Rassidakis, G.Z., Admirand, J.H., and Medeiros, L.J. (2004) Immunohistochemical detection of BCL-3 in lymphoid neoplasms: A survey of 353 cases. *Mod Pathol* 17:911–917.

Carter, R.F., and Valli, V.E.O. (1988) Advances in the cytologic diagnosis of canine lymphoma. *Sem Vet Med Surg (Sm An)* 3(3):167–175.

Chan, J.K.C., Ng, C.S., and Tung, S. (1986) Multilobated B-cell lymphoma, a variant of centroblastic lymphoma. Report of four cases. *Histopathol* 10:601–612.

Copie-Bergman, C., Plonquet, A., Alonso, M.A., Boulland, M.L., Marquet, J., Divine, M., Moller, P., Leroy, K., and Gaulard, P. (2002) MAL expression in lymphoid cells: Further evidence for MAL as a distinct molecular marker of primary mediastinal large B-cell lymphomas. *Mod Pathol* 15(11): 1172–1180.

Dhodapkar, M., Yale, S.H., and Hoagland, H.C. (1993) Hemorrhagic pleural effusion and pleural thickening as a complication of chronic lymphocytic leukemia. *Am J Hematol* 42:221–224.

Dobson, J.M., Blackwood, L.B., McInnes, E.F., Bostock, D.E., Nicholls, P., Hoather, T.M., and Tom, B.D.M. (2001) Prognostic variables in canine multicentric lymphosarcoma. *J Sm An Pract* 42:377–384.

Evert, M., Lehringer-Polzin, M., Mobius, W., and Pfeifer, U. (2000) Angiotropic large-cell lymphoma presenting as pulmonary small vessel occlusive disease. *Human Pathol* 31(7):879–882.

Haralambieva, E., Pulford, K.A.F., Lamant, L., Pileri, S., Roncador, G., Gatter, K.C., Delsol, G., and Mason, D.Y. (2000) Anaplastic large-cell lymphomas of B-cell phenotype are anaplastic lymphoma kinase (ALK) negative and belong to the spectrum of diffuse large B-cell lymphomas. *Brit J Haematol* 109:584–591.

Harris, N.L., Jaffe, E.S., Stein, H., Banks, P.M., Chan, J.K.C., Cleary, M.L., Delsol, G., De Wolf-Peeters, C., Falini, B., Gatter, K.C., Grogan, T.M., Isaacson, P.G., Knowles, D.M., Mason, D.Y., Muller-Hermelink, H.K., Pileri, S.A., Piris, M.A., Ralfkiaer, E., and Warnke, R.A. (1994) A revised European-American classification of lymphoid neoplasms: A proposal from the International Lymphoma Study Group. *Blood* 84(5):1361–1392.

Higgins, J.P., and Warnke, R.A. (1999) CD30 expression is common in mediastinal large B-cell lymphoma. *Am J Clin Pathol* 112:241–247.

Hill, M.E., MacLennan, K.A., Cunningham, D.C., Vaughan Hudson, B., Burke, M., Clarke, P., Di Stefano, F., Anderson, L., Vaughan Hudson, G., Mason, D., Selby, P., and Linch, D.C. (1996) Prognostic significance of BCL-2 expression and *bcl-2* major breakpoint region rearrangement in diffuse large cell non-Hodgkin's lymphoma: A British National Lymphoma Investigation Study. *Blood* 88(3):1046–1051.

Jacobson, J.O., Aisenberg, A.C., Lamarre, L., Willett, C.G., Linggood, R.M., Miketic, L.M., and Harris, N.L. (1988) Mediastinal large cell lymphoma: An uncommon subset of adult lymphoma curable with combined modality therapy. *Cancer* 62(9):1893–1898.

Keung, Y.K., Cobos, E., Morgan, D., and McConnell, T.S. (1996) Non-pyothorax-associated primary pleural lymphoma with complex karyotypic abnormalities. *Leuk and Lymph* 23:621–624.

Kojima, M., Nakamura, S., Ichimura, K., Suzuki, R., Kagami, Y., Kondo, E., Motoori, T., Hosomura, Y., Oyama, T., Itoh, H., Ban, S., Yoshida, K., Ohno, Y., Shimizu, K., Masawa, N., and Sugihara, S. (2002) Centroblastic and centroblastic/centrocytic lymphoma associated with a prominent epithelioid granulomatous response: A clinicopathologic study of 50 cases. *Mod Pathol* 15(7):750–758.

Lossos, I.S., Okada, C.Y., Tibshirani, R., Warnke, R., Vose, J.M., Greiner, T.C., and Levy, R. (2000) Molecular analysis of immunoglobulin genes in diffuse large B-cell lymphomas. *Blood* 95(5):1797–1803.

McDonough, S.P., Van Winkle, T.J., Valentine, B.A., vanGessel, Y.A., and Summers, B.A. (2002) Clinicopathological and immunophenotypical features of canine intravascular lymphoma (malignant angioendotheliomatosis). *J Comp Path* 126:277–288.

Menestrina, F., Chilosi, M., Bonetti, F., Lestani, M., Scarpa, A., Novelli, P., Doglioni, C., Todeschini, G., Ambrosetti, A., and Fiore-Donati, L. (1986) Mediastinal large-cell lymphoma of B-type, with sclerosis: Histopathological and immunohistochemical study of eight cases. *Histopathol* 10: 589–600.

Menke, D.M., Horny, H.P., Griesser, H., Tiemann, M., Katzmann, J.A., Kaiserling, E., Parwaresch, R., and Kyle, R.A. (2001) Primary lymph node plasmacytomas (plasmacytic lymphomas). *Am J Clin Pathol* 115:119–126.

Nador, R.G., Cesarman, E., Chadburn, A., Dawson, D.B., Ansari, M.Q., Said, J., and Knowles, D.M. (1996) Primary effusion lymphoma: A distinct clinicopathologic entity associated with the Kaposi's sarcoma—associated herpes virus. *Blood* 88(2):645–656.

Ottensmeier, C.H., and Stevenson, F.K. (2000) Isotype switch variants reveal clonally related subpopulations in diffuse large B-cell lymphoma. *Blood* 96(7):2550–2556.

Robertson, L.E., Redman, J.R., Butler, J.J., Osborne, B.M., Velasquez, W.S., McLaughlin, P., Swan, F., Rodriguez, M.A., Hagemeister, F.B., Fuller, L.M., and Fernando, C. (1991) Discordant bone marrow involvement in diffuse large-cell lymphoma: A distinct clinical-pathologic entity associated with a continuous risk of relapse. *J Clin Oncol* 9(2): 236–242.

Steinberg, H. (1996) Multisystem angiotropic lymphoma (malignant angioendotheliomatosis) involving the humerus in a dog. *J Vet Diagn Invest* 8:502–505.

Todeschini, G., Ambrosetti, A., Meneghini, V., Pizzolo, G., Menestrina, F., Chilosi, M., Benedetti, F., Veneri, D., Cetto, G.L., and Perona, G. (1990) mediastinal large B-cell lymphoma With sclerosis: A clinical study of 21 patients. *J Clin Oncol* 8(5):804–808.

Valli, V.E., Jacobs, R.M., Norris, A., Couto, C.G., Morrison, W.B., McCaw, D., Cotter, S., Ogilvie, G., and Moore, A. (2000) The histologic classification of 602 cases of feline lymphoproliferative disease using the National Cancer Institute Working Formulation. *J Vet Diagn Invest* 12: 295–306.

Vernau, W., Valli, V.E.O., Dukes, T.W., Jacobs, R.M., Shoukri, M., and Heeney, J.L. (1992) Classification of 1,198 cases of bovine lymphoma using the National Cancer Institute Working Formulation for human non-Hodgkin's lymphomas. *Vet Pathol* 29:183–195.

Wakely, Jr., P.E., Menezes, G., and Nuovo, G.J. (2002) Primary effusion lymphoma: Cytopathologic diagnosis using in situ molecular genetic analysis for human herpesvirus 8. *Mod Pathol* 15(9):944–950.

Williams, L.E., Broussard, M.T., Johnson, J.L., and Neel, J. (2005) Comparison of results of clinicians' assessments, cytologic examination of fine-needle lymph node aspirates, and flow cytometry for determination of remission status of lymphoma in dogs. *JAVMA* 226(4):562–566.

Wright, K.N., Gompf, R.E., and DeNovo, Jr., R.C. (1997) Peritoneal effusion in cats: 65 cases (1981–1997). *JAVMA* 214(3):375–381.

Xu, Y., McKenna, R.W., and Kroft, S.H. (2002) Comparison of multiparameter flow cytometry with cluster analysis and immunohistochemistry for the detection of CD10 in diffuse large B-cell lymphomas. *Mod Pathol* 15(4):413–419.

Zinzani, P.L., Bendandi, M., Martelli, M., Falini, B., Sabattini, E., Amadori, S., Gherlinzoni, F., Martelli, M.F., Mandelli, F., Tura, S., and Pileri, S.A. (1996) Anaplastic large-cell lymphoma: Clinical and prognostic evaluation of 90 adult patients. *J Clin Oncol* 14(3):955–962.

T-Cell Rich Large B-Cell Lymphoma/ Lymphomatoid Granulomatosis

Definition

Diffuse lymphoma of the T-cell rich large B-cell lymphoma (TCRLBCL) type is not defined as an entity in the revised REAL/WHO classification but rather as one of the variant types of large B-cell lymphoma. This variant type of large B-cell lymphoma was known as the "Diffuse Mixed" small and large cell type in the Working Formulation (WF) and had a similar name in the British National Lymphoma Investigation Classification, but did not have a clear counterpart in the Kiel classification of 1974. In general terms, this variant was felt to be the diffuse counterpart of follicular mixed small-cleaved and large cell lymphoma. With the advent of immunohistochemistry it became apparent that the small centrocytes and large centroblasts of the FL type neoplasms were both B-cell type, and the small cells of the TCRLBCL were T-cells likely present in reaction to a smaller number of neoplastic large B-cells. The treatment of this neoplasm as a separate entity in this description is not to deviate from the WHO system but to give more emphasis to the TCRLBCL variant of large B-cell lymphoma because it is a common and characteristic neoplasm in several domestic animals.

The status of lymphomatoid granulomatosis (LYG) is currently still under investigation. The LYG is now felt to be a type of diffuse large B-cell lymphoma that in humans has, in the majority of cases, the EBV (Epstein-Barr virus) intranuclear but not apparently integrated into the genome of the neoplastic cells. LYG was compared to TCRLBCL and suggested to be a variant type of that disease, but this is no longer considered valid. Whatever the cause of the tumor seen occasionally in the lung of the dog, it has similarities to the human tumor of the same name, including the predominance of T-lymphocytes, numerous atypical giant cells, and large locally extensive areas of ischemic necrosis. There is a mixed cell reaction with large atypical cells and irregular infiltration of eosinophils, both singly and irregularly in small clusters. Some of the cases in dogs presenting with a large mass in a caudal dorsal area of one lung were described as LYG, but it is likely that some of these are cases of the non-phagocytic type of histiocytic sarcoma. At present, the status of LYG in animals, principally dogs, is undetermined and it may be that the animal counterpart of the human lesion may not exist or may not have been adequately described. Lung lesions in the dog that are negative for CD18 (Fig. 3.435) on immunohistochemistry are characterized by a large focal sclerosing mass in the caudal lung lobes with a mixture of cell types present, including very atypical giant cells that have tentacular cytoplasmic tendrils and several hundred nuclei (Fig. 3.436). There are irregular large areas of ischemic necrosis bordered by benign inflammatory cells (Figs. 3.437,

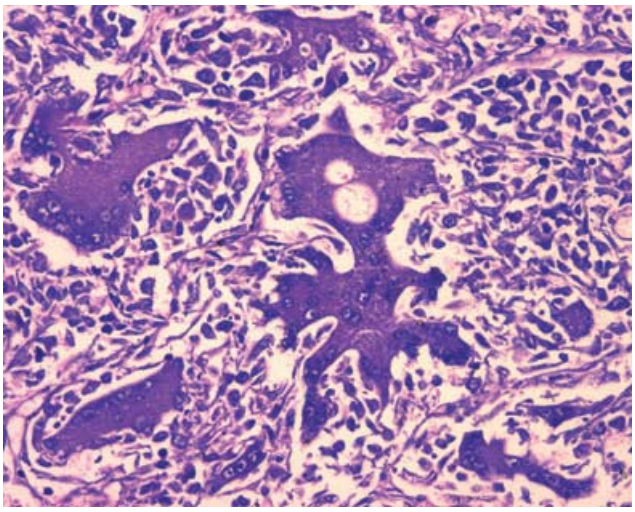

Figure 3.435. Dog: lung, lymphomatoid granulomatosis. A presumptive interpretation on an ill-defined lesion with very atypical giant cells and a background of lymphocytic and histiocytic proliferation.

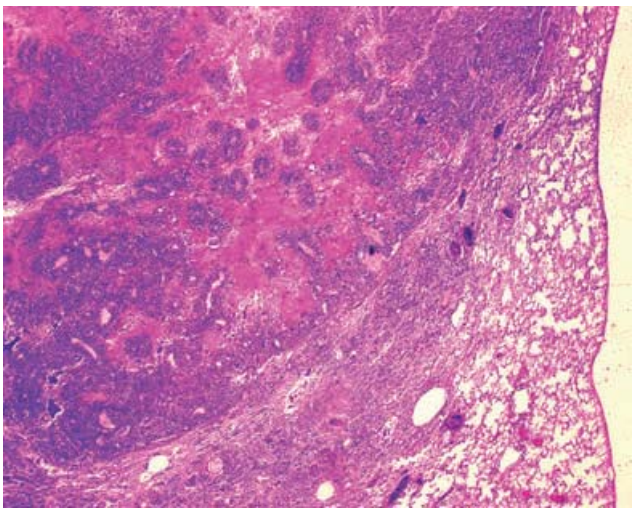

Figure 3.436. Dog: lung, lymphomatoid granulomatosis. Typical large focal lesions, spreading by compression of surrounding lung. There are multifocal areas of necrosis that appear as pink homogenous areas in the center. Focal areas of cells surviving in these areas surround vessels and are more properly "collar lesions" of cells surviving around vessels in an ischemic area than an indication of angiocentricity.

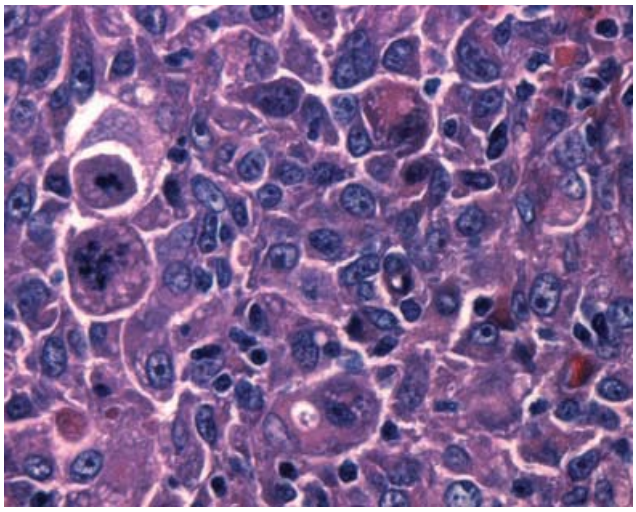

Figure 3.437. Dog: lung, lymphomatoid granulomatosis. Detail of Figure 3.435. There are 2 large cells at the left with abnormal mitotic figures. Two larger above left and below center resemble the popcorn cells of T-cell rich large B-cell lymphoma with multinucleation, large nucleoli, and a tendency to undergo necrosis with nuclear pyknosis and hyaline eosinophilic cytoplasm, as in the large and smaller binucleated cell at top.

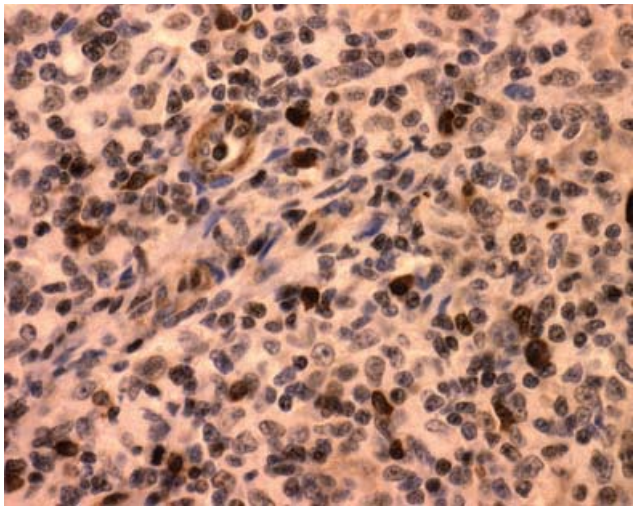

Figure 3.438. Dog: lung, lymphomatoid granulomatosis. Phenotype of Figure 3.435. On staining with CD79, there is strong marking of residual plasma cells and a few of the large atypical cells as well as nonspecific nuclear labeling.

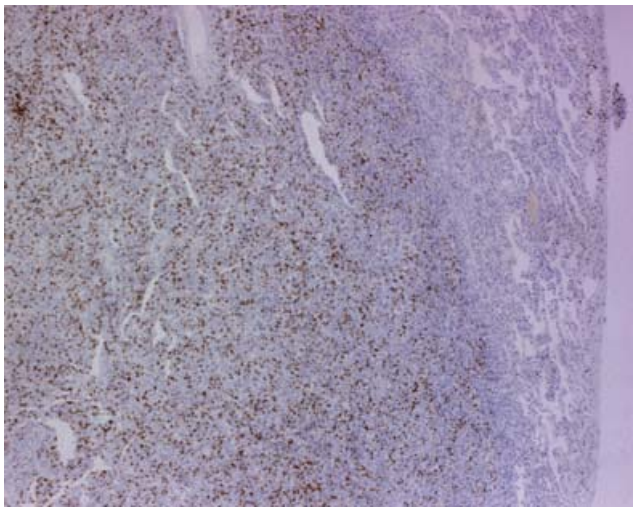

Figure 3.439. Dog: lung, lymphomatoid granulomatosis. Phenotype of Figure 3.435. With CD3 staining, there is a much more general marking throughout the mass with reduced density in ischemic areas (center). The pattern is similar to that of T-cell rich large B-cell lymphoma.

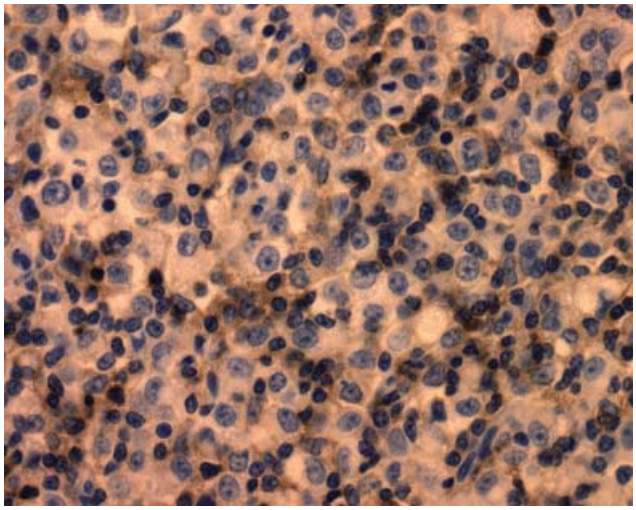

Figure 3.440. Dog: lung, lymphomatoid granulomatosis. Phenotype of Figure 3.435. On staining with CD18, there is marking of residual alveolar macrophages with the large atypical cells interpreted to be neoplastic lymphocytes completely negative.

3.438). In immunohistochemical staining, there are cells positive for both CD79 (Fig. 3.439) and CD3 (Fig. 3.440), but no convincing pattern or reactivity on the large atypical cells is present. In the dog, there does not appear to be the angiocentricity described for the human form of LYG, but vessels and airways are compressed and invaded as part of general encirclement.

Epidemiology and Incidence

The T-cell rich large B-cell variant of large B-cell lymphomas is seen in all domestic animals, but it is most common in the horse and cat. In a review of 751 cases of feline lymphoma, mostly prior to routine immunophenotyping, there were 56 cases of TCRLBCL or diffuse mixed (DM) type for 56/751 or 7.5% of total cases. In a similar review of 118 cases of equine lymphoma, there were 39

cases of TRCB type for 39/118 or 33% of total cases. In other animals, the proportion of neoplasms of TCRLBCL type is much lower. In 1,198 cases of bovine lymphoma, there were only 26 cases of TRCB for 26/1,198 (2.2%) of total cases. In 502 cases of canine lymphoma, there were 10 cases of TCRLBCL for 10/502, about 2.0% of cases. In the same group of dogs, there were 2 cases diagnosed as of lymphomatoid granulomatosis type. In a review of 136 cases of lymphoma in domestic swine, there were 4 cases felt to be of TCRLBCL type for 4/136 (3%) of cases. For comparison in the study of 1,104 cases of human lymphoma reviewed in the development of the Working Formulation, there were 77 cases of diffuse mixed or TCRLBC lymphoma for 6.7% of cases.

Clinical Presentation and Features

In the horse, the TCRLBCL tumor appears most often in the skin type of lymphoma and occasionally as a very large single subcutaneous mass that may weigh 10–20 pounds. The presentation in the horse is characteristically in animals over 10 years of age and with a strong female predominance of 3–4:1 (Fig. 3.441). Topographically the common presentation is with multiple (<100 or more) skin lesions that are discoid 1–3 cm in diameter and are mobile beneath the skin, lying in a thin panniculus overlying the skeletal muscle (Fig. 3.442). In the early stages, the owners may be more bothered by this development than the horse that remains in good health and vigor but becomes less useful for riding because the tumor nodules are present over the withers, flank, and limb areas, as well as along the back in the area normally covered by the saddle and cinch. Oddly, in mares the lesions have been known to regress during pregnancy only to recur following foaling. Rarely, horses present with a proliferative lymphoid lesion over one eye, which is a dermal and subdermal infiltration that tends to recur after excisional biopsy. These are cohesive neoplasms that have typical cytomorphology of TCRLBC lymphoma.

Topographically of 56 cases of TRCB in the cat, 17 cases were multicentric; 14 affecting one node only; 13 cases involving the gastrointestinal tract; and 2 cases for each of mediastinal, renal, skin, and generalized lymphadenopathy. Other sites occurring only once included brain and spinal cord, liver, nasal cavity, and skin. In terms of the tissues on which the diagnosis was made, in these 56 cases the most frequent was peripheral node; site not indicated, 20; small intestine, 10; node cervical area, 9; liver, 6; and mesenteric node, 5. Other tissues were mentioned only once. In recent years, it has become apparent that a typical presentation for TCRLBCL in the cat is a single very large node in the "cervical area" described both as mandibular and neck locations. These nodes may be up to 4 cm in length and flattened 1–1.5 cm in depth, several cm in width, and lying over the jugular vein. The tissues are firmly encapsulated but remain mobile and are usually removed intact. A characteristic history is for a second mass to occur in the same area and for successive nodes to be removed at about yearly inter-

Figure 3.441. A 10-year-old female quarter horse was presented first with a few subcutaneous skin nodules and over a period of a year developed many nodules of varying size from 1–2 cm in diameter, lightly mobile and not fixed to the skin.

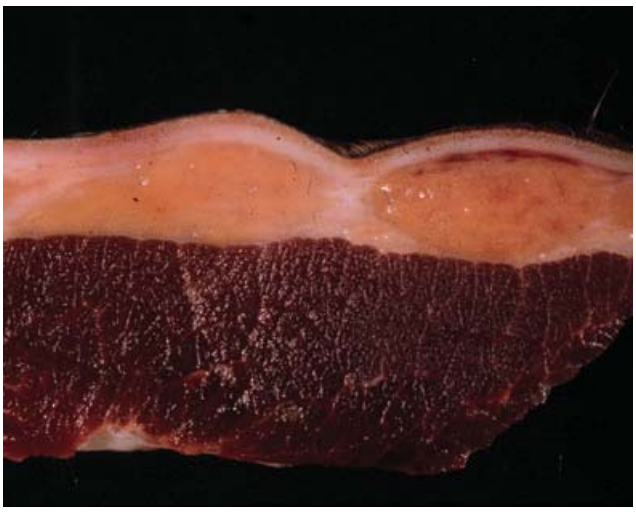

Figure 3.442. Equine: skin, T-cell rich large B-cell lymphoma. The subcutaneous nodules are discoid masses beneath the skin that do not invade either muscle or skin until very late in the disease or the individual lesions become very large and cause skin ulceration. The lesions do not bulge on the cut surface and are very cohesive with a high level of fine fibrovascular tissue.

vals from the same region with spread from the initial site always to a contiguous node, either prescapular or mediastinal. In this respect, this neoplasm in the cat is very like human Hodgkin's lymphoma, which spreads by contiguity to neighboring nodes without "skip lesions" affecting distant sites.

Pathologic Features

Blood

Blood seems not to be involved in TCRLBCL, or at least it is not a presenting abnormality or a tissue that is mentioned in the follow-up of diagnosed cases.

Bone Marrow

Bone marrow is involved in TCRLBCL in the cat and likely occurs as a late manifestation and in animals noted to present likely for necropsy as having multicentric tissue involvement. At the architectural level, the infiltration is apparent as an area with complete exclusion of all fat cells. Cytologically, the lesion appears the same in marrow as in node but with less prominent vascular structures. Adjacent areas may not have complete phthisis of normal marrow cells, but the extent of marrow involvement in the areas sampled suggest that some effect on the blood picture was likely present.

Lymph Node

One of the most characteristic features of the TCRLBCL lesion in all animals is the presence of a very fine but dense fibrovascular network that is most apparent because the tissues, though very large, do not fragment on sectioning (Figs. 3.443–3.447). In this respect the TCRLBCL lesion differs from the high-grade lymphomas that tend to be very friable and have cracks and tears, particularly if the tissue is large. The capsule is thin and taut, and there is not usually involvement of perinodal tissues even in very large tumors (Fig. 3.448). At the architectural level, there

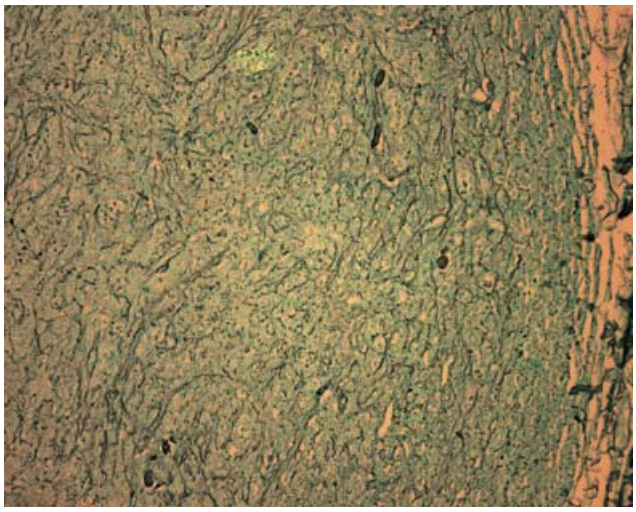

Figure 3.443. Dog: subcutaneous mass, possibly node, T-cell rich large B-cell lymphoma. Reticulin stain demonstrates the very fine arborization of reticulin fibers within this type of lymphoma. The darker-staining focal structures in the upper right and lower left are residual collagen bands associated with the subcutaneous tumor.

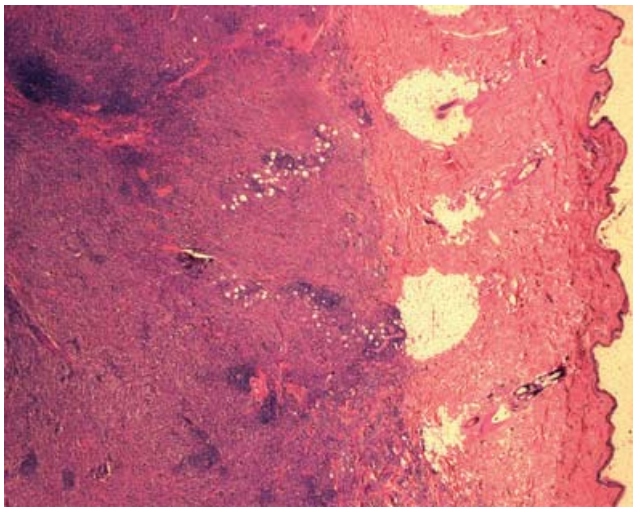

Figure 3.444. Dog: subcutaneous mass, T-cell rich large B-cell lymphoma. The neoplasm is pressed tightly against the skin that has focal areas of fatty infiltration. The neoplasm is diffuse and cohesive, with the darker areas representing irregular areas of small T-cell infiltration.

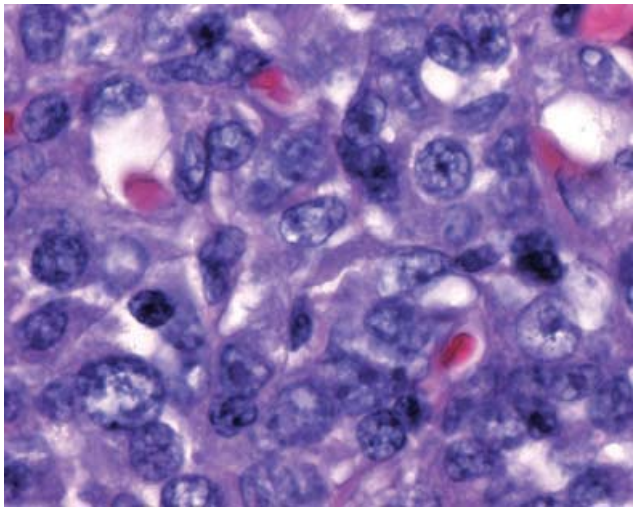

Figure 3.445. Dog: S/C mass, T-cell rich large B-cell lymphoma. Detail of Figure 3.443. The lesion is characterized by a consistent intermixing of small mature lymphocytes with compact chromatin and nuclei only slightly larger than red cells. The large cells have vesicular nuclei with a branched chromatin pattern and irregularly prominent nucleoli. The cytoplasm is moderate in volume and staining density with the large cells more prominent than usual in early lesions.

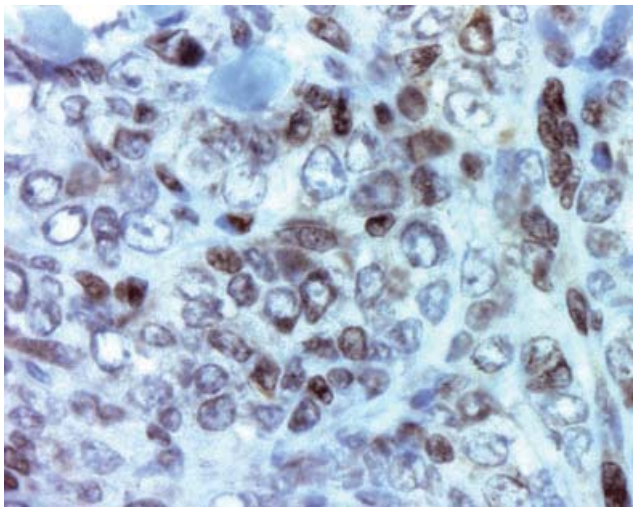

Figure 3.446. Dog: S/C mass, T-cell rich large B-cell lymphoma. Phenotype of Figure 3.443. With CD79 staining, there is irregular marking of the large cells as well as some of intermediate size, with many cells unmarked but with quite a lot of artifactual nuclear staining of smaller cells.

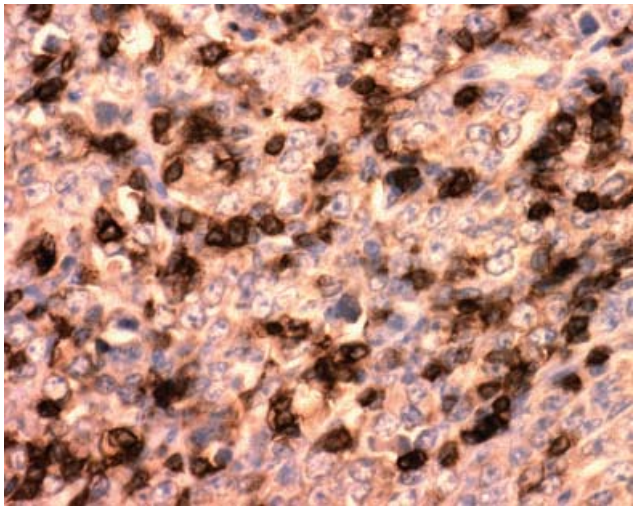

Figure 3.447. Dog: S/C mass, T-cell rich large B-cell lymphoma. Phenotype of Figure 3.443. With CD3 staining, the small cell population is largely labeled, with many of the unmarked cells having visible vesicular nuclei and prominent nucleoli.

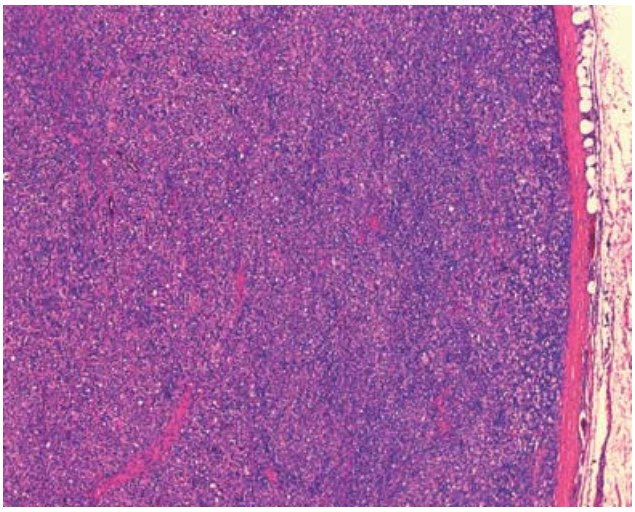

Figure 3.448. Cat: submandibular lymph node, T-cell rich large B-cell lymphoma. The capsule is thin and taut without invasion of perinodal structures, and the peripheral sinus is compressed. The tissue has a diffuse dense appearance with the focal, pink areas representing fine collage bands; and the mixed cell population presents a varied background. *Slide from F. A. Juck, DVM.*

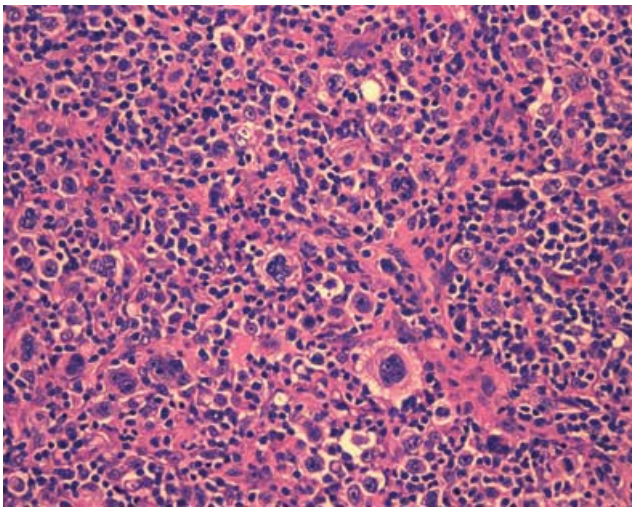

Figure 3.449. Cat: node, T-cell rich large B-cell lymphoma. Detail of Figure 3.448. Typical of this lesion in the cat, there are focal areas where the large cells may be very large and multinucleated with very prominent central nucleoli. There may be binucleated cells with peripheralized chromatin that resemble Reed-Sternberg cells of Hodgkin's lymphoma. Typically, the larger cells irregularly undergo necrosis with eosinophilic cytoplasm and dense pyknotic nuclei (upper and lower right).

are often fading germinal centers beneath the nodal peripheral sinus and often deep within the node, indicating a heritage of benign hyperplasia prior to the onset of neoplastic infiltration. The interior of the node has a completely diffuse involvement, usually with destruction of the medullary cords and sinuses (Fig. 3.449). Cytologically, the cell complement is "mixed" with small and medium lymphocytes predominating and cells with large and vesicular nuclei 3 red cells in diameter constituting as low as 5% and as high as 70% of the cells present (Fig. 3.450). It is not clearly established, but it appears that the proportion of larger cells increases as the disease progresses. In the horse, the same changes are present in nodes, but the diagnosis is almost always made on sub-

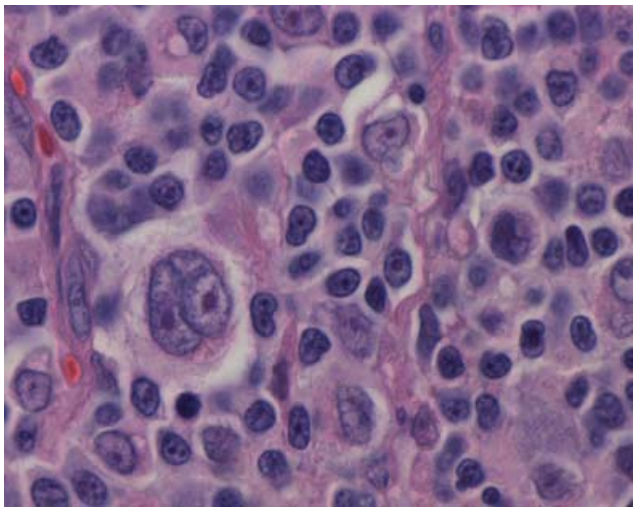

Figure 3.450. Cat: lymph node, T-cell rich large B-cell lymphoma. Detail of Figure 3.448. The large cells typically do not have the peripheralized chromatin of Reed-Sternberg cells and are large and may be very large. The cell in the right center with the indented nucleus has a very large nucleolus and is undergoing degenerative change. Density of the more mature T-lymphocytes is typical, with some of these of intermediate size and with nucleoli suggesting in situ proliferation of the benign cell population.

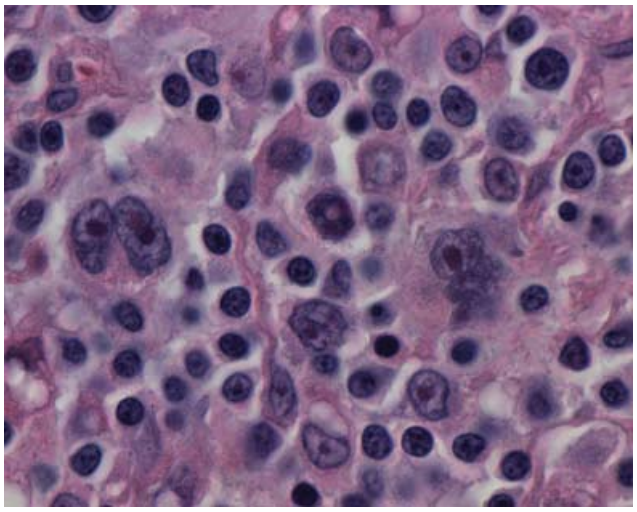

Figure 3.451. Cat: node, another area of Figure 3.450. Binucleation and multinucleation are common in the large atypical cells that have very prominent central nucleoli and fine granular chromatin patterns with variable parachromatin clearing.

cutaneous nodules that lack the evidence of prior nodal architecture and likely arise along subcutaneous lymphatic chains. In cats, but not in horses or dogs, there are cases with variant histology, usually those arising in the neck area where a low proportion of the cells present, less than 1%, are huge with round to oval nuclei 10 red cells or more in diameter. These cells have nucleoli as large as red cells and with a branched chromatin pattern without the peripheralization of chromatin that is an essential criterion of the classic type Reed-Sternberg (RS) cell of human Hodgkin's disease (Fig. 3.453).

Because the cat type of TCRLBCL has been compared to human Hodgkin's lymphoma, some description of that disease is required in order to put the cat tumor in perspective in terms of comparative pathology. Hodgkin's lymphoma (HL) has been divided in the WHO classification into two major groups on the basis of molecular pathology. The larger group of "classic types" of HL has RS cells that are clonally stable, postgerminal center B-cells that have rearranged Ig genes with hypermutated variable regions; the second group, consisting of the lymphocyte predominance type, has RS cells with ongoing Ig gene mutations. The RS cells tend to vary in morphologic type with the overall histology of the lesion. Within the classic group, the nodular sclerosis type (Fig. 3.452) of HL has RS cells of the lacunar type that are favored in their recognition by formalin fixation in which the contraction of the cells in processing tends to highlight the

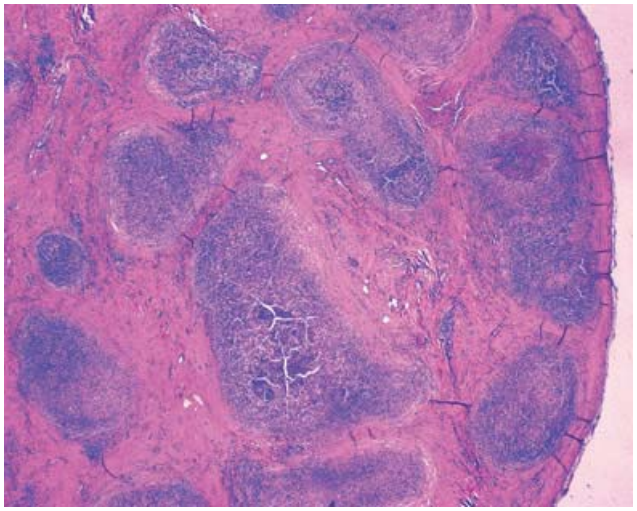

Figure 3.452. Human: lymph node, Hodgkin's lymphoma, nodular sclerosis type. Remnants of lymphoid tissue are isolated by heavy bands of connective tissue that are brightly birefringent of mature collagen on polarized light. *Slide from Cornell Tutorial.*

lacunar cell separation from surrounding cells (Fig. 3.453). The mixed cellularity (lymphocytic/histiocytic, (Fig. 3.454) type of HL has RS cells that have the classic type of chromatin peripheralization and very large nucleoli with binucleate (Fig. 3.455) and multinucleated cells (Fig. 3.456). The lymphocyte depletion type of HL (Fig. 3.457) has RS cells that are more pleomorphic with deeply stained nuclei and nucleoli often indistinct (Fig. 3.458). In contrast the nonclassical variant of lymphocyte predominance type HL has the "popcorn" or wrinkled,

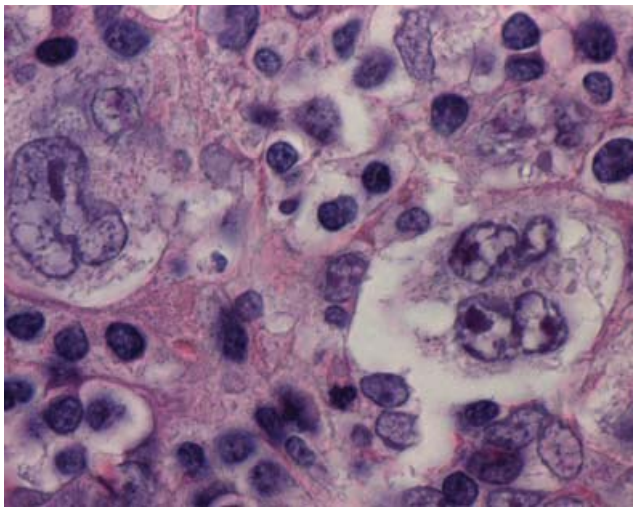

Figure 3.453. Human: node, Hodgkin's lymphoma, nodular sclerosis type. Detail of Figure 3.452. The cell at the top has multiple nuclei with very large nucleoli and peripheralized chromatin typical of Reed-Sternberg cell type. The cytoplasm has retracted from the surrounding tissues, making the structure more obvious at low-power observation.

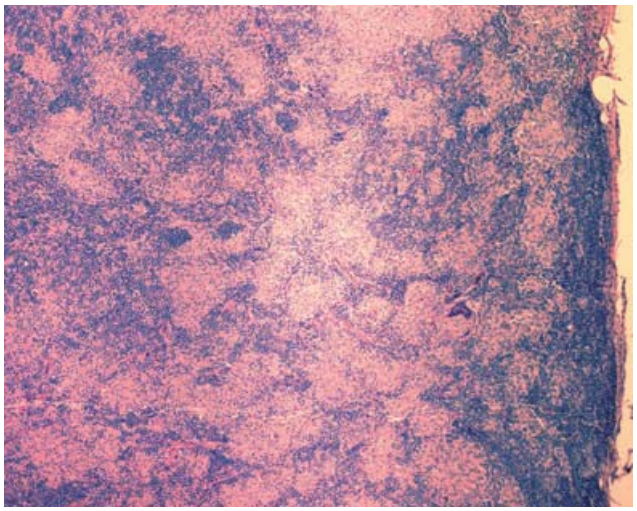

Figure 3.454. Human: node, Hodgkin's lymphoma, mixed cellularity type. The node has a variegated appearance at the architectural level due to the presence of many large epithelioid macrophages with focal areas of dense lymphoid cellularity. *Slide from Cornell Tutorial.*

twisted, creased, and folded nuclei with small or variable sized nucleoli (Figs. 3.459–3.462). In the human literature, these popcorn cells are also referred to as the *L&H* cells that are characteristic of the lymphocyte predominance type of HL that was historically known as the diffuse lymphocytic and histiocytic type of HL, as well the nodular type of L&H HL that is more common than the diffuse form.

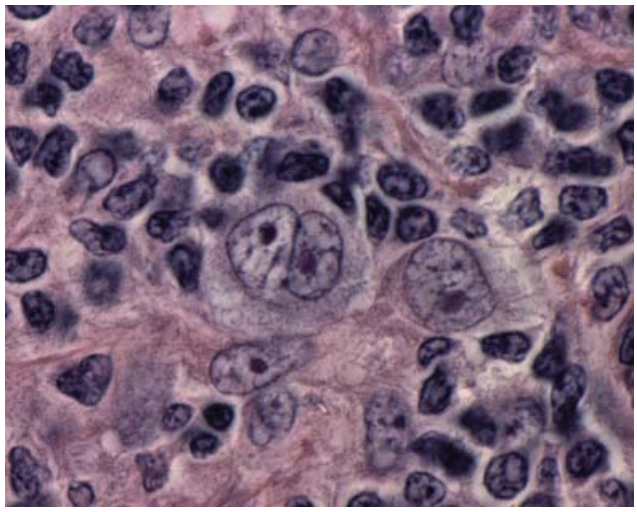

Figure 3.455. Human: lymph node, Hodgkin's lymphoma, mixed cellularity type. Detail of Figure 3.454. The background has low cellularity of small lymphocytes with the RS cells of the classic type with peripheralized chromatin and large central nucleoli.

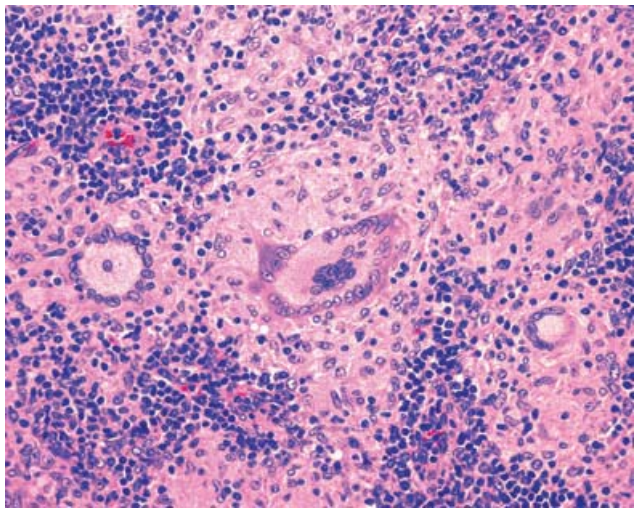

Figure 3.456. Human: lymph node, Hodgkin's lymphoma, mixed cellularity type. Multiple giant cells characteristic of the mixed cellularity subtype of HL. *Slide from Cornell Tutorial.*

The large cells in the cat have abundant cytoplasm and are often seen undergoing both degeneration, which is more correctly necrosis than apoptosis (Fig. 3.463), as well as mitosis (Fig. 3.464). In the early stages of degeneration, the cytoplasm of these large cells retracts from the neighboring tissue and makes these cells obvious at low-power observation and similar to the human "lacunar type" of RS cell. They may have a multilobated nucleus and may resemble the popcorn cells of Hodgkin's lymphoma of the lymphocyte predominance type. Nodular sclerosis is not seen in animal lymphomas in the

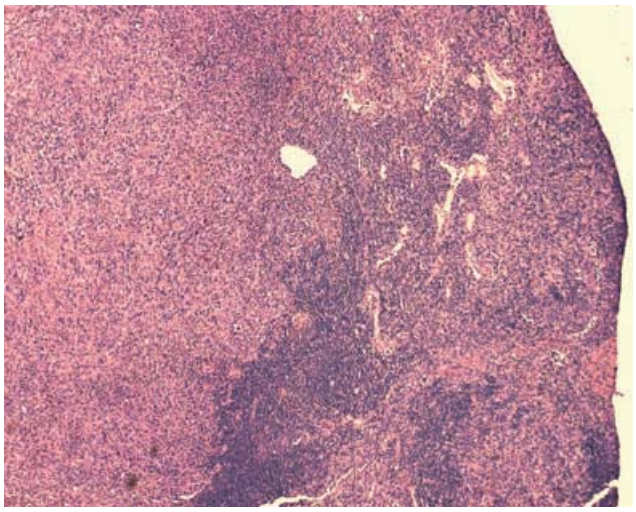

Figure 3.457. Human: node, excisional biopsy, Hodgkin's lymphoma, lymphocyte depletion type. The tissue has a coarsely variegated appearance with focal areas of fading germinal centers and paracortex with large diffuse areas of no lymphoid cellularity and focal areas of ischemic necrosis. *Slide from Cornell Tutorial.*

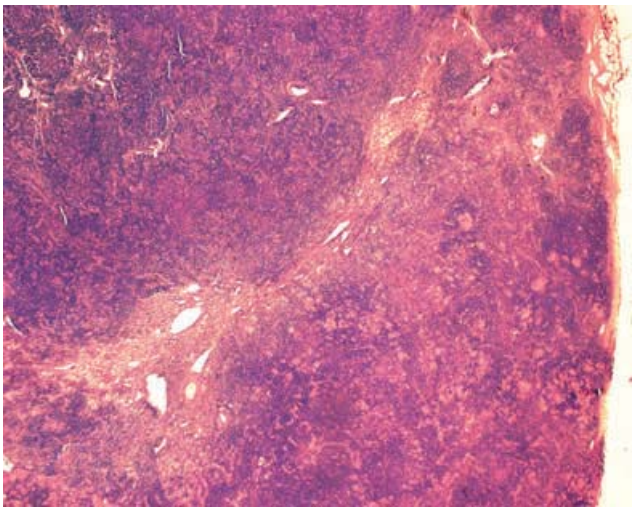

Figure 3.459. Human: lymph node, Hodgkin's lymphoma, lymphocyte predominance type. The capsule is thinned with the peripheral sinus compressed or destroyed but without areas of perinodal colonization. There is destruction of the internal architecture with densely cellular areas and adjacent focal areas of increased stroma but no areas of ischemic necrosis. *Slide from Cornell Tutorial.*

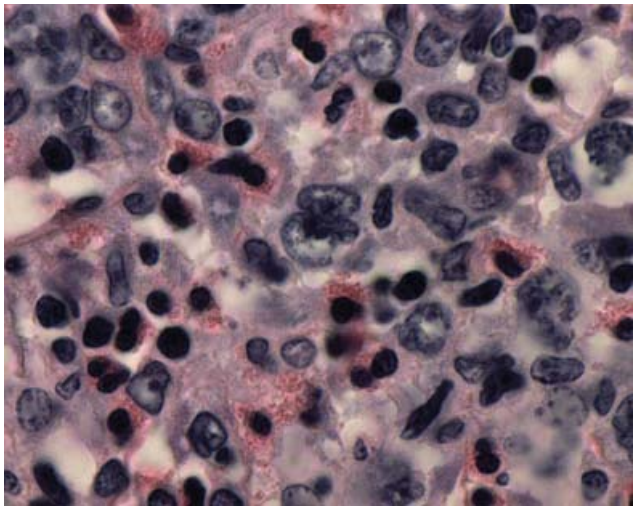

Figure 3.458. Human: node, Hodgkin's lymphoma, lymphocyte depletion type. Detail of Figure 3.457. A Reed-Sternberg cell with incomplete peripheralization of chromatin (center) surrounded by numerous eosinophils and increased stromal cells with small lymphocytes.

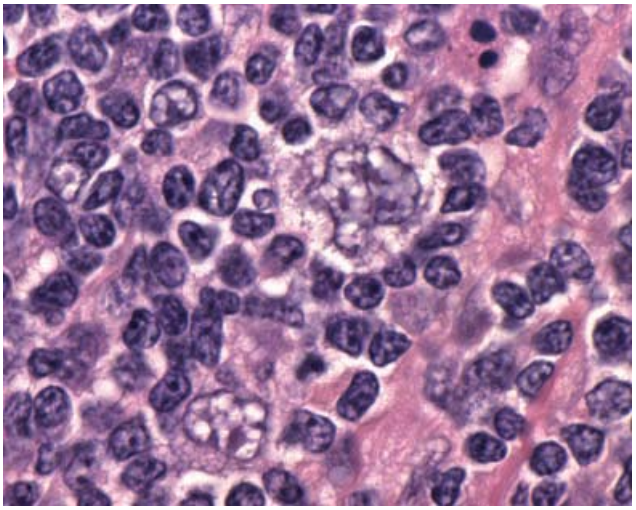

Figure 3.460. Human: node, Hodgkin's lymphoma, lymphocyte predominance type. Large cells with multilobulated "popcorn"-type nuclei and multiple nucleoli are present in a background of small and medium lymphocytes. *Slide from Cornell Tutorial.*

same context as in the human cases, but all animal TCRLBCL cases have diffuse sclerosis as noted above that accounts for the cohesive nature of the biopsied tissues. Recently, a new subtype of HL has been defined termed *lymphocyte rich*, which differs from the lymphocyte predominance type in having very few RS cells that are of the classic type and distinguish this subtype from the lymphocyte predominance type that has variant type of RS cells. Morphologic overlap is recognized and immunophenotype is required to distinguish these two forms of HL. The biological similarities of the cat TCRLBC lymphoma to HL are in the tendency to spread by contiguity and in the mixture of cells present accompanied by the large atypical popcorn-type cells and in animal terms, a relatively indolent course.

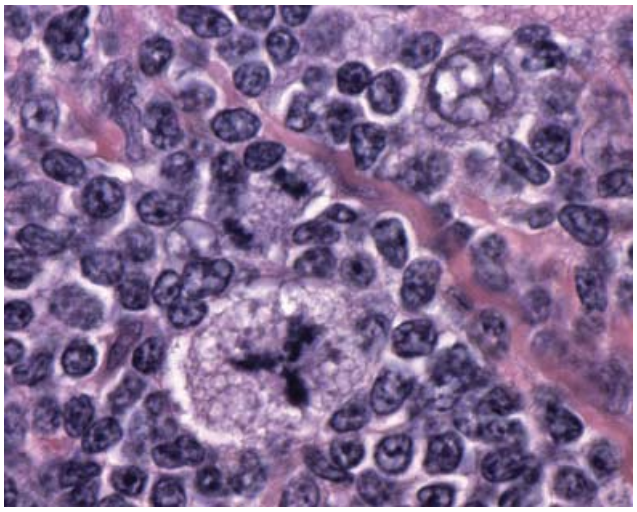

Figure 3.461. Human: lymph node, Hodgkin's lymphoma, lymphocyte predominance type. Detail of Figure 3.460. Popcorn-type cell has an abnormal tripolar mitosis and more normal-appearing anaphase to the above. The large cell in the upper left is of the same cell type as the more lobulated forms of popcorn-type cells.

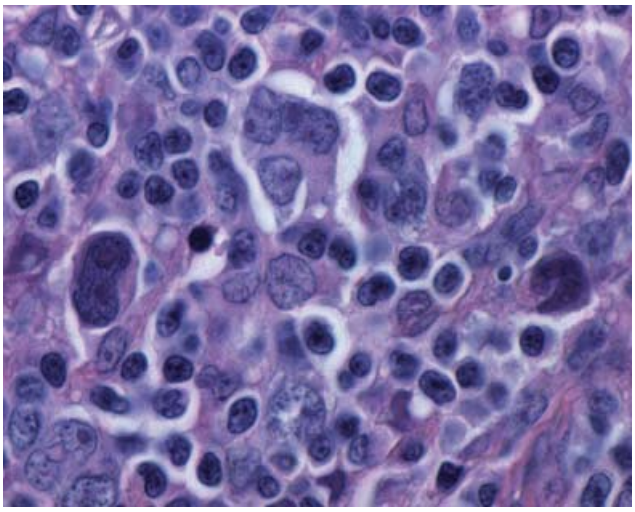

Figure 3.463. Cat: lymph node, T-cell rich large B-cell lymphoma. Detail of Figure 3.462. The popcorn-type cells of this type of lymphoma are frequently found undergoing contraction from surrounding tissues with increased cytoplasmic eosinophilia and nuclear condensation and hyperchromicity with progression to complete necrosis.

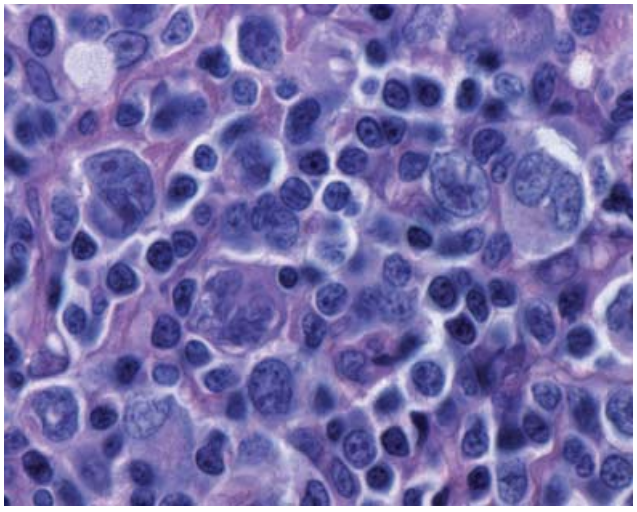

Figure 3.462. Cat: lymph node, T-cell rich large B-cell lymphoma. There are popcornlike cells, multinucleated cells with delicate folded and overlapping nuclear membranes, with large nucleoli and abundant cytoplasm. *Slide from F. A. Juck, DVM.*

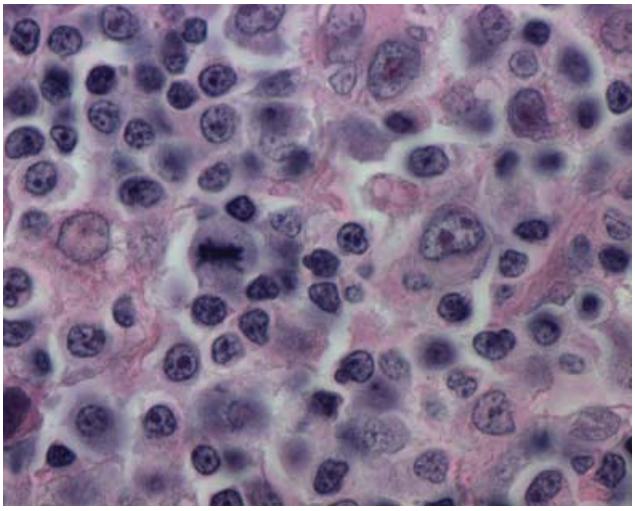

Figure 3.464. Cat: lymph node, T-cell rich large B-cell lymphoma, same case as Figure 3.462. A large popcorn-type cell is undergoing mitosis.

Spleen

The lymphomas in the equine spleen appear to be of small cell or other than TCRLBCL type. In the cat, the spleen is seldom involved in TCRLBCL, and when present there is only mild enlargement of the spleen in the early stages, with complete loss of germinal centers and relatively broad areas of cellular proliferation around each arteriole. Cytologically, the cells are predominantly of small and intermediate types, with the large cells with vesicular nuclei and prominent nucleoli relatively infrequent and tending to be at the periphery of the focal mass. TCRLBCL occurs in the spleen of the mouse and may arise there as a primary site (Figs. 3.465, 3.466).

Other Organs

The skin may be involved with TCRLBCL in both the cat and dog as well as in the horse where the disease is most often found. It appears that in both cat (Figs.

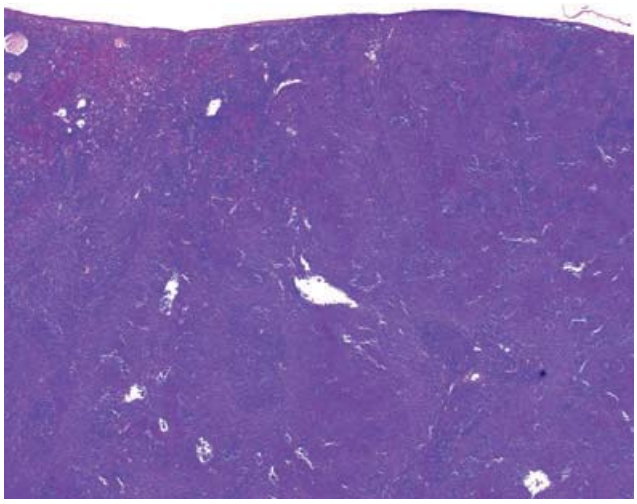

Figure 3.465. Mouse: lymphoma, diffuse mixed cell type. There is marked thinning of the capsule and wide separation of the trabeculae indicating splenomegaly. There is complete loss of architecture with only vague outlines of periarteriolar lymphoid sheaths. *Slide from J. M. Ward, DVM.*

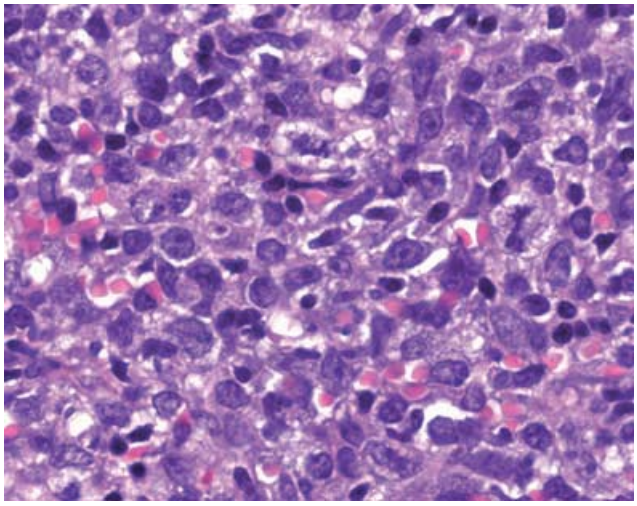

Figure 3.466. Mouse: lymphoma, diffuse mixed cell type. Detail of Figure 3.465. The neoplasm resembles T-cell rich large B-cell lymphoma of other species with numerous small lymphocytes in the background and a neoplastic population of cells with large vesicular nuclei that have 1–2 prominent nucleoli. The cytoplasm is moderate in volume and staining density and cell boundaries are generally indistinct. There are 2 cells in mitosis. The red cells provide an index of cell size.

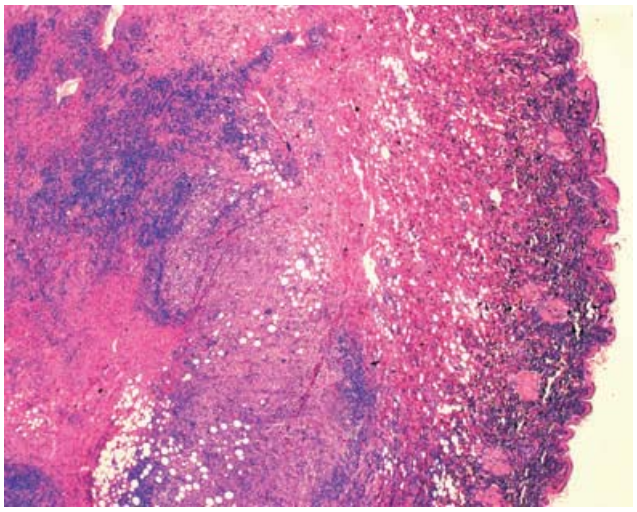

Figure 3.467. Cat: skin, T-cell rich large B-cell lymphoma. The tumor is arising in the panniculus and displacing fat with the overlying skin largely uninvolved.

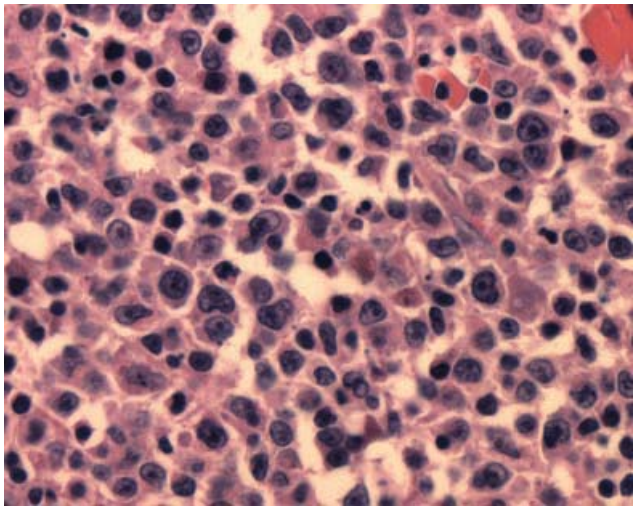

Figure 3.468. Cat: skin, T-cell rich large B-cell lymphoma. Detail of Figure 3.467. The histology is much like that of a node with atypical large cells in a background of small and medium lymphocytes with an unobtrusive reticular and fibrovascular network.

3.467–3.470) and dog (Figs. 3.471, 3.472), TCRLBCL in the skin presentation is largely a disease of the panniculus as in the horse, with the skin largely uninvolved until the tumor has become large when ulceration may occur. The TCRLBC lymphomas involve many tissues and, in comparison to other lymphomas, are occasionally found in the lung. The latter finding may be less a statement of the degree of aggression of the tumor and more a function of the animal surviving a relatively long time and providing more opportunity for spread. The liver and kidney are often involved, as is the small intestine and mesenteric nodes. Involvement of the liver is often in very large solid foci rather than a diffuse clustering around portal and central vein areas. Renal involvement is primarily cortical with focal clusters in inner areas that appear to follow in cuffs around the larger vessels.

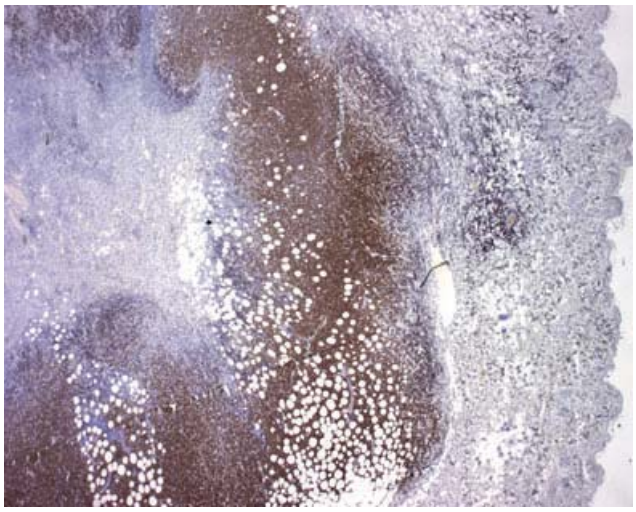

Figure 3.469. Cat: skin, T-cell rich large B-cell lymphoma. Phenotype of Figure 3.467. On staining with CD79, the lesion is more like cutaneous large B-cell lymphoma with the B-cells greatly predominating.

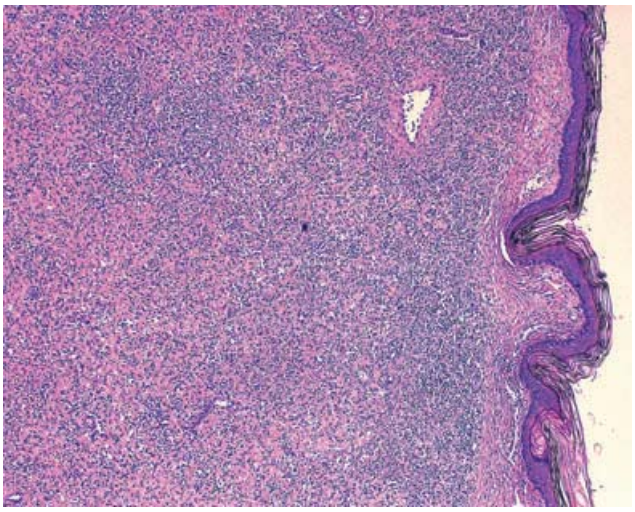

Figure 3.471. Dog: skin, T-cell rich large B-cell lymphoma. There is a broad Grenz zone sparing most of the dermis with a diffuse neoplasm extending into the panniculus.

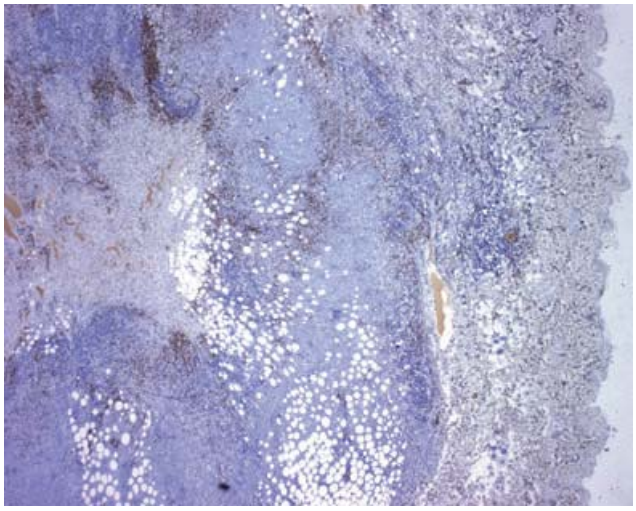

Figure 3.470. Cat: skin, T-cell rich large B-cell lymphoma. Phenotype of Figure 3.467. On staining with CD3, there are many cells labeled, but the intermixing is not as uniform as in the nodal form of this type of lymphoma.

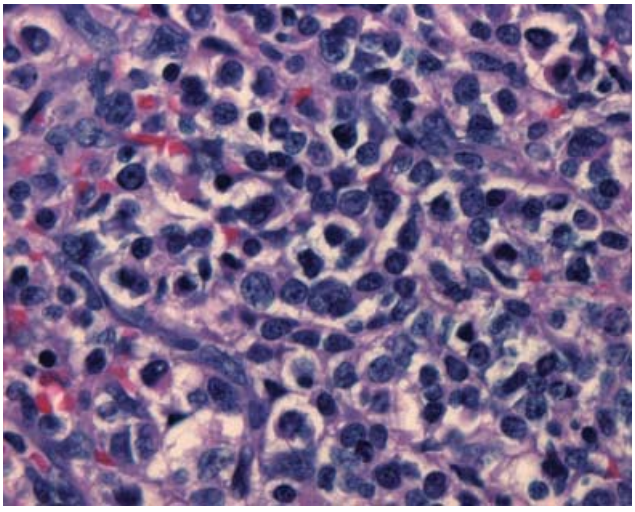

Figure 3.472. Dog: skin, T-cell rich large B-cell lymphoma. Detail of Figure 3.471. Throughout much of the tumor, there is a constant intermixing between large cells with obvious nucleoli and a predominant population of small more mature cells with compact nuclei.

Immunologic Features

The small cells of the TCRLBC lymphoma mark normally with CD3, and the large cells of the horse mark consistently with CD79 alpha and likely with CD20. In the cat, the small cells mark with CD3 (Fig. 3.473), but the largest cells with the vesicular nuclei mark about 2–5% with B cell reagents (Fig. 3.474). The cells, with nuclei 2.5–3.0 red cells in diameter, tend to mark much more consistently with CD79 than with CD20, but CD79 will as an artifact mark the nuclei of many of the large atypical cells (see Fig. 3.474). BLA36 antibody is derived by vaccination with human RS cells and marks the large cells in the cat more frequently than CD79, but it also marks a lot of the cells that otherwise stain with CD3. The staining of TCRLBCL for light chain restriction does not appear to have been well evaluated at least in animals and neither has the staining for surface or cytoplasmic imunoglobulin. Because the disease is so heterogenous in humans, it has not survived as a clear-cut immunologic entity that

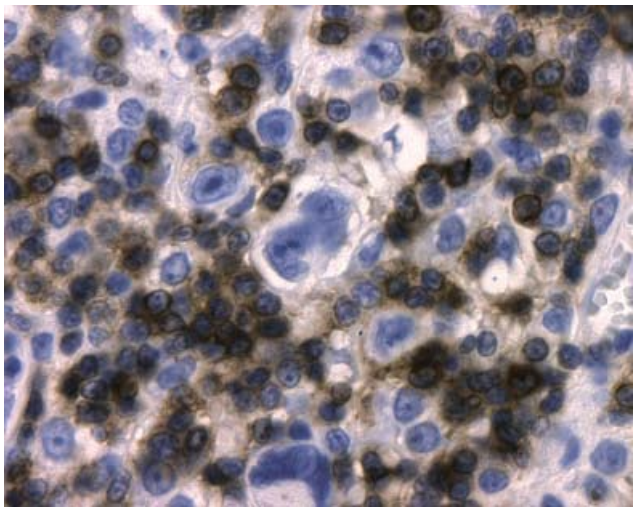

Figure 3.473. Cat: lymph node, T-cell rich large B-cell lymphoma. Phenotype of Figure 3.448. On staining with CD3, the large atypical cells with prominent nucleoli are completely negative and the small and some medium-sized lymphocytes are strongly and uniformly marked throughout all areas of the tissue.

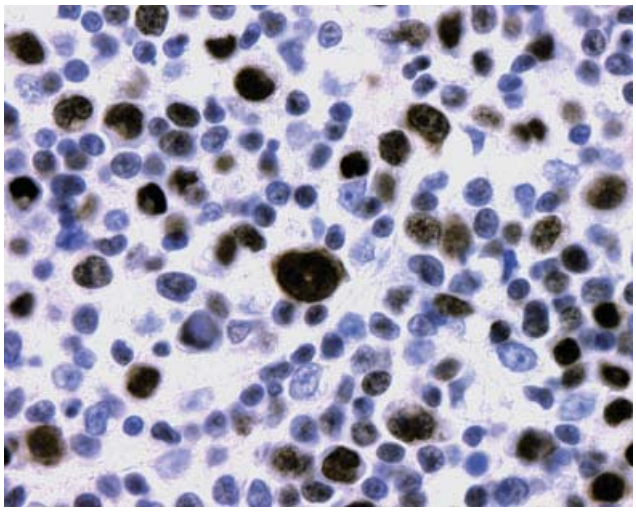

Figure 3.474. Cat: node, T-cell rich large B-cell lymphoma. Phenotype of Figure 3.448. With CD79 staining, there is extensive artifactual nuclear marking of the large atypical cells, with a low percentage having actual cytoplasmic labeling (center). The small cells are uniformly negative.

has lead to its inclusion as a variant of diffuse large B-cell lymphoma.

Cytogenetic and Molecular Features

In the human cases considered to be of TCRLBCL type, PCR techniques have demonstrated rearrangement of the IgH and IgL genes, but the T-cells present are found to be polyclonal and reactive. In single cell analysis obtained my micromanipulation the DNA from single large cells that were CD20 positive were clonal for the variable region of the IgH and IgL genes. In addition the *BCL2* gene was found to be rearranged in some human cases, which suggests a relation to follicular lymphoma. No studies of this type are available for animals bearing TCRLBC type lymphomas.

Cell of Origin

In studies on human TCRLBCL, the findings of rearranged Ig genes strongly indicates that the neoplastic B-cells of this variant have, like other diffuse large B-cell lymphomas, all arisen from postgerminal center cells. Because some intraclonal diversity has been found, it is still unclear whether this is due to the stage of cell differentiation at the time of testing or whether in the TCRLBCL variant there may be some continuing mutation of the variable portion of the Ig gene as occurs in the lymphocyte predominance type of Hodgkin's lymphoma.

Diagnostic Criteria

In the horse and the cat, the presentation of multiple small subcutaneous masses in the horse and a single large cervical node in an elderly cat are very highly suggestive of TCRLBC type lymphoma. At the architectural level, a subcutaneous mass from a horse or a node from a cat with a diffuse proliferation of mixed cell type is likely to be TCRLBC lymphoma. In addition the very cohesive nature of these tissues with no artifactual cracking or tearing of the tissue is suggestive of a very fine and cohesive fibrovascular supporting network. Cytologically, in these lesions the major difference with other neoplasms is that the homogeneity generally associated with lymphoma is replaced by a mixed cellular population. In most cases of TRCB, the small mature-appearing T-cells predominate by a wide margin with the vascular background relatively inconspicuous. About half of these cells have nuclei slightly larger than a red cell, and the rest have nuclei of intermediate cell size, round and oval, and often with shallow indentations about 1.5–2.0 red cells in diameter. Both of these cell types have a coarse granular chromatin pattern without parachromatin clearing and with most of the larger cells having a small inapparent nucleolus. The large cells may be only 5% or less of the population and have nuclei 2.5–3.0 red cells in size but with vesiculation and peripheralized chromatin and a prominent nucleolus. That pattern is uniformly seen in the horse, but in the cat some cases will have this description plus a few of the very large nuclei of the classical round, oval, or binucleated type or of the multilobated popcorn nuclear type. All of these larger cells have relatively abundant cytoplasm that may be apparent because of increased staining density associated with onset of apoptosis.

Differential Diagnosis

Presentation for the horse and the cat is very suggestive of the microscopic diagnosis of TCRLBCL. Architecturally, in all animals there is a diffuse proliferation with few remaining germinal centers beneath the node capsule and filling and compression of the medullary structures. Cytologically, T-cell rich large B-cell lymphoma needs to be differentiated from benign hyperplasia that is more likely to be the case if there are numerous remaining germinal centers with the paracortex typically having a mixture of small lymphocytes, a few large cells of dendritic type, and usually some macrophages.

Staging

In horses, the multifocal type of skin presentation tends to persist, and extension is a late occurrence that is usually preceded by elective destruction. In contrast, the disease occasionally occurs as a single very large subcutaneous mass often in the pectoral region that may reach 30–40 cm in diameter with ulceration and elective termination. In the cat, if the presentation is a peripheral node, the attention needs to be directed at contiguous regional nodes or the mediastinum if the index node is cervical. If the disease presents in the intestinal tract, the mesenteric nodes are almost always involved. In the intestine itself, the disease begins as a mucosal lesion and will extend widely laterally before bridging the intestinal muscular wall.

Transformation and Progression

Progression of TCRLBC lymphoma occurs without cell transformation but with an increasing proportion of large neoplastic B-cells and with fewer small benign T-cells. A diagnosis once established for TCRLBCL can be expected to be consistently confirmed at subsequent biopsies, even if repeated on recurring lesions at yearly intervals. Larger nodal lesions with progression are likely to have large areas of ischemic necrosis. Animals with mediastinal lesions may present with acute respiratory distress because a large mass that had been tolerated without symptoms increased rapidly in size due to spreading ischemic necrosis. Animals with intestinal lesions develop ulceration of the mucosa and have a neutrophilic leukocytosis with toxic changes in granulocytes, but they seldom have perforation of the bowel and peritonitis as occurs in more high-grade lymphomas.

Evaluation of the Treated Animal

In human cases of TCRLBC type of lymphoma, the response to treatment is still likely to provide a durable complete remission, even in cases that present with well-established bone marrow involvement. Because the nodal tumors as well as those involving other tissues have a high proportion of supporting stroma, even an effective destruction of neoplastic cells may not result in complete resolution of nodal or other lesional enlargement, and in measuring response to therapy the nature of the histology needs to be kept in mind.

Treatment and Survival

In human medicine, the standard of care treatment for diffuse large cell lymphoma was radiation until about 1980, and with this regimen alone survival at 5 years of up to 80% was achieved in some studies. More recently, doxorubicin-based therapy has been used accompanied by radiation, particularly for patients who present with bulky disease of 10 cm diameter or more, and survival has still been in the range of 80% at 5 years and 50% at 10 years. Newer strategies include combination therapies using anthracycline drugs in younger patients with extensive disease, and bone marrow transplant has been tried that provided long-term failure-free survival for 60–80% of patients. In the treatment of older patients, the use of the antibody Rituximab plus CHOP gave superior results to the use of CHOP alone. The TCRLBC lymphoma has not been segregated for treatment as an entity in animals, and the particular problems, if any, associated with management of this neoplasm are yet to be determined.

REFERENCES

Anagnostopoulos, I., Dallenbach, F., and Stein, H. (2001) Diffuse large cell lymphomas. In Knowles, D.M. (ed.), *Neoplastic Hematopathology,* 2nd ed., Lippincott Williams & Wilkins, Philadelphia, pp. 855–914.

Aquino, S.M., Hamor, R.E., Valli, V.E., Kitchell, B.E., Tunev, S.S., Bailey, K.L., and Ehrhart, E.J. (2000) Progression of an orbital T-cell rich B-cell lymphoma to a B-cell lymphoma in a dog. *Vet Pathol* 37:465–469.

Armitage, J.O., Mauch, P.M., Harris, N.L., Dalla-Favera, R., and Bierman, P.J. (2004) Diffuse large B-cell lymphoma. In Mauch, P.M., Armitage, J.O., Coiffier, B.C., Dalla-Favera, R., and Harris, N.L. (eds.), *Non-Hodgkin's Lymphomas*. Lippincott Williams & Wilkins, Philadelphia, pp. 427–453.

Brauninger, A., Kuppers, R., Spieker, T., Siebert, R., Strickler, J.G., Schlegelberger, B., Rajewsky, K., and Hansmann, M.L. (1999) Molecular analysis of single B cells from T-cell–rich B-cell lymphoma shows the derivation of the tumor cells from mutating germinal center B cells and exemplifies means by which immunoglobulin genes are modified in germinal center B cells. *Blood* 93(8):2679–2687.

Brousset, P., Chittal, S.M., Schlaifer, D., and Delsol, G. (1995) T-cell rich B-cell lymphoma in the lung. *Histopathol* 26:371–373.

Chang, C.C., Bunyi-Teopengco, E., Eshoa, C., Chitambar, C.R., and Kampalath, B. (2002) $CD5^+$ T-cell/histiocyte-rich large B-cell lymphoma. *Mod Pathol* 15(10):1051–1057.

Day, M.J., Kyaw-Tanner, M., Silkstone, M.A., Lucke, V.M., and Robinson, W.F. (1999) T-cell-rich B-cell lymphoma in the cat. *J Comp Path* 120:155–167.

Detilleux, P.G., Cheville, N.F., and Sheahan, B.J. (1989) Ultrastructure and lectin histochemistry of equine cutaneous histiolymphocytic lymphosarcomas. *Vet Pathol* 26:409–419.

De Wolf-Peeters, C., and Pittaluga, S. (1995) T-cell rich B-cell lymphoma: A morphological variant of a variety of non-Hodgkin's lymphomas or a clinicopathological entity? *Histopathol* 26:383–385.

Dunphy, C.H., and Nahass, G.T. (1999) Primary cutaneous T-cell–rich B-cell lymphomas with flow cytometric immunophenotypic findings. Report of 3 cases and review of the literature. *Arch Pathol Lab Med* 123:1236–1240.

Ferraro, P., Trastek, V.F., Adlakha, H., Deschamps, C., Allen, M.S., and Pairolero, P.C. (2000) Primary non-Hodgkin's lymphoma of the lung. *Ann Thorac Surg* 69:993–997.

Fitzgerald, S.D., Wolf, D.C., and Carlton, W.W. (1991) Brief communications and case reports. Eight cases of canine lymphomatoid granulomatosis. *Vet Pathol* 28:241–245.

Greer, J.P., Macon, W.R., Lamar, R.E., Wolff, S.N., Stein, R.S., Flexner, J.M., Collins, R.D., and Cousar, J.B. (1995) T-cell-rich B-cell lymphomas: Diagnosis and response to therapy of 44 patients. *J Clin Oncol* 13(7):1742–1750.

Harris, N.L., Jaffe, E.S., Stein, H., Banks, P.M., Chan, J.K.C., Cleary, M.L., Delsol, G., De Wolf-Peeters, C., Falini, B., Gatter, K.C., Grogan, T.M., Isaacson, P.G., Knowles, D.M., Mason, D.Y., Muller-Hermelink, H.K., Pileri, S.A., Piris, M.A., Ralfkiaer, E., and Warnke, R.A. (1994) A revised European-American classification of lymphoid neoplasms: A proposal from the International Lymphoma Study Group. *Blood* 84(5):1361–1392.

Henson, K.L., Alleman, A.R., Cutler, T.J., Ginn, P.E., and Kelley, L.C. (1998) Regression of subcutaneous lymphoma following removal of an ovarian granulose-theca cell tumor in a horse. *JAVMA* 212(9):1419–1422.

Jaffe, E.S., and Wilson, W.H. (1997) Lymphomatoid granulomatosis: Pathogenesis, pathology and clinical implications. *Cancer Surveys: Lymphoma* 30:233–248.

Lones, M.A., Cairo, M.S., and Perkins, S.L. (2000) T-cell–rich large B-cell lymphoma in children and adolescents. A clinicopathologic report of six cases from the Children's Cancer Group Study CCG-5961. *Cancer* 88(10):2378–2386.

Michishita, M., Nakamura, S., Sakakibara, I., Ono, F., Fujimoto, K., Kamiya, K., Ishii, Y., Hayashi, K., Yoshikawa, Y., and Takahashi, K. (2003) Spontaneous T-cell-rich B-cell lymphoma in a cynomolgus monkey (Macaca fascicularis). *Exp An* 52(4):339–344.

Miller, W.H., Tamke, P.G., and Scott, D.W. (1990) A spontaneously regressing pseudolymphoma in a dog resembling pseudo-Hodgkin's disease. *Vet Derm* 1:171–176.

Rudiger, T., Ott, G., Ott, M.M., Muller-Deubert, S.M., and Muller-Hermelink, H.K. (1998) Differential diagnosis between classic Hodgkin's lymphoma, T-cell-rich B-cell lymphoma, and paragranuloma by paraffin immunohistochemistry. *Am J Surg Pathol* 22(10):1184–1191.

Schmidt, U., Metz, K.A., and Leder, L.D. (1995) T-cell-rich B-cell lymphoma and lymphocyte-predominant Hodgkin's disease: Two closely related entities? *Brit J Haematol* 90: 398–403.

Steele, K.E., Saunders, G.K., and Coleman, G.D. (1997) T-cell-rich B-cell lymphoma in a cat. *Vet Pathol* 34:47–49.

Tanimoto, T., and Ohtsuki, Y. (1998) T-cell-rich B-cell lymphoma in a pig. *Vet Pathol* 35:147–149.

Valentine, B.A., Blue, J.T., Zimmer, J.F., Yeager, A.E., and McDonough, S.P. (2000) Pulmonary lymphomatoid granulomatosis in a cat. *J Vet Diagn Invest* 12:465–467.

Valli, V.E., Jacobs, R.M., Norris, A., Couto, C.G., Morrison, W.B., McCaw, D., Cotter, S., Ogilvie, G., and Moore, A. (2000) The histologic classification of 602 cases of feline lymphoproliferative disease using the National Cancer Institute Working Formulation. *J Vet Diagn Invest* 12:295–306.

Vernau, B., and Moore, P. (2001) Immunophenotyping in the dog. *Vet Cancer Soc Newsl* 25(1):1–12.

Vernau, W., Valli, V.E.O., Dukes, T.W., Jacobs, R.M., Shoukri, M., and Heeney, J.L. (1992) Classification of 1,198 cases of bovine lymphoma using the National Cancer Institute Working Formulation for human non-Hodgkin's lymphomas. *Vet Pathol* 29:183–195.

Walton, R.M., and Hendrick, M.J. (2001) Feline Hodgkin's-like lymphoma: 20 cases (1992–1999). *Vet Pathol* 38:504–511.

Chapter 4

T-Cell and NK-Cell Neoplasms

PRECURSOR T-CELL NEOPLASMS

Precursor T-Cell Lymphoblastic Lymphoma and Lymphoblastic Leukemia

Definition

Acute lymphoblastic leukemia (T-ALL) is a malignant lymphoproliferative disease arising in the thymus and bone marrow usually in young animals and characterized by the rapid onset of marrow failure. T-lymphoblastic lymphoma (LBL) is a neoplasm of peripheral tissues characterized by involvement of peripheral nodes with very rapid spread to parenchymal organs and bone marrow and by short remission and survival of treated animals. Both T-ALL and LBL are positive with CD3 and negative with CD79 and CD20.

Epidemiology and Features

In general, the T-cell lymphoid neoplasms are more common in animals than in humans. On an overall basis, LBL in humans is relatively rare and accounts for about 2% of all non-Hodgkin's lymphomas. There is a consistent male predominance in human LBL. In children, acute lymphoblastic leukemia (ALL) is very predominantly of B-cell type with the T-ALL making up about 15% of pediatric ALL and about 20% of adult ALL. In contrast, in dogs about 75% of chronic lymphocytic leukemia (CLL) is of T-cell type, again in contrast to the human incidence, and the proportion of T-ALL is less well characterized but is likely about half of cases. In 502 cases of a canine hematopoietic neoplasia, 69/502 or 13.7% were of T-cell derivation by immunohistochemical determination. On a topographic basis, almost all of these cases were lymphomas, with 6 cases of LBL and 3 cases of T-ALL. Three of the 6 cases of LBL were presented with generalized lymphadenopathy, with one in each of node, skin, and mediastinum. The cases of ALL were presented with blood and marrow involvement in all 3. The gender was known in 8, with 4 males and 4 females, and ages ranged from 2 years (ALL) to 14 (ALL) with a mean of 8 years.

In 751 cases of feline hematopoietic neoplasia, 22/751 or 2.9% were of ALL (12) or LBL (10) type without phenotypic determination. The gender was known in 21 cases, with 13 male and 8 female. The presentation of the LBL cases was mediastinal in 6 and most likely of T-cell type and multicentric in the other 4. The cases diagnosed as ALL had marrow involved in 9, with marrow not submitted in 3, and on these 3 cases the diagnosis was made on node in 2 and liver in 1.

Clinical Presentation and Features

In general, the animals with acute lymphoblastic tumors, whether of leukemic or nodal presentation, tend to be in animals in good general condition and indicative of an acute onset. In contrast to the more indolent lymphoid neoplasms, these animals are most often symptomatic and have reduced appetite and activity, with the diagnosis arrived at following presentation and routine clinical and laboratory examination. A small proportion of cases occur in young cats and dogs 1–2 years of age that develop a mediastinal mass that rapidly involves the bone marrow and generally presents with ALL, with the LBL in the thymic tissue discovered in subsequent examinations. It appears to be the case in animals as in adolescent humans that the cases of T-ALL have higher total leukocyte counts in the 50×10^3/ul and may have tumors in other areas besides the mediastinal mass and marrow. In older animals, LBL presents with peripheral involvement of lymph nodes or skin and becomes generalized with low levels of neoplastic cells in the blood, progression to hepatosplenomegaly, and heavy colonization of marrow, and it is likely diagnosed as ALL.

Pathologic Features

Blood

Historical perceptions of acute leukemia where the determinations were carried out without the benefit of immune detection, either by flow cytometry or immunocytochemistry, are likely to err in underestimating the cases of acute myeloid leukemia (AML) and without distinction of B- or T-cell types of ALL. Recent studies indicate that a least

half of acute leukemias in dogs are undifferentiated or poorly differentiated myeloid leukemias of the M0 or M1 level of development, as defined in the FAB (French-American-British, see Chapter 5, "Acute Myeloid Leukemias") classification system. About 70–80% of ALL in dogs is of T-cell type in similar proportion to that of CLL. The ALL of T- and B-cell type are not distinguishable on routine blood stains, and neither is distinguishable from poorly differentiated AML. About half of the cases of ALL of T-cell type are large granular lymphocytes (LGL), and of those about half are not marked by CD3 and are likely of NK-cell type. In terms of morphology, most of the cases of ALL in horses, dogs, and cats are of the L1 (Figs. 4.1–4.3) and L2 type, and most in the cow are of the L3 type by the FAB system (Figs. 4.4–4.7). ALL of T-cell type is likely to have a high leuko-

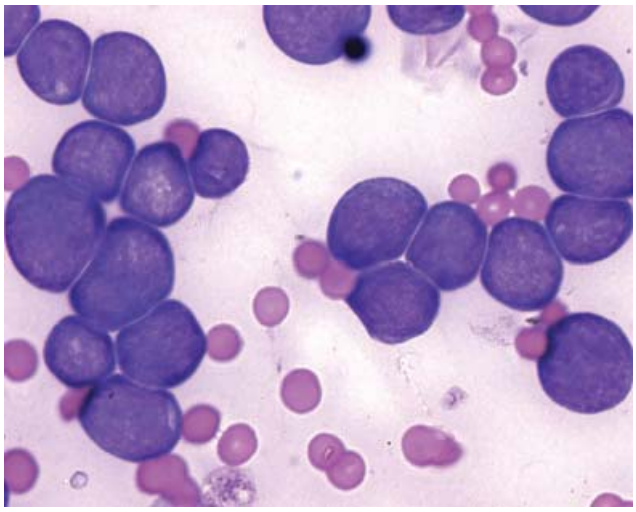

Figure 4.1. Cat: blood, acute lymphoblastic leukemia. A 5-year-old cat that presented with anorexia and depression was found to have splenomegaly with a leukocyte count of 338,000 on examination of blood. Over 90% of the peripheral cells were primitive lymphocytes with round nuclei and a narrow rim of highly basophilic cytoplasm. The chromatin is uniformly dispersed and deeply stained with inapparent nucleoli.

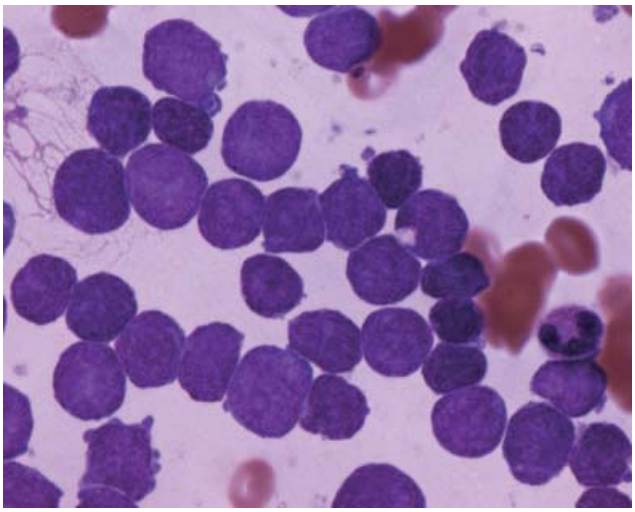

Figure 4.3. Human: marrow aspirate, ALL. Detail of Figure 4.2. The cells are small with some nuclei only slightly larger than red cells. They are regularly round with densely stained chromatin and a very narrow rim of cytoplasm. There are multiple nucleoli of moderate size that are irregularly apparent. These characteristics are typical of ALL of L1 type.

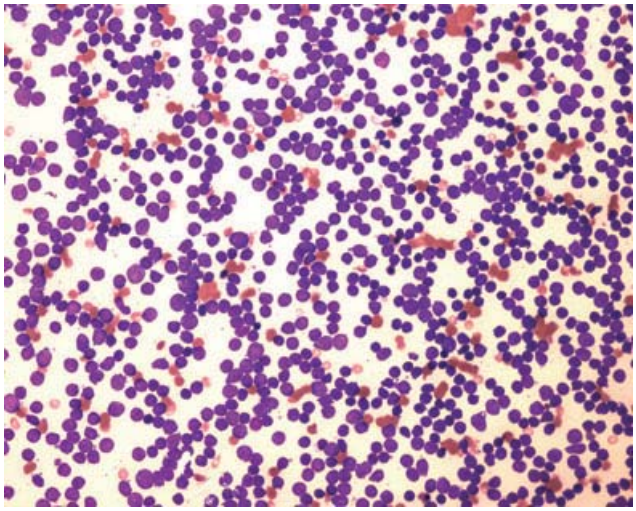

Figure 4.2. Human: marrow aspirate, precursor T-cell leukemia. There is complete phthisis of normal marrow cells with a homogenous population of undifferentiated leukocytes of intermediate size. *Slide from Cornell Tutorial.*

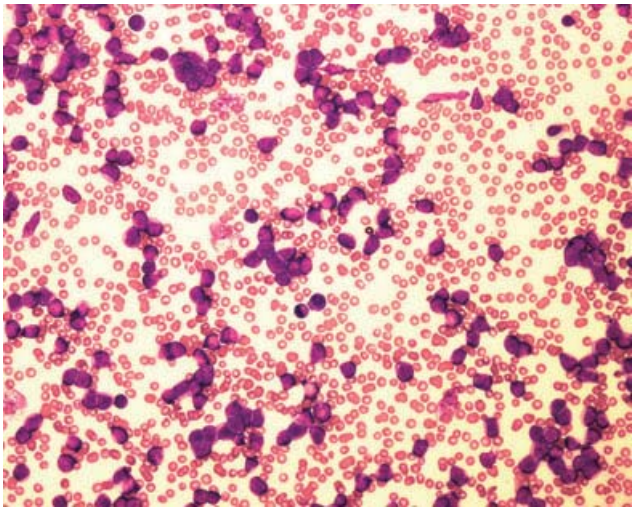

Figure 4.4. Dog: blood, acute lymphoblastic leukemia. The dog presented with a total leukocyte count of 422,000 with hemoglobin of 8.9 g per dl and platelets of 67,000 per ul. Note the tendency of the neoplastic cells to cohere.

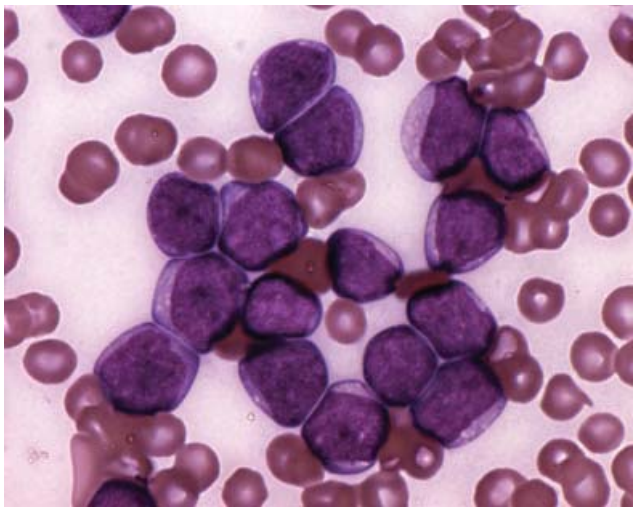

Figure 4.5. Dog: blood, ALL, L3 type. Note the fine nuclear indentations and fine cytoplasmic vacuolations. The chromatin pattern is fine and generally dispersed with nucleoli that are small, multiple, and inapparent.

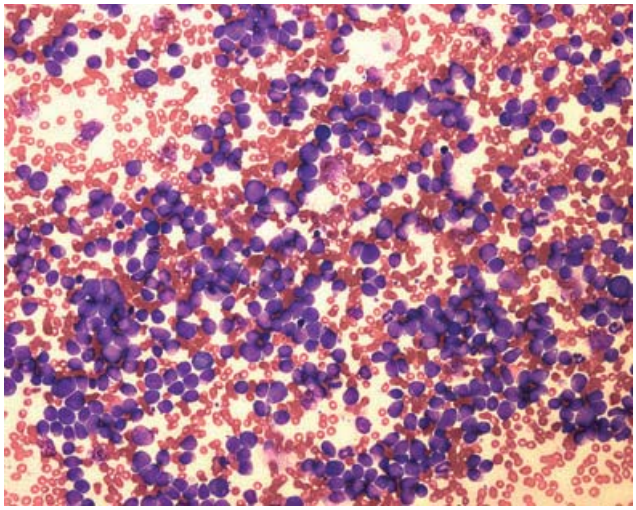

Figure 4.6. Dog: marrow aspirate, ALL, L3 type. There is almost complete phthisis of normal marrow elements with the uniform population of neoplastic cells of intermediate size.

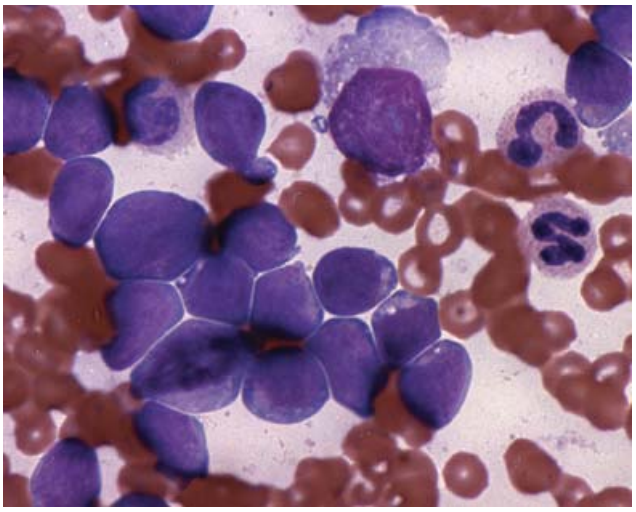

Figure 4.7. Dog: marrow aspirate, ALL. Detail of Figure 4.6. The nuclei are round to oval, moderately irregular, and 1.5–2.5 red cells in diameter. The chromatin is fine and uniformly dispersed with nucleoli small and generally inapparent but more obvious with rupture of the nuclear membrane (upper right). The cytoplasm is deeply basophilic with fine peripheral vacuoles. The cell with oval nucleus and irregular outline in the lower left is in metaphase.

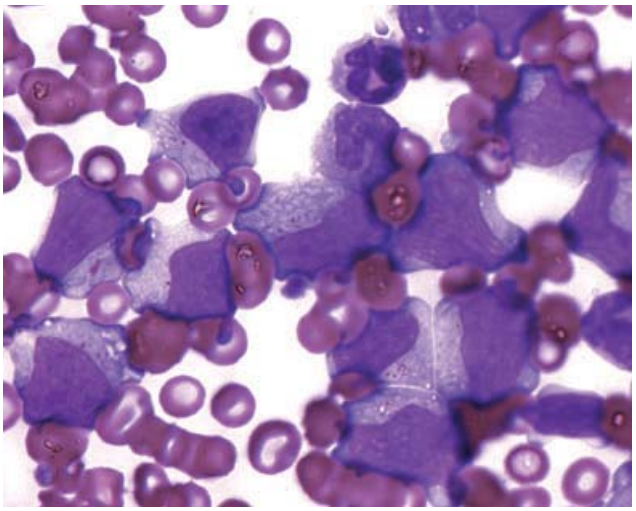

Figure 4.8. Dog: blood, acute lymphoblastic leukemia. Morphologically, these cells resemble the L2 type of ALL with irregular-shaped nuclei that have more abundant cytoplasm containing a small number of distinctly stained azurophilic granules. The neutrophil (top) is indication that the animal is not neutropenic.

cyte count, generally in excess of 100,000/ul, and accompanied by anemia of moderate to severe degree and thrombocytopenia of less that 50,000/ul. Oddly, the cases of ALL of LGL type are also characterized by anemia and thrombocytopenia of similar degree, but unlike the cases in humans are not neutropenic (Fig. 4.8).

Bone Marrow

As a general rule of thumb, there is little evidence of marrow insufficiency in the peripheral blood until at least half of the bone marrow is involved with tumor. Therefore in animals that present with ALL and some degree of anemia or thrombocytopenia, it can be expected that the marrow will be heavily involved (see Figs. 4.6, 4.7). The pattern of marrow involvement was described for the dog in various types of leukemia, with animals with ALL likely to have a mixed focal and interstitial pattern (Figs. 4.9–4.11) or largely interstitial pattern with the tumor

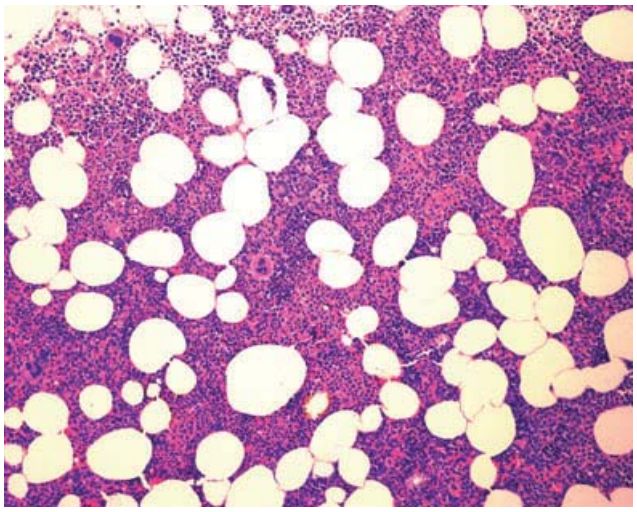

Figure 4.9. Dog: bone marrow, ALL. Both diaphyseal and femoral marrow have small focal areas of increased cellularity and density composed of diffuse infiltration of neoplastic cells.

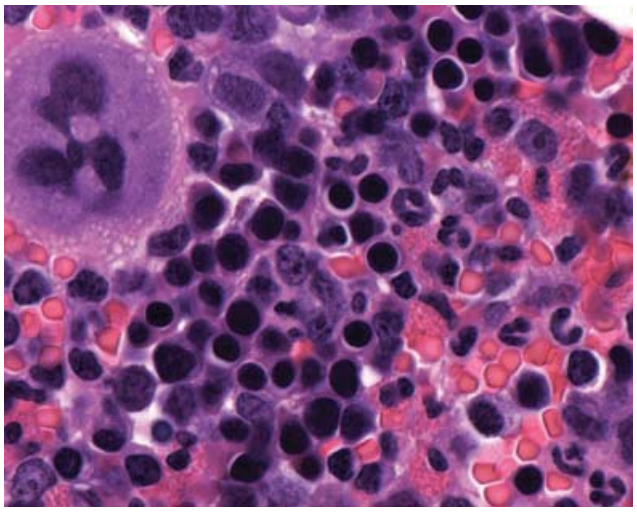

Figure 4.10. Dog: bone marrow, ALL. Detail of Figure 4.9. The neoplastic cells have infiltrated the marrow in small dense clusters that displace normal marrow cells and are apparent by their nuclear homogeneity.

displacing normal hematopoiesis, including fat cells in large foci that span trabecular spaces. As in other leukemias, the involved areas of marrow are apparent at low power magnification due to the absence of fat cells in focal areas and at greater detail by the homogeneity of cell type with an absence of the typical small, densely stained, round nuclei of developing rubricytes.

Lymph Node

Lymphoblastic lymphoma usually has expanded beyond the nodal capsule at the time of diagnosis and has

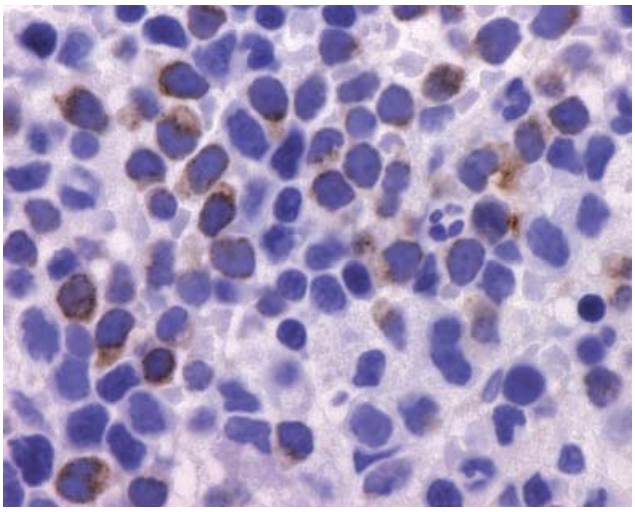

Figure 4.11. Dog: marrow. Phenotype of Figure 4.9. With CD3 staining, the neoplastic cells are marked to varying degrees depending on their low cytoplasmic volume. The nuclei appear bland, with dispersed chromatin, and slightly larger as a result of the antigen retrieval process.

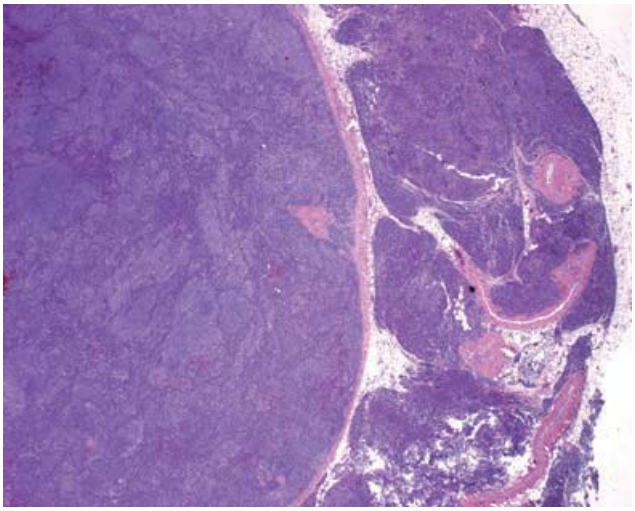

Figure 4.12. Dog: lymph node, lymphoblastic lymphoma. The capsule is thinned, with the peripheral sinus compressed and a broad area of involvement of perinodal fatty tissue. There is complete loss of germinal centers, with the node having diffuse architecture and varying levels of focal congestion.

advanced in several "tide marks" into the surrounding perinodal tissue (Fig. 4.12). There may be a scalloping effect in the original nodal margin that represents growth of the neoplasm around the residual subcapsular germinal centers. The peripheral sinus is destroyed around most or all of the nodal margins with solid tissue on either side of the remaining nodal capsule. The arrangement of the neoplastic cells in the peripheral areas and in infiltrating

the capsule is characteristically in linear columns referred to as "indian file" arrangement. The interior of the node has a diffuse architecture and, unlike the indolent lymphomas, there is likely to be ischemic necrosis of the center of the node rather than sclerosis of medullary supporting structures. Medullary cord and sinus structures are invariably absent, and the increase in nodal size tends to dilute any clusters of residual plasma cells in the medullary region. It is almost essential in dealing with LBL with nodal excision that the tissue be examined near the outer margin of tissue in order for the chromatin pattern typical of this neoplasm to be recognized (Figs. 4.13–4.15).

Cytologically, the cells of LBL are of intermediate size—that is, larger than a thymic cortical lymphocyte and smaller than large cell lymphoma. In working terms, the nuclei are 1.5–2.0 red cells in diameter, are round to oval, and may have sharp shallow indentations in the lymphoblastic convoluted (LBC, Fig. 4.16) form of the disease. There does not appear to be a survival value in the presence or absence of the nuclear indentations in humans or animals, but their presence should be anticipated for diagnostic recognition. The two most important criteria in the recognition of LBL are the fine uniform chromatin pattern and the inapparent nucleoli. The reason for examining the cells at the edge of the tissue is that unless fixation is rapid there is aggregation of chromatin and parachromatin clearing of the cells with delayed fixation and the major diagnostic criteria lost (Figs. 4.17–4.20, see also Fig. 4.16). A further, most important, observation is the presence of a high mitotic rate, usually 5–15/400× field (see Fig. 4.18). If a high mitotic rate is found in a diffuse lymphoma of intermediate nuclear size, LBL should be considered and cells at the periphery closely examined for fine chromatin distribution. The mitoses of LBL are oddly not easily identified, and unlike other lymphomas the metaphases do not have sharp chromosomal boundaries and are often seen in polar aspect, with the chromosomes arranged in a circular pattern of slightly greater diameter than an intact

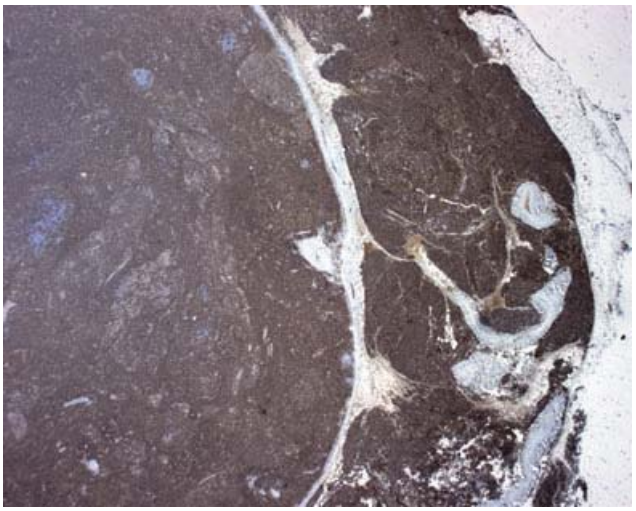

Figure 4.14. Dog: node, lymphoblastic lymphoma. Phenotype of Figure 4.12. With CD3 staining, the tissue is solidly and uniformly labeled.

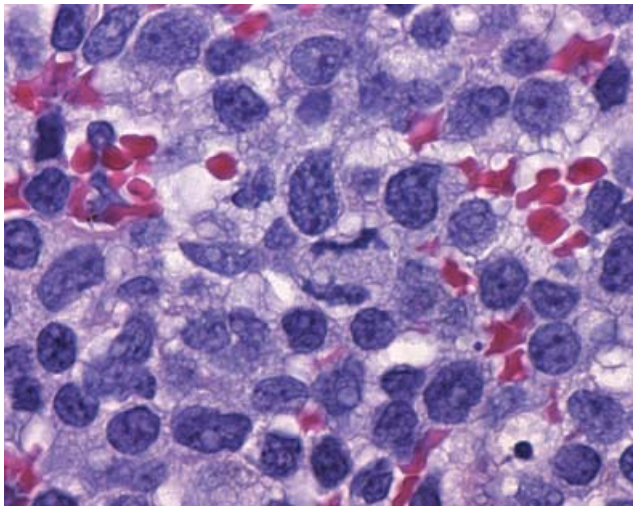

Figure 4.13. Dog: lymph node, lymphoblastic lymphoma. Detail of Figure 4.12. Image from near the edge of the specimen, for optimal fixation. The nuclei are round to oval, 1.5 red cells in diameter with dispersed chromatin and small or inapparent nucleoli. There is an anaphase in the center that is characteristically unobtrusive and easily overlooked.

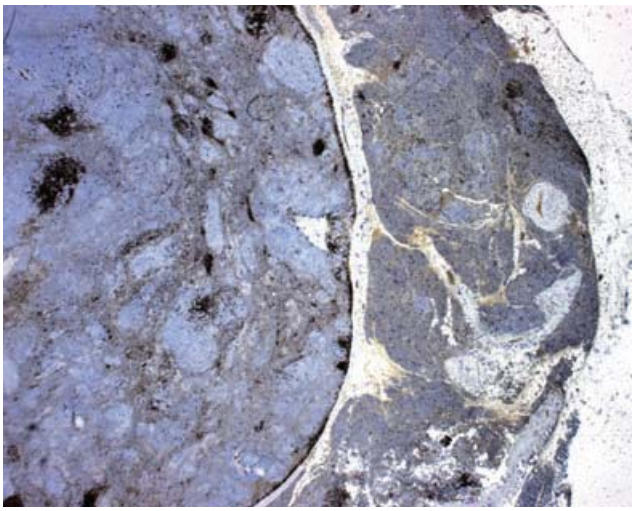

Figure 4.15. Dog: node, lymphoblastic lymphoma. Phenotype of Figure 4.12. With CD20 staining for B-lymphocytes, the tissue is very largely negative with a thin rim of residual benign cells beneath the capsule and irregularly within the node cortex and outer areas of infiltration.

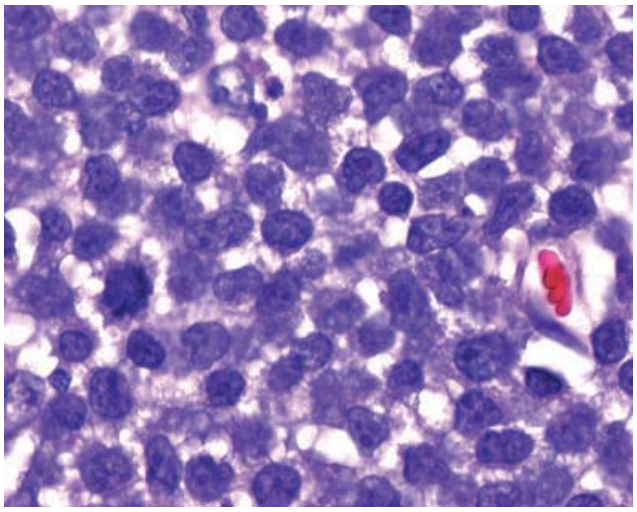

Figure 4.16. Dog: lymph node, lymphoblastic lymphoma. This tissue demonstrates the lymphoblastic convoluted type of LBL. The nuclei are generally 1.5 red cells in diameter but more variable in size and have sharp, shallow irregular nuclear indentations. The chromatin is generally dispersed with small, often multiple nucleoli, as evident in several nuclei. The cytoplasm is moderate in volume and staining density with cell boundaries indistinct. There is a cell in metaphase in the axial plane in the left center that is unusually apparent for this type of neoplasm and a second mitotic cell in the center of the field that is not in sharp focus and appears as a blurred column of basophilia between the adjacent cells. The latter type of mitotic figure at right angles to the centriolar axis is much more common and more easily overlooked. Without recognition of the high mitotic rate, the small cell character of the neoplasm may suggest a less aggressive lesion.

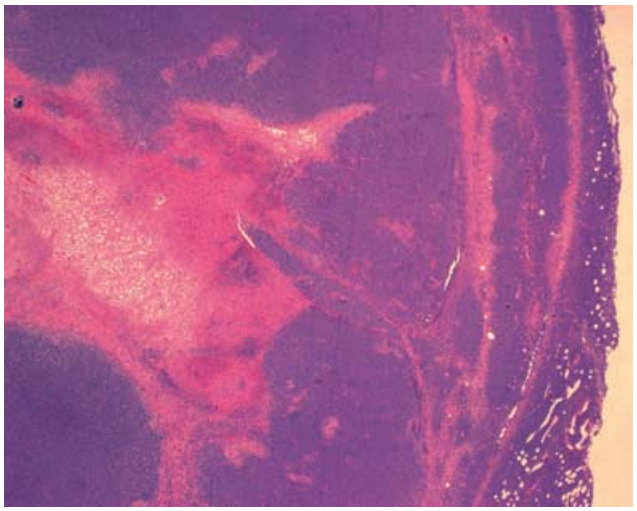

Figure 4.17. Dog: node, lymphoblastic lymphoma. The central area of the node is infarcted with a rim of intact tissue at one end. Note the tide marks near the right representing successive invasions of peripheral encapsulation.

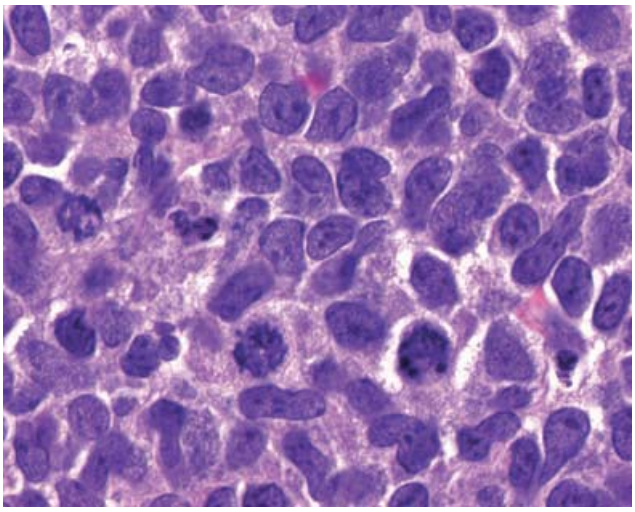

Figure 4.18. Dog: node, lymphoblastic lymphoma. Detail of Figure 4.17. Image from the edge of the tissue, with early fixation. The nuclear membranes are delicate and well defined with uniformly dispersed chromatin and small nucleoli evident in about half of the cells. The nuclear irregularities would classify this as lymphoblastic convoluted. There are 3 cells in metaphase in the field and 4 undergoing apoptosis. The cytoplasm is typically moderate in volume and staining density with cell boundaries undefined.

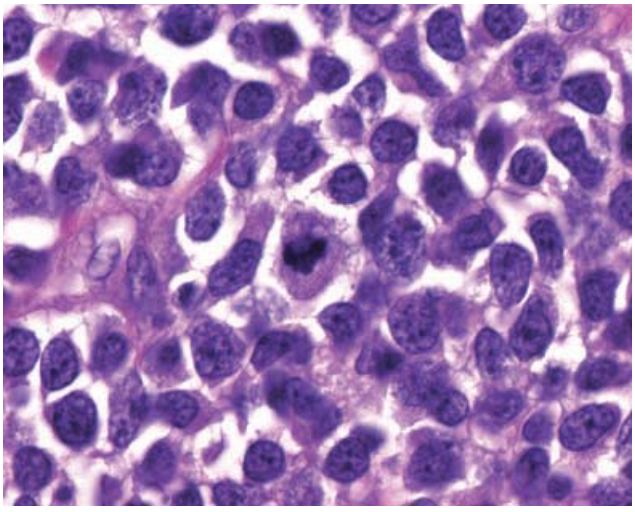

Figure 4.19. Dog: lymph node, lymphoblastic lymphoma. Detail of Figure 4.17. This image was taken from an inner area of the node where the cells are viable but fixation was delayed due to the depth of tissue. There are fewer mitoses and more stromal tissue with nuclei appearing more vesicular and the chromatin irregularly aggregated and nucleoli generally more prominent. These changes lose the qualities of chromatin dispersion and inapparent nucleoli that are key to recognition of lymphoblastic lymphoma.

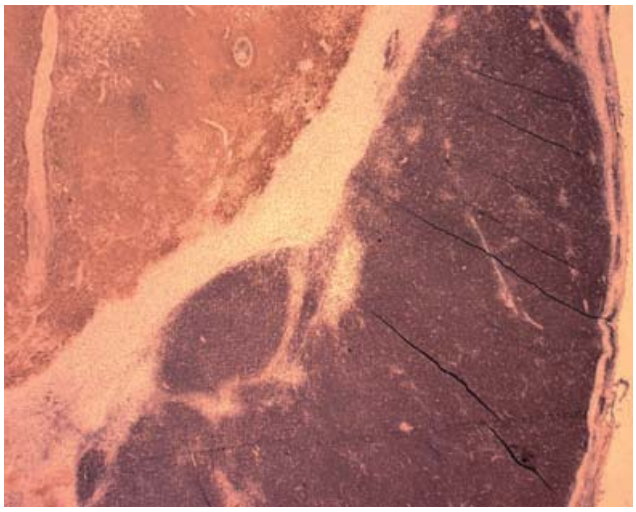

Figure 4.20. Dog: node. Phenotype of Figure 4.17. With CD3 stain, the viable outer rim is solidly and uniformly labeled with a broad boundary of connective tissue separating the infarcted inner mass from the surrounding area of viable tissue. This would suggest that the infarction occurred some weeks earlier when the node was in the process of rapid enlargement.

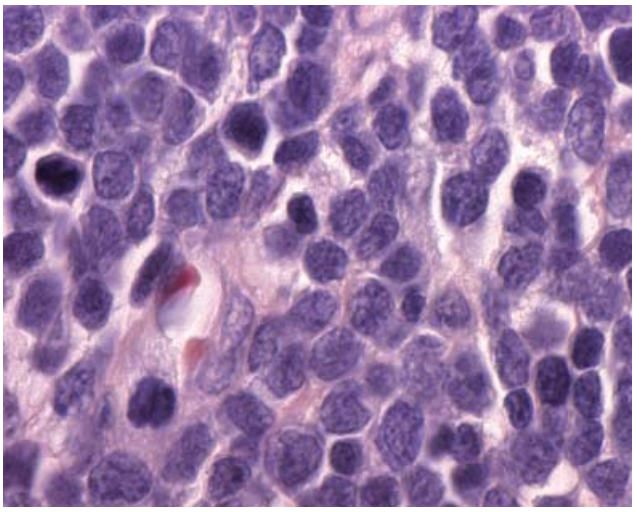

Figure 4.22. Human: mediastinal mass, lymphoblastic lymphoma. Detail of Figure 4.21. In early and well-fixed areas, the nuclear membranes are thin and delicate with the chromatin dispersed and nucleoli generally inapparent. There are 2 cells in metaphase near the left and the darker cell at lower left is likely undergoing apoptosis. The size of the nuclei can be deduced from the red cell. Cytoplasm is minimal and cell boundaries are indistinct.

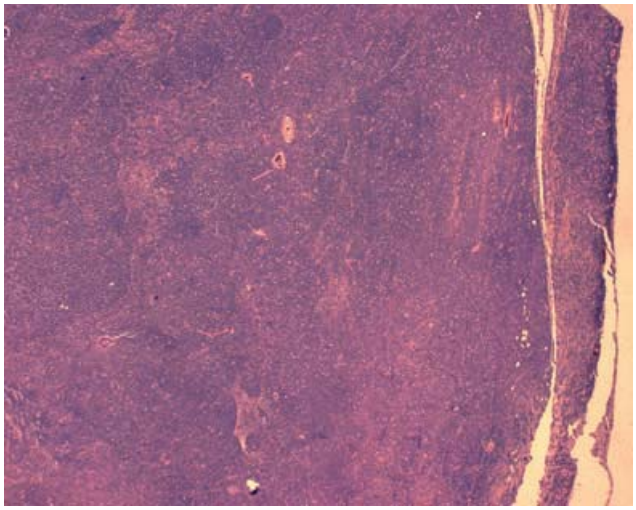

Figure 4.21. Human: mediastinal mass, lymphoblastic lymphoma. The tissue has no natural borders and consists of a diffuse proliferation that has the density of small nuclei closely packed. The pinpoint light speckling is a starry sky effect due to numerous tingible body macrophages. *Slide from Cornell Tutorial.*

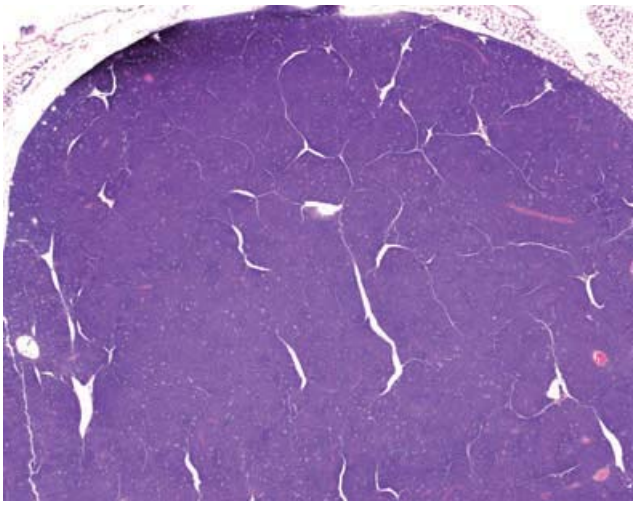

Figure 4.23. Mouse: pancreatic lymph node, acute lymphoblastic leukemia. *Slide from J. M. Ward, DVM.*

nucleus. The densely stained and uniformly distributed chromatin of LBL renders the nuclei a uniform density across the surface with no accentuation of the nuclear membrane by peripheralization of chromatin, as is seen to some degree in most other lymphomas (see Fig. 4.18). Nucleoli are present in about half of the cells, but these are small and obscured by the chromatin. The cytoplasm in LBL is scanty and moderately deeply stained, and cell boundaries are usually not distinct. The cells are CD3 positive and negative for B-cell markers. Tingible body macrophages are not prominent and may be seen in about 10% of cases, but not to the extent of a starry sky appearance at low magnification (Figs. 4.21, 4.22). Similar changes are seen in other species (Figs. 4.23, 4.24).

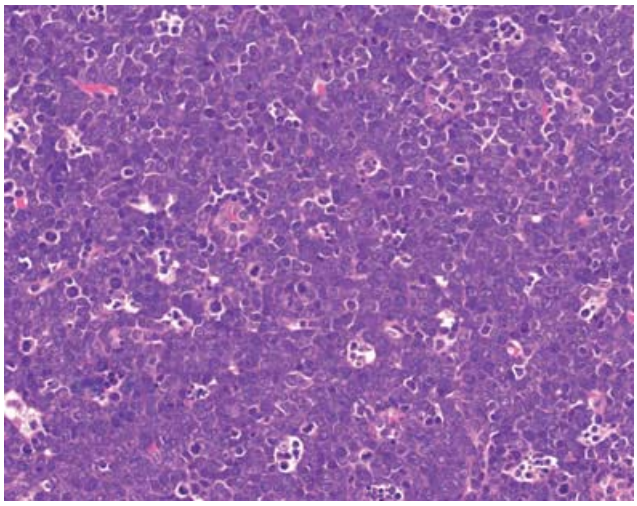

Figure 4.24. Mouse: lymph node, acute lymphoblastic leukemia. Detail of Figure 4.23. The tissue consists of tightly packed small cells with a high mitotic rate that can be deduced from the starry sky appearance due to the presence of many tingible body macrophages.

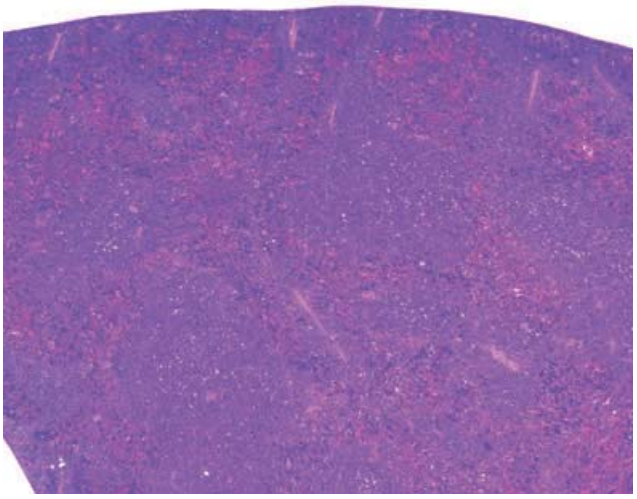

Figure 4.25. Mouse: spleen, acute lymphoblastic leukemia. The periarteriolar lymphoid sheaths have increased greatly in size and are beginning to coalesce with compression of the surrounding areas of sinus characterized by clusters of small dark cells representing foci of erythropoiesis. *Slide from J. M. Ward, DVM.*

Spleen

The spleen is generally not involved in lymphoblastic lymphoma in early stages of nodal involvement even if generalized. The involvement of the spleen in LBL appears to parallel the involvement of bone marrow and begins with focal masses arising on the arteriolar cuffs and coalescing in focal areas (Figs. 4.25, 4.26). In contrast, T-ALL always involves the spleen and tends to do so with sinus colonization that proceeds to generalized involvement and splenomegaly. Involvement of the spleen by LBL progresses from atrophy of the small lymphocytes of the periarteriolar lymphoid sheaths to loss of mantle cell cuffs around the follicles and then to gradual atrophy of the follicles themselves as neoplastic cells appear irregularly around arterioles and in sinus areas. In aggressive lymphomas, there is usually focal subendothelial colonization of the large muscular veins, which heralds the involvement of the liver. As the spleen becomes infiltrated, so does the liver and hepatosplenomegaly is present in about half of the cases of lymphoblastic disease. As LBL becomes leukemic it is indistinguishable form ALL, and in similar fashion as ALL progresses to solid involvement of parenchymal organs it is indistinguishable form LBL. For these very good reasons the two diseases are considered together, and in a particular case the term of *ALL* or *LBL* is applied according to the tissue that has the greatest volume of tumor. Thus, lymphoblastic disease with heavy marrow involvement, regardless of the blood picture and minimal tumor in other tissues, would be considered ALL and if there was lymphadenopathy without marrow involvement the disease is LBL.

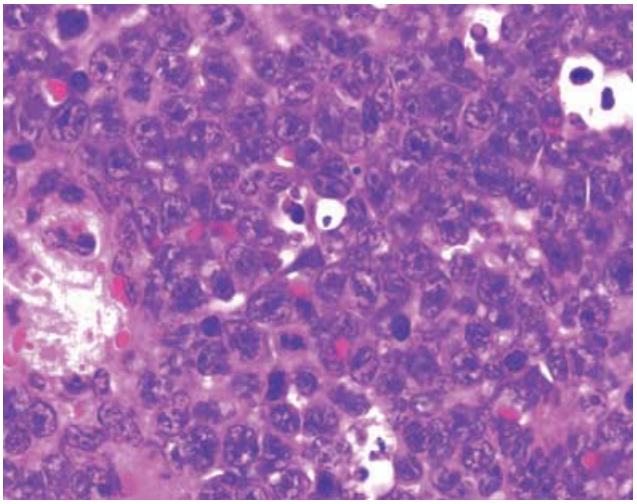

Figure 4.26. Mouse: spleen, acute lymphoblastic leukemia. Detail of Figure 4.25. The cell size is similar to that in other species, but the nuclei have a more aggressive appearance, with parachromatin clearing and prominent nucleoli in contrast to the criteria for lymphoblastic cells in larger mammals.

Other Organs

If the LBL arises in the mediastinum, there is rapid involvement of the marrow with presentation as ALL (see Figs. 4.21, 4.22). If LBL arises in peripheral nodes or skin, there is a longer period of peripheral spread, but ultimately the liver (Figs. 4.27, 4.28) and spleen (see Figs. 4.25, 4.26) become involved, followed by the bone marrow (Fig. 4.29), and then virtually all other tissues

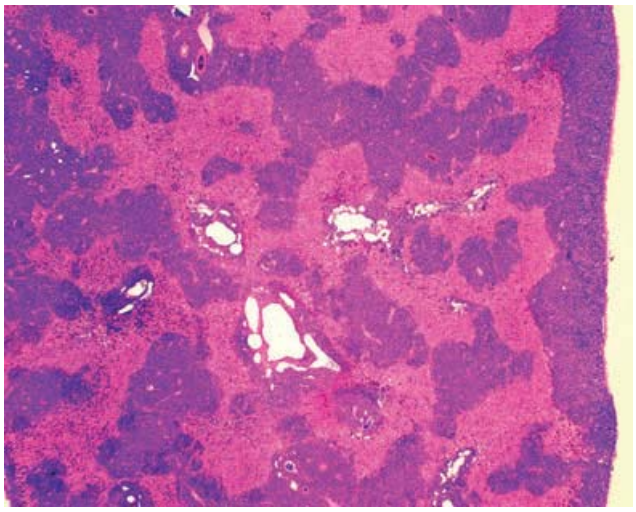

Figure 4.27. Dog: liver, lymphoblastic lymphoma. The involvement is primarily periportal, coalescing with the hepatic veins dilated (center), and surrounded by dilated lymphatics with a narrow zone of tumor infiltration. There is a broad laminar subcapsular infiltration surrounding the biopsy.

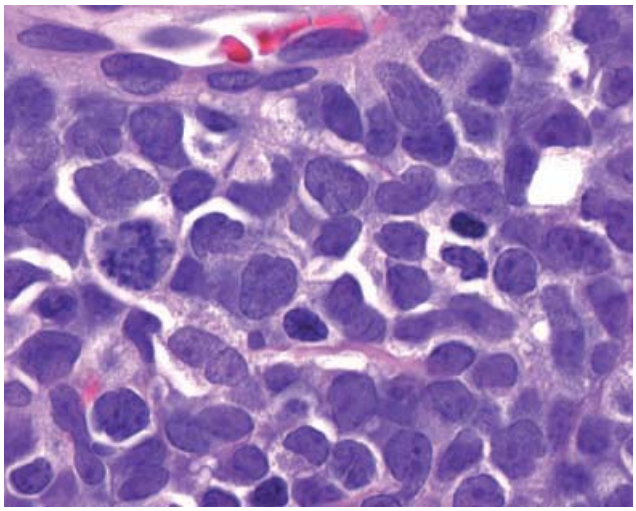

Figure 4.28. Dog: liver, lymphoblastic lymphoma. Detail of Figure 4.27. In areas of ideal fixation, the nuclear membranes are thin and delicate with the chromatin dispersed and surrounding small frequently inapparent nucleoli. There is marked variation in the nuclear outline, with sharp, shallow indentations indicating that this is lymphoblastic lymphoma of convoluted type. The nuclei are 1.5–2 red cells in diameter and the cytoplasm is minimal and lightly stained. The cell in left center is in metaphase.

may be involved, including brain, tonsil, gonads, adrenals, bone, and kidneys.

Immunologic Features

Lymphoblastic lymphoma of T-cell type is predominantly CD3 positive and negative for CD79, but rarely it may be positive with CD20. Many of the canine and feline cases of LBL may have azurophilic granulation, and those of LGL type are CD3 positive, but others that are granulated may be negative and are presumably of NK-cell type. A small group of canine LBL cases were reported to be about half CD4 and CD8 positive (double positive) and half negative for both (double negative). Currently in any group of acute leukemias, there will be cases of AML that are morphologically not distinguishable from T- or B-cell LBL and other cases that must be considered acute and undifferentiated by current technology. It is unclear whether T-cell ALL is positive for CD34, but B-cell ALL is likely to be positive; a solid tumor of LBL type is likely to be negative, which may be a useful reagent in differentiating ALL from LBL in early stages.

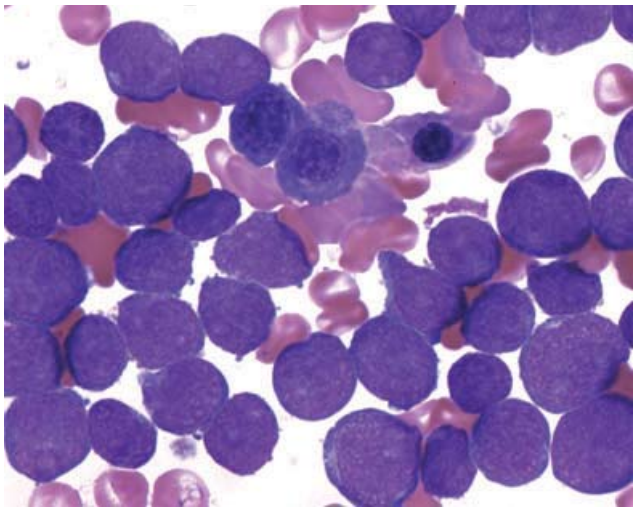

Figure 4.29. Human: marrow aspirate, precursor cell leukemia lymphoma. The marrow is hypercellular with a predominant population of neoplastic cells. Three rubricytes are present in upper center, as a residue of benign marrow cells. The neoplastic cells have round to oval nuclei generally 1.5 red cells in diameter with a cribriform chromatin pattern and multiple small but quite prominent nucleoli. The cytoplasm is minimal and highly basophilic. *Slide from Cornell Tutorial.*

Cytogenetic and Molecular Features

T-cell ALL and LBL that have differentiated to the extent of expression of the T-cell receptor (TCR) can be identified in paraffin-embedded tissues and in flow cytometry by anti-CD3 antibody, as noted above. The assembly of the T-cell receptor requires expression of a mutually exclusive pair of loci from a group of four identified as alpha (α), beta (β), gamma (γ), and delta (δ). In the assembly of the T-cell receptor, the products of these gene loci assemble as either αβ or γδ pairings of the TCR. The TCR can be identified by appropriate primers in PCR (polymerize chain reaction) testing of cellular DNA derived

from both benign or neoplastic and clonal populations. The amplified product of these probes separated on acrylamide gels has a smear or ladderlike banding result with polyclonal benign cells and a single sharp band with clonal populations. By these techniques, it has been determined that about 80% of human LBLs and 20% of ALLs are of T-cell origin, with the remainder of cases from each category found to be of B-cell type. In dogs, the majority of ALL cases are of T-cell type and for LBL it is less clear, but for all types of canine lymphoma about 80% are of B-cell type and 20% of T-cell type, a much higher proportion of T-cell neoplasms than is seen in humans. At least 10% of canine ALL is of the undifferentiated type without indication of B- or T-cell lineage. In human cases of prothymocyte ALL, the cells may be positive for TdT (terminal deoxynucleotidyl transferase, CD99), but they may not have rearranged or expressed any of the TCR genes or only the γ chain of TCR, with the other loci remaining in germline configuration. One of the problems of molecular identification of cell lineage (not clonality) is that there is a level of *lineage promiscuity* in both B- and T-cell neoplasms of both primitive and well-differentiated types. In human pathology, the TCR genes rearrange more frequently in B-cell neoplasms than do the immunoglobulin genes in T-cell ALL and LBL. In canine lymphoma, about 10% of one series of indolent B-cell neoplasms were clonal for both B- and T-cell receptors. The lineage, as determined by immunophenotype, does not have this overlap, or only very rarely; for this reason, both clonality and phenotype as determined on paraffin-embedded tissues and histology are required for definitive categorization. Clonality cannot be determined by flow cytometry alone because the predominant cell type present may not be the malignant population, as is seen in the T-cell rich large B-cell lymphomas. The specific recognition of the subtypes of ALL, LBL, and AML, along with those that are undifferentiated (AUL), represent the cutting edge of diagnostic interpretation.

Cell of Origin

T-cell lymphoblastic disease is derived from a naive T-cell that may be at various stages of TCR 4gene rearrangements. Most human cases do not have surface CD3 but have cytoplasmic positivity that is not distinguishable in immunohistochemistry but can be determined in flow cytometry.

Diagnostic Criteria

Lymphoblastic lymphoma is always characterized by a diffuse architecture, and in nodal disease there is destruction of the peripheral sinus and colonization of the capsule and perinodal tissues in one or more areas. There may be nodal infarction, with the central area of the node having undergone ischemic necrosis. Unlike the more indolent lymphomas, fading germinal centers are almost always absent, and the medullary areas lack sclerosis of supporting and vascular structures more associated with long-term benign hyperplasia.

Cytologically, lymphoblastic lymphoma is composed of medium-sized cells with intermediate-sized nuclei that are round or oval and have densely stained, finely dispersed, chromatin and nucleoli are present and small but inconspicuous and obscured by the chromatin. There is a high mitotic rate of 15–25/400× field, and metaphases are less well defined and less obvious than in other lymphomas. There are numerous apoptotic bodies and moderate numbers of tingible body macrophages. The nuclear membrane may be smooth and entire or have sharp shallow indentations that are of no clinical significance. The cytoplasm is minimal, and cell boundaries are generally indistinct.

Differential Diagnosis

Lymphoblastic lymphoma of T-cell type is indistinguishable from LBL of B-cell type and from cases of acute myeloid leukemia on oversight stains. LBL generally has cells of L1 type, and cell boundaries are indistinct. This feature assists distinction from the Burkitt's-type lymphoma, which has more cytoplasm like the L2 type cell of the FAB classification and evident cell boundaries emphasized by the "squaring-off" artifact of formalin fixation (Figs. 4.30, 4.31). The Burkitt's-lymphoma also has prominent nucleoli and more consistent starry sky accumulation of tingible body macrophages (see Fig. 4.30). LBL must be differentiated from lymphoid thymoma, which will also have a T-cell phenotype but the chromatin pattern of the lymphocytes is more typically of large dense

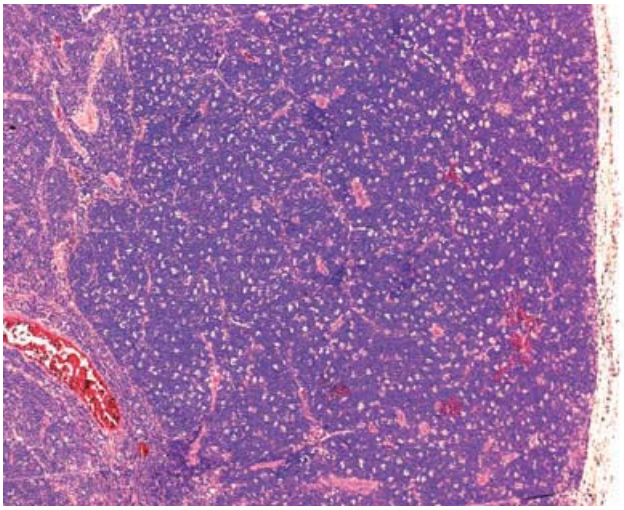

Figure 4.30. Human: lymph node, Burkitt's type lymphoma. High grade B-cell lymphoma, with prominent starry sky tingible body, macrophage formation. *Slide from Cornell Tutorial.*

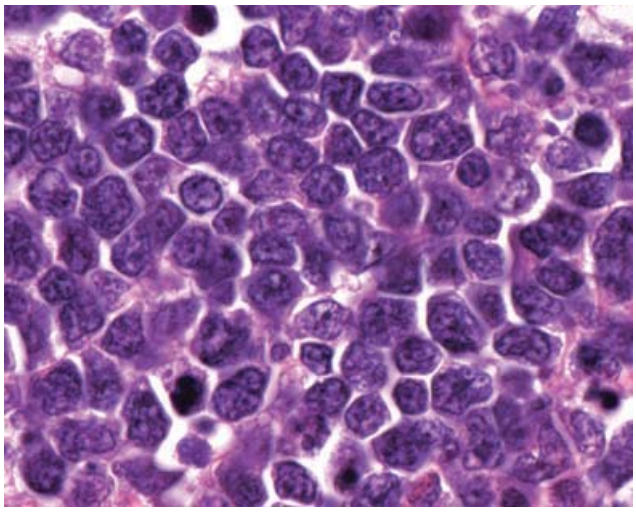

Figure 4.31. Human: node, Burkitt's lymphoma. Detail of Figure 4.30. In inner areas of the tissue with some cellular contraction, the cytoplasm of the interfacing cells tends to have sharply defined parallel interfaces referred to as the *squaring off* appearance.

chromocenters rather than dispersed, and also by a lower mitotic rate of these benign thymic lymphocytes and the presence of epithelial cells.

Staging

Because all animals diagnosed with lymphoblastic lymphoma or T-cell ALL must be given intensive therapy, the treatment will be the same in all cases. There appears to be no difference in survival with human B- or T-cell LBL despite concerns that B-cell LBL in adults had a worse prognosis, which was likely based on inadequate data because these cases are relatively rare. In human studies, it is felt that the prognostic factors for lymphoblastic leukemia were well defined and those for lymphoblastic lymphoma were largely nonexistent. A well-recognized, negative prognostic finding in the dog with T-cell LBL is the presentation with hypercalcemia due to a paraneoplastic production of parathormone type products. Some factors from Sweetenham and Borowitz felt to be of adverse significance in adult human LBL are

- Advanced age
- Ann Arbor stage
- Bone marrow involvement
- Central nervous system involvement
- Leukemic overspill
- Elevated serum LDH
- B symptoms
- Time to attainment of complete remission

Transformation and Progression

Because T-LBL and ALL are already blastic diseases, there is no further change that heralds a worse prognosis other than the spread of the tumor to the central nervous system, heart, liver, kidneys, and other vital organs. Because animals with intractable diseases are usually humanely destroyed, the progression of the neoplasm beyond multicentric involvement is not of common occurrence. Currently, in humans rescue treatment involves autologous and more recently allogeneic stem cell transplantation.

Evaluation of the Treated Animal

Because ALL *presents* with marrow involvement and LBL tends to *spread to* marrow involvement, most cases of advanced ALL/LBL will have some degree of marrow failure with anemia, thrombocytopenia, and likely bacterial invasion due to neutropenia. The latter may not be characterized by fever in the absence of adequate numbers of granulocytes. Most animals with advanced LBL are acutely ill and do not present a good case for aggressive therapy.

Treatment and Survival

The history of clinical management of LBL in humans is one of recognition of the need for very aggressive therapy for a disease characterized by relapse with leukemic spread to the CNS and gonads in cases treated as for other aggressive non-Hodgkin's lymphomas. As LBL began to be treated, as for ALL where there was a much larger database, longer survivals were achieved. With experience, radiation to the brain was added to more intensive chemotherapy for longer-term survivals. It is unlikely that animals will ever be subjected to curative levels of treatment. Currently, with aggressive therapy the response rate for human LBL varies from 73–100% and overall 5-year survival from 40–69% of cases. It is noted in the treatment of human LBL that these tumors are very sensitive to chemotherapy and cases with large tumor burdens are at risk of developing tumor lysis syndrome on the induction of aggressive therapy; this needs to be considered in provision of supportive measures. In studies conducted in dogs where the diagnosis was verified as T-cell LBL, the mean survival time of treated animals was in the range of 60–90 days.

REFERENCES

Borowitz, M.J., and DiGiuseppe, J.A. (2001) Acute lymphoblastic leukemia. In Knowles, D.M. (ed.), *Neoplastic Hematopathology*. 2nd ed.. Lippincott Williams & Wilkins, Philadelphia, Pennsylvania, pp. 1643–1665.

Brownell, M.D., Sheibani, K., Battifora, H., Winberg, C.D., and Rappaport, H. (1987) Distinction between undifferentiated (small noncleaved) and lymphoblastic lymphoma. An immunohistologic study on paraffin-embedded, fixed tissue sections. *Am J Surg Pathol* 11(10):779–787.

Burnett, R.C., Vernau, W., Modiano, J.F., Olver, C.S., Moore, P.F., and Avery, A.C. (2003) Diagnosis of canine lymphoid neoplasia using clonal rearrangements of antigen receptor genes. *Vet Pathol* 40:32–41.

Coleman, L.A., Erdman, S.E., Schrenzel, M.D., and Fox, J.G. (1998) Immunophenotypic characterization of lymphomas from the mediastinum of young ferrets. *AJVR* 59(10): 1281–1286.

Dabaja, B.S., Ha, C.S., Thomas, D.A., Wilder, R.B., Gopal, R., Cortes, J., Bueso-Ramos, C., Hess, M.A., Cox, J.D., and Kantarjian, H.M. (2002) The role of local radiation therapy for mediastinal disease in adults with T-cell lymphoblastic lymphoma. *Cancer* 94(10):2738–2744.

Doige, C.E. (1987) Bone and bone marrow necrosis associated with the calf form of sporadic bovine leukosis. *Vet Pathol* 24:186–188.

Fournel-Fleury, C., Ponce, F., Felman, P., Blavier, A., Bonnefont, C., Chabanne, L., Marchal, T., Cadore, J.L., Goy-Thollot, I., Ledieu, D., Ghernati, I., and Magnol, J.P. (2002) Canine T-cell lymphomas: A morphological, immunological, and clinical study of 46 new cases. *Vet Pathol* 39:92–109.

Gassmann, W., Löffler, H., Thiel, E., Ludwig, W.D., Schwartz, S., Haferlach, T., Maurer, J., Rieder, H., Fonatsch, C., Gökbuget, N., and Hoelzer, D. (1997) Morphological and cytochemical findings in 150 cases of T-lineage acute lymphoblastic leukaemia in adults. *Brit J Haematol* 97:372–382.

Gibson, D., Aubert, I., Woods, J.P., Abrams-Ogg, A., Kruth, S., Wood, R.D., and Bienzle, D. (2004) Flow cytometric immunophenotype of canine lymph node aspirates. *J Vet Intern Med* 18:710–717.

Grindem, C.B., and Buoen, L.C. (1989) Cytogenetic analysis in nine leukaemic cats. *J Comp Path*101:21–30.

Grindem, C.B., Stevens, J.B., and Perman, V. (1986) Cytochemical reactions in cells from leukemic dogs. *Vet Pathol* 23:103–109.

Hyjek, E., Chadburn, A., Liu, Y.F., Cesarman, E., and Knowles, D.M. (2001) BCL-6 protein is expressed in precursor T-cell lymphoblastic lymphoma and in prenatal and postnatal thymus. *Blood* 97(1):270–276.

Keller, R.L., Avery, A.C., Burnett, R.C., Walton, J.A., and Olver, C.S. (2004) Detection of neoplastic lymphocytes in peripheral blood of dogs with lymphoma by polymerase chain reaction for antigen receptor gene rearrangement. *Vet Clin Pathol* 33(3):145–149.

Knowles, D.M. (2001) Lymphoblastic lymphoma. In Knowles, D.M. (ed.), *Neoplastic Hematopathology*. Lippincott Williams & Wilkins, Philadelphia, pp. 915–951.

Kröber, S.M., Greschniok, A., Kaiserling, E., and Horny, H.P. (2000) Acute lymphoblastic leukaemia: Correlation between morphological/immunohistochemical and molecular biological findings in bone marrow biopsy specimens. *J Clin Pathol: Mol Pathol* 53:83–87.

Lilleyman, J.S., Hann, I.M., Stevens, R.F., Richards, S.M., Eden, O.B., Chessells, J.M., and Bailey, C.C. (1992) Cytomorphology of childhood lymphoblastic leukemia: A prospective study of 2000 patients. *Brit J Haematol* 81:52–57.

Longui, C.A., Vottero, A., Adamson, P.C., Cole, D.E., Kino, T., Monte, O., and Chrousos, GP. (2000) Low glucocorticoid receptor α/β ratio in T-cell lymphoblastic leukemia. *Horm Metab Res* 32:401–406.

Malec, M., van der Velden, V., Björklund, E., Wijkhuijs, J.M., Söderhäll, S., Mazur, J., Björkholm, M., and Porwit-MacDonald, A. (2004) Analysis of minimal residual disease in childhood acute lymphoblastic leukemia: Comparison between RQ-PCR analysis of Ig/TcR gene rearrangements and multicolor flow cytometric immunophenotyping. *Leukemia* 18:1630–1636.

Matus, R.E., Leifer, C.E., and MacEwen, G. (1983) Acute lymphoblastic leukemia in the dog: A review of 30 cases. *JAVMA* 183(8):859–862.

Spodnick, G.J., Berg, J., Moore, F.M., and Cotter, S.M. (1992) Spinal lymphoma in cats: 21 cases (1976–1989). *JAVMA* 200(3):373–376.

Suzumiya, J., Ohshima, K., Kikuchi, M., Takeshita, M., Akamatsu, M., and Tashiro, K. (1997) Terminal deoxynucleotidyl transferase staining of malignant lymphomas in paraffin sections: A useful method for the diagnosis of lymphoblastic lymphoma. *J Pathol* 182:86–91.

Sweetenham, J.W., and Borowitz, M.J. (2004) Precursor B- and T-cell lymphoblastic lymphoma. In Mauch, P.M., Armitage, J.O., Coiffier, B.C., Dalla-Favera, R., and Harris, N.L. (eds.), *Non-Hodgkin's Lymphomas*. Lippincott Williams & Wilkins, Philadelphia, pp. 503–513.

Thomas, X., Le, Q.-H., Danaïla, C., Lhéritier, V., and French, M. (2002) Bone marrow biopsy in adult acute lymphoblastic leukemia: Morphological characteristics and contribution to the study of prognostic factors. *Leukemia Res* 26:909–918.

Troxel, M.T., Vite, C.H., Van Winkle, T.J., Newton, A.L., Tiches, D., Dayrell-Hart, B., Kapatkin, A.S., Shofer, F.S., and Steinberg, S.A. (2002) Feline intracranial neoplasia: Retrospective review of 160 cases (1985–2001). *J Vet Intern Med* 17:850–859.

Vernau, B., and Moore, P. (2001) Immunophenotyping in the dog. *Vet Cancer Soc Newsl* 2001, 25(1):1–12.

Vernau, W., and Moore, P.F. (1999) An immunophenotypic study of canine leukemias and preliminary assessment of clonality by polymerase chain reaction. *Vet Immunol Immunopathol* 69:145–164.

von Euler, H., Einarsson, R., Olsson, U., Lagerstedt, A.S., and Eriksson, S. (2004) Serum thymidine kinase activity in dogs with malignant lymphoma: A potent marker for prognosis and monitoring the disease. *J Vet Intern Med* 18:696–702.

Weiss, D.J. (2001) Flow cytometric and immunophenotypic evaluation of acute lymphocytic leukemia in dog bone marrow. *J Vet Intern Med* 15:589–594.

Weng, A.P., Ferrando, A.A., Lee, W., Morris IV, J.P., Silverman, L.B., Sanchez-Irizarry, C., Blacklow, S.C., Look, A.T., and Aster, J.C. (2004) Activating mutations of *NOTCH1* in human T-cell acute lymphoblastic leukemia. *Science* 306:269–271.

MATURE (PERIPHERAL) T-CELL AND NK-CELL NEOPLASMS

Chronic Lymphocytic Leukemia

Definition

Chronic lymphocytic leukemia (CLL) can be defined as a persistent lymphocytosis of relatively small mature type cells that tends to increase slowly over time in the absence of any identifiable cause. In the dog and cat, CLL appears to be similar to the extent of morphology, presentation, and pathology. Phenotypic and clonal studies have been reported for CLL in the dog but not in the cat.

Epidemiology and Features

CLL is not commonly encountered or is underdiagnosed. There were 10 cases of CLL in 751 cases of feline hematopoietic neoplasm, with 11 cases of small cell lymphocytic lymphoma (SLL). The presentation was multicentric in all cats diagnosed as CLL with marrow examined and heavily involved. Five of the cats diagnosed as SLL had splenomegaly, with marrow examined on 2 of these and others having involvement of liver in 2 and mediastinum in 1. Thus even if some of the cases considered SLL were leukemic, the total number is still small. The age of cats with CLL ranged from 2–16 years with a mean of 8 years. Gender was available in 7 cases with 5 male and 2 female. Only 1 case of CLL was diagnosed in 503 cases of canine hematopoietic neoplasms with 13 cases of SLL (T-zone lymphoma) and 12 cases diagnosed as small cell lymphoma of intermediate type. Others have found a mean age of dogs with CLL to be 10 years with a range of 1.5–15 years. Males have outnumbered females in most reports of canine CLL, but in large granular lymphocytic leukemia (LGL) the ratio seems to be reversed. The cases reported from personal collections consist almost entirely of histologic preparations; it is likely that in both the cat and the dog, these numbers very likely do not reflect the true incidence of chronic lymphocytic leukemia. Because most of the leukemias would have been diagnosed on examination of blood and marrow on cytologic specimens, they would not have been submitted for consultative interpretation.

Clinical Presentation and Features

The presentation of both dogs and cats with CLL is likely to be on the basis of an unsuspected condition identified on a routine blood examination. In that respect, CLL in animals is very like the same disease in humans. In humans, the proliferative rate in CLL is very low, and the disease is predominantly of B-cell type. Human CLL is considered primarily a disease of accumulation because the cells express high levels of Bcl-2 protein product and resist apoptosis. In animals, the phenotype of CLL has only recently been reported and is the reverse of the predominant B-cell presentation of humans. In normal dogs, the lymphocytes subsets are about 80% T-cells that are CD3 positive and of these 45% are of CD4 (helper) and 25% CD8 (cytotoxic) type with 15% of lymphocytes of B-cell type and positive for CD79, CD20, and CD21. The remaining lymphocytes are of NK-cell type (CD3 negative) with some double negative ($CD4^-$,$CD8^-$) types. Normal cats are similar to dogs with slightly less (75%) peripheral blood T-cells. In young animals, the proportion of B-cells in blood is higher (25%) and decreases with age while the proportion of CD8 positive T-cells increases from 15% in young to 25% in adults, as reported by Workman and Vernau. In dogs, most of the T-cell receptors are of the $\alpha\beta$ type with the $\gamma\delta$ less that 2% of blood lymphocytes. The large granular lymphocytes in blood of normal dogs range from 0–10%. The presentation of CLL may involve any one of these phenotypic subsets.

As noted, most animals presenting CLL are found incidental to other examinations, but when symptomatic the complaints are most often lethargy, reduced appetite, and gradual weight loss. As the disease progresses, animals become mildly to moderately anemic but may show little change in behavior as a result, and the low mitotic rate of the neoplasm does not appear to present a metabolic cost that results in fever or extensive weight loss. Physical examination usually identifies splenomegaly, even in dogs not showing other signs, and less often hepatomegaly and pallor of anemia. The presenting level of lymphocytosis is variable in both dogs and cats and may vary from near normal to 1–200 $\times$ 10^3/ul, with counts over a million having been found (Fig. 4.32). The anemia is normocytic, normochromic, and nonresponsive and of mild (Hct of 30%) to moderate (Hct of 20–30%) degree. Thrombocytopenia is usually present and mild (100 $\times$ 10^3/ul) and the animals are not neutropenic.

Pathologic Features

Blood

Cytologically, the cells in CLL are of two types, with the most common having small round nuclei slightly larger than red cells that have densely stained, large chromocenters without parachromatin clearing that, on examination at moderate or low magnification, appear solid and relatively structureless (Fig. 4.33). Nucleoli are not present in cells in blood, but they may be found in tissues in small clusters of cells with slightly larger nuclei called *proliferation centers* that form the dividing segment of the population. Mitoses are absent and the cytoplasm is scanty and forms a tight, slightly eccentric rim around the nuclei. The second type is less common and has nuclei 1.5–2.0 red cells in diameter that are of irregular shape but generally not indented and have a dense uniform chromatin structure that appears bland and structureless

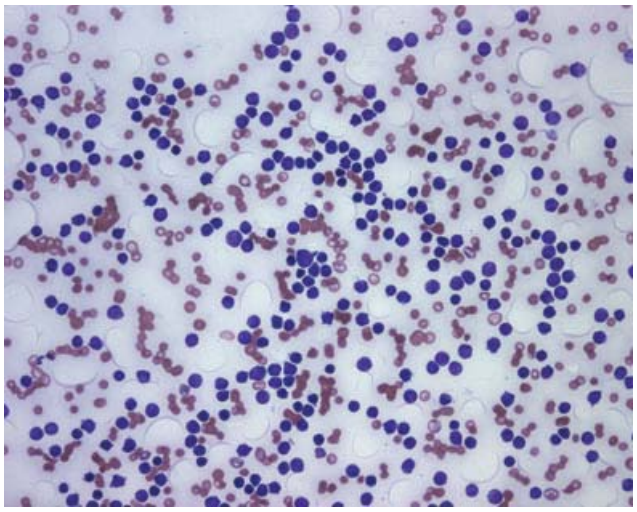

Figure 4.32. Dog: blood, chronic lymphocytic leukemia. A mature dog was presented with mild reduction and activity and weight loss, with an extremely high leukocyte count found on examination of the blood. There is mild anemia that is mildly responsive and platelet levels are normal.

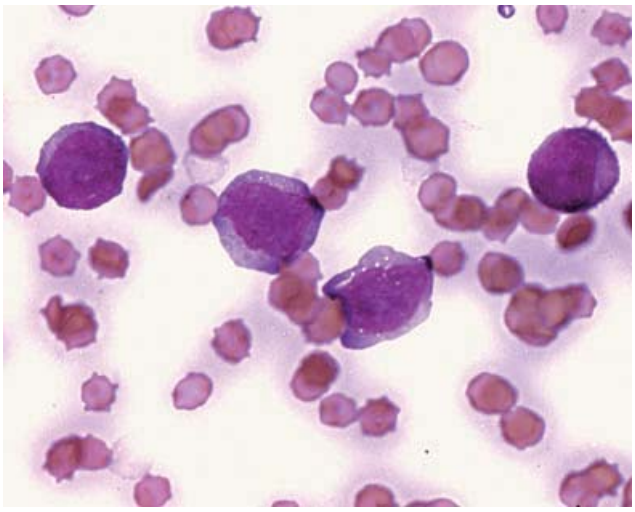

Figure 4.34. Cat: blood, CLL. At this examination, the animal had over 600,000 lymphocytes per microliter with only mild anemia. The neoplasm is likely entering an accelerated phase characterized by the more central cells. The cytoplasm is more abundant and nucleoli are not readily discernible.

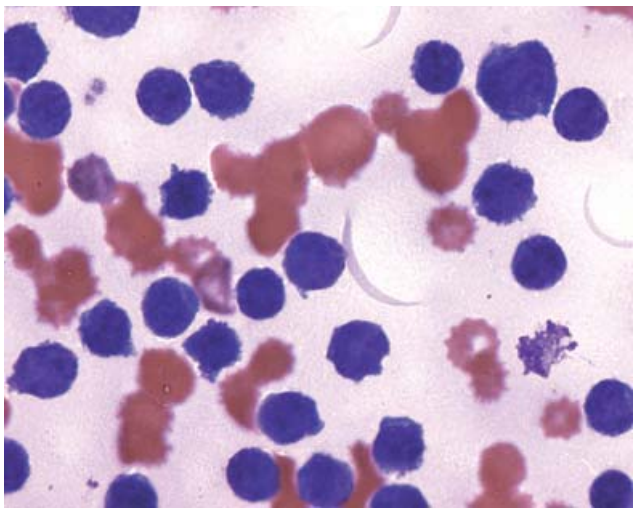

Figure 4.33. Dog: blood, CLL. Detail of Figure 4.32. The nuclei are round and densely stained and only slightly larger than red cells. The cytoplasm is a narrow rim that is highly basophilic. The lenticular artifacts in the densely stained background are suggestive of gammopathy similar to that of the Waldenstrom Macroglobulinemia.

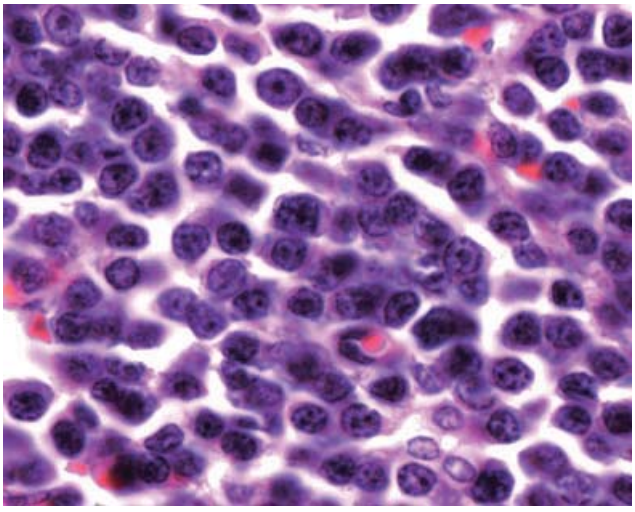

Figure 4.35. Cat: liver, CLL, same case as Figure 4.34. In comparison to nodal tumor, the neoplastic cells in liver are more widely dispersed providing easier evaluation of cell detail. The larger more irregular nuclei present in the blood are inapparent in tissue evaluation.

and lacks nucleoli (Fig. 4.34). The cytoplasm is relatively abundant and pale-staining with characteristic reduction in density near the nuclear membrane. Mitoses are again absent. In tissues, both forms have a dense, deeply stained appearance at low power magnification due to the density of nuclei and the relative tight packing of the cells (Figs. 4.35–4.40).

Bone Marrow

Bone marrow is always involved, is usually 30% or more infiltrated with neoplastic cells at presentation, and clinically significant cytopenias generally do not occur until at least 50% of marrow is involved. Similar results are found in cats (Fig. 4.41), which often have more advanced disease than dogs before becoming symptomatic (Fig. 4.42). An exception to these findings occurs

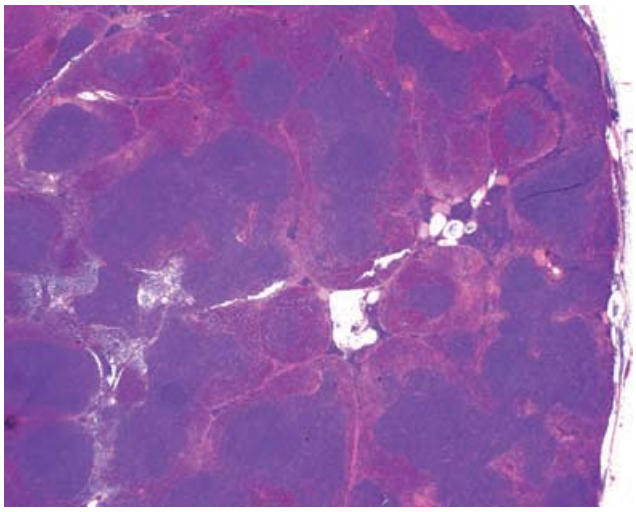

Figure 4.36. Horse: lymph node, CLL. There is an irregular colonization of lymph node with the capsule thinned and taut and the sinus intact without involvement of perinodal tissues. The medullary cords are at the lower left of the image with filling of these areas typical of chronic lymphocytic leukemia without destruction of node architecture.

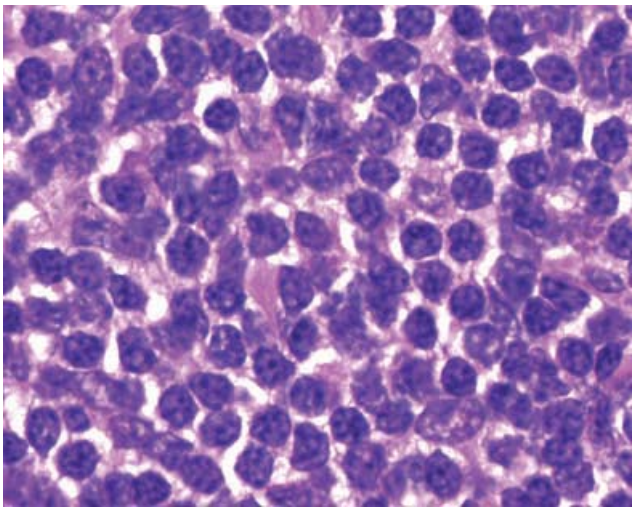

Figure 4.38. Equine: node, CLL. Detail of Figure 4.36. The neoplastic cells have small nuclei slightly larger than red cells, with large dense chromocenters with irregular parachromatin clearing. Nucleoli are not apparent, and the cytoplasm is minimal and moderately stained with cell boundaries generally indistinct.

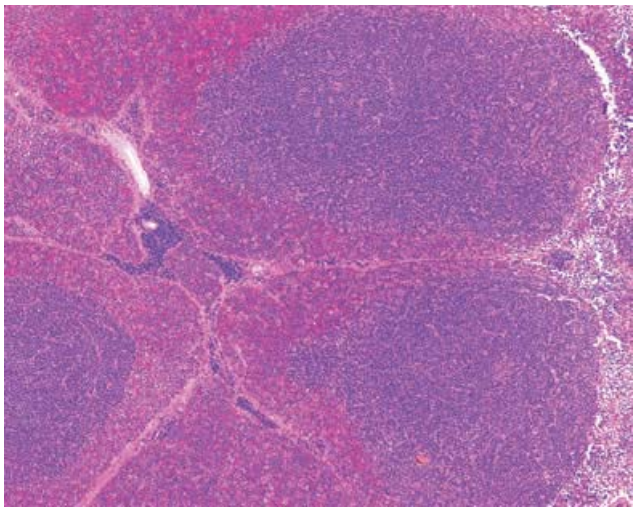

Figure 4.37. Horse: node, CLL. Detail of Figure 4.36. Colonization of the node medulla occurs with large focal areas of neoplastic proliferation filling the medullary cords and sinuses. The preservation of node architecture is indicative of slow proliferative activity unlike that of high grade lymphomas.

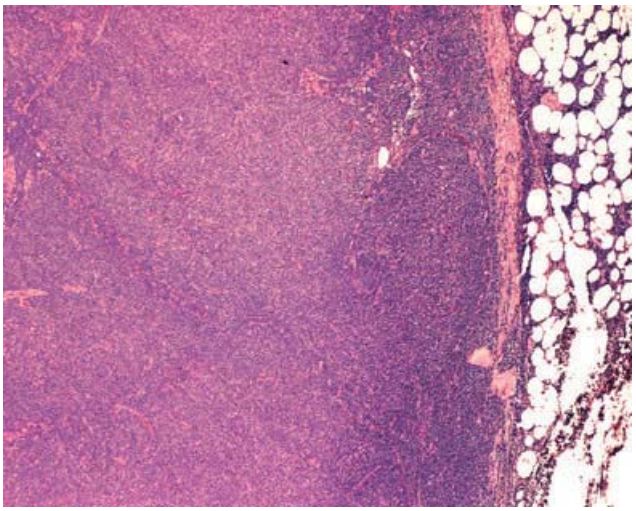

Figure 4.39. Human: lymph node, CLL. There is complete loss of normal node architecture with compression and apparent destruction of the peripheral sinus with irregular colonization of the capsule and perinodal fat. *Slide from Cornell Tutorial.*

in dogs that have CLL of LGL type that present with a leukemic blood picture and splenomegaly but with relatively normal bone marrow (Figs. 4.43, 4.44). These cases consistently express CD11d, and the disease is like that of the Fisher 344 rat where the neoplasm is felt to originate in the spleen.

Lymph Node

Lymph nodes may be involved, characteristically by filling of the medullary cords, with compression of relatively empty sinuses (Fig. 4.45, see also Figs. 4.36, 4.39), or they may be atrophic and reflect the loss of normal cellular replacement, as in the spleen. A characteristic CLL in cats is that the postcapillary venules may retain quite high and vesicular endothelial nuclei, but there is almost

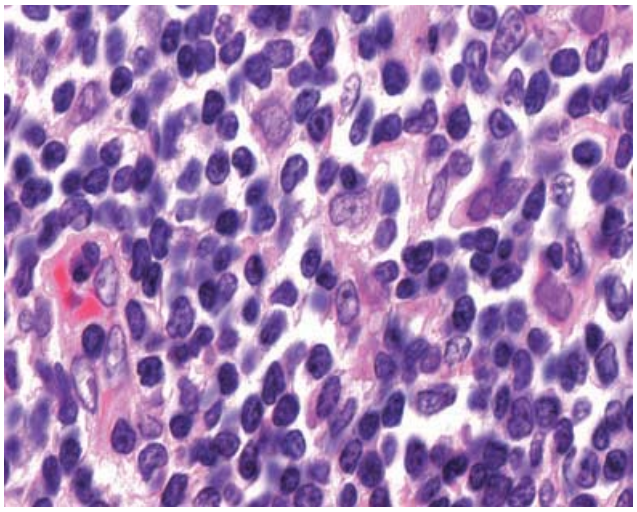

Figure 4.40. Human: node, CLL. Detail of Figure 4.39. The nuclei are small, round to oval, and occasionally indented with compact chromatin, large chromocenters, and most cells lacking nucleoli. The cytoplasm is minimal and lightly stained, and there is an absence of mitotic and apoptotic figures.

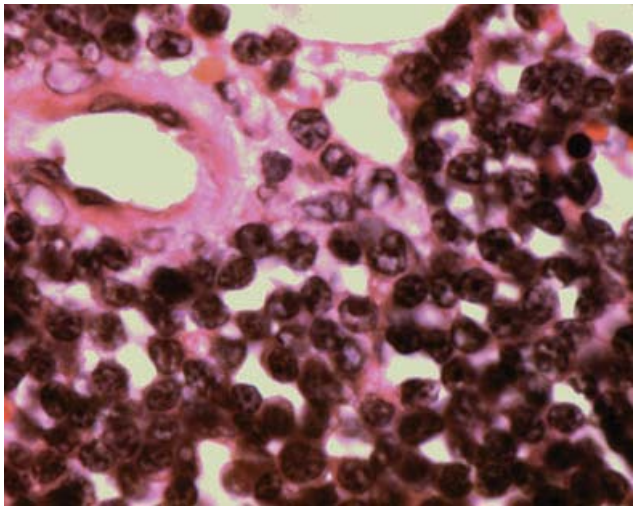

Figure 4.41. Cat: bone marrow, CLL, same case as Figure 4.34. The bone marrow has solid involvement with neoplastic cells, with only a few fat cells remaining (top). There is almost complete phthisis of normal marrow cells with a single late-stage rubricyte present in the upper right.

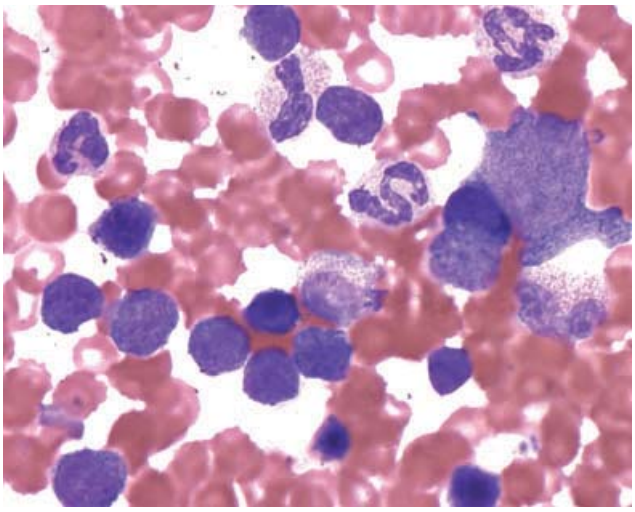

Figure 4.42. Dog: bone marrow aspirate, CLL. There are 5 tumor cells in a row (lower right) that have round nuclei with minimal highly basophilic cytoplasm. Residual marrow cells include developing eosinophils and a polychromatic rubricyte.

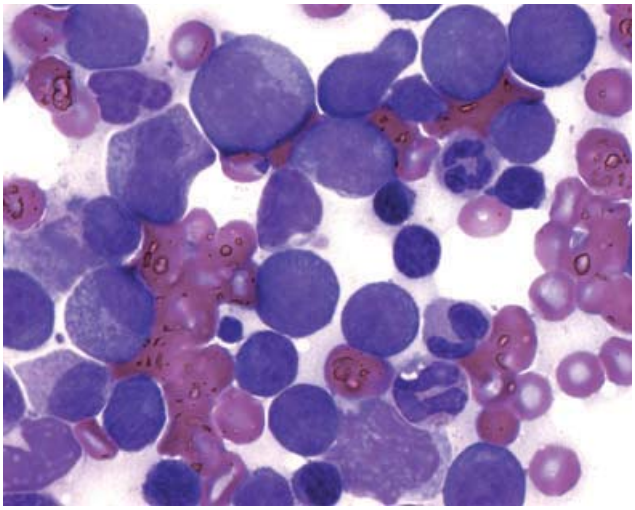

Figure 4.43. Dog: marrow aspirate, chronic lymphocytic leukemia. The dog has a peripheral blood leukemic picture with cells of large granular lymphocyte type, but the marrow is relatively uninvolved. Both normal myeloid and erythroid lineages are present and there is no evidence of tumor cells.

no translmural lymphocytic traffic across the walls of these vessels despite very high circulating lymphocyte levels (Fig. 4.46). This is presumably because the neoplastic cells lack the intercellular adhesion molecules (ICAMs) to marginate, exit the vessel, and enter the node cortex. Macrophages and apoptotic cells are not present in viable areas of tumor that has a diffuse architecture in nodal tissues and aligns along tissue boundaries in parenchymal organs. Cytologically, there are large dense chromocenters with more internal detail than is seen in thymic cortical cells with irregular parachromatin clearing, and nucleoli are again absent as are mitotic figures.

Spleen

Splenic involvement is sinusoidal, with atrophy of the follicular areas that may remain identified by pink areas of protein insudation from earlier events causing follicular hyalinosis. There is concurrent atrophy of the periarteri-

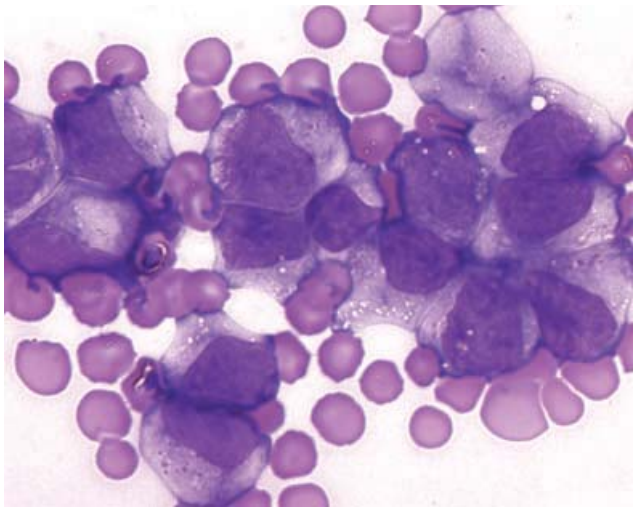

Figure 4.44. Dog: blood, CLL of LGL type, same animal as in Figure 4.43. There is an apparent disparity between the very leukemic blood picture of intermediate-sized cells with abundant cytoplasm with azurophilic granulation and the apparent normal bone marrow. The origin of these cells in the spleen requires a new concept of leukemia with marrow not the source of the neoplastic cells.

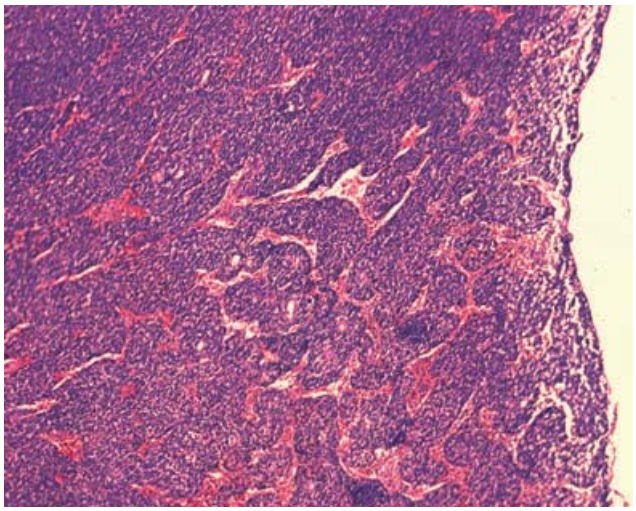

Figure 4.45. Cat: node, CLL, same case as Figure 4.34. The hilar area of the node is characterized by filling of the medullary cords with relatively empty medullary sinuses containing primarily red cells. The changes are characteristic of slow colonization of the lymph node without destruction of nodal architecture.

olar lymphoid sheaths that may be reduced to a few small lymphocytes around arterioles that stain darker than the infiltrating neoplastic lymphocytes (Figs. 4.47–4.49). The splenic sinus involvement is at first patchy and gradually becomes confluent (Fig. 4.50). Extramedullary hematopoiesis is well established in the early stages of the

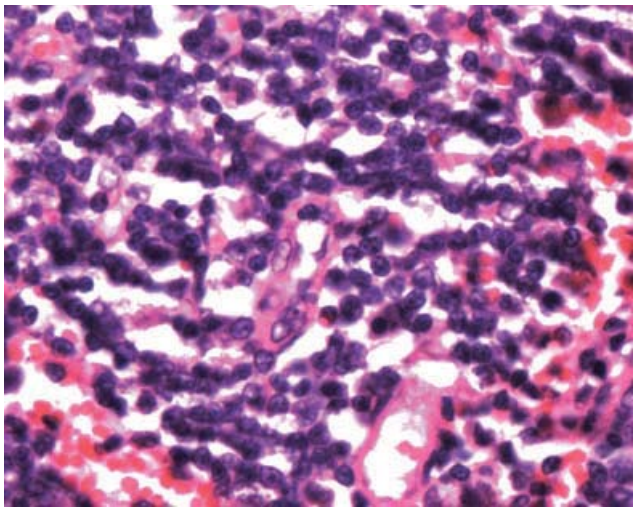

Figure 4.46. Cat: node, chronic lymphocytic leukemia. Detail of Figure 4.45. A postcapillary venule in the center has vesicular nuclei but very low transmural cellular traffic characteristic of CLL.

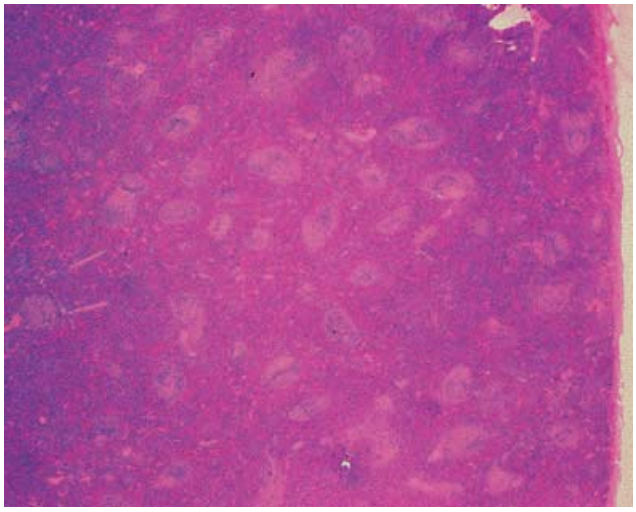

Figure 4.47. Cat: spleen, chronic lymphocytic leukemia. The spleen is markedly enlarged with thinning of the capsule and widely separated smooth muscle trabeculae. There is irregular colonization of the periarteriolar lymphoid sheaths as well as the sinuses, which greatly expands splenic size.

CLL, and with progression there is phthisis of these cells that tend to be in paratrabecular areas and identified by isolated megakaryocytes (Fig. 4.51). Colonization of the large muscular venous sinuses occurs as a subendothelial infiltration that heralds extensive involvement of the liver.

Other Organs

With progression, virtually all tissues may become involved, but the liver is most consistently involved beside the spleen (Figs. 4.52, 4.53). Hepatic involvement is also

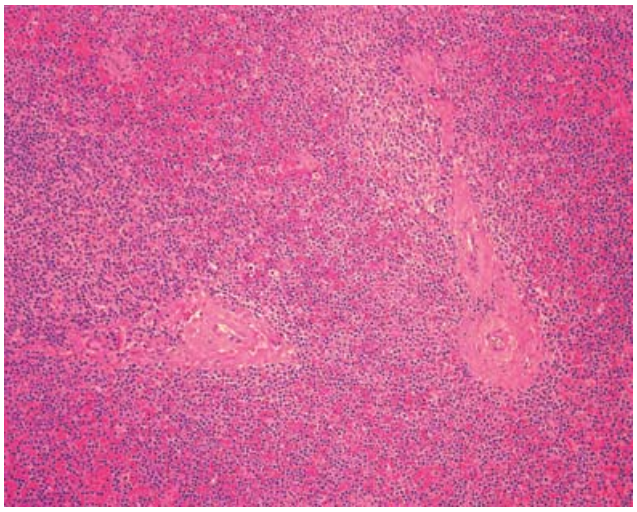

Figure 4.48. Cat: spleen, CLL. Detail of Figure 4.47. Adjacent arterioles with almost complete loss of the small cell cuff of normal lymphocytes and with irregular colonization of the surrounding splenic sinus areas.

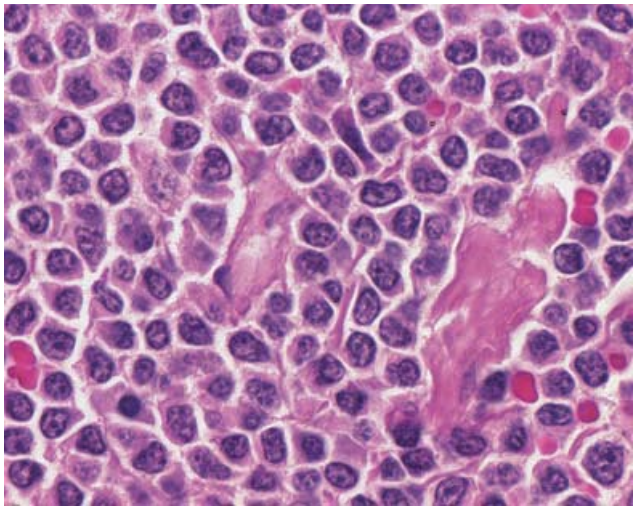

Figure 4.49. Cat: spleen, CLL. Detail of Figure 4.47. There is marked thinning of smooth muscle trabeculae at right surrounded by a dense infiltration of sinus areas by neoplastic lymphocytes. The cellular morphology is of intermediate-sized nuclei that are round or irregularly indented with a moderate volume of cytoplasm and with cell boundaries generally distinct.

sinusoidal, but oddly the level of lymphocytes in the sinus areas does not seem to correlate with the degree of lymphocytosis as measured in the circulating blood. Similar findings occur in cattle with CLL; occur occasionally in horses (Figs. 4.54–4.56); and occur rarely in sheep, goats, and rabbits.

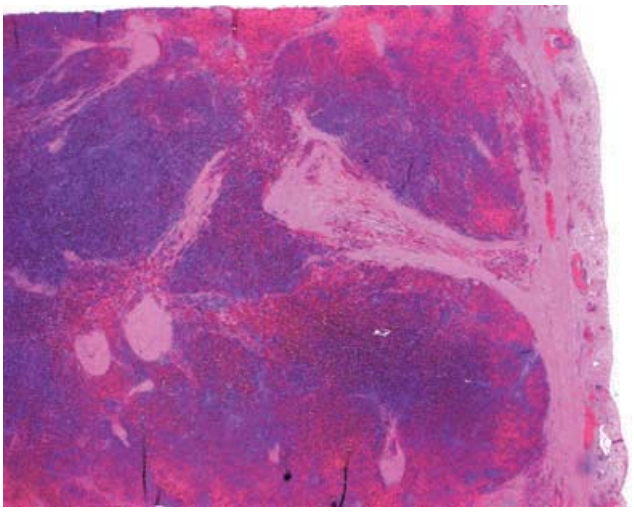

Figure 4.50. Horse: spleen, CLL. Grossly, there was splenomegaly and large areas of ischemic infarction and other areas of irregular congestion. The darker areas represent more dense, but not solid, areas of infiltration with apparent atrophy of normal periarteriolar lymphoid sheaths. The cytologic appearance is similar to that of the node in Figure 4.38.

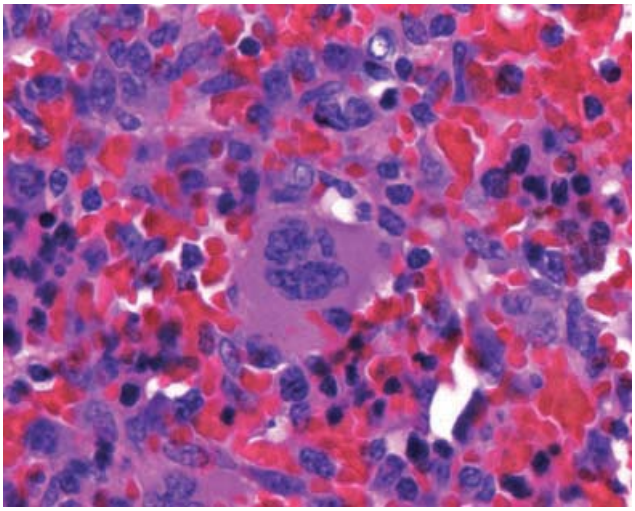

Figure 4.51. Horse: spleen, CLL. Detail of Figure 4.50. A focal area of normal but congested, area of splenic sinus with residual hematopoiesis, primarily megakaryocytic and erythroid.

Differential Diagnosis

CLL needs to be differentiated from reactive hyperplasia, especially in cats. If the level of lymphocytosis is in the range of 25 × 10^3/ul and the animal feels well, it is rational to repeat the examination of blood at intervals of 1–2 months and only examine marrow if there is splenomegaly and a gradual increase in lymphocyte count, with continuing homogeneity of cell type. If the

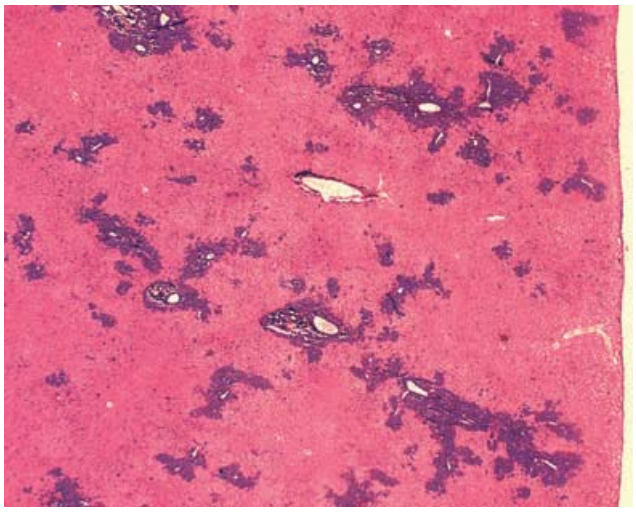

Figure 4.52. Cat: liver, CLL, same case as Figure 4.41. There is sharply defined focal colonization of vascular structures that is most prominent around portal areas but also involves larger central veins. There is extensive sinus involvement not apparent at this magnification.

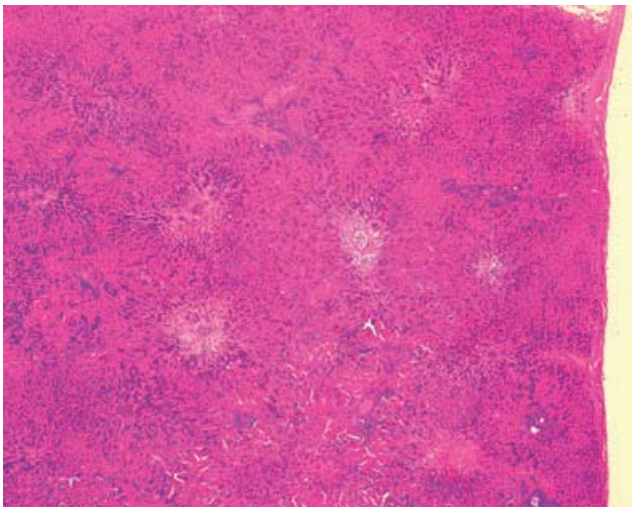

Figure 4.54. Horse: liver, CLL, same case as node in Figure 4.36. The pale areas represent foci of ischemic necrosis with loss of hepatocytes. There is heavy focal colonization of all vascular structures plus heavy sinus colonization.

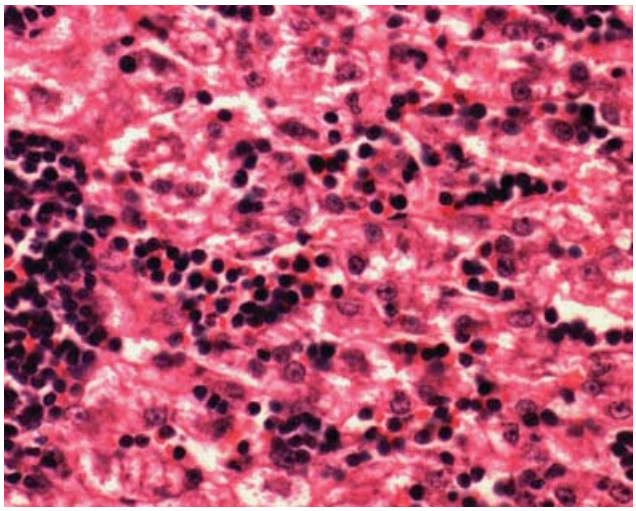

Figure 4.53. Cat: liver, CLL. Detail of Figure 4.52. The edge of a large colonization is at the left with extensive sinus involvement apparent across the functional lobule. Cytologic detail of neoplastic lymphocytes appears in Figure 4.35.

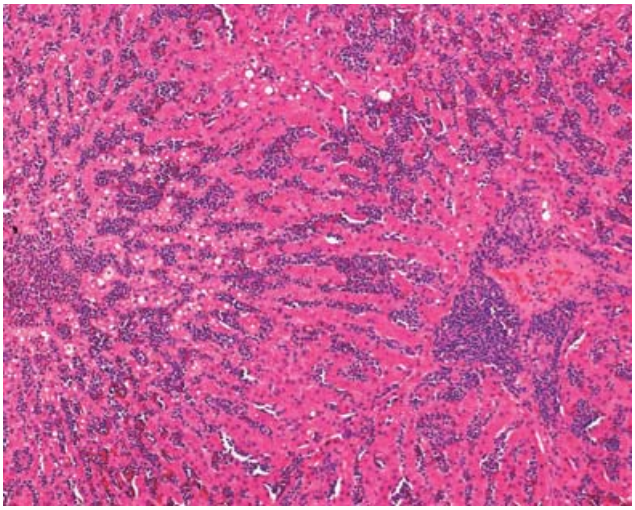

Figure 4.55. Horse: liver, CLL. Detail of Figure 4.54. Hepatic functional lobule, with portal area right and central vein area left. There is extensive involvement of both vascular structures with heavy colonization of hepatic sinusoids. Due to progressive ischemia, there is extensive fallout of hepatocytes surrounding the central vein area.

case appears complex for other reasons, clonality can be determined on blood or even on the DNA from an unstained blood film.

Treatment and Survival

There is little information on the survival of animals with CLL where only cats and dogs are generally given the opportunity to advance to a late stage of the disease. The disease is generally indolent, and it is likely that animals have had the disease for a year or more at the time of presentation or diagnosis. CLL is not curable in humans, and treatment strategies should be aimed at palliation that alone may provide for survival of several years.

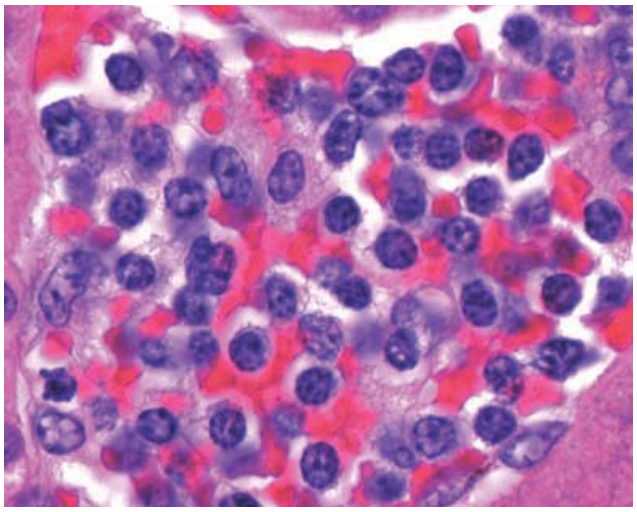

Figure 4.56. Horse: liver, CLL. Detail of Figure 4.54. Hepatic sinusoids are dilated with neoplastic lymphocytes that have round to oval nuclei 1.5 red cells in diameter with densely stained large chromocenters and incomplete parachromatin clearing. Nucleoli are not apparent and the cytoplasm is minimal with moderate staining density.

REFERENCES

Bennett, J.M., Catovsky, D., Daniel, M.T., Flandrin, G., Galton, D.A.G., Gralnick, H.R., and Sultan, C. (1989) Proposals for the classification of chronic (mature) B and T lymphoid leukaemias. *J Clin Pathol* 42:567–584.

Fournel-Fleury, C., Magnol, J.P., Chabanne, L., Ghernati, I., Marchal, T., Bonnefond, C., Bryon, P.A., and Felman, P. (1997) Growth fractions in canine non-Hodgkin's lymphomas as determined in situ by the expression of the Ki-67 antigen. *J Comp Pathol* 117:61–72.

Gilbert, S., Affolter, V.K., Gross, T.L., Moore, P.F., and Ihrke, P.J. (2004) Clinical, morphological and immunohistochemical characterization of cutaneous lymphocytosis in 23 cats. *Vet Dermatol* 15:3–12.

Harvey, J.W., Terrell, T.G., Hyde, D.M., and Jackson, R.I. (1981) Well-differentiated lymphocytic leukemia in a dog: Long-term survival without therapy. *Vet Pathol* 18:37–47.

Hoyer, J.D., Ross, C.W., Li, C.Y., Witzig, T.E., Gascoyne, R.D., Dewald, G.W., and Hanson, C.A. (1995) True T-cell chronic lymphocytic leukemia: A morphologic and immunophenotypic study of 25 cases. *Blood* 86(3):1163–1169.

Kurec, A.S., Threatte, G.A., Gottlieb, A.J., Smith, J.R., Anderson, J., and Davey, F.R. (1992) Immunophenotypic subclassification of chronic lymphocytic leukaemia (CLL). *Brit J Haematol* 81:45–51.

Raskin, R.E., and Krehbiel, J.D. (1988) Histopathology of canine bone marrow in malignant lymphoproliferative disorders. *Vet Pathol* 25:83–88.

Valli, V.E., Jacobs, R.M., Norris, A., Couto, C.G., Morrison, W.B., McCaw, D., Cotter, S., Ogilvie, G., and Moore, A. (2000) The histologic classification of 602 cases of feline lymphoproliferative disease using the National Cancer Institute Working Formulation. *J Vet Diagn Invest* 12:295–306.

Vernau, W., and Moore, P.F. (1999) An immunophenotypic study of canine leukemias and preliminary assessment of clonality by polymerase chain reaction. *Vet Immunol Immunopathol* 69:145–164.

Wong, K.F., Chan, J.K.C., and Sin, V.C. (1996) T-cell form of chronic lymphocytic leukaemia: A reaffirmation of its existence. *Brit J Haematol* 93:157–159.

Workman, H.C., and Vernau, W. (2003) Chronic lymphocytic leukemia in dogs and cats: The veterinary perspective. *Vet Clin Sm An* 33:1379–1399.

Mature (Peripheral) Nodal T-Cell (T-Zone) Lymphoma

Definition

Peripheral T-cell lymphoma of small cell type can be defined as an indolent lymphoma involving peripheral lymph nodes that has a tendency to remain localized for very long periods and is characterized by little impairment of general health and activity and with very long survival with minimal therapy.

Epidemiology and Features

The term "T-zone lymphoma" was first applied in the Kiel classification of 1974 and was described as a rarely encountered small cell nodal lymphoma with the nomenclature providing both phenotypic and architectural identity. T-zone lymphoma (TZL) is a unique neoplasm that is relatively common in dogs and quite uncommon in other species. There were 13 cases of TZL in dogs in a collection of 502 cases of hematopoietic neoplasms. This level of cases is without recognition that this unique neoplasm was not recognized as an entity until the latter part of the 1990s. From the first recorded case of canine TZL at case number 348 the 13 cases constitutes 13/154 or about 8% of cases. Only 1 of these cases was in a mesenteric node and the rest were in peripheral nodes and in submandibular in 5 and generalized in 4 cases. The ages of these animals ranged from 2 to 11 years with a mean of 7 and the gender where known was 7 female and 5 male. Almost the same number of cases, were found in 751 cases of feline lymphoma determined without the benefit of immunophenotyping in all, but 150 more recent cases with no increase in case recognition in cats in the light of better architectural understanding and phenotypic staining. The prevalence of this type of neoplasm is virtually unknown on other species with less than 2% of 1198 cases of bovine lymphoma of small lymphocytic type and these identified on oversight staining without phenotypic selection. In 157 cases of hematopoietic neoplasms in swine there was one case of small lymphocytic lymphoma and 2 cases of CLL one verified as of T-cell type.

Clinical Presentation and Features

The presentation of TZL in the dog is consistent with usually only one or two nodes involved and usually found incidentally as a result of examination for vaccination, dental care or in grooming by the owner. Invariably the dog is in apparent good health with normal appetite and activity. The nodes are always fully mobile and nontender to palpation and easily removed or aspirated with the latter determination indicating benign hyperplasia.

Pathologic Features

Blood and Bone Marrow

As far as is known the blood is not involved at the numerical level in TZL of the dog, and not likely in other species either. It is likely that at a molecular level of examination the neoplastic cells may circulate but are not apparent on routine examinations.

Lymph Node

The architectural features are constant and consist of a taut and usually thinned capsule without involvement of perinodal tissues (Fig. 4.57). The peripheral sinus may be focally compressed but is never destroyed by neoplastic infiltration (Fig. 4.58). Like late stage MZL there is usually some degree of irregular dilation of cortical sinuses with filling by red cells and small lymphocytes (Fig. 4.59). Almost invariably there is at least moderate sclerosis of the medullary supporting raphe some of which may send branches out to the peripheral capsule (Fig. 4.60). There are numerous fading germinal centers or follicles that consist of collapsed mantle cell foci tightly applied to the peripheral sinus and irregularly throughout the interior of the node. In contrast to marginal zone lymphoma (MZL) where the fading follicles are separated from the peripheral sinus by a wide layer of marginal zone proliferation in TZL the cellular population that is growing is *eccentric* to the follicles rather than surrounding them (see Fig. 4.60). In the interior of the node the

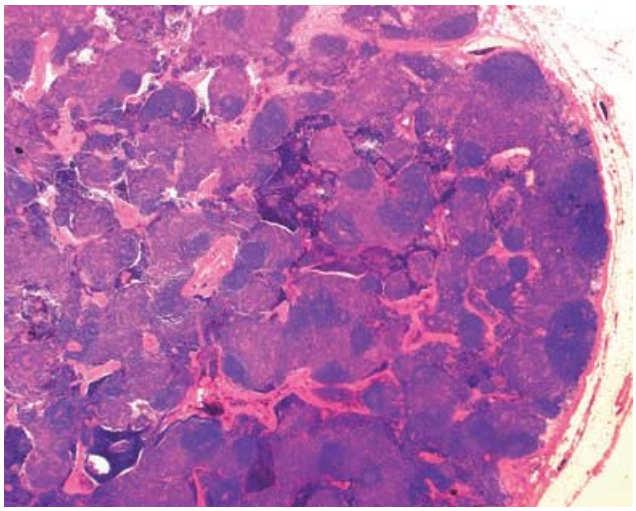

Figure 4.57. Dog: node, T-zone lymphoma. The capsule is focally thinned and taut with multiple densely stained clusters of cells representing the mantle cells of fading germinal centers. There is a moderate and irregular medullary sclerosis with thickening of the collagenous supporting structures against which the fading follicles are frequently located. The more darkly stained areas represent irregular sinus dilation filled with red cells characteristic of later stage TZL.

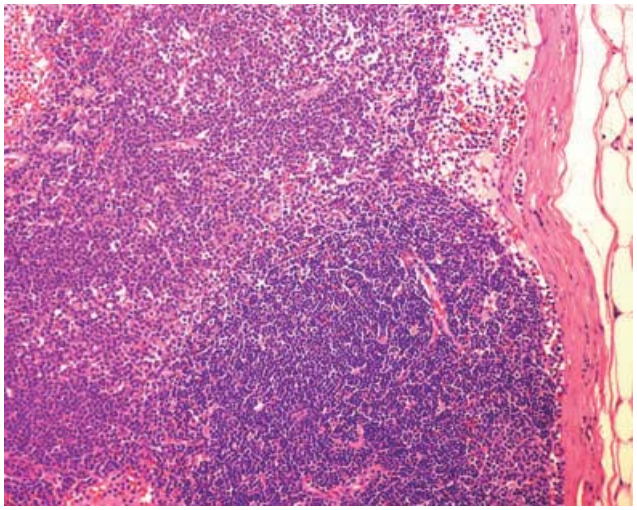

Figure 4.58. Dog: node, T-zone lymphoma. Detail of Figure 4.57. The peripheral sinus is irregularly dilated in the upper right and compressed below but is intact throughout the nodal circumference.

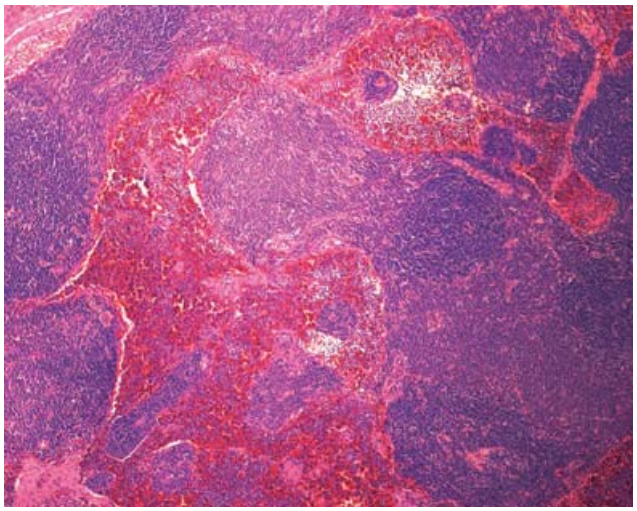

Figure 4.59. Dog: lymph node, T-zone lymphoma. Detail of Figure 4.57. Sinus ectasia, within the interior of the node, that is largely blood-filled with a high level of small lymphocytes is a characteristic change in TZL.

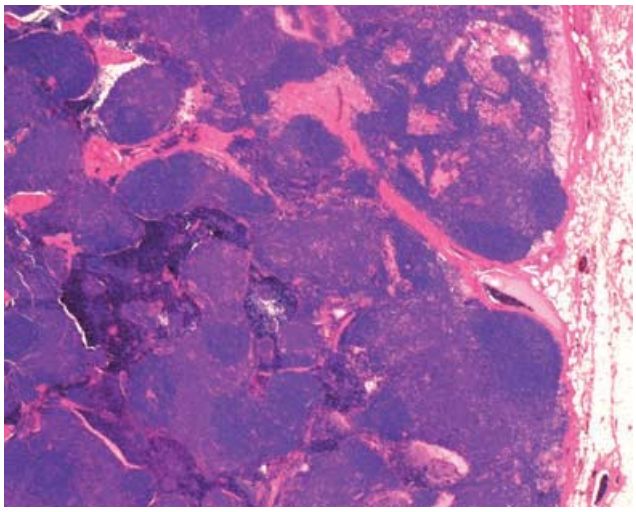

Figure 4.60. Dog: node, TZL. Detail of Figure 4.57. Thickened fibrous raphe associated with vascular structures extend from the capsule of the medullary areas.

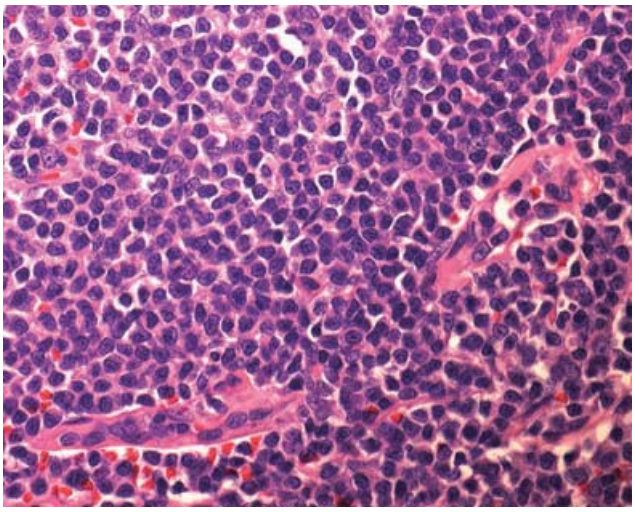

Figure 4.62. Dog: node, TZL. Detail of Figure 4.57. Cortical postcapillary venules, with intraluminal, but few transmural, lymphocytes.

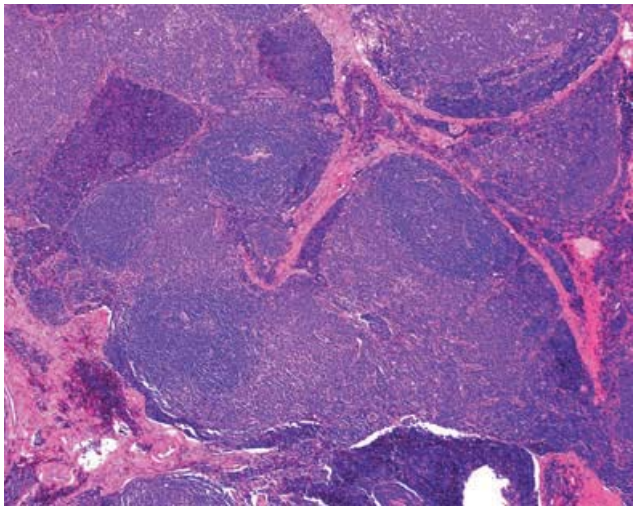

Figure 4.61. Dog: node, TZL. Detail of Figure 4.57. Fading follicular hyperplasia identified as round clusters of darkly stained mantle cells are peripheralized against connective tissue barriers by expanding paracortical proliferation.

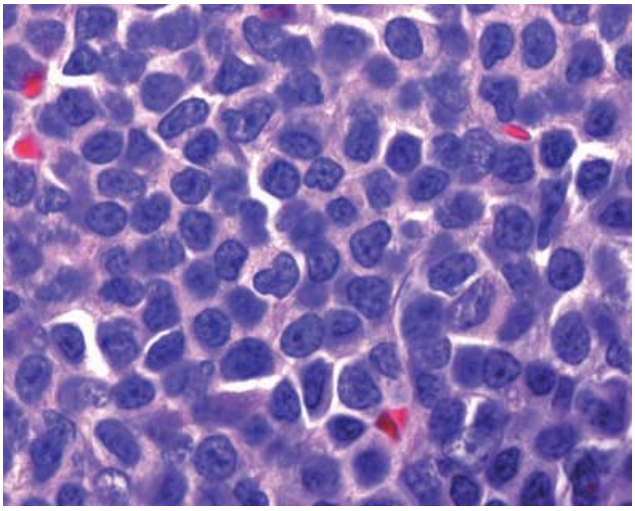

Figure 4.63. Dog: node, TZL. Detail of Figure 4.62. Cytologically the cells of the paracortical expansion have nuclei slightly larger than red cells with densely stained chromatin with large chromocenters and dispersed intervening areas without parachromatin clearing. Nucleoli are present in some cells but are generally small and inapparent. Note the sharp shallow nuclear indentations that are characteristic of this cell population. The cytoplasm is relatively abundant, and lightly stained, giving the nuclei an appearance of relatively even spacing. Finally, mitoses are characteristically absent from most fields.

fading follicles tend to be compressed against the connective tissue supporting structures with the paracortical proliferation extending from the outer cortex to the medulla with filling of the medullary cords and compression of the sinuses (Fig. 4.61). The postcapillary venules of the paracortex retain a high level of endothelial nuclear vesiculation and numerous small lymphocytes of the type in the surrounding areas of proliferation are present within the vessels but the level of translmural cellular migration is relatively low (Fig. 4.62).

The cytologic identity of the TZL is in the small cells that constitute the diffuse paracortical proliferation. These cells have nuclei only slightly larger than the red cells that appear round at low power magnification but have sharp shallow nuclear indentations on detailed examination (Fig. 4.63). They have densely stained finely

distributed chromatin with very small more densely stained aggregations and no parachromatin clearing and rarely nucleoli. The cytoplasm is relatively abundant for small cells and very lightly stained so that the nuclei appear to be very uniformly spaced though cell boundaries are not perceived (Fig. 4.64, see also 4.63). A most important further criterion is that there are virtually no mitotic figures to be found in the neoplastic population. The TZL neoplasm remains unique in progression and is characterized by the irregular areas of sinus dilation becoming larger and the capsule thinner with the node more likely to fragment on sectioning. This change is barely apparent in TZL in the early stage and mid-stage of development (Figs. 4.65–4.69) and becomes more apparent in the later stages of TZL (Fig. 4.70).

Other Organs

No tissues other than lymph node are known to be involved.

Immunologic Features

On phenotypic staining the B-cell reagents CD79 and CD20 give a remarkable picture, with the fading follicles standing out sharply against a completely negative interior of the node (see Figs. 4.65, 4.66). In contrast with CD3, the neoplastic population is uniformly but not heavily marked, and this does not appear to be due to antibody depletion but to the character of the TCR expression (see Figs. 4.67–4.69).

There is a slightly larger variant of the canine TZL that has nuclei the same size as the mantle cells of the fading follicles. These cells have round nuclei with fewer indentations than the smaller, more common, type. The chromatin pattern is more open, with partial parachromatin

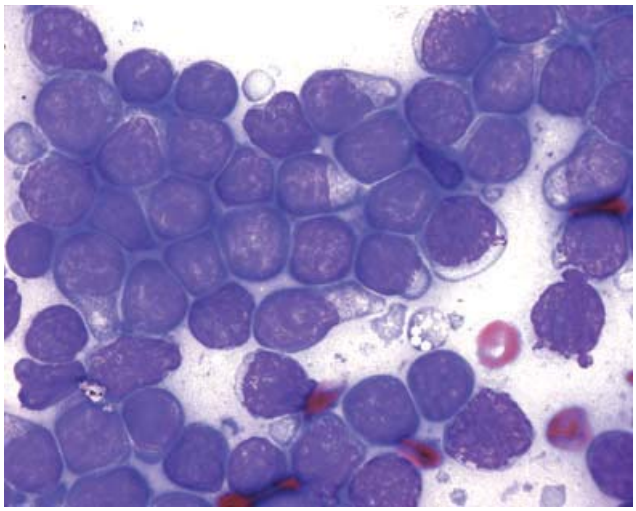

Figure 4.64. Dog: node, T-zone lymphoma, fine needle aspirate. Cytologically, the nuclei are relatively uniform in size and about 1.5 red cells in diameter. The nuclei sharply in focus, on the top and lower margins, have sharp, shallow nuclear indentations, but the irregularities seen histologically are relatively inapparent on cytologic preparations. The chromatin pattern is irregularly dense without parachromatin clearing and nucleoli are generally absent. The cytoplasm is moderate in volume and occasionally eccentric giving rise to hand mirror–type configurations.

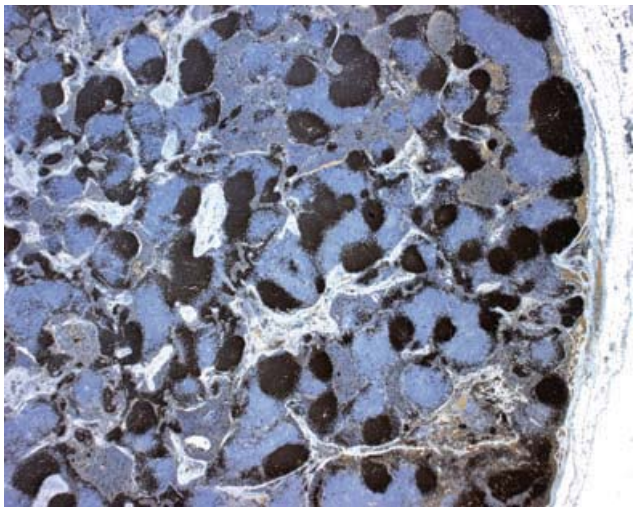

Figure 4.65. Dog: node, T-zone lymphoma. Phenotype of Figure 4.57. On staining with CD20 for B-lymphocytes, the tightly clustered mantle cells provide a striking contrast to the unstained surrounding areas of paracortical proliferation and areas of stroma and sinus ectasia. On phenotypic staining, the eccentric nature of the fading follicles to the surrounding areas of paracortical expansion becomes more readily apparent.

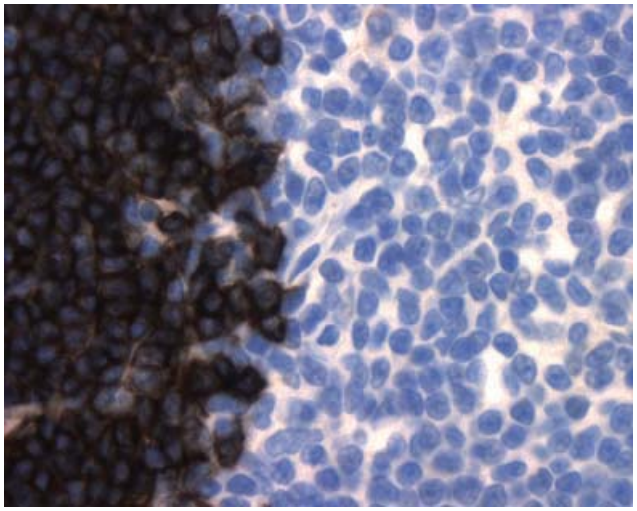

Figure 4.66. Dog: node, TZL phenotype. There is a sharp transition between the densely stained focus of residual mantle cells stained with CD20 and the background of unstained and neoplastic paracortical lymphocytes.

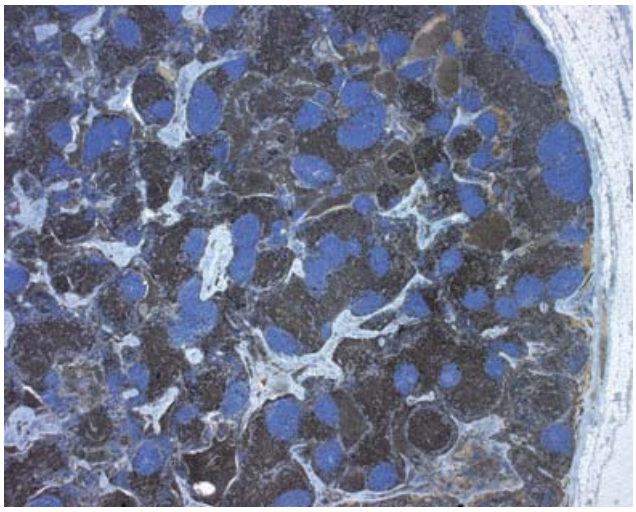

Figure 4.67. Dog: node, TZL. Phenotype of Figure 4.57. On staining with CD3, the focal areas of residual benign mantle cells and areas of supporting stroma are negative, in contrast with the areas of paracortical expansion, uniformly and strongly labeled.

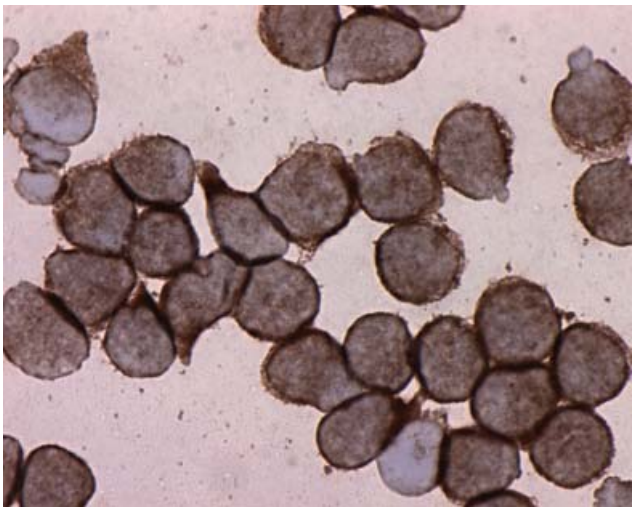

Figure 4.69. Dog: node, T-zone lymphoma. Phenotype of Figure 4.64. CD3 staining of node aspirate with strong cytoplasmic marking.

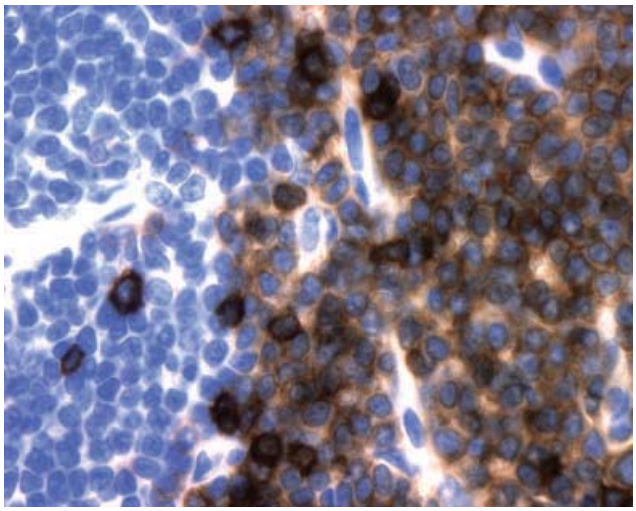

Figure 4.68. Dog: node, TZL phenotype. In a similar interface to Figure 4.66, the benign mantle cells at the bottom are negative with CD3 staining, and the small cells of paracortical expansion are uniformly positive. The small population of the cells most strongly -marking with CD3 may be benign T-cells from the original mantle cell layer since they are not uniformly distributed in the adjacent areas of T-cell proliferation.

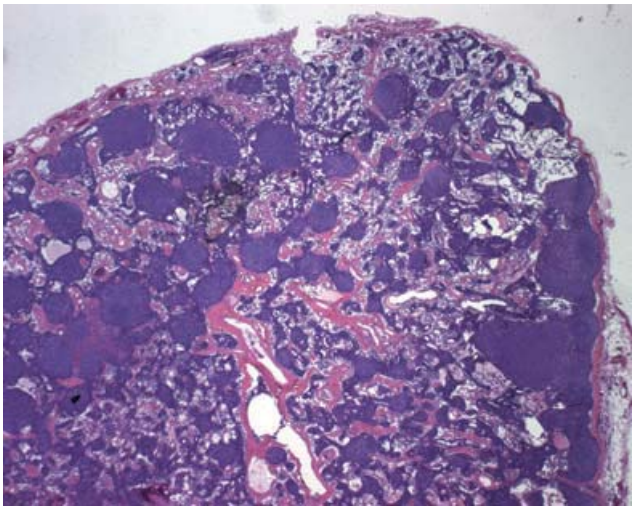

Figure 4.70. Dog: node, TZL. With progression, T-zone lymphoma frequently becomes less cellular with atrophy of the fading follicles that remain primarily subcapsular and with the areas of paracortical expansion increasingly separated by areas of sinus ectasia. The node capsule becomes very thinned and fragile on histologic processing.

clearing between dense chromocenters and with some cells having small nucleoli but no mitoses (Figs. 4.71, 4.72). The architecture is similar but usually with a greater proportion of surviving B-cell population. Some of the cells in these neoplasms are unstained by either CD20 (Fig. 4.73) or CD3 (Figs. 4.74, 4.75), and there may be a separate entity underlying this variant that has not had the benefit of clonal identification by PCR techniques. A neoplasm in human pathology that has similar cytomorphology lacks the architectural characteristics of fading germinal centers and has been referred to as *peripheral T-cell lymphoma, not otherwise specified (PTCL, NOS)* (Figs. 4.76, 4.77). TZL in the cat is similar to the dog but less commonly encountered (Figs. 4.78–4.82).

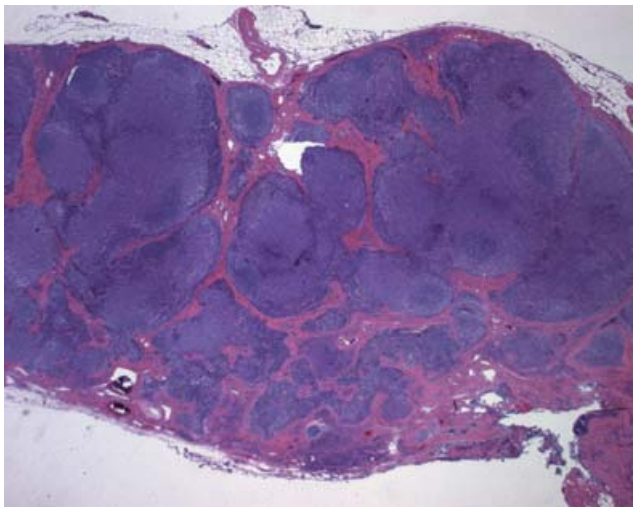

Figure 4.71. Dog: node, T-zone lymphoma, larger cell type. There is marked generalized sclerosis with heavy collagenous connective tissue outlining the areas of lymphoid proliferation. The darkly stained foci are of mantle cells, from fading follicles, usually peripheralized against the connective tissue boundaries.

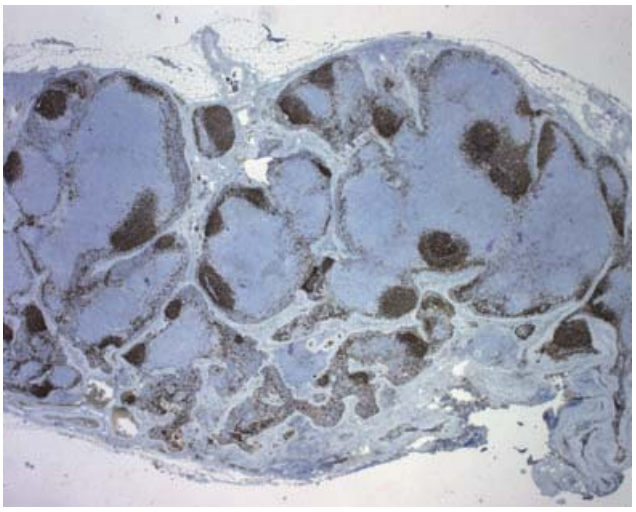

Figure 4.73. Dog: node, TZL. Phenotype of Figure 4.71. With CD20 staining for B-cells, the peripheralized clusters of mantle cells are finely and sharply defined, with the areas of paracortical expansion uniformly negative but with a narrow rim of mantle cells in surrounding sinus areas.

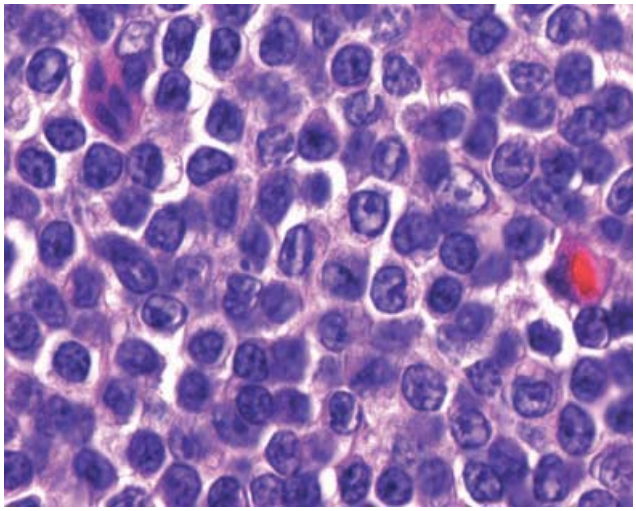

Figure 4.72. Dog: node, T-zone lymphoma, larger cell type. Detail of Figure 4.71. With the red cell at the right as an index of size, it can be seen that the cells are not markedly enlarged, but the chromatin pattern differs with greater aggregation into large chromocenters and clear parachromatin areas. About half the cells have small nucleoli, and the cytoplasm is again moderate in volume and staining density with cell boundaries generally indistinct. An important similarity to the more common smaller cell variant is that the mitotic rate remains very low.

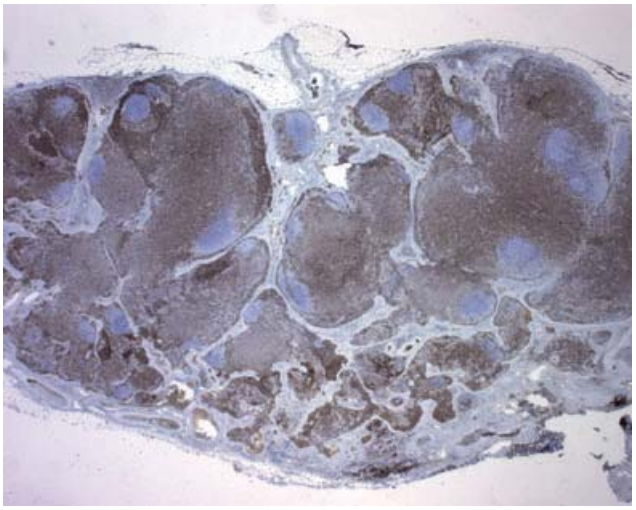

Figure 4.74. Dog: node, TZL. Phenotype of Figure 4.71. On staining with CD3, the diffuse areas of paracortical expansion are uniformly labeled, with the foci of residual mantle cells and stromal areas unmarked.

Transformation and Progression

The biological features of TZL are more compelling than the histocytology, with the animals with this diagnosis living to old age in a number of cases in which the neoplasm was confirmed clonal by PCR. The dogs with this disease may develop bulky nodal enlargement described in one as "orange-sized," but they retain normal activity and apparent vigor. Conservative therapy is currently recommended. The owners rapidly perceive that the dogs do about as well with no therapy as when it is given and consequently tend not to follow regimes of intensive therapy. Combination chemotherapy seems to be less effective in reducing nodal size as compared to that for more aggres-

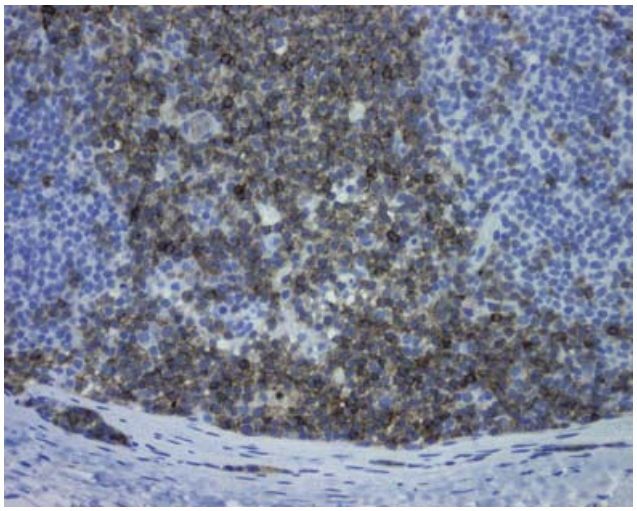

Figure 4.75. Dog: node, T-zone lymphoma, larger cell type. Phenotype of Figure 4.71. With CD3 staining, a junctional area between two foci of fading mantle cells and a portion of peripheral sinus demonstrates that the cell type in the residual B- and T-cell areas are very similar in size and other characteristics at all but the highest magnification. Neoplasms of this type are likely similar to those in human medicine referred to as peripheral T-cell lymphoma, not otherwise specified (PTCL NOS).

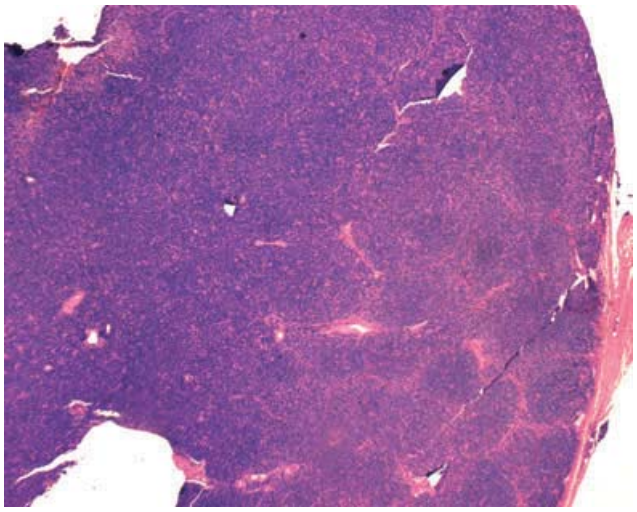

Figure 4.76. Human: node, peripheral T-cell lymphoma. A small cell lymphoma with dense relatively uniform architecture was characterized as peripheral T-cell lymphoma, not otherwise specified. *Slide from Cornell Tutorial.*

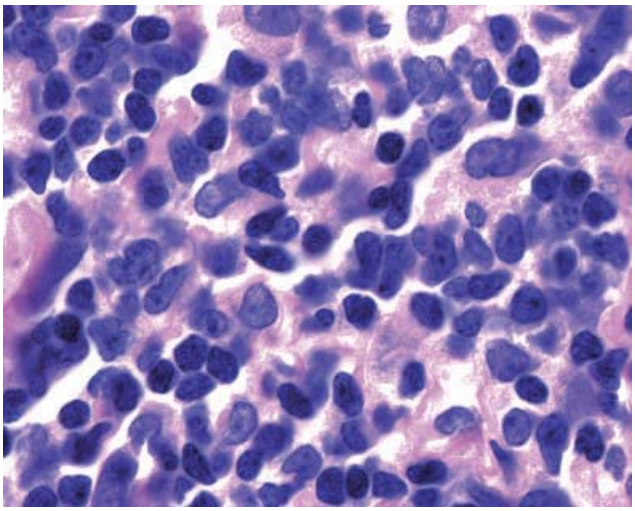

Figure 4.77. Human: lymph node, peripheral T-cell lymphoma. Detail of Figure 4.76. Cytologically, the smaller more densely stained cells are very similar to those of the smaller type of T-zone lymphoma of the dog. The larger cells with more vesicular nuclei but irregular boundaries are more like the cells of the larger form of canine TZL. Like the canine neoplasms of similar type, there is a very low mitotic and apoptotic rate.

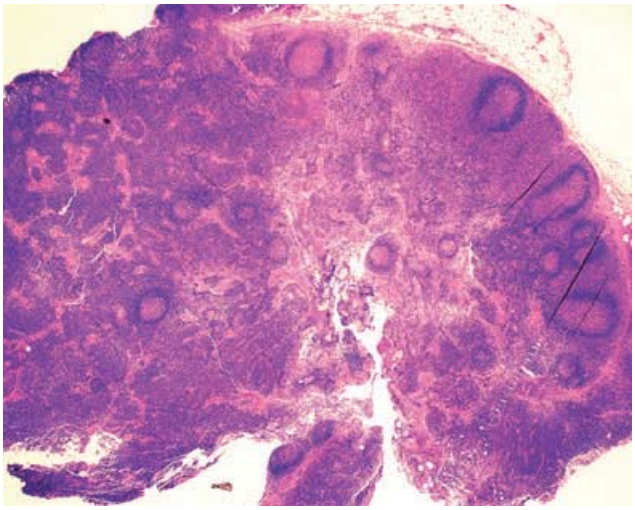

Figure 4.78. Cat: node, T-zone lymphoma. The changes are similar to the dog in that there is evidence of fading follicular hyperplasia, with germinal centers appearing in the medullary areas and usually some degree of medullary sclerosis. There is capsular thinning, and generally peripheral nodal tissue is not involved.

sive lymphomas and appears less required because of the apparent normal function of the nontreated animal.

Differential Diagnosis

TZL must be distinguished from SLL of T- or B-cell type, which is much less common and tends to involve multiple tissues including the spleen and liver. There are significant cytologic differences, with TZL having fine, sharp, shallow nuclear indentations as a constant finding in the small cell variant, less common in the large cell variant, and not seen in CLL. In isolated tissues, areas of CLL might appear similar, but the widespread organ and blood involvement in CLL would be definitive.

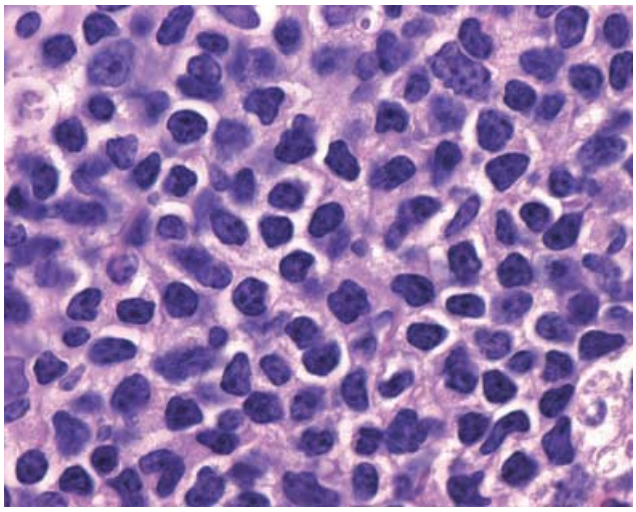

Figure 4.79. Cat: node, T-zone lymphoma. Detail of Figure 4.78. Cytologically, these cells are similar to those in the dog, with small compact nuclei slightly larger than red cells with large densely stained chromocenters without parachromatin clearing and most cells lacking nucleoli. There is, as with the dog, a moderate volume of lightly stained cytoplasm, with the nuclei tending to be very uniformly separated but with cell boundaries indistinct. The mitotic and apoptotic rate are both very low.

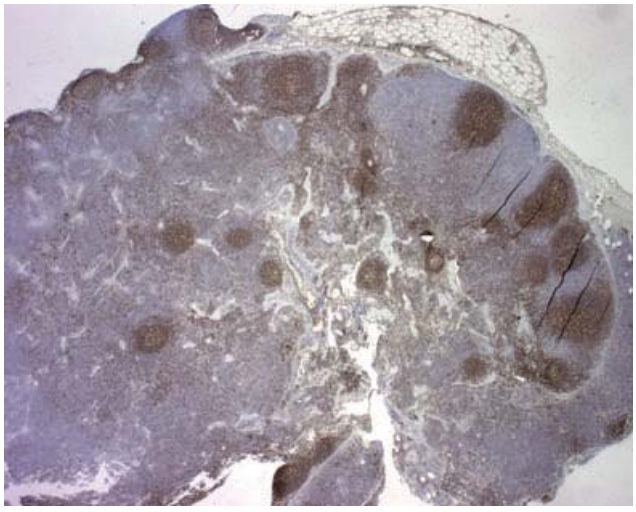

Figure 4.80. Cat: node, T-zone lymphoma. Phenotype of Figure 4.78. On staining with CD20, the peripheral and central fading germinal centers are strongly and uniformly labeled, with the areas of paracortical proliferation primarily marked with the counter stain.

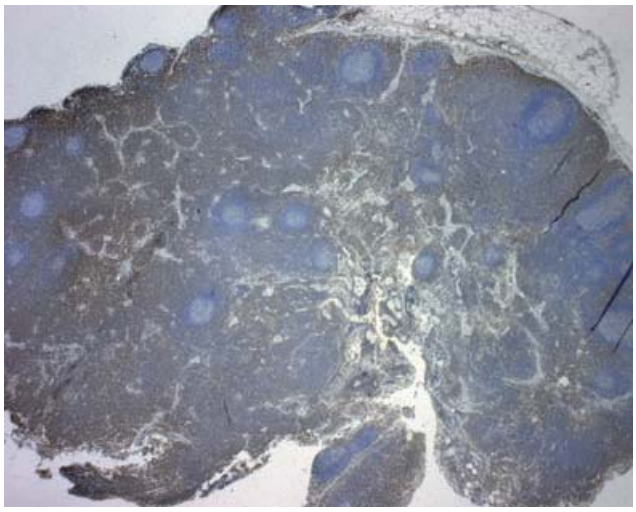

Figure 4.81. Cat: node, T-zone lymphoma. Phenotype of Figure 4.78. With CD3 staining, the fading areas of medullary and peripheral centers are unmarked, with the surrounding paracortical areas solidly and uniformly labeled.

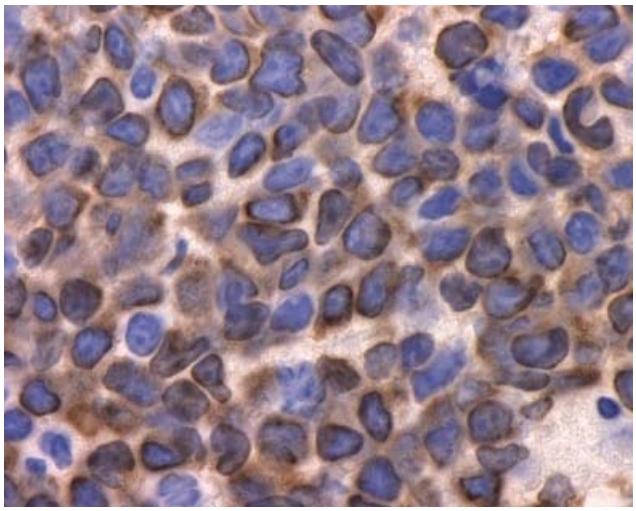

Figure 4.82. Cat: node, T-zone lymphoma. Phenotype of Figure 4.78. The process of antigen retrieval causes the nuclei to swell slightly in the more vesicular lymphomas with generally little effect in most neoplasms like TZL. The irregular shape of the nuclei is still apparent as well as uniform marking for the T-cell receptor.

TZL or small T-cell lymphocytic lymphoma (SLL) is less distinctive in other animals and less common than what has become the TZL of dogs. In cats, the node with SLL has a diffuse, very dense appearance at low magnification that is like an entire node filled with cells of mantle cell size and staining characteristics and unlike the fading follicle architecture of TZL. In SLL, the capsule is taut and very thinned and the peripheral sinus is compressed. There are often foci of bridging of the capsule with involvement of the perinodal tissues. Cytologically, the neoplastic cells are about the size and staining character of thymic cortical cells with round densely stained nuclei, inapparent cytoplasm, no nucleoli, and no mitoses. There are the occasional foci of slightly larger cells that are the "proliferation centers" described in human cases, and small lymphatics in the cortical areas may be seen tightly

packed with small lymphocytes similar to those in the surrounding tissue. These clusters are surrounded by very thin-walled vessels, and there are no accompanying red cells that support this interpretation.

Treatment and Survival

The biological behavior of TZL in dogs is not a matter of much record, but others have noted long survival in these animals with minimal or no treatment.

REFERENCES

Carter, R.F., and Valli, V.E.O. (1988) Advances in the cytologic diagnosis of canine lymphoma. *Sem Vet Med Surg (Sm An)* 3(3):167–175.

Carter, R.F., Valli, V.E.O., and Lumsden, J.H. (1986) The cytology, histology and prevalence of cell types in canine lymphoma classified according to the National Cancer Institute Working Formulation. *Can J Vet Res* 50:154–164.

Fournel-Fleury, C., Magnol, J.P., Bricaire, P., Marchal, T., Chabanne, L., Delverdier, A., Bryon, P.A., and Felman, P. (1997) Cytohistological and immunological classification of canine malignant lymphomas: Comparison with human non-Hodgkin's lymphomas. *J Comp Path* 117:35–59.

Hanson, C.A., Bockenstedt, P.L., Schnitzer, B., Fox, D.A., Kueck, B., and Braun, D.K. (1991) S100-positive, T-cell chronic lymphoproliferative disease: An aggressive disorder of an uncommon T-cell subset. *Blood* 78(7):1803–1813.

Kelley, L.C., and Mahaffey, E.A. (1998) Equine malignant lymphomas: Morphologic and immunohistochemical classification. *Vet Pathol* 35:241–252.

Nakamura, S., Suchi, T., Koshikawa, T., Suzuki, H., Oyama, A., Kojima, M., Motoori, T., Ueda, R., and Takahashi, T. (1993) Clinicopathologic study of 212 cases of peripheral T-cell lymphoma among the Japanese. *Cancer* 72(5):1762–1772.

The Non-Hodgkin's Lymphoma Classification Project. (1997) A clinical evaluation of the International Lymphoma Study Group Classification of Non-Hodgkin's Lymphoma. *Blood* 89(11):3909–3918.

Pandolfi, F., Zambello, R., Cafaro, A., and Semenzato, G. (1992) Biology of disease: Biologic and clinical heterogeneity of lymphoproliferative diseases of peripheral mature T lymphocytes. *Lab Invest* 67(3):274–302.

Rüdiger, T., Ichinohasama, R., Ott, M.M., Müller-Deubert, S., Miura, I., Ott, G., and Müller-Hermelink, H.K. (2000) Peripheral T-cell lymphoma with distinct perifollicular growth pattern: A distinct subtype of T-cell lymphoma? *Am J Surg Pathol* 24(1):117–122.

Shimoyama, M., and Members of The Lymphoma Study Group (1991) Diagnostic criteria and classification of clinical subtypes of adult T-cell leukaemia-lymphoma. *Brit J Haematol* 79:428–437.

Uherova, P., Ross, C.W., Finn, W.G., Singleton, T.P., Kansal, R., and Schnitzer, B. (2002) Peripheral T-cell lymphoma mimicking marginal zone B-cell lymphoma. *Mod Pathol* 15(4):420–425.

Vernau, W., Jacobs, R.M., Davies, C., Carter, R.F., and Valli, V.E.O. (1998) Morphometric analysis of bovine lymphomas classified according to the National Cancer Institute Working Formulation. *J Comp Path* 118:281–289.

T-Cell Prolymphocytic Leukemia

Prolymphocytic proliferation in animals has a much firmer basis in cell recognition than in disease characterization. The name does describe a unique stage of lymphoid cell morphology but is otherwise inappropriate. In neoplasms of B-cell prolymphocytic leukemia, the cells have surface Ig but their precursors do not; in T-cell prolymphocytic leukemia, the cells have well-developed TCR development and are more mature than their precursors and therefore are ill termed as prolymphocytic. The use of the name *prolymphocytic* is somewhat analogous to that of the "hand mirror" cytoplasmic extrusion, which is seen in cytological preparations and largely attributed to T-cell lineage but occurs in both T- and B-cells and is indicative of a generic stage of maturation rather than of lineage.

T-cell prolymphocytic leukemia (PLL) is a relatively rare type of neoplasm that has a chronic or subacute course that is seen in cattle and dogs and likely occurs in all domestic animals. The disease presents with reduced performance, and anemia is present and accompanied by a leukemic lymphocytosis of 50–100 $\times$ 10^3/ul. There is usually not neutropenia or thrombocytopenia, but on marrow aspiration there is multifocal marrow involvement. The spleen is usually moderately and diffusely enlarged and there is minor cuffing of hepatic portal vessels, but the peripheral lymph nodes are not enlarged.

Cytologically, the nuclei in PLL are round to oval and 1.5 red cells in diameter. They are not indented or cleft, but they may be compressed into hourglass or smoothly indented forms. The cytoplasm is moderate in volume and staining density with the cell diameter about 2 red cells in total. The cytoplasm is of uniform density and basophilia without the usual perinuclear clear areas of lymphoid neoplasms and it is always agranular. The unique distribution of the chromatin gives the cell its most characteristic feature, with 20 or so large dense chromocenters that are separated by areas of parachromatin clearing. The chromocenters are irregularly linked by coarse chromatin bands that give an overall appearance of a "spotted" nucleus at low magnification (Fig. 4.83). Nucleoli are not present but there is a low percentage (<1%) of larger cells present that represent the dividing population. These larger cells have the same overall shape, but the nuclei are a full 2 red cells in diameter, and the chromatin is more dispersed with only a few smaller chromocenters and no parachromatin clearing. About half of these larger cells have small nucleoli. Similar

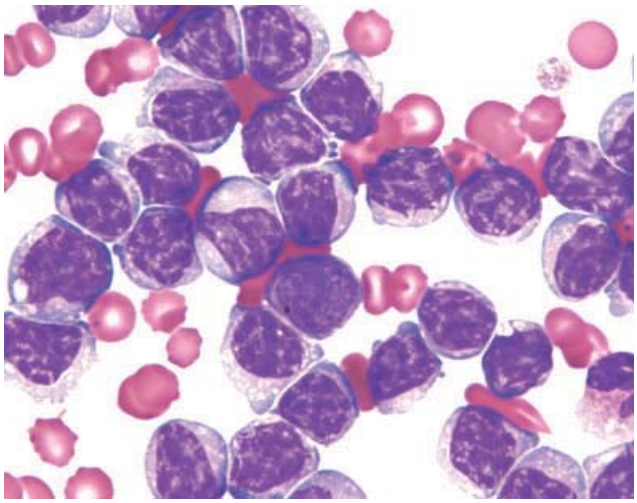

Figure 4.83. Dog: blood, prolymphocytic leukemia. The nuclei are round to oval and generally 1.5 red cells in diameter, with the chromatin pattern characteristic and consisting of large chromocenters separated by broad chromatin bands with intervening areas of parachromatin clearing. The cytoplasm is moderate in volume and lightly stained, with characteristic perinuclear clearing and peripheral increased basophilia of lymphocytes. Most cells lack nucleoli but the cell directly in the center with the finer chromatin pattern has a small nucleolus and is likely one of the dividing cells of the population. *Slide from W. Vernau, BVSc.*

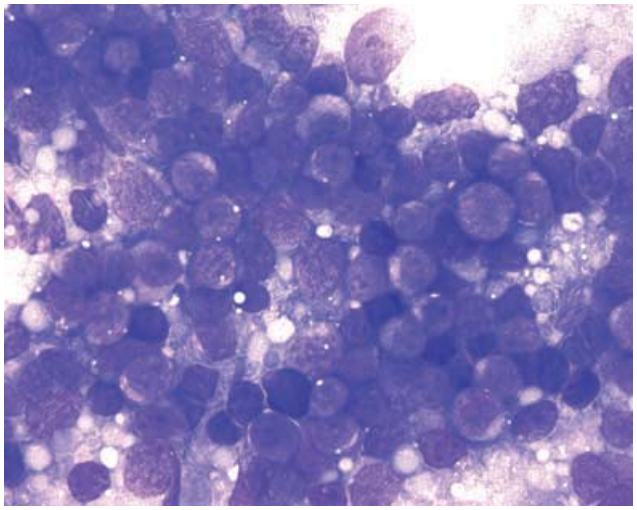

Figure 4.84. Dog: node, prolymphocytic lymphoma. The nuclear pattern appears stippled at the intermediate level of magnification without the apparent parachromatin clearing seen with cells of similar cell type in blood.

changes are present in node and splenic tissues involved with PLL cellular infiltration. The chromatin patterns are most evident in areas of cytologic preparations where the cells are not too crowded (Figs. 4.84, 4.85) but characteristic changes are always more evident in blood (Figs. 4.86, 4.87).

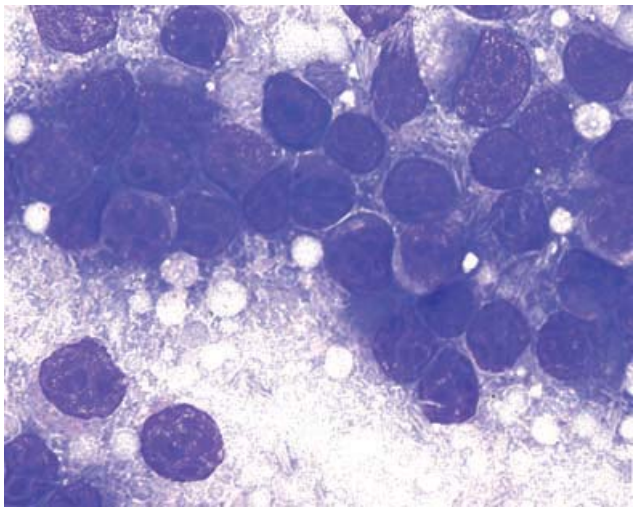

Figure 4.85. Dog: node, prolymphocytic lymphoma. Detail of Figure 4.84. The chromatin pattern on most of the cells is characterized by large chromocenters irregularly joined by chromatin bands with intervening areas of parachromatin clearing. Most cells do not have obvious nucleoli. The cytoplasm is moderate in volume and staining density. The mitotic rate is generally quite low.

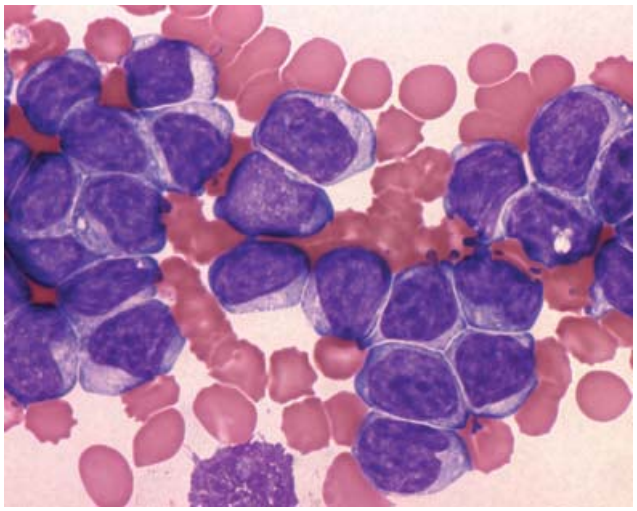

Figure 4.86. Dog: node, prolymphocytic leukemia. Most cells have the characteristic large chromocenters that are irregularly outlined by parachromatin clearing. The cell in the center has a more uniform chromatin pattern and a nucleolus and likely constitutes the proliferating population. *Slide from R. M. Jacobs, DVM.*

In immunocytochemical staining, the cells are CD3 positive and negative for CD79 and likely for CD20 as well. Cells that correspond to this type of morphology but are CD3 negative have been presumptively considered to be of NK-cell type. In histological preparations, the PLL cells

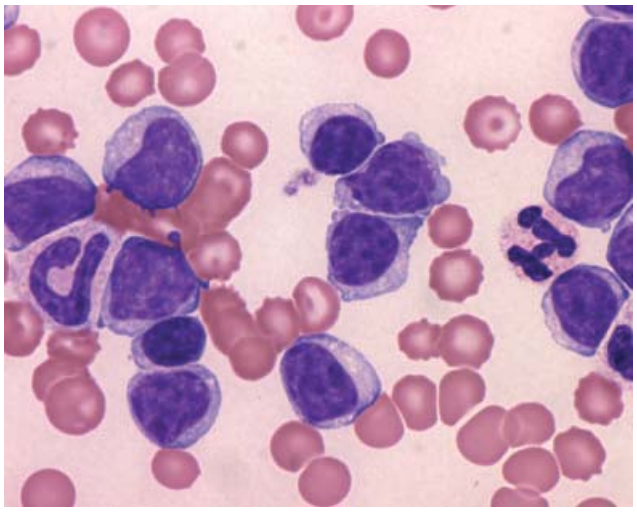

Figure 4.87. Dog: node, PLL, same case as Figure 4.86, body of the slide with greater cell diversity. These smaller cells are more typical of the predominant period of leukemia, with the dog feeling quite well while the larger cells tend to herald an accelerating process. Note that the neutrophil at the right tends to hypersegmentation that is likely an indication of splenic overload.

resemble intermediate type or size of lymphoma with slightly more internal nuclear detail and, again, can be seen to lack nucleoli that may be confused with the often round but dense chromocenters.

In human studies, the PLL neoplasm is described as a post-thymic tumor, usually of αβ type of TCR expression. Nothing is known about the etiology of the neoplasm in animals, but in humans some association has been made with the HLV-1 provirus.

The diagnosis of PLL is based on the blood picture as a whole, including the elevated lymphocyte count and the unique chromatin structure. PLL must be differentiated from CLL of B- or T-cell type, with both tending to have much more generally aggregated chromatin without the parachromatin clearing. Cases that completely correspond to T-PLL but are CD3 negative are considered to be a form of NK-cell leukemias.

Because the disease has not been recognized as an entity, there is no information on the response of T-PLL to therapy or to expected outcome. Because a few larger cells are characteristically present, it is likely that with progression these cells increase as in CLL and that terminally there is a shift to a more aggressive neoplasm with widespread organ involvement.

REFERENCES

Domingo-Doménech, E., Gonzalez-Barca, E., Salar, A., Claros, A.D., and Granerna, A. (1999) Indolent course as presentation in t-prolymphocytic leukaemia. *Brit J Haematol* 105:840.

Herling, M., Khoury, J.D., Washington, L.T., Duvic, M., Keating, M.J., and Jones, D. (2004) A systematic approach to diagnosis of mature T-cell leukemias reveals heterogeneity among WHO categories. *Blood* 104(2):328–335.

Kojima, K., Hara, M., Sawada, T., Miyata, A., Saito, H., Matsuo, Y., Yasukawa, M., Fujita, S., and Harada, M. (2000) Human T-lymphotropic virus type I provirus and T-cell prolymphocytic leukemia. *Leuk and Lymph* 38(3–4):381–386.

Serra, A., Estrach, M.T., Marti, R., Villamor, N., Rafel, M., and Montserrat, E. (1998) Cutaneous involvement as the first manifestation in a case of T-cell prolymphocytic leukaemia. *Acta Derm Venereol (Stockh)* 78:198–200.

Soma, L., Cornfield, D.B., Prager, D., Nowell, P., and Bagg, A. (2002) Unusually indolent T-cell prolymphocytic leukemia associated with a complex karyotype: Is this T-cell chronic lymphocytic leukemia? *Am J Hematol* 71:224–226.

Sugimoto, T., Imoto, S., Matsuo, Y., Kojima, K., Yasukawa, M., Murayama, T., Kohfuku, J., Mizuno, I., Yakushijin, K., Sada, A., Nishimura, R., and Koizumi, T. (2001) T-cell receptor γδ T-cell leukemia with the morphology of T-cell prolymphocytic leukemia and a post-thymic immunophenotype. *Ann Hematol* 80:749–751.

Tamayose, K., Sato, N., Ando, J., Sugimoto, K., and Oshimi, K. (2002) CD3-negative, CD20-positive T-cell prolymphocytic leukemia: Case report and review of the literature. *Am J Hematol* 71:331–335.

Wong, K.F., Chan, J.K., and Sin, V.C. (1996) T-cell form of chronic lymphocytic leukaemia: A reaffirmation of its existence. *Brit J Haematol* 93:157–159.

T-Cell Granular Lymphocytic Leukemia/Lymphoma

Leukemias involving large granulated lymphocytes (LGL) are likely widely distributed in nature and are described in dogs, cats, horses, and birds, but oddly not in the cow where LGLs are frequently seen in inflammatory conditions. Unlike other types of lymphoid neoplasms where a specific cell type has a similarity of disease presentation, in most species the LGL cell diseases are more diagnoses of cell type rather than of specific disease entities. Thus, the associated conditions need to be defined by their unique presentation in each species.

In the cat, LGL proliferation is most likely to present as a lymphoma involving the lower small intestine and the associated lymph nodes of the mesentery. Typically, the animals present with anorexia, vomiting, and diarrhea, usually of recent onset, but often weight loss has been noted. The animals are not anemic or only mildly so, usually have a mild to moderate neutrophilic leukocytosis, and are not thrombocytopenic; neoplastic LGL cells are present in blood in less than half of cases. On examination of marrow, there is myeloid hyperplasia, and erythropoiesis may be depressed with large lymphocytes present and generally in the 10% range of nucleated cells. With progression, there is involvement of the sinus areas

of the spleen and the sinusoids of the liver (Fig. 4.88) and kidney may be involved without liver colonization (Figs. 4.89, 4.90). Cytologically, the LGL cells of cats are distinctive in being large with nuclei round, oval, or indented at least 3 red cells in diameter with densely stained chromatin with absent or obscured nucleoli. The cytoplasm is abundant and lightly basophilic. The granules are characteristically larger than in other species, round, azurophilic on blood stains, and mainly about 1 micron in diameter, but they may be as large as 3 um in diameter and grouped in perinuclear areas. Most of the cases described were accessed before the era of immunohistochemical phenotyping and are described as likely of NK-cell type. The disease in the cat is much more consistent than in the dog and it is likely that a consistent phenotypic pattern will be described.

In the dog, LGL disease has a whole range of presentations that include benign lymphocytosis in reaction to ehrlichiosis or other chronic antigenemia or frank leukemia. In contrast to the cat, a dog with LGL disease has lymphocytosis that may be mild or very marked and as high as 200×10^3/ul. Lymphocytosis of cells with LGL characteristics in the dog is likely to be associated with anemia of mild to moderate degree, but in contrast to the human disease (Fig. 4.91) dogs are not neutropenic (Figs. 4.92, 4.93). The LGL leukemias in the dog are unique for other reasons that may require a redefinition of the concept of leukemia because the bone marrow has little involvement, and the neoplasms arise in the splenic sinuses. Normal dogs are found to have 0–500 LGLs/ul in peripheral blood that constitutes 1–10% of the circulating pool of lymphocytes. Most of the LGLs in blood are CD3 positive, with something less than 10% being negative for both T- and B-cell markers and are presumptively of NK-cell type. Most (60%) of blood LGLs are of αβ T-cell receptor type, and half that level (32%) are of γδ type T-cell receptor. However, the most basic characteristic of the LGL cells is their leukointegrin expression of α_d/β_2 type, which is not limited to LGL cells but is shared by macrophages, T-cells of both αβ and γδ receptor types, and NK-cells. The importance of this leukointegrin status as defined by McDonough and Moore is that cells with

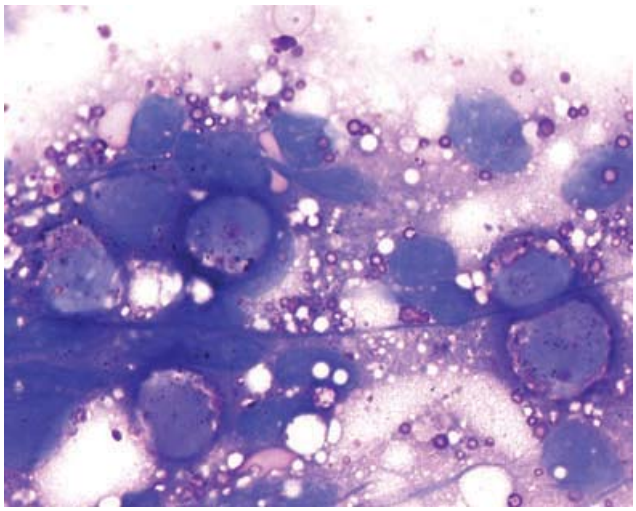

Figure 4.88. Cat: node, large granular lymphocytic lymphoma. Imprint of hepatic Tru-cut biopsy. The nuclei are large, and the granules are remarkably large and prominent. *Slide from R. M. Jacobs, DVM.*

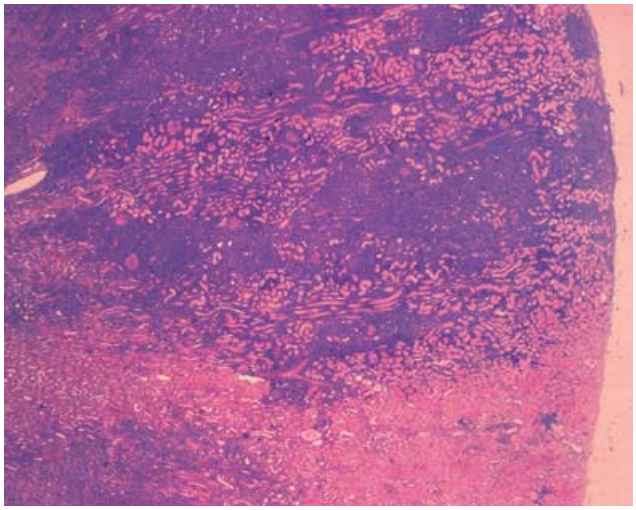

Figure 4.89. Cat: kidney, LGL lymphoma. There is extensive infiltration of the entire cortex extending from the capsule to the cortical medullary junction in an irregular fashion.

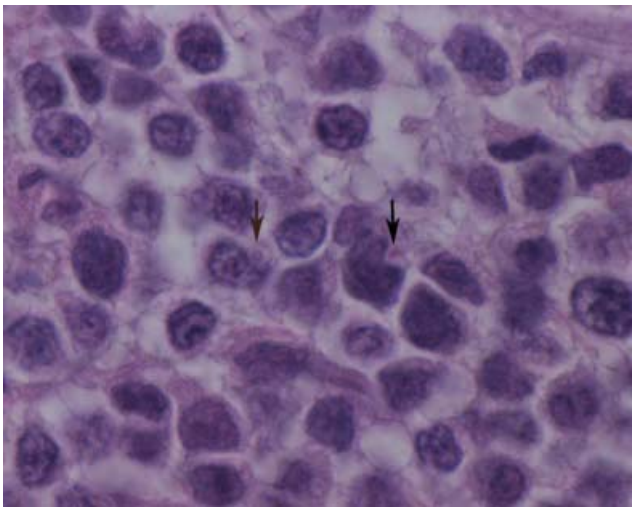

Figure 4.90. Cat: renal LGL lymphoma. Detail of Figure 4.89. Even with quite large granules (arrows), the diagnosis is unlikely to be made histologically if the granules have not been recognized on cytologic examination. This lesion was negative on staining with CD3, which suggests the cells may be of NK-cell type.

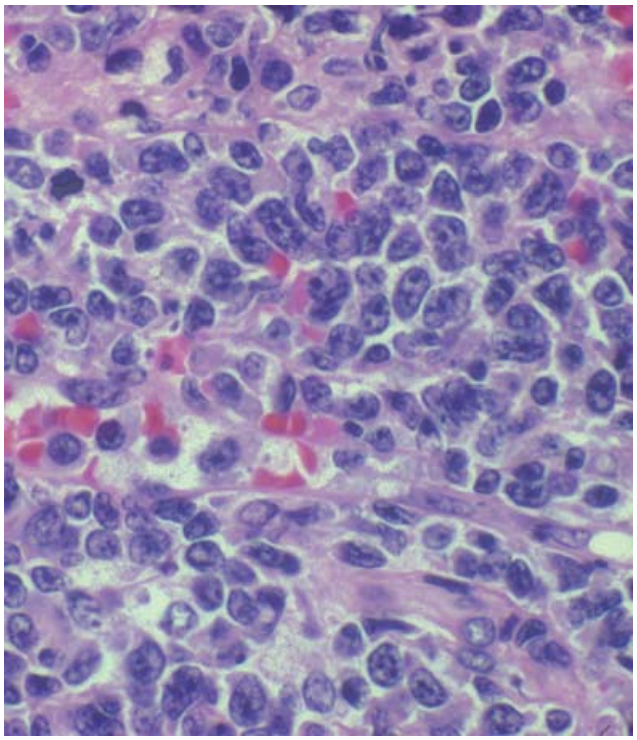

Figure 4.91. Human: spleen, hepatosplenic lymphoma. There is diffuse filling of sinus areas with cells with quite variable-shaped nuclei, with irregular chromatin patterns with parachromatin clearing and most cells having nucleoli. The cytoplasm is inapparent and cell boundaries are irregularly distinct. *Slide from Cornell Tutorial.*

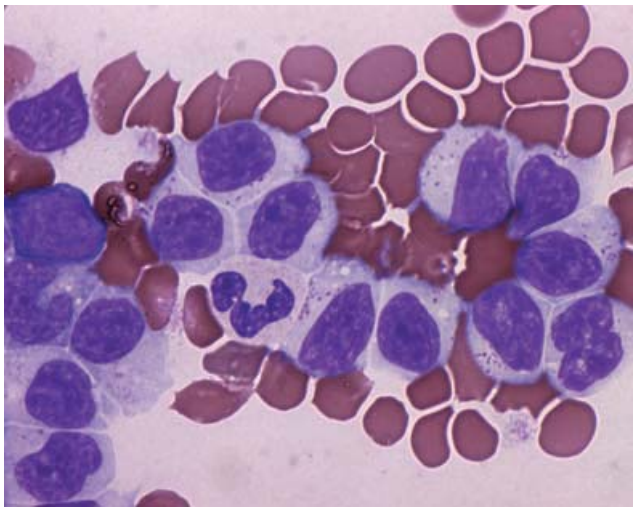

Figure 4.92. Dog: blood, CLL of LGL type. Tip of smear with aggregates of cells. Nuclei are typically 2 red cells in diameter with a broad envelope of lightly stained cytoplasm. The dog presented with a leukocyte count of 144,000 per ul. *Slide from R. M. Jacobs, DVM.*

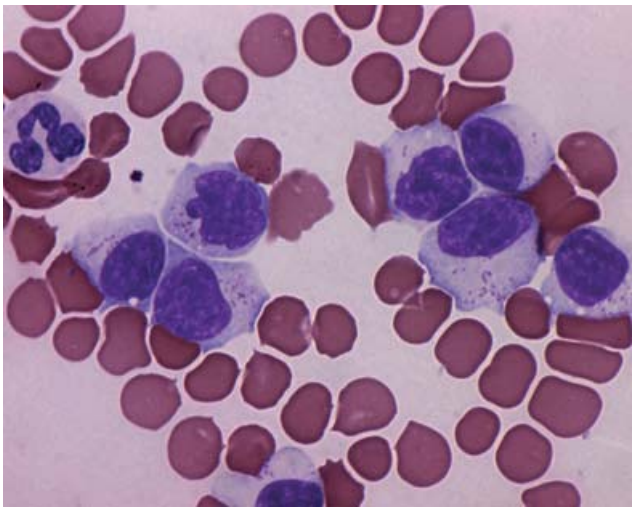

Figure 4.93. Dog: blood, CLL, LGL type, same case as Figure 4.92, body of the blood field. Note the marked variation in nuclear shape and chromatin pattern like that of prolymphocytic leukemia.

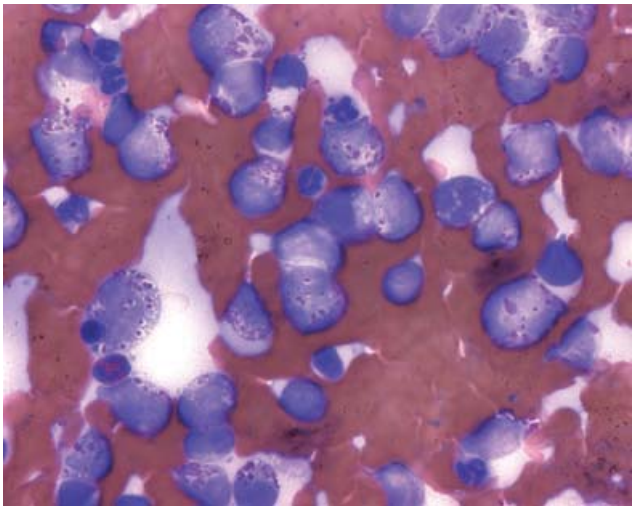

Figure 4.94. Dog: spleen, hepatosplenic lymphoma. Fine needle aspirate of spleen. There is a uniform population of large cells with large and multiple granules.

that specific surface binding complement are in high proportion in normal circumstances in the splenic red pulp sinuses. It follows that in hyperplastic and neoplastic states, these same homing preferences would prevail, and in LGL leukemia in the dog there is heavy colonization of the splenic sinuses with splenomegaly. Remarkably, the marrow involvement appears to be largely cells in transit.

In dogs with acute leukemia of LGL cells the disease may be very rapidly progressive or slowly but relentlessly progressive with survival of 1–2 years. These animals have hepatosplenomegaly at diagnosis that persists, and terminally there may be neoplastic infiltrates in virtually all tissues but particularly spleen (Figs. 4.94, 4.95) and

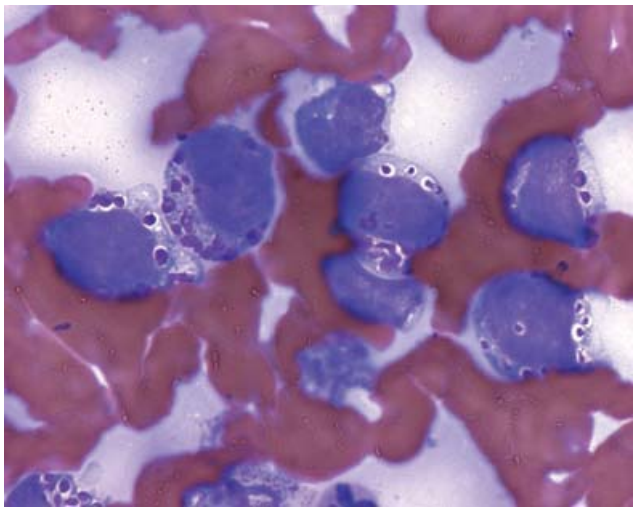

Figure 4.95. Dog: spleen, hepatosplenic lymphoma. Detail of Figure 4.94. With focus on the granules, the nuclei have densely stained, relatively uniform, and evenly dispersed chromatin with some cells having a multiple prominent nucleoli.

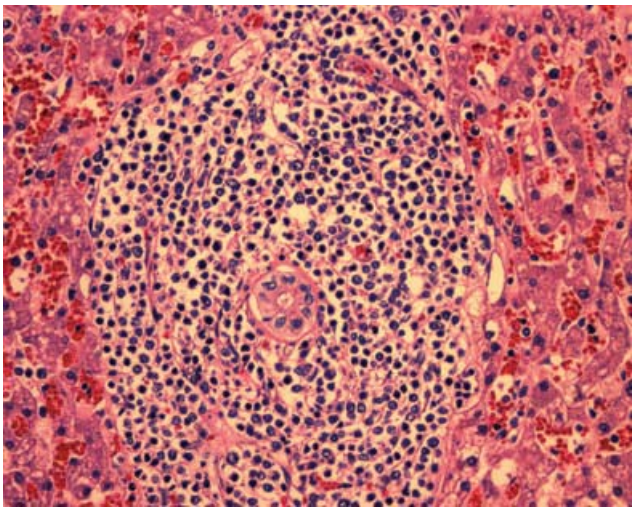

Figure 4.97. Dog: liver, LGL. Detail of Figure 4.96. Isolated bile ducts are surrounded by neoplastic infiltration that compresses hepatocytes in a broad front manner without penetrating the periportal surrounding connective tissue.

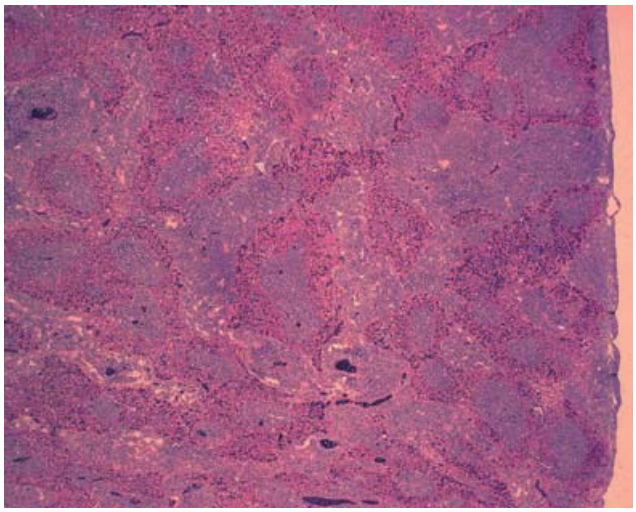

Figure 4.96. Dog: liver, LGL. There is encircling infiltration around vascular structures that is coalescing to isolate hepatocytes to those remaining in mid-zone areas.

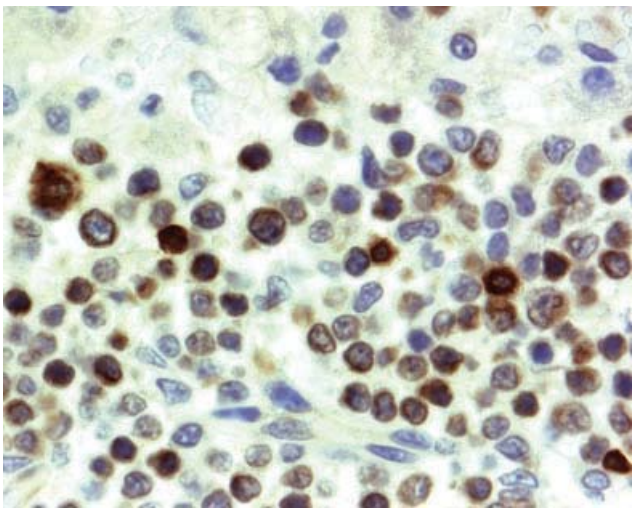

Figure 4.98. Dog: liver, LGL. Phenotype of Figure 4.96. With CD3 staining, the cells are strongly but irregularly marked, with the tissues suffering autolytic changes prior to fixation.

liver (Figs. 4.96–4.98). The blood picture is one of progressively severe leukocytosis of LGL cells with anemia and thrombocytopenia, but not neutropenia, and the marrow tends to retain granulocyte production (Fig. 4.99). In the blood, the LGL cells always predominate, but other lymphocytes remain in circulation. Cytologically, the neoplastic LGL cells have round to oval and reniform nuclei with densely stained and irregularly aggregated chromatin without apparent nucleoli. The cytoplasm is abundant, lightly basophilic with <20 granules lying near the nuclear membrane. The granules vary widely in size from less than 1–2 um and stain a light pink with blood stains.

Although lymphocytosis of LGL type cells may occur in a variety of inflammatory conditions in the cat and dog, there is no consistent agent that might be considered causative. However, a retroviral agent has been derived from an LGL neoplasm in a dog from which a cell line was derived with the virus found in the cells in culture.

In other species where LGL leukemia has been found, including the Fischer 344 rat (Figs. 4.100, 4.101), the disease is primarily in the spleen as in the dog, with the

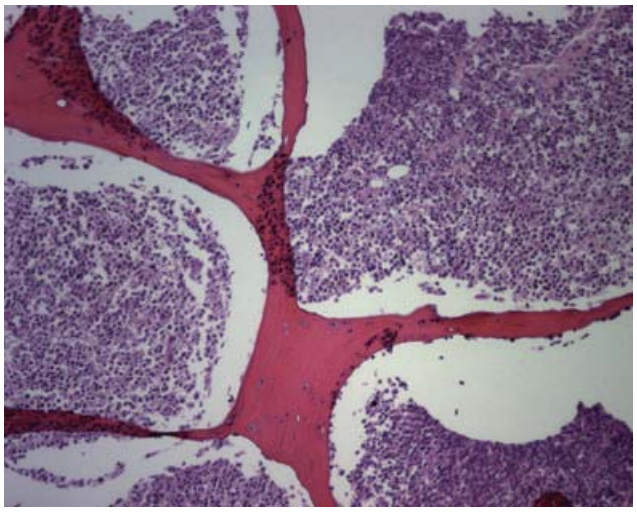

Figure 4.99. Dog: bone marrow, LGL. The bone marrow is extensively infiltrated with the dog presenting very late in the disease. There is extensive replacement of all fat cells and a uniform population of large round cells with phthisis of normal marrow elements.

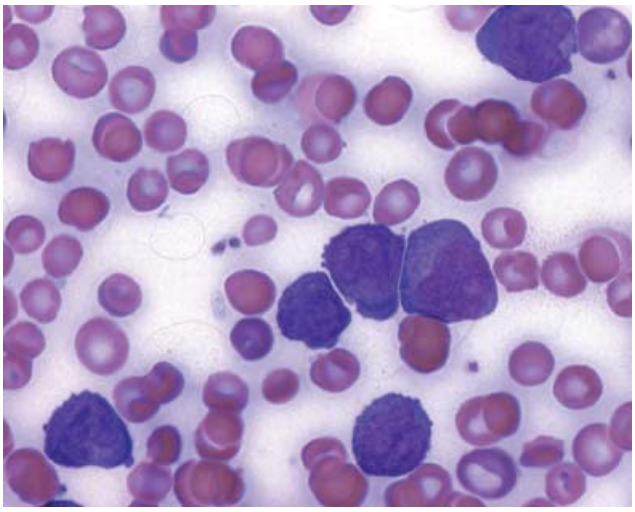

Figure 4.101. Rat: blood, large granulocytic leukemia, same animal as in Figure 4.100. In this area, the larger cell in the right center has visible cytoplasmic granules beside the nucleus. The cell in the upper right has very fine cytoplasmic granulation in the nuclear notch with the other cells likely of the same type.

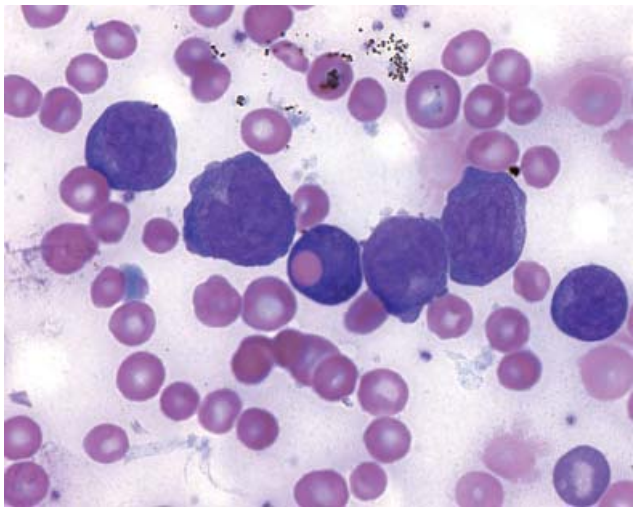

Figure 4.100. Fischer rat: blood, large granular lymphocyte leukemia. There are fine cytoplasmic granulations barely apparent in the cells closest to that in the center, which has ingested a red cell. Erythrophagocytosis by a primitive cell occurs in other T-cell lymphomas in the cat and dog and is an indication of malignancy since monocytic cells at that stage of development would not be erythrophagocytic.

LGL cells lacking CD3 and considered of NK-cell type and having the same $alph_d/beta_2$ leukointegrin as the dog. In the horse, the presentation and topographical distribution of the tumor is hepatoenteric, as in the cat. Differential diagnoses that need to be considered include the globular leukocyte tumor that has been described in cats.

REFERENCES

Cheney, C.M., Rojko, J.L., Kociba, G.J., Wellman, M.L., Di Bartola, S.P., Rezanka, L.J., Forman, L., and Mathes, L.E. (1990) A feline large granular lymphoma and its derived cell line. *In Vitro Cell Dev Biol* 26:455–463.

Cho, K.H., Kim, C.W., Kwon, O.S., Yang, S.G., Park, K.C., Park, M.H., Cho, H.I., and Kim, J.G. (1997) Epstein-Barr virus–associated lymphoproliferative eruption with progression to large granular lymphocytic leukaemia. *Brit J Dermatol* 137:426–430.

Darbès, J., Majzoub, M., Breuer, W., and Hermanns, W. (1998) Large granular lymphocyte leukemia/lymphoma in six cats. *Vet Pathol* 35:370–379.

Foucar, K., Matutes, E., and Catovsky, D (2004) T-cell large granular lymphocytic leukemia, T-cell prolymphocytic leukemia, and aggressive natural killer–cell leukemia/lymphoma. In Mauch, P.M., Armitage, J.O., Coiffier, B.C., Dalla-Favera, R., and Harris, N.L. (eds.), *Non-Hodgkin's Lymphomas*. Lippincott Williams & Wilkins, Philadelphia, pp. 283–293.

Franks, P.T., Harvey, J.W., Calderwood Mays, M., Senior, D.F., Bowen, D.J., and Hall, B.J. (1996) Feline large granular lymphoma. *Vet Pathol* 23:200–202.

Ghernati, I., Corbin, A., Chabanne, L., Auger, C., Magnol, J.P., Fournel, C., Monier, J.C., Darlix, J.L., and Rigal, D. (2000) Canine large granular lymphocyte leukemia and its derived cell line produce infectious retroviral particles. *Vet Pathol* 37:310–317.

Grindem, C.B., Roberts, M.C., McEntee, M.F., and Dillman, R.C. (1989) Large granular lymphocyte tumor in a horse. *Vet Pathol* 26:86–88.

Henson, K.L., Alleman, A.R., Kelley, L.C., and Mahaffey, E.A. (2000) Immunohistochemical characterization of estrogen and progesterone receptors in lymphoma of horses. *Vet Clin Pathol* 29(2):40–46.

Herraez, P., Berridge, B., Marsh, P., Weeks, B., and Ramiro-Ibañez, F. (2001) Small intestine large granular lymphoma in a horse. *Vet Pathol* 38:223–226.

Kariya, K., Konno, A., and Ishida, T. (1997) Perforin-like immunoreactivity in four cases of lymphoma of large granular lymphocytes in the cat. *Vet Pathol* 34:156–159.

Kramer, J., Tornquist, S., Erfle, J., and Sloeojan, G. (1993) Large granular lymphocyte leukemia in a horse. *Vet Clin Pathol* 22(4):126–128.

Lamy, T., and Loughran, T.P. (1999) Currents concepts: Large granular lymphocyte leukemia. *Blood Rev* 13:1–11.

Losco, P.E., and Ward, J.M. (1984) The early stage of large granular lymphocyte leukemia in the F344 rat. *Vet Pathol* 21:286–291.

Matsumoto, Y., Tsujimoto, H., Fukasawa, M., Hirota, Y., Miura, T., Hayami, M., Goitsuka, R., Ono, K., and Hasegawa, A. (1990) Molecular cloning of feline leukemia provirus genomes integrated in the feline large granular lymphoma cells. *Arch Virol* 111:177–185.

McDonough, S.P., and Moore, P.F. (2000) Clinical, hematologic, and immunophenotypic characterization of canine large granular lymphocytosis. *Vet Pathol* 37(6):637–646.

McEntee, M.F., Horton, S., Blue, J., and Meuten, D.J. (1993) Granulated round cell tumor of cats. *Vet Pathol* 30:195–203.

Miyajima, R., Hosoi, M., Yamamoto, S., Mikami, S.I., Yamakawa, S., Iwata, H., and Enomoto, M. (1999) Eosinophilic granulated cells comprising a tumor in a Fischer rat. *Toxicol Pathol* 27(2):233–236.

Patnaik, A.K. (1993) Histologic and immunohistochemical studies of granular cell tumors in seven dogs, three cats, one horse, and one bird. *Vet Pathol* 30:176–185.

Staempfli, H.R., McAndrew, K.H., Valli, V.E.O., and McEwen, B.J. (1988) An unusual case of lymphoma in a mare. *Equine Vet J* 20(2):141–143.

Wellman, M.L., Hammer, A.S., DiBartola, S.P., Carothers, M.A., Kociba, G.J., and Rojko, J.L. (1992) Lymphoma involving large granular lymphocytes in cats: 11 cases (1982–1991). *JAVMA* 201(8):1265–1269.

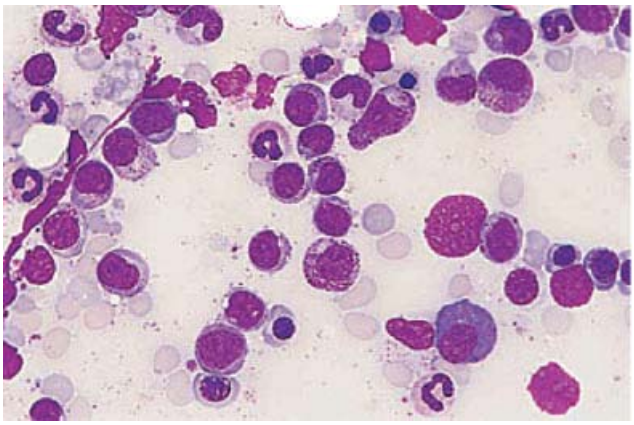

Figure 4.102. Human: blood, Aggressive NK-cell leukemia. Multiple neoplastic cells with round nuclei 1.5 red cells in diameter have a dense cribriform chromatin pattern with small nucleoli and a moderate lightly stained cytoplasm with numerous azurophilic granules. *Reprinted from* Surgical Pathology, *9th Edition, Volume 2, by Rosai and Ackerman, 2004, Chapter 23, page 2089, with permission from Elsevier and J. K. C. Chan, MD.*

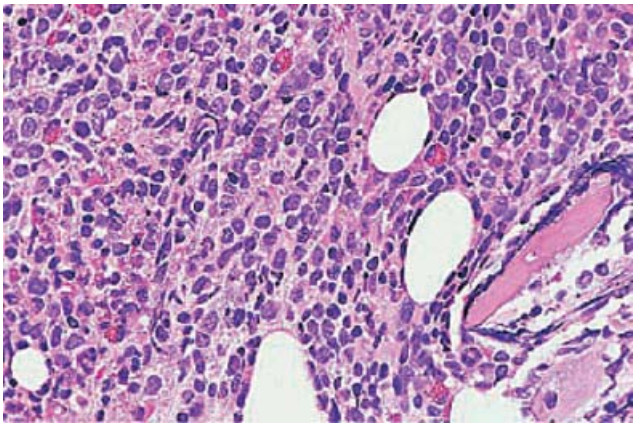

Figure 4.103. Human: bone marrow, aggressive NK-cell leukemia, same patient as in Figure 4.102. There is very heavy involvement of marrow with intermediate-sized cells with round nuclei and relatively abundant cytoplasm with phthisis of normal marrow cells.

Aggressive NK-Cell Leukemia and Blastic NK-Cell Lymphoma

Aggressive NK-Cell Leukemia

In the WHO classification, the aggressive NK-cell leukemias and the blastic NK-cell lymphomas are considered as separate entities. Because so little is known of these diseases in humans where overlap in these diseases is seen to occur, they are considered together here to define roughly the diseases that likely have animal counterparts as yet undescribed. In humans, the NK-cell aggressive leukemia is a rare disease seen most frequently in the Mideastern countries and often associated with Epstein-Barr virus (EBV) infection (Figs. 4.102, 4.103). The disease is seen in adults and without male or female predominance. The diagnosis in humans is considered difficult, which may be one reason why the entity is not defined in animals. NK-cells can be defined on functional properties and have similarities to other mature or postthymic T-cells, but the morphologic identification is difficult because there is no phenotypic specificity to the NK-cells. The two major classes of postthymic T-cells are defined on the structure of the T-cell receptor as α-β or γ-δ types. NK-cells have largely germline T-cell receptor genes but usually express the ε chain that is part of the CD3 complex and, as a consequence, most NK-cells have cytoplasmic labeling with CD3 but not membrane TCR.

The primary phenotypic marker for human NK-cells is CD56 (N-CAM), but this antigen also occurs on acute myeloid neoplasms of monocytoid type and on lymphoblastic lymphomas, cytotoxic lymphocytes, and dendritic cell neoplasms. CD56 does not mark cells with NK-cell function in any known animal species, including nonhuman primates.

Despite these limitations, the human neoplastic NK-cells are consistently of LGL type and of intermediate-sized nuclei, are round with densely stained chromatin, and with abundant cytoplasm that is granulated. There is bone marrow involvement that is of diffuse distribution with rapid extension to other tissues with interstitial type infiltration.

The immunophenotype of the aggressive NK-cell leukemia is identical to that of the nasal type NK-cell lymphoma, and it is likely that these diseases represent leukemic and solid or lymphomatous presentations of the same cell type. Both are associated with EBV integration in a clonal manner. Both diseases are positive for CD56, CD2, TIA-1, and granzyme. The T-cell receptor genes are unrearranged and remain germline.

The clinical presentation of human NK-cell leukemia is of patients with systemic disease having fever, weight loss, organomegaly, and multiorgan failure. One-third to one-half of cases present with skin lesions that may have preceded the onset of systemic illness. Most cases have extensive hepatosplenomegaly, and half have lymphadenopathy. The blood findings are of anemia, thrombocytopenia, and neoplastic cells in circulation. Therapy has included a variety of chemotherapeutic agents, with splenectomy and immunotherapy effective in isolated cases that have survived for several years.

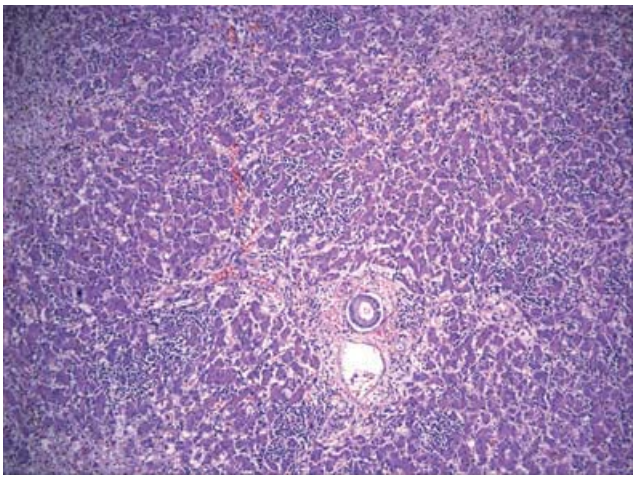

Figure 4.104. Dog: liver, Aggressive T-cell lymphoma. The liver is very heavily involved with the primarily sinus colonization with ischemic degeneration of hepatocytes in central vein areas. With fine needle aspirate, the neoplasm was found to be lymphoid of large granular lymphocyte (LGL) type. *Image from P. F. Moore, BVSc.*

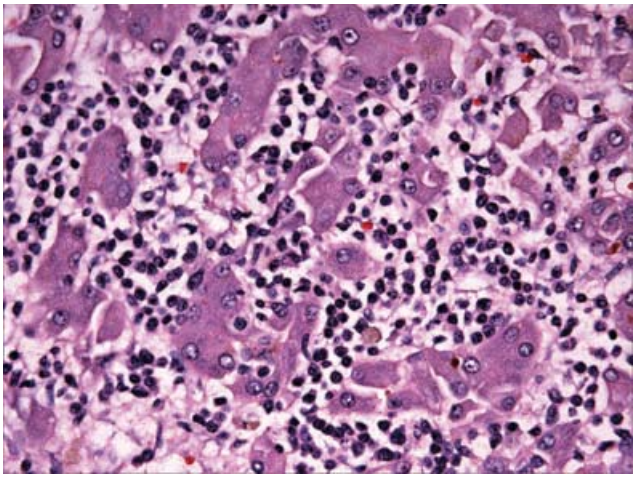

Figure 4.105. Dog: liver, aggressive NK-cell lymphoma. Detail of Figure 4.104. The hepatic cords are broken up by very extensive infiltration of leukocytes of intermediate size with a relative narrow rim of lightly stained cytoplasm.

Blastic NK-Cell Lymphoma

The extranodal nasal lymphoma of NK-cell type is the prototypic solid tumor of NK-cell type. This disease formerly known as lethal midline granuloma occurs in other regions of the upper airway system and is now known as *nasal type* as an all-encompassing term. Although usually focal and facial, a small portion of human cases present with severe systemic disease and hepatic and marrow failure.

A disease in dogs may be of similar type in presenting with hepatomegaly and splenic masses with abdominal nodal involvement, rapid progression, and an LGL cell type on cytological examination. The liver was very heavily infiltrated with primarily sinus colonization (Figs. 4.104, 4.105), and on staining with CD3 there is distinct cytoplasmic labeling (Fig. 4.106). On characterization of the neoplasm by PF Moore BVSc, the cells had cytoplasmic positivity for epsilon fraction of CD3 but negative for T-cell receptor in frozen sections (Figs. 4.107, 4.108). PCR probing of the T-cell receptor and immunoglobulin genes did not demonstrate gene rearrangement from germline. The cytoplasmic positivity was determined to be due to expression of the epsilon chain, and the case was concluded to be lymphoma of NK-cell type. This nasal type of this neoplasm is not recognized in animals, although some of the facial rodent ulcers of cats have similarities to this disease.

In humans, the nasal form of NK-cell lymphoma is rare and has a strong geographic distribution seen in southern China and in Japan and Korea. In Hong Kong, where there is a long history of very competent diagnostic

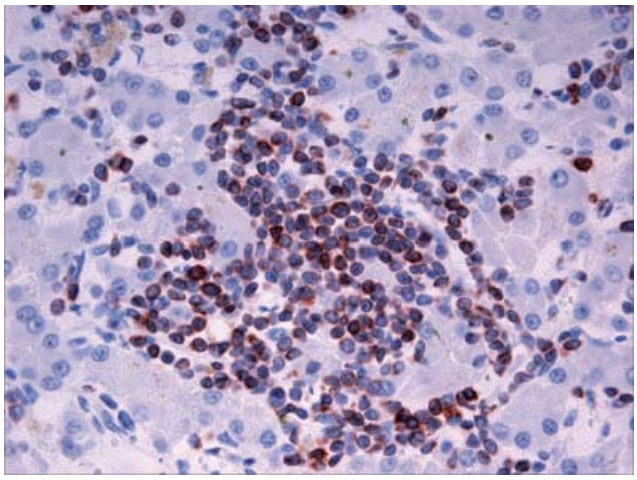

Figure 4.106. Dog: liver, Aggressive NK-cell lymphoma. Phenotype of Figure 4.104. On staining with CD3, there is marking of the cytoplasm with molecular studies demonstrating that the T-cell receptor gene was not rearranged. *Image from P. F. Moore, BVSc.*

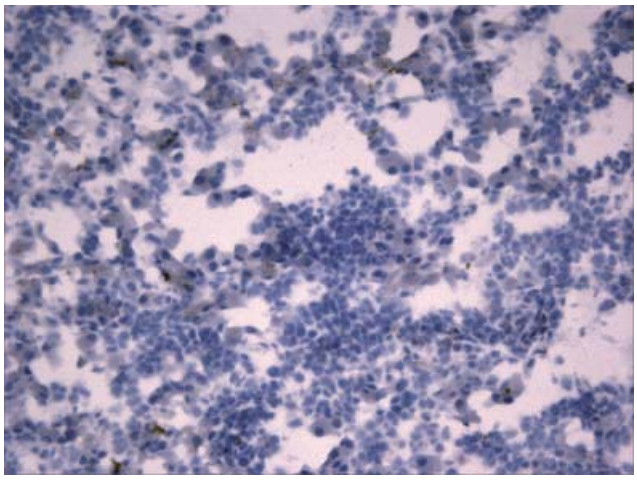

Figure 4.107. Dog: liver, aggressive NK-cell lymphoma. On immunohistochemical staining (liver frozen section) for the γδ type of T-cell receptor, the infiltrating lymphocytes are completely negative indicating that this form of the receptor could not have been responsible for the positive cytoplasmic CD3 reaction (Figure 4.106). *Image from P. F. Moore, BVSc.*

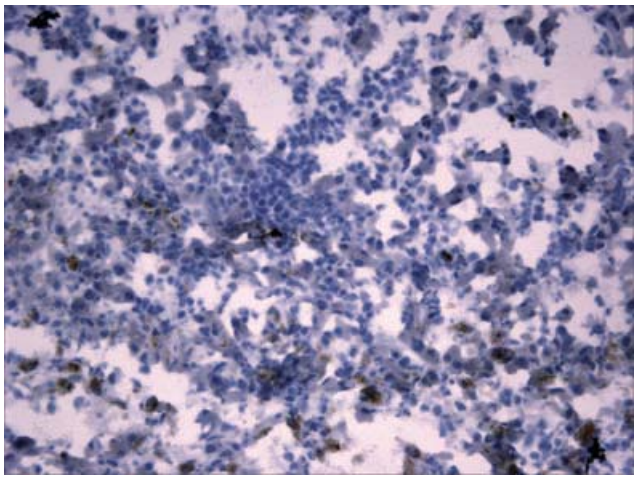

Figure 4.108. Dog: liver, aggressive NK-cell lymphoma. On immunohistochemical staining of a frozen section of liver for the αβ beta form of T-cell receptor, the infiltrating neoplastic cells are completely unlabeled. These findings are consistent with the positive cytoplasmic CD3 reaction of Figure 4.106 to cytoplasmic but not membrane expression of the epsilon component of the T-cell receptor. *Image from P. F. Moore, BVSc.*

expertise, the nasal type NK-cell tumor constitutes 8% of all non-Hodgkin's lymphomas. In the Americas, the disease occurs in native Americans, in Mexico, and in Central and South America, but it does not occur in Caucasians. In Europe and North America, the NK-cell nasal neoplasm accounts for less than 1% of non-Hodgkin's lymphomas and is rarely seen in transplant and immunosuppressed individuals.

Pathologically, the nasal NK-cell disease has a wide cellular variation, and the small cell variant may be difficult to distinguish from benign inflammation. Because most cases of this disease involve ulceration of the skin and mucus membranes, there is always extensive necrosis present that further complicates the distinction from inflammation. Pathologically, the lesion is characterized by vascular invasion and obstruction that was the reason an earlier name was *angiocentric lymphoma*. Because almost all cases are associated with EBV infection, the detection of EBV-encoded nuclear RNA (EBER) is a useful diagnostic tool. Oddly, the EBV present is always of the same p-ala subtype that is never found in other EBV-associated neoplasms. In immunophenotypic terms, the cells are positive for CD2 and CD56 and may have nonspecific cytoplasmic CD3 in paraffin-embedded tissue, but the molecular studies show that the T-cell receptor genes are not rearranged.

The presentation is more common in men of middle age with nasal complaints ranging from bleeding and obstruction to involvement of the eyes, nasal sinuses, nasopharynx, oropharynx, palate, and larynx. The disease with progression metastasizes to the skin, enteric tract, and testis, all sites where CD56 is normally expressed. The disease is treated by combined chemotherapy and radiation, with either alone ineffective.

REFERENCES

Armitage, J.O., Liang, R.H.S., Sweetenham, J.W., Reyes, F., Jaffe, E.S., and Raffeld, M. (2004) Mature nodal and extranodal T-cell and non-Hodgkin–cell lymphomas (peripheral

T-cell, angioimmunoblastic, nasal natural killer/T-cell, hepatosplenic T-cell, enteropathy-type T-cell, and subcutaneous panniculitis-like T-cell lymphomas). In Mauch, P.M., Armitage, J.O., Coiffier, B.C., Dalla-Favera, R., and Harris, N.L. (eds.), *Non-Hodgkin's Lymphomas*. Lippincott Williams & Wilkins, Philadelphia, pp. 405–426.

Bayerl, M.G., Rakozy, C.K., Mohamed, A.N., Vo, T.D., Long, M., Eilender, D., and Palutke, M. (2002) Blastic natural killer cell lymphoma/leukemia. A report of seven cases. *Am J Clin Pathol* 117:41–50.

Felgar, R.E., Macon, W.R., Kinney, M.C., Roberts, S., Pasha, T., and Salhany, K.E. (1997) TIA-1 expression in lymphoid neoplasms: Identification of subsets with cytotoxic T lymphocyte or natural killer cell differentiation. *Am J Pathol* 150(6):1893–1900.

Kenna, T., Mason, L.G., Porcelli, S.A., Koezuka, Y., Hegarty, J.E., O'Farrelly, C., and Doherty, D.G. (2003) NKT cells from normal and tumor-bearing human livers are phenotypically and functionally distinct from murine NKT cells. *J Immunol* 171(4)1775–1779.

Kinney, M.C. (1999) The role of morphologic features, phenotype, genotype, and anatomic site in defining extranodal T-cell or NK-cell neoplasms. *Am J Clin Pathol* 111(Suppl.1):S104–S118.

Kuroda, J., Kimura, S., Akaogi, T., Hayashi, H., Nishida, K., Kakazu, N., and Abe, T. (2000) Aggressive natural killer cell leukemia/lymphoma: A comprehensive cytogenetic study by spectral karyotyping. *Ann Hematol* 79:519–522.

Mhawech, P., Medeiros, L.F., Bueso-Ramos, C., Coffey, D.M., Gei, A.F., and Shahab, I. (2000) Natural killer–cell lymphoma involving the gynecologic tract. *Arch Pathol Lab Med* 124:1510–1513.

Moretta, L., Bottino, C., Pende, D., Mingari, M.C., Biassoni, R., and Moretta, A. (2002) Human natural killer cells: Their origin, receptors and function. *Eur J Immunol* 32:1205–1211.

Ooi, G.C., Chim, C.S., Liang, R., Tsang, K.W.T., and Kwong, Y.L. (2000) Nasal T-cell/natural killer cell lymphoma: CT and MR imaging features of a new clinicopathologic entity. *AJR* 174:1141–1145.

Rakozy, C.K., Mohamed, A.N., Vo, T.D., Khatib, G., Long, P.M., Eilender, D., and Palutke, M. (2001) $CD56^{+}/CD4^{+}$ lymphomas and leukemias are morphologically, immunophenotypically, cytogenetically, and clinically diverse. *Am J Clin Pathol* 116:168–176.

Sadahira, Y., Wada, H., Nakamura, E., Terayama, K., Sugihara, T., Yamada, O., Mikami, Y., and Shirabe, T. (2000) Nasal NK/T cell lymphoma presenting as transverse myelopathy. *Virchows Arch* 436:393–397.

Yoon, T.Y., Lee, H.T., and Chang, S.H. (1999) Nasal-type T/natural killer cell angiocentric lymphoma, Epstein-Barr virus-associated, and showing clonal T-cell receptor γ gene rearrangement. *Brit J Dermatol* 140:505–508.

Mature Nodal and Extranodal T-Cell Lymphoma

Angioimmunoblastic T-Cell Lymphoma

Angioimmunoblastic T-cell lymphoma (AILT) was formerly known as *angioimmunoblastic lymphoma with dysproteinemia*. The condition was characterized as a disease of the elderly with male predominance. The presentation included generalized lymphadenopathy, fever, weight loss, skin manifestations, polyclonal gammopathy, and frequently autoimmune disease, including positive Coomb's test and recurrent infections. With experience, it was suggested that the disease was neoplastic from the outset, and this acceptance has resulted in the WHO terminology designating it as a type of T-cell lymphoma. The disease in animals is rare and seen primarily in mature large breed dogs with insufficient cases to conclude a predominant gender. The presentation is of weight loss and generalized lymphadenopathy. The presence of concurrent skin lesions with fever and any serum protein abnormalities is unrecorded, but the history of recurrent infections has been noted in some dogs. There is no information on the general blood picture and adequacy of bone marrow responses.

The tissue submitted is usually lymph node, but subcutaneous masses that may have been node have also been seen. Early cases have a thinned capsule and compressed peripheral sinus but no involvement of perinodal tissues. There are few fading germinal centers in cortical areas and none in the inner cortex, and there is medullary sclerosis that suggests a long period of benign hyperplasia (Figs. 4.109, 4.110). The architectural appearance is of benign involution ("burnt out follicles"). The nodal structure is essentially diffuse, with the few fading mantle cell areas giving the appearance of a T-zone lymphoma without the sharp definition of the fading follicles or the loss of architecture that might suggest T-zone lymphoma

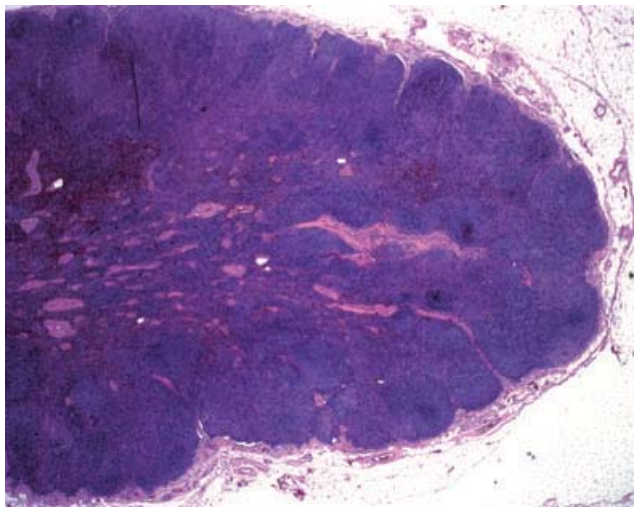

Figure 4.109. Dog: node, angioimmunoblastic T-cell lymphoma. The node is moderately enlarged with the capsule intact and the peripheral sinus compressed but not encompassed by tumor. There are fading germinal centers in subcortical areas and medullary sclerosis indicative of prior period of chronic benign hyperplasia.

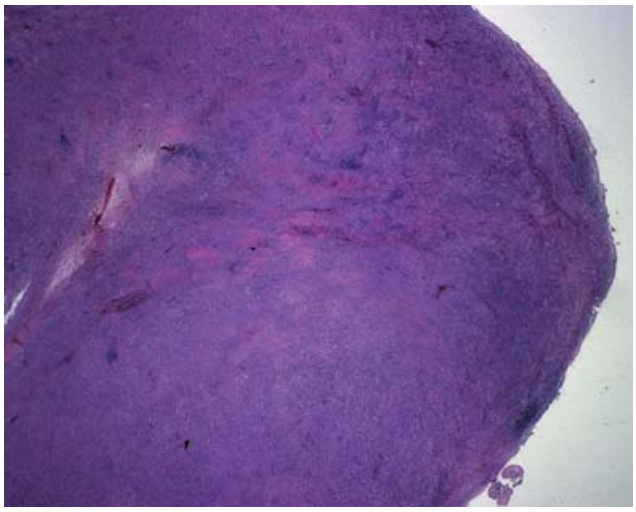

Figure 4.110. Dog: node, angioimmunoblastic T-cell lymphoma. Different animal and later stage case, than Figure 4.109. There is loss of normal node capsule and architecture with a few small clusters of darkly stained cells representing residual mantle cells and a diffuse architecture traversed by irregular columns of collagen bands.

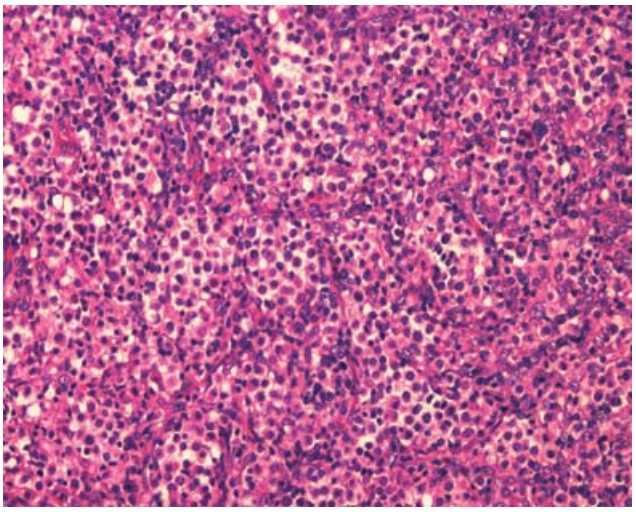

Figure 4.112. Dog: node, angioimmunoblastic T-cell lymphoma. Detail of Figure 4.111. In less dense areas of node tissue, the vascular proliferation presents a striking network of prominent vessels surrounding the neoplastic population.

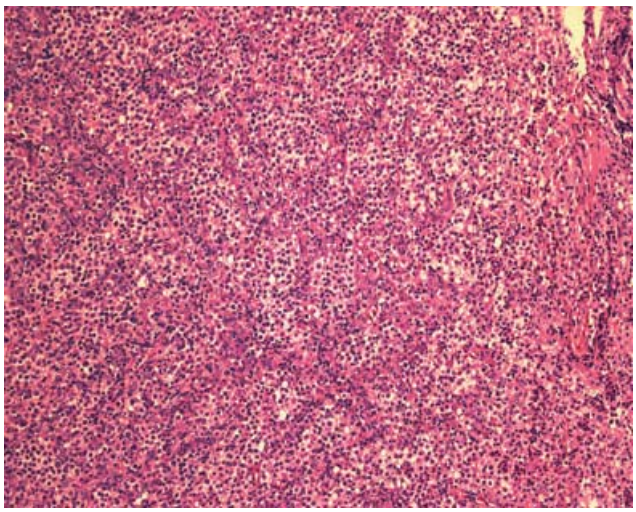

Figure 4.111. Dog: node, angioimmunoblastic T-cell lymphoma. Detail of Figure 4.110. The fading capsule is at the right, with the cortex replaced by an interlacing network of vessels with quite deeply eosinophilic cytoplasm enclosing areas of relatively lightly stained cells.

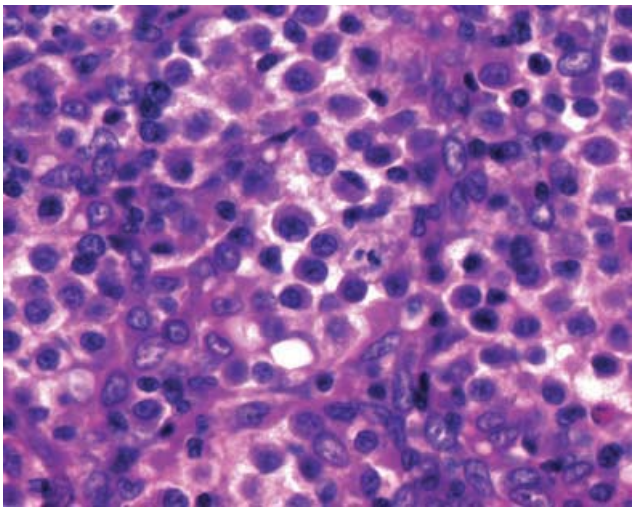

Figure 4.113. Dog: node, angioimmunoblastic T-cell lymphoma. Detail of Figure 4.112. A dense network of endothelial and perivascular cells with abundant eosinophilic cytoplasm constitutes the reticular and vascular network surrounding clusters of atypical cells with round nuclei and eccentrically placed, highly amphophilic cytoplasm.

or T-cell rich large B-cell lymphoma. A higher magnification view presents a cortical region that has lost the normal heterogeneity of the paracortex, with a predominance of small cells with abundant clear cytoplasm and a very prominent vascular network of vessels of the size and staining characteristics of postcapillary venules (Figs. 4.111–4.113). The cytoplasm of the vascular walls is unusually pink with the H&E staining; the endothelial nuclei retain a high vesicular appearance, but the transmural cellular traffic is low. There are cells with much larger nuclei lying adjacent to the vessels, including some with very large lobated nuclei and large nucleoli, as well as medium-sized lymphocytes with round nuclei 1.5 red cells in diameter with dense uniformly distributed chromatin that obscures a large single central nucleolus (Fig. 4.114). Occasional plasma cells are present but

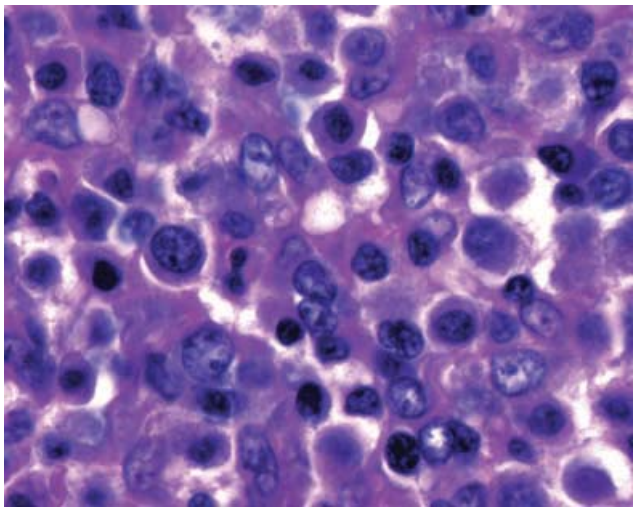

Figure 4.114. Dog: node, immunoblastic T-cell lymphoma. Detail of Figure 4.113. The cellular population is variable with cells of intermediate size with round nuclei and obscured large central nucleoli (center) and other cells with more centroblastic appearing nuclei with peripheralized nucleoli (upper and lower left and right) as well as small lymphocytes and others with a broad rim of highly amphophilic cytoplasm.

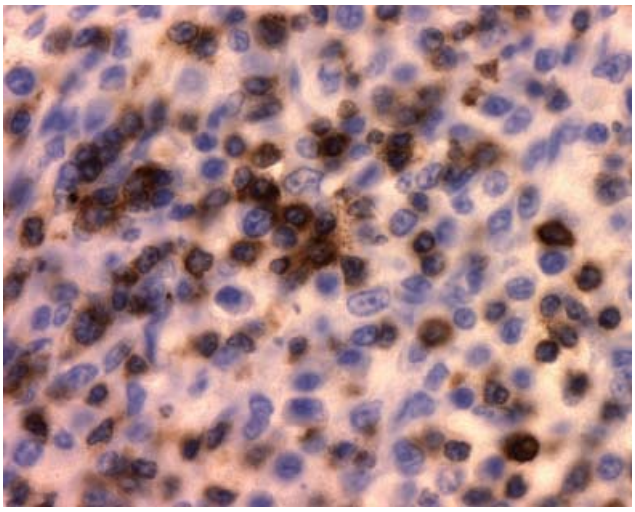

Figure 4.115. Dog: node, angioimmunoblastic T-cell lymphoma. Phenotype of Figure 4.110. There is a cluster of atypical plasmacytoid cells with CD3 in the center, as well as in the upper center and right, that are strongly labeled. Small lymphocytes and larger cells with irregular-shaped nuclei are irregularly but often strongly labeled.

always singly and never in sheets, as often seen in nodes with evidence of past follicular hyperplasia. The vascular compartments contain small foci of 50 or more cells apparent because of abundant cytoplasm that is deeply eosinophilic that have irregular-shaped nuclei more typical of Langerhans type cells.

With progression of AILT there is a complete loss of the node capsule forming large tissues with no normal boundaries and multiple foci of small darkly stained cells resembling benign mantle cells but clearly arising around small veins. There are small irregular areas of ischemic degeneration and of fibrous septation. The prominent vascular pattern is the most characteristic feature, and in these tissues the proportion of larger cells is greater, but with the small round cells with clear cytoplasm still predominating. A major difference from the lesion described as an earlier form of AILT is the frequent presence in all fields of cells with round densely stained nuclei and abundant deeply amphophilic, eccentrically placed cytoplasm. These cells have an indistinct cell boundary that is "furry" but not normally smooth, and they resemble plasma cells but are CD3 positive (Fig. 4.115). There are typical plasma cells present, again singly, that mark with CD79 (Fig. 4.116). In general, with immunostaining the small and medium cells are CD3 positive and the most atypical cells are irregularly positive (see Fig. 4.115). The clusters of cells with more abundant cytoplasm that strongly resemble Langerhans type of histiocytic cells are less apparent and their lineage has not been verified.

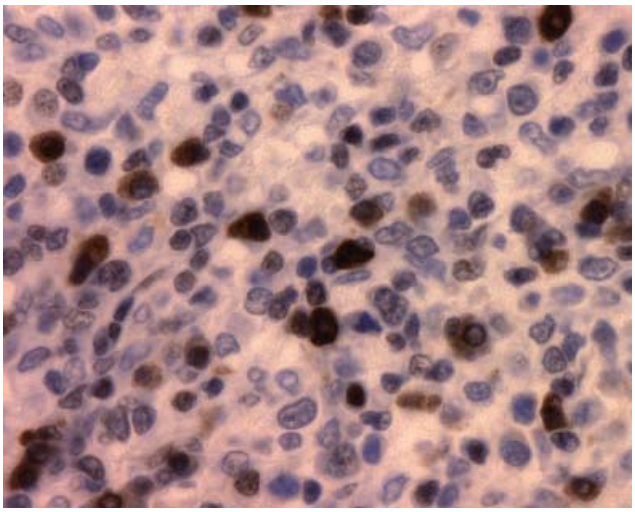

Figure 4.116. Dog: node, angioimmunoblastic T-cell lymphoma. Phenotype of Figure 4.110. With CD79 staining, morphologically typical plasma cells are strongly labeled, with most of the atypical cells having vesicular nuclei unmarked.

Nothing is known of the biological behavior of this neoplasm in animals or of response to treatment. There are descriptions of lesions in animals that resemble AILT but are described as one of a group of T-cell neoplasms with recognition of hyperplastic postcapillary venules but without comparison to the AILT lesion as described in humans. A disease in cats like AILT with prominent signs of fever and weight loss has been described. Morpholog-

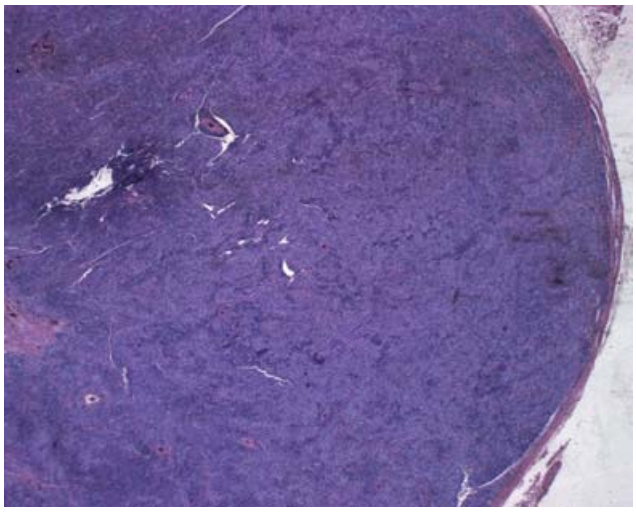

Figure 4.117. Human: lymph node, angioimmunoblastic T-cell lymphoma. The node capsule is thinned with compression and focal obliteration of the peripheral sinus with lymphoid infiltration of the capsule, likely benign. There is destruction of node architecture with a diffuse filling of the cortex that has focal clusters of deeply stained cells in subcapsular areas indicative of fading germinal centers. *Slide from Cornell Tutorial.*

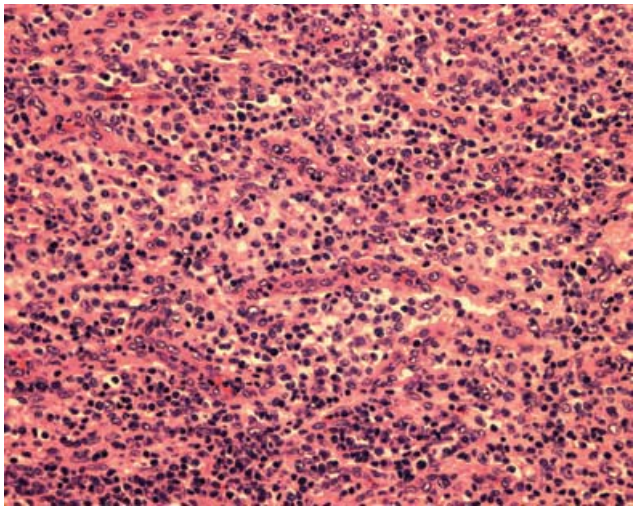

Figure 4.118. Human: lymph node, angioimmunoblastic T-cell lymphoma. Detail of Figure 4.117. Prominent vessels with plump endothelial cells and unusually eosinophilic cytoplasm enclose loose clusters of cells of varying types.

ically, the putative entity in animals closely resembles the human counterpart neoplasm (Figs. 4.117–4.119).

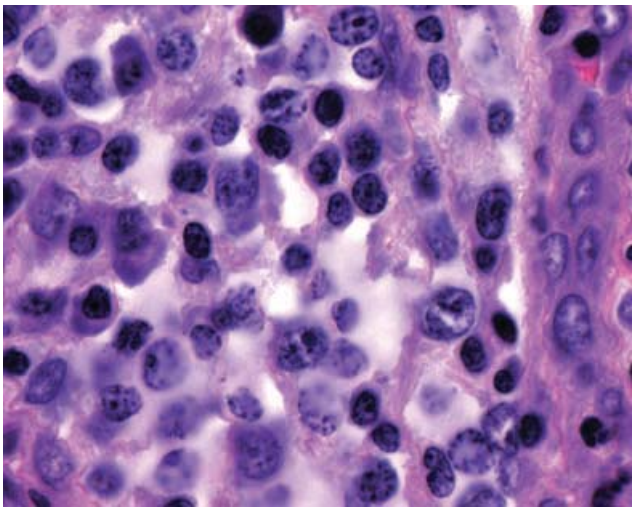

Figure 4.119. Human: node, angioimmunoblastic T-cell lymphoma. Detail of Figure 4.117. A typical small vessel is at the right lying next to a variety of cells that include small and medium lymphocytes with coarse chromatin patterns and moderately prominent nucleoli. There are 3 prominent benign-appearing plasma cells at left.

REFERENCES

Danon, A.D., Krishnan, J., and Frizzera, G. (1993) Morpho-immunophenotypic diversity of Castleman's disease, hyaline-vascular type: With emphasis on a stroma-rich variant and a new pathogenetic hypothesis. *Virchows Archiv A Pathol Anat* 423:369–382.

Fournel-Fleury, C., Ponce, F., Felman, P., Blavier, A., Bonnefont, C., Chabanne, L., Marchal, T., Cadore, J.L., Goy-Thollot, I., Ghernati, D., Ledieu, I, and Magnol, J.P. (2002) Canine T-cell lymphomas: A morphological, immunological, and clinical study of 46 New Cases. *Vet Pathol* 39:92–109.

Frizzera, G., Moran, E.M., and Rappaport, H. (1975) Angioimmunoblastic lymphadenopathy: Diagnosis and clinical course. *Am J Med* 59:803–818.

Hineman, V.L., Phyliky, R.L., and Banks, P.M. (1982) Angiofollicular lymph node hyperplasia and peripheral neuropathy: Association with monoclonal gammopathy. *Mayo Clin Proc* 57:379–382.

Houston, D.M., Clark, E.G., Matwichuk, C.L., and Teachout, D.J. (1993) A case of cutaneous sterile pyogranuloma/granuloma syndrome in a golden retriever. *Can Vet J* 34:121–122.

Leung, C.Y., Ho, F.C.S., Srivastava, G., Loke, S.L., Liu, Y.T., and Chan, A.C.L. (1993) Usefulness of follicular dendritic cell pattern in classification of peripheral T-cell lymphomas. *Histopathol* 23:433–437.

Pangalis, G.A., Moran, E.M., Nathwani, B.N., Zelman, R.J., Kim, H., and Rappaport, H. (1983) Angioimmunoblastic lymphadenopathy: Long-term follow-up study. *Cancer* 52(2):318–321.

Patsouris, E., Noël, H., and Lennert, K. (1989) Angioimmunoblastic lymphadenopathy-type of T-cell lymphoma with a high content of epithelioid cells: Histopathology and comparison with lymphoepithelioid cell lymphoma. *Am J Surg Pathol* 13(4):262–275.

Shimokawa, I., Ushijima, N., Moriuchi, R., Okimoto, T., Ikeda, T., Iwasaki, K., and Matsuo, T. (1993) A case of angiocentric

immunoproliferative lesions (angiocentric lymphoma) associated with human T-cell lymphotropic virus type 1. *Hum Pathol* 24(8):921–923.

Swanson, S., Innes, D.J., Frierson, H.F., and Hess, C.E. (1987) T-immunoblastic lymphoma mimicking B-immunoblastic lymphoma. *Arch Pathol Lab Med* 111:1077–1080.

Tobinai, K., Minato, K., Ohtsu, T., Mukai, K., Kagami, Y., Miwa, M., Watanabe, S., and Shimoyama, M. (1988) Clinicopathologic, immunophenotypic, and immunogenotypic analyses of immunoblastic lymphadenopathy-like T-cell lymphoma. *Blood* 73(3):1000–1006.

Weiss, L.M., Jaffe, E.S., Liu, X.F., Chen, Y.Y., Shibata, D., and Medeiros, L.J. (1992) Detection and localization of Epstein-Barr viral genomes in angioimmunoblastic lymphadenopathy and angioimmunoblastic lymphadenopathy-like lymphoma. *Blood* 79(7):1789–1795.

Hepatosplenic Lymphoma

Hepatosplenic T-cell lymphoma (HSTL), also known as *hepatosplenic γδ T-cell lymphoma*, is a rare neoplasm occurring in humans and dogs and likely other animals. HSTL comprises less than 5% of all human T-cell lymphomas and may have the same prevalence in the dog, where the presentation is similar to humans but the disease is not often recognized. In humans, this disease is primarily seen in young men; in dogs, males may be affected more often, but it is seen most often in dogs 10 years and older.

The presentation is of an animal with lethargy, anorexia, weight loss, and often diarrhea, all of recent onset. On clinical examination, the peripheral lymph nodes are normal but there is muscle wasting, and hepatomegaly and/or splenomegaly are noted; both are present on ultrasound examination. The blood changes include poorly responsive anemia, thrombocytopenia that may include spherocytosis, and toxic changes in neutrophils but with negative Coomb's test. Most animals don't have neoplastic cells in blood that are noted on morphologic examination. Needle aspiration of liver, spleen, and marrow produces cells of similar type in all locations characterized by large nuclei 3 red cells in diameter and irregular in outline, with sharp, shallow nuclear indentations and some more reniform. The chromatin pattern is densely stained and uniformly dispersed with multiple small inconspicuous nucleoli (Fig. 4.120). The cytoplasmic volume varies from a narrow rim on more blastic cells to relatively abundant in the largest cells. Remarkably, these neoplastic cells are erythrophagocytic with ingested red cells estimated to occur in 5% of tumor cells in one case (Fig. 4.121). There is concurrent erythrophagocytosis by benign macrophages, which makes the diagnosis of this neoplasm obscure unless it is realized that red cells within the blastic population are a different cell population from the macrophages (Fig. 4.122). The latter point is a unique differentiation, with ingested red cells observed not only in blastic-appearing cells but, rarely, in primitive cells in mitosis! There is marrow erythroid and megakaryocytic hyperplasia with 10–20% of the cells present of neoplastic type.

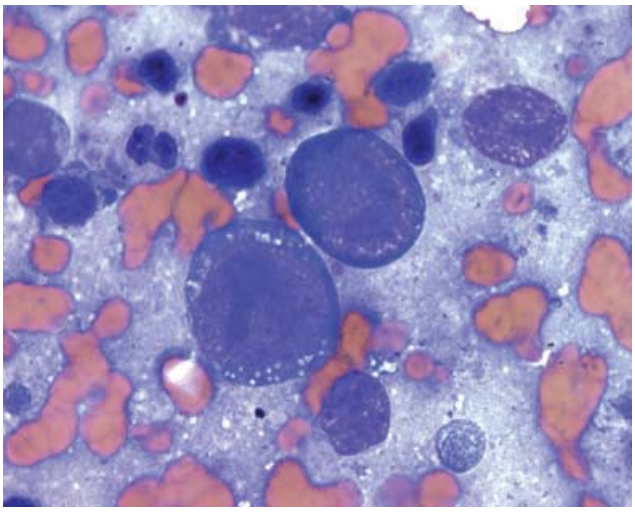

Figure 4.120. Cat: splenic aspirate, hepatosplenic lymphoma. The neoplastic cells are large and densely stained with a cribriform chromatin pattern and multiple poorly defined nucleoli. The cytoplasm is moderate in volume, very highly basophilic, and focally vacuolated.

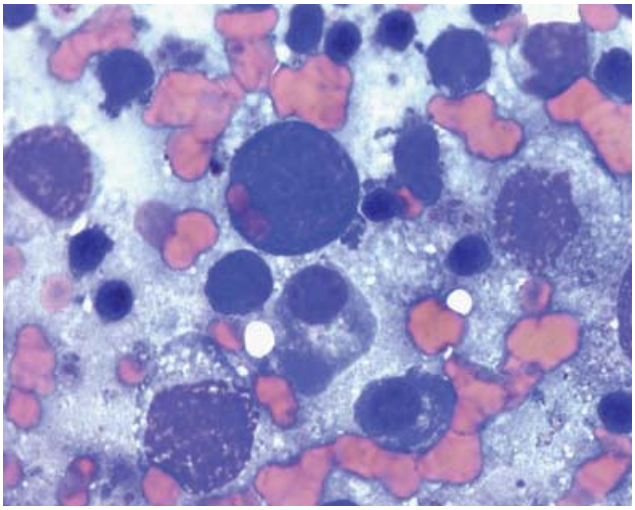

Figure 4.121. Cat: splenic aspirate, hepatosplenic lymphoma. Neoplastic cell, typical of tumor population, with erythrophagocytic activity. There is an absence of any type of differentiation that would suggest the erythrophagocytic cell is of macrophage origin.

The dogs with HSTL follow a rapid downhill course and are usually euthanized on the advice of clinicians, with treatment, if attempted, ineffective. Pathologically, there is hepatosplenomegaly with neoplastic spread to most parenchymal organs, unlike the human disease

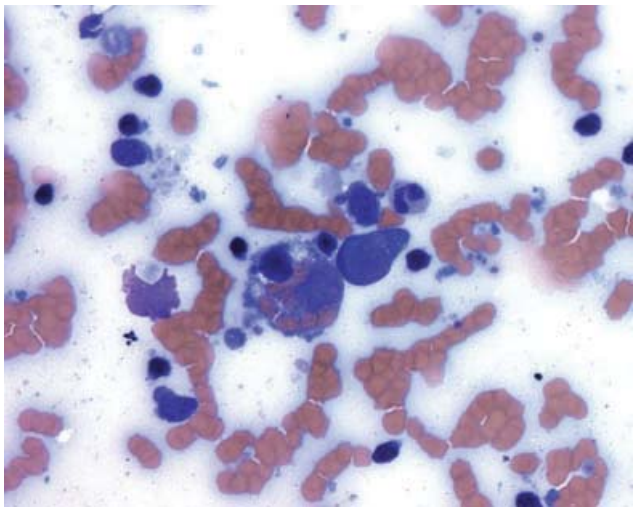

Figure 4.122. Cat: splenic aspirate, hepatosplenic lymphoma. A benign macrophage from the spleen heavily involved with T-cell lymphoma, likely of γδ type. Note that the nucleus is smaller than that of an adjacent neoplastic cell with the benign phage having abundant cytoplasm and containing hemosiderin as well as ingested red cells. Erythrophagocytosis by fully differentiated macrophages is morphologically distinct from that of the neoplastic cells.

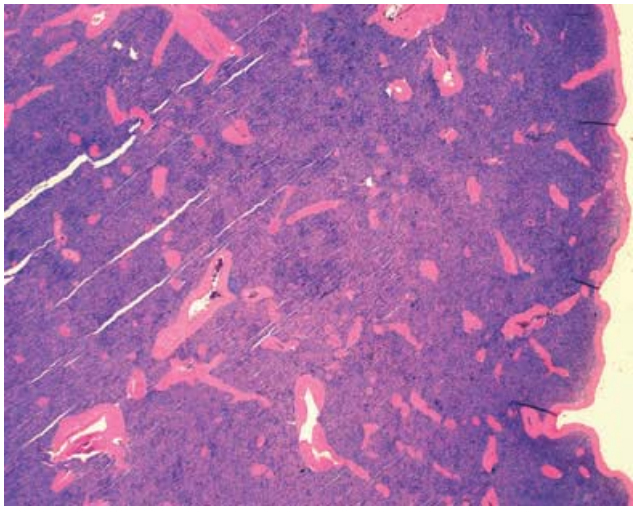

Figure 4.123. Dog: spleen, hepatosplenic lymphoma. The organ is moderately enlarged with thinning of the capsule and thinned and widely spaced muscular trabeculae. Note the diffuse appearance of the splenic architecture with a complete loss of germinal centers and periarteriolar lymphoid sheaths and with diffuse sinus colonization.

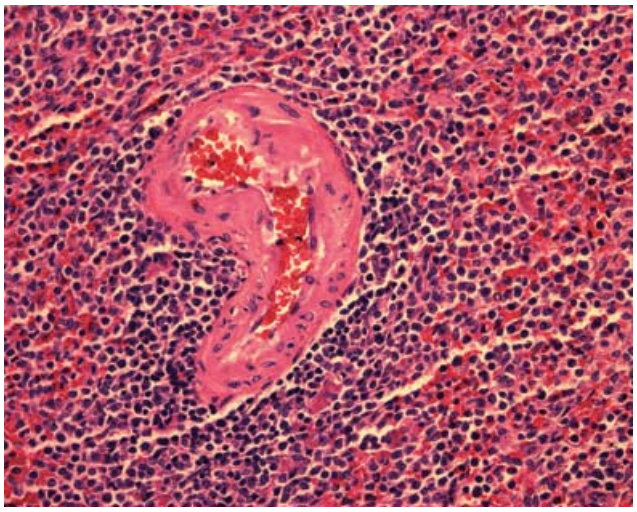

Figure 4.124. Dog: spleen, hepatosplenic lymphoma. Detail of Figure 4.123. The arteriolar lymphoid sheath is atrophic and barely surrounds the small arteriole, with the surrounding sinus areas loosely invaded by the neoplastic γδ T-cells.

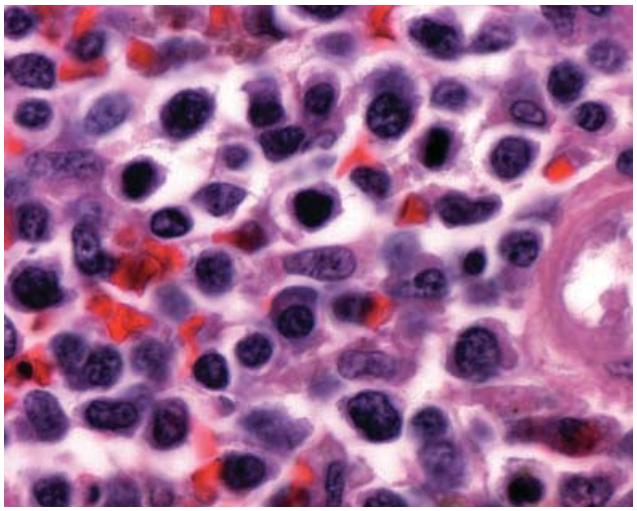

Figure 4.125. Dog: spleen, hepatosplenic lymphoma. Detail of Figure 4.123. Periarteriolar sinus area, devoid of normal small lymphocytes. The neoplastic cells have nuclei that are round, oblong, and occasionally lobated (left) with relatively abundant highly amphophilic cytoplasm and relatively inapparent nucleoli.

where marrow, liver, and splenic involvement predominate. Pathologically, the tissue tropism is distinctive with splenic involvement primarily in sinus areas (Figs. 4.123–4.125) and with both vascular cuffing and sinusoidal involvement in the liver (Figs. 4.126, 4.127). In the dog, the disease may present in more advanced stages than in humans, and infiltration has been found in the renal cortex and medullary areas and even in the lung with locally extensive plugging of alveolar capillaries. The molecular characteristics of HSTL in the dog include expression of a TCR of γδ type and also of the CD11d integrin that is characteristic of the cells of LGL, macrophage, and T-cell type that home to the sinus areas of the spleen.

Hepatosplenic lymphoma in the dog presents like the macrophage form of malignant histiocytosis with

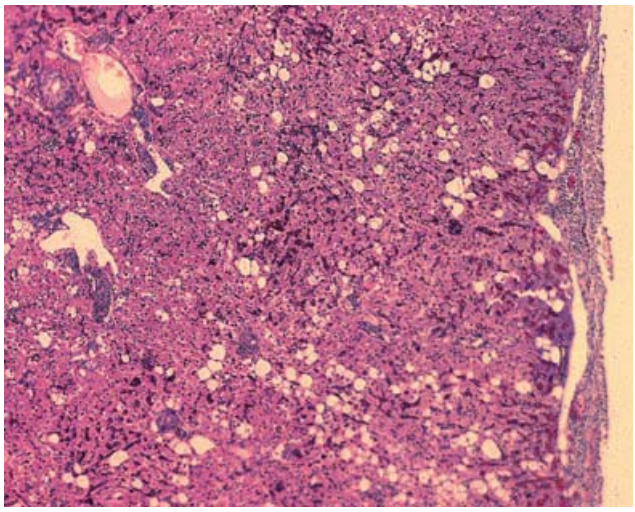

Figure 4.126. Dog: liver, hepatosplenic lymphoma. There is extensive capsular infiltration as well as irregular sinus congestion and tumor infiltration with narrow cuffing around vessels.

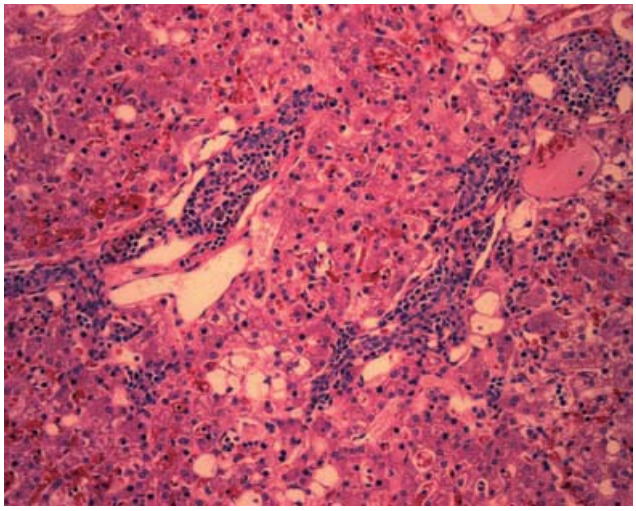

Figure 4.127. Dog: liver, hepatosplenic lymphoma. There is cuffing around both portal and venous areas and mild irregular sinus involvement, with focal areas of the liver more heavily infiltrated.

unrelenting anemia and hepatosplenomegaly. In the latter disease, the neoplastic cells are much more avidly erythrophagocytic, with 50–100 red cells in some tumor cells and many with hemosiderin granules. In malignant histiocytosis of the macrophage type, the neoplastic cells have huge nuclei, and it is clearly the neoplastic cells that are the cause of the anemia.

REFERENCES

Armitage, J.O., Liang, R.H.S., Sweetenham, J.W., Reyes, F., Jaffe, E.S., and Raffeld, M. (2004) Mature nodal and extranodal T-cell and non-Hodgkin–cell lymphomas (peripheral T-cell, angioimmunoblastic, nasal natural killer/T-cell, hepatosplenic T-cell, enteropathy-type T-cell, and subcutaneous panniculitis-like T-cell lymphomas). In Mauch, P.M., Armitage, J.O., Coiffier, B.C., Dalla-Favera, R., and Harris, N.L. (eds.), *Non-Hodgkin's Lymphomas*. Lippincott Williams & Wilkins, Philadelphia, pp. 405–426.

Cooke, C.B., Krenacs, L., Stetler-Stevenson, M., Greiner, T.C., Raffeld, M., Kingma, D.W., Abruzzo, L., Frantz, C., Kaviani, M., and Jaffe, E.S. (1996) Hepatosplenic T-cell lymphoma: A distinct clinicopathologic entity of cytotoxic γδ T-cell origin. *Blood* 88:4265–4274.

de Wolf-Peeters, C., and Achten, R. (2000) γδ T-cell lymphomas: A homogeneous entity? *Histopathol* 36:294–305.

Farcet, J.P., Gaulard, P., Marolleau, J.P., Le Couedic, J.P., Henni, T., Gourdin, M.F., Divine, M., Haioun, C., Zafrani, S., Goosens, M., Hercend, T., and Reyes, F. (1990) Hepatosplenic T-cell lymphoma: Sinusal/sinusoidal localization of malignant cells expressing T-cell receptor γδ. *Blood* 75:2213–2219.

Fry, M.M., Vernau, W., Pesavento, P.A., Brömel, C., and Moore, P.F. (2003) Hepatosplenic lymphoma in a dog. *Vet Pathol* 40:556–562.

Gorczyca, W., Weisberger, J., Liu, Z., Tsang, P., Hossein, M., Wu, C.D., Dong, H., Wong, J.Y.L., Tugulea, S., Dee, S., Melamed, M.R., and Darzynkiewicz, Z. (2002) An approach to diagnosis of T-cell lymphoproliferative disorders by flow cytometry. *Cytometry (Clin Cytometry)* 50:177–190.

Khan, W.A., Yu, L., Eisenbrey, A.B., Crisan, D., Saadi, A.A., Davis, B.H., Hankin, R.C., and Mattson, J.C. (2001) Hepatosplenic gamma/delta T-cell lymphoma in immunocompromised patients: Report of two cases and review of literature. *Am J Clin Pathol* 116:41–50.

Macon, W.R., Levy, N.B., Kurtin, P.J., Salhany, K.E., Elkhalifa, M.Y., Casey, T.T., Craig, F.E., Vnencak-Jones, C.L., Gulley, M.L., Park, J.P., and Cousar, J.B. (2001) Hepatosplenic αβ T-cell lymphomas: A report of 14 cases and comparison with hepatosplenic gammadelta T-cell lymphomas. *Am J Surg Pathol* 25:285–296.

McDonough, S.P., and Moore, P.F. (2000) Clinical, hematologic, and immunophenotypic characterization of canine large granular lymphocytosis. *Vet Pathol* 37:637–646.

Murakami, K., Sentsiu, H., Inoshima, Y., and Inumaru, S. (2004) Increase in γδ T cells in the blood of cattle persistently infected with bovine leukemia virus following administration of recombinant bovine IFN-γ. *Vet Immunol and Immunopathol* 101:61–71.

Roccabianca, P., Paltrinieri, S., Gallo, E., and Giuliani, A. (2002) Hepatosplenic T-cell lymphoma in a mare. *Vet Pathol* 39(4):508–511.

Weidmann, E. (2000) Hepatosplenic T-cell lymphoma. A review on 45 cases since the first report describing the disease as a distinct lymphoma entity in 1990. *Leuk* 14:991–997.

Enteropathy-Type T-Cell Lymphoma

Intestinal lymphoma has been progressively reviewed and renamed with the advent of phenotypic marking and better understanding of pathogenesis. In humans, the lymphoplasmacytic enteritis known as Crohn's disease and

ulcerative colitis are primarily granulomatous and B-cell proliferations now felt to derive from a deficient function of an immunoregulatory subset of $CD25^{+}CD4^{+}$ T-cells. In contrast, the enteropathy-type T-cell lymphoma (ETCL) is primarily seen in patients who have a gluten-sensitive intestine (celiac disease), usually of long standing. In animals, a variety of immunoproliferative small intestinal diseases occur, all of which are associated with a presentation of weight loss associated with intermittent diarrhea and vomition in dogs and cats. There is at least anecdotal information from skilled clinicians that these diseases, particularly in the cat, are primarily of lymphoplasmacytic and B-cell type in younger animals and more likely to be of T-cell type in animals over 10 years old. A form of noninfectious inflammatory bowel disease occurs in the cat, dog, and horse—and likely in other species. Most of the enteridities in the pig and cow have an infectious etiology, and small ruminants appear to be similar. A breed-associated immunoproliferative disease has been described in Basenji dogs that also have abnormalities in thyroid function and skin disease.

A common history of weight loss over the previous 6 months or longer is found in animals that have ETCL. Additional common findings in presentation are anorexia and recurrent diarrhea or loose stools and vomition in dogs and cats. Laboratory findings include mild to moderate anemia with hypoproteinemia, and there may be elevation of hepatic enzymes. Neutrophilic leukocytosis may be present and marked and is an indication of intestinal ulceration. There is no apparent breed association in cats; a report on 44 dogs found the boxer and sharpei breeds to be overrepresented, but not all 44 dogs had T-cell lymphoma. All of the small intestine is involved, with increasing severity in the jejunum and ileum in the cat, dog, and pig, and in the horse the colon may be involved as well. Although the disease tends to be segmental there appears to be sufficient involvement of the duodenum that the diagnosis can be made on endoscopic biopsy of the gastric and duodenal mucosa.

On histological examination of the intestine, there is villus shortening, stumping, and fusion, with a reduction in overall thickness of the villus portion of the mucosa, often with an increase in thickness of the lamina propria or glandular region (Fig. 4.128). All regions of the intestine have a heavy infiltration of small lymphocytes in the villus epithelium and a variable lymphocytic plasmacytic infiltration in the lamina propria that extends down to surround and separate the glands (Fig. 4.129). In areas of apparent benign epitheliotropic infiltration of the villus surface cells, the infiltrating lymphocytes have nuclei that are of the same diameter as red cells and are surrounded by a very narrow zone of relatively water-clear cytoplasm. These cells lie between cytoplasmic membranes of the intestinal epithelial cells and generally in the middle and upper third of these columnar cells. The nuclei are lightly compressed into an oval shape by the surrounding epithelium and have completely dense and uniformly distributed chromatin without internal nuclear detail and lacking nucleoli (Figs. 4.130, 4.131). As the disease progresses, the number of larger lymphocytes and plasma cells in the lamina propria decreases and the number of small

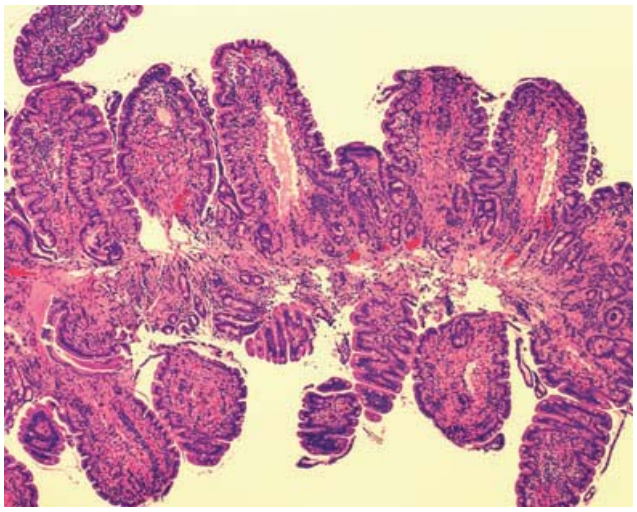

Figure 4.128. Dog: duodenum, enteric epitheliotropic T-cell infiltration. The dog presented with dependent edema, hypoproteinemia, and a syndrome of diarrhea with protein losing enteropathy. The duodenal mucosa has marked widening and general shortening of the villi with villous smooth muscle hypertrophy and irregular dilation of the central lacteals.

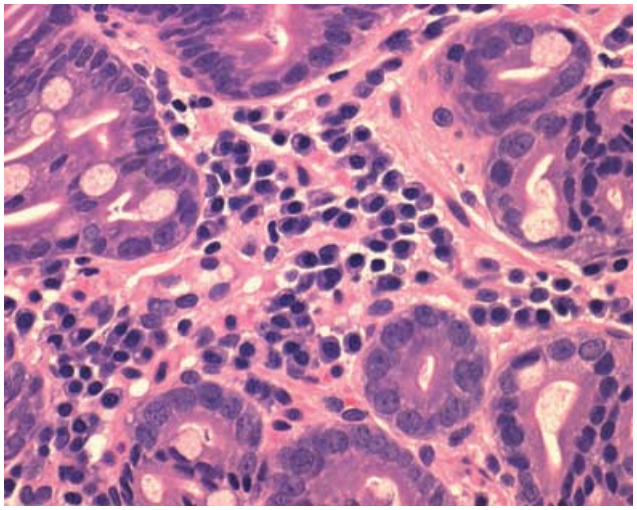

Figure 4.129. Dog: duodenum, lamina propria layer, same case as Figure 4.128. In the deeper areas of the mucosa, there is mild irregular sclerosis with increased connective tissue surrounding glands and solid areas of plasma cells in contrast to the small T-lymphocyte population in the villous lamina propria and epithelium.

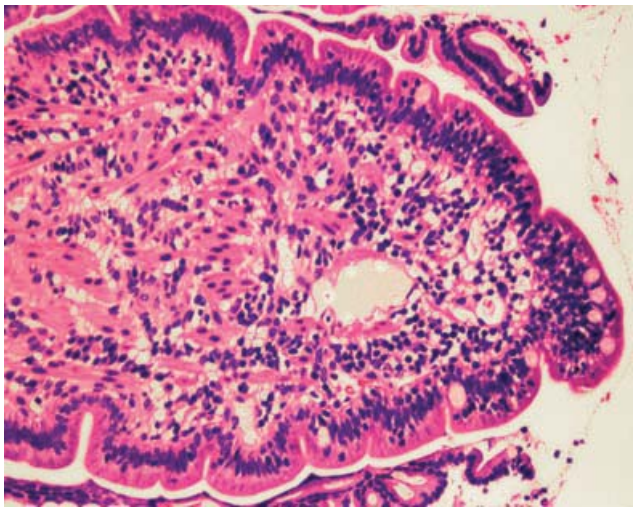

Figure 4.130. Dog: duodenum, enteric epitheliotropic infiltration. Detail of Figure 4.129. There is irregular infiltration of small lymphocytes into the epithelial layer with the lamina propria dilated by quite marked smooth muscle hypertrophy and small lymphocytic infiltration into the lamina propria and dilation of the central lacteal.

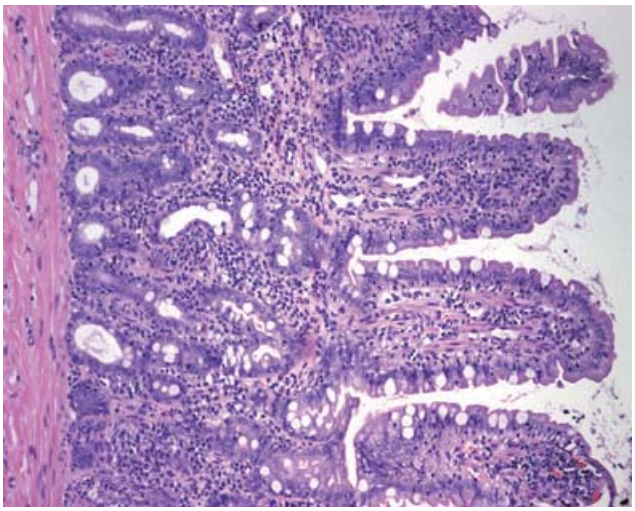

Figure 4.132. Cat: jejunum, enteric epitheliotropic infiltration. The villi are shortened with mild smooth muscle hypertrophy and small cell infiltration into the epithelium with infiltration continuing into the lamina propria layer with irregular displacement of glands.

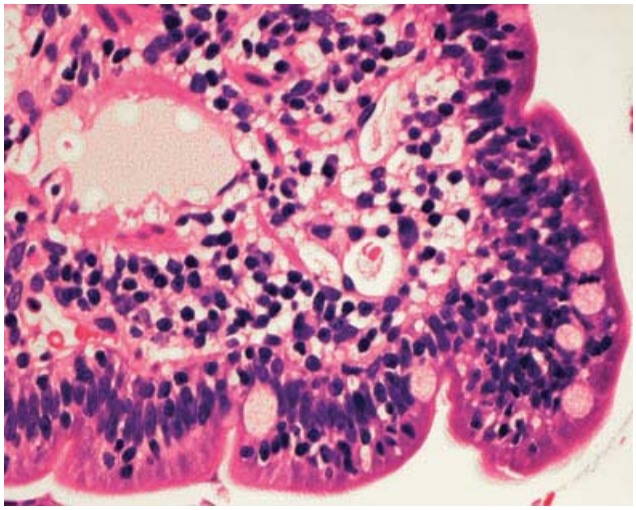

Figure 4.131. Dog: duodenum, epitheliotropic T-cell infiltration. Detail of Figure 4.129. The small cell infiltration into the epithelium can be seen to have nuclei similar to those in the lamina propria. There are a few plasma cells present and no apparent eosinophils.

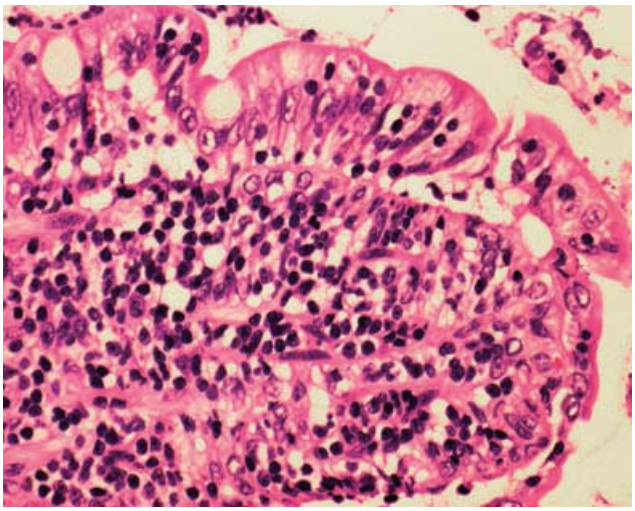

Figure 4.133. Cat: jejunum, enteric epitheliotropic infiltration. Detail of Figure 4.132. There is a heavy and irregular infiltration of small lymphocytes into the intestinal epithelium and thinning of epithelium over the crown of the villus. There is a very heavy small cell infiltration into the lamina propria with very few lymphocytes of another type present.

lymphocytes of T-cell type increases till they predominate (Figs. 4.132–4.135). The lymphocytes in the lamina propria have round nuclei with some internal detail but with very compact chromatin and no nucleoli. These changes in the infiltrating cells are accompanied by smooth muscle hypertrophy of the villus fibers and usually by irregular dilatation of the central lacteal. If the villi are cut in cross section, the overall diameter will be 2–3 times normal (Figs. 4.136, 4.137). The glandular infiltration retains a high proportion of larger lymphocytes and plasma cells that irregularly infiltrate the epithelium of the glandular crypts. Eosinophils are present and may be numerous in the lamina propria of the villi and in the glandular mucosa and may form a continuous layer with small lymphocytes on the deeper surface of the glands just above the muscularis mucosa (Fig. 4.138). There are usually focal areas of B-cell proliferation at the

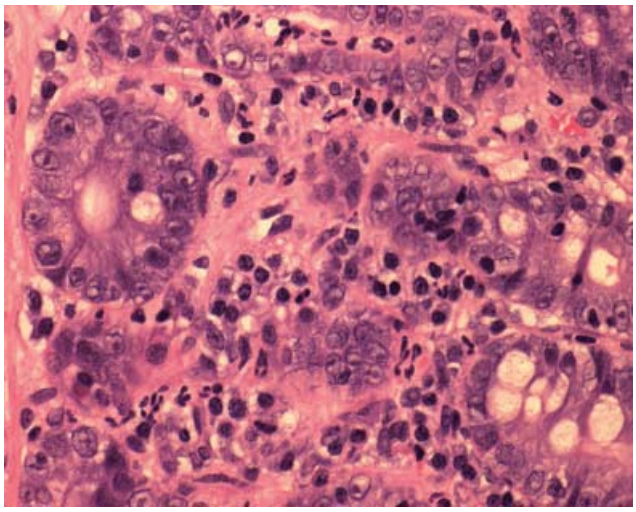

Figure 4.134. Cat: jejunum, enteric epitheliotropic infiltration. Detail of Figure 4.132. The lamina propria layer of the small intestine contains numerous small lymphocytes similar to those in the lamina propria of the villi, with relatively few plasma cells. There are quite numerous neutrophils and small lymphocytes that continue to invade the epithelium of the glands but to a lesser extent than in villus areas.

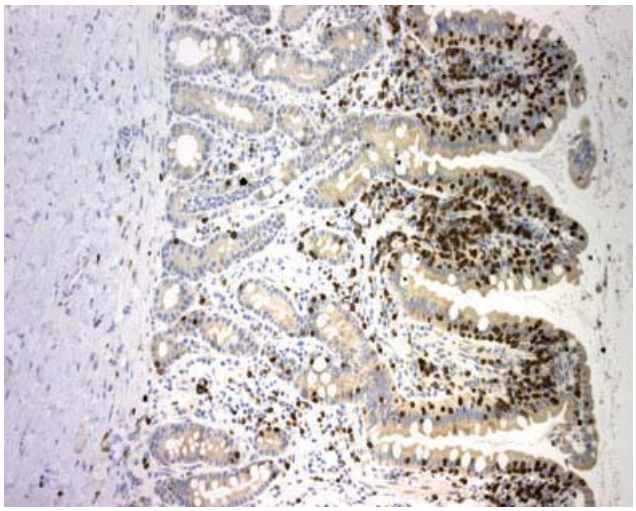

Figure 4.135. Cat: jejunum, epitheliotropic infiltration. Phenotype of Figure 4.132. On staining with CD3, the concentration of positive cells in the upper area of the small intestine is apparent as well as a continuation of the positively marking cells into the lamina propria layer with continued epithelial infiltration.

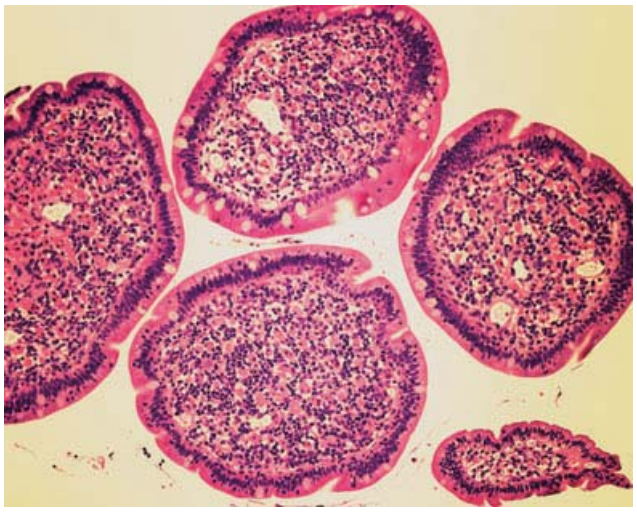

Figure 4.136. Dog: duodenum, epitheliotropic infiltration, same case as Figure 4.128. A more normal villus is in the lower right with the other four profiles having marked smooth muscle hypertrophy and accompanying small lymphocytic infiltration.

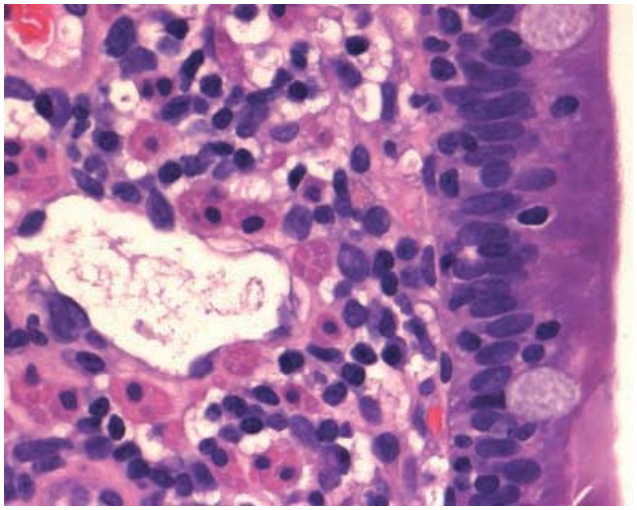

Figure 4.137. Dog: duodenum, enteric epitheliotropic infiltration. Detail of Figure 4.136. The small lymphocytes in the epithelium are clearly differentiated from the surrounding epithelial nuclei and similar to those in the lamina propria with very few plasma cells present.

level of the muscularis mucosa, and these lack a mantle cell cuff and can be seen to be germinal centers in decline (Fig. 4.139). At this stage, neoplastic change may be present in isolated cells, but the overall impression is of severe but benign epitheliotropic inflammatory bowel disease (Figs. 4.140, 4.141) that may include a characteristic laminar sclerosis of the lamina propria layer (Fig. 4.142). In the inflammatory stage, there is commonly minor focal lymphoid proliferation in the gastric mucosa that has a loose, widely spaced distribution in the superficial glandular areas and focal areas of nodular proliferation that may have included a germinal center that is fading as the surrounding T-cells increase in density (Figs. 4.143, 4.144).

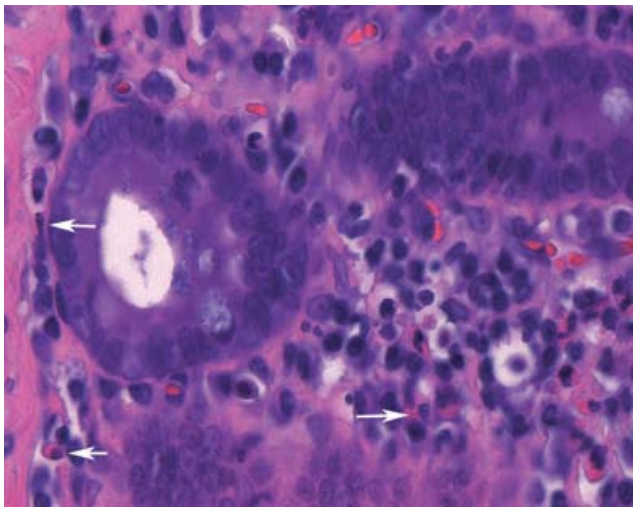

Figure 4.138. Cat: small intestine, enteric epitheliotropic infiltration. Lamina propria with extensive eosinophil infiltration into the deeper mucosa also forms a linear band between the glands and the muscularis mucosa (arrows).

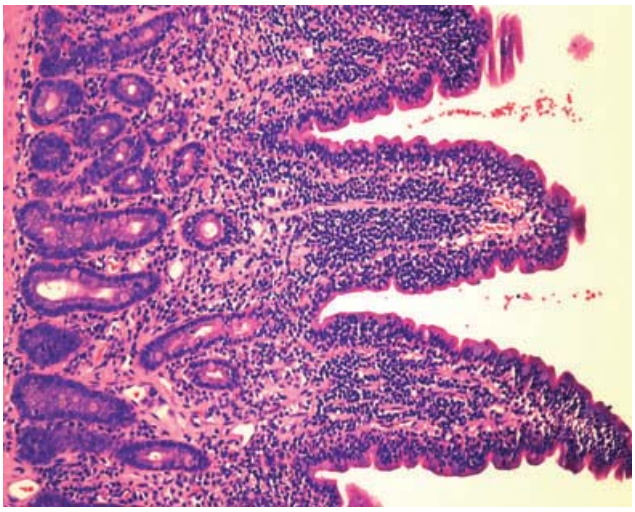

Figure 4.140. Cat: duodenum, epitheliotropic infiltration. An animal with advanced epitheliotropic inflammatory bowel disease, with heavy infiltration of the lamina propria and epithelium and mild sclerosis of the lamina propria layer.

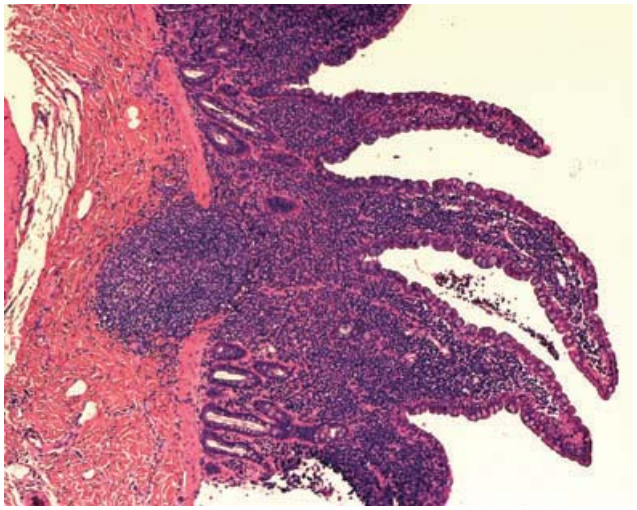

Figure 4.139. Cat: small intestine, enteric epitheliotropic infiltration. A B-cell follicle at the base of the glandular mucosa lacks a well-defined germinal center and a mantle cell cuff.

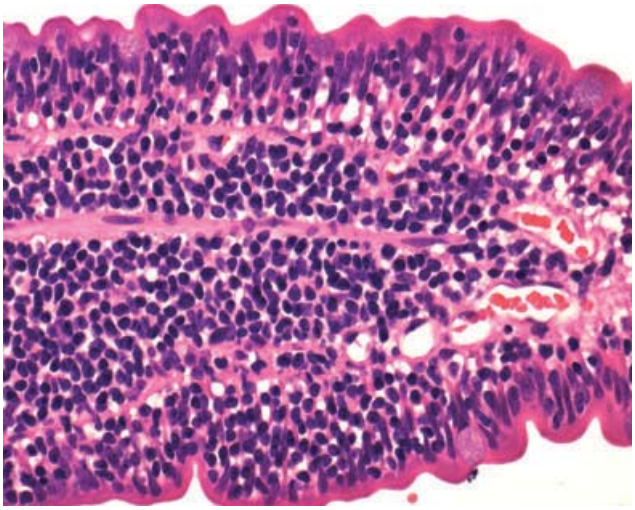

Figure 4.141. Cat: duodenum, epitheliotropic infiltration. Detail of Figure 4.140. There is very dense colonization of villus epithelium by small lymphocytes. The basement membrane becomes indefinite and the density of nuclei in the epithelium may be close to that in the lamina propria and exceed the number of epithelial nuclei.

The transition to frank neoplasia is subtle and recognized as one of the most difficult interpretations of anatomic surgical pathology in both humans and animals. The determination of cancer cannot be made on the depth of inflammatory cell infiltration or on frank mucosal ulceration but is made on the change in character of the infiltrating cells. The neoplastic cells of ETCL have nuclei that are larger, 1.5 red cells in diameter, and irregular in shape, with elongated and lobated shapes more like the larger cells of T-zone lymphoma (Figs. 4.145–4.147). The chromatin is densely stained and uniformly dispersed, with a single small central nucleolus obscured by the chromatin, as in lymphoblastic lymphoma (Fig. 4.148). These lymphocytes have a very narrow rim of lightly stained cytoplasm, which is barely perceptible in the well-fixed tissues taken by endoscopic biopsy but is more apparent in the larger tissues taken at necropsy with some artifactual contraction of surrounding tissues. An astute observation by Jim Carpenter, DVM, is that, at the stage of benign inflammatory bowel disease, the infiltration of the

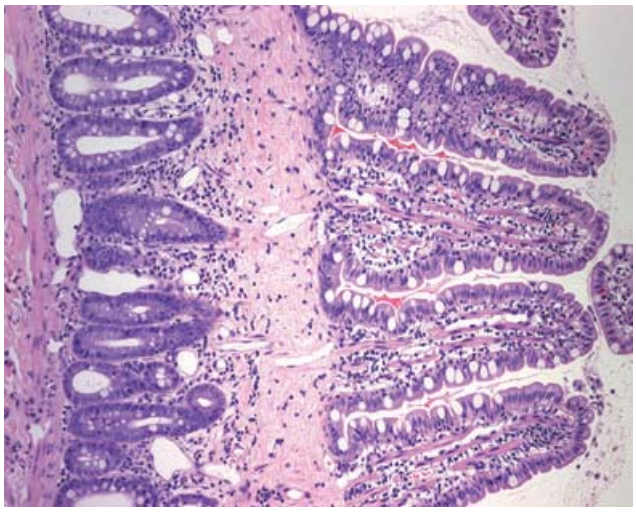

Figure 4.142. Cat: jejunum, epitheliotropic infiltration. A late stage of T-cell inflammatory bowel disease with sclerosis of the lamina propria that is mildly birefringent on polarized light. There is mild dilation of villus lacteals and dilation of lymphatics throughout the mucosa and muscularis.

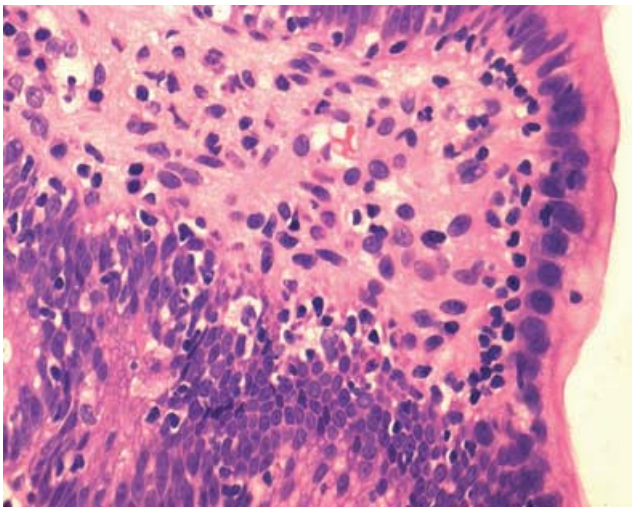

Figure 4.144. Dog: gastric epitheliotropic inflammatory bowel disease. Detail of Figure 4.143. The linear arrangement of small lymphocytes beneath the basement membrane resembles the string-of-pearls arrangement of lymphoid infiltration in early stages of mycosis fungoides. There are very few plasma cells present in the deeper mucosa with moderate lymphoid infiltration of the adjacent epithelium.

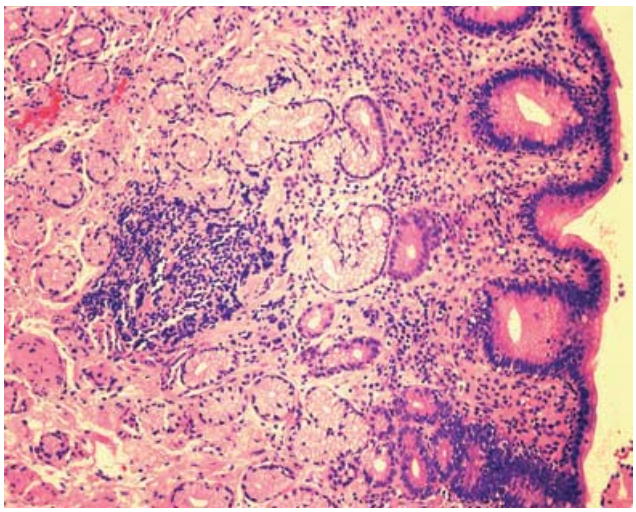

Figure 4.143. Dog: gastric mucosa, epitheliotropic inflammatory bowel disease. There is moderate sclerosis of the superficial and deep mucosa with dense lymphoid proliferation that lines the basement membrane but with minor epithelial colonization. The deeper lymphoid cluster has pale eosinophilic material in the center that resembles the follicular hyalinosis of the fading germinal center.

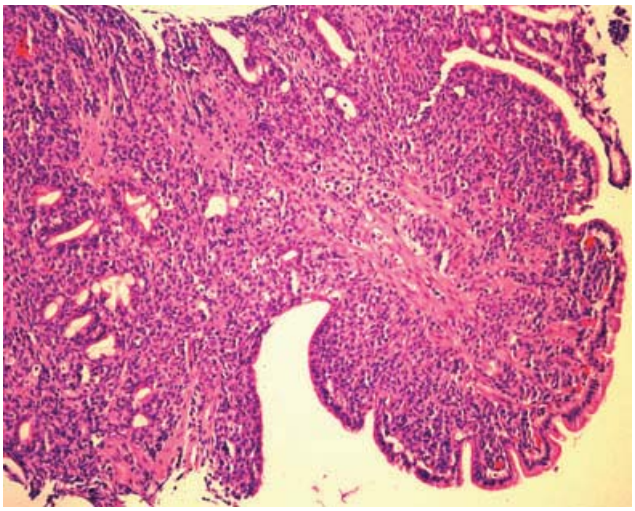

Figure 4.145. Dog: duodenum, enteric T-cell lymphoma. In frank neoplasia, there may be less involvement of residual epithelium, but there is greater destruction of the intestinal architecture with loss of villi and destruction of glands in the lamina propria layer.

epithelium will be relatively uniform across a group of villi best observed in cross section. In contrast, in ETCL the involvement is much more variable, and although all villi will have some infiltration, some may be relatively lightly involved with an adjacent villus heavily infiltrated. Mitoses are rarely observed, and the picture is one of dense infiltration by cells of much more homogeneous type. It is frequently the case that in situ lymphoma may be observed, with a focal area of uniform cell type filling the glandular tissue and villi with adjacent areas of fading follicles and more mixed cellular infiltration. These changes are not apparent on examination at the architectural level, but they become apparent on phenotypic staining with solid areas of T-cell marking. The extension of

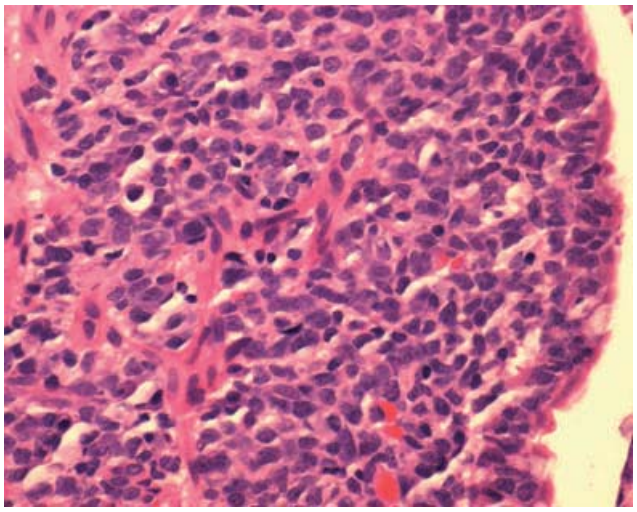

Figure 4.146. Dog: duodenum, enteric T-cell lymphoma. Detail of Figure 4.145. Infiltrating cells are more densely packed, and the nuclei are larger with dense but relatively uniform staining with inapparent nucleoli.

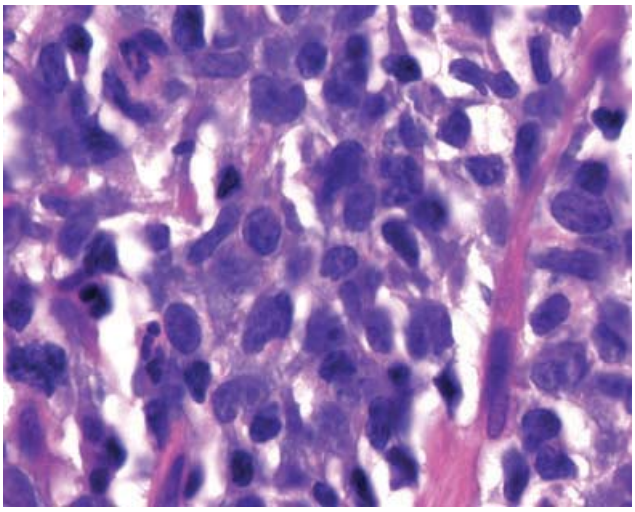

Figure 4.148. Dog: duodenum, enteric T-cell lymphoma. Detail of Figure 4.145. The infiltrating cells have sharp, shallow nuclear indentations, generally a hyperchromatic but finely dispersed chromatin pattern that obscures nucleoli that are occasionally multiple.

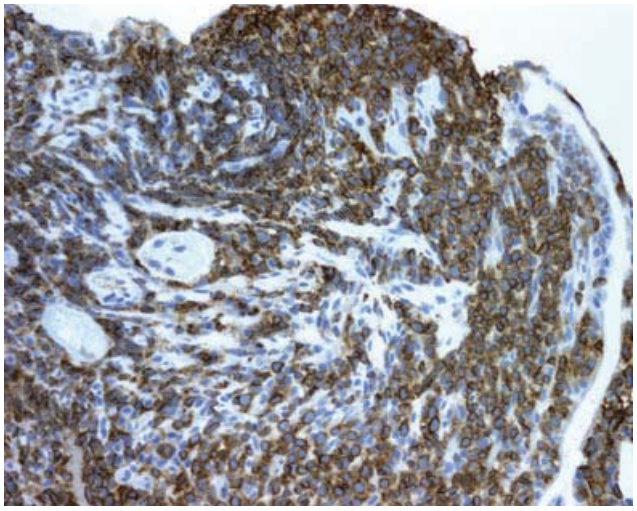

Figure 4.147. Dog: duodenum, enteric T-cell lymphoma. Phenotype of Figure 4.145. There is dense and quantitative staining of the cellular infiltrate with CD3. The epithelium is intact at the surface (right) heavy infiltration by neoplastic cells. The same area is completely negative on staining with CD 79.

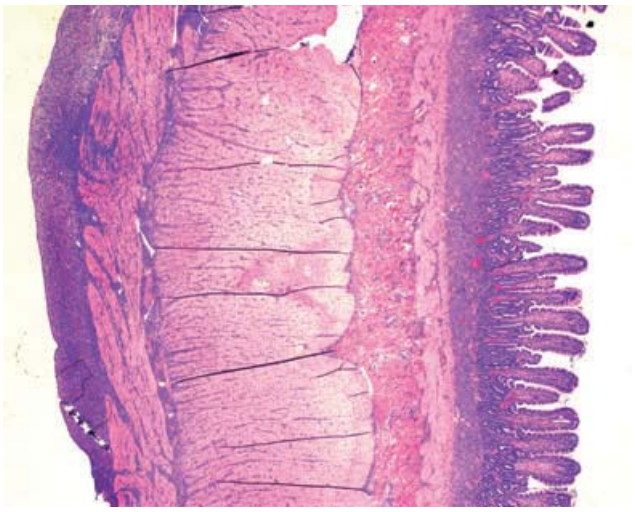

Figure 4.149. Dog: duodenum, enteric T-cell lymphoma. A case with hepatoenteric distribution. The villus mucosa is relatively intact with very heavy infiltration of the lamina propria layer and transmural colonization of the tunica muscularis.

the neoplastic process to invasion of the tunica muscularis and focal colonization of the subserosal layer can be found at some levels (Fig. 4.149), but the level of infiltration may be greatly exceeded in a MALT tumor of B-cell type, with a large mass lesion surrounding the intestinal lumen but with far less prognostic importance. The spread of ETCL within the intestine appears to be by direct extension and not by linear movement along longitudinal lymphatics as occurs in other types of intestinal lymphoma.

Extension of the ETCL to other tissues includes the liver (Fig. 4.150). When the intestine is extensively involved, it is usual for the liver to have focal areas of neoplastic colonization (Figs. 4.151, 4.152). In terms of diagnostic strategies, if there is some generalized thickening of the small intestine but no mass lesion and any areas of altered echogenicity of the liver, a fine

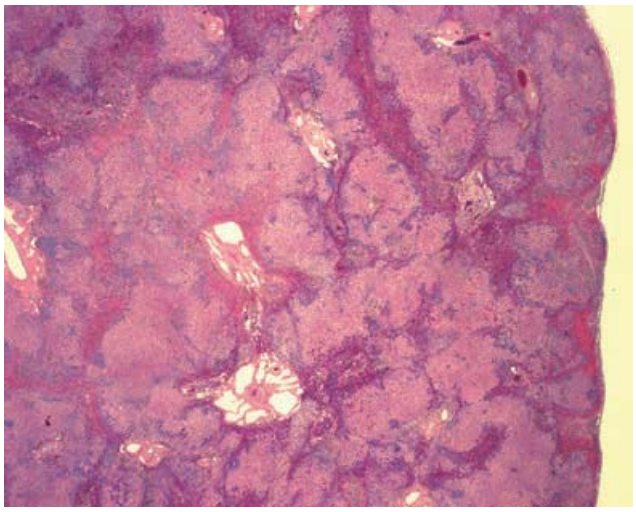

Figure 4.150. Dog: liver, enteric T-cell lymphoma, same case as Figure 4.149. There is irregular loss of hepatocytes and sinus filling, with red cells outlining islands of residual hepatocytes that are lightly encapsulated by a narrow rim of neoplastic lymphoid cells. There is marked lymphatic dilation surrounding the central veins (center).

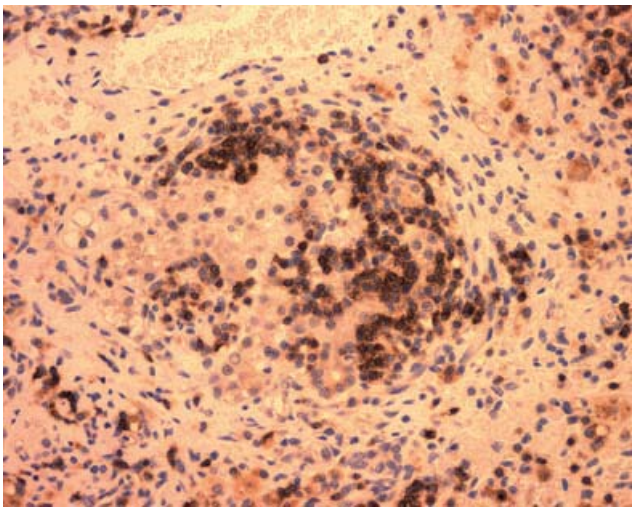

Figure 4.152. Dog: liver, enteric T-cell lymphoma. Phenotype of Figure 4.150. The area is similar to that of Figure 4.151, with a central area of residual hepatocytes surrounded by infiltrating T-lymphocytes with a heavy surrounding layer of desmoplastic connective tissue.

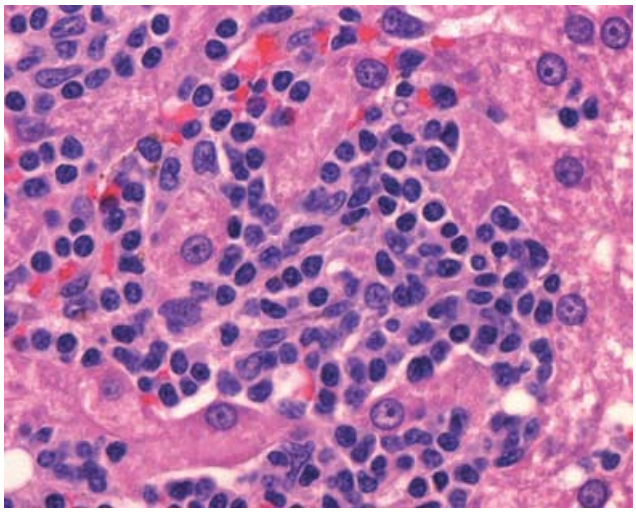

Figure 4.151. Dog: liver, enteric T-cell lymphoma. Detail of Figure 4.150. The cell type is very similar to that of T-zone lymphoma of the node, with small dense nuclei with occasional sharp, shallow indentations and a narrow rim of lightly stained cytoplasm.

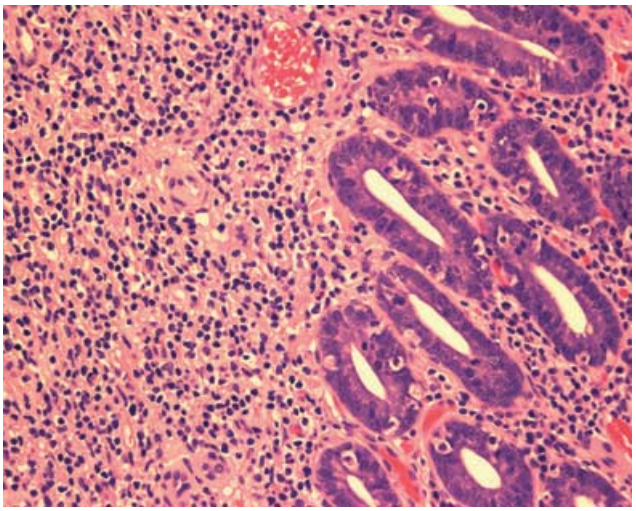

Figure 4.153. Dog: duodenum, enteric T-cell lymphoma. Detail of Figure 4.149. There is scattered small cell infiltration of the epithelium of the glands in the lamina propria layer with a broad area of small cell infiltration separating the base of the glands from the muscularis mucosa.

needle aspiration of those hepatic sites is likely to give a definitive diagnosis because a high level of lymphoid cells in the liver is easily interpreted, but the recognition of small neoplastic cells from the intestine may be interpreted to be benign or equivocal (Figs. 4.153–4.155). Extension of the ETCL to other tissues also includes the gastric mucosa and mesenteric nodes (Figs. 4.156, 4.157), which may not be involved before the liver and to a lesser extent.

The treatment of ETCL is not very successful, and even a good reduction of neoplastic cells has the risk of inducing perforation and peritonitis. Because most cases are diagnosed late in the disease this contributes to difficulty in management.

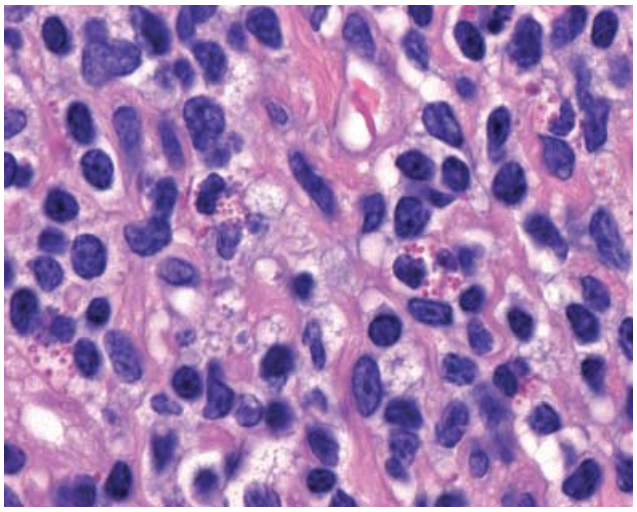

Figure 4.154. Dog: duodenum, enteric T-cell lymphoma. Detail of Figure 4.153. The nuclei of the neoplastic cells are deeply stained without parachromatin clearing and nucleoli are irregularly apparent. The cells have a narrow rim of lightly stained cytoplasm similar to those found in lymph node with the same typical nuclear separation. There are numerous eosinophils present within the neoplastic cells both in the intestine and in the liver.

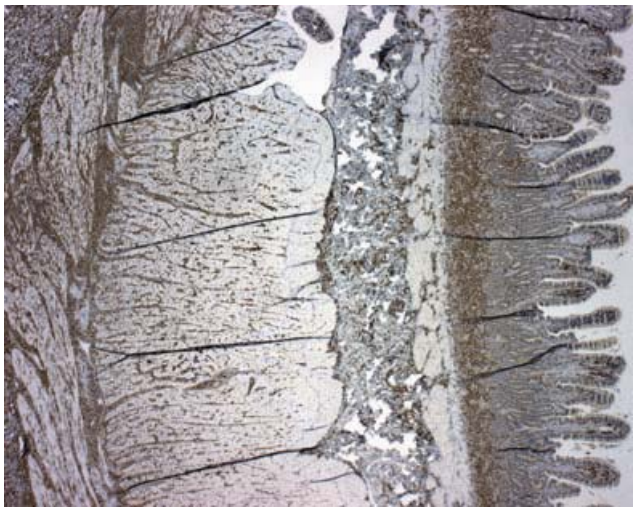

Figure 4.155. Dog: duodenum, enteric T-cell lymphoma. Phenotype of Figure 4.149. With CD3 staining, the infiltrating cells are uniformly and strongly labeled with heavy population of neoplastic cells within the villi as well as the solid laminar infiltration beneath the lamina propria layer.

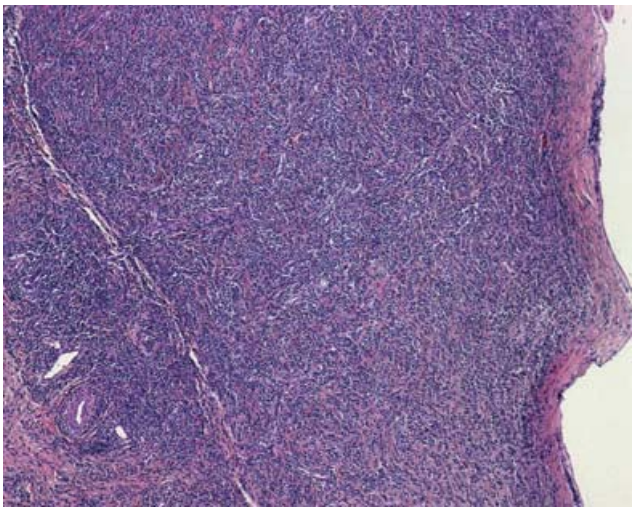

Figure 4.156. Dog: mesenteric node, enteric T-cell lymphoma. There is marked thickening of the capsule with obliteration of the peripheral sinus and diffuse infiltration of cells with loss of normal architecture and fine fibrovascular sclerosis.

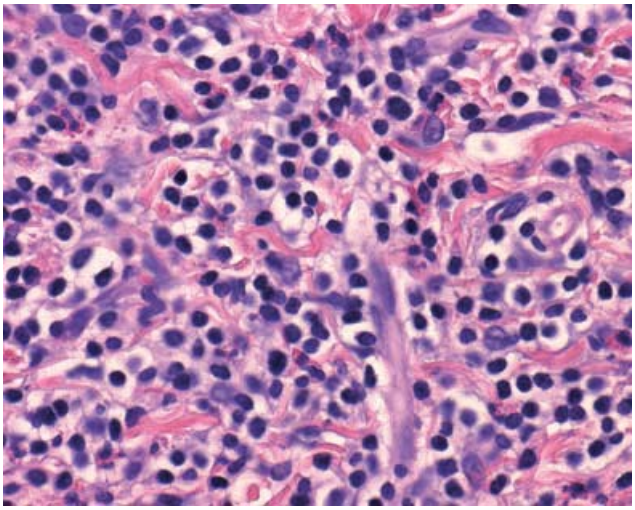

Figure 4.157. Dog: mesenteric node, enteric T-cell lymphoma. Detail of Figure 4.156. The cell type is similar to that of peripheral nodal T-cell lymphoma, but the connective tissue proliferation is unusual and may be related to the heavy chemotaxis for eosinophils.

REFERENCES

Alfsen, G.C., Beiske, K., Bell, H., and Marton, P.F. (1989) Low-grade intestinal lymphoma of intraepithelial T lymphocytes with concomitant enteropathy-associated T cell lymphoma: Case report suggesting a possible histogenetic relationship. *Hum Pathol* 20(9):909–913.

Armitage, J.O., Liang, R.H.S., Sweetenham, J.W., Reyes, F., Jaffe, E.S., and Raffeld, M. (2004) Mature nodal and extranodal T-cell and non-Hodgkin–cell lymphomas (peripheral T-cell, angioimmunoblastic, nasal natural killer/T-cell, hepatosplenic T-cell, enteropathy-type T-cell, and subcutaneous panniculitis-like T-cell lymphomas). In Mauch, P.M., Armitage, J.O., Coiffier, B.C., Dalla-Favera, R., and Harris, N.L. (eds.), *Non-Hodgkin's Lymphomas*. Lippincott Williams & Wilkins, Philadelphia, pp. 405–426, 2004.

Bagriacik, E.U., Okabe, M., and Klein, J.R. (2000) Origins of intestinal intraepithelial lymphocytes: Direct evidence for

a thymus-derived γδ T cell component. *Immunol Lttrs* 75:77–83.
Couto, C.G., Rutgers, H.C., Sherding, R.G., and Rojko, J. (1989) Gastrointestinal lymphoma in 20 dogs: A retrospective study. *J Vet Intern Med* 3:73–78.
Coyle, K.A., and Steinberg, H. (2004) Characterization of lymphocytes in canine gastrointestinal lymphoma. *Vet Pathol* 41:141–146.
Eberl, G., and Littman, D.R. (2004) Thymic origin of intestinal αβ T cells revealed by fate mapping of RORγt cells. *Science* 305:248–251.
Erdman, S.E., Moore, F.M., Rose, R., and Fox, J.G. (1992) Malignant lymphoma in ferrets: Clinical and pathological findings in 19 cases. *J Comp Pathol* 106:37–47.
French, R.A., Seitz, S.E., and Valli, V.E.O. (1996) Primary epitheliotropic alimentary T-cell lymphoma with hepatic involvement in a dog. *Vet Pathol* 33:349–352.
Gale, J., Simmonds, P.D., Mead, G.M., Sweetenham, J.W., and Wright, D.H. (2000) Enteropathy-type intestinal T-cell lymphoma: Clinical features and treatment of 31 patients in a single center. *J Clin Oncol* 18(4):795–803.
Katoh, A., Ohshima, K., Kanda, M., Haraoka, S., Sugihara, M., Suzumiya, J., Kawasaki, C., Shimazaki, K., Ikeda, S., and Kikuchi, M. (2000) Gastrointestinal T cell lymphoma: Predominant cytotoxic phenotypes, including alpha/beta, gamma/delta T cell and natural killer cells. *Leuk and Lymph* 39(1–2):97–111.
Krecic, M.R., and Black, S.S. (2000) Epitheliotropic T-cell gastrointestinal tract lymphosarcoma with metastases to lung and skeletal muscle in a cat. *JAVMA* 216(4):524–528.
Ochoa, R., Breitschwerdt, E.B., and Lincoln, K.L. (1984) Immunoproliferative small intestinal disease in Basenji dogs: Morphologic observations. *Am J Vet Research*, 45(3):482–490.
Pinkerton, M.E., Bailey, K.L., Thomas, K.K., Goetz, T.E., and Valli, V.E. (2002) Primary epitheliotropic intestinal T-cell lymphoma in a horse. *J Vet Diagn Invest* 14:150–152.
Platt, H. (1986) Chronic inflammatory and lymphoproliferative lesions of the equine small intestine. *J Comp Pathol* 96: 671–684.
Tanimoto, T., Minami, A., Yano, S., and Ohtsuki, Y. (1994) Natural disease: Ileal lymphoma in swine. *Vet Pathol* 31:629–636.
Tsujimura, K., Obata, Y., Matsudaira, Y., Ozeki, S., Yoshikawa, K., Saga, S., and Takahashi, T. (2001) The binding of thymus leukemia (TL) antigen tetramers to normal intestinal intraepithelial lymphocytes and thymocytes. *J Immunol* 167:759–764.
Willard, M.D., Dalley, J.B., and Trapp, A.L. (1985) Lymphocytic-plasmacytic enteritis in a cat. *JAVMA*186(2):181–182.
Wright, D.H. (1997) Enteropathy associated T cell lymphoma. Cancer surveys. *Lymph* 30:249–261.
Yatabe, Y., Mori, N., Oka, K., Nakazawa, M., and Asai, J. (1994) Primary gastric T-cell lymphoma: Morphological and immunohistochemical studies of two cases. *Arch Pathol Lab Med* 118:547–550.
Zettl, A., Ott, G., Makulik, A., Katzenberger, T., Starostik, P., Eichler, T., Puppe, B., Bentz, M., Müller-Hermelink, H.C., and Chott, A. (2002) Chromosomal gains at 9q characterize enteropathy-type T-cell lymphoma. *Am J Pathol* 161: 1635–1645.

Subcutaneous Panniculitis-like T-Cell Lymphoma

The subcutaneous panniculitis-like T-cell lymphoma (SPTCL) is the least common of the subtypes of peripheral T-cell lymphoma in humans and has only recently been reported in the dog. The SPTCL neoplasm was first described in human pathology in the last 15 years, and in that time only 100 cases have been described. SPTCL presents as subcutaneous masses that are painful and in humans tend to follow nodular lesions that have a waxing and waning character over a period of several years before progression to ulceration.

In a case seen in a dog, the presentation was of a subcutaneous mass with extensive fat necrosis deep in the panniculus, with the reaction extending 2–3 cm below the skin (Figs. 4.158, 4.159) and accompanied by a very mixed cell reaction (Figs. 4.160, 4.161). There are coalescing areas of inflammatory cell reaction with surrounding areas that are about half fat cells that architecturally resembles bone marrow (Fig. 4.162). The remaining fat cells are separated by a mixed population of large atypical lymphocytes and many lipid-bearing macrophages and neutrophils. The disease, while rare, is likely underdiagnosed because the panniculitis is so necrotizing that an underlying neoplasm may not be suspected. The diagnosis rests on the recognition that there are large lymphocytes with vesicular nuclei and prominent nucleoli (Fig. 4.163) that are present in the spreading areas of the lesion and occur in clusters in some areas, particularly around small vessels. The neoplastic cells mark strongly with CD3 and are negative with B-cell markers (Fig. 4.164). This case was included in a study of canine cutaneous lymphoma studied for the presence of retinoid receptors and was found to be positive. Follow-up was

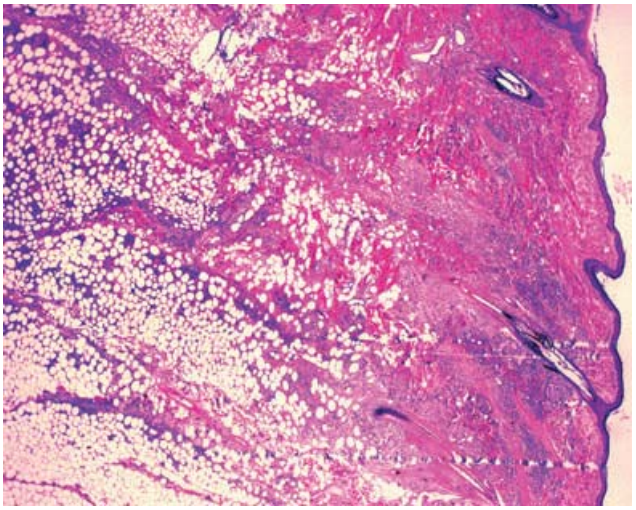

Figure 4.158. Dog: skin, subcutaneous panniculitis-like T-cell lymphoma. There is heavy infiltration of the dermis, which extends with infiltration in the underlying panniculus.

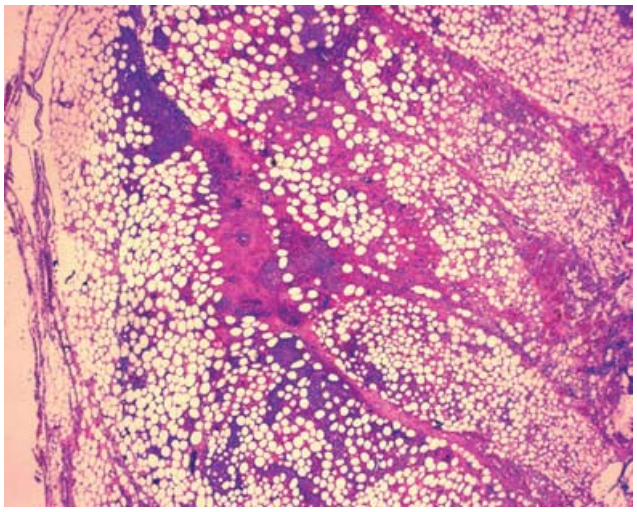

Figure 4.159. Dog: skin, subcutaneous panniculitis-like T-cell lymphoma, deeper portion of tissue from Figure 4.158. The lesion is remarkably extensive and consists of an area of involvement of the panniculus 1.5 cm in length and 1 cm in depth besides the infiltration of the dermis. The panniculus is traversed by fibrous bands of varying thickness with focal areas of hemorrhage and cellular reaction that is multifocal and locally extensive, unlike most other neoplasms.

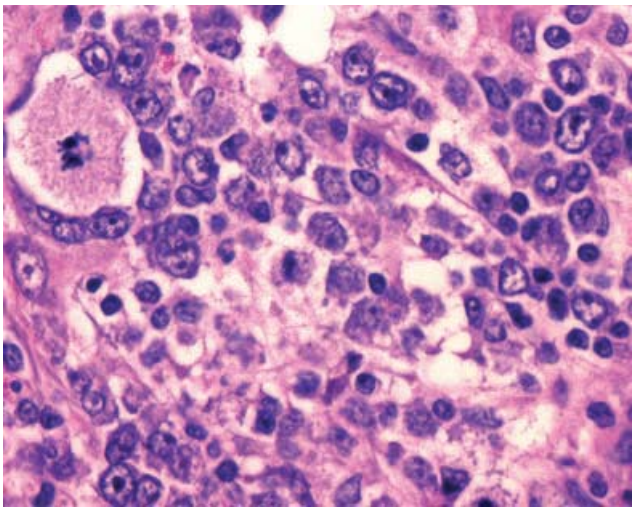

Figure 4.161. Dog: skin, subcutaneous panniculitis-like T-cell lymphoma. Detail of Figure 4.160. There is an abnormal mitotic figure in a huge cell at the upper left with the most prominent other cells having irregularly shaped nuclei, frequently with sharp and deep indentations and with peripheralized chromatin and multiple nucleoli. There are numerous small cells with densely stained nuclei that are presumably benign cells. There is a single eosinophil in the lower left.

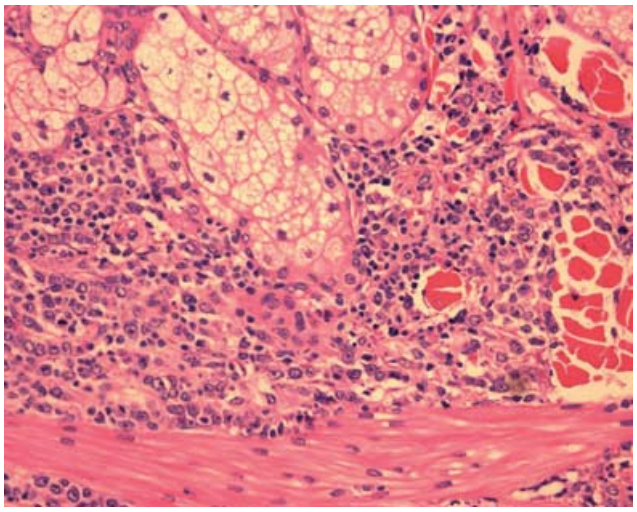

Figure 4.160. Dog: mid-dermal area with erector pili muscle at bottom and collagen fibers at the right. A highly variable population of cells are infiltrating the adnexa with the heterogeneity of cells suggesting inflammation.

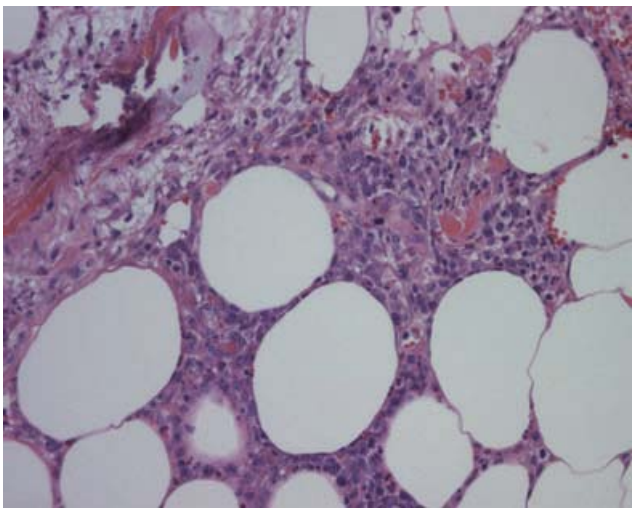

Figure 4.162. Dog: skin, subcutaneous panniculitis-like T-cell lymphoma. An area of solid tumor is interfacing with deeper areas of fatty tissue. There is a focus of collagen necrosis in the upper left similar to that seen in a mast cell tumor. The neoplastic cells irregularly infiltrate between adipocytes in a pattern like panniculitis.

not done, and the outcome not known; however, this subtype of peripheral T-cell lymphoma in humans is characterized by a short remission on chemotherapy and better response to local irradiation, with many cases following an indolent course. A dog with a diagnosis of SPTCL was apparently well after removal of the lesion and presented a year later with a similar lesion and diagnosis (Fig. 4.165). The case is similar to that illustrated in Figures 4.158–4.164 and suggests that a diagnosis of SPTCL does not infer systemic disease (Figs. 4.166–4.168).

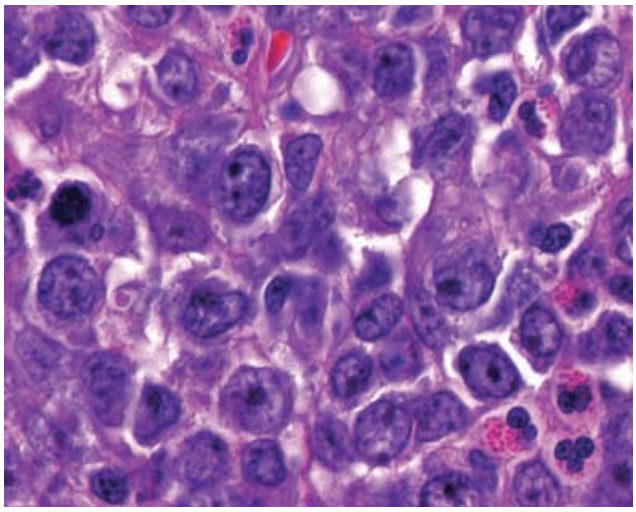

Figure 4.163. Dog: skin, subcutaneous panniculitis-like T-cell lymphoma. Detail of deep dermal lesion. The neoplastic cells have nuclei that are 2–2.5 red cells in diameter, with a hyperchromatic branched chromatin pattern with irregular parachromatin clearing and 1–2 prominent nucleoli that appear both centered and peripheralized. The cytoplasm is moderate in volume and staining density. There are numerous eosinophils present and a cell in mitosis at the left center. There are few smaller lymphocytes of benign type in this field and no neutrophils that are irregularly present in other areas.

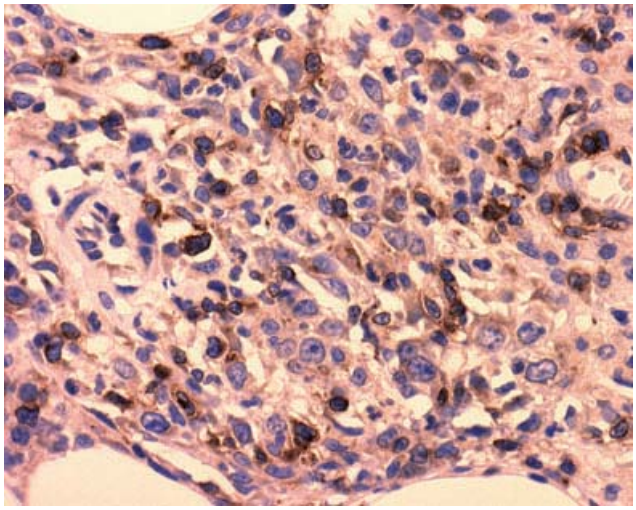

Figure 4.164. Dog: skin, subcutaneous panniculitis-like T-cell lymphoma. Phenotype of Figure 4.162. With CD3 staining, the neoplastic cells are strongly but irregularly marked with frequent reactive mesenchymal cells in the background that are unlabeled. This same area and virtually all areas are completely negative with CD79.

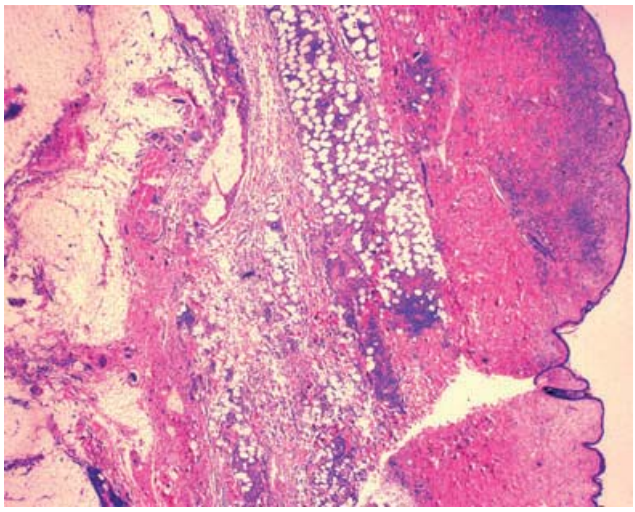

Figure 4.165. Dog: skin, subcutaneous panniculitis-like T-cell lymphoma. The dog presented a year earlier with the same diagnosis given. The case illustrates that these lesions may not be indicative of systemic disease.

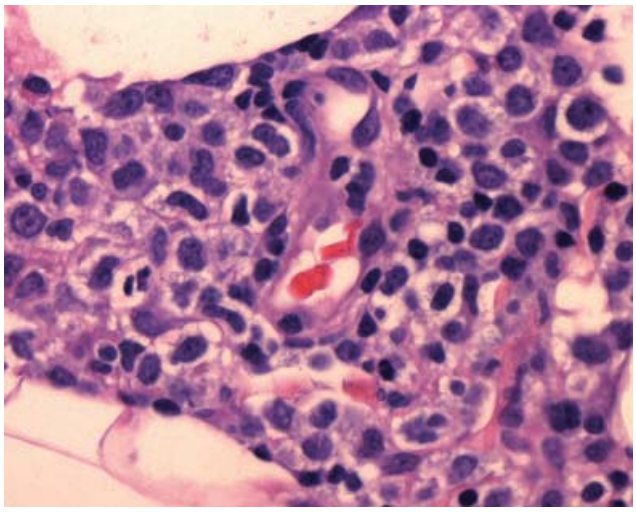

Figure 4.166. Dog: skin, subcutaneous panniculitis-like T-cell lymphoma. Detail of Figure 4.165. The cellular infiltrate is of mixed character: a number of cells with small densely stained nuclei, likely benign cells, particularly in perivascular regions and a small number of larger cells with vesicular nuclei and prominent nucleoli.

Molecular analysis has not been carried out in the dog; however, in humans, most cases of SPTCL have $CD8^+$ αβ type of expression with a minority of $CD4^-CD8^-$ type and express a γδ type of T-cell receptor. All of the human cases of SPTCL are of the cytotoxic T-cell phenotype and are TIA-1^+, and most tested are perforin positive. It appears that the human cases with the γδ type T-cell receptor follow a more aggressive course, and some patients with SPTCL later develop a local form of the hemophagocytic syndrome.

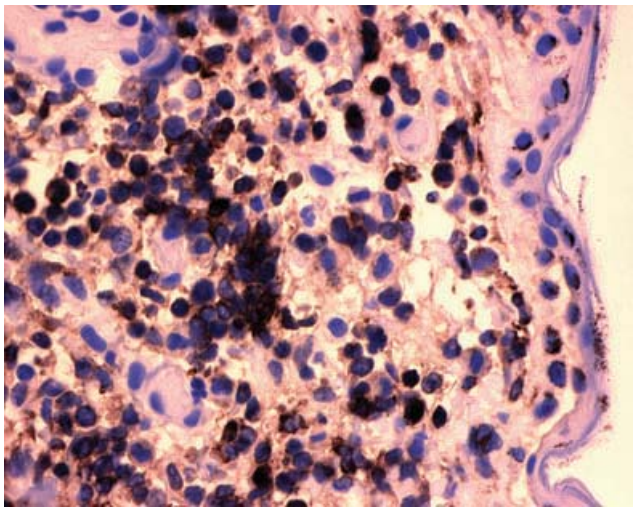

Figure 4.167. Dog: skin, subcutaneous panniculitis-like T-cell lymphoma. Phenotype of Figure 4.165. With CD3 staining, the cells in the superficial dermis are strongly and relatively uniformly labeled.

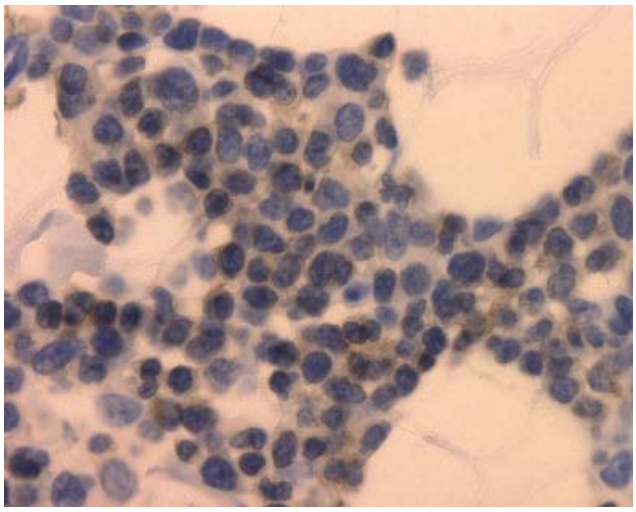

Figure 4.168. Dog: skin, subcutaneous panniculitis-like T-cell lymphoma. Phenotype of Figure 4.165. In the panniculus area, the cell type is more consistently of the large neoplastic type, again with some irregular-shaped nuclei and hyperchromatic chromatin with irregularly prominent nucleoli. The cytoplasm is relatively abundant with cell boundaries generally not distinct. Despite this being a recurrent lesion, the cells do not look more anaplastic than that of the primary diagnosis (Figure 4.163).

REFERENCES

Armitage, J.O., Liang, R.H.S., Sweetenham, J.W., Reyes, F., Jaffe, E.S., and Raffeld, M. (2004) Mature nodal and extranodal T-cell and non-Hodgkin–cell lymphomas (peripheral T-cell, angioimmunoblastic, nasal natural killer/T-cell, hepatosplenic T-cell, enteropathy-type T-cell, and subcutaneous panniculitis-like T-cell lymphomas). In Mauch, P.M., Armitage, J.O., Coiffier, B.C., Dalla-Favera, R., and Harris, N.L. (eds.), *Non-Hodgkin's Lymphomas*. Lippincott Williams & Wilkins, Philadelphia, pp. 405–426, 2004.

Beale, K.M., Dill-Macky, E., Meyer, D.J., and Calderwood-Mays, M. (1990) An unusual presentation of cutaneous lymphoma in two dogs. *J Am An Hosp Assoc* 26:429–432.

Day, M.J. (1995) Immunophenotypic characterization of cutaneous lymphoid neoplasia in the dog and cat. *J Comp Pathol* 112:79–96.

Kelley, L.C., and Mahaffey, E.A. (1998) Equine malignant lymphomas: Morphologic and immunohistochemical classification. *Vet Pathol* 35:241–252.

Kempf, W., Dummer, R., and Burg, G. (1999) Approach to lymphoproliferative infiltrates of the skin: The difficult lesions. *Am J Clin Pathol* 111(Suppl1):S84–S93.

Kumar, S., Krenacs, L., Medeiros, J., Elenitoba-Johnson, K.S.J., Greiner, T.C., Sorbara, L., Kingma, D.W., Raffeld, M., and Jaffe, E.S. (1998) Subcutaneous panniculitic T-cell lymphoma is a tumor of cytotoxic T lymphocytes. *Hum Pathol* 29(4): 397–403.

The Non-Hodgkin's Lymphoma Classification Project. (1997) A clinical evaluation of the International Lymphoma Study Group Classification of Non-Hodgkin's Lymphoma. *Blood* 89(11):3909–3918.

Salhany, K.E., Macon, W.R., Choi, J.K., Elenitsas, R., Lessin, S.R., Felgar, R.E., Wilson, D.M., Przybylski, G.K., Lister, J., Wasik, M.A., and Swerdlow, S.H. (1998) Subcutaneous panniculitis-like T-cell lymphoma: Clinicopathologic, immunophenotypic, and genotypic analysis of alpha/beta and gamma/delta subtypes. *Am J Surg Pathol* 22(7):881–893.

Şen, F., Rassidakis, G.Z., Jones, D., and Medeiros, L.J. (2002) Apoptosis and proliferation in subcutaneous panniculitis-like T-cell lymphoma. *Mod Pathol* 15(6):625–631.

Takeshita, M., Akamatsu, M., Ohshima, K., Kimura, N., Suzumiya, J., Kikuchi, M., Okamura, T., Nakayama, J., Imayama, S., Uike, N., and Nakayama, H. (1995) Angiocentric immunoproliferative lesions of the skin show lobular panniculitis and are mainly disorders of large granular lymphocytes. *Hum Pathol* 26(12):1321–1328.

Takeshita, M., Kimura, N., Suzumiya, J., Ohshima, K., Kikuchi, M., Watanabe, R., Okamura, T., and Goto, H. (1994) Angiocentric lymphoma with granulomatous panniculitis in the skin expressing natural killer cell and large granular T-cell phenotypes. *Virchows Archiv* 425:499–504.

Tobey, J.C., Houston, D.M., Breur, G.J., Jackson, M.L., and Stubbington, D.A. (1994) Cutaneous T-cell lymphoma in a cat. *JAVMA* 204(4):606–609.

Valli, V.E.O., and Gentry, P.A. (1990) Hematopoietic system. Subcutaneous panniculitis-like T-cell lymphoma. In Maxie, M.G., Slocombe, R., Barker, I.K. (In press) *Jubb, Kennedy and Palmer's Pathology of Domestic Animals,* 5th ed. Elsevier Ltd. Health Sciences, Oxford, U.K.

Vernau, W., Jacobs, R.M., Davies, C., Carter, R.F., and Valli, V.E.O. (1998) Morphometric analysis of bovine lymphomas classified according to the National Cancer Institute Working Formulation. *J Comp Pathol* 118:281–289.

Mycosis Fungoides and Sézary Syndrome

Mycosis Fungoides (MF) is a type of cutaneous lymphoma characterized by a linear interface infiltration of small, mature, irregularly cleft lymphocytes that are epitheliotropic and form focal clusters of neoplastic cells in hyperplastic epidermis known as a *Pautrier's microabscess* (Figs. 4.169, 4.170). A variant type of epitheliotropic lymphoma of MF type has an almost complete homing to the epidermal layer itself and is known as *pagetoid reticulosis (PR)* (Figs. 4.171–4.173). The disease presents as a patch of interface dermatitis that is pruritic and progresses to patch/plaque stage, and in humans to an erythroderma not obvious in animals with densely haired skin. The normal biological progression, if untreated, is for the skin disease to become widespread and eventually to involve the blood where the characteristic irregularly cleft cells are known as *Sézary cells* (Fig. 4.174) and the stage as *Sézary syndrome*. In human cases,

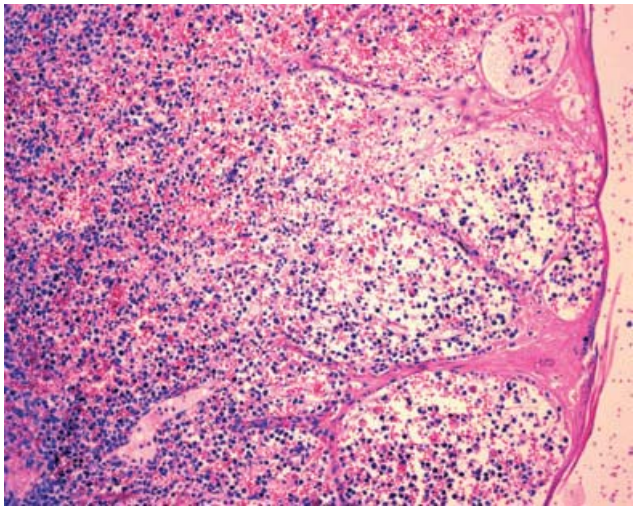

Figure 4.169. Cat: skin, mycosis fungoides. There are multiple epidermal vesicles filled with edema fluid and neoplastic cells.

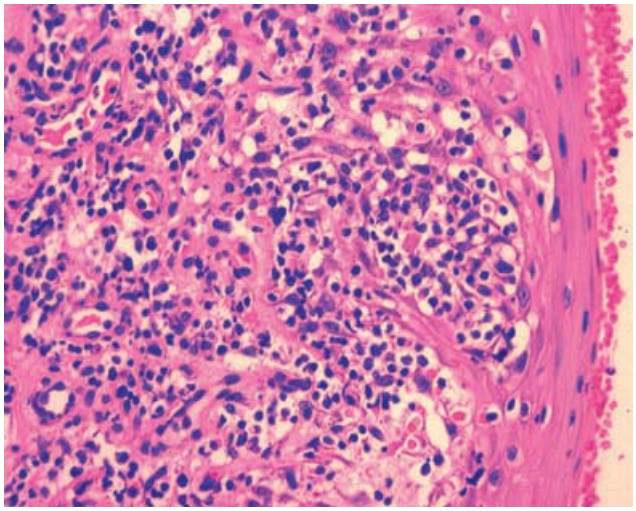

Figure 4.170. Dog: skin, mycosis fungoides. More typical of Pautrier's microabscess with pockets of cells invading the epidermis singly and in large clusters forming intraepithelial vesicles.

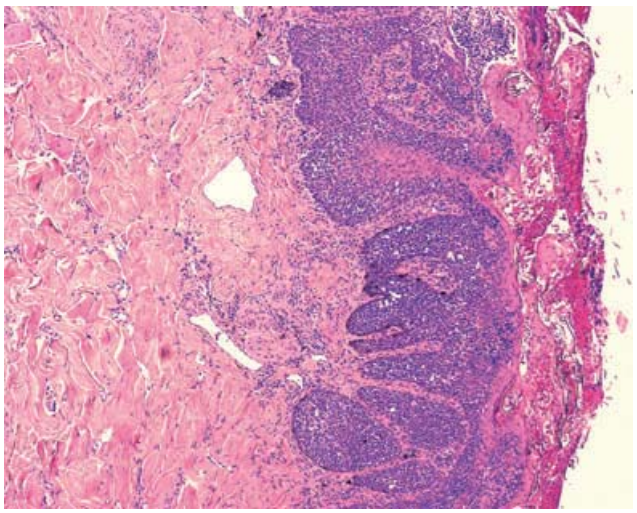

Figure 4.171. Dog: skin, pagetoid reticulosis. There is an intense infiltration of neoplastic cells into a characteristically thickened epithelial layer with an overlying crust of variable density. There is only a very mild accumulation of cells in the papillary dermis beneath the basement membrane that are primarily of B-cell type; those in the epidermis are entirely of T-cell type.

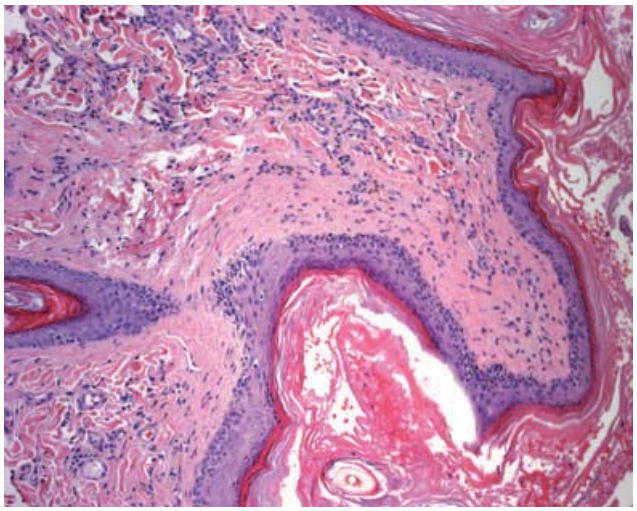

Figure 4.172. Dog: skin, pagetoid reticulosis. This is the early stage of the disease, with a narrow laminar band of lymphocytes, the string-of-pearls–type lesion, infiltrating just above the basement membrane.

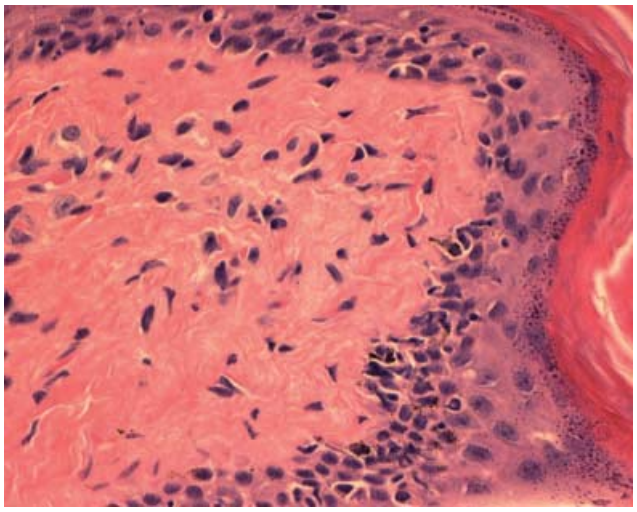

Figure 4.173. Dog: skin, pagetoid reticulosis. Detail of Figure 4.172. There is dense and laminar infiltration into the basal layer of the epidermis with the superficial dermis virtually uninvolved.

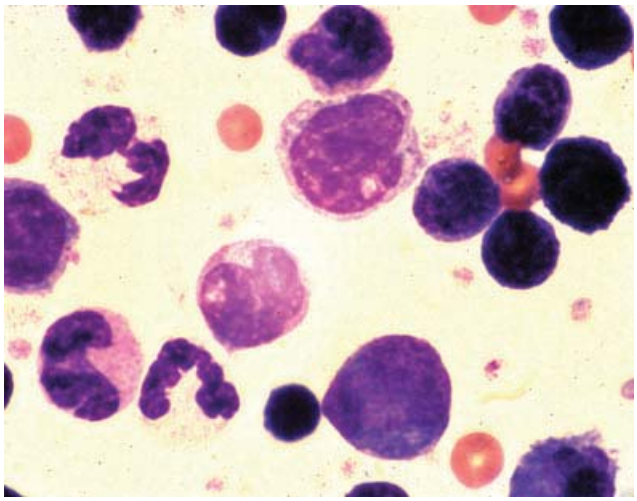

Figure 4.174. Horse: blood, buffy coat, Sézary syndrome. The 3 larger cells are of Sézary type, of which 2 can be seen to have sharp nuclear clefts with cerebriform nuclear membrane convolutions.

the infiltrating cells are predominantly of $CD4^+$ type, but in the dog at least the infiltration is of $CD8^+$ lymphocytes. In animals, an outwardly identical neoplasm to the human MF neoplasm is seen most often in the dog and occurs in the cat, horse, 2-year-old cattle, and in a number of laboratory animals.

In humans, MF accounts for 2% of non-Hodgkin's lymphomas and characteristically is seen in older adults with a median age of 55–60 years with a 2:1 male predominance. In 502 cases of canine lymphoma, there were 13 cases (13/502 = 2.5%) that presented with lymphoma in the skin and of these 2 were in the facial area, 5 were on

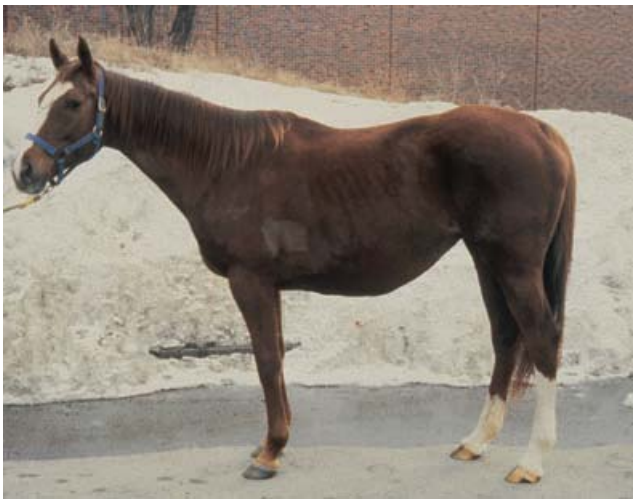

Figure 4.175. A 10-year-old thoroughbred mare in the last month of pregnancy was presented because of difficulty breathing and was found to have pleural and pericardial effusion with an atypical persistent peripheral blood lymphocytosis. The animal was subsequently found to have the Sézary syndrome stage of mycosis fungoides.

lip or gingival area, and 6 cases were of pagetoid reticulosis type. Gender was known in 9, of which 6 were male and 3 were female, and the mean of 10 recorded ages was 10.3 years. In a group of 751 cases of feline lymphoma, 15 cases presented with skin neoplasm, including 1 case of gingival biopsy (15/751 = 2%). Gender was known in 12 cases, with 6 male and 6 female, and the mean age was 11.9 years.

The history at presentation is usually of an animal with exfoliative dermatitis extending over many months or several years for which a number of treatments, including antibacterial and antifungal agents and steroids, have given some improvement but with eventual progression leading to surgical biopsy. A mare in late gestation had pericardial fluid and atypical "monocytes" in blood; there was no apparent skin disease but brick-red oral mucosa that did not blanch on pressure (Figs. 4.175, 4.176). A mucosal biopsy was diagnostic, and the cells in the skin (Figs. 4.177, 4.178), blood, and pericardial fluid were recognized to be lymphocytes with convoluted nuclear folds and Sézary-like cells in blood. The histological changes are similar in most species and consist of interface dermatitis with a dense cellular infiltrate that extends from the basement membrane irregularly around the adnexa (Fig. 4.179). The most minimal involvement is of the string-of-pearls type with a single row of lymphocytes lying beneath and above the basement membrane (see Figs. 4.172, 4.173). There is always some degree of epidermal hypertrophy with mild to moderate parakeratosis and some crusting that is easily dislodged in skin prepa-

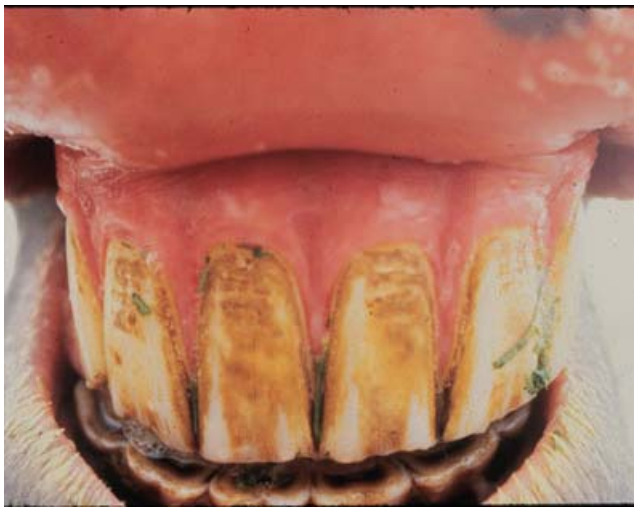

Figure 4.176. Horse: oral mucosa, Sézary syndrome. The mucus membranes were brick red and did not blanch on digital pressure.

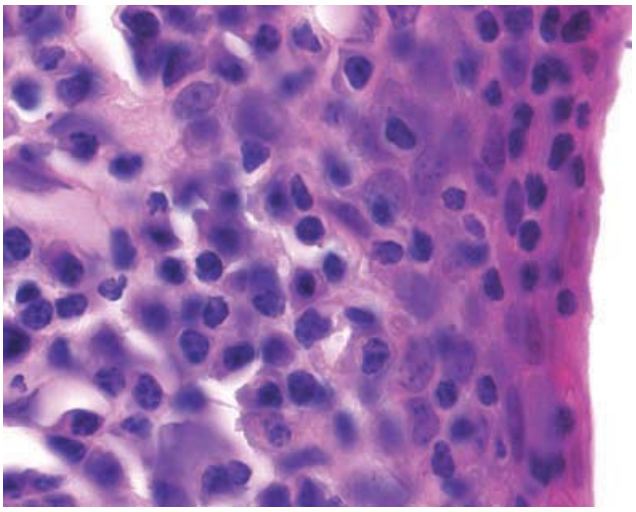

Figure 4.178. Horse: oral mucosa, Sézary syndrome. Detail of Figure 4.177. The irregular contours of the nuclei in the infiltrating cells are apparent as well as focal cells with irregular chromatin aggregation and parachromatin clearing.

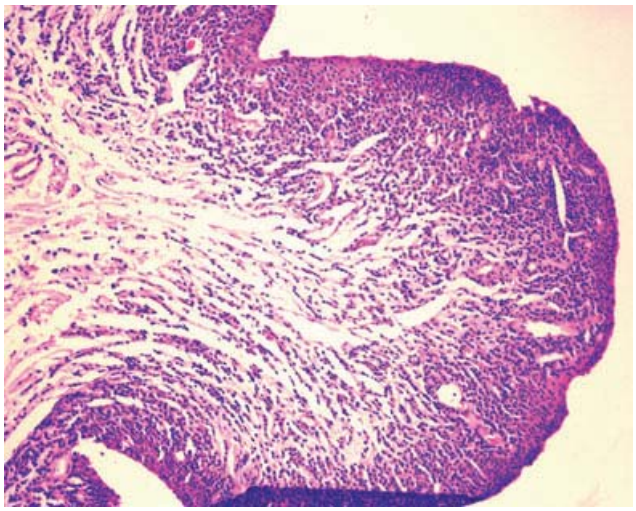

Figure 4.177. Horse: oral mucosa, Sézary syndrome. Tissue from the mouth area that appeared red on gross examination. There is very heavy lymphoid infiltration into the epithelium and superficial dermal mucosa.

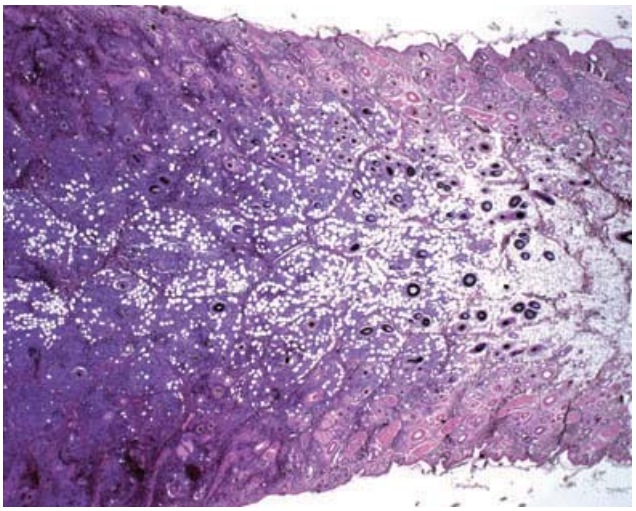

Figure 4.179. Cat: skin, mycosis fungoides. The lesion involved the tip of the tail with a ball-like thickening that began with an increase in interface dermatitis that progressively surrounds the adnexa and becomes confluent at the bottom of the image.

ration for surgery or in tissue processing (Fig. 4.180). In early lesions, the cellular infiltrate is heterogeneous with plasma cells and small and medium lymphocytes. With progression, there is invasion of the epithelium in single cell and small clusters of cells that appear prominent because of a relatively clear halo around each lymphoid nucleus (Fig. 4.181). In advanced lesions, the cellular infiltrate becomes very homogeneous small cell type. There may be central ulceration with the epitheliotropism remaining evident in the mural invasion of hair follicles and in the flanking areas of skin. Cytologically, the neoplastic cells are distinct and very closely resemble those of T-zone lymphoma (TZL) (Fig. 4.182). The nuclei appear round at low magnification and oval with greater detail, and they are only slightly larger than red cells. The nuclei have sharp shallow indentations of the nuclear membrane with some nuclei appearing reniform and others with the more "notched" appearance of the small-cleaved cells of T-cell type. The chromatin is densely stained and dispersed with nucleoli very small and generally not perceived (see Fig. 4.182). Mitoses are virtually absent, and there are no apoptotic cells or tingible body macrophages.

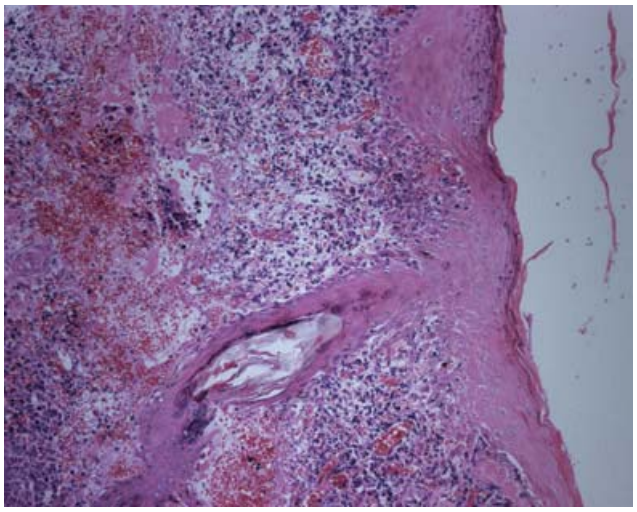

Figure 4.180. Cat: skin, mycosis fungoides. An area of epidermal hypertrophy, with marked hyperkeratosis, that was lost in surgical preparation.

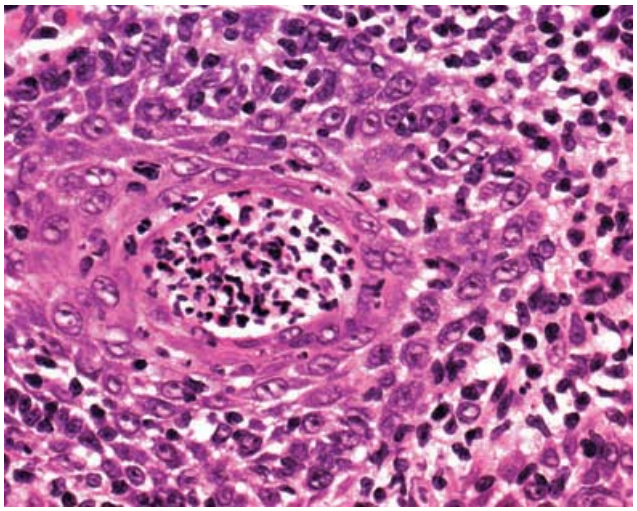

Figure 4.181. Dog: skin, epitheliotropic T-cell lymphoma. There is extensive infiltration into the epithelial cells surrounding a hair follicle, with the basement membrane intact over most of the upper side of the follicle and inapparent on the lower side. The invading cells have small irregularly shaped, densely stained nuclei that are irregularly surrounded by a clear halo that is likely an artifact of tissue contracture during processing. The nuclei are quite plastic and deform into various shapes as they move between the epithelial cells, and they occasionally resemble granulocytes.

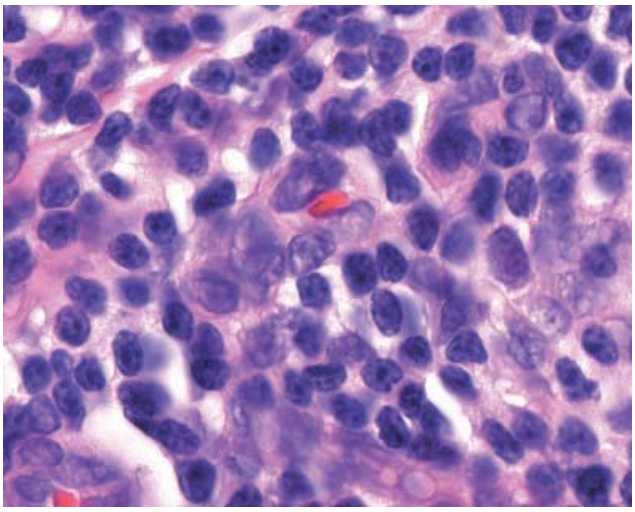

Figure 4.182. Cat: skin, deep dermis, epitheliotropic T-cell lymphoma. The connective tissue membrane in the upper left is a capsule that surrounds a hair follicle heavily infiltrated with small lymphocytes. The nuclei are approximately the same diameter as red cells with the nuclei deeply stained without parachromatin clearing and with sharp, shallow nuclear indentations. The perinuclear clear areas are variably present due to differential shrinking of the epithelial and stromal elements.

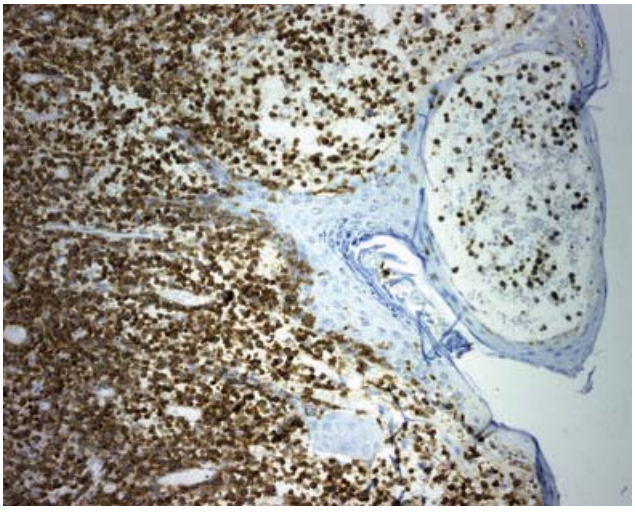

Figure 4.183. Cat: skin, mycosis fungoides. Phenotype of Figure 4.179. With CD3 staining, the infiltrating cells are solidly and uniformly labeled, including those infiltrating the intraepithelial cavities.

The cytoplasm is moderate in volume and generally lightly stained with cell boundaries indistinct; the nuclei have a very uniform spacing and are seldom in contact. These cells are uniformly, but often not strongly, marked with CD3 (Fig. 4.183). In advanced cases, the neoplastic cells extend in large and small clusters that separate the dermal collagen fibers and advance in loose scattered fashion in the panniculus. There may be more deeply stained clusters of lymphocytes in the deep dermis that are fading germinal centers consisting of closely aggregated mantle cells that are sharply differentiated in immune staining by CD79 or CD20 (Fig. 4.184).

MF in cattle is a distinctive neoplasm with a defining history of occurring in cattle at 2 years of age. In cattle,

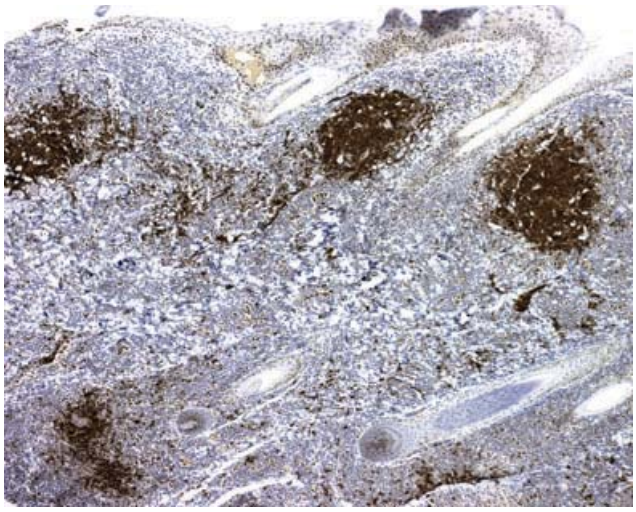

Figure 4.184. Cat: skin, cutaneous T-cell lymphoma. Phenotype of Figure 4.182. With CD79 staining, the collapsed mantle cells of fading germinal centers stain very sharply against a negative background of T-cell infiltration.

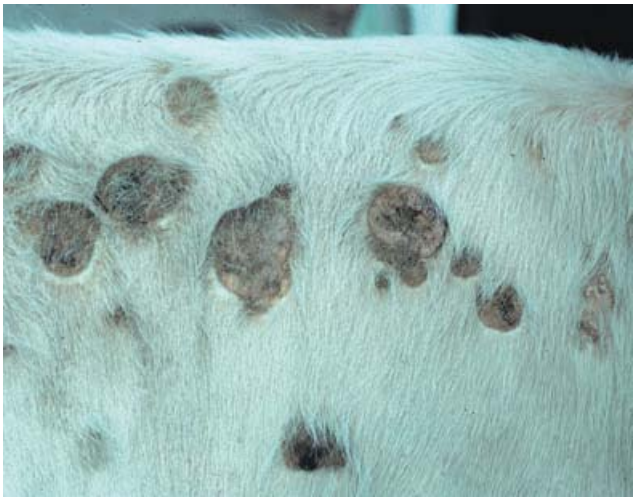

Figure 4.186. Cow: mycosis fungoides. Detail of Figure 4.185. The lesions are sharply demarcated and moderately raised with extensive hair loss over the areas of involvement. The lesions wax and wane over a period of months.

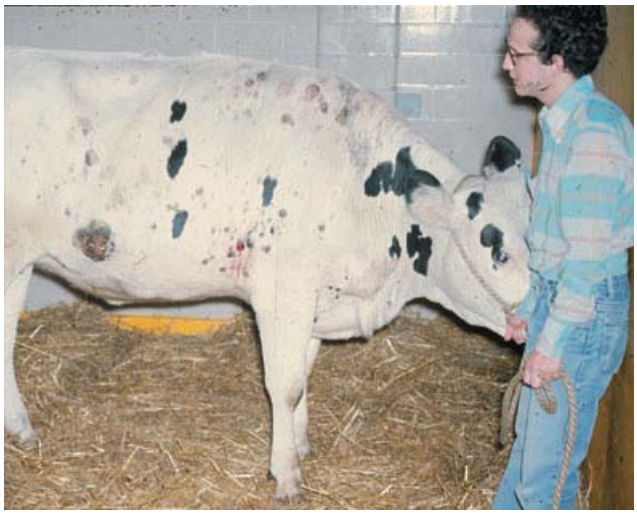

Figure 4.185. A 2-year-old Holstein cow with mycosis fungoides. There are multifocal raised and depilated lesions, some of which are ulcerated, likely due to self trauma. The animal is restrained by R. M. Jacobs, DVM.

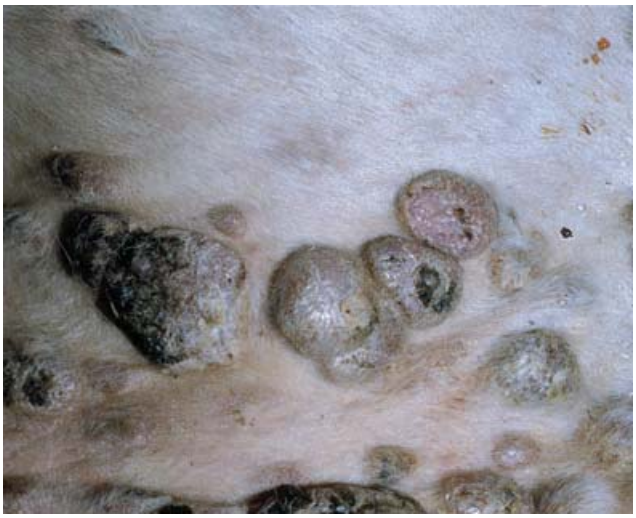

Figure 4.187. Cow: mycosis fungoides. Occasionally, the lesions may be raised and ulcerated with depilation and mild reddening.

cutaneous lymphoma is of the sporadic form not associated with bovine leukemia virus infection (BLV) and the disease is characterized by focal, often circular skin lesions of 2–20 cm in diameter on abdomen, flanks, and limbs (Figs. 4.185–4.187). These lesions depilate and ulcerate and then often heal to appear elsewhere. The lesions have been mistaken for ringworm infection because of their focal nature, with the animals remaining in good health in the early stages of the disease. Over a period of a year or less, there is invariably progression of the disease to involve all internal organs, including spleen, liver, nodes, and marrow, with the disease not distinguishable from the enzootic BLV-related multicentric lymphoma.

The histological lesions in the skin are like those described for the dog, with a much greater thickness of dermis (Fig. 4.188). The irregularity of the lymphocyte nuclear membranes, seen in Sézary syndrome in humans, is also present in cattle, but it is less apparent than in the dog where thin sections of skin are more easily obtained.

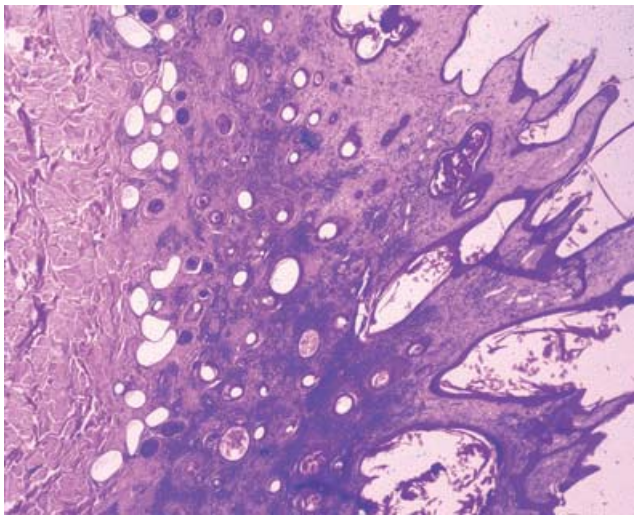

Figure 4.188. Cow: skin, mycosis fungoides. In the margins of the plaquelike lesions, there is irregular infiltration into the adnexa with marked thickening of the superficial dermis and irregular proliferation of the overlying epithelium.

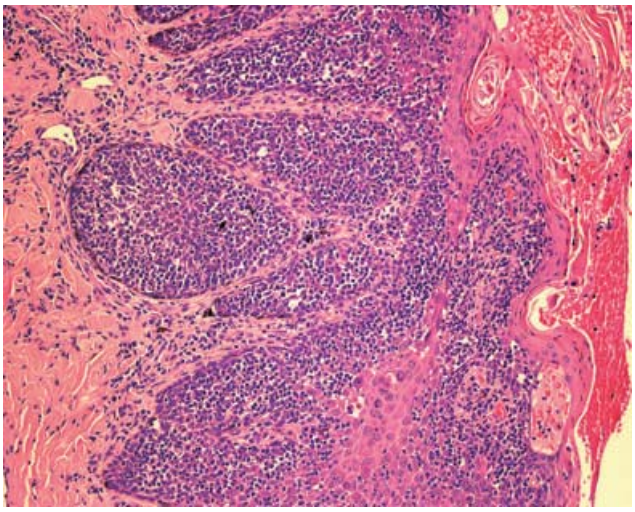

Figure 4.190. Dog: skin, pagetoid reticulosis. Detail of Figure 4.189. There is very heavy infiltration into the epidermal layer by small cells with the characteristic perinuclear halo giving the tissue a moth-eaten appearance. The cells in the superficial dermis are a much more variable type.

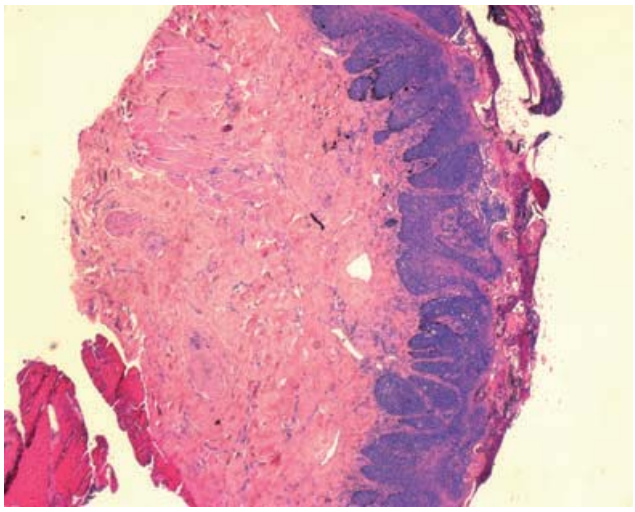

Figure 4.189. Dog: skin, pagetoid reticulosis. There is marked thickening of the epidermal layer with lengthened rete ridges and narrowed dermal pegs. There is adherent overlying debris. There is very heavy lymphoid infiltration into the epithelium itself but very little reaction in the underlying dermis.

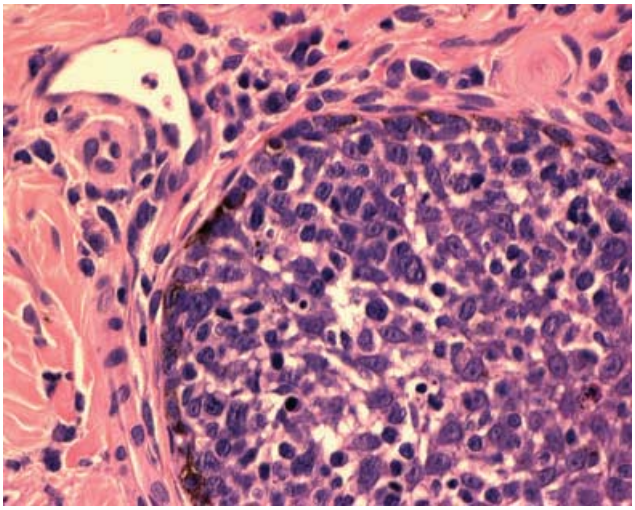

Figure 4.191. Dog: skin, pagetoid reticulosis. Detail of Figure 4.189. The number of small lymphocytes within the epidermal layer is about equal to the number of epithelial nuclei. The cells in the surrounding superficial dermis include a number of plasma cells (above) and other lymphocytes of B-cell lineage.

The neoplastic cells of cattle are slightly larger than in the dog, with nuclei about 1.5 red cells in diameter. There is no known cause of MF/SS in humans or animals, but a retroviral agent has been isolated from the MF cells of a dog in long-term culture.

Pagetoid reticulosis (PR), also known as *Woringer-Kolopp* disease, is considered a verrucose variant of MF and, in humans, has a similar biology to MF. The histology of this variant is distinctive, and the lesions should be identified as separate diseases until our database can determine otherwise. In PR, the neoplastic infiltration is virtually all above the basement membrane, and this may include deep mural invasion of the hair follicles and areas of the adnexa (Figs. 4.189–4.191). There is an interface dermal cellular reaction that may be intense in areas but is of a mixed cellular population. These neoplasms give a remarkable reaction on immunohistochemical staining,

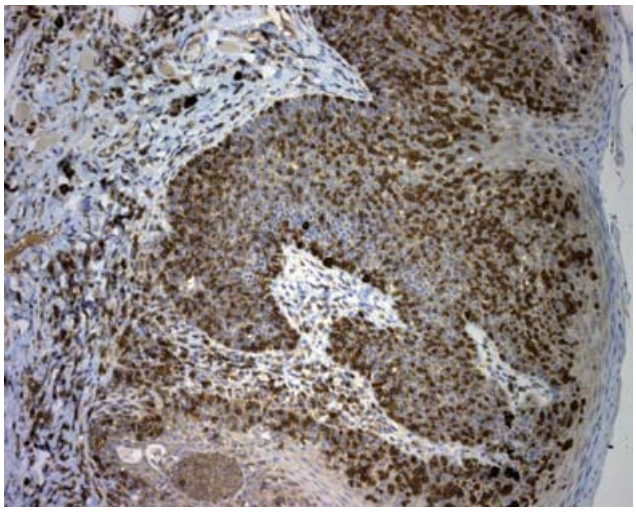

Figure 4.192. Dog: skin, pagetoid reticulosis. Phenotype of Figure 4.189. With CD3 staining, there is strong reactivity of the cells within the epidermal layer and scattered staining of cells in the superficial dermis.

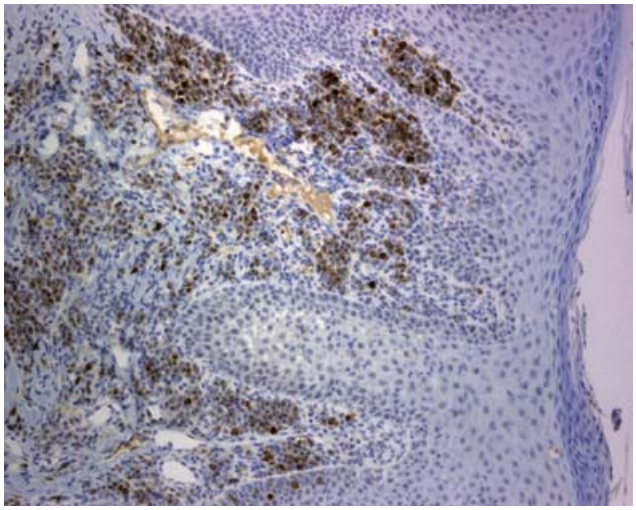

Figure 4.193. Dog: skin, pagetoid reticulosis. Phenotype of Figure 4.192. On staining with CD79, there are a few plasma cells in the superficial dermis with the heavy cell infiltration into the epidermal layer completely unlabeled.

with the cells in the epithelial layers uniformly marked with CD3 (Fig. 4.192) and those in the superficial dermis largely of B-cell type and marking with CD79 or CD20 (Fig. 4.193).

The treatment of MF and PR is largely one of topical treatments in humans, which is not an option in animals that regularly lick affected areas of skin. In general, it is felt that unless and until there is erythrodema or evidence of systemic spread there is little advantage in systemic chemotherapy. In humans, most cases remain as skin involvement, and only about 15–20% progress to systemic disease. There does not appear to be a transformation to a more aggressive form of lymphoma with MF/SS in humans or animals, but in cattle, at least, there are more apparent nucleoli in the cells in the blood in cases with visceral involvement. It appears likely that in the dog many cases of cutaneous T-cell lymphoma have retinoid receptors and, barring cost, may respond to alltrans-retinoic acid therapy (Fig. 4.194).

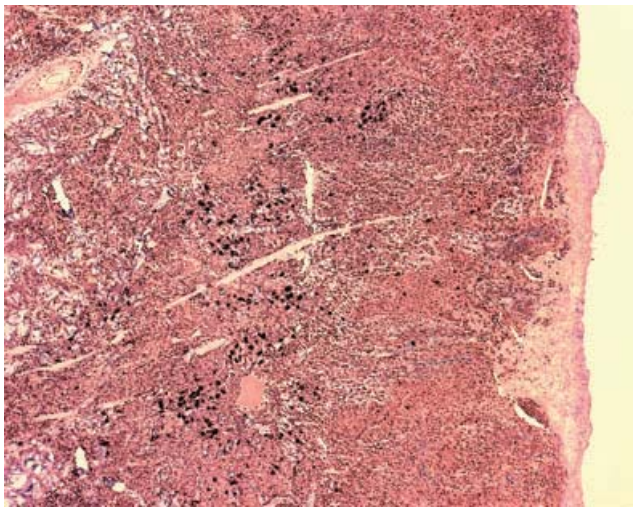

Figure 4.194. Dog: skin, epitheliotropic T-cell lymphoma stained for the retinoic acid receptor alpha subtype with strong positive reaction. The very dark cells are melanocytes.

There is little opportunity to see the viscera in these cases as a function of tumor progression. In human cases that have advanced to Sézary syndrome (Figs. 4.195–4.200), there are nodular lesions in the liver and in the bone marrow and irregular involvement of peripheral nodes, most of which have overlapping changes of nonspecific dermatopathic lymphadenopathy with many melanin-bearing cells and macrophages in the outer cortices.

REFERENCES

Baker, J.L., and Scott, D.W. (1989) Mycosis fungoides in two cats. *JAAHA* 25:97–101.

Bellei, B., Pacchiarotti, A., Perez, M., and Faraggiana, T. (2004) Frequent β-catenin overexpression without exon 3 mutation in cutaneous lymphomas. *Mod Pathol* 17:1275–1281.

DeBoer, D.J., Turrel, J.M., and Moore, P.F. (1990) Mycosis fungoides in a dog: demonstration of T-cell specificity and response to radiotherapy. *JAAHA* 26:566–572.

Fournel-Fleury, C., Ponce, F., Felman, P., Blavier, A., Bonnefont, C., Chabanne, L., Marchal, T., Cadore, J.L., Goy-Thollot, I., Ledieu, D., Ghernati, I., and Magnol, J.P. (2002) Canine

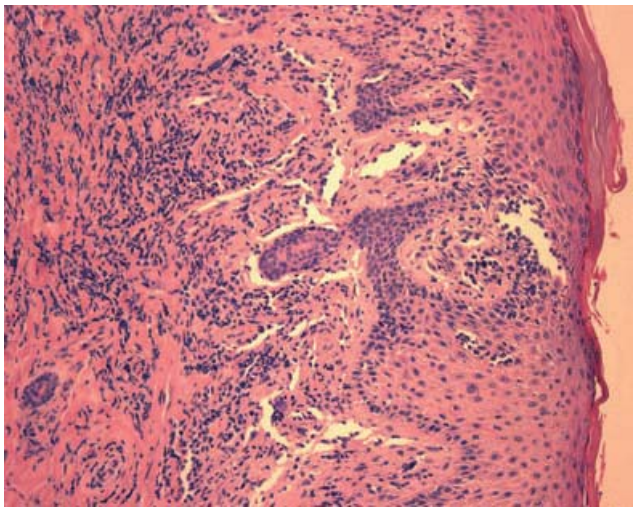

Figure 4.195. Human: skin, mycosis fungoides. There is characteristic epidermal thickening with mild interface small lymphocytic infiltration and focal clusters of lymphocytes within the epidermal layer. *Slide from Cornell Tutorial.*

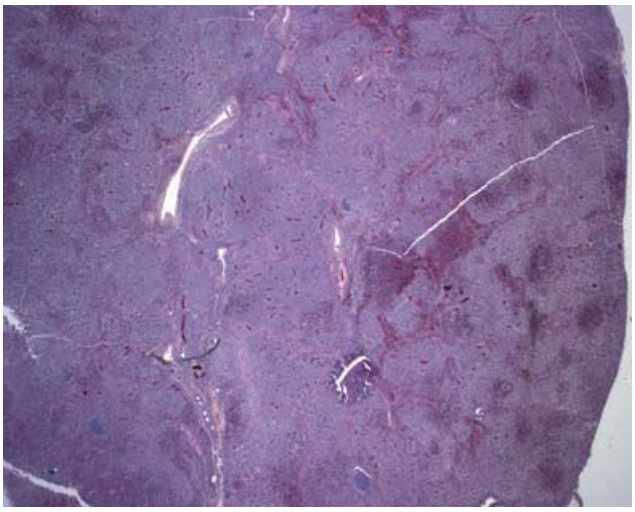

Figure 4.197. Human: lymph node, mycosis fungoides. The capsule is markedly thinned, with the peripheral sinus compressed or obliterated and the node architecture replaced by diffuse proliferation with focal areas of sinus congestion. *Slide from Cornell Tutorial.*

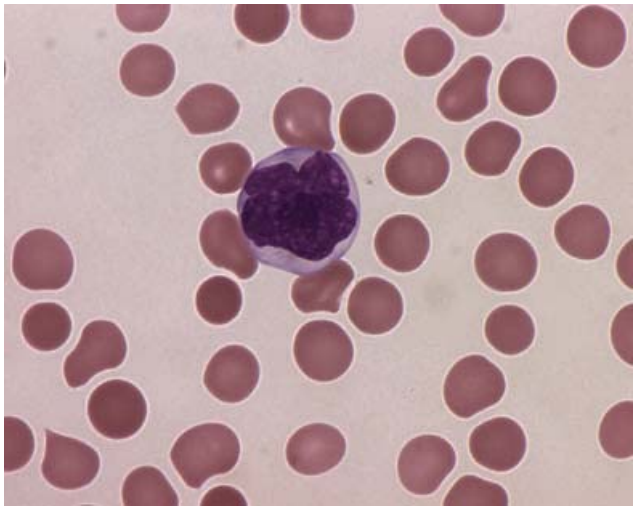

Figure 4.196. Human: blood, Sézary syndrome. Characteristic multiple deep nuclear clefts known as *convoluted* or *cerebriform nuclei* are apparent in this cell. The patient was only moderately leukemic but platelets were deficient. *Slide from Cornell Tutorial.*

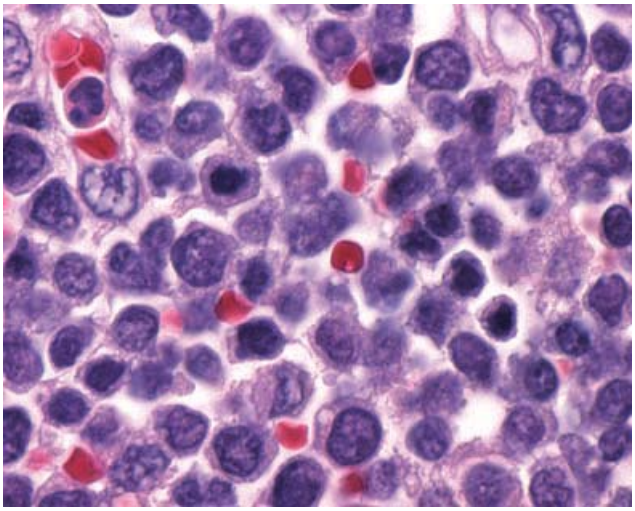

Figure 4.198. Human: node, mycosis fungoides. Detail of Figure 4.197. The cells are larger than in the dog and more like the cow, with moderate anisokaryosis and some irregularities in nuclear outline apparent. There is much higher mitotic rate than generally seen with this disease in animals.

T-cell lymphomas: A morphological, immunological, and clinical study of 46 new cases. *Vet Pathol* 39:92–109.

Ghernati, I., Auger, C., Chabanne, L., Corbin, A., Bonnefont, C., Magnol, J.P., Fournel, C., Rivoire, A., Monier, J.C., and Rigal, D. (1999) Characterization of a canine long-term T cell line (DCL 01) established from a dog with Sézary syndrome and producing retroviral particles. *Leukemia* 13:1281–1290.

Girardi, M., Oppenheim, D.E., Steele, C.R., Lewis, J.M., Glusac, E., Filler, R., Hobby, P., Sutton, B., Tigelaar, R.E., and Hayday, A.C. (2001) Regulation of cutaneous malignancy by γδ T cells. *Science* 294:605–609.

Graham, S.J., Sharpe, R.W., Steinberg, S.M., Cotelingam, J.D., Sausville, E.A., and Foss, F.M. (1993) Prognostic implications of a bone marrow histopathologic classification system in mycosis fungoides and the Sézary syndrome. *Cancer* 72:726–734.

Hoppe, R.T., Harvell, J.D., and Kim, Y.H. (2004) Mycosis fungoides. In Mauch, P.M., Armitage, J.O., Coiffier, B.C., Dalla-Favera, R., and Harris, N.L. (eds.), *Non-Hodgkin's Lymphomas*. Lippincott Williams & Wilkins, Philadelphia, pp. 307–318.

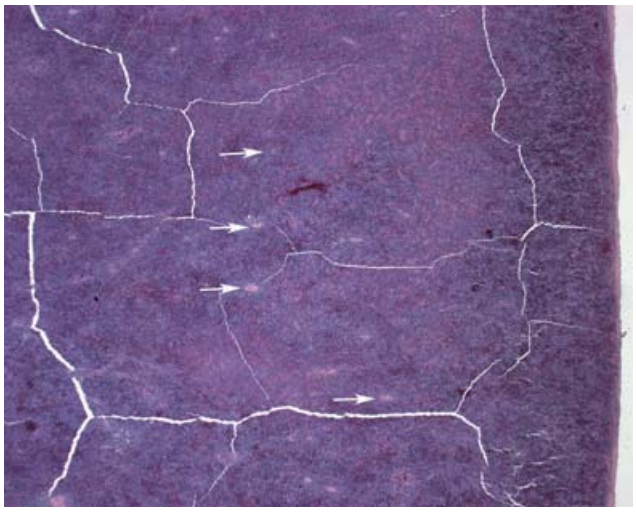

Figure 4.199. Human: spleen, mycosis fungoides. There is marked thinning of the capsule, and the smooth muscle trabeculae are thinned and widely separated indicating splenomegaly. There are few arterioles present (arrows), and these have markedly atrophic periarteriolar lymphoid sheaths and there is a complete absence of germinal centers. *Slide from Cornell Tutorial.*

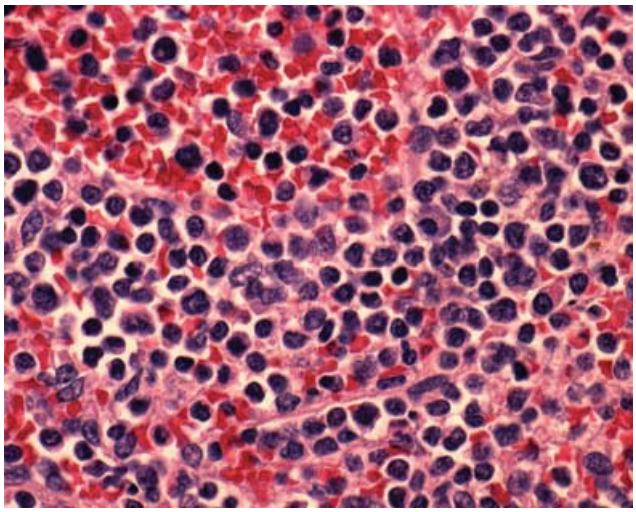

Figure 4.200. Human: spleen, mycosis fungoides. Detail of Figure 4.199. There is diffuse infiltration of the splenic parenchyma with irregular dilation of a large sinus in the upper left.

Prats, M., Fondevila, D., Rabanal, R.M., Marco, A., Domingo, M., and Ferrer, L. (1994) Epidermotropic cutaneous lymphoma (mycosis fungoides) in an SD rat. *Vet Pathol* 31:396–398.

Rosenbaum, M.R., Affolter, V.K., Usborne, A.L., and Beeber, N.L. (1996) Cutaneous epitheliotropic lymphoma in a ferret. *JAVMA* 209(8):1441–1444.

Shohat, M., Hodak, E., Hannig, H., Bodemer, W., David, M., and Shohat, B. (1999) Evidence for the cofactor role of human T-cell lymphotropic virus type 1 in mycosis fungoides and Sézary syndrome. *Brit J Dermatol* 141:44–49.

Tobey, J.C., Houston, D.M., Breur, G.J., Jackson, M.L., and Stubbington, D.A. (1994) Cutaneous T-cell lymphoma in a cat. *JAVMA* 204(4):606–609.

Vermeer, M.H., Geelen, F.A.M.J., Kummer, J.A., Meijer, C.J.L.M., and Willemze, R. (1999) Expression of cytotoxic proteins by neoplastic T cells in mycosis fungoides increases with progression from plaque stage to tumor stage disease. *Am J Pathol* 154:1203–1210.

Anaplastic Large Cell Lymphoma

Anaplastic large cell lymphoma (ALCL) occurs in two major forms of primary cutaneous and primary systemic presentations. There are 2 variants of ALCL recognized in the WHO classification, but the spectrum is wider with the *common* or large cell type constituting about 70% of human cases not included in the last WHO classification. The *small-cell variant* and the *lymphohisticytic variant* each make up about 5–10% of human cases and are given status of disease entities in the WHO system. Other variant types more rarely encountered have been proposed, including sarcomatoid, neutrophil-rich, hypocellular, and signet ring forms. A particular morphologic correlate known as the *hallmark cell*, which has a roughly horseshoe-shaped nucleus, rates its name because it is common to all suggested subtypes. One unifying identification of the ALCL subtypes is that they all express the CD30 (Ki-1) transmembrane molecule on at least some cells. The latter marker is the cytokine receptor of the tumor necrosis factor family receptor with ligand CD30L. The expression of CD30 is not uniform even in single variants; it is on the cell membrane and in the Golgi area and most commonly present on the largest cells found near blood vessels. Although not grouped together in the WHO system of classification, the text by Mauch et al., recognizes the distribution of $CD30^+$ neoplasms in a grouping of cutaneous lymphoproliferative diseases that includes all forms of ALCL and lymphomatoid papulosis. The latter disease is virtually unrecognized in animals, but in human patients about 10% of those with lymphomatoid papulosis have a prior history of mycosis fungoides or Hodgkin's disease.

The second and more generally relied-upon marker is for the anaplastic lymphoma kinase (ALK) protein expression. The ALCL neoplasm is associated with a t(2;5) translocation that results in the ALK gene fusing with the NPM (nucleophosmin) gene. The NPM protein is a multifunctional agent involved in nuclear transport and in controlling centrosome duplication and thus entry and successful exit from mitosis. The ALK gene encodes for a transmembrane receptor with a large extracellular domain. The function of ALK is unknown, and in physiologic states it is found only in nervous tissue. In the t(2;5)

translocation, the fusion gene forms an 80-kDa chimeric protein that loses the extracellular and transmembrane domains of ALK but produces the entire cytoplasmic region of the ALK protein. In the fusion protein part of the NPM, carrying the nuclear localization signals is lost. The functional implications of this chimeric protein is that the ALK gene comes under control of the strong NPM promoter, which results in constitutively high-level production of the NPM-ALK fusion protein. This protein can form homodimers that mimic ALK binding to its normal ligand and unregulated activation of the tyrosine kinase catalytic domain of the ALK protein. The chimeric NPM-ALK protein can also form heterodimers with any wild type NPM that can result in nuclear staining by the anti-ALK diagnostic reagent. Finally, the NPM-ALK fusion is felt to be the oncogene in causation of ALCL.

The use of these two reagents for detection of CD30 and ALK proteins is the primary means of identifying the various subtypes of ALCL. The most common form of systemic ALCL has a T or null phenotype, with the latter felt to be derived from a T-cell because of rearranged T-cell antigen receptor genes and because of common expression of cytotoxic molecules perforin, granzyme B, and TIA-1. A B-cell form of ALCL has been proposed in humans and occurs in animals, at least in cats and dogs (Figs. 4.201, 4.202; see also Chapter 3, "B-Cell Neoplasms," Figs. 3.430–3.433), as identified by the hallmark cells. In human cases, B-cell types of ALCL may be derived from follicular lymphomas and have been identified by the detection of somatic mutations in the immunoglobulin H-variable regions genes.

Because the ALK protein is not found outside of neural tissue, its presence is considered indicative of the t(2;5) translocation and positive identification of ALCL. A number of staining patterns with ALK are found that reflect these various molecular dimerizations. About 60% of the T or null type of ALCL, mark with the ALK reagent in immunohistochemical staining. The positive cells have reactive protein in both the cytoplasm and nucleus as a result of binding to wild-type NPM. Cells with positive ALK marking only in the nucleus can be considered to be labeling benign cells with wild type NPM and likely of neural origin. ALCL may occur where the ALK gene has fused with other than the NPM gene, and this leads to an immunohistochemical reaction with only cytoplasmic labeling. Other loci that have formed fusion genes and chimeric proteins with ALK include TPM3 (nonmuscle tropomyosin) and can transform both lymphoid and mesenchymal tissues. Also, the CLTCL-ALK (clathrin heavy polypeptide-like) gene and Moesin-ALK fusion gene have been found, each of which has some unique cytoplasmic staining characteristics in immune recognition.

There are important variations in presentation found in human cases of ALCL where the primary systemic type accounts for 2–8% of all lymphomas but 10–15% of childhood non-Hodgkin's lymphomas. Patients with the ALK^- form of systemic ALCL tend to be male, be over 60 years old, and have a wider range of extranodal tissues involved, including skin, bone, and many other soft tissues. The ALK^+ cases of ALCL tend to occur in younger patients, again with male predominance, and have a much better response to therapy. Negative prognostic factors identified in pediatric patients include mediastinal

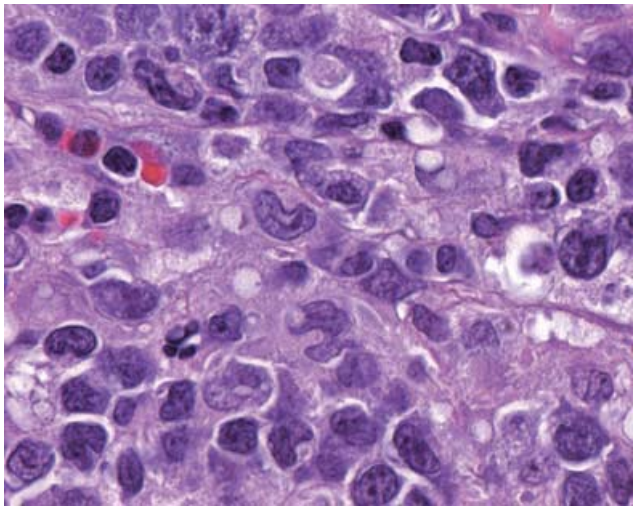

Figure 4.201. Cat: node, anaplastic large cell lymphoma. There are 2 cells in the center, one with reniform shape and the second with a definite horse-shoe indentation. These are the so-called "hallmark cells" of anaplastic large cell lymphoma.

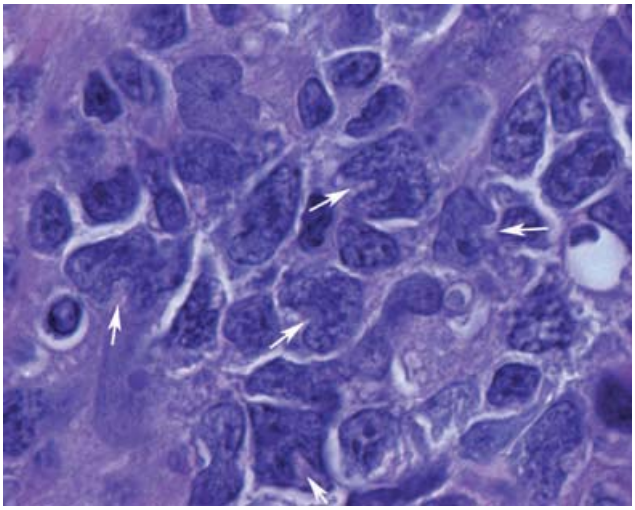

Figure 4.202. Cat: node, ALCL. Multiple cells are present with deeply and smoothly indented nuclei indicated by arrows at putative hallmark-type cells.

involvement; visceral involvement if including spleen, lung or liver; and skin lesions.

In human cases, the remission rate is higher for ALCL than for nonanaplastic large cell lymphomas, and those with T-ALCL had a better survival rate than those with large T-cell lymphoma on nonanaplastic large cell type.

Primary Cutaneous Anaplastic Large Cell Lymphoma of T-Cell Type

Primary cutaneous anaplastic large cell lymphoma of T-cell type in animals is a rarely encountered neoplasm seen most often in dogs, and it likely occurs and is underrecognized in other domestic animals. The hallmark cell configuration is not rare and is seen as well in B-cell as well as in T-cell neoplasms (see Chapter 3, Figs. 3.430–3.433). In humans, primary cutaneous ALCL is defined by greater than 70% of the atypical lymphocytes marking positively for CD30 and without evidence of extracutaneous disease within 6 months of diagnosis. Although not included in the definition, but of importance, most of the atypical cells are negative for ALK.

In animals, the presentation is usually in dogs under 5 years, with single or multiple lesions that have had a variety of treatments without effect and are followed by biopsy as deeper tissues become affected. In the skin, the T-cell variant of ALCL is a "high-up" neoplasm that extends from the basement membrane with no sparing of the Grenz zone and advances irregularly throughout the dermis and into the panniculus. There is likely to be central ulceration with the relationship of the neoplasm to the basement membrane evident in flanking areas. The neoplasm at the architectural level has solid areas of large cell proliferation that are irregularly interspersed by foci of smaller darker staining cells, usually a mixture of benign reactive small lymphocytes, plasma cells, and histiocytes. Cytologically, the neoplastic cells have large nuclei 3–4 red cells in diameter than vary from round to oval, with a recurring tendency to oblong cells with a reniform shape and a smooth not sharp concavity (Figs. 4.203, 4.204). Binucleated cells are relatively numerous, and occasionally 2–3 cells in near proximity may be found that appear more eosinophilic and that have a definite U- or C-shaped nucleus. That slight change in tinctorial quality may indicate some regressive change in the cells, as is seen in the large atypical B-cells of T-cell rich large B-cell lymphoma in the cat. Occasionally, the horseshoe configuration may be made up of several oblong nuclei in ring formation. The chromatin pattern is coarsely granular or branched with accentuation of the nuclear membrane and marked parachromatin clearing. Nucleoli are multiple (1–3), prominent, and central, and they stand out against the peripheralized chromatin. There are usually 5–10 mitoses/400× field and occasional apoptotic bodies, but generally there are few or no tingible body macrophages (Fig. 4.205). The cytoplasm is always abundant and irregularly placed with only moderate amphophilia, it reacts strongly with CD3 (Fig. 4.206), and cell boundaries may be in close contact or with narrow separation but generally distinct.

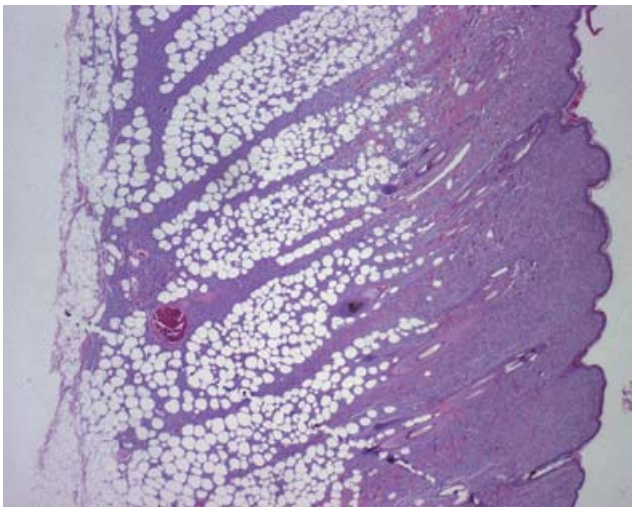

Figure 4.203. Dog: skin, cutaneous anaplastic large cell lymphoma of T-cell type. The lesion extends solidly from the dermal/epidermal junction through the dermis and irregularly invades the panniculus.

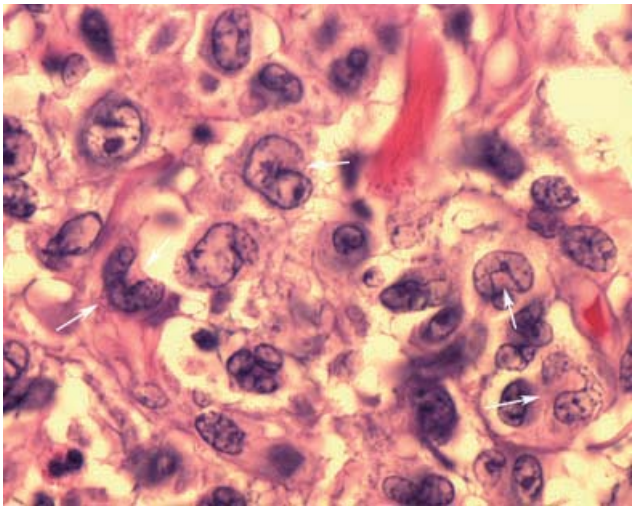

Figure 4.204. Dog: skin, anaplastic large cell lymphoma. Superficial dermis, containing multiple diagnostic cells with horseshoe-type nuclear configurations (arrows) typical of ALCL.

The variety of morphological variants described in humans are either not seen in animals or are not as yet identified and may be part of the peripheral T-cell lymphomas of "not otherwise specified" type. Treatment of primary cutaneous ALCL is usually effectively made by wide excision with only one or two lesions present.

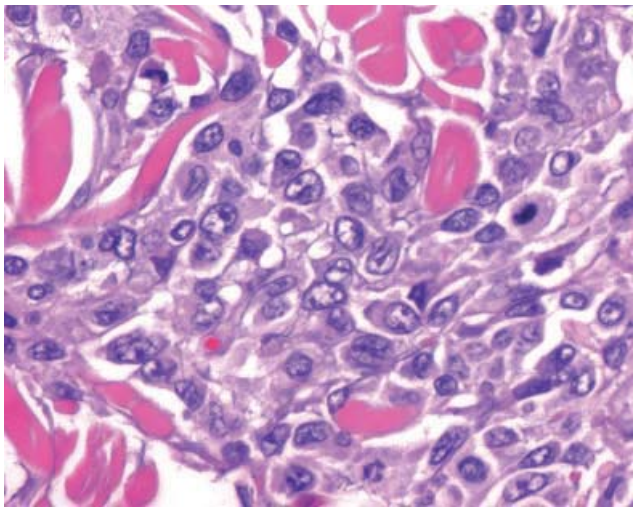

Figure 4.205. Dog: skin, anaplastic large cell lymphoma. The nuclei vary widely in size and can be seen to be as much as 4 times the diameter of the red cell in the lower left center. The chromatin pattern is coarse granular and branched with very marked parachromatin clearing that adds prominence to the generally central nucleoli. There is a cell in mitosis in the right center with cells undergoing apoptosis in the right center and upper left. The cytoplasm is relatively abundant, often eccentrically placed, and of irregular density with cell boundaries irregularly apparent.

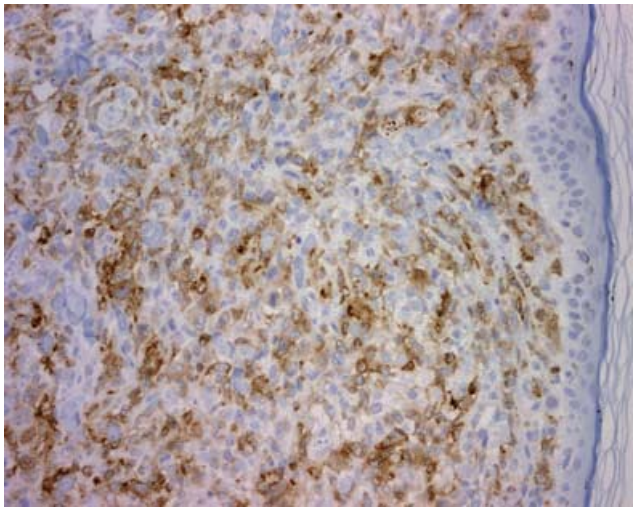

Figure 4.206. Dog: skin, anaplastic large cell lymphoma. Phenotype of Figure 4.203. With CD3 staining, the cells are strongly but irregularly labeled, with heavily marked cells immediately adjacent to others of similar appearance that are relatively unmarked. Some of the atypical cells were also marked with CD79.

Primary Systemic Anaplastic Large Cell Lymphoma of T-Cell Type

Primary systemic anaplastic large cell lymphoma of T-cell type is seen most often as a nodal presentation and may affect most other tissues, but skin appears to be the extranodal tissue most often involved. The disease is rare and has been seen in a large breed dog 1 year old that presented with generalized skin disease with dependent edema and peripheral lymphadenopathy and was severely ill. An involved node capsule is thin and taut, and the sinus is generally intact with little involvement of perinodal tissues (Figs. 4.207–4.209). If cutaneous disease is present and deep, there may be coalescence of nodal and

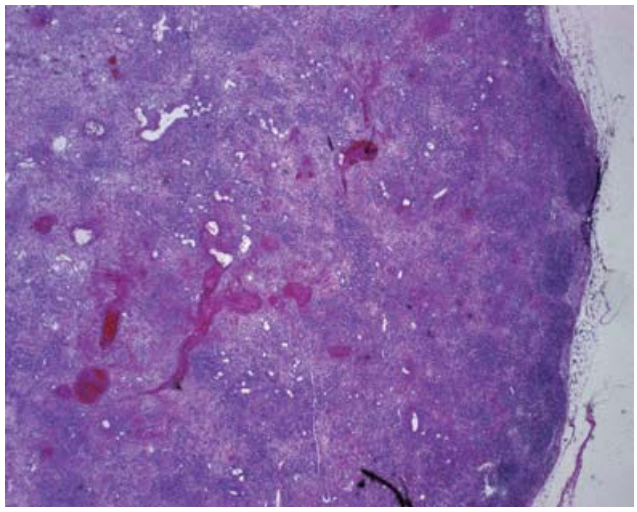

Figure 4.207. Dog: lymph node, systemic anaplastic large cell lymphoma of T-cell type. The node capsule is taut with the peripheral sinus compressed and a few fading germinal centers beneath the subcapsular sinus. The node is markedly and irregularly congested, with many of the larger vessels undergoing dilation and thrombosis.

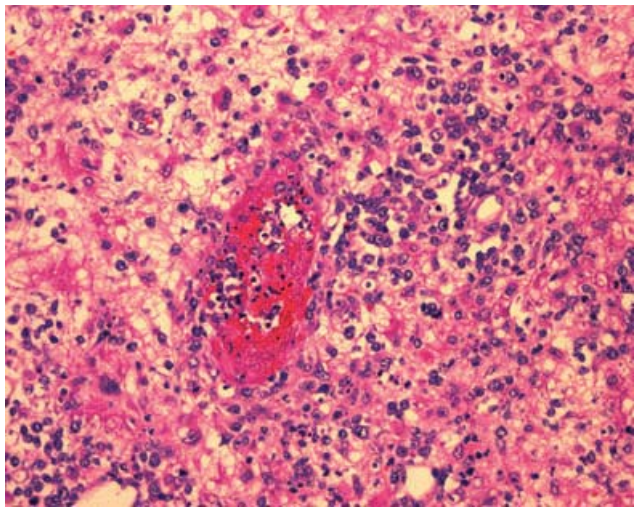

Figure 4.208. Dog: node, systemic anaplastic large cell lymphoma. Detail of Figure 4.207. The parenchyma of the node is characterized by patchy areas of necrosis with marked edema associated with vasculitis and thrombosis of both arterioles and veins.

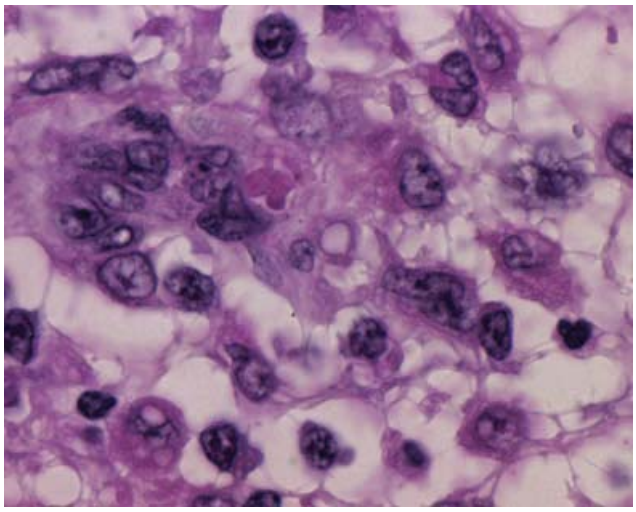

Figure 4.209. Dog: node, systemic anaplastic large cell lymphoma. Detail of Figure 4.207. There is marked variability in cell type with numerous binucleated cells that have coarsely branched chromatin with marked parachromatin clearing and prominent nucleoli. The cytoplasm is relatively abundant, with cell boundaries distorted by the surrounding edema.

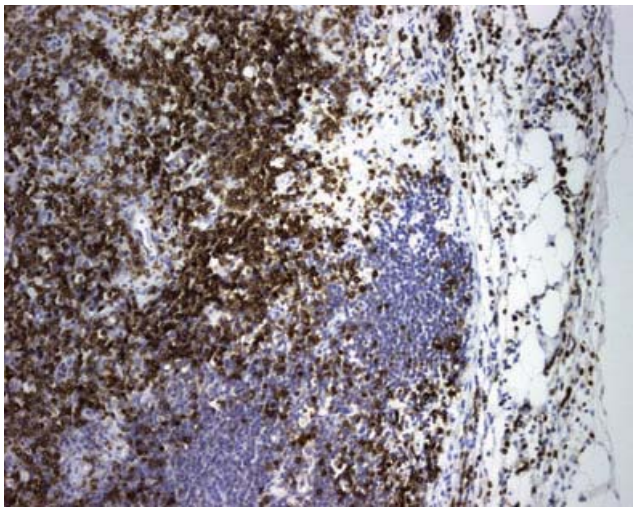

Figure 4.210. Dog: node. Phenotype of Figure 4.207. The node capsule is at the right. The fading area of germinal center at the right and right lower, are conspicuously unlabeled with CD3 staining; the surrounding neoplastic cells are strongly and uniformly marked.

cutaneous lesions. The cortical involvement is patchy with extensive areas of subcapsular homogenous neoplastic proliferation that extends irregularly throughout the interior of the node. There may be serpentine involvement of the medullary sinuses, with the large neoplastic cells standing out against the small benign lymphocytes of the medullary cords. The cells are as described for skin with large nuclei 3–4 red cells in longest dimension and with a recurring tendency for reniform shapes, but not with the nuclear folds or creases of the neoplastic Langerhans cells. The nuclei with reniform shape prompt surveillance for the typical horseshoe-shaped variants. The chromatin is usually peripheralized, which renders additional prominence to the large central nucleoli, though within the same tissue there may be areas with very finely dispersed chromatin that suggest fixation effects may be present. The cytoplasm is always abundant and tends to be lightly stained with cell boundaries generally distinct but is strongly positive with CD3 staining (Fig. 4.210). Vascular invasion is not a feature of the neoplasm, and foci of necrosis are generally not present, which assists distinction from histiocytic sarcoma. There is a very high mitotic rate with 20–25 mitoses/400× field; these are large, dark metaphases often in planar section with the radially arranged chromosomes standing out clearly against the surrounding lightly stained cytoplasm. There are equally numerous apoptotic bodies but very few tingible body macrophages. The morphology of the tumor in other tissues is a matter of speculation, either because the biopsy diagnosis results in termination or successful treatment. Similar changes are present in the human counterpart neoplasm (Figs. 4.211, 4.212).

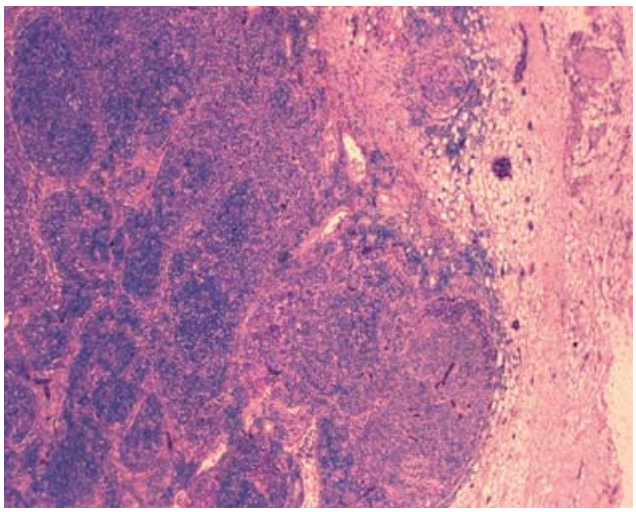

Figure 4.211. Human: lymph node, anaplastic large cell lymphoma. There is irregular invasion of the node capsule with destruction of the peripheral sinus and displacement of normal small lymphocytes that are more darkly stained by the proliferating cells in the outer cortex. *Slide from Cornell Tutorial.*

REFERENCES

Abdulkader, I., Cameselle-Teijeiro, J., Fraga, M., Rodriguez-Núnez, A., Allut, A.G., and Forteza, J. (1999) Primary anaplastic large cell lymphoma of the central nervous system. *Human Pathol* 30(8):978–981.

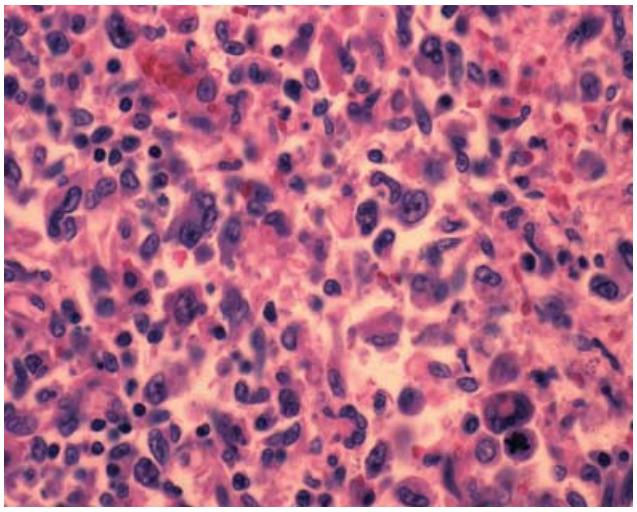

Figure 4.212. Human: lymph node, anaplastic large cell lymphoma. Detail of Figure 4.211. There is very marked variation in cell size and nuclear shape, with numerous binucleated cells and a multinucleated cell in the lower right with multiple nuclei and a semicircular ring next to an atypical mitotic figure. There is a horseshoe-shaped nucleus in the upper-right center typical of hallmark-type cells.

Banks, P.M., Metter, J., and Allred, D.C. (1990) Anaplastic large cell (Ki-1) lymphoma with histiocytic phenotype simulating carcinoma. *Am J Clin Pathol* 94:445–452.

Bayle, C., Charpentier, A., Duchayne, E., Manel, A.M., Pages, M.P., Robert, A., Lamant, L., Dastugue, N., Bertrand, Y., Dijoud, F., Emile, J.F., Machover, D., Brugières, L., and Delsol, G. (1999) Leukaemic presentation of small cell variant anaplastic large cell lymphoma: Report of four cases. *Brit J Haematol* 104:680–688.

Bittner, C., Feller, A.C., Renauld, J.C., Lange, K., Pietrzik, R., Jenetzky, C., Briese, J., Gaiser, T., Müller, A., Wiedemann, G.J., Van Snick, J., and Merz, H. (2000) An animal model for anaplastic large cell lymphoma in the immunocompetent syngeneic C57Bl/6 mouse. *Lab Invest* 80(10):1523–1531.

Carey, M.J., Medeiros, L.J., Roepke, J.E., Kjeldsberg, C.R., and Elenitoba-Johnson, K.S.J. (1999) Primary anaplastic large cell lymphoma of the small intestine. *Am J Clin Pathol* 112:695–701.

Chan, J.K.C., Buchanan, R., and Fletcher, C.D.M. (1990) Sarcomatoid variant of anaplastic large-cell Ki-1 lymphoma. *Am J Surg Pathol* 14(10):983–988.

Chikatsu, N., Kojima, H., Suzukawa, K., Shinagawa, A., Nagasawa, T., Ozawa, H., Yamashita, Y., and Mori, N. (2003) ALK^+, $CD30^-$, $CD20^-$ large B-cell lymphoma containing anaplastic lymphoma kinase (*ALK*) fused to clathrin heavy chain gene (*CLTC*). *Mod Pathol* 16(8):828–832.

Cross, P.A., Eyden, B.P., and Harris, M. (1989) Signet ring cell lymphoma of T cell type. *J Clin Pathol* 42:239–245.

De Bruin, P.C., Beljaards, R.C., Van Heerde, P., Van Der Valk, P., Noorduyn, L.A., Van Krieken, J.H.J.M., Kluin-Nelemans, J.C., Willemze, R., and Meijer, C.J.L.M. (1993) Differences in clinical behaviour and immunophenotype between primary cutaneous and primary nodal anaplastic large cell lymphoma of T-cell or null cell phenotype. *Histopathol* 23:127–135.

Felgar, R.E., Salhany, K.E., Macon, W.R., Pietra, G.G., and Kinney, M.C. (1999) The expression of TIA-1^+ cytolytic-type granules and other cytolytic lymphocyte-associated markers in $CD30^+$ anaplastic large cell lymphomas (ALCL): Correlation with morphology, immunophenotype, ultrastructure, and clinical features. *Human Pathol* 30(2):228–236.

Gisselbrecht, C., and Falini, B. (2004) Anaplastic large-cell lymphoma. In Mauch, P.M., Armitage, J.O., Coiffier, B.C., Dalla-Favera, R., and Harris, N.L. (eds.), *Non-Hodgkin's Lymphomas*. Lippincott Williams & Wilkins, Philadelphia, pp. 389–403.

Harris, N.L., Jaffe, E.S., Stein, H., Banks, P.M., Chan, J.K.C., Cleary, M.L., Delsol, G., De Wolf-Peeters, C., Falini, B., Gatter, K.C., Grogan, T.M., Isaacson, P.G., Knowles, D.M., Mason, D.Y., Muller-Hermelink, H.K., Pileri, S.A., Piris, M.A., Ralfkiaer, E., and Warnke, R.A. (1994) A revised European-American classification of lymphoid neoplasms: A proposal from the International Lymphoma Study Group. *Blood* 84(5):1361–1392.

Kinney, M.C., and Kadin, M.E. (1999) The pathologic and clinical spectrum of anaplastic large cell lymphoma and correlation with *ALK* gene dysregulation. *Am J Clin Pathol* 111(Suppl.1):S56–S67.

Krenacs, L., Wellmann, A., Sorbara, L., Himmelmann, A.W., Bagdi, E., Jaffe, E.S., and Raffeld, M. (1997) Cytotoxic cell antigen expression in anaplastic large cell lymphomas of T- and null-cell type and Hodgkin's disease: Evidence for distinct cellular origin. *Blood* 89(3):980–989.

Nakamura, S., Shiota, M., Nakagawa, A., Yatabe, Y., Kojima, M., Motoori, T., Suzuki, R., Kagami, Y., Ogura, M., Morishima, Y., Mizoguchi, Y., Okamoto, M., Seto, M., Koshikawa, T., Mori, S., and Suchi, T. (1997) Anaplastic large cell lymphoma: A distinct molecular pathologic entity. A reappraisal with special reference to p80NPM/ALK expression. *Am J Surg Pathol* 21(12):1420–1432.

Penny, R.J., Blaustein, J.C., Longtine, J.A., and Pinkus, G.S. (1991) Ki-1-positive large cell lymphomas, a heterogenous group of neoplasms. Morphologic, immunophenotypic, genotypic and clinical features of 24 cases. *Cancer* 68(2):362–373.

Saffer, H., Wahed, A., Rassidakis, G.Z., and Medeiros, L.J. (2002) Clusterin expression in malignant lymphomas: A survey of 266 cases. *Mod Pathol* 15(11):1221–1226.

Sgrignoli, A., and Abati, A. (1997) Cytologic diagnosis of anaplastic large cell lymphoma. *Acta Cytologica* 41(4): 1048–1052.

Skinnider, B.F., Connors, J.M., Sutcliffe, S.B., and Gascoyne, R.D. (1999) Anaplastic large cell lymphoma: A clinicopathologic analysis. *Hematol Oncol* 17:137–148.

Tort, F., Pinyol, M., Pulford, K., Roncador, G., Hernandez, L., Nayach, I., Kluin-Nelemans, H.C., Kluin, P., Touriol, C., Delsol, G., Mason, D., and Campo, E. (2001) Molecular characterization of a new *ALK* translocation involving *Moesin* (*MSN-ALK*) in anaplastic large cell lymphoma. *Lab Invest* 81(3):419–426.

Villamor, N., Rozman, M., Esteve, J., Aymerich, M., Colomer, D., Aguilar, J.L., Montserrat, E., and Campo, E. (1999)

Anaplastic large-cell lymphoma with rapid evolution to leukemic phase. *Ann Hematol* 78:478–482.

Zinzani, P.L., Martelli, M., Magagnoli, M., Zaccaria, A., Ronconi, F., Cantonetti, M., Bocchia, M., Marra, R., Gobbi, M., Falini, B., Gherlinzoni, F., Moretti, L., De Renzo, A., Mazza, P., Pavone, E., Sabattini, E., Amendola, A., Bendandi, M., Pileri, S.A., Mandelli, F., and Tura, S. (1998) Anaplastic large cell lymphoma Hodgkin's-like: A randomized trial of ABVD versus MACOP-B with and without radiation therapy. *Blood* 92(3):790–794.

Lymphomatoid Papulosis

Lymphomatoid papulosis (LYP) in humans has a peak incidence in the 5th decade with a slight male predominance. LYP is largely absent from veterinary literature, but the similarities in the presenting signs and histological changes in the human disease and in animals plus the frequency of skin disease in domestic animals suggests that an animal counterpart exists. Human patients with LYP have an exaggerated reaction to insect bites, especially mosquitoes, and to a variety of other environmental antigens and have a high frequency of concurrent atopy. The disease, when reliably diagnosed as LYP, tends to persist in some degree throughout life regardless of treatment. In humans, despite the indolent course of the majority of cases the atypical cells of LYP have repeatedly been shown to be clonal. Although a minority of human cases evolve into a T-cell lymphoma, in some of these cases the cells of the LYP lesion and the subsequent lymphoma were shown to share the same clonal changes. The cell of origin for human LYP is an early lymphoid precursor and believed to be of Th2 cell type, and it is the progeny of these cells that express the CD30 antigen.

The constellation of signs and risk factors for human LYP are commonly mentioned in the causation for chronic skin disease in the dog. The histological changes present in canine dermatitis span those described for the human LYP syndrome. In humans, LYP is divided into three forms, with Type A most common, and resembles Hodgkin's lymphoma because of the frequency of large atypical cells with very large nucleoli. The aggressive appearance of the lesion coupled with a predominantly benign course with prolonged survival resulted in the early description of LYP as histologically malignant and clinically benign. These atypical cells have frequent mitoses and are accompanied by neutrophils and a mixture of other inflammatory cells. There is superficial perivascular exocytosis of the mixed cell population, and the endothelial cells have plump nuclei of a reactive host (Figs. 4.213, 4.214).

The type B lesion is more like mycosis fungoides (MF) with a thickened epidermis and focal, largely single cell infiltration of the epithelial layer without formation of microabscesses. A further similarity to MF is the convoluted outlines of nuclei in the infiltrating cells, but in distinction to MF the plaquelike lesions have a marked tendency to regress in most cases of LYP.

Type C of LYP resembles ALCL of large cell type cytologically, but architecturally the infiltrate tends to remain in the superficial dermis in LYP in contrast to invasion of the panniculus in ALCL. All of these combinations are seen in the dog, but in the absence of a CD30 reagent and tissue target there is no specificity in the same type of lesions in animal dermatopathology.

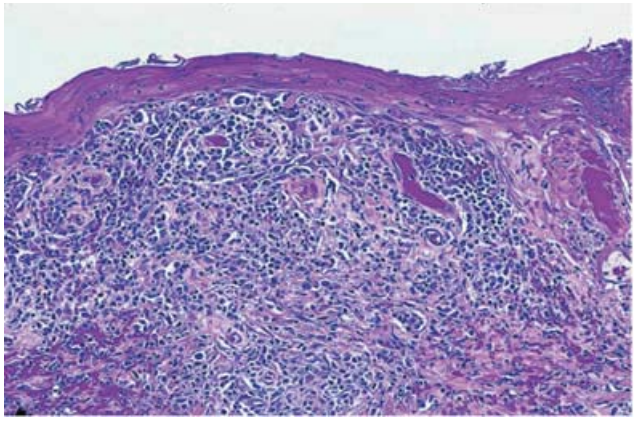

Figure 4.213. Human: skin, lymphomatoid papulosis. There is epidermal thinning with a heavy interface infiltration of mononuclear cells. *Reprinted from* Surgical Pathology, *9th Edition, Volume 1, Juan Rosai, 2004, Chapter 4, "Skin," Figure 181, Page 199, with permission from Elsevier*.

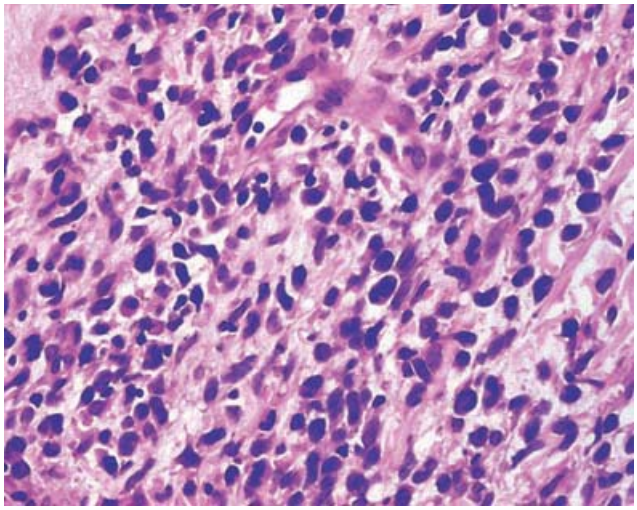

Figure 4.214. Human: skin, lymphomatoid papulosis. Detail of Figure 4.213. There is dense infiltration of variably shaped lymphocytes surrounding the superficial dermal vessels. *Reprinted from* Surgical Pathology, *9th Edition, Volume 1, Juan Rosai, 2004, Chapter 4, "Skin," Figure 182, Page 199, with permission from Elsevier.*

REFERENCES

Demierre, M.F., Goldberg, L.J., Kadin, M.E., and Koh, H.K. (1997) Is it lymphoma or lymphomatoid papulosis? *J Am Acad Dermatol* 36(5):765–772.

Kadin, M.E., Liu, H.L., Kim, Y.H., and Hoppe, R.T. (2004) $CD30^+$ cutaneous lymphoproliferative disease (anaplastic large-cell lymphoma and lymphomatoid papulosis. In Mauch, P.M., Armitage, J.O., Coiffier, B.C., Dalla-Favera, R., and Harris, N.L. (eds.), *Non-Hodgkin's Lymphomas*. Lippincott Williams & Wilkins, Philadelphia, pp. 333–343.

Karp, D.L., and Horn, T.D. (1994) Lymphomatoid papulosis. *J Am Acad Dermatol* 30:379–395.

MacAulay, W.L. (1968) Lymphomatoid papulosis: A continuing self-healing eruption, clinically benign–histologically malignant. *Arch Dermatol* 97:23–30.

Willemze, R., Kerl, H., Sterry, W., Berti, E., Cerroni, L., Chimenti, S., Diaz-Peréz, J.L., Geerts, M.L., Goos, M., Knobler, R., Ralfkiaer, E., Santucci, M., Smith, N., Wechsler, J., van Vloten, W.A., and Meijer, C.J.L.M. (1997) EORTC classification for primary cutaneous lymphomas: A proposal from the Cutaneous Lymphoma Study Group of the European Organization for Research and Treatment of Cancer. *Blood* 90(1):354–371.

Zirbel, G.M., Gellis, S.E., Kadin, M.E., and Esterly, N.B. (1995) Lymphomatoid papulosis in children. *J Am Acad Dermatol* 33:741–748.

Adult T-Cell Lymphoma/Leukemia

The human form of this disease has an endemic viral association occurring in the South Island of Japan and in the Caribbean basin. The oncogenic retrovirus of the adult T-cell leukemia/lymphoma is the human T-cell leukemia virus HTLV-I. In Japan, the seroprevalence varies from 0.2% in low endemic areas to 13% in highly infected areas and with a conversion to neoplastic disease of about 1.5/1000 infected males over 40 years and 0.5/1000 infected females. There are remarkable similarities in many aspects of this disease in humans and those neoplastic diseases caused by the oncogenic retroviruses in cats by the feline leukemia virus (FeLV) and in cattle by the bovine leukemia virus (BLV). All three viruses are exogenous retroviruses, but recently the cat has been shown to be carrying endogenous retrovirus that is passed in germline cells to offspring and is homologous to the exogenous virus but have large deletions that render them noninfectious. Exogenous FeLV infects T-cells and causes T-cell leukemia/lymphoma but is also capable of causing myeloid leukemia and a putative disease like Hodgkin's lymphoma with Reed-Sternberg–like cells that are BLA36 positive and therefore likely derived from B-lymphocytes. The HTLV-I virus is carried in T-cells and produces leukemia/lymphoma of T-cell phenotype. The BLV invades B-lymphocytes and is integrated into the DNA of B-lymphocytes of BLV-associated lymphomas, although, rarely, adult types of BLV-associated lymphoma have been negative for both B- and T-cell markers. In addition, BLV has been found as provirus in neoplastic lymphocytes from a case of sporadic lymphoma of thymic type that was also seropositive for BLV. Exogenous retrovirus of lentiviral subtype occur in sheep, goats, and horses and cause chronic inflammatory diseases not associated with immune depression, as occurs in the lentiviral infections of macaques (SIV) and humans (HIV).

In Japan, the prevalence of HTLV-I infection is dropping with education and the knowledge that the virus is spread in breast milk, with the risk of infection in children from seropositive mothers ranging from 10–30%. This finding was made many years ago in defining the vertical spread of BLV in cattle. Some major differences exist. Both HTLV-I and BLV are highly cell-associated, and viremia is ephemeral or does not occur. In contrast, in cats there may be high viremia with virus shed in saliva but with short survival of the virus in the environment. In both humans and cattle, the virus may be spread in sexual contact generally from male to female, with provirus in lymphocytes present in semen. In all three species, the virus can be spread by blood transfusions and by reuse of needles, as occurs in intravenous drug users and in vaccinations, especially in cattle. In cattle, all forms of minor injury, such as dehorning, ear tagging, and exposed barbwire, as well as habits of cows to sniff and lick genitalia as well as fresh placenta, can result in transmission of virus. In cats, grooming and fighting (spitting) can result in direct contact with virus in saliva. Much has been learned in cattle, where the virus is easily spread by natural breeding, but infected bulls do not transmit the virus in frozen semen. It is likely that in closely related cattle the virus is more easily spread because there is less likelihood of an infecting lymphocyte being destroyed by the histocompatability system before dividing and generating new provirus. In cattle, the spread of virus can easily be prevented between groups of cattle by separate pastures and milking the infected animals last.

In all three species, there is along latency period that is likely shortest in the cat in terms of total potential life span. In HLV-I infected individuals, about 5% of all carriers will develop adult T-cell leukemia/lymphoma. In cattle, the conversion rate to neoplastic disease is likely in the range of 1%, though it is usually quoted as high as 5% in reports aimed at prevention or economic impact. The BLV is much more prevalent in dairy cattle than in beef breeds, and dairy cattle in current production conditions seldom live to the 7–8-year peak period of lymphoma occurrence. As a consequence, the incidence of the enzootic form of bovine lymphoma is less common today. Lymphoma is not the only cost of infection, and it is expected that cattle infected with BLV will have a higher

culling rate for a variety of causes, including mastitis, infertility, and lameness. Infection of cattle with BLV is followed by a very predictable sequence of events, including seroconversion, lifelong infection, and benign B-cell lymphocytosis (persistent lymphocytic leukocytosis PLL). Only a small proportion of cases develop lymphoma, which suggests another agent, such as bovine herpesvirus, may perform a triggering effect. In contrast, in cats infection may be followed by a variety of outcomes, including persistent viremia as occurs in about 30% of cases, self-limiting infection in 60%, transient viremia in 30–40%, and an atypical unstable interaction with sequestered infection in 5–10%. Lymphoma may develop in the first year of life or after 20 or more years. It has been felt that there was an age-related incidence of certain topographical types of lymphoma, with the thymic type occurring in young cats under 3 years and multicentric in older cats, but in a study of over 600 cases of feline lymphoma the thymic form developed as often in older cats.

The types of host/viral interaction in humans is very variable—more like that in the cat—with acute, chronic, and smoldering forms of neoplastic induction. In the smoldering type of presentation, which is felt to be an early manifestation, there is focal involvement of nodes with paracortical expansion of intermediate-sized cells with little cytoplasm and interspersed Reed-Sternberg–like cells and giant cells with lobated nuclei that are positive for Epstein-Barr virus and express CD30 and CD15. The atypical EBV expression is felt to be a result of immunosuppression by the HTLV-I, and these patients usually progress to frank leukemia/lymphoma within months. In the chronic form of presentation there is moderate to a quite marked level of lymphoid leukemia but few other signs of disease. Lymph node involvement is usually present, and there may be skin disease with epidermotropism and even Pautrier's-like microabscess formation.

The acute form of the disease is characterized by hypercalcemia and often hyperbilirubinemia with very high levels of leukemia and with lymphadenopathy and hepatosplenomegaly. The cells in blood may be markedly polylobated and are referred to as *flower cells*. The leukemic cells are $CD4^+$, $CD3^+$, $CD7^-$, and strongly $CD25^+$.

Similarities are present in the mode of viral integration, which is random in all three species with the virus capable of *transactivation* from any site of integration. As a result of the random mode integration, a promoter insertion mechanism of *cis* activation oncogenesis has long been denied in favor of transactivation, with the Tax factor considered the initiating agent. There are more often multiple integration sites in a single cell with some being defective or with mutated regions for the Tax transacting viral factor. Tax in the HTLV-I infected cells is a primarily nuclear 40-kDa phosphoprotein, which causes potent activation of viral transcription mediated through three 21-bp repeats that each contain a cyclic AMP response element core flanked by 5′ G-rich and 3′ C-rich sequences. These cAMP response elements are bound by the host cellular basic domain-leucine zipper protein (CREB) and activating transcription factor-1- that sequentially recruit Tax into stable ternary complexes. Tax recruits the coactivators, a CREB binding protein, p300, and a CPB-associated factor that results in potent transcriptional activation. Tax also impacts cellular genes by transcriptional regulation via the enhancer binding proteins like CREB, nuclear factor (NF)-*k*B, serum response factor, and by tethering coactivators to the DNA-bound transcription factors. Other cellular genes that are targets of Tax include those with growth-promoting activities such as IL-6 and lymphokine receptors such as IL-2, receptor alpha, and c-fos. Other genes targeted include those with growth retardation, including transrepression of p181NK4c and LcK. The net result being that Tax effectively promotes cell proliferation and proviral transcription of viral-infected lymphocytes. It appears that the process of transactivation is similar in other host species, with the BLV Tax acting via an enhancer in the long terminal repeat (LTR) region that contains the same three 21-bp repeats that in turn engage the bovine CREB2 protein.

The bovine virus given to lambs by injection of bovine lymphocytes bearing provirus causes multicentric lymphoma in a high proportion of animals. Transmission between sheep appears to be controlled by histocompatibility genes, with easy transmission between related animals and less-efficient replication of donor lymphocytes with production of virus in more distantly related animals. The susceptibility of cattle to infection with BLV seems to follow a similar pattern, with the observation that the introduction of the virus into a herd with little inbreeding results in very slow spread and a low stable level of infected animals. In contrast, as often occurs in high-producing dairy herds with many animals being the progeny of a single valued sire, the rate of infection is higher, presumably again related to the ease of transmitting live lymphocytes from animal to animal. Specific loci in cattle have been identified that are associated with susceptibility and resistance to infection with BLV.

The pathology of neoplasms caused by HTLV-I, FeLV, and BLV also have remarkable similarities. In the human neoplasms of adult T-cell leukemia/lymphoma, there is predominant involvement of nodes, marrow, and skin; there is also involvement of spleen and liver, GI tract, central nervous system (CNS), and often lung. All of these are found in the lymphoproliferative diseases of the cat and cow, with the lung likely the least affected organ, but with relatively frequent involvement of the eye and spinal

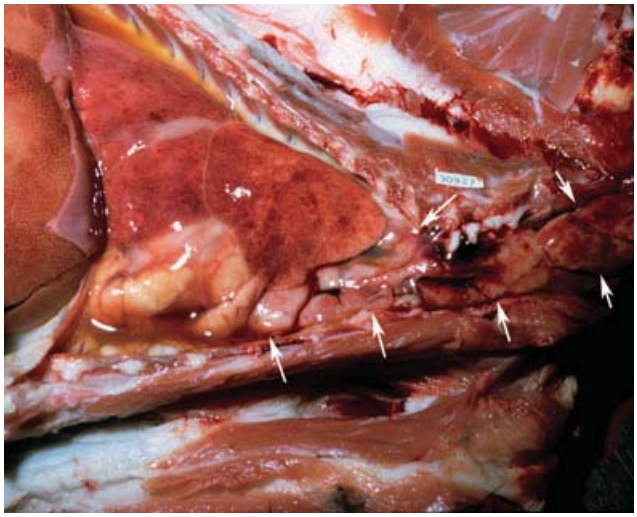

Figure 4.215. Cat: thymic lymphoma. A large mass (arrows) occupies the anterior mediastinum extending from the base of the heart through the entrance to the thoracic cavity and extending up the neck. This is an early lesion, with advanced cases causing displacement of the heart and much greater compression of the lung.

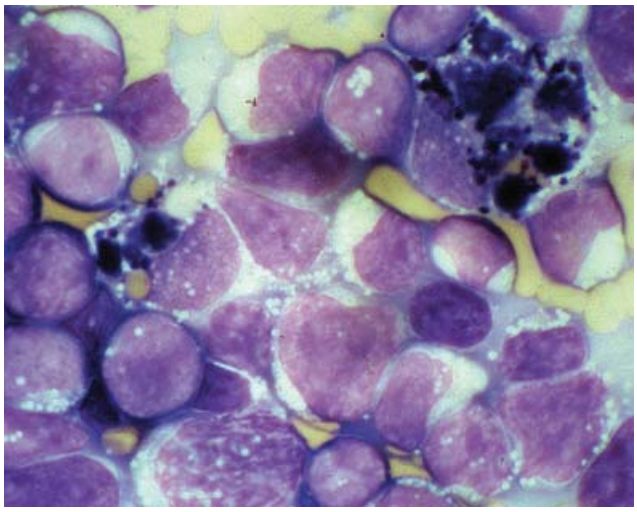

Figure 4.216. Cat: pleural fluid, thymic lymphoma. Two macrophages are present with deeply stained phagocytic debris. The lymphocytes are large and with variable diameter, with chromatin largely dispersed and relatively abundant cytoplasm. The fine cytoplasmic vacuolation is likely due to sojourn in the fluid cavity rather than an indication of lipid formation.

cord and even brain, bone, and skeletal muscle. There are recurring topographical presentations characteristic of each species, with the cat having thymic lymphoma (Figs. 4.215, 4.216) less frequently since the advent of anti-FeLV vaccination plus lymphadenopathy, hepatosplenomegaly (Fig. 4.217), and gastrointestinal involvement, with occa-

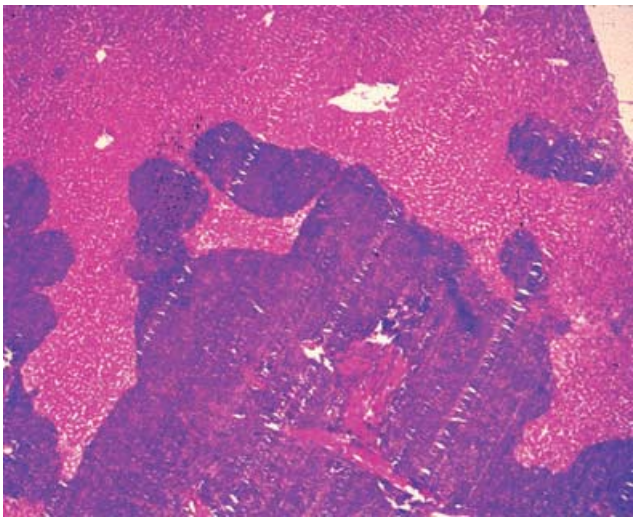

Figure 4.217. Cat: liver, lymphoma. There is an unusual pattern of hepatic involvement, with massive solid lobular infiltration rather than colonization of vessels throughout the liver.

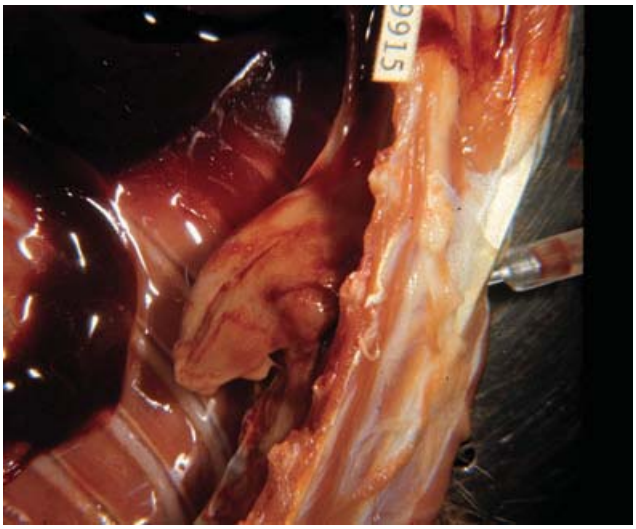

Figure 4.218. Cat: ventral spinal node in caudal thoracic area. The tumor invaded the spinal nerves and the spinal canal causing compression of the cord with the cat presenting with ataxia.

sional involvement of the spinal cord (Figs. 4.218, 4.219) and eye (Fig. 4.220) as well as presentation with frank leukemia. In the cow, the presentation is often of a single enlarged peripheral node (Fig. 4.221), but often retrobulbar (Fig. 4.222), cephalic, cervical, and sublumbar with invasion of the spinal cord (Figs. 4.223–4.225). The neoplasm may be primary in the heart (Figs. 4.226, 4.227), enteric tract (Figs. 4.228, 4.229), and even in the urogenital systems (Fig. 4.230). The gastric wall is frequently involved in cattle and the presentation is of an anemic animal with melena. In addition, cattle with advanced

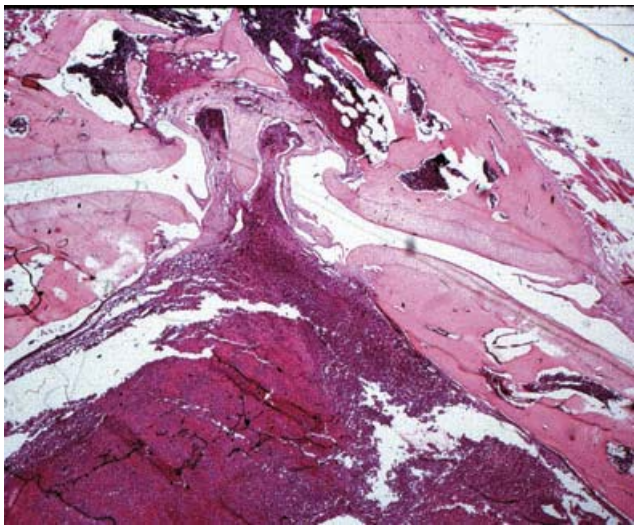

Figure 4.219. Cat: spinal column, lymphoma. Histology of Figure 4.218. Cross section of spinal column with lymphoma entering the subdural space and forming a large mass compressing the spinal cord located to the right of the tumor mass.

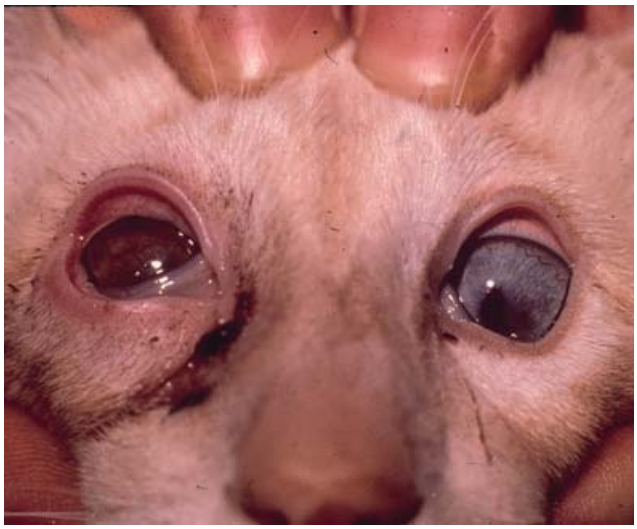

Figure 4.220. Cat: ocular lymphoma. The cat was presented with epiphora and on examination, corneal clouding with chemosis of conjunctiva was found with lymphoma diagnosed on fine needle aspirate of the anterior chamber.

Figure 4.221. Mature cow: prescapular node, lymphoma. Typical presentation of the adult type of enzootic bovine lymphoma with a single enlarged peripheral lymph node. The cow has a glossy hair coat and has likely presented with a modest reduction in milk production.

Figure 4.222. Cow: retrobulbar lymphoma. There is bilateral epiphora and proptosis due to invasion and paralysis of the extrinsic oculi muscles as well as to space-occupying effects of the neoplasm in the retrobulbar region.

lymphoma almost always have involvement of the spleen and liver with the presentation rarely primary in these sites and clinical disease onset because of rupture of the organ capsule with abdominal hemorrhage. Adult cattle and bulls are occasionally diagnosed by inadvertent blood sampling for other purposes, and like the human adult T-cell leukemia they have a total leukocyte count in the range of 100×10^3/ul and are asymptomatic but with incipient marrow failure.

Cytologically, most of the bovine lymphomas are of the large cell type (Figs. 4.231–4.233) constituting 66% of a large review. About 20% are of intermediate cell size that includes high-grade types like lymphoblastic and Burkitt's-like, and 10% are of small cell lymphoma (Figs. 4.234–4.236). The flower or floral type of multilobated nucleus as seen in the adult T-cell leukemia/lymphoma in blood is seen in the blood of cattle with BLV-associated

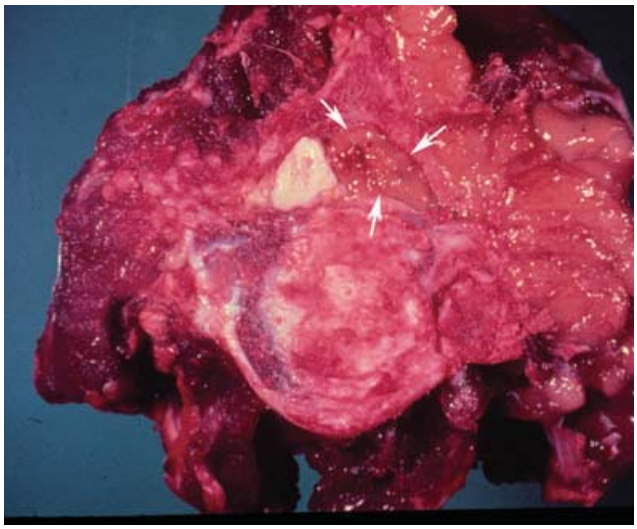

Figure 4.223. Cow: cross section of spinal column, lymphoma. The spinal body is below with the spinal cord, the white triangular structure that is compressed to the side of the spinal canal by infiltration of lymphoma outlined by arrows. There is also neoplastic tissue above and to the right of the mass in the spinal canal.

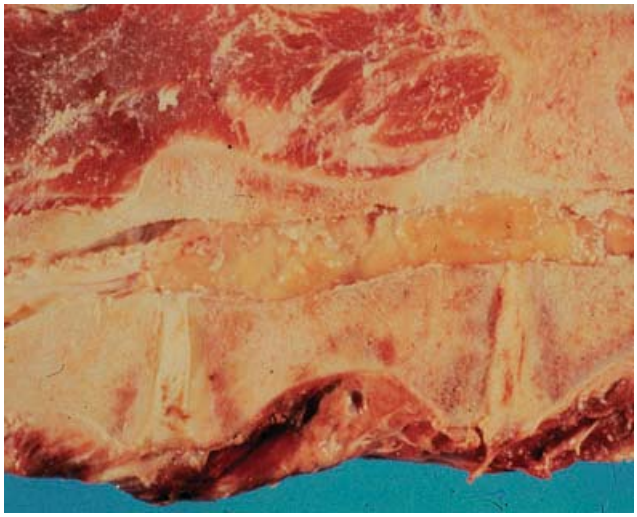

Figure 4.224. Cow: spinal canal, longitudinal section, lymphoma. The spinal cord appears white at the bottom and is obscured through the center of the image by a yellowish infiltration of solid lymphoma. Infiltrates may appear like normal fatty tissue requiring an imprint to identify the tissue as neoplastic.

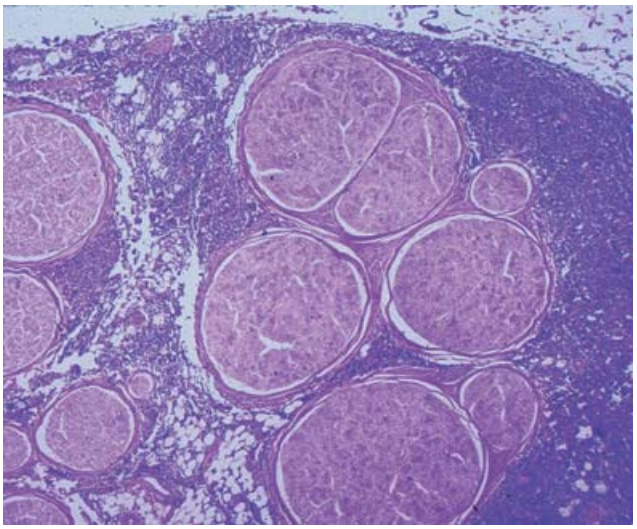

Figure 4.225. Mature bull: sciatic nerve, lymphoma. The animal was owned by an artificial breeding unit and was in excellent condition with an examination requested because of mild unilateral hindlimb lameness. A routine blood sample was taken and the animal was found to be quite markedly leukemic, with the animal rapidly progressing to recumbency. This section is of the sciatic nerve with extensive lymphomatous infiltration.

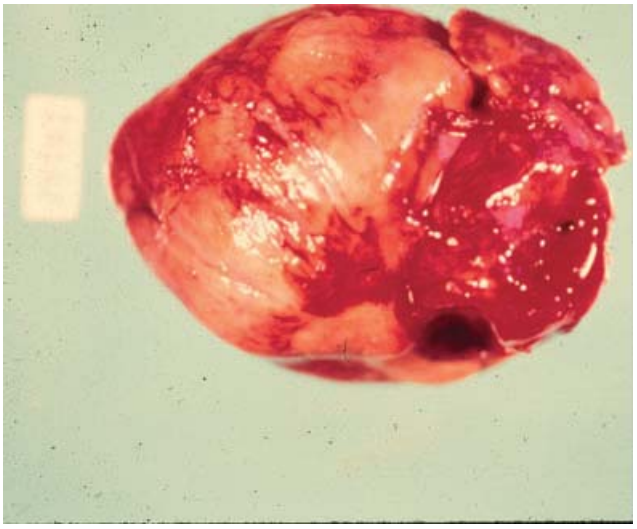

Figure 4.226. Bovine: heart, lymphoma. The pale areas on the surface of the heart extend past the fat normally at the base of the heart and can be seen to be infiltrating the muscle fibers down the length of the ventricle.

leukemia. In the cat, of 602 cases, most (54%) of the lymphomas are of large cell type (Fig. 4.237), with 18% of intermediate type, 17% of small cell type including lymphoma and leukemia (Figs. 4.238, 4.239), and 8% of mixed small and large cell types (Fig. 4.240), which includes the T-cell rich large B-cell lymphoma, with just under 4% of acute leukemia.

Collectively, this group represents one of the largest and most frequently encountered types of lymphomas seen in cats and cattle. As more is learned of viral oncogenesis in the dog, it is likely that other disease entities besides Mycosis Fungoides will be added to this comparison of retroviral-induced lymphoma in animals.

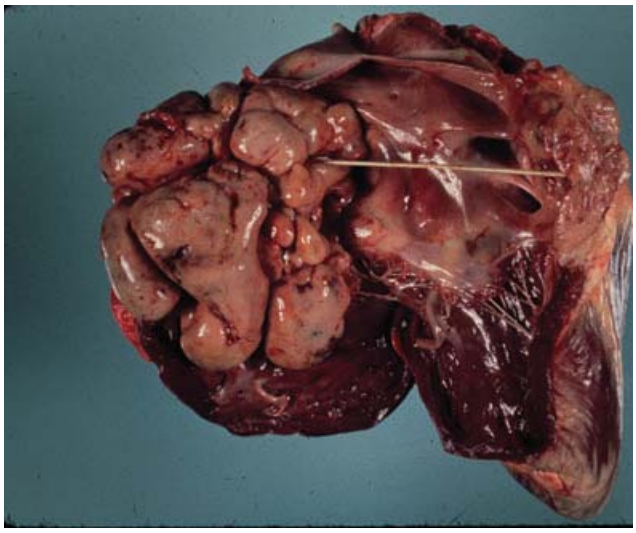

Figure 4.227. Bovine: heart, lymphoma. The tumor typically begins in the right atrium and may involve all of the heart. Multiple protruding masses are arising from the right ventricular free wall, greatly reducing ventricular capacity, and extend across the atrioventricular valve.

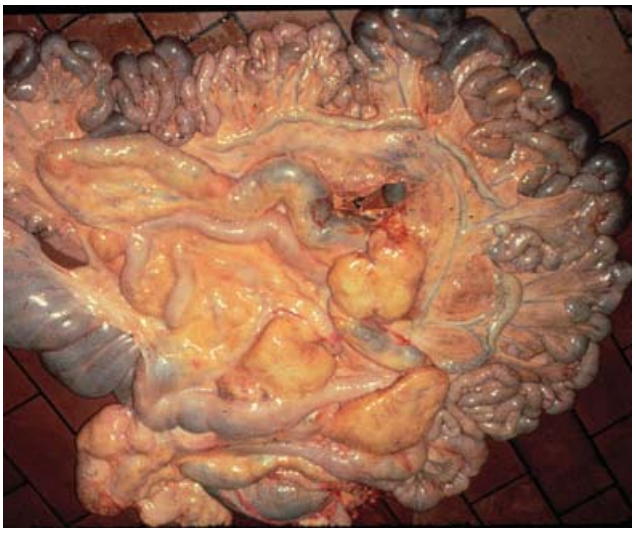

Figure 4.229. Cow: small intestinal tract, lymphoma, with massive enlargement of mesenteric nodes. The initial involvement is usually with the abomasal wall, with a nodal involvement in the abdominal cavity that may cause intestinal obstruction due to space-occupying effects but not usually with tumor involvement of the intestinal wall.

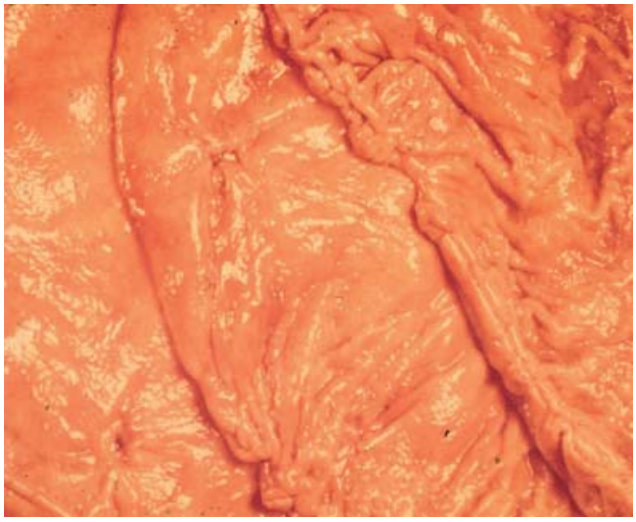

Figure 4.228. Cow: abomasum, lymphoma. The abomasal folds have multiple areas of plication surrounding areas of focal ulceration due to heavy laminar infiltration with lymphoma.

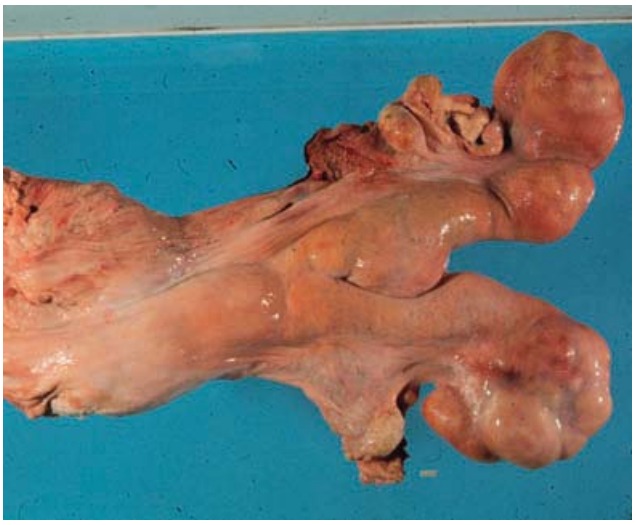

Figure 4.230. Cow: uterus, lymphoma. There is extension from the corpus to both ovaries and the uterine horns. The lesion may be primarily in the body of the uterus, creating a mass large enough to mimic pregnancy on rectal examination.

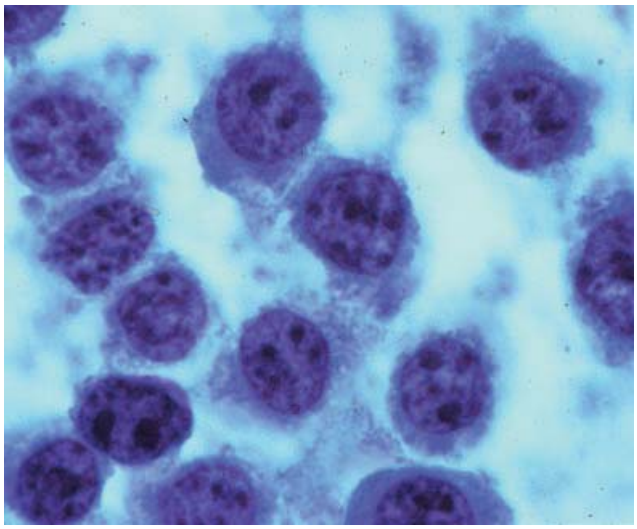

Figure 4.231. Cow: node imprint, lymphoma. With wet fixation and Papanicolaou stain, the chromatin pattern mimics that seen in histology with a coarse chromatin pattern and multiple prominent nucleoli. The cytoplasm is moderate in volume and staining density with the nuclei generally exceeding 2 red cells in diameter.

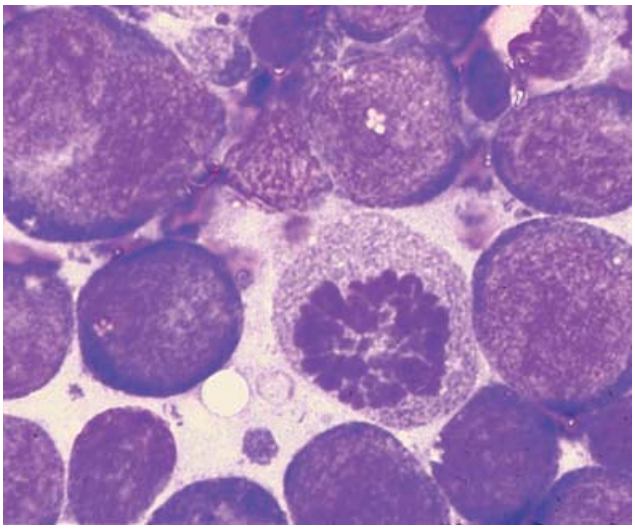

Figure 4.233. Cow: lymph node imprint, lymphoma. With Wright's staining, the nuclei appear larger and 3–4 red cells in diameter. There are a number of red cells between the lymphocytes that are somewhat crenated. The chromatin pattern is largely cribriform, and the number and positioning of the nucleoli is less apparent than with wet-fixed cytologic preparations or histology. The cells in Figures 4.231–4.233 are representative of bovine large cell lymphoma.

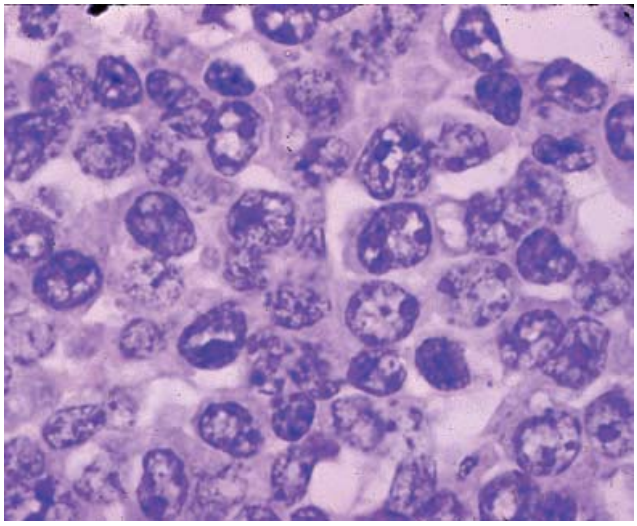

Figure 4.232. Cow: lymph node, lymphoma. With H&E staining on a lymphoma of similar type to that in Figure 4.231, there is a branched chromatin pattern, with the nucleoli frequently impinging on the nuclear membrane mimicking centroblastic cells of benign type. The cytoplasm is relatively abundant but lightly stained and cell boundaries are irregularly distinct.

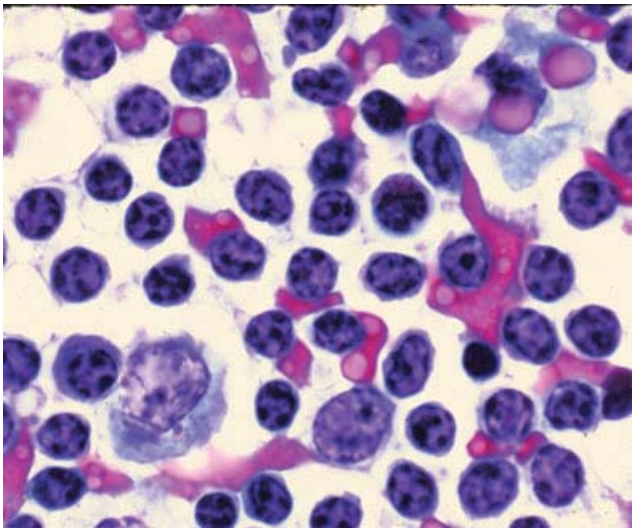

Figure 4.234. Cow: lymph node imprint, small cell lymphocytic lymphoma. On wet fixation and staining with the Papanicolaou method, the nuclei that appear dense with little internal nuclear detail have large chromocenters with partial parachromatin clearing and small nucleoli. The cytoplasm appears minimal by this technique, and the nuclei can be seen to be only slightly larger than red cells with fresh cells wet-fixed.

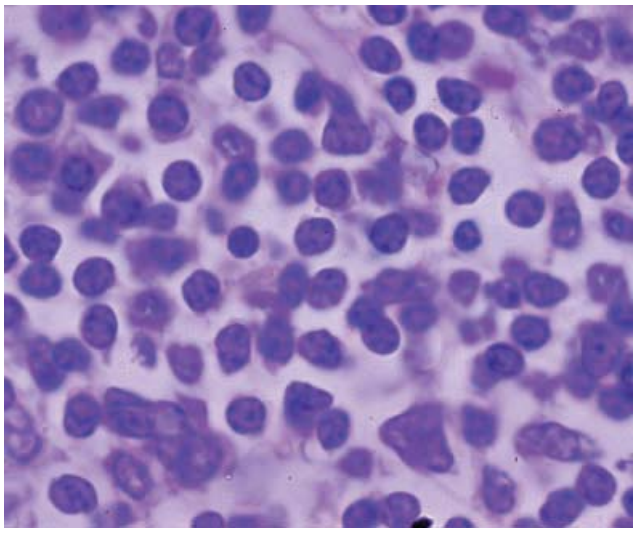

Figure 4.235. Cow: lymph node histology, same case as Figure 4.234. With tissue processing and hematoxylin and eosin staining, the cells at the same magnification appear small with relatively round irregular nuclei with similar chromatin patterns but less internal nuclear detail and little apparent cytoplasm.

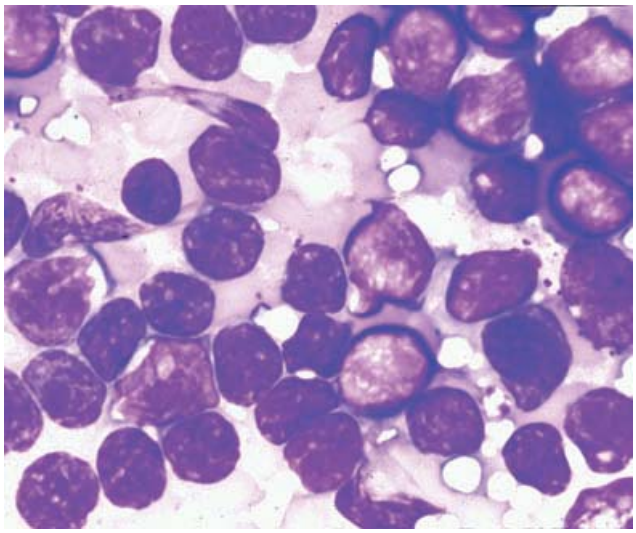

Figure 4.236. Cow: lymph node imprint, same case as Figure 4.234. With Wright's stain, the cells are flattened and appear larger but are about the same proportion in size and comparison to red cells. The chromatin pattern is apparent, with large chromocenters and small areas of parachromatin clearing with multiple small nucleoli. The cytoplasm is minimal on these smaller cells and more abundant on the larger cells with finer chromatin patterns that are likely the dividing cell population.

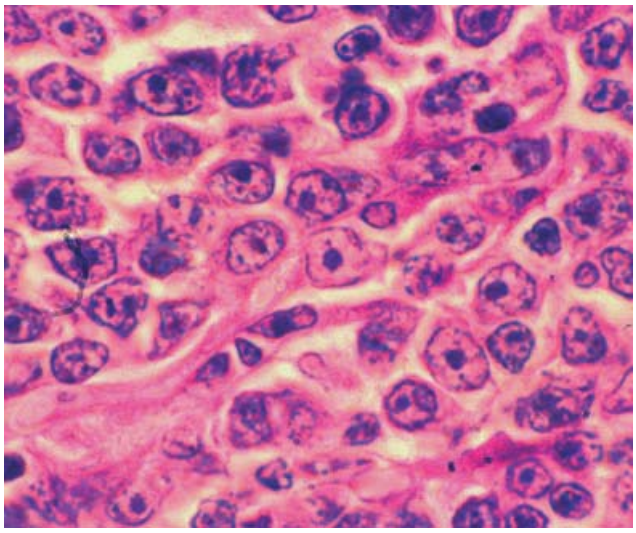

Figure 4.237. Cat: liver, large cell lymphoma. The nuclei are 2–3 red cells in diameter with peripheralized chromatin and moderate parachromatin clearing with a single prominent central nucleolus. The cytoplasm is moderate in volume and quite deeply stained with cell boundaries generally distinct.

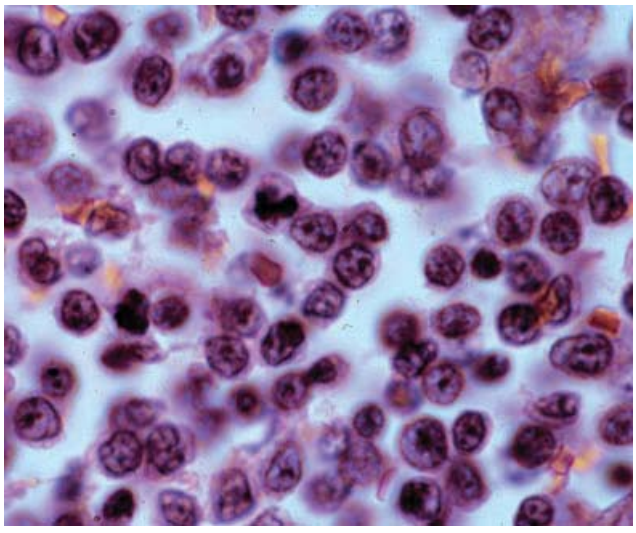

Figure 4.238. Cat: lymph node, lymphoblastic lymphoma. The cells are small but with vesicular-appearing nuclei with parachromatin clearing (due to delayed fixation) and multiple small nucleoli. The cytoplasm is minimal and there is a high mitotic and apoptotic rate.

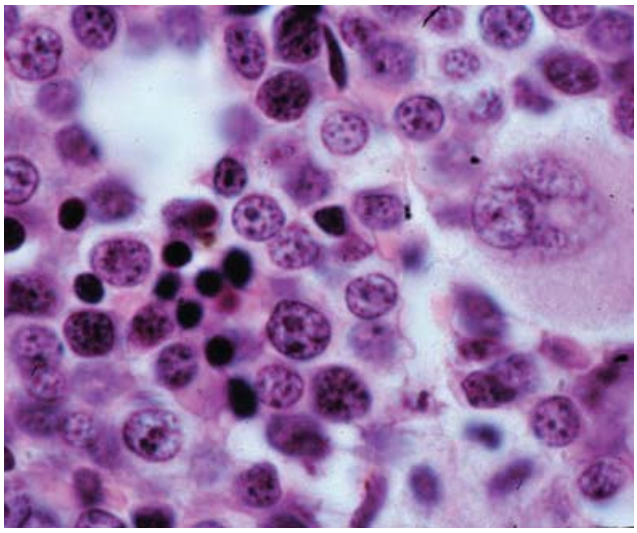

Figure 4.239. Cat: bone marrow, acute lymphoblastic leukemia. There is a megakaryocyte at the top with residual metarubricytes at the lower center. Most of the cells present are the infiltrating lymphocytes that have round nuclei and 1–2 small nucleoli.

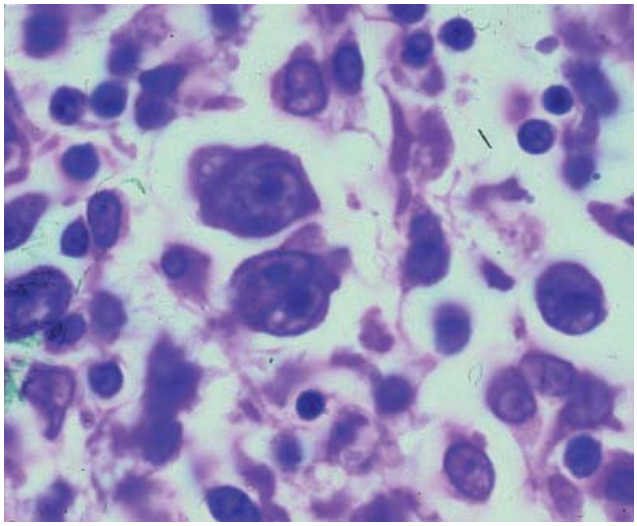

Figure 4.240. Cat: node, large cell lymphoma. The large binucleate cell with large nucleoli and peripheralized chromatin is typical of those that have been compared to Reed-Sternberg cells.

REFERENCES, HUMAN

Fujii, M., Sassone-Corsi, P., and Verma, I.M. (1998) C-fos promoter trans-activation by the Tax1 protein of human T-cell leukemia virus type I. *Pro Natl Acad Sci USA* 85:8526–8530.

Giebler, H.A., Loring, J.E., van Orden, K., et al. (1997) Anchoring of CREB binding protein to the human T-cell leukemia virus type 1 promoter: A molecular mechanism of Tax transactivation. *Mol Cell Biol* 17:5156–5164.

Inoue, J., Seiki, M., Taniguchi, T., et al. (1986) Induction of interleukin 2 receptor gene expression by p40x encoded by human T-cell leukemia virus type 1. *Embo J* 5:2883–2888.

Kwok, R.P., Laurance, M.E., Lundblad, J.R., et al. (1996) Control of cAMP-regulated enhancers by the viral transactivator Tax through CREB and the co-activator CBP. *Nature* 380:642–646.

Lemasson, I., Robert-Hebmann, V., Hamaia, S., et al. (1997) Transrepression of lck gene expression by human T-cell leukemia virus type 1-encoded p40tax. *J Virol* 71:1975–1983.

Mori, N., Shirakawa, F., Shimizu, H., et al. (1994) Transcriptional regulation of the human interleukin-6 gene promoter in human T-cell leukemia virus type I-infected T-cell lines: Evidence for the involvement of NF-kappa B. *Blood* 84:2904–2911.

Suzuki, T., Hirai, H., and Yoshida, M. (1994) Tax protein of HTLV-1 interacts with the Rel homology domain of NF-kappa B p65 and c-Rel proteins bound to the NF-kappa B binding site and activates transcription. *Oncogene* 9:3099–3105.

Suzuki, T., Narita, T., Uchida-Toita, M., et al. (1999) Down-regulation of the INK4 family of cyclin-dependent kinase inhibitors by Tax protein of HTLV-1 through two distinct mechanisms. *Virol* 259:384–391.

Tobinai, K., Watanabe, T., and Jaffe, E.S. (2004) Human T-cell leukemia virus type I–associated adult T-cell leukemia-lymphoma. In Mauch, P.M., Armitage, J.O., Coiffier, B.C., Dalla-Favera, R., and Harris, N.L. (eds.), *Non-Hodgkin's Lymphomas*. Lippincott Williams & Wilkins, Philadelphia, pp. 295–305.

Wagner, S., and Green, M.R. (1984) HTLV-I Tax protein stimulation of DNA binding of bZIP proteins by enhancing dimerization. *Science* 225:381–385.

Yoshida, M. (2001) Multiple viral strategies of HTLV-1 for dysregulation of cell growth control. *Ann Rev Immunol* 19:475–496.

Zhao, L.J., and Giam, C.Z. (1992) Human T-cell lymphotropic virus type I (HTLV-I) transcriptional activator, Tax, enhances CREB binding to HTLV-I 21-base-pair repeats by protein-protein interaction. *Proc Natl Acad Sci USA* 89:7070–7074.

REFERENCES, FELINE

Anderson, M.M., Lauring, A.S., Robertson, S., Dirks, C., and Overbaugh, J. (2001) Feline Pit2 functions as a receptor for subgroup B feline leukemia viruses. *J Virol* 75(22):10563–10572.

Fujino, Y., Satoh, H., Hisasue, M., Masuda, K., Ohno, K., and Tsujimoto, H. (2003) Detection of the integrated feline leukemia viruses in a cat lymphoid tumor cell line by fluorescence in situ hybridization. *J Hered* 94(3):251–255.

Hoover, E.A., and Mullins, J.I. (1991) Feline leukemia virus infection and diseases. *JAVMA* 199(10):1287–1297.

Richter, K.P. (2003) Feline gastrointestinal lymphoma. *Vet Clin Sm An* 33:1083–1098.

Roca, A.L., Pecon-Slattery, J., and O'Brien, S.J. (2004) Genomically intact endogenous feline leukemia viruses of recent origin. *J Virol* 78(8):4370–4375.

Rojko, J.L., and Kociba, G.J. (1991) Pathogenesis of infection by the feline leukemia virus. *JAVMA* 199(10):1305–1310.

Toth, S.R., Onions, D.E., and Jarrett, O. (1986) Histopathological and hematological findings in myeloid leukemia induced by a new feline leukemia virus isolate. *Vet Pathol* 23:462–470.

Troxel, M.T., Vite, C.H., Van Winkle, T.J., Newton, A.L., Tiches, D., Dayrell-Hart, B., Kapatkin, A.S., Shofer, F.S., and Steinberg, S.A. (2003) Feline intracranial neoplasia: Retrospective review of 160 cases (1985–2001). *J Vet Intern Med* 17:850–859.

Valli, V.E., Jacobs, R.M., Norris, A., Couto, C.G., Morrison, W.B., McCaw, D., Cotter, S., Ogilvie, G., and Moore, A. (2000) The histologic classification of 602 cases of feline lymphoproliferative disease using the National Cancer Institute Working Formulation. *J Vet Diagn Invest* 12:295–306.

Walton, R.M., and Hendrick, M.J. (2001) Feline Hodgkin's-like lymphoma: 20 cases (1992–1999). *Vet Pathol* 38:504–511.

REFERENCES, BOVINE AND OVINE

Adam, E., Kerkhofs, P., Mammerickx, M., Burny, A., Kettmann, R., and Willems, L. (1996) The CREB, ATF-1, and ATF-2 transcription factors from bovine leukemia virus-infected B lymphocytes activate viral expression. *J Virol* 70(3):1990–1999.

Altreuther, G., Llames, L., Neuenschwander, S., Langhans, W., and Werling, D. (2001) Morphologic and functional changes in bovine monocytes infected in vitro with the bovine leukaemia virus. *Scand J Immunol* 54:459–469.

Asahina, M., Kimura, K., Murakami, K., Ajito, T., Wu, D., Goryo, M., Aida, Y., Davis, W.C., and Okada, K. (1995) Phenotypic analysis of neoplastic cells from calf, thymic, and intermediate forms of bovine leukosis. *Vet Pathol* 32:683–691.

Duncan, R.B., Scarratt, W.K., and Buehring, G.C. (2005) Detection of bovine leukemia virus by in situ polymerase chain reaction in tissues from a heifer diagnosed with sporadic thymic lymphosarcoma. *J Vet Diagn Invest* 17:190–194.

Gatot, J.S., Callebaut, I., Van Lint, C., Demonté, D., Kerkhofs, P., Portetelle, D., Burny, A., Willems, L., and Kettmann, R. (2002) Bovine leukemia virus SU protein interacts with zinc, and mutations within two interacting regions differently affect viral fusion and infectivity in vivo. *J Virol* 76(16):7956–7967.

Gorrell, M.D., Brandon, M.R., Sheffer, D., Adams, R.J., and Narayan, O. (1992) Ovine lentivirus is macrophagetropic and does not replicate productively in T lymphocytes. *J Virol* 66(5):2679–2688.

Heeney, J.L., and Valli, V.E.O. (1990) Transformed phenotype of enzootic bovine lymphoma reflects differentiation-linked leukemogenesis. *Lab Invest* 62(3):339–346.

Lewin, H.A. (1994) Host genetic mechanism of resistance and susceptibility to a bovine retroviral infection. *An Biotechnol* 5(2):183–191.

Nagaoka, Y., Kabeya, H., Onuma, M., Kasai, N., Okada, K., and Aida, Y. (1999) Ovine MHC Class II *DRB1* alleles associated with resistance or susceptibility to development of bovine leukemia virus-induced ovine lymphoma. *Cancer Res* 59:975–981.

Taylor, J.A., and Jacobs, R.M. (1993) Effects of plasma and serum on the in vitro expression of bovine leukemia virus. *Lab Invest* 69(3):340–346.

Valli, V.E.O., McSherry, B.J., Lumsden, J.H., Smart, M.E., Grenn, H.H., and Heath, B. (1973) Blood cell types associated with bovine lymphosarcoma. The occurrence and significance of nuclear malignancy associated changes in the blood of normal and leucotic cattle. *Cancer Detect Prev* 322:598–607.

Vernau, W., Valli, V.E.O., Dukes, T.W., Jacobs, R.M., Shoukri, M., and Heeney, J.L. (1992) Classification of 1,198 cases of bovine lymphoma using the National Cancer Institute Working Formulation for human Non-Hodgkin's lymphomas. *Vet Pathol* 29:183–195.

Willems, L., Burny, A., Collete, D., Dangoisse, O., Dequiedt, F., Gatot, J.S., Kerkhofs, P., Lefèbvre, L., Merezak, C., Peremans, T., Portetelle, D., Twizere, J.C., and Kettmann, R. (2000) Genetic determinants of bovine leukemia virus pathogenesis. *Aids Res Hum Retrovir* 16(16):1787–1795.

Willems, L., Gatot, J.S., Mammerickx, M., Portetelle, D., Burny, A., Kerkhofs, P., and Kettmann, R. (1995) The YXXL signalling motifs of the bovine leukemia virus transmembrane protein are required for in vivo infection and maintenance of high viral loads. *J Virol* 69(7):4137–4141.

Wu, D., Takahashi, K., Liu, N., Koguchi, A., Makara, M., Sasaki, J., Goryo, M., and Okada, K. (1999) Distribution of T-lymphocyte subpopulation in blood and spleen of normal cattle and cattle with enzootic bovine leukosis. *J Comp Pathol* 120:117–127.

Intravascular Large T-Cell Lymphoma

Intravascular large T-cell lymphoma occurs in both humans and animals, although only the B-cell variant that is more frequent in human cases is given status as a disease entity in the WHO classification system. In both humans and animals, cases of actual angiocentric and angioinvasive neoplasms are quite rare, with that occurring in histiocytic sarcoma the most commonly occurring example in animals. The latter is an example of angioinvasion and not of primary intravascular neoplasm. A number of reports of intravascular lymphoma in humans treat the disease in a generic sense and include both B- and T-cell types with emphasis on the presentation and management. In many lymphoid neoplasms, the vessels in the area are invaded by the advancing tumor without specificity for vessels per se but with the result of ischemic necrosis in the surrounding tumor. In these cases, neoplastic cells may survive in "collar lesions" surrounding the remaining functional vessels to a depth of about 20 cells, which appears to represent the distance that diffusion from the vessel can sustain the surrounding cells (Figs. 4.241–4.244). In contrast, in a histiocytic sarcoma of Langerhans cell type there is true angioinvasion of small arterioles that results in patchy ischemic necrosis in the surrounding neoplasm. In this disease, the neoplastic

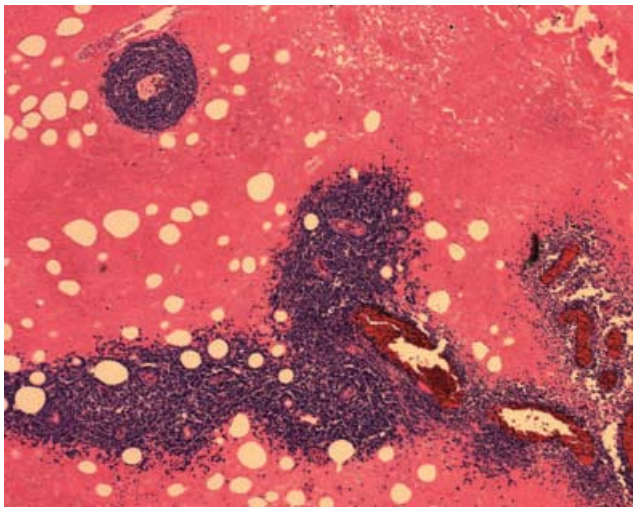

Figure 4.241. Cat: skin, lymphoma with a collar lesion. There is widespread ischemic necrosis of the tumor within the panniculus with islands of surviving tissue surrounding small vessels. The spaces consist of fat cells of the panniculus invaded by the neoplasm.

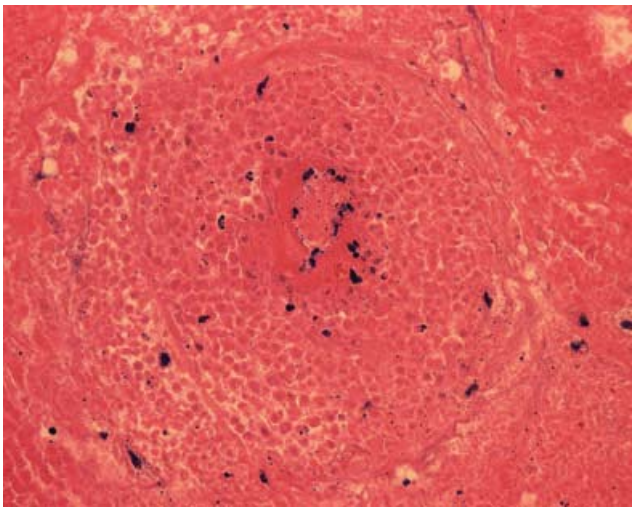

Figure 4.243. Cat: skin, vaccination sarcoma, same tissue as Figure 4.241. Remnants of a collar lesion. The tumor cells infiltrated the pericytes of a venule with the entire structure now necrotic like the surrounding tissue.

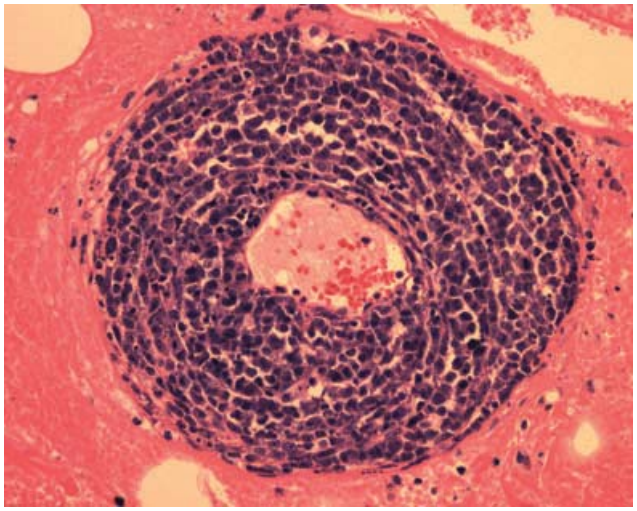

Figure 4.242. Cat: skin, vaccination site sarcoma. Detail of Figure 4.241. The cells survive around thin-walled vessels with the neoplastic cells having permeated the outer vascular sheath, which is thinned and distended and apparent at the boundary with necrotic tissue.

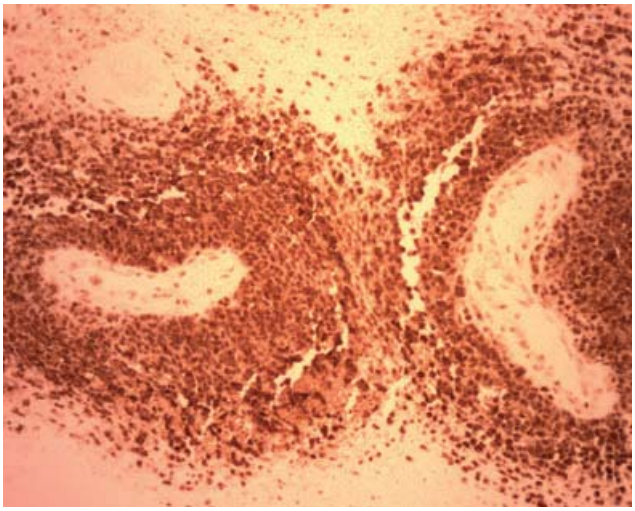

Figure 4.244. Cat: skin, collar lesion. Phenotype of Figure 4.241. On staining with CD79, the surrounding viable cells are strongly and uniformly labeled. Lesions of this type can occur with a variety of neoplasms not limited to B- or T-lymphocytes.

cells labeled with CD18 can be seen to be within the muscular walls of small arterioles that are still functional, as well as in others that are completely embolized without dilation of the arteriole in the process (Figs. 4.245–4.247).

In lymphomas, a number of forms of vascular involvement occur that involve the vessels at different levels of invasion. The most peripheral involvement is characterized by marked infiltration of the venous pericyte sheath, which is greatly dilated with neoplastic lymphocytes filing the intervening space with gradual compression of the venous wall till the vascular lumen is reduced to a slitlike cavity or completely obstructed; there is generally no marked congestion or local ischemic necrosis as a result (Figs. 4.248–4.250). A second more intrusive type of involvement of arteries results from the passage of the neoplastic cells from either blood or tissue to accumulate under an intact endothelium that retains continuity but is again compressed to obliteration. This type of neoplasm

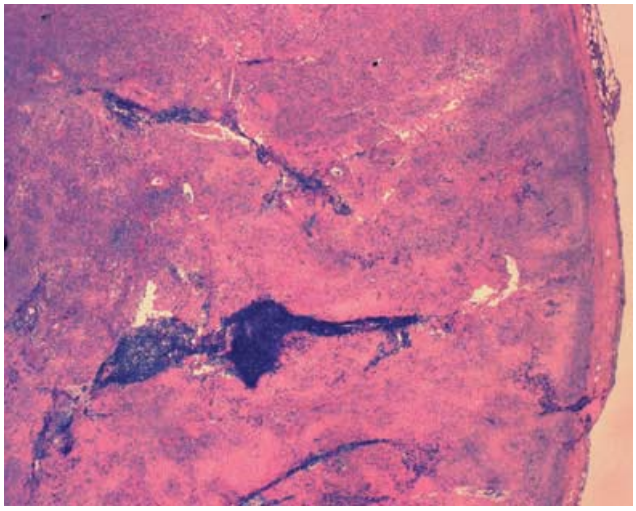

Figure 4.245. Dog: popliteal node, histiocytic sarcoma. There is marked thickening of the node capsule with destruction of the peripheral sinus and obliteration of nodal architecture with multifocal pale areas of ischemic necrosis.

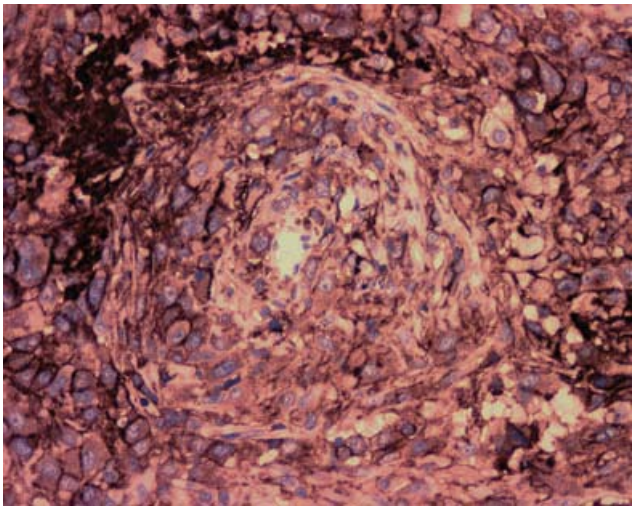

Figure 4.247. Dog: node, histiocytic sarcoma. Phenotype of Figure 4.245. On staining with CD18, the infiltrating cells are uniformly positive. The darker area to the upper left is the result of focal necrosis with deeper staining by benign macrophages.

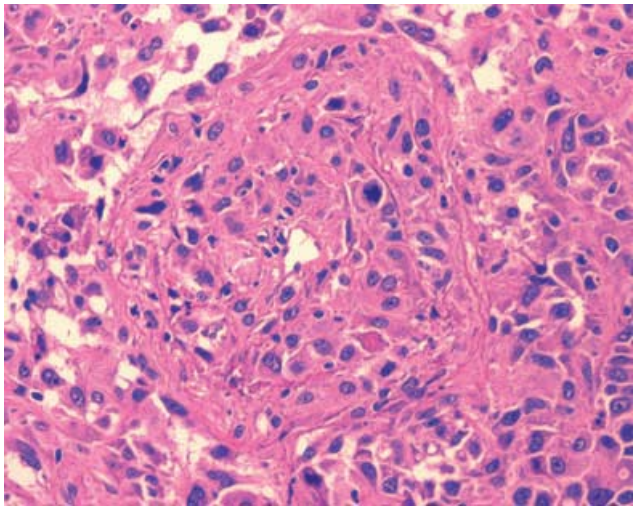

Figure 4.246. Dog: node, histiocytic sarcoma. Detail of Figure 4.245. There is heavy infiltration of the wall of a small arteriole with neoplastic histiocytic cells.

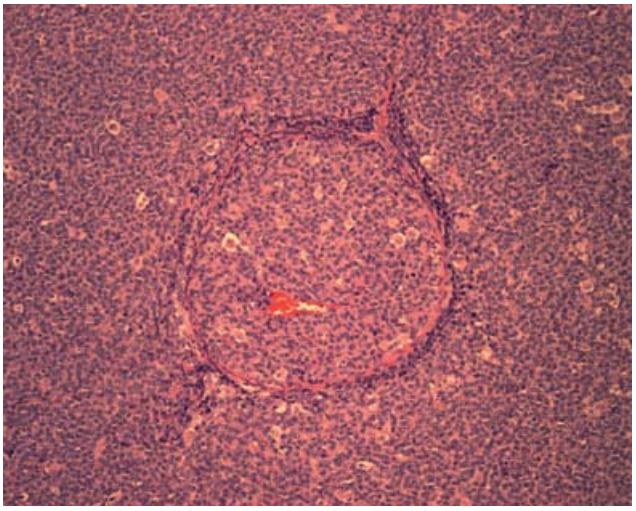

Figure 4.248. Dog: lymph node, venous occlusion. B-cell lymphoma of large cell type has infiltrated the perivascular tissues and markedly compressed the lumen of a quite large vein.

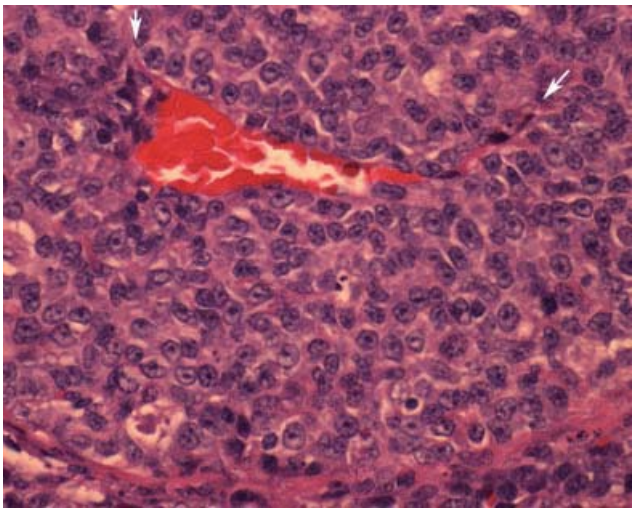

Figure 4.249. Dog: node, lymphoma. Detail of Figure 4.248. The perivascular mantle is at the lower border of the image with the vein boundaries indicated by arrows that indicate marked compression of the initial lumen. The endothelium remains intact with the nuclei irregularly crowded.

has been found in the heart of a dog, with rapid extension to the lung (Figs. 4.251, 4.252) and death was due to cardiac blockage. With the development of immune staining and specifically identifying the cells as of lymphoid origin, the terminology has changed from *angioendotheliomatosis* to a more specific reference to the most common form of the neoplasm now termed *intravascular large cell lymphoma*. In the T-cell variant of this neoplasm, there is actually homing to the vascular lumen of arterioles, with progression largely by local expansion as well as by metastatic spread by tumor emboli. This type of neoplasm was found in a mature large breed dog in the vessels of the nasal turbinates that were infarcted with tumor (Figs. 4.253–4.255), which spread through the

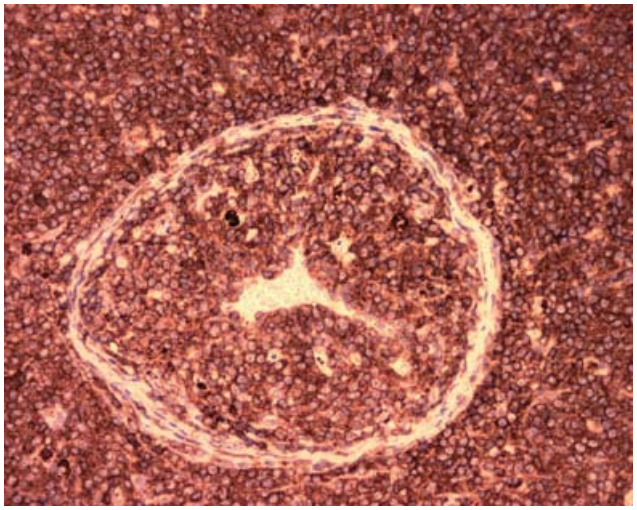

Figure 4.250. Dog: node, lymphoma. Phenotype of Figure 4.248. On staining with CD79, the infiltrating cells are strongly and uniformly positive. This form of vascular occlusion is less common than the invasion of arterioles as seen in histiocytic sarcoma.

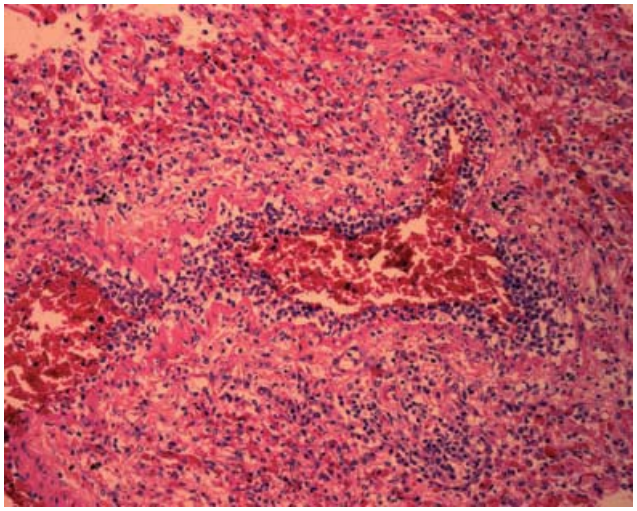

Figure 4.251. Dog: lung, angiotropic lymphoma. A pulmonary artery with thickened wall and irregularly plicated muscularis has mild lymphocytic colonization of perivascular areas and a very heavy laminar subendothelial colonization irregularly reducing the luminal area.

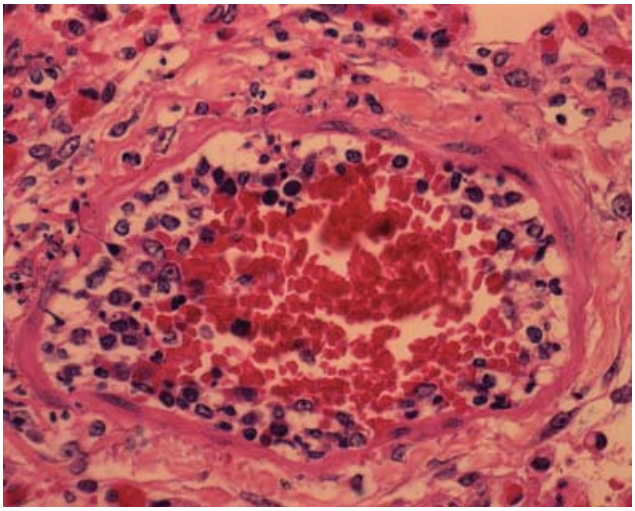

Figure 4.252. Dog: lung, angiotropic lymphoma, same tissue as Figure 4.251. The smaller artery has a markedly dilated muscularis with an inner cuff of lymphocytes displacing the endothelium. There appears to be a vacuolar space-occupying effect like the presence of lipid or edema with the lymphocytes having a moderate volume of quite deeply staining cytoplasm. The lesion was not phenotyped.

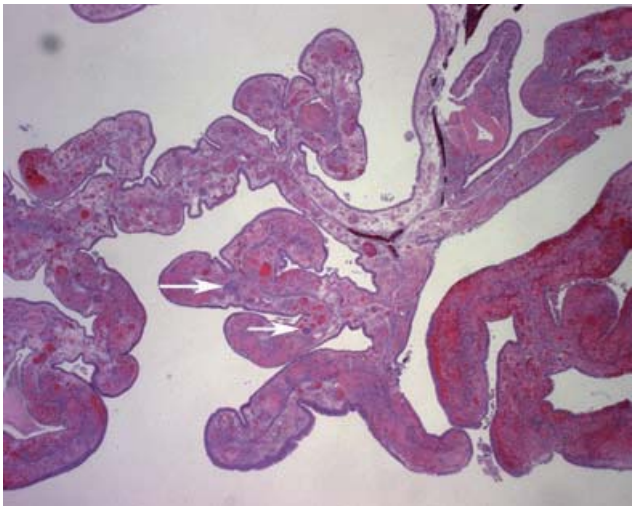

Figure 4.253. Dog: nasal turbinates, angiotropic T-cell lymphoma. A mature large-breed dog with persistent epistaxis developed convulsions and was euthanized. Turbinates are thickened and edematous with focal areas of hemorrhage due to multiple areas of embolism by neoplastic lymphocytes. *Case from J. J. Andrews, DVM.*

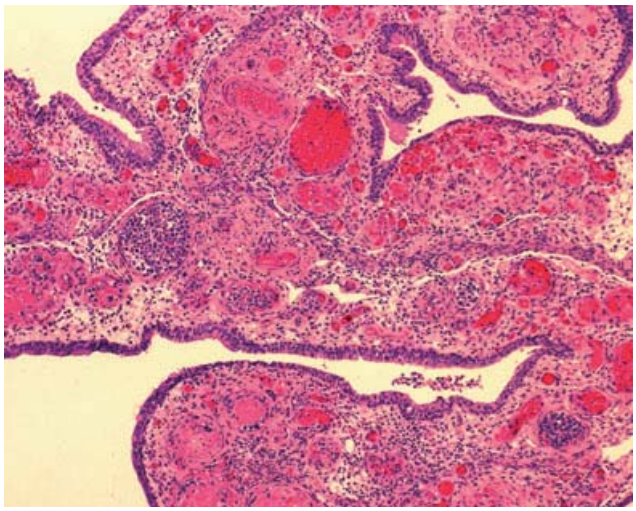

Figure 4.254. Dog: turbinate, angiotropic T-cell lymphoma. Detail of the areas indicated by arrows in Figure 4.253. Several vessels can be seen to be filled with densely packed nuclei that are arterioles while the veins frequently are distended with fibrin.

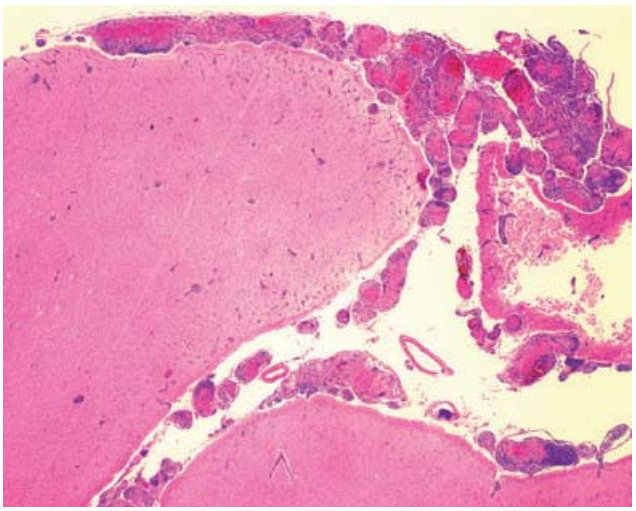

Figure 4.256. Dog: brain, olfactory meninges, angiotropic T-cell lymphoma, same case as Figure 4.253. There is marked colonization and embolism of meningeal vessels with some direct extension into the superficial neuropil of the upper left.

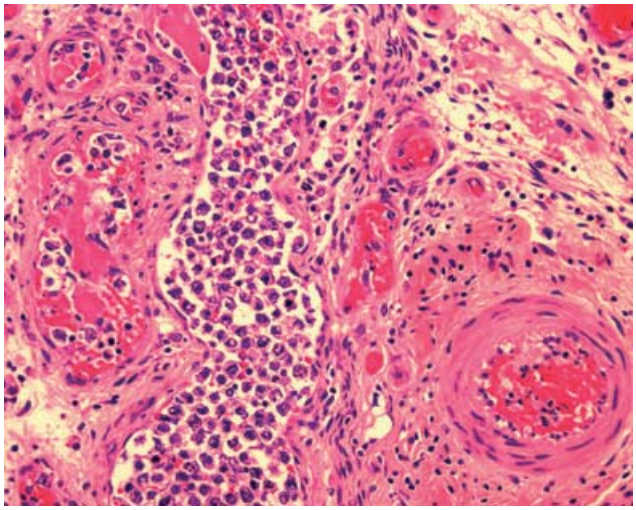

Figure 4.255. Dog: turbinate, angiotropic T-cell lymphoma. Detail of Figure 4.253. The lesions appear to develop by blood delivered by intact arterioles (lower right) continuing to distend veins that are irregularly blocked with fibrin and neoplastic cells (left center).

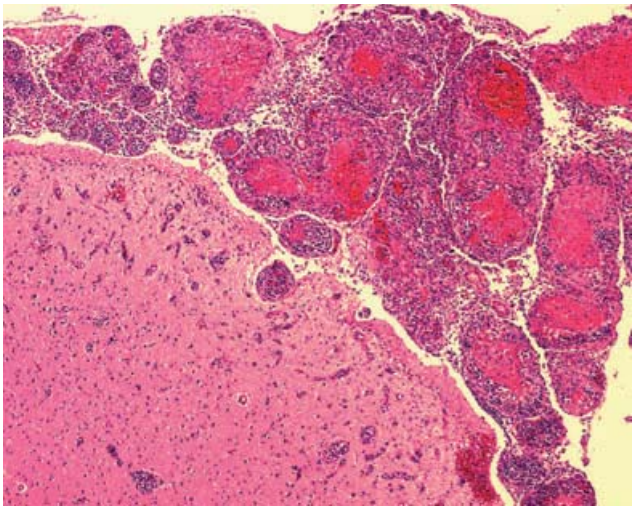

Figure 4.257. Dog: meninges, angiotropic T-cell lymphoma. Detail of Figure 4.256. There is widespread infiltration and thrombosis of meningeal vessels with extension into the superficial vessels of the olfactory bulb.

cribriform plate involving the meninges and superficial vessels of the olfactory bulbs. In these tissues, the venous walls were greatly distended and thinned with the neoplastic cells solidly blocking vascular channels (Figs. 4.256–4.259).

In oversight stains, it is not possible to determine the phenotypic lineage of the invading cells on the basis of the mode of invasion or colonization. Oddly in both humans and animals, the intravascular lymphomas of B- and T-cell type are characterized by early spread to the central nervous system that may begin in the spinal cord with ascending paralysis and rapid progression resulting in death.

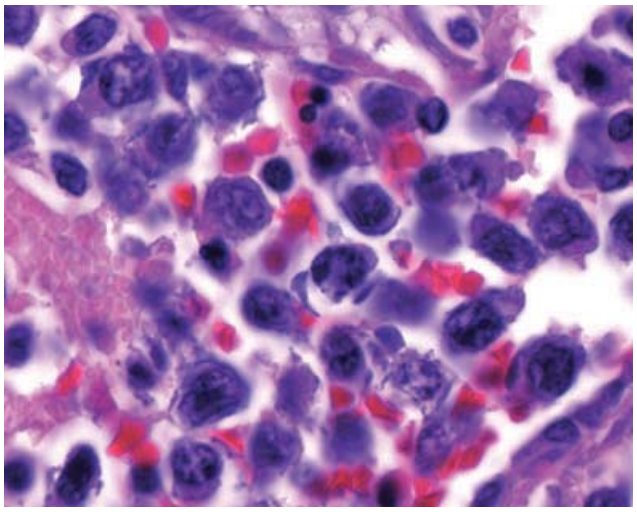

Figure 4.258. Dog: meninges, angiotropic T-cell lymphoma. The neoplastic cells are autolytic but of large cell type with large dense chromocenters and prominent parachromatin clearing with multiple large nucleoli. The cytoplasm is relatively abundant and deeply stained with the cells appearing noncohesive.

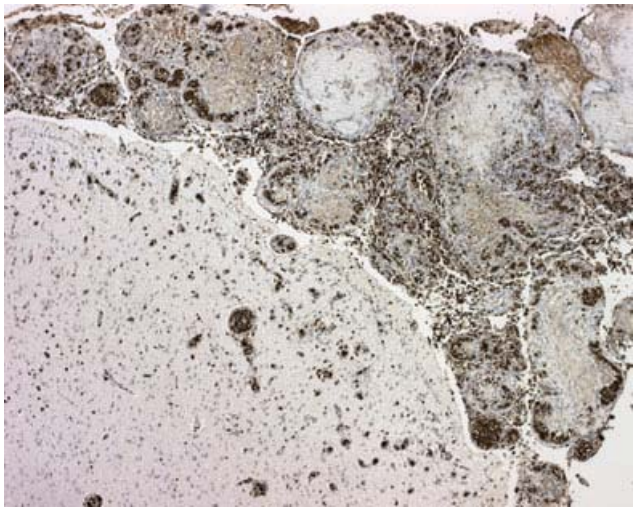

Figure 4.259. Dog: meningeal angiotropic T-cell lymphoma. Phenotype of Figure 4.257. On staining with CD3, the neoplastic cells are strongly and uniformly labeled. The neoplastic cells tend to line subendothelial spaces with dilated vessels containing fibrin and red cells. This pattern is likely due to vessels passing a column of blood around the central obstruction with mural dilation in each cardiac systole.

REFERENCES

DiGiuseppe, J.A., Nelson, W.G., Seifter, E.J., Boitnott, J.K., and Mann, R.B. (1994) Intravascular lymphomatosis: A clinicopathologic study of 10 cases and assessment of response to chemotherapy. *J Clin Oncol* 12(12):2573–2579.

Lapointe, J.M., Higgins, R.J., Kortz, G.D., Bailey, C.S., and Moore, P.F. (1997) Intravascular malignant T-cell lymphoma (malignant Angioendotheliomatosis) in a cat. *Vet Pathol* 34:247–250.

Malicki, D.M., Suh, Y.K., Fuller, G.N., and Shin, S.S. (1999) Angiotropic (intravascular) large cell lymphoma of T-cell phenotype presenting as acute appendicitis in a patient with acquired immunodeficiency syndrome. *Arch Pathol Lab Med* 123:335–337.

McDonough, S.P., Van Winkle, T.J., Valentine, B.A., vanGessel, Y.A., and Summers, B.A. (2002) Clinicopathological and immunophenotypical features of canine intravascular lymphoma (malignant Angioendotheliomatosis). *J Comp Path* 126:277–288.

Misago, N., Ohshima, K., Aiura, S., Kikuchi, M., and Kohda, H. (1996) Primary cutaneous T-cell lymphoma with an angiocentric growth pattern: Association with Epstein-Barr virus. *Brit J Dermatol* 135:638–643.

Mosqueda-Taylor, A., Meneses-Garcia, A., Zárate-Osorno, A., Ruiz-Godoy, R.L.M., Ochoa-Carrillo, F.J., and Mohar-Betancourt, A. (1997) Angiocentric lymphomas of the palate: Clinico-pathological considerations in 12 cases. *J Oral Pathol Med* 26:93–97.

Roux, S., Grossin, M., De Bandt, M., Palazzo, E., Vachon, F., and Kahn, M.F. (1995) Angiotropic large cell lymphoma with mononeuritis multiplex mimicking systemic vasculitis. *J Neurol Neurosurg and Psychiat* 58:363–366.

Stroup, R.M., Sheibani, K., Moncada, A., Purdy, L.J., and Battifora, H. (1990) Angiotropic (intravascular) large cell lymphoma: A clinicopathologic study of seven cases with unique clinical presentations. *Cancer* 66:1781–1788.

Thiel, R., Sarbia, M., Gerharz, C.D., Ebert, T., Schmitz-Dräger, B., and Ackermann, R. (1995) Angiocentric lymphoma of the kidney in the acquired immunodeficiency syndrome. *J Urol* 153:137–139.

Peripheral T-Cell Lymphoma, NOS

The REAL and WHO systems of classification included categories of peripheral T-cell lymphoma (PTCL) that were not otherwise specified (NOS). In later publications on human lymphoma, this category has largely been omitted, with grouping of multiple categories initially considered entities and since shown to be related by common factors of cellular size and low mitotic rate in the Mature T-Cell Leukemia-Lymphoma (SLL,TZL); further, by topographical and immunophenotypic characteristics in Mature Nodal and Extranodal Lymphoma with Angioimmunoblastic (AILT), Hepatosplenic (HSTL), Enteropathy (ETCL) and Subcutaneous Panniculitis-like (SPTCL) types of T-cell lymphoma; and finally, immunophenotypic and morphological characteristics of ALK and CD30 plus the Hallmark cells in Anaplastic Large Cell Lymphomas of Primary Cutaneous, Primary Systemic, and Lymphomatoid Papulosis types. However, for animal lymphomas without the array of specific antibodies and in situ probes now available for diagnostic

work on human tissues, there are still undefined neoplasms that require a generic category like NOS. The PTCL of NOS types can be defined in general terms. They may be in lymph node with a paracortical pattern, but they may be in the dermis and panniculi and may be focal or systemic. They lack a specific mode of growth that would label them as angiocentric or angioinvasive, but often invade vessels causing focal necrosis as part of general tissue invasion. Most of the neoplasms in this category are found in dogs simply because they are the animal species most often biopsied, but they can occur in all mammals and in birds and fish as well. Some of the general features of PTCL of NOS types listed here are derived from Chapter 29 of *Neoplastic Hematopathology* by Pinkus and Said:

- Extensive morphologic heterogeneity
- Spectrum of lymphoid cells; single cell size may predominate
- Various degrees of nuclear complexity
- Abundant pale or clear cytoplasm with formalin fixation
- Large transformed cells usually with fine chromatin, single to several distinct nucleoli, and delicate nuclear membranes
- Large bizarre or Reed-Sternberg–like cells may occur Increased vascularity, prominent in angioimmunoblastic lymphomas
- Histiocytes present and may be abundant
- Eosinophils variable and present in Hodgkin's-like lymphomas
- Prominent necrosis in NK-cell types
- Sinusoidal filling may occur as in the ALCL types; T-zone pattern may be present in nodal forms
- Transformation in cell type may occur

One form of PTCL of NOS type is rare and typically seen in a young large breed dog that presented with generalized skin disease with dependent edema, with peripheral lymphadenopathy, and severely ill. The disease resembles inflammatory carcinoma in that there is widespread plugging and distension of small vessels with severe congestion of surrounding tissues (Figs. 4.260–4.262). There is a generalized infiltration with large cells with round to oval and elongated nuclei, prominent nucleoli and marked parachromatin clearing. Because of the edema and congestion there is a mixture of inflammatory cells present, with a cellulitis or mycotic vasculitis felt to be the basis of the lesion. On immunohistochemical staining, the large atypical cells mark strongly with CD3 and are negative with reagents for B-cell and histiocytes.

A second type of presentation is of a mature dog in good health with a single mass in the panniculus that may have been interpreted to be a puncture wound and has multiple small foci of necrosis surrounded by hyaline bars and many eosinophils (Figs. 4.263, 4.264). The lesions look distinctly inflammatory with a gradient of granulocytes, histiocytes, and granulation tissue surrounding the areas of necrosis. As a consequence, cases of this type may have been stained for all manner of infectious agents before neoplasm is considered. The tissues surrounding the areas of necrosis have early sclerosis and a prominent fine vascular pattern that may be considered part of a

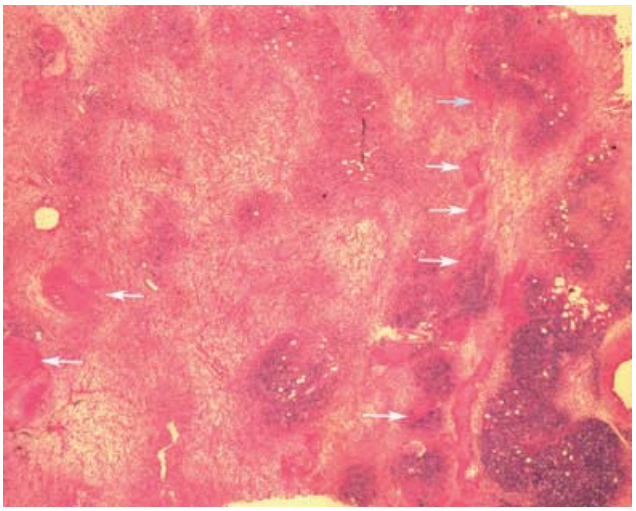

Figure 4.260. Dog: skin, systemic aggressive T-cell lymphoma. The biopsy is a core of very edematous skin with the surface lying below the left margin of the image. The arrows point to dilated and obstructed veins with the darker areas consisting of foci of neoplastic cells surrounding and invading small arterioles.

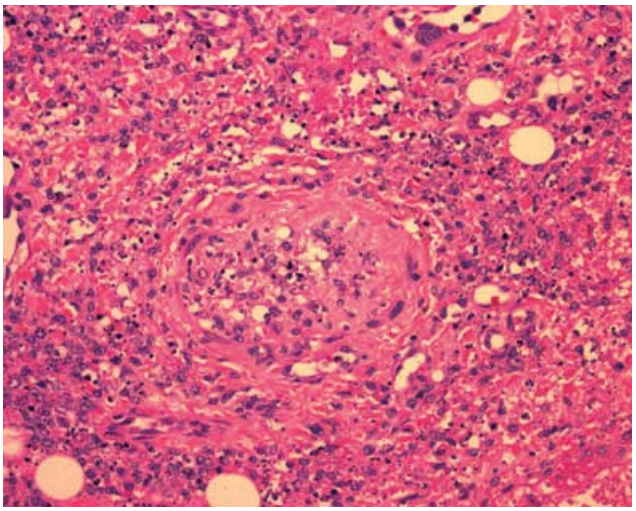

Figure 4.261. Dog: skin, cutaneous T-cell lymphoma. Detail of Figure 4.260. An arteriole surrounded by neoplastic lymphocytes that are undergoing apoptosis due to generalized ischemia of the area with multiple foci of vascular invasion.

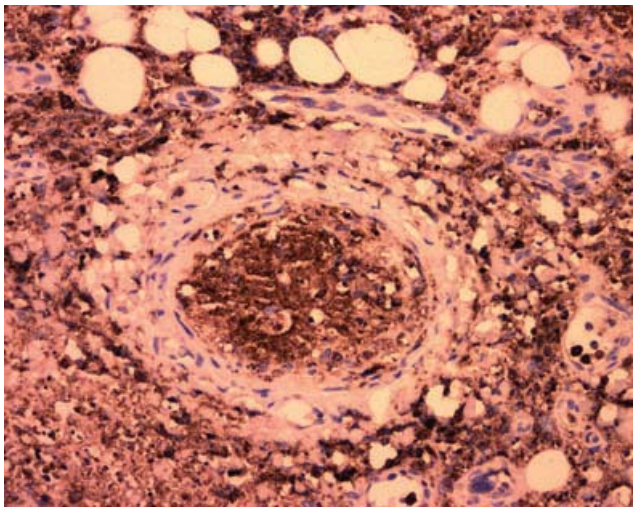

Figure 4.262. Dog: skin, cutaneous T-cell lymphoma. Phenotype of Figure 4.261. The same vessel as depicted in Figure 4.260 has strongly positive cytoplasmic marking with CD3 that is largely on cellular debris that leaves the muscle fibers of the arteriolar wall sharply defined.

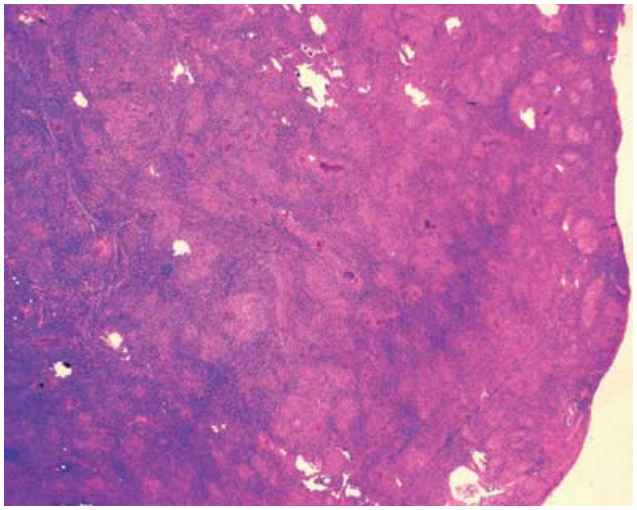

Figure 4.263. Dog: subcutaneous mass, mixed cellularity type peripheral T-cell lymphoma. The mass has no natural borders, with a reticulated appearance due to very prominent fine vascularity with lighter areas consisting of masses of histiocytes. The general appearance of the tissue suggests granulomatous inflammation. The fine pink areas of varying size are palisading areas of immunoprecipitates of the Splendore-Hoeppli reaction. *Slide from Doug Hoefling, DVM.*

granulation tissue response. The neoplastic cells are of medium to large cell type with vesiculation and peripheralization of chromatin, but they do not attract attention in the mixture of cells present. They are usually adjacent to small veins and have relatively abundant water-clear cytoplasm and prominent central nucleoli (Fig. 4.265).

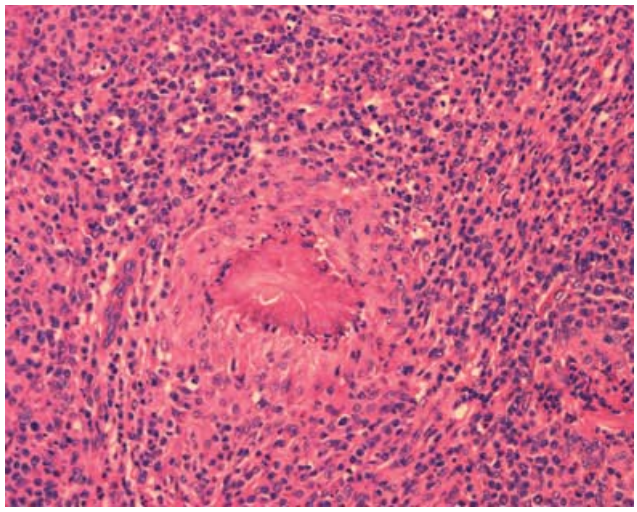

Figure 4.264. Dog: subcutaneous mass, mixed type peripheral T-cell lymphoma. Detail of Figure 4.263. The central area of immune precipitates is surrounded by a discontinuous layer of eosinophils and a broad outer rim of epithelioid macrophages and connective tissue, with a surrounding area of mixed inflammation with many neutrophils and eosinophils. The presence of the Splendore-Hoeppli aggregations promoted staining for infectious agents, all of which were negative.

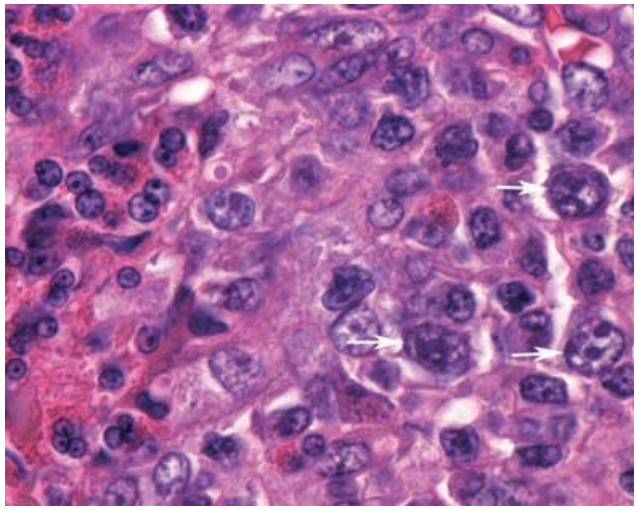

Figure 4.265. The edge of a small granuloma (below) is surrounded, with eosinophils and epithelioid macrophages. The arrows indicate nuclei of lymphocytes with peripheralized chromatin and 3–4 very large nucleoli. The cells have marked parachromatin clearing with a moderate volume of cytoplasm that has a deeper stained perinuclear area and a relatively water-clear periphery. The mass was diagnosed on these tissues as peripheral extranodal T-cell lymphoma by L. Dehner, MD, of St. Louis. The animal initially responded to treatment with steroids and 6 months later was euthanized because of generalized lymphadenopathy with lymphoma confirmed.

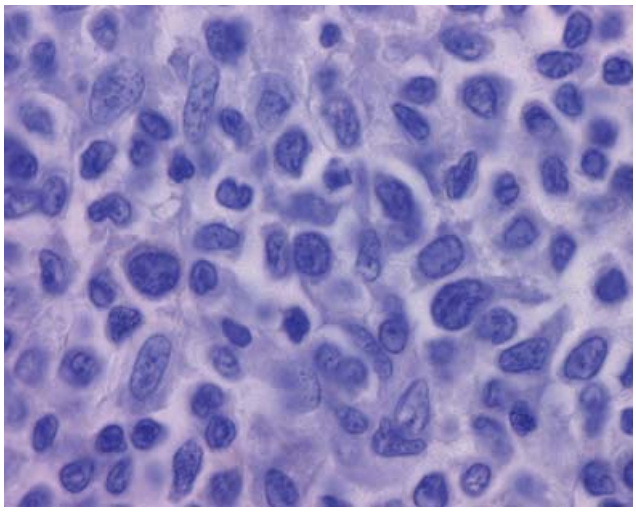

Figure 4.266. Dog: lymph node, peripheral T-cell lymphoma, mixed cell type. Tissue at necropsy from the same animal as in Figure 4.263. The marked variation of cell type is evident in this weakly stained CD3 preparation, with marked variation in both size and nuclear contours. There is a consistent peripheralization of chromatin and quite prominent nucleoli with a narrow rim of more deeply stained cytoplasm and a peripheral area of clearing.

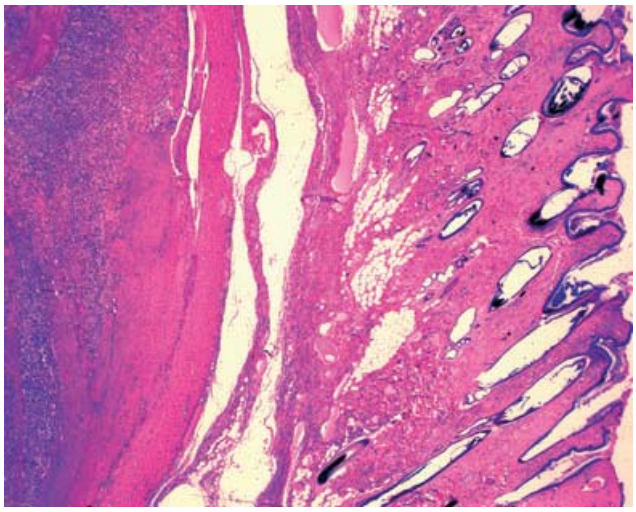

Figure 4.267. Dog: skin, peripheral T-cell lymphoma, large cell type. The skin is not invaded by neoplasm but there is widespread hair loss over a heavily encapsulated subcutaneous mass.

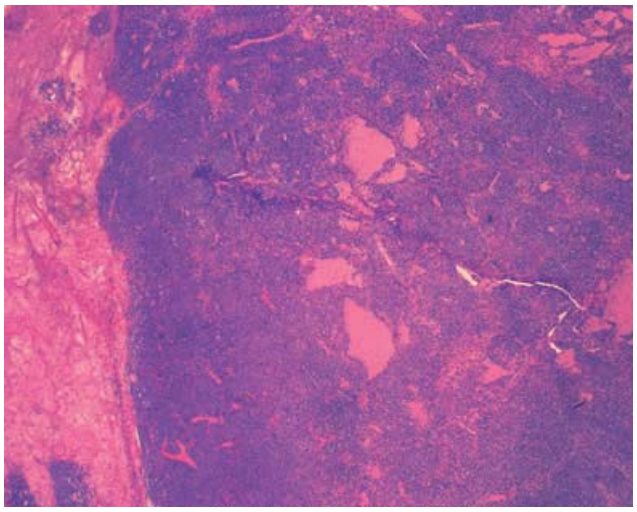

Figure 4.268. Dog: skin, peripheral T-cell lymphoma of large cell type. Deep area of Figure 4.267. The lesion is densely cellular with focal areas of ischemic necrosis and vascular ectasia. The lighter area at the left has undergone ischemic necrosis with the darker structures in the lower left collar lesions of viable tumor cells surrounding small vessels.

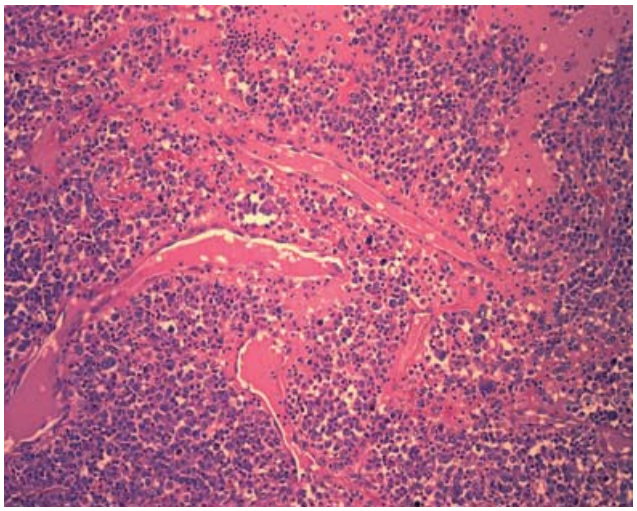

Figure 4.269. Dog: skin, peripheral T-cell lymphoma, large cell type. Detail of Figure 4.268. The lesion is characterized by an abnormal vascular accompaniment with irregular dilation of thin-walled vessels and irregular areas of laking necrosis filled with highly proteinaceous fluid (upper right).

They may make up only 10–20% of the overall cellular population and only when immunohistochemical staining is carried out do they become apparent in terms of homogeneity of cell type and proximity to small vessels. One case of this type was treated with steroids and made a complete local recovery, but 6 months later there was generalized lymphadenopathy that was not responsive to chemotherapy. The involved nodes had diffuse paracortical expansion and a heterogenous cell type of varying size and shape and irregularly CD3 positive, likely due to prolonged storage in wet fixation (Fig. 4.266). Other types of peripheral T-cell lymphomas are seen, which appear as isolated subcutaneous proliferations. Although these neoplasms have the cytologic characteristics of aggressive behavior, they may be amenable to excision without other therapy (Figs. 4.267–4.272). There is not currently a

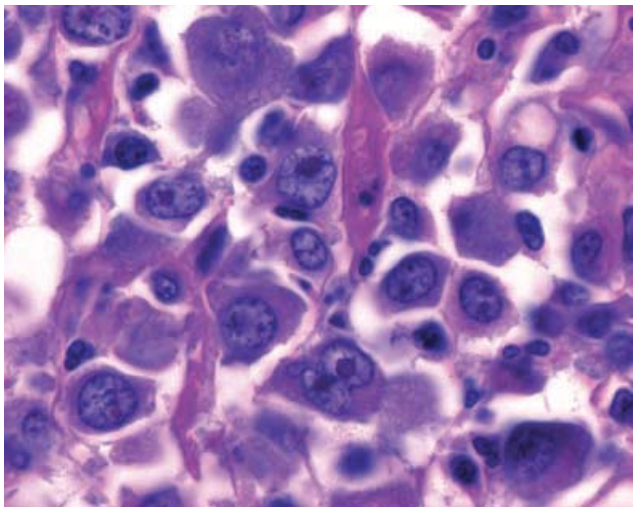

Figure 4.270. Dog: skin, peripheral T-cell lymphoma, large cell type. Detail of Figure 4.268. The cells vary quite markedly in size and shape with bilobed and multinucleated forms, all of which have peripheralized chromatin with parachromatin clearing and very prominent central nucleoli. The cytoplasm is relatively abundant and highly amphophilic with cell boundaries generally distinct. The cell in the lower right with more eosinophilic cytoplasm is likely in early stages of degeneration.

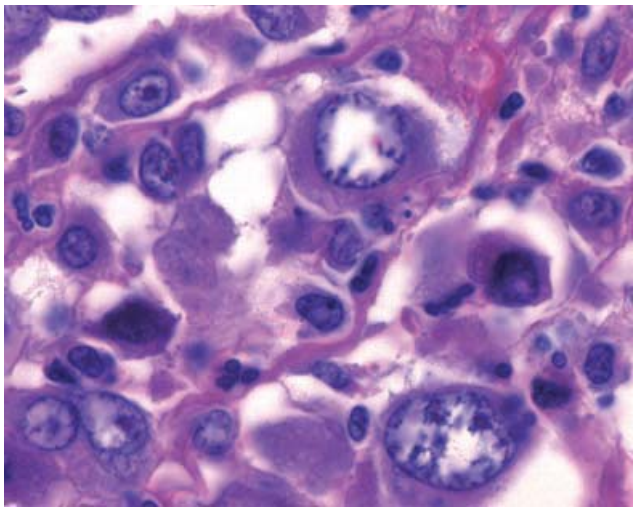

Figure 4.271. Dog: skin, peripheral T-cell lymphoma, large cell type. Detail of Figure 4.269. In other areas of the tumor mass, there are cells with very large vesicular nuclei with relatively abundant cytoplasm. Two cells in the same field have cytoplasm retracted from surrounding cells and are undergoing degeneration.

classification system for these lesions, but if their biological behavior is distinctively focal and late or unlikely to disseminate they constitute a management, if not morphologic entity.

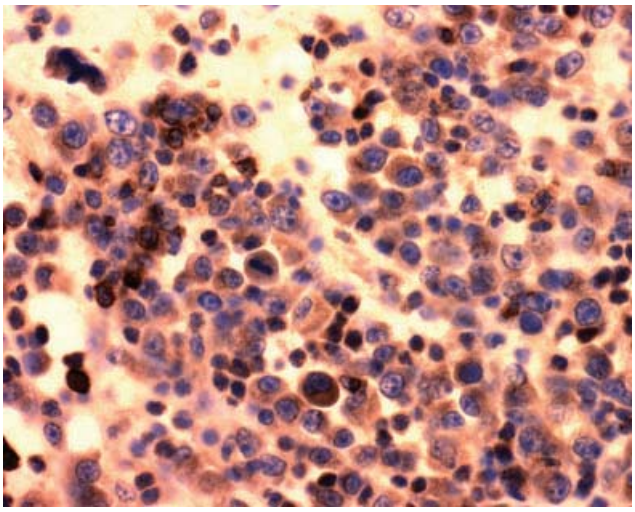

Figure 4.272. Dog: skin, peripheral T-cell lymphoma of large cell type. Phenotype of Figure 4.269. With CD3 staining, the neoplastic cells are strongly and uniformly labeled. There is a metaphase in the center and a tripolar mitosis in the lower left. The tissue is completely negative on staining with CD79.

REFERENCES

Baron, B.W., Anastasi, J., Montag, A., Huo, D., Baron, R.M., Karrison, T., Thirman, M.J., Subudhi, S.K., Chin, R.K., Felsher, D.W., Fu, Y.X., McKeithan, T.W., and Baron, J.M. (2004) The human BCL6 transgene promotes the development of lymphomas in the mouse. *PNAS* 101(39):14198–14203.

Brizard, A., Brizard, F., Babin, P., Agius, G., Delwail, V., Guilhot, F., and Tanzer, J. (1994) Unclassifiable high grade malignant T-cell lymphoma with clonal evolution. *Leuk and Lymph* 13:349–352.

Chott, A., Augustin, I., Wrba, F., Hanak, H., Öhlinger, W., and Radaszkiewicz, T. (1990) Peripheral T-cell lymphomas: A clinicopathologic study of 75 cases. *Hum Pathol* 21:1117–1125.

Coleman, L.A., Erdman, S.E., Schrenzel, M.D., and Fox, J.G. (1998) Immunophenotypic characterization of lymphomas from the mediastinum of young ferrets. *AJVR* 59(10): 1281–1286.

de Lorimier, L.P., Alexander, S.D., and Fan, T.M. (2003) T-cell lymphoma of the tympanic bulla in a feline leukemia virus-negative cat. *Can Vet J* 44:987–989.

Diez-Martin, J.L., Lust, J.A., Witzig, T.E., Banks, P.M., and Li, C.Y. (1991) Unusual presentation of extranodal peripheral T-cell lymphomas with multiple paraneoplastic features. *Cancer* 68(4):834–841.

Fournel-Fleury, C., Magnol, J.P., Bricaire, P., Marchal, T., Chabanne, L., Delverdier, A., Bryon, P.A., and Felman, P. (1997) Cytohistological and immunological classification of canine malignant lymphomas: Comparison with human non-Hodgkin's lymphomas. *J Comp Path* 117:35–59.

Fournel-Fleury, C., Ponce, F., Felman, P., Blavier, A., Bonnefont, C., Chabanne, L., Marchal, T., Cadore, J.L., Goy-Thollot, I.,

Ledieu, D., Ghernati, I., and Magnol, J.P. (2002) Canine T-cell lymphomas: A morphological, immunological, and clinical study of 46 new cases. *Vet Pathol* 39:92–109.

Friedman, H.D., Hutchison, R.E., Smith, J.R., Gonchoroff, N.J., Stein, C.K., and Poiesz, B.J. (1994) $CD8^+$ polylobated T-cell leukemia/lymphoma. A case report with immunophenotypic, ultrastructural, gene rearrangement, karyotypic, and DNA content analysis and autopsy description. *Arch Pathol Lab Med* 118:722–727.

Harris, N.L., Jaffe, E.S., Stein, H., Banks, P.M., Chan, J.K.C., Cleary, M.L., Delsol, G., De Wolf-Peeters, C., Falini, B., Gatter, K.C., Grogan, T.M., Isaacson, P.G., Knowles, D.M., Mason, D.Y., Muller-Hermelink, H.K., Pileri, S.A., Piris, M.A., Ralfkiaer, E., and Warnke, R.A. (1994) A revised European-American classification of lymphoid neoplasms: A proposal from the International Lymphoma Study Group. *Blood* 84(5):1361–1392.

Kato, H., Nagasaka, T., Ichikawa, A., Kinoshita, T., Murate, T., Tsushita, K., Hotta, T., and Saito, H. (1994) Tumor necrosis factor-β gene expression and its relationship to the clinical features and histopathogenesis of peripheral T-cell lymphomas. *Leuk and Lymph* 16:125–133.

Kelley, L.C., and Mahaffey, E.A. (1998) Equine malignant lymphomas: Morphologic and immunohistochemical classification. *Vet Pathol* 35:241–252.

Kern, W.F., Spier, C.M., Hanneman, E.H., Miller, T.P., Matzner, M., and Grogan, T.M. (1992) Neural cell adhesion molecule-positive peripheral T-cell lymphoma: A rare variant with a propensity for unusual sites of involvement. *Blood* 79(9):2432–2437.

Koduru, P.R.K., Susin, M., Kolitz, J.E., Soni, M., Teichberg, S., Siques, M.J., Sun, T., Amorosi, E., and Budman, D.R. (1995) Morphological, ultrastructural, and genetic characterization of an unusual T-cell lymphoma in a patient with sinus histiocytosis with massive lymphadenopathy. *Am J Hematol* 48:192–200.

Marker, L., Munson, L., Basson, P.A., and Quackenbush, S. (2003) Multicentric T-cell lymphoma associated with feline leukemia virus infection in a captive Namibian cheetah (Acinonyx jubatus). *J Wildl Dis* 39(3):690–695.

Montalban, C., Obeso, G., Gallego, A., Castrillo, J.M., Bellas, C., and Rivas, C. (1993) Peripheral T-cell lymphoma: A clinicopathological study of 41 cases and evaluation of the prognostic significance of the updated Kiel classification. *Histopathol* 22:303–310.

The Non-Hodgkin's Lymphoma Classification Project. (1997) A Clinical evaluation of the International Lymphoma Study Group Classification of Non-Hodgkin's Lymphoma. *Blood* 89(11):3909–3918.

Patsouris, E., Noël, H., and Lennert, K. (1988) Histological and immunohistological findings in lymphoepithelioid cell lymphoma (Lennert's lymphoma). *Am J Surg Pathol* 12(5):341–350.

Pinkus, G.S., and Said, J.W. (2001) Peripheral T-cell lymphomas. In Knowles, D.M. (ed.), *Neoplastic Hematopathology,* 2nd ed. Lippincott Williams & Wilkins, Philadelphia, pp. 1091–1125.

Ponce, F., Magnol, J.P., Marchal, T., Chabanne, L., Ledieu, D., Bonnefont, C., Felman, P., and Fournel-Fleury, C. (2003) High-grade canine T-cell lymphoma/leukemia with plasmacytoid morphology: A clinical pathological study of nine cases. *J Vet Diagn Invest* 15:330–337.

Remotti, D., Pescarmona, E., Burgio, V.L., Gastaldi, R., Guglielmi, C., Martelli, M., Mandelli, F., and Baroni, C.D. (1992) Prognostic value of the histologic classification of peripheral T-cell lymphoma: A clinico-pathologic study of 71 HTLV-1 negative cases. *Leuk and Lymph* 8:371–380.

Steinberg, H. (2000) Disseminated T-cell lymphoma in a guinea pig with bilateral ocular involvement. *J Vet Diagn Invest* 12:459–462.

Tachibana, J., Shimizu, S., Takiguchi, T., Ueno, Y., Kishimoto, I., Wada, M., and Konda, S. (1993) Lymphomatous polyarthritis in patients with peripheral T-cell lymphoma. *Leuk and Lymph* 11:459–467.

Zettl, A., Rüdiger, T., Konrad, M.A., Chott, A., Simonitsch-Klupp, I., Sonnen, R., Müller-Hermelink, H.K., and Ott, G. (2004) Genomic profiling of peripheral T-cell lymphoma, unspecified, and anaplastic large T-cell lymphoma delineates novel recurrent chromosomal alterations. *Am J Pathol* 164(5): 1837–1848.

Chapter 5

Acute Myeloid Leukemias

MYELOPROLIFERATIVE DISEASES

Myeloproliferative disease is a general categorization of disease characterized by medullary and extramedullary proliferation of one or more or marrow cell lineages with exclusion of the lymphoid leukemias and lymphomas. Myeloid neoplasms are classified by cellular lineage into four major categories of granulocytic, including neutrophils, eosinophils, and basophils; monocytic; erythroid; and megakaryocytic. In addition, myeloid neoplasms are divided into acute and chronic types based on the presentation and the proliferative rate of the neoplastic clone. Current classifications and terminology divide the myeloid neoplasms into the acute (AML) and chronic (CML) leukemias, with the latter grouped as the chronic myeloproliferative diseases (CMPD). A third group, the myelodysplastic diseases (MDS), are bone marrow disorders characterized by dysplastic changes in one or more marrow cell lines that may include an increase in the myeloblasts in blood and marrow that is below the 20% threshold level required for a diagnosis of AML.

Acute myeloid leukemias (AML) present most often with single involvement of one cell line, or multiple cell lines may be involved in a panmyelopathy. The presentation of AML is usually at the stage of marrow involvement approaching marrow failure with anemia and or thrombocytopenia. The peripheral blood manifestations may vary widely, with a marked elevation in total leukocyte count with blasts present or severe leukopenia with few neoplastic cells in circulation. The classification used in describing the myeloid neoplasms in animals is from the WHO system that is modified from the French-American-British (FAB) system that has earlier been applied to animal hematopathology (Table 5.1). The major differences in the FAB and WHO systems are a general lowering of the level of blast cells required for the diagnosis of AML from 30% of blasts in marrow to 20% of blasts in blood or marrow (Table 5.2). In addition, much more emphasis was given to the presence of cytogenetic changes and molecular markers in human neoplasms as they relate to the biology of the various leukemic subtypes. Most of the latter information is not applicable to animals, but the emphasis on the additional criterion of multilineage dysplasia based on morphologic criteria is readily apparent when present in animals. In humans, the prior or concurrent presence of myelodysplastic changes with AML is associated with a more aggressive neoplasm and a shorter course, and these principles also appear to apply in animals. Because of the importance of concurrent dysplasia to outcome, these associations are specifically stated to identify AML arising from progression of a myelodysplastic syndrome. In addition, if there is no prior history of MDS but dysplastic changes accompany AML at the time of diagnosis, the designation of the neoplasm would be AML with MDS. A third category of AML recognized in the WHO classification is the development of AML and/or MDS that arises subsequent to antineoplastic chemotherapy, generally of alkylating agent type.

The diagnosis of AML by morphologic means is based on the presence of at least 20% of blast cells in the marrow or peripheral blood. In order for these interpretations to be made it is essential that strict criteria be followed in the recognition and enumeration of myeloid blast cells, of which three levels of differentiation are defined.

The type I myeloblast has a round nucleus, or has only very shallow nuclear indentations, 2 red cells in diameter. The cytoplasm is scanty, with high peripheral basophilia, and agranular. The nucleus is densely stained with a poorly defined cribriform chromatin pattern and contains 2–4 nucleoli of varying prominence (Figs. 5.1–5.3).

The type II myeloblast is like type I with the presence of a few, generally less than 20, fine azurophilic granules. There may be slightly more cytoplasmic volume and some darker aggregations of nuclear chromatin (Figs. 5.4, 5.5).

The type III myeloblast has the nuclear features of type II with prominent nucleoli and small crescentic areas of chromatin aggregation at the edge of one or more nucleoli. The major difference from type I is the more abundant cytoplasmic volume and more numerous

Table 5.1. World Health Organization proposal for the classification of acute myeloid leukemia.

1. Acute Myeloid Leukemia with Recurrent Cytogenetic Abnormalities
Acute myeloid leukemia t(8;21)(q22;q222)
Acute promyelocytic leukemia t(15;17)(q22;q21)
Acute myeloid leukemia inv(16)(p13;q22)
Acute myeloid leukemia (v;11q23)
2. Acute Myeloid Leukemia with Myelodysplasia-Related Features
Acute myeloid leukemia evolvingfrom myelodysplastic syndrome
Acute myeloid leukemia with multilineage dysplasia without prior history of a myelodysplastic syndrome
3. Acute Myeloid Leukemia, Therapy-Related
Alkylating agent-related type
Topoisomerase II-related type
4. Acute Myeloid Leukemia, Not Otherwise Categorized
Acute myeloblastic leukemia, minimally differentiated (M0)
Acute myeloblastic leukemia without maturation (M1)
Acute myeloblastic leukemia with maturation (M2)
Acute promyelocytic leukemia (9M3) or microgranular (hypogranular) variant (M3V)
Acute myelomonocytic leukemia (M4) or acute myelomonocytic leukemia with increased marrow eosinophils (M4E0)
Acute monocytic leukemias
Acute monoblastic leukemia (M5A)
Acute monocytic leukemia (M5B)
Acute erythroid leukemias
Erythroleukemia (M6A)
Pure acute erythroid leukemia (M6B)
Acute megakaryoblastic leukemia (M7)
Acute basophilic leukemia
Acute panmyelosis with myelofibrosis

cytoplasmic granules (Figs. 5.6–5.9). Myeloblasts of type III differentiation are distinguished from promyelocytic leukemia (Figs. 5.10, 5.11) by their fine chromatin pattern, less cytoplasmic volume, and less prominent granules that are not discernible overlying the nucleus.

In the application of these criteria it is not important which type (I–III) of blasts are present, but for animal pathology as for human, it is not possible to distinguish the type I myeloblast from a large primitive lymphocyte on routine staining. For this reason, the level of poorly differentiated myeloid leukemia in animals has not been fully recognized, and consequently the incidence of AML is underestimated. In animals, one of the least common types of AML is the promyelocytic type for which the level of promyelocytes themselves is the criterion of diagnosis rather than of types I–III blast cells. Similarly, in pure erythroid leukemia (erythremic myelosis) the

Table 5.2. Summary of bone marrow changes in subtypes of acute myeloid leukemia.

AML M0
≥20% blasts <3% blasts MPO/SBB-positive ≥20% Blasts express one or more myeloid-associated bantigens (i.e., CD13, CD33) Negative for lymphocyte antigens
AML M1
≥20% blasts ≥3% blasts MPO/SBB-positive <10% promyelocytes and more mature neutrophils
AML M2
≥20% blasts ≥3% blasts MPO/SBB-positive ≥10% promyelocytes or more mature neutrophils
AML M3
≥20% myeloblasts and abnormal promyelocytes Blasts and promyelocytes with multiple Auer rods (faggot cells) Intense MPO/SBB positivity
AML M4
≥20% myeloblasts, monoblasts, and promonocytes ≥20% neutrophils ≥20% monocytic cells Monocytosis: $\geqslant 5 \times 10^9/L$[b]
AML M5A
≥20% myeloblasts, monoblasts, and promonocytes ≥80% monocytic cells with ⩾80% monoblasts
AML M5B
>20% myeloblasts, monoblasts, and promonocytes ≥80% monocytic cells with ⩾80% monoblasts Predominance of promonocytes
AML M6A
≥50% erythroblasts ≥20% of nonerythroid cells are myeloblasts Myeloblasts may contain Auer rods
AML M6B
≥80% proerythroblasts and basophilic erythroblasts with dyserythropoiesis Myeloblasts may or may not be increased
AML M7
≥20% blasts ≥50% megakaryocytic cells (megakaryoblasts, promegakaryocytes, and megakaryocytes) by immunologic markers or ultrastructural study

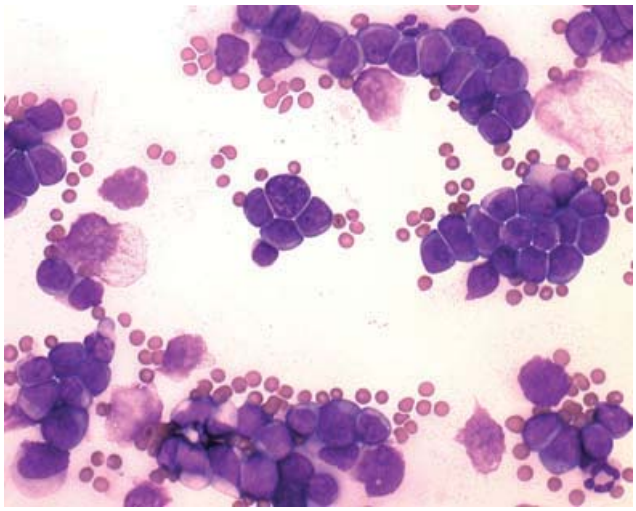

Figure 5.1. Cat: blood, acute myeloid leukemia. The tip of the blood smear from a sample with marked anemia and thrombocytopenia with abundant large atypical cells. Note that only 2 neutrophils are present. The cell in the center with the variegated nuclear appearance is entering metaphase. *Slide from R. M. Jacobs, DVM.*

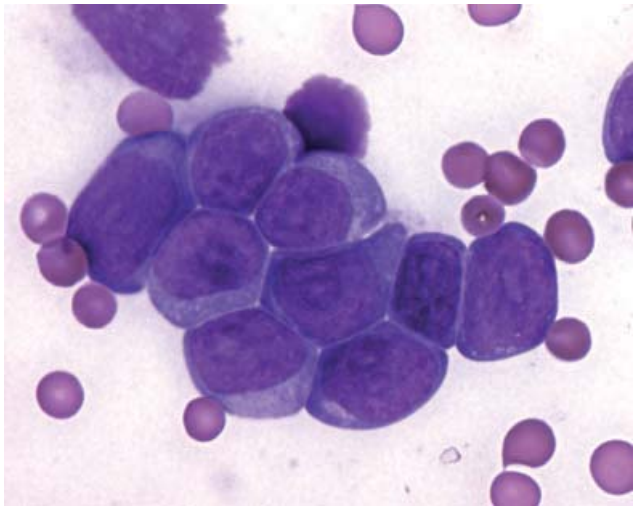

Figure 5.2. Cat: blood, acute myeloid leukemia. Detail of Figure 5.1. The nuclei are large and generally round with the cytoplasm varying in amounts from minimal to moderate with high basophilia and absent granulation. The chromatin pattern is dispersed and hyperchromatic with multiple large nucleoli. Without special staining, the cells are not distinguishable from acute lymphoid leukemia.

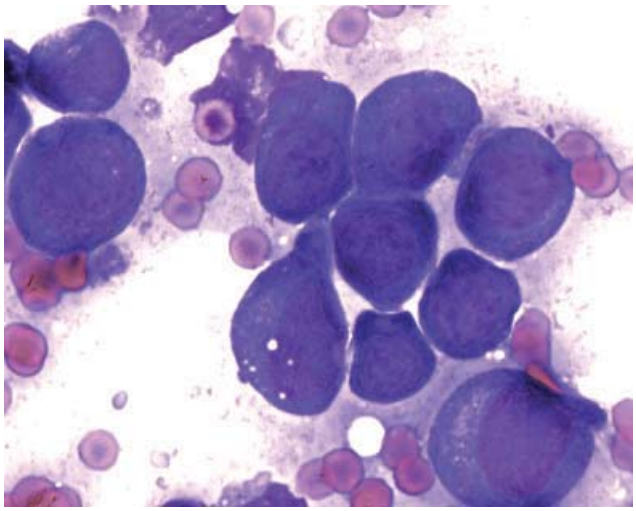

Figure 5.3. Cat: marrow, acute myeloid leukemia, likely M0. The nuclei are round without indentation and vary from 2–3 red cells in diameter, with a dense cribriform chromatin pattern with the cytoplasm variable in volume and very highly basophilic. Some of the larger cells appear to have focal granulation that may suggest some degree of differentiation. *Slide from R. M. Jacobs, DVM.*

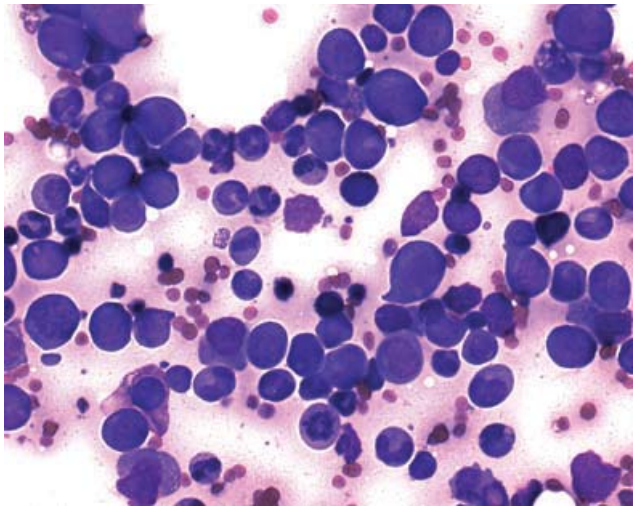

Figure 5.4. Cat: marrow, acute myeloid leukemia, type II myeloblasts. Note the preponderance of blast cells with few maturing cells of myeloid type that are likely the progeny of residual benign precursors. The nuclei vary moderately in size with the larger cells having slightly more cytoplasm, which retains a very deep basophilia and is largely agranular. *Slide from R. M. Jacobs, DVM.*

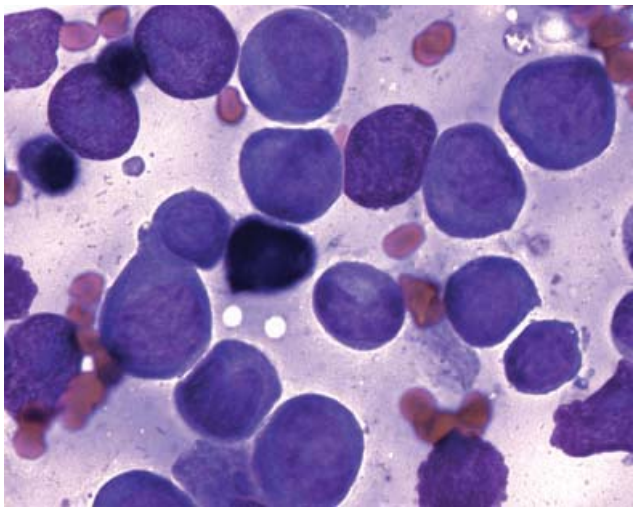

Figure 5.5. Cat: marrow, acute myeloid leukemia, type II myeloblasts. Detail of Figure 5.4. The nuclear chromatin is less cribriform with focal dense areas of chromocenter formation and nuclei containing 1–3 large nucleoli that tend to be obscured by the cytoplasmic basophilia. Some granulation is present in the cell just to the right of top center.

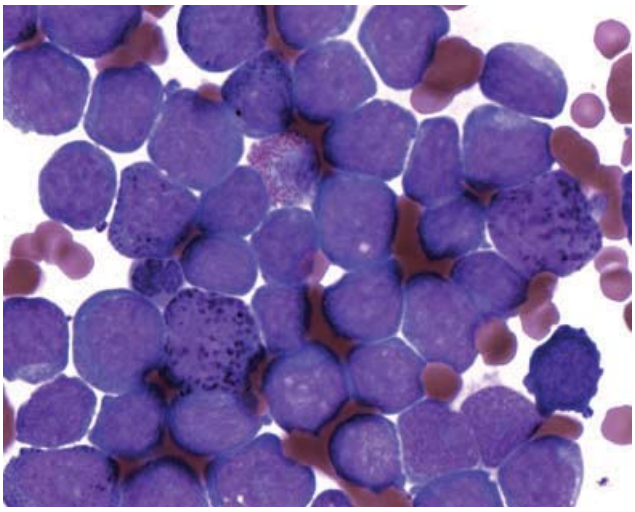

Figure 5.7. Cat: bone marrow, acute myeloid leukemia, myeloblasts type III. Detail of Figure 5.6. The nuclei have numerous areas of chromatin aggregation, but an important feature is the crescentic aggregation of chromatin that partially surrounds and defines many of the nucleoli. The cytoplasm is moderate in volume with little granulation except for cells that appear to be in basophil lineage.

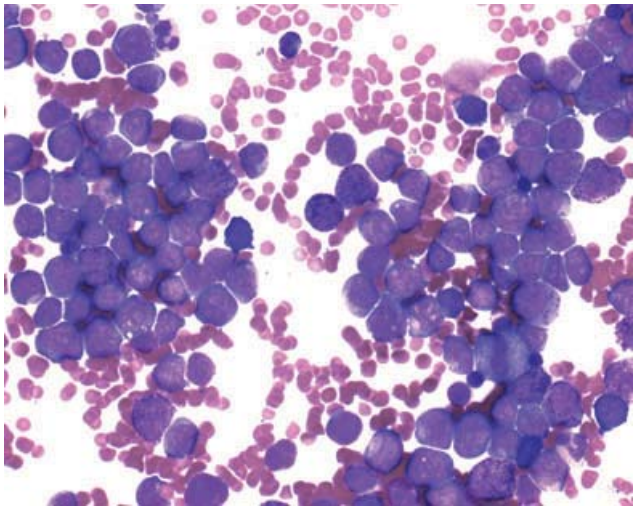

Figure 5.6. Cat: marrow, acute myeloid leukemia, type III myeloblasts. The chromatin aggregation is apparent at this magnification with several cells present having early differentiation to basophils (right center).

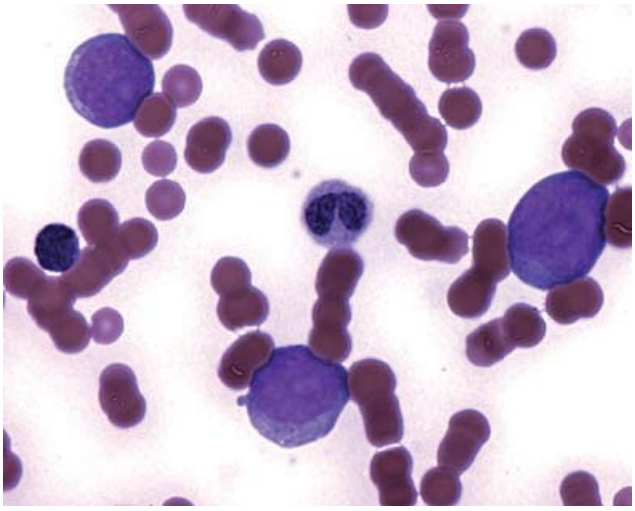

Figure 5.8. Cat: blood, acute myeloid leukemia, type III myeloblasts. The concentric ringing of chromatin around nucleoli is more apparent in the peripheral blood cells. The bilobed neutrophil in the center is typical of the abnormal maturation of neutrophils that enter the blood at a primitive stage and don't develop a normal segmentation.

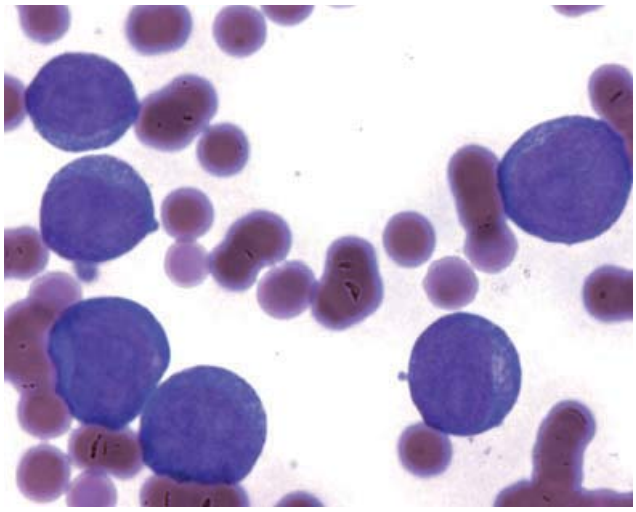

Figure 5.9. Cat: blood, acute myeloid leukemia type III myeloblasts. There are a few large chromocenters within the nuclei but there is more definite chromatin ringing of the nucleoli characteristic of the type III blasts.

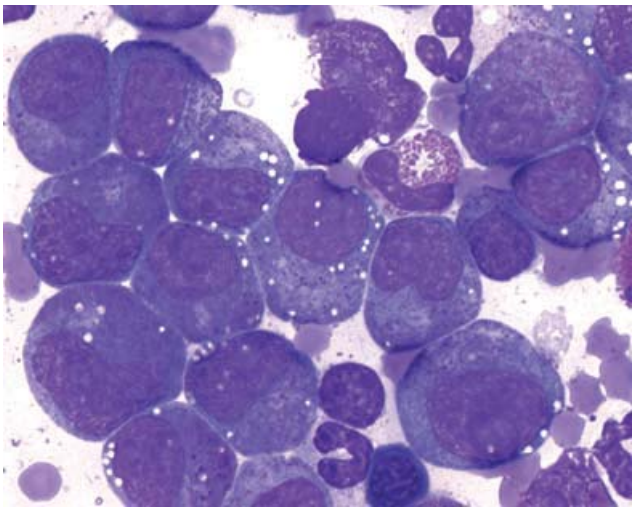

Figure 5.11. Cat: marrow aspirate, promyelocytic leukemia. Detail of Figure 5.10. These cells are among the largest seen in acute myeloid leukemias. The nuclei are 2.5–3 red cells in diameter with very abundant highly granulated cytoplasm. There are multiple prominent nucleoli irregularly accentuated by chromatin aggregation.

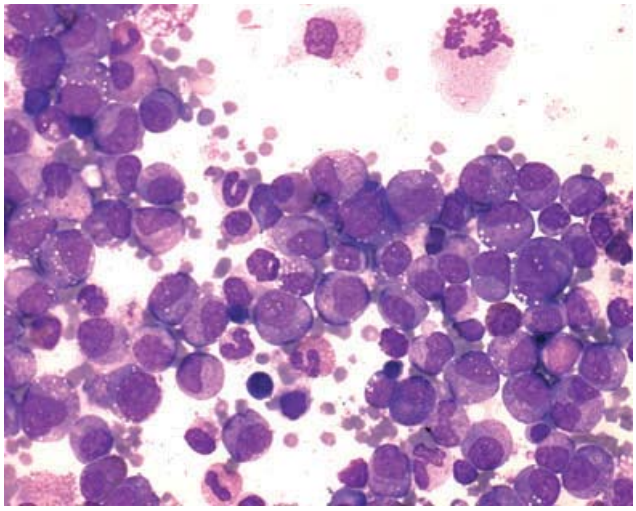

Figure 5.10. Cat: bone marrow aspirate, promyelocytic leukemia. The aspirate is very cellular and primarily composed of large cells with abundant highly granulated cytoplasm. There are a few residual marrow cells with a marked reduction in erythropoiesis and maturing myelopoiesis. There is a metaphase in the upper right, and the neoplastic cell in the lower right is binucleated. *Slide from R. M. Jacobs, DVM.*

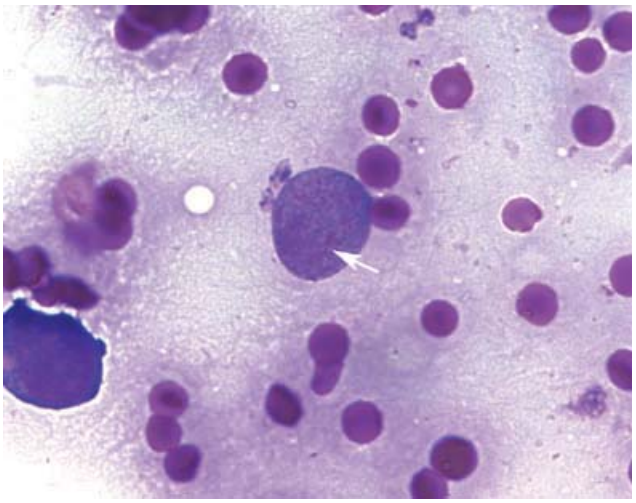

Figure 5.12. Dog: marrow aspirate, acute myeloid leukemia. The fragment of shed cytoplasm from a primitive cell has a number of azurophilic granules with a rodlike structure indicated by the arrow.

diagnosis is based on the combined presence of 80% or more of prorubricytes (also known as proerythroblasts) and basophilic rubricytes in place of a blast count. A rare neoplasm in humans and animals involving both erythroid and myeloid cell lineages is called *erythroleukemia*, also known as M6A. Erythroleukemia is identified by a count on the myeloid precursor blasts only, with the blast level in the erythroid line not included in the total, which needs to exceed 20% for lesion identification. In humans and only very rarely in animals, myeloblasts may contain azurophilic rods of aggregated and crystallized granule material known as *Auer rods* that are 2–3 um in length and about 0.5 um in width (Fig. 5.12). The presence of these bodies is taken as indication that the blasts are of type II level of differentiation.

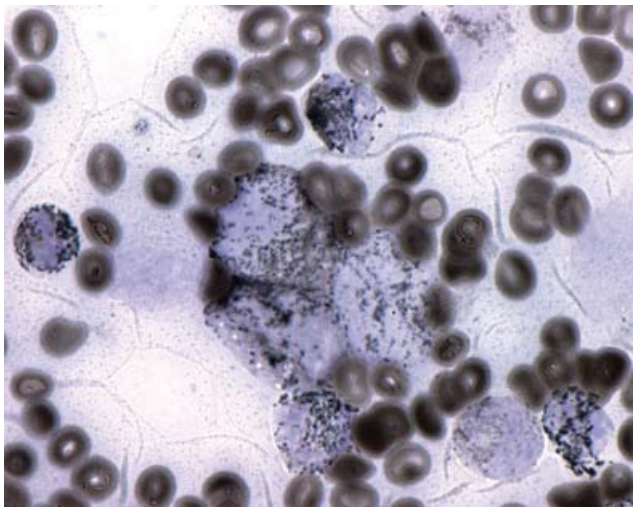

Figure 5.13. Dog: marrow, acute myelomonocytic leukemia, Sudan Black-B stain. The SBB stain marks the cytoplasmic granules of both precursors (center) and mature granulocytes at the margins of the image. *Slide from R. M. Jacobs, DVM.*

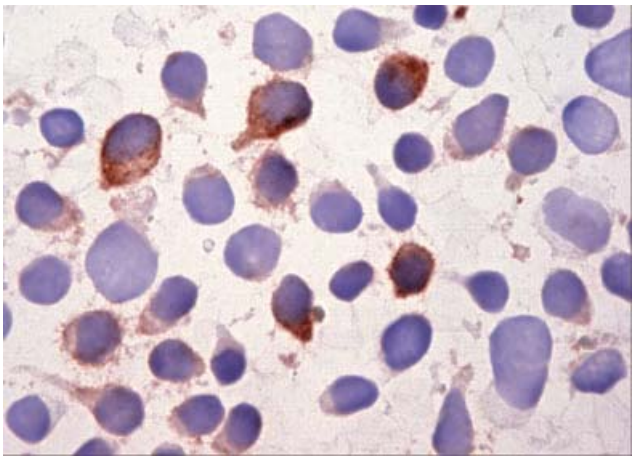

Figure 5.15. Dog: marrow, acute myeloid leukemia. Detail of Figure 5.14. There is irregular staining not related to cell size or cytoplasmic volume. The cellular morphology and staining pattern is exactly as described for human AML of minimally differentiated type. *Image from W. Vernau BVSc, reprinted with permission of the American Society for Veterinary Clinical Pathology.*

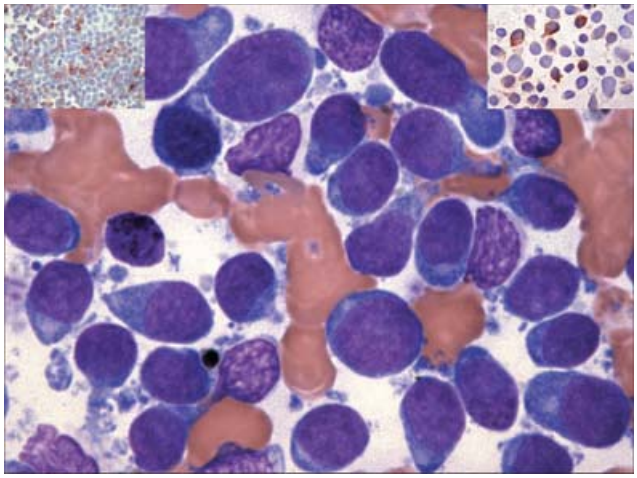

Figure 5.14. Dog: marrow, acute myeloid leukemia. Myeloperoxidase (MPO) stain in the upper right (cytology) and in the upper left (histology of marrow). A rapidly progressive poorly differentiated leukemia has a fine chromatin structure with a variable volume of cytoplasm, often eccentrically placed and without cytoplasmic granulation. The cells were negative with immunocytochemical staining for B- and T-cell lymphocytes and (typically) irregularly positive staining in both cytologic and histologic preparations with a monoclonal antibody against canine myeloperoxidase. *Images from W. Vernau, BVSc, reprinted with permission of the American Society for Veterinary Clinical Pathology.*

The identification of myeloblasts is based on cytochemical and immunohistochemical identification of cytoplasmic myeloperoxidase (MPO). In general for marrow and blood in cytologic preparations, the cytochemical detection of MPO is efficient and can be roughly substituted for by Sudan Black-B (SBB) staining, which marks the azurophilic granules and is therefore not as reliable for myeloblasts of the type I level of differentiation (Fig. 5.13). For formalin-fixed and paraffin-embedded tissues, an immunohistological reaction is standard in human preparations, and a monoclonal antibody with this reactivity in fixed tissues has now been developed with activity against dog and cat tissue and likely other animals as well (Figs. 5.14, 5.15). In cytologic preparations, the identification of cells of monocytic lineage can be reliably made with the nonspecific esterase (NSE) reaction (Figs. 5.16, 5.17). Again on cytologic preparations, the chloroacetate esterase (CAE) reaction is positive on neutrophils to the level of promyelocytes, but it is not present in blasts at any level of differentiation and therefore is less useful than SBB and MPO for that purpose (Fig. 5.18). However, although the blasts may not be specifically identified, the old axiom that "they can be identified by the company they keep" applies, and if the progeny are of granulocytic type as identified by CAE it can be inferred that the precursors must be myeloblasts.

REFERENCES

Ackerman, G.A. (1950) Microscopic and histochemical studies on the Auer bodies in leukemic cells. *Blood* 5:847–863.

Bennett, J.M., Catovsky, D., Daniel, M.T., et al. (1976) Proposals for the classification of the acute leukaemias. *Br J Haematol* 33:451–458.

Bennett, J.M., Catovsky, D., Daniel, M.T., et al. (1985) Proposed revised criteria for the classification of acute myeloid

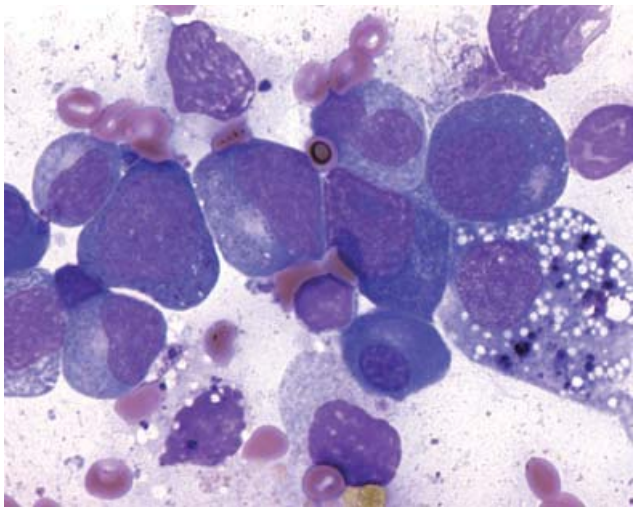

Figure 5.16. Dog: marrow aspirate, acute myelomonocytic leukemia. The abundant cytoplasm and fine cytoplasmic granulation identifies these as primitive myeloid cells. The fine cytoplasmic vacuolation in some of the primitive cells is consistent with, but not specific for, early monocytic differentiation. Benign macrophage (right) has a smaller nucleus with nucleolus and abundant phagocytized debris. *Slide from R. M. Jacobs, DVM.*

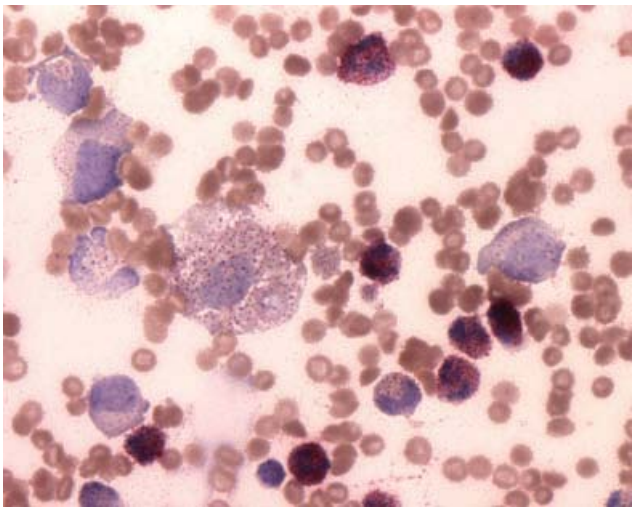

Figure 5.18. Dog: marrow aspirate, acute myelomonocytic leukemia. Phenotype of Figure 5.16. With chloroacetate esterase staining for the myeloid or granulocytic line, the neutrophils and their precursors are strongly labeled and the macrophage in the center and monocytic precursors are negative with fine artifactual marking. *Slide from R. M. Jacobs, DVM.*

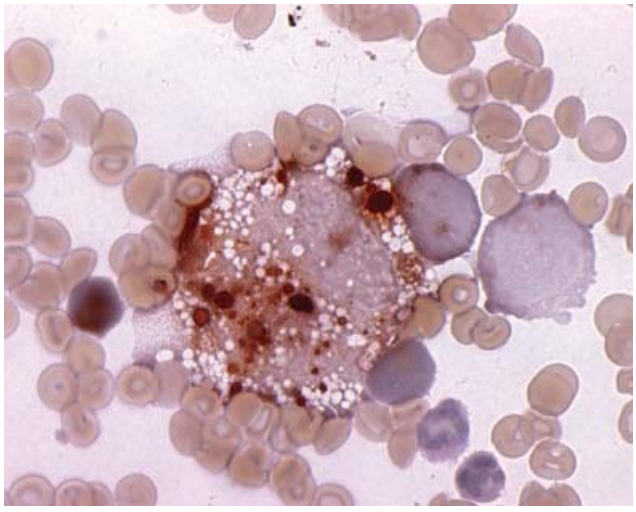

Figure 5.17. Dog: marrow, acute myelomonocytic leukemia. Phenotype of Figure 5.16. With nonspecific or alpha naphthyl esterase staining, the benign macrophages in the center are very positive, as are the smaller neoplastic cell at the left and the large oval cell to the right of the macrophage. The largest cell at the right and the precursor at the lower right of the macrophage are negative indicating the specificity of the stain and that these precursors negatively stained are of myeloid rather than monocytic lineage. *Slide from R. M. Jacobs, DVM.*

leukemia: A report of the French-American-British cooperative group. *Ann Intern Med* 103:626–629.

Berger, R., Bernheim, A., Daniel, M.T., et al. (1982) Cytologic characterization and significance of normal karyotypes in t(8;21) acute myeloblastic leukemia. *Blood* 59:171–178.

Brunning, R. (1999) Proposed World Health Organization (WHO) classification of acute leukemia and myelodysplastic syndromes. *Mod Pathol* 12:102.

Brunning, R., and McKenna, R.W. (1994) *Tumors of the Bone Marrow*, 3rd series, fasc. 9. Armed Forces Institute of Pathology, Washington, D.C. pp. 19–100.

Brunning, R.D. (2001) Acute myeloid leukemia. In Knowles, D.M. (ed.), *Neoplastic Hematopathology*, 2nd ed. Lippincott Williams & Wilkins, Philadelphia, pp. 1667–1715.

Buccheri, V., Shetty, V., Yoshida, A., et al. (1992) The role of an anti-myeloperoxidase antibody in the diagnosis and classification of acute leukaemia: A comparison with light and electron microscopy, cytochemisty. *Br J Haematol* 80:489–498.

Cheson, B.D., Cassileth, P.A., Head, D.R., et al. (1990) Report of the National Cancer Institute–sponsored workshop on definitions of diagnosis and response in acute myeloid leukemia. *J Clin Oncol* 8:813–819.

Head, D.R. (1996) Revised classification of acute myeloid leukemia. *Leuk* 10:1826–1831.

Rumke, C.L. (1960) Variability of results in differential counts on blood smears. *Triangle* 4:154–158.

MYELOID AML

Minimally Differentiated M0 and Without Maturation M1

These two entities, as defined in the WHO classification, are considered together here since in animal pathology they are not distinguishable by technologies currently in use. Acute myeloid leukemia (AML) of these types are more rarely recognized than rarely occurring. Vernau and Moore found that in dogs with acute leukemia, 55% of these were AML with the remainder being acute lymphoid leukemia (ALL), of which more than a third were of LGL type. On routine blood, staining these groups can't be reliably differentiated.

Definition

AML of minimal differentiation is a peracute disease of clonal proliferation of poorly differentiated myeloid precursors that lack evidence of myeloid lineage on routine blood stains and most cells on specific cytochemical staining. Fewer than 3% of the blast cells are positive for myeloperoxidase (MPO) and Sudan Black-B (SBB), and at least 20% of nucleated marrow cells must be of blast cell type.

Epidemiology and Incidence

Nothing is known of the causation of AML, but it is assumed that the uncontrolled proliferation results from chromosomal injury in a primitive precursor of myeloid lineage. Historically, AML has been identified most often in the cat but it is likely that AML of more differentiated type was more frequent in cats prior to control of FeLV. The true incidence of AML of minimal differentiation is likely much higher than recognized and occurs in all domestic and wild animals, but it is more common in cats and dogs, is occasionally found in swine, and is rare or rarely recognized in other species.

Clinical Presentation and Features

Animals presented with AML of M0 and M1 levels of maturation are typically young, less than 5 years old, in good body condition, and with a shiny hair coat indicative of a disease of very rapid onset. Astute animal owners may present animals because of reduced activity and appetite that have obvious leukemia on examination of blood. However, in many cases the animals are presented in collapse with anemia, thrombocytopenia, and epistaxis.

Pathologic Features

Blood

In general, the total leukocyte count in AML is usually lower than in CLL and may be lower than normal, but wide variation occurs with the only maxim that blast cells are always present in peripheral blood. In a review of a small number of cases in the dog, the total leukocyte counts ranged from 3,800–9,600/ul, with platelets 30,000–111,000/ul and hemoglobin levels 4.3–12.0 g/dl. Typically, the mature neutrophils make up less than 20% of the total differential, with the rest about evenly divided between blasts and immature myeloid cells and lymphocytes. The only neutrophils present are the progeny of benign precursors, and these have reduced normal granulation with mild toxic granulation and vacuolation (Figs. 5.19–5.21). Residual lymphocytes are small and mature and eosinophils and monocytes are absent. The platelets may be rare, but they are generally severely reduced in numbers. Those present are small, usually half the size of a red cell, poorly granulated, and with faint peripheral cytoplasmic basophilia. There are often numerous fine stellate, cytoplasmic projections, particularly if there are bleeding and widespread endothelial injury (Fig. 5.22). One of the major difficulties in interpreting the platelets in AML is that the neoplastic cells are fragile and lose their cytoplasm, and these fragments will be counted as platelets by flow cytometers causing the degree of thrombocytopenia to be underestimated. The anemia is normochromic and nonresponsive with mild anisocytosis, no polychromasia, and numerous spherocytes. The spherocytes are present because of splenic overload as a result of the numbers of degenerating neoplastic cells causing hypofunction in clearing aged blood cells of all types. These spherocytes and red cells injured in areas of endothelial damage may be accompanied by red cells with

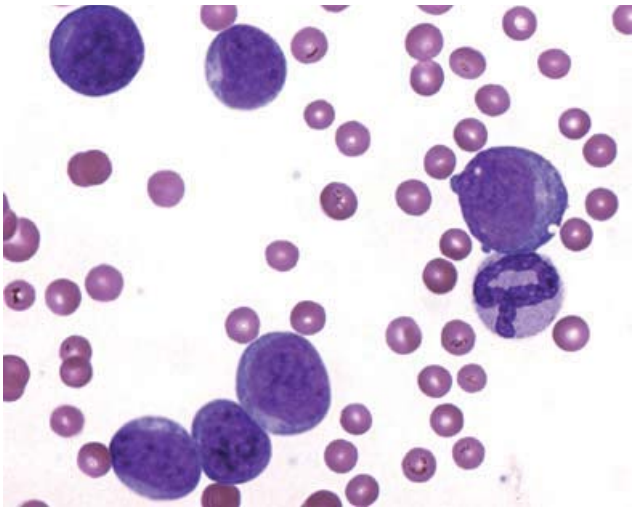

Figure 5.19. Cat: blood, acute myeloid leukemia. There is an absence of platelets with a single granulocyte too large for a neutrophil and likely a poorly granulated basophil. *Slide from R. M. Jacobs, DVM.*

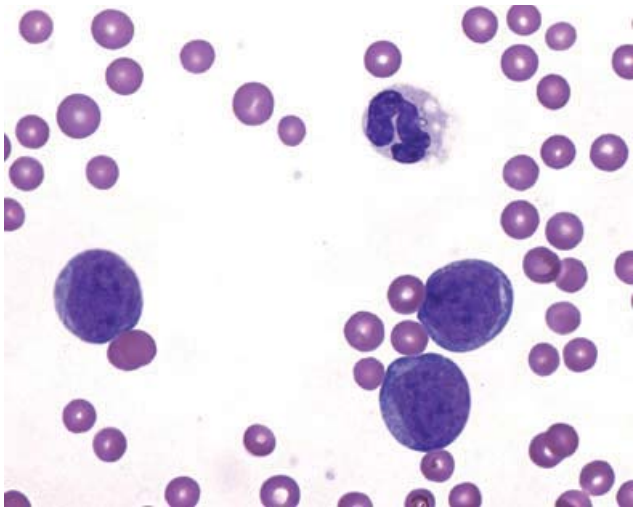

Figure 5.20. Cat: blood, acute myeloid leukemia, same case as Figure 5.19. The neutrophil (top) has a mild reduction in cytoplasmic volume with an almost complete absence of granulation and multiple large cytoplasmic vacuolations. The nucleus is progressing to hypersegmentation suggesting prolonged peripheral blood sojourn due to reduced clearance.

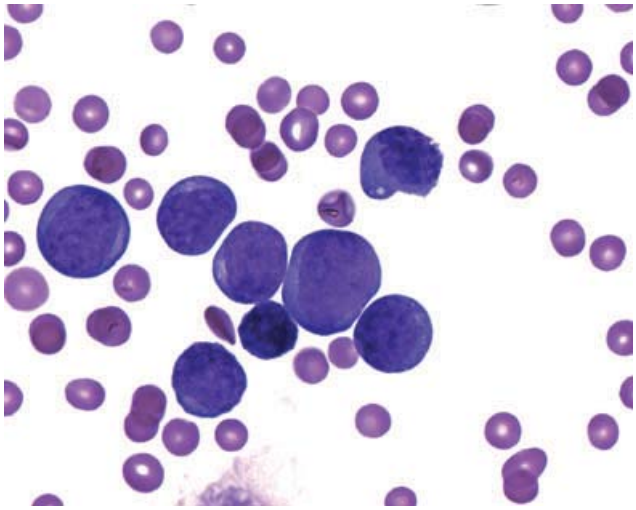

Figure 5.21. Cat: blood, acute myeloid leukemia, same case as Figure 5.19. The cell in the upper right is degenerating, and its presence in the peripheral blood is indicative of impaired splenic function due to sinus colonization by tumor cells and increased numbers of cells degenerating in the peripheral circulation. The smaller cell in the field is likely a benign lymphocyte of medium size.

Howell-Jolly bodies (Fig. 5.23). Erythropoiesis is severely depressed and the reticulocyte count is usually less than the normal level of 1% or 60,000/ul, but an occasional rubricyte may be present and these may be immature to the level of prorubricytes due to leukemic myelophthisis.

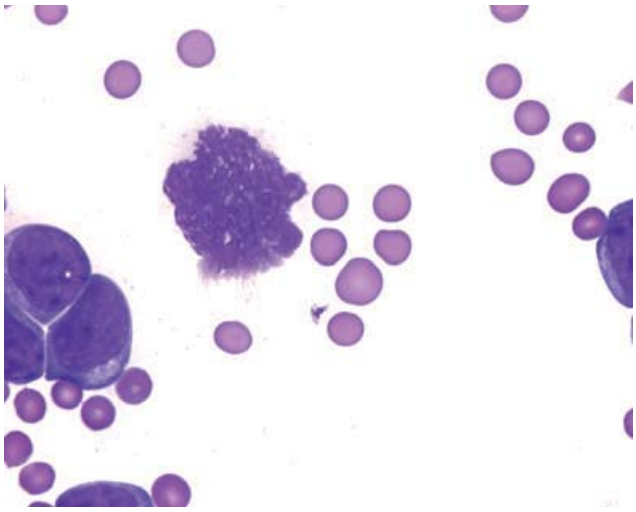

Figure 5.22. Cat: blood, acute myeloid leukemia, same case as Figure 5.19. There is a single small platelet in center field. The granules are aggregated and the cytoplasm is stellate suggestive of thrombocytopenic endothelial injury.

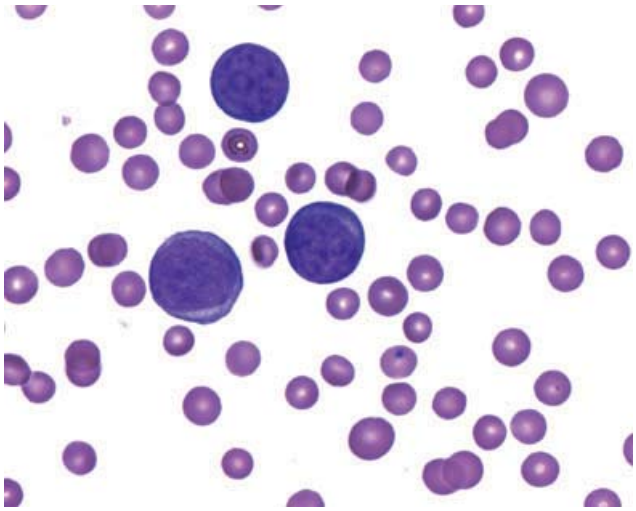

Figure 5.23. Cat: blood, acute myeloid leukemia, same case as Figure 5.19. The neoplastic precursor cells are accompanied by a Howell-Jolly body (lower right) that is a further indication of impaired splenic function.

Bone Marrow

The animal with AML of M0–M1 level of maturation may require a blood transfusion to increase the platelet level to where a bone marrow aspiration or core can be carried out. A Jamshidi procedure with an aspiration followed by a core biopsy is always the preferred method of confirming the diagnosis. This strategy permits the widest range of diagnostic procedures to be carried out with SBB reactive on a marrow aspirate but not on paraffin-embedded sections. The marrow is always hypercellular,

and in aspirated samples there are few fat cells and almost complete phthisis of normal cell lines (Fig. 5.24). The hemosiderin pattern is coarse but not markedly elevated. The cells present are primarily of primitive type with round nuclei and metamyelocytes may be the most mature cell present of myeloid type and these are likely the progeny of residual benign precursors (Fig. 5.25). If a core biopsy is taken, there may be focal hemorrhagic necrosis, especially if thrombocytopenia has been severe. The cellularity is usually 90% or greater with loss of most fat cells, and the cell proliferation is closely related to the bone trabeculae (Fig. 5.26). There is an apparent absence of megakaryocytes (Fig. 5.27) and few apparent rubricytes (Fig. 5.28). The neoplastic cells are of type I blast cells with round nuclei that are deeply stained and on cytological preparations have a coarse ropy type of chromatin pattern that looks like overstained cribriform type

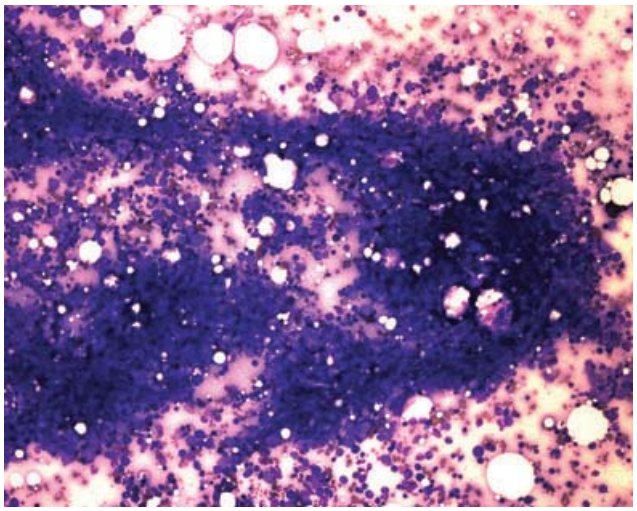

Figure 5.24. Cat: marrow aspirate, acute myeloid leukemia. The marrow granules have very high density with few fat cells and few fat cells in the surrounding cellular area. These changes would equate to a marrow cellularity of over 80% on histological examination. *Slide from R. M. Jacobs, DVM.*

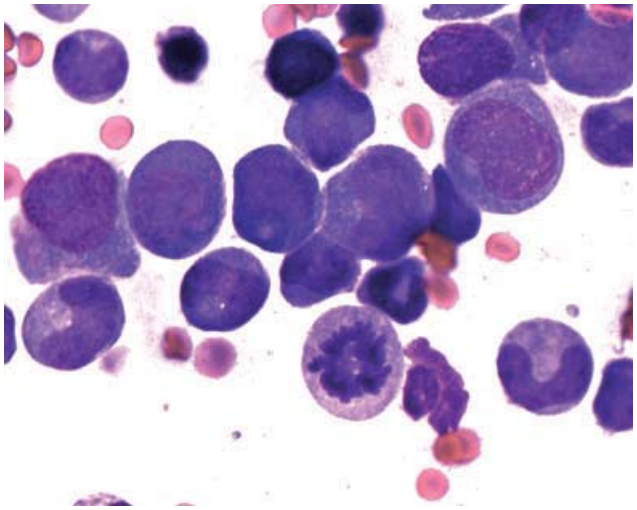

Figure 5.25. Cat: marrow aspirate, acute myeloid leukemia, same case as Figure 5.24. The most prevalent granulocytes are large metamyelocytes that may be hyperdiploid due to myelodysplasia and or tumor-induced folate deficiency.

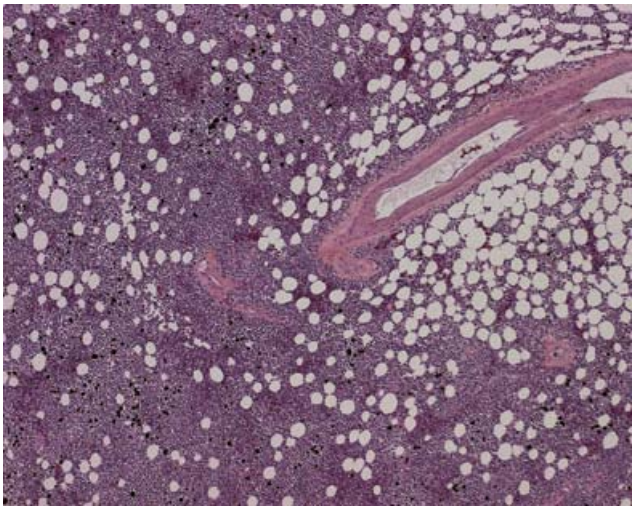

Figure 5.26. Dog: bone marrow, acute myeloid leukemia, midshaft femoral tissue. The entire area is hypercellular with the tissue in the upper right of normal cellularity for a dog in homeostasis, however, the entire area would be completely fatty in a normal adult dog. The small dark foci are hemosiderin-bearing macrophages typical of the coarse iron pattern of cancer.

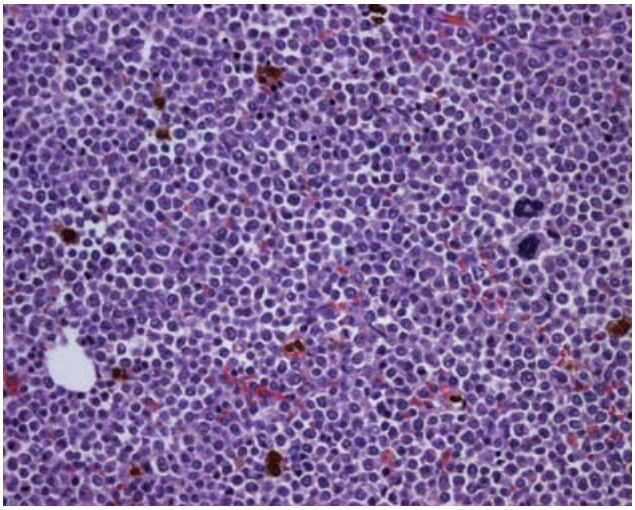

Figure 5.27. Dog: bone marrow, acute myeloid leukemia. The marrow in this region is almost solidly cellular, but megakaryocytes are remarkably reduced in numbers with those present having reduced cytoplasmic volume.

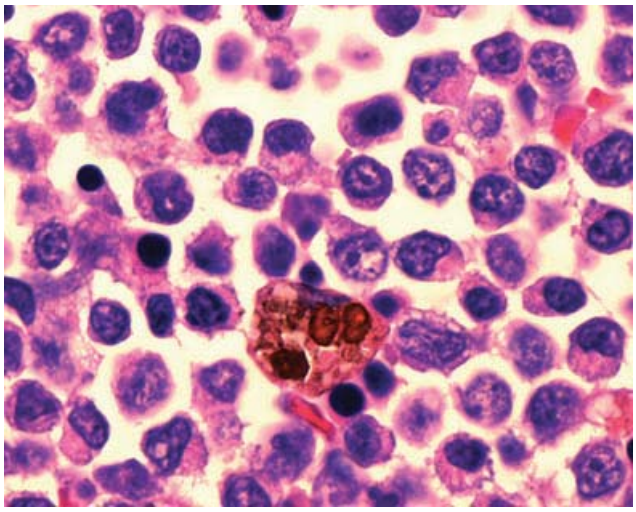

Figure 5.28. Dog: marrow, acute myeloid leukemia. Detail of Figure 5.26. There is a macrophage containing coarse aggregates of hemosiderin lower center with a single polychromatic rubricyte below and a second in left center. These cells are markedly deficient and normally appear in clusters with a range of differentiation from blasts to metarubricytes. There is also a complete loss of marrow granulocyte reserves with an absence of neutrophils.

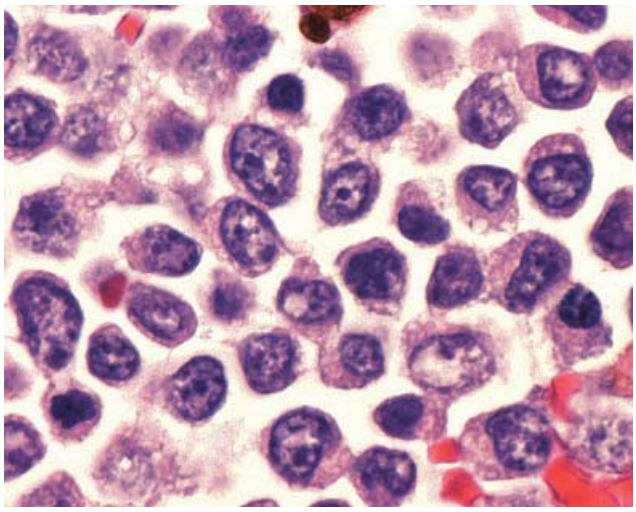

Figure 5.29. Dog: marrow, acute myeloid leukemia. Detail of Figure 5.26. On histological preparations, the nuclei are vesicular with the chromatin largely peripheralized and marked parachromatin clearing but with the nucleoli prominently apparent. The small volume of cytoplasm that is deeply stained is apparent as well as apparent cell boundaries.

with marked parachromatin clearing on histological section (Fig. 5.29). One to three nucleoli are present but no evidence of larger chromocenters of more differentiated cells. There is minimal cytoplasm that has a pale perinuclear halo and is darker at the outer margin. There are no cytoplasmic granules on routine Wright's or Giemsa staining.

Lymph Node

All lymph nodes will have a degree of lymphoid atrophy even if uninvolved with metastatic myeloid neoplasm. There is atrophy of germinal centers and thinning of the paracortex (Fig. 5.30), usually with some crenation of the nodal capsule that may have neoplastic colonization if the node is extensively involved. Unlike high-grade lymphoma, AML tends not to bridge the peripheral sinus and involves the cortex and capsule without filling the peripheral sinus. Initially at least, the tumor cells home to the medullary cords (Fig. 5.31), and the progression of the neoplasm can be gauged by the presence and displacement of benign extramedullary hematopoiesis (Fig. 5.32). As marrow phthisis develops, the mobile benign stem cells migrate to other areas of the body with a fine reticular vascular network like the nodes, spleen, adrenals, pituitary, and liver. There is initial colonization of the medullary cords by the benign cells, which are made most obvious by the presence of megakaryocytes, but trilineage hematopoiesis will be present to some degree (Fig. 5.33).

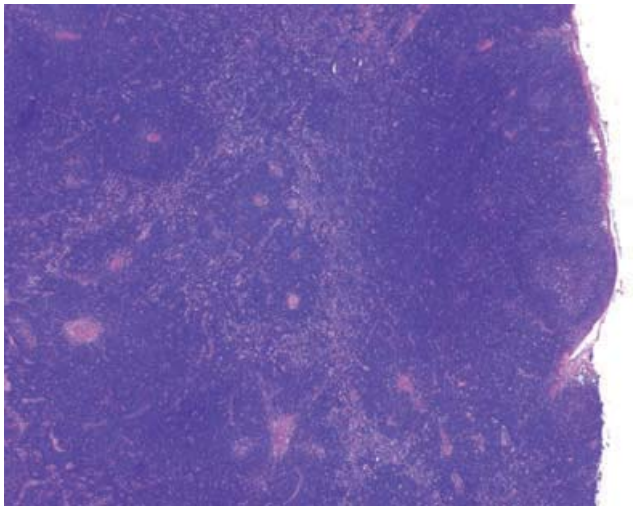

Figure 5.30. Cat: lymph node, acute myeloid leukemia. There is a small fading follicle (right center) with cortical atrophy and heavy infiltration of the medullary cords and sinuses with neoplastic myeloid cells.

As the neoplasm progresses, there is displacement of the benign cells to the medullary sinuses with the more monomorphic neoplastic cells occupying the medullary cords. The presence of these cells is not apparent unless looked for, and on architectural examination it appears that a larger lymphoid population has replaced the plasma cells and medium lymphocytes that normally occupy the area. The megakaryocytes, if present, again

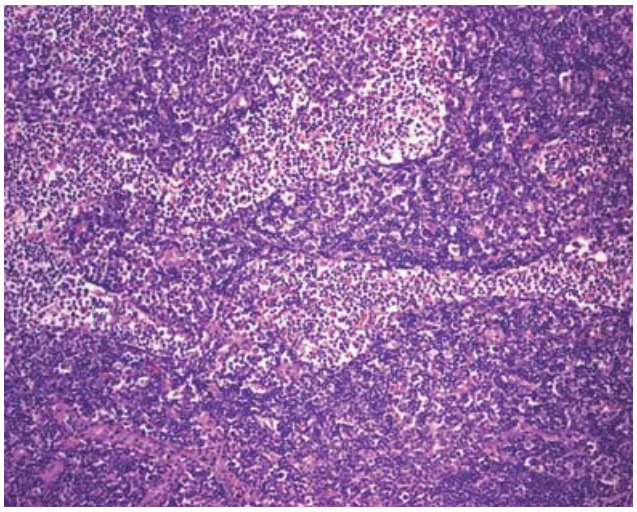

Figure 5.31. Cat: lymph node, acute myeloid leukemia, same tissue as Figure 5.30. There is marked irregular dilation of medullary sinuses that are heavily infiltrated with neoplastic cells, and medullary cords are irregularly infiltrated with focal bridging of sinus membranes.

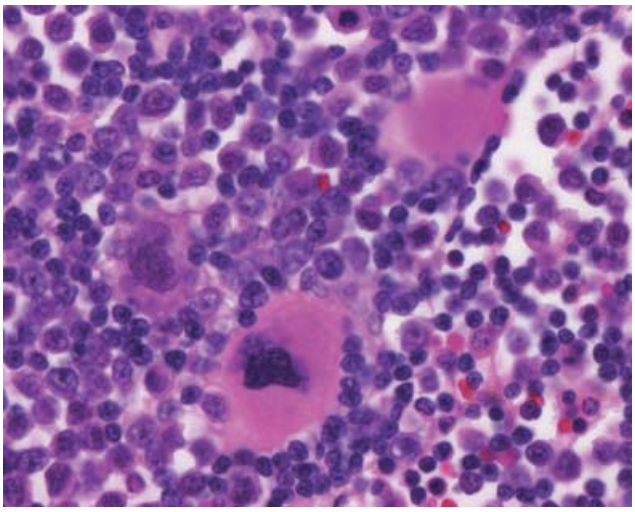

Figure 5.33. Cat: node, acute myeloid leukemia, same tissue as Figure 5.30. Three megakaryocytes are part of an area of extramedullary hematopoiesis along with a few rubricytes that remain within the medullary cord with the medullary sinus lying below to the right.

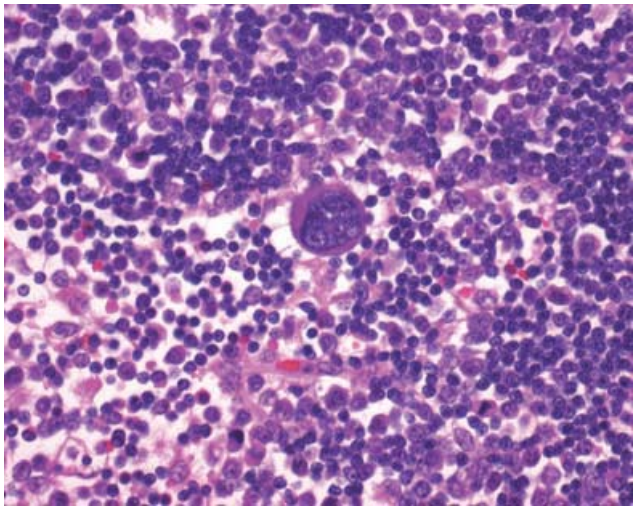

Figure 5.32. Cat: node, acute myeloid leukemia, same tissue as Figure 5.30. There is extensive colonization of medullary sinus by neoplastic myeloid cells center with an intervening area of the medullary cord that is heavily infiltrated with neoplastic cells (above). In this medullary sinus at upper center, a single megakaryocyte has been displaced from the medullary cord to the sinus area by aggressive colonization of the medullary cord by neoplastic cells.

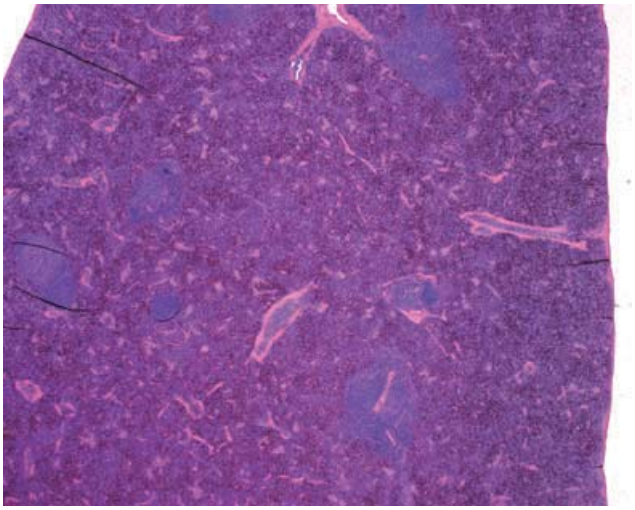

Figure 5.34. Cat: spleen, acute myeloid leukemia, same case as Figure 5.30. There is an absence of germinal centers and moderate irregular atrophy of periarteriolar lymphoid sheaths. The sinus areas are solidly cellular with uniform infiltration of neoplastic cells.

indicate the presence of benign hematopoiesis in the sinus areas that is apparently not as fertile an area for cellular proliferation by either benign or malignant hematopoiesis.

Spleen

The spleen is symmetrically enlarged and almost never with focal tumor, which changes the contour of the capsule as is common in lymphomas. Architecturally, there is complete loss of germinal centers (Fig. 5.34) that may be evident in areas of follicular hyalinosis adjacent to terminal arterioles (Fig. 5.35). There is atrophy of the thymic-dependent periarteriolar lymphoid sheaths, with most reduced to a layer of small lymphocytes 1–2 cells in depth surrounding the small arterioles, and on cytologic level of examination even some of these may be seen to

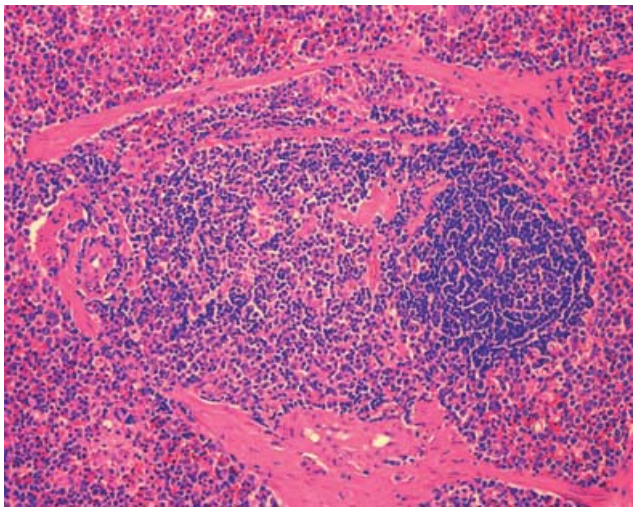

Figure 5.35. Cat: spleen, chronic myelogenous leukemia, same tissue as Figure 5.34. There is a terminal arteriole at the left with complete loss of lymphoid sheath, with the central area an involuted germinal center with insudation of amorphous proteinaceous material of follicular hyalinosis type left of a small foci of residual small lymphocytes of mantle cell type.

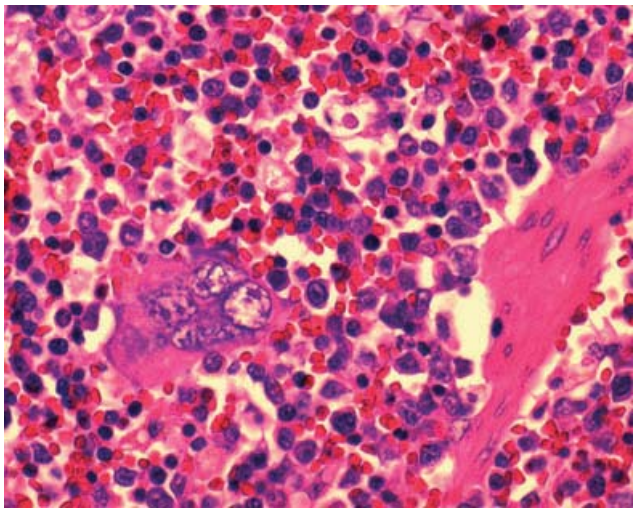

Figure 5.36. Cat: spleen, acute myelogenous leukemia, same tissue as Figure 5.34. A single megakaryocyte with dysplastic changes of delayed nuclear fusion and reduced cytoplasmic volume is surrounded by a few rubricytes with infiltrating neoplastic cells occupying the area between the megakaryocyte and smooth muscle trabeculae.

be plasma cells rather than the typical small lymphocyte investment. The main change in the spleen on architectural examination is a bland diffuse appearance due to loss of the lymphoid complement and absence of areas of sinus congestion. Cytologically, there is complete and diffuse filling of the sinus areas with neoplastic cells. The

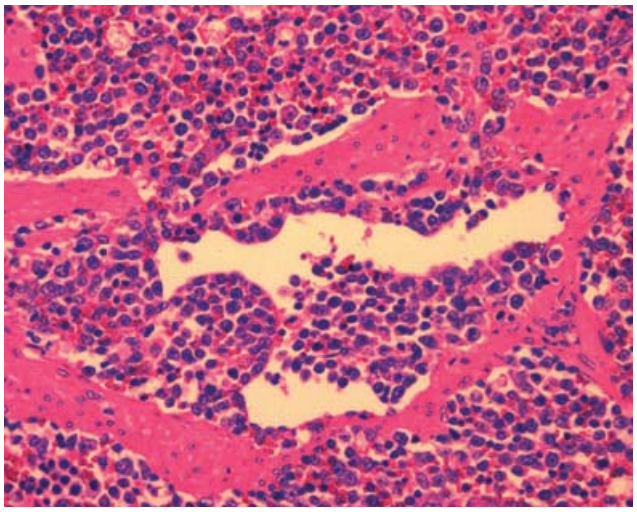

Figure 5.37. Cat: spleen, acute myeloid leukemia, same tissue as Figure 5.34. There is extensive subendothelial colonization of the large muscular vein or sinus typical of advanced AML.

hemosiderin pattern is coarse granular, and benign hematopoiesis is generally restricted to paratrabecular areas and identified by an occasional megakaryocyte (Fig. 5.36). In advanced cases, there is usually subendothelial colonization of the large muscular veins (Fig. 5.37).

Other Organs

The liver is always involved to some degree, and the most apparent effects may be centrolobular ischemic degeneration and focal areas of hemorrhagic infarction. The neoplastic cells primarily involve the hepatic sinuses, and if there is a low leukocyte level they are not obvious. There may be some portal colonization, but unlike the lymphomas this is focal and may be mixed with residual benign hematopoiesis (Figs. 5.38, 5.39). If examined, the thymus is atrophic and usually not involved with neoplasm (Figs. 5.40, 5.41). Changes secondary to marrow failure (Figs. 5.42, 5.43) include hemorrhage and septic foci in lung, skin, and other areas with little cellular reaction due to the severe neutropenia.

Cytogenetic and Molecular Features

This is now an area of investigation in animals more related to the lymphomas because they are much more commonly diagnosed if encountered. A high incidence of chromosomal changes is found in human AML of M0 and M1 types, including monosomy 5q or 7q and rearrangements involving 12p12–13 and 2p12–15.

Cell of Origin

A primitive precursor of committed myeloid lineage with capability of continued proliferation without maturation or differentiation is the accepted progenitor of AML.

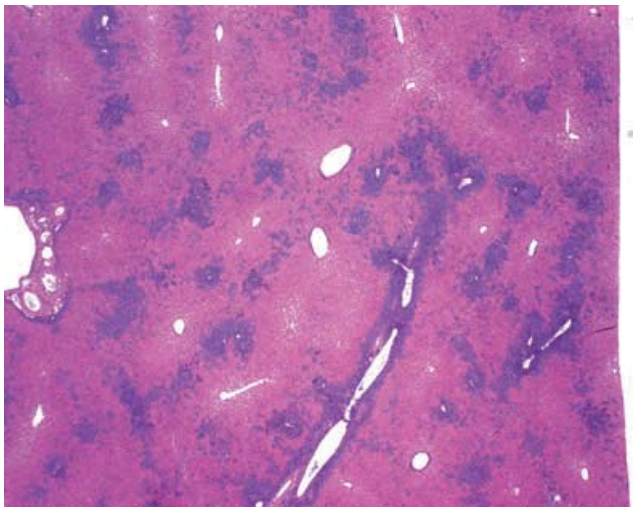

Figure 5.38. Cat: liver, acute myeloid leukemia, same case as Figure 5.30. There is perivascular colonization most prominent around portal areas.

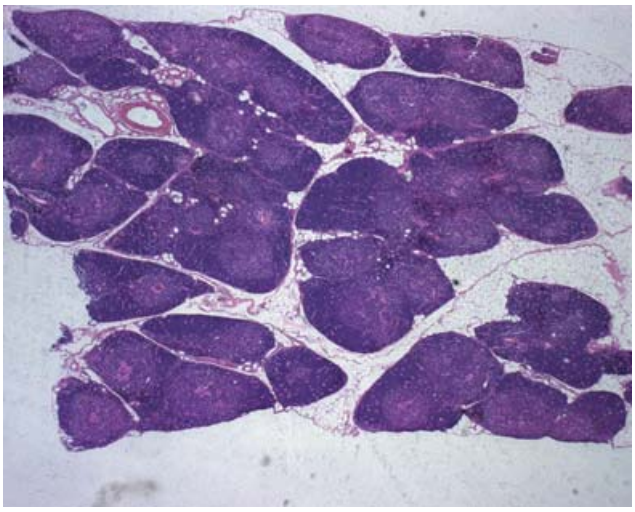

Figure 5.40. Cat: thymus, acute myeloid leukemia, same case as Figure 5.30. There is marked atrophy involving the cortical areas to a greater extent than the medulla with reduced follicle size and wide lobular separation.

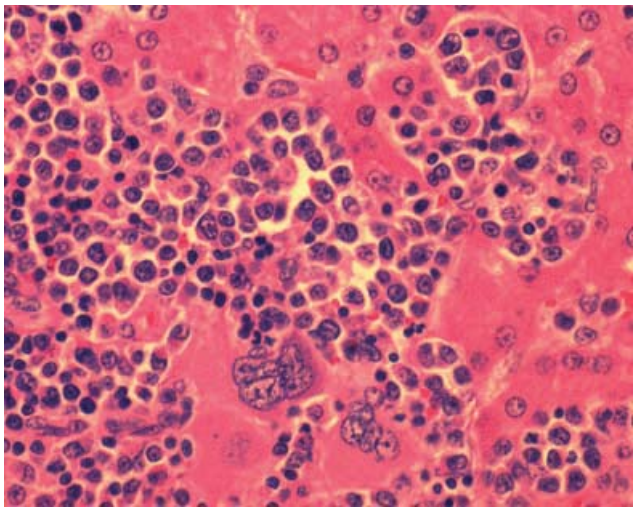

Figure 5.39. Cat: liver, acute myeloid leukemia. Detail of Figure 5.38. There is irregular colonization of hepatic sinuses with compression and displacement of hepatocytes and a mixture of neoplastic myeloid cells and extramedullary hematopoiesis.

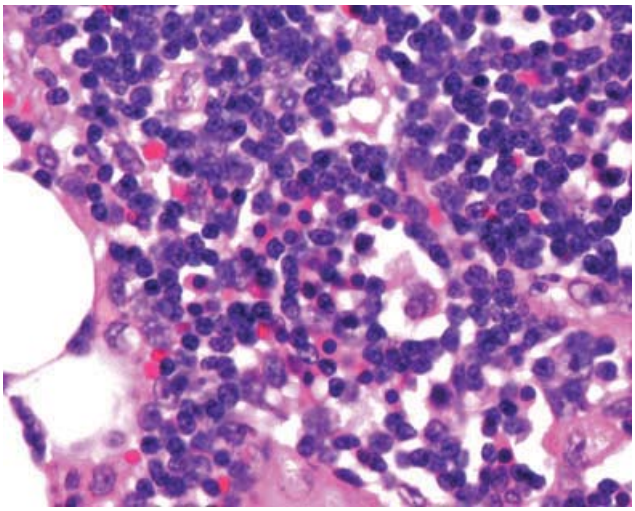

Figure 5.41. Cat: thymus, acute myeloid leukemia. Detail of Figure 5.40. The center of the image is at the cortico-medullary junction with a small foci of extramedullary erythropoiesis but no apparent colonization by neoplastic myeloid cells.

Diagnostic Criteria

The diagnosis is usually not obvious and is outwardly ALL. The severity of onset may raise suspicion of AML, and if a Sudan Black-B stain (SBB) is done on buffy coat cells only a rare cell will be positive in the range of 1% of total cells. It is essential to interpret these few positive cells properly because positive precursors are almost literally never in the peripheral blood in benign conditions. The few positive cells must be recognized to be indistinguishable from the general population of peripheral blood blasts for the diagnosis to be realized. If a myeloperoxidase reagent is available, only a similar proportion of cells (1–3%) can be expected to be labeled, and in this regard a light stain of both SBB and MPO is preferable in order that the nuclear criteria can be properly evaluated in the labeled cells with fine chromatin pattern and nucleoli visualized. The diagnosis needs to be verified by complete negative reactions for pan B- and T-lymphocyte receptors, and if the neoplasm is very primitive it may need to be verified of hematopoietic origin with CD34 and general

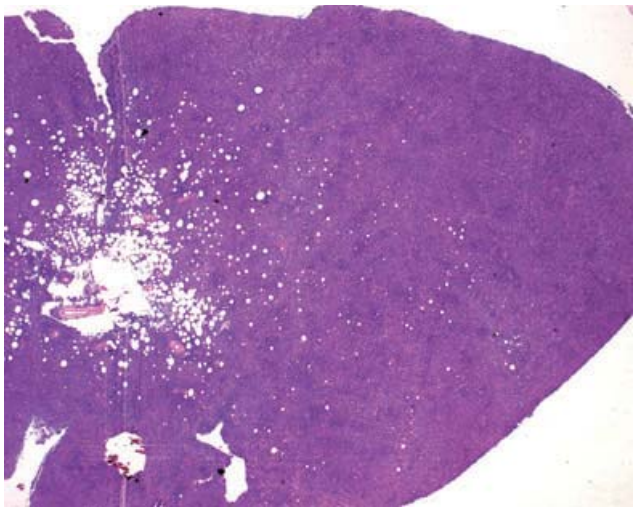

Figure 5.42. Cat: bone marrow, acute myeloid leukemia, mid-femoral shaft. The marrow is almost 100% cellular with this level of phthisis of fat cells likely to correlate with an equivalent phthisis of normal marrow elements.

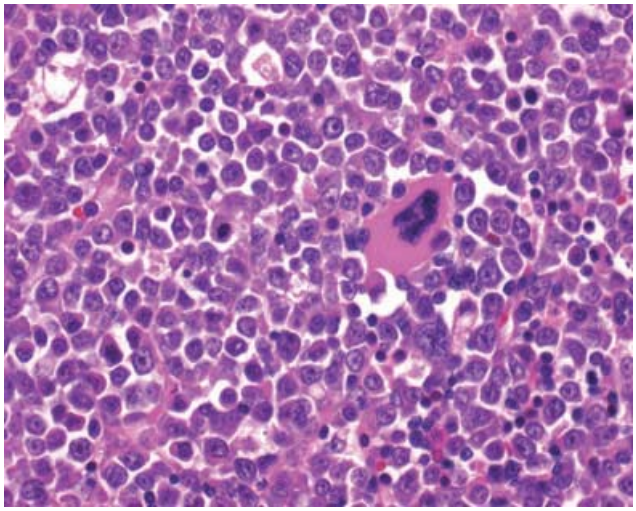

Figure 5.43. Cat: marrow, acute myeloid leukemia. Detail of Figure 5.42. There is complete loss of marrow granulocyte reserves with scattered residual megakaryocytes and erythroid precursors. At this level of marrow infiltration, with over half of the marrow occupied by neoplastic cells, there will be inadequate numbers of peripheral blood cells of all three normal lineages.

leukocyte antigens such as CD45, CD49, or CD18. MPO may be available for both cytological and histological interpretation, and it is best interpreted in the light of marrow architecture as seen in section. The diagnosis rests on complete negativity for lymphocyte antigens, and the level of blast cells must equal or exceed 20% of total nucleated marrow cells.

Differential Diagnosis

AML of M0 and M1 type must be differentiated from acute lymphoid leukemia of large cell type and from AML of M2 type with differentiation. The differentiation from ALL of large cell type must be made on the basis of immunocytochemical and histochemical staining, with complete negativity for lymphoid antigens. The differentiation from AML of M2 type can be made on the absence of any morphological evidence of cell lineage in AML of M0 and M1 types on routine blood stains, in contrast to evident azurophilic granulation in the type II and III blasts that predominate in AML of M2 type. In addition, the level of marking with MPO and SBB is much higher than in the occasional cell of AML M0 and M1, and cytologically there is evident maturation to promyelocytes in up to 10% of cells in AML M2.

Staging

Because AML is by definition a disseminated disease at diagnosis, staging is less a matter of determining the degree of spread than evaluating the residual productive capacity of the bone marrow for benign cells essential for life.

Evaluation of the Treated Animal

The most likely treatments to have been given to animals with relatively undifferentiated AML are usually antibiotics that do not change the character of the neoplastic cells plus steroids and blood transfusions. Transfused animals will have widespread erythrophagocytosis in nodes, spleen, liver, and marrow, but this is unlikely to obscure the underlying neoplasm evident on examination of blood and marrow. Chemotherapy appears to cause a small reduction in size of the cells of the neoplastic clone, but all other parameters remain unchanged, including the mitotic rate. The major change likely to be encountered in marrow is the presence of dysplastic changes in both the benign myeloid and erythroid cells and in the neoplastic cells with nuclear lobulation and binucleation and incipient myelofibrosis.

Treatment and Survival

AML of M0 and M1 types are virtually untreatable in animals, although some have been used in trials of bone marrow transplant that seem to have some chance of prolonging life but not in a currently practical manner.

REFERENCES

Ackerman, G.A. (1950) Microscopic and histochemical studies on the Auer bodies in leukemic cells. *Blood* 5:847–863.

Bennett, J.M., Catovsky, D., Daniel, M.T., et al. (1976) Proposals for the classification of the acute leukaemias. *Br J Haematol* 33:451–458.

Bennett, J.M., Catovsky, D., Daniel, M.T., et al. (1985) Proposed revised criteria for the classification of acute myeloid leukemia: A report of the French-American-British cooperative group. *Ann Intern Med* 103:626–629.

Berger, R., Bernheim, A., Daniel, M.T., et al. (1982) Cytologic characterization and significance of normal karyotypes in t(8;21) acute myeloblastic leukemia. *Blood* 59:171–178.

Brunning, R. (1999) Proposed World Health Organization (WHO) classification of acute leukemia and myelodysplastic syndromes. *Mod Pathol* 12:102.

Brunning, R., and McKenna, R.W. (1994) *Tumors of the Bone Marrow*, 3rd series, fasc. 9. Armed Forces Institute of Pathology, Washington, D.C. pp. 19–100.

Brunning, R.D. (2001) Acute myeloid leukemia. In Knowles, D.M. (ed.), *Neoplastic Hematopathology*, 2nd ed. Lippincott Williams & Wilkins, Philadelphia, pp. 1667–1715.

Buccheri, V., Shetty, V., Yoshida, A., et al. (1992) The role of an anti-myeloperoxidase antibody in the diagnosis and classification of acute leukaemia: A comparison with light and electron microscopy, cytochemistry. *Br J Haematol* 80:489–498.

Cheson, B.D., Cassileth, P.A., Head, D.R., et al. (1990) Report of the National Cancer Institute–sponsored workshop on definitions of diagnosis and response in acute myeloid leukemia. *J Clin Oncol* 8:813–819.

Cuneo, A., Ferrant, A., Michaux, J.L., et al. (1995) Cytogenetic profile of minimally differentiated (FAB-MO) acute myeloid leukemia: Correlation with clinicobiologic findings. *Blood* 85:3688–3694.

Estey, E.H. (2001) Prognostic factors in acute myelogenous leukemia. *Leuk* 15:670–672.

Grimwade, E., Walker, H., Oliver, F., et al. (1998) The importance of diagnostic cytogenetics on outcome in AML: Analysis of 1,612 patients entered into the MRC AML 10 trial. *Blood* 92:2322–2333.

Haferlach, T., Kern, W., Schoch, C., Schnittger, S., Sauerland, M.C., Heinecke, A., Büchner, T., and Hiddemann, W. (2004) A new prognostic score for patients with acute myeloid leukemia based on cytogenetics and early blast clearance in trials of the German AML Cooperative Group. *Haematologica* 89(4):408–418.

Harris, N.L., Jaffe, E.S., Diebold, J., Flandrin, G., Muller-Hermelink, H.K., Vardiman, J., Lister, T.A., and Bloomfield, C.D. (2000) The World Health Organization classification of neoplastic diseases of the haematopoietic and lymphoid tissues: Report of the Clinical Advisory Committee Meeting, Airlie House, Virginia, November 1997. *Histopathol* 36:69–87.

Head, D.R. (1996) Revised classification of acute myeloid leukemia. *Leuk* 10:1826–1831.

Jordan, C.T. (2004) Cancer stem cell biology: From leukemia to solid tumors. *Curr Opin Cell Biol* 16:708–712.

Kaleem, Z., and White, G. (2001) Diagnostic criteria for minimally differentiated acute myeloid leukemia (AML-MO). *Am J Clin Pathol* 115:876–884.

Kogan, S.C., Ward, J.M., Anver, M.R., Berman, J.J., Brayton, C., Cardiff, R.D., Carter, J.S., de Coronado, S., Downing, J.R., Fredrickson, T.N., Haines, D.C., Harris, A.W., Harris, N.L., Hiai, H., Jaffe, E.S., MacLennan, I.C.M., Pandolfi, P.P., Pattengale, P.K., Perkins, A.S., Simpson, R.M., Tuttle, M.S., Wong, J.F., and Morse III, H.C. (2002) Bethesda proposals for classification of nonlymphoid hematopoietic neoplasms in mice. *Blood* 100(1):238–245.

Lichtman, M.A. (2001) The stem cell in the pathogenesis and treatment of myelogenous leukemia: A perspective. *Leuk* 15:1489–1494.

Loh, M.L., Reynolds, M.G., Vattikuti, S., Gerbing, R.B., Alonzo, T.A., Carlson, E., Cheng, J.W., Lee, C.M., Lange, B.J., and Meshinchi, S. (2003) *PTPN11* mutations in pediatric patients with acute myeloid leukemia: Results from the Children's Cancer Group. *Leuk* 1–4.

Lowenberg, B. (2004) Strategies in the treatment of acute myeloid leukemia. *Haematologica* 89(9):1029–1034.

Raskin, R.E. (1996) Myelopoiesis and myeloproliferative disorders: Veterinary clinics of North America. *Sm An Pract* 26(5):1023–1042.

Repp, R., Schaekel, U., Helm, G., Thiede, C., Soucek, S., Pascheberg, U., Wandt, H., Aulitzky, W., Bodenstein, H., Sonnen, R., Link, H., Ehninger, G., Gramatzki, M., and the AML-SHG Study Group (2003) Immunophenotyping is an independent factor for risk stratification in AML. *Cytometry Part B (Clin Cytometry)* 53B:11–19.

Rubnitz, J.E., Lensing, S., Zhou, Y., Sandlund, J.T., Razzouk, B.I., Ribeiro, R.C., and Pui, C.H. (2004) Death during induction therapy and first remission of acute leukemia in childhood. *Cancer* 101(7):1677–1684.

Rumke, C.L. (1960) Variability of results in differential counts on blood smears. *Triangle* 4:154–158.

Scott, C.S., Den Ottolander, G.J., Swirsky, D., Pangalis, G.A., Vives Corrons, J.L., De Pasquale, A., Van Hove, L., Bennett, J.M., Namba, K., Flandrin, G., Lewis, S.M., and Polliack, A. (1993) Recommended procedures for the classification of acute leukaemias. *Leuk and Lymph* 11:37–49.

Stone, R.M., DeAngelo, D.J., Klimek, V., Galinsky, I., Estey, E., Nimer, S.D., Grandin, W., Lebwohl, D., Wang, Y., Cohen, P., Fox, E.A., Neuberg, D., Clark, J., Gilliland, D.G., and Griffin, J.D. (2005) Patients with acute myeloid leukemia and an activating mutation in FLT3 respond to a small-molecule FLT3 tyrosine kinase inhibitor, PKC412. *Blood* 105(1):54–60.

Tchinda, J., Volpert, S., McNeil, N., Neumann, T., Kennerknecht, I., Ried, T., Büchner, T., Serve, H., Berdel, W.E., Horst, J., and Hilgenfeld, E. (2003) Multicolor karyotyping in acute myeloid leukemia. *Leuk and Lymph* 44(11):1843–1853.

Vernau, W., and Moore, P.F. (1999) An immunophenotypic study of canine leukemias and preliminary assessment of clonality by polymerase chain reaction. *Vet Immunol and Immunopathol* 69:145–164.

Acute Myeloblastic Leukemia with Maturation M2

Definition

AML M2 is an acute leukemia of myeloid lineage in which the bone marrow or blood contains 20% or more of type I and type II myeloblasts. AML M2 is distinguished from AML M1 by the presence of cells maturing to the level of promyelocyte or more mature stages in at least 10% of marrow cells.

Epidemiology and Incidence

AML M2 is the disease that historically has been assumed to be the most primitive acute myeloid leukemia occurring in animals because it can be diagnosed by the recognition of azurophilic granules in the type II and III myeloblasts that are apparent on routine blood stains. The disease is uncommon and recognized most often in young mature cats and dogs and rarely in other domestic animals.

Clinical Presentation and Features

The presentation of animals with AML M2 is similar to that of M1. Most cases have anemia, thrombocytopenia, and leukocytosis. There are few case descriptions, but it appears that there may be a bimodal age distribution, with most cases occurring in animals 2–3 years old and a lesser number of cases in mature animals, and with the same pattern observed in cats and dogs. A male predominance has been suggested, but the cases well enough defined to be included in AML of M2 type don't support a difference in occurrence with gender. The history is not as explosive as in the undifferentiated types of AML, with owners reporting loss of weight and activity over the previous weeks or months. There may be history of vomition and diarrhea or other relatively nonspecific signs that, if present for some months and resulting in cachexia, suggest that the animal may have had chronic myeloid leukemia for a year or more and the presentation is of an animal in blastic crisis.

Pathologic Features

Blood

Animals with AML M2 present with mucosal pallor and usually hepatosplenomegaly, but with normal or small lymph nodes. The hematocrit is usually less than 25% and the total leukocyte count less than 50,000/ul, with mature neutrophils less than 10% of total blood cells and less than normal levels on the basis of absolute numbers (Figs. 5.44, 5.45). Cases presenting with a mature neutrophilic leukocytosis, even with blast cells present, are unlikely to be AML of neutrophil or other granulocyte (eosinophil or basophil) type. Because the character of the neoplasm is one of impaired maturation, any neutrophils present are the progeny of residual benign precursors. The differential count on blood will reflect the maturation arrest in marrow, with the presence of some blast cells of type II and III accompanied by some promyelocytes (Fig. 5.46) and possibly a few poorly granulated myelocytes that may be mistaken for lymphocytes or monocytes (Fig. 5.47). There are usually some bilobed granulocytes present that represent the abnormal maturation of cells entering the blood earlier than the metamyelocyte stage. The disease tends to become clinical when marrow failure results in the reduction in numbers of peripheral blood neutrophils and platelets to sustain homeostasis. There is always thrombocytopenia, although in the context of the myeloproliferative disease involving all cell lineages there is a human syndrome of AML M2 that presents with thrombocytosis (associated with chromosomal inversion inv (3)(q21;q26) or translocation t(3;3)(q21;q26), with a counterpart syndrome in animals not recognized. A subgroup of human patients with AML M2 that have a translocation of t(8;21) type constitutes a younger

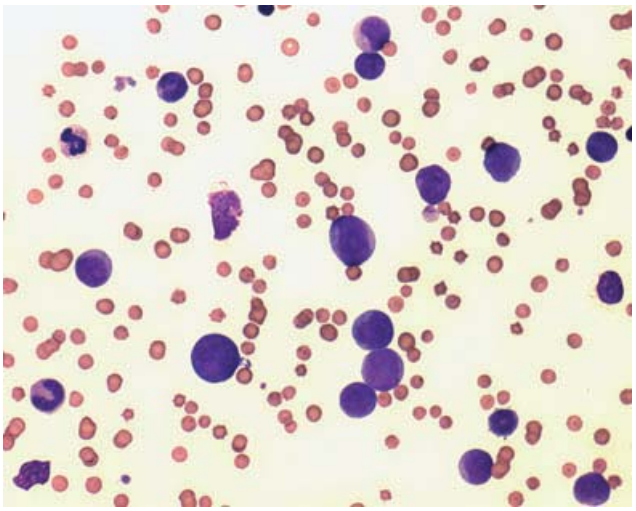

Figure 5.44. Dog: blood, acute myeloid leukemia. The M2 type of acute myeloid leukemia is characterized by a low percentage of neutrophils in the peripheral blood with the presence of type I and II blast cells with anemia and thrombocytopenia. *Slide from R. M. Jacobs, DVM.*

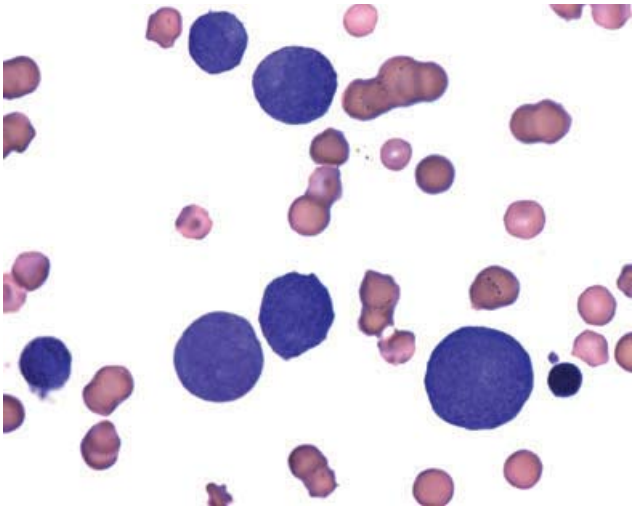

Figure 5.45. Dog: blood, acute myeloid leukemia. Detail of Figure 5.44. The large cell at the lower right is a type I blast, with the cells to the left type II blasts with the nucleolus becoming encircled by condensed chromatin. Cytoplasmic granulation is not apparent.

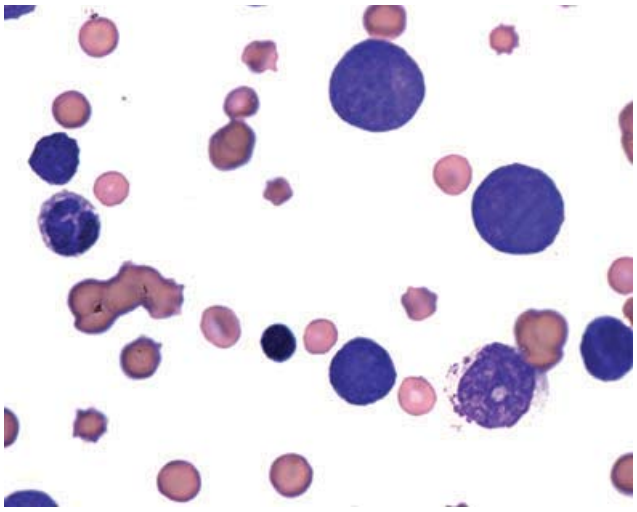

Figure 5.46. Dog: blood, acute myeloid leukemia, same slide as Figure 5.44. Two promyelocytes (upper right) and an atypical donut-type cell with granulated cytoplasm present in the lower right, likely a dysplastic metamyelocyte. The neutrophil in the center left has atypical segmentation and reduced cytoplasmic volume with increased basophilia and poor granulation.

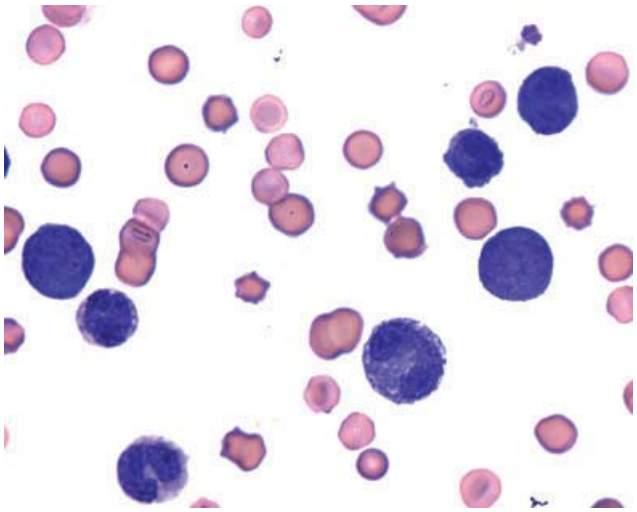

Figure 5.47. Dog: blood, acute myeloid leukemia, same slide as Figure 5.44. There is a type II blast at the right center with chromatin ring around a prominent central nucleolus. Below to the left is a giant metamyelocyte, likely tetraploid type, and at left it 2 later stage neutrophils with abnormally shaped nuclei. There is a single platelet in the upper right.

population and has a more favorable prognosis with high-dose cytarabine in combination therapy. Patients with the translocation t(8;21) have a high likelihood of developing extramedullary granulocytic sarcoma. This is associated with a less-favorable prognosis in adults with AML who also have the translocation, but not in a pediatric population that has AML and the same translocation. Extramedullary granulocytic sarcoma in association with AML has been seen in animals, but rarely, and is felt to be a sign of recurrence in treated cases in remission.

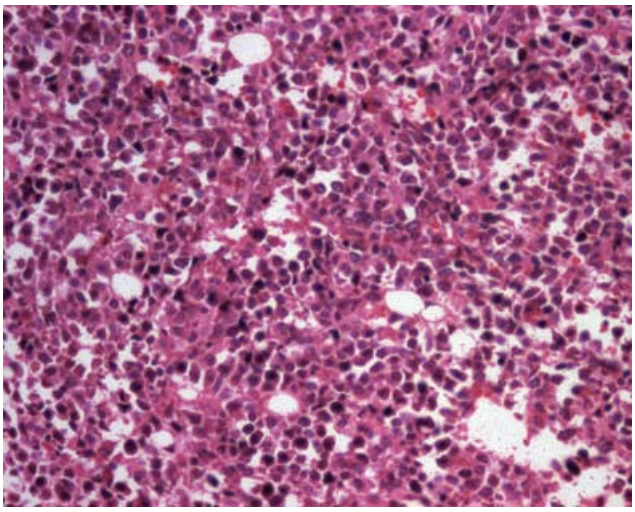

Figure 5.48. Dog: marrow, acute myeloid leukemia. The marrow is hypercellular with over 90% of cell volume occupied by hematopoietic tissue and few fat cells remaining. Note the absence of megakaryocytes and of clusters of cells with densely stained nuclei typical of colonies of erythropoiesis.

Bone Marrow

The bone marrow is always hypercellular with 10% or less of tissue area occupied by fat cells, and in areas of nodular neoplastic proliferation the fat is completely lost (Figs. 5.48, 5.49). Dysplastic changes may be present in all benign cell lines with hypolobate megakaryocytes and giant metamyelocytes or donut "rodent-cell" forms (Figs. 5.50–5.52). The erythroid precursors may have mitoses in late stage rubricytes and binucleated forms with nuclei varying widely in diameter (Figs. 5.53, 5.54). The most predominant benign mature granulocytes are usually eosinophils. The neoplastic cells form solid areas of monomorphous proliferation and resemble foci of large cell lymphoma on H&E staining. A few cells with similar or larger nuclei and greater cytoplasmic volume may be recognized as promyelocytes, and a few more mature cells can be recognized in the neoplastic clone. The azurophilic granulation that is the basis of lineage recognition in the blood or on marrow cytologic preparations are not reliably discerned on routine histological stains. If thrombocytopenia has been severe, there are large foci of marrow hemorrhagic infarction which seem to be more prominent in midshaft areas and prominent grossly, but they are less likely to be encountered in the cancellous areas chosen for marrow core biopsy. On staining with reagents for pan B- and T-lymphocytes, the tissue is completely negative;

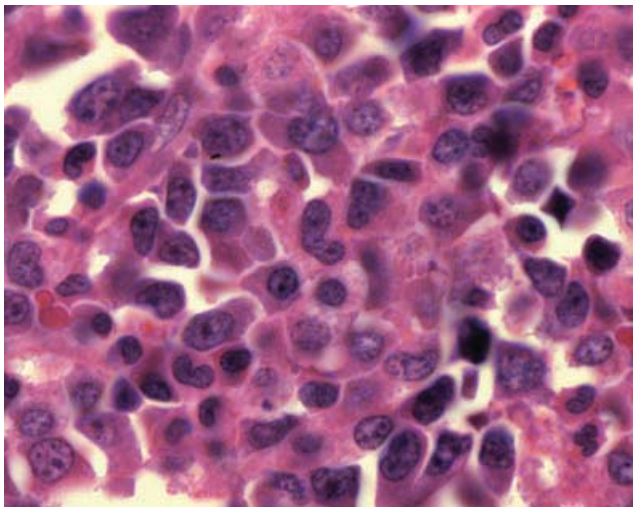

Figure 5.49. Dog: marrow, acute myeloid leukemia. Detail of Figure 5.48. Typical of the M2 type of AML, there is almost a complete loss of marrow granulocyte reserves and erythropoiesis, with the cells dominated by primitive precursors with a giant metamyelocyte in the center and another with atypical maturation in the lower left.

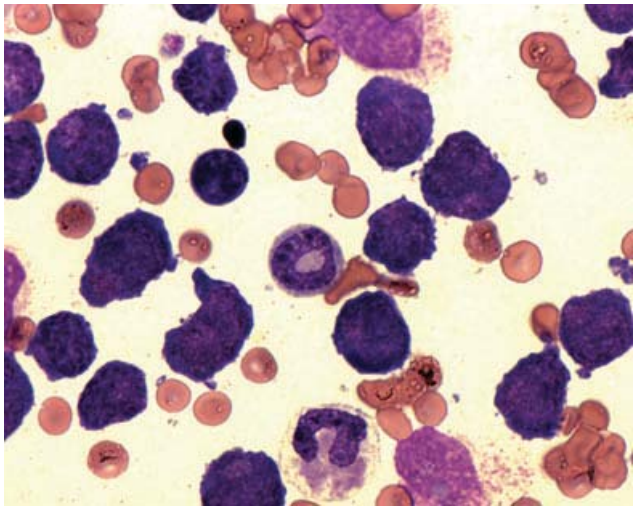

Figure 5.50. Dog: marrow aspirate, acute myeloid leukemia. Small blasts and promyelocytes surround a donut-type metamyelocyte (center) with an atypical band at lower center with very poorly granulated cytoplasm. *Slide from R. M. Jacobs, DVM.*

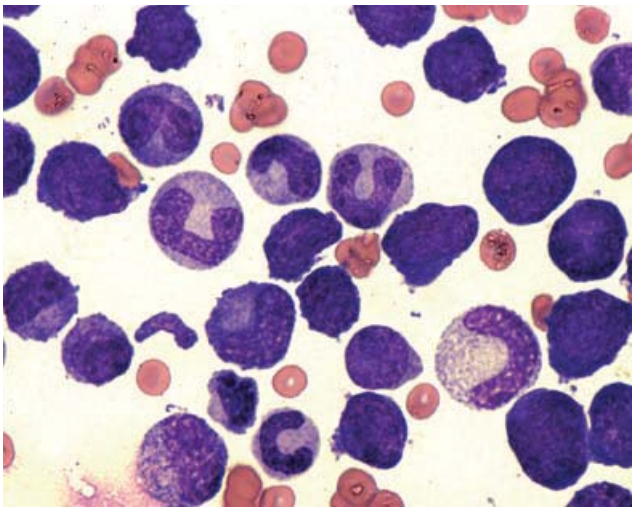

Figure 5.51. Dog: marrow aspirate, acute myeloid leukemia, same slide as Figure 5.50. There are 7 metamyelocytes in this field of giant cell type with a single band and segmented neutrophil in the lower center right.

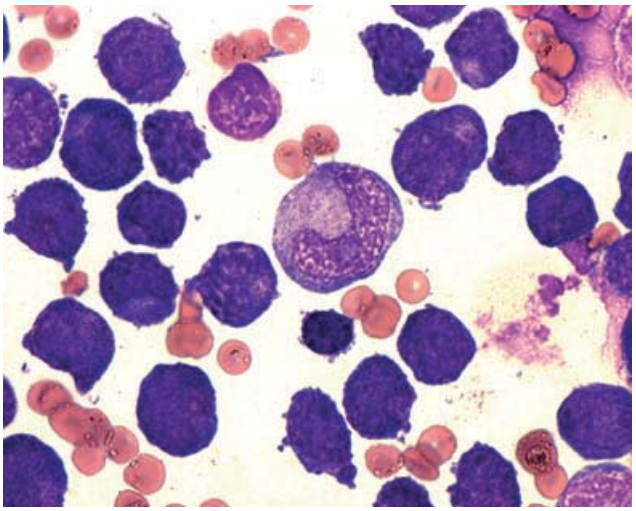

Figure 5.52. Dog: marrow aspirate, acute myeloid leukemia, same slide as Figure 5.50. A remarkably enlarged metamyelocyte in the center with fine azurophilic granules is flanked by small atypical promyelocytes above to the right and below to the left. Surrounding cells are primarily atypical type I and II blasts. Giant metamyelocytes can occur in benign states due to folate deficiency and are likely present in myeloid neoplasia for that reason as well as accompanying dysplasia.

staining with MPO generally marks 10% or more of the atypical blastic population. A variant form of human AML M2 has a specific translocation found to be associated with bone marrow basophilia and rapidly progressive myelofibrosis.

Other Organs

There is diffuse involvement of the splenic sinus areas as described for AML M0/M1, with severe lymphoid atrophy of both the follicular and thymic-dependent periarteriolar sheath areas (Figs. 5.55–5.57). There is usually colonization of the subendothelial areas of the large

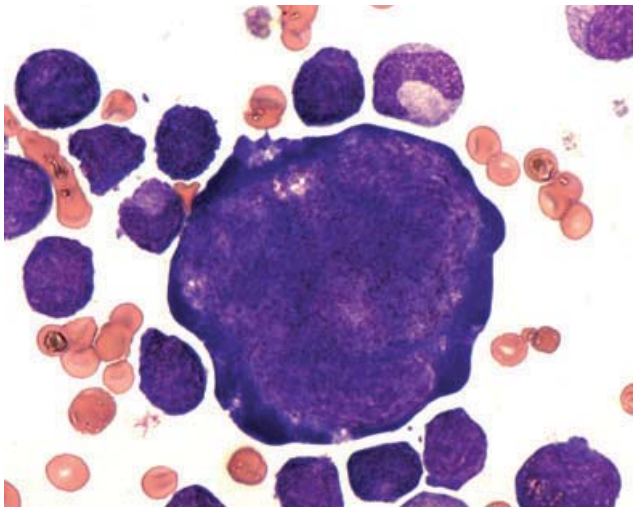

Figure 5.53. Dog: marrow aspirate, acute myeloid leukemia, same slide as Figure 5.50. A young megakaryocyte with asynchronous development appears to have incomplete nuclear fusion with irregular cytoplasmic granulation prior to development of normal cytoplasmic volume.

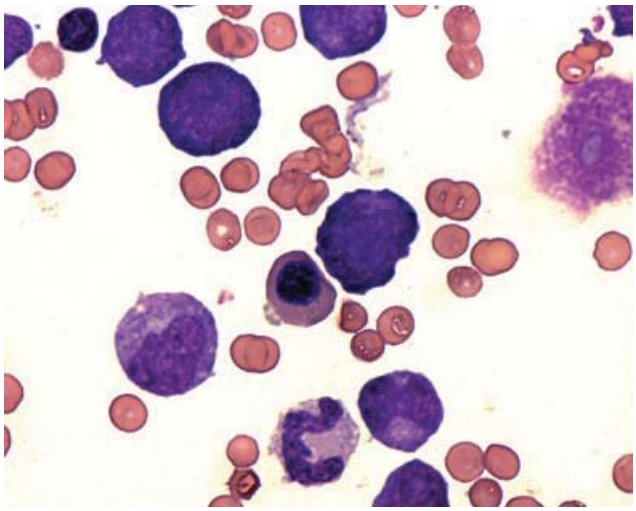

Figure 5.54. Dog: marrow, acute myeloid leukemia, same slide as Figure 5.50. The single polychromatic rubricyte in the center has a much larger cytoplasmic envelope than normal and may indicate an impending late stage mitosis.

muscular veins, and there may be focal hemorrhagic infarction. The liver is always involved, and the architecture will vary with the leukocyte count, but there are perivascular foci of solid neoplasm (Figs. 5.58, 5.59), some portal areas with mixed benign extramedullary hematopoiesis (EMH), and neoplastic proliferation. There is thymic atrophy even in young animals, and the nodes are usually small with some having mixed EMH

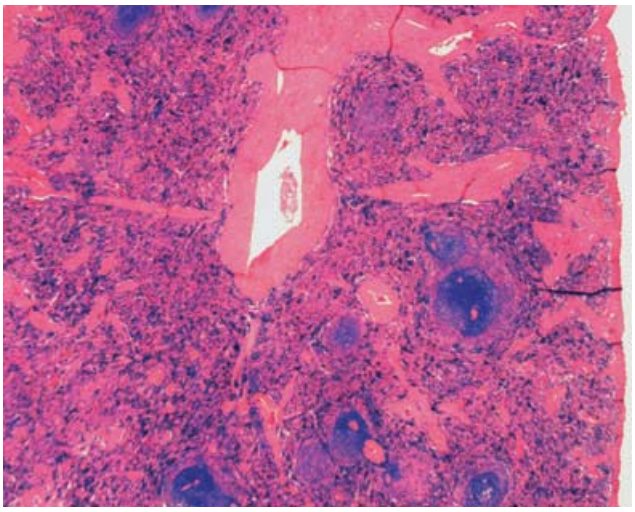

Figure 5.55. Dog: spleen, acute myeloid leukemia, same case as Figure 5.48. The organ is contracted with broad and dense muscular trabeculae. There is complete atrophy of germinal centers and moderate atrophy of periarteriolar lymphoid sheaths. There is a prominent perifollicular sinus around most germinal centers, most prominent in the right center. There is heavy sinus hemosiderosis apparent in small dense granulation.

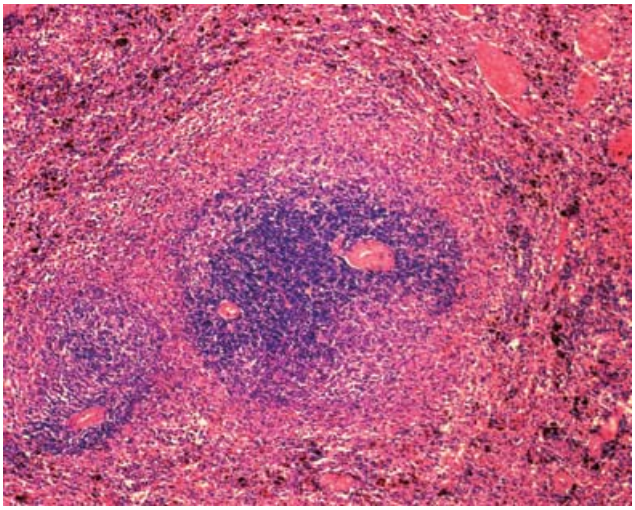

Figure 5.56. Dog: spleen, acute myeloid leukemia. Detail of Figure 5.55. The arterioles are surrounded by an atrophic lymphoid sheath, with a lighter area representing areas of the involuted germinal center. There is a prominent perifollicular sinus separating the lymphoid area from the surrounding areas of sinus that are heavily laden with hemosiderin.

and neoplastic colonization (Figs. 5.60, 5.61). If neutropenia has been severe, foci of sepsis may be present in the lung and in areas of cellulitis with minimal cell reaction, mainly of monocytic type.

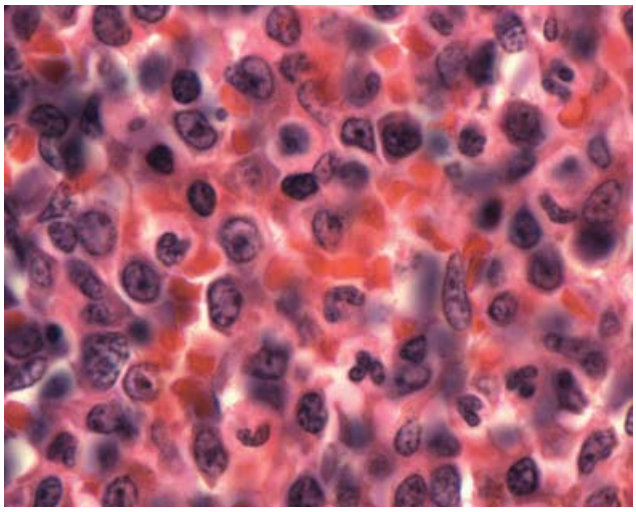

Figure 5.57. Dog: spleen, acute myeloid leukemia. Detail of Figure 5.56. The edge of the lymphoid sheath is at the left with the perifollicular sinus area in the center. The cells in the perifollicular sinus are primarily vesicular with prominent nucleoli representing a predominant population of cells in circulation. There is a metamyelocyte in the center and likely a band neutrophil at the lower center. The trilobulated cell below the metamyelocyte is likely a hypersegmented neutrophil.

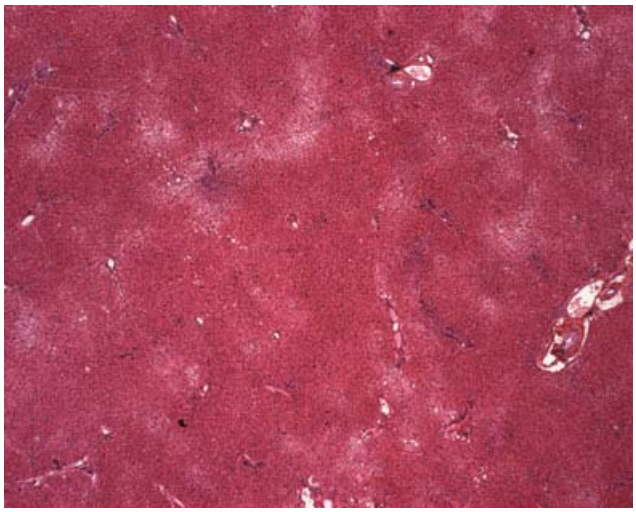

Figure 5.58. Dog: liver, acute myeloid leukemia. There is irregular accentuation of zonation due to ischemic degeneration and steroid-like hepatopathy affecting centrilobular areas.

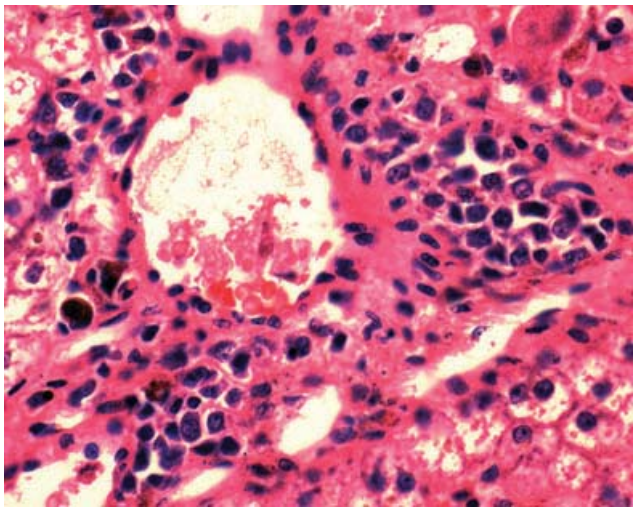

Figure 5.59. Dog: liver, acute myeloid leukemia. Detail of Figure 5.57. The portal area is surrounded by large primitive cells without an apparent direction of differentiation. The dense round structure to the lower left of the portal vein is a hemosiderin-laden macrophage that, with the hemosiderosis in the spleen, suggests chronic anemia or hemolysis preceding the development of acute leukemia.

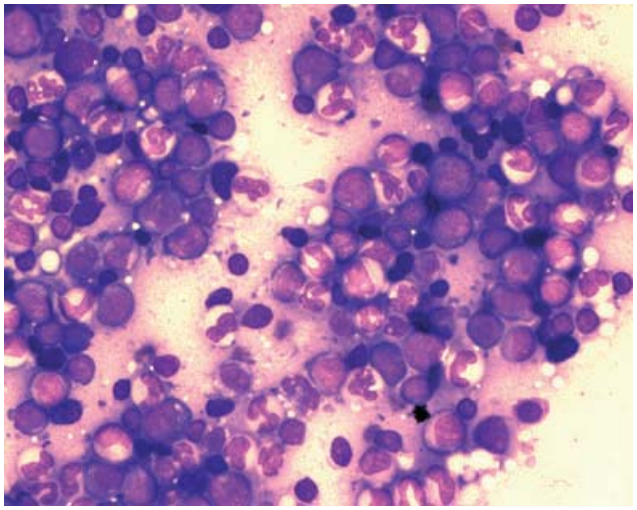

Figure 5.60. Dog: node, acute myelogenous leukemia. Imprint of AML felt to be at M2 differentiation. The cellularity is not much different than the marrow of the same case of Figures 5.49–5.54. Most of the cells are blasts and poorly granulated promyelocytes with few myelocytes but quite numerous neutrophils undergoing abnormal segmentation. The lymphocytes are the small darkly stained nuclei that appear at 20% or less of the total population.

Diagnostic Criteria

At least 3% of the blastic forms of type II and III type must stain positively with SBB in cytologic preparations (Fig. 5.62) and at least 3% must mark with MPO in cytologic or histologic preparations. The neoplastic cells are negative, with all markers specific for lymphoid antigens. At least 10% of marrow cells must have evident maturation to the promyelocyte stage to distinguish AML M2 from less-differentiated M0 or M1. The total of the combined types of neoplastic blast cells must exceed 20% of the total nucleated marrow cells to be accepted as a neoplastic process. The level of granulation in the type II and

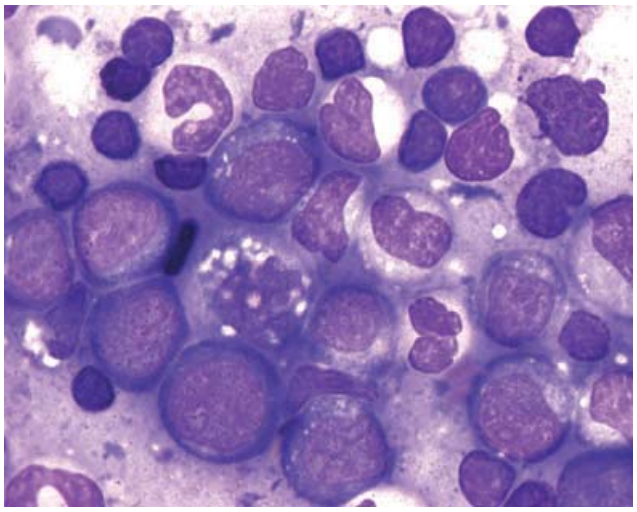

Figure 5.61. Dog: node, acute myelogenous leukemia. Detail of Figure 5.59. An area selected for frequent lymphocytes (top), which are primarily small and medium type with a very narrow rim of cytoplasm likely reflecting long-lived memory cells.

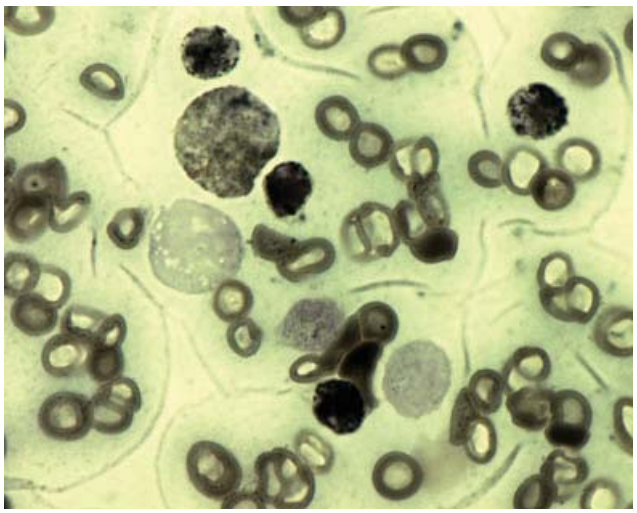

Figure 5.62. Dog: marrow, acute myeloid leukemia. Sudan Black-B stain. The large blast in the upper left is positive with the 3 precursors below unlabeled. More mature granulocytes are strongly labeled. *Slide from R. M. Jacobs, DVM.*

III blasts is usually sufficiently evident to obviate the need for more generalized leukocyte-type stains like CD45.

Differential Diagnosis

AML M2 must be differentiated from other forms of acute myeloid leukemia on the level of maturation of the neoplastic clone that largely ends at the promeyelocyte stage. Differentiation from ALL is made on negative reaction of the atypical blast cells for pan B- and T-lymphocyte receptors. AML of all types must be differentiated from benign hyperplasia on the presence of 20% or more of all marrow nucleated cells being blast cell II and III types.

Treatment and Survival

Animals with AML differentiated to the M2 stage may be candidates for therapy, and some of these may respond well to the anthracycline class of chemotherapeutic agents.

REFERENCES

Alsabeth, R., Brynes, R.K., Slovak, M.L., et al. (1997) Acute myeloid leukemia with the t(6;9)(p23;q34): Association with myelodysplasia, basophilia, and initial CD34 negative immunophenotype. *Am J Clin Pathol* 107:430–437.

Bernstein, R., Pinto, M.R., Behr, A., et al. (1992) Chromosome 3 abnormalities in acute nonlymphocytic leukemia (ANLL) with abnormal thrombopoiesis: Report of three patients with a "new" inversion anomaly and a further case of homologous translocation. *Blood* 60:613–617.

Bitter, M.A., Neilly, M.E., LeBeau, M.M., et al. (1985) Rearrangements of chromosome 3 involving bands 3q21 and 3q26 are associated with normal or elevated platelet counts in acute nonlymphocytic leukemia. *Blood* 60:1362–1370.

Brunning, R.D. (2001) Acute myeloid leukemia. In Knowles, D.M. (ed.), *Neoplastic Hematopathology*, 2nd ed. Lippincott Williams & Wilkins, Philadelphia, pp. 1667–1715.

Byrd, J.C., Weiss, R.C., Arthur, D.C., et al. (1997) Extramedullary leukemia adversely affects hematologic complete remission rate and overall survival in patients with t(8;21)(q22;q22): Results from Cancer and Leukemia Group B 8461. *J Clin Oncol* 15:466–475.

Fonatsch, C., Gudat, H., Langfelder, E., et al. (1994) Correlation of cytogenetic findings with clinical features in 18 patients with in(3)(q21;q26) or t(3;3)(q21;q26). *Leuk* 8:1318–1326.

Fraser, C.J., Joiner, G.N., Jardine, J.H., and Gleiser, C.A. (1974) Acute granulocytic leukemia in cats. *JAVMA* 164(4):355–359.

Grimwade, D., Walker, H., Oliver, F., et al. (1998) The importance of diagnostic cytogenetics on outcome in AML: Analysis of 1,612 patients entered into the MRC AML 10 trial. *Blood* 92:2322–2333.

Keller, P., Sager, P., Freudiger, U., and Speck, B. (1985) Acute myeloblastic leukaemia in a dog. *J Comp Pathol* 95:619–632.

Schalm, O.W., Jain, N.C., and Carroll, E.J. (1975) The leukemia complex in the dog. In *Veterinary Hematology*, 3rd ed. Lea & Febiger, Philadelphia, pp. 558–565.

Schalm, O.W., Jain, N.C., and Carroll, E.J. (1975) The Feline leukemia complex. In *Veterinary Hematology*, 3rd ed. Lea & Febiger, Philadelphia, pp. 583–587, 1975.

Valli, V.E.O. (1993) The hematopoietic system. In Jubb, K.V.F., Kennedy, P.C., and Palmer, N. (eds.), Pathology of Domestic Animals, 4th ed. Harcourt Brace Jovanovich, Orlando, Florida, pp. 116–119, 1993.

Acute Promyelocytic Leukemia M3

Acute promyelocytic leukemia (APL), or AML M3, is characterized not by the blast cells but by the promyelocytes that prominently outnumber the blasts, with most being of neoplastic type. The diagnosis is based on a combination of myeloblasts and promyelocytes that together must exceed 20% of total marrow cells. In human APL, the median level of promyelocytes is 8% of total marrow cells, which gives a proportionate level at which the promyelocytes exceed the number of blast cells.

In humans, AML M3 or APL occurs in two forms of hypergranular and microgranular or hypogranular types. The disease is extremely rare in animals with only a well-granulated form recognized. Because of evident morphology with the large heavily granulated cells, it is likely truly rare and not just underrecognized. In dogs, the neoplastic clones are poorly granulated by human standards, with the neoplastic cells most resembling the human microgranular form because the nucleus is clearly visible. But the granules are few—about 20–50 per cell—and of distinct azurophilic staining, 0.2–0.5 microns in diameter, and resembling the granules of normal promyelocytes. In the human hypergranular form, the granules so frequently coalesce into the Auer bodies that their presence becomes a function of the diagnosis with cells, with many of these bodies known as "faggot cells." The human hypergranular type AML M3 presents with anemia, leukopenia, and thrombocytopenia. The hypogranular variant presents with marked leukocytosis of about 50,000/ul with the abnormal promyelocytes predominating, and most patients have severe coagulopathy or are at risk of it developing on the initiation of therapy.

A major interest in this disease has been the determination of the specific translocations involved in the pathogenesis of the clinical syndrome and the development of a very effective therapy with relatively nontoxic alltrans-retinoic acid (ATRA). A chromosomal translocation t(15;17)(q22;q11–12) is felt to be the specific change in initiating both forms of human APL. This translocation puts the *RARA* retinoic acid receptor-alpha gene on chromosome 17 in fusion with the gene encoding the zinc finger binding transcription factor on chromosome 15 called the *PML* (promyelocytic leukemia) gene. The resulting fusion protein is called *PML-RARA* product. There are two major facets of this pathogenesis and the resulting neoplasm that are unique. First, the APL neoplasm can be effectively treated in about 90% of cases, with durable remission effected by the primitive neoplastic cells undergoing differentiation into neutrophils. Second, the mechanism of this form of oncogenesis is by epigenetic means defined as heritable changes in gene function resulting in cell proliferation that cannot be explained by changes in DNA sequence. In APL, the neoplastic phenotype is maintained by an increased proliferation of blast cells as a result of two factors. First, there is a block to maturation and differentiation that prevents the neoplastic clone from reaching a postmitotic stage and programmed cell death. Second, there is an increased capacity of the neoplastic precursors to maintain a state of self renewal. There is overall hypomethylation in APL as a result of the action of the PML/RARA-alpha fusion protein with regional hypermethylation. This has the net result of inducing cell proliferation and down-regulating the normal repressor genes and their product by enzymes causing specific and limited hypermethylation, heterochromatin formation, and gene silencing. The ATRA results in a reprogramming of the neoplastic APL cells, which induces differentiation and reduces proliferation. Much of the mechanism of the histone acetylation and cytosine methylation leading to these interactions was derived by the study of in vitro metabolism in APL cell lines.

Clinical Presentation and Blood

In animals, APL is seen in dogs and cats and appears to be in more mature animals than are the acute myeloid leukemias of M0–M2 type. The Auer bodies are not seen and, if present, are uncommon in contrast to the human forms of APL. The presentation is of an animal that has lost weight, appetite, and activity and is anemic, is thombocytopenic, and may be febrile if there is severe neutropenia. The blood is diagnostic, and if misinterpreted the marrow is unmistakably a proliferation of abnormal large and very large cells with abundant cytoplasm that has a slate gray basophilia with evident but not abundant azurophilic granulation (Fig. 5.63). The nuclei are round, and most are 2.5–3.0 red cells in diameter with an occasional huge cell, all with abundant cytoplasm that give the APL cells an overall diameter of 5–6 red cells (Fig. 5.64).

In the bone marrow, there are few actual blasts that are much smaller cells, many forms of aberrant maturation with myelocytes and huge metamyelocytes, and no neutrophils. The large cells referred to as *metamyelocytes* are considered reniform promyelocytes in human pathology, and because they lack any other signs of maturation like less-cytoplasmic basophilia or more granulation, they should be counted as part of the dividing cell population (Fig. 5.65, see also Fig. 5.64). Oddly, somewhat like the human cases of APL, there are some forms of maturing cells of eosinophil type that appear to be derived from the APL precursors and occasional large myelocytic basophils (Fig. 5.66). Mitoses are frequently found, and there is almost complete phthisis of normal hematopoietic cells. The donut type of metamyelocyte frequently seen in normal rodents is present, as well as binucleate types of atypical promyelocytic precursors (Figs. 5.67, 5.68).

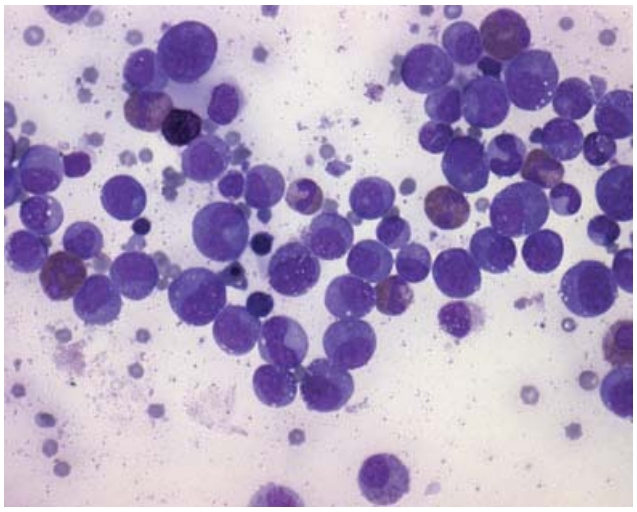

Figure 5.63. Cat: marrow, acute myeloid leukemia, M3. There is a predominant population of large atypical promyelocytes with round nuclei that are 3 red cells in diameter surrounded by abundant eccentrically placed cytoplasm that has uniformly increased basophilia and reduced azurophilic granulation. There is a donut-type metamyelocyte in the right center indicating mild accompanying dysplasia. Most of the mature granulocytes are of the eosinophil type. *Slide from R. M. Jacobs, DVM.*

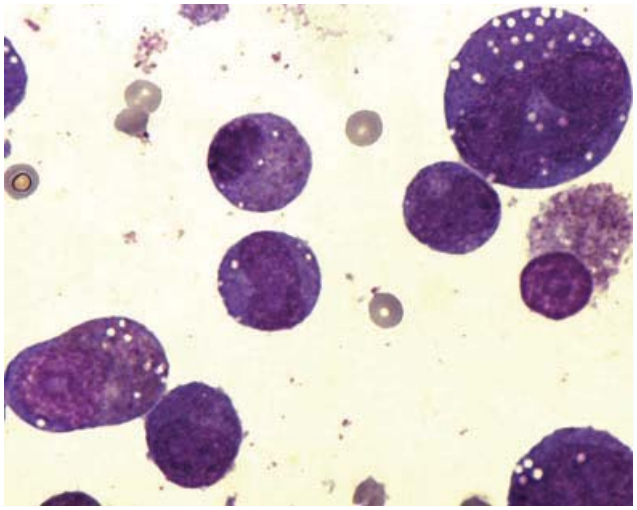

Figure 5.64. Cat: marrow, acute myeloid leukemia, M3. There is marked anisokaryosis; the cell in the upper right is huge with an irregular donut-type nucleus and retaining chromatin rimming around the very large nucleolus.

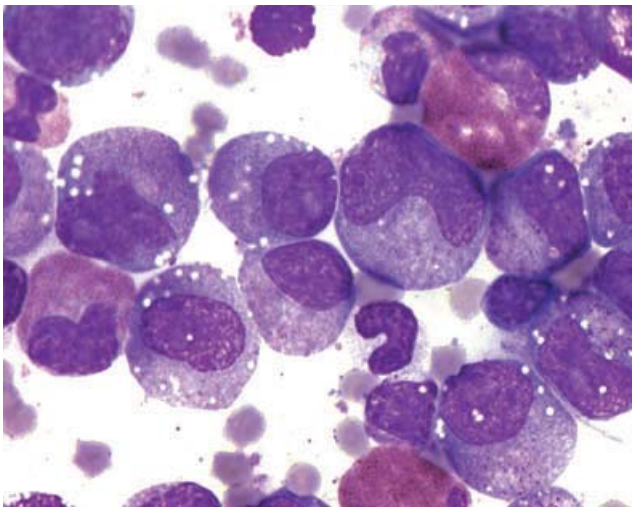

Figure 5.65. Cat: marrow, acute myeloid leukemia, M3. The giant types of metamyelocyte, (right center) are included in the count of promyelocytic cells for diagnostic purposes.

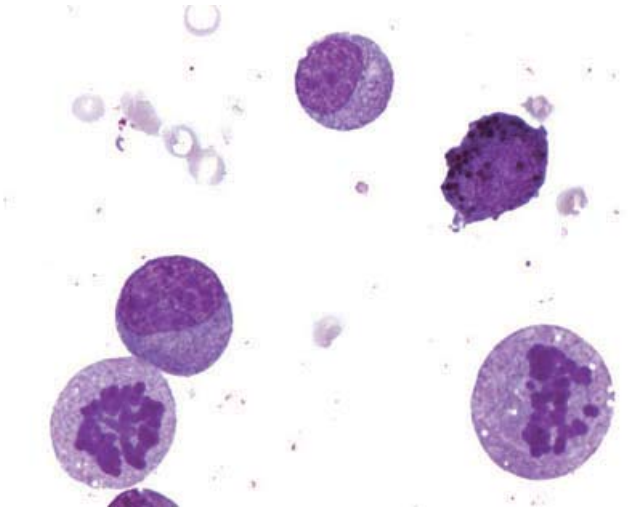

Figure 5.66. Cat: bone marrow, acute promyelocytic leukemia (APL) or M3. There are 2 promyelocytes in metaphase and 2 smaller cells that may be atypical myelocytes. The cell in the upper right is likely a dwarf myelocyte basophil. *Slide from R. M. Jacobs, DVM.*

APL had been largely recognized as an acute myeloid leukemia of specific cell type with little indication of pathology in organs other than bone marrow in human pathology; less is known of the general pathologic picture in animals. It can be assumed that there will be involvement of the spleen and liver with primarily sinusoidal colonization.

The diagnosis of APL can largely be made on routine blood stains, but APL cells stain strongly positive with MPO and SBB and are positive with chloroacetate esterase (CAE). The granulation is easily missed in histological preparations, and in the absence of specific staining or knowledge of blood examination the large cells might be mistaken for acute monocytic leukemia or even lymphoid leukemia. APL cells are negative with all markers specific for lymphoid-derived neoplasms.

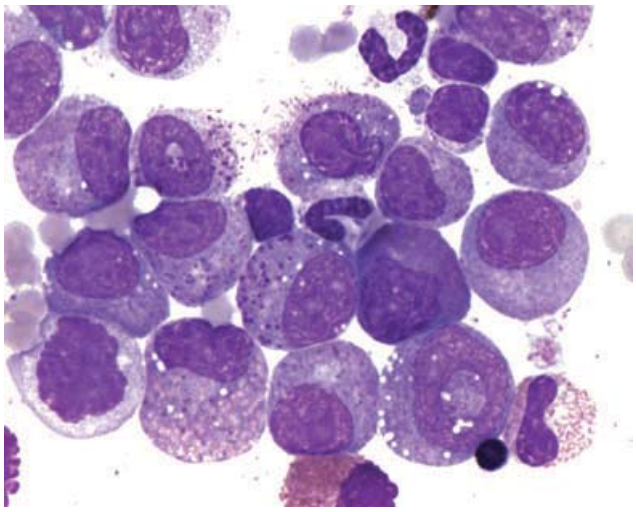

Figure 5.67. Cat: acute myeloid leukemia, M3. There are 2 cells in this field with ringed nuclei, with the largest in the lower right, still being included in the progranulocyte count. There is a cell in metaphase in the lower left. Note the very poor granulation of both neutrophils and maturing eosinophils.

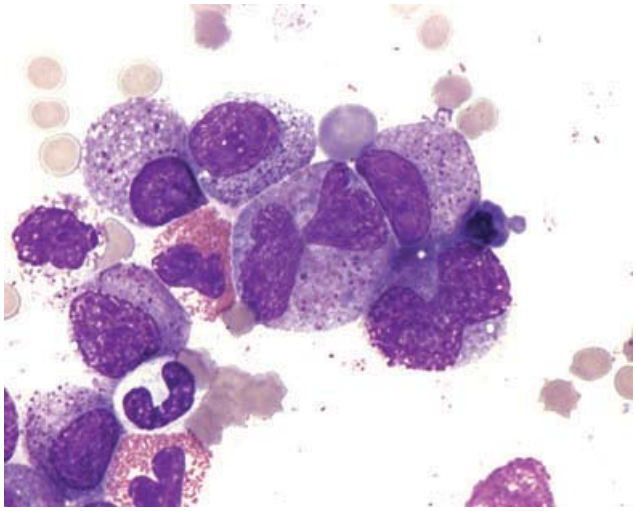

Figure 5.68. Cat: marrow, M3. The 2 cells in the center with hourglass-shaped nuclei suggest a genesis of binucleate cells from the usual atypical nuclear maturation, like that of cells in the peripheral blood that become binucleate rather than band cells.

REFERENCES

Avvisati, G., Lo Coco, F., and Mandelli, F. (2001) Acute promyelocytic leukemia: Clinical and morphologic features and prognostic factors. *Semin Hematol* 38(1):4–12.

Brunning, R.D. (2001) Acute myeloid leukemia. In Knowles, D.M. (ed.), *Neoplastic Hematopathology*, 2nd ed. Lippincott Williams & Wilkins, Philadelphia, pp. 1667–1715.

Castoldi, G.L., Liso, V., Specchia, G., et al. (1994) Acute promyelocytic leukemia: Morphological aspects. *Leuk* 8(Suppl 2):S27–S32.

Di Croce, L., Raker, V.A., Corsaro, M., Fazi, F., Fanelli, M., Faretta, M., Fuks, F., Lo Coco, F., Kouzarides, T., Nervi, C., Minucci, S., and Pelicci, P.G. (2002) Methyltransferase recruitment and DNA hypermethylation of target promoters by an oncogenic transcription factor. *Science* 295:1079–1082.

Falanga, A., and Barbui, T. (2001) Coagulopathy of acute promyelocytic leukemia. *Acta Haematol* 106:43–51.

Fenaux, P., Chomienne, C., and Degus, L. (1997) Acute promyelocytic leukemia: Biology and treatment. *Semin Oncol* 24:92–102.

Grimwade, D. (1999) The pathogenesis of acute promyelocytic leukaemia: Evaluation of the role of molecular diagnosis and monitoring in the management of the disease. *Brit J Haematol* 106:591–613.

Kadota, K., Yamazaki, M., Ishino, S., and Nei, T. (1984) Ultrastructure and C-type particles in myeloid leukemia of a pig. *Vet Pathol* 21:263–265.

Li, S.W., Tang, D., Ahrens, K.P., She, J.X., Braylan, R.C., and Yang, L. (2003) All-trans-retinoic acid induces CD52 expression in acute promyelocytic leukemia. *Blood* 101(5):1977–1980.

McKenna, R.W., Parkin, J., Bloomfield, C.D., et al. (1982) Acute promyelocytic leukaemia: A study of 39 cases with identification of a hyperbasophilic microgranular variant. *Br J Haematol* 50:201–214.

Murate, T., Suzuki, M., Hattori, M., Takagi, A., Kojima, T., Tanizawa, T., Asano, H., Hotta, T., Saito, H., Yoshida, S., and Tamiya-Koizumi, K. (2002) Up-regulation of acid sphingomyelinase during retinoic acid-induced myeloid differentiation of NB4, a human acute promyelocytic leukemia cell line. *J Biol Chem* 277(12):9936–9943.

Nouzova, M., Holtan, N., Oshiro, M.M., Isett, R.B., Munoz-Rodriguez, J.L., List, A.F., Narro, M.L., Miller, S.J., Merchant, N.C., and Futscher, B.W. (2004) Epigenomic changes during leukemia cell differentiation: Analysis of histone acetylation and cytosine methylation using CpG island microarrays. *J Pharmacol and Experim Therapeut* 311(3):968–981.

Puccetti, E., and Ruthardt, M. (2004) Acute promyelocytic leukemia: PML/RARα and the leukemic stem cell. *Leuk* 18:1169–1175.

Sham, R.L., and Tallman, M.S. (2004) Treatment of acute promyelocytic leukemia in the very elderly: Case report and review of the literature. *Leuk Res* 28:1347–1350.

Tallman, M.S., Kwaan, H.C. (1992) Assessing the hemostatic disorder associated with acute promyelocytic leukemia. *Blood* 79:543–553.

Villa, R., De Santis, F., Gutierrez, A., Minucci, S., Pelicci, P.G., and Di Croce, L. (2004) Epigenetic gene silencing in acute promyelocytic leukemia. *Biochem Pharmacol* 68:1247–1254.

Acute Myelomonocytic Leukemia M4

Definition

Acute myelomonocytic leukemia M4 is characterized by a marrow population of at least 20% monocytic cells

made up of monoblasts, promonocytes, and monocytes, plus 20% or more of neutrophils and their precursors. The neutrophil precursors include type I and II myeloblasts, and the monocytic precursors are represented by monoblasts and promonocytes.

Clinical Presentation and Features

Blood, Bone Marrow, and Other Tissues

Dogs tend to present with lymphadenopathy, and the blast cells in the blood are likely to be interpreted as lymphoid leukemia. In dogs, there is characteristically a leukocyte count in the 4,000/ul range with the severe neutropenia and the monocytic progeny predominating, but blasts of both lineages are present. With progression, there is a blastic crisis with the leukocyte count rising to over 400×10^3/ul and the lymphadenopathy accompanied by hepatosplenomegaly and marked neutropenia, anemia, and thrombocytopenia. Dogs with M4 may present with skin lesions or develop cutaneous manifestations over the course of the disease. Pathologically, there is widespread neoplastic proliferation, with the marrow largely devoid of fat and with solid neoplastic cells (Figs. 5.69, 5.70). The spleen has diffuse sinus infiltration with lymphoid atrophy and the liver has both sinus and perivascular infiltrates. The nodes are heavily infiltrated, and if there is a unique architectural pattern of nodal colonization it has not been documented.

The presentation of M4 in the horse is similar, but because palpation of nodes is less accurate in this heavily muscled species, enlargement of the submandibular nodes is usually noted; other sites of lymphadenopathy are largely found only on necropsy. The leukocyte count in the horse at presentation is even lower than the dog, again with severe neutropenia and accompanied by anemia and thrombocytopenia. Pathologically, there is widespread tumor with prominent splenomegaly and focal hepatic involvement and a packed marrow.

M4 in the cat may differ from other species in a much higher total leukocyte count at presentation, with a normal level of neutrophils and trilineage myelodysplastic changes that progress to severe anemia and thrombocytopenia. The cytochemical staining characteristics and anatomic pathology are as described for M4 in other animals.

The diagnosis rests on demonstration of blasts and progeny of both neutrophil and monocytic lineages in both marrow and blood, with 20% or more of marrow myeloblasts, monoblasts, and promonocytes. In addition, the marrow must contain 20% or more of both neutrophilic and monocytic progeny. These lineages are identified by the neutrophil lineage marking for MPO and SBB in precursors and progeny and the monocytic lineage marks with nonspecific esterase (NSE).

A variant form of M4 occurs in humans that is characterized by increased marrow eosinophils and is associated with a specific inversion inv(16) or t(16;16) and has a very good prognosis with cytarabine therapy. It is unknown whether this variant occurs in animals, but it has useful diagnostic differences with the eosinophilic precursors having atypical granulation with eosinophilic and basophilic granules.

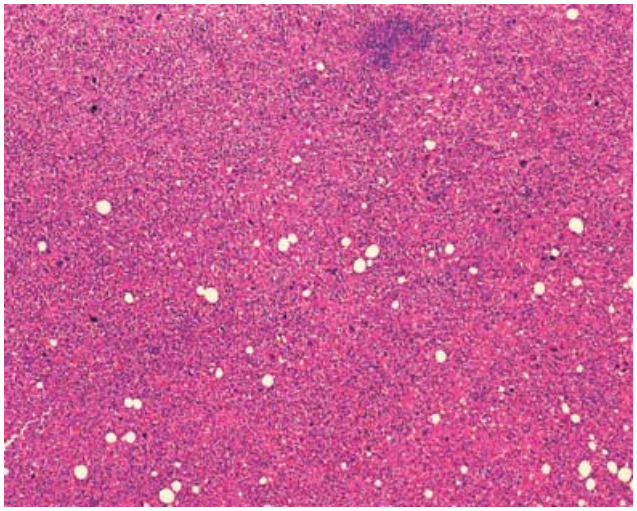

Figure 5.69. Cat: bone marrow, acute myeloid leukemia, likely M4. The marrow is hypercellular in the midfemoral shaft with solidly cellular proliferation. A cluster of dark cells at the upper margin is a fading lymphoid follicle.

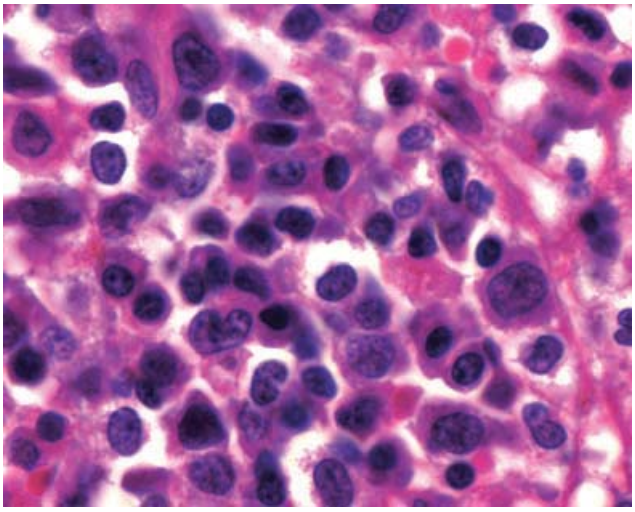

Figure 5.70. Cat: marrow, acute myeloid leukemia. Detail of Figure 5.69. There are large blasts present with a loss of marrow granulocyte reserves and erythropoietic cells with suggestion of myeloid differentiation in the large indented cell in the left center and lower right.

In the blood, with M4 the major difference with the more acute leukemias is that mature neutrophils are numerous and platelets may be reduced but not to a level associated with petechiation. The neutrophils have reduced normal granulation and very pale cytoplasm. The most mature monocytes are slightly smaller than normal with remarkably lobulated nuclei that resemble those of basophils with broad nuclear segments that retain a bland chromatin pattern without formation of dense chromocenters. The neutrophil precursors include metamyelocytes with broad nuclear arms that resemble the giant type of myelodysplastic marrow, and the myelocytes have lightly basophilic cytoplasm with little granulation. The promyelocytes are of normal size with more than normal cytoplasmic basophilia and less than normal granulation. The blasts are of both type I and II types and are relatively numerous. The monocytic precursors include very large cells with reniform nuclei that have finely dispersed chromatin, without dense chromocenters, and abundant lightly basophilic agranular cytoplasm that has occasional fine vacuoles. The monoblasts and promonocytes are very large cells 5–6 red cells in total diameter, with round to oval nuclei with abundant quite highly basophilic cytoplasm that has an occasional azurophilic granule and many fine vacuoles.

The bone marrow in M4 is highly cellular with few fat cells and few megakaryocytes or rubricytes. Some time must be spent in looking for the intermediate stages of maturation on both the neutrophil and monocytic line because both lineages are atypical in appearance and larger than normal (Fig. 5.71). In the neutrophil lineage, the blasts are like M1 and M2, but the promyelocytes are poorly granulated and have an increased nuclear cytoplasmic ratio, due to a larger nucleus and less cytoplasm, that is often eccentrically placed with the nuclear and cytoplasmic membranes often in contact (Fig. 5.72). The myelocytes are more like large lymphocytes with an occasional azurophilic granule and unusual cytoplasmic basophilia. The monocytic series normally has a shorter proliferative sequence with only blast, promonocyte, and monocytic stages (Fig. 5.73). In M4, some of the promonocytes appear to be in aberrant maturation, with very basophilic cytoplasm that is highly vacuolated and appears somewhat toxic and degenerate and with vacuolations perforating the nucleus, which has larger dense chromocenters and chromatin bands (Fig. 5.74). There is a remarkable phthisis of normal marrow elements with few rubricytes or megakaryocytes.

M4 must be differentiated from AML of M2 type and from M5B AML on the criteria of diagnosis for each entity. The M2 form of AML has much fewer monocytes than M4, and all primitive cells are negative with NSE staining (Figs. 5.75, 5.76) although the myeloid precursors are positive with CAE (Figs. 5.77, 5.78). The M5 AML has many more maturing marrow monocytes than M4.

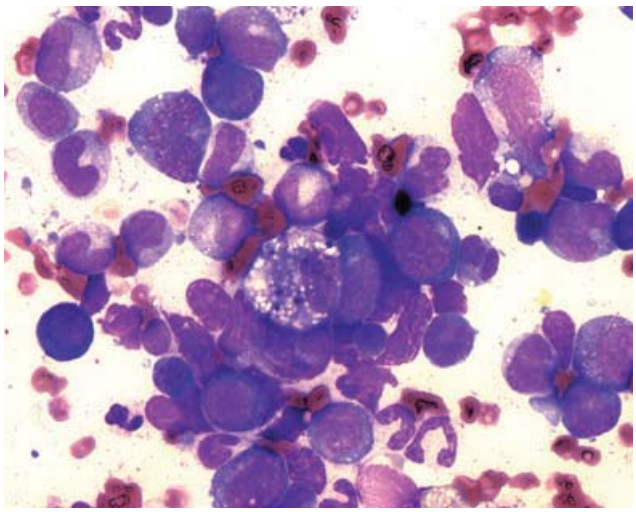

Figure 5.71. Cat: marrow aspirate, acute myelomonocytic leukemia. The neoplastic blasts are from both the myeloid and monocytic lineages. Those cells in the upper left are likely of granulocytic lineage; the cells in the upper right with irregular-shaped nuclei and fine cytoplasmic vacuolations are more likely of monocytic lineage. There are mature neutrophils and some erythroid cells present indicative of less severe phthisis of normal marrow cells.

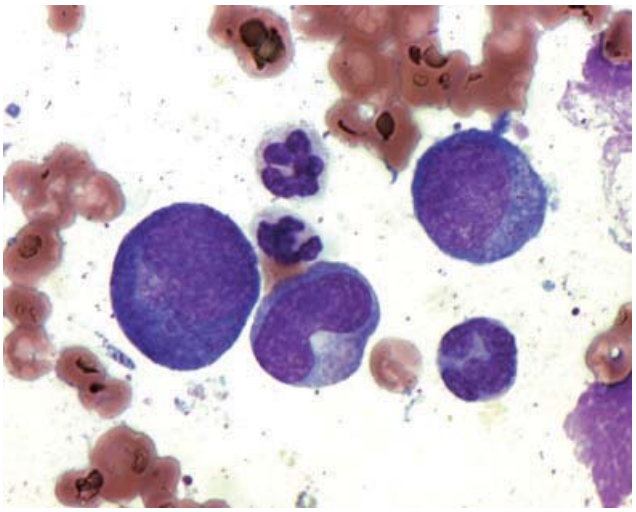

Figure 5.72. Cat: acute myelomonocytic leukemia. Detail of Figure 5.71. Two large cells with eccentric cytoplasm are likely promyelocytes with reduced cytoplasmic volume and granulation. The very large cell with an indented nucleus is likely myelocytic or metamyelocytic, with the 2 cells above poorly granulated neutrophils and the cell in lower right a small atypical monocytic cell with low cytoplasmic volume.

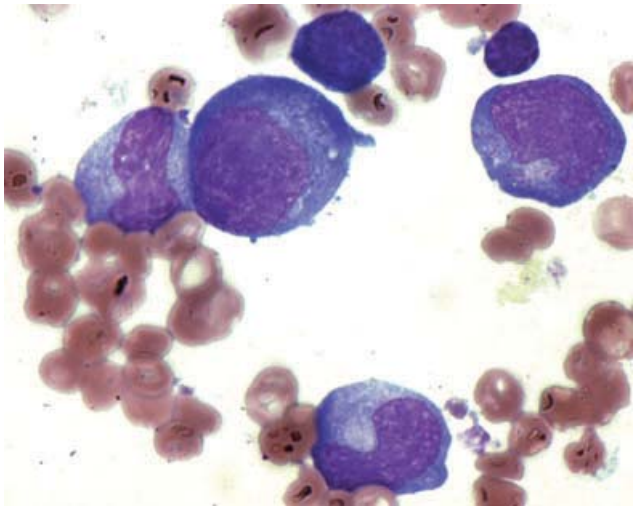

Figure 5.73. Cat: acute myelomonocytic leukemia. Detail of Figure 5.71. A large cell at the center left is likely a blastic cell of the monocytic series with early cytoplasmic vacuolation and minor indentations in nuclear outline. The other 3 cells have irregular-shaped nuclei with fine cytoplasmic vacuolations with the cell at the top having scattered cytoplasmic granulation smaller than granules of a promyelocyte.

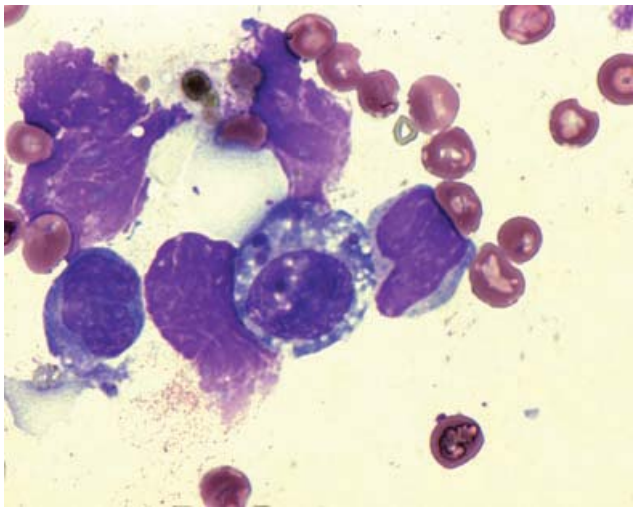

Figure 5.74. Cat: acute myelomonocytic leukemia. An atypical monocytic precursor, (center) with cytoplasmic vacuolation that also perforates the nucleus. The cell retains a nucleolus and has ingested hemosiderin granules. The intact cells left and right are of more mature monocytic progeny.

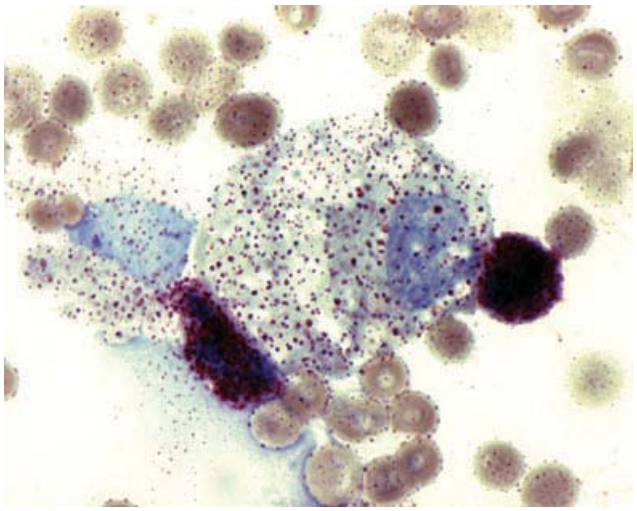

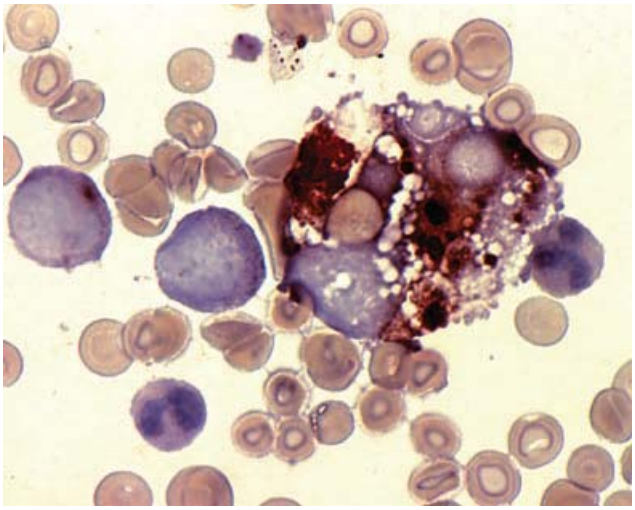

Figure 5.75. Cat: marrow, acute myelomonocytic leukemia. With nonspecific esterase (NSE) staining, the specificity of the stain is indicated by strong focal cytoplasmic marking of a large macrophage with the surrounding myeloid precursors unlabeled. *Slide from R. M. Jacobs, DVM.*

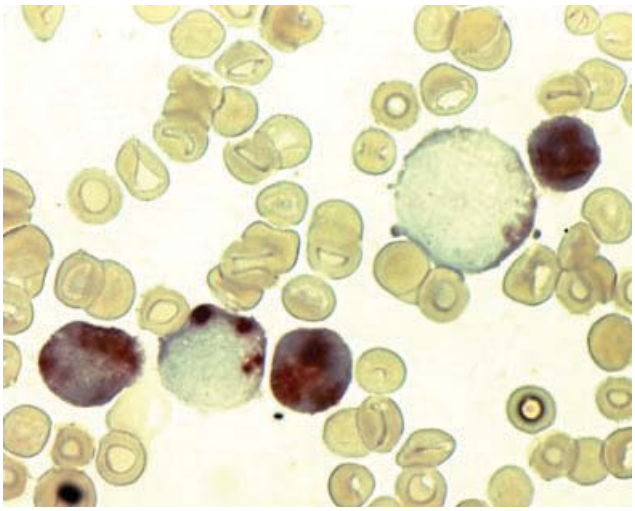

Figure 5.76. Cat: marrow, acute myelomonocytic leukemia. Phenotype of Figure 5.71. With NSE staining, the large promyelocyte (right) is negative while 3 maturing monocytic cells have strong labeling and a blast at lower left with strong focal cytoplasmic marking indicating early monocytic differentiation.

Figure 5.77. Cat: marrow, acute myelomonocytic leukemia. Phenotype of Figure 5.71. With chloroacetate esterase (CAE) staining, 2 macrophages are negative with fine focal artifactual background staining with 2 adjacent maturing granulocytes strongly positive indicating the specificity of the stain for myeloid differentiation. *Slide from R. M. Jacobs, DVM.*

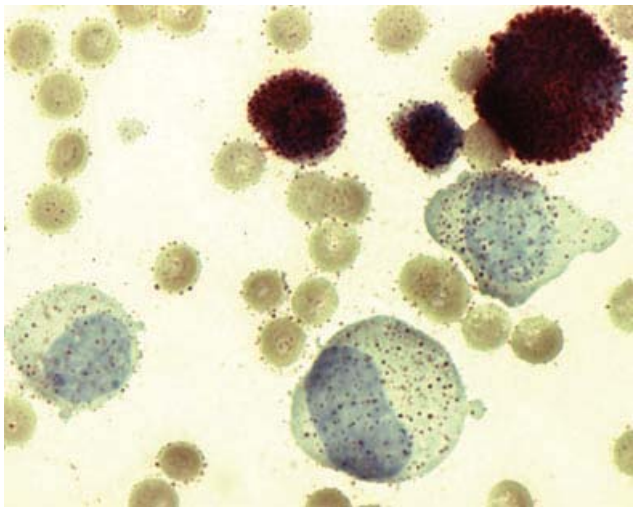

Figure 5.78. Cat: marrow, acute myelomonocytic leukemia with CAE staining. The cell of promyelocytic size in the upper right and 2 maturing granulocytes are strongly positive while 3 adjacent cells of large mononuclear type, the largest of which has fine cytoplasmic vacuoles, are negative.

REFERENCES

Aricò, M., Biondi, A., and Pui, C.H. (1997) Juvenile myelomonocytic leukemia. *Blood* 90(2):479–488.

Beran, M., Kantarjian, H., O'Brien, S., Koller, Ch., Al-Bitar, M., Arbuck, S., Pierce, S., Moore, M., Abbruzzese, J.L., Andreeff, M., Keating, M., and Estey, E. (1996) Topotecan, a topoisomerase I inhibitor, is active in the treatment of myelodysplastic syndrome and chronic myelomonocytic leukemia. *Blood* 88(7):2473–2479.

Bienzle, D., Hughson, S.L., and Vernau, W. (1993) Acute myelomonocytic leukemia in a horse. *Can Vet J* 34:36–37.

Brumbaugh, G.W., Stitzel, K.A., Zinkl, J.G., and Feldman, B.J. (1982) Myelomonocytic myeloproliferative disease in a horse. *JAVMA* 180(3):313–316.

Brunning, R.D. (2001) Acute myeloid leukemia. In Knowles, D.M. (ed.), *Neoplastic Hematopathology*, 2nd ed., Lippincott Williams & Wilkins, Philadelphia, pp. 1667–1715.

Domínguez, J., Ezquerra, A., Alonso, F., McCullough, K., Summerfield, A., Bianchi, A., Zwart, R.J., Kim, Y.B., Blecha, F., Eicher, S., Murtaugh, M., Pampusch, M., and Burger, K. (1998) Porcine myelomonocytic markers: Summary of the second international swine CD workshop. *Vet Immunol and Immunopathol* 60:329–341.

Galton, D.A.G. (1992) Haematological differences between chronic granulocytic leukaemia, atypical chronic myeloid leukaemia, and chronic myelomonocytic leukaemia. *Leuk and Lymph* 7:343–350.

Graves, T.K., Swenson, C.L., and Scott, M.A. (1997) A potentially misleading presentation and course of acute myelomonocytic leukemia in a dog. *J Am An Hosp Assoc* 33:37–41.

Jain, N.C., Madewell, B.R., Weller, R.E., and Geissler, M.C. (1981) Clinical-pathological findings and cytochemical characterization of myelomonocytic leukemia in 5 dogs. *J Comp Pathol* 91:17–31.

Kass, L. (1977) Esterase reactions in acute myelomonocytic leukemia. *Am J Clin Pathol* 67(5):485–488.

Larson, R.A., Williams, S.F., Le Beau, M.M., Bitter, M.A., Vardiman, J.W., and Rowley, J.D. (1986) Acute myelomonocytic leukemia with abnormal eosinophils and inv(16) or t(16;16) has a favorable prognosis. *Blood* 68(6):1242–1249.

Mori, T., Ishida, T., Washizu, T., Yamagami, T., Umeda, M., Sugiyama, M., and Motoyoshi, S. (1991) Acute myelomonocytic leukemia in a horse. *Vet Pathol* 28:344–346. (1977) Nagata, T., Mugishima, H., Yoden, A., Yoshikawa, K., Oguni, T., Yamashiro, K., Yamamori, S., and Harada, K. (2000) A case of monoclonal gammopathy associated with acute myelomonocytic leukemia with eosinophilia suggested to be the result of lineage infidelity. *Am J Hematol* 65:66–71.

Raskin, R.E., and Krehbiel, J.D. (1985) Myelodysplastic changes in a cat with myelomonocytic leukemia. *JAVMA* 187(2):171–174.

Rohrig, K.E. (1983) Acute myelomonocytic leukemia in a dog. *JAVMA* 182(2):137–141.

Rosen, A.M., Haines III, K., Tallman, M.S., Hakimian, D., and Ramsey-Goldman, R. (1995) Rapidly progressive cutaneous vasculitis in a patient with chronic myelomonocytic leukemia. *Am J Hematol* 50:310–312.

Shifrine, M., Bulgin, M.S., Dollarhide, N.E., Wolf, H.G., Taylor, N.J., Wilson, F.D., Dungworth, D.L., and Zee, Y.C. (1971) Transplantation of radiation-induced canine myelomonocytic leukaemia. *Nature* 232(5310):405–406.

Acute Monoblastic Leukemia M5A and Acute Monocytic Leukemia M5B

Definition

Acute leukemia involving the monocytic lineage occurs in two forms with a peracute monoblastic form known as M5A and a more differentiated form known as acute monocytic leukemia M5B. M5 closely resembles AML M2 and AML M4, and these entities need to be carefully distinguished on the proportions of primitive myeloid and monocytic cells present. Both types of M5 are characterized by marrow containing 80% or more of monoblasts, promonocytes, and monocytes but including some neutrophils, erythroid progenitors, and some of the lymphoid lineage with both lymphocytes and plasma cells. The distinctions between these entities are subtle, the criteria for M5A (acute monoblastic leukemia) is 20% or more of marrow cells consisting of myeloblasts, monoblasts, and promonocytes, but with more than 80% of marrow monocytic cells being true monoblasts. In contrast M5B (acute monocytic leukemia) is defined as having 80% of marrow cells of monocytic type, but fewer of these are of

blast cell type. Succinctly stated, the monoblast predominates in M5A and the promonocyte predominates in M5B.

AML M5A—Epidemiology and Incidence

AML M5A is a rare disease or is at least rarely convincingly identified. In the dog, M5A occurs in young animals generally less than 3 years old, and no sex predilection has been noted. In human M5A, translocations involving 11q23 and a variety of partner chromosomes are the most common cytogenetic abnormalities.

Clinical Presentation and Features

Typically in animals, there is a history of declining weight and appetite over a period of a month or less and they may be pyrexic on presentation. The animals have pale mucus membranes often with petechiation, generalized lymphadenopathy, and hepatosplenomegaly. The clinical period following diagnosis is typically 2 weeks or less.

Pathologic Features

Blood

The packed red cell volume (PCV) is in the 20–25% range, and there is a moderate leukocytosis of 25,000–35,000/ul with neutrophils in the normal range or mildly elevated, mild lymphopenia, and a predominant population of monoblasts and progeny with marked predominance (>80%) of blasts (Figs. 5.79–5.82). There is always thrombocytopenia and it may be marked and in the 10,000/ul range attributing to the anemia and the petechiation. Some animals will have patchy erythematous skin lesions due to neoplastic perivascular infiltration and deep dermal vessels.

Bone Marrow

The marrow is solidly infiltrated with the neoplastic cells, with the animals typically becoming clinical when more

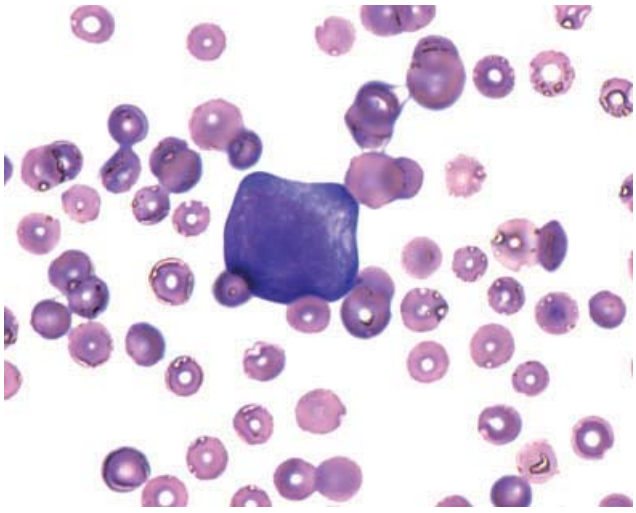

Figure 5.79. Cow: blood, acute monoblastic leukemia. The monoblastic cells are typically softer than myeloblasts and more likely to be indented by surrounding cells. The nucleus is oval with multiple small nucleoli and with a dense chromatin pattern without large chromocenters. The cytoplasm is abundant and highly basophilic but without vacuolation.

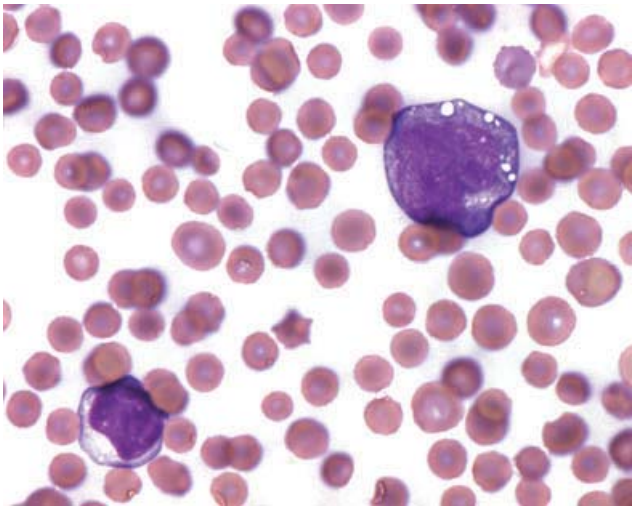

Figure 5.80. Cow: blood, acute monoblastic leukemia, same slide as Figure 5.79. The larger cell is a promonocyte that retains nucleolus but has early nuclear indentation and several large chromocenters. The cytoplasm is abundant and highly basophilic with fine and larger cytoplasmic vacuolations.

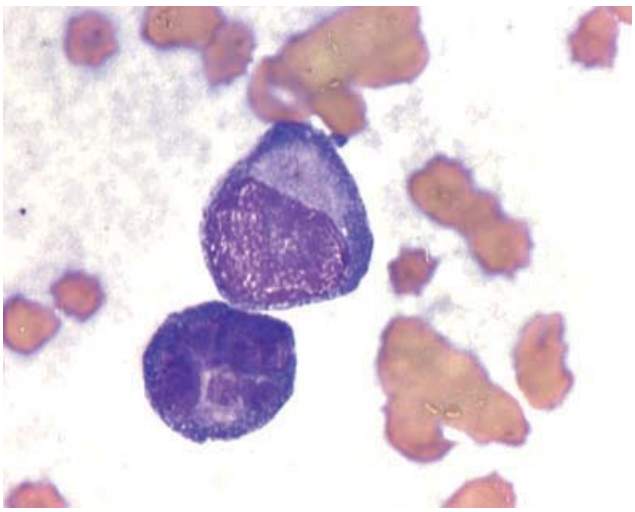

Figure 5.81. Dog: blood, acute monoblastic leukemia. The cell in center is a blast with a poorly delineated large nucleolus without formation of the large chromocenters. The cytoplasm is highly basophilic and relatively abundant. The more densely stained cytoplasm in the periphery is atypical and likely related to location at the base of the blood film. The cell on the left is more differentiated and likely a late promonocyte.

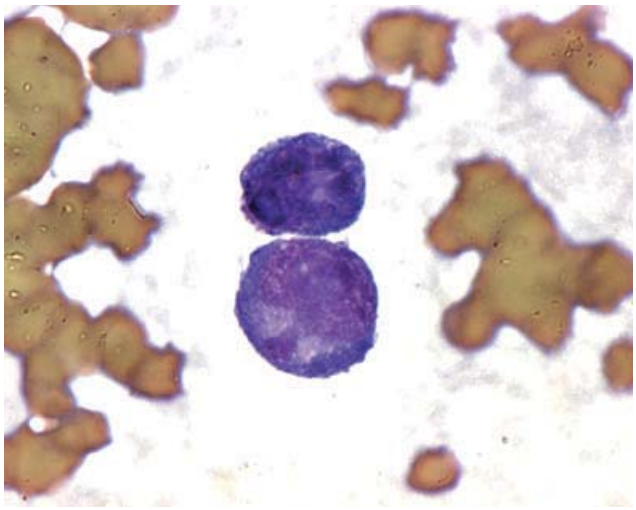

Figure 5.82. Dog: blood, acute monoblastic leukemia. Two large cells have asynchronous nuclear maturation, hyperchromatic cribriform chromatin with multiple nucleoli and without large chromocenters but with advanced nuclear indentations. The cytoplasm is very densely stained and with only focal vacuolation.

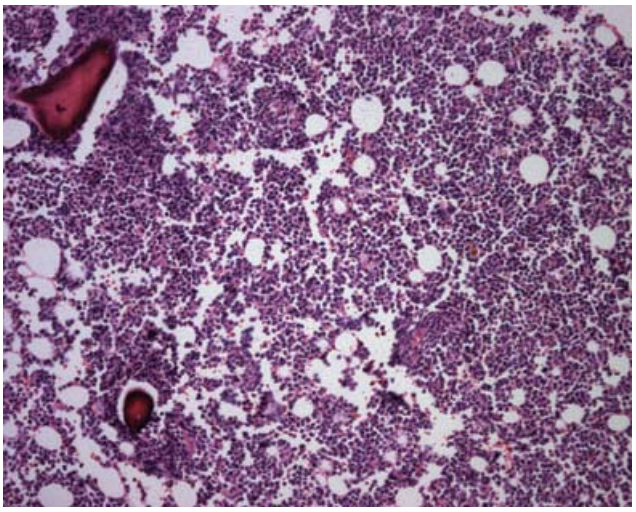

Figure 5.84. Dog: marrow, acute monoblastic leukemia. There is very high cellularity of the marrow in the femoral diaphyseal area. This image was taken at an architectural level to demonstrate a complete absence of megakaryocytes.

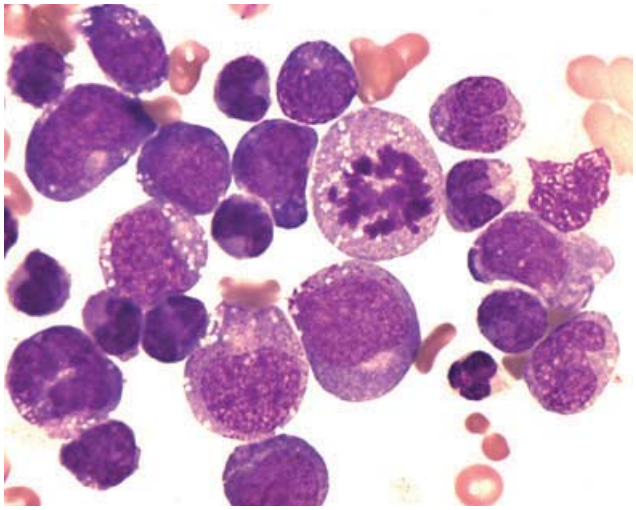

Figure 5.83. Dog: marrow, acute monoblastic leukemia. The larger primitive cells with cytoplasmic vacuoles are typical of monocytic differentiation with a few azurophilic granules. The cell in the lower left with an irregularly shaped nucleus with smooth nuclear membranes is typical of a maturing monocyte. There is an absence of erythroid precursors.

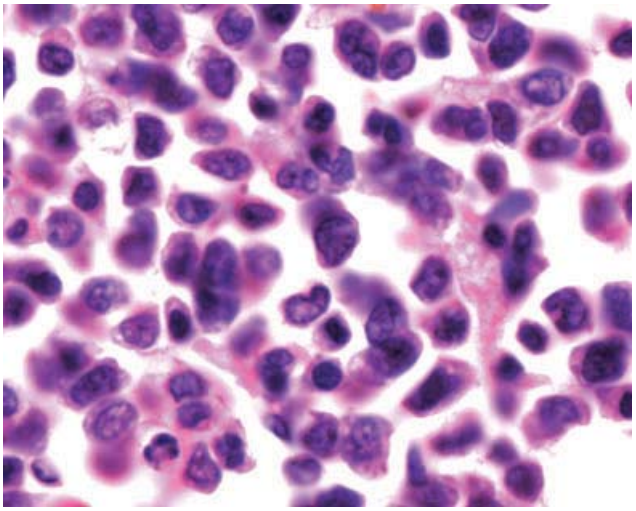

Figure 5.85. Dog: marrow, acute monoblastic leukemia. Detail of Figure 5.84. The marrow is completely occupied by cells of monocytoid appearance, with the precursors having more rounded nuclei and the maturing stages having indented or lobulated nuclei. The cytoplasm is moderate in volume and staining density; there is a complete absence of erythroid precursors and marrow granulocyte reserves except for a single neutrophil in the lower left.

than 50% of marrow is occupied by tumor and there is phthisis of the erythroid and megakaryocytic lineages (Figs. 5.83–5.85). The splenic sinuses are expanded with a monoblastic population and there is marked lymphoid atrophy (Figs. 5.86, 5.87). Cytologically, the monoblasts have round to oval nuclei 3 red cells in diameter with densely stained chromatin with a diffuse cribriform pattern, no large chromocenters, and 1–3 relatively prominent nucleoli (Fig. 5.88). The cytoplasm is moderate in volume, agranular, and very highly basophilic, and it may have a few very fine marginal vacuoles. In some cases, the cytoplasm is less basophilic and an occasional azurophilic granule may be present. The promonocytes may be larger than blasts, especially in the cow (see Fig.

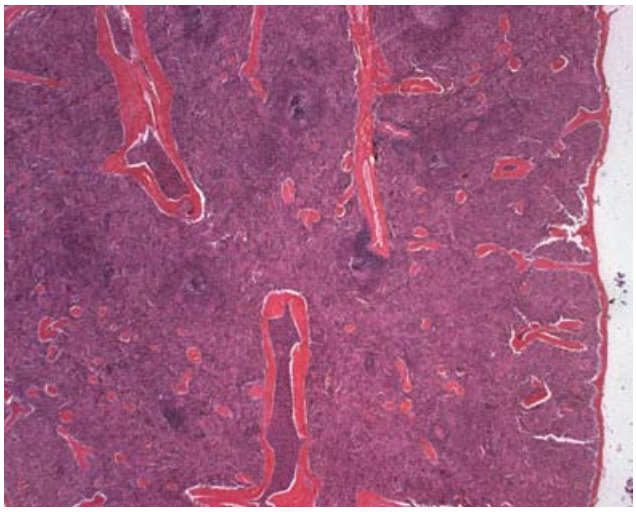

Figure 5.86. Dog: spleen, acute monoblastic leukemia, same case as Figure 5.83. The spleen is moderately enlarged with thinning of the capsule and separation of muscular trabeculae by diffuse sinus expansion. There is a complete absence of germinal centers with one fading in the upper right and marked atrophy of periarteriolar lymphoid sheaths.

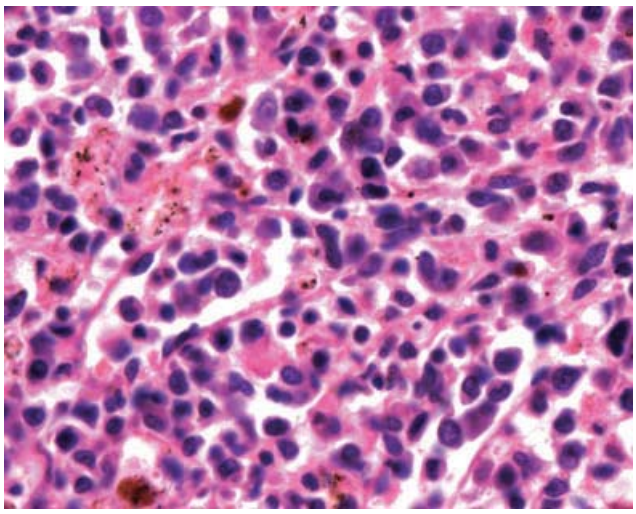

Figure 5.87. Dog: spleen, acute monoblastic leukemia. Detail of Figure 5.86. The sinus areas are solidly filled with neoplastic cells very similar to that of the marrow with a complete absence of extramedullary hematopoiesis.

5.80), with round to oval nuclei 4 red cells in diameter with a smooth nonindented margin and 5–10 large chromocenters that may abut the several nucleoli. The cytoplasm is abundant and slate gray with even density from the nuclear margin to the cell boundary, and it may have

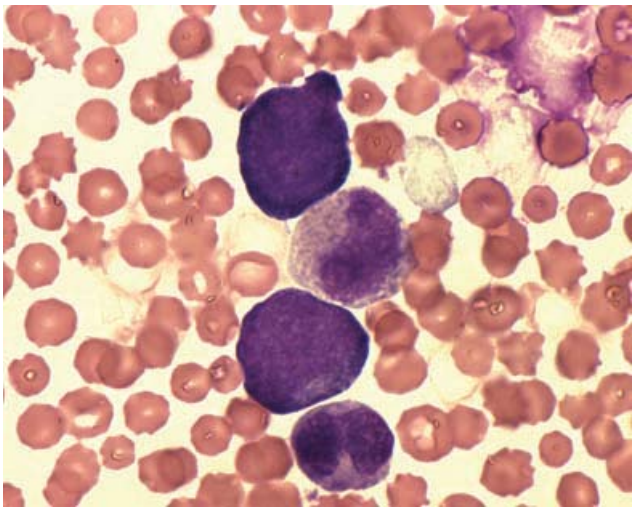

Figure 5.88. Cow: marrow, acute monocytic leukemia. There are 2 blast cells in the center flanking a differentiating cell of metamyelocyte type. The cell at the bottom with bilaterally indented nucleus is likely a differentiating monocytic cell.

many fine peripheral vacuoles. Most cells are agranular or have a very few dustlike pink granules, but none of azurophilic type of promyelocytes (see Fig. 5.88). Both monoblasts and promonocytes have a cytoplasmic tendency for focal pseudopodia that is like that of megakaryoblastic leukemia. The more mature monocytic cells are larger than their normal counterpart and have very irregular-shaped nuclei that may be trilobated and or with multiple deep clefts. The chromatin pattern retains a relatively young appearance, but the larger chromocenters become more apparent as the cells age and nucleoli are still evident in the maturing cells. Platelets are rare or absent, small, and poorly granulated with fine irregular basophilia.

Diagnostic Criteria

The neoplastic cells from blood and tissues are strongly or moderately positive with alpha naphthyl acetate esterase or N-butyl acetate esterase in about 80% of cells, and all are negative or, rarely, only very weakly and irregularly positive for chloroacetate esterase and completely negative for SBB and leukocyte peroxidase.

Differential Diagnosis

M5A must be differentiated from M2 on the basis of NBE positivity and from M4 myelomonocytic leukemia by the monocytic blastic population being less than 80% of the cells of monocytic lineage in blood and marrow. Because of the tendency of the primitive cells to have

cytoplasmic pseudopodia and the accompanying thrombocytopenia, it is necessary to differentiate M5A from M7 acute megakaryoblastic leukemia that is negative or only weakly positive for nonspecific esterase (ANAE, NBE).

AML M5B—Definition

M5B is an acute leukemia in which the predominant cell in both blood and marrow are of promonocyte type.

Epidemiology and Incidence

M5B is much more common than M5A, and most of the cases described are of this type. Some cases described as acute monocytic leukemia, with hepatosplenomegaly of mononuclear cells that occasionally have ingested red cells but with minimal involvement of bone marrow if not verified by positive staining for NBE, may in fact be hepatosplenic T-cell lymphoma. The latter neoplasm is characterized by erythrophagocytic activity by blast cells, and this activity does not ensure monocytic lineage. In human M5B, a variant type occurs with a t(8;16)(p11;p13) translocation characterized by neoplastic monocytes that are erythrophagocytic. These cells have a few azurophilic granules, and the patients have a poor prognosis due to a tendency to involve the central nervous system. Dogs with M5B are typically under 3 years old and horses are young mature with several reports on 6-year-old animals with no gender predilection.

Clinical Presentation and Features

The presentation in all species is similar with a history of declining appetite and weight over a period of 3–4 months. On physical examination there is again mucosal pallor, but not petechiation, and mild lymphadenopathy and hepatosplenomegaly.

Pathologic Features

Blood

All animals are mild to moderately anemic with variable leukocytosis that may be marked in the dog, and in excess of 100,000/ul and in the horse in the 20,000–30,000/ul range, but platelets may be only mildly reduced (Fig. 5.89). Most of the cells in the blood are of monocytic origin and blasts are present but much fewer than the maturing forms (Fig. 5.90).

Bone Marrow

The bone marrow is always involved with at least 20% of marrow cells myeloblast, monoblast, and promonocyte type. Megakaryocytes are few and there is very extensive erythroid phthisis. Treatment is again rarely undertaken because of the very poor prognosis, and most animals do not survive long following diagnosis. Cytologically, the

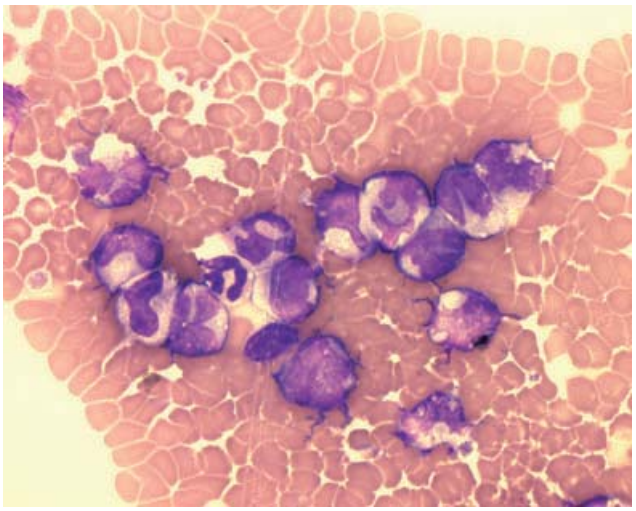

Figure 5.89. Dog: blood, acute monocytic leukemia. At the M5B level of differentiation, the peripheral blood cells consist primarily of monocytes. There is a single neutrophil near the left center and several platelets in the upper left, left center, and lower right. The animal is only mildly anemic.

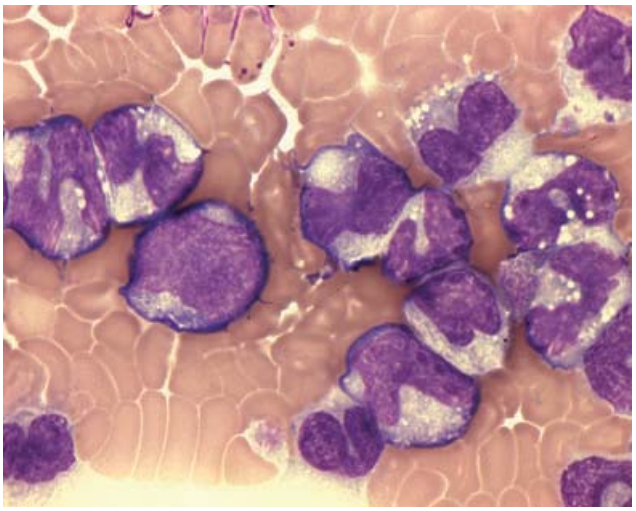

Figure 5.90. Dog: blood, acute monocytic leukemia. Detail of Figure 5.89. Most of the cells are relatively mature monocytes that retain a fine chromatin pattern with few large chromocenters that lack nucleoli. The cytoplasm tends to be of similar density throughout with the more mature cells developing cytoplasmic vacuoles. The cell in the left center is likely promonocytic.

blasts and promonocytes are like those of M5A, but the proportions are greatly shifted to a predominance of promonocytes and atypical monocytes with blast cells in minor proportion (Figs. 5.91, 5.92).

Pathologically, the neoplastic cells are in marrow, spleen, and liver (Figs. 5.93, 5.94), but they are also in the intestinal wall, kidneys, adrenals, and even the choroid plexus.

Differential Diagnosis

M5B must be differentiated from the poorly granulated type of M4 promyelocytic leukemias that are always strongly positive for myeloperoxidase and SBB and negative for NBE. In M5B there is phthisis of the myeloid system; in M4 the neutrophils exceed 20% of marrow cells, but they do not in M5B.

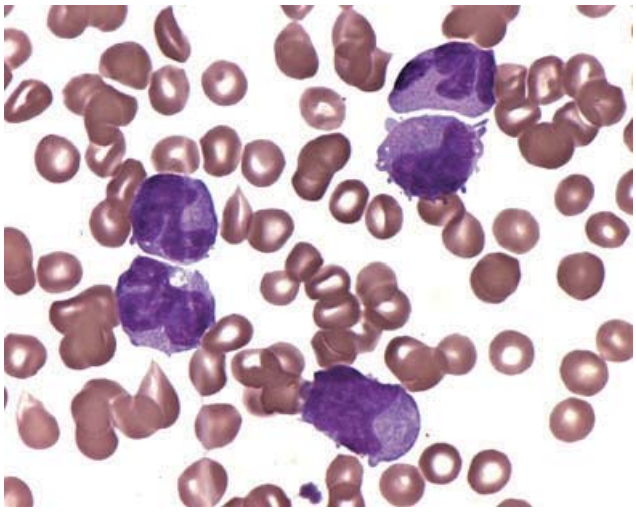

Figure 5.91. Dog: marrow, acute monocytic leukemia. The monocytes predominate in the marrow with greater immaturity than in the blood but with similar cytoplasmic development with uniform basophilia.

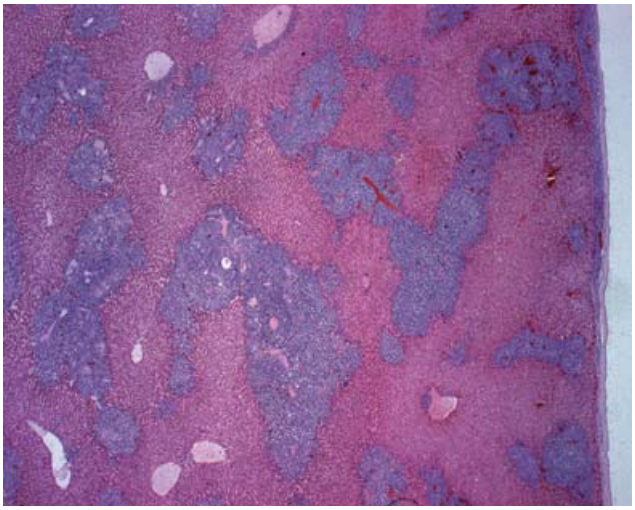

Figure 5.93. Dog: liver, acute monocytic leukemia. There is very extensive involvement of the liver that remains highly focal and centered on portal areas.

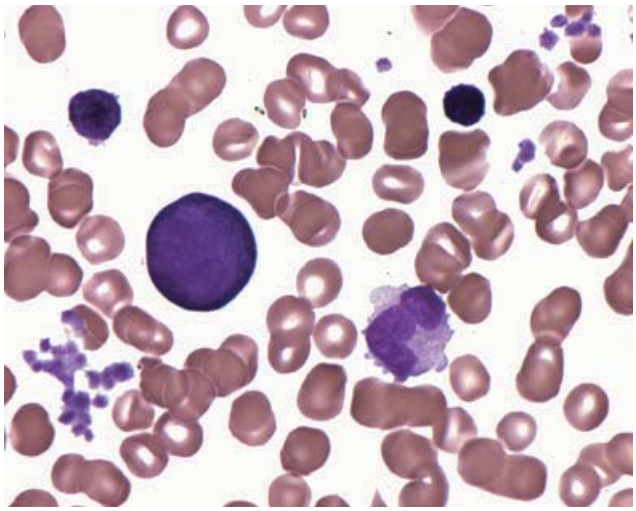

Figure 5.92. Dog: marrow, acute monocytic leukemia, same case as Figure 5.90. The large cell is a blast presumably of monocytic center lineage with an early monocyte above. The 2 small dense cells are rubricytes that with the presence of platelets indicates less severe phthisis of normal marrow elements than in AML MO-2.

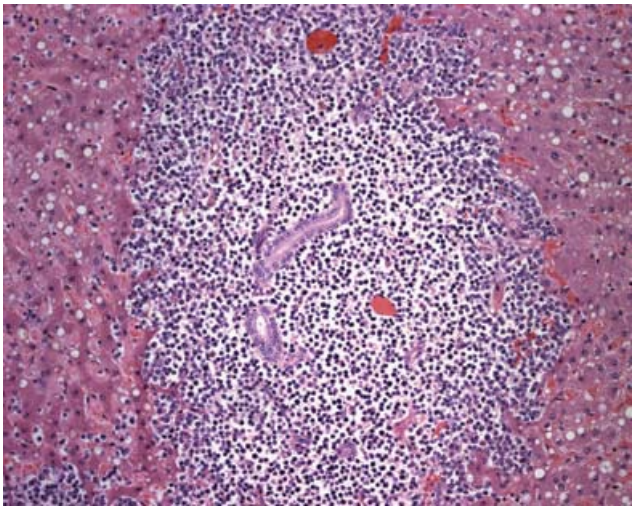

Figure 5.94. Dog: liver, acute monocytic leukemia. Detail of Figure 5.93. The infiltration of the liver is remarkably limited to the portal areas, with a relatively solid front of compressive expansion at the interface with the surrounding parenchyma with few neoplastic cells in hepatic sinuses. Benign extramedullary hematopoiesis is not present either focally or intermixed with the neoplastic cells.

REFERENCES

Bertheas, M.F., Jaubert, J., Vasselon, C., et al. (1989) A complex t(3;8;17) involving breakpoint 8p11 in a case of M5 acute non-lymphoblastic leukemia with erythrophagocytosis. *Cancer Genet Cytogenet* 2:62–73.

Brunning, R. (1999) Proposed World Health Organization (WHO) classification of acute leukemia and myelodysplastic syndromes. *Mod Pathol* 12:102.

Brunning, R.D. (2001) Acute myeloid leukemia. In Knowles, D.M. (ed.), *Neoplastic Hematopathology*, 2nd ed. Lippincott Williams & Wilkins, Philadelphia, pp. 1667–1715.

Burkhardt, F., Saldern, F., and Huskamp, B. (1984) Monocytic leukemia in a horse. *Vet Pathol* 21:394–398.

Cheson, B.D., Cassileth, P.A., Head, D.R., et al. (1990) Report of the National Cancer Institute-sponsored workshop on definitions of diagnosis and response in acute myeloid leukemia. *J Clin Oncol* 8:813–819.

Hanslip, J.I., Swansbury, R., Pinkerton, R., et al. (1992) The translocation (t8;16)(p11;p13) defines an AML subtype with distinct cytology and clinical features. *Leuk Lymph* 6:479–486.

Heim, S., Avanzi, G., Billstrom, R., et al. (1987) A new chromosomal rearrangement (t8;16)(p11;p13) in acute monocytic leukemia. *Brit J Haematol* 66:323–326.

Koziner, B., McKenzie, S., Straus, D., Clarkson, B., Good, R.A., and Siegal, F.P. (1997) Cell marker analysis in acute monocytic leukemias. *Blood* 49(6):895–901.

Lai, J.L., Zandecki, M., Joulet, J.P., et al. (1987) Three cases of translocation (8;16)(p11;p13) observed in acute myelomonocytic leukemia: A new specific group? *Cancer Genet Cytogent* 27:101–109.

Latimer, K.S., and Dykstra, M.J. (1984) Acute monocytic leukemia in a dog. *JAVMA* 184(7):852–855.

Mackey, L.J., Jarrett, W.F.H., and Wiseman, A. (1972) Monocytic leukaemia in a cow. *Res Vet Sci* 13:289–291.

McKenna, R.W., Bloomfield, C.D., Dick, F., Nesbit, M.E., and Brunning, R.D. (1975) Acute monoblastic leukemia: Diagnosis and treatment of ten cases. *Blood* 46(4):481–494.

Milligan, D.W., Roberts, B.E., Limbert, H.J., and Jalihal, S. (1984) Cytochemical and immunological characteristics of acute monocytic leukaemia. *Brit J Haematol* 58:391–397.

Modiano, J.F., Smith III, R., Wojcieszyn, J., Thomas, J.S., Rosenbaum, B.A., Ball, C., Nicholds, E.A., Anthony, M.A., and Barton, C.L. (1998) The use of cytochemistry, immunophenotyping, flow cytometry, and in vitro differentiation to determine the ontogeny of a canine monoblastic leukemia. *Vet Clin Pathol* 27(2):40–49.

Monteith, C.N., and Cole, D. (1995) Monocytic leukemia in a horse. *Can Vet J* 36:765–766.

Nakano, K., Kusakabe, H., and Kiyokane, K. (1999) Acute monocytic leukemia presenting as cutaneous involvement. *Dermatol* 199:349–352.

Passantino, L., Patruno, R., Cianciotta, A., Passantino, G., Tafaro, A., Gadaleta, C., and Ranieri, G. (2003) A phylogenetic comparison between acute monocytic leukemia cells and monocytes—Macrophages in lower vertebrates. *Immunopharmacol and Immunotoxicol* 25(1):87–99.

Peterson, L., Dehner, L.P., and Brunning, R.D. (1981) Extramedullary masses as presenting features of acute monoblastic leukemia. *Am J Clin Pathol* 75:140–148.

Piquemal, D., Commes, T., Manchon, L., Lejeune, M., Ferraz, C., Pugnère, D., Demaille, J., Elalouf, J.M., and Marti, J. (2002) Transcriptome analysis of monocytic leukemia cell differentiation. *Genomics* 80(3):361–371.

Ridge, S.A., and Wiedemann, L.M. (1994) Chromosome 11q23 abnormalities in leukaemia. *Leuk Lymph* 14:11–17.

Scott, C.S., Stark, A.N., Limbert, H.J., Master, P.S., Head, C., and Roberts, B.E. (1988) Diagnostic and prognostic factors in acute monocytic leukaemia: An analysis of 51 cases. *Brit J Haematol* 69:247–252.

Stanley, M., McKenna, R.W., Ellinger, G., et al. (1985) Classification of 358 cases of acute myeloid leukemia by FAB criteria: Analysis of clinical and morphologic features. In Bloomfield, C.D. (ed.), *Chronic and Acute Leukemias in Adults*. Martinus Nijhoff Publishers, Boston pp. 147–174.

Walter, R.B., Bächii, E.B., Schaer, D.J., Rüegg, R., and Schoedon, G. (2003) Expression of the hemoglobin scavenger receptor (CD163/HbSR) as immunophenotypic marker of monocytic lineage in acute myeloid leukemia. *Blood* 101(9):3755–3756.

Acute Erythroid Leukemia M6

The revised WHO classification recognizes two forms of erythroid leukemia:

- M6A AML, or erythroleukemia, which involves neoplasia in both the myeloblast and erythroblast cell lineages
- M6B AML, or pure erythroid leukemia, formerly referred to as *erythremic myelosis*

M6A is the most common erythroid leukemia in humans; in animals, M6B is seen much more frequently than M6A. M6B was seen with even greater frequency prior to the control of FeLV infection in cats.

Much has been learned of the mechanisms of erythroid leukemia by study of the Friend F-MuLV or spleen focus forming virus (SFFV), which integrates in specific sites in the mouse genome in common integration sites (*cis*) and acts by *insertional mutagenesis* rather than by the transacting retroviruses of HTLV-1 and the BLV types that have multiple random sites of insertion. Part of the process of oncogenesis is the production of a membrane glycoprotein by the virus that is able to bind to the erythropoietin binding site and thus mimics the action of erythropoietin. In the standard model of F-MuLV infection in the mouse, there is first a partially compensated hemolytic anemia that becomes more severe with the onset of massive splenomegaly to 10–20 times normal size by colonization of clonal erythroblasts. A second syndrome occurs in which a different strain of the Friend leukemia virus is able to cause a disease that resembles

polycythemia vera with massive increase in the red cell mass by anatomically normal-appearing red cells. These syndromes have enabled the recognition of two loci of control of erythroid proliferation, with one operating at a primitive stage of cell maturation resulting in erythremic myelosis or M6b and the other operating at a much later stage of differentiation resulting in polycythemia vera or a chronic leukemia of mature red cells.

Definition

In the clinical syndromes in humans and animals, both M6A and M6B result in anemia and ultimately marrow failure. M6A is defined as having erythroblasts totaling at least 50% of nucleated marrow cells with at least 20% of the nonerythroid cells consisting of myeloblasts. In this criterion, the term *erythroblasts* is used loosely to include rubricytes at all stages of maturation. In the human type of M6A, the true rubriblasts and prorubricytes have the typical very high cytoplasmic basophilia that is highly vacuolated, and these vacuoles are SBB negative but highly PAS positive. This vacuolation occurs to a much less extent in animals, but the staining pattern is identical and weak PAS positivity can usually be demonstrated in marrow sections of animals with AML of M6 type in paraffin-embedded tissues.

Epidemiology and Incidence

Little is known of the causation of M6 in humans or animals other than a loose association that has been made between FeLV infection and M6 in the cat. In animals, M6 is seen primarily in cats, less often in dogs, and rarely in other species. Cats with M6B are usually in the 3-year-old range or mature and 7–8 years of age. A case was identified in a 12-year-old cow presented because of declining appetite and milk production.

Clinical Presentation and Features

Animals with M6 are presented with a history of declining appetite, weight, and activity over a period usually exceeding a month. On clinical examination, there is marked mucosal pallor and mild depression. The hemoglobin level lies between 3 and 5 g/dl and the total nucleated blood cell count between 50,000 and 120,000/ul. There is usually a near-normal level of neutrophils, but levels vary between 1,000 and 5,000/ul with platelets at 10,000–20,000/ul. Oddly, the lymphocyte count tends to be in the normal range or elevated as high as 10,000/ul. There is often mild pyrexia, and in historical cases "hemobartonella" was a usual prime differential. On physical examination, the lymph nodes are normal or small and an abdominal mass is found that is due to splenomegaly.

Pathologic Features

Blood

On examination of blood in cases of M6A, the anemia and rubricytosis dominate the findings. Other accompanying blood changes include the presence of rare myeloblasts in the peripheral blood that are easily missed in the many large prorubricytes present. The neutrophils are characteristically large and the size of basophils, and they have hypersegmented nuclei likely as a consequence of folate deficiency (Fig. 5.95). The platelets are usually rare, and those present are activated with villous cytoplasmic projections (Fig. 5.96). There are many bare erythroid nuclei present, and as a consequence many rounded-up foci of rubricyte cytoplasm that is basophilic, may have a few azurophilic granules, and may be mistaken for huge shift platelets. The lymphocytes present often have a few pink granules and are likely of benign LGL type. The anemia and thrombocytopenia are severe; neutrophils generally remain present but have very little granulation with almost water-clear cytoplasm (Fig. 5.97). Blast cells of both myeloid and erythroid lineage are present in peripheral blood (Fig. 5.98).

Bone Marrow

The bone marrow in M6A is solidly cellular with very little fat area remaining and has foci of small benign lymphocytes (Figs. 5.99, 5.100). Maturing megakaryocytes

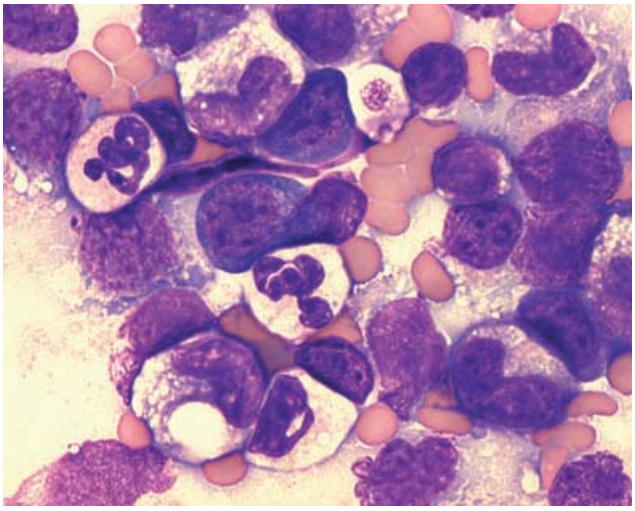

Figure 5.95. Cat: blood, erythroleukemia. End of the blood smear from a 7-year-old FeLV positive cat, Animal presented anemic and jaundiced, with lethargy for the past 5 days. The neutrophils in the center and upper left are hypersegmented, with reduced normal granulation and mild vacuolation and a Doehle body in the cell in the center. There are numerous cells of metamyelocytic type with 3 intact precursor cells with highly basophilic cytoplasm that are uncharacteristically distorted by compression of surrounding cells. There are numerous cells present with burst cytoplasmic and or nuclear membranes.

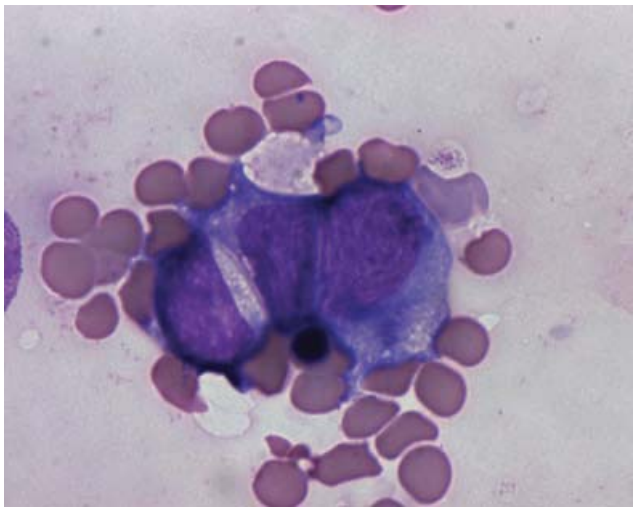

Figure 5.96. Cat: blood, erythroleukemia. There is a platelet with fine azurophilic granulation and a complete absence of basophilia adherent to the cluster of cells in the upper right. The red cell (right center) has a Howell-Jolly body that is not in focus. The nucleated cells have primitive nuclei with relatively abundant agranular cytoplasm. The 2 at center are likely myeloid precursors and the lower cell at left a lymphocyte. There is a metarubricyte attached to the cluster below.

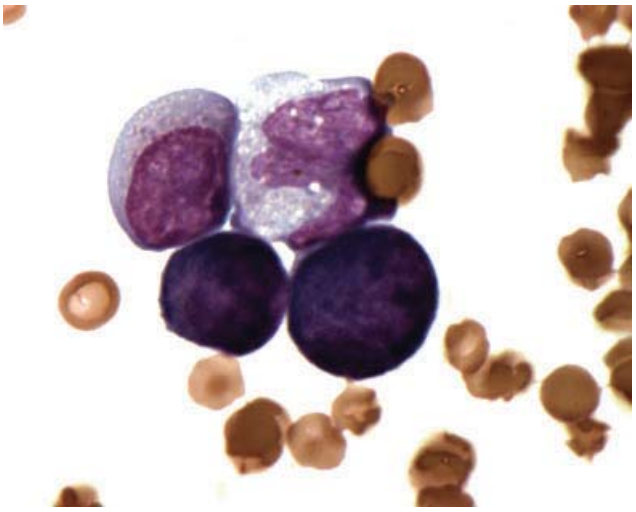

Figure 5.98. Cat: blood, erythroleukemia. There are putative blasts of both erythroid and myeloid lineages present in the peripheral blood and rarely found in association. The basophilic cell at the lower center is likely a myeloblast and the one at left is an erythroblast. The cell at the upper right with the cytoplasmic and nuclear vacuolations is likely monocytic and the one at left with a large nucleolus and a few azurophilic granules is likely a myelocyte.

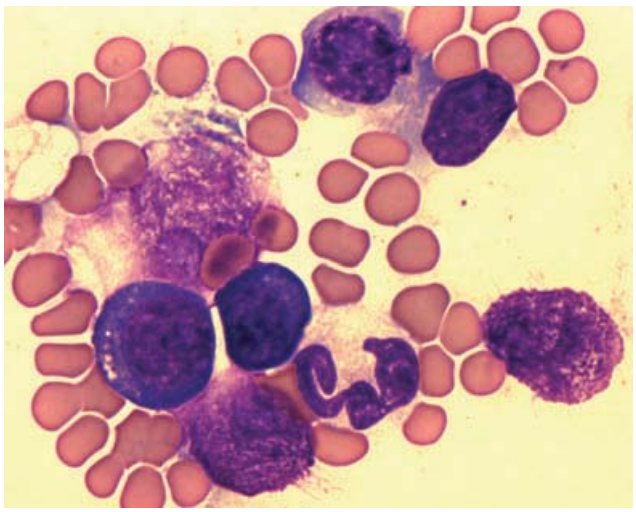

Figure 5.97. Cat: blood, erythroleukemia. Cluster of 2 intact neoplastic rubricytes and 1 at top, with a burst cytoplasmic membrane. There are 4 bare nuclei, and there is a nucleolus apparent in the nuclei that is located at bottom. The neutrophil is large with an atypical immature chromatin, abnormal segmentation, and very pale, almost agranular, cytoplasm with numerous fine vacuolations.

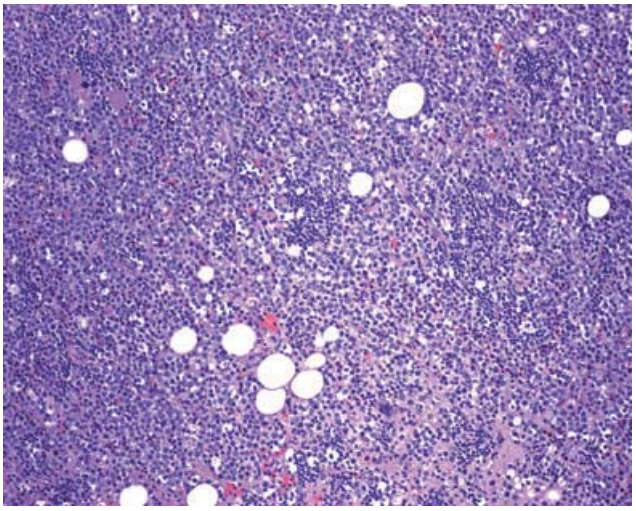

Figure 5.99. Cat: bone marrow, erythroleukemia. Histologically, the marrow in the midfemoral cavity is solidly cellular with 80–90% cellularity. The scattered dark foci represent areas of lymphocytic infiltration, with 2 megakaryocytes apparent in the upper left and 1 in the lower center. The vascular pattern is inapparent, partially because with the extreme anemia, the marrow is ischemic.

are rare, and the major abnormality is the presence of a majority of erythroid precursors despite a lack of peripheral blood reticulocytosis and severe anemia. The benign erythroid component is labile and tends to be displaced in favor of residual myelopoiesis and thrombopoiesis in the face of marrow phthisis. Thus, conditions of severe anemia with reticulocytopenia, blast cells in the peripheral blood, and a high proportion of marrow erythroid cells should suggest that one of the M6 neoplasms needs to be considered in the differential diagnosis. The marrow is characterized by many late stage rubricytes, but the connection to the precursor cells is not as apparent as in

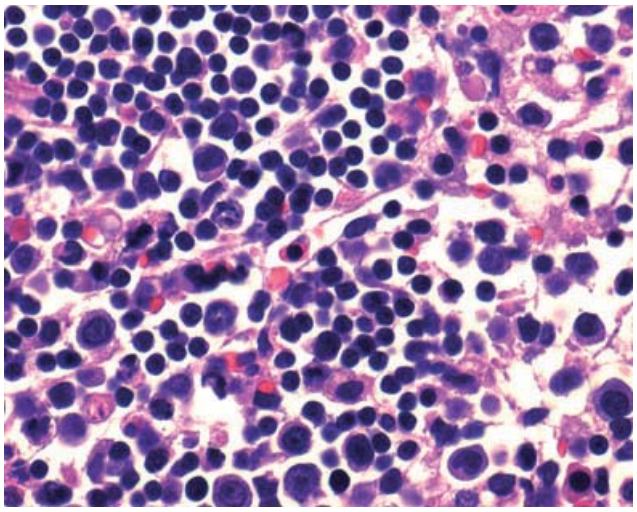

Figure 5.100. Cat: marrow, erythroleukemia. Detail of Figure 5.99. The area of lymphoid colonization with a single metarubricyte in the center with maturing red cytoplasm distinguishes the surrounding erythroid population from the small lymphocytes with an inapparent narrow rim of cytoplasm.

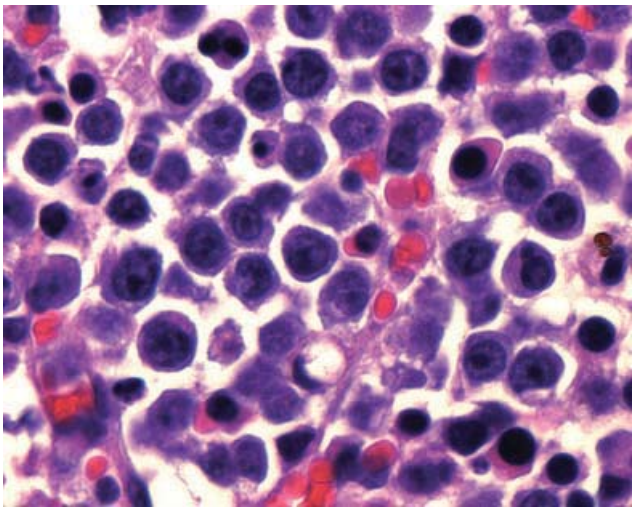

Figure 5.101. Cat: marrow, erythroleukemia, same case as Figure 5.99. Dyserythropoiesis is evident in the cell in the right center with the small satellite nucleus above. Most of the precursors are of erythroid lineage with a single neutrophil in the upper left.

benign erythroid hyperplasia. Another subtle but important difference between M6 and benign hyperplasia is that in hyperplasia there is an apparent increase in the number of marrow macrophages with ingested metarubricyte nuclei. Under normal conditions, marrow macrophages serve as erythroid nurse cells that provide iron and nucleotides to the rubricytes developing in deep cavitations within their cytoplasm. On maturation, the metarubricyte nucleus is withdrawn from the erythrocyte membrane, leaving the nucleus with both a nuclear membrane and a covering of the red cell membrane visible in electron microscopic examination. The nucleus is then degraded to the nucleotide level with these provided as large building blocks to neighboring rubricytes undergoing nuclear synthesis phase. In the absence of sufficient cells of phagocytic type, the late stage rubricytes persist in a form of late stage asynchrony such that the progeny greatly outnumber the progenitors. A further clue to the nature of the M6 marrow lesion is that the erythroid nuclei remain perfectly round and most are uniformly dense and structureless from the basophilic rubricyte stage on, which results in a field of cells that vary in diameter and degree of cytoplasmic hemoglobin but not in nuclear shape or chromatin density (Fig. 5.101). Thus, the morphologic diagnosis of M6 rests on "knowing the progenitors by the company they keep," and if most of the progeny are late stage rubricytes, most of the unidentified precursors must be of erythroid lineage.

Another factor that makes the diagnosis of M6A difficult, particularly on a histological basis, is that although there are numerous myeloblasts present they are difficult to identify, and their progeny are not in evidence since myeloid cells later than myelocytes will have been released due to the peripheral need for granulocytes. In both types of M6, there are many erythroid cells indicative of dysplastic maturation with binucleated late stage rubricytes, often with marked asynchrony between the two nuclei. Other indications are rubricytes at the basophilic and polychromatic stage that have a single sharply projecting nuclear lobation and others with Howell-Jolly body nuclear remnants. Myeloid dysplasia is evident in the presence of giant metamyelocytes and even donut types with a ring nucleus and a central cavity.

The lesions in other organs include the spleen with marked sinus colonization by neoplastic erythroid precursors (Fig. 5.102) but also by increased numbers of megakaryocytes. The lymphoid compartments are atrophic with marked atrophy of the thymic-dependent periarteriolar lymphoid sheaths and the germinal centers remaining as "bare" involuting centers, with complete loss of mantle cells and many with a center of amorphous proteinaceous material of follicular hyalinosis. The usual reddish rim around the follicles is absent due to the anemia and presence of so many nucleated red cells (Fig. 5.103). The sinus areas have a high level of coarse hemosiderin and myelopoiesis is difficult to identify, again by loss of association of precursors with progeny. Neoplastic cells colonize the subendothelial areas of large muscular veins (Fig. 5.104).

The liver has accentuation of zonation due to ischemic degeneration of hepatocytes around central veins. Focal

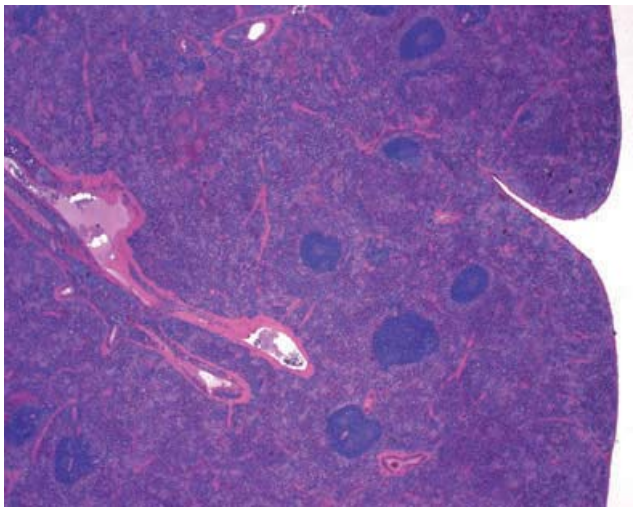

Figure 5.102. Cat: spleen, erythroleukemia. There is irregular lymphoid atrophy with dense cuffs around fading germinal centers and almost complete atrophy of periarteriolar lymphoid sheaths. There is a fine irregular paleness around the lymphoid nodules that defines the perifollicular sinus that is relatively devoid of mature red cells. The sinus is markedly hyperplastic and uniformly filled with neoplastic cells. There is intramural colonization of the large muscular sinuses evident in the lower center.

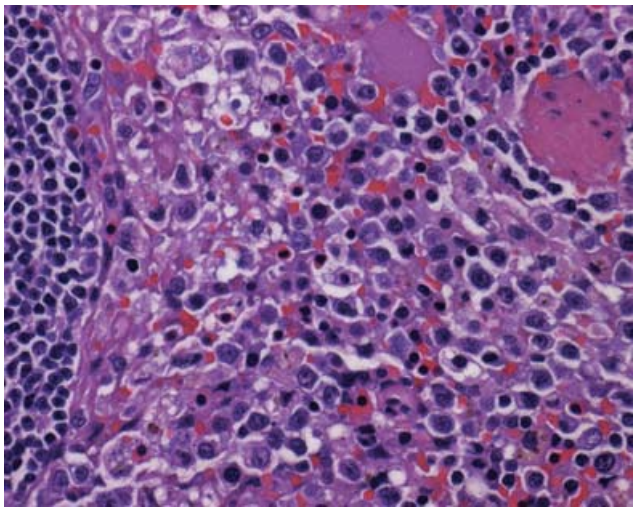

Figure 5.103. Cat: spleen, erythroleukemia. Detail of Figure 5.102. The edge of a lymphoid follicle is at the left with the empty peripheral sinus adjacent and a solid area of neoplastic sinus erythropoiesis at the right.

areas of ischemic necrosis may be present and there is a marked increase in sinus hemosiderin-bearing Kupffer cells. The pattern of colonization appears to be random with vascular structure more often missed than involved (Fig. 5.105). Most neoplastic cells occur in a tight round cluster of 20–50 cells that displaces adjoining parenchyma

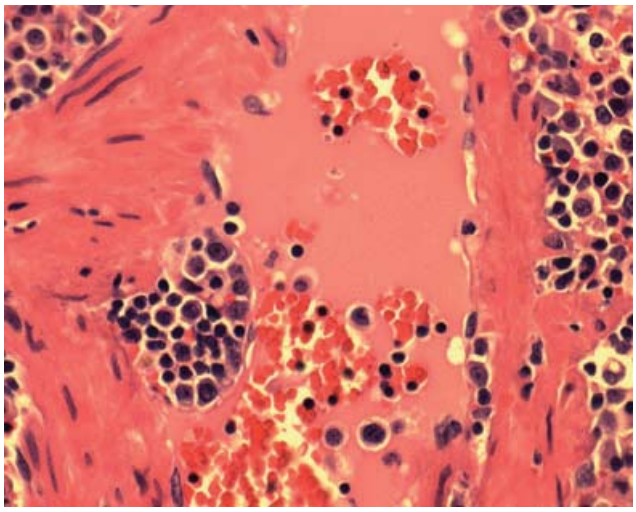

Figure 5.104. Cat: spleen, erythroleukemia. Subendothelial colonization of a large muscular vein or sinus by neoplastic hematopoietic precursors. The vascular implants are in a narrow laminar row at right, and in a larger colony at the left endothelial margin.

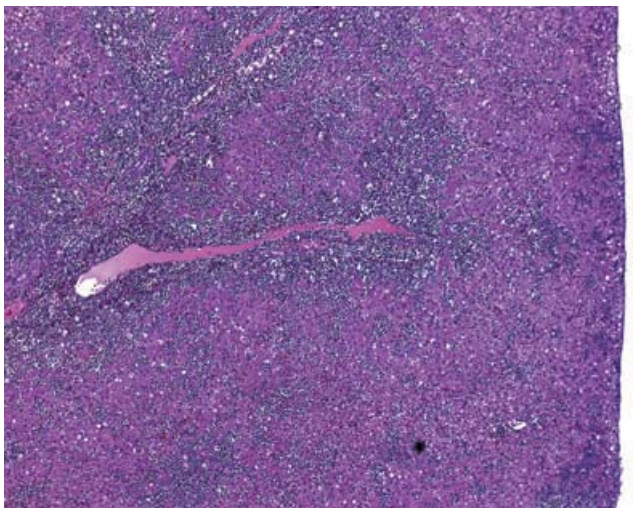

Figure 5.105. Cat: liver, erythroleukemia. There is extensive periportal venous colonization as well as multiple small foci throughout the hepatic lobule.

and is present in mid-zone areas (Fig. 5.106). Extramedullary hematopoiesis is not a feature of the hepatic changes.

All lymph nodes are of normal size, and most if not all are involved to some extent with neoplastic colonization (Figs. 5.107, 5.108). It is difficult to distinguish between sinus dilation due to lymphoid atrophy and active invasion, but the typical pattern is of all sinuses including peripheral and internal, expanded by the late stage rubricytes with complete loss of germinal centers and filling of medullary sinuses. In situ colonization appears as focal

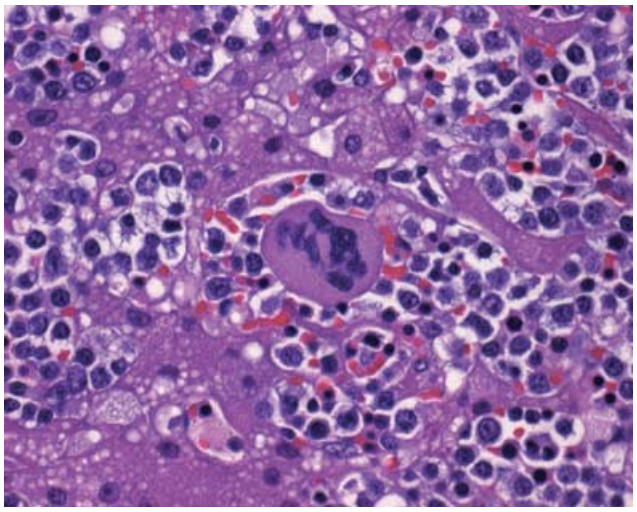

Figure 5.106. Cat: liver, erythroleukemia. Hepatic sinus, with area of neoplastic colonization, primarily of erythroid and platelet precursors, with few apparent myeloid cells.

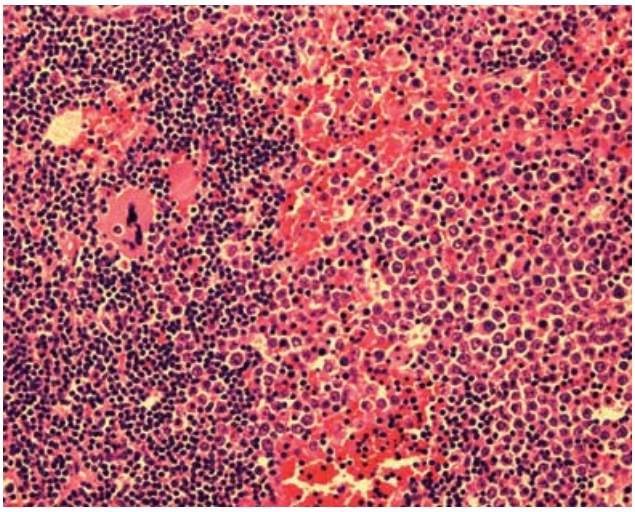

Figure 5.108. Cat: node, erythroleukemia. The medullary area with extramedullary hematopoiesis in the medullary cord (left) with an intervening sinus largely occupied by red cells and metarubricytes with the medullary cord area at the right occupied by large precursors with round nuclei that might be mistaken for lymphoid neoplasm.

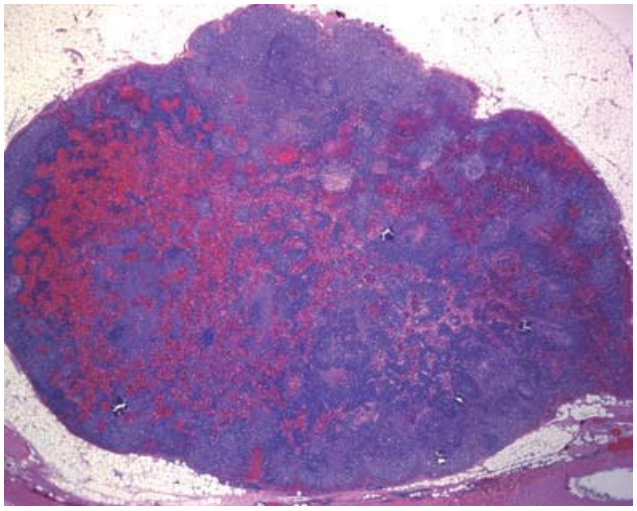

Figure 5.107. Cat: node, erythroleukemia. There are fading germinal centers in subcortical areas with the pale diffuse areas in subcapsular regions. There is irregular infiltration in medullary cords and in the diffuse areas at the center above with solid areas of neoplastic colonization.

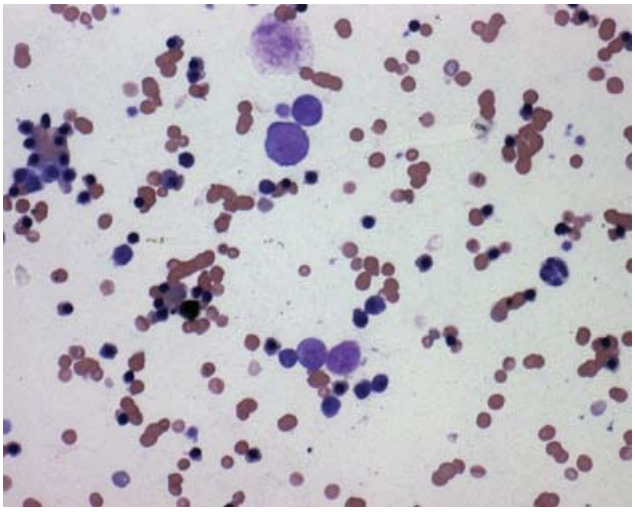

Figure 5.109. Cat: blood, pure erythroid leukemia (erythremic myelosis). The predominant nucleated cells are maturing rubricytes with numerous bare nuclei and quite frequent blast cells (center) and an occasional lymphocyte but few granulocytes. There is severe anemia and thrombocytopenia.

areas of larger cells in the midst of a paracortical small lymphocyte area that may resemble the edge of a germinal center; on closer examination the typical very large round nuclei are apparent as the only cell type present. Typically in the stage at which most animals come to necropsy, there is no evidence of extramedullary hematopoiesis in node medullary areas.

Pure Erythroid Leukemia (Erythremic Myelosis) M6B

Blood

In M6B there is a remarkable peripheral blood rubricytosis that may exceed 100,000/ul in the cat and is usually accompanied by lymphocytosis of 10,000/ul or more

(Figs. 5.109, 5.110). There is quite marked anisocytosis but very few true basophilic red cells with occasional basophilic stippling and Howell-Jolly body (Fig. 5.111). The late stage rubricytes predominate and there are very many bare nuclei. There appears to be a gap between the clusters of cells at metarubricyte stage and the large atypical cells present that are not immediately apparent as the precursor stages. The prorubricytes are very large cells with round nuclei 4 red cells in diameter that stain deep red on Wright's stain with a coarse cribriform chromatin pattern with irregularly apparent nucleoli and a few large chromocenters in more mature forms (Fig. 5.112). Their cytoplasm is moderately basophilic and often with small vacuoles. The rubriblasts are less numerous and have nuclei that are more dense and much more basophilic staining with nucleoli present but not apparent and with very basophilic cytoplasm (Fig. 5.113). Both cell types have occasional azurophilic granules that are most obvious in the shed cytoplasm of injured cells. The neutrophils are at about the same level as in M6A, and they have very little normal cytoplasmic granulation but have diffuse basophilia with occasional Doehle bodies and toxic vacuolations (Fig. 5.114). The lymphocytes present are of small and medium size with a narrow rim of pale blue cytoplasm and are easily overlooked with the basophilic rubricytes of similar size (Fig. 5.115).

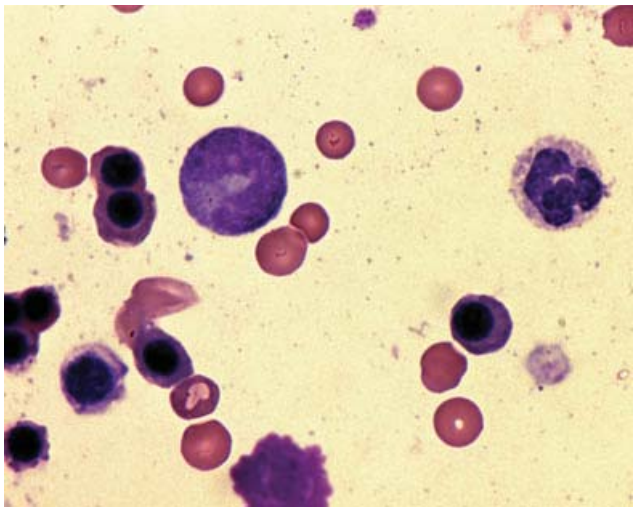

Figure 5.110. Cat: blood, erythroid leukemia. Detail of Figure 5.109. The neutrophil at the right is approaching hypersegmentation and has low cytoplasmic volume with very low cytoplasmic density and inapparent granulation. The large cell may be a metamyelocyte and there is a single platelet with low granulation and basophilia in the lower right.

Bone Marrow

The bone marrow in M6B is over 90% hematopoietic with few fat cells remaining (Fig. 5.116, 5.117). There are relatively numerous maturing megakaryocytes as scattered foci of small lymphocytes with nuclei of the same size as the metarubricytes but with no obvious cytoplasmic margins. Like M6A, tingible body macrophages that

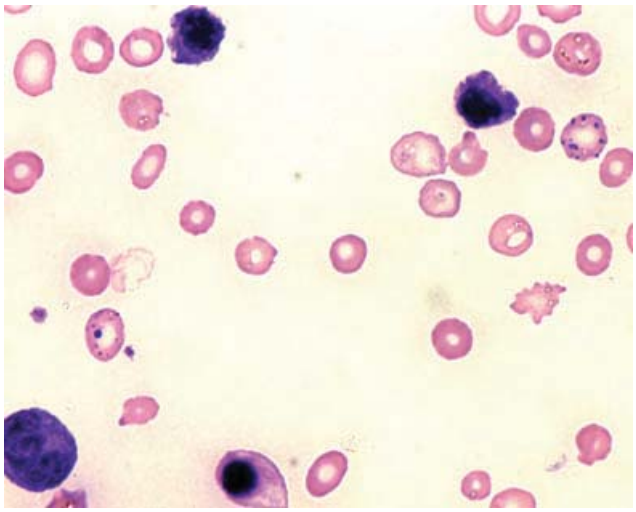

Figure 5.111. Cow: blood, erythroid leukemia. There is severe anemia with hypochromasia and oval red cells suggesting abnormal marrow stromal proliferation. There is red cell basophilic stippling and a Howell-Jolly body in the bottom right and a cell with basophilic stippling only in the upper left. The other cells present are a lymphocyte and late stage rubricytes.

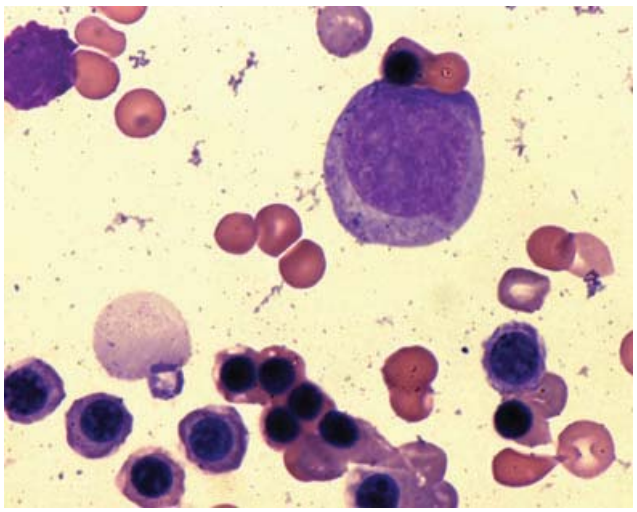

Figure 5.112. Cat: blood, erythroid leukemia. The very large cell in the upper right with a round nucleus, multiple large nucleoli with chromatin rimming and abundant moderately basophilic cytoplasm, is likely a neoplastic erythroid blast. The pale round object in the lower left is shed cytoplasm from an injured cell accompanied by numerous polychromatic and metarubricytes.

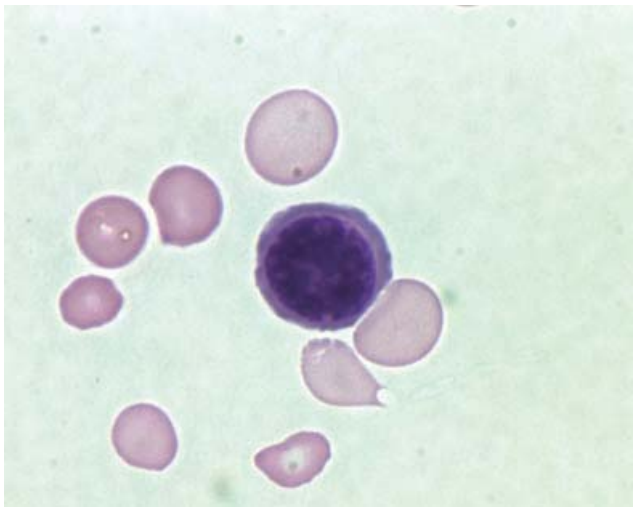

Figure 5.113. Cow: blood, erythroid leukemia. The nucleated cell is a rubriblast with densely stained nucleus and with multiple nucleoli of moderate size, quite heavily rimmed with chromatin. The size and staining density are characteristic.

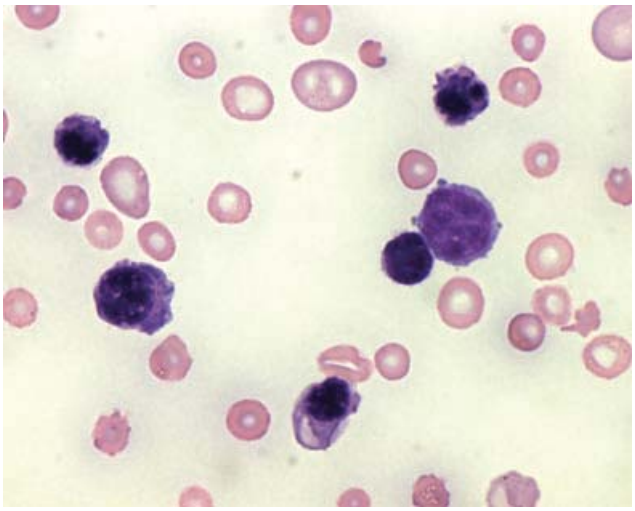

Figure 5.115. Cow: blood, erythroid leukemia. There is a medium lymphocyte in the right center, with a small lymphocyte immediately below it with a dense nucleus and a very narrow rim of cytoplasm. The size of the small lymphocyte is similar to that of the maturing rubricytes.

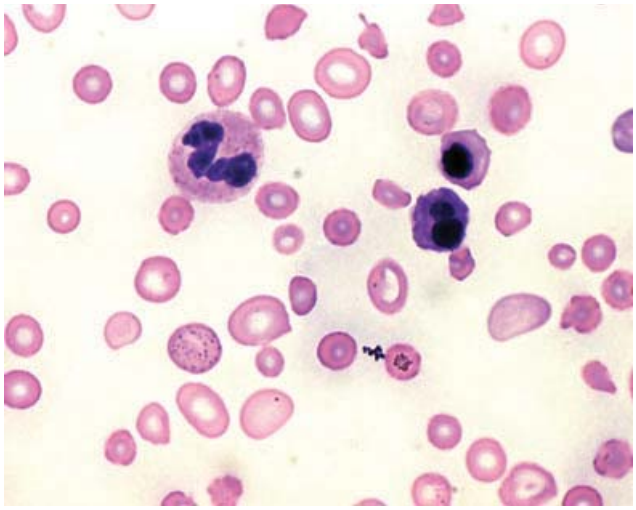

Figure 5.114. Cow: blood, erythroid leukemia. The neutrophil has reduced normal granulation and mild toxic granulation without vacuolation. There is basophilic stippling in the red cell below and at right a binucleated late stage rubricyte indicating marrow dyserythropoiesis.

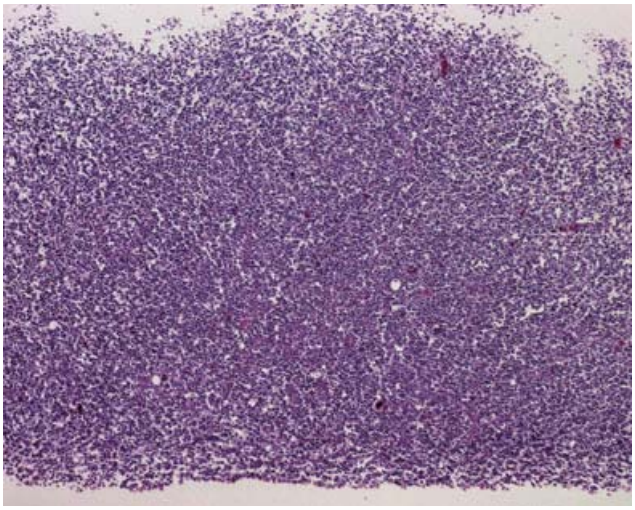

Figure 5.116. Cat: bone marrow, erythroid leukemia. The marrow in the central femoral cavity is solidly cellular with 2 fat cells remaining in this area in the center and lower right. There is homogeneity to the marrow pattern at low power with M6B that is not present in M6A, which has much greater cellular heterogeneity.

might be expected to be present with the level of rubricyte nuclei being produced are conspicuously absent, likely as a function of the neoplastic rubricytes inability to mature and shed their cytoplasmic envelope. Cytologically, the impression is not unlike that of large cell lymphoma with a majority of cells with very round densely stained nuclei that have nucleoli and parachromatin clearing and abundant highly amphophilic cytoplasm (Fig. 5.118). Their progeny, the basophilic rubricytes, have slightly smaller nuclei that are also very evenly round, are completely densely stained with no internal nuclear detail, and also have abundant deeply stained cytoplasm (Fig. 5.119). It is the anisokarosis that is the key to recognition of the cellular lineage with gradations of cells with round densely stained nuclei that vary mainly in diameter plus the apparent hemoglobin content of the late stage cells

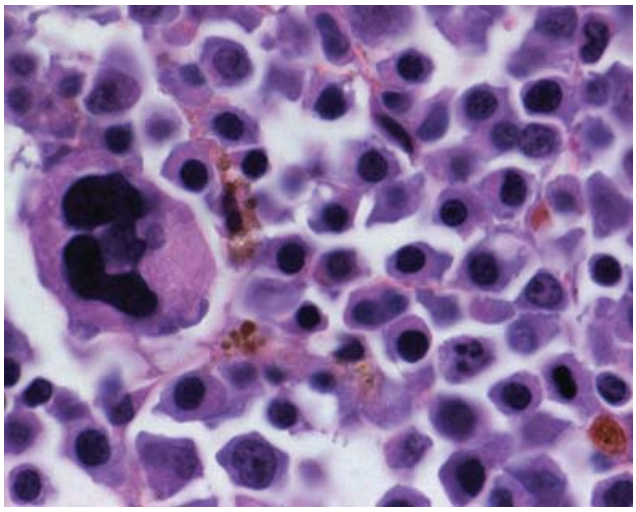

Figure 5.117. Cat: bone marrow, erythroid leukemia. Detail of Figure 5.116. A single megakaryocyte with reduced nuclear fusion is present at left with several hemosiderin-bearing macrophages. Four rubricytes with prominent nucleoli are present in the upper left and more maturing rubricytes with round densely stained nuclei that vary slightly in diameter make up most of the field.

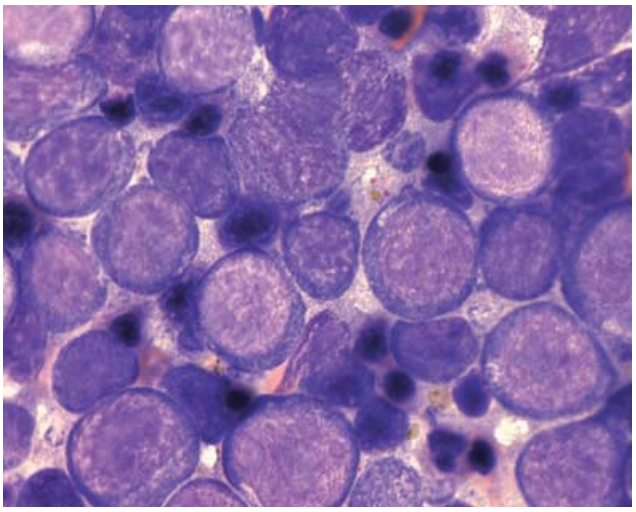

Figure 5.119. Cow: marrow aspirate, erythroid leukemia. Detail of Figure 5.118. The smaller cells in the center are likely erythroblasts with the larger cells with less densely stained nuclei and prominent nucleoli prorubricytes. The basophilic and polychromatic rubricytes are less apparent, but there are many cells of metarubricyte stage nestled between the larger cells.

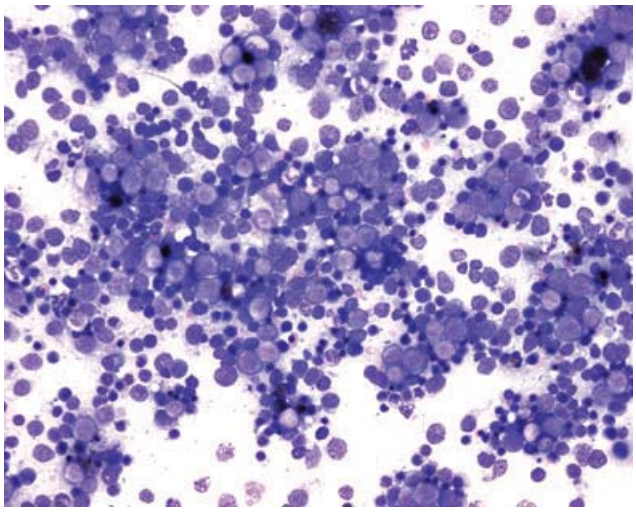

Figure 5.118. Cow: bone marrow aspirate, erythroid leukemia. The field is dominated by large cells of prorubricyte type, with a narrow rim of highly basophilic cytoplasm with an apparent gap of cells of intermediate maturation with the primitive cells accompanied by many polychromatic and metarubricytes. There is a single megakaryocyte in the upper left and a large hemosiderin-bearing macrophage in the upper right.

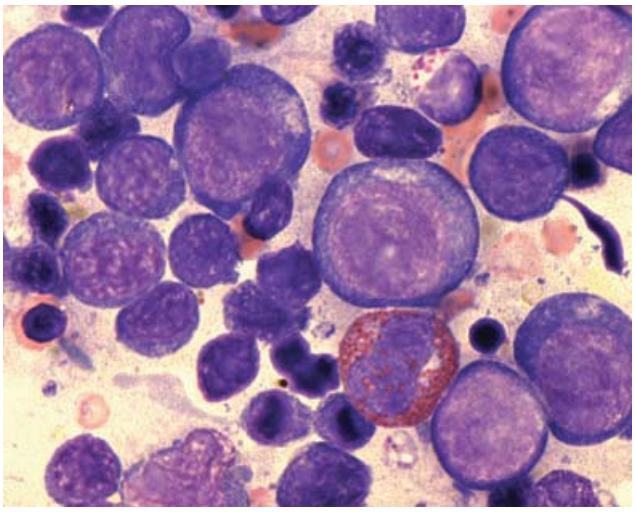

Figure 5.120. Cow: bone marrow, erythroid leukemia. In a less-crowded field, the lineage continuity is more apparent. There are rubriblasts in the upper left, with a row of maturing rubricytes with a metarubricyte in the left center with more saturated cytoplasm. Adjacent, there are 2 basophilic rubricytes and next to them 2 cells of polychromatic rubricytes stage that retain basophilic cytoplasm. The largest cells are prorubricytes and there is a large granular lymphocyte in the upper left.

(Figs. 5.120, 5.121). With erythropoiesis tending to be lost in neoplasms causing myelophthisis, the sheer numbers of late stage rubricytes points to the primitive cells as their precursors.

In advanced cases of M6B 30–40% of the liver may be involved with metastatic tumor now surrounding both veins and portal areas and colonizing the mid-zonal areas in small clusters of cells (Figs. 5.122, 5.123). At the architectural level, scattered megakaryocytes are present and

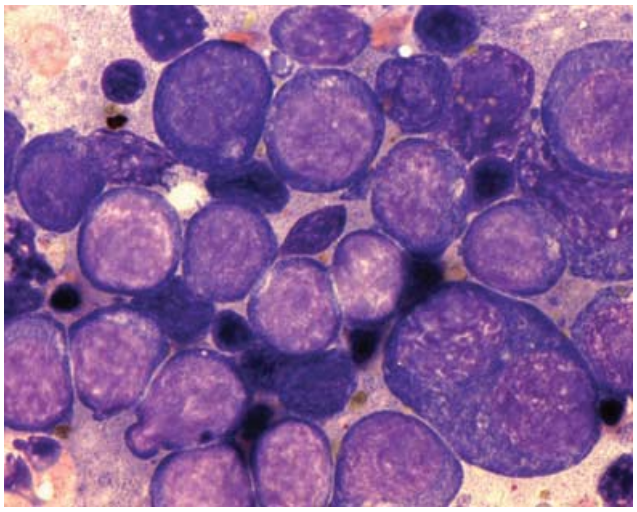

Figure 5.121. Cow: marrow, erythroid leukemia. The field is dominated by rubriblasts and prorubricytes with a binucleated cell in the lower right with 2 interphase nuclei, most likely the first stage of differentiation of a megakaryoblast.

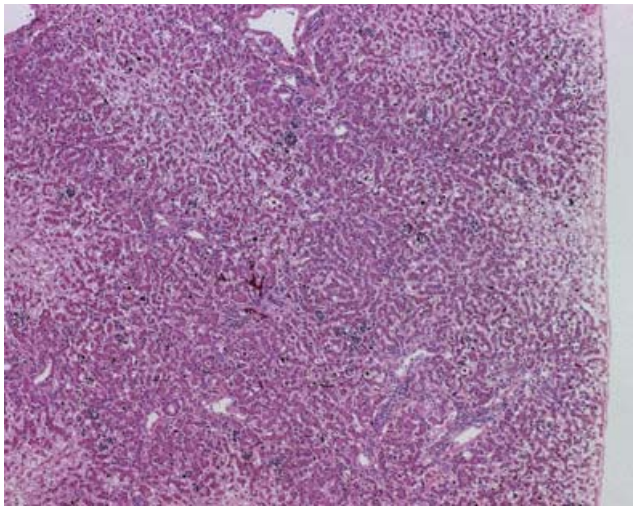

Figure 5.122. Cat: liver, erythroid leukemia. The major change is ischemic degeneration around central veins due to the severe anemia. The small sinusoidal accumulation of red cells in the center stands out against the absence of red cells throughout most of the tissue. There is widespread focal colonization by neoplastic cells without apparent homing to larger vascular structures.

the neoplastic cells colonize the subendothelial areas of the large muscular hepatic veins.

The splenic changes are like that of M6A with thinned capsule and widely spaced muscular trabeculae indicative of splenomegaly. The sinuses are densely cellular with numerous scattered megakaryocytes and solid tumor colonization. There are no germinal centers, but the B-cell nodules remain densely cellular and an occasional area of larger cells is not a residual follicle center but invasion by

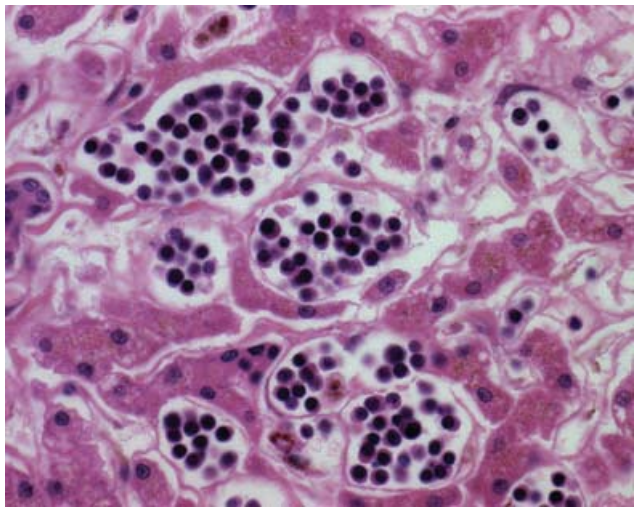

Figure 5.123. Cat: liver, erythroid leukemia. Detail of Figure 5.122. Focal colonies of neoplastic erythropoiesis are dilating the sinuses. There is widespread separation of the endothelium from the hepatocytes that is part of the ischemic change and heavy hepatocyte pigmentation, likely lipofuscin but often considered both bile and iron pigment.

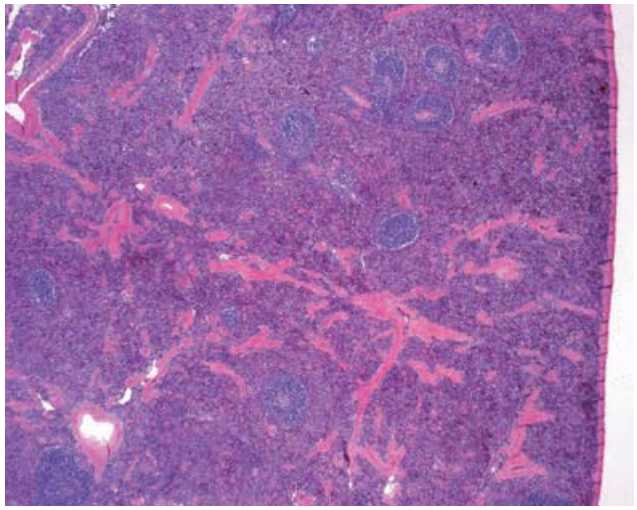

Figure 5.124. Cat: spleen, erythroid leukemia. There is marked and uniform sinus filling with neoplastic cells. The residual areas of B-lymphocytes are small and sharply defined with pale centers or focal follicular hyalinosis, and periarteriolar lymphoid sheaths are markedly atrophic.

the neoplastic cells. There is again complete loss of mantle cell cuffs, with the B-nodules very sharply defined and surrounded by a pale margin occupied by the rubricytes instead of red cells. The periarteriolar lymphoid sheaths are almost completely absent and reduced to a narrow cuff of 1–2 cells thick (Figs. 5.124, 5.125). The nodal changes are like those of M6A.

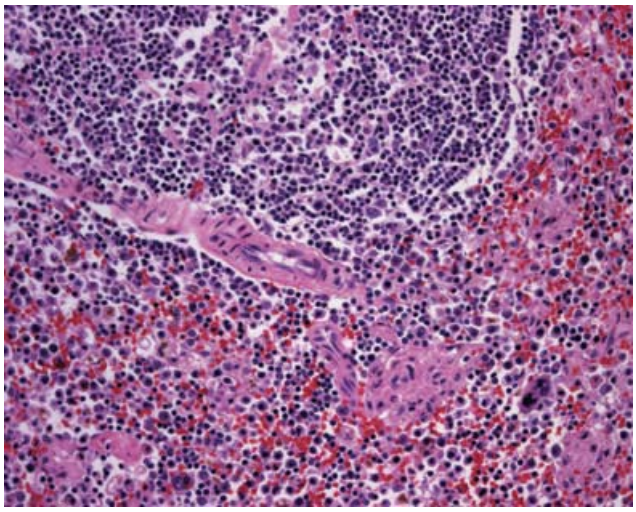

Figure 5.125. Cat: spleen, erythroid leukemia. Detail of Figure 5.124. The fading follicle in the upper left has a hypocellular center with sinus areas primarily occupied by neoplastic erythropoiesis. There are megakaryocytes in the lower left and right. The arteriole (center) has almost complete loss of a small lymphocytic cuff of cells consisting of a single row of small lymphocytes intermixed with erythroid precursors.

There is very little information on the treatment of M6 of either type, and most animals seem to be euthanized, either on making the diagnosis or to confirm it.

REFERENCES

Bennett, J.M., Catovsky, D., Daniel, M.T., et al. (1985) Proposed revised criteria for the classification of acute myeloid leukemia: A report of the French-American-British cooperative group. *Ann Intern Med* 103:626–629.

Brunning, R., McKenna, R.W. (1994) *Tumors of the Bone Marrow*, 3rd Series, fasc.9. Armed Forces Institute of Pathology, Washington, D.C., pp. 19–100.

Brunning, R.D. (2001) Acute myeloid leukemia. In Knowles, D.M. (ed.), *Neoplastic Hematopathology*, 2nd ed. Lippincott Williams & Wilkins, Philadelphia, pp. 1667–1715.

Davey, F.R., Abraham, Jr., N., Brunetto, V.L., MacCallum, J.M., Nelson, D.A., Ball, E.D., Griffin, J.D., Baer, M.R., Wurster-Hill, D., Mayer, R.J., chiffer, C.A., and Bloomfield, C.D. (1995) Morphologic characteristics of erythroleukemia (acute myeloid leukemia; FAB-M6): A CALGB study. *Am J Hematol* 49:29–38.

Fouillard, L., Labopin, M., Gorin, N.C., Polge, E., Prentice, H.G., Meloni, G., Reiffers, J., Pigneux, A., Willemze, R., Schattenberg, A., Sica, S., Lagrange, M., Fenneteau, O., Perot, C., and Frassoni, F. (2002) Hematopoietic stem cell transplantation for de novo erythroleukemia: A study of the European Group for Blood and Marrow Transplantation (EBMT). *Blood* 100(9):3135–3140.

Garand, R., Duchayne, E., Blanchard, D., Robillard, N., Kuhlein, E., Fenneteau, O., Salomon-Nguyen, F., Grange, M.J., Rousselot, P., Demur, C., Talmant, P., Radford, I., Flandrin, G., and the Groupe Français d'Hématologie Cellulaire. (1995) Minimally differentiated erythroleukaemia (AML M6 'variant'): A rare subset of AML distinct from AML M6. *Brit J Haematol* 90:868–875.

Harris, N.L., Jaffe, E.S., Diebold, J., Flandrin, G., Muller-Hermelink, H.K., Vardiman, J., Lister, T.A., and Bloomfield, C.D. (1997) The World Health Organization classification of neoplastic diseases of the haematopoietic and lymphoid tissues: Report of the Clinical Advisory Committee Meeting, Airlie House, Virginia, November 1997. *Histopathol* 36:69–87.

Kass, L. (1975) Cytochemical abnormalities of atypical erythroblasts in acute erythremic myelosis. *Acta Haematologica* 54:321–327.

Kogan, S.C., Ward, J.M., Anver, M.R., Berman, J.J., Brayton, C., Cardiff, R.D., Carter, J.S., de Coronado, S., Downing, J.R., Fredrickson, T.N., Haines, D.C., Harris, A.W., Harris, N.L., Hiai, H., Jaffe, E.S., MacLennan, I.C.M., Pandolfi, P.P., Pattengale, P.K., Perkins, A.S., Simpson, R.M., Tuttle, M.S., Wong, J.F., and Morse III, H.C. (2002) Bethesda proposals for classification of nonlymphoid hematopoietic neoplasms in mice. *Blood* 00(1):238–245.

Li, J.P., D'Andrea, A.D., Lodish, H.F., and Baltimore, D. (1990) Activation of cell growth by binding of Friend spleen focus-forming virus gp55 glycoprotein to the erythropoietin receptor. *Nature* 343:762–764.

Maede, Y., and Murata, H. (1980) Erythroleukemia in a cat with special reference to the fine structure of primitive cells in its peripheral blood. *Jpn J Vet Sci* 42:531–541.

Mazella, F.M., Kowal-Vern, A., Shrit, A., et al. (1998) Acute erythroleukemia: Evaluation of 48 cases with reference to classification proliferation, cytogenetics and prognosis. *Am J Clin Pathol* 110:590–598.

Olopade, O.I., Thangavelu, M., Larson, R.A., et al. (1992) Clinical, morphologic and cytogenetic characteristics of 26 patients with acute erythroblastic leukemia. *Blood* 80:2873– 2882.

Park, S., Picard, F., Azgui, Z., Viguie, F., Merlat, A., Guesnu, M., Leblond, V., and Dreyfus, F. (2002) Erythroleukemia: A comparison between the previous FAB approach and the WHO classification. *Leuk Res* 26:423–429.

Rietveld, L.E.G., Caldenhoven, E., and Stunnenberg, H.G. (2001) Avian erythroleukemia: A model for corepressor function in cancer. *Oncogene* 20:3100–3109.

Roggli, V.L., and Saleem, A. (1982) Erythroleukemia: A study of 15 cases and literature review. *Cancer* 48(1):101–108.

Seki, M., and Shirasawa, H. (1965) Role of the reticular cells during maturation process of the erythroblast report III. The fate of phagocytized nucleus. *Acta Path Jap* 15(4):387–405.

Selby, D.M., Valdez, R., Schnitzer, B., Ross, C.W., and Finn, W.G. (2003) Diagnostic criteria for acute erythroleukemia. *Blood* 101(7):2895–2896.

Sels, F.T., Langer, S., Schulz, A.S., Silver, J., Sitbon, M., and Friedrich, R.W. (1992) Friend murine leukaemia virus is integrated at a common site in most primary spleen tumours of erythroleukaemic animals. *Oncogene* 7:643–652.

Shibuya, T., Niho, Y., and Mak, T.W. (1982) Erythroleukemia induction by Friend leukemia virus: A host gene locus controlling early anemia or polycythemia and the rate of proliferation of late erythroid cells. *J Exp Med* 156:398–414.
Villeval, J.L., Cramer, P., Lemoine, F., et al. (1986) Phenotype of early erythroblastic leukemias. *Blood* 68:1167–1174.
Watanabe, Y., Sekine, T., Yabe, M., and Kadota, K. (1998) Myeloproliferative disease in a calf. *J Comp Pathol* 119: 83–87.

Acute Megakaryoblastic Leukemia M7

Definition

Acute megakaryoblastic leukemia is diagnosed on the basis of excess blasts and the evidence of their relation to the platelet progenitor lineage. Officially, there must be at least 20% of blasts in the blood or marrow, and 50% of these cells must be of megakaryocytic lineage as determined by immunologic markers.

Epidemiology and Incidence

Little is known of the demographics of M7 in animals. In humans, the disease is relatively rare and accounts for about 8–10% of human AML. Although M7 occurs in humans in all age groups, most cases are seen in the young because of the high risk and incidence of AML in children with Downs syndrome. In animals, M7 is seen in dogs and cats, with most in the 1–3-year-old range and some cases in mature dogs with no breed or gender predilection.

Clinical Presentation and Features

The presentation of animals with M7 is of an animal in poor condition but with a history of illness of relatively recent onset, usually within a month or 2 weeks of clinical examination. On physical examination there are pale mucus membranes, occasionally with petechiation and mild icterus. Generalized lymphadenopathy is almost always present, and even tonsillar enlargement has been noted along with hepatosplenomegaly.

Pathologic Features

Blood

On laboratory examination, there is moderate to severe anemia with the PCV of 10–20% and a total leukocyte count of 4,000–6,000/ul of which 1,000–2,000/ul are neutrophils and thrombocytopenia, with platelets ranging from 7,000–16,000/ul. On examination of blood there is a nonresponsive anemia with reticulocytes at about the same level as the platelets or less than a third of the 60,000/ul that would be seen in a dog with a normal hematocrit. There is usually mild mature rubricytosis with macrocytosis and hypochromia, with an occasional fragmented red cell due to the widespread areas of microvascular injury of thrombocytopenia. The neutrophils are poorly granulated, and lymphocytes tend to be small to medium with the presence of mononuclear large blast cells. The blastic cells have round to oval nuclei with hyperchromatic coarsely cribriform chromatin and 1–2 prominent nucleoli. The cytoplasm is moderate in volume forming a complete, often eccentric enclosure of the nucleus and is highly basophilic with occasional fine vacuolations and azurophilic granules. A most significant aspect of these blasts is the characteristic narrow based cytoplasmic blebbing that is recapitulating normal platelet shedding (Fig. 5.126). M7 blasts have a much greater tendency to anisokaryosis than the blasts of other types of AML, which is a further significant characteristic. In general, the most mature megakaryocytes of M7 are smaller than their benign counterparts and much smaller than those of benign megakaryocytic hyperplasia. The neoplastic blasts mimic benign precursors in binucleation, which is much more common than in normal marrow. The blast forms of M7 may be small and in the same size range as large lymphocytes and are known as *dwarf* or *micromegakaryocytes*, but they retain the characteristic of a focal cytoplasmic protrusion or budding (Figs. 5.127, 5.128)

Bone Marrow

The bone marrow in AML of M7 type may be difficult to obtain if there is focal sclerosis, which tends to yield a preponderance of injured cells on aspiration (Figs. 5.129, 5.130). On histological section, there is patchy hypercellularity with reduced proportion of fat cells and with

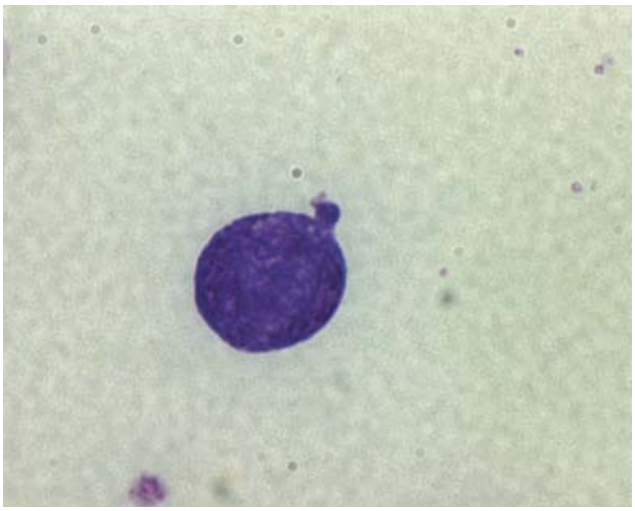

Figure 5.126. Dog: blood, megakaryoblastic leukemia. The blast cells in the peripheral blood have a hyperchromatic chromatin pattern and retained nucleoli that are lightly rimmed by chromatin and have a narrow rim of highly basophilic cytoplasm with characteristic broad-based pseudopodia.

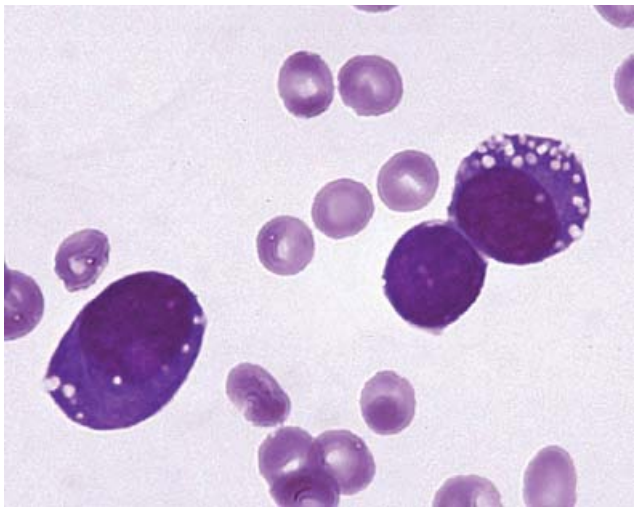

Figure 5.127. Dog: blood, megakaryoblastic leukemia. There are 2 blastic cells of relatively normal size with that in the center possibly a dwarf-type megakaryoblast. *Image from J. W. Harvey, DVM.*

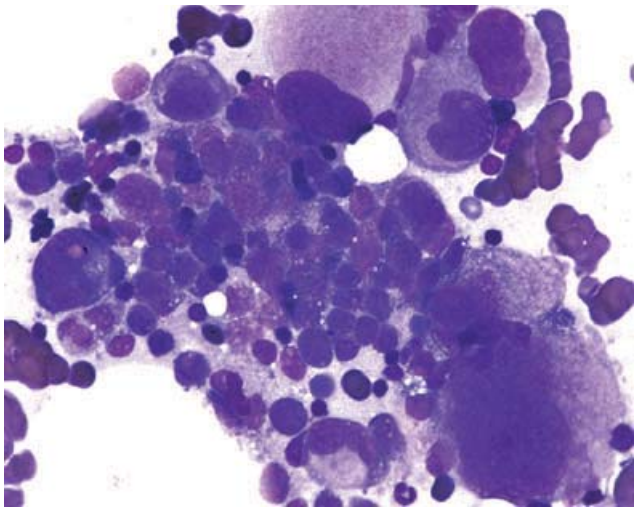

Figure 5.128. Dog: marrow, megakaryoblastic leukemia. There are multiple large atypical megakaryocytes and many smaller blastic cells in the center that may be of the same lineage. *Image from J. W. Harvey, DVM.*

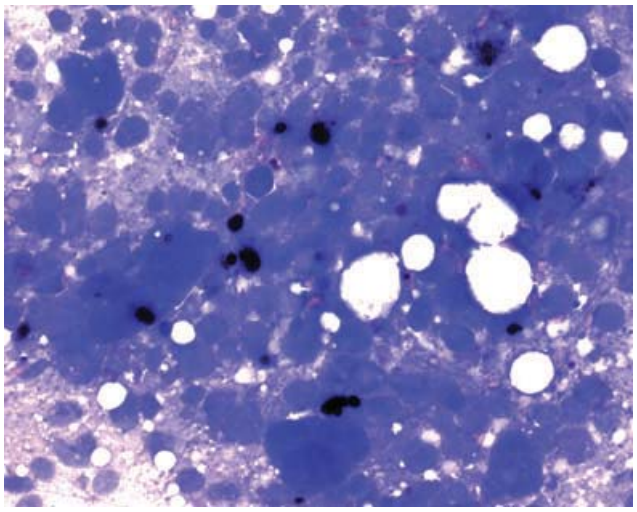

Figure 5.129. Dog: marrow aspirate, megakaryoblastic leukemia. There is marked anisokaryosis of the densely stained cells in the lower left with many bare nuclei. There is quite marked anisokaryosis within the developing megakaryocyte in the lower center and a complete absence of marrow granulocyte reserves and very few erythropoietic cells.

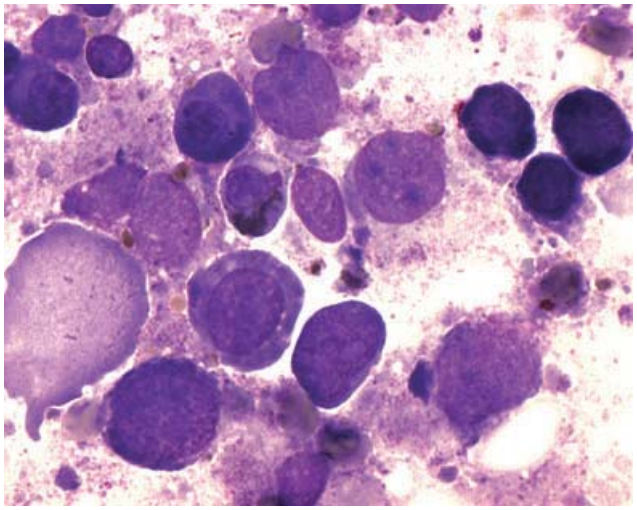

Figure 5.130. Dog: marrow aspirate, megakaryoblastic leukemia. Detail of Figure 5.129. The 3 cells in the upper right are blastic with the 3 larger cells in the lower center left likely promegakaryocytes. There are numerous bare nuclei with prominent multiple nucleoli and irregular tags of cytoplasm with fine granulation suggesting megakaryocytic differentiation.

increased connective tissue consisting of reticulin sclerosis and marked irregular dilation of marrow sinusoids (Figs. 5.131, 5.132). In areas of megakaryocytic proliferation, there is remarkable phthisis of normal marrow cells with complete loss of myelopoiesis and scattered residual rubricytes and foci of small lymphocytes (Fig. 5.133). The rubricytes have dysplastic changes, including binucleation with anisokaryosis and cells with nuclear budding. The neoplastic cells have marked variability, from large blasts with very little cytoplasm to others with multinucleation and irregular lobulation, with some cells with very large nuclei and some small nuclei remaining that have not been included in the initial nuclear melding (Fig. 5.134). An occasional neutrophil is present in megakaryocytic cytoplasm. Most neoplastic nuclei are markedly hyperchromatic and may be found in elongated shapes, particularly in dilated sinuses. The vascular changes in marrow are

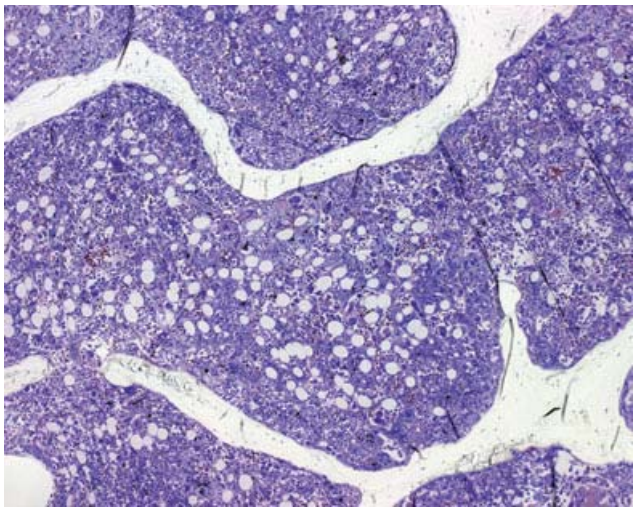

Figure 5.131. Dog: marrow, megakaryoblastic leukemia, plastic section. The marrow has focal areas of increased cellularity with massive numbers of large nuclei of megakaryocytic precursors. *Slide from F. Colbatzky, DVM.*

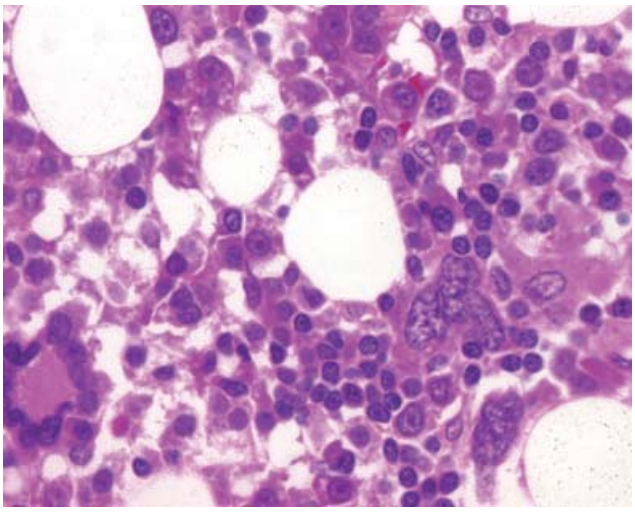

Figure 5.133. Dog: marrow, megakaryoblastic leukemia. A small foci of lymphocytes is surrounded by neoplastic megakaryocytes. *(Slide from F. Colbatzky, DVM.)*

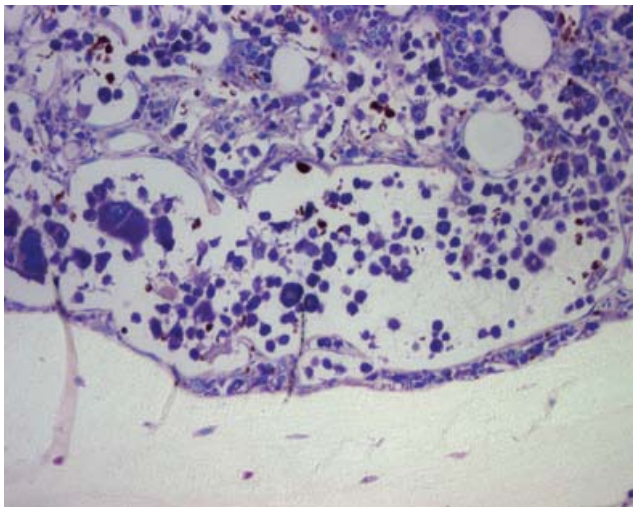

Figure 5.132. Dog: marrow, megakaryoblastic leukemia. The center of the image is occupied by a curving area of marked sinus dilation characteristic of M7 leukemia and regressive marrow sclerosis. *Slide from F. Colbatzky, DVM.*

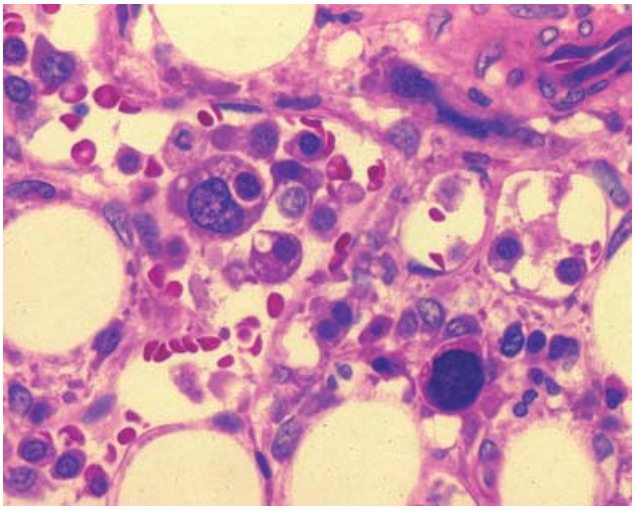

Figure 5.134. Dog: marrow, megakaryoblastic leukemia, same case as Figure 5.133. The neoplastic cells vary from that in the upper right, which is markedly elongated with a long single nucleus to round cells with varying amounts of cytoplasm.

not seen in other forms of AML and consist of markedly irregular dilation of thin-walled sinuses that contain few red cells and large, often irregularly elongated, megakaryocytes. If there is sufficient differentiation to conclude that the neoplastic lineage is of megakaryocytic type, the diagnosis may be made on H&E-stained bone marrow. In most cases, immunologic confirmation can be made by demonstrating that the cytoplasm of the neoplastic cells mark with antibodies against factor VIII–related antigen. Reagents demonstrating platelet glycoprotein are most specific (Fig. 5.135). Most of the blasts and maturing megakaryocytes will show some reactivity to PAS, but the blasts are routinely negative with MPO and SBB. There is always reticulin sclerosis of marrow with M7, but the reaction lacks specificity except in speed of development and extent of proliferation.

Other Organs

Other tissues regularly involved include spleen, nodes, liver, and even lungs. Nodes of normal size may be par-

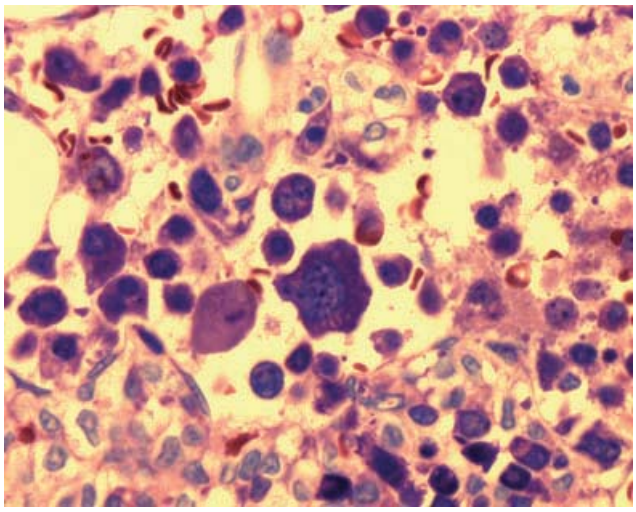

Figure 5.135. Dog: marrow, megakaryoblastic leukemia. Immunohistochemical stain for platelet glycoprotein demonstrating differentiated megakaryocytes and their precursors with other marrow cells at top and bottom unlabeled. *Slide from F. Colbatzky, DVM.*

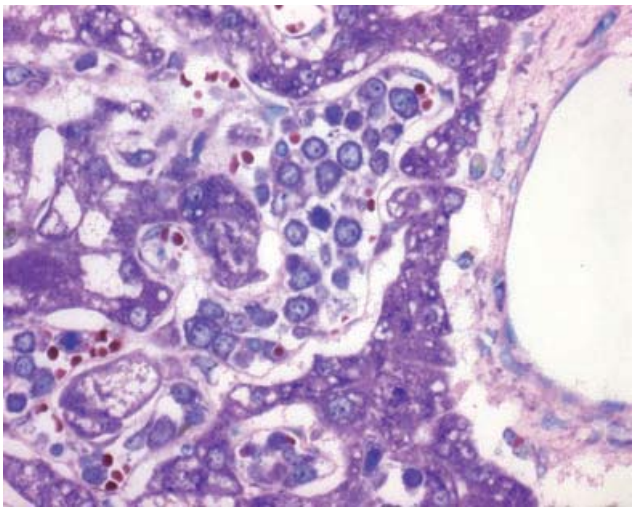

Figure 5.137. Dog: liver, megakaryoblastic leukemia. Detail of Figure 5.136. Atypical megakaryocytes and precursors occupy dilated sinuses near a central vein. Hepatocytes contain bile and iron pigment and are markedly atrophic.

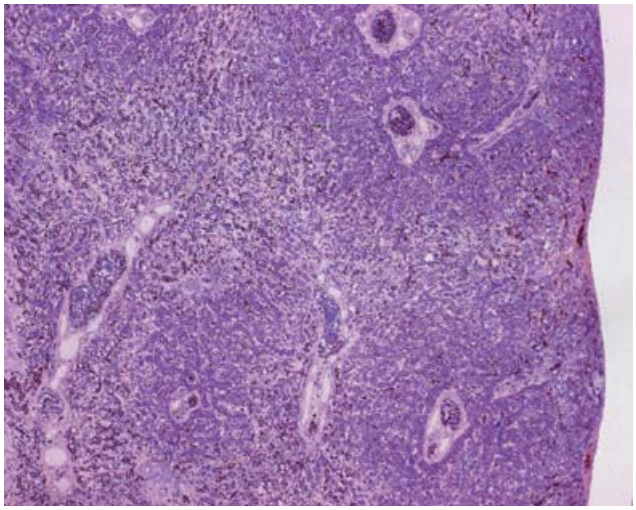

Figure 5.136. Dog: liver, megakaryoblastic leukemia. There is accentuation of zonation with reduced density of hepatocellular staining in the mid-zone and perivenous areas. There is a focal area of neoplastic colonization in the subcapsular area (right).

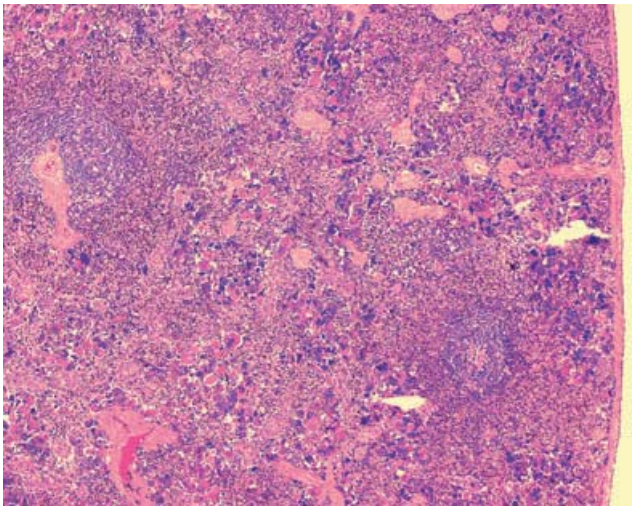

Figure 5.138. Dog: spleen, megakaryoblastic leukemia. A fading germinal center in the lower-right area has a pink proteinaceous insudation of follicular hyalinosis and there is accentuation of the sinus around that area as well as the upper left. The sinuses are irregularly and diffusely occupied by neoplastic megakaryocytes. *Slide from F. Colbatzky, DVM.*

tially invaded, with architecture still evident, and enlarged nodes have complete effacement of lymphoid tissue with diffuse colonization by neoplastic cells. The liver may resemble other types of AML with diffuse sinusoidal involvement, or there may be focal areas of complete parenchymal destruction by solid tumor proliferation (Figs. 5.136, 5.137). The spleen is always enlarged with thinning of the capsule and widely separated and thinned muscular trabeculae. There is marked atrophy of the periarteriolar lymphoid sheaths and germinal centers that are replaced by an amyloidlike amorphous proteinaceous deposition (Fig. 5.138). The sinus areas are devoid of most other cells, with irregular sinus dilation and presence of megakaryocytes at all stages of maturation (Fig. 5.139). Megakaryocytic nuclei are occasionally seen in normal animals lodged in the pulmonary alveolar capillaries. In M7, where there are many large cells in

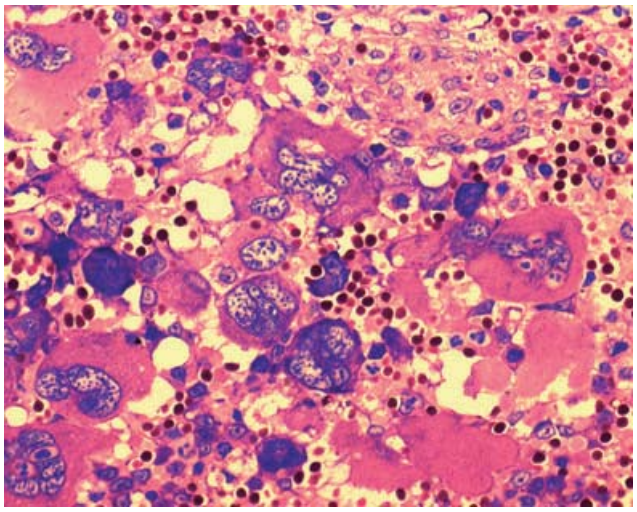

Figure 5.139. Dog: spleen, megakaryoblastic leukemia. Detail of Figure 5.138. The sinus is dominated by megakaryocytes at varying stages of development. There are 3 neutrophils migrating through the cytoplasm of the megakaryocyte in the right center. There is a splenic ellipsoid surrounding small vessels in the upper right. *Slide from F. Colbatzky, DVM.*

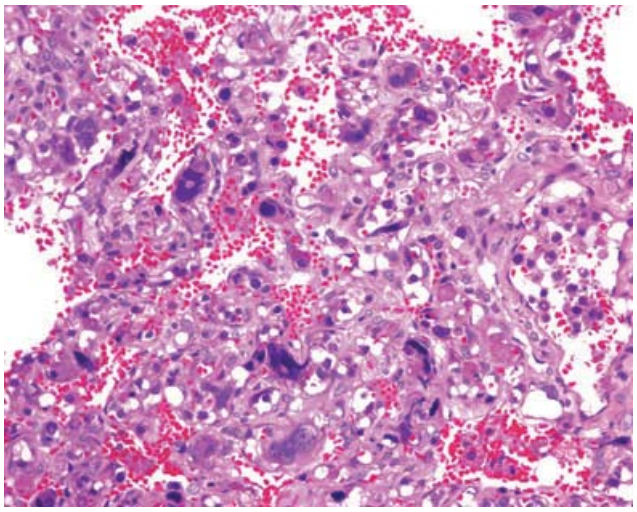

Figure 5.140. Dog: lung, megakaryoblastic leukemia. There is a markedly dilated vein in the left center with distortion of architecture due to widespread embolism of vessels by megakaryocytes at all stages of development. *Slide from F. Colbatzky, DVM.*

circulation, many of the blastic cells with larger nuclei are present in smaller vessels in the lung with irregular distension by the nuclei often bare of any discernible cytoplasm (Fig. 5.140).

M7 may present as an even more aggressive neoplasm with major involvement of the marrow, and, although there is involvement of the spleen and other organs, the neoplasm is less differentiated and the disease resembles a large cell leukemia/lymphoma with irregular binucleation and rapidly advancing myelofibrosis.

REFERENCES

Bene, M.C., Castoldi, G., Knapp, W., et al. (1995) European group for the immunological characterization of leukaemias (EGIL): Proposals for the immunological classification of acute leukaemias. *Leuk* 9:1783–1786.

Bennett, J.M., Catovsky, D., Daniel, M.T., et al. (1985) Criteria for the diagnosis of acute leukemia of megakaryocytic lineage (M7): A report of the French-American-British cooperative group. *Ann Intern Med* 103:460–462.

Bolon, B., Buergelt, C.D., Harvey, J.W., Meyer, D.J., and Kaplan-Stein, D. (1989) Megakaryoblastic leukemia in a dog. *Vet Clin Pathol* 18(3):69–72.

Brunning, R. (1999) Proposed World Health Organization (WHO) classification of acute leukemia and myelodysplastic syndromes. *Mod Pathol* 12:102.

Brunning, R.D. (2001) Acute myeloid leukemia. In Knowles, D.M. (ed.), *Neoplastic Hematopathology*, 2nd ed. Lippincott Williams & Wilkins, Philadelphia, pp. 1667–1715.

Chuang, S.-S., and Li, C.-Y. (1977) Useful panel of antibodies for the classification of acute leukemia by immunohistochemical methods in bone marrow trephine biopsy specimens. *Am J Clin Pathol* 107:410–418.

Colbatzky, F., and Hermanns, W. (1993) Acute megakaryoblastic leukemia in one cat and two dogs. *Vet Pathol* 30:186–194.

Cuneo, A., Mecucci, C., Kerim, S., Vandenberghe, E., Dal Cin, P., Van Orshoven, A., Rodhain, J., Bosly, A., Michaux, J.L., Martiat, P., Boogaerts, M., Carli, M.G., Castoldi, G., and Van Den Berghe, H. (1989) Multipotent stem cell involvement in megakaryoblastic leukemia: Cytologic and cytogenetic evidence in 15 patients. *Blood* 74(5):1781–1790.

Erber, W.N., Breton-Gorius, J., Villeval, J.L., et al. (1987) Detection of cells of megakaryocyte lineage in haematological malignancies by immunoalkaline phosphatase labeling cell smears with a panel of monoclonal antibodies. *Brit J Haematol* 65:87–94.

Holscher, M.A., Collins, R.D., Glick, A.D., and Griffith, B.O. (1978) Megakaryocytic leukemia in a dog. *Vet Pathol* 15:562–565.

Jiang, S., Levine, J.D., Fu, Y., Deng, B., London, R., Groopman, J.E., and Avraham, H. (1994) Cytokine production by primary bone marrow megakaryocytes. *Blood* 84(12):4151–4156.

Kitamura, N., Koshiba, M., Horie, O., and Ryo, R. (2002) Expression of granulysin mRNA in the human megakaryoblastic leukemia cell line CMK. *Acta Haematol* 108:13–18.

Koike, T., Aoki, S., Maruyama, S., et al. (1987) Cell surface phenotyping of megakaryoblasts. *Blood* 69:957–960.

Ledieu, D., Palazzi, X., Marchal, T., and Fournel-Fleury, C. (2005) Acute megakaryoblastic leukemia with erythrophagocytosis and thrombosis in a dog. *Vet Clin Pathol* 34(1):52–56.

Ma, Z., Morris, S.W., Valentine, V., Li, M., Herbrick, J., Cui, X., and Bouman, D. (2001) Fusion of two novel genes, RBM15 and MKL1, in the t(1;22)(p13;q13) of acute megakaryoblastic leukemia. *Nat Genet* 28:220–221.

Matsuo, T., and Bennett, J.M. (1988) Acute leukemia of megakaryocytic lineage (M7). *Cancer Genet Cytogenet* 34:1–3.

McClellan, J.E., Maddox, J.C., and Innes, D.J. (1989) Platelet vacuoles in acute megakaryoblastic leukemia. *Am J Clin Pathol* 92(5):700–702.

Messick, J., Carothers, M., and Wellman, M. (1990) Identification and characterization of megakaryoblasts in acute megakaryoblastic leukemia in a dog. *Vet Pathol* 27:212–214.

Miyamoto, T., Hachimura, H., and Amimoto, A. (1996) A case of megakaryoblastic leukemia in a dog. *J Vet Med Sci* 58:177–179.

Pucheu-Haston, C.M., Camus, A., Taboada, J., Gaunt, S.D., Snider, T.G., and Lopez, M.K. (1995) Megakaryoblastic leukemia in a dog. *JAVMA* 207(2):194–196.

Ramsfjell, V., Borge, O.J., Veiby, O.P., Cardier, J., Murphy, Jr., M.J., Lyman, S.D., Lok, S., and Jacobsen, S.E.W. (1996) Thrombopoietin, but not erythropoietin, directly stimulates multilineage growth of primitive murine bone marrow progenitor cells in synergy with early acting cytokines: Distinct interactions with the ligands for c-*kit* and FLT3. *Blood* 88(12):4481–4492.

Ribeiro, R.C., Oliveira, M.S.P., Fairclough, D., Hurwitz, C., Mirro, J., Behm, F.G., Head, D., Silva, M.L.M., Raimondi, S.C., Crist, W.M., and Krance, R. (1993) Acute megakaryoblastic leukemia in children and adolescents: A retrospective analysis of 24 cases. *Leuk and Lymph* 10:299–306.

Schmitz, B., Thiele, J., Kaufmann, R., Witte, O., Wickenhauser, C., Kuhn-Regnier, F., and Fischer, R. (1993) Megakaryocytes and fibroblasts—Interactions as determined in normal human bone marrow specimens. *Leuk Res* 19(9):629–637.

Shull, R.M., DeNovo, R.C., and McCracken, M.D. (1986) Megakaryoblastic leukemia in a dog. *Vet Pathol* 23:533–536.

Thiele, J., Titius, B.R., Kopsidis, C., and Fischer, R. (1992) Atypical micromegakaryocytes, promegakaryoblasts and megakaryoblasts: A critical evaluation by immunohistochemistry, cytochemistry and morphometry of bone marrow trephines in chronic myeloid leukemia and myelodysplastic syndromes. *Virchows Archiv B Cell Pathol* 62:275–282.

Zunino, R., Li, Q., Rosé, S.D., Romero-Benítez, M.M.I., Lejen, T., Brandan, N.C., and Trifaró, J.M. (2001) Expression of scinderin in megakaryoblastic leukemia cells induces differentiation, maturation, and apoptosis with release of plateletlike particles and inhibits proliferation and tumorigenesis. *Blood* 98(7):2210–2219.

Acute Panmyelosis with Myelofibrosis M8

A rapidly progressive myelofibrosis with marrow failure and short course is a rare disease in humans and is largely unrecognized in animals. Acute panmyelosis is distinguished from myeloid metaplasia with myelofibrosis, which occurs rarely in animals, and is a chronic disease characterized by persistent neutrophilic leukocytosis without apparent cause that is followed by splenomegaly, myelofibrosis, and marrow failure with anemia and finally pancytopenia.

Acute panmyelosis of humans is a disease of acute onset in adults and in children that presents with pancytopenia and without splenomegaly. The red cells have few changes other than deficient numbers. Blast cells may be present in low numbers in blood, and neutrophils are abnormally segmented with both hypolobulated and hypersegmented forms (Fig. 5.141). Marrow aspiration results in a "dry tap," and a core is essential to obtain a sample due to the rapidity of onset of myelosclerosis. Cytologically, the marrow is hypercellular with hyperplasia of all three lineages (Fig. 5.142). Blasts are increased and megakaryocytes are increased with dysplastic forms present, including micromegakaryocytes and multilobulated forms (Figs. 5.143, 5.144). Reticulin stains provide evidence of early but widespread fibrosis, and collagen is generally not present (Fig. 5.145).

The differential diagnosis in humans includes M7 and chronic idiopathic myelofibrosis or agnogenic myeloid metaplasia. Clonality is not indicated, but the implication is of a primitive progenitor that is driving proliferation of all cell lines, with the megakaryocytic proliferation resulting in early and fatal sclerosis.

A fatal disease characterized by myelofibrosis has been described in pygmy goats that may not be an animal counterpart of the human syndrome of panmyelosis. The disease in goats occurs in related progeny of apparently normal dams and sires. The disease in goats is characterized by slow growth from birth followed by anemia and death of marrow failure by 3 months of age. The presentation is of a poor-doing animal with severe anemia,

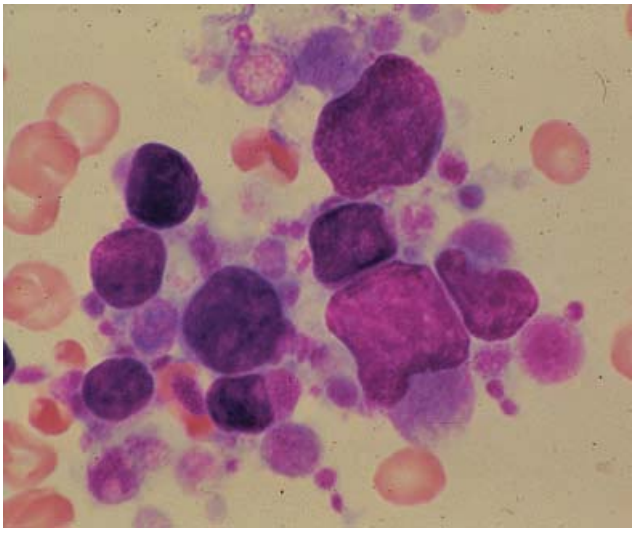

Figure 5.141. Human: bone marrow aspirate, acute panmyelosis with myelofibrosis in blastic crisis. There is typically a poor yield to aspiration. The larger cells are likely atypical micromegakaryocytic nuclei, with the small darkly stained nuclei likely atypical erythroid precursors. Note that some nuclei are bereft of cytoplasm and the multiple cytoplasmic fragments, some with fine azurophilic granulation, are an indication of cellular damage during tissue aspiration and slide preparation. *Image from R. D. Brunning, MD.*

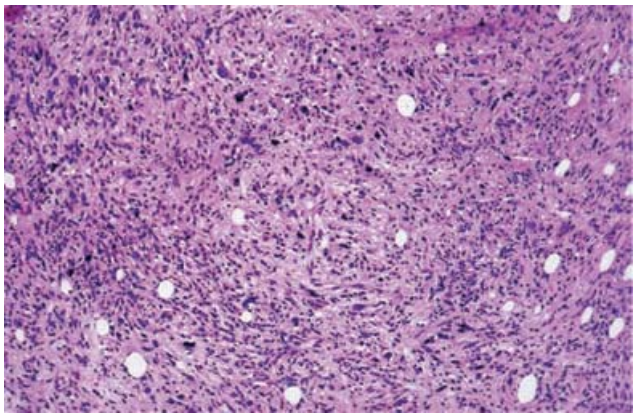

Figure 5.142. Human: bone marrow, acute panmyelosis. Architectural level to demonstrate solid cellularity with few fat cells remaining in streaming patterns of stromal cells with marked reduction of most benign marrow elements except for megakaryocytes which are increased in numbers and vary greatly in size and shape. *Reprinted from* Rosai and Ackerman's Surgical Pathology, *9th Edition, Volume 2 by J. Rosai, page 2064, 2004, Permission from Elsevier and A. Orazi M.D. FIGURE 23.35A.*

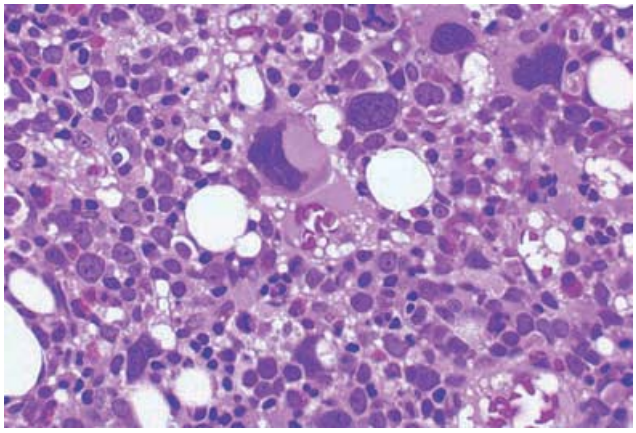

Figure 5.143. Human: marrow, acute panmyelosis. Same case as Figure 5.142. There is early asynchrony with increased numbers of primitive cells with atypical appearing megakaryocytes. There is a tripolar mitosis top center. *Reprinted from Rosai and Ackerman's Surgical Pathology, 9th Edition, Volume 2 by J. Rosai, page 2064, 2004, Permission from Elsevier and A. Orazi M.D. FIGURE 23.35B.*

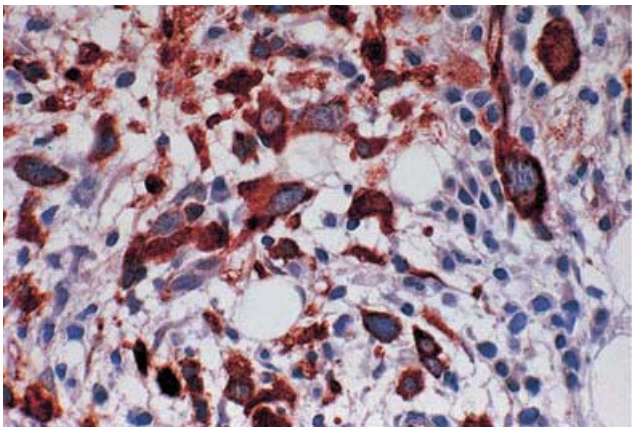

Figure 5.144. Human: bone marrow, acute panmyelosis. Same case as Figure 5.142. Immunoperoxidase staining for factor VIII, demonstrating the high level of megakaryocytic precursors. *Reprinted from Rosai and Ackerman's Surgical Pathology, 9th Edition, Volume 2 by J. Rosai, page 2064, 2004, Permission from Elsevier and A. Orazi M.D. FIGURE 23.35C.*

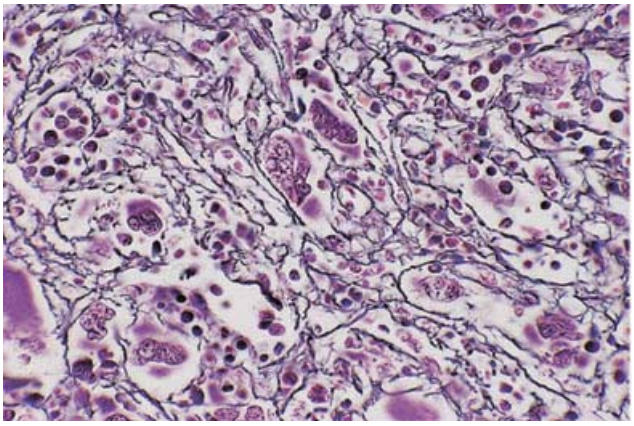

Figure 5.145. Human: marrow, acute panmyelosis. Marrow with reticulin stain demonstrating encirclement of marrow cells by continuous columns of reticulin fibers [wilder reticulin stain]. *Reprinted from Rosai and Ackerman's Surgical Pathology, 9th Edition, Volume 2 by J. Rosai, page 2064, 2004, Permission from Elsevier and A. Orazi M.D. FIGURE 23.36.*

moderate leukopenia but severe neutropenia, and a responsive reticulocytosis. The leukocytes are morphologically normal, but there is quite marked red cell poikilocytosis with ovalocytosis not specifically noted. The marrow is extensively fibrotic with actual collagen formation and areas of complete exclusion of all hematopoiesis. In residual areas of hematopoietic marrow, there is megakaryocytic hyperplasia with focal degenerative cells and emperipolesis with other marrow cells within megakaryocytic cytoplasm. Other significant findings are the presence of extramedullary hematopoiesis in most other organs, including tonsil, lymph nodes, liver, and thymus (Figs. 5.146–5.148). The disease is suggested to result from dyspoiesis of the megakaryocytic system with the overproduction of a series of growth-promotant cytokines, including platelet-derived growth factor, transforming growth factor-B, and epidermal growth factor.

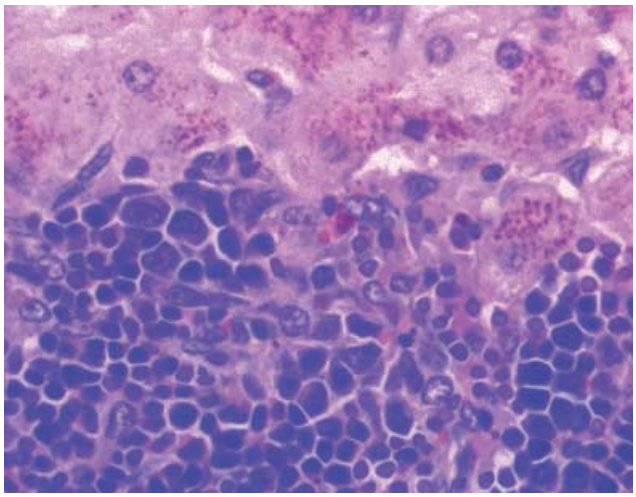

Figure 5.146. Pygmy goat: myelofibrosis. Liver with hepatocytes above and extramedullary hematopoiesis below. The hepatocytes have abundant fine granular pigment that was identified as hemosiderin. The hematopoieis appears to be primarily erythroid type. *Image from K. S. Latimer, DVM.*

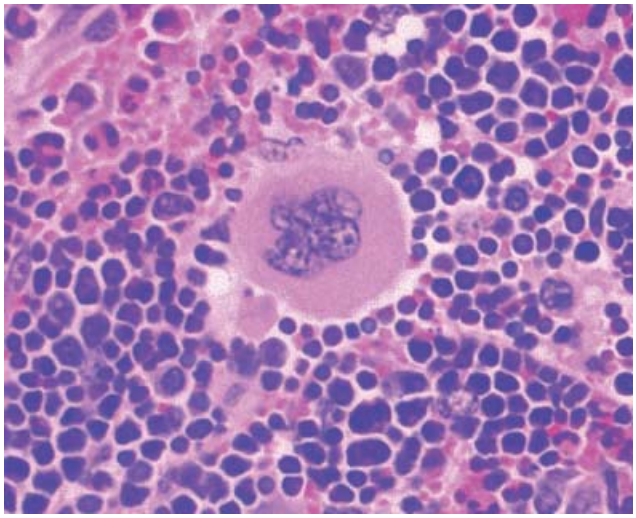

Figure 5.147. Pygmy goat: bone marrow, myelofibrosis. Image taken from a residual area of marrow, with solid trilineage hematopoiesis. There is a small area of stromal proliferation in the upper left. *Image from K. S. Latimer, DVM.*

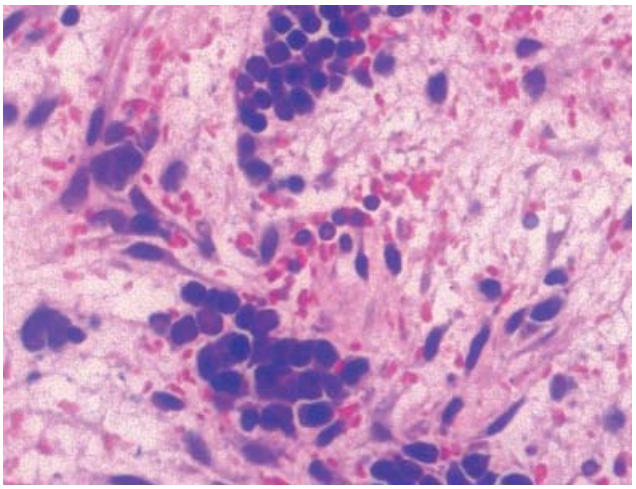

Figure 5.148. Goat: bone marrow, myelofibrosis. Image taken from an area of marrow with extensive fibrillar proliferation and phthisis of normal marrow elements. The disease is not unlike that of human CIMF in that there is early proliferation of all cell lines with reticulin but not collagen fibrosis and minimal atypia in the proliferative fibroblasts. *Image from K. S. Latimer, DVM.*

REFERENCES

Bearman, R.M., Gerassimas, A., Panglis, A., et al. (1979) Acute (malignant) myelosclerosis. *Cancer* 43:279–293.

Brunning, R.D. (2001) Acute myeloid leukemia. In Knowles, D.M. (ed.), *Neoplastic Hematopathology*, 2nd ed. Lippincott Williams & Wilkins, Philadelphia, pp. 1667–1715.

Cain, G.R., East, N., and Moore, P.F. (1994) Myelofibrosis in young pygmy goats. *Comp Haematol Int* 4:167–172.

Harris, N.L., Jaffe, E.S., Diebold, J., Flandrin, G., Muller-Hermelink, H.K., Vardiman, J., Lister, T.A., and Bloomfield, C.D. (2000) The World Health Organization classification of neoplastic diseases of the haematopoietic and lymphoid tissues: Report of the Clinical Advisory Committee Meeting, Airlie House, Virginia, November 1997. *Histopathol* 36:69–87.

Hruban, R.H., Kahajda, F.P., and Mann, R.B. (1987) Acute myelofibrosis. Immunohistochemical study of four cases and comparison with acute megakaryoblastic leukemia. *Am J Clin Pathol* 88:578–588.

Rameshwar, P., Chang, V.T., Thacker, U.F., and Gascón, P. (1998) Systemic transforming growth factor-beta in patients with bone marrow fibrosis—Pathophysiological implications. *Am J Hematol* 59:133–142.

Sultan, C., Sigaux, F., Imbert, M., et al. (1981) Acute myelodysplasia with myelofibrosis: A report of eight cases. *Brit J Haematol* 49:11–16.

Granulocytic Sarcoma

Granulocytic sarcoma (GS) is a focal mass of extramedullary proliferation of myeloid precursors that can be of any lineage but in animals is composed of neutrophils or most often eosinophilic cells of varying maturity with myelocytes and mature eosinophils predominating. The gross lesions may have a green appearance on exposure of a cut surface to air due to the high level of cellular myeloperoxidase, which has resulted in the alternate designation of *chloroma*. GS occurs in cattle, primarily in skeletal muscle, and in dogs and cats in the lung (Figs. 5.149–5.153), gut (Figs. 5.154, 5.155),

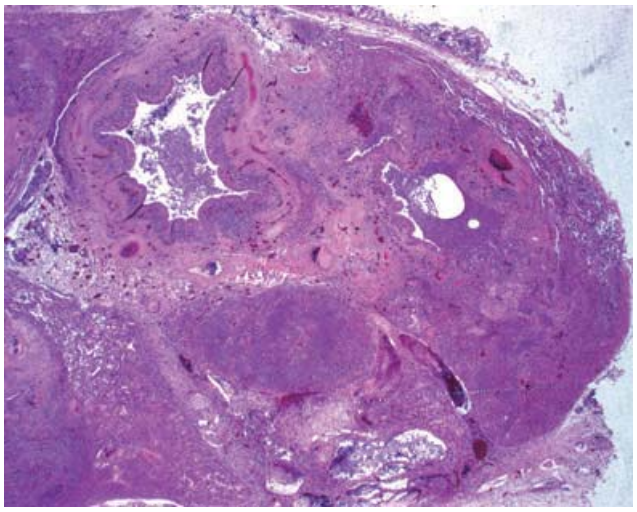

Figure 5.149. Cat: lung, granulocytic sarcoma. There is complete lobular collapse with a very large airway surrounded by completely collapsed pulmonary parenchyma that is heavily infiltrated with neoplastic cells.

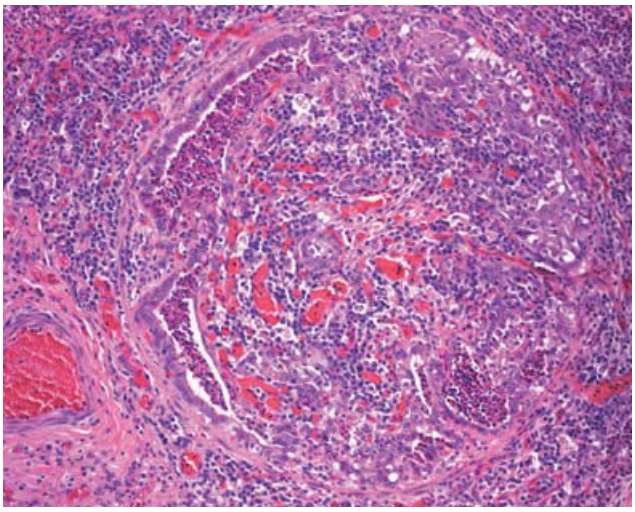

Figure 5.151. Cat: lung, granulocytic sarcoma. The destructive nature of this neoplasm is apparent in this example of neoplastic bronchiectasis with infiltration, colonization, and vascularization of a neoplastic granulomatous reaction within the airway lumen.

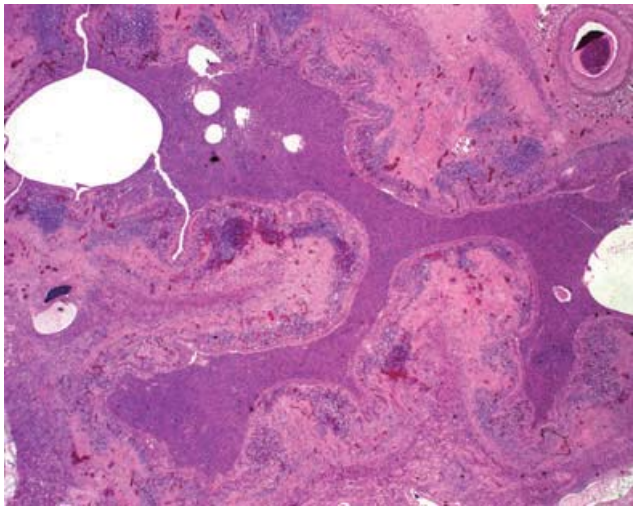

Figure 5.150. Cat: lung, granulocytic sarcoma, another area of same case as Figure 5.149. The section demonstrates the major airways of the lung that are largely filled with cellular debris but remain lined by intact epithelium and irregularly surrounded by benign lymphoid proliferation that appears as an irregular laminar line of increased density with focal dark areas of residual lymphoid nodules. The surrounding lung has become completely solid tissue with cellular exudate and some areas of fibrosis.

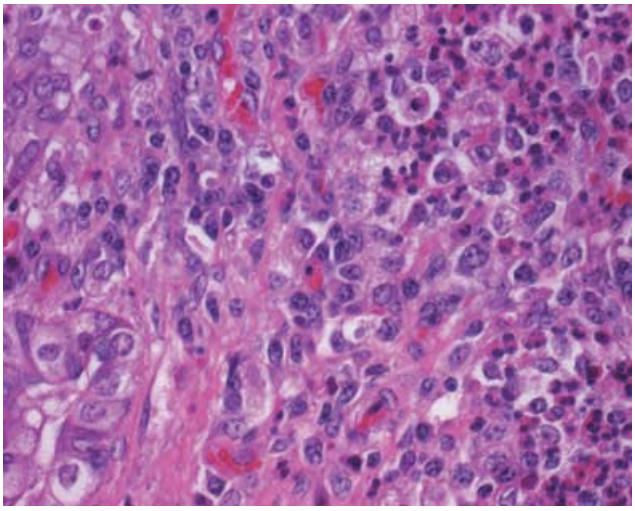

Figure 5.152. Cat: lung, granulocytic sarcoma. Detail of Figure 5.151. The epithelium at the left of the image is at the top margin of Figure 5.151. There are numerous plasma cells and benign inflammatory cells in the organizing tissue within the airway. The pulmonary parenchyma is heavily infiltrated with mononuclear-appearing cells with vesicular nuclei and mature eosinophils with evident brightly stained granules.

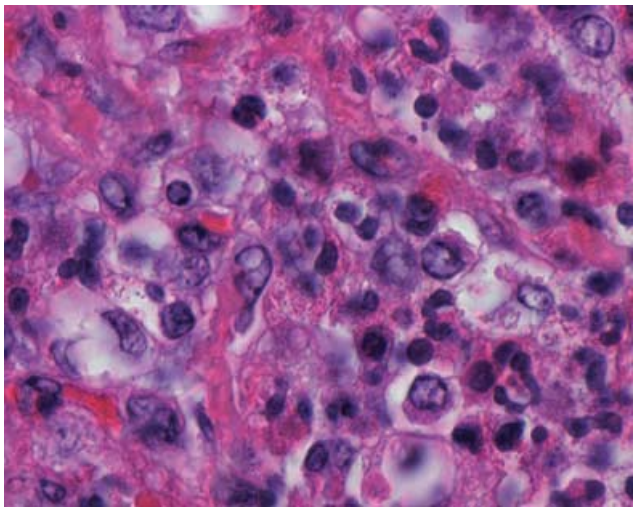

Figure 5.153. Cat: lung, granulocytic sarcoma. Detail of Figure 5.152. The cell in the center with round nuclei and evident granules is an eosinophil myelocyte. The large cells with abundant cytoplasm are residual alveolar macrophages. The characteristic tendency of eosinophils to segment into a bilobed structure is evident in a number of the surrounding maturing cells that have abundant atypical granulation.

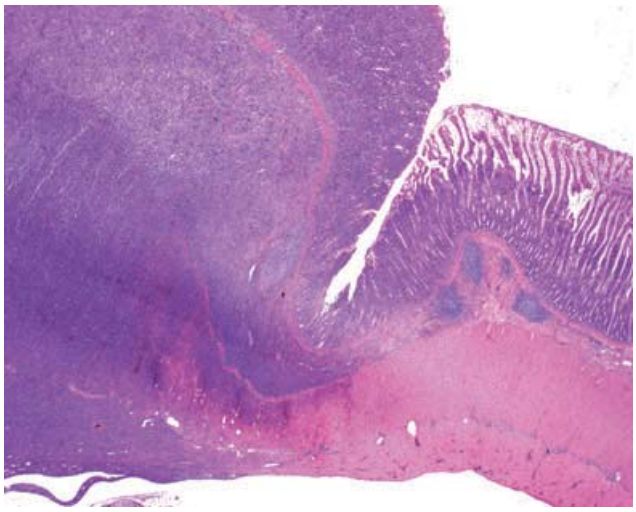

Figure 5.154. Cat: ileum, granulocytic sarcoma. There is an abrupt transition from normal mucosa at the top with several submucosal lymphoid follicles adjacent to a massive transmural infiltration of neoplastic cells.

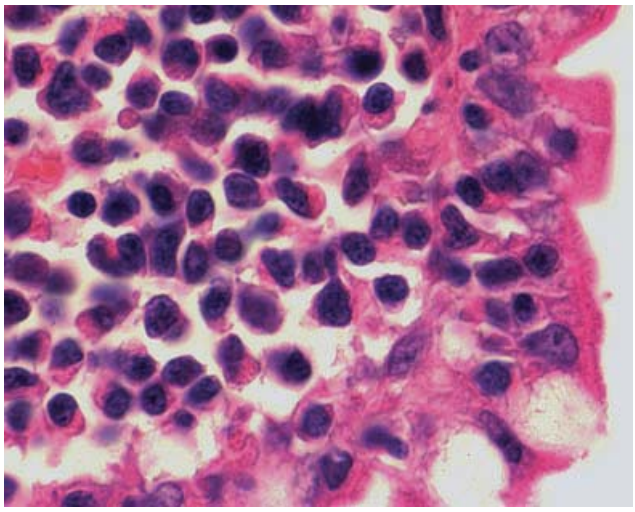

Figure 5.155. Cat: ileum, granulocytic sarcoma. Detail of Figure 5.154, Ileal epithelium near junction with normal intestine. The infiltration in the lamina propria is primarily of cells at the myelocyte stage accompanied by a few residual plasma cells in the left center.

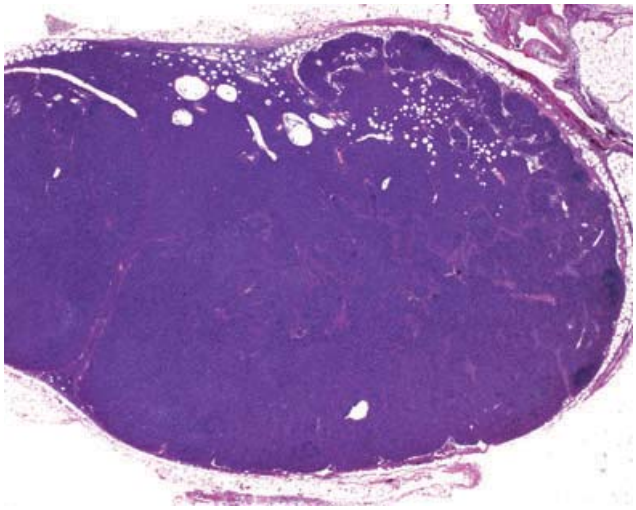

Figure 5.156. Cat: mesenteric node, granulocytic sarcoma, same case as Figure 5.154. The node is diffusely enlarged with a taut and thinned capsule with compression of the peripheral sinus and almost complete loss of normal internal architecture. There are 3 fading germinal centers in subcapsular sinus areas at the right of the image.

node (Figs. 5.156, 5.157), liver (Figs. 5.158, 5.159), and skin, but the lesions may occur in any sites. In cases of longer standing, there is the characteristic tissue injury caused by the eosinophil granule peptide that results in sclerosis of whatever tissue is involved (Figs. 5.160, 5.161).

In humans, the disease is seen either preceding or following a diagnosis of acute myeloid leukemia, and this association makes proper diagnosis an important distinction. In animals, the occurrence of chloroma or myeloid sarcoma is generally an incidental finding and has not been associated with the subsequent onset of AML.

The presence of a focal mass diagnosed as GS is not expected to be associated with the presence of atypical

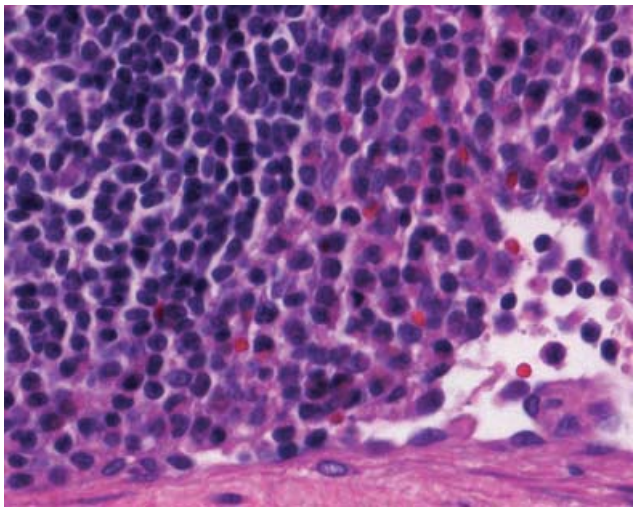

Figure 5.157. Cat: mesenteric node, granulocytic sarcoma. Detail of Figure 5.156. The node capsule is at the bottom margin with an adjacent area of open subcapsular sinus. A fading germinal center is in the upper left with the center and upper areas of the field filled with eosinophils and their precursors, many at a metamyelocyte stage of maturation. The entire remaining areas of node were involved to the same extent.

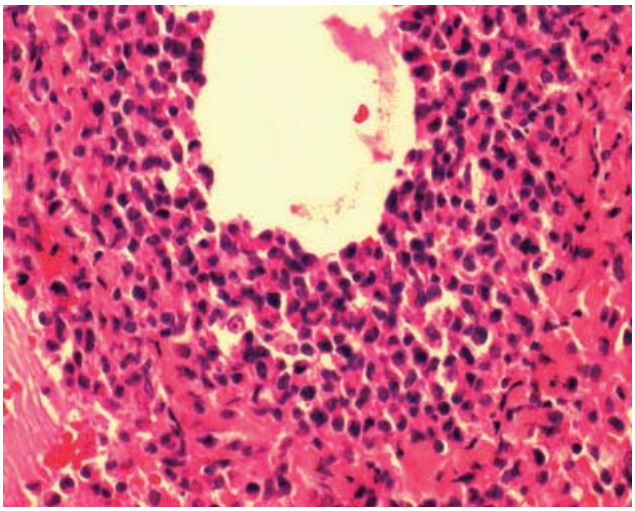

Figure 5.159. Cat: liver, granulocytic sarcoma. Detail of Figure 5.158. A large hepatic vein is likely quite markedly dilated and has a very heavy subendothelial colonization of neoplastic eosinophils. The smooth muscle wall appears discontinuous at the left and bottom with the vessel largely uninvolved on the outer surface. Similar changes are present in other areas mimicking the subendothelial colonization of large veins that occurs with other leukemias particularly in the spleen. Arteries are uninvolved.

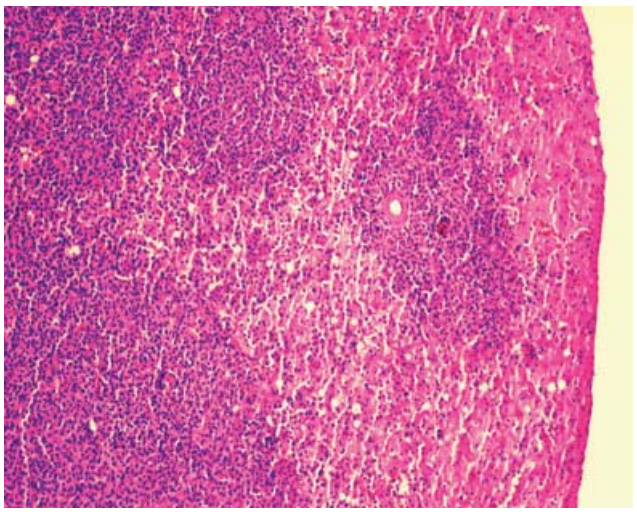

Figure 5.158. Cat: liver, granulocytic sarcoma, same case as Figure 5.154. There is a focal area of hepatic involvement, several centimeters in diameter, that arises on vessels and progresses to coalescence.

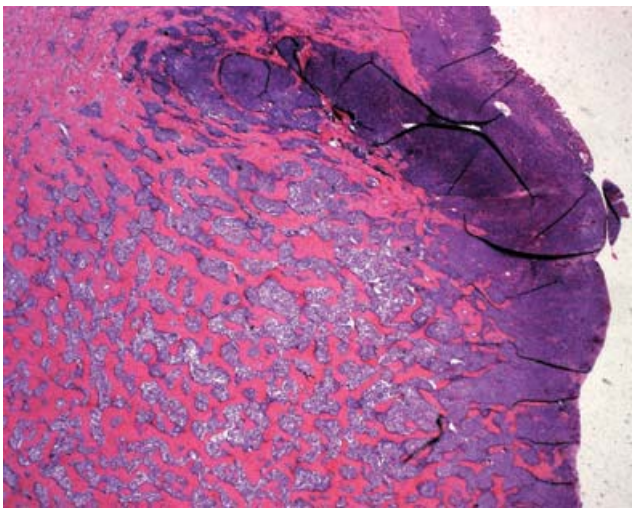

Figure 5.160. Cat: jejunum, granulocytic sarcoma. The effects of chronic eosinophil degranulation in tissues is evident in this image in which there is an interlacing pattern of mature collagen throughout the area occupied by the neoplastic cells.

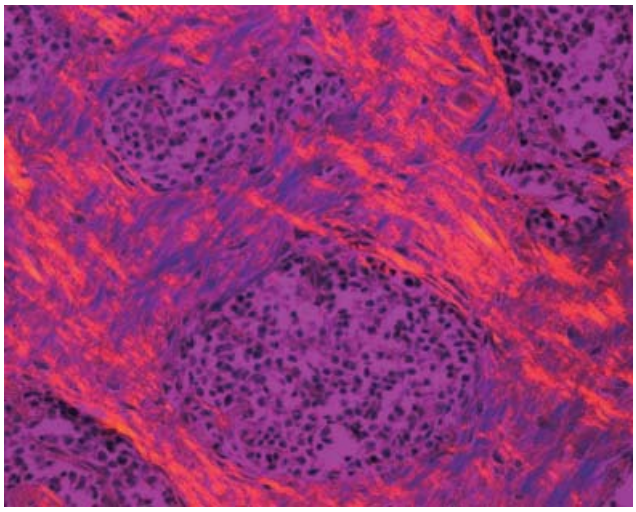

Figure 5.161. Cat: jejunum, granulocytic sarcoma. Detail of Figure 5.160. With polarized light, the network of pink fibers in the submucosal area can be demonstrated to be solid mature collagen, likely a result of chronic eosinophil deposition in the area.

cells in the blood, but in domestic animals that association has not been tested or noted if present. The lesions form solid nodules with destruction of the parent tissue, and the cells are strongly positive for MPO in histological preparations and for chloroacetate esterase staining in cytologic preparations.

In both humans and cattle, the GS lesions occur in the young, pediatric in humans and yearlings in cattle—with the disease in dogs relatively poorly described. In cats, the mean age of four cases was 10.1 years, with a further case examined from a mature cat of unknown age. In humans, the foci of myeloid sarcoma are found in the axial skeleton with the orbit, paranasal sinuses, lymph nodes, breast, and skin, and in the body systems of peripheral and central nervous, gastrointestinal, respiratory, and genitourinary tracts.

The morphology of the GS lesions may vary widely, and this is a major reason for accurately recognizing the cellular lineage to eliminate diseases of similar-appearing cells. In humans, three levels of maturation are recognized, including blastic, immature, and differentiated. The blastic types are composed primarily of myeloblasts with few better-granulated cell types to exclude lymphoma from diagnostic consideration. The immature types consist of myeloblasts and promyelocytes, and the differentiated types have promyelocytes as the most immature cell and most of the mass is of more mature granulocytes. Because these lesions in cattle are almost always diagnosed by gross examination and in histology, the cellular detail to distinguish these various levels is usually lacking.

In humans, the differential diagnosis includes Burkitt's lymphoma and lymphoblastic lymphoma for the poorly differentiated types, with the chloroacetate esterase (CAE) stain required to rule out high-grade lymphoma.

REFERENCES

Brunning, R.D. (2001) Acute myeloid leukemia. In Knowles, D.M. (ed.), *Neoplastic Hematopathology*, 2nd ed. Lippincott Williams & Wilkins, Philadelphia, pp. 1667–1715.

Fellbaum, C., and Hansmann, M.L. (1990) Immunohistochemical differential diagnosis of granulocytic sarcomas and malignant lymphomas on formalin-fixed material. *Virchows Archiv A Pathol Anat* 416:351–355.

Hudock, J., Chatten, J., Miettinen, M. (1994) Immunohistochemical evaluation of myeloid leukemia infiltrates (granulocytic sarcomas) in formaldehyde-fixed, paraffin-embedded tissue. *Am J Clin Pathol* 102:55–60.

Inborn, R.C., Aster, J.C., Roach, S.A., et al. (1995) A syndrome of lymphoblastic lymphoma, eosinophilia, and myeloid hyperplasia/malignancy associated with a t(8;13)(p11;q11): Description of a distinctive clinicopathologic entity. *Blood* 85:1881–1887.

Krishnamurthy, M., Nusbacher, N., Elguezabal, A., and Seligman, B.R. (1977) Granulocytic sarcoma of the brain. *Cancer* 39(4):1542–1546.

Landis, D.M., and Aboulafia, D.M. (2003) Granulocytic sarcoma: An unusual complication of aleukemic myeloid leukemia causing spinal cord compression. A case report and literature review. *Leuk and Lymph* 44(10):1753–1760.

Meis, J.M., Butler, J.J., Osborne, B.M., et al. (1986) Granulocytic sarcoma in nonleukemic patients. *Cancer* 58:2697–2709.

Mrad, K., Abid, L., Driss, M., Abid, H.B., and Romdhane, K.B. (2004) Granulocytic sarcoma of the small intestine in a child without leukemia. Report of a case with cytologic findings and immunophenotyping pitfalls. *Acta Cytol* 48:641–644.

Neiman, R.S., Barcos, M., Berard, C., et al. (1981) Granulocytic sarcoma: Clinicopathologic study of 61 biopsied cases. *Cancer* 48:1426–1437.

Perkins, S.E., Murphy, J.C., and Alroy, J. (1996) Eosinophil granulocytic sarcoma in a New Zealand white rabbit. *Vet Pathol* 33:89–91.

Pettinato, G., De Chiara, A., Insabato, L., and De Renzo, A. (1988) Fine needle aspiration biopsy of a granulocytic sarcoma (chloroma) of the breast. *Acta Cytologica* 32(1):67–71.

Reinhardt, D., and Creutzig, U. (2002) Isolated myelosarcoma in children—Update and review. *Leuk and Lymph* 43(3):565–574.

Roth, M.J., Medeiros, L.J., Elenitoba-Johnson, K., Kuchnio, M., Jaffe, E.S., and Stetler-Stevenson, M. (1995) Extramedullary myeloid cell tumors. An immunohistochemical study of 29 cases using routinely fixed and processed paraffin-embedded tissue sections. *Arch Pathol Lab Med* 119:790–798.

Sevinc, A., Buyukberber, S., Camci, C., Koruk, M., Savas, M.C., Turk, H.M., Sari, I., and Buyukberber, N.M. (2004) Granulocytic sarcoma of the colon and leukemic infiltration of the liver in a patient presenting with hematochezia and jaundice. *Digestion* 69:262–265.

Walker, B.R., and Cartwright, P.C. (2001) Granulocytic sarcoma presenting as testicular and paratesticular masses in infancy. *J Urol* 165:224.

Yavuz, S., Paydas, S., Disel, U., and Erdogan, S. (2004) Ovarian granulocytic sarcoma. *Leuk and Lymph* 45(1):183–185.

Chapter 6

Chronic Myeloproliferative Diseases

CHRONIC MYELOID LEUKEMIA

The myeloproliferative diseases (MPDs) in humans are an irregular proliferation of one or more marrow cell lines within a single individual and anchored by the presence of a specific chromosomal translocation. In contrast, the myeloproliferative diseases in animals are an assortment of different proliferative entities with species-specific characteristics occurring in many animals and not anchored by any known molecular characteristic. It is thus hazardous to apply a classification system developed around many years of experience within a single (human) species to relatively much less well-characterized disease entities in a variety of animal species.

Chronic myeloproliferative disease in the human context consists of a spectrum of related disorders, all resulting from a chromosomal translocation occurring in a pluripotential marrow stem cell. The disease results in the overproduction of one or more of the four myeloid cell lines producing the disease entities of chronic myeloid leukemia (CML), polycythemia vera (PV), essential thrombocythemia (ET), and idiopathic myelofibrosis, formerly known as *agnogenic myeloid metaplasia*.

Human CML

In many ways, the entity of CML in humans has been the focus of many high-impact developments in the area of hematopathology. CML was the disorder that prompted Virchow to coin the term *leukemia* and Neumann to add the topographical origin of *myelogene*. CML was the first disease found to be associated with a chromosomal translocation and the first where the genetic change was found to result in a fusion gene that produced a fusion protein leading to the uncontrolled proliferation. Currently, CML is again a leading subject of high impact in the development of effective and relatively nontoxic modalities of chemotherapy. The central oncogenic role of the BCR-ABL fusion gene characteristic of human CML results from the reciprocal translocation t(9;22). The role of this fusion gene was further demonstrated by its insertion by retroviral vector in marrow cells given to irradiated mice that then develop a CML-like syndrome. It has subsequently been shown that each stem cell lineage that becomes infected with the vector will contribute to the CML-like syndrome, thus confirming the primary oncogenic role of the BCR-ABL oncogene.

The gene product of this oncogene has tyrosine kinase-like activity that is able to adopt an active tertiary conformation, as determined by X-ray diffraction in both the phosphorylated and unphosphorylated states. An effective inhibitor of the activity of this protein tyrosine kinase Bcr-Abl is a 2-phenylaminopyrimidine agent called *ST1571,* also *imatinib* or *Gleevec*. The mechanism of action of Gleevec, as determined on primary cell cultures derived from CML patients, has been to inhibit the activity of both the phosphorylated and unphosphorylated forms of the Bcr-Abl tyrosine kinase. The net effect of this inhibition is to down-regulate the proliferation of the neoplastic clones while not inhibiting the benign precursors permitting them to recover. A secondary role suggested for Gleevec of enhancing apoptosis of the neoplastic lineages was not found to occur. This inhibition does not necessarily result in the elimination of the neoplastic precursors, but it effectively silences them. In current trials, Gleevec appears able to induce remission in patients in the chronic phase of CML and even to have efficacy in those entering the accelerated and blast phases. Cases that are resistant to Gleevec or become resistant after therapy appear to result from a second mutation that changes the shape of the mutant tyrosine kinase that prevents the binding and inactivation by Gleevec. With the understanding of the mechanism of resistance, a second compound designated BMS-354825 has been developed that has a high level of activity in Gleevec-resistant cases. In humans, CML, occurs at a fairly constant rate of 1–1.5 cases/100,000/year and is by far the most common of the chronic myeloproliferative diseases, with the eosinophilic subtype quite rare. In contrast, in animals—in cats at least—the eosinophilic variant appears more common than the more general multilineage involvement,

characteristic of human CML. Unlike the lymphomas where the presence or absence of a clear-cut animal counterpart is more readily apparent, it is less clear in the MPDs where the diseases themselves alter with time, making the identification of a direct animal counterpart less apparent. In the spirit of comparative medicine it would seem most efficient to define the MPDs in human terms and then describe the range of chronic myeloid leukemias in animals to direct the need for further definition in animal neoplasms.

Human CML is a chronic myeloproliferative disease characterized in hematologic terms by marked leukocytosis with basophilia and esosinophilia with moderate anemia and very variable platelet levels. The leukocytosis is primarily of mature neutrophils accompanied by a lesser number of immature forms but with a greater number of myelocytes than of metamyelocytes, known as the *myelocyte bulge* and noted because it is not a feature of human reactive neutrophilia (Figs. 6.1, 6.2). The disease is characterized by an initial chronic phase, at which time most patients are diagnosed, followed by an accelerated phase (Figs. 6.3–6.6) and finally a blast phase. The accelerated phase is defined as an increase in the sum of the promyelocytes and blasts and an increase in reticulin fibrosis. The disease invariably terminates in a blast phase of several months' duration that resembles AML, is refractory to treatment, and may be of lymphoid blast type (Figs. 6.7–6.9). The conversion to the acute phase may be focal in the marrow, or it may occur in the periphery and appear as an enlarged node like granulocytic sarcoma.

Virtually all cases of human CML have the t(9;22) chromosomal translocation whereby the ABL protooncogene from chromosome 9 is placed adjacent to the BCR (breakpoint cluster region) region on chromosome 22 forming the *BCR-ABL* fusion gene capable of being tran-

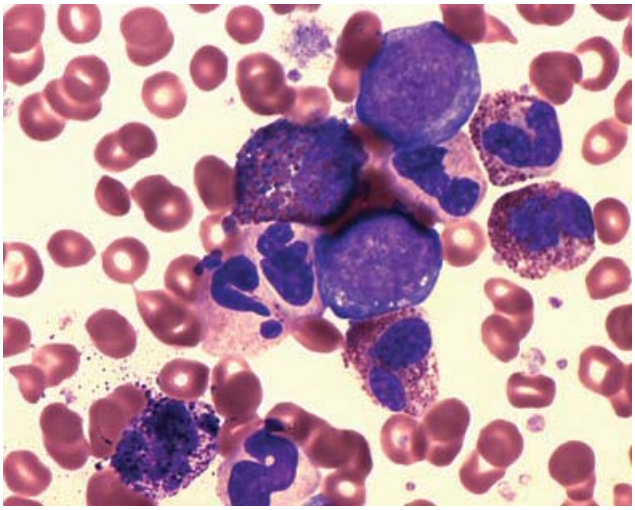

Figure 6.2. Human: blood, chronic myeloid leukemia. This image demonstrates the plurality of cell types present in the human CML. The large cells at top and center are late blastic stages lying adjacent an eosinophil promyelocyte. There are 3 maturing eosinophils and a basophil in the lower left characteristic of neoplastic myeloid proliferation. The 3 neutrophils in the center and right have very low cytoplasmic granulation. *Slide from Cornell Tutorial.*

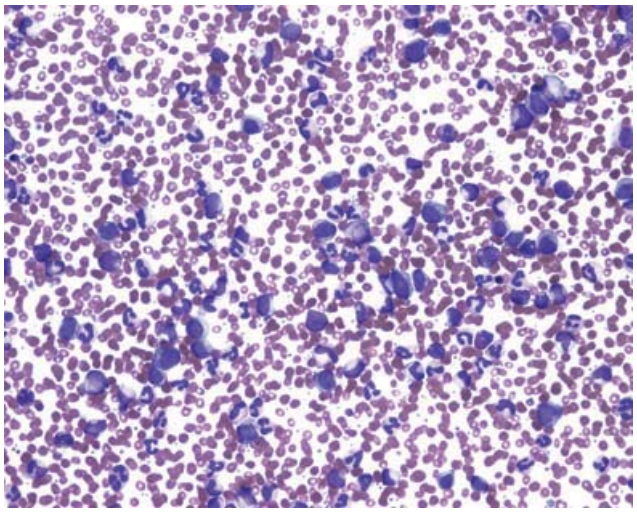

Figure 6.1. Human: blood, chronic myeloid leukemia in chronic phase. There is peripheral blood neutrophilia but with quite marked immaturity and characteristically a greater number of myelocytes than of metamyelocytes constituting the characteristic "myelocyte bulge" of human CML in chronic phase. *Slide from Cornell Tutorial.*

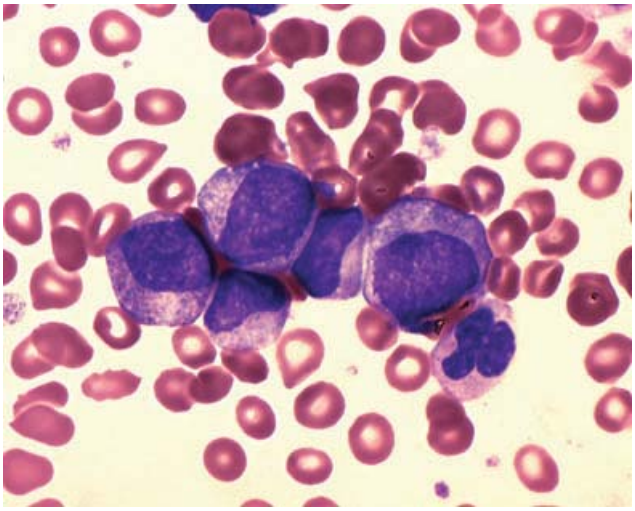

Figure 6.3. Human: blood, chronic myeloid leukemia, same case as Figure 6.1. Illustration of the "myelocyte bulge" with 3 myelocytes accompanied by 2 metamyelocytes and a maturing neutrophil. The disproportionate number of myelocytes is characteristic of CML and is not found in the active or rebound leukocytosis.

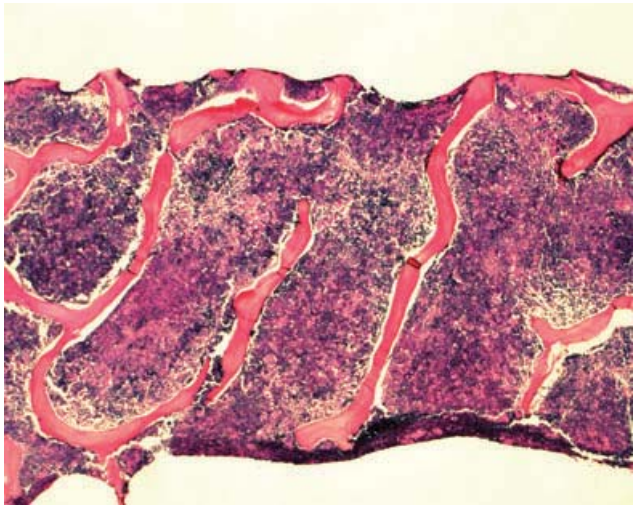

Figure 6.4. Human: bone marrow core, chronic myeloid leukemia, accelerated phase. The marrow is solidly cellular and there is likely some degree of osteopenia with reduced density of cancellous bone.

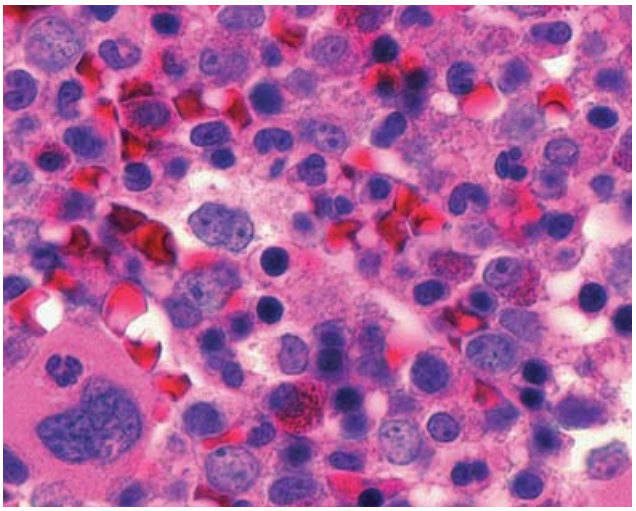

Figure 6.6. Human: marrow, chronic myeloid leukemia. Detail of Figure 6.5. There is an increase in immaturity with more numerous precursors and decreased numbers of maturing neutrophils. Emperipolesis is present with a neutrophil in megakaryocytic cytoplasm in the lower left.

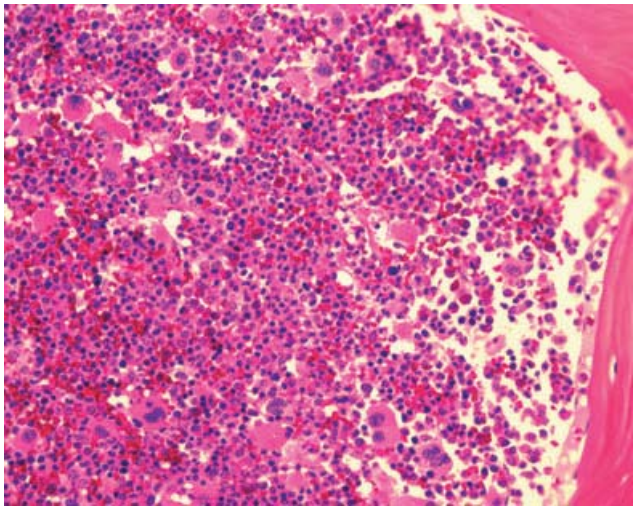

Figure 6.5. Human: bone marrow core, chronic myeloid leukemia. Detail of Figure 6.4. There is diffuse hypercellularity with a loss of fat cells with increased proportions of myeloid cells and reduced erythropoiesis. Megakaryocytes are small and have irregular nuclear fusion with foci of emperipolesis at the lower left.

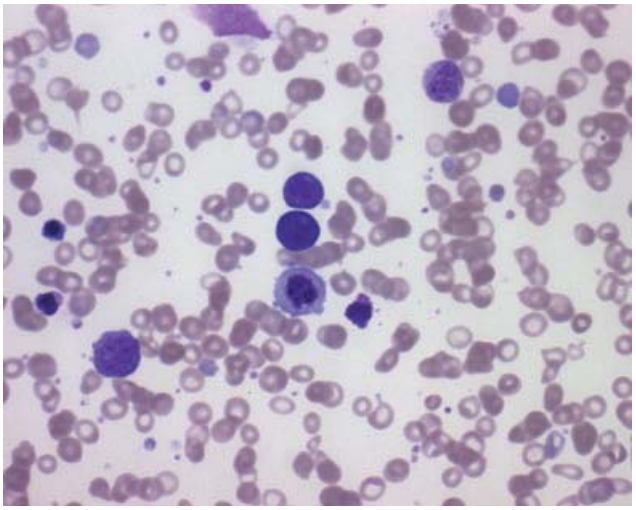

Figure 6.7. Human: blood, chronic myeloid leukemia in blast crisis. Terminally, there is an increasing presence of blasts in the peripheral blood and marrow with reduced mature cell types. *Slide from Cornell Tutorial.*

scribed into a chimeric protein with abnormal tyrosine kinase activity.

CML is primarily a disease of adults in the 5th and 6th decade, with the disease in children unusual except for those with Downs syndrome. Most patients present with hepatosplenomegaly and leukocyte counts in excess of 100×10^3/ul. The mature neutrophils predominate in blood, but blasts are always present at 1–2% level with promyelocytes and a greater number of myelocytes than metamyelocytes (the myelocyte bulge), which is not found in rebound reactive conditions. Importantly, there are always some basophils present and often eosinophilia as well. Monocytes are low on a proportional basis but may be increased in absolute terms. The lymphocyte count varies widely, and the T-cell type may be increased.

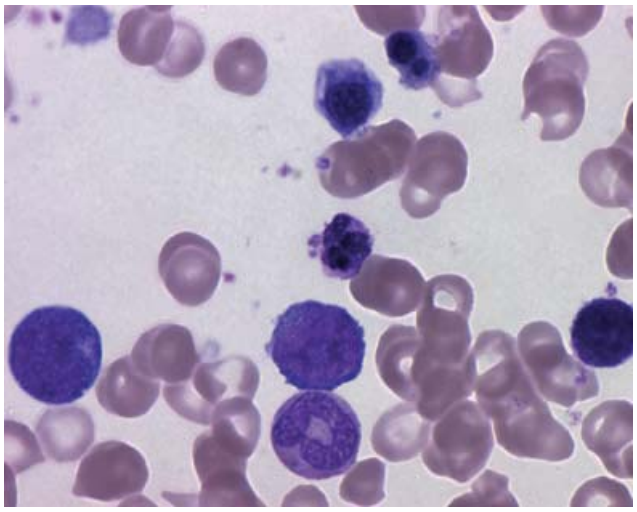

Figure 6.8. Human: blood, chronic myeloid leukemia, blast crisis. Detail of Figure 6.7. The cell in the lower center with the central nucleolus is a blast cell, as well as that directly to the left. The neutrophil at the bottom is enlarged with hyposegmentation. The two cells at the top are a polychromatic rubricyte and metarubricyte with dyserythropoiesis characterized by a satellite nucleus and basophilic stippling. The cell in the center may be a degenerating basophil.

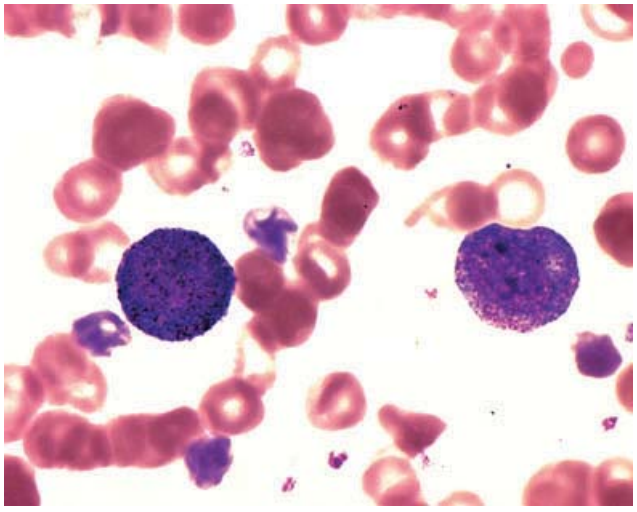

Figure 6.9. Human: blood, chronic myeloid leukemia, blast crisis. Detail of Figure 6.7. The cell in the center right is a neutrophil promyelocyte and the cell at left is a basophil promyelocyte that would otherwise be a cell not seen in the peripheral blood.

Platelets may be as high as 1000 × 10^3/ul, and most patients are not thrombocytopenic. The anemia is normochromic and nonresponsive. Those symptomatic have lethargy and weight loss due partially to anemia, often of occult bleeding, plus sweats, bone pain, and discomfort due to splenomegaly.

In the chronic phase of human CML, the marrow is always hypercellular with almost no fat cells remaining. The myeloid expansion mimics what is seen in the blood with a myelocyte bulge but with a low blast count, with blasts and promyelocytes together totaling less than 10% of marrow nucleated cells. Basophils and eosinophils are almost always seen, as well as abnormal macrophages with birefringent crystals called *pseudo-Gaucher cells*. Histologically, the marrow is characterized by a wider layer of subperiosteal myeloid proliferation, increased in depth over the normal level of 2–3 cells to 5–10 cells with centripetal maturation, radiating inward. Megakaryocytes are increased in numbers but not in size, and they tend to be in the intertrabecular areas and have reduced nuclear lobulation.

The spleen and liver are involved, as in other myeloid neoplasms, with lymphoid atrophy and sinus hyperplasia in the spleen and sinus distension in the liver with minor portal involvement.

The accelerated phase is characterized by lack of response to therapy and increasing systemic signs due to the anemia, splenomegaly, and bone pain. There is an increasing peripheral blood immaturity, with blasts as high as 15% and basophils up to 20% of peripheral blood cells. The total of the blasts and promyelocytes reaches 30% of blood cells, and thrombocytopenia may be present as well as rubriblasts in the peripheral blood.

The blast phase of human CML occurs in most patients after 4–5 years and may become apparent by an altered prominence of blood cell lineage, with a number of types occurring. These include predominance of myeloid blasts or of a mixture of myeloid and monocytic blasts that are similar to the AML of M1, M2, and M4 types. These changes are accompanied or preceded by additional cytogenetic alterations characteristic of the phenotypic change. Some types of blast phase cells may be of erythroid type and, more frequently, of lymphoid type.

Human CML must be differentiated from a severe leukemoid reaction that lacks the myelocyte bulge and peripheral blood basophilia. The leukemoid reaction tends to be ephemeral and generally not accompanied by splenomegaly and, if persistent, the causative lesion is usually identified. CML is usually diagnosed by examination of blood and marrow, but in borderline cases the presence of the t(9;22) translocation and BCR-ABL fusion are considered the gold standard for identifying unusual presentations.

REFERENCES

Anastasi, J., and Vardiman, J.W. (2001) Chronic myelogenous leukemia and the chronic myeloproliferative diseases. In Knowles, D.M. (ed.), *Neoplastic Hematopathology*, 2nd ed. Lippincott Williams & Wilkins, Philadelphia, pp. 1745–1790.

Atwell, S., Adams, J.M., Badger, J., Buchanan, M.D., Feil, I.K., Froning, K.J., Gao, X., Hendle, J., Keegan, K., Leon, B.C., Müller-Dieckmann, H.J., Nienaber, V.L., Noland, B.W., Post, K., Rajashankar, K.R., Ramos, A., Russell, M., Burley, S.K., and Buchanan, S.G. (2004) A novel mode of Gleevec binding is revealed by the structure of spleen tyrosine kinase. *J Biol Chem* 279(53):55827–55832.

Bartam, C.R., de Klein, A., Hagemeijer, A., et al. (1983) Translocation of c-abl oncogene adjacent to a translocation breakpoint in chronic myelogenous leukaemia. *Nature* 306:277–280.

Brunning, R.D., and McKenna, R.W. (1994) Chronic myeloproliferative diseases. In *Tumors of the Bone Marrow*. Armed Forces Institute of Pathology, Washington, D.C., pp. 195–254.

Call, T.G., Noel, P., Habermann, T.M., et al. (1994) Incidence of leukemia in Olmstead County, Minnesota 1975 through 1989. *Mayo Clin Proc* 69:315–322.

Casperson, T., Gahrtoin, G., Lindsten, J., et al. (1970) Identification of the Philadelphia chromosome as number 22 by quinacrine mustard fluorescence analysis. *Exp Cell Res* 63:238–240.

Chang, H., Sutherland, R., Nayar, R., Li, D., Kamel-Reid, S., Mile, M.A., Messner, H., and Lipton, J. (2004) Chronic lymphocytic leukemia in the course of chronic myelocytic leukemia: Evidence of independent clonal origin as shown by interphase fluorescence in situ hybridization and fluorescence-activated cell sorting. *Cancer Genet and Cytogenet* 152:146–148.

Cortes, J. (2004) Natural history and staging of chronic myelogenous leukemia. *Hematol Oncol Clin N Am* 18:569–584.

Cortes, J., and Kantarjian, H. (2003) Advanced-phase chronic myeloid leukemia. *Sem Hematol* 40(1):79–86.

Cortes, J., and O'Dwyer, M.E. (2004) Clonal evolution in chronic myelogenous leukemia. *Hematol Oncol Clin N Am* 18:671–684.

Cortes, J.E., O'Brien, S.M., Giles, F., Alvarez, R.H., Talpaz, M., and Kantarjian, H.M. (2004) Investigational strategies in chronic myelogenous leukemia. *Hematol Oncol Clin N Am* 18:619–639.

Daley, G.Q., Van Etten, R.A., and Baltimore, D. (1990) Induction of chronic myelogenous leukemia in mice by the P210$^{bcr/abl}$ gene of the Philadelphia chromosome. *Science* 247:824–830.

Druker, B.J. (2003) Imatinib alone and in combination for chronic myeloid leukemia. *Sem in Hematol* 40(1):50–58.

Graham, S.M., Jørgensen, H.G., Allan, E., Pearson, C., Alcorn, M.J., Richmond, L., and Holyoake, T.L. (2002) Primitive, quiescent, Philadelphia-positive stem cells from patients with chronic myeloid leukemia are insensitive to STI571 in vitro. *Blood* 99(1):319–325.

Groffen, J., Stephenson, J.R., Heisterkamp, N., et al.(1984) Philadelphia chromosomal breakpoints are clustered within a limited region bcr on chromosome 22. *Cell* 36:93–99.

Harris, N.L., Jaffe, E.S., Diebold, J., Flandrin, G., Muller-Hermelink, H.K., Vardiman, J., Lister, T.A., and Bloomfield, C.D. (2000) The World Health Organization Classification of neoplastic diseases of the haematopoietic and lymphoid tissues: Report of the Clinical Advisory Committee Meeting, Airlie House, Virginia, November 1997. *Histopathol* 36:69–87.

Hasford, J., Pfirrmann, M., Hehlmann, R., Baccarani, M., Guilhot, F., Mahon, F.X., Kluin-Nelemans, H.C., Ohnishi, K., Thaler, J., and Steegmann, J.L., for the Collaborative CML Prognostic Factors Project Group. (2004) Prognosis and prognostic factors for patients with chronic myeloid leukemia: Nontransplant therapy. *Sem in Hematol* 40(1):4–12.

Holtz, M.S., Slovak, M.L., Zhang, F., Sawyers, C.L., Forman, S.J., and Bhatia, R. (2002) Imatinib mesylate (STI571) inhibits growth of primitive malignant progenitors in chronic myelogenous leukemia through reversal of abnormally increased proliferation. *Blood* 99(10):3792–3799.

Johansson, B., Fioretos, T., and Mitelman, F. (2002) Cytogenetic and molecular genetic evolution of chronic myeloid leukemia. *Acta Haematol* 107:76–94.

Konopka, J.B., Witte, O.N. (1985) Detection of c-abl tyrosine kinase activity in vitro permits direct comparison of normal and altered abl gene products. *Mol Cell Biol* 5:3116–3123.

Larson, R.A., Daley, G.Q., Schiffer, C.A., Porcu, P., Pui, C.H., Marie, J.P., Steelman, L.S., Bertrand, F.E., and McCubrey, J.A. (2003) Normal and malignant hemopoiesis. Treatment by design in leukemia, a meeting report, Philadelphia, Pennsylvania, December 2002. *Leuk* 17(12):1–25.

Neumann, E. (1878) Uber myelogene leukaemie. *Berl Klin Wochenschur* 15:69.

Nowell, P.C., Hungerford, D.A. (1960) A minute chromosome in human chronic granulocytic leukemia. *Science* 132:1497–1500.

Ohmine, K., Ota, J., Ueda, M., Ueno, S., Yoshida, K., Yamashita, Y., Kirito, K., Imagawa, S., Nakamura, Y., Saito, K., Akutsu, M., Mitani, K., Kano, Y., Komatsu, N., Ozawa, K., and Mano, H. (2001) Characterization of stage progression in chronic myeloid leukemia by DNA microarray with purified hematopoietic stem cells. *Oncogene* 20:8249–8257.

Radich, J.P., Olavarria, E., and Apperley, J.F. (2004) Allogeneic hematopoietic stem cell transplantation for chronic myeloid leukemia. *Hematol Oncol Clin N Am* 18:685–702.

Rowley, J.D. (1973) A new consistent abnormality in chronic myelogenous leukemia identified by quinicrine fluorescence and Giemsa staining. *Nature* 243:290–293.

Shah, N.P., Tran, C., Lee, F.Y., Chen, P., Norris, D., and Sawyers, C.L. (2004) Overriding Imatinib resistance with a novel ABL kinase inhibitor. *Science* 305:399–401.

Shtivelman, E., Lifshitz, B., Gale, R.P., et al. (1985) Fused transcripts of abl and bcr genes in chronic myeloid leukaemia. *Nature* 315:550–554.

Virchow, R. (1845) Weisses blut. *Froiep's Notizen* 1845, 36:151–156.

Xu, Y., Dolan, M.M., and Nguyen, P.L. (2003) Diagnostic significance of detecting dysgranulopoiesis in chronic myeloid leukemia. *Am J Clin Pathol* 120:778–784.

Young, J.L., Jr., Percy, C.L., Asire, A.J., et al. (1981) Cancer incidence and mortality in the United States, 1973–1977. *Natl Cancer Inst Monogr* 57:1–187.

Animal CML

One of the difficulties in recognizing the different subtypes of MPDs in animals is that the diseases likely go through the same three phases of chronic, accelerated, and blast, with the animals electively terminated relatively

soon after diagnosis so that the full range of presentations is not seen. It is recognized that long-lived domestic animals, including dogs, cats, horses, and cattle, may be presented with relatively stable high leukocyte counts with the presence of marrow and peripheral blood myeloid immaturity. It is less apparent that each of these animals tends to present with a syndrome unique to that species. Dogs, cats, and cows are most like humans, with hyperplastic marrow and high leukocyte counts; horses may have a packed marrow and a peripheral blood picture like pancytopenia with a few blasts.

Clinical Presentation and Features

CML in all animals tends to be in mature individuals that have had slow loss of condition and activity, or CML, like CLL, may be discovered on routine blood examination and be very unexpected. Alternatively, animals with CML that have been in a relatively stable condition may present with disease of apparent acute onset if complicated by infectious disease or trauma due to reduced activity or agility.

Most animals are presented with a history of reduced appetite and weight loss and on examination are found to be anemic and to have splenomegaly or hepatosplenomegaly. The median age of animals at presentation is about the same as for AML, but the mean age is a bit greater. In 7 dogs with a form of CML, the ages ranged from 2–9 years with those involving the monocytic lineage having the most apparent variability.

Pathologic Features

Blood

Cats are most likely to present with a disease like that described for human CML, with neutrophil predominance in the marrow and peripheral blood and with anemia and thrombocytopenia but not with petechiation. The total leukocyte count is usually above 50,000/ul and below the 100,000/ul level (Fig. 6.10). Neutrophils predominate with bands, but myelocytes are most prominent (Fig. 6.11), and promyelocytes are very large with nuclei alone 3–4 red cells in diameter (Figs. 6.12, 6.13). The promyelocyte cytoplasm is poorly granulated and diffusely basophilic and often vacuolated, and an occasional nucleus may be indented rather than round donut, or rodent forms, are present (Fig. 6.14). If monocytes are prominent, the promonocytes, which are also very large and have vacuolations, poorly granulated cytoplasmic basophilia, and irregularly shaped nuclei, may be confused with promyelocytes (Fig. 6.15). True blasts are present but rare, and they won't be found in a differential count of 100 cells (Fig. 6.16). Basophils are present, but they are less than 1% of nucleated cells and easily missed because, although their granules fill the cytoplasm they are not basophilic but more of a tan shade with Wright's staining (Fig. 6.17). The neutrophils do not segment normally and may have smooth nuclear margins

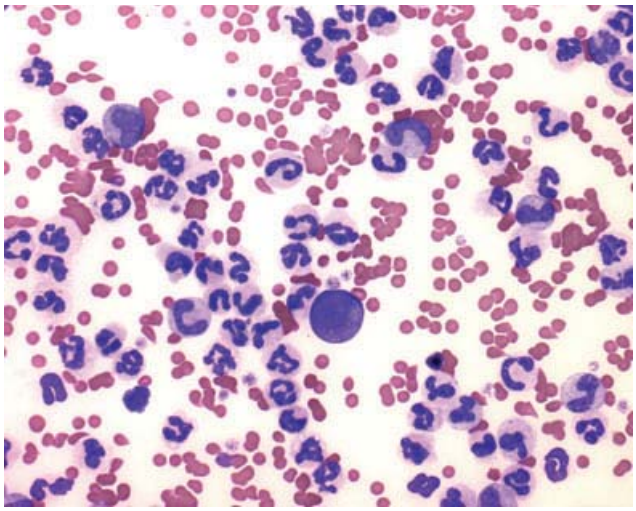

Figure 6.10. Cat: blood, chronic myeloid leukemia of neutrophil type. The total leukocyte count exceeded 500,000 per microliter with most cells maturing neutrophils. In this field, there are large and atypical metamyelocytes as well as a large promyelocyte in the center.

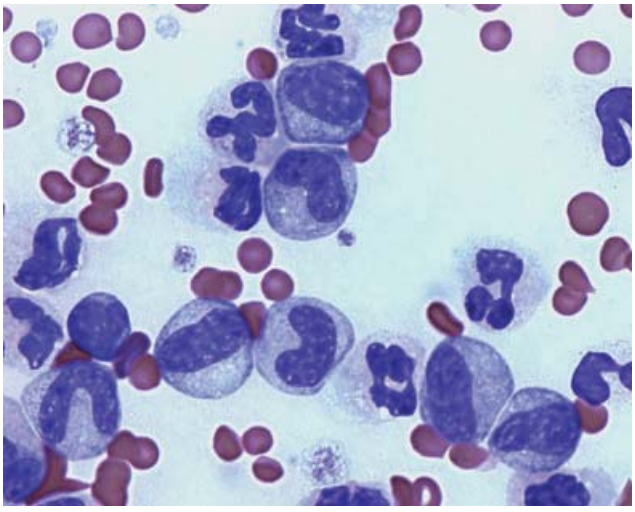

Figure 6.11. Cat: blood, CML. Detail of Figure 6.10. There is an early myelocyte in the upper center and 3 cells below in later stage along with 2 metamyelocytes and a band neutrophil in the lower left. There is a small lymphocyte in the lower left for size comparison and numerous platelets indicating competence of the bone marrow even at this high count. The red cells tend to be normochromic and normocytic, with the anemia severe and packed red cell volume of 11%.

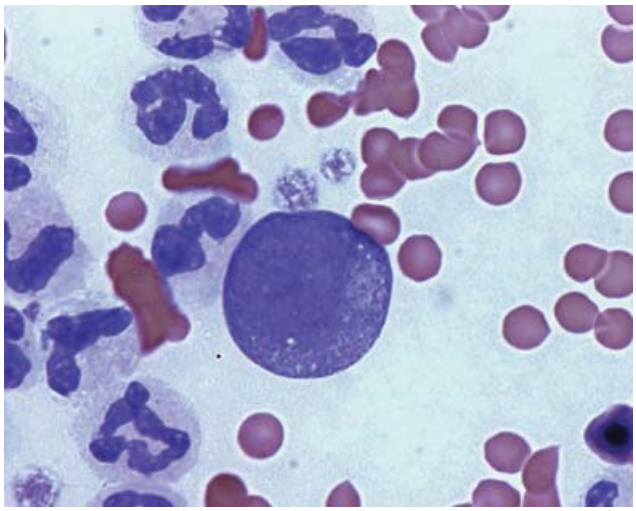

Figure 6.12. Cat: blood, chronic myelogenous leukemia. There is a promyelocyte in the center, with the nucleus nearly 4 red cells in diameter with abundant cytoplasm and heavy azurophilic granulation with greater than normal cytoplasmic basophilia. There is a tendency for surrounding neutrophils to be hypersegmented.

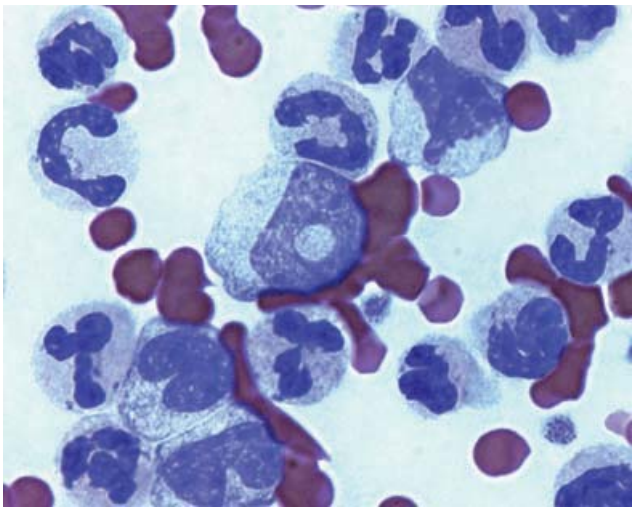

Figure 6.14. Cat: blood, chronic myeloid leukemia. There is a donut or rodent cell type of metamyelocyte in the center with diffuse basophilia and almost no specific granulation. The surrounding neutrophils are poorly granulated and there are Doehle bodies in the neutrophil in the lower left. The cell in the upper right with an atypical-shaped nucleus is likely a monocyte that has faint granulation.

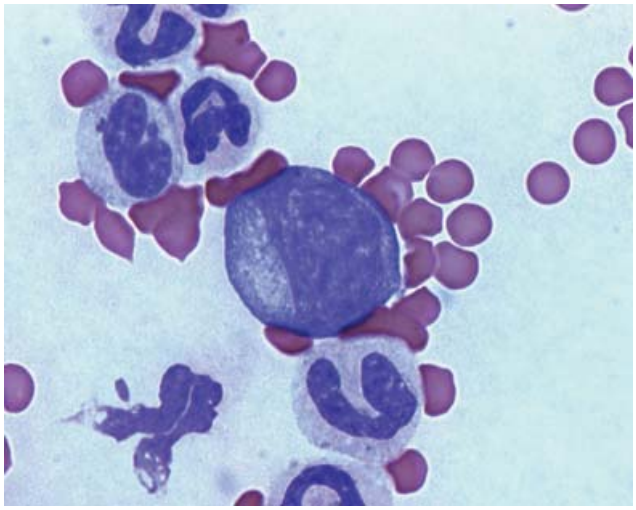

Figure 6.13. Cat: blood, chronic myeloid leukemia. In the center, an early promyelocyte with several nucleoli and abnormally few azurophilic granules. The neutrophils have very pale cytoplasm with less than normal granulation and the one below center has a small Doehle body.

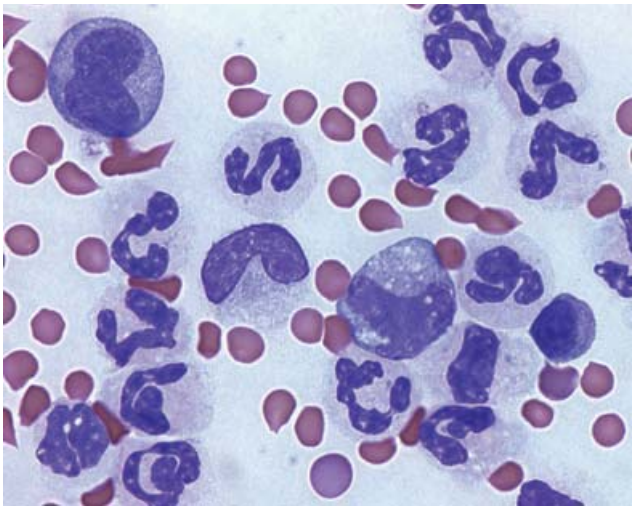

Figure 6.15. Cat: blood, chronic myeloid leukemia. A young monocyte in the right center is roughly the same size as the promyelocytes, with irregularly shaped nucleus and vacuolated cytoplasm that is typically the same density from the nucleus to the cell margin.

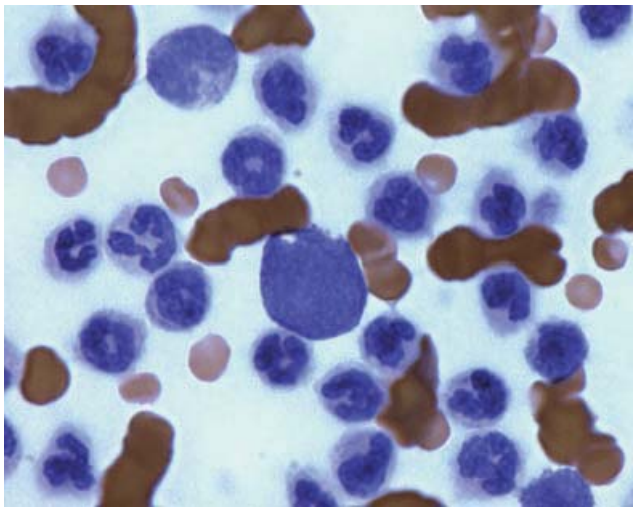

Figure 6.16. Cat: blood, chronic myeloid leukemia. A true myeloblast of stage I or II type with dense cribriform chromatin pattern without the formation of large chromocenters has multiple small nucleoli without chromatin rimming.

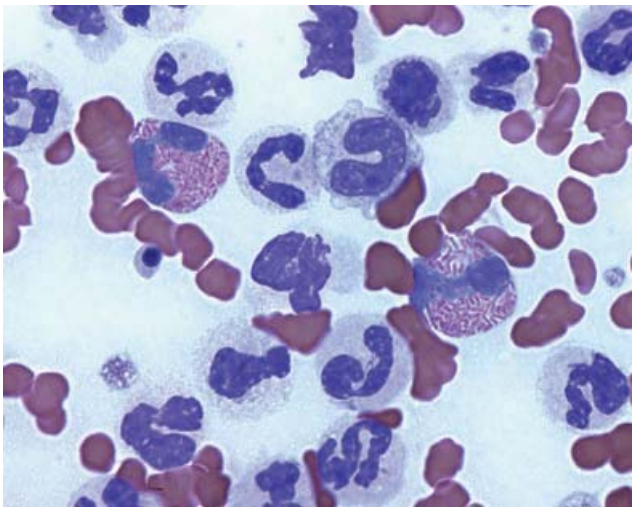

Figure 6.18. Cat: blood, chronic myeloid leukemia. Two well-granulated mature eosinophils are present with neutrophils having reduced normal granulation with generalized basophilia and hypolobulation (below left) and generally hypersegmentation of nuclei.

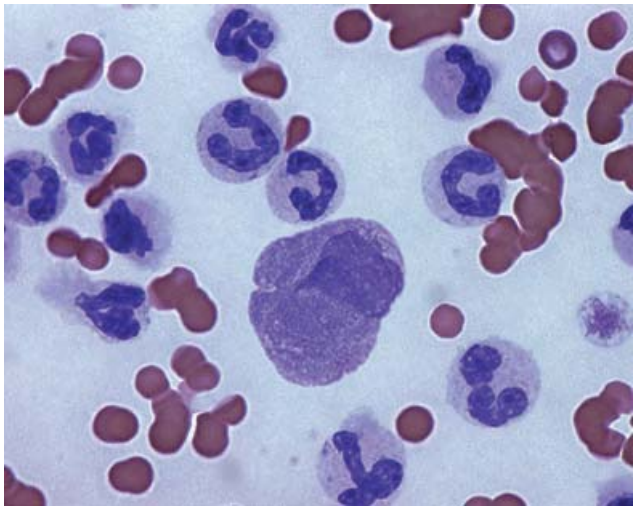

Figure 6.17. Cat: blood, chronic myeloid leukemia. An early basophil, likely myelocyte stage with injured nucleus, has the typical smooth nuclear contours that persist into the segmented stage and granules that consist of a few residual azurophilic type of the promyelocyte stage in a background of poorly defined specific granulation with mild metachromatic properties.

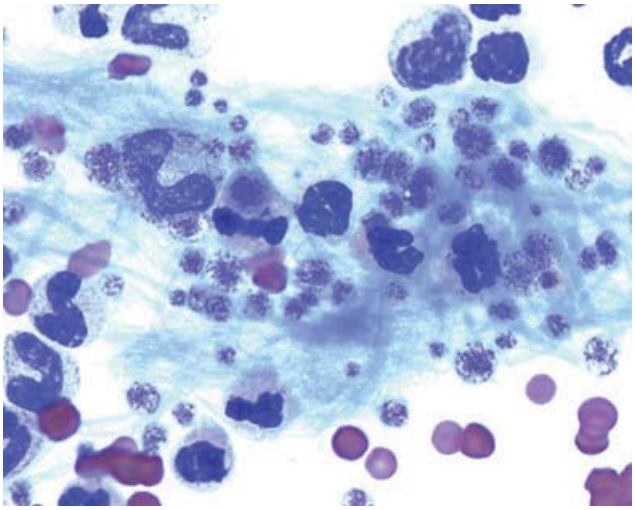

Figure 6.19. Cat: blood, chronic myeloid leukemia. The tip of the blood film with a cluster of platelets and leukocytes enmeshed in fibrin strands. The platelets in this animal have marked size variation, which tends to suggest they are present in adequate numbers. They are well granulated but generally have low basophilia.

like normal basophils and tend to hypersegmentation (see Fig. 6.17). In other cases, they are smaller and have broader nuclear segments and tend to 2 nuclear segments, as seen in benign states with marked left shift. The cytoplasm of neutrophils is pale with reduced, or absent, specific granulation and 1–3 residual azurophilic ("toxic") granules, and they may have an occasional Doehle body (see Fig. 6.14). Cats, in particular, are generally not lymphopenic and may have a normal level of eosinophils (Fig. 6.18) and quite marked monocytosis with late stage rubricytosis. The persistence of monocytes may be indicative of clonal change in a very primitive precursor affecting several competing cell lineages. The platelets have wide size variation but reduced granulation and basophilia (Fig. 6.19).

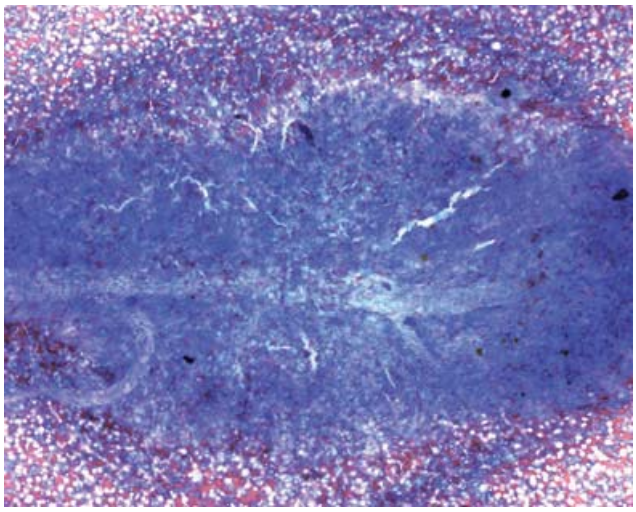

Figure 6.20. Dog: bone marrow aspirate, chronic myeloid leukemia. Crush preparation between 2 slides with large core of marrow flattened around the prominent central vessel. There is a complete absence of fat cells.

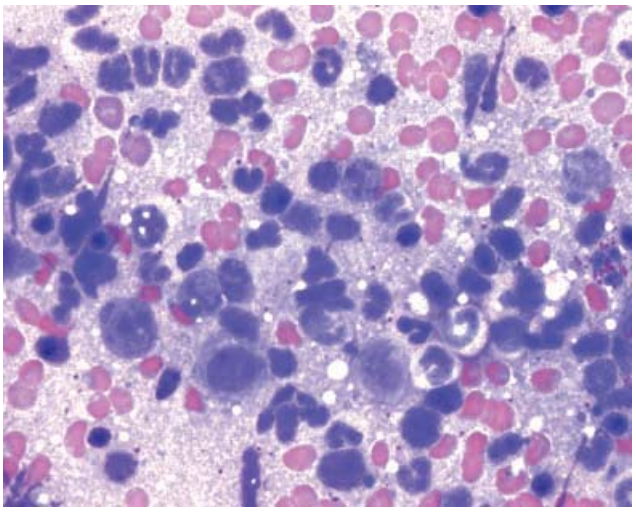

Figure 6.21. Dog: marrow aspirate, chronic myeloid leukemia. There are numerous maturing neutrophils in the upper left and lower right with a number of myelocyte stage cells in the center.

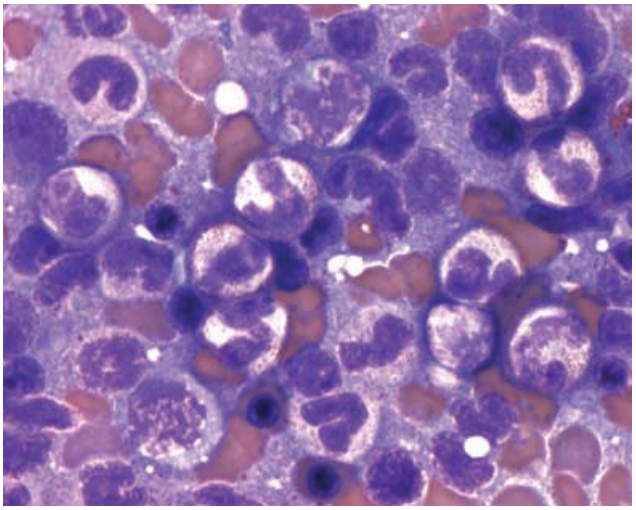

Figure 6.22. Dog: marrow aspirate, chronic myeloid leukemia. There are numerous poorly granulated neutrophils and several giant metamyelocytes in the left center and cells of similar type in the lower.

Bone Marrow

The bone marrow is always hyperplastic, and marrow aspirates are very cellular in early stages of the disease (Fig. 6.20) but may become less so as reticulin sclerosis develops. There are numerous neutrophils (Fig. 6.21), but the promyelocytes and myelocytes are most prominent with usually some giant metamyelocytes (Fig. 6.22). Blasts are increased but not numerous, and the blasts and promyelocytes together may total 10%, as in the human cases. Megakarocytes may be increased but with reduced cytoplasmic volume and hypolobulation. Rubricytes are present but not prominent, and most are in late stage of maturation. There is strong staining with MPO that marks the myeloblasts, promyelocytes, myelocytes, and, weakly, in neutrophils. The monocytic series remains unmarked, but in cytolological preparations can be demonstrated with the alpha naphthyl acetate esterase (ANAE) reaction.

Lymph Node

The lymph nodes are usually of normal size or atrophic, with fading germinal centers in subcapsular areas and narrowed paracortex with most of the node occupied by medullary cords and sinuses. In the early or chronic phase, there are megakaryocytes in the medullary cords that are likely of benign precursors, and other lineages of hematopoiesis surround them. Later, the neoplastic clones occupy the cords and benign cells are largely excluded or present in sinus areas in scattered small foci.

Spleen

The spleen has lymphoid atrophy and marked sinus hyperplasia. There are focal areas of granulocytic colonization of the muscular trabeculae and walls of large muscular veins but less tendency to colonize the subendothelial areas than in the lymphoid leukemias. Megakarocytes are most prominent near the muscular trabeculae and subcapsular areas. Maturing neutrophils are less prominent than in the marrow, and the pattern of maturation may not be as apparent. There is scattered erythropoiesis and a general background of coarse hemosiderin accumulation.

Other Organs

The liver has both portal and sinus colonization and there may be a mixture of benign and neoplastic hematopoiesis that is not possible to distinguish accurately. There are often some areas of central lobular ischemic degeneration and colonization of the larger veins and lymphatic channels.

With progression, there is increasing anemia and thrombocytopenia with the occurrence of poor healing of skin abrasions and persistence of oral ulcers. Ultimately, there is termination due to sepsis or elective decision as the animals become weak and recumbent.

REFERENCES

Dunn, J.K., Jeffries, A.R., Evans, R.J., et al. (1987) Chronic granulocytic leukaemia in a dog with associated bacterial endocarditis, thrombocytopenia and preretinal and retinal hemorrhages. *J Sm An Pract* 28(1):1079–1086.

Gorman, N.T., and Evans, R.J. (1987) Myeloproliferative disease in the dog and cat: Clinical presentations, diagnosis and treatment. *Vet Rec* 121:490–496.

Grindem, C.B., Stevens, J.B., Brost, D.R., et al. (1992) Chronic myelogenous leukaemia with meningeal infiltration in a dog. *Comp Haematol Int* 2(3):170–174.

Harvey, J.W., Shields, R.P., and Gaskin, J.M. (1978) Feline myeloproliferative disease. Changing manifestations in the peripheral blood. *Vet Pathol* 15:437–448.

Joiner, G.N., Fraser, C.J., Jardine, J.H., and Trujillo, J.M. (1976) A case of chronic granulocytic leukemia in a dog. *Can J Comp Med* 40(2):153–160.

Leifer, C.E., Matus, R.E., Patnaik, A.K., et al. (1983) Chronic myelogenous leukemia in the dog. *J Am Vet Med Assoc* 183:686–689.

Lucke, V.M., and Sumner-Smith, G. (1963) A case of myeloid leukaemia in the dog. *J Sm An Pract Suppl* 4:23–28.

Ndikuwera, J., Smith, D.A., Obwolo, M.J., et al. (1992) Chronic granulocytic leukaemia/eosinophilic leukaemia in a dog. *J Sm An Pract* 33(11):553–557.

Pollet, L., Van Hove, W., and Matheeuws, D. (1978) Blastic crisis in chronic myelogenous leukaemia in a dog. *J Sm An Pract* 19:469–475.

Rouse, B.T., Osborne, A.D., Grunsell, C.S., and Hooper, R.B. (1967) Acute granulocytic leukaemia in a bitch. *Vet Rec* 80(13):1–3.

Schalm, O.W., and Theilen, G.H. (1970) Myeloproliferative disease in the cat, associated with C-type leukovirus particles in bone marrow. *JAVMA* 157(11):1686–1696.

Searcy, G.P., and Orr, J.P. (1981) Chronic granulocytic leukemia in a horse. *Can Vet J* 22:148–151.

Tarrant, J.M., Stokol, T., Blue, J.T., McDonough, S.P., and Farrell, P. (2001) Diagnosis of chronic myelogenous leukemia in a dog using morphologic, cytochemical, and flow cytometric techniques. *Vet Clin Pathol* 30(1):19–24.

Thomsen, M.K., Jensen, A.L., Skak-Nielsen, T., et al. (1991) Enhanced granulocyte function in a case of chronic granulocytic leukemia in a dog. *Vet Immunol Immunopathol* 28(2):143–165.

CHRONIC NEUTROPHILIC LEUKEMIA

Chronic neutrophilic leukemia is an extremely rare disease in humans, with less than a hundred cases reported, and these lack the t(9;22) translocation of human CML. It is not clear whether an animal counterpart exists, but a pure neutrophilic leukemia would be very like what has been called *myeloid metaplasia with myelofibrosis* (*MMM*) or *agnogenic myeloid metaplasia*. MMM is characterized by a prolonged period of mature neutrophilic leukocytosis with splenomegaly and without apparent cause followed by marrow failure due to myelofibrosis. In MMM there are no apparent blasts in the peripheral blood and insufficient criteria for a diagnosis of neoplasia. A putative case of neutrophil-type CML in the cat had a total leukocyte count greater than 500,000/ul and a packed cell volume of 11% (see Figs. 6.10–6.19). The animal had a massive mature neutrophilia and blast cells in the peripheral blood.

In the human cases, a recurring clonal karyotypic lesion has been found in the neutrophilic and eosinophilic lineages but not in the lymphoid, monocytic, or erythroid lines. As more information is gained on the cytogenetic changes in the dog and cat in hematopoietic neoplasms, it may become possible to verify a clonal state in animals without a high blast count that corresponds to a pure neutrophilic leukemia. A type of CML that appears to be of pure neutrophil type occurs in the mouse. Because blood is seldom the means of diagnosis, most cases are identified on subsequent histological examination. The usual

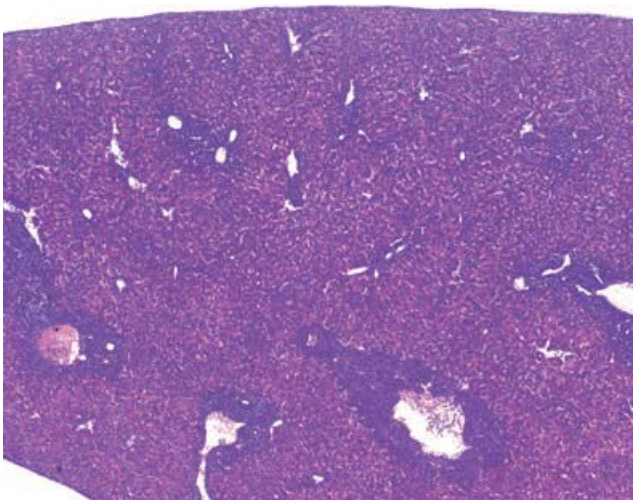

Figure 6.23. Mouse: liver, chronic myeloid leukemia of neutrophil type. There is extensive perivascular cuffing and infiltration involving both portal and venous areas. *Slide from J. M. Ward, DVM.*

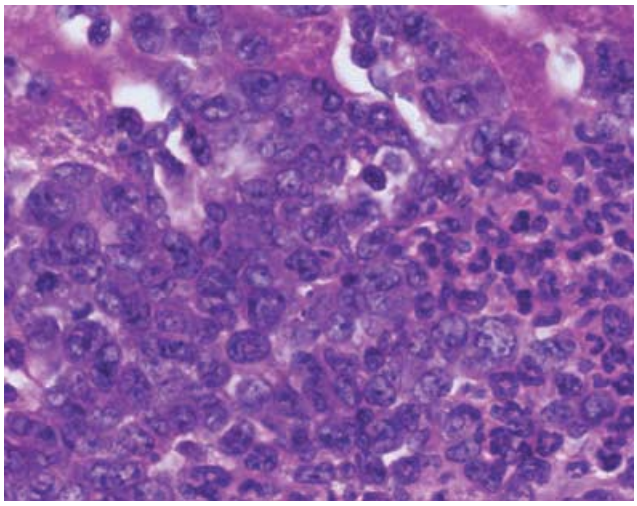

Figure 6.24. Mouse: liver, chronic myeloid leukemia. Detail of Figure 6.23. There are a few residual hepatocytes at left with maturing neutrophils at the top and more primitive proliferative stages below. The proliferation is clearly of neutrophil type.

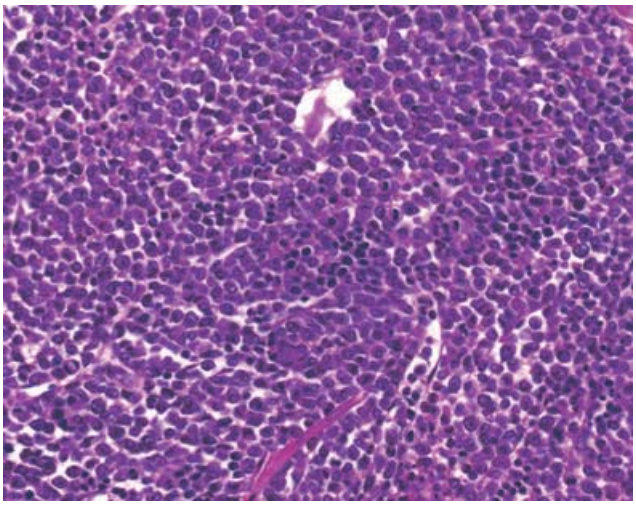

Figure 6.26. Mouse: spleen, chronic myeloid leukemia, same tissue as Figure 6.25. The sinus areas are solidly filled with proliferating myeloid cells, with the more darkly stained cells indicative of residual benign erythroid proliferation. There is a very thinned smooth muscle trabeculae at the lower center.

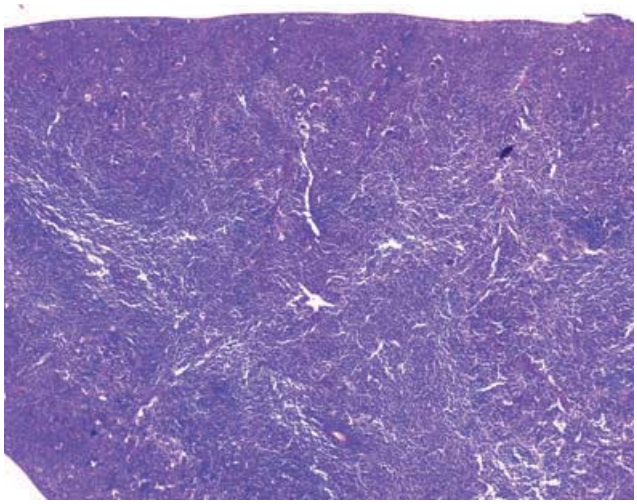

Figure 6.25. Mouse: spleen, chronic myeloid leukemia, same case as Figure 6.23. The organ is markedly enlarged with a greatly thinned capsule and thinned and widely separated smooth muscle trabeculae. There is almost complete loss of periarteriolar lymphoid sheaths with massive sinus colonization by neoplastic cells. *Slide from J. M. Ward, DVM.*

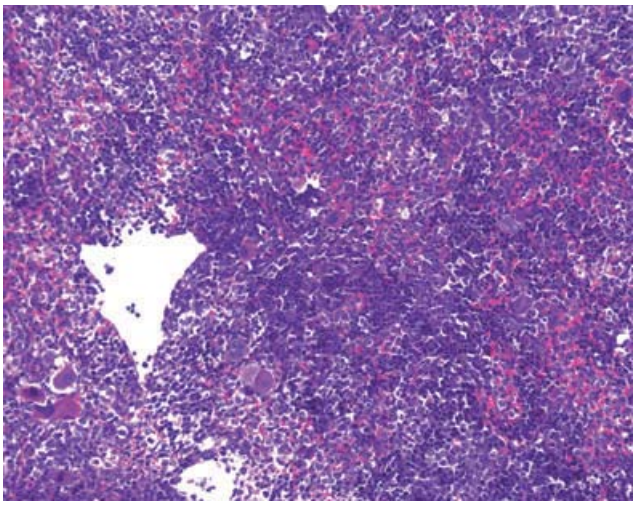

Figure 6.27. Mouse: bone marrow, chronic myeloid leukemia. The marrow is completely solid with loss of all fat cells. Irregular dark areas represent residual erythropoiesis with intervening areas consisting of massive myeloid proliferation. Residual megakaryocytes are evident in the center, and lower left. *Slide from J. M. Ward, DVM.*

organs of liver (Figs. 6.23, 6.24), spleen (Figs. 6.25, 6.26), and marrow (Figs. 6.27, 6.28) are heavily involved. Other tissues may be heavily involved as well, including the small intestine (Figs. 6.29, 6.30).

In cases that might be of this type, there is a different morphology to the peripheral blood neutrophils with hyposegmentation and irregular nuclear membranes but only 2–3 segments. There is low cytoplasmic granulation and only moderate peripheral blood immaturity. Peripheral blood basophils are present, which has added to the interpretation of this disease as a type of myeloproliferative disease.

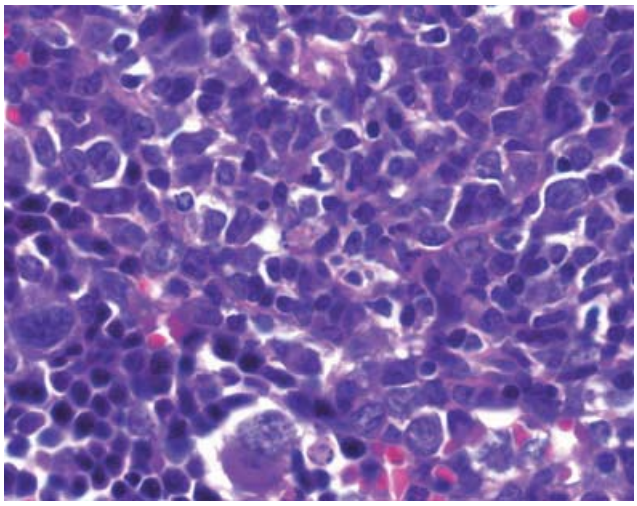

Figure 6.28. Mouse: marrow, chronic myeloid leukemia. Same tissue as Figure 6.26. A residual area of erythropoiesis and thrombopoiesis is in the lower left. There is solid myeloid proliferation in surrounding areas with greater immaturity than is present in peripheral tissues.

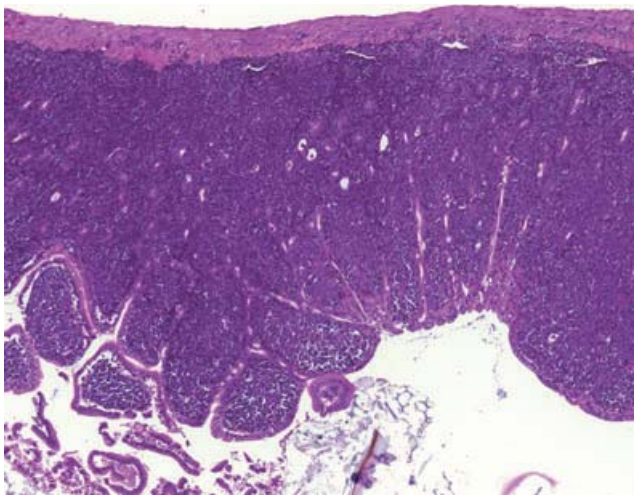

Figure 6.29. Mouse: small intestine, chronic myeloid leukemia, same case as Figure 6.28. There is massive involvement of the intestinal lamina propria with filling and loss of villi but with epithelium largely retained and with only minor involvement of the tunica muscularis. *Slide from J. M. Ward, DVM.*

REFERENCES

Cervantes, F., Marti, J.M., Rozman, C., et al. (1988) Chronic neutrophilic leukemia with marked myelodysplasia terminating in blast crisis. *Blut* 56:75–78.

DiDonato, C., Croci, G., Lazzari, S., et al. (1986) Chronic neutrophilic leukemia: Description of a new case with karyotypic abnormalities. *Am J Clin Pathol* 85:369–371.

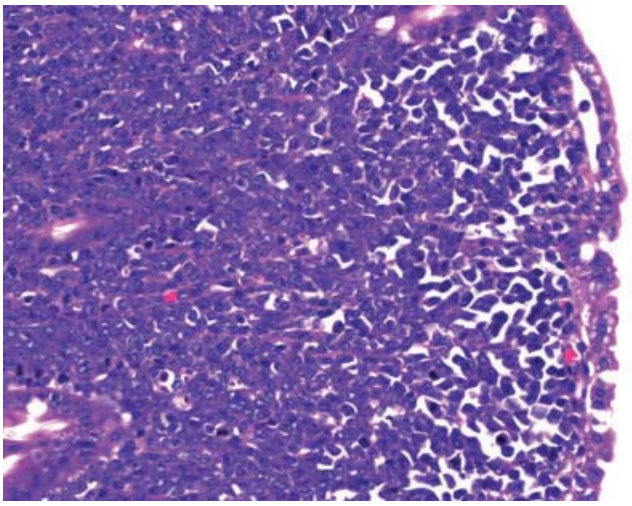

Figure 6.30. Mouse: small intestine, chronic myeloid leukemia. Detail of Figure 6.29. The mucosal surface is at the right with the epithelium thin to cuboidal and lying above a dense infiltration of neoplastic myeloid proliferation that is destroying and displacing residual glands at the bottom.

Foa, P., Iurlo, A., Saglio, G., et al. (1991) Chronic neutrophilic leukemia associated with polycythemia vera: Pathogenetic implications and therapeutic approach. *Brit J Haematol* 72:285–288.

Froberg, M.K., Brunning, R.D., Dorion, P., et al. (1998) Demonstration of clonality in neutrophils using FISH in a case of chronic neutrophilic leukemia. *Leuk* 12:623–626.

Kwong, Y.L., and Cheng, G. (1993) Clonal nature of chronic neutrophilic leukemia. *Blood* 82:1035–1036.

Masini, L., Salvarani, C., Macchioni, P., et al. (1992) Chronic neutrophilic leukemia (CNL) with karyotypic abnormalities associated with plasma cell dyscrasia: A case report. *Haematologica* 77:277–279.

Wolman, S.R., McMorrow, L.E., and Cohen, M.W. (1982) Animal model of human disease. Myelogenous leukemia in the RF mouse. *AJP* 107(2):280–284.

Zittoun, R., Rea, D., Ngoc, L.H., et al. (1994) Chronic neutrophilic leukemia: A study of four cases. *Ann Hematol* 68:55–60.

Zoumbos, N.C., Symeonidis, A., and Kourakli-Symeonidis, A. (1989) Chronic neutrophilic leukemia with dysplastic features: A new variant of the myelodysplastic syndromes? *Acta Haematol* 82:156–160.

CHRONIC EOSINOPHILIC LEUKEMIA AND HYPEREOSINOPHILIC SYNDROME

Chronic eosinophilic leukemia (CEL) is primarily a disease of cats, as is the hypereosinophilic syndrome (HES). Dogs get HES and eosinophilic granuloma, but rarely get CEL if at all. In the cat, both diseases have been found in association with FeLV infection, but they have

been found as often in animals free of that virus. A useful meta analysis of feline HES and CEL concluded that both occurred in middle-aged cats with a female predominance in HES but not in CEL. Marrow eosinophilic hyperplasia occurs in both conditions, but all cells appear normal in HES; in the leukemic condition of CEL, some cases had atypical primitive cells. The shift to myelopoiesis is greater in cats with CEL that have myeloid:erythroid (M:E) ratios greater than 10:1; cats with HES tend to have an M:E of less than 10. These changes in M:E translate into similar changes in the peripheral blood where the immature eosinophils constitute a higher proportion of total leukocytes in the leukemic cats, as compared to cats with HES. In addition, in accord with the M:E shift, the PCV in cats with CEL is 10% lower with an average of 25%, as compared to a mean of 34% in cats with HES. Equally important, both diseases are characterized by eosinophil infiltration of the marrow, spleen, lymph nodes, and liver, but the kidney, heart, and mediastinum are more likely to be involved in CEL. Further, the immaturity of the infiltrating cells is greater in CEL and of relatively mature cells in HES. HES is a chronic disease of smoldering inflammation with resultant fibrosis; CEL is like other myeloid leukemias and has a poor prognosis.

Cats with both diseases present with a history of anorexia, often with fever and weight loss associated with recurrent vomition. The clinical examination rules out parasitism, and no apparent inciting agent is evident for either HES or CEL, but both can occur as a result of experimental infection with FeLV. Cats with CEL have total leukocyte counts of 75,000–150,000/ul (Figs. 6.31–6.34), and cats with HES tend to have total leukocyte counts between 50,000 and 75,000/ul (Figs. 6.35, 6.36). Eosinophils are likely to exceed neutrophils in the

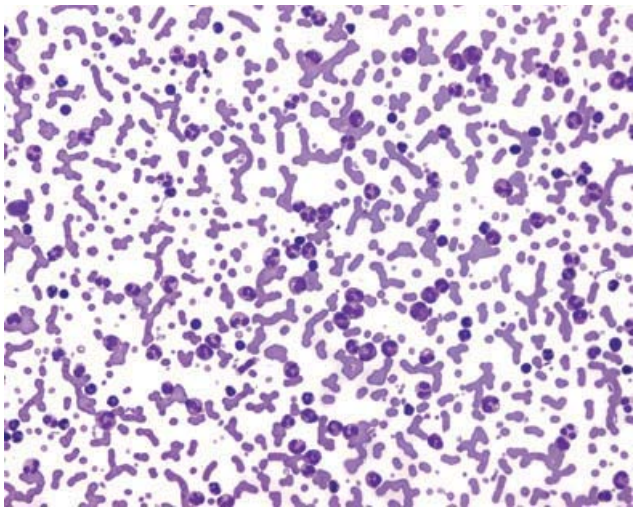

Figure 6.31. Cat: blood, chronic myeloid leukemia, eosinophil type. The cat presented with a total leukocyte count of 120,000/microliter and a packed cell volume of 23% with a platelet count of 86,000/microliter. The counts remained in that region over a period of months. On low power examination, it is apparent that most of the cells in the peripheral blood are of segmented type cells of greater size and more density of cytoplasm than would be found with neutrophils and accompanied by reduced numbers of red cells with extensive rouleau formation.

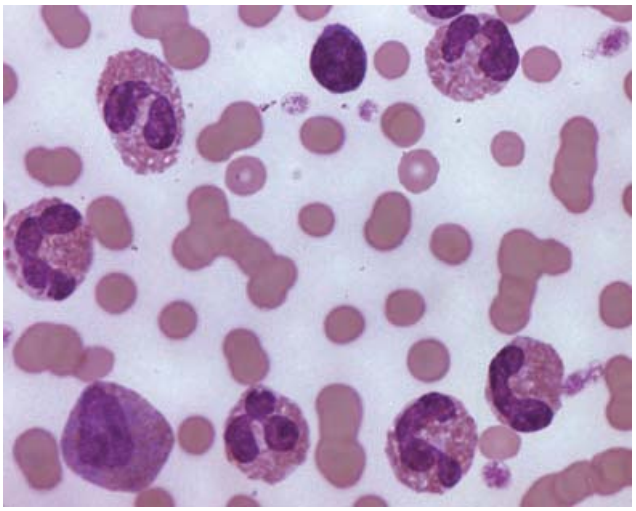

Figure 6.32. Cat: blood, chronic myelogenous leukemia of eosinophil type. Detail of Figure 6.31. There is an eosinophil myelocyte in the lower left that retains a fairly high level of cytoplasmic basophilia but has specific eosinophil type granulation. There is a small lymphocyte in the top center. Note the tendency for bilobation in the eosinophils. Platelets are present, unlike acute myeloid leukemia.

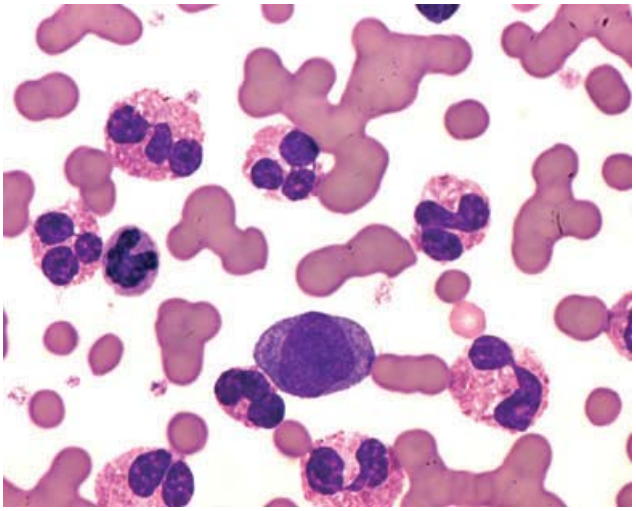

Figure 6.33. Cat: blood, chronic myeloid leukemia, eosinophil type. The cell in the lower center is a promyelocyte that has early nuclear condensation and retains a nucleolus. There is very faint and fine granulation without apparent specific granulation.

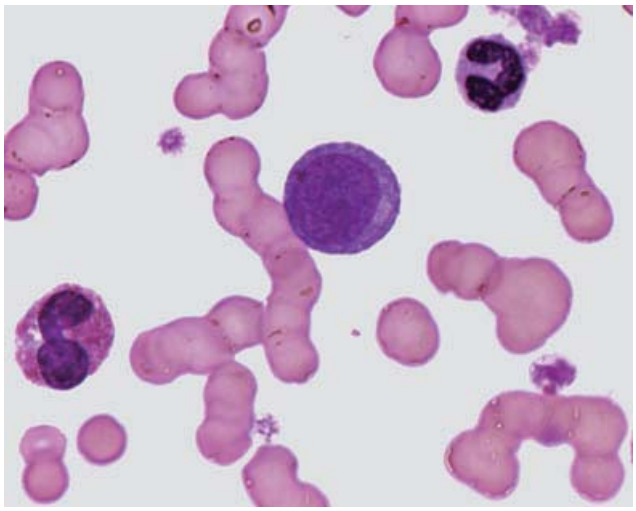

Figure 6.34. Cat: blood, chronic myeloid leukemia, eosinophil type. There is a putative blast cell above center with a fine chromatin pattern and several small nucleoli. There are a few, very faint fine granules near the Golgi zone. Note the disparity in size between the neutrophil and eosinophil.

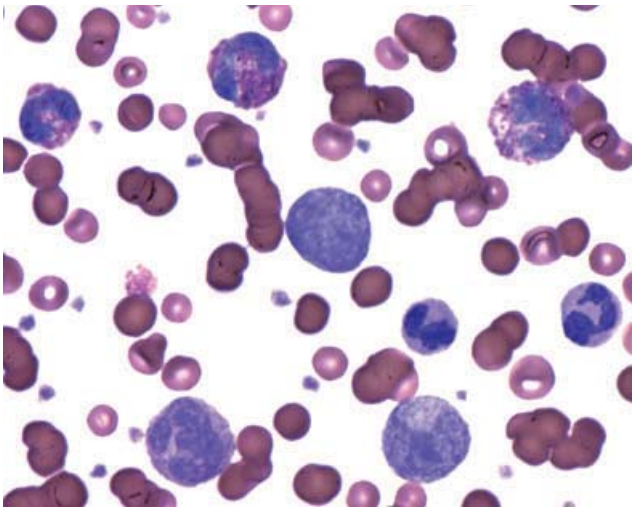

Figure 6.36. Cat: blood, hypereosinophilic syndrome. Detail of Figure 6.35. The cell in the center and in the lower right are likely eosinophil progenitors. The cell with lobulated and smooth surface nuclear contours in the lower left is likely a basophil precursor and its presence is suggestive that the disease may in fact be CML of eosinophil type.

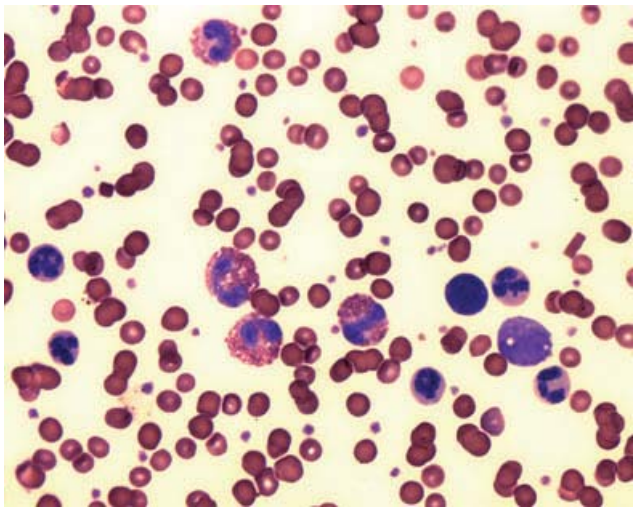

Figure 6.35. Cat: blood, hypereosinophilic syndrome. The cat was presented for examination because of weight loss over the past year. Total leukocyte count was 68,000 per microliter and the packed red cell volume was 20%. Note that neutrophils outnumber the eosinophils, and the anemia is less severe than in chronic myeloid leukemia and platelets are numerous. *Slide from R. M. Jacobs, DVM.*

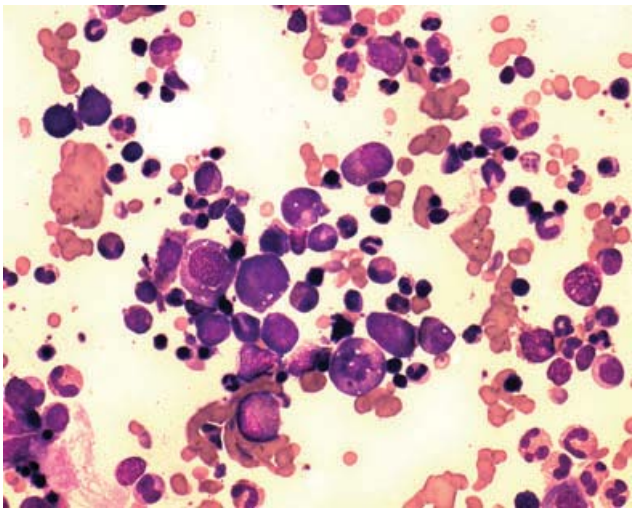

Figure 6.37. Cat: bone marrow, chronic myeloid leukemia of eosinophil type, same case as Figures 6.31–6.34. There is a cluster of immature precursors in the center, primarily myeloid surrounded by eosinophils and neutrophils with quite numerous maturing rubricytes.

blood in HES but the opposite holds in CEL where very high neutrophil counts are found in the range of 5,000–50,000/ul often with a very high band neutrophil count. Lymphocytosis occurs in both conditions but thrombocytopenia is likely only in cats with CEL.

All organs have the same character of diffuse infiltration that is periportal in the liver, sinusoidal in the spleen, and starts in the medullary region in nodes and extends to destroy the architecture and even spreads to pericapsular fat. The marrow is solidly involved in both diseases with greater immaturity in CEL (Figs. 6.37–6.41), and the kidney in CEL has solid focal infiltrates.

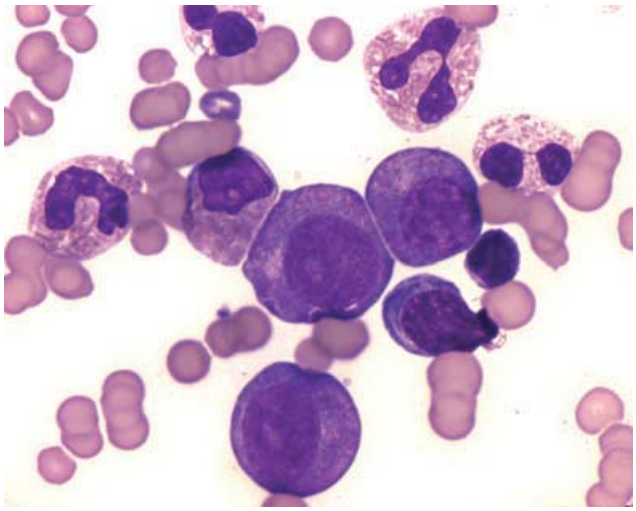

Figure 6.38. Cat: marrow, chronic myeloid leukemia of eosinophil type. The 3 large cells are eosinophil promyelocytes with an eosinophil myelocyte in the left center and a small lymphocyte in the upper right. The injured cell is likely a basophilic rubricyte.

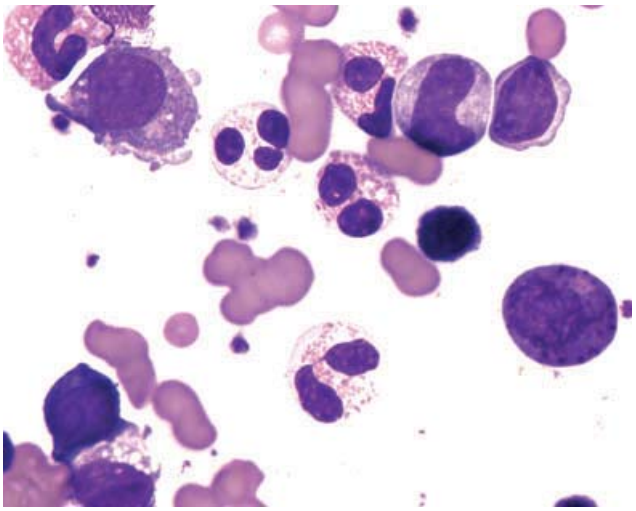

Figure 6.40. Cat: marrow, chronic myeloid leukemia of eosinophil type. The cell with fine granulation in the upper left is likely a promyelocyte and a very basophilic cell in the lower left an erythroid precursor. The cell in the right center is a basophil myelocyte. The presence of these basophils and their progeny in the peripheral blood increases the likelihood that the disease process is neoplastic.

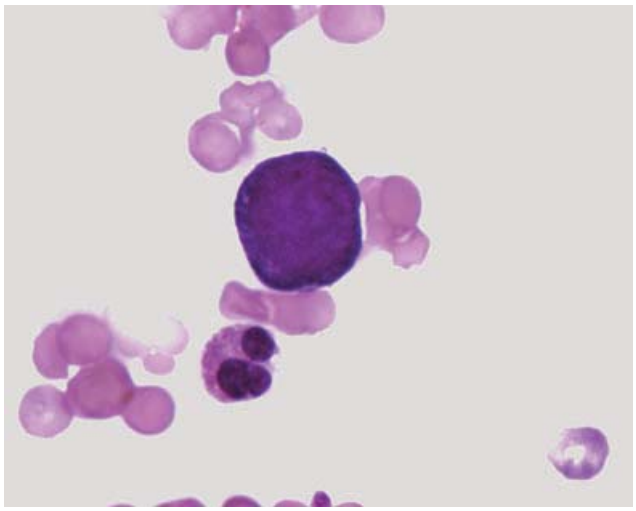

Figure 6.39. Cat: bone marrow, chronic myeloid leukemia of eosinophil type. A myeloblast with a large poorly defined nucleolus and very high cytoplasmic basophilia. The asymmetrical segmentation of the eosinophil is typical.

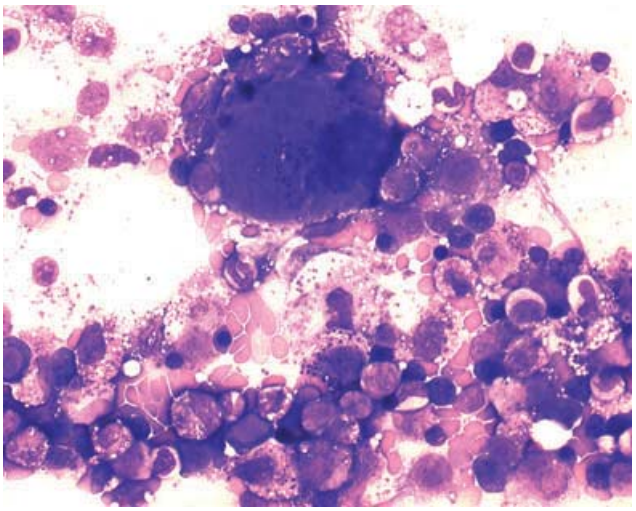

Figure 6.41. Cat: marrow, hypereosinophilic syndrome, same case as Figures 6.35 and 6.36. There is less immaturity than in the animal with chronic myeloid leukemia (Figures 6.37–6.40) with most of the cells in the myelocyte stage. The distinction between chronic myeloid leukemia of eosinophil type and hypereosinophilic syndrome is equivocal, and the presence of the basophils with distinct deeply basophilic granules at the center top and below would increase the likelihood that this case is also a true neoplasm. *Slide from R. M. Jacobs, DVM.*

Hypereosinophilic syndrome was found in three Rottweiler dogs aged 1–3 years. They were presented with a short history of inappetence and were found to have total leukocyte counts in the 25,000–50,000/ul range with eosinophils predominating in one dog. None of the dogs were lymphopenic. The accompanying lesions included marrow myeloid hyperplasia with a high proportion of eosinophils and precursors and focal ulceration throughout the GI tract. Two dogs had splenomegaly and the

third had organs of normal size but heavy infiltration of both liver and spleen with mature eosinophils. All three animals had extensive involvement of abdominal lymph nodes, and all three had significant pulmonary infiltrates although pulmonary infiltrates with eosinophilia (PIE) was not considered as a primary diagnosis in any if these animals.

CEL in cats needs to be differentiated from the benign counterpart of HES on the basis of degree of immaturity in blood and marrow, with peripheral blood blasts present in CEL but not in HES. Cats frequently have eosinophilic granuloma complex, focal peripheral diseases of the skin and oral cavity with few systemic changes. HES in dogs needs to be differentiated from chronic eosinophilic leukemia if it occurs and from T-cell lymphoma with marked eosinophilic reaction. In the latter condition, the eosinophils greatly outnumber the lymphocytes, which are of intermediate size and relatively inconspicuous without specific immunological staining. Dogs may present with Loefflers syndrome, which is generally a self-limiting disease, whereas the PIE syndrome is much more prolonged and may involve pericardial infiltration and mimic the hypereosinophilic syndrome. Granulocytic sarcoma is seldom a consideration because the disease is almost always focal and is more a differential for AML or recurrent AML.

REFERENCES

Anastasi, J., and Vardiman, J.W. (2001) Chronic myelogenous leukemia and the chronic myeloproliferative diseases. In Knowles, D.M. (ed.), *Neoplastic Hematopathology,* 2nd ed. Lippincott Williams & Wilkins, Philadelphia, pp. 1745–1790.

Bain, B.J. (1996) Eosinophilic leukaemias and the idiopathic hypereosinophilic syndrome. *Brit J Haematol* 95:2–9.

Blomme, E.A.G., Foy, S.H., Chappell, K.H., and La Perle, K.M.D. (1999) Hypereosinophilic syndrome with Hodgkin's-like lymphoma in a ferret. *J Comp Pathol* 120:211–217.

Bredal, W.P., Gunnes, G., Vollset, I., and Ulstein, T.L. (1996) Oral eosinophilic granuloma in three Cavalier King Charles spaniels. *J Sm An Pract* 37:499–504.

Cassi, E., De Paoli, A., Fava, S., Luoni, M., Tosi, A., Turri, C., and Grimi, E. (1992) Idiopathic hypereosinophilic syndrome and eosinophilic leukemia. *Haematologica* 77:430–432.

Center, S.A., Randolph, J.F., Erb, H.N., and Reiter, S. (1990) Eosinophilia in the cat: A retrospective study of 312 cases (1975 to 1986). *J Am An Hosp Assoc* 26:349–358.

Chang, H.W., Leong, K.H., Koh, D.R., et al. (1999) Clonality of isolated eosinophils in the hypereosinophilic syndrome. *Blood* 93:1651–1657.

Chusid, M.J., Dale, D.C., West, B.C., et al. (1975) The hypereosinophilic syndrome: Analysis of fourteen cases with review of the literature. *Medicine* 54:1–27.

Davis, T. (1971) Eosinophilic leukemia in a cat. *JAVMA* 158(2):199.

Finlay, D. (1985) Eosinophilic leukaemia in the cat: A case report. *Vet Rec* 116:567.

Hardy, W.R., and Anderson, R.E. (1968) The hypereosinophilic syndrome. *Ann Intern Med* 68:1220–1228.

Hendrick, M. (1981) A spectrum of hypereosinophilic syndromes exemplified by six cats with eosinophilic enteritis. *Vet Pathol* 18:188–200.

Huibregtse, B.A., and Turner, J.L. (1994) Hypereosinophilic syndrome and eosinophilic leukemia: A comparison of 22 hypereosinophilic cats. *J Am An Hosp Assoc* 30:591–599.

Kueck, B.D., Smith, R.E., Parkin, J., et al. (1991) Eosinophilic leukemia: A myeloproliferative disorder distinct from the hypereosinophilic syndrome. *Hematol Pathol* 5:195–205.

Lewis, M.G., Kociba, G.J., Rojko, J.L., Stiff, M.I., Haberman, A.B., Velicer, L.F., and Olsen, R.G. (1985) Retroviral-associated eosinophilic leukemia in the cat. *Am J Vet Res* 46(5):1066–1070.

McEwen, S.A., Valli, V.E.O., and Hulland, T.J. (1985) Hypereosinophilic Syndrome in cats: A report of three cases. *Can J Comp Med* 49:248–253.

Sanderson, C.J. (1992) Interleukin-5, eosinophils, and disease. *Blood* 79:3101–3109.

Saxon, B., Hendrick, M., and Waddle, J.R. (1991) Restrictive cardiomyopathy in a cat with hypereosinophilic syndrome. *Can Vet J* 32:367–369.

Sellon, R.K., Rottman, J.B., Jordan, H.L., Wells, M.R., Simpson, R.M., Nelson, P., and Keene, B.W. (1992) Hypereosinophilia associated with transitional cell carcinoma in a cat. *JAVMA* 210(4):591–593.

Spry, C.J.F., Davies, J., Tai, P.C., et al. (1983) Clinical features of fifteen patients with the hypereosinophilic syndrome. *QJM* 205:1–22.

Swenson, C.L., Carothers, M.A., Wellman, M.L., and Kociba, G.J. (1993) Eosinophilic leukemia in a cat with naturally acquired feline leukemia virus infection. *J Am An Hosp Assoc* 29:497–501.

Sykes, J.E., Weiss, D.J., Buoen, L.C., Blauvelt, M.M., and Hayden, D.W. (2001) Idiopathic hypereosinophilic syndrome in 3 rottweilers. *J Vet Intern Med* 15:162–166.

Weller, P.F., and Bubley, G.J. (1994) The idiopathic hypereosinophilic syndrome. *Blood* 83:2759–2779.

Wilson, S.C., Thomson-Kerr, K., and Houston, D.M. (1996) Hypereosinophilic syndrome in a cat. *Can Vet J* 37:679–680.

POLYCYTHEMIA VERA

Polycythemia vera (PV) is a neoplastic disorder of erythropoietic stem cells that produce increased levels of normally functional red cells without response to normal controls of proliferation. In humans, the early proliferative phase of PV is characterized by multilineage overproliferation with erythrocytosis accompanied by leukocytosis, thrombocytosis, and blood volume expansion, in addition to the increase in red cell mass. In animals there is only mild leukocytosis, no thrombocytosis, and no increase in blood volume.

In humans, PV is relatively uncommon, with an annual incidence of 1 case per 100,000 population. There is equal frequency in sexes and a mean age at diagnosis of 60 years. In dogs, the ages range from 1–9 years, and there may be increased frequency in males. Cats with PV ranged in age from 10–15 years and likely with male predominance, and calves with PV have all been under a year of age with no apparent difference in frequency with sex.

The presentation in humans is related to headache and dizziness with visual impairment and tingling paresthesias. One-quarter of human patients are first identified as having PV because of thrombotic complications, including deep vein thrombophlebitis or myocardial ischemia or cerebrovascular accident. Dogs are presented for examination because of polydipsia and polyuria, vomiting, anorexia, lethargy, and lameness due to aortic or leg vein thrombosis. On physical examination, the reddened mucus membranes are a prominent feature that leads to discovery of a PCV in the range of 65–80% and hemoglobin in the 23–26g/dl range. Calves and cats are similar.

Blood

There is moderate neutrophilia with minimal left shift and normal lymphocyte and platelet counts (Figs. 6.42, 6.43). The reticulocyte counts are at 0–1%, and a few late stage rubricytes may be present, usually with a few basophils (Fig. 6.44). The red cell morphology is normochromic normocytic; on examination of bone marrow, the M:E is more often above 1.0 and in the range of 1.1–1.8:1, and in those with erythroid predominance the shift is in the range of 0.7–0.8:1. Cytologically, all cases have hyperplastic marrow with an apparent increase in rubricytes and megakaryocytes. The maturation of all marrow lineages is normal. If hemorrhage has occurred, there may be depletion of marrow iron stores that will be reflected in reduced red cell saturation. There is a mild increase in the blood urea nitrogen that, due to consistency, is more likely due to impaired renal perfusion as a result of blood hyperviscosity rather than intestinal bleeding.

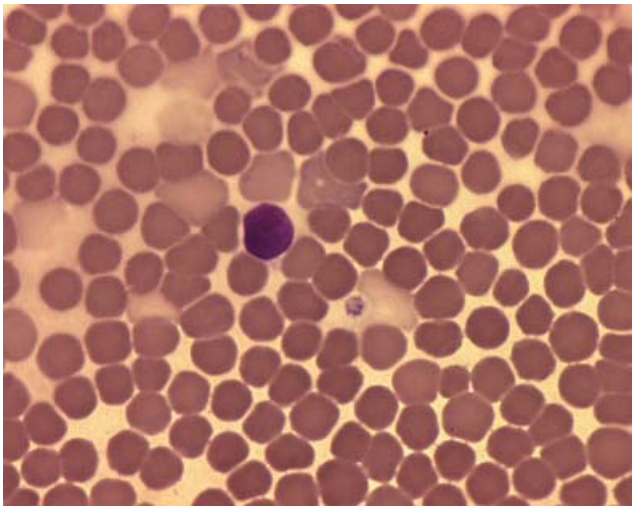

Figure 6.43. Dog: blood, polycythemia vera. An image taken near the edge of the blood film with the red cells very largely normochromic normocytic. There are several larger and less saturated cells near the lymphocyte that may be younger cells with the level of anisocytosis quite low.

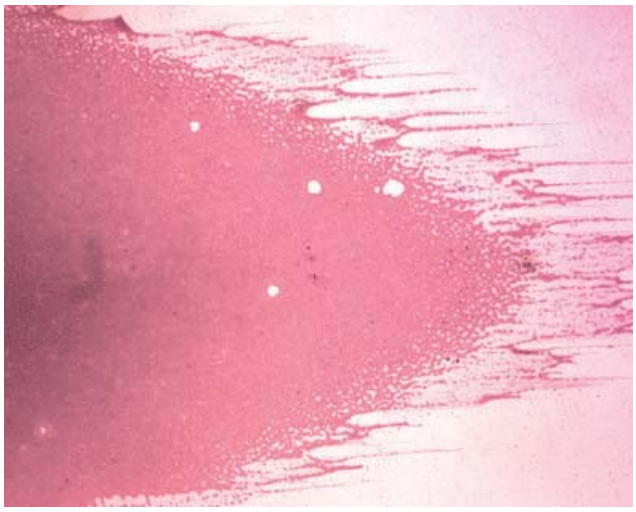

Figure 6.42. Dog: blood, polycythemia vera. A mature dog presented in collapse with a packed red cell volume of 80%. Blood smear is extremely dense due to the low proportion of plasma.

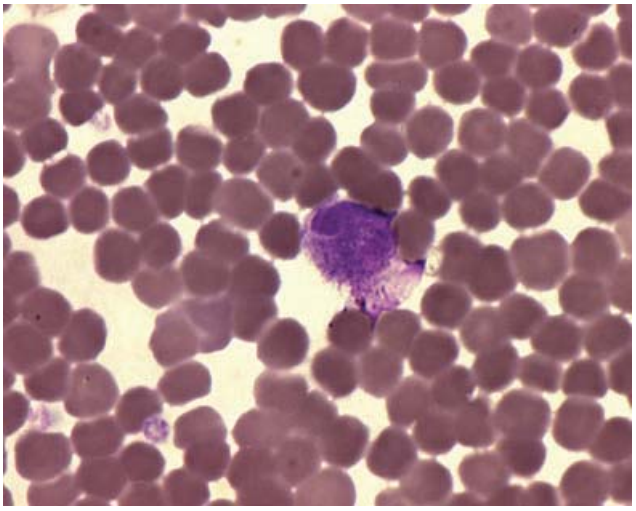

Figure 6.44. Dog: blood, polycythemia vera, same case as Figure 6.42. The nucleated cell is an injured basophil whose presence in the peripheral blood increases the likelihood that this is a primary neoplastic lesion not secondary to low oxygen tension.

Most cases require vigorous phlebotomy, which relieves the symptoms at least temporarily. In the early proliferative phase, there is constant hepatosplenomegaly that is due to sinus dilation and plethora and not to extramedullary hematopoiesis.

Cases of human PV that survive the proliferative phase enter a "spent" phase, in which marrow proliferation wanes to the point that there may be homeostasis for a time characterized by splenomegaly, now with EMH, in the face of progressive myelofibrosis. At this point there is significant thrombocytopenia and the survival is about 5 years from the onset of the spent phase.

Unlike the other types of CML there are no characteristic cytogenetic abnormalities in PV, but there are demonstrable functional changes in the erythroid stem cells that will grow in culture in the absence of erythropoietin (EPO). The latter feature has been demonstrated to be present in the marrow erythroid precursors in a case of PV in a cat. There are no known risk factors for PV in humans other than familial tendencies; viral etiology has been proposed but not demonstrated. Subspecies of the Friend leukemia virus can be demonstrated to cause either erythroleukemia or PV, depending on which host genes are impacted.

The differential diagnosis must include secondary erythrocytosis that is EPO-dependent and due to impaired oxygenation that can be red cell–dependent and exacerbated by tobacco smoking in humans. In dogs, secondary erythrocytosis may be due to the presence of a primary or metastatic neoplasm in the kidney that causes regional ischemia and overproduction of EPO. In EPO-dependent secondary erythrocytosis there is always an increased reticulocyte count that is absent in PV and, if EPO levels are measured, the hormone drops to low or undetectable levels in the autonomous cases of primary PV. A further clinically apparent difference is that splenomegaly is constant in PV and absent in secondary erythrocytosis.

REFERENCES

Anastasi, J., and Vardiman, J.W. (2001) Chronic myelogenous leukemia and the chronic myeloproliferative diseases. In Knowles, D.M. (ed.), 2nd ed. Lippincott Williams & Wilkins, Philadelphia, pp. 1745–1790.

Crow, S.E., Allen, D.P., Murphy, C.J., and Culbertson, R. (1995) Concurrent renal adenocarcinoma and polycythemia in a dog. *J Am An Hosp Assoc* 31:29–33.

Eid, J., Ebert, R.F., Gesell, M.S., and Spivak, J.L. (1987) Intracellular growth factors in polycythemia vera and other myeloproliferative disorders. *Proc Natl Acad Sci USA* 84:532–536.

Ellis, J.T., Peterson, P., Geller, S.A., and Rappaport, H. (1986) Studies of the bone marrow in polycythemia vera and the evolution of myelofibrosis and second hematologic malignancies. *Sem Hematol* 23(2):144–155.

Evans, L.M., and Caylor, K.B. (1995) Polycythemia vera in a cat and management with hydroxyurea. *J Am An Hosp Assoc* 31:434–438.

Fowler, M.E., Cornelius, C.E., and Baker, N.F. (1964) Clinical and erythrokinetic studies on a case of bovine polycythemia vera. *Cornell Vet* 54:153–160.

Gentz, E.J., Pearson, E.G., Lassen, E.D., Snyder, S.P., and Sharpnack, E. (1994) Polycythemia in a llama. *JAVMA* 204(9):1490–1492.

Kaneko, J.J., Zinkl, J., Tennant, B.C., and Mattheeuws, D.R.G. (1968) Iron metabolism in familial polycythemia of jersey calves. *Am J Vet Res* 29(5):949–952.

Khanna, C., and Bienzle, D. (1994) Polycythemia vera in a cat: Bone marrow culture in erythropoietin-deficient medium. *J Am An Hosp Assoc* 30:45–49.

Lundberg, L.G., Lerner, R., Sundelin, P., Rogers, R., Folkman, J., and Palmblad, J. (2000) Bone marrow in polycythemia vera, chronic myelocytic leukemia, and myelofibrosis has an increased vascularity. *Am J Pathol* 157(1):15–19.

McGrath, C.J. (1974) Polycythemia vera in dogs. *JAVMA* 164(11):1117–1122.

Miller, R.L., Purvis, J.D., and Weick, J.K. (1989) Familial polycythemia vera. *Cleve Clin J Med* 56:813–818.

Najean, Y., and Rain, J.D., for the French Polycythemia Study Group. (1997) Treatment of polycythemia vera: The use of hydroxyurea and pipobroman in 292 patients under the age of 65 years. *Blood* 90:3370–3377.

Najean, Y., Mugnier, P., Dresch, C., et al. (1987) Polycythaemia vera in young people: An analysis of 58 cases diagnosed before 40 years. *Brit J Haematol* 67:285–291.

Pahl, H.L. (2000) Towards a molecular understanding of polycythemia rubra vera. *Eur J Biochem* 267:3395–3401.

Price, C.M., Kanfer, E.J., Colman, S.M., et al. (1992) Simultaneous genotypic and immunophenotypic analysis of interphase cells using dual-color fluorescence: A demonstration of lineage involvement in polycythemia vera. *Blood* 80:1033–1038.

Reed, C., Ling, G.V., Gould, D., and Kaneko, J.J. (1970) Polycythemia vera in a cat. *JAVMA* 157(1):85–91.

Remacha, A.F., Montserrat, I., Santamaria, A., et al. (1997) Serum erythropoietin in the diagnosis of polycythemia vera: A follow-up study. *Haematologica* 82:406–410.

Shibuya, T., and Mak, T.W. (1982) A host gene controlling early anaemia or polycythemia induced by Friend erythroleukaemia virus. *Nature* 296(5857):577–579.

Watson, A.D.J., and Yeats, J.A. (1984) Primary polycythaemia in a dog. *Austral Vet J* 61(2):61–63.

Weinberg, R.S., Worsley, A., Gilbert, H.S., Cuttner, J., Berk, P.D., and Alter, B.P. (1989) Comparison of erythroid progenitor cell growth in vitro in polycythemia vera and chronic myelogenous leukemia: Only 0polycythemia vera has endogenous colonies. *Leuk Res* 13(4):331–338.

Wolf, B.C., Banks, P.M., Mann, R.B., et al. (1988) Splenic hematopoiesis in polycythemia vera: A morphologic and immunohistologic study. *Am J Clin Pathol* 89:69–75.

Wolff, L., Kaminchik, J., Hankins, W.D., and Ruscetti, S.K. (1985) Sequence comparisons of the anemia- and polycythemia-inducing strains of Friend spleen focus-forming virus. *J Virol* 53(2):570–578.

ESSENTIAL THROMBOCYTHEMIA

Essential thrombocythemia (ET), or formerly megakaryocytic myelosis, is a clonal neoplasm of the megakaryocytic system characterized by a marked and persistent increase in platelets in the peripheral blood and megakaryocytes in the bone marrow. The clinical implications of this proliferation are thrombotic and hemorrhagic foci throughout the blood vascular system. There are no definitive markers that distinguish the benign and ephemeral increases in blood platelets from those of the neoplastic precursors. The diagnosis of ET is therefore a matter of excluding other causes of thrombocytosis of both benign causes and MPDs with related effects on platelet proliferation like polycythemia vera.

In terms of incidence in humans, ET is the least common of the MPDs occurring at a rate less than that of PV at 1 per 100,000 population. ET may occur at any time throughout life, but has a peak incidence in the 7th decade, and there is no difference in incidence between sexes. In animals, ET is rarely reported and the disease must be considered to be of rare occurrence. Reported cases in the cat range from 9 months to 6 years and in the dog from 7–10 years with even sex incidence in a very small sample.

In humans, many cases present with thrombotic or hemorrhagic complaints, but at least half are asymptomatic with a markedly elevated platelet count found on examination of blood for routine purposes. Signs of microvascular upset include paresthesias or peripheral gangrene with most thrombotic events in deep veins, but stroke and myocardial infarcts may be the initial event. On examination, about half of human patients have at least mild splenomegaly and half of those with splenomegaly have hepatomegaly. In dogs, vomiting and depression lasting several weeks, lethargy, weakness, and pica are mentioned as presenting signs. In cats, weight loss and anorexia are mentioned as chronic indicators of ill health, and sudden onset of hindlimb lameness as an acute sign of thromboembolism. On examination, animals are usually described as having pale mucus membranes and even signs of icterus. Splenomegaly is usually reported on further examination but hepatomegaly is not.

The blood picture in humans is primarily of marked thrombocytosis with platelet anisocytosis. The leukocyte count is minimally elevated with little neutrophil immaturity, basophils are irregularly present, and other MPDs are considered if basophilia is sustained. The marrow is hypercellular, with megakaryocytic hyperplasia the most obvious change; many of these are unusually large, but some are also equally smaller than normal (Figs. 6.45–6.48). Emperipolesis is common with red cells and granulocytes found within the megakaryocytic cytoplasm.

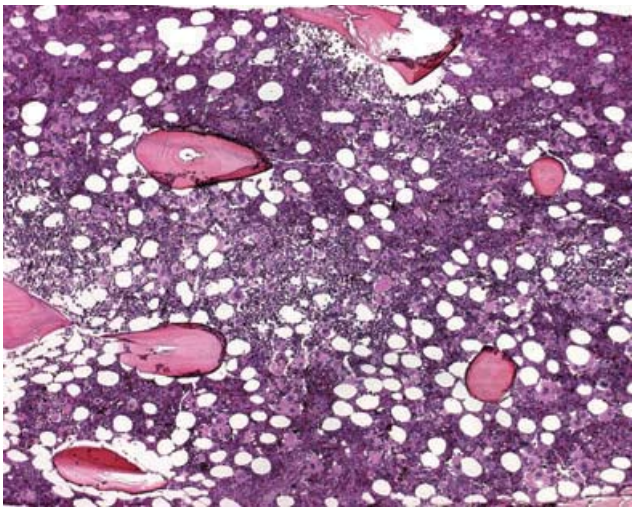

Figure 6.45. Human: marrow core, essential thrombocythemia. The marrow is hyperplastic with focal reductions in fat cells. There are increased numbers of megakaryocytes with relatively uniform size, most apparent in the upper left, lower center, and right center. *Slide from Cornell Tutorial.*

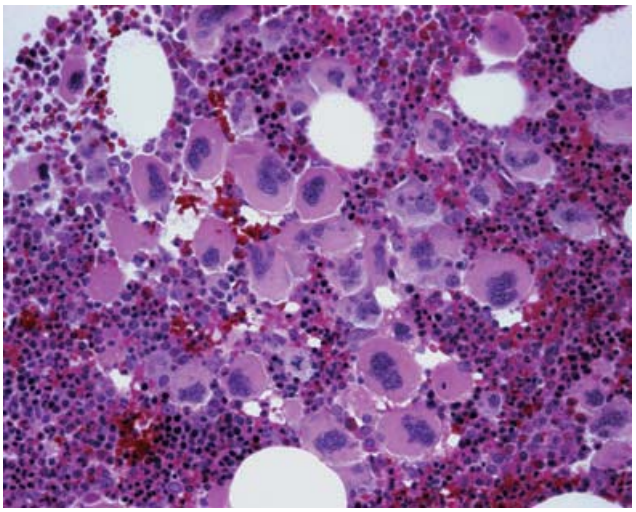

Figure 6.46. Human: marrow, essential thrombocythemia. Detail of Figure 6.45. There is irregular clustering of megakaryocytes that are reported to be larger than normal with increased nuclear ploidy but with proportionate levels of cytoplasm. There appears to be less anaplasia in the human form than in animals and there is little phthisis of other normal cell lineages.

In animals, the blood picture is remarkable due to the number and variation in platelet size. The platelet count may reach several million/ul and if there is even moderate basophilia of the platelet cytoplasm the slide has a blue tinge, as seen with very high leukocyte and platelet counts (Fig. 6.49). The platelets range in size from 2 times the size of red cells to as small as 1/4–1/3 of red cell

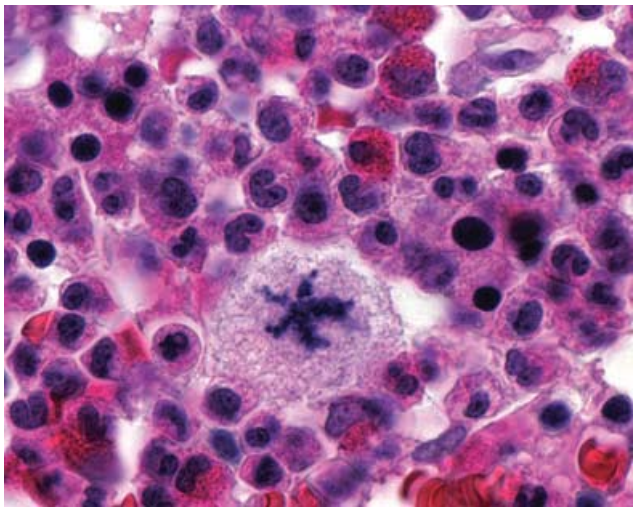

Figure 6.47. Human: bone marrow, essential thrombocythemia. The megakaryocyte with a 5-polar metaphase indicates its neoplastic lineage. There is densely cellular tissue surrounding of normal erythropoiesis and myelopoiesis.

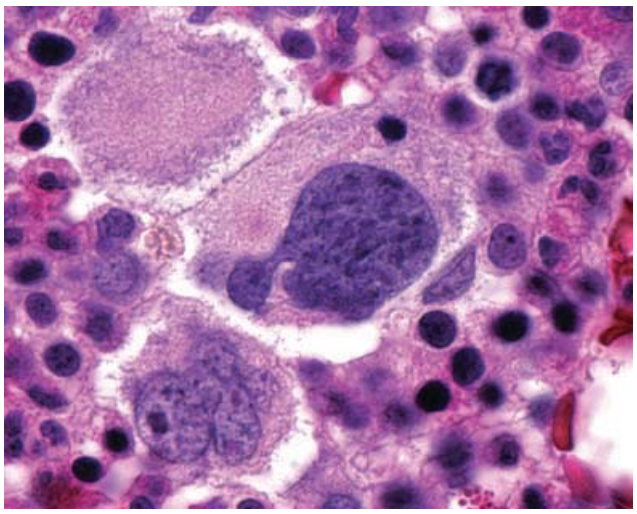

Figure 6.48. Human: bone marrow, essential thrombocythemia. Megakaryocytes are present with atypical nuclear lobulation and prominent nucleoli. The upper cell has an intracytoplasmic nucleus likely of a small lymphocyte typical of emperipolesis seen in this neoplasm.

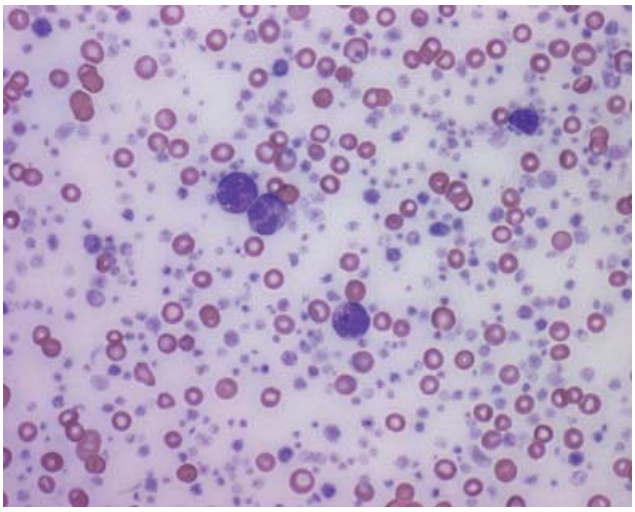

Figure 6.49. Dog: blood, essential thrombocythemia. The animal presented with a platelet count in excess of 2,000,000 per microliter. The total leukocyte count was 44,000 per ul and a packed cell volume of 8%. There is massive thrombocytosis with platelets varying greatly in size accompanied by severe anemia without signs of regeneration and with 4 basophils present suggestive of myeloproliferative disease.

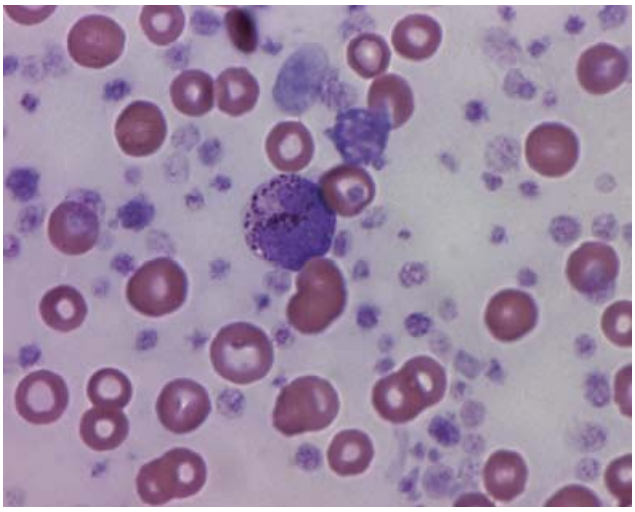

Figure 6.50. Dog: blood, essential thrombocythemia. Detail of Figure 6.49. There is remarkable platelet anisocytosis that varies from twice the size of a red cell in the top center to 1/4 to 1/3 the diameter of a red cell. Granulation also varies widely from near normal, as in the upper left, to almost absent, as in some of the smaller platelets. There is also wide variation in shape as well as in basophilia that varies from very low to very dark, as in the lower right.

diameter (Fig. 6.50). They have mild diffuse basophilia and varying levels of pink granulation, with the larger platelets often having large clear vacuoles. There is usually at least moderate anemia and mild anisocytosis of red cells, but red cell basophilia is rare. Some dogs have numerous basophils that are poorly granulated (Fig. 6.51) and also poorly granulated eosinophils (Fig. 6.52). The neutrophils have reduced granulation, and some will appear hypersegmented (Fig. 6.53). There are rare blast cells present of uncertain lineage that may be due to phthisis and dislodgment of normal precursors (Fig. 6.54). Some animals have what appears to be very atypical

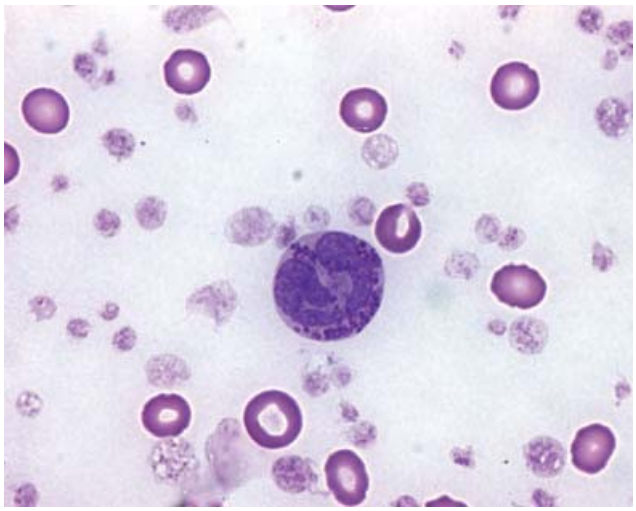

Figure 6.51. Dog: blood, essential thrombocythemia. The peripheral leukocyte picture is dominated by the number and size of atypical basophils that retain characteristic smooth nuclear margins with hyposegmentation and varying levels of granulation.

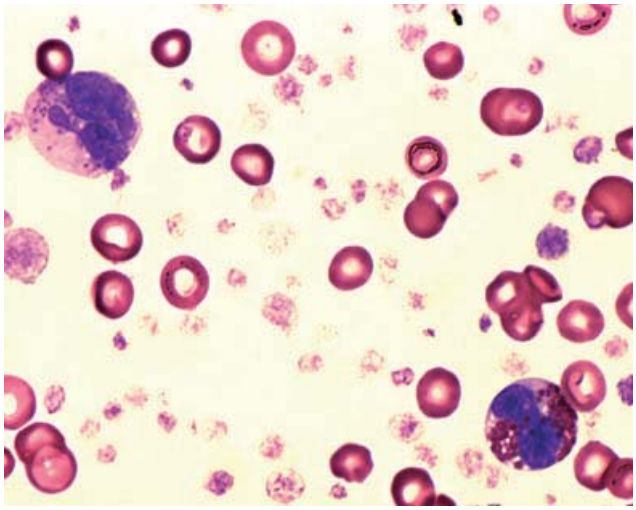

Figure 6.52. Dog: blood, essential thrombocythemia. The dog was a female, and the basophil appears to have the drumstick type nuclear projection. The eosinophil has a reduced number of granules of normal density and size.

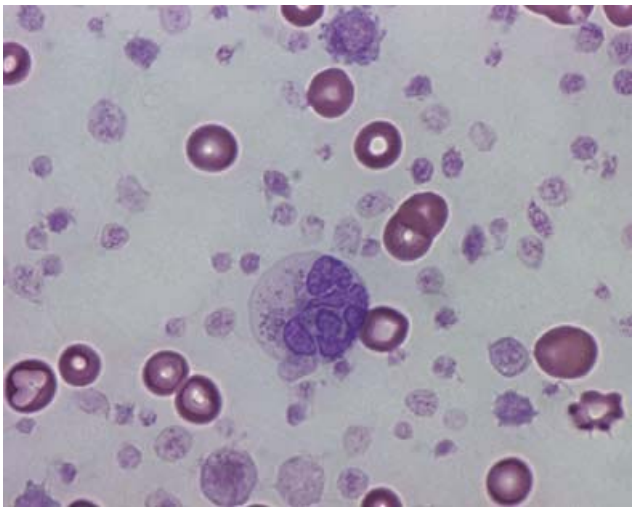

Figure 6.53. Dog: blood, essential thrombocythemia. The neutrophils have very low granulation, with cytoplasm only slightly more densely stained than the surrounding background of serum. There are multifocal small cytoplasmic vacuolations and the nucleus is approaching hypersegmentation.

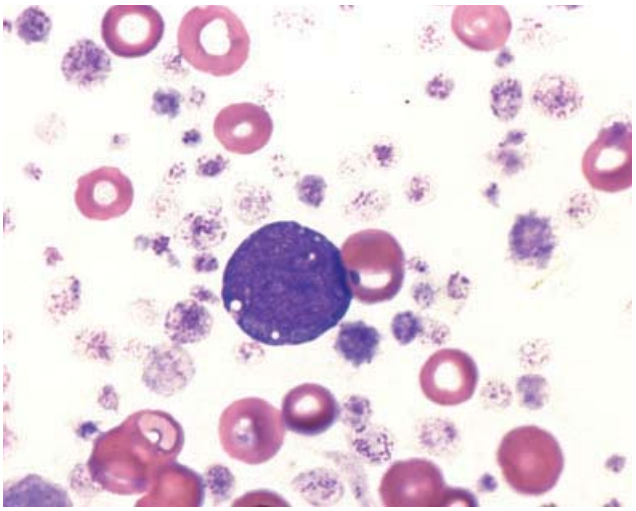

Figure 6.54. Dog: blood, essential thrombocythemia. The blast cell has a fine cribriform chromatin pattern and multiple nucleoli with narrow chromatin rimming and several cytoplasmic and nuclear vacuoles likely as a result of the degeneration. The level of differentiation does not indicate intended lineage.

megakaryocytes in circulation that are 4–5 red cells in cellular diameter and have three nuclear lobes with thin joining segments or appear as trinucleated. The cytoplasm has pale basophilia like the surrounding platelets and are usually lightly granulated (Fig. 6.55).

The bone marrow in both dogs and cats is hyperplastic with myeloid predominance but with few mature neutrophils and numerous eosinophil precursors and late stage basophils (Fig. 6.56). Giant metamyelocytes are present and suggestive of dysplastic myelopoiesis. The field is dominated by megakaryocytes, and in cytological preparations there may be 10 or more large megakaryocytes with lobulated nuclei in a 400× field and many more of smaller type. The binucleated form of promegakaryocytes are numerous, but the stages with nuclear proliferation are less apparent (Figs. 6.57, 6.58). There is a predominant population of primitive cells of

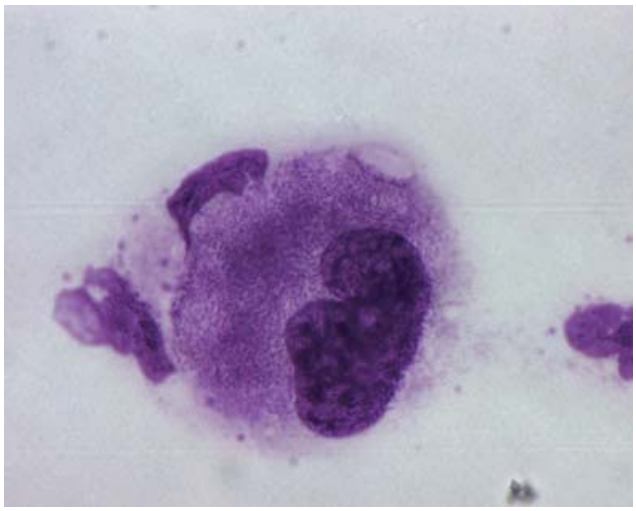

Figure 6.55. Dog: blood, essential thrombocythemia. Image from the tip of the blood film where larger cells and cell aggregates are often deposited. A megakaryocyte of moderate size is present with quite high cytoplasmic granulation and very low basophilia. These cells are present in blood at low numbers in normal animals and end up as emboli in the lung.

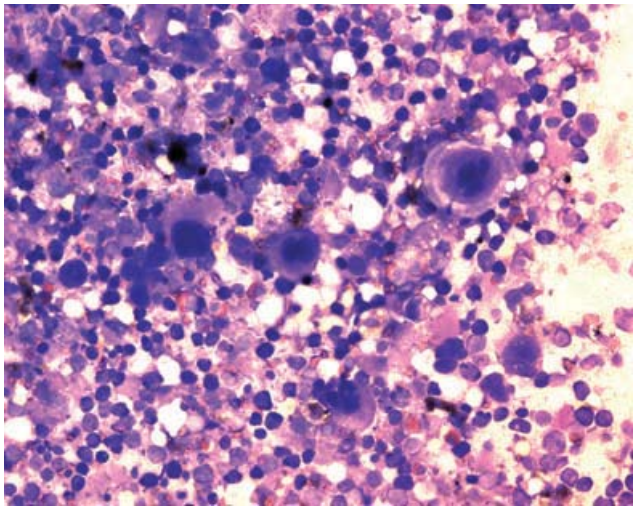

Figure 6.56. Dog: bone marrow imprint, essential thrombocythemia. The marrow is hyperplastic with increased numbers of megakaryocytes of varying size and maturity but without phthisis of other marrow elements. In general, the cytoplasmic volume is reduced compared to nuclear size and ploidy in comparison to normal megakaryocytes.

about the same size as erythroblasts, although the maturing cells of rubricyte type are markedly diminished and occur in small clusters. Because the anemia in ET is usually of moderate degree, there must be an overall level of erythropoiesis of about normal volume that is less apparent because of the greatly increased marrow volume

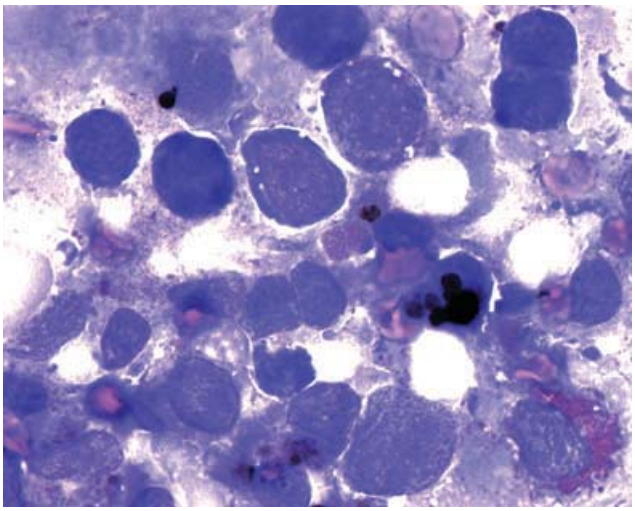

Figure 6.57. Dog: bone marrow imprint, essential thrombocythemia. The binucleated cell in a single envelope in the upper right is likely the first recognizable stage of megakaryocytic development. The large cell to the left is a basophil promyelocyte and below it is a blast cell with a prominent nucleolus. The 3 darkly stained cells in the left center and upper corner are basophils at the early stage of development. The very dark object in the right center is hemosiderin, and there is an eosinophil myelocyte in the lower right. The cell in the lower left with an oval-shaped nucleus and relatively abundant lightly stained cytoplasm is a neutrophil myelocyte.

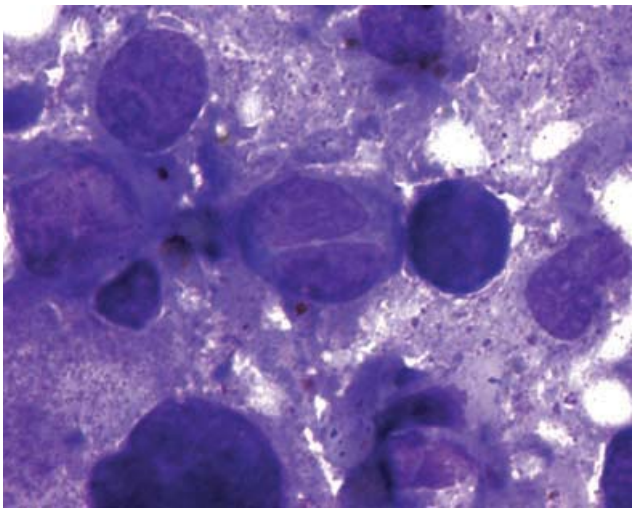

Figure 6.58. Dog Marrow, Essential Thrombocythemia. A neoplastic blast cell of the megakaryocyte series identified by binucleation of a primitive cell is in the center. The chromatin is fine and hyperchromatic with inapparent nucleoli and the cytoplasm is typically very highly basophilic. A blast cell of unidentified lineage lies on the left margin.

with red marrow in the central femoral cavity. Monocytic cells are completely inapparent, as are lymphocytes. Unlike M7, the acute leukemia of the same cell lineage where marrow fibrosis is early and results in myelophthisis, in ET only rarely does myelofibrosis become clinically significant.

The spleen and liver in ET in animals are not well described. The spleen is uniformly enlarged and tends to be turgid grossly as if the capsule were in active contraction. Histologically, there is a complete absence of germinal centers and marked atrophy of the periarteriolar lymphoid sheaths (Fig. 6.59). The sinus areas are solidly cellular with megakaryocytic prominence due to the proportion of larger cells, but many smaller cells are present at the binucleated stage and stages of nuclear proliferation with minimal cytoplasm (Fig. 6.60). Platelet sequestration is described in the spleen, but storage iron is not prominent and neither are macrophages. The liver has central lobular ischemic injury that tends to be a diffuse change and more likely related to the platelet numbers than the reduction in red cells (Fig. 6.61). There is sinus dilation, and megakaryocytes are present in sinuses in extended form, which appears more thrombotic than colony forming. In the mouse, the nodes may be very much enlarged and resemble lymphoma grossly. There is peripheral sinus dilation and complete loss of normal nodal architecture (Fig. 6.62). Cytologically, the megakaryocytes in murine ES may have peripheralized nuclei, unlike the normal counterpart, but are distinguished from macrophage-derived giant cells by nuclear fusion (Fig. 6.63).

The human literature suggests that ET needs to be differentiated from polycythemia vera and from reactive causes of thrombocytosis. Because the blood picture is so different in these diseases in the developed state, there appears little likelihood of confusion of these conditions if the blood is repeatedly examined over a period of several weeks. If the platelet count remains markedly

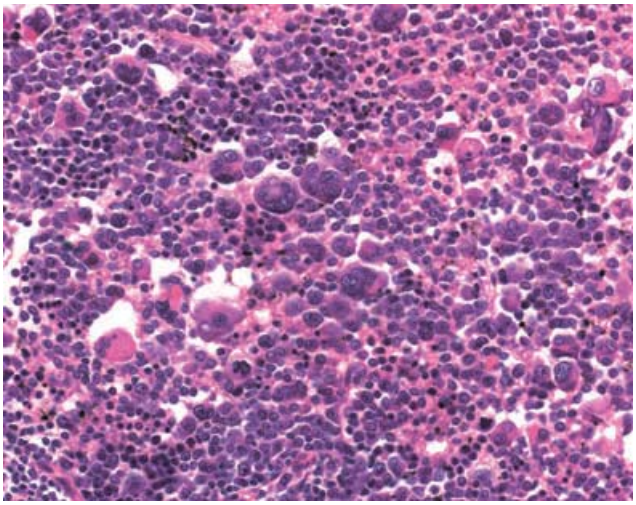

Figure 6.60. Mouse: spleen, essential thrombocythemia. Detail of Figure 6.59. Megakaryocytic cells are greatly increased in number and vary markedly in size. The cytoplasmic volume does not reach normal volume in proportion to nuclear ploidy.

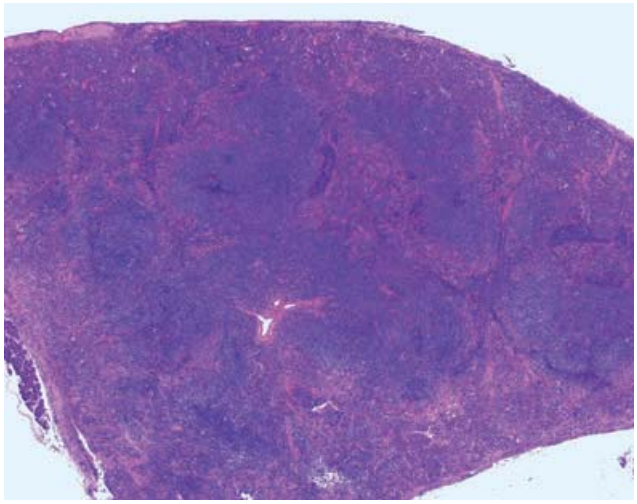

Figure 6.59. Mouse: spleen, essential thrombocythemia. The organ is markedly enlarged with the capsule greatly thinned and smooth muscle trabeculae thinned and widely separated. Periarteriolar sheath areas are discernible as irregular areas of darker staining with the surrounding sinus areas greatly expanded. *Slide from J. M. Ward, DVM.*

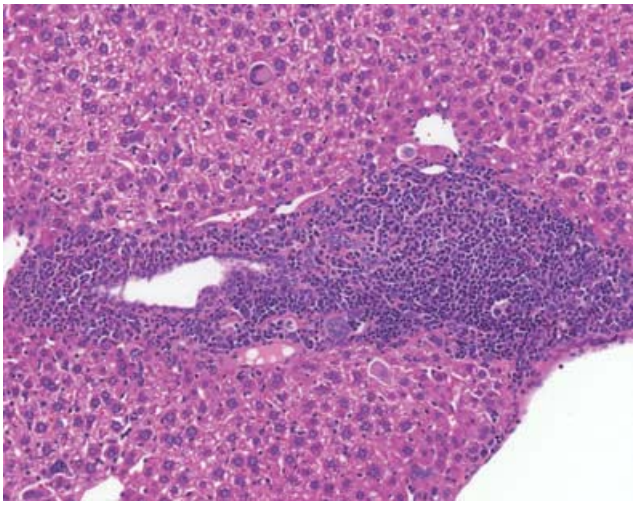

Figure 6.61. Mouse: liver, essential thrombocythemia. Unlike the spleen that has massive involvement with essential thrombocythemia, the liver has scattered large but focal areas of perivascular infiltration that is of mixed lineage and benign extramedullary hematopoiesis. *Slide from J. M. Ward, DVM.*

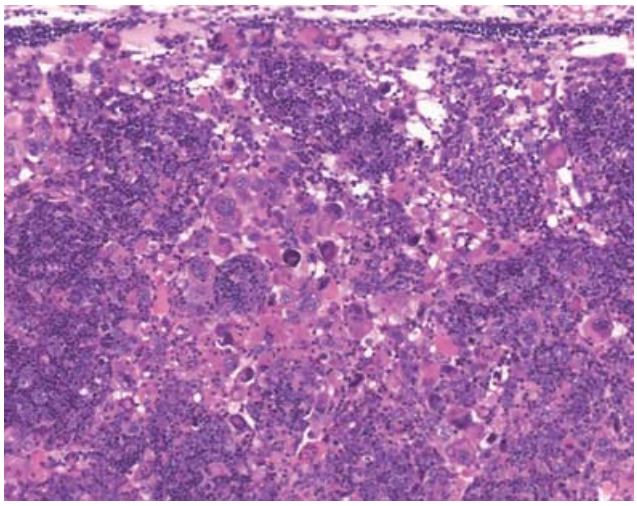

Figure 6.62. Mouse: lymph node, essential thrombocythemia. The nodal capsule is at top and greatly thinned, with the peripheral sinus open and irregularly dilated with large atypical megakaryocytes filling sinus areas and irregular areas of mixed myelopoiesis occupying more solid areas of the tissue. *Slide from J. M. Ward, DVM.*

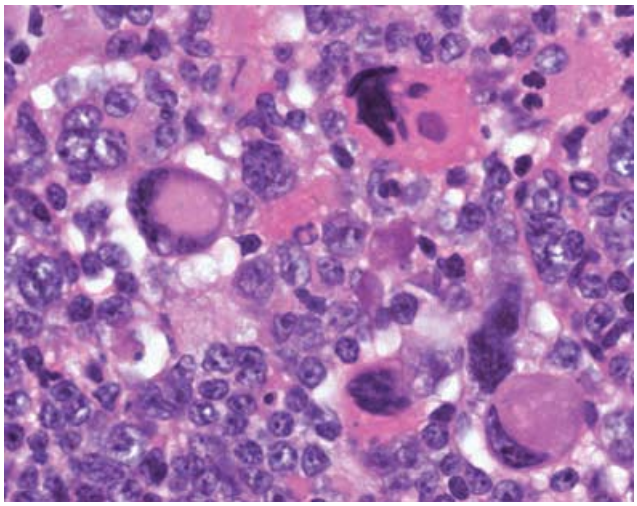

Figure 6.63. Mouse: lymph node, essential thrombocythemia. Detail of Figure 6.62. The developing megakaryocytes vary in size, with irregular nuclear conformations occasionally resembling phagocytic giant cells but with nuclear fusion. There is emperipolesis in megakaryocytes in the upper right.

elevated in the range of 800,000 to 1,000,000 or more, especially if accompanied by basophilia, the diagnosis of ET may be made with assurance.

REFERENCES

Anastasi, J., and Vardiman, J.W. (2001) Chronic myelogenous leukemia and the chronic myeloproliferative diseases. In Knowles, D.M. (ed.), *Neoplastic Hematopathology,* 2nd ed. Lippincott Williams & Wilkins, Philadelphia, pp. 1745–1790.

Bass, M.C., and Schultze, A.E. (1998) Essential thrombocythemia in a dog: Case report and literature review. *J Am An Hosp Assoc* 34:197–203.

Buhr, T., Georgii, A., Schuppan, O., Amor, A., and Kaloutsi, V. (1992) Histologic findings in bone marrow biopsies of patients with thrombocythemic cell counts. *Ann Hematol* 64:286–291.

Degen, M.A., Feldman, B.F., Turrel, J.M., Goding, B., Kitchell, B., and Mandell, C.P. (1989) Thrombocytosis associated with a myeloproliferative disorder in a dog. *J Am Vet Med Assoc* 194:1457–1459.

Hammer, A.S. (1991) Thrombocytosis in dogs and cats: A retrospective study. *Comp Haematol Int* 1:181–186.

Hammer, A.S., Couto, C.G., Getzy, D., and Bailey, M.Q. (1990) Essential thrombocythemia in a cat. *J Vet Int Med* 4:87–91.

Hofmann, W.K., Kalina, U., Koschmieder, S., Seipelt, G., Hoelzer, D., and Ottmann, O.G. (2000) Defective megakaryocytic development in myelodysplastic syndromes. *Leuk and Lymph* 38(1–2):13–19.

Hogan, D.F., Dhaliwal, R., Sisson, D.D., and Kitchell, B.E. (1999) Paraneoplastic thrombocytosis-induced systemic thromboembolism in a cat. *J Am An Hosp Assoc* 35:483–486.

Hopper, P.E., Mandell, C.P., Turrel, J.M., Jain, N.C., Tablin, F., and Zinkl, J.G. (1989) Probable essential thrombocythemia in a dog. *J Vet Int Med* 3:79–85.

Kobayashi, S., Teramura, M., Hoshino, S., Motoji, T., Oshimi, K., and Mizoguchi, H. (1993) Circulating megakaryocyte progenitors in myeloproliferative disorders are hypersensitive to interleukin-3. *Brit J Haematol* 83:539–544.

Kutti, J., and Wadenvik, H. (1996) Diagnostic and differential criteria of essential thrombocythemia and reactive thrombocytosis. *Leuk and Lymph* 22(Suppl.1):41–45.

Matolcsy, A., Nador, R., Wéber, E., and Kónya, T. (1992) Nucleolar organizer regions of megakaryocytes in chronic myeloproliferative disorders. *Virchows Archiv A Pathol Anat* 420:441–445.

Metcalf, D., Mifsud, S., and Di Rago, L. (2005) Murine megakaryocyte progenitor cells and their susceptibility to suppression by G-CSF. *Stem Cells* 23:55–62.

Michel, R.L., O'Handley, P., and Dade, A.W. (1976) Megakaryocytic myelosis in a cat. *J Am Vet Med Assoc* 168(11):1021–1025.

Michiels, J.J. (1999) Normal life expectancy and thrombosis-free survival in aspirin treated essential thrombocythemia. *Clin Appl Thrombosis/Hemostasis* 5(1):30–36.

Michiels, J.J., Kutti, J., Stark, P., Bazzan, M., Gugliotta, L., Marchioli, R., Griesshammer, M., van Genderen, P.J.J., Brière, J., Kiladjian, J.J., Barbui, T., Finazzi, G., Berlin, N.I., Pearson, T.C., Green, A.C., Fruchtmann, S.M., Silver, R.T., Hansmann, E., Wehmeier, A., Lengfelder, E., Landolfi, R., Kvasnicka, H.M., Hasselbalch, H., Cervantes, F., Reilly, J.T., Demory, J.L., Gisslinger, H., Guardiola, P., Martyré, M.C., Le Bousse-Kerdilès, M.C., and Thiele, J. (1999) Diagnosis, pathogenesis and treatment of the myeloproliferative disorders essential thrombocythemia, polycythemia vera and essential megakaryocytic granulocytic metaplasia and myelofibrosis. *Netherlands J Med* 54:46–62.

Pitcher, L., Taylor, K., Nichol, J., Selsi, D., Rodwell, R., Marty, J., Taylor, D., Wright, S., Moore, D., Kelly, C., and Rentoul, A. (1997) Thrombopoietin measurement in thrombocytosis: Dysregulation and lack of feedback inhibition in essential thrombocythaemia. *Brit J Haematol* 99:929–932.

Randi, M.L., Putti, M.C., Fabris, F., Sainati, L., Zanesco, L., and Girolami, A. (2000) Features of essential thrombocythaemia in childhood: A study of five children. *Brit J Haematol* 108:86–89.

Robak, T., Urbańska-Ryś, H., Góra-Tybor, J., Wawrzyniak, E., Korycka, A., Bartkowiak, J., Kordek, R., and Polliack, A. (2003) Coexistence of chronic lymphocytic leukemia and essential thrombocythemia. *Leuk and Lymph* 44(8):1425–1431.

Sacchi, S., Vinci, G., Gugliotta, L., Rupoli, S., Gargantini, L., Martinelli, V., Baravelli, S., Lazzarino, M., and Finazzi, G. (2000) Diagnosis of essential thrombocythemia at platelet counts between 400 and 600 × 10^9/L. *Haematologica* 85:492–495.

Simpson, J.W., Elsa, R.W., and Honeyman, P. (1990) Successful treatment of suspected essential thrombocythaemia in the dog. *J Sm An Pract* 31:345–348.

Tablin, F., Jain, N.C., Mandell, C.P., Hopper, P.E., and Zinkl, J.G. (1989) Ultrastructural analysis of platelets and megakaryocytes from a dog with probable essential thrombocythemia. *Vet Path* 26:289–293.

Thiele, J., Kvasnicka, H.M., Diehl, V., Fischer, R., and Michiels, J.J. (1999) Clinicopathological diagnosis and differential criteria of thrombocythemias in various myeloproliferative disorders by histopathology, histochemistry and immunostaining from bone marrow biopsies. *Leuk and Lymph* 33(3–4):207–218.

Thiele, J., Schneider, G., Hoeppner, B., Wienhold, S., Zankovich, R., and Fischer, R. (1988) Histomorphometry of bone marrow biopsies in chronic myeloproliferative disorders with associated thrombocytosis—Features of significance for the diagnosis of primary (essential) thrombocythaemia. *Virchows Archiv A Pathol Anat* 413:407–417.

Wehmeier, A., Daum, I., Jamin, H., and Schneider, W. (1991) Incidence and clinical risk factors for bleeding and thrombotic complications in myeloproliferative disorders. *Ann Hematol* 63:101–106.

CHRONIC IDIOPATHIC MYELOFIBROSIS

Chronic idiopathic myelofibrosis (CIMF) is a clonal proliferation arising in bone marrow characterized by a period of hyperproliferation of relatively normal-appearing hematopoietic cells and followed by deposition of connective tissue in bone marrow. This proliferation and subsequent sclerosis results in marrow failure due to myelofibrosis with splenomegaly and widespread compensatory extramedullary hematopoiesis. CIMF was formerly known as *myeloid metaplasia with myelofibrosis (MMM)* and *agnogenic myeloid metaplasia*. The term *CIMF,* indicating an unknown cause, is used for those cases presenting with primary myeloid metaplasia followed by myelofibrosis, and it is not used to describe cases that arise as "spent" cases of polycythemia vera or essential thrombocythemia.

As indicated by the name, the cause of CIMF is unknown. It is known that the clonality is limited to a primitive stage of marrow stem cell and that the marrow stroma retains a normal karyotype with the fibrosis an epiphenomenon. In some human cases, the lymphocytes of both lineages are also clonal, but apparently in others the lymphocytes are normal. Extramedullary hematopoiesis is considered a hallmark of CIMF, as is leukoerythroblastosis or the appearance of normal but immature blood precursors of both myeloid and erythroid types in the peripheral blood, along with oval and teardrop-shaped red cells indicative of stromal proliferation. The cause of the myelofibrosis is also unknown, but a direct relation has been shown between the levels of serum thrombopoietin (TPO) and numbers and mass of marrow megakaryocytes and the degree of marrow fibrosis. Further, there is a direct relationship between the cytokines required for fibrogenesis and the alpha granules of the megakaryocytes and platelets. Active participants include platelet-derived growth factor, platelet-derived collagenase inhibitors, calmodulin, and abnormal secretion of TGF beta. The latter factor increases the biosynthesis of collagen types I, II, and III.

In humans, the incidence of CIMF is very low and estimated to be 0.5 per 100,000, with men affected more often than women. The peak incidence is between the 6th and 7th decades, and the disease is rarely seen in children. The disease is rarely recognized in animals with the emphasis on recognition, not incidence, but even if all cases of this type were correctly identified the disease would still be exceedingly unusual. One-third of human cases are asymptomatic at diagnosis, and this appears to follow for dogs where cases are seen with idiopathic neutrophilic leukocytosis without apparent cause. In humans, the leukocyte count varies widely depending on the stage at which the disease is recognized, and it is usually between 10,000 and 20,000/ul but may be as high as 60,000/ul. In dogs, the leukocyte count is usually between 25,000 and 50,000/ul but with progression may be less than normal. Cats are more likely to have below-normal levels of neutrophils, and leukopenia was present in a single case in a marmoset that had extensive marrow fibrosis at the time of diagnosis. The blood platelet count varies widely in humans, with one-third of cases having platelet counts less than 150,000/ul and 10% or more having platelet counts over 500,000/ul, with some exceeding 1 million/ul. In cats, cases are reported as having platelet counts from 250,000–500,000/ul, which is likely representative of animals in a well-developed but not terminal stage of disease. In humans, 70–90% of cases have splenomegaly at diagnosis and 50% have hepatomegaly.

In animals, hepatosplenomegaly is present in most cases at necropsy and presumably would be detectable with current technology in the live animal. All animals have anemia of mild to severe degree, and all have a leukoerythroblastic picture with distorted or oval red cells (Figs. 6.64, 6.65). In humans with CIMF, blast cells are commonly seen in the peripheral blood and may reach 10% of total cells in leukopenic phase without indicating transformation to an acute leukemia. In animals, the blast cell level in bone marrow had been noted to be below the level required for a diagnosis of leukemia, but the presence of blasts in the blood has not received comment. In summary, the clinical picture prior to attempts at marrow aspiration or core biopsy is of an animal with progressive weight loss and loss of activity and appetite, an abnormal leukocyte level either increased or decreased with nonresponsive anemia, low platelet levels, leukoerythroblastic reaction, and splenomegaly.

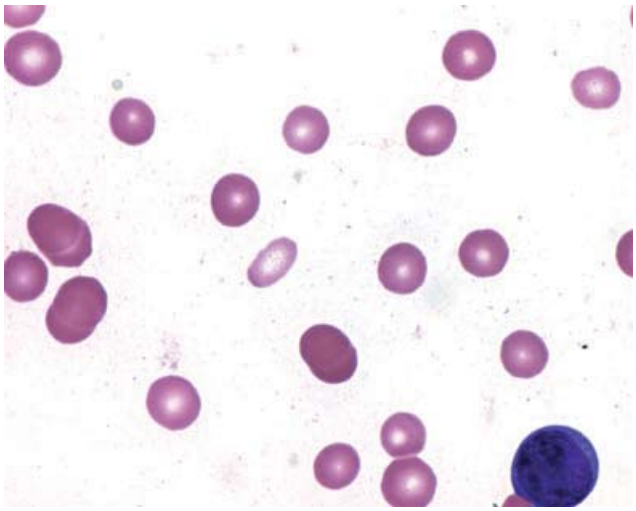

Figure 6.64. Dog: blood, myelofibrosis. The dog presented with weakness and mucosal pallor with a total leukocyte count of 6,300/ul and a hemoglobin of 3.7 grams per dl with platelets at 16,000/ul. The oval red cells in upper center is indicative of a marrow stromal proliferation. The presence of these oval red cells in the absence of indication of erythroid response in severe anemia are presumptive evidence of extensive marrow stromal proliferation.

The variability in the peripheral blood findings is a reflection of changes in the marrow that may be hypercellular in the early stages of the disease and hypocellular as fibrosis develops. In human patients, the marrow is hypercellular at diagnosis in 20–40% of cases that present in the stage of myeloid metaplasia (Figs. 6.66, 6.67). The most characteristic change in marrow of humans with CIMF is in the megakaryocytes that are increased in number with greater variability in size but may be found in clusters of 3–10 cells adjacent to or very significantly within irregularly dilated marrow sinusoids (Fig. 6.68). Dysplastic changes are present in marrow megakaryocytes with hyperchromatic irregularly lobulated large cells as well as micromegakaryocytes or "dwarf" cells that may be almost devoid of cytoplasm (see Fig. 6.67). Myeloid maturation is synchronous and erythroid cells are normoblastic, but some megaloblastic forms may be present. Eosinophils may be increased and there may be increased basophils, usually predictable by peripheral

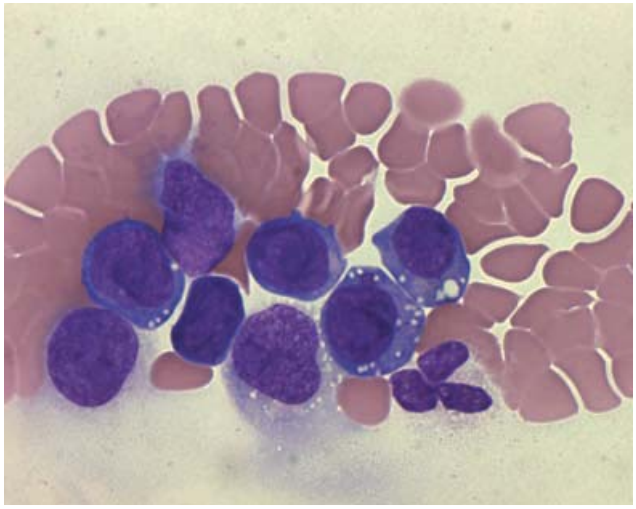

Figure 6.65. Dog: blood, myelofibrosis, same case as Figure 6.64. A foci of atypical blast cells at the tip of the slide, some with fine azurophilic granulation. The neutrophil in the lower right has very low cytoplasmic density and very few specific granules.

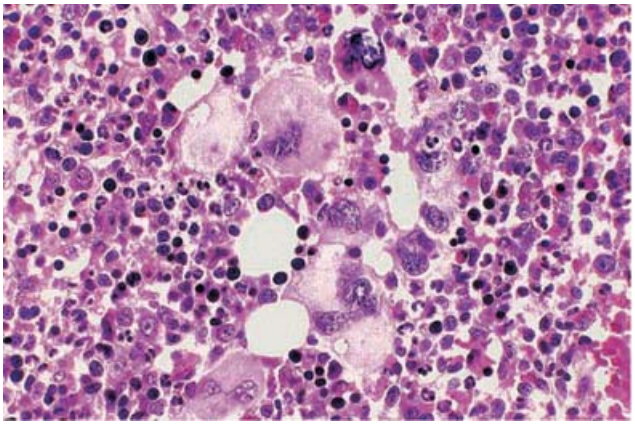

Figure 6.66. Human: bone marrow, chronic idiopathic myelofibrosis. The lesion is taken in an early prefibrotic stage of disease progression. The marked variation in size of megakaryocytes is characteristic as well as the level of variation in nuclear cytoplasmic ratio. *Reprinted from* Surgical Pathology, *9th edition, Volume 2, by Rosai and Ackerman, 2004, Chapter 23, page 2072, with permission from Elsevier and J. Thiele, MD.*

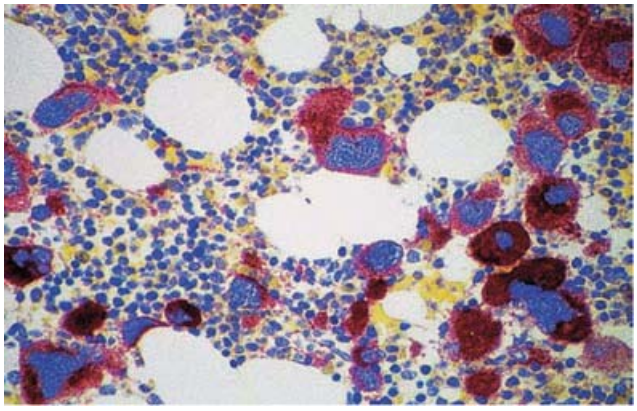

Figure 6.67. Human: bone marrow, chronic idiopathic myelofibrosis. Bone marrow taken at a prefibrotic stage of progression with immunohistochemical staining for megakaryocytes using CD61. The megakaryocytes vary markedly in cell size as well as in nuclear size and shape and have atypical ropy chromatin aggregation. *Reprinted from* Surgical Pathology, *9th edition, Volume 2, by Rosai and Ackerman, 2004, Chapter 23, page 2072, with permission from Elsevier and J. Thiele, MD.*

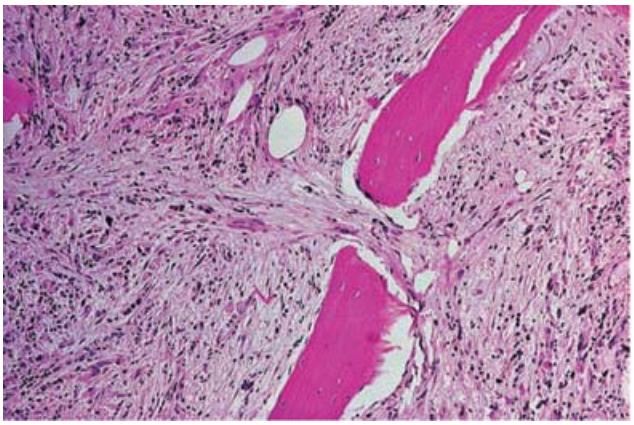

Figure 6.69. Human: marrow, chronic idiopathic myelofibrosis. The tissue from a patient diagnosed 7 years earlier with agnogenic myeloid metaplasia. There is now very extensive fibrosis that has resulted in phthisis and exclusion of most hematopoietic precursors and their progeny. *Reprinted from* Surgical Pathology, *9th edition, Volume 2, by Rosai and Ackerman, 2004, Chapter 23, page 2072, with permission from Elsevier and J. Thiele, MD.*

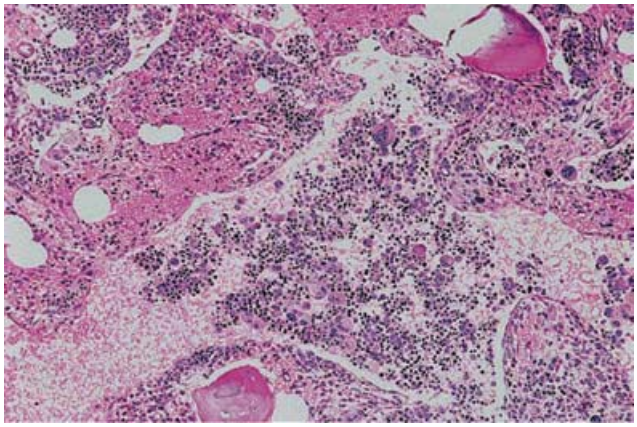

Figure 6.68. Human: bone marrow, chronic idiopathic myelofibrosis. This image demonstrates extensive intrasinusoidal hematopoiesis that consists primarily of erythroid precursors and megakaryocytes at varying stages of maturation. The irregular dilation of sinuses and adjacent interstitial areas with low cellularity are indications of disease progression. *Reprinted from* Surgical Pathology, *9th edition, Volume 2, by Rosai and Ackerman, 2004, Chapter 23, page 2072, with permission from Elsevier and J. Thiele, MD.*

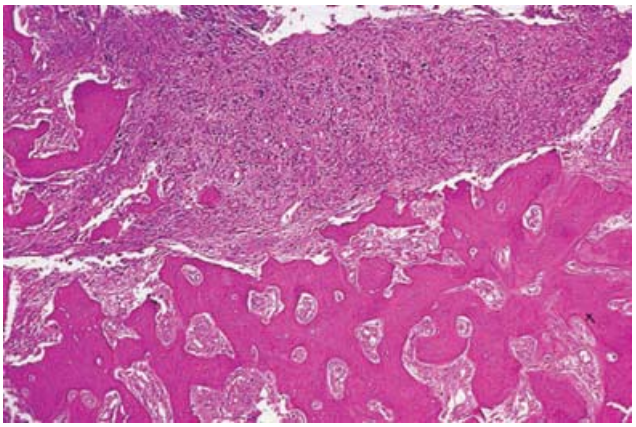

Figure 6.70. Human: bone marrow, chronic idiopathic myelofibrosis. There is extensive osteosclerosis evident in the thickened trabecular bone, with a solid area of marrow to the left containing primarily primitive cells. *Reprinted from* Surgical Pathology, *9th edition, Volume 2, by Rosai and Ackerman, 2004, Chapter 23, page 2072, with permission from Elsevier and J. Thiele, MD.*

blood basophilia. Besides the early reticulin sclerosis and later actual formation of collagen, some cases have proliferation of dense cancellous bone with phthisis of all marrow elements (Figs. 6.69, 6.70). At diagnosis, 50–60% of human patients have some degree of one or more of the latter three types of myelofibrosis.

CIMF in animals is the disease most characteristic of a "dry tap" on attempts at marrow aspiration. Further indication of the degree of sclerosis is apparent when a "roll imprint" of a marrow core is made with little and irregular free cell exfoliation. In animals, the early fibrotic response is more likely to be seen in cats than in dogs; however, the osteosclerotic changes seen in humans are less common in animals or don't tend to occur because of elective termination at an earlier stage of sclerosis. Where described, there is irregular periosteal new bone production that is more like the changes seen in pulmonary hypertrophic osteopathy than the medullary proliferation

of bone seen in humans. Much of the sclerosis previously seen in marrow of cats has been due to infection with FeLV and part of a myelodysplastic syndrome. Cats tend to have less extensive cancellous bone in metaphyses than in dogs, and on gross examination the marrow may shell out from the central femoral marrow cavity in a shiny dense cohesive cylinder that in color and texture resembles a venous thrombus. In dogs, the marrow is more irregularly fibrotic with focal sinus ectasia (Fig. 6.71). In both animals, there is abundant sclerosis on silver staining for reticulin fibers that is more irregularly dense in dogs and with less actual collagen than is seen in humans or nonhuman primates (Figs. 6.72, 6.73).

The spleen in animals with CIMF is uniformly enlarged with sinus hyperplasia and lymphoid atrophy. The EMH is trilineage, but in all tissues the megakaryocytes are most apparent; there is quite marked and irregular sinus ectasia and increased sinus stromal tissue, but the spleen is never as involved in sclerosis as the marrow. The liver has sinus dilation with EMH and general involvement of portal areas that have more myeloid progenitors and progeny than of megakaryocytes. The nodes may be small or enlarged and involved in EMH, which is largely neoplastic and tends to be paracortical (Fig. 6.74) and medullary in location with intrasinus EMH (Fig. 6.75) in medullary cords and sinuses (Figs. 6.76, 6.77). Scattered foci of fibrotic areas of hematopoiesis may appear in almost any tissue in the body, but in humans the spleen and liver are almost always involved. Other tissues include most of the anatomy, but kidney, adrenals, gastrointestinal tract, lung, pleura, skin, breast, and dura mater of the central nervous system may be involved in the process of EMH. The small or micromegakaryocytes may be underestimated in all tissues and are more apparent on staining with CD31, where irregular thin wisps of cytoplasm are seen to be marked in cells with round nuclei about the size of large lymphocytes and even smaller.

CIMF must be distinguished from PV and ET and some forms of myelodysplasia, with the diagnosis not apparent without some history of the blood picture over previous

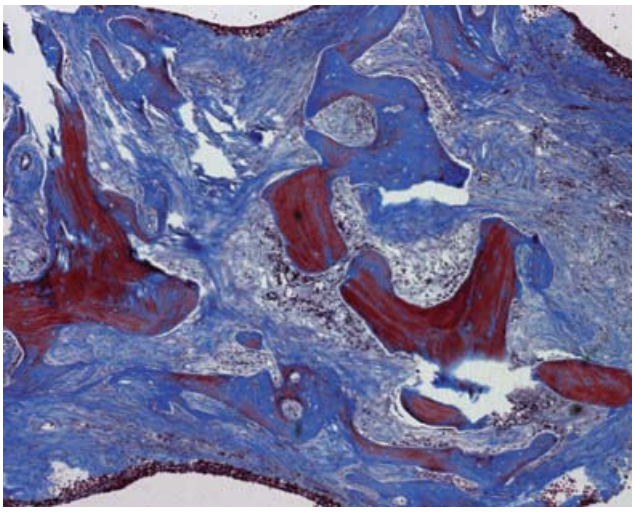

Figure 6.72. Dog: marrow, myelofibrosis. Masson's stain on same tissue as Figure 6.71. The level of blue staining fibers is indicative of a high level of mature collagen at previous areas of hematopoiesis.

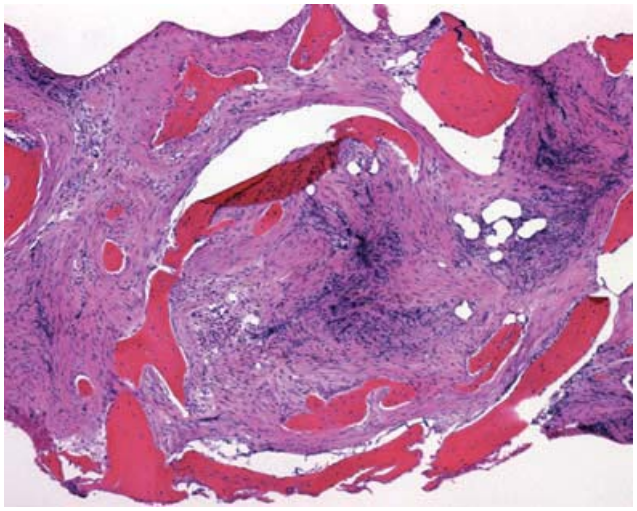

Figure 6.71. Dog: bone marrow core, myelofibrosis. A 5-year-old dog presented with mucosal pallor on clinical examination and a history of progressive weight loss over the past 6 months. There is very extensive myelofibrosis that has progressed to almost complete myelophthisis.

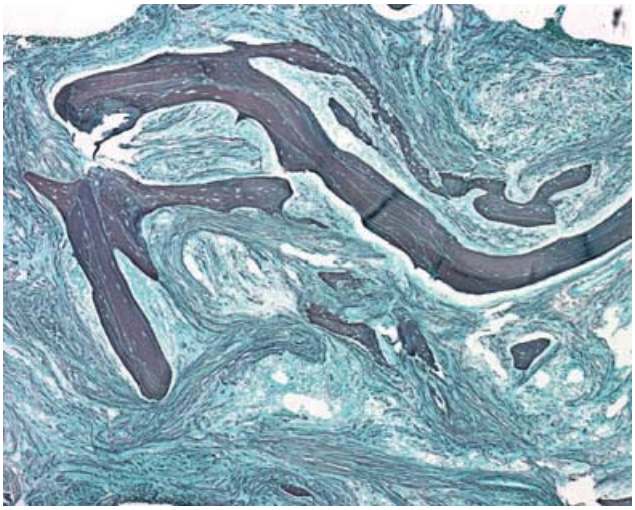

Figure 6.73. Dog: marrow, myelofibrosis, silver stain for reticulin fibers. There is a dense fine fibrillar network occupying the majority of the soft tissue space indicating that even those areas not occupied by actual collagen have a high level of sclerotic change.

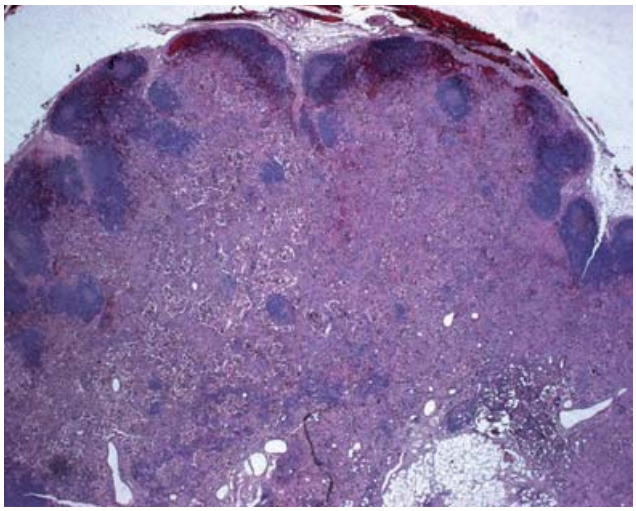

Figure 6.74. Human: lymph node, chronic idiopathic myelofibrosis. The residual normal lymphoid tissue consists of peripheralized fading germinal centers in subcapsular areas with a very narrow and irregular adjacent band of darkly stained residual paracortex. The interior of the node has a diffuse architecture with irregularities of sinus distension. *Slide from Cornell Tutorial.*

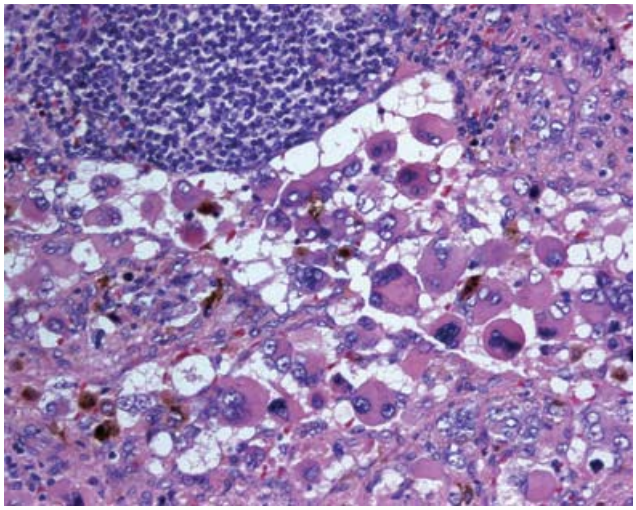

Figure 6.75. Human: lymph node, chronic idiopathic myelofibrosis. Detail of Figure 6.74. The subcapsular area of fading paracortex is at the top with an irregular area of sinus dilation below containing many very atypical megakaryocytes with apparent irregularities in nuclear fusion.

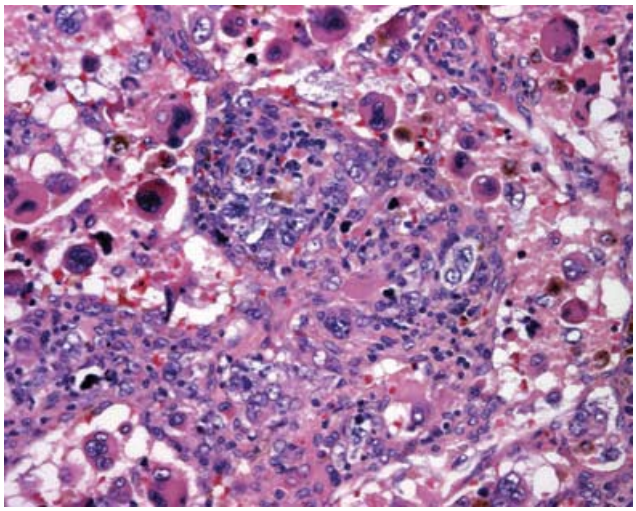

Figure 6.76. Human: lymph node, chronic idiopathic myelofibrosis. The upper third of the image is an area of medullary sinus partially occupied by neoplastic megakaryocytes and hemosiderin-bearing macrophages. The solid area of tissue immediately below the center is a medullary cord that also contains neoplastic megakaryocytes evident by the vesicular nuclei. There is extensive fine sclerosis of cortex as well as interstitial areas of medullary cords.

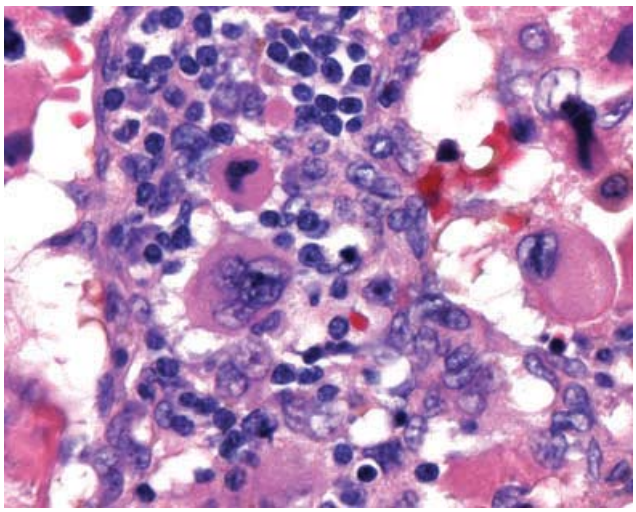

Figure 6.77. Human: lymph node, chronic idiopathic myelofibrosis. Detail of Figure 6.76. The central 1/3 of the image is of medullary cord that contains megakaryocytic precursors and small lymphocytes with prominent adjacent fibroblast nuclei. Virtually no cells of neutrophil or erythroid lineage are present due to phthisis of fibrosis similar to that occurring in bone marrow.

months and access to marrow histology. The presence of the leukoerythroblastic blood picture with distorted red cells of oval and teardrop-shaped types in an animal with chronic weight loss and anemic with splenomegaly is highly suggestive of CIMF. A history of atypical high leukocyte counts that seem to have no particular target would be strong supporting evidence for a diagnosis of CIMF. The presence of marrow megakaryocytes of variable size and shape without a blast count that would support a diagnosis of leukemia and marrow sinus ectasia with intravascular hematopoiesis are very strong supportive evidence for CIMF.

A rare disease known as *acute panmyelosis* or *malignant myelosclerosis* occurs rarely in humans and is considered a subtype of AML (see Chapter 5, "Acute Myeloid Leukemias"). In this disease, there is pancytopenia with myelofibrosis, multilineage myelodysplasia, and circulating blasts. The marrow is extensively involved with sclerotic foci and appears hypocellular with all cell lineages present and with evidence of maturation, but with very variable megakaryocytes. A major point of difference is that 20% or more of marrow cells are blasts. These cases lack splenomegaly and hepatomegaly, and the higher blast cell level distinguishes this disease from CIMF.

REFERENCES

Anastasi, J., and Vardiman, J.W. (2001) Chronic myelogenous leukemia and the chronic myeloproliferative diseases. In Knowles, D.M. (ed.), *Neoplastic Hematopathology,* 2nd ed. Lippincott Williams & Wilkins, Philadelphia, pp. 1745–1791.

Bianco, P., and Robey, P.G. (2000) Marrow stromal stem cells. *J Clin Invest* 105(12):1663–1668.

Blue, J.T. (1988) Myelofibrosis in cats with myelodysplastic syndrome and acute myelogenous leukemia. *Vet Pathol* 25:154–160.

Breuer, W., Darbès, J., Hermanns, W., and Thiele, J. (1999) Idiopathic myelofibrosis in a cat and in three dogs. *Comp Haematol Int* 9:17–24.

Brunning, R.D., and McKenna, R.W. (1993) Chronic idiopathic myelofibrosis (agnogenic myeloid metaplasia. In *Tumors of the Bone Marrow. Atlas of Tumor Pathology*. Armed Forces Institute of Pathology, pp. 238–246.

Dupriez, B., Morel, P., Demory, J.L., Lai, J.L., Simon, M., Plantier, I., and Bauters, F. (1996) Prognostic factors in agnogenic myeloid metaplasia: A report on 195 cases with a new scoring system. *Blood* 88(3):1013–1018.

Hirose, Y., Masaki, Y., Shimoyama, K., Sugai, S., and Nojima, T. (2001) Granulocytic sarcoma of megakaryoblastic differentiation in the lymph nodes terminating as acute megakaryoblastic leukemia in a case of chronic idiopathic myelofibrosis persisting for 16 years. *Eur J Haematol* 67: 194–198.

Khan, K.N.M., Logan, A.C., and Blomquist, E.M. (1997) Idiopathic myelofibrosis (agnogenic myeloid metaplasia) in a marmoset (Callithrix jacchus): Hematologic and histopathologic changes. *Vet Pathol* 34:341–345.

Kreipe, H., Jaquet, K., Felgner, J., and Parwaresch, M.R. (1992) Clonal analysis of agnogenic myeloid metaplasia. *Leuk and Lymph* 8:459–464.

Kumar, S., Mow, B.M.F., and Kaufmann, S.H. (1999) Hypercalcemia complicating leukemic transformation of agnogenic myeloid metaplasia-myelofibrosis. *Mayo Clin Proc* 74: 1233–1237.

Kvasnicka, H.M., Thiele, J., Regn, C., Zankovich, R., Diehl, V., and Fischer, R. (1999) Prognostic impact of apoptosis and proliferation in idiopathic (primary) myelofibrosis. *Ann Hematol* 78:65–72.

Le Brousse-Kerdilès, M.C., and Martyré, M.C. (2000) Myelofibrosis: Pathogenesis of myelofibrosis with myeloid metaplasia. *Springer Sem Immunopathol* 21:491–508.

Loewy, G., Mathew, A., and Distenfeld, A. (1994) Skin manifestation of agnogenic myeloid metaplasia. *Am J Hematol* 45:167–170.

Mesa, R.A., Elliott, M.A., and Tefferi, A. (2000) Splenectomy in chronic myeloid leukemia and myelofibrosis with myeloid metaplasia. *Blood Rev* 14:121–129.

Orazi, A., O'Malley, D.P., Jiang, J., Vance, G.H., Thomas, J., Czader, M., Fang, W., An, C., and Banks, P.M. (2005) Acute panmyelosis with myelofibrosis: An entity distinct from acute megakaryoblastic leukemia. *Mod Pathol* 18:603–614.

Tefferi, A. (2000) Myelofibrosis with myeloid metaplasia. *New England J Med* 342:1255–1265.

Tefferi, A., Mesa, R,A., Nagomey, D.M., Schroeder, G., and Silverstein, M.N. (2000) Splenectomy in myelofibrosis with myeloid metaplasia: A single-institution experience with 223 patients. *Blood* 95(7):2226–2233.

Zenoble, R.D., and Rowland, G.N. (1979) Hypercalcemia and proliferative, myelosclerotic bone reaction associated with feline leukovirus infection in a cat. *JAVMA* 175(6):591–595.

BASOPHIL LEUKEMIA AND MAST CELL TUMOR

Basophil leukemia is a rare disease occurring primarily in dogs, cats, and possibly pigs. Oddly, dogs and cats are known to have basophils in the peripheral blood only rarely in normal animals; normal pigs have peripheral blood basophils present in very low numbers. Systemic mast cell disease is much more common and is characterized by cells with round vesicular nuclei and variable basophilic granulation. Basophil leukemia is characterized by numerous myelocytes in peripheral blood with round nuclei and abundant cytoplasm but with an apparent continuum to more mature basophils with segmenting nuclei, although these may not predominate in early progression. The basophils are larger than neutrophils, and they have wider nuclear segments with smooth contours and retain a fine dispersed chromatin pattern. These characteristics are important in the recognition of morphologic linkage from promyelocytes to myelocytes and segmenting cells of basophil-type lineage. The disease is recognized by the persistence of high levels of blood basophils, with the presence of a low level of circulating blasts that distinguishes the neoplastic syndrome from ephemeral basophilia associated with hypersensitivity reactions.

Animals present with a history of weight loss and loss of appetite and activity but no specific indications until a blood sample is examined. The disease appears to be more typical of chronic myeloid leukemia similar to those with neutrophil and eosinophil predominance in a background of general myeloid hyperplasia. The peripheral blood

basophils are generally poorly granulated, but they are recognizable because of being larger than neutrophils and retaining the characteristic smooth nuclear membranes (Figs. 6.78, 6.79). There is a continuity of immaturity to myelocytes and promyelocytes with rare blastic forms present. The neutrophils and often eosinophils are usually increased and also poorly granulated, and neutrophils may be hypersegmented. With few cases reported, some had the same "myelocyte bulge" or more numerous myelocytes than metamyelocytes in the peripheral blood, as seen in CML of eosinophil or neutrophil type. There is moderate nonresponsive anemia, and platelet levels may vary greatly with suggestions that levels may rise to as high as 1 million/ul. Because basophil leukemia must be differentiated from essential thrombocythemia, with basophilia, cases with extremely high platelet counts should be carefully evaluated for marrow megakaryocyte predominance and atypia and likelihood of a diagnosis of ET. Mahaffey et al. reported that putative basophils are negative with the chloroacetate esterase reaction, whereas mast cells react strongly with this reagent and this would seem to be a useful means of distinguishing between neoplasms characterized by metachromatic granules. In addition, because the basophils progress to segmentation but mast cells tend to retain a round or oval-shaped nucleus, staining of cytologic or histologic preparations with hematoxylin and eosin that less strongly marks the granules assists in the interpretation of nuclear shape.

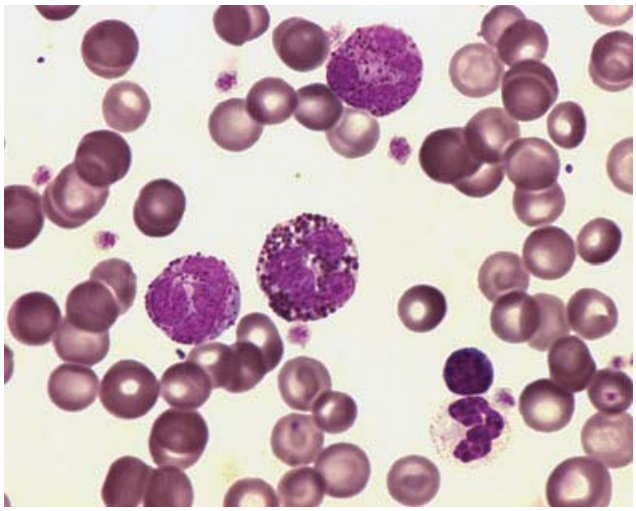

Figure 6.78. Dog: blood, chronic myeloid leukemia of basophil type. The dog has a mild upward shift in the mean cell volume of red cells that appear slightly larger than normal. There are atypical hypersegmented basophils in the left center and lower center with an eosinophil between. These 3 cells are larger than normal and with reduced granulation. A small lymphocyte is in the upper right along with a neutrophil that has reduced normal cytoplasmic granulation. The platelets in the background are at an adequate level. *Slide from R. E. Raskin, DVM.*

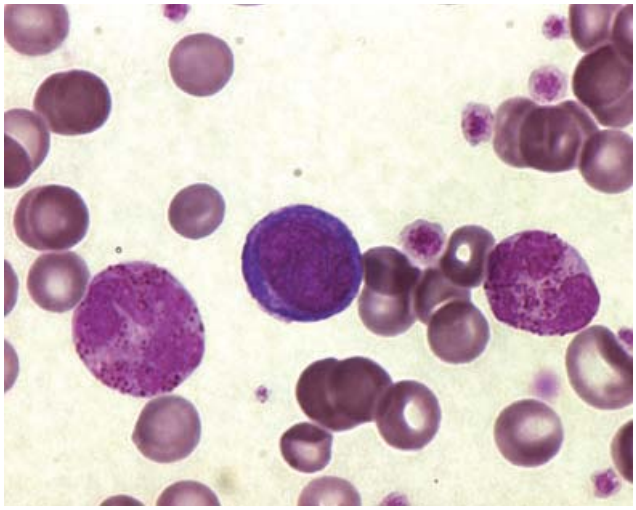

Figure 6.79. Dog: blood, chronic myeloid leukemia of basophil type. There is a type III blast in the center flanked by atypical basophils and numerous platelets. *Slide from R. E. Raskin, DVM.*

The bone marrow is hypercellular with myeloid predominance (Figs. 6.80, 6.81) and numerous megakaryocytes of normal size and morphology; erythroid cells are limited to focal islands but have normoblastic morphology. With progression, the basophilic precursors predominate and the immaturity becomes more apparent.

There is widespread organ infiltration, with liver and spleen most heavily affected. In tissues, the basophils are

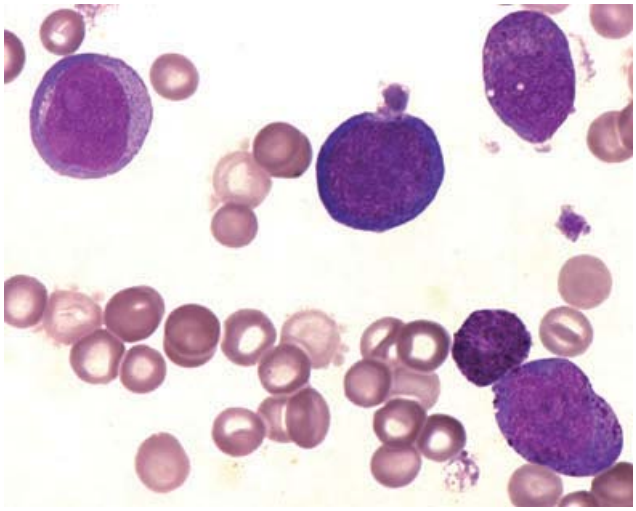

Figure 6.80. Dog: marrow, chronic myeloid leukemia of basophil type, same case as Figure 6.78. There are basophil promyelocytes in the upper and lower right and a maturing basophil in the lower right. The cell in the center is a type II blast and that in the upper left a type III blast with chromatin rimming of a large nucleolus. The blast cells may not be of the same lineage. *Slide from R. E. Raskin, DVM.*

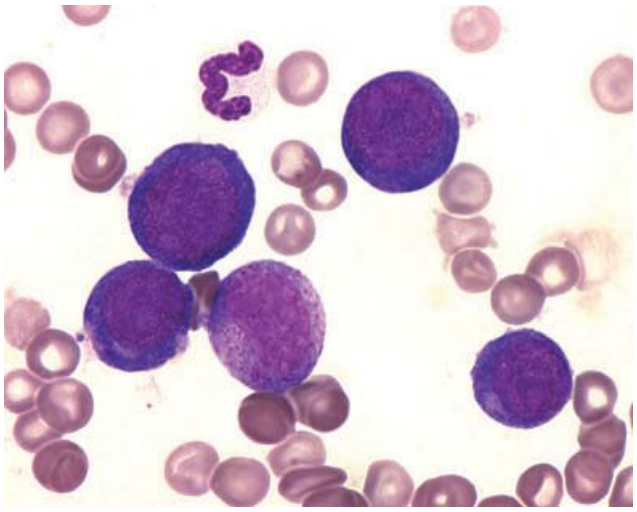

Figure 6.81. Dog: bone marrow, chronic myeloid leukemia of basophil type. The field contains 4 blast cells of myeloid type and a promyelocyte that has a mixture of azurophilic granules with a few metachromatic granules indicating basophilic lineage. The neutrophil is approaching hypersegmentation and has very low cytoplasmic density. *Slide from R. E. Raskin, DVM.*

poorly granulated, but they react normally with a few granules of metachromatic type in most cells and their precursors to the level of promyelocytes.

Basophil leukemia must be differentiated from systemic mast cell disease and from other types of chronic myeloid leukemia that present with basophilia and occasionally eosinophilia. It has not been widely noted that animals, as in humans, have basophilia with chronic myeloid leukemia of neutrophil or eosinophil type, as well as with essential thrombocythemia. Therefore, it is essential to ensure that the most primitive cells of the neoplastic clone are of basophil lineage. It is suggested that these differences can be verified by basophils being negative for chloroacetate esterase; mast cells react positively in this assay. Clonality has not been demonstrated but is assumed to be present. If other cell lineages share the same clonal changes, it is possible that there will be hyperplasia in several lines, and these may make the diagnosis less clear if there is not clear predominance of the basophil line.

The reference by MacEwen et al. notes a remarkable response in a dog with what appears to be a reliable diagnosis of CML of basophil type that had a very good response on treatment with hydroxyurea.

REFERENCES

Alroy, J. (1972) Basophilic leukemia in a dog. *Vet Pathol* 9:90.

Bounous, D.I., Latimer, K.S., Campagnoli, R.P., and Haynes, P.F. (1994) Acute myeloid leukemia with basophilic differentiation (AML, M-28) in a cat. *Vet Clin Pathol* 23:15–18.

Dvorak, A.M. (1998) Cell biology of the basophil. *Int Rev Cytol* 180:87–236.

Dvorak, A.M., and Ackerman, S.J. (1989) Ultrastructural localization of the Charcot-Leyden crystal protein (Lysophospholipase) to granules and intragranular crystals in mature human basophils. *Lab Invest* 60(4):557–567.

Holzworth, J. (1960) Leukemia and related neoplasms in the cat. II Malignancies other than lymphoid. *J Am Vet Med Assoc* 136:107.

MacEwen, E.G., Drazner, F.H., McClelland, A.J., and Wilkins, R.J. (1975) Treatment of basophilic leukemia in a dog. *J Am Vet Med Assoc* 166:376.

Mahaffey, E.A., et al. (1987) Basophilic leukemia in a dog. *J Comp Pathol* 97:393.

Mears, E.A., Raskin, R.E., and Legendre, A.M. (1997) Basophilic leukemia in a dog. *J Vet Intern Med* 11(2):92–94.

Ragan, H.A. (1999) Comparative hematology. In Greer, J.P., Foerster, J., Lukens, J.N., Rodgers, G.M., Paraskevas, F., Glader, B. (eds.), *Wintrobe's Clinical Hematology,* 10th ed. Lippincott Williams & Wilkins, Philadelphia, pp. 2708–2719.

MAST CELL TUMORS

Mast cell tumors (MCT) occur frequently in dogs; less commonly in cats; and rarely in horses, pigs, and primates. In dogs, most mast cell tumors occur in the skin, topographically tend to be more common in caudal areas, and may be ventral and involve the external genitalia. MCT are breed associated and occur most frequently in boxers, pugs, Boston terriers, Weimaraners, and Labrador retrievers. They have a wide age range most frequent in mature middle-aged dogs, and there is no sex predilection. The disease is widely studied and is regularly capable of causing disseminated and fatal disease. The problem is not the diagnosis, which tends to be rather straightforward, but rather in relating the architectural and histological characteristics of the individual tumor to prognosis.

In cats, the disease appears to be more homogeneous, and classification systems have not been predictive of clinical behavior. The disease in other animal species is too infrequent to define other than as a generic diagnosis. In humans, mast cell tumors are defined as cutaneous (urticaria pigmentosa) or systemic and involving marrow spleen and nodes. Grade I tumors in humans tend to have only focal lesions in marrow and are primarily in skin; the Type II and III lesions did not involve skin and were systemic. The Grade II lesion is often associated with myeloproliferative diseases of both AML and CML type and the Type III lesion usually presented as mast cell leukemia. In human MCT, the chloroacetate esterase stain is used to identify mast cells, as well as the mast cell tryptase and, more commonly, toluidine blue and Giemsa

stains. The positive staining of human mast cells with chloroactetate esterase would cast doubt on the use of this reagent to distinguish basophils from mast cells in animals.

A system of grading for canine MCT by Patnaik et al. showed wide separation of survival curves based on a morphological grading system of I–III, but repeated studies show that pathologists, in applying this system, have a high level of interobserver variability. Consequently, grading of MCT appears to be relatively unreliable in predicting outcome. Goldschmidt has summarized the cytologic features of MCT in what might be expected to be a system that could be applied in a consistent and reproducible manner by individuals and with agreement between observers.

Work has shown that the frequency of nucleolar organizer regions correlates well with tumor grade and might be expected to correlate negatively with survival. A recent study on 100 cases of canine MCT, which was reviewed partially blinded by pathologists from a number of institutions, concluded that immunohistochemical staining for KIT and tryptase gave the most reproducible means of predicting survival. Because the determination of the nucleolar organizer areas is, in effect, a measure of cytologic anaplasia, it would seem that a careful and consistent application of the cellular criteria as already defined would have clinical relevance. In the study of the 100 dogs in which the outcome was known, there were 9 cases felt to be Grade III tumors by the organizers, and presumably these cases were also known to have resulted in dissemination. By one observer, 6 of these 9 cases were identified on histocytologic grounds as Grade III MCT, and the remaining 3 cases were noted to have increased anisokaryosis. This blind study did show that the depth of the lesion in the panniculus was not a measure of likelihood of dissemination. Thus, it would seem that criteria that included a careful cytologic evaluation, including nuclear size, chromatin distribution and staining density, nucleolar presence number, and shape with anisokaryosis and mitotic rate would relate to the level of tumor aggression, as it does for many other neoplasms. The examples of tumor grading presented here as Grade I (Figs. 6.82–6.84), Grade II (Figs. 6.85–6.89) and Grade III (Figs. 6.90–6.92) are selected to present these criteria in a manner that not only assists the differentiation of MCT from basophils but also relates to the biological behavior of the MCT neoplasm. An untested feature of both mast cell neoplasms and cutaneous plasmacytomas is the presence of more cytologic anaplasia in deeper areas of the mass (see Figs. 6.86, 6.87). Changes include greater anisokaryosis and more variation in chromatin distribution, less dense and more variable cytoplasmic granulation (see Figs. 6.88, 6.89, 6.91), and more prominent nucleoli (see Fig. 6.92).

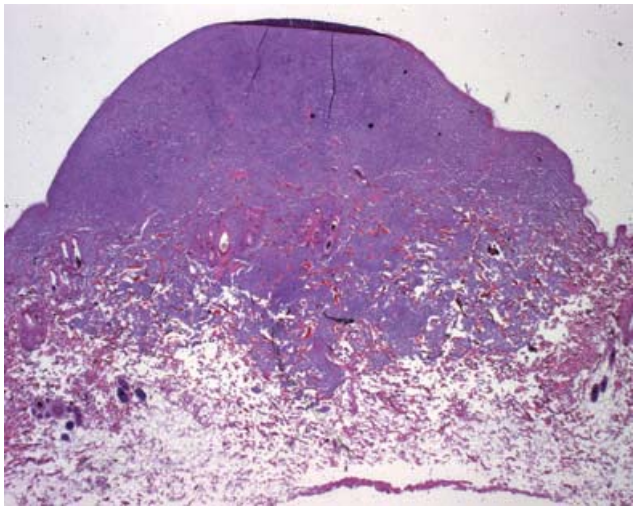

Figure 6.82. Cat: skin, mast cell tumor, Grade I. An intradermal mass 0.5 cm in diameter removed from the left rib of an 8-year-old domestic shorthair cat. The lesion is a high-up infiltration of the superficial dermis extending through the dermis with minimal penetration of the panniculus and flanked by normal-haired skin.

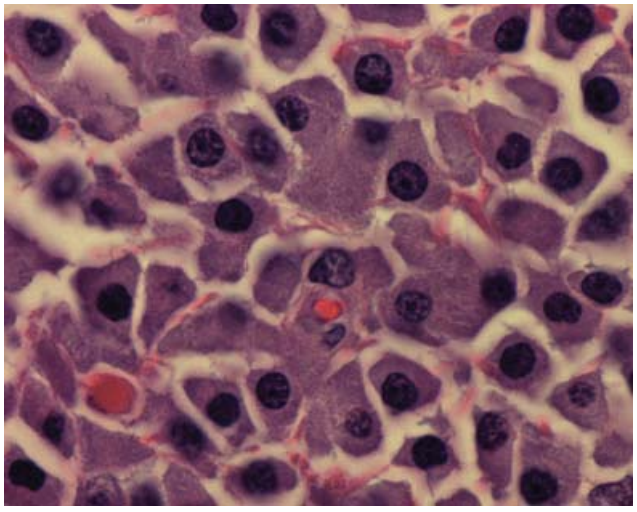

Figure 6.83. Cat: skin, mast cell tumor. Detail of Figure 6.82. Under high magnification, the nuclei, which appear very uniform at 400× magnification can be seen to have considerable variation in diameter, staining density, and chromatin patterns. A single red cell (center) provides an index of size. Most nuclei contain 1–2 small nucleoli that are generally obscured and may be mistaken for large chromocenters. The animal had recurrent mast cell tumors considered Grade I.

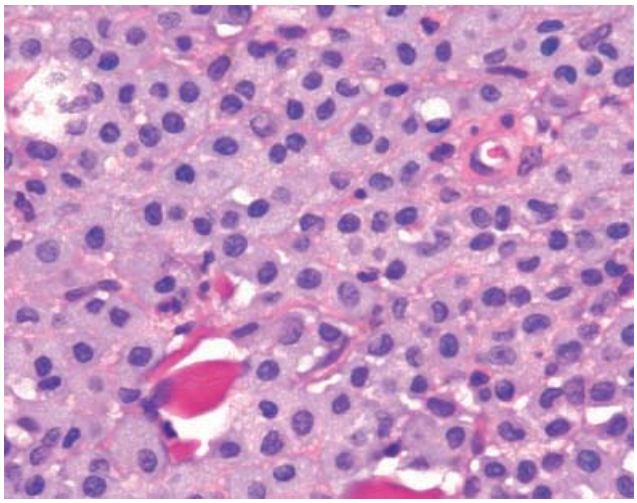

Figure 6.84. Dog: skin, mast cell tumor, Grade I. A single red cell in the upper right provides an index of size. The nuclei are relatively round and uniform with a finely branched chromatin pattern and a few large chromocenters with occasional cells having a single small nucleolus. Mitotic figures were not found.

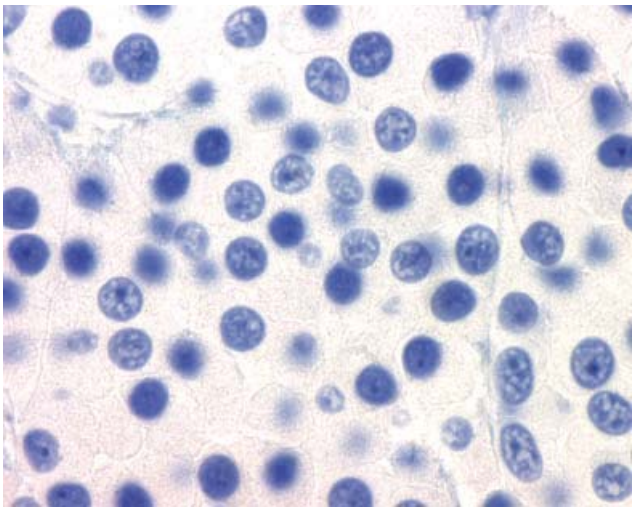

Figure 6.86. Dog: skin, mast cell tumor, Grade II. Detail of Figure 6.85. The nuclei are moderately and uniformly larger and retain a round to oval outline. The chromatin pattern varies from agranular and dispersed to coarse granular with most cells having 1–2 small nucleoli. The cytoplasm remains relatively abundant and binucleation is more prominent. Tissue preparation is of negative immunological stain with only nuclear counterstain to enhance nuclear detail.

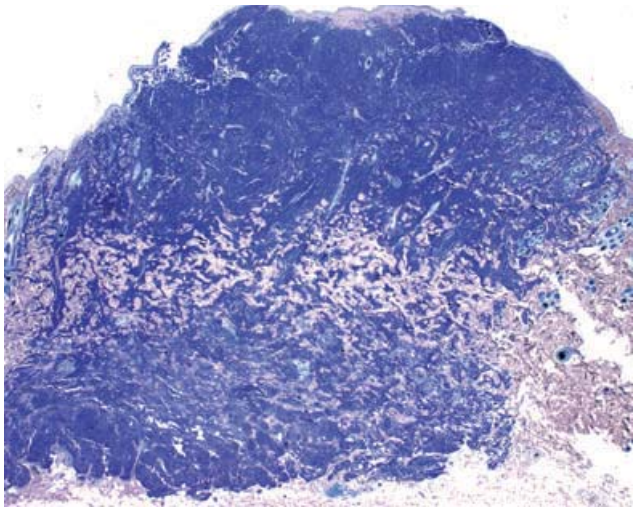

Figure 6.85. Dog: skin, mast cell tumor, Grade II. The lesion is a high-up infiltration of the superficial and deep dermis that extends in a deep band into the panniculus. The deep penetration is eccentric to the surface mass and well within the boundaries of the raised surface area on the right but extends beneath normal haired skin on the left. With Giemsa staining, it is apparent that the cells in the more superficial areas are much more deeply stained and presumably more heavily granulated than those in deeper areas of the mass.

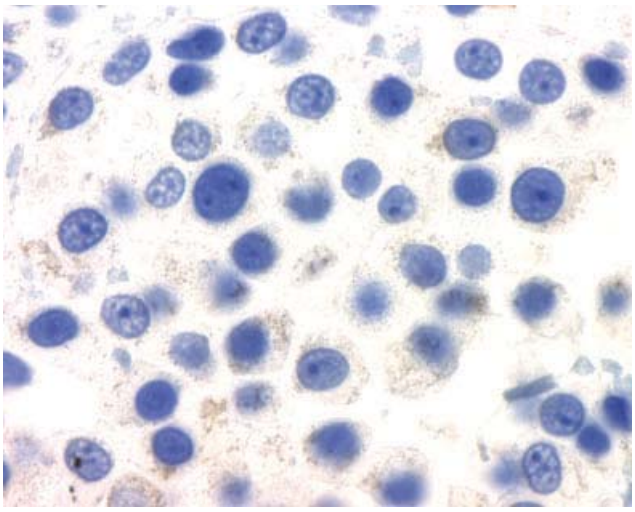

Figure 6.87. Dog: skin, mast cell tumor, Grade II, same tissue as Figure 6.86. The image is from an area adjacent to the deep margin of tumor with greater anisokaryosis. The nuclei vary more widely in size and shape, with the larger cells having an irregularly branched chromatin pattern with parachromatin clearing and 1–3 small nucleoli.

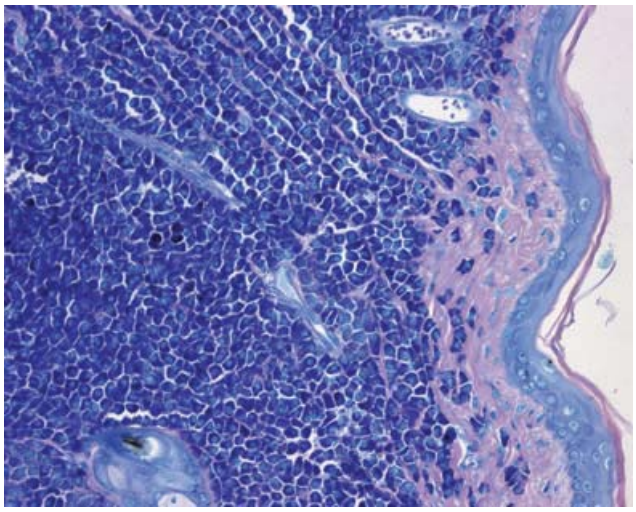

Figure 6.88. Dog: skin, mast cell tumor. Detail of Figure 6.85. Giemsa staining provides a uniformly dense representation of tumor cell granulation in the superficial dermis.

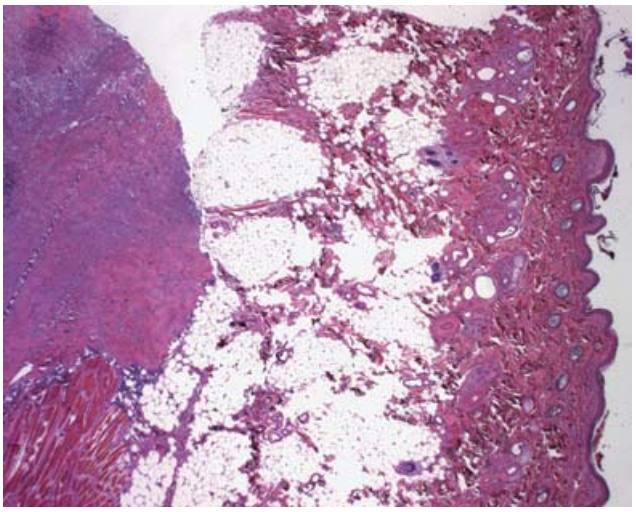

Figure 6.90. Dog: skin, mast cell tumor, Grade III. The tumor mass lies within the panniculus, beneath an area of thickened skin. There is irregular infiltration of superficial skeletal muscle in the lower left.

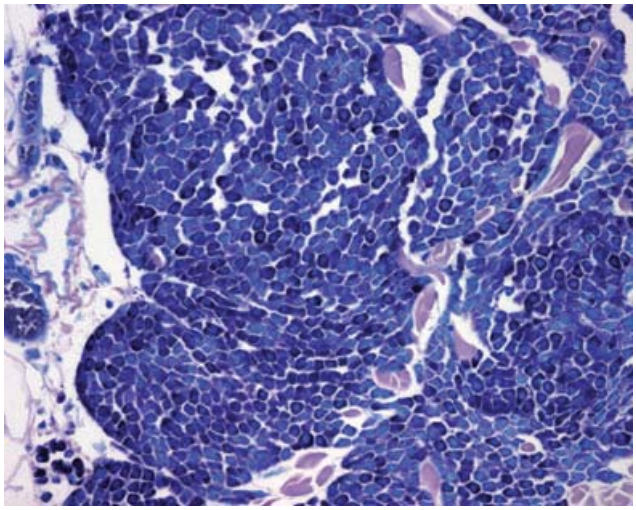

Figure 6.89. Dog: skin, mast cell tumor. Detail of Figure 6.85 at a junctional area of deep tumor margin and underlying tissue. There is marked variation in depth of metachromatic staining in cells at the deeper surface of the tumor.

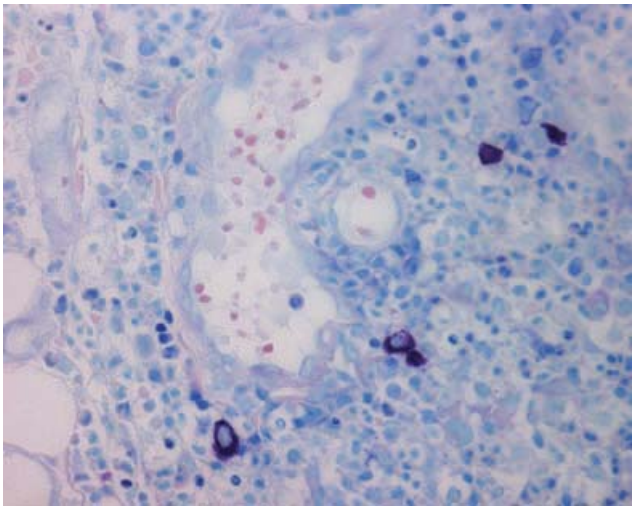

Figure 6.91. Dog: skin, mast cell tumor, Grade III. Deep area of interface of Grade III tumor with underlying tissues. Giemsa stain demonstrates very low granulation with most of the tumor mass having an irregular interface with benign tissues. The deeply stained cells have large nuclei and are likely benign mast cells.

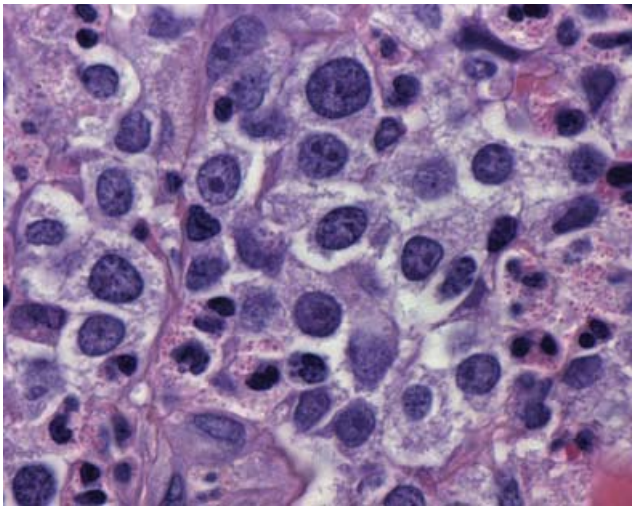

Figure 6.92. Dog: skin, mast cell tumor, Grade III. Detail of Figure 6.91. There is marked anisokaryosis with all cells having hyperchromatic coarse granular chromatin with parachromatin clearing and typically one prominent nucleolus. There is moderate variation in nuclear shape with some cells elongated and with both smooth and sharp nuclear indentations. The cytoplasm is greatly reduced in volume and granule content and there are frequent binucleated cells, but mitotic figures are absent from most fields at 400×.

REFERENCES

Goldschmidt, M.H., and Shofer, F.S. (1998) Mast cell tumors. In *Skin Tumors of the Dog and Cat*, Chapter 28. Butterworth-Heinemann, Oxford, pp. 231–244.

Hottendorf, G.H., and Nielsen, S.W. (1968) Pathologic report of 29 necropsies on dogs with mastocytoma. *Pathol Vet* 5:102–121.

Kiupel, M., Webster, J.D., Kaneene, J.B., Miller, R., and Yuzbasiyan-Gurkan, V. (2004) The use of KIT and tryptase expression patterns as prognostic tools for canine cutaneous mast cell tumors. *Vet Pathol* 41:371–377.

Kravis, L.D., Vail, D.M., Kisseberth, W.C., Ogilvie, G.K., and Volk, L.M. (1996) Frequency of argyrophilic nucleolar organizer regions in fine-needle aspirates and biopsy specimens from mast cell tumors in dogs. *JAVMA* 209(8):1418–1420.

Molander-McCrary, H., Henry, C.J., Potter, K., Tyler, J.W., and Buss, M.S. (1998) Cutaneous mast cell tumors in cats: 32 cases (1991–1994). *J Am An Hosp Assoc* 34:281–284.

Northrup, N.C., Harmon, B.G., Gieger, T.L., Brown, C.A., Carmichael, K.P., Garcia, A., Latimer, K.S., Munday, J.S., Rakich, P.M., Richey, L.J., Stedman, N.L., Cheng, A.L., and Howerth, E.W. (2005) Brief communications: Variation among pathologists in histologic grading of canine cutaneous mast cell tumors. *J Vet Diagn Invest* 17:245–248.

Northrup, N.C., Howerth, E.W., Harmon, B.G., Brown, C.A., Carmichael, K.P., Garcia, A.P., Latimer, K.S., Munday, J.S., Rakich, P.M., Richey, L.J., Stedman, N.L., and Gieger, T.L. (2005) Brief communications: Variation among pathologists in the histologic grading of canine cutaneous mast cell tumors with uniform use of a single grading reference. *J Vet Diagn Invest* 17:561–564.

Ozaki, K., Yamagami, T., Nomura, K., and Narama, I. (2002) Mast cell tumors of the gastrointestinal tract in 39 dogs. *Vet Pathol* 39:557–564.

Patnaik, A.K., Ehler, W.J., and MacEwen, E.G. (1984) Canine cutaneous mast cell tumor: Morphologic grading and survival time in 83 dogs. *Vet Pathol* 21:469–474.

Séguin, B., Leibman, N.F., Bregazzi, V.S., Ogilvie, G.K., Powers, B.E., Dernell, W.S., Fettman, M.J., and Withrow, S.J. (2001) Clinical outcome of dogs with grade-II mast cell tumors treated with surgery alone: 55 cases (1996–1999). *JAVMA* 218(7):1120–1123.

Simoes, J.P.C., Schoning, P., and Butine, M. (1994) Prognosis of canine mast cell tumors: A comparison of three methods. *Vet Pathol* 31:637–647.

Simpson, A.M., Ludwig, L.L., Newman, S.J., Bergman, P.J., Hottinger, H.A., and Patnaik, A.K. (2004) Evaluation of surgical margins required for complete excision of cutaneous mast cell tumors in dogs. *JAVMA* 224(2):236–240.

Strefezzi, R.D.F., Xavier, J.G., and Catão-Dias, J.L. (2003) Morphometry of canine cutaneous mast cell tumors. *Vet Pathol* 40:268–275.

Chapter 7

Myeloproliferative/Myelodysplastic Diseases

Myelodysplastic syndrome/myeloproliferative diseases (MDS/MPD) is a new category of chronic myeloid disorders introduced by the revisions of the REAL and revised WHO classification systems. The pathologists engaged in these discussions felt that the three previously described entities of atypical or Philadelphia chromosome negative—chronic myeloid leukemia (aCML), chronic myelomonocytic leukemia (CMML), and juvenile myelomonocytic leukemia (jMML)—had many features in common. To reflect these commonalities, they are included as subtypes in the MDS/MPD category.

The logic in the classification systems that preceded this subdivision cited several criteria as the basis for differentiation of chronic myeloproliferative diseases (CMPD) and the disorders known as myelodysplastic diseases (MDS). The distinctions between these entities were that in CMPD hematopoiesis was effective; in MDS it was ineffective. The MDS lesions were identified by significant cytologic dysplasia at the time of diagnosis; any degree of dysplasia is uncommon in the initial presentation of CMPD. Further, organomegaly of spleen and liver is almost always present in cases of CMPD but is not a feature of the MDS conditions, or is of minor development. Although it is clear that CMPD and MDS are separable, entities with overlapping features were given the designation of *MDS/MPD*. Although this degree of disease distinction is not now made in the classification of hematopoietic neoplasms in animals, it is important that veterinarians understand the background for these disease categories in order that this level of discrimination can be brought to the diagnosis of myeloid tumors in animals.

ATYPICAL CHRONIC MYELOID LEUKEMIA

The nomenclature for this entity might suggest that it is like CML with minor differences, but in contrast aCML is a unique human disorder in which the characteristic t(9;22) chromosomal translocation (Ph chromosome) is lacking. aCML has the leukocytosis comprised of mature and immature neutrophils of CML, but it also has a constant level of evident dysplasia that may involve one or all cell lineages. aCML is not difficult to distinguish from CML in the chronic phase. However, it is more difficult to distinguish from the accelerated phase of CML and the differentiation from CMML that presents with dysplasia may be very difficult.

The presentation of aCML in humans is characteristically in an individual in the 7th decade that presents with symptoms related to anemia, thrombocytopenia, or splenomegaly. The presenting leukocyte count is in the range of 30,000–50,000/ul and composed primarily of neutrophils and immature precursors, including blasts. The blasts alone don't exceed 5% of total cells, and the lesser stages of immaturity—including promyelocytes, myelocytes, and metamyelocytes—may total 10–20% of total peripheral blood leukocytes. Monocytes are a minor population at 3–10% of total cells but may be increased in absolute terms. Unlike CML, basophilia is uncommon in aCML. The most significant distinguishing feature of aCML is dysplasia, as seen in the neutrophil series as very characteristic clumping of chromatin and hyposegmentation of Pelger-Huët type. Anemia is always present, and blood manifestations of marrow dyserythropoiesis include giant oval red cells accompanied by thrombocytopenia of moderate degree with increased anisocytosis.

The marrow is hypercellular due to myelopoiesis with increased blasts that occur singly in colonies of myeloid progeny. Megakaryocytes may be reduced, but the most reliable finding is the presence of the abnormal hyperchromicity and apparent aggregation of chromatin in maturing granulocytes. The dyspoiesis is also present in the erythroid and megakaryocytic systems, with the latter series having hypolobulation and micromegakaryocytic forms present.

Human patients with aCML have a poor survival pattern with median durations following diagnosis of 20 months, often with progression into AML. A syndrome like aCML has not been recognized in animals.

REFERENCES

Arico, M., Biondi, A., and Pui, C.-H. (1997) Juvenile myelomonocytic leukemia. *Blood*, 90:479–488.

Bennett, J., Catovsky, D., Daniel, M.T., et al. (1994) The chronic myeloid leukaemias: Guidelines for distinguishing chronic granulocytic, atypical chronic myeloid, and chronic myelomonocytic leukaemias. Proposals by the French-American-British cooperative leukaemia group. *Brit J Haematol* 87:746–754.

Felman, P., Bryon, P., Gentilhomme, O., et al. (1988) The syndrome of abnormal chromatin clumping in leucocytes: A myelodysplastic disorder with proliferative features? *Brit J Haematol* 70:49–54.

Galton, D.A.G. (1992) Haematological differences between chronic granulocytic leukemia, atypical chronic myeloid leukaemia, and chronic myelomonocytic leukaemia. *Leuk Lymph* 7:343–350.

Harris, N.L., Jaffe, E.S., Diebold, J., Flandrin, G., Muller-Hermelink, H.K., Vardiman, J., Lister, T.A., and Bloomfield, C.D. (2000) The World Health Organization classification of neoplastic diseases of the haematopoietic and lymphoid tissues: Report of the Clinical Advisory Committee Meeting, Airlie House, Virginia, November 1997. *Histopathol* 36:69–87.

Invernizzi, R., Custodi, P., De Fasio, P., et al. (1990) The syndrome of abnormal chromatin clumping in leucocytes: Clinical and biological study of a case. *Haematol* 75:532–536.

Michaux, J., and Martiat, P. (1993) Chronic myelomonocytic leukaemia (CMML): A myelodysplastic or myeloproliferative syndrome? *Leuk Lymph* 9:35–41.

Montefusco, E., Alimena, G., Lo Coco, F., et al. (1992) Ph-negative and bcr-negative atypical chronic myelogenous leukemia: Biological features and clinical outcome. *Ann Hematol* 7:343–350.

Pugh, W.C., Pearson, M.C., Vardiman, J.W., et al. (1985) Philadelphia chromosome-negative chronic myelogenous leukemia: A morphologic reassessment. *Brit J Haematol* 60:457–467.

Shukrulla, N., Finiewicz, K.J., Roulston, D., et al. (1997) Is atypical chronic myeloid leukemia a high white cell count myelodysplastic syndrome? *Mod Pathol* 10:134a.

CHRONIC MYELOMONOCYTIC LEUKEMIA

Chronic myelomonocytic leukemia (CMML) occurs in dogs, cats, and cows and is likely unrecognized in other animals. Historically, CMML was first known as a *preleukemic syndrome* and characterized by the presence of increasing numbers of blasts in the bone marrow and a high incidence of monocytoid leukemic transformation. This preceded our understanding of MDS as *myelokathexis* to indicate that the marrow was hyperplastic but the cells were being destroyed in situ and not released into the blood. As the syndrome of MDS began to be understood, the concept of *ineffective hematopoiesis* was described for conditions characterized by progressive cytopenias, functional abnormalities, and bone marrow hypercellularity. Because of the presence of prominent dysplastic changes, CMML was classified within the MDSs by the FAB Group (Bennett et al., 1982). However, proliferative features of CMML, including the presence of a peripheral monocytosis and sometimes the development of a marked leukocytosis, were uncharacteristic of MDS. Based on this combination of dysplastic and proliferative features, CMML was recently reclassified as one of the myelodysplastic and myeloproliferative disorders. To recognize the powerful prognostic weighting of bone marrow blast cell counts in this disease, CMML was further split into CMML-1 with <10% blasts and CMML-2 with 11–20% blasts.

In animals, the term *CMML* was used to indicate a paradoxical disease characterized by ineffective hematopoiesis, peripheral blood cytopenias with a packed bone marrow, and death of cells in the marrow. In a limited number of dogs observed by this author, the presentation is of a mature animal that presents in chronic ill health with no localizing signs, and on examination of blood there is a variable total leukocyte count of 4,000–15,000/ul with rising counts progressing to 30,000–35,000/ul. A characteristic of the blood picture is a monocytosis that remains in the region of 4,000/ul with mild anemia, low normal lymphocytes, and often neutropenia.

Dogs with CMML tend to be 5–8 years of age, but cases occur in 2-year-old animals. Cats also tend to be older, usually greater than 10 years of age, and a single case was found in an older dairy cow. The animals are usually only mildly anemic and the blood picture is normochromic normocytic. The total leukocyte count in one dog seen by this observer and followed over a period of months presented at 4,300/ul and rose to 14,900/ul and finally to 35,800/ul, with the monocytes over that period ranging from 3,700/ul to 4,700/ul and finally to 12,500/ul. The peripheral blood monocytes retain a slate gray cytoplasm that has the same density from the nuclear membrane to the cytoplasmic membrane and is frequently vacuolated (Figs. 7.1, 7.2) The nuclei tend to be deeply cleft, almost binucleated, and the nuclear chromatin pattern is characteristic and has large dense chromocenters surrounded by lighter staining areas (Fig. 7.3), but without parachromatin clearing or the fine chromatin bands seen in prolymphocytic leukemia. The promonocytes are large cells with nuclei 3 red cells in diameter and cell diameter of 4 red cells. The promonocytic nuclei have a fine woven-appearing chromatin pattern with 2–3 prominent nucleoli, and they appear more lobulated than indented. The cytoplasm is more deeply basophilic and may not be vacuolated, but the vacuoles, when present, may penetrate the nucleus at all stages of maturation (Fig.

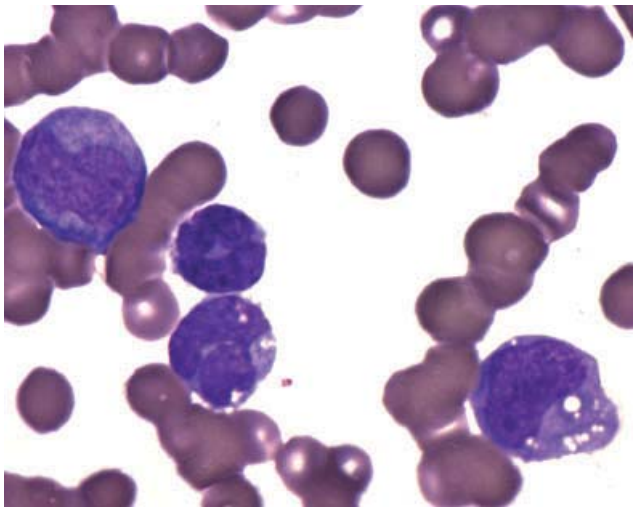

Figure 7.1. Dog: blood, chronic myelomonocytic leukemia. Two larger cells with typical monocytic features have irregularly shaped nuclei retaining a fine chromatin pattern and uniformly dense cytoplasm without perinuclear clearing. There are irregular cytoplasmic vacuolations and faint fine pink granulation. The 2 smaller cells have irregular shaped nuclei with smooth nuclear contours and are likely typical small monocytic cells.

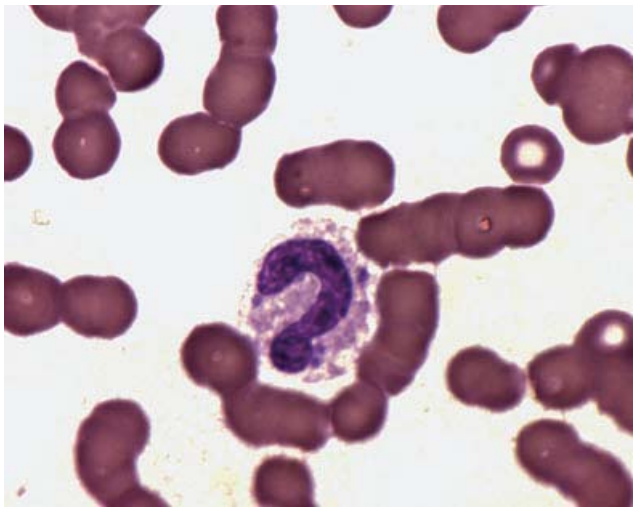

Figure 7.2. Dog: blood, chronic myelomonocytic leukemia. The young neutrophil has smooth nuclear contours but typical large chromocenters and small areas of chromatin clearing. The cytoplasm lacks normal granular density but has abnormal basophilia with multiple vacuolations and multiple Doehle bodies.

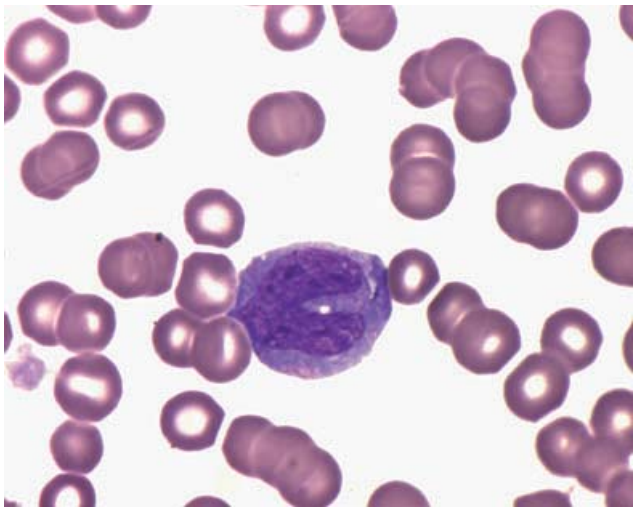

Figure 7.3. A large young monocyte with typical focal chromatin aggregations and a small almost inapparent nucleolus and relatively abundant cytoplasm.

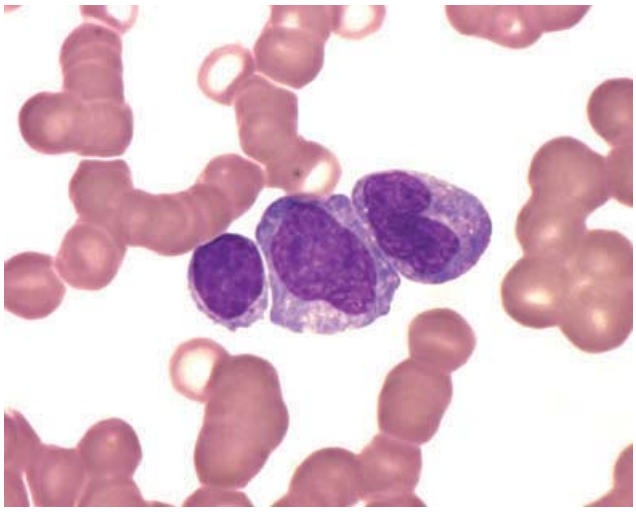

Figure 7.4. Dog: blood, chronic myelomonocytic leukemia. Two young monocytes with nuclear lobulations with small nucleoli in the cell at left and both have relatively dense cytoplasm with few very small vacuolations. A medium-sized lymphocyte is at left.

7.4, see also Fig. 7.3). Blasts are present, but rare, and are larger than myeloblasts with mild irregularities of nuclear membrane and high cytoplasmic basophilia (Fig. 7.5). Granulation is subdued in the whole lineage with very few finely azurophilic granules. There is prominent dysplasia in the neutrophil series with many giant metamyelocytes in the blood that may mimic the maturing monocytes, but they have much more deeply stained large chromocenters that contrast more clearly against the lighter-stained areas (Fig. 7.6). The metamyelocyte cytoplasm lacks basophilia and has very light granulation, often with fine vacuolation. These features are also present in neutrophils that may reflect the origin of this cell from a primitive precursor in common to the monocyte. An occasional basophil is present, and these have immaturity and dysplastic changes with large nuclei almost twice the size of neutrophils but with characteristic smooth nuclear

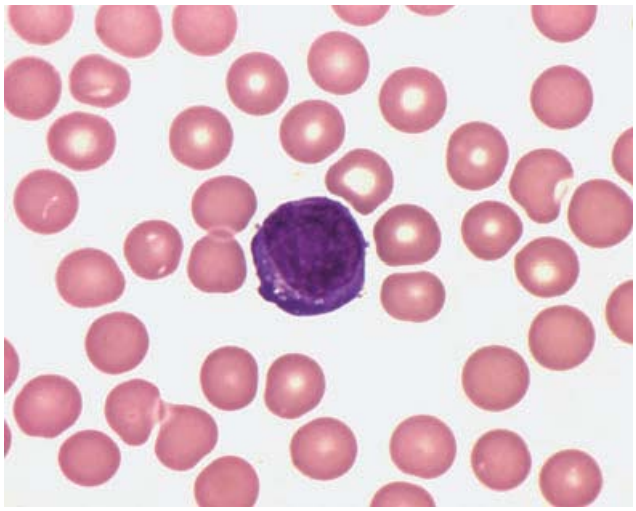

Figure 7.5. Dog: blood, chronic myelomonocytic leukemia. A blast cell of uncertain lineage. The nucleus retains several small nucleoli with increased density of chromatin likely representing a long time in circulation. The cytoplasm is moderate in volume, eccentrically placed, highly basophilic, and lightly vacuolated.

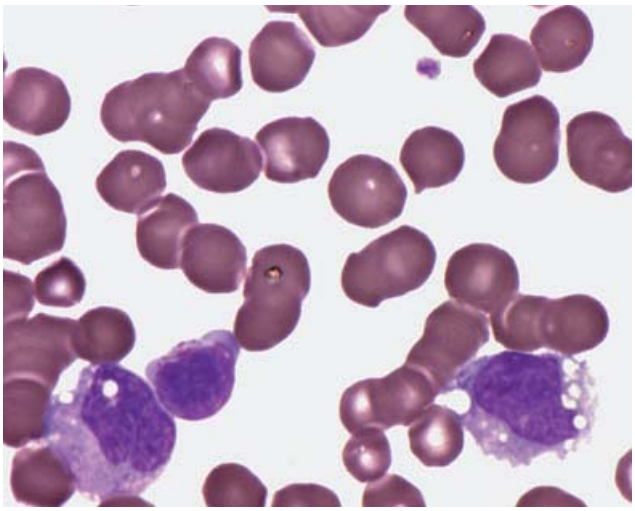

Figure 7.7. The 2 monocytes are heavily vacuolated and accompany a small lymphocyte with prominent pink granulation. There is a single platelet in the upper right that is small with normal granulation and has moderate basophilia.

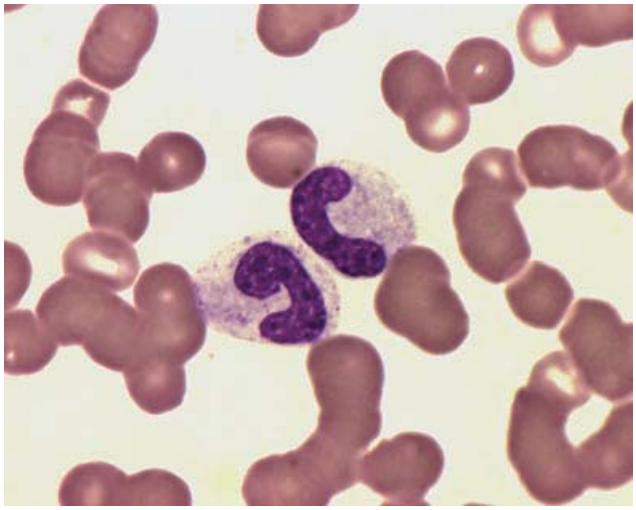

Figure 7.6. Dog: blood, chronic myelomonocytic leukemia. The lower cell is an early segmented neutrophil and the one above is a late metamyelocyte. Both have very low cytoplasmic granulation with abnormal levels of basophilia and fine vacuolations. Large dense chromocenters are typical and have progressed out of phase with nuclear segmentation.

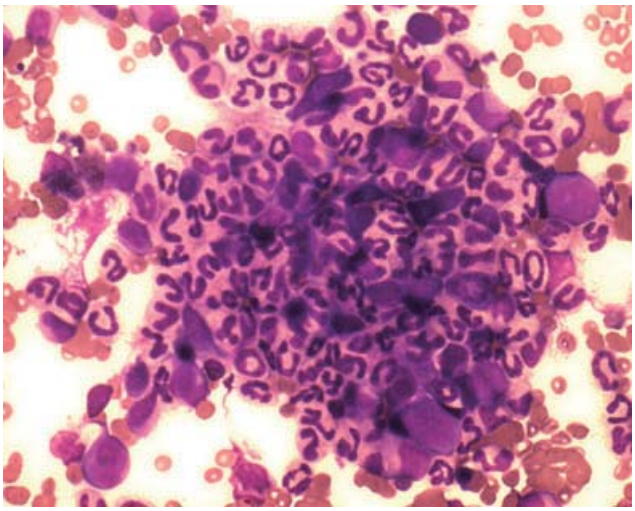

Figure 7.8. Dog: bone marrow aspirate, chronic myelomonocytic leukemia. Marrow granule is solidly hematopoietic with a complete absence of fat cells. There is a marked myeloid shift with an abundance of myeloid precursors and maturing neutrophils with relatively few erythroid cells.

contours and only 5–10 metachromatic granules of larger than normal size. Lymphocytes are of medium size and not remarkable for immaturity or basophilia, as in reactive states, and platelets are small and in deficient numbers (Fig. 7.7).

The bone marrow is hyperplastic and characteristically with a marked myeloid shift and the appearance of many large myeloid cells similar in size to the promonocytes in the peripheral blood (Figs. 7.8, 7.9). These cells appear to predominate with blasts only mildly increased. The promyelocytes in marrow have lightly or poorly granulated cytoplasm and there are numerous giant metamyelocytes (Fig. 7.10). The dysplastic changes appear in the erythroid system, with late stage divisions (Fig. 7.11) and an occasional late stage rubricyte with a satellite nucleus of much smaller size, but larger than a Howell-Jolly body

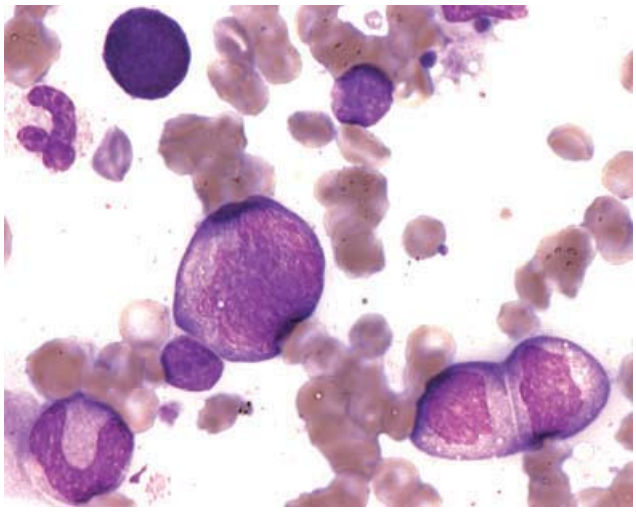

Figure 7.9. Dog: bone marrow aspirate, chronic myelomonocytic leukemia. The very large cell in the center is typical of promonocytes of marrow and blood with a fine chromatin pattern and large faintly outlined nucleoli. There is a metamyelocyte in the lower left and a segmented neutrophil in the upper left. The promonocyte is accompanied by a small lymphocyte to the left and a larger one above and to the right. The cell in the lower right is likely a myelocyte in late telophase. The very basophilic cell in the upper left is most likely an early erythroid precursor.

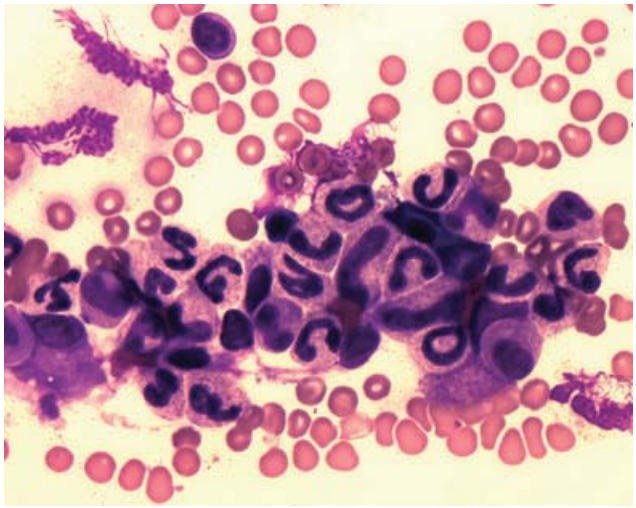

Figure 7.10. Dog: bone marrow aspirate, chronic myelomonocytic leukemia. The image is of a cluster of developing myeloid cells with numerous giant metamyelocytes and an almost complete absence of rubricytes except for one with polychromatic cytoplasm adjacent to the myeloid cells in the center. The irregular chromatin clusters in the upper left likely represent an injured anaphase of a developing myeloid cell.

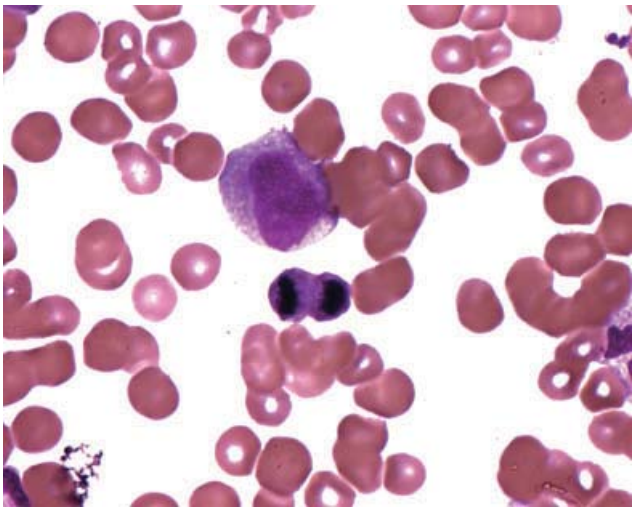

Figure 7.11. Dog: bone marrow aspirate, chronic myelomonocytic leukemia. A young monocyte is next to an example of dyserythropoiesis in the form of late stage anaphase. Erythroid nuclear division normally ends at the basophilic rubricyte stage.

(Fig. 7.12). At termination, there is hepatosplenomegaly and variable involvement of lymph nodes. The differentiation in spleen and liver is less apparent than in the marrow, with most descriptions indicating a primarily monocytic proliferation in these sites.

The diagnosis for CMML in the dog rests on recognition of a process of chronic monocytosis that is combined with relatively low leukocyte count and immaturity, as well as the presence of dysplastic changes in the neutrophil and erythroid lineages. Because there are both immaturity and dysplastic changes in the neutrophil and monocytic series, it is essential to carry out chloroacetate esterase stains for identification of the neutrophil lineage and nonspecific or butyl acetate esterase for the monocytic cells. The differential diagnosis of CMML includes aCML and may include CML and acute monocytic leukemia. If there is marked immaturity in the peripheral blood, the bone marrow should be examined for a level of blasts exceeding 20%, which would indicate AML M5B.

There are striking similarities between human CMML and the disease identified as CMML in animals. Human cases present with leukocyte counts in the range of 15,000–30,000/ul, with some much higher and lower. In most cases, the absolute monocyte count is less than 5,000/ul, but it also may vary widely above and below that level. Anemia is always mild and severe thrombocytopenia is rarely seen. In human CMML, the blood monocytes make up at least 10% of leukocytes and may account for 30–50% of the total count. These are atypical with hypolobulation and granulation maybe increased or decreased. Blasts and promonocytes make up less than 5% of peripheral blood leukocytes. There is significant

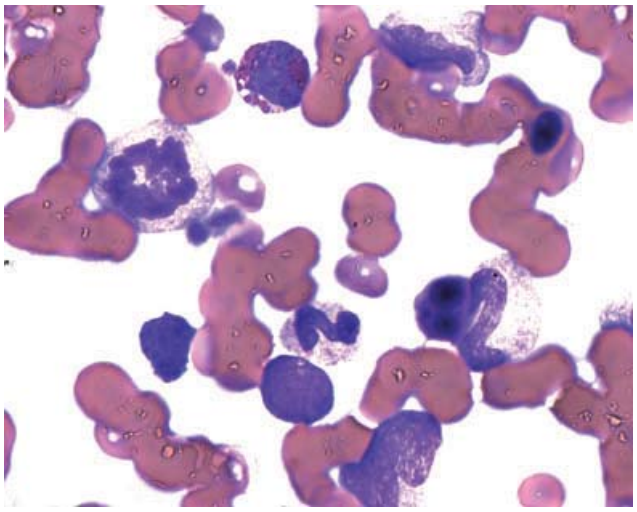

Figure 7.12. Dog: bone marrow aspirate, chronic myelomonocytic leukemia. Multiple indications of dyserythropoiesis are present in the densely stained late stage rubricyte with round dense structureless nuclei characteristic of metarubricyte stage that contains 2 Howell-Jolly bodies (lower right). The dark oval cell in the upper right is likely a metarubricyte with a young eosinophil (center) and to the left a myelocyte in metaphase. The atypical metarubricyte is flanked by neutrophils and a primitive cell of uncertain lineage (center) and an injured rubricyte in the lower left.

dysplasia of the neutrophil series with pseudo Pelger-Huët (bisegmented) changes, and most cases have reduced granulation. The marrow in human CMML is always hypercellular and has a myeloid appearance, with nonspecific esterase stains required to assess the level and immaturity accurately in that lineage. Blasts are below 5% of marrow cells, and if as many as 20% of cells are blastic there is conversion to acute leukemia.

CMML is characterized as an entity that has monocytic proliferation coupled with dysplasia that often involves all three lineages. In half of human cases, there is leukocytosis due to monocytosis and neutrophilia with splenomegaly, skin involvement, and effusions in serous cavities. These cases have minimal dysplasia and are more like a case of CMPD. In the other half of cases, there is low or normal leukocyte counts with absolute monocytosis and usually without splenomegaly but with significant dysplasia, making this variant more like MDS. These characteristics have led to suggestions that CMML be divided into myeloproliferative and myelodysplastic variants; however, there is no clinical difference in the two forms that would lend relevance to a subclassification. An additional reason against making these distinctions is that some cases that present with the dysplastic form with low leukocyte levels may, with time, become more like the proliferative variant, as in the case of the canine case described above.

REFERENCES

Anastasi, J., and Vardiman, J.W. (2001) Chronic myelogenous leukemia and the chronic myeloproliferative diseases. In Knowles, D.M. (ed.), *Neoplastic Hematopathology,* 2nd ed. Lippincott Williams & Wilkins, Philadelphia, pp. 1745–1790.

Bennett, J.M., Catovsky, D., Daniel, M.T., et al. (1982) Proposals for the classification of the myelodysplastic syndromes. *Brit J Haematol* 51:189–199.

Bennett, J.M., Catovsky, D., Daniel, M.T., et al. (1994) The chronic myeloid leukaemias: Guidelines for distinguishing chronic granulocytic, atypical chronic myeloid, and chronic myelomonocytic leukaemias. Proposals by the French-American-British cooperative leukaemia group. *Brit J Haematol* 87:746–754.

Bourantas, K.L., Tsiara, S., Panteli, A., Milionis, C., and Christou, L. (1998) Pleural effusion in chronic myelomonocytic leukemia. *Acta Haematol* 99:34–37.

Buresh, A., Perentesis, J., Rimsza, L., Kurtin, S., Heaton, R., Sugrue, M., and List, A. (2005) Hyperleukocytosis complicating lonafarnib treatment in patients with chronic myelomonocytic leukemia. *Leuk* 19:308–310.

Couto, C.G., and Kallet, A.J. (1984) Preleukemic syndrome in a dog. *JAVMA* 184(11):1389–1392.

Galton, D.A.G. (1992) Haematological differences between chronic granulocytic leukemia, atypical chronic myeloid leukaemia, and chronic myelomonocytic leukaemia. *Leuk Lymph* 7:343–350.

Germing, U., Gattermann, N., Minning, H., et al. (1998) Problems in the classification of CMML: Dysplastic versus proliferative type. *Leuk Res* 22:871–878.

Germing, U., Strupp, C., Aivado, M., and Gattermann, N. (2002) New prognostic parameters for chronic myelomonocytic leukemia? *Blood* 100(2):731–733.

Harris, N.L., Jaffe, E.S., Diebold, J., Flandrin, G., Muller-Hermelink, H.K., Vardiman, J., Lister, T.A., and Bloomfield, C.D. (2000) The World Health Organization classification of neoplastic diseases of the haematopoietic and lymphoid tissues: Report of the Clinical Advisory Committee Meeting, Airlie House, Virginia, November 1997. *Histopathol* 36:69–87.

Hyde, J., and Sun, T. (2003) Chronic myelomonocytic leukemia with abnormal bone marrow eosinophils. *Arch Pthol Lab Med* 127:1214–1216.

Maschek, H., Georgii, A., Kaloutsi, V., et al. (1992) Myelofibrosis in primary myelodysplastic syndromes: A retrospective study of 352 patients. *Eur J Haematol* 48:208–214.

Michaux, J., and Martiat, P. (1993) Chronic myelomonocytic leukaemia (CMML): A myelodysplastic or myeloproliferative syndrome? *Leuk Lymph* 9:35–41.

Montefusco, E., Alimena, G., Lo Coco, F., et al. (1992) Ph-negative and bcr-negative atypical chronic myelogenous leukemia: Biological features and clinical outcome. *Ann Hematol* 65:17–21.

Oscier, D., and Chapman, R. (1998) The classification of chronic myelomonocytic leukaemia. *Leuk Res* 22:879–880.

Raskin, R.E., and Krehbiel, J.D. (1985) Myelodysplastic changes in a cat with myelomonocytic leukemia. *JAVMA* 187(2):171–174.

Shepherd, P.C.A., Ganesan, T.S., and Galton, D.A.G. (1987) Haematological classification of the chronic myeloid leukaemias. *Bailliers Clin Haematol* 1:887–906.

Steensma, D.P., Tefferi, A., and Li, C.Y. (2003) Splenic histopathological patterns in chronic myelomonocytic leukemia with clinical correlations: Reinforcement of the heterogeneity of the syndrome. *Leuk Res* 27:775–782.

Storniolo, A.M., Moloney, W.C., Rosenthal, D.S., et al. (1990) Chronic myelomonocytic leukemia. *Leuk* 11:766–770.

Tefferi, A., Hoagland, H.C., Therneau, T.M., et al. (1989) Chronic myelomonocytic leukemia: Natural history and prognostic determinants. *Mayo Clin Proc* 64:1246–1254.

Voglová, J., Chrobák, L., Neuwirtová, R., Malasková, V., and Straka, L. (2001) Myelodysplasic and myeloproliferative type of chronic myelomonocytic leukemia—Distinct subgroups or two stages of the same disease? *Leuk Res* 25:493–499.

JUVENILE MYELOMONOCYTIC LEUKEMIA

Juvenile myelomonocytic leukemia (jMML) is a distinct chronic myeloid disorder of human infants now grouped within the MDS/MPD category in the revised WHO classification system. It is unknown whether a corresponding entity occurs in animals; however, cases of atypical myeloid proliferation in very young animals have been observed. jMML is a neoplasm of monocytes and neutrophils that accounts for about one-third of the cases of childhood leukemias that present with dysplastic changes. The mean age at diagnosis has been reported to lie between 1.5–2.0 years, with more than two-thirds of cases less than 3 years of age. Like the other diseases in this group of MDS/MPD, the cause of jMML is unknown. The unique aspects of this neoplasm that justify its recognition rest mainly with the need for aggressive treatment, and even then the prognosis is poor with marrow transplant as the only type of management that alters the outcome. Genetically, 30% of jMML cases have mutations of the *RAS* gene that is felt to link the risk for this disease to children with neurofibromatosis type 1. The leukemic cells of jMML are hypersensitive to GM-CSF, and if they are placed in culture in the absence of any added growth factors they will form granulocyte-macrophage colonies. This capability can be eliminated either by removing the monocytes and other adherent cells from the culture systems or by the addition of anti–GM-CSF. These results indicate that in culture the monocytic fraction is producing small amounts of growth factors and likely does the same in vivo. Because the level of GM-CSF in the unsorted cell cultures is not above control levels, it strongly suggests that the leukemic cells must be extremely sensitive to the growth factors to respond to such low levels. This characteristic of the jMML leukemic cells can be used as a diagnostic test for the disease itself.

Children with jMML present with a fever and usually evidence of infection and splenomegaly is a constant finding, with hepatomegaly and lymphadenopathy present in over half of cases. On presentation, there is leukocytosis accompanied by anemia and thrombocytopenia. The median leukocyte count lies between 25,000 and 35,000/ul, is always above 10,000/ul, and consists of immature granulocytes and monocytes. The median monocyte level lies between 5,000 and 7,000/ul and is always above 1,000/ul. The blast and promonocyte levels are fewer than 5% of total leukocytes and never rise to the 20% level that would cause consideration for AML. Nucleated red cells are often present, and the thrombocytopenia may be severe and accompanied by bleeding.

The marrow is hypercellular with a left shift in the myeloid maturation and blasts and promonocytes are usually below 10% of marrow nucleated cells. Monocytes make up 5–10% of marrow cells but may be higher. Although megakaryocytes are deficient in numbers, those present are morphologically normal. Accompanying dysplastic changes include reduced granularity and hyposegmentation of the neutrophil series and megaloblastic changes in the erythroid lineage.

Other tissues likely to be involved include the skin, lung, and splenic sinuses with homing to the larger vessels. Lymph nodes, if involved, have a leukemic pattern of involvement with colonization of the paracortical and medullary areas. A useful diagnostic test is the demonstration of hemoglobin F (fetal) that is present in 70% of cases, as is polyclonal gammopathy. There is as yet no definitive genetic abnormality associated with jMML.

It is unclear whether a proliferative syndrome of very young animals associated with dysplastic changes occurs as an animal counterpart of jMML. However, the only possibility for a disease of this type to be recognized in animals is if veterinarians are aware of this entity and have an index of suspicion on seeing similar hematologic changes. If a syndrome like jMML were to occur in an animal, it would likely be at about weaning age, if comparable to the condition in human infants in which the peak incidence lies between 1–2 years. Animals presenting at this age with rapidly advancing diseases are usually felt to have an infectious process, and if they are associated with hematologic dyscrasia an inborn error in neutrophil function might be considered. Because companion animals reproduce in litters, siblings might be affected if familial disease is considered. Alternatively, neoplastic diseases would be less likely to affect multiple offspring.

An animal disease with presenting signs like the human syndrome was seen by this author in a 6-week-old Corgi dog that succumbed to a fulminating disease with fixed tissues submitted for histologic examination. The blood and bone marrow were not examined prior to death. The

animal had a focal purulent alveolitis with a pure culture of a widely antibiotic susceptible Bordetella bronchiseptica recovered in pure culture (Figs. 7.13, 7.14). There are focal areas of myeloid proliferation around each vessel in the liver that consist of areas of myelopoiesis to a metamyelocyte level (Figs. 7.15–7.17) and some areas of blasts only (Fig. 7.18). The spleen had complete lymphoid atrophy (Figs. 7.19, 7.20) and massive sinus hematopoiesis, with marked immaturity and myeloid predominance (Figs. 7.21–7.23). There was massive atrophy of the small intestinal Peyer's Patches (Fig. 7.24), as well as very reduced villus and lamina propria lymphocytes and plasma cells—even for a young animal (Fig. 7.25). The heart and kidney were normal and no other tissues were examined. The tissues were negative on immunohistochemical staining for canine distemper antigen. The extent of myelopoiesis in this animal and of lymphoid atrophy would suggest that the pneumonia was due more to cellular incompetence than cellular deficit.

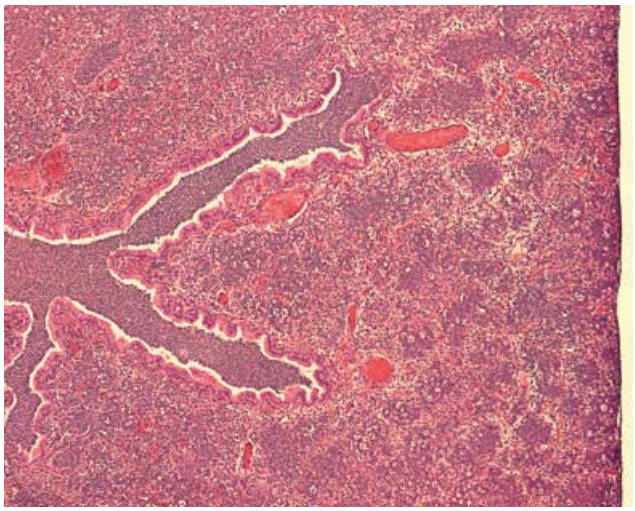

Figure 7.13. Dog: lung, myeloproliferative disease resembling juvenile CMML. Purulent bronchopneumonia and alveolitis with a focal area of lung solidly infiltrated with inflammatory cells, primarily neutrophils.

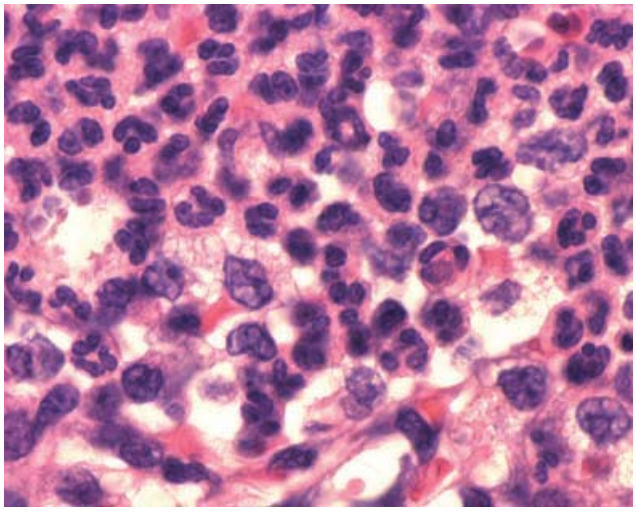

Figure 7.14. Dog: lung, resembles juvenile CMML. At the alveolar level the cellular reaction includes immature neutrophils with numerous large mononuclear cells with more abundant cytoplasm. The neutrophils appear to have a normal level of cytoplasmic granulation and density.

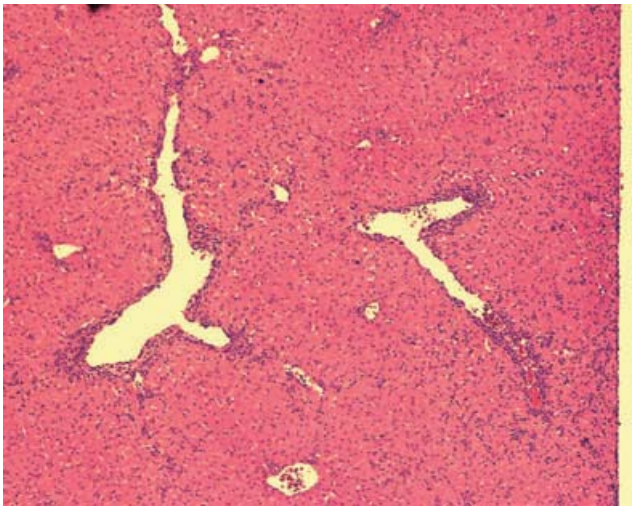

Figure 7.15. Dog: liver, resembles juvenile CMML. There is widespread vascular cuffing with irregular small areas of colonization of hepatic sinuses.

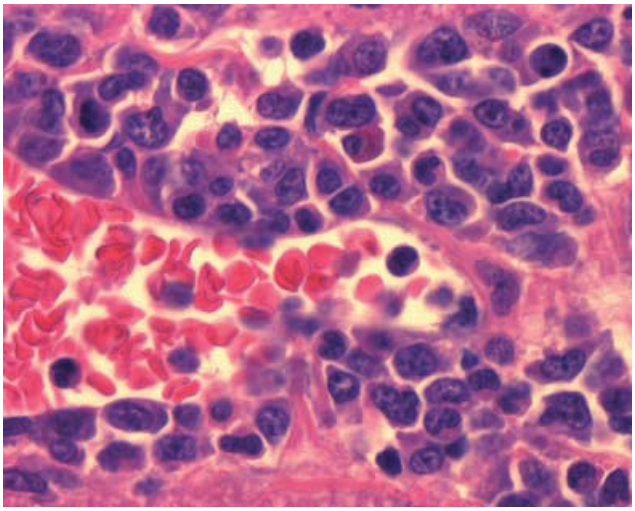

Figure 7.16. Dog: liver, resembles juvenile CMML. There are numerous cells within vascular cuffs with lobulated nuclei and relatively abundant cytoplasm unlike neutrophil precursors that suggests a mixed monocytic-neutrophilic differentiation.

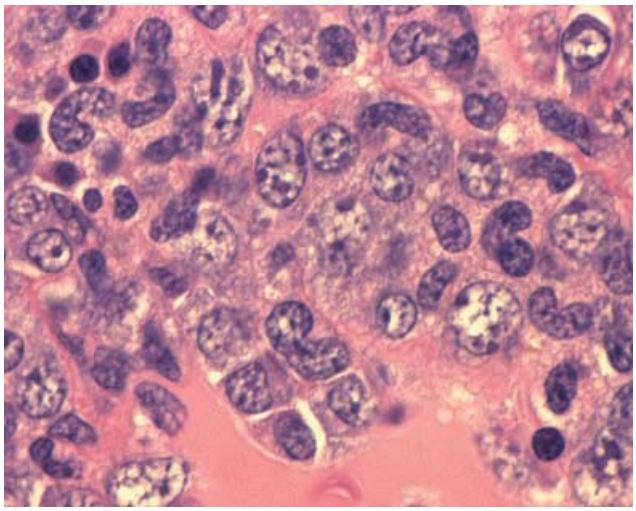

Figure 7.17. Dog: liver, resembles juvenile CMML. Focal perivenous cuff of hematopoietic cells with giant metamyelocytes and early asynchrony with large vesicular blast cells with marginated nucleoli approximately equal to the number of maturing cells.

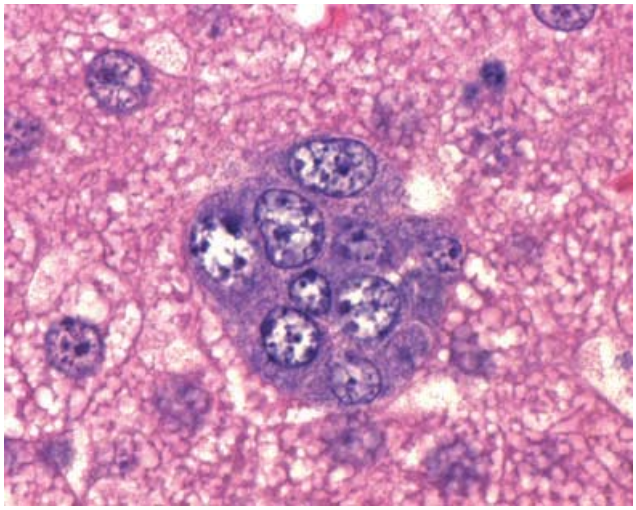

Figure 7.18. Dog: liver, resembles juvenile CMML. An interstitial area of atypical cell proliferation, which consists entirely of blastic cells in one plane of section.

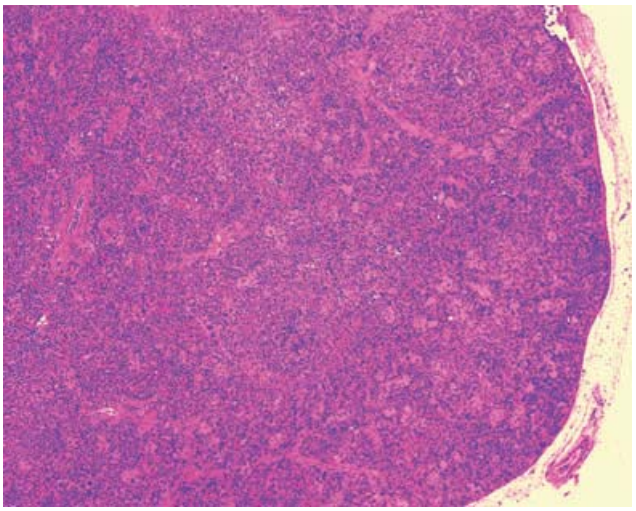

Figure 7.19. Dog: spleen, myeloproliferative disease, possible juvenile myelomonocytic leukemia. The spleen has a completely diffuse architecture with virtually complete atrophy of periarteriolar lymphoid sheaths. There is marked thinning of the peripheral capsule and thinning and wide separation of internal muscular trabeculae. There is marked and diffuse sinus colonization.

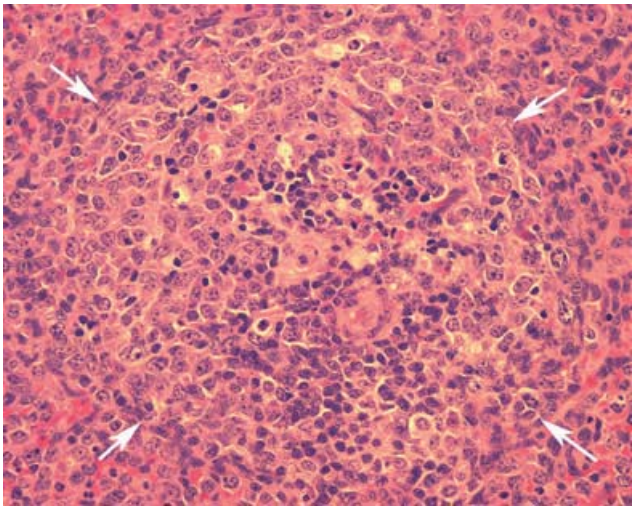

Figure 7.20. Detail of Figure 7.19. An arteriole cut in cross section has a very small cuff of small lymphocytes and is surrounded by a larger cuff of primitive stromal-appearing cells possibly endothelial (arrows), with vesicular nuclei, and elongated bipolar cytoplasm.

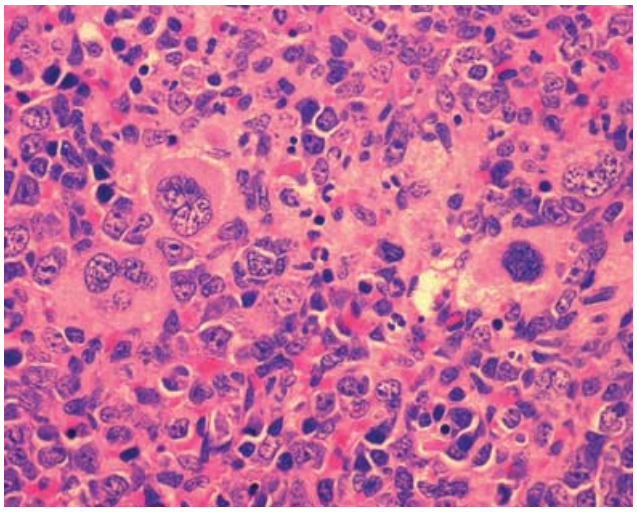

Figure 7.21. Dog: spleen, resembles juvenile CMML. Detail of splenic sinus with mixed myeloid cellular proliferation with several developing megakaryocytes, few erythroid precursors, and large numbers of relatively undifferentiated cells.

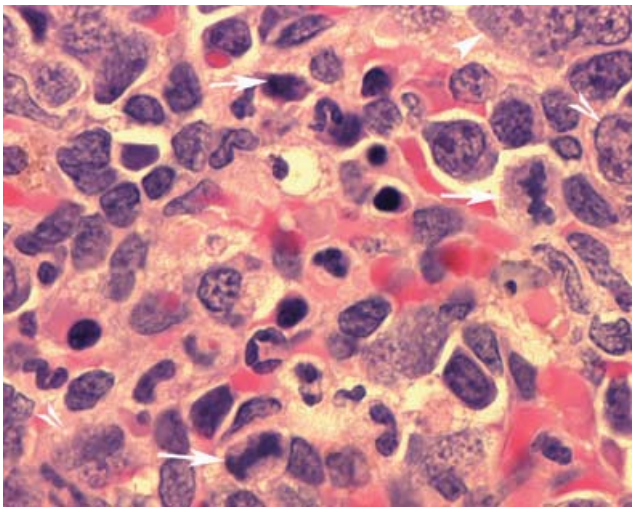

Figure 7.23. Dog: spleen, resembles juvenile CMML. Splenic sinus with a cellular cluster of more apparent myeloid differentiation. There are metaphases in upper right and lower center (arrows). There are large blastic cells in the upper right and lower left (arrow heads) with mononuclear cells with irregularly shaped nuclei in the lower left and apparent neutrophil differentiation in the lower center.

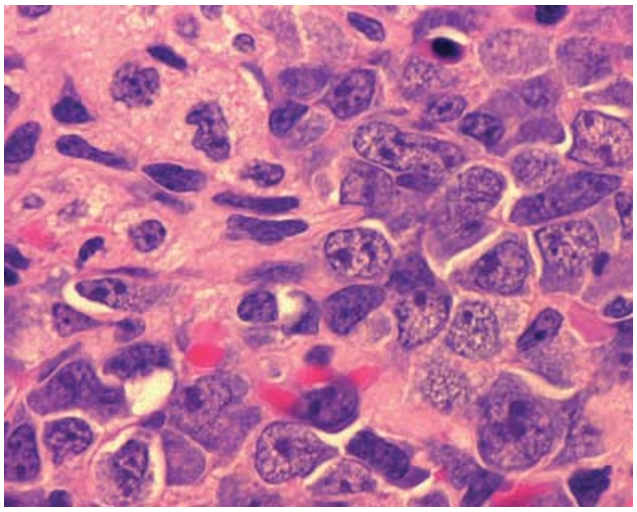

Figure 7.22. Dog: spleen, resembles juvenile CMML. Oval nuclei in the upper left are likely of endothelial cells surrounded by larger pale cells of an ellipsoid sheath. Those cells are surrounded by a cluster of relatively undifferentiated blast cells. There is a single rubricyte in the upper right.

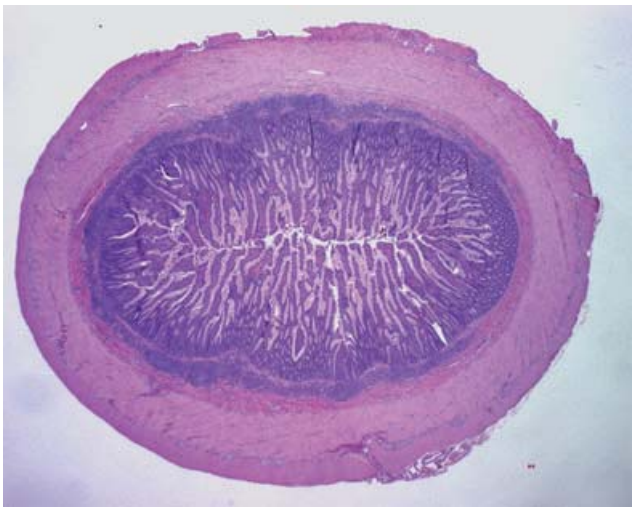

Figure 7.24. Dog: lower small intestine, myeloproliferative disease, possible juvenile myelomonocytic leukemia. The Peyer's patch lymphoid tissue is reduced to a thin ellipse that surrounds the mucosa in the lateral and ventral areas.

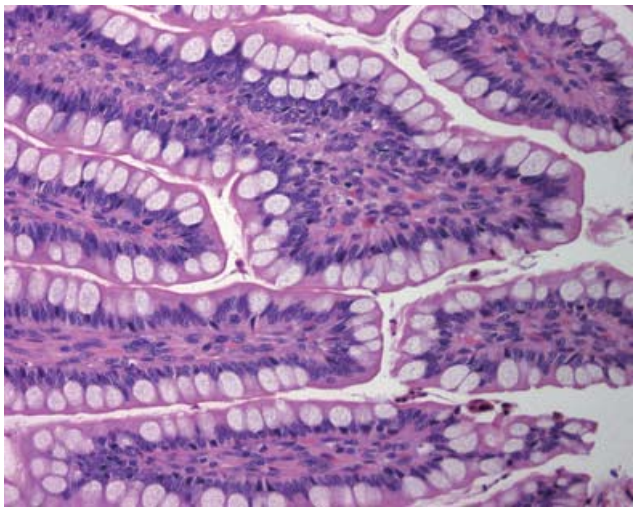

Figure 7.25. Dog: small intestine. Detail of Figure 7.24 of ileal villi with intestinal lumen at the top. Note the contracted villous lamina propria that consists primarily of smooth muscle and stromal cells with absence of lymphocytes and plasma cells.

It is certainly not clear that the dog had a canine form of jMML, but it is very likely that the dog did have a form of leukemia. That in itself is remarkable because it is so unsuspected that it may not be considered as a possible diagnosis. It is unusual, but well recognized, that calves may be born with lymphoma, so cancer in neonates of other species is not unknown. jMML is not a new disease, but the recognition of its aggressive nature is. In comparative terms we are well advised to realize that neoplasms of this type may also occur in animals.

REFERENCES

Anastasi, J., and Vardiman, J.W. (2001) Chronic myelogenous leukemia and the chronic myeloproliferative diseases. In Knowles, D.M. (ed.), *Neoplastic Hematopathology*, 2nd ed. Lippincott Williams & Wilkins, Philadelphia, pp. 1745–1790.

Arico, M., Biondi, A., and Pui, C.-H. (1997) Juvenile myelomonocytic leukemia. *Blood* 90:479–488.

Castro-Malaspina, H., Schaison, G., Passe, et al. (1984) Subacute and chronic myelomonocytic leukemia in children (juvenile CML): Clinical and hematologic observations, and identification of prognostic factors. *Cancer* 54:675–686.

Emmanuel, P., Bates, L.J., Castleberry, R.P., et al. (1991) Selective hypersensitivity to granulocyte macrophage colony stimulating factor by juvenile chronic myeloid leukemia hematopoietic progenitors. *Blood* 77:925–931.

Emmanuel, P., Bates, L.J., Zy, S.W., et al. (1991) The role of monocyte-derived hematopoietic growth factors in the regulation of myeloproliferation in juvenile chronic myelogenous leukemia. *Exp Hematol* 19:1017–1020.

Haas, O.A., and Gadner, H. (1996) Pathogenesis, biology, and management of myelodysplastic syndromes in children. *Semin Hematol* 33:225–235.

Luna-Fineman, S., Shannon, K.M., Atwater, S.K., et al. (1998) Myelodysplastic and myeloproliferative disorders of childhood: A study of 167 patients. *Blood* 93:459–466.

Niemeyer, C.M., Arico, M., Basso, G., et al. (1997) Chronic myelomonocytic leukemia in childhood: A retrospective analysis of 110 cases. *Blood* 89:3534–3543.

Chapter 8

Myelodysplastic Syndromes

Myelodysplastic syndromes are hematologic disorders of bone marrow characterized by defined abnormalities of precursor cell maturation of dysplastic or regressive nature that may affect one or more cell lineages and result in ineffective production and cytopenias. The paradoxical nature of the MDS syndromes is peripheral blood cell deficiencies with a hypercellular marrow as a result of ineffective hematopoiesis. These dysplastic changes are most often characterized by normal levels of blasts in marrow without their appearance in the peripheral blood, and if blasts are increased the levels are below the 20% required for diagnosis of AML. In humans, the MDS conditions may occur as primary afflictions (de novo) or secondary to chemotherapeutic or irradiation therapy. Virtually all of the types of dysplastic change described for human blood and marrow are found in animals, with the possible exception of ringed sideroblasts. Rubricytes with these cytoplasmic features can be recognized on routine blood staining of human cells and can be proven by simple stains for iron. Rubricytes with lesser amounts of iron are seen in dogs, and the ringed form may have subtle presence in animal tissue and be underrecognized.

In animals, as in humans, the MDS changes are seen in mature dogs and cats and less commonly in horses and cattle, but they are likely present in any domestic mammal that is kept into maturity. The presentation is also similar and related to cytopenias with infection due to neutropenia or bleeding due to thrombocytopenia. In humans, hepatosplenomegaly is not usually a presenting sign, although there may be associated autoimmune disease, and both criteria also appear to apply in animals. The diagnosis of MDS is based on both a subjective assessment of abnormal cellular morphology and an objective assessment of the degree of immaturity. In two types of MDS in humans specifically, refractory anemia and refractory anemia with ringed sideroblasts, there are the dysplastic changes but no increase in blast cells. In contrast, in other types of MDS there are both dysplastic changes and increased blasts in marrow and blood. The third category is the refractory cytopenia with multilineage dysplasia that has dysplastic changes in two or more cell lineages and less than 5% marrow blasts.

The definition of dysplasia in each cell line is the key to recognition of the various combinations by which the current six types of MDS are identified. In neutrophils, the dysplastic changes consist of decreased or abnormal granulation and errors in nuclear segmentation. These may be less than normal with pseudo–Pelger-Huët with large lobed bisegmentation or more than normal with six or more small segments. In the erythroid lineage, the dysplastic changes include asynchronous nuclear and cytoplasmic maturation. These include megaloblastoid-type fine nuclear chromatin and abnormal lobulation with multinucleated cells of varying nuclear size, as well as both karyorrhexis and actual nuclear fragmentation. In humans, ringed sideroblasts occur in each subtype of MDS, but, as noted above, rubricytes with these changes are rarely recognized in animals. The peripheral blood progeny of these precursors also have changes, which include marked anisocytosis, oval macrocytes, and dacryocytes or teardrop-shaped red cells. In the megakaryocytic lineage, the dysplastic changes include very small megakaryocytes without nuclear lobulation that might be mistaken for large lymphocytes with ragged cytoplasmic margins. Cells of this same size range may be binucleated and appear similar to the normal pattern of promegakaryocytic development except that the nuclei do not flatten against each other and appear as round nuclei within a single cytoplasmic envelope. At the other extreme, very large megakaryocytes may be present with nonlobulated nuclei and with very fine dispersed chromatin patterns. As in the erythroid series, the progeny may reflect the abnormal development with peripheral blood platelets as large lymphocyte nuclei and with decreased or absent granulation.

With omission of the one MDS category in humans identified by molecular genetic changes (5q-syndrome), the five categories listed above are likely seen in animals. Many of the cases described in animals are given a more general diagnosis of myelodysplastic syndrome without designation to a specific subtype, as are described in

human MDS. This may be appropriate because the animal cases may not be directly comparable with the human forms of MDS. However, the subclassifications applied to human cases have important prognostic implications that, if applicable, to MDS in animals would be useful for planning management strategies. With this background for the syndromes of myelodysplasia, these references are included as a basis for understanding the scope of these disorders, with more specific treatment given to the individual entities.

REFERENCES

Billström, R., Johansson, H., Johansson, B., and Mitelman, F. (1995) Immune-mediated complications in patients with myelodysplastic syndromes—Clinical and cytogenetic features. *Eur J Haematol* 55:42–48.

Blue, J.T. (2003) Myelodysplasia: Differentiating neoplastic from nonneoplastic syndromes of ineffective hematopoiesis in dogs. *Toxicol Pathol* 31(Suppl.):44–48.

Boone, L.E., Knauer, K.W., Rapp, S.W., Stewart, J.F., and Modiano, J.F. (1998) Use of human recombinant erythropoietin and prednisone for treatment of myelodysplastic syndrome with erythroid predominance in a dog. *JAVMA* 213(7):999.

Breuer, W., Hermanns, W., and Thiele, J. (1999) Myelodysplastic syndrome (MDS), acute myeloid leukaemia (AML) and chronic myeloproliferative disorder (CMPD) in cats. *J Comp Pathol* 121:203–216.

Brunning, R. (1999) Proposed World Health Organization (WHO) classification of acute leukemia and myelodysplastic syndromes. *Mod Pathol* 12:102.

Brunning, R.D. (2001) Myelodysplastic syndromes. In Knowles, D.M. (ed.), *Neoplastic Hematopathology*, 2nd ed. Lippincott Williams & Wilkins, Philadelphia, pp. 1717–1743.

Brunning, R.D., and McKenna, R.W. (1994) Myelodysplastic syndromes. In *Tumors of the Bone Marrow. Atlas of Tumor Pathology*, 3rd series, fasc 9. Armed Forces Institute of Pathology, Washington, D.C., pp. 143–194.

Casadevall, N., Durieux, P., Dubois, S., Hemery, F., Lepage, E., Quarré, M.-C., Damaj, G., Giraudier, S., Guerci, A., Laurent, G., Dombret, H., Chomienne, C., Ribrag, V., Stamatoullas, A., Marie, J.-P., Vekhoff, A., Maloisel, F., Navarro, R., Dreyfus, F., and Fenaux, P. (2004) Health, economic, and quality-of-life effects of erythropoietin and granulocyte colony-stimulating factor for the treatment of myelodysplastic syndromes: A randomized, controlled trial. *Blood* 104(2):321–327.

Dreyfus, B. (1976) Preleukemic states: I. Definition and classification. II. Refractory anemia with excess of myeloblasts in the bone marrow (smouldering acute leukemia). *Blood Cells* 2:33–45.

Enright, H., Jacob, H.S., Vercellotti, G., et al. (1995) Paraneoplastic autoimmune phenomena in patients with myelodysplastic syndromes: Response to immunosuppressive therapy. *Brit J Haematol* 91:403–408.

Farhi, C.D. (1995) Myelodysplastic syndromes and acute myeloid leukemia: Diagnostic criteria and pitfalls (review). *Pathol Ann* 30:29–57.

Felman, P., Bryon, P.-A., Gentilhomme, O., Ffrench, M., Charrin, C., Espinouse, D., and Viala, J.-J. (1988) The syndrome of abnormal chromatin clumping in leucocytes: A myelodysplastic disorder with proliferative features? *Brit J Haematol* 70:49–54.

Fontenay-Roupie, M., Bouscary, D, Guesnu, M., Picard, F., Melle, J., Lacombe, C., Gisselbrecht, S., Mayeux, P., and Dreyfus, F. (1999) Ineffective erythropoiesis in myelodysplastic syndromes: Correlation with Fas expression but not with lack of erythropoietin receptor signal transduction. *Brit J Haematol* 106:464–473.

Germing, U., Gattermann, N., Strupp, C., Aivado, M., and Aul, C. (2000) Validation of the WHO proposals for a new classification of primary myelodysplastic syndromes: A retrospective analysis of 1,600 patients. *Leuk Res* 24:983–992.

Groupe Francais de Morphologie Hematologique. (1987) French Registry of acute leukemia and myelodysplastic syndromes: Age distribution and hemogram analysis of the 4,496 cases recorded during 1982–1983 and classified according to FAB criteria. *Cancer* 60:1385–1394.

Hellström-Lindberg, E., Ahlgren, T., Beguin, Y., Carlsson, M., Carneskog, J., Dahl, I.M., Dybedal, I., Grimfors, G., Kanter-Lewensohn, L., Linder, O., Luthman, M., Löfvenberg, E., Nilsson-Ehle, H., Samuelsson, J., Tangen, J.-M., Winqvist, I., Öberg, G., Österborg, A., and Öst, À. (1998) Treatment of anemia in myelodysplastic syndromes with granulocyte colony-stimulating factor plus erythropoietin: Results from a randomized phase II study and long-term follow-up of 71 patients. *Blood* 92(1):68–75.

Hisasue, M., Okayama, H., Okayama, T., Suzuki, T., Mizuno, T., Fujino, Y., Naganobu, K., Hasegawa, A., Watari, T., Matsuki, N., Masuda, K., Ohno, K., and Tsujimoto, H. (2001) Hematologic abnormalities and outcome of 16 cats with myelodysplastic syndromes. *J Vet Intern Med* 15:471–477.

Juneja, S.K., Imbert, M., Joualt, H., et al. (1983) Haematological features of primary myelodysplastic syndromes (PMDS) at initial presentation: A study of 118 cases. *J Clin Pathol* 36:1129–1135.

Koeffler, H.P. (1996) Introduction: Myelodysplastic syndromes. *Semin Hematol* 33:87–94.

McManus, P.M., and Hess, R.S. (1998) Myelodysplastic changes in a dog with subsequent acute myeloid leukemia. *Vet Clin Pathol* 27(4):112.

Miyamoto, T., Horie, T., Shimada, T., Kuwamura, M., and Baba, E. (1999) Long-term case study of myelodysplastic syndrome in a dog. *J Am An Hosp Assoc* 35:475–481.

Rosati, S., Mick, R., Xu, F., et al. (1996) Refractory cytopenia with multilineage dysplasia: Further characterization of an "unclassifiable" myelodysplastic syndrome. *Leuk* 10:20–26.

Weiss, D.J., and Aird, B. (2001) Cytologic evaluation of primary and secondary myelodysplastic syndromes in the dog. *Vet Clin Pathol* 30(2):67–75.

Weiss, D.J., and Smith, S.A. (2000) Primary myelodysplastic syndromes of dogs: A report of 12 cases. *J Vet Intern Med* 14:491–494.

Yashige, H., Horiike, S., Taniwaki, M., Misawa, S., and Abe, T. (1999) Micronuclei and nuclear abnormalities observed in erythroblasts in myelodysplastic syndromes and in de novo acute leukemia after treatment. *Acta Haematol* 101:32–40.

REFRACTORY ANEMIA

MDS of Refractory Anemia Without Ringed Sideroblasts

Refractory anemia (RA) without ringed sideroblasts is likely one of the more common types of MDS occurring in animals. In the author's experience and from published reports, all animals with refractory anemia were presented with some degree of depression and reduced activity and appetite. Pale mucus membranes are seen on physical examination, and at least mild splenomegaly is often mentioned. In dogs, the anemia is moderate to severe with packed cell volumes (PCV) in the range of 15–25%; it is more severe in cats, with a mean PCV of less than 20%. The peripheral blood red cell morphology is not well recorded, but anisocytosis and poikilocytosis are present to some degree and may be moderate to marked. Most cases are not thrombocytopenic, and therefore the red cell changes are more likely attributable to abnormal production and not to vascular injury. There is mild neutrophilic leukocytosis in most cases without peripheral blood blasts.

The bone marrow is hypercellular (Fig. 8.1), and most reports have followed the human criterion that blasts cells must not exceed 5% of marrow cells. In both cats and dogs, there is usually erythroid predominance (Fig. 8.2), but the M:E ratio may be variable, which likely reflects some cases in transition to more aggressive states. Dyserythropoiesis is present in all cases, with some having more megaloblastoid features (Fig. 8.3), and others more

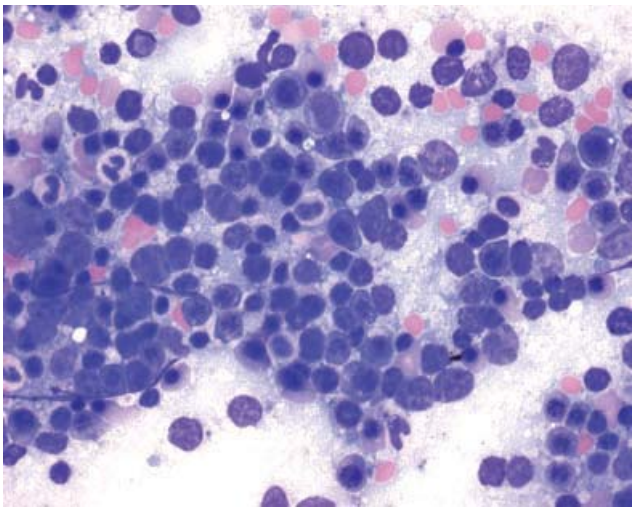

Figure 8.2. Dog: bone marrow, refractory anemia of myelodysplastic syndrome. Typical area of thinly distributed cells where dominance of rubricytes are apparent. There is a single neutrophil in the lower center.

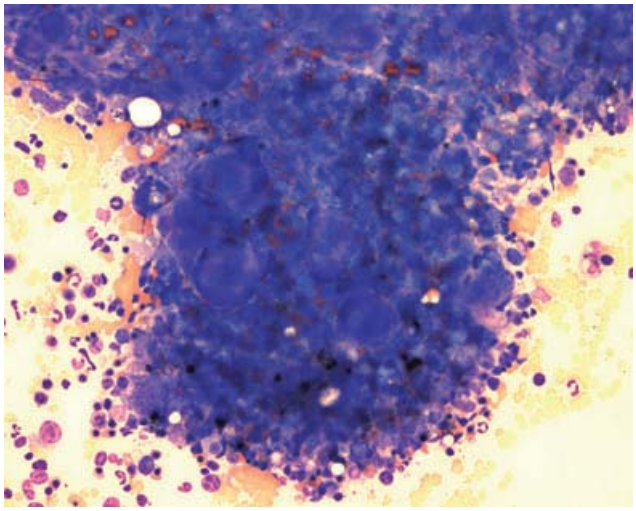

Figure 8.1. Dog: bone marrow aspirate, refractory anemia due to myelodysplastic syndrome. There is marked hypercellularity with a granule almost completely devoid of fat cells. The marrow tissue can be seen to be solidly cellular with numerous megakaryocytes and many late stage rubricytes apparent at the outer edge of the nodule. Dense, irregular-shaped small masses at bottom center are hemosiderin granules in marrow macrophages with their size and density typical of anemia of chronic disease with poor iron utilization.

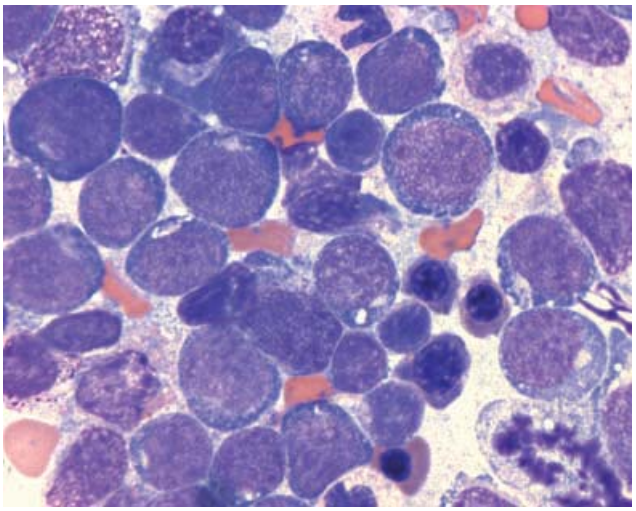

Figure 8.3. Dog: bone marrow, refractory anemia of myelodysplasia. An area of maturing rubricytes in the upper right with a background of relatively undifferentiated cells that have large round nuclei with a fine chromatin pattern and a narrow rim of highly basophilic cytoplasm. Most of these large cells are megaloblastoid type erythroid precursors. There is a normal-appearing plasma cell and neutrophil at the bottom center and an injured cell in metaphase in the lower right.

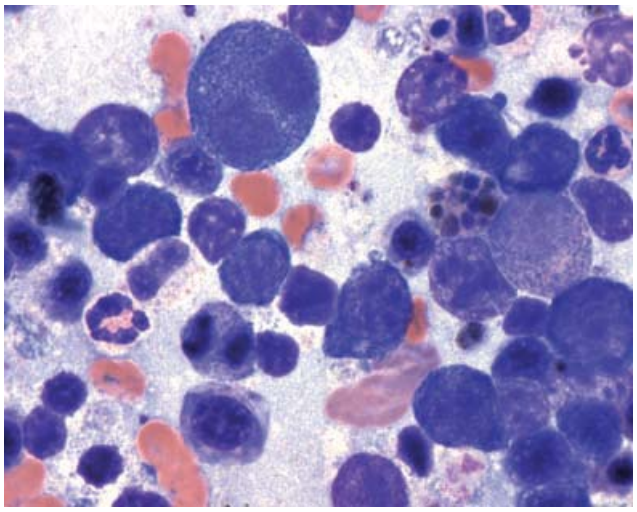

Figure 8.4. Dog: marrow, refractory anemia due to myelodysplasia. The late stage anaphase in the left center is likely an erythroid precursor. The cluster of small round bodies of varying size and density in the upper right is cytoplasm of a macrophage with nuclei of ingested rubricytes indicating a level of marrow proliferation, some of which is associated with an effective peripheral blood response.

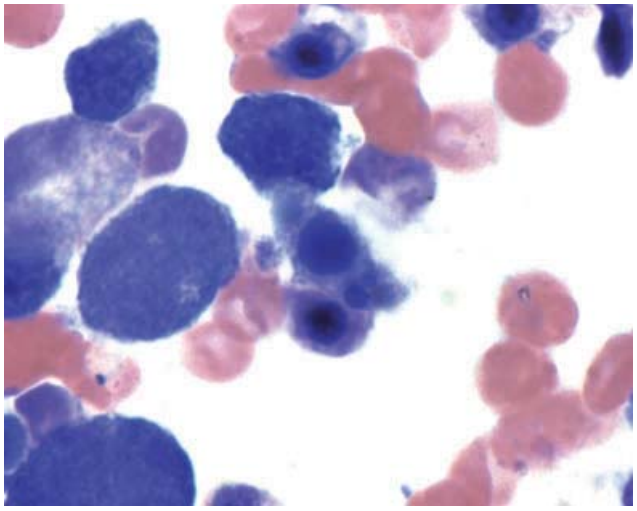

Figure 8.5. Dog: marrow, refractory anemia due to myelodysplasia. The cell in the center is a metarubricyte with cytoplasm that has a high level of basophilia and an asynchronously low level of hemoglobin. The cell immediately above and in contact with the rubricyte is the cytoplasm of a marrow phagocyte with the homogenous dark staining structures of varying density representing 5 nuclei that are in various stages of digestion. The presence of these cells signifies that there is a high level of erythroid turnover within the marrow that, coupled with a low reticulocyte count, indicates ineffective erythropoiesis.

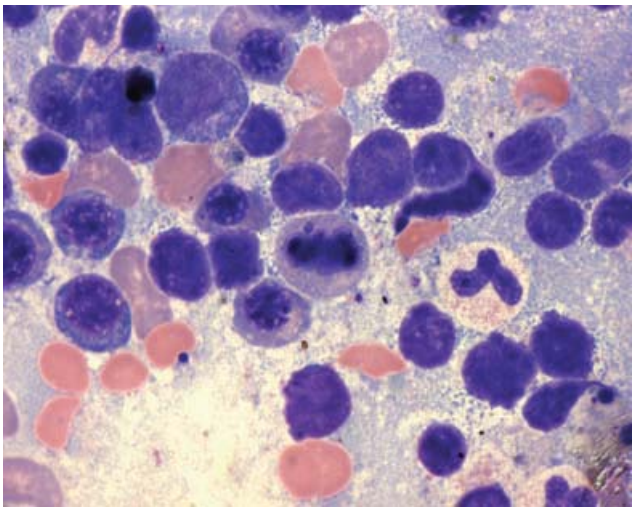

Figure 8.6. Dog: bone marrow, refractory anemia due to myelodysplastic syndrome. A cluster of erythroid cells includes one in metaphase (center) with an apparent lagging chromosomal fragment that will likely appear as a Howell-Jolly body in a red cell after denucleation.

mature rubricytes, with binucleation (Fig. 8.4) and multinucleation more prominent. Marrow phagocytes are present but not prominent with ingested evidence of erythroid proliferation that is ineffective because the cytoplasmic envelope does not appear in the peripheral blood (Fig. 8.5). Abnormal mitoses may be seen in developing rubricytes (Fig. 8.6). Ringed sideroblasts are not usually mentioned and generally at less than 1% of maturing rubricytes; that level is well within the criterion of less than 15% to include in the category of refractory anemia without ringed sideroblasts.

In the human cases of RA, some 10–15% have hypocellular marrow, and these tend to be in older individuals with aplastic anemia a consideration. These cases have increased numbers of immature marrow cells positive for CD34, as is seen in AML but not in aplastic anemia. Some human patients in this category have specific cytogenetic changes, including 20q- and may have few dysplastic changes. About 20% of human patients with RA without ringed sideroblasts respond to treatment with growth factors, usually G-CSF given with erythropoietin (epo).

REFERENCES

Brunning, R.D. (2001) Myelodysplastic syndromes. In Knowles, D.M. (ed.), *Neoplastic Hematopathology*, 2nd ed. Lippincott Williams & Wilkins, Philadelphia, pp. 1717–1743.

Hisasue, M., Okayama, H., Okayama, T., Suzuki, T., Mizuno, T., Fujino, Y., Naganobu, K., Hasegawa, A., Watari, T., Matsuki, N., Masuda, K., Ohno, K., and Tsujimoto, H. (2001) Hematologic abnormalities and outcome of 16 cats with myelodysplastic syndromes. *J Vet Intern Med* 15:471–477.

Nand, S., and Godwin, J.E. (1988) Hypoplastic myelodysplastic syndrome. *Cancer* 62:958–964.
Orazi, A., Albiter, M., Heerema, N.A., et al. (1997) Hypoplastic myelodysplastic syndrome can be distinguished from acquired aplastic anemia by CD34 and PCNA immunostaining of bone marrow biopsy specimens. *Am J Clin Pathol* 107:268–274.
Weiss, D.J., and Aird, B. (2001) Cytologic evaluation of primary and secondary myelodysplastic syndromes in the dog. *Vet Clin Pathol* 30:67–75.
Weiss, D.J., and Smith, S.A. (2000) Primary myelodysplastic syndromes of dogs: A report of 12 cases. *J Vet Intern Med* 14:491–494.
Yoshida, Y., Oguma, H., and Maekawa, T. (1995) Refractory myelodysplastic anaemias with hypocellular bone marrow. *J Clin Pathol* 41:763–767.

MDS of Refractory Anemia with Ringed Sideroblasts

MDS characterized by refractory anemia with ringed sideroblasts (RARS) has been rarely described in animals.

In humans, anemia is always present, and siderocytes may be present in peripheral blood red cells as "Pappenheimer bodies" (Fig. 8.7). Neutrophils tend to have normal levels and morphology, as do platelets. There is usually marrow erythroid hyperplasia, and the critical level of 15% of rubricytes must have ringed sideroblast formations as well as prominent dyserythropoiesis. Megakaryocytes and myelopoietic cells appear normal. A relatively small proportion of human patients with RARS, estimated at 7–10%, progress to AML. Others in this category are characterized by inborn errors in erythroid proliferation that in maturity renders them more susceptible to the addition of dysplastic changes and higher risk of AML. Because patients with RARS are expected to have normal-appearing myelopoiesis and thrombopoiesis with dysplasia limited to the erythroid series, any sign of dysplasia in the other lineages should suggest the alternative diagnosis of sideroblastic anemia with multilineage dysplasia that has a higher incidence of progression to AML.

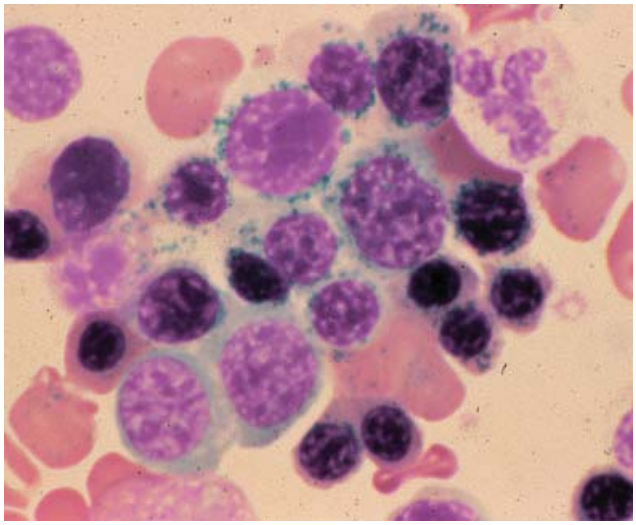

Figure 8.7. Human: bone marrow, sideroblastic anemia. Wright's on Perl's stain for iron demonstrating ringed rubricytes in sideroblastic anemia. Small positive bodies can also be seen in red cells in the upper right and lower center. *Image from R. D. Brunning, MD.*

REFERENCES

Boudard, D., Vasselon, C., Berthéas, M.-F., Jaubert, J., Mounier, C., Reynaud, J., Viallet, A., Chautard, S., Guyotat, D., and Campos, L. (2002) Expression and prognostic significance of Bcl-2 family proteins in myelodysplastic syndromes. *Am J Hematol* 70:115–125.
Brunning, R.D. (2001) Myelodysplastic syndromes. In Knowles, D.M.(ed.), *Neoplastic Hematopathology*, 2nd ed. Lippincott Williams & Wilkins, Philadelphia, pp. 1717–1743, 2001.
Canfield, P.J., Watson, A.D., Ratcliffe, R.C. (1987) Dyserythropoeisis, sideroblasts/siderocytes and hemoglobin crystallization in a dog. *Vet Clin Pathol* 16(1):21–28.
Ganser, A., and Karthaus, M. (1997) Clinical use of hematopoietic growth factors in the myelodysplastic syndromes. *Leuk and Lymph*26(Suppl.1):13–27.
Juneja, S.K., Imbert, M., Joualt, H., et al. (1983) Haematological features of primary myelodysplastic syndromes (PMDS) at initial presentation: A study of 118 cases. *J Clin Pathol* 36:1129–1135.
Nusbaum, N.J. (1991) Concise review: Genetic bases for sideroblastic anemia. *Am J Hematol* 37:41–44.
Orazi, A., Albiter, M., Heerema, N.A., et al. (1997) Hypoplastic myelodysplastic syndrome can be distinguished from acquired aplastic anemia by CD34 and PCNA immunostaining of bone marrow biopsy specimens. *Am J Clin Pathol* 107:268–274.
Weiss, D.J., Lulich, J. (1999) Myelodysplastic syndrome with sideroblastic differentiation in a dog. *Vet Clin Pathol* 28(2):59–63.

REFRACTORY ANEMIA WITH EXCESS BLASTS

The primary distinction of refractory anemia with excess blasts (RAEB) from the other types of refractory anemia is the presence of a higher level of blasts in both the blood and marrow, which ranges from 5–15% but remains below the level of 20% that would designate AML. Of these diseases, the RAEB category appears to have the most supporting descriptive pathology in the dysplastic diseases of animals. It may also be that RAEB is simply more frequent in animals than some of the other types of MDS. In humans, the higher level of blasts appeared

related to the prognosis, and subsequent studies have shown that the proportion of cases that progress to AML is significantly lower in patients with RAEB that have blast counts in the region of 5–10%, as compared to those with blast levels that range from 11–19%. These subtypes of RAEB are now officially designated as *RAEB-1* for those cases with the lower blast count and *RAEB-2* for cases with higher percentages. If cases in the lower level with less than 11% blasts have some with Auer rods, these cases have a higher risk of transition to AML and are also then classed as type RAEB-2. Further, in cases where there are more blasts in the blood than in the marrow, the level in the blood is used to determine the prognostic level. These changes in criteria of classification removed a conflict that resulted from the lowering of the criteria for AML to 20% blasts from 30% in previous criteria. With the former criteria, the category of RAEBt for the higher grade variant (RAEB in transition to AML) was set at a boundary of 20% blasts, which equals the level for actual AML by the newer criteria.

The presentation of human cases with RAEB is always with anemia that is normochromic and maybe macrocytic with large oval red cells and occasional peripheral blood rubricytes. There is usually neutropenia and thrombocytopenia and often pancytopenia. These findings associated with the presentation of humans with RAEB are very similar to those described as present in cats suggested to have an animal counterpart of RAEB. Most animals diagnosed as having myelodysplastic syndromes present with a history of reduced appetite and activity over several months accompanied by weight loss (Fig. 8.8).

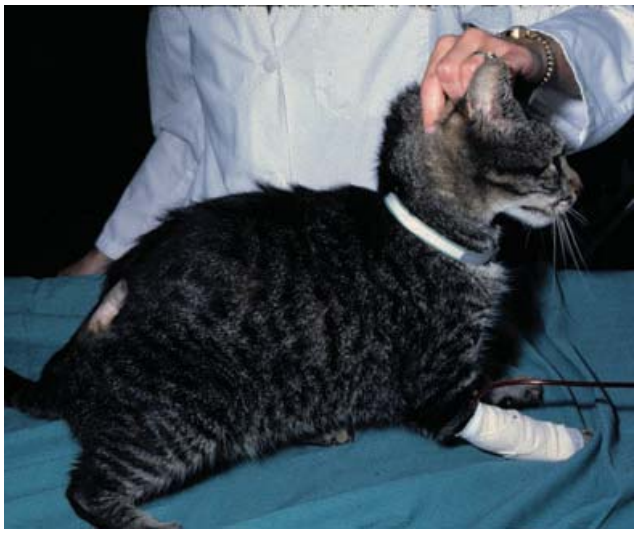

Figure 8.8. Cat: refractory anemia. The cat presented with lethargy and anorexia and was found to have weight loss and pale mucous membranes with severe and unresponsive anemia identified on examination of blood.

In humans, the changes in blood on presentation are mirrored from those in the marrow where there is an increase in myeloblasts that in many cases is accompanied by an increase in promyelocytes. This seems to be less the case in animals where the blast compartment seems to stand out without a well-defined lineage of following maturation (Figs. 8.9–8.11). On histological examination of

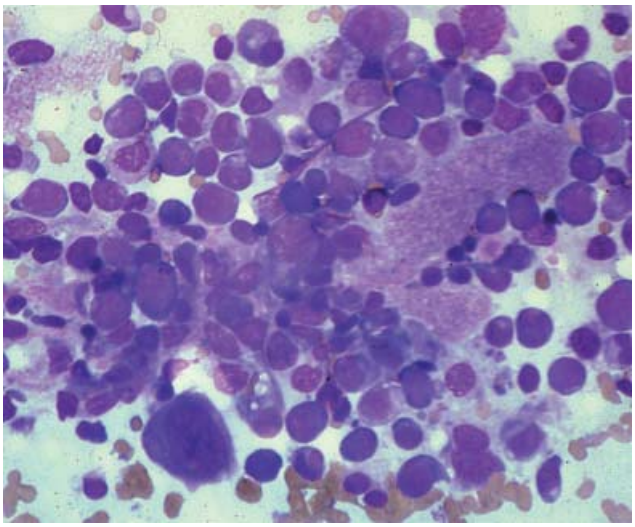

Figure 8.9. Cat: bone marrow aspirate, refractory anemia with excess blasts. There is paradoxical hypercellularity with moderate peripheral pancytopenia. The marrow contains a predominance of primitive cells with some apparent later stage rubricytes but with marked reduction in marrow granulocyte reserves.

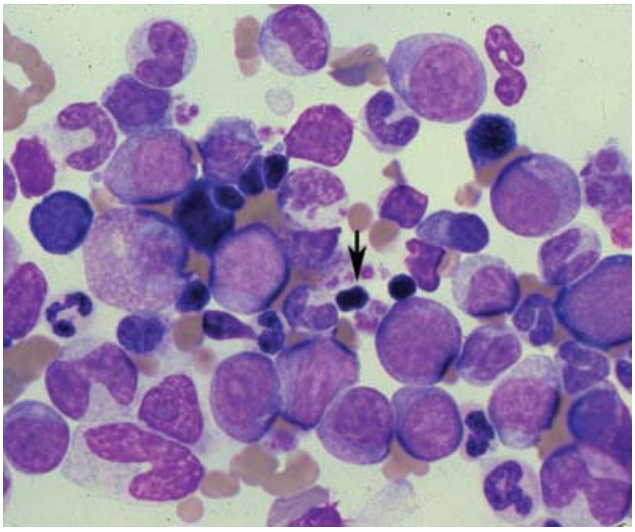

Figure 8.10. Cat: marrow aspirate, refractory anemia with excess blasts. There is marked early asynchrony with numerous blast cells but more indication of maturation of both erythroid and myeloid systems. There is a binucleate late stage rubricyte in the center indicative of dyserythropoiesis (arrow).

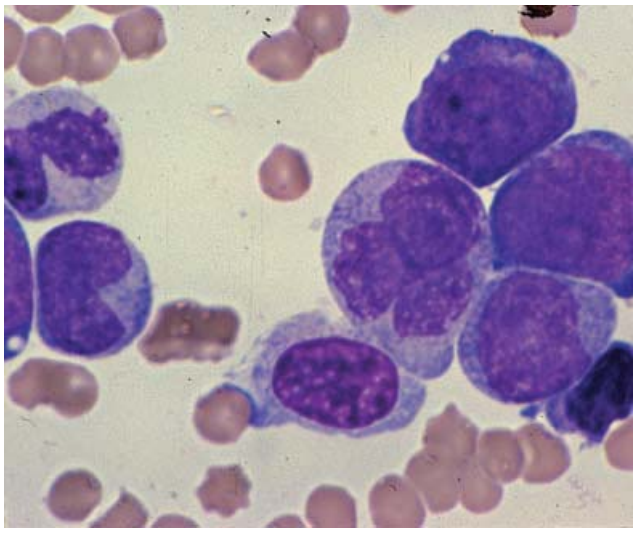

Figure 8.11. Cat: bone marrow, refractory anemia with excess blasts. The cell in the upper right is an early promyelocyte with a type III myeloblast (below right). The trinucleated cell could be an atypical megakaryocyte precursor. The cell at the lower right with deeply stained nucleus is likely a basophilic rubricyte with the other cells possibly developing myeloid cells with very little cytoplasmic granulation.

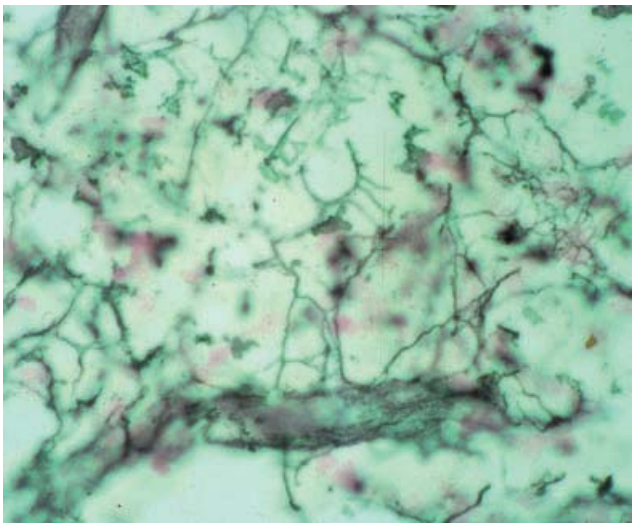

Figure 8.13. Cat: marrow, refractory anemia with excess blasts. Silver stain for reticulin on the same bone marrow as Figure 8.12. There is a small vessel at the bottom that is sheathed in reticulin fibers, which normally are not observed in an interdigitating pattern in interstitial areas. This level of sclerosis is sufficient to inhibit a normal level of hematopoiesis.

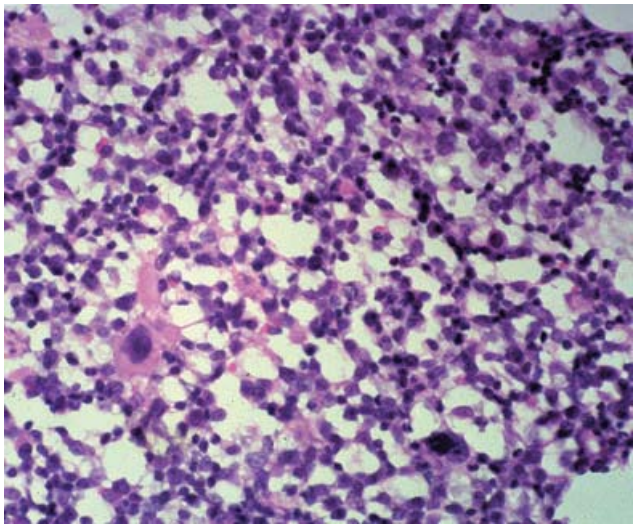

Figure 8.12. Cat: bone marrow, refractory anemia with excess blasts. Histologically, there is loss of fat, with possible areas of serous atrophy with spaces occupied by thin proteinaceous material. There is a preponderance of young cells with immature chromatin and round nuclei, a general lack of maturation in all three lineages, and an appearance of increased reticular stroma.

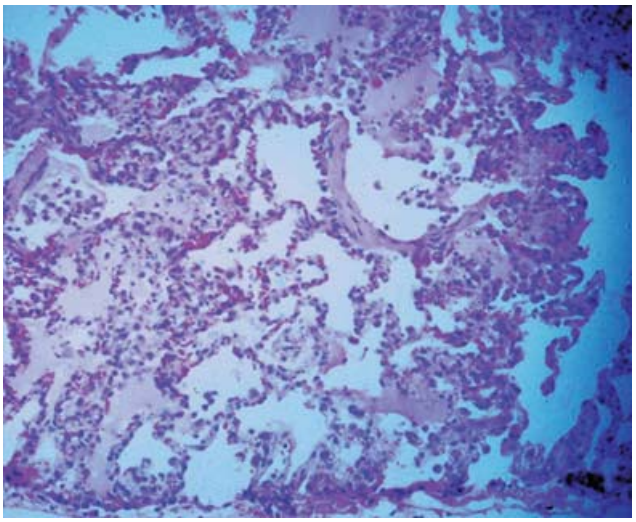

Figure 8.14. Cat: lung, marrow failure due to refractory anemia with excess blasts. There is patchy collapse and flooding with proteinaceous fluid but little apparent aggregation of cell reaction as a reflection of chronic neutropenia.

marrow, there is usually a complete loss of fat cells, but the marrow cells are more widely separated than in normally hyperplastic states, and the tissue is cohesive, which is indicative of reticulin (Fig. 8.12) but not collagen sclerosis (Fig. 8.13). The peripheral lack of neutrophils may make some lesions appear atypical, and inflammatory foci in lung will be almost devoid of mature neutrophils (Figs. 8.14, 8.15). In humans, dysplastic changes in the myeloid system may be present, and those in the erythroid system are most apparent. These are mirrored in animals and consist of megaloblastoid nuclei (Fig. 8.16), nuclear lobulation, and multinucleation (Fig. 8.17), which is most

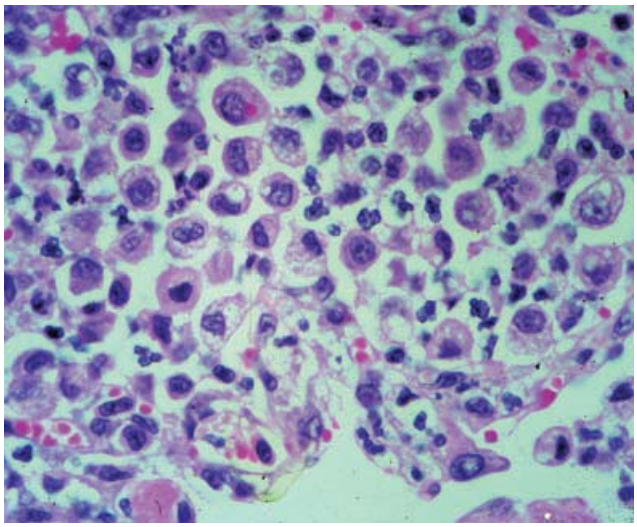

Figure 8.15. Cat: lung, pneumonia due to pancytopenia of refractory anemia. An area of alveolitis with a large number of alveolar macrophages and an unusually low number of neutrophils, some of which are degenerating with fragmentation of nuclei.

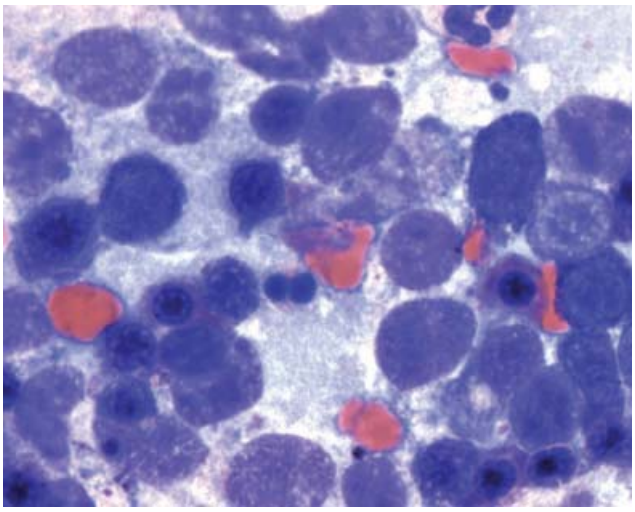

Figure 8.17. Dog: bone marrow, refractory anemia with excess blasts. A cluster of largely erythroid precursors contains a dyspoietic metarubricyte in the center, which has very lightly eosinophilic cytoplasm containing 2 nuclei of slightly varying diameters.

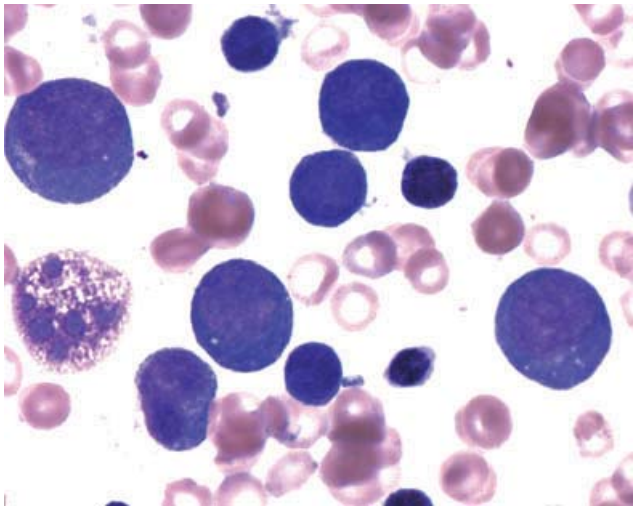

Figure 8.16. Cat: marrow, refractory anemia with excess blasts. Erythroid precursors retain a fine nuclear chromatin pattern with the nuclei decreased in size but with the cytoplasm having reduced density of hemoglobin in late stage cells that retain abnormal basophilia. The bare nucleus in the lower left is likely of an erythroid precursor that illustrates the fine chromatin pattern and multiple nucleoli that would be at the stage of a basophilic rubricyte.

apparent in animals with nuclei varying widely in diameter. In humans, but not in animals, the ringed sideroblasts may be present at levels above the 15% criterion level for RARS, and there may be Auer bodies in the blasts. As an indicator of prognostic significance the levels of sideroblasts are an accompaniment, but the levels of blasts and the Auer rods, when identified, dictate the category of classification. In the megakaryocytic lineage, dysplastic changes include micromegakaryocytes that have round nuclei, neither indented nor lobulated, and these may be numerous. Reminiscent of the "proliferation centers" seen in nodes in SLL in human RAEB there may be foci of increased immaturity in the marrow. If these foci are in interstitial areas and present in three or more areas, these areas are known as *abnormal localization of immature precursors* and are suggested to be indicative of increased risk of evolution to AML. These foci of increased immaturity have not been recognized in animals.

The confirmation of diagnosis is assisted by special staining that includes the periodic acid-Schiff stain or Factor VIII stain that helps identify the micromegakaryocytes that, with round nuclei, are less apparent if the cytoplasm is not identified as of megakaryocytic lineage. If the blast level is equivocal, staining with CD34 is of assistance in recognizing the level of precursors present.

REFERENCES

Baker, R.J., and Valli, V.E.O. (1986) Dysmyelopoiesis in the cat: A hematological disorder resembling refractory anemia with excess blasts in man. *Can J Vet Res* 50:3–6.

Fuchigami, K., Mori, H., Matsuo, T., Iwanaga, M., Nagai, K., Kuriyama, K., and Tomonaga, M. (1999) Absolute number of circulating $CD34^+$ cells is abnormally low in refractory anemias and extremely high in RAEB and RAEB-t; novel pathologic features of myelodysplastic syndromes identified by highly sensitive flow cytometry. *Leuk Res* 24:163–174.

Germing, U., and Gattermann, N. (2001) Refractory anemia with excess of blasts in transformation: A dying category? *Leuk Res* 25:1095–1096.

Guerci, A.-P., Feldmann, L., Humbert, J.-C., and Guerci, O. (1995) Refractory anemia with excess of blasts: A multivariate analysis of prognostic factors in 91 patients and a simplified scoring system for predicting survival. *Eur J Haematol* 54:241–244.

Hisasue, M., Okayama, H., Okayama, T., Suzuki, T., Mizuno, T., Fujino, Y., Naganobu, K., Hasegawa, A., Watari, T., Matsuki, N., Masuda, K., Ohno, K., and Tsujimoto, H. (2001) Hematologic abnormalities and outcome of 16 cats with myelodysplastic syndromes. *J Vet Intern Med* 15:471–477.

Juneja, S.K., Imbert, M., Sigaux, F., et al. (1983) Prevalence and distribution of ringed sideroblasts in primary myelodysplastic syndromes. *J Clin Pathol* 36:566–569.

Lester, S.J., and Searcy, G.P. (1981) Hematologic abnormalities preceding apparent recovery from feline leukemia virus infection. *JAVMA* 178(5):471–474.

Majluf-Cruz, A., Hurtado, R., Vargas-Vorackova, F., and Labardini-Méndez, J. (1999) Refractory anemia with excess of blasts: Increased survival when treated with cyclophosphamide, methotrexate and 6-mercaptopurine. *Eur J Haematol* 62:213–218.

Nand, S., and Godwin, J.E. (1988) Hypoplastic myelodysplastic syndrome. *Cancer* 62:958–964.

Orazi, A., Albiter, M., Heerema, N.A., et al. (1997) Hypoplastic myelodysplastic syndrome can be distinguished from acquired aplastic anemia by CD34 and PCNA immunostaining of bone marrow biopsy specimens. *Am J Clin Pathol* 107:268–274.

Seigneurin, D., and Audhuy, B. (1983) Auer rods in refractory anemia with excess of blasts: Presence and significance. *Am J Clin Pathol* 80:359–362.

Strupp, C., Gattermann, N., Giagounidis, A., Aul, C., Hildebrandt, B., Haas, R., and Germing, U. (2003) Refractory anemia with excess of blasts in transformation: Analysis of reclassification according to the WHO proposals. *Leuk Res* 27:397–404.

Tricot, G., De Wolf-Peeters, C., Hendrickx, B., et al. (1984) Bone marrow histology in myelodysplastic syndromes: I. Histological findings in myelodysplastic syndromes and comparison with bone marrow smears. *Brit J Haematol* 57: 423–430.

Tricot, G., Vlietinck, R., Boogaers, M.A., et al. (1985) Prognostic factors in the myelodysplastic syndromes: Importance of initial data on peripheral blood counts, bone marrow cytology, trephine biopsy and chromosomal analysis. *Brit J Haematol* 60:19–32.

Yokose, N., Ogata, K., An, E., Tamura, H., Kamikubo, K., Dan, K., and Nomura, T. (1995) Lineage-unrestricted hematologic response to granulocyte colony-stimulating factor in a patient with refractory anemia with excess blasts. *Ann Hematol* 70:163–167.

Yoshida, Y., Oguma, H., and Maekawa, T. (1995) Refractory myelodysplastic anaemias with hypocellular bone marrow. *J Clin Pathol* 41:763–767.

REFRACTORY CYTOPENIA WITH MULTILINEAGE DYSPLASIA

Refractory cytopenia (RC) with multilineage dysplasia includes those cases that present with varying levels of marrow failure having peripheral blood cytopenia that involves one or all three cell lineages and accompanied dysplastic changes in all lines but lack increased blasts or monocytes or the presence of Auer rods. Alternative and descriptive names include *refractory anemia with severe dysplasia*. A succinct description of RC is that it is like RAEB without increased blasts. Like other types of MDS, RC is paradoxical in that the marrow is hypercellular as distinguished from hyperplastic, but it is accompanied by peripheral blood cytopenia of one or more elements (Fig. 8.18). The blasts are only mildly increased and not above 5% in marrow, and blasts do not appear in the peripheral blood (Fig. 8.19). The marrow dysplastic changes are as have been described for RAEB (Figs. 8.20–8.22), and the megakaryocytic changes are always present, but they tend to be occult due to the presence of many micromegakaryocytes (Fig. 8.23). These cells with nonlobulated round nuclei may not be recognized as such in the absence of special stains to identify the cytoplasmic differentiation.

Many cases of MDS in humans are initiated by alkylating agent therapy and have multilineage marrow dysplasia. Where cytogenetic relationships have been determined, those with the 5q- and 20q-chromosomal defects tend to show the multilineage dysplasia, and these

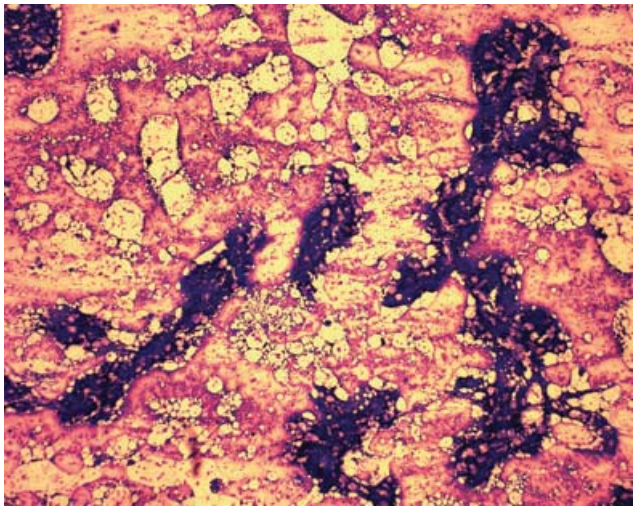

Figure 8.18. Mature cat with a history of weight loss found to have a total leukocyte count of 2.7×10^3/ul, with 9 grams per dl of Hb and moderately reduced platelet count. The marrow aspirate obtained relatively abundant marrow with the preparation demonstrating very cohesive masses with relatively poor single cell exfoliation. The marrow is moderately hypocellular.

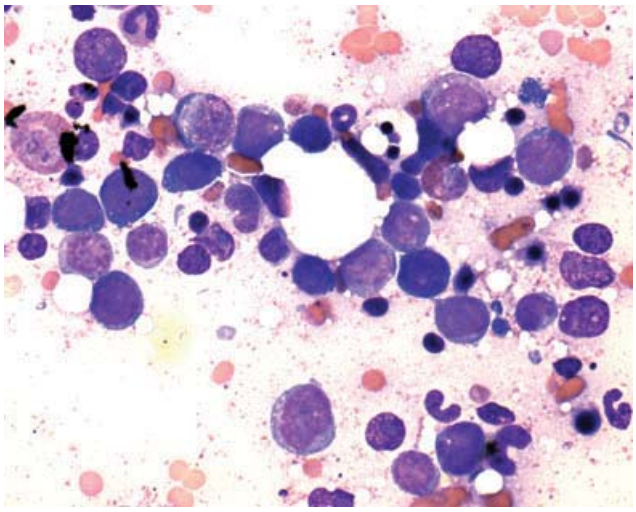

Figure 8.19. Cat: marrow, refractory cytopenia. Detail of Figure 8.18, with moderate early asynchrony with increased numbers of blastic cells with the presence of maturing rubricytes and myeloid cells. There is a giant metamyelocyte in the lower right and several late stage rubricytes.

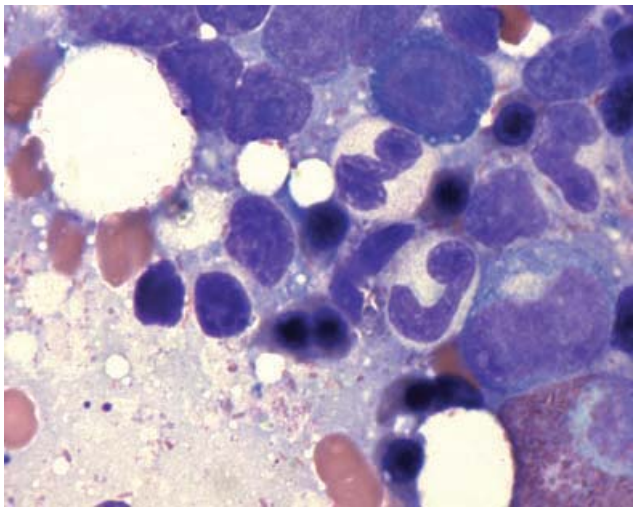

Figure 8.20. Cat: bone marrow, refractory cytopenia with multilineage dysplasia. There are numerous primitive proliferative cells in the upper area with a binucleated late stage rubricyte in the center.

genetic changes are found in both the erythroid and megakaryocytic lineages.

REFERENCES

Aguayo, A., Giles, F., and Albitar, M. (2003) Vascularity, angiogenesis and angiogenic factors in leukemias and myelodysplastic syndromes. *Leuk and Lymph* 44(2):213–222.

Blue, J.T. (2003) Myelodysplasia: Differentiating neoplastic from nonneoplastic syndromes of ineffective hematopoiesis in dogs. *Toxicol Pathol* 31(Suppl.):44–48.

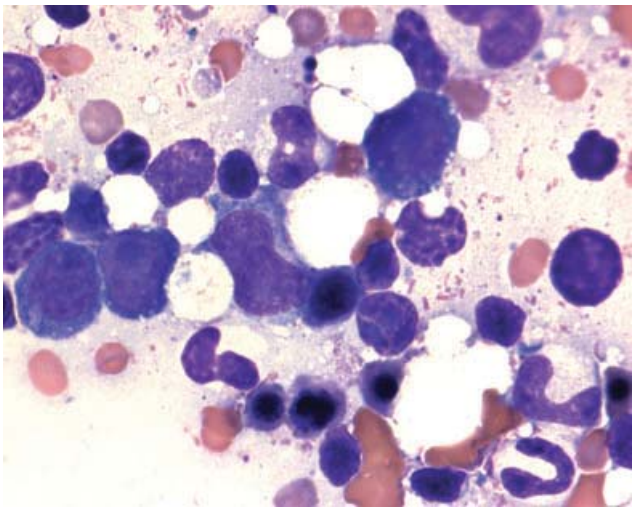

Figure 8.21. Cat: marrow, refractory cytopenia. There is a normal band neutrophil with a giant metamyelocyte adjacent in the lower right. There is a binucleated polychromatic rubricyte in the lower right and an eosinophil myelocyte in the upper left. The presence of dysplasia in both myeloid, erythroid series in the same area is relatively common.

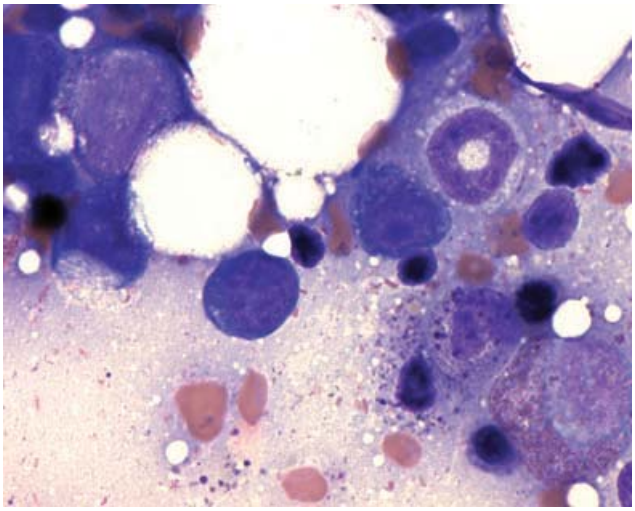

Figure 8.22. Cat: marrow, refractory cytopenia. The ringed nuclear metamyelocyte in the upper right is normal in rodents and is an indication of dysplasia in the myeloid system in larger mammals. The presence of more frequent basophil myelocytes in the lower right is a frequent accompaniment of dysplastic changes. The large cell in the upper left adjacent to the 2 fat cells has basophilic cytoplasmic granules suggesting that it is a basophil promyelocyte. The basophilic rubricytes in the center have asynchronously large nucleoli and fine chromatin.

Breuer, W., Hermanns, W., and Thiele, J. (1999) Myelodysplastic syndrome (MDS), acute myeloid leukaemia (AML) and chronic myeloproliferative disorder (CMPD) in cats. *J Comp Pathol* 121:203–216.

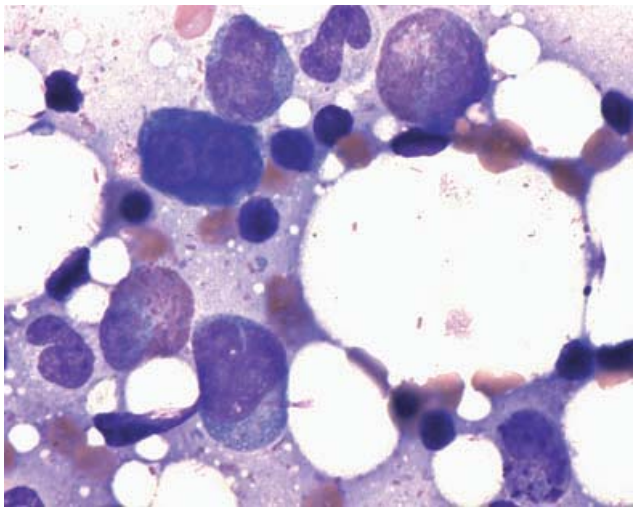

Figure 8.23. Cat: marrow, refractory cytopenia. The binucleated cell in the upper left is a dwarf megakaryoblast. The nuclei are approximately half normal size. Two interphase nuclei in a basophilic cytoplasmic envelope is the earliest recognizable stage of thrombopoiesis. There is a maturing basophil in the lower right that increases the likelihood of myeloid dysplasia, and the neutrophil at top and lower left have reduced normal granulation and typically persistent basophilia.

Brunning, R.D. (2001) Myelodysplastic syndromes. In Knowles, D.M. (ed.), *Neoplastic Hematopathology*, 2nd ed. Lippincott Williams & Wilkins, Philadelphia, pp. 1717–1743.

Brunning, R.D., and McKenna, R.W. (1994) Myelodysplastic syndromes. In *Tumors of the Bone Marrow. Atlas of Tumor Pathology*, 3rd series, fasc 9. Armed Forces Institute of Pathology, Washington, D.C., pp. 143–194.

Čermák, J., Michalová, K., Březinová, J., and Zemanová, Z. (2003) A prognostic impact of separation of refractory cytopenia with multilineage dysplasia and 5q-syndrome from refractory anemia in primary myelodysplastic syndrome. *Leuk Res* 27:221–229.

Chen, Y.-C., Chou, J.-M., Ketterling, R.P., Letendre, L., and Li, C.-Y. (2003) Histologic and immunohistochemical study of bone marrow monocytic nodules in 21 cases with myelodysplasia. *Am J Clin Pathol* 120:874–881.

Goasguen, J.E., Mielot, F., Buisine, J., Fenneteau, O., Duchayne, E., Mallet, M., and Groupe Français D'Hématologie Cellulaire. (1997) Prognostic factors in myelodysplastic syndromes: Specific prospects for children. *Intern J Ped Hematol/Oncol* 4(3):203–208.

Howe, R., Micallef, I.N.M., Inwards, D.J., Ansell, S.M., Dewald, G.W., Dispenzieri, A., Gastineau, D.A., Gertz, M.A., Geyer, S.M., Hanson, C.A., Lacy, M.Q., Tefferi, A., and Litzow, M.R. (2003) Secondary myelodysplastic syndrome and acute myelogenous leukemia are significant complications following autologous stem cell transplantation for lymphoma. *Bone Marrow Transpl* 32:317–324.

Lambertenghi Deliliers, G., Annaloro, C., Soligo, D., and Oriani, A. (1998) The diagnostic and prognostic value of bone marrow immunostaining in myelodysplastic syndromes. *Leuk and Lymph* 28:231–239.

Mathew, P., Tefferi, A., Dewald, G.W., et al. (1993) The 5q-syndrome: A single institution study of 43 cases. *Blood* 81:1040–1045.

Matsuda, A., Jinnai, I., Yagasaki, F., et al. (1998) Refractory anemia with severe dysplasia: Clinical significance of morphological features in refractory anemia. *Leuk* 12:482–485.

Metayer, C., Curtis, R.E., Vose, J., Sobocinski, K.A., Horowitz, M.M., Bhatia, S., Fay, J.W., Freytes, C.O., Goldstein, S.C., Herzig, R.H., Keating, A., Miller, C.B., Nevill, T.J., Pecora, A.L., Rizzo, J.D., Williams, S.F., Li, C.-Y., Travis, L.B., and Weisdorf, D.J. (2003) Myelodysplastic syndrome and acute myeloid leukemia after autotransplantation for lymphoma: A multicenter case-control study. *Blood* 101(5):2015–2023.

Nand, S., and Stock, W. (1997) Treatment of primary myelodysplastic syndromes: Lessons from the adult patient population. *Intern J Ped Hematol/Oncol* 4(3):239–253.

Rosati, S., Mick, R., Xu, F., et al. (1996) Refractory cytopenia with multilineage dysplasia: Further characterization of an "unclassifiable" myelodysplastic syndrome. *Leuk* 10:20–26.

Smith, S.M., Le Beau, M.M., Huo, D., Karrison, T., Sobecks, R.M., Anastasi, J., Vardiman, J.W., Rowley, J.D., and Larson, R.A. (2003) Clinical-cytogenetic associations in 306 patients with therapy-related myelodysplasia and myeloid leukemia: The University of Chicago series. *Blood* 102(1):43–52.

Tefferi, A., Mathew, P., and Noel, P. (1994) The 5q-syndrome: A scientific and clinical update. *Leuk Lymph* 14:375–378.

MYELODYSPLASTIC SYNDROME, UNCLASSIFIED

Human patients may present with an MDS-like syndrome which may not fit the criteria for any of the described syndromes, and are then recorded as unclassified. This would seem to be most often the case with MDS in animals where it may appear that some criteria are missing or other criteria are present that render cases unlike any of the major human types of MDS. The characteristics for unclassifiable cases of MDS in humans are

1. Minimal or no increase in blasts in the marrow or blood
2. Dysplasia found in only one lineage
3. Cytopenia occurring in one, two, or all cell lines with pancytopenia

A recurring human syndrome that fits these criteria is seen in patients that present with severe anemia and sometimes pancytopenia, but with marked marrow erythroid hyperplasia with severe dysplastic changes in that cell line alone. The overall changes are suggestive of AML of M6B type or erythremic myelosis without the level of blasts required for that diagnosis. These patients frequently have genetic changes involving chromosomes 5 or 7 and a short clinical course. In these cases, the differential diagnosis lies between AML of M6 type, refractory cytopenia with

multilineage dysplasia, or MDS unclassified. The major point made here is that in the absence of a sufficient blast level to justify a diagnosis of AML the patients should be treated with aggressive therapy. This is an important distinction that should be kept in mind in cases of this type arising in animals where the clinician in the absence of a firm diagnosis of neoplasia may be reluctant to treat as such. In animals, this type of presentation might be considered RAEB if the dysplastic changes in the myeloid system are subtle or missed (Figs. 8.24, 8.25).

In a further departure from the types of MDS seen in animals, there are a number of human syndromes that are associated with specific genetic abnormalities, none of which are known in animals as of this writing. These cases may, however, be instructive in terms of defining clinical syndromes associated with specific genetic dysfunction because the same genes seem to be present in animals but with different chromosomal relationships. Based on the prognostic impact of various cytogenetic changes, a system of grading or scoring human cases of MDS have been proposed with categories of good, intermediate, and poor. Those cases in the good category have normal chromosomes, 5q only, or 20q only, with those in the intermediate grading with abnormalities of other areas and poor with complex and multiple chromosomal changes.

The human 5q-syndrome is seen as a *de novo* disorder that involves an interstitial deletion of the long arm of chromosome 5 that loses bands q12 to q32. The clinical syndrome is seen most often in mature females and is characterized by hematologic changes resembling RAEB or refractory cytopenia with multilineage dysplasia. There is a macrocytic anemia requiring repeated transfusions, and leukocyte and platelet counts are generally maintained. The marrow has erythroid hypoplasia and myeloid dysplasia with increased numbers of dysplastic megakaryocytes without nuclear lobation, and with focal lymphoid and plasmacytic infiltrates. Some patients have splenomegaly. The course is generally chronic with some cases evolving to AML.

A case with similar marrow findings including erythroid hypoplasia with myeloid and megakaryocytic dysplasia was present in an 11-year-old female spayed Labrador retriever with persistent low-grade neutrophilia (Figs. 8.26–8.30).

A human syndrome with 17p deletion is characterized by dyplasia of the myeloid lineage with small neutrophils with hypolobulation of Pelger-Huët type accompanied by cytoplasmic vacuoles. Some neutrophils have contracted round nuclei, and the syndrome is frequently therapy related. The changes include dysregulation of the p53 suppressor gene and a poor prognosis.

A dysplastic syndrome that presents with increased platelet counts is seen with abnormalities of chromosome 3, which involves a paracentric inversion of bands q21–26 involving both arms. The marrow changes include dysthrombopoiesis with small hypolobulated megakary-

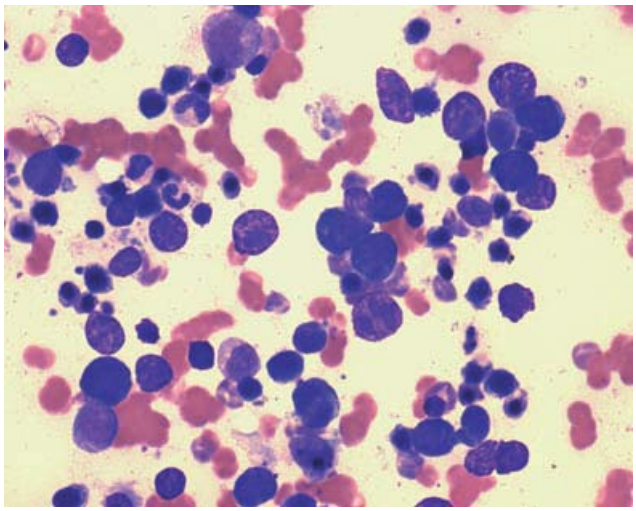

Figure 8.24. An 11-year-old male schnauzer was presented because of repeated episodes of syncope. Total leukocyte count was 7.5 × 10^3/ul, with 7.1 g per dl of Hb and 255 × 10^3/ul of platelets. On aspiration, the bone marrow was hypercellular with a marked erythroid predominance and early asynchrony. There are 6 putative blasts in this field with the rest of the cells in varying stages of erythroid differentiation, all of which have increased cytoplasmic basophilia and deficient hemoglobin production with a paucity of myeloid cells.

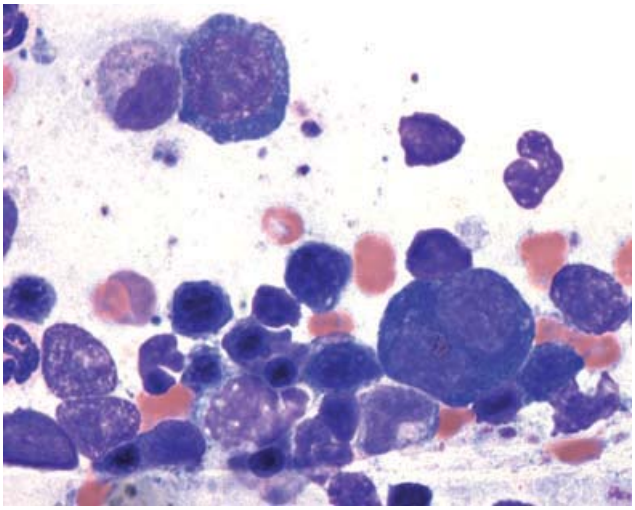

Figure 8.25. Dog: marrow, anemia due to myelodysplasia. Detail of Figure 8.24. There is an unidentified blast in the upper left with binucleated megakaryoblast in the lower right. To the left of that cell there are 2 basophilic rubricytes with abnormally vacuolated cytoplasm, and adjacent to them 2 rubricytes of polychromatic stage that may be binucleated with a prominent nuclear lobulation on the surface of the larger nucleus.

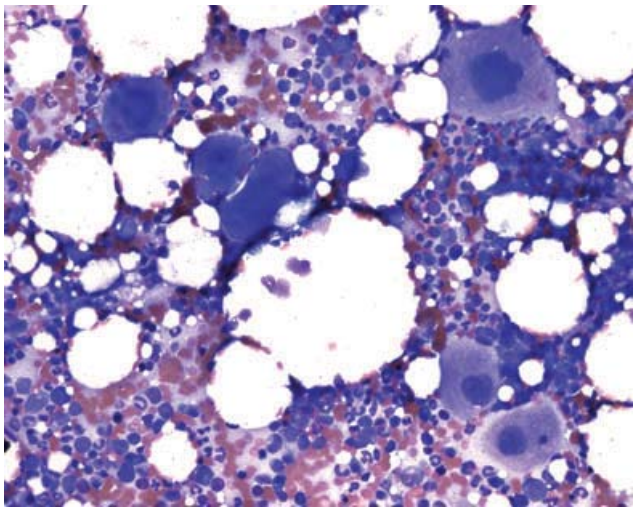

Figure 8.26. An 11-year-old female spayed Labrador retriever presented with a syndrome of chronic unexplained neutrophilia with thrombocytosis and early asynchrony. On aspiration of marrow, the megakaryocytes were increased in number and tended to have round lobulated but not segmented nuclei. There is binucleate emperipolesis in the upper right and in a single (lymphoid?) nucleus in the lower right.

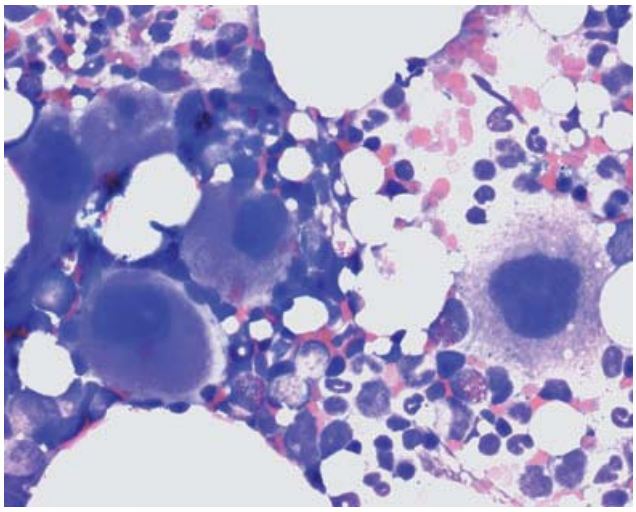

Figure 8.27. Dog: bone marrow, neutrophilia with myelodysplasia. Detail of Figure 8.26. This field contains 5 megakaryocytes, of which 3 have rounded nuclei and 2 have emperipolesis in the upper left and possibly at the lower left.

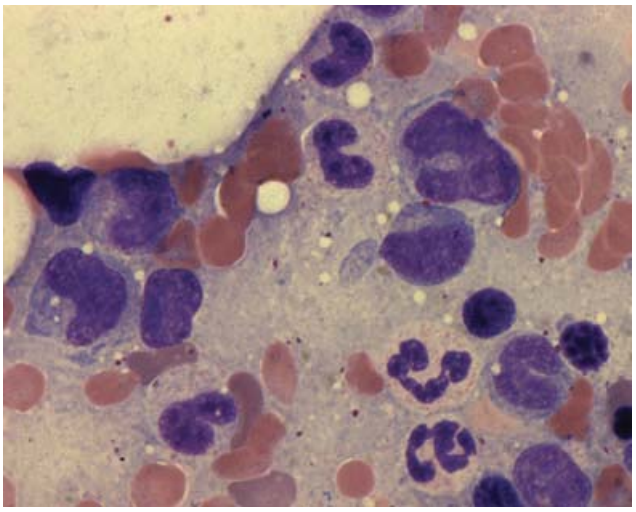

Figure 8.28. Dog: marrow, dysmyelopoiesis, same case as Figure 8.27. There are 9 cells in the field with characteristics of giant metamyelocytes. The neutrophils are approaching hypersegmentation.

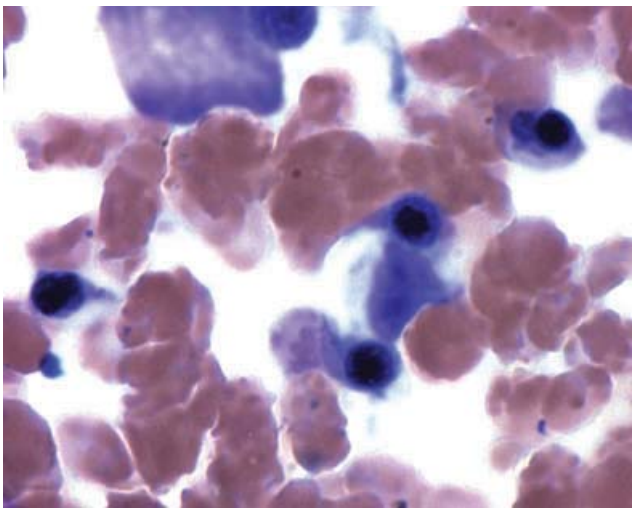

Figure 8.29. Dog: marrow, dyserythropoiesis, same case as Figure 8.26. There is a binucleated metarubricyte in the upper right with a cytoplasmic envelope retaining basophilia and with inadequate hemoglobin. The same asynchrony of maturation is present in the 2 metarubricytes in the center field, which may be ingested in a macrophage as ongoing ineffective erythropoiesis. The rubricyte at the left is bilobed with sharp shallow indentations of the metarubricyte nucleus and a small cytoplasmic envelope with tinctorial characteristics similar to that in the upper right.

ocytes that are increased in number. These patients have a poor prognosis and may have a history of exposure to mutagenic agents.

A disorder seen most often in males, and generally under a year of age, is associated with monosomy 7, which has presentation with anemia and neutrophilia and frequently thrombocytopenia. There may be recurrent infections and hepatosplenomegaly. Neutrophils have defective chemotaxis with dysplastic changes in precursors and a very low level of peripheral blood blasts. There is accompanying monocytosis and recurring leukoerythroblastosis. Dysplastic changes may be present in the erythroid lineage, but the megakaryocytic line appears

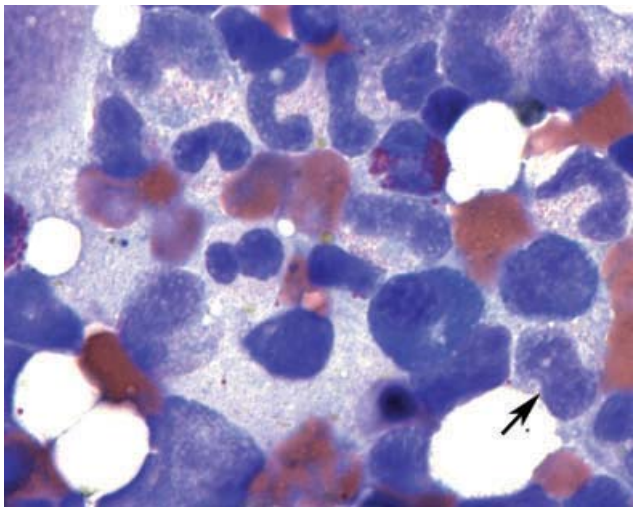

Figure 8.30. Dog: marrow, myelodysplasia, same case as Figure 8.26. There is a prominent plasmacytosis throughout the marrow with a characteristic well-differentiated plasma cell in the center right. In the left center a neutrophil with a bilobed nucleus is characteristic of the Pelger-Huët type of maturation anomaly and one with an hourglass-shaped nucleus to the right of the plasma cell (arrow).

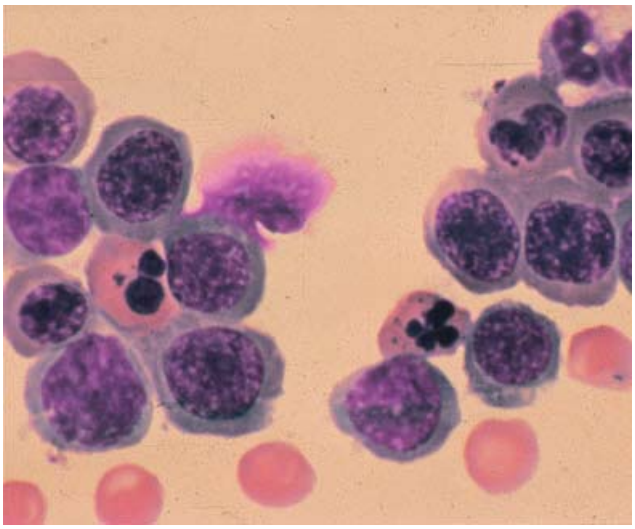

Figure 8.31. Human: bone marrow aspirate, arsenic poisoning. There is marked dyserythropoiesis primarily evident in maturing rubricytes with multinuclearity and binucleation. *Image from R. D. Brunning, M.D.*

normal but reduced in number. This constellation of changes may be seen in AML and must be differentiated from juvenile myelomonocytic leukemia (jMML) with the distinction not always possible on morphologic grounds alone.

MDS in Perspective: Differential Diagnosis of Myelodysplastic Syndromes

The diagnosis of MDS must include a careful consideration of clinical history and any environmental or lifestyle exposure that may have led to genetic injury. In general, the entities included in the spectrum of MDS disorders can be considered as two main groups characterized by requisite morphologic changes plus increased blasts or with normal levels of blasts. Those types with increased blasts and/or Auer rods include RAEB-1 and RAEB-2. Those types of MDS without increased blasts include refractory anemia (RA), RA with ringed sideroblasts (RARS), refractory cytopenia with multilineage dysplasia, and finally MDS unclassified.

The differentials for subtypes of MDS with low blast counts are instructive in indicating mechanisms for the various morphologic changes observed. Cases presenting with RA, RARS, and MDS unclassified have changes in blood and marrow that resemble those of specific deficiency (megaloblastoid) or toxic exposures (multinuclearity). The most important are the megaloblastic changes in the erythroid system that may be caused by vitamin B_{12} and/or folic acid deficiency, and assays for these vitamins are essential before other treatment is given. Exposure to heavy metals such as arsenic (Fig. 8.31) causes dysplastic changes that are limited to the erythroid lineage. The erythroid changes in animals, which include mild anemia, rubricytosis, and basophilic stippling associated with lead poisoning, have been well described. The human syndrome of congenital dyserythropoietic anemia known to be associated with rubricyte multinuclearity is usually apparent at an early age; however, examples in animals likely exist, including the anemia and marrow failure of the adult black rhinoceros (Fig. 8.32). Most chronic anemias in humans and animals are associated with abnormal accumulations of iron, but the ringed sideroblasts characteristic of that form of human refractory "sideroblastic" anemia (see Fig. 8.7) are not generally recognized in animals. Porphyria, which occurs in cattle and other animals as an inherited disease, is associated with morphologic changes of erythroid nuclei that mimic changes of MDS and might be misinterpreted in the absence of a full history and examination. HIV infection is associated with bone marrow dysplastic changes involving all three lineages, and similar changes may occur in nonhuman primates infected with SIV. Other viral agents that may cause serious marrow changes include the parvoviral infections of humans and animals, which are characterized by aplasia followed by a regenerative burst that includes a stage of marked early asynchrony resembling the maturation arrest of MDS. Finally, as treatment with GM-CSF becomes more common in animals, it is important to recognize that the response to this therapy results

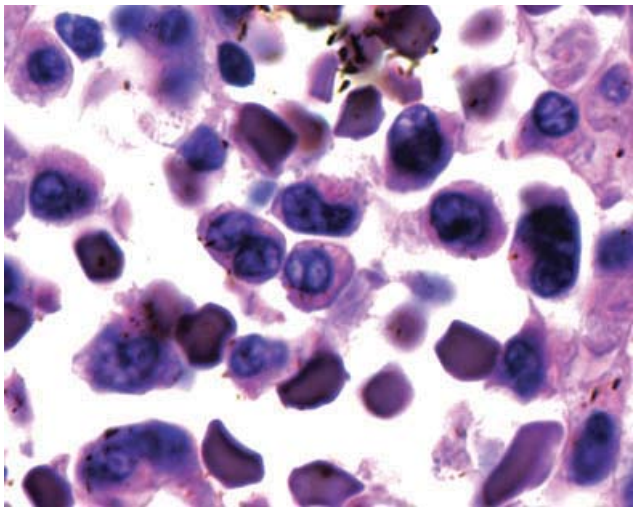

Figure 8.32. Black rhinoceros: bone marrow, chronic (congenital?) anemia now with myelofibrosis, hemosiderosis, and marrow failure. Autolytic changes are present in the marrow with most of the cells present of erythroid type. There is a binucleate late stage rubricyte in the left center and immediately below out of focus is a late stage rubricyte with a broad-based nuclear lobe, both indicative of dyserythropoiesis. Crystalline granules in the left above center are hemosiderin crystals.

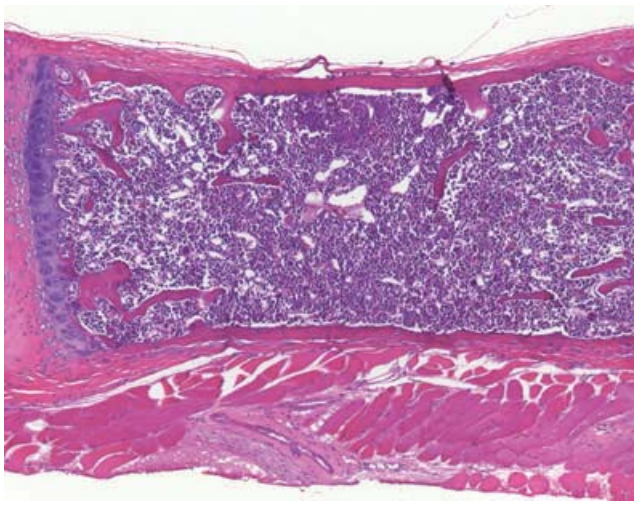

Figure 8.33. Mouse: sternal marrow, myelodysplasia. The marrow is solidly cellular with an absence of fat cells and there may be mild osteopenia. *Slide from J. M. Ward, DVM.*

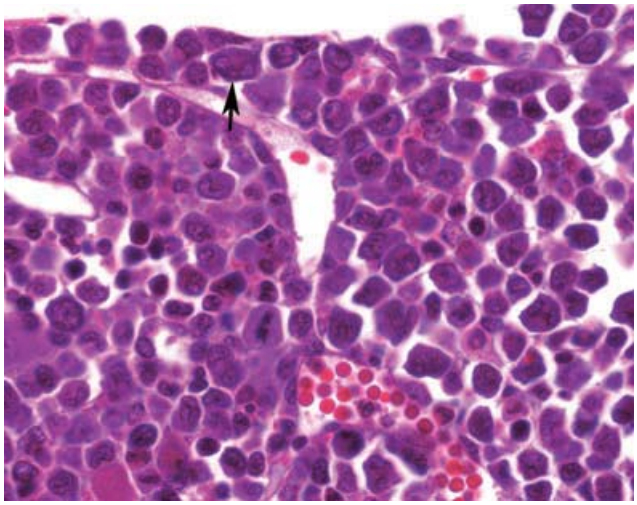

Figure 8.34. Mouse: marrow, myelodysplasia. Detail of Figure 8.33. The marrow is solidly cellular with myeloid predominance, early asynchrony with blasts less than 10%. These blastic changes are present in all lineages with a giant metamyelocyte evident at upper center (arrow). Note the anisocytosis of red cells. *Slide from J. M. Ward, DVM.*

in the presence of blasts in the peripheral blood and hypolobulation of neutrophils with marked atypical cytoplasmic granulation and Dohle bodies that may be misinterpreted as a form of MDS.

For those types of MDS associated with an increased blast count, which includes RAEB types 1 and 2, the differential diagnosis includes corresponding types of AML, including M2 AML with maturation, M4 acute myelomonocytic leukemia, and M6 the acute erythroid leukemias. Myelodysplastic changes are described in the mouse, and these appear to be more in the nature of generalized myeloproliferative disease with myeloid rather than erythroid predominance and very solid and diffuse involvement of spleen and marrow (Figs. 8.33–8.36). The dysplastic changes seen in the mouse are almost invariably found at necropsy, and as a result the tissue changes are not correlated with the evidence of MDS as seen in the peripheral blood. In comparison to descriptions of MDS in humans, the tissue changes in the mouse are most like the syndrome of refractory cytopenia in humans.

MDS: Prognosis

In humans, those types of MDS associated with an increased blast count like RAEB have a poorer prognosis and generally shorter survival, with one review finding a median survival of 2.1 years for patients with a marrow blast count lying between 5–10% and 0.7 years for those with a blast count of 11–20%. The survival for cases with RA and RARS is longer because these tend not to evolve to AML, but over time they have increased cytopenias and tend to terminate in marrow failure. Patients with MDS of refractory cytopenia with multilineage dysplasia are more likely to have an intermediate risk of progression to AML and of intermediate prognosis.

A workshop on prognostic factors determined that there are three major criteria that strongly relate to risk

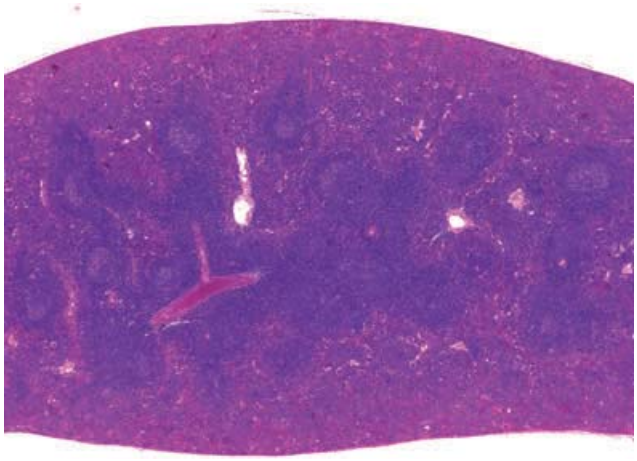

Figure 8.35. Mouse: spleen, myelodysplasia. The organ is markedly enlarged with the germinal centers unusually well defined. The periarteriolar lymphoid sheaths are reduced in proportion but not likely in total overall mass. There is massive sinus infiltration, with hematopoietic cells with many megakaryocytes that are evident at the architectural level of examination. *Slide from J. M. Ward, DVM.*

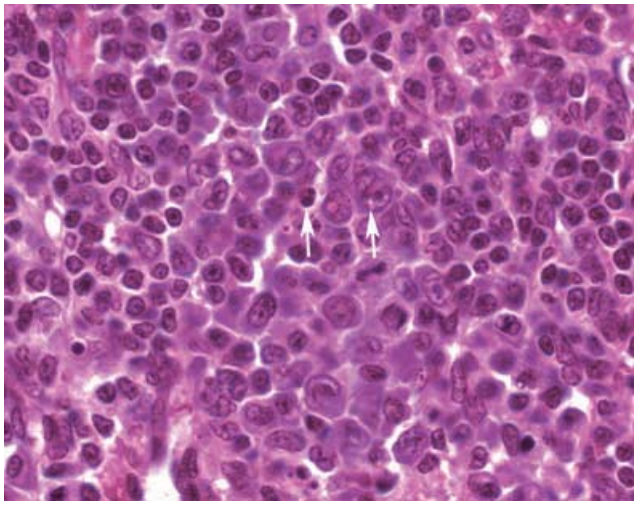

Figure 8.36. Mouse: spleen, myelodysplasia. Detail of Figure 8.35. The sinus areas of the spleen are similar to bone marrow with a solid proliferation that has myeloid predominance. Myeloid dysplasia is evident in the giant metamyelocyte to the left of center (right arrow) and to the left what appears to be a binucleated late stage rubricyte (left arrow). There are numerous mitoses (center) but the level of immaturity does not approach that of leukemia.

of evolution to AML: presence and type of genetic aberration, level of myeloblasts in marrow, and number of cell lineages in deficient numbers and at cytopenic level. Other important factors are patient age and gender. Based on these criteria, four levels of risk groups for evolution to AML and with short survival were defined with the poorest having complex cytogenetic abnormalities, higher marrow blast counts, and multiple cytopenias.

MDS: Management

Those human cases that have the higher blast counts and are at high risk of evolving to AML may enter remission on treatment with topotecan and cytarabine. The cases with more chronic types of MDS, especially with neutropenia, may benefit from treatment with recombinant drugs for stem cell stimulation.

REFERENCES

Baranger, L., Baruchel, A., Leverger, G., et al. (1990) Monosomy-7 in childhood hemopoietic disorders. *Leuk* 4:345–349.

Beran, M., Estey, E., O'Brien, S., et al. (1999) Topotecan and cytarabine is an active combination regimen in myelodysplastic syndromes and chronic myelomonocytic leukemia. *J Clin Oncol* 17:2819–2830.

Bitter, M.A., Neilly, M.E., LeBeau, M.M., et al. (1985) Rearrangements of chromosome 3 involving bands 3q21 and 3q26 are associated with normal or elevated platelet counts in acute nonlymphocytic leukemia. *Blood* 66:1362–1370.

Brown, K., and Young, N. (1995) Parvovirus B19 infection and hematopoiesis. *Blood Rev* 9:176–182.

Brunning, R.D. (2001) Myelodysplastic syndromes. In Knowles, D.M. (ed.), *Neoplastic Hematopathology*, 2nd ed. Lippincott Williams & Wilkins, Philadelphia, pp. 1717–1743.

Brunning, R.D., and McKenna, R.W. (1994) Myelodysplastic syndromes. In *Tumors of the Bone Marrow: Atlas of Tumor Pathology*, 3rd series, fasc 9. Armed Forces Institute of Pathology, Washington, D.C., pp. 143–194.

Butcher, M., Frenck, R., Emperor, J., et al. (1995) Molecular evidence that childhood monosomy 7 syndrome is distinct from juvenile chronic myelogenous leukemia and other childhood myeloproliferative disorders. *Genes Chrom Cancer* 12:50–57.

Coiffier, B., Adeleine, P., Gentilhomme, O., et al. (1987) Myelodysplastic syndromes: A multi-parametric study of prognostic factors in 336 patients. *Cancer* 60:3029–3032.

Evans, J.P.M., Czepulkowski, B., Gibbons, B., et al. (1988) Childhood monosomy 7 revisited. *Brit J Haematol* 69:41–45.

Fenaux, P., Morel, P., and LucLai, J. (1996) Cytogenetics in myelodysplastic syndromes. *Sem Hematol* 33:127–138.

Fonatsch, C., Gudat, H., Lengfelder, E., et al. (1994) Correlation of cytogenetic findings with clinical features in 18 patients with inv(3)(q21;q26) or t(3:3)(q21;q26). *Leuk* 8:1318–1326.

Foucar, K., Langdon, R.M., Armitage, J.O., et al. (1985) Myelodysplastic syndromes: A clinical and pathologic analysis of 109 cases. *Cancer* 56:553–561.

Greenberg, P., Cox, C., Lebeau, M., et al. (1997) International scoring system for evaluation prognosis in myelodysplastic syndromes. *Blood* 89:2079–2088.

Guillermo, F., Sanz, M.A., Vallespi, T., et al. (1989) Two regression models and a scoring system for predicting survival and planning treatment in myelodysplastic syndromes: A multi-

variate analysis of prognostic factors in 370 patients. *Blood* 74:395–408.

Hasle, H. (1994) Myelodysplastic syndromes in childhood. Classification, epidemiology, and treatment. *Leuk Lymp* 13:11–26.

Hasle, H., Arico, M., Basso, G., et al. (1999) Myelodysplastic syndrome, juvenile myelomonocytic leukemia and acute myeloid leukemia associated with complete or partial monosomy 7. *Leuk* 13:376–385.

Hutter, J.J., Hecht, F., Kaiser-McCaw, B., et al. (1984) Bone marrow monosomy 7: Hematologic and clinical manifestations in childhood and adolescence. *Hematol Oncol* 2:5–12.

Jary, L., Mossafa, H., Fourcase, C, et al. (1997) The 17-p-syndrome: A distinct myelodysplastic syndrome entity? *Leuk Lymph* 25:163–168.

Jenkins, R.B., Tefferi, A., Solberg, L.A., et al. (1989) Acute leukemia with abnormal thrombopoiesis and inversions of chromosome 3. *Cancer Genet Cytogenet* 39:167–179.

Jotterand, M., and Parlier, V. (1996) Diagnostic and prognostic significance of cytogenetics in adult primary myelodysplastic syndromes. *Leuk Lymph* 23:253–266.

Kerkhofs, H., Hagemeijer, A., Leeksma, C.H.W., et al. (1982) The 5q-chromosome abnormality in haematological disorders: A collaborative study of 34 cases from the Netherlands. *Brit J Haematol* 52:365–381.

Kerkhofs, H., Hermans, J., Haak, H.L., et al. (1987) Utility of the FAB classification for myelodysplastic syndromes: Investigation of prognostic factors in 237 cases. *Brit J Haematol* 65:73–81.

Kurtin, P.J., DeWald, G.W., Shields, D.J., et al. (1996) Hematologic disorders associated with deletions of chromosome 20q-. *Am J Clin Pathol* 106:680–688.

Kyle, R.A., and Pease, G.L. (1965) Hematologic aspects of arsenic intoxication. *N Engl J Med* 273:18–23.

Lai, H., Preudhomme, C., Zandecki, M., et al. (1995) Myelodysplastic syndromes and acute myeloid leukemia with 17p deletion: An entity characterized by specific dysgranulopoiesis and a high incidence of P53 mutations. *Leuk* 9:370–381.

List, A.F., Harinder, S., Garewal, S., et al. (1990) The myelodysplastic syndromes: Biology and implications for management. *J Clin Oncol* 8:1424–1441.

Luna-Fineman, S., Shannon, K.M., and Lange, B.J. (1995) Childhood monosomy 7: Epidemiology, biology, and mechanistic implications. *Blood* 85:1985–1999.

Passmore, S.J., Hann, I.M., Stiller, C.A., et al. (1995) Pediatric myelodysplasia: A study of 68 children and a new prognostic scoring system. *Blood* 85:1742–1750.

Pintado, T., Ferro, M.T., San Roman, C.L., et al. (1985) Clinical correlations of the 3q21;q26 cytogenetic anomaly: A leukemia or myelodysplastic syndrome with preserved or increased platelet production and lack of response to cytotoxic therapy. *Cancer* 55:535–541.

Sanz, G.F., Sanz, M.A., Vallespi, T., et al. (1989) Two regression models and a scoring system for predicting survival and planning treatment in myelodysplastic syndromes: A multivariable analysis of prognostic factors in 370 patients. *Blood* 74:395–408.

Shannon, K.M., Waterson, J., Johnson, P., et al. (1992) Monosomy 7 myeloproliferative disease in children with neurofibromatosis, type 1: Epidemiology and molecular analysis. *Blood* 79:1311–1318.

Sieff, C.A., Chessells, J.M., Harvey, B.A.M., et al. (1981) Monosomy 7 in childhood: A myeloproliferative disorder. *Brit J Haematol* 49:235–249.

Soenen, V., Preudhomme, C., Roumier, C., et al. (1998) 17p deletion in acute myeloid leukemia and myelodysplastic syndrome: Analysis of breakpoints and deleted segments by fluorescence in situ. *Blood* 91:1008–1015.

Sokal, G., Michaux, J.L., Van Den Berghe, H., et al. (1975) A new hematologic syndrome with a distinct karyotype: The 5q-chromosome. *Blood* 46:519–533.

Sterkers, Y., Preudhomme, C., Lai, J.-L., et al. (1998) Acute myeloid leukemia and myelodysplastic syndromes following essential thrombocythemia treated with hydroxyurea: High proportion of cases with 17p deletion. *Blood* 91:616–622.

Suciu, S., Kuse, R., Weh, H., et al. (1990) Results of chromosome studies and their relation to morphology, course, and prognosis in 120 patients with de novo myelodysplastic syndrome. *Cancer Genet Cytogenet* 44:15–26.

Tefferi, A., Matthew, P., and Noel, P. (1994) The 5q-syndrome: A scientific and clinical update. *Leuk Lymph* 14:375–378.

Third MIC Cooperative Study Group. (1988) Recommendations for a morphologic, immunologic, and cytogenetic (MIC) working classification of the primary and therapy related myelodysplastic disorders. *Cancer Genet Cytogenet* 32: 1–10.

Tricot, G., Boogaerts, M.A., De Wolf-Peeters, C., et al. (1985) The myelodysplastic syndromes: Different evolution patterns based on sequential morphological and cytogenetic investigations. *Brit J Haematol* 59:659–670.

Van den Berge, H., Vermaelen, K., Mecucci, C., et al. (1985) The 5q-anomaly. *Cancer Genet Cytogenet* 17:189–255.

Westhoff, D.D., Samaha, R.J., Barnes, A., Jr. (1975) Arsenic intoxication as a cause of megaloblastic anemia. *Blood* 45:241–246.

Young, N. (1995) B19 parvovirus. *Baillieres Clin Haematol* 8:25–27.

Yunis, J.J., and Brunning, R.D. (1986) Prognostic significance of chromosomal abnormalities in acute leukemias and myelodysplastic syndromes. *Clin Haematol* 15:597–620.

Yunis, J.J., Lobell, M., Arnesen, M.A., et al. (1988) Refined chromosome study helps define prognostic subgroups in most patients with primary myelodysplastic syndrome and acute myelogenous leukaemia. *Brit J Haematol* 68:189–194.

Yunis, J.J., Rydell, R.E., Oken, M.M., et al. (1986) Refined chromosome analysis as an independent prognostic indicator in de novo myelodysplastic syndromes. *Blood* 67:1721–1730.

Chapter 9

Hodgkin's Lymphoma

Lymphoma of the Hodgkin's type is rare in animals, but cases acceptable to human pathologists have rarely been reported. More often, cases are suggested to be a counterpart of the human disease, but these are also more often less well defined. In the last WHO revision of classifications, it was suggested that the name of the disease be changed from *Hodgkin's disease* to *Hodgkin's lymphoma,* because patients given the traditional diagnosis were unaware that they had a malignant neoplasm. The Reed-Sternberg (RS) cell, the hallmark of Hodgkin's lymphoma (HL) or Hodgkin's disease (HD), has been the object of much study over the last century and been an enigmatic marker that has yielded its biological lineage to the tools of molecular pathology. The development of the laser capture microscope permitted the harvesting of individual cells that could be identified in histologic preparations by standard methods of morphology and staining. By this means, individual RS cells were retrieved from patients with HL and, by molecular probes and PCR techniques, were found to have rearranged immunoglobulin genes. These rearrangements included the variable region of the immunoglobulin gene that defined the RS cells as having passed through a germinal center selection process and were, therefore, aberrant B-cells. Further, in a number of cases, the RS cells were found to be clonal, and in further studies subtypes of RS cells were identified as nonclonal. Subsequently, those cases in which the RS cells were clonal were found to occur in those cases of HL identified as the classic types. In a small proportion of cases of human HL, the RS cells appear to be derived from dendritic cells and in others from T-cells with characteristics of NK cells. These findings have led to a revised classification system for Hodgkin's lymphoma for the most common types.

CLASSIFICATION OF HODGKIN'S LYMPHOMA

The advent of molecular probes has resulted in the addition of a new category of HL known as *lymphocyte predominance,* which identifies the subtype of HL in which the RS cells have rearranged immunoglobulin genes but continue to mutate the variable region gene. The remaining categories have RS cells with clonal rearrangements of the immunoglobulin gene and appear as normal postgerminal center B-cells, and these are now known as the classic types of HL. The previous category of lymphocyte predominance is now split into two, with the new category with the mutating variable region gene retaining the older name of *lymphocyte predominance* and the category in the classic group now named *lymphocyte-rich classic*. The following is the WHO classification:

- Nodular lymphocyte predominance
- Lymphocyte-rich classic
- Nodular sclerosis grades I and II
- Lymphocyte depletion

A major interest of veterinary medicine in HL is that the type of lymphoma known as *diffuse mixed* in the Working Formulation and currently as *T-cell rich large B-cell lymphoma (TCRLBCL)* is an important differential for the Lymphocyte-rich classic type of HL. As noted in the description of subtypes of large B-cell lymphoma, TCRLBCL is seen frequently in domestic animals, particularly in the cat and the horse. Reports of HL type of lymphoma in animals are usually of the TCRLBCL type. It is known that in humans, and to a lesser extent in animals, the RS type of cells may occur in a number of other diseases particularly infectious mononucleosis and non-Hodgkin's type lymphomas. Therefore, in an attempt to define the Hodgkin's type lymphoma in humans, it has been stressed that the diagnosis rests on finding diagnostic RS-type cells in an appropriate cellular background or environment. Unfortunately, because HL consists of a spectrum of diseases, the cellular background can have a lot of variation, and the definition is not specific or explicit.

THE MORPHOLOGY OF THE RS CELLS

In human pathology, a great deal of emphasis is placed on the fact that the RS cells themselves have different characteristics in each of the subtypes of HL. Some

general characteristics are that the *diagnostic* RS cells are usually binucleated but can be lobated or multinucleated. The nuclei are large, generally 2–3 red cells in diameter, and with peripheralized chromatin such that the very large nucleoli are described as *inclusion-body–like*. The nucleoli themselves are distinctly eosinophilic and homogeneous and generally about one-quarter of the diameter of the nucleus. The cytoplasm is abundant and deeply amphophilic. Cells in animals that are compared to diagnostic human RS cells may be large and have large nucleoli, but they frequently lack the peripheralization of chromatin that gives the large nucleolus its evident prominence.

The variations of RS cell types include the "popcorn" type characteristic of the lymphocyte predominance form of HL. These cells are mononuclear and have multiple deep nuclear folds or lobulations, each of which may have a prominent nucleolus but one that is smaller than that of the binucleated type. These cells also have abundant cytoplasm. Cells of this type are seen in the TCRLBC type of lymphoma in cats. The lymphocyte-rich classic type of HL has the classic type of RS cell as described above, with binucleated or multinucleated forms and the very large nucleoli. The RS cells of the nodular sclerosis type of HL are again unique in having one to several nuclei with smaller but prominent nucleoli that are often basophilic staining and abundant pale-staining cytoplasm that retracts from the surrounding cells. The latter characteristic gives these cells their descriptive name of *lacunar cells*, and these cells are frequently seen in various stages of degeneration and necrosis with very eosinophilic cytoplasm. This type of change is also seen frequently in the large neoplastic B-cells of TCRLBCL of the cat. Finally, the RS cells of the lymphocyte depletion type of HL are very variable and pleomorphic with mononuclear and binucleated forms and nuclei of various shapes. In the lymphocyte depletion type of HL, the pleomorphic RS cells are characteristically numerous; an older name for this category is *HL of sarcomatous type*.

THE PHENOTYPIC CHARACTERISTICS OF THE RS CELLS

In the diagnosis of HL, pathologists are assisted by distinct antigenic patterns and immunophenotypic reactions of RS cells in the various types of HL. In the lymphocyte predominance type of HL, the RS cells have unique features that have resulted in suggestions that this entity is more like the non-HL type of lymphoid neoplasms. These RS cells are consistently positive with CD20 and CD45 but are negative for CD15 and vimentin and usually also negative for CD30.

In the lymphocyte-rich classic HL, both the diffuse and nodular forms express the constellation of antigens characteristic of the classic types of HL, namely CD15 and CD30 positive and CD20 and CD45 negative, and these staining characteristics are also present in the nodular sclerosis, mixed cellularity, and lymphocyte depletion types of HL. Other immunologic criteria commonly positive in the classic types of HL include vimentin, fascin, and CD40.

GENERAL PATHOLOGY OF HL

Lymphocyte Predominance

The lymphocyte predominance or, more commonly, nodular lymphocyte predominance (NLPHL) type of HL includes about 5% of cases of which only about 10% are of diffuse lymphocytic and histiocytic type, and the name is generally synonymous with nodular HL. The disease is most common in men in their forties who present with persistent nodal enlargement, are in stages 1-IIA, and have a relatively indolent course. Most of the cells in the lymphocyte predominance type are a mixture of small lymphocytes and histiocytes with the distinction that, in the nodular forms, half of the small lymphocytes mark for B-cells. In nodes, the residual germinal centers are largely subcapsular with the nodules of HL poorly delineated and variable in size, and they may require a reticulin stain to better visualize them (Fig. 9.1). The most characteristic feature is the presence of the L&H or popcorn type of RS cells that may make up 10% of the cells present; the

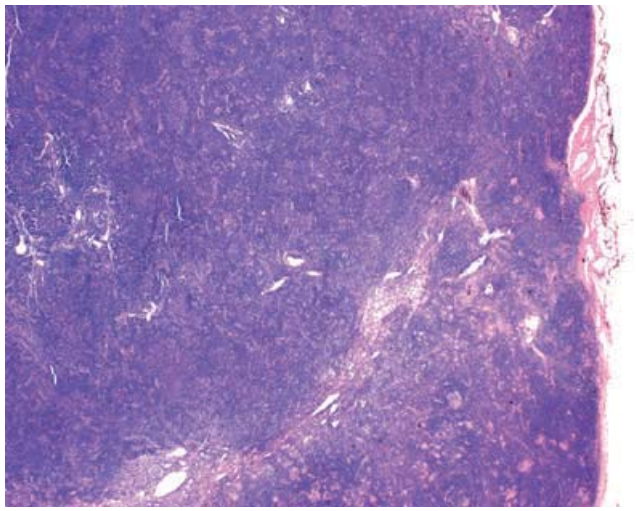

Figure 9.1. Human: node, Hodgkin's lymphoma, lymphocyte predominance type. The architecture is largely diffuse, but focal lightly stained areas with a border of increased density representing faint nodularity are apparent in the left center. The capsule is compressed but there is no apparent extra nodal colonization. *Slide from Cornell Tutorial.*

mononuclear type of RS cell is rare and may not be found. Characteristically, the small lymphocytes ringing the popcorn type RS cells are all of T-cell type with their presence known as the *rosetting pattern* (Figs. 9.2–9.4). The absence of the mononuclear-type RS cells is as significant as the abundance of small lymphocytes, and if RS cells of this type are present the diagnosis is more likely lymphocyte-rich classic HL or mixed cellularity HL. The architectural appearance of HL of lymphocyte predominance type strongly resembles that of nodes with reactive hyperplasia undergoing "progressive transformation of germinal centers" where there is marked variation in size of nodules; however, in the reactive form the L&H type of popcorn RS cells is not present.

Lymphocyte-Rich Classic HL

The classic type of HL now includes all other types of HL that are linked by similar phenotype of neoplastic cells and differ in topographical areas involved, clinical presentations, growth patterns, levels of fibrosis, and cellular atypia. The subtypes include nodular sclerosis, mixed cellularity, lymphocyte-rich, and lymphocyte depletion. The lymphocyte-rich classic HL is the most recent addition to the classification and is defined as a diffuse lymphoid neoplasm with relatively infrequent RS cells of the classic type with very large nucleoli. The background population is of small lymphocytes, occasional eosinophils, and plasma cells. The nodular form of this subtype has many mantle cell–type lymphocytes and dendritic cells in an irregular background. Both the classic and lacunar types of RS cells are found around the borders of the nodules. The main differential diagnosis of the lymphocyte-rich classic form of HL is the T-cell rich large B-cell lymphoma that has a small cell lymphoid background and even very large cells that may mimic the classic and L&H type of RS cells. The T-cell rich large B-cell lymphoma of cats shares many of these characteristics (Figs. 9.5–9.7).

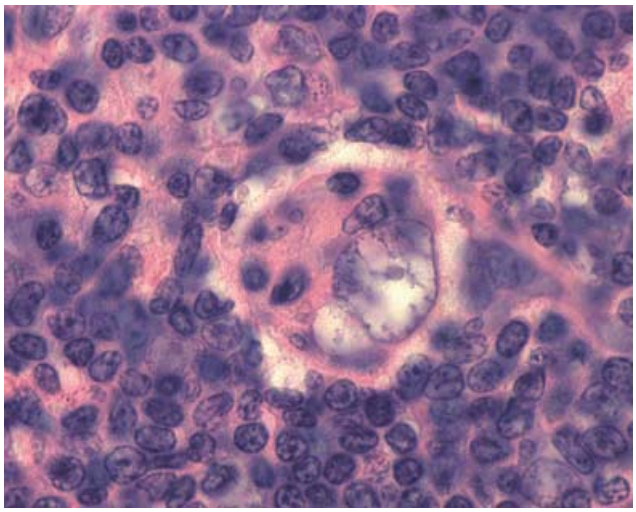

9.2

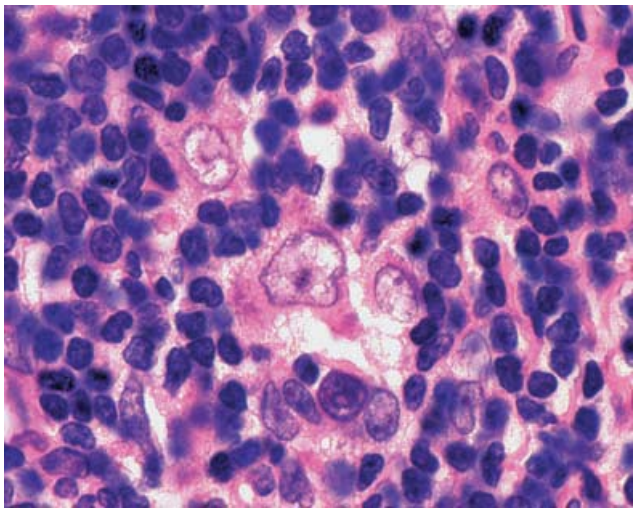

9.3

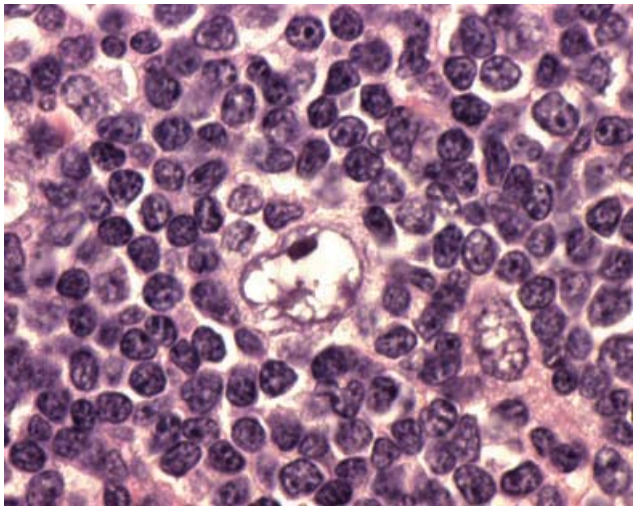

9.4

Figures 9.2, 9.3, and 9.4. Human: lymph node, Hodgkin's lymphoma, lymphocyte predominance type L&H or popcorn type of Reed-Sternberg cells. The cells are large with very vesicular and lobulated nuclei with a branched chromatin pattern and prominent nucleolus. The cytoplasm is of variable density and encircled or invaded by small lymphocytes. *Slides from Cornell Tutorial.*

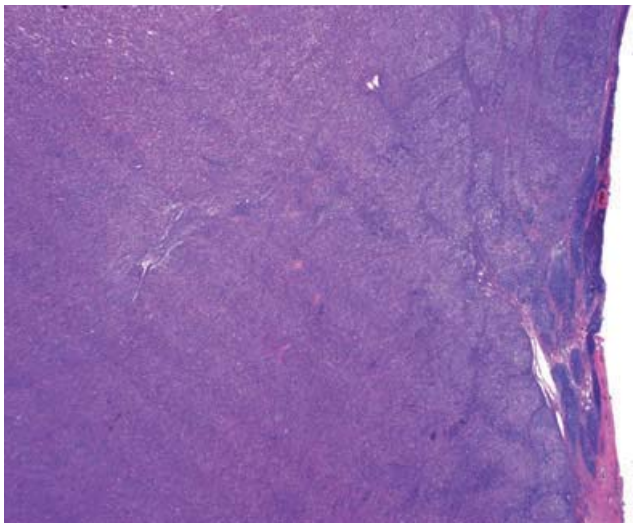

Figure 9.5. Cat: lymph node, T-cell rich large B-cell lymphoma. The capsule is irregularly thickened but without involvement of perinodal structures. There is a fading nodularity in subcapsular areas representing residual normal node architecture with the interior of the mass of completely diffuse architecture. The tissue is remarkably cohesive due to fine sclerosis. *Slide from F. Juck, DVM.*

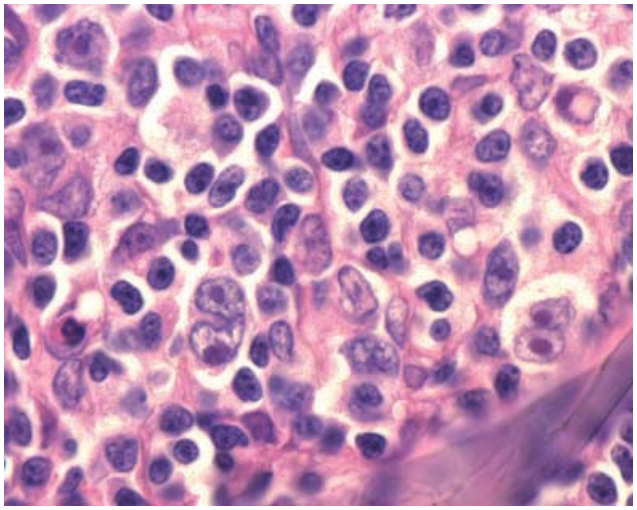

Figure 9.6. Cat: node, T-cell rich large B-cell lymphoma. Detail of Figure 9.5. The cell in the lower right has many of the characteristics of Reed-Sternberg cells, including peripheralized chromatin and very large nucleoli in a binucleated cell. A similar cell type lies to the left of center.

Another differential is lymphoma and leukemia of small lymphocytic type, particularly with the presence of large epithelioid histiocytes that may have RS cell features. A useful criterion of distinction between these types of lymphoid proliferation is that in CLL and ALL there is frequent invasion of the nodal capsule, but this rarely occurs in HL.

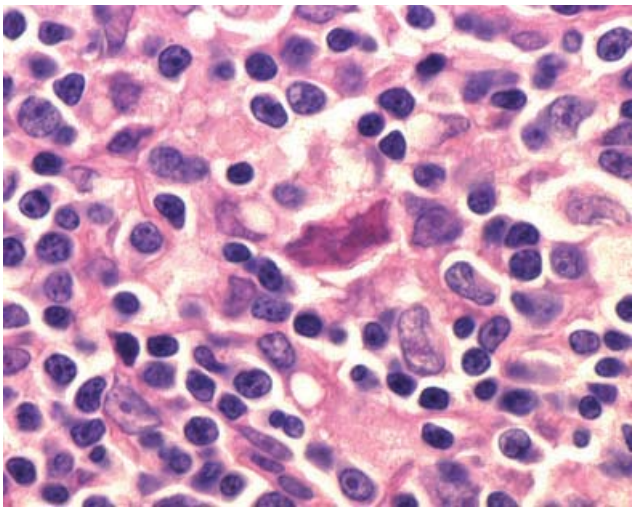

Figure 9.7. Cat: node, T-cell rich large B-cell lymphoma. Typical form of Reed-Sternberg–like cell, undergoing necrosis with eosinophilic cytoplasm contracted from surrounding cells and loss of nuclear detail.

Nodular Sclerosis HL

The nodular sclerosis is the most common type of HL, making up more than 60% of cases, and has the highest level of agreement on review by different pathologists. The nodular sclerosis type of HL is more common in females generally under 50 years old and tends to present in the lymph nodes of the lower cervical, supraclavicular, and mediastinal areas. Oddly, these are exactly the age (10+ years), gender, and sites of presentation of the T-cell rich large B-cell lymphoma of cats. The diagnosis of nodular sclerosis type of HL may be apparent on gross examination and on trimming the fixed tissue by the regular dissection of the nodal tissue by broad bands of translucent collagenous tissue (Fig. 9.8). On histological examination, these bands are mature to the extent of birefringence with polarized light, and these bands irregularly segment the interior of the node and are associated with marked fibrous thickening of the node capsule (Fig. 9.9). The background cellular population is variable and mixed with small and medium lymphocytes with relatively numerous neutrophils, eosinophils, and prominent fine vascularity (Fig. 9.10). The RS cells are numerous and of the lacunar type that, in slides prepared from formalin-fixed tissues, characteristically has cytoplasmic borders retracting from the surrounding cells (Figs. 9.11–9.13). This facet greatly aids identification of these cells on histological examination at low magnification. This feature is lost in tissues fixed in Zenker's or B5 processes. The classic type of RS cells may be difficult to find or it may be absent, despite the lacunar type of RS cells occurring

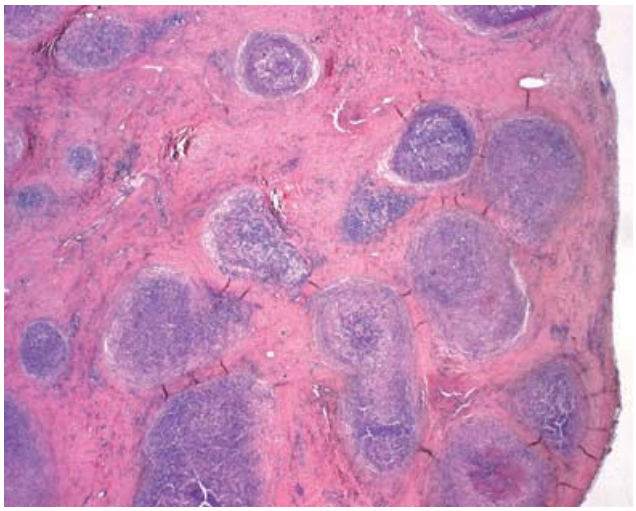

Figure 9.8. Human: node, Hodgkin's lymphoma, nodular sclerosis type. The tissue is largely sclerotic with lymphoid areas surviving as islands in a background of solid collagenous proliferation. *Slide from Cornell Tutorial.*

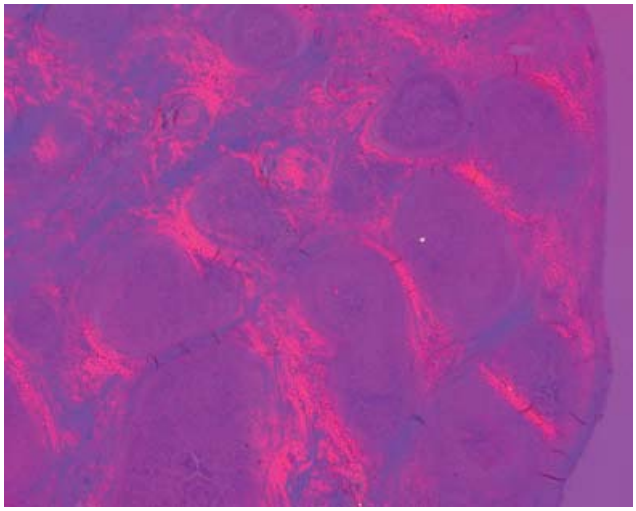

Figure 9.9. Human: lymph node, Hodgkin's lymphoma, nodular sclerosis, same tissue as Figure 9.8. With polarized light there is a remarkable level of birefringent mature collagen, separating the darker-appearing residual nodules.

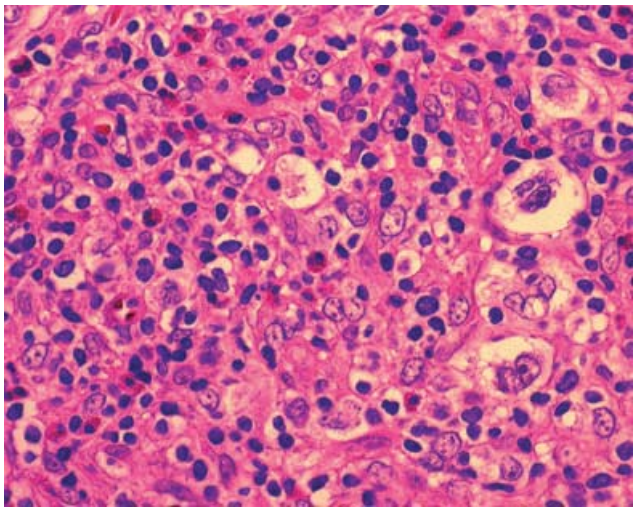

Figure 9.10. Human: lymph node, Hodgkin's lymphoma, nodular sclerosis type, same tissue as Figure 9.8. The nodular nonfibrous areas of the node have a mixed cellularity with small and medium lymphocytes and numerous eosinophils. The lacunar type of Reed-Sternberg cells are frequent as seen at the right with cytoplasmic tendrils retracting from surrounding tissues.

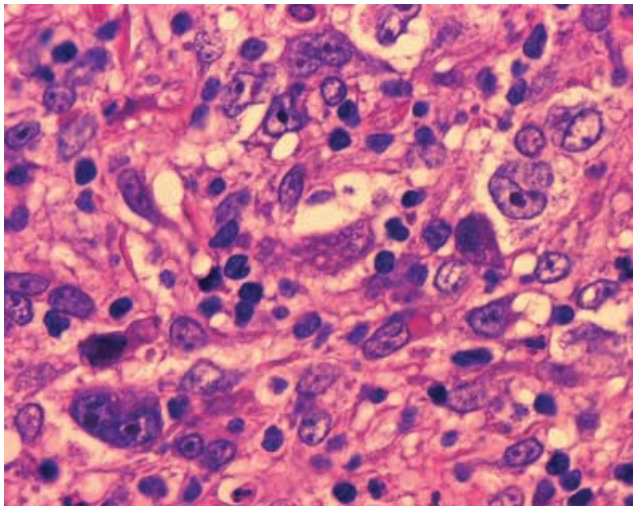

Figure 9.11. Human: lymph node, Hodgkin's lymphoma, nodular sclerosis type, same case as Figure 9.8. A more rarely encountered classic Reed-Sternberg cell in the lower left is present as well as lacunar type cells in the upper right.

frequently. In the WHO classification, the nodular sclerosis category was divided into type I, as described above, that constitutes 70–80% of human cases and a type II that has focal areas of lymphocyte depletion and or foci of anaplastic-appearing lacunar cells. The basis for this separation was studies that indicated that patients with the characteristics ascribed to the type II category had poor response to initial treatment, increased relapse rate, and shortened survival. The diagnosis rests on the internodular collagen bands, the thickened nodal capsule, and the presence of the lacunar cells. The extent of the sclerosis may vary, but it must include at least one fibrous band extending into the nodal interior from the capsule. There is a survival benefit associated with the maturity of the fibrous bands with more collagen fibers and less cellularity characterized by longer relapse-free survival.

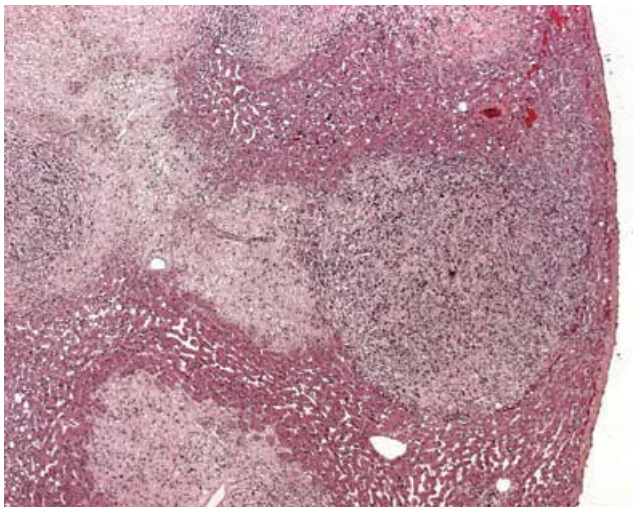

Figure 9.12. Human: liver, Hodgkin's lymphoma, nodular sclerosis type. The hepatic parenchyma is destroyed by multifocal coalescing nodules of neoplastic proliferation. *Slide from Cornell Tutorial.*

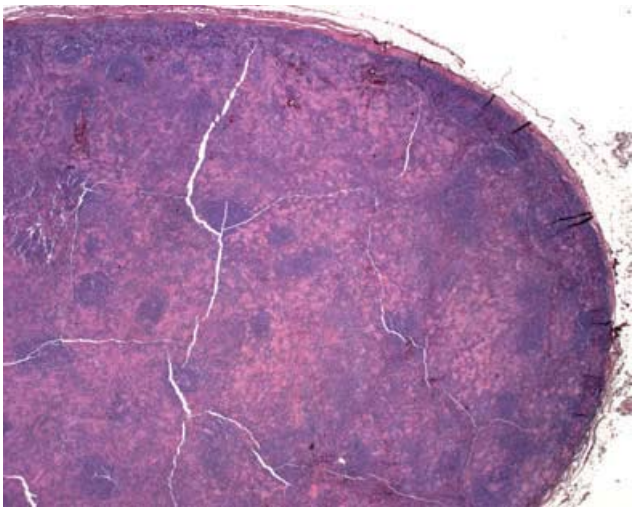

Figure 9.14. Human: lymph node, Hodgkin's lymphoma, mixed cellularity type. The node capsule is thinned with subcortical and internal fading germinal centers with a diffuse background of variable density. *Slide from Cornell Tutorial.*

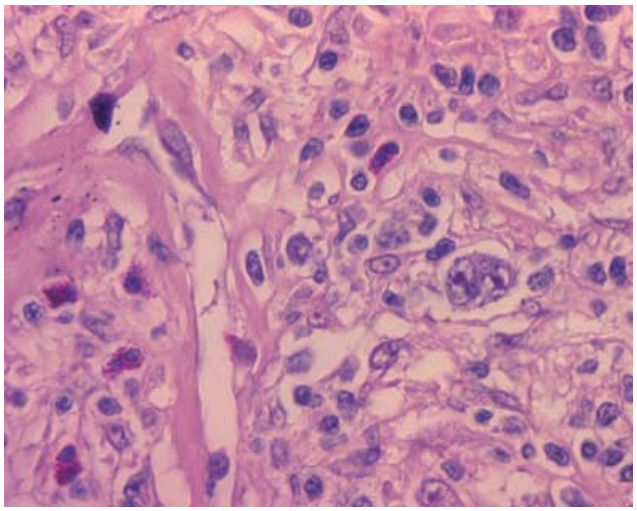

Figure 9.13. Human: liver, Hodgkin's lymphoma, nodular sclerosis type. Detail of Figure 9.12. The cellularity is variable between cases with eosinophils and lacunar cells common, and in this case, smaller lymphocytes are accompanied by a rare typical Reed-Sternberg cell (right center).

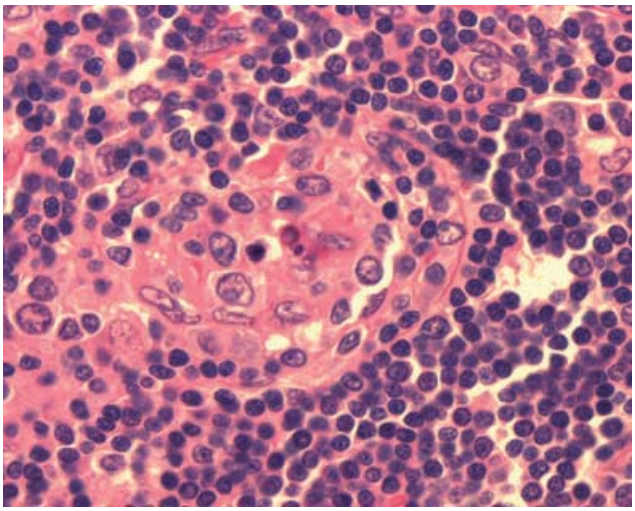

Figure 9.15. Human: node, Hodgkin's lymphoma, mixed cellularity type, same tissue as Figure 9.14. A cluster of macrophages in the center is surrounded by a typical population of small lymphocytes with round nuclei.

Mixed Cellularity HL

Mixed cellularity HL is the second most common type; it is more common in males and often presents with systemic symptoms, but it may be at all stages and prognostically is intermediate between lymphocyte predominance and lymphocyte depletion types. Nodal architecture may be partially or completely effaced (Fig. 9.14) and RS cells of the classic type tend to be readily identified. Some cases that have RS cells of other types with very few of the classic type remain included in the mixed cellularity subcategory. As the name indicates, the background cells are a mixture of small lymphocytes, with variable levels of neutrophils, eosinophils, plasma cells, and histiocytes, often in homogenous clusters that resemble what has been known as *Lennert's lymphoma* (Figs. 9.15–9.17). It is stressed that the small lymphocytes of the mixed type of HL have round nuclei with compact

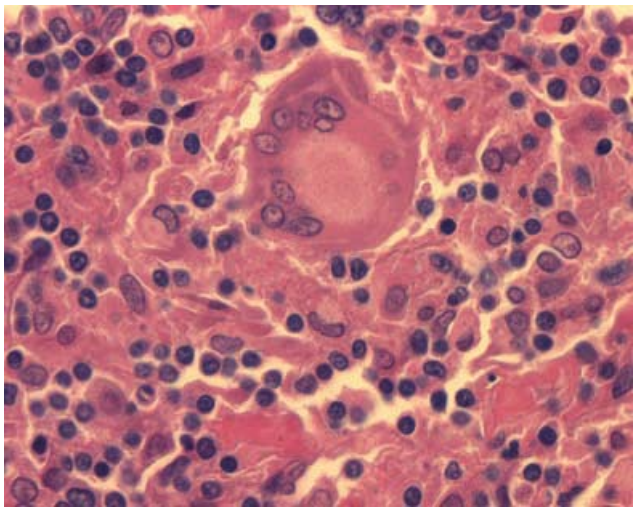

Figure 9.16. Human: lymph node, Hodgkin's lymphoma, mixed cell type, same tissue as Figure 9.14. A Langerhans type of giant cell is present in a background of macrophages and mixed cellularity.

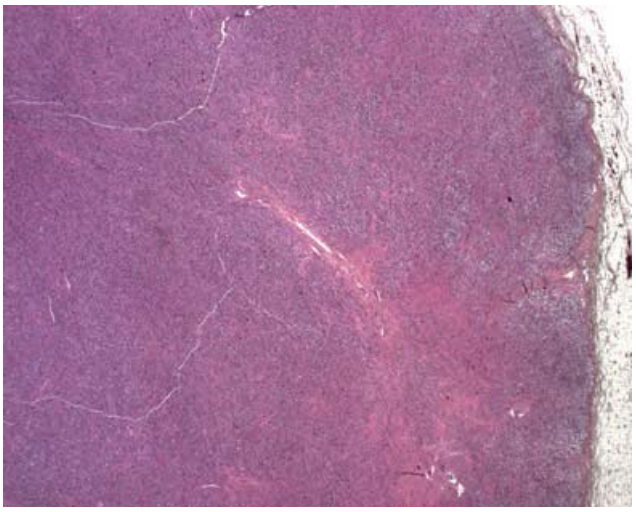

Figure 9.18. Human: node, Hodgkin's lymphoma, lymphocyte depletion type. There is thinning of the capsule with compression of the peripheral sinus and complete loss of normal architecture with irregular patterns of diffuse fibrosis without apparent areas of necrosis. *Slide from Cornell Tutorial.*

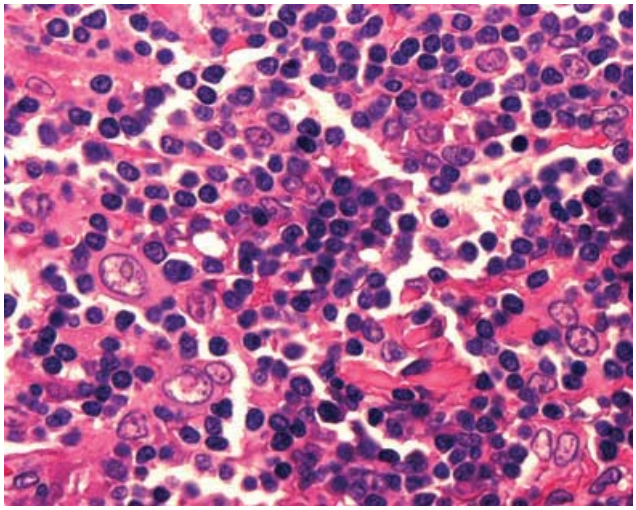

Figure 9.17. Human: node, Hodgkin's lymphoma, mixed cellularity type. Detail of Figure 9.14. There is a near-classic type of Reed-Sternberg cell at the right, with atypical lacunar cells in the lower left with a background of lymphocytes, plasma cells, and occasional eosinophil in a background of fine sclerosis.

chromatin that lack nucleoli and appear normal; the small lymphocytes of similar-appearing conditions have atypical-appearing small cells with irregularly indented nuclear contours. There is minimal or fine fibrosis, but foci of necrosis may be present. The differential diagnosis of the mixed cellularity type of HL is understandably broad because of the numbers of other entities that share the general features and include angioimmunoblastic lymphadenopathy (AILD) and peripheral T-cell lymphomas of the mixed medium and large cell type, as well as lymphoepithelioid cell or Lennert's lymphoma. These conditions are generally characterized by nodal capsular invasion not seen in mixed cellularity HL and by lack of RS cells.

Lymphocyte Depletion HL

Lymphocyte depletion HL is the least common type, comprising about 1% of human cases, and tends to be seen in older patients that present with constitutional symptoms and stage III or IV at diagnosis. Patients often present with fever and marked weight loss and indication of hepatic dysfunction or failure but not peripheral lymphadenopathy. On physical and laboratory examination, there is extensive disease below the diaphragm, including involvement of the liver, spleen, retroperitoneal nodes, and bone marrow. This form of HL has the shortest survival; it has a better prognosis for those cases with diffuse fibrosis and a poorer prognosis in patients with the atypical-appearing RS cells known as the *reticular type*. This form of HL is characterized by diffuse fibrosis of nonbirefringent maturation, with irregular areas of increased density (Figs. 9.18–9.21). The cell depletion is mainly of lymphocytes, and there may be foci of increased numbers of RS cells. There are two general patterns of nodal change, with one resembling the mixed cellularity type of HL with increased numbers of RS cells. The second type has the increased numbers of RS cells, but these are atypical and sarcomatous-appearing, known as the

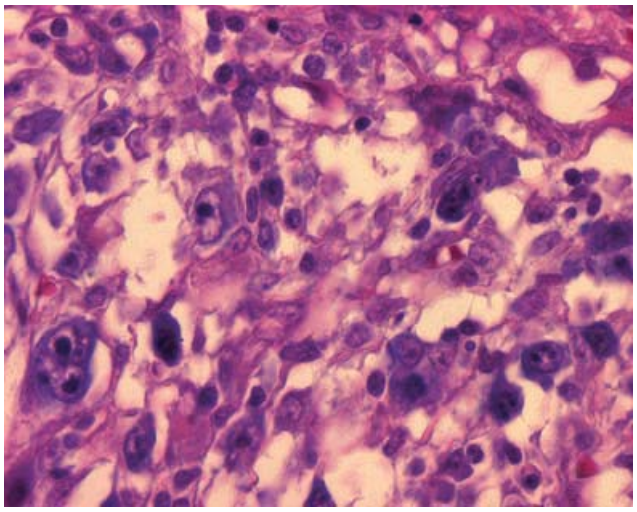

Figure 9.19. Human: node, Hodgkin's lymphoma, lymphocyte depletion type. Detail of Figure 9.18. There is a classic Reed-Sternberg cell in the lower left and a number of other cells with very atypical morphology in a background primarily of connective tissue. There is a cell in metaphase partially in focus lower right.

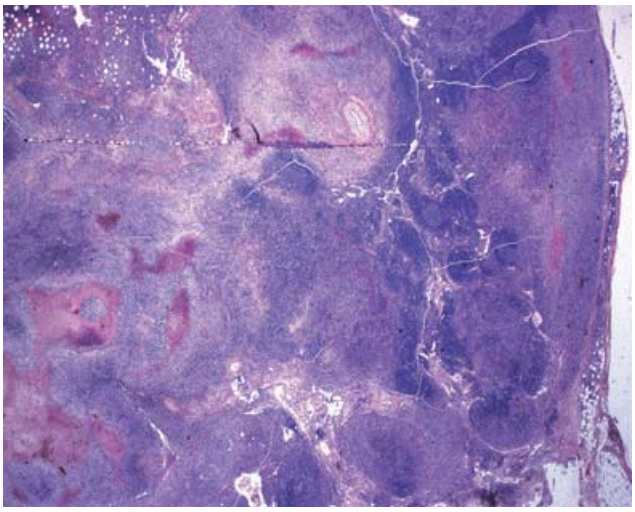

Figure 9.21. Human: node, Hodgkin's lymphoma, lymphocyte depletion type. There is thinning of the node capsule with the darker stained areas representing small foci of residual benign lymphocytes and several fading germinal centers. There are broad areas of sclerosis and focal areas of ischemic necrosis at upper center and lower left. *Slide from Cornell Tutorial.*

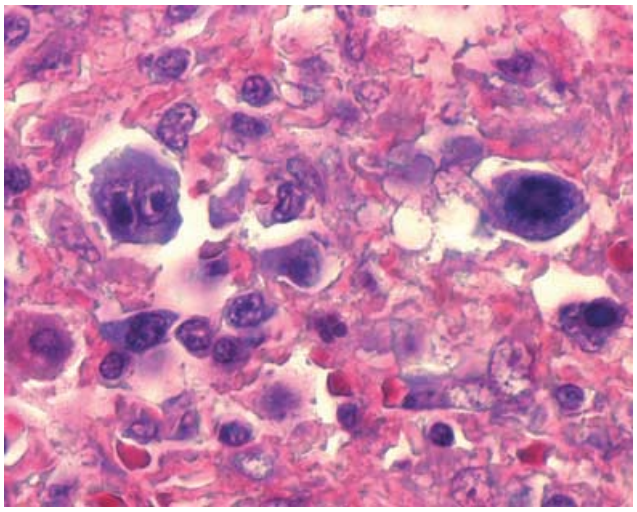

Figure 9.20. Human: node, Hodgkin's lymphoma, lymphocyte depletion type. Detail of Figure 9.18. A classic Reed-Sternberg cell in the lower upper and a large cell in metaphase in the upper right are surrounded by a small number of lymphocytes of medium size and numerous pale-staining vesicular nuclei of background of connective tissue.

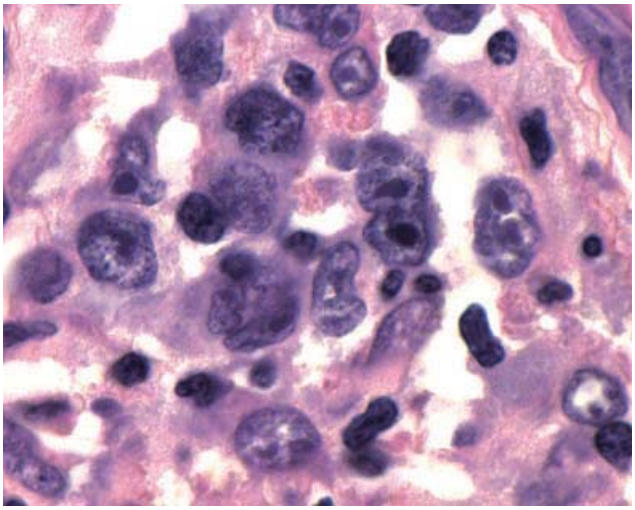

Figure 9.22. Human: node, Hodgkin's lymphoma, lymphocyte depletion type. Detail of Figure 9.21. A cluster of very atypical cells, including several with lobulated nuclei and multiple very large nucleoli. Lacking peripheralized chromatin, these cells would not qualify as acceptable Reed-Sternberg cells despite a very typical background population.

reticular type, and with RS cells in almost all fields at high-power histological examination (Fig. 9.22). HL of the lymphocyte depletion type needs to be differentiated from the anaplastic types of large cell lymphoma and from other types of HL, particularly the type II of nodular sclerosis.

REGIONAL PATHOLOGY AND STAGING OF HL

Hodgkin's lymphoma is unique in its mode of spread, which is unlike the non-Hodgkin's type lymphomas that tend to be more regional or organ associated, as

in peripheral lymphadenopathy or hepatosplenic. With HL, the spread is almost invariably to contiguous tissues without "skip" lesions between. With the discovery that HL was curable by irradiation, it became essential to identify the extent of tissue involvement in order to ensure treatment of all areas. This was done by laparotomy with metal clips placed in the tumor margins so that these landmarks could be identified by radiography and used to direct the therapeutic beam. With the advent of tomography and MRI, laparotomy is now seldom employed.

Splenic involvement in HL occurs in about 40% of cases, with splenic size and weight having little bearing on tumor load, which is usually multifocal and miliary. It has been shown that five or more nodules of HL in the spleen is associated with an unfavorable outcome, and it has become common to record the number of splenic foci of HL. However, because these foci may not be visible from the capsular surface and too small to be readily visualized on imaging, it is essentially a matter of sectioning the spleen at 2–3 mm intervals to determine the level of splenic colonization accurately. Within the spleen, the localization is usually associated with the periarteriolar lymphoid sheaths or the marginal areas of follicles. In general, the diagnosis is made prior to splenectomy and the criteria for the spleen are the same as those for nodes, but because the human spleen, as in animals, may have foci of lymphoid nodular hyperplasia or lymphoid pseudotumor, these nodules can not be counted grossly as foci of HL, even in a diagnosed case. Further, because the spleen may have foci of histiocytic proliferation for a variety of causes, the diagnosis of HL in the spleen is not as accurate as for lymph nodes.

The involvement of abdominal nodes by HL produces lesions the same as seen elsewhere, but nodes may be involved with HL and not enlarged and may be considered positive or suspicious in the basis of lymphangiography. The splenic hilar nodes are often involved with the spleen, but mesenteric nodes, unlike in non-Hodgkin's lymphoma, are rarely involved with HL.

An initial diagnosis of HL from other than a lymph node is taken very cautiously because these are most likely to be other diseases, often non-Hodgkin's lymphoma. Until the advent of AIDS, a primary diagnosis of HL in other than nodal sites was considered to be extremely rare. The same criteria are followed for liver and marrow in cases of diagnosed HL, and because these are usually cutting needle biopsies and relatively small tissue areas, diagnostic RS cells may not be found and are not taken as required if the initial diagnosis is firmly established and the cellular background is typical. In the liver, foci of HL are usually located in portal areas and are large, so their distinction from small periportal lymphoid aggregates is not usually a problem and can be partially avoided by taking multiple site biopsies. Bone marrow is similarly taken from multiple sites and marrow involvement does not in itself infer a poor prognosis. Primary HL in bone has been recorded and with focal invasion of cancellous bone and even in reparative new bone production. The lung is second to the liver in nonlymphatic tissue invaded by HL, and even at that is rarely involved. Lung involvement is usually with the nodular sclerosis type and by direct extension from a primary site of mediastinal tumor.

HODGKIN'S-LIKE LYMPHOMA IN ANIMALS

The descriptions of the various types of HL occurring in humans does not suggest that there is a population of HL in animals that has been overlooked. The most likely type of HL to be missed in animal pathology would be the lymphocyte predominance type or the lymphocyte-rich classic type because these could be mistaken as small lymphocytic lymphoma with no history to suggest that a search for classic or other type RS cell be undertaken. The most obvious animal counterpart is the T-cell rich large B-cell lymphoma, particularly of the cervical area of cats, that has the uncanny habit of spread by local extension to the prescapular nodes or the mediastinum. The lesions characteristically have fine diffuse sclerosis with prominent fine vascularity, but the putative RS cells in these lesions don't consistently have the peripheralization of chromatin and typically huge nucleoli. More often in the cat, these cells have the L&H or popcorn type of large atypical cells that mark for B-cells, at a level of about 10–20% of cells in most cases. A skunk from a small zoo was presented for pathological examination and had lesions like lymphocyte predominance HL. The zoo had noted several deaths in adult animals from the same group, but only one had pathologic examination. The lesions were suggestive of HL of mixed cell type, and that diagnosis was felt appropriate by a consulting MD hematopathologist. There were focal lesions in the nodes, liver, and spleen, and the animal was in very good flesh with abundant fat (Figs. 9.23–9.28). It is not a matter of import whether there is a direct animal counterpart of human HL, but in those hematopoietic neoplasms of animals that appear like the human lesion of the same name there is a close correlation in cell type, mitotic rate, phenotypic type, response to therapy, and survival. For this reason, it is desirable for veterinary pathologists to be aware of the types of HL and progress of knowledge made in understanding and identifying them in order that this information can be tested against what may be rare events in animal diagnostic pathology.

Figure 9.23. Skunk: lymph node, Hodgkin's-like Lymphoma of mixed cellularity. The node has a variegated appearance with dark areas representing residual foci of benign lymphocytes and the pale areas of cellularity with a variety of cell types. The capsule is intact and there is no involvement of perinodal tissues.

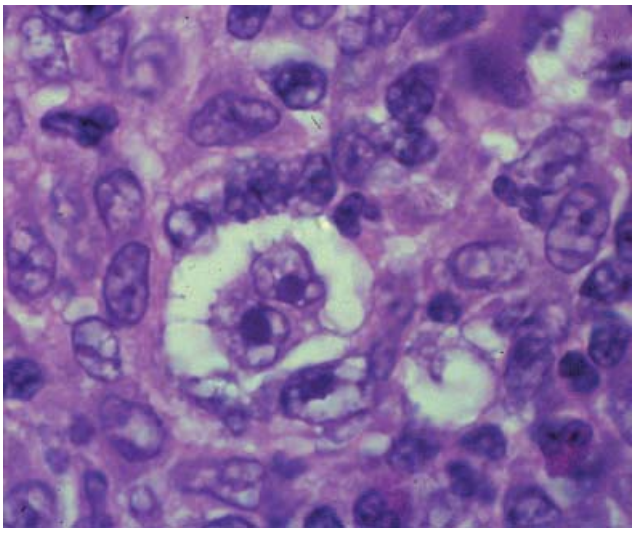

Figure 9.25. Skunk: lymph node, Hodgkin's-like lymphoma of mixed cellularity type. A Reed-Sternberg–like cell is present surrounded by connective tissue and small lymphocytes. There is an indication of the mixed cellularity in the lower right with eosinophils and small and medium lymphocytes.

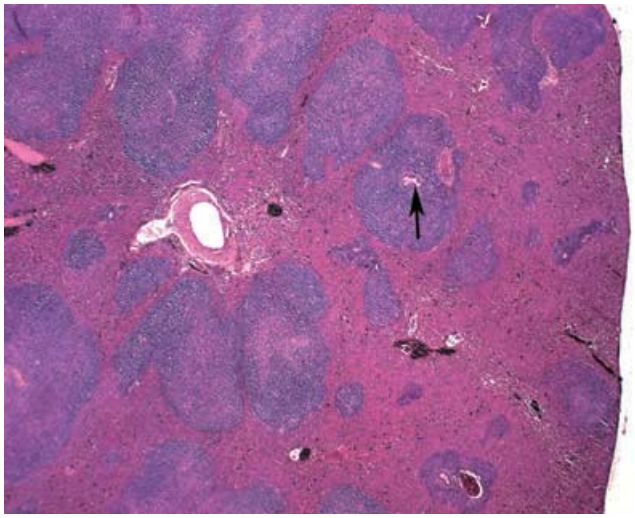

Figure 9.24. Skunk: liver, Hodgkin's-like lymphoma of mixed cellularity type. Multiple sharply defined foci of tumor are present in the liver lobe, with most arising on portal areas (arrow) with another smaller periportal focus in the lower right. The pale areas are largely of connective tissue proliferation.

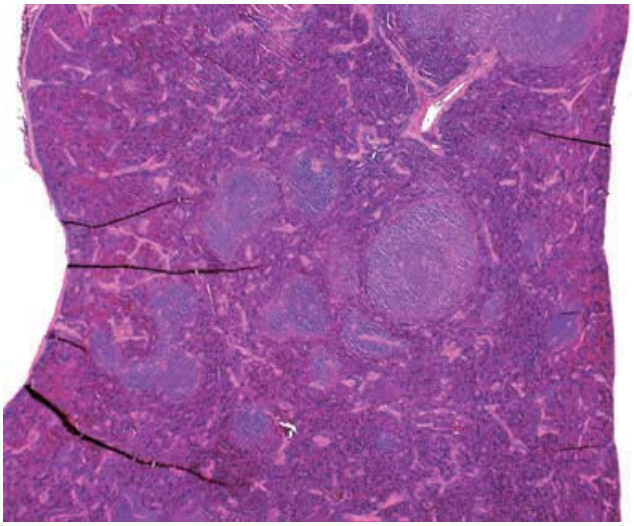

Figure 9.26. Skunk: spleen, Hodgkin's-like lymphoma, mixed cellularity type. There is marked thinning of the splenic capsule with the smooth muscle trabeculae thinned and widely spaced. The periarteriolar lymphoid sheaths are atrophic and there are multifocal areas of neoplastic infiltration.

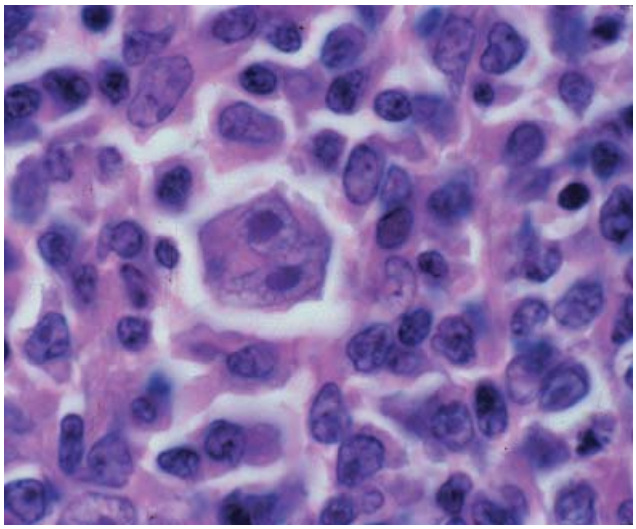

Figure 9.27. Skunk: spleen, Hodgkin's-like lymphoma. Detail of Figure 9.26. The classic type of Reed-Sternberg cell with peripheralized chromatin and very large prominent nucleoli is present in a background of mixed lymphocytes and a mild increase in stroma.

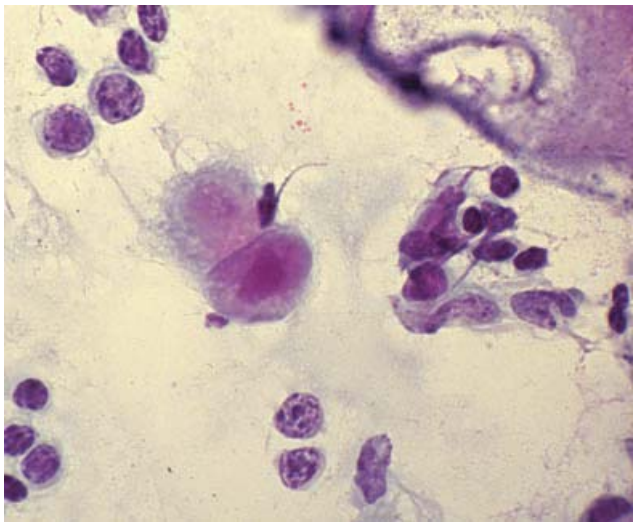

Figure 9.28. Skunk: node, Hodgkin's-like lymphoma. A tissue imprint, wet-fixed with Papanicolaou stain and with a putative Reed-Sternberg cell. The nucleus in the center is in focus, with an irregularly shaped nucleolus with very fine chromatin pattern. The second nucleus has insufficient detail for confirmation.

REFERENCES, HUMAN

Aisenberg, A.C. (1999) Problems in Hodgkin's disease management. *Blood* 93:761–779.

Ashton-Key, M., Thorpe, P.A., Allen, J.P., et al. (1995) Follicular Hodgkin's disease. *Am J Surg Pathol* 19:1294–1299.

Austin-Seymour, M.M., Hoppe, R.T., Cox, R.S., et al. (1984) Hodgkin's disease in patients over sixty years old. *Ann Intern Med* 100:13–18.

Baur, A.S., Meugé-Moraw, C., Michel, G., et al. (1998) Prognostic value of follicular dendritic cells in nodular sclerosing Hodgkin's disease. *Histopathol* 32:512–520.

Bearman, R.M., Pangalis, G.A., Rappaport, H. (1978) Hodgkin's disease, lymphocyte depletion type: A clinicopathologic study of 39 patients. *Cancer* 41:293–302.

Ben-Ezra, J., Sheibani, K., Swartz, W., et al. (1989) Relationship between eosinophil density and T-cell activation markers in lymph nodes of patients with Hodgkin's disease. *Hum Pathol* 20:1181–1185.

Braeuninger, A., Kuppers, R., Strickler, J.G., et al. (1997) Hodgkin and Reed-Sternberg cells in lymphocyte predominance Hodgkin's disease represent clonal populations of germinal center-derived tumor cells. *Proc Natl Acad Sci USA* 94:9337–9342.

Burke, J.S. (1981) Surgical pathology of the spleen: An approach to the differential diagnosis of splenic lymphomas and leukemias. Part I. Diseases of the white pulp. *Am J Surg Pathol* 5:551–563.

Burke, J.S. (2001) Hodgkin's disease: Histopathology and differential diagnosis. In Knowles, D.M. (ed.), *Neoplastic Hematopathology,* 2nd ed. Lippincott Williams & Wilkins, Philadelphia, pp. 623–665.

Burke, J.S., and Butler, J.J. (1976) Malignant lymphoma with a high content of epithelioid histiocytes (Lennert's lymphoma). *Am J Clin Pathol* 66:1–9.

Butler, J.J. (1971) Relationship of histological findings to survival in Hodgkin's disease. *Cancer Res* 31:1770–1775.

Butler, J.J., and Pugh, W.C. (1993) Review of Hodgkin's disease. *Hematol Pathol* 7:59–77.

Carbone, P.P., Kaplan, H.S., Musshoff, K., et al. (1971) Report of the committee on Hodgkin's disease staging classification. *Cancer Res* 31:1860–1861.

Coppleson, L.W., Rappaport, H., Strum, B., et al. (1973) Analysis of the Rye classification of Hodgkin's disease: The prognostic significance of cellular composition. *J Natl Cancer Inst* 51:379–390.

Delabie, J., Tierens, A., Gavril, T., et al. (1996) Phenotype, genotype and clonality of Reed-Sternberg cells in nodular sclerosis Hodgkin's disease: Results of single cell study. *Brit J Haematol* 94:198–205.

Devaney, K., and Jaffe, E.S. (1991) The surgical pathology of gastrointestinal Hodgkin's disease. *Am J Clin Pathol* 95:794–801.

Dich, N.H., Goodman, Z.D., and Klein, M.A. (1989) Hepatic involvement in Hodgkin's disease: Clues to histologic diagnosis. *Cancer* 64:2121–2126.

Dorfman, R.F. (1971) Relationship of histology to site in Hodgkin's disease. *Cancer Res* 31:1786–1793.

Ferry, J.A., Linggood, R.M., Convery, K.M., et al. (1993) Hodgkin's disease, nodular sclerosis type: Implications of histologic subclassification. *Cancer* 71:457–463.

Frizzera, G., Moran, E.M., and Rappaport, H. (1975) Angioimmunoblastic lymphadenopathy: Diagnosis and clinical course. *Am J Med* 59:803–818.

Gamble, J.F., Fuller, L.M., Martin, R.G., et al. (1975) Influence of staging celiotomy in localized presentations of Hodgkin's disease. *Cancer* 35:817–825.

Gascoyne, R.D., Delabie, J., de Wolfe-Peeters, C., et al. (1999) "Paragranulomatype" T-cell rich B-cell lymphoma: A report of 50 cases. *Mod Pathol* 137A(abst).

Gonzalez, C.L., Medeiros, L.J., and Jaffe, E.S. (1991) Composite lymphoma: A clinicopathologic analysis of nine patients with Hodgkin's disease and B-cell non-Hodgkin's lymphoma. *Am J Clin Pathol* 96:81–89.

Harris, N.L. (1999) Hodgkin's disease: Classification and differential diagnosis. *Mod Pathol* 12:159–176.

Harris, N.L., Jaffe, E.S., Stein, H., et al. (1994) A revised European-American classification of lymphoid neoplasms: A proposal from the International Lymphoma Study Group. *Blood* 84:1361–1392.

Hoppe, R.T., Rosenberg, S.A., Kaplan, H.S., et al. (1980) Prognostic factors in pathological stage IIIA Hodgkin's disease. *Cancer* 46:1240–1246.

Kadin, M.E. (2001) Hodgkin's disease: Cell of origin, immunobiology, and pathogenesis. InKnowles, D.M. (ed.), *Neoplastic Hematopathology*. Lippincott Williams & Wilkins, Philadelphia, pp. 667–690.

Kanzler, H., Kuppers, R., Hansmann, M.L., et al. (1996) Hodgkin and Reed/Sternberg cells in Hodgkin's disease represent the outgrowth of a dominant tumor clone derived from (crippled) germinal center B cells. *J Exp Med* 184:1495–1505.

Kinney, M.C., Greer, J.P., and Collins, R.D. (1991) Assessment of lymphocyte depleted Hodgkin's disease, reticular variant (LDHD-R) by monoclonal antibodies reactive in paraffin sections. *Mod Pathol* 4:75A(abst).

Kuppers, R., and Rajewsky, K. (1998) The origin of Hodgkin and Reed/Sternberg cells in Hodgkin's Disease. *Ann Rev Immunol* 16:471–493.

Lister, T.A., Crowther, D., Sutcliffe, S.B., et al. (1989) Report of a committee convened to discuss the evaluation and staging of patients with Hodgkin's disease: Cotswolds meeting. *J Clin Oncol* 7:1630–1636.

Lukes, R.J. (1971) Criteria for involvement of lymph node, bone marrow, spleen, and liver in Hodgkin's disease. *Cancer Res* 31:1755–1767.

Lukes, R.J., Butler, J.J., and Hicks, E.B. (1966) Natural history of Hodgkin's disease as related to its pathologic picture. *Cancer* 19:317–344.

MacMahon, B. (1966) Epidemiology of Hodgkin's disease. *Cancer Res* 26:1189–1200.

Marafioti, T.R., Hummel, M., Anagnostopoulous, I., et al. (1997) Origin of nodular lymphocyte-predominant Hodgkin's disease from a clonal expansion of highly mutated germinal-center B cells. *N Engl J Med* 337:453–458.

Mason, D.Y., Banks, P.M., Chan, J., et al. (1994) Nodular lymphocyte predominance Hodgkin's disease: A distinct clinicopathological entity. *Am J Surg Pathol* 18:526–530.

McBride, J.A., Rodriguez, J., Luthra, R., et al. (1996) T-cell-rich B large-cell lymphoma simulating lymphocyte-rich Hodgkin's disease. *Am J Surg Pathol* 20:193–201.

Munker, R., Hasenclever, D., Brosteanu, O., et al. (1995) Bone marrow involvement in Hodgkin's disease: An analysis of 135 consecutive cases. *J Clin Oncol* 13:403–409.

Nakamura, S., Nagahama, M., Kagami, Y., et al. (In press) Hodgkin's disease expressing follicular dendritic cell marker CD21 without any other B-cell marker: A clinicopathologic study of nine cases. *Am J Surg Pathol.*

Neiman, R.S., Rosen, P.J., and Lukes, R.J. (1973) Lymphocyte-depletion Hodgkin's disease: A clinicopathological entity. *N Engl J Med* 288:751–754.

Nguyen, P.L., Ferry, J.A., and Harris, N.L. (1999) Progressive transformation of germinal centers and nodular lymphocyte predominance Hodgkin's disease: A comparative immunohistochemical study. *Am J Surg Pathol* 23:27–33.

Oudejans, J.J., Kummer, J.A., Jiwa, M., et al. (1996) Granzyme B expression in Reed-Sternberg cells of Hodgkin's disease. *Am J Pathol* 148:233–240.

Patsouris, E., Noel, H., and Lennert, K. (1989) Cytohistologic and immunohistochemical findings in Hodgkin's disease, mixed cellularity type, with a high content of epithelioid cells. *Am J Surg Pathol* 13:1014–1022.

Pinkus, G.S., and Said, J.W. (1988) Hodgkin's disease, lymphocyte predominance type, nodular—Further evidence for a B cell derivation: L&H variants of Reed-Sternberg cells express L26, a pan B cell marker. *Am J Pathol* 133:211–217.

Pinkus, G.S., Pinkus, J.L., Langhoff, E., et al. (1997) Fascin, a sensitive new marker for Reed-Sternberg cells of Hodgkin's disease: Evidence for a dendritic or B cell derivation: *Am J Pathol* 150:543–562.

Poppema, S. (1992) Lymphocyte-predominance Hodgkin's disease. *Semin Diagn Pathol* 9:257–264.

Poppema, S., Kaiserling, E., and Lennert, K. (1979) Hodgkin's disease with lymphocytic predominance, nodular type (nodular paragranuloma) and progressively transformed germinal centres—A cytohistological study. *Histopathol* 3:295–308.

Rappaport, H., Berard, C.W., Butler, J.J., et al. (1971) Report of the committee on histopathological criteria contributing to staging of Hodgkin's disease. *Cancer Res* 31:1864–1865.

Rosenberg, S.A. (1985) Laparotomy and splenectomy in Hodgkin's disease: A reappraisal after twenty years. *Scand J Haematol* 34:289–292.

Rüdiger, T., Ott, G., Ott, M.M., et al. (1998) Differential diagnosis between classic Hodgkin's lymphoma, T-cell–rich B-cell lymphoma, and paragranuloma by paraffin immunohistochemistry. *Am J Surg Pathol* 22:1184–1191.

Strum, S.B., Park, J.K., and Rappaport, H. (1970) Observation of cells resembling Sternberg-Reed cells in conditions other than Hodgkin's disease. *Cancer* 26:176–190.

Suster, S., and Moran, C.A. (1996) Pleomorphic large cell lymphomas of the mediastinum. *Am J Surg Pathol* 20:224–232.

Thomas, R.M., Jaffe, E.S., Zarate-Osorno, A., et al. (1993) Inflammatory pseudotumor of the spleen: A clinicopathologic and immunophenotypic study of eight cases. *Arch Pathol Lab Med* 117:921–926.

von Wasielewski, R., Seth, S., Franklin, J., et al. (1999) Prevalence, presentation and prognosis of lymphocyte-rich classic Hodgkin's disease. *Mod Pathol* 12:147A(abst).

Wijlhuizen, T.J., Vrints, L.W., Jairam, R., et al. (1989) Grades of nodular sclerosis (NSI-NSII) in Hodgkin's disease: Are they of independent prognostic value? *Cancer* 63:1150–1153.

Wood, N.L., and Coltman, C.A., Jr. (1973) Localized primary extranodal Hodgkin's disease. *Ann Intern Med* 78:113–118.

REFERENCES, ANIMAL

Majeed, S.K., and Gopinath, C. (1985) Hodgkin's disease-like lesion in a rat. *J Comp Pathol*95:123–126.

Smith, D.A., and Barker, I.K. (1983) Four cases of Hodgkin's disease in striped skunks (Mephitis mephitis). *Vet Pathol* 20:223–229.

Walton, R.M., and Hendrick, M.J. (2001) Feline Hodgkin's-like lymphoma: 20 cases (1992–1999). *Vet Pathol* 38:504–511.

Wells, G.A.H. (1974) Hodgkin's disease-like lesions in the dog. *J Pathol* 112(1):5–10.

Chapter 10

Histiocytoses

HISTIOCYTIC AND DENDRITIC CELL PROLIFERATIONS

The histiocytic diseases of animals are largely diseases of dogs, but forms of histiocytic proliferation occur in cats and likely in all domestic animals, albeit in rare and unique presentation. Lesions of the histiocytic type derive from two major lineages, which include the monocyte-macrophage cells of the innate immune system that are largely phagocytic in nature and the dendritic and Langerhans cells that are largely antigen presenting cells of the adaptive immune system. Both of these lineages originate from a CD34 positive bone marrow precursor and develop into morphologically and functionally different cells. This development takes place under the inductive pressure of a variety of stimuli that include granulocyte-macrophage colony-stimulating factor (GM-CSF), tumor necrosis factor α (TNF-α), and interleukin (IL-4). Early differentiation results in cutaneous lymphocyte-associated antigen$^+$ (CLA$^+$) lines that are destined to become intraepithelial dendritic antigen presenting cells (APC) of the Langerhans system or CLA$^-$ lines that form the interstitial dendritic cells. The Langerhans cells home to the epidermis and epidermal structures of the adnexa and epithelia of mucosa on internal body surfaces; the interstitial dendritic cells occupy nonlymphoid tissues as well as superficial dermal perivascular APC. These myeloid-derived APC cells occupy the peripheral tissues and are exposed to environmental antigens that are ingested and carried by their migration to the regional draining lymph nodes where, as interdigitating cells, they present antigen in context of MHC class I, MHC class II, or CD1 to naive lymphocytes for specific immune response. The macrophage lineage arises from a branch-point in the interstitial dendritic cell lines with the CD14$^+$, CD1α$^-$ precursors differentiating under the inductive pressure of macrophage colony-stimulating factor (M-CSF) into the CD1$^-$, CD14$^+$, MHC II$^+$, CD11c$^-$, CD11b$^+$ phagocytes of the peripheral tissues.

A third lineage of myeloid dendritic cells identified in humans develops from a CD34$^+$ marrow precursor that expresses a high level of IL-3α receptors (IL-3Rα). In an apparently random process unrelated to antigen exposure or inflammatory process, these IL-3Rα^{high}, CD45RA$^+$, CD4$^+$ dendritic cells migrate from the marrow directly to nodal paracortical areas to become the APCs of the T-cell–dependent areas analogous to those of the B-cell–dependent follicular areas. These cells are an important part of the innate immune system and are a major source of antiviral interferon. In proliferative lesions, these cells are known as the interdigitating dendritic cell sarcomas in distinction from those neoplasms of the nodal follicular dendritic cells.

The progeny of these cell streams appear largely to remain lineage specific, but there is some evidence that interchange between the systems may occur likely at early stages of development. The macrophage system is primarily phagocytic and digestive but with capability for production of a wide range of cytokines and growth factors. The dendritic and Langerhans cells have the remarkable ability to recognize and ingest foreign material, but rather than breaking these down to elemental level they can simplify ingested material to just the level of specific antigenicity. That antigenic information can then be retained for indefinite periods until the cells are in a lymphoid organ where they become involved in a B–T-cell antigen processing system for development of specific antibody or cell-mediated specificity. In the process of their committed differentiation, the macrophages and dendritic cells develop specific phenotypic profiles by which they can be recognized. These phenotypic changes are paralleled by functional changes of the dendritic cells that, in the immature state, are active in antigen capture by endocytosis, but are limited in ability to activate T-lymphocytes. Immature dendritic cells have MHC II molecules in cytoplasmic lysosomal containment and in effect inactivated. In contrast, in the mature state the dendritic cells can present antigen internalized, days earlier in the form of the antigen peptides linked to the MHC II presented at

the cell membrane. In this manner, the mature dendritic cell moves from selective phagocytic ability without impact on naive T-cells to effective antigen presenting cells (APC) without phagocytic ability but now able to engage and activate T-cells.

The macrophage lineage has been identified by cytoplasmic reactivity with butyl acetate esterase and lysozyme, but in tissues the current most useful reagents for delineation of these lineages include CD1, CD11b, CD11c, CD14, CD68, and MHC class II. With these reagents, the dendritic cells are characteristically $CD1^+$, and $CD11c^+$, and the macrophage cells are $CD11b^+$, $CD14^+$, and $CD68^+$.

The diseases resulting from abnormal proliferation of these defensive cells have been heavily documented over the last 50 years, particularly as other cells of the immune system have yielded to specific identification. Over this period there has been a series of changes in nomenclature, from an initial approach in which most of the lesions were felt to be of macrophage origin to the current era where the interstitial dendritic and Langerhans cells have also been identified in both benign and malignant conditions. The changes driven by specific cellular identification have resulted in major changes in nomenclature. In view of the relative plasticity of the antigen processing and presenting cells the term *histiocyte* is now used in a generic sense to form the root for a family of cells closely related in lineage and immune function, much as "lymphocyte" forms the basis for the many B- and T-cell subtypes. To proceed in describing the diseases resulting from proliferation of all three of these histiocytic lineages (macrophage, dendritic cell, Langerhans cell) it is necessary to define terminology as assigned by current understanding and usage. The cryptic definitions provided here are intended to avoid the confusion of former usage and to assist orientation to current terminology.

VARIANT TYPES OF HISTIOCYTIC NEOPLASMS

Cutaneous Histiocytoma

Cutaneous histiocytoma is a common benign dermal proliferation of epidermal Langerhans cells most often arising as a single lesion and frequently occurring on the head or ear of young dogs.

Cutaneous Histiocytosis (Cutaneous Reactive Histiocytosis)

Cutaneous histiocytosis is a relatively rare condition that occurs in young mature to aged dogs with wide breed distribution and is characterized by multifocal dermal proliferations of plaque or nodular form and composed of interstitial (dermal) dendritic cells and T-cells.

Systemic Histiocytosis (Systemic Reactive Histiocytosis)

Systemic histiocytosis is a familial disease of Bernese mountain dogs, and sporadically in other breeds, characterized by proliferation of large and solid masses of non-neoplastic interstitial dendritic cells occurring in many tissues, but particularly in skin, peripheral lymph nodes, and ocular and nasal mucosa.

Histiocytic Sarcoma

Histiocytic sarcoma is an aggressive malignant neoplasm of dogs, and less often of cats, characterized by proliferation of histiocytic cells that are not hemophagocytic.

Hemophagocytic Histiocytic Sarcoma

Hemophagocytic histiocytic sarcoma is an aggressive and rapidly fatal neoplasm of dogs that present with Coomb's negative anemia, thrombocytopenia, and hypoalbuminemia with splenomegaly and usually hepatomegaly due to proliferation of neoplastic macrophages that are avidly hemophagocytic, arise in the spleen and marrow, and spread to liver and lung via blood vascular invasion. The disease occurs rarely in cats.

REFERENCES

Affolter, V.K., and Moore, P.F. (2002) Localized and disseminated histiocytic sarcoma of dendritic cell origin in dogs. *Vet Pathol* 39:74–83.

Calabi, F., and Bradbury, A. (1991) The CD1 system. *Tissue Antigens* 37:1–9.

Caux, C., Dezutter-Dambuyant, C., Schmitt, D., and Banchereau, J. (1992) GM-CSF and TNF-alpha cooperate in the generation of dendritic Langerhans cells. *Nature* 360:258–261.

Caux, C., Vanbervliet, B., Massacrier, C., Durand, I., and Banchereau, J. (1996) Interleukin-3 cooperates with tumor necrosis factor alpha for the development of human dendritic/Langerhans cells from cord blood $CD34^+$ hematopoietic progenitor cells. *Blood* 87:2376–2385.

Furue, M., Nindl, M., Kawabe, K., Nakamura, K., Ishibashi, Y., and Sagawa, K. (1992) Epitope mapping of CD1a, CD1b, and CD1c antigens in human skin: Differential localization on Langerhans cells, keratinocytes, and basement membrane zone. *J Invest Dermatol* 99(Suppl):23–26.

Galy, A., Christopherson, I., Ferlazzo, G., Liu, G., Spits, H., and Georgopoulos, K. (2000) Distinct signals control the hematopoiesis of lymphoid-related dendritic cells. *Blood* 95(1):128–137.

Huang, Q., Liu, D., Majewski, P., Schulte, L.C., Korn, J.M., Young, R.A., Lander, E.S., and Hacohen, N. (2001) The plasticity of dendritic cell responses to pathogens and ytheir components. *Science* 294:870–875.

Moore, P.F., Schrenzel, M.D., Affolter, V.K., Olivry, T., and Naydan, D. (1996) Canine cutaneous histiocytoma is an epidermotropic Langerhans cell histiocytosis that expresses CD1 and specific beta 2-integrin molecules. *Am J Pathol* 148:1699–1708.

Moore, P.F., Affolter, V.K., Olivry, T., and Schrenzel, M.D. (1998) The use of immunological reagents in defining the pathogenesis of canine skin diseases involving proliferation of leukocytes. In Kwochka, K.W., Willemse, T., and von Tscharner, C. (eds.), *Advances in Veterinary Dermatology*. Butterworth-Heinemann, Oxford, pp. 77–94.

Olweus, J., BitMansour, A., Warnke, R., Thompson, P.A., Carballido, J., Picker, L.J., and Lund-Johansen, F. (1997) Dendritic cell ontogeny: A human dendritic cell lineage of myeloid origin. *Proc Natl Acad Sci USA* 94:12551–12556.

Porcelli, S.A., Segelke, B.W., Sugita, M., Wilson, I.A., and Brenner, M.P. (1998) The CD1 family of lipid antigen presenting molecules. *Immunol Today* 19:362–368.

Saraya, K., and Reid, C.D. (1995) Synergistic interaction between c-kit ligand (SCF), GM-CSF and TNF promotes optimal dendritic Langerhans cell proliferation from primitive progenitors in human bone marrow. *Adv Exp Med Biol* 378:13–16.

Shortman, K., and Caux, C. (1997) Dendritic cell development: Multiple pathways to nature's adjuvants. *Stem Cells* 15:409–419.

Stingl, G., and Bergstresser, P.R. (1995) Dendritic cells: A major story unfolds. *Immunol Today* 16:330–333.

Strunk, D., Rappersberger, K., Egger, C., Strobl, H., Kromer, E., Elbe, A., Maurer, D., and Stingl, G. (1996) Generation of human dendritic cells/Langerhans cells from circulating $CD34^+$ hematopoietic progenitor cells. *Blood* 87:1292–1302.

Sugiura, K., Shamoto, M., Sakamoto, N., Shinzato, M., Osada, A., Sugiura, M., Hayakawa, R., and Kato, Y. (2003) It is true that, when Langerhans cells migrate from the skin to the lymph node, they are transported via lymph vessels. *Dermatol* 206:222–224.

Traver, D., Akashi, K., Manz, M., Merad, M., Miyamoto, T., Engleman, E.G., and Weissman, I.L. (2000) Development of CD8α-positive dendritic cells from a common myeloid progenitor. *Science* 290:2152–2154.

Trombetta, E.S., Ebersold, M., Garrett, W., Pypaert, M., and Mellman, I. (2003) Activation of lysosomal function during dendritic cell maturation. *Science* 299:1400–1403.

Vandenabeele, S., and Wu, L. (1999) Dendritic cell origins: Puzzles and paradoxes. *Immunol and Cell Biol* 77:411–419.

HISTIOCYTIC NEOPLASMS

Cutaneous Histiocytoma

Canine cutaneous histiocytoma (CCH) is a commonly occurring benign neoplasm generally encountered in dogs less than 2 years old but occurring in older dogs as well. The presentation is usually of a young dog in good health with a single nonpruritic skin nodule 1–2 cm in diameter that is raised and dome-shaped, often hairless, and prone to central ulceration. Less often, the lesion may be a thickened skin plaque, and either type of mass tends to occur on the head, ears, neck, and limbs. Lesions are remarkable; if left unattended, they spontaneously involute with complete healing. Animals may present with more than one lesion but seldom more than two. Multiple lesions may be concurrent or appear successively, and shar-pei dogs are most prone to this type of involvement. In cases with ulceration of the overlying skin, there may be superficial sepsis and enlargement of regional nodes; however, this is unusual because most cases resolve or are removed surgically prior to any secondary involvement.

Histologically, the typical CCH lesion is a high-up infiltration of round cells that extends from the dermal epidermal junction (Fig. 10.1), separating the dermal collagen bundles and extending past the deep adnexa to deep margin of the dermis and panniculus, The infiltrating cells may invade the epidermal layer and resemble epitheliotropic lymphoma (Fig. 10.2). Cytologically, the infiltrating cells have vesicular nuclei of variable shape, but they are usually 1.5–2.0 red cells in the longest dimension (Fig. 10.3). It is the variable shape of the nuclei that gives this lesion its histological signature. Typically, those cells near the skin surface have relatively round nuclei with a single deep infolding that is more divisive than reniform. In deeper areas, the nuclei have variable shapes,

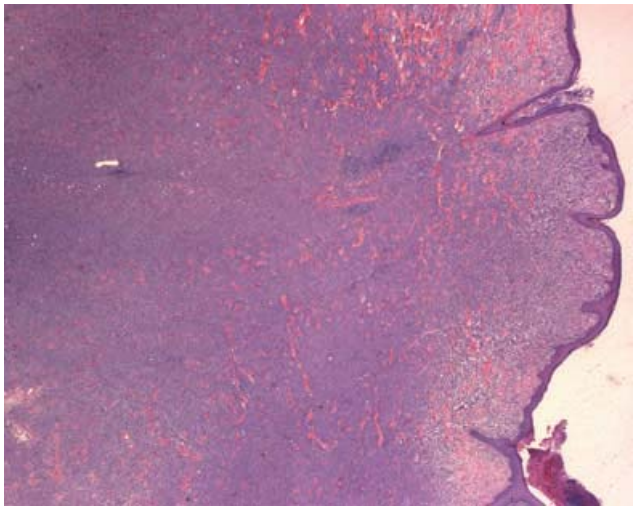

Figure 10.1. Dog: skin, cutaneous histiocytoma, early lesion. There is marked thinning of the overlying skin with central ulceration (lower). The infiltrating cells extend in a solid infiltration through the dermal collagen fibers and through the panniculus indicated by intralesional fat cells to the level of deep connective tissue and superficial skeletal muscle.

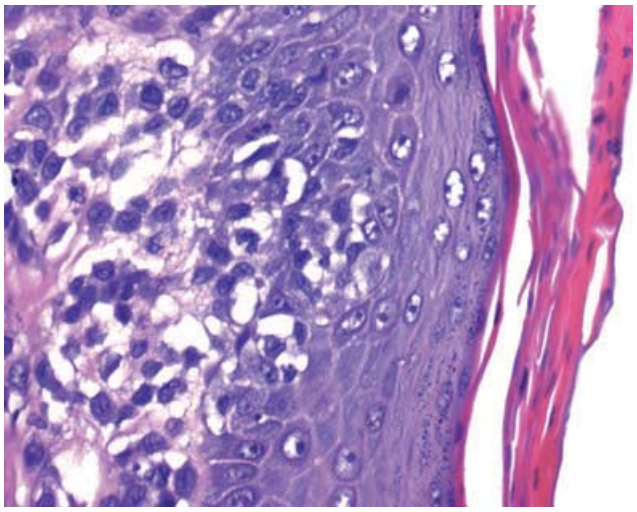

Figure 10.2. Dog: skin, cutaneous histiocytoma. Detail of dermal/epidermal junction in Figure 10.1. The basis for the descriptions of CCH as a high-up lesion are apparent in this image that demonstrates the infiltrating histiocytoma cells in close apposition to the epidermal basement membrane with irregular infiltration into the epidermis that may be misinterpreted as epitheliotropic lymphoma.

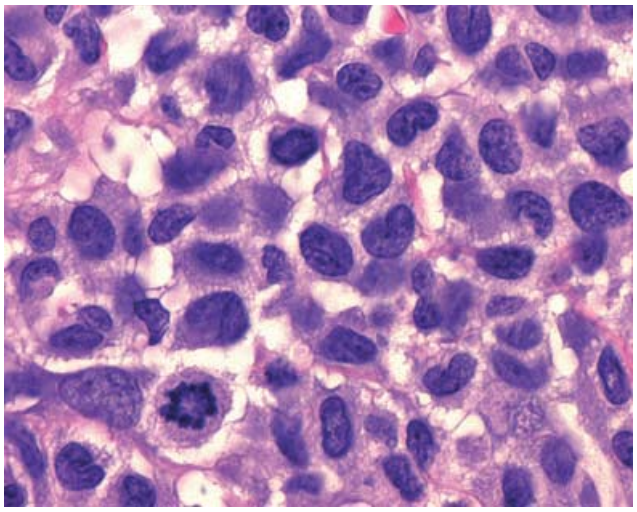

Figure 10.3. Dog: skin, cutaneous histiocytoma. The image is taken at a focal plane to demonstrate the prominent nuclear crease through the oval nucleus in the center. The surrounding cells that tend to be rounded with a deep sharp indentation are typical, as well the more reniform shape as in the nucleus third from the edge in the lower right. The cytoplasmic density is typical with deeper cytoplasmic stain near the nucleus and irregularly fading to the exterior with fine vacuolations.

but typically they have a "bent sausage" appearance with one side convex and slightly curved and the other with a sharp nuclear infolding. Other shapes are present, but a characteristic finding in about 1 in 20–50 nuclei is a sharply defined nuclear crease running linearly across the

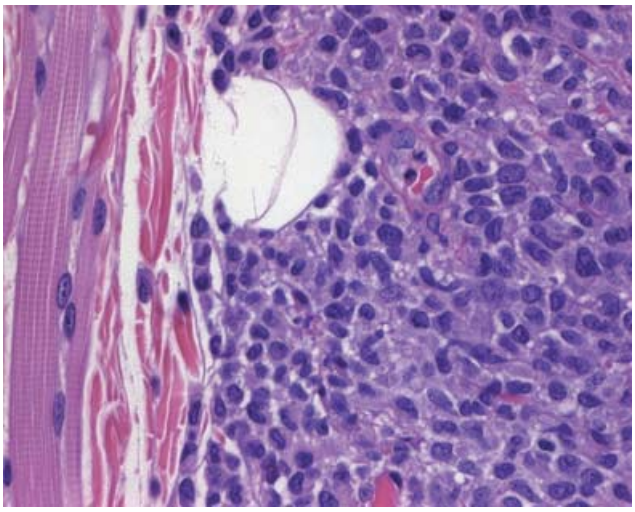

Figure 10.4. Dog: skin, cutaneous histiocytoma. Detail of early lesion, at the junction of infiltrating cells and the deep dermal surface. The infiltrating cells are identical to those seen at the dermal/epidermal junction without evidence of host cell response or corresponding degeneration of infiltrating cells.

nucleus that is the hallmark of the Langerhans cell in histological section. There are 2–5 mitoses/400× field most evident in the more superficial areas. The cytoplasm is abundant and lightly basophilic with cell boundaries generally distinct in superficial areas and coalescing in deeper areas. In early lesions there is solid infiltration of the invading cells to the level of the panniculus or deeper to the superficial skeletal muscle (Fig. 10.4). In lesions that have been present for several months, there are varying levels of involution present that are evident in much more variation in the depth of staining, particularly in deep areas due to lymphoid infiltration (Fig. 10.5). With regression, there is less dense infiltration at the epidermal junction (Fig. 10.6), and the infiltrating cells become more variable in size and nuclear shape with single cytoplasmic vacuolation and focal single cell necrosis (Fig. 10.7). The lymphoid reaction is usually most prominent around the deep adnexa, and lymphocytes usually outnumber the infiltrating cells (Fig. 10.8, see also Fig. 10.5). The lymphocytes are of small type, with shallow nuclear cleavage and a positive staining with CD3, and are of $CD8^+$ cytotoxic type, although there are always a lesser number of B-cells present. In some cases, the extent of the lymphoid infiltration may obscure the primary cellular infiltration and is immediately recognized as reactive.

Phenotypically, Moore et al. have shown that the histiocytoma cells are $CD1^+$, $CD4^-$, $CD11c^+$, MHC II^+, ICAM-1^+, and CD90 or Thy-1^+ and variably E-cadherin$^+$. This array of surface antigens identifies the histiocytoma cells as nonactivated *epidermal* dendritic APC or Langerhans cells. Because the CCH lesion tends to resolve without

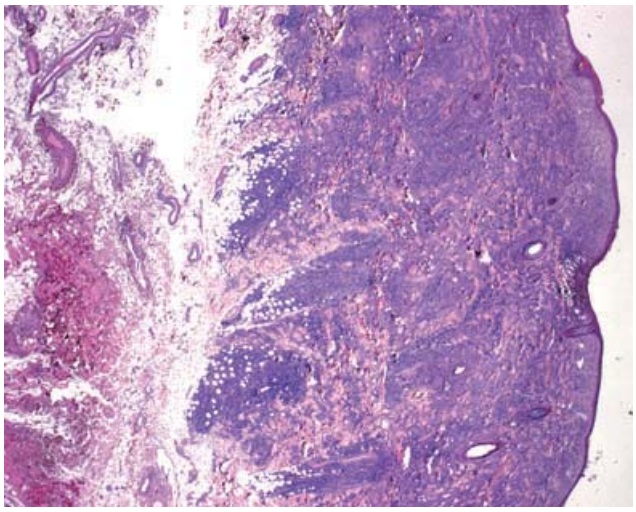

Figure 10.5. Dog: skin, cutaneous histiocytoma, lesion at an advanced stage of involution. The infiltrating cells appear less dense with the darker areas at the deeper surface of the lesion representing areas of dense lymphoid infiltration.

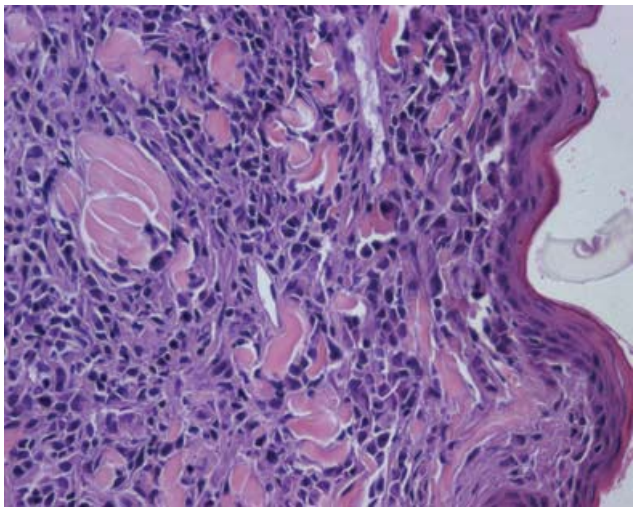

Figure 10.6. Dog: skin, cutaneous histiocytoma in mid-involution dermal/epidermal junction. There is reduced density of the infiltrating cells in the superficial dermis and the cells appear more contracted with hyperchromatic angular nuclei.

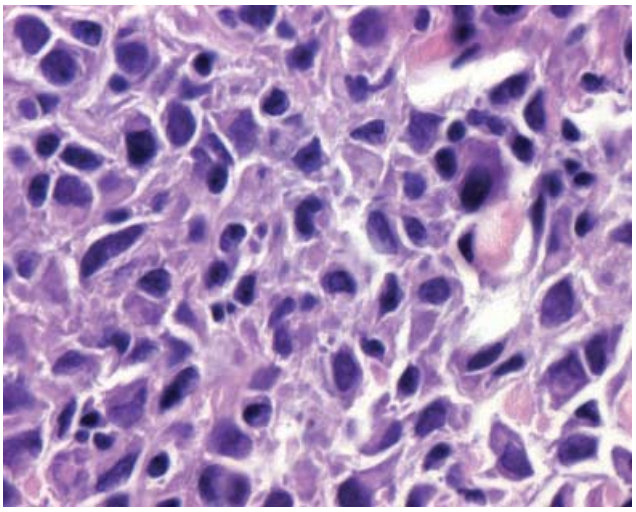

Figure 10.7. Dog: skin, cutaneous histiocytoma, infiltrating cells at the stage of involution. The nuclei of the infiltrating cells remain irregular in shape but tend to become smaller and more angular and deeply stained. The oval and indented cell in the center retains a characteristic conformation. The cytoplasm appears more homogenous and less granular and cell boundaries may become more apparent. There are numerous small lymphocytes present at the top and lower left.

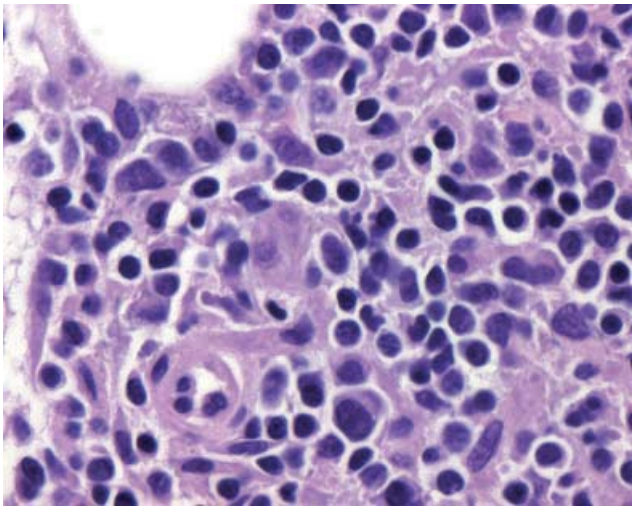

Figure 10.8. Dog: skin, cutaneous histiocytoma at stage of involution at junction of lesion with panniculus. Most of the cells present are small lymphocytes with round densely stained nuclei, occasionally with sharp shallow indentations. The infiltrating cells are less apparent with some retaining the elongated nucleus with smooth unilateral indentation (upper center).

treatment, it may be allowed to resolve spontaneously; however, this is seldom done because the cytologic diagnosis may be less apparent due to the mixture of cells present and because of ulceration, bleeding, and risk of infection or other neoplasm. Because the resolution of the CCH is by host cellular immune response, treatment with steroids is contraindicated.

The CCH lesion needs to be differentiated from cutaneous lymphoma and from more aggressive or persistent types of histiocyosis. The age of the dog and location of the lesion are important factors in the clinical recognition of cutaneous histiocytoma.

Cutaneous histiocytoma occurs in dogs at 5–7 years old and, rarely, older usually as a single lesion and may be

more persistent than in younger dogs. The lesions have a similar topography, with possibly more often on limbs than in young dogs, and tend to be larger and more spreading with lesions 2–3 cm in diameter and more thickened and plaquelike than the dome-shaped mass of young dogs (Fig. 10.9). The lesions are typically high-up infiltrations about 1 cm in depth and may ulcerate less often than in young dogs.

Histologically, the invading cells are similar to those of cutaneous histiocytoma, with nuclei slightly more vesicular and larger but with the same shape irregularities and nuclear creases (Fig. 10.10). The proliferation extends from the dermal epidermal junction down to the panniculus. The major difference from younger dogs is that lymphoid infiltration is sparse, which may account for the apparent lack of spontaneous involution although foci of intratumoral degeneration are present.

Phenotypically, cutaneous histiocytoma in older dogs marks strongly with CD18, and the lymphocytic infiltration is more mixed with the T-cell component much less prevalent. Biologically, these lesions tend to be cured by simple excision, whether or not clean margins were obtained. Histiocytoma in older dogs is not sufficiently different from that in younger animals that it is likely to be mistaken for other neoplasms, but it needs to be differentiated from cutaneous lymphoma and from more aggressive and anaplastic types of histiocytic proliferation.

Recently, a further subtype of histiocytoma has been recognized that has a different presentation, with multifocal dermal lesions that are not distinguishable from the usual disease of solitary lesion type but have an aggressive and unrelenting progression not responsive to therapy (P. F. Moore BVSc, personal communication).

Langerhans cell histiocytosis in humans (histiocytosis X) is a disease of the young, generally less than 5 years old, and there is a male predominance. Unlike the presentation in animals, bone is often involved and lack of bone lesions is a poor prognostic sign. The disease in lymph nodes is characterized by sinus dilation with colonization by cells that have the characteristic nuclear creases of the Langerhans histiocytes (Figs. 10.11–10.13).

Cutaneous Histiocytosis (Cutaneous Reactive Histiocytosis)

Cutaneous histiocytosis (CH) is a disease recognized by multifocal proliferation of *interstitial* dendritic cell proliferation. The immunological characteristics of these cells include expression of CD1, CD11c, and MHC class II similar to cutaneous histiocytoma, but they also express CD90 (Thy-1), a marker of dermal dendritic cells, and CD4, a marker of cellular activation. The CH proliferations have an anterior predilection for the skin of the head, neck, or, caudally, for the flanks, perineum, and scrotum. The syndrome is much less common than cutaneous histiocytoma and apparently has no breed predilec-

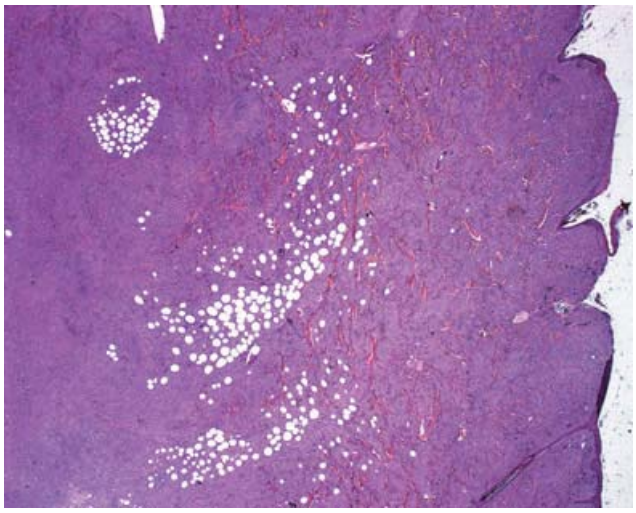

Figure 10.9. Dog: skin, histiocytoma in older animal. The cutaneous lesions are solidly cellular with thinning of the epithelium that is focally ulcerated with complete displacement of adnexa and relatively solid separation of dermal fibers extending down into the panniculus. In contrast to the more common histiocytoma of younger dogs the dense lymphocytic infiltration is not present.

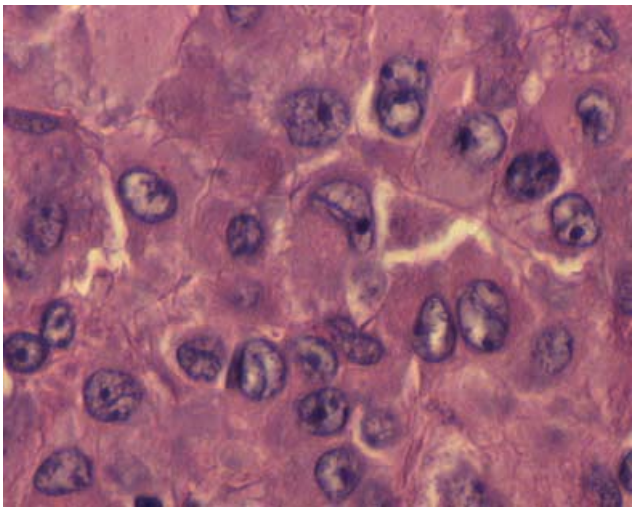

Figure 10.10. Dog: skin, histiocytoma in older animal. Detail of Figure 10.9. The nuclei tend to be vesicular and round to oval with a smaller number of cells with reniform-shaped nuclei like those in the center. The chromatin is coarsely granular and peripheralized with cells having 1–2 prominent nucleoli. Multiple cells in this field have prominent nuclear creases appearing as a dense line across the nucleus. The cytoplasm is abundant and highly amphophilic with the cytoplasm tending to be more dense in perinuclear areas and with cell boundaries indistinct.

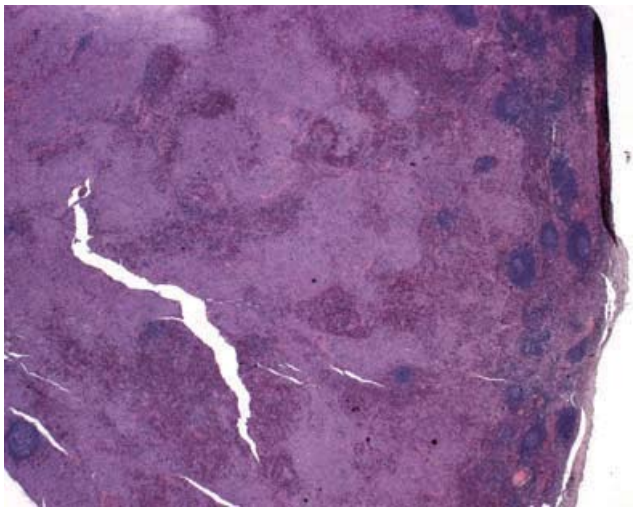

Figure 10.11. Human: lymph node, Langerhans cell histiocytosis (histiocytosis X). The capsule is thinned and taut with cortical colonization by foci of pale-staining cells with multiple small fading germinal centers. *Slide from Cornell Tutorial.*

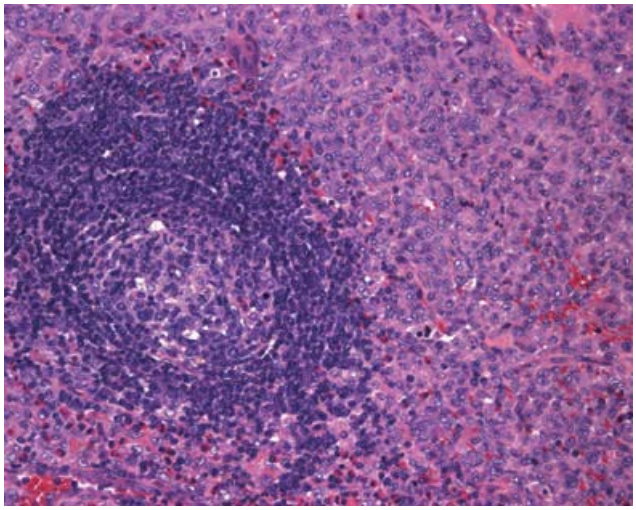

Figure 10.12. Human: lymph node, Langerhans cell histiocytosis, same case as Figure 10.11. The node cortex contains diffuse areas of histiocytic proliferation accompanied by numerous normal-appearing eosinophils.

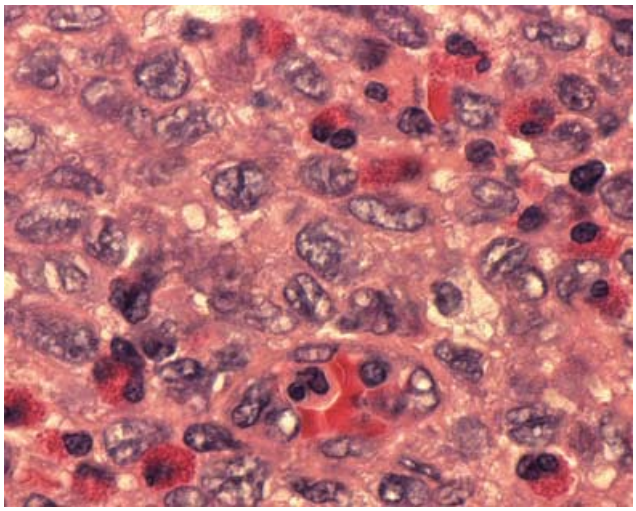

Figure 10.13. Human: lymph node, Langerhans cell histiocytosis. Detail of Figure 10.11. The area contains numerous cells with folded nuclear membranes and a range of shapes, with some sharply indented and others elongated and more reniform. There is abundant cytoplasm that has moderate amphophilia and mild irregular vacuolation with cell boundaries indistinct. The background of eosinophils is characteristic.

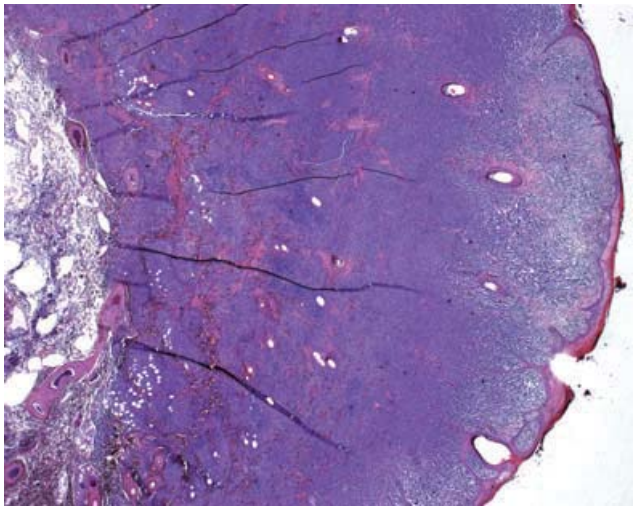

Figure 10.14. Dog: skin, cutaneous histiocytosis. Tissue from a 7 cm diameter dermal mass in the flank of an 8-year-old female spayed Great Dane. There is thinning of the epidermis with displacement of adnexa and solid infiltration through to the panniculus. The darker staining areas are due to focal lymphoid infiltration with most of the pale areas representing serpiginous areas of ischemic necrosis.

tion. The age range affected by CH is broad and generally in animals 3 years to maturity.

The presentation of CH differs from the solitary lesion of cutaneous histiocytoma with multiple dermal plaques or nodules and with a deep orientation within the skin.

Histologically, the infiltrating cells are of mixed cell type forming nodular, almost granulomatous-appearing lesions that spare the superficial dermis (Figs. 10.14, 10.15) and have a "bottom-heavy" infiltration, which differs from the "high-up" lesion characteristic of cutaneous histiocytoma. Architecturally, the cellular proliferation is angiocentric and focally angioinvasive and consists of an initial perivascular cellular proliferation that includes lymphocytes that may focally predominate and other leukocytes, as well as the activated histiocytic population. With progression, these foci coalesce and invade

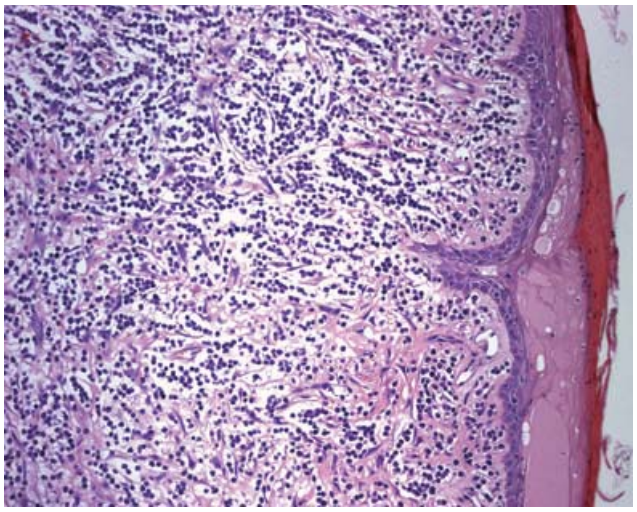

Figure 10.15. Detail of Figure 10.14 with severe laminar superficial dermal edema.

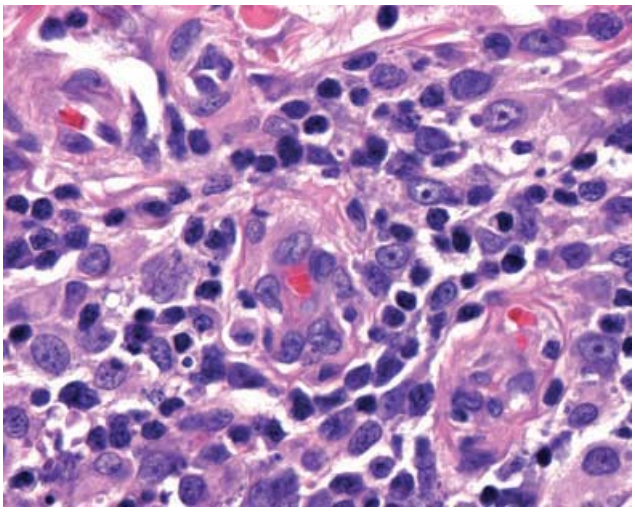

Figure 10.17. Dog: skin, cutaneous histiocytosis. Three small arterioles in the deeper area of the tissue have medial infiltration by irregular-shaped nuclei of histiocytic cells. The vessel in the lower right has almost complete luminal occlusion.

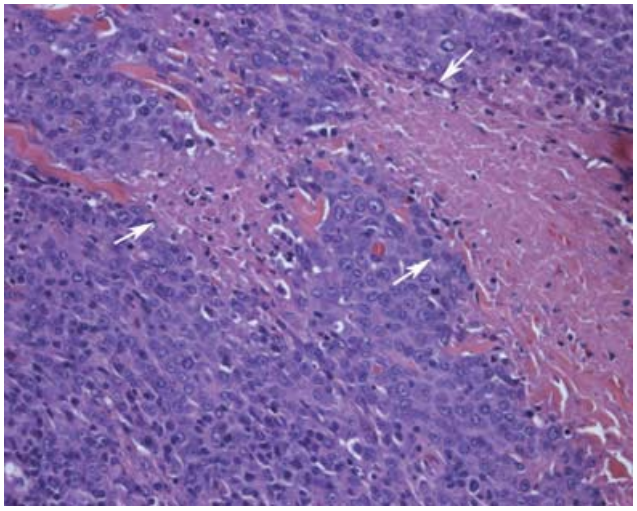

Figure 10.16. Dog: skin, cutaneous histiocytosis. Area of serpiginous necrosis, (left) has focal infiltration of small lymphocytes (left).

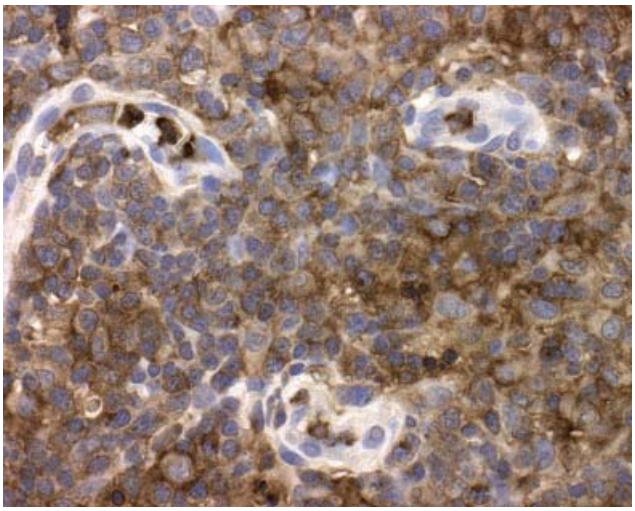

Figure 10.18. Dog: skin, cutaneous histiocytosis, arteriolar infiltration by histiocytic cells in a deep area of the lesion. The CD18 stain strongly marks the surrounding population as well as those cells infiltrating the arteriolar vessel walls and lumen.

the deep dermis and panniculus with a waxing and waning habit of focal nodular proliferation followed by regression and then recurrence in previously uninvolved areas. Large lesions have scattered foci of ischemic necrosis (Fig. 10.16) that result from foci of angioinvasion and obstruction of small muscular arterioles (Figs. 10.17, 10.18), but apparently less often small veins. The cell types are larger and more varied than those of histiocytoma and have more nuclei that are round to oval without hyperchromicity and have a dispersed very fine granular chromatin pattern with small but prominent central nucleoli. The rest of the nuclei are more reminiscent of the Langerhans cell type with the elongated nuclei with one-sided indentation and occasional nuclear creases (Fig. 10.19). Mitoses are present but not in all fields, and large clusters of the atypical cells may be present surrounded by a quite prominent fibrovascular network (Fig. 10.20). The CH cells have abundant, finely granular cytoplasm of even density throughout that resembles that of macrophages and differs from the perinuclear clear areas characteristic of lymphocytes. Cell boundaries are indistinct (Figs. 10.21, 10.22).

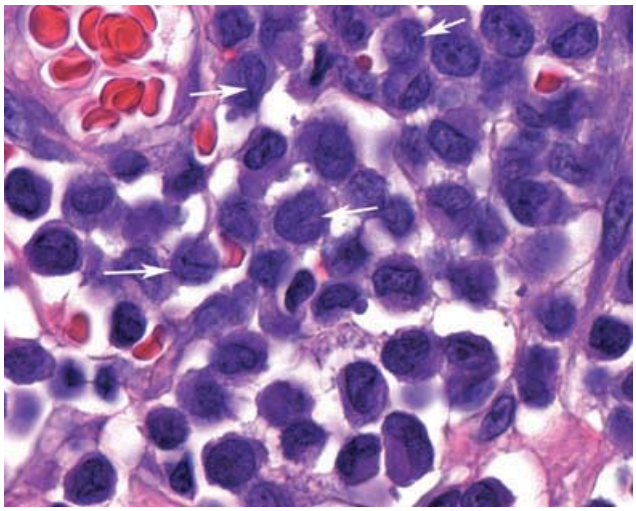

Figure 10.19. Dog: skin, cutaneous histiocytosis. Cytologic detail of infiltrating cells, which have more rounded and vesicular nuclei when compared to the cells of CCH. In addition there are more prominent, often multiple, nucleoli. The recurring nuclear shapes with reniform indentation are present as well as prominent nuclear creases appearing as a curved dark line across the nuclei (arrows).

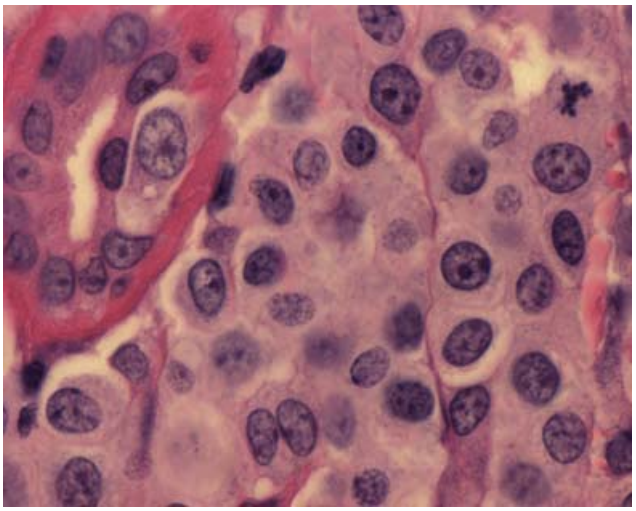

Figure 10.21. Dog: skin, cutaneous histiocytosis. The nuclei tend to be round with a coarse granular chromatin pattern and generally 1–2 small nucleoli. The cytoplasm is relatively abundant, finely granular, and fades in density toward the outer membrane. The cells are closely in contact with cell boundaries generally finely outlined. There is a cell in metaphase in the upper right and binucleated in the lower center. A single cell is invading the epithelium of a shrunken and isolated apocrine gland in the upper left.

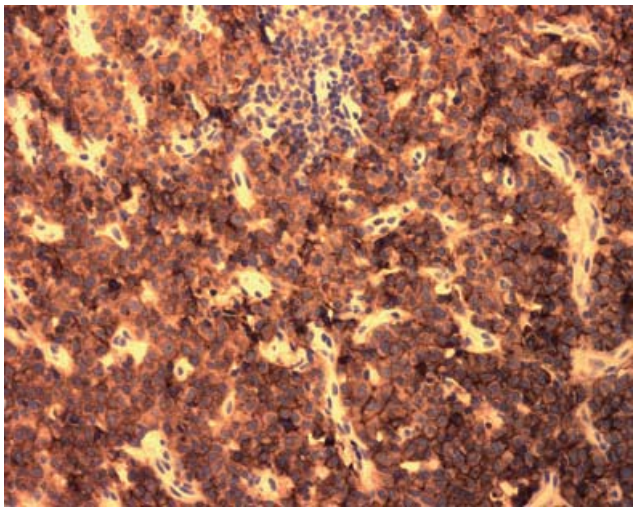

Figure 10.20. Canine: skin, cutaneous histiocytosis, same case as Figure 10.19. With CD18 staining, the infiltrating cells are strongly and uniformly labeled. There is a vibrant fine fibrovascular network in more superficial areas of the tumor that are apparent and unlabeled and, unlike arterioles, are not invaded by the infiltrating cells. The lesions generally have very little host reaction with a small focus of lymphoid cells in the uppper center.

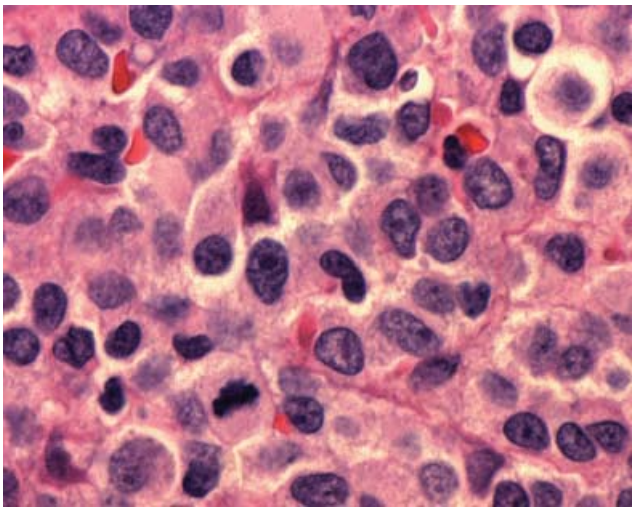

Figure 10.22. Dog: skin, cutaneous histiocytosis, same case as Figure 10.21. A typical area, with Langerhans type cells, which have a unilateral indented cell like that in the center and smaller cells with sharp shallow nuclear indentations in the upper and lower center. There is a cell in metaphase in the lower center and one, upper center, undergoing pyknosis with eosinophilic cytoplasm.

The variability of cell type present in CH may suggest pyogranulomatous dermatitis and special staining to rule out an infectious etiology. A useful feature distinguishing CH from lesions of infectious nature are the very atypical configurations of the histiocytic nuclei in CH. In addition, there is no "inflammatory gradient" of granulation tissue to macrophages and neutrophils as seen in granulomas. CH lesions may have foci of necrosis related to vascular invasion with angiocentricity, and embolism of arterioles by inflammatory cells is an unlikely feature of infectious disease. Lesions of similar appearance that involve the mucosal surfaces, particularly of conjunctival and nasal areas, need to be considered within the category of systemic histiocytosis. Cutaneous histiocytosis is an immunoregulatory rather than neoplastic disorder. CH lesions respond irregularly to corticosteroids but much more consistently to more potent immunosuppression by cyclosporin A or leflunomide.

Phenotypically, the cells of reactive histiocytosis are identified as activated dermal dendritic APC that have the phenotype of $CD1^+$, $CD11c^+$, $CD11b^+$, $MHCII^+$, $ICAM\text{-}1^+$ and CD90 or $Thy\text{-}1^+$ and $E\text{-}cadherin^-$. The CH cells are thus distinguished from Langerhans cells, as described for cutaneous histiocytoma. The associated cell types present include $CD8^+$ T-cells with the $TCR\alpha\beta^+$ type of receptor profile and $CD11b^+$ neutrophils. The CH cells react strongly and uniformly with the CD18 monoclonal antibody (source: Dr. P. F. Moore, U.C. Davis), and with this reagent it is possible to identify flattened cells invading the muscular layers of small arterioles that are still functional, as well as solid infiltration into vessels that have undergone complete obliteration (see Fig. 10.15). The necrosis and the vascular invasion are not found in the same area, but they are likely related with the foci of ischemic necrosis observed, likely the downstream effects of arteriolar emboli in an adjacent area of the tissue.

Systemic Histiocytosis (Systemic Reactive Histiocytosis)

Systemic histiocytosis (SH) is a disorder characterized by proliferation of interstitial dendritic cells in a multifocal presentation. Thus, the cells of SH express the identical phenotype of cutaneous histiocytosis CH) and have the signature of $CD1b^+$, $CD1c^+$, $CD4^-$, $CD11c^+$, $MHC\ II^+$ and $ICAM\text{-}1^+$ and mark strongly with CD18. The breed predilection for this disease includes rottweiler, Bernese mountain dog, golden retriever, Labrador retriever, flat-coated retriever, shar-pei, beagle, and crossbred dogs. The disease is most commonly seen in mature dogs, but it has been seen in animals 3–11 years old.

SH may present as a solitary lesion that appears as a rapidly progressive, deeply located soft tissue mass. Skin is almost always involved, predominantly of the limbs, and when multifocal in presentation the sites include one or more of other areas, including the spleen, lung, bone, brain, and, less often, nasal or oral cavity. The lesions may become very large locally or may invade local lymph nodes by the time of presentation.

Histologically, the lesions of SH are identical to those of CH with focal ischemic necrosis of angiocentric and angioinvasive localization accompanied by a mixed cellular reaction, which may look pyogranulomatous and of infectious origin. Architecturally, the SH lesions are unencapsulated and have poorly demarcated margins and irregular narrow bands of collagenous stroma. The cell type may be predominantly of large round cells with discrete cell margins or of stellate spindle cells with vesicular oval nuclei, or there may be regions with either cell type focally predominating in the same lesion (Fig. 10.23). The nucleolar pattern is variable, with some cells having a prominent single nucleolus and others having several nucleoli, which are smaller and often peripheralized. The mitotic rate is variable with some present in contiguous fields at 400× magnification. The cytoplasm is abundant and irregularly amphophilic, generally more deeply stained near the nucleus, and fading to the cell boundaries with some cells having focal prominent Golgi areas. There are areas with more anisokaryosis with some nuclei both large and deeply stained (Fig. 10.24). Reactive cells

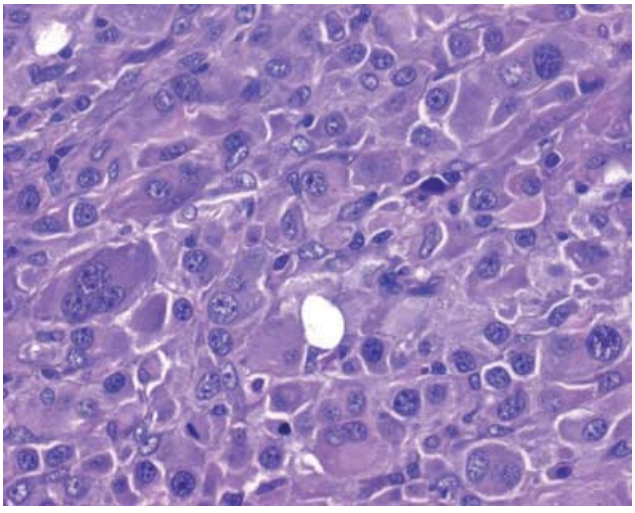

Figure 10.23. Dog: subcutaneous mass, systemic histiocytosis. Cytologically, the cells are more variable than in the cutaneous types of histiocytosis (CH). The nuclei are largely round and vesicular, but folded and indented types are present. There is single cell necrosis present in the upper right center and a trinucleated cell in the lower left. The chromatin pattern is coarse granular with irregular parachromatin clearing and 1–2 prominent nucleoli. The cytoplasm is abundant and deeply amphophilic in perinuclear areas, with fading to the outer membrane and some cells having lighter perinuclear areas that resemble Golgi zones.

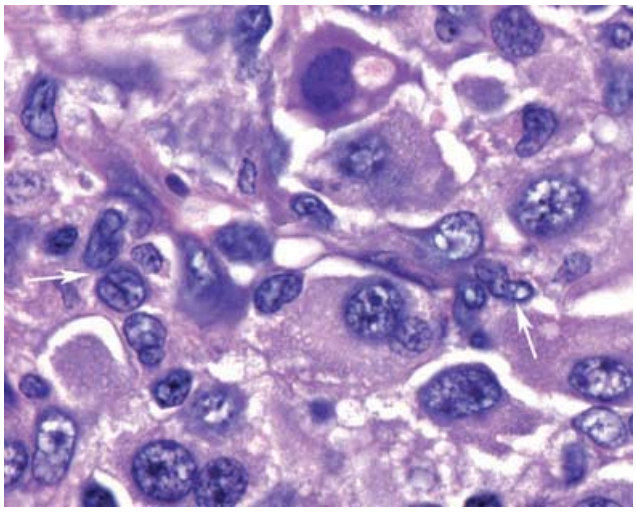

Figure 10.24. Dog: subcutaneous mass, systemic histiocytosis. Detail of Figure 10.23. There is remarkable variation in nuclear shape with vesiculation more common and with some cells remaining elongated and folded with occasional fine nuclear creases (arrow). The chromatin pattern is coarsely granular with irregular parachromatin clearing and 1–2 nucleoli that vary in prominence. The cytoplasm is relatively abundant and moderately amphophilic with cell boundaries irregularly distinct. Mitoses are present in other fields.

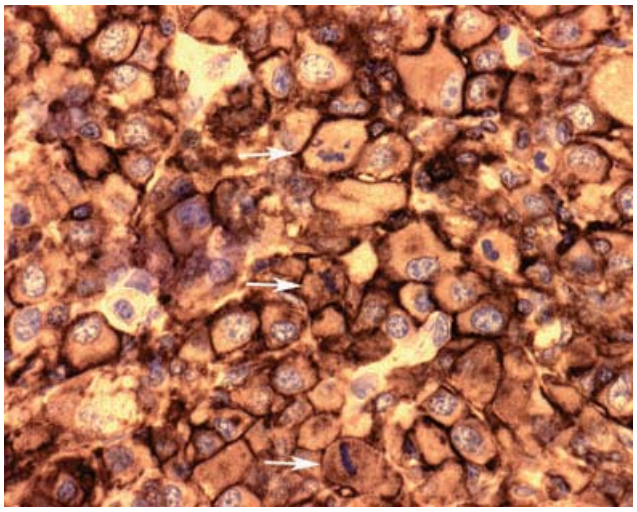

Figure 10.25. Dog: subcutaneous mass, systemic histiocytosis. Phenotype of Figure 10.23. On staining with CD18, the cells are strongly and uniformly labeled. There are 3 cells in metaphase in the center of the image. The tissue was negative for lymphoid markers and lightly positive with vimentin and negative with cytokeratin.

present include neutrophils and macrophages in areas of necrosis with relatively few lymphocytes occurring in small clusters. Multinucleated cells are irregularly present and SH cells may have vacuolated cytoplasm, rarely with phagocytosis of red cells or neutrophils. The cells of SH are strongly and uniformly labeled with CD18 (Fig. 10.25).

Biologically, SH is a nonneoplastic immunoregulatory disorder that is managed as for CH with corticosteroids generally ineffective and immunosuppressive therapy with cyclosporin A or leflunomide generally very effective. SH must be differentiated from the neoplastic histiocytic sarcomas as well as from other soft tissue sarcomas, including malignant fibrous histiocytoma. Those neoplasms occurring near joints must be distinguished from synovial cell sarcoma, and with the degree of anisokaryosis and variability of cell type, amelanotic melanoma may appear to be a consideration.

Histiocytic Sarcoma

Histiocytic sarcoma (HS) may present as solitary or multiple lesions characterized by rapid dissemination. The primary sites for HS when solitary are on the limbs and typically lying above a joint or encircling it in a manner that defeats curative excision. The lesions arise beneath the skin and in the subsynovium below the synovial lining and likely from perivascular interstitial dendritic cells. Less often, a solitary presentation of HS may occur elsewhere in a dermal or subdermal site. When disseminated the more common sites of involvement are the skin, lung, lymph node, bone marrow, spleen, and even brain. The lesions of HS, if correctly identified, are due to proliferation of dendritic antigen presenting cells (APCs). In lymphoid tissues the normal cell counterpart is likely the interdigitating dendritic cell population, but the cellular origin in proliferations arising in other sites is unknown. With the origin as dendritic APC, the tumors arising have the immunological expression of CD1, CD11C, and MHC class II. They have variable expression of CD90 and are negative for CD4. HS is therefore like cutaneous histiocytoma, although negative for E-cadherin, and cytomorphologically HS has the appearance of a much more aggressive lesion. It is important to differentiate the antigen expression of HS with that of the variant disease characterized by avid hemophagocytic activity and now known as *hemophagocytic histiocytic sarcoma (HHS)*, which arises from the macrophage population and express MHC class II and the β2 integrin, CD11d. The HHS cells have low or inconsistent expression of CD1 and CD11c, which distinguishes them from histiocytic sarcoma (HS).

The breed predilection of HS is similar to that of the systemic reactive histiosis (SH) for the most commonly represented breeds, with slight female predominance. Animals are presented with multiorgan involvement, and it is unclear whether this represents metastatic disease from a single site of tumor induction or if predisposed animals develop multiple metachronous neoplasms

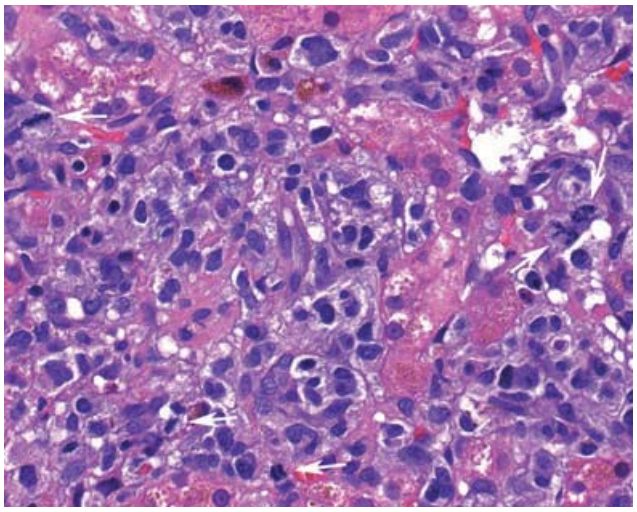

Figure 10.26. Dog: liver, histiocytic sarcoma. There are interlacing columns of neoplastic cells infiltrating hepatic parenchyma along sinusoids. The nuclei are hyperchromatic and vary from round to oval and indented with a dispersed fine chromatin pattern with nucleoli not evident. The cytoplasm is moderate in volume and finely vacuolated. There are 4 mitotic figures indicated by arrows.

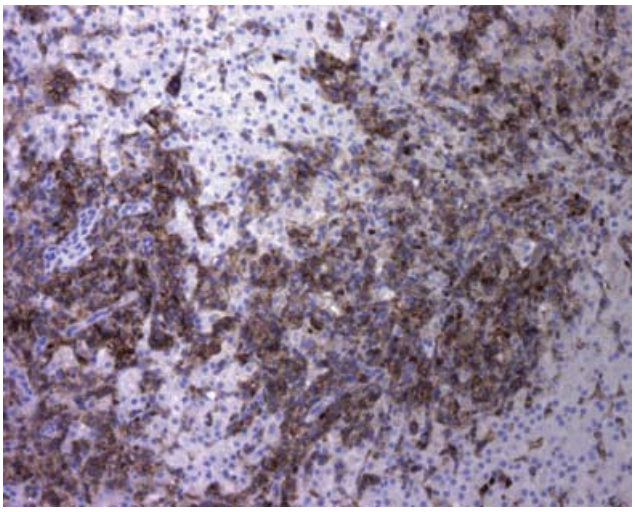

Figure 10.28. Dog: liver, histiocytic sarcoma. Phenotype of Figure 10.26. With CD18 staining, the infiltrating cells are solidly and uniformly labeled. There is also scattered positivity along the sinusoids in unaffected areas due to marking by normal benign Kupffer cells. The tissues were negative with staining for lymphocyte antigens.

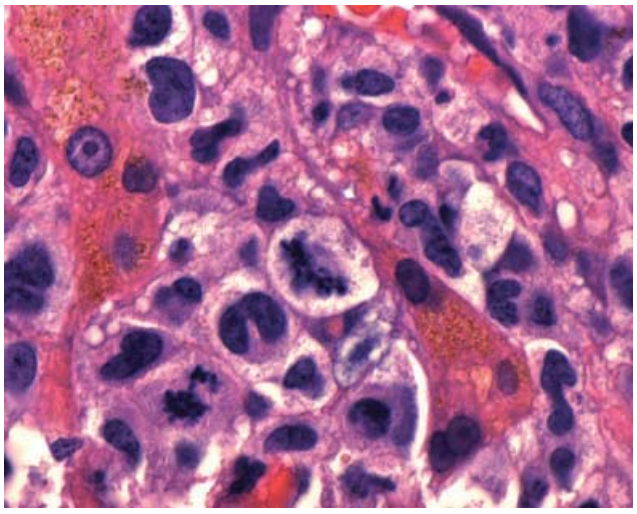

Figure 10.27. Dog: liver, histiocytic sarcoma. Detail of Figure 10.26. The nuclei vary in shape with markedly hyperchromatic, dispersed chromatin that obscures nucleoli of moderate size. The cytoplasm is abundant, finely granular, and typically more densely stained near the nucleus and fading to the exterior with cell boundaries generally distinct. There are a few other cells apparent besides hepatocytes and endothelial cells. The hepatocytes have intracellular pigment.

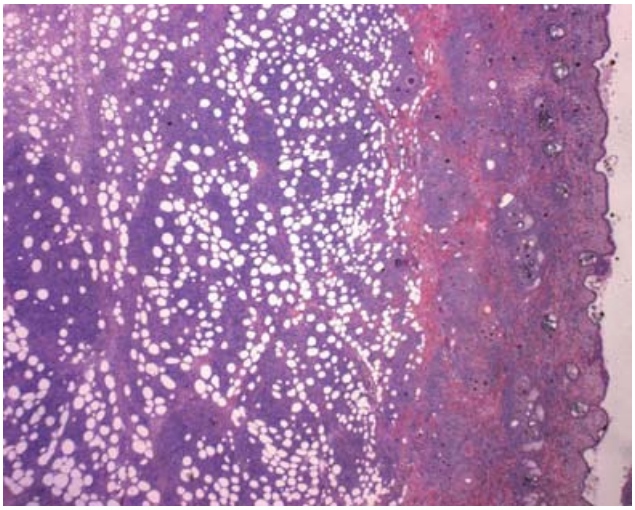

Figure 10.29. Dog: skin, histiocytic sarcoma. A 9-year-old female blue heeler presented with multiple oozing lesions on the back and sides with five biopsies received from multiple sites. The skin is thickened, largely due to solid cellular infiltration around deep adnexa with multifocal lesions extending through the panniculus. There are multifocal pale areas of ischemic necrosis and the lesion was originally thought to be panniculitis-like T-cell lymphoma.

developing sequentially in different sites. The spleen is most often involved, followed in descending order by the liver (Figs. 10.26–10.28), bone marrow and adjacent vertebral bone, lung, lymph nodes, subcutaneous tissues (Figs. 10.29–10.35), kidney, and more unusual occurrences in myocardium, nasal and oral cavities, brain prostate, adrenals, and gonads.

Histologically and phenotypically, the cells of HS are as described for the localized form of the neoplasm. The disseminated form of this disease must be differentiated from malignant fibrous histiocytoma, which may present with

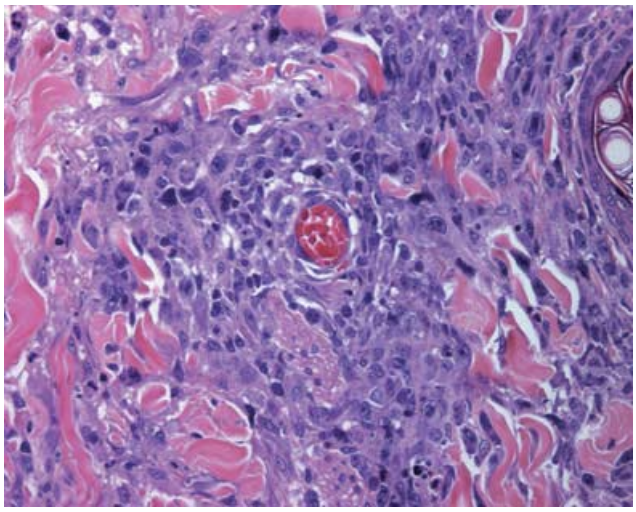

Figure 10.30. Dog: skin, histiocytic sarcoma. Detail of Figure 10.29. There is remarkably tight cuffing of neoplastic cells around superficial dermal vessels similar to types of epitheliotropic lymphoma.

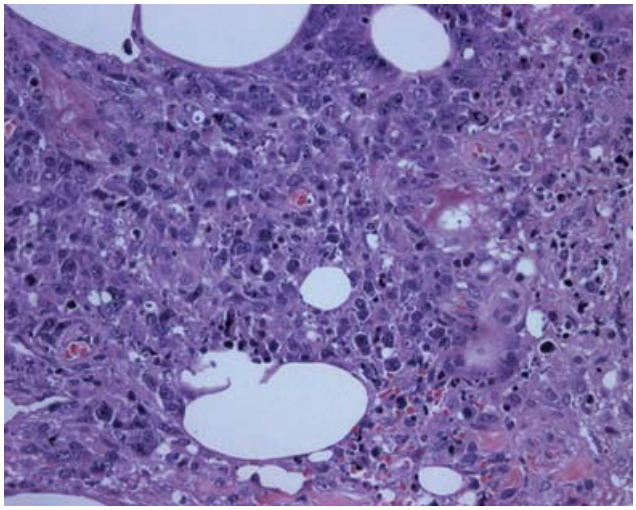

Figure 10.31. Dog: skin, histiocytic sarcoma, same case as Figure 10.29. An area of deep panniculus has viable cells in the center and is bordered by an area of ischemic necrosis at the right.

multiorgan involvement, and from hemophagocytic HS of macrophage origin on the basis of cell and phenotype and by the latter neoplasm having avid phagocytic activity that is evident in all tumor sites. HS tends to have more cellular variability in the accompaniment of inflammatory cells that are generally present only in the various soft tissue sarcomas in areas of necrosis.

Biologically, the disseminated form of histiocytic sarcoma is poorly responsive or not responsive to current therapies and has a poor prognosis.

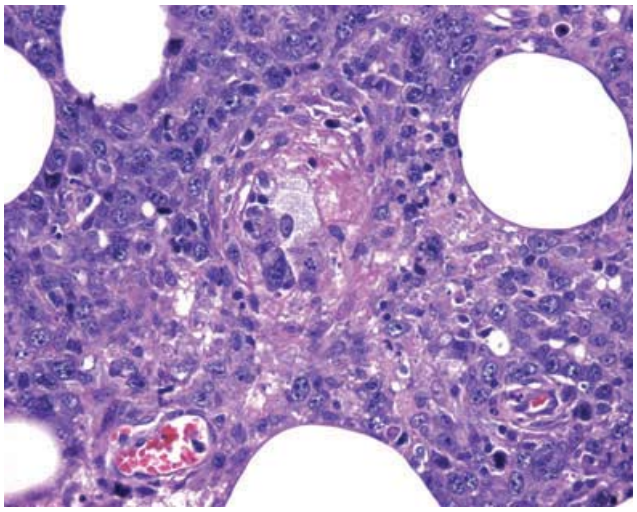

Figure 10.32. Dog: skin, histiocytic sarcoma, same case as Figure 10.29. An area of deep panniculus with two small vessels (lower); with that in right with neoplastic cellular infiltration into the media. The oval area in the upper center is likely a larger vessel that has become completely occluded with the central area now containing serum and neoplastic cells.

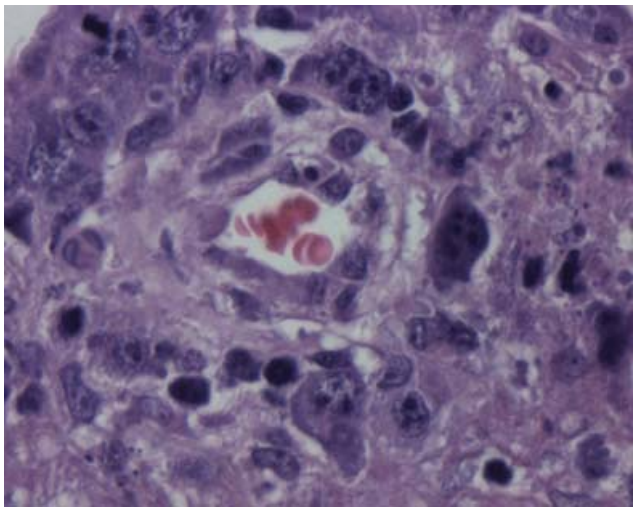

Figure 10.33. Dog: skin, histiocytic sarcoma. Detail of Figure 10.29. The small vessel (center) can be seen to have concentric laminations of the media with apparent infiltration of neutrophils at left and an atypical cell possibly of tumor type at the right.

Hemophogocytic Histiocytic Sarcoma

Hemophagocytic histiocytic sarcoma (HHS), formerly known as *malignant histiocytosis*, has had a several names in both human and veterinary pathology, and other terms used from time to time are best left undisturbed. In human pathology, many of the earlier descriptions of this disease have been since been questioned by limited review

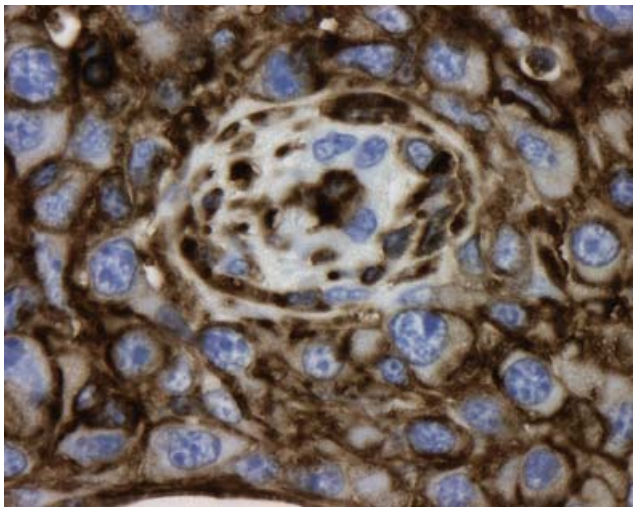

Figure 10.34. Dog: skin, histiocytic sarcoma. Phenotype of arteriolar infiltration. With CD18 staining, the neoplastic cells are strongly and uniformly labeled. An arteriole similar to that in Figure 10.33 has labeled cells, presumably neoplastic, infiltrating the media and compressing the lumen. The tissue was negative with immunologic stains for lymphocytes.

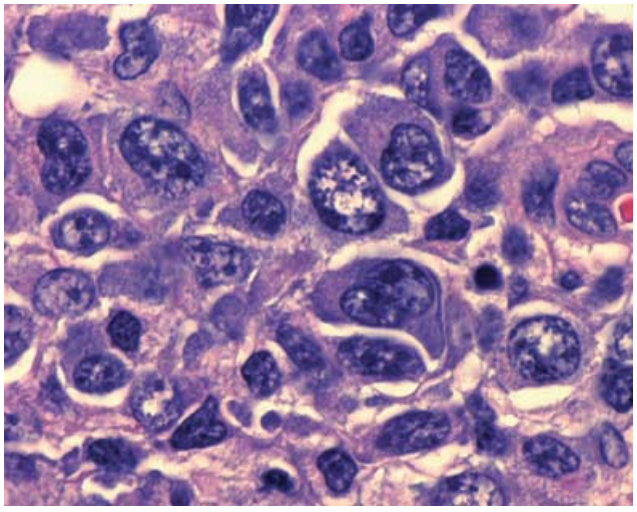

Figure 10.35. Dog: skin, histiocytic sarcoma. Detail, deep dermal area of Figure 10.29. As the disease becomes more aggressive, the neoplastic cells become more vesicular. There are 2 nuclei with reniform shape in the upper left and a binucleated cell in the center. The nucleus in the lower right has a sharp shallow indentation and the one lower center with the oval outline has a central linear density that may indicate a nuclear crease. The cytoplasm is relatively abundant and highly amphophilic, and cell boundaries are only irregularly apparent. There is likely an occasional small lymphocyte present but most of the small dark bodies are pyknotic.

of collections originally diagnosed as malignant histiocytosis. In cases where retrieval of the paraffin-embedded tissue was possible, followed by examination using current technology, many of these were shown to be peripheral T-cell lymphoma and, less often, large B-cell lymphoma. Others were shown to be null for CD68, the macrophage marker, or positive for CD30, which recognizes activated T- or B-cells and Reed-Sternberg cells. Currently in human pathology, the guidelines for the diagnosis of HHS require that the lesion be shown to have germline status for both the T-cell receptor and immunoglobulin genes. Further, even demonstration of germline lymphoid receptor genes is not adequate evidence for diagnosis of HHS unless there is also convincing phenotypic proof of macrophage origin.

HHS is very rare in animals and apparently also in humans. In my own experience, I have tissue from two dogs and have seen HHS in two cats that were verified by nonspecific esterase staining. There may as well be regional differences in the incidence of SSH because some well-experienced pathologists feel they have not been presented with cases that fit this description. Because SSH appears to be rarely encountered in humans or veterinary practice, the descriptions here will include reference to this condition in both humans and animals. In humans, SSH is primarily a disease of older adults, although it has been reported in children. In animals, it appears to occur primarily in mature dogs and in cats older than 10 years. There is no sex predilection for HHS in humans.

Too few verified cases have been reported in animals to be clear on incidence by gender, but one report of 4 cases diagnosed without phenotypic confirmation included 3 males and 1 female with ages ranging from 2–11 years, with a mean of 6.5 years. In a more extensive review of HHS, 17 dogs were described, including Bernese mountain dog (6), golden retriever (4), rottweiler (3), Labrador retriever (2), schnauzer (1) and 1 mixed breed, with ages ranging from 2.5–13 years. These comprised 8 females (2 intact) and 9 males (3 intact). The presentation of these animals was distinctly different from that of HS, and consists of Coomb's negative responsive anemia, thrombocytopenia, hypoalbuminemia, and hypocholesterolemia, with this spectrum of changes occurring together in a high proportion of cases. The course was rapidly fatal in all cases, either naturally or elective due to intractable disease. All animals had diffuse splenomegaly with poorly defined masses, and microscopically lesions were present in the spleen, liver, lung, and bone marrow. Metastatic spread was by vascular spread with minimal local mass formation (P. F. Moore BVSc, personal communication).

The neoplastic cells vary from single to multinucleated with widely varying degrees of atypia that is most marked in the spleen. The neoplastic cells are remarkably erythrophagocytic, and the larger cells, presumably older,

contain both red cells and hemosiderin. The HHS cells arise from the splenic red pulp sinus areas and express MHC class II and the β2 integrin, CD11d. The hemophagocytic HS cells have low or inconsistent expression of CD1 and CD11c, which are dominantly expressed by the nonphagocytic dendritic APC of histiocytic sarcoma (HS).

On physical examination, there is anemia, abdominal distension, irregular lymphadenopathy, and hepatosplenomegaly. The HHS lesions are usually in spleen (Figs. 10.36–10.40) and liver, some nodes, and focally in marrow, with lesions arising in any other site. In cats, there is a similar loss of weight in an older animal, irregular lymphadenopathy, and usually splenomegaly. In one case of this author's experience, the diagnosis was made on fine needle aspiration of an enlarged mandibular salivary gland, with the disease later determined to be multicentric.

Cytologically, the diseases in the dog and cat are the same and consist of cells with marked anisokaryosis, including large cells that may have massive, deeply stained nuclei with nucleoli as large as red cells and abundant highly basophilic cytoplasm with marked erythrophagocytosis (see Figs. 10.38, 10.39). Cells are present with no evidence of phagocytic activity, but in every field there are some with many ingested red cells and occasionally neutrophils or lymphocytes (see Fig. 10.40). A constant accompaniment of these cells are others that have very abundant cytoplasm and iron pigment at various stages of protein complexing that is granular and diffuse and highly basophilic on cytologic examination.

Histologically, the lesions in the spleen are characterized by complete lymphoid atrophy (Fig. 10.41) and marked sinus distension by large and very large cells with abundant cytoplasm that are irregularly phagocytic and some with evident golden hemosiderin cytoplasmic pigment (Fig. 10.42). There are occasional foci of subendothelial colonization by the neoplastic cells, as seen in leukemias (Fig. 10.43), and the neoplastic cells appear to

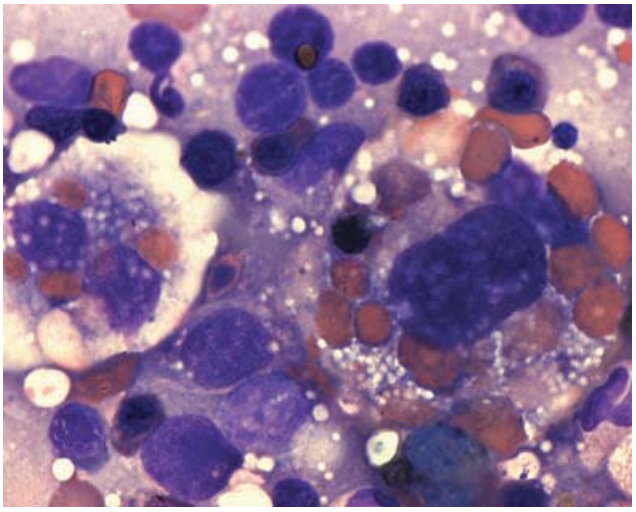

Figure 10.37. Dog: spleen, hemophagocytic histiocytic sarcoma. There are 2 large neoplastic histiocytes at the left and right that contain ingested erythrocytes. The larger cell had very deeply stained chromatin and both may be binucleated.

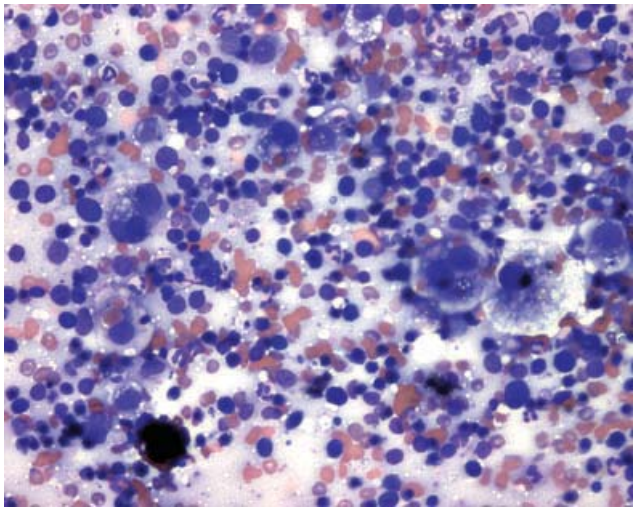

Figure 10.36. Dog: spleen, imprint hemophagocytic histiocytic sarcoma. The background population includes increased numbers of neutrophils and a marked increase in large cells with abundant cytoplasm that is finely vacuolated. Erythrophagocytosis is apparent in cells in the lower left. The anemia is accompanied by evident splenic erythropoiesis.

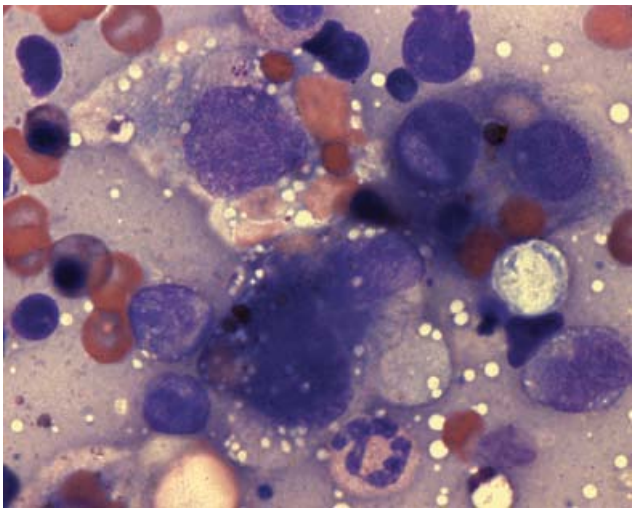

Figure 10.38. Dog: spleen, hemophagocytic histiocytic sarcoma. Large phagocytic cells; the one in the upper left has a single large nucleus and contains numerous ingested red cells.

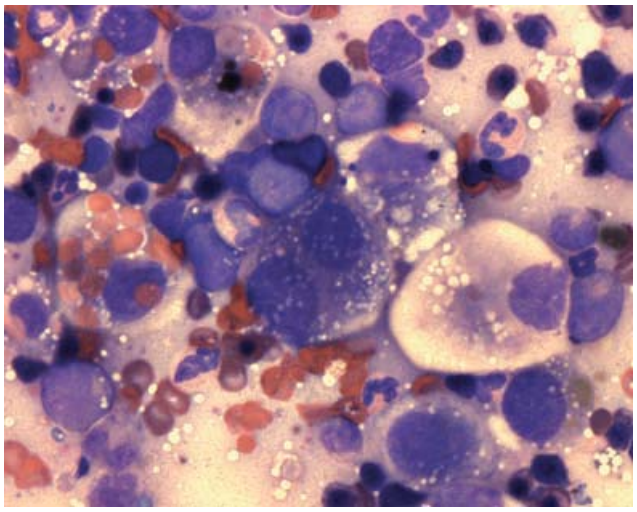

Figure 10.39. Dog: spleen, hemophagocytic histiocytic sarcoma. A group of cells with 4 large macrophages in the center with a binucleated cell centrally and one with numerous ingested red cells at the left. Macrophages at an earlier stage of development are at the center and lower right.

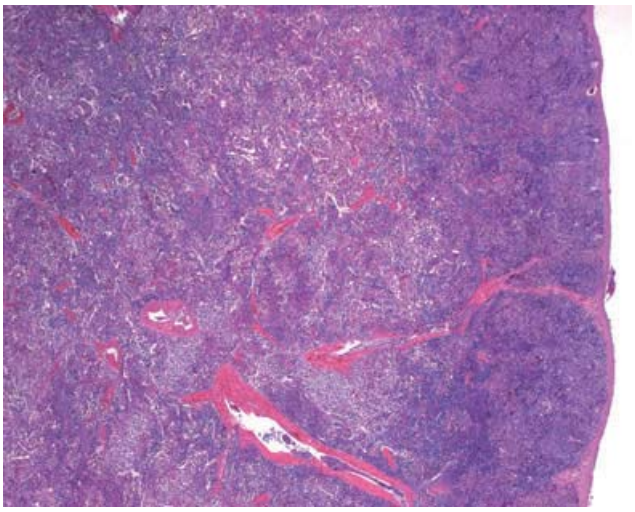

Figure 10.41. Dog: spleen, hemophagocytic histiocytic sarcoma. There is thinning of the capsule with thinned and widespread smooth muscle trabeculae indicating splenomegaly. There is a completely diffuse architecture with loss of periarteriolar lymphoid sheaths and follicular lymphoid development. There is solid sinus filling with a patchy appearance due to clusters of lighter-staining phagocytic cells.

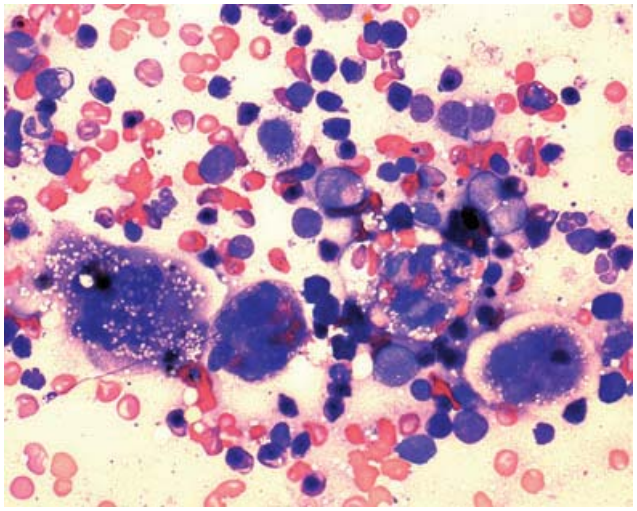

Figure 10.40. Dog: spleen, hemophagocytic histiocytic sarcoma. There are four malignant histiocytes; all are apparently multinucleated, with that second from the right containing ingested granulocytes as well as red cells. The cell left of center has less cytoplasm with 5–6 nuclei and numerous ingested red cells. The phages at the left and right have large darkly stained granules of hemosiderin as evidence of previous red cell destruction.

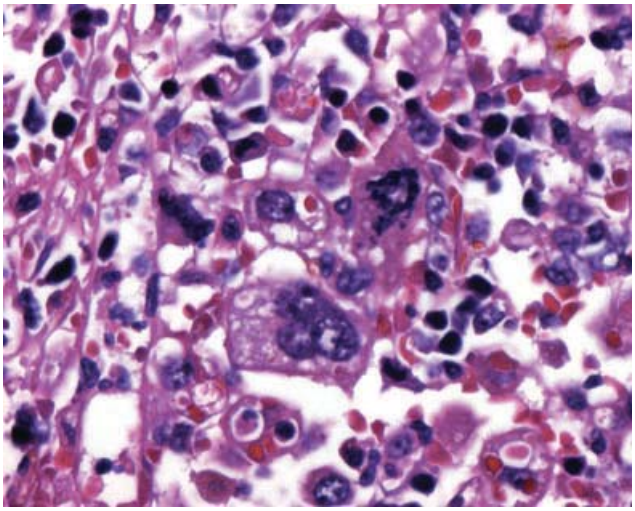

Figure 10.42. Dog: spleen, hemophagocytic histiocytic sarcoma. The large cell in the upper left and right are in metaphase. They are surrounded by neoplastic, often multinucleated, phagocytes that are identified by cytoplasmic vacuolation and both erythrophagocytosis and hemosiderin.

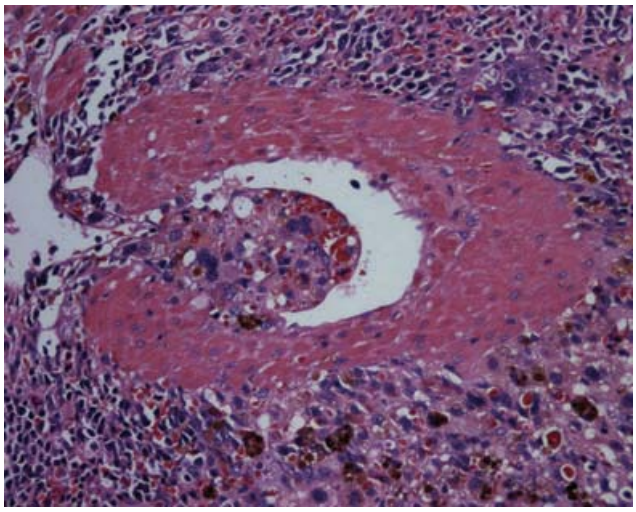

Figure 10.43. Dog: spleen, hemophagocytic histiocytic sarcoma. A large trabecular vein is invaded with a subendothelial colonization of neoplastic cells.

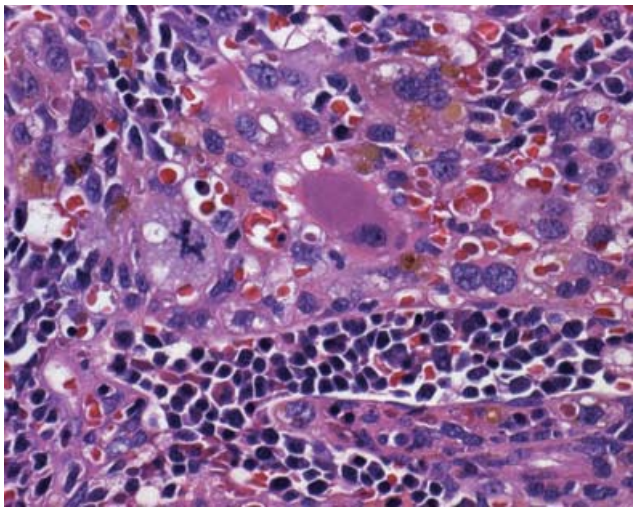

Figure 10.44. Dog: spleen, hemophagocytic histiocytic sarcoma. The interstitial areas of the spleen have been occupied by the neoplastic macrophages (above), one of which is in phased mitosis. There is abundant hemosiderin in the neoplastic cells that are both binucleated and multinucleated. The adjacent sinus below contains primarily erythroid cells that have been displaced from interstitial to open sinus structures.

occupy the splenic sinus interstitial areas with displacement of benign hematopoiesis to dilated vascular channels (Fig. 10.44). In the human cases, hemophagocytosis is seen but not prominent, which would seem to be a clear difference from the form of this neoplasm in animals. In animals, the liver lesions in a cat were focal and solid with expansion of broad front or pushing type of expansion with a light pseudoencapsulation caused by compression of benign supporting tissue at the boundaries. The lesions in liver are more sinusoidal in the dog. The nuclei are round to oval with smooth nuclear contours and vary from 3–8 or more red cells in diameter with hyperchromatic cribriform and branched chromatin patterns and very large, usually single, nucleoli. Binucleation and multinucleation are relatively common with marked anisokaroyosis of individual cells and even within multinucleated cells. The cytoplasm is abundant, relatively evenly centered around the nucleus, deeply amphophilic, and irregularly vacuolated with frequent evidence of phagocytic capability. Mitoses are present in most fields but not with the frequency expected in a lymphoid or histiocytic neoplasm of Langerhans type. The disease in nodes is not well characterized, and it appears to be primarily medullary in early stages with solid sinus filing and compression of the medullary cords; with progression, it becomes regional and locally extensive with destruction of nodal architecture in both dogs and cats. The disease in the marrow is focal and irregularly solid, with irregular sinus dilations as seen in megakaryocytic neoplasms.

Few cases in older literature have had adequate phenotypic characterization, but in one report of a single case in a dog, the neoplastic cells were positively marked with both alpha naphthyl acetate esterase (ANAE) and alpha naphthyl butyrate esterase (ANBE), and negative with chloroacetate esterase (CAE) and Sudan Black-B (SBB). Current identification of HHS in animals is assisted by CD18 staining and specific integrins.

HHS must be differentiated from large cell B- or T-cell lymphoma, anaplastic large cell lymphoma, hepatosplenic γδ T-cell lymphoma, acute monocytic leukemia, and one of the dendritic cell neoplasms. Confirmation of HHS in animals would seem to require assurance of negative reaction with B- or T-cell reagents and myeloperoxidase; and in cytological preparations, assurance of negative with SBB and positive with one of the nonspecific (ANAE or ANBE) esterase stains; and at least multifocal highly avid erythrophagocytosis.

Human Lesions of Significance for Differential Diagnosis

A number of human disorders of histiocytic type that do not appear to have an animal counterpart are considered in the discussion of the histiocytic and dendritic diseases. These conditions are defined here only to signify that there are a range of other well-defined proliferative disorders of the hematopoietic system that are not in the lexicon of animal diseases.

Sinus histiocytosis with massive lymphadenopathy (SHML) is a benign disease of children and young adults that present with huge isolated cervical

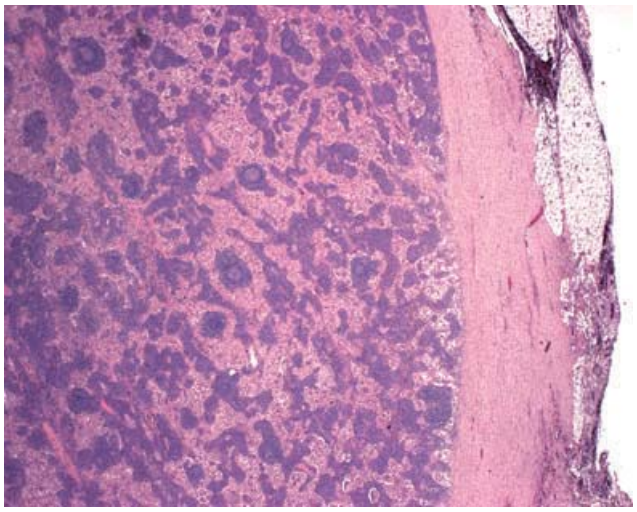

Figure 10.45. Human: lymph node, sinus histiocytosis with massive lymphadenopathy. The node is markedly enlarged with very marked thickening of the node capsule. The peripheral sinus is compressed, with nodal tissue compressed into serpiginous islands surrounded by dilated sinuses crowded with large pale-staining cells. *Slide from Cornell Tutorial.*

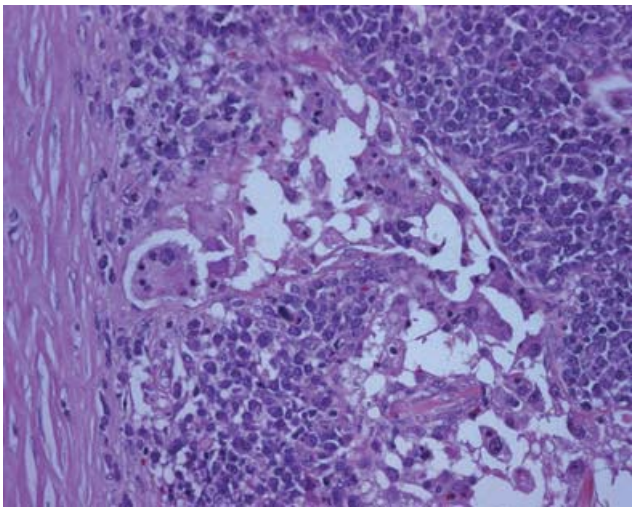

Figure 10.46. Human: lymph node, sinus histiocytosis with massive lymphadenopathy, same case as Figure 10.45. A subcapsular sinus is dilated with large macrophages containing ingested leukocytes, primarily lymphocytes.

lymphadenopathy. Other nodes may be involved, including axillary, inguinal, and mediastinal, accompanied by fever, night sweats, weight loss, malaise, and often joint pain, but no involvement of spleen or liver. The lesions include marked distension of nodal sinuses by huge phagocytic cells that may contain many normal-appearing lymphocytes (Figs. 10.45–10.47). Most cases appear to undergo spontaneous remission.

Infection associated hemophagocytic syndrome (IAHS) is a nonneoplastic proliferation of cytologically benign histiocytes that are avidly erythrophagocytic. The condition was initially called *viral associated hemophagocytic syndrome,* but it has become apparent that a variety of inflammatory conditions can induce this condition including herpesvirus of various types, bacteria, fungi, and Leishmaniasis. There are two main categories of patients with this syndrome, those with no apparent underlying disease and those with immunosuppression. The presentation is of severely ill patients with systemic illness characterized by fever, skin rash, lymphadenopathy, hepatosplenomegaly, and often bilateral, pulmonary infiltrates. There is accompanying pancytopenia and abnormalities in clotting factors with prolonged PT and PTT. The histologic lesions are cortical expansion of nodes due to phagocytic proliferation with ingestion of platelets, red cells, and leukocytes. The disease is of benign cellular proliferation and may be self limiting, but about half of the patients die of organ failure and superinfection because of the cytopenia and immune dysfunction. A morphologically closely related condition called *familial hemophagocytic lymphohistiocytosis* is a rare and fatal disease of children characterized by multiorgan infiltration with lymphocytes and histiocytes accompanied by fever and hepatosplenomegaly. The disease appears to be inherited as an autosomal recessive trait that has no ethnic predilection, and parental consanguinity is often present.

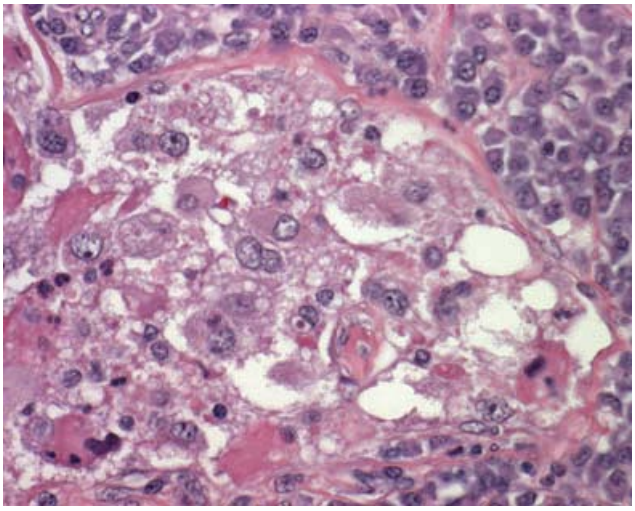

Figure 10.47. Human: lymph node, sinus histiocytosis with massive lymphadenopathy, same case as Figure 10.45. The surviving areas of nodal tissue resemble medullary cords and contain mature plasma cells, with the dilated sinuses containing a syncytium of large macrophages with vacuolated cytoplasm that frequently contain normal-appearing lymphocytes.

REFERENCES

Affolter, V.K., and Moore, P.F. (1999) Canine histiocytic proliferative disease. *15th Proc AAVD/ACVD Mtng* pp. 79–86.

Affolter, V.K., and Moore, P.F. (2000) Canine cutaneous and systemic histiocytosis: Reactive histiocytosis of dermal dendritic cells. *Am J Dermatopathol* 22(1):40–48.

Affolter, V.K., and Moore, P.F. (2002) Localized and disseminated histiocytic sarcoma of dendritic cell origin in dogs. *Vet Pathol* 39:74–83.

Azumi, N., Sheibani, K., Swartz, W.G., et al. (1988) Antigenic phenotype of Langerhans cell histiocytosis: An immunohistochemical study demonstrating the value of LN-2, LN-3 and vimentin. *Hum Pathol* 19:1376–1382.

Bazzocchi, C., Mortarino, M., Comazzi, S., Bandi, C., Franceschi, A., and Genchi, C. (2005) Expression and function of toll-like receptor 2 in canine blood phagocytes. *Vet Immunol and Immunophenotyp* 104:15–19.

Bottomly, K. (1999) T cells and dendritic cells get intimate. *Science* 283:1124–1125.

Carioto, L. (1997) Malignant histiocytosis in a Bernese mountain dog presenting as a mandibular mass. *Can Vet J* 38:105–107.

Cattoretti, G., Villa, A., Vezzoni, P., et al. (1990) Malignant histiocytosis: A phenotypic and genotypic investigation. *Am J Pathol* 136:1009–1019.

Favara, B.E., and Feller, A.C. (with members of the WHO Committee on Histiocytic/Reticulum Cell Proliferations) (1997) Contemporary classification of histiocytic disorders. *Med and Ped Oncol* 29:159–1166.

Foucar, E., Rosai, J., and Dorfman, R.F. (1990) Sinus histiocytosis with massive lymphadenopathy (Rosai-Dorfman disease): Review of the entity. *Sem Diagn Pathol* 7:19–73.

Franchino, C., Reich, C., Distenfeld, A., et al. (1988) A clinicopathologically distinctive primary splenic histiocytic neoplasm: Demonstration of its histiocytic derivation by immunophenotypic and molecular genetic analysis. *Am J Surg Pathol* 12:398–404.

Hayden, D.W., Waters, D.J., Burke, B.A., and Manivel, J.C. (1993) Disseminated malignant histiocytosis in a golden retriever: Clinicopathologic, ultrastructural, and immunohistochemical findings. *Vet Pathol* 30:256–264.

Isaacson, P., Wright, D.H., and Jones, D.B. (1983) Malignant lymphoma of true histiocytic (monocyte-macrophage) origin. *Cancer* 51:80.

Janka, G.E. (1983) Familial hemophagocytic lymphohistiocytosis: Review. *Eur J Pediatr* 140:221–230.

Kamel, O.W., Gocke, C.D., Kell, D.L., et al. (1995) True histiocytic lymphoma: A study of 12 cases based on current definition. *Leuk Lymph* 18:81–86.

Kerlin, R.L., and Hendrick, M.J. (1996) Malignant fibrous histiocytoma and malignant histiocytosis in the dog—Convergent or divergent phenotypic differentiation? *Vet Pathol* 33:713–716.

Lieberman, P.H., Jones, C.R., Steinman, R.M., et al. (1996) Langerhans cell (eosinophilic) granulomatosis: A clinicopathologic study encompassing 50 years. *Am J Surg Pathol* 20:519–552.

Miettinen, M., Fletcher, C.D.M., and Lasota, J. (1993) True histiocytic lymphoma of small intestine: Analysis of two S-100 protein-positive cases with features of interdigitating reticulum cell sarcoma. *Am J Surg Pathol* 100:285–292.

Moore, P.F. (1984) Systemic histiocytosis of Bernese mountain dogs. *Vet Pathol* 21:554–563.

Moore, P.F. (1986) Utilization of cytoplasmic lysozyme immunoreactivity as a histiocytic marker in canine histiocytic disorders. *Vet Pathol* 23:757–762.

Moore, P.F., Affolter, V.K., Olivry, T., and Schrenzel, M.D. (1998) The use of immunological reagents in defining the pathogenesis of canine skin diseases involving proliferation of leukocytes. In Kwochka, K.W., Willemse, T., and von Tscharner, C. (eds.), *Advances in Veterinary Dermatology*. Butterworth Heinemann, Oxford, pp. 77–94.

Ost, A., Nilsson-Ardnor, S., and Henter, J.-I. (1998) Autopsy findings in 27 children with haemophagocytic lymphohistiocytosis. *Histopathol* 32:310–316.

Pace, L.W., Kreeger, J.M., Miller, M.A., Turk, J.R., and Fischer, J.R. (1994) Immunohistochemical staining of feline malignant fibrous histiocytomas. *Vet Pathol* 31:168–172.

Paulli, M., Bergamaschi, G., Tonon, L., et al. (1995) Evidence for a polyclonal nature of the cell infiltrate in sinus histiocytosis with massive lymphadenopathy (Rosai-Dorfman disease), *Brit J Haematol* 91:415–418.

Perez-Ordonez, B., and Rosai, J. (1998) Follicular dendritic cell tumor: Review of the entity. *Sem Diagn Pathol* 15:144–154.

Risdall, R.J., McKenna, R.W., Nesbitt, M.E., et al. (1979) Virus associated hemophagocytic syndrome: A benign histiocytic proliferation distinct from malignant histiocytosis. *Cancer* 44:993–1002.

Scherlie, P.H., Smedes, S.L., Feltz, T., Dougherty, S.A., and Riis, R.C. (1992) Ocular manifestation of systemic histiocytosis in a dog. *JAVMA* 201(8):1229–1232.

Soini, Y., and Miettinen, M. (1990) Immunohistochemistry of markers of histiomonocytic cells in malignant fibrous histiocytomas. A monoclonal antibody study. *Pathol Res Pract* 186:759–767.

Steinman, R.M., and Inaba, K. (1999) Myeloid dendritic cells. *J Leukoc Biol* 66:205–208.

Vos, J.A., Abbondanzo, S.L., Barekman, C.L., Andriko, J.W., Miettinen, M., and Aguilera, N.S. (2005) Histiocytic sarcoma: A study of five cases including the histiocyte marker CD163. *Mod Pathol* 18:693–704.

Walton, R.M., Modiano, J.F., Thrall, M.A., and Wheeler, S.L. (1996) Bone marrow cytological findings in 4 dogs and a cat with hemophagocytic syndrome. *J Vet Internal Med* 10(1):7–14.

Weiss, D.J. (2001) Cytologic evaluation of benign and malignant hemophagocytic disorders in canine bone marrow. *Vet Clin Pathol* 30(1):28–34.

Weiss, D.J. (2002) Flow cytometric evaluation of hemophagocytic disorders in canine bone marrow. *Vet Clin Pathol* 31(1):36.

Weiss, L.M. (2001) Histiocytic and dendritic cell proliferations. In Knowles, D.M. (ed), *Neoplastic Hematopathology*. Lippincott Williams & Wilkins, Philadelphia, pp. 1815–1845.

Wellman, M.L., Davenport, D.J., Morton, D., and Jacobs, R.M. (1985) Malignant histiocytosis in four dogs. *JAVMA* 187(9):919–921.

Wellman, M.L., Krakowka, S., Jacobs, R.M., and Kociba, G.J. (1988) A macrophage-monocyte cell line from a dog with malignant histiocytosis. *In Vitro Cellul & Devel Biol* 24(3):223–229.

Wilson, M.S., Weiss, L.M., Gatter, K.C., Mason, D.Y., Dorfman, R.F., and Warnke, R.A. (1990) Malignant histiocytosis: A reassessment of cases previously reported in 1975 based on paraffin section immunophenotype studies. *Cancer* 66:530–536.

Yu, R.C., Chu, C., Buluwela, L., et al. (1994) Clonal proliferation of Langerhans cells in Langerhans cell histiocytosis. *Lancet* 343:767–768.

Index

Page references followed by f denote figures. References followed by t denote tables.

A
Abnormal localization of immature precursors, 480
Acetic acid, 59
Acetone, 26
Acetylcholine receptors, 88, 90
Acid hemolysis, 106
ACML (atypical chronic myeloid leukemia), 461
Acute erythroid leukemia (M6), 401–411
  erythroid leukemia, 406–411
  erythroleukemia, 401–406
Acute lymphoblastic leukemia (ALL)
  B-cell (B-ALL)
    cell of origin, 135–136
    clinical presentation and features, 124–125, 125f–127f
    definition, 124
    diagnostic criteria, 136
    differential diagnosis, 136
    epidemiology, 124
    evaluation of treated animals, 136
    immunologic features, 134–135
    incidence, 124
    pathologic features
      blood, 128, 128f–130f
      bone marrow, 130–131, 131f–132f
      liver, 134, 135f
      lymph node, 131, 133–134, 133f–134f
      spleen, 134, 134f
    staging, 136
    transformation and progression, 136
    treatment and survival, 136
  Burkitt's lymphoma distinguished from, 141
  L1 type, 120
  L2 type, 120
  T-cell (T-ALL)
    cell of origin, 284
    clinical presentation and features, 275
    cytogenetic and molecular features, 283–284
    definition, 275
    diagnostic criteria, 284–285
    epidemiology and features, 275
    evaluation of the treated animal, 285
    immunologic features, 283
    pathologic features, 275–283
      blood, 275–277, 276f–277f
      bone marrow, 277–278, 277f–278f
      other organs, 282
      spleen, 282, 282f
    staging, 285
    transformation and progression, 285
Acute lymphoid leukemia
  neoplastic cell colonization of bone marrow, 101
Acute monoblastic leukemia (M5A), 395–399, 396f–398f
  clinical presentation and features, 396
  definition, 395–396
  diagnostic criteria, 398
  differential diagnosis, 398–399
  epidemiology and incidence, 396
  pathologic features, 396–398, 396f–398f
Acute monocytic leukemia (M5B), 399–400, 399f–400f
  clinical presentation and features, 399
  definition, 395–396, 399
  differential diagnosis, 400
  epidemiology and incidence, 399
  pathologic features, 399–400
Acute myeloid leukemia (AML), 367–423
  aCML progression to, 461
  acute lymphoblastic leukemia (ALL) compared, 136
  granulocytic sarcoma, 419–423, 420f–423f
  M0 (minimally differentiated) and M1 (without maturation), 374–381
    cell of origin, 379
    clinical presentation and features, 374
    cytogenetic and molecular features, 379
    definition, 374
    diagnostic criteria, 380–381
    differential diagnosis, 381
    epidemiology and incidence, 374
    evaluation of the treated animal, 381
    pathologic features, 374–379, 374f–380f
      blood, 374–375, 374f–375f
      bone marrow, 375–377, 376f–377f, 381f
      lymph node, 377–378, 377f–378f
      other organs, 379, 380f
      spleen, 378–379, 378f–379f
    staging, 381
    treatment and survival, 381
  M2 (AML with maturation), 382–388
    clinical presentation and features, 383
    definition, 382
    diagnostic criteria, 387–388, 388f

Acute myeloid leukemia (AML) (*cont.*)
differential diagnosis, 388
epidemiology and incidence, 383
pathologic features
blood, 383–384, 383f–384f
bone marrow, 384–385, 384f–386f, 388f
liver, 386, 387f
lymph nodes, 386, 387f–388f
spleen, 385–386, 386f–387f
treatment and survival, 388
M3 (acute promyelocytic leukemia), 389–390, 390f–391f
M4 (acute myelomonocytic leukemia), 391–393, 392f–395f
M5A (acute monoblastic leukemia), 395–399, 396f–398f
clinical presentation and features, 396
definition, 395–396
diagnostic criteria, 398
differential diagnosis, 398–399
epidemiology and incidence, 396
pathologic features, 396–398, 396f–398f
M5B (acute monocytic leukemia), 399–400, 399f–400f
clinical presentation and features, 399
definition, 395–396, 399
differential diagnosis, 400
epidemiology and incidence, 399
pathologic features, 399–400
M6A (erythroleukemia)
classification, 401–402
clinical presentation and feature, 402
definition, 402
epidemiology and incidence, 402
pathologic features, 402–406, 402f–406f
M6B (pure erythroid leukemia), 406–411
blood, 406–407, 406f–408f
bone marrow, 407–409, 408f–410f
classification, 401–402
definition, 402
epidemiology and incidence, 402
liver, 409–410, 410f
spleen, 410, 410f–411f
M7 (acute megakaryoblastic leukemia), 412–416, 412f–416f
clinical presentation and features, 412
definition, 412
epidemiology and incidence, 412
pathologic features, 412–416, 412f–416f
M8 (acute panmyelosis with myelofibrosis), 417–418, 417f–419f
myelodysplastic syndromes compared, 473, 476–478, 480, 483–484, 486–488
myeloproliferative diseases, 367–368, 368t, 369f–373f, 371–372
bone marrow changes in subtypes, 368t
classification, 367–368, 368t, 371–372
neoplastic cell colonization of bone marrow, 101
refractory anemia progression to, 477, 478
underdiagnosis of, 120
Acute myelomonocytic leukemia (M4), 391–393, 392f–395f
Acute panmyelosis, 454
Acute panmyelosis with myelofibrosis (M8), 417–418, 417f–419f
Acute promyelocytic leukemia (APL), 389–390, 390f–391f
Adult T-cell lymphoma/leukemia, 346–350, 348f–354f
AE1-AE3 anticytokeratin cocktail, 43
African swine fever, 35
Aggressive NK-cell leukemia, 309–310, 309f
Agnogenic myeloid metaplasia, 425, 434, 449
AIDS
bone marrow dysplastic changes in HIV infection, 486
Hodgkin's lymphoma and, 499
AILD (angioimmunoblastic lymphadenopathy with dysproteinemia), 312, 497
ALCL (anaplastic large cell lymphoma), 240, 257, 339
ALCL-B (anaplastic large cell lymphoma) variant, 256, 256f–257f, 257
Aleutian mink, 111, 112
ALK. *See* Anaplastic lymphoma kinase (ALK) protein
Alkylating agents
bone marrow effects, 116
for lymphoplasmacytic lymphoma (LPL), 214
ALL. *See* Acute lymphoblastic leukemia (ALL)
Alltrans-retinoic acid (ATRA), 337, 389
ALPDs (atypical lymphoproliferative disorders), 119
Alpha naphthyl acetate esterase (ANAE), 398f, 433, 521
Alpha naphthyl butyrate esterase (ANBE), 521
Alpha naphthyl esterase, 373f
American Registry of Pathology, 3
AML. *See* Acute myeloid leukemia (AML)
Amyloidosis
in Chédiak Higashi anomaly, 112
in plasma cell dyscrasias, 202
spleen, 64
ANAE (alpha naphthyl acetate esterase), 398f, 433, 521
Anaplastic large cell lymphoma (ALCL), 240, 257, 339
Anaplastic large cell lymphoma (ALCL-B) variant, 256, 256f–257f, 257
Anaplastic lymphoma kinase (ALK) protein, 73, 339–341
ANBE (alpha naphthyl butyrate esterase), 521
Anemia
in acute lymphoblastic leukemia (ALL), 277
in acute megakaryoblastic leukemia, 412
in acute monoblastic leukemia M5A, 396
in acute monocytic leukemia, 399
in acute myeloid leukemia (AML), 374, 383
in acute myelomonocytic leukemia, 392
in acute panmyelosis, 417
in acute promyelocytic leukemia (APL), 389
in atypical chronic myeloid leukemia, 461
in chronic idiopathic myelofibrosis, 450
in chronic lymphocytic leukemia (CLL), 287
in chronic myeloid leukemia, 426, 428, 430
in erythroid leukemia, 402–403
in essential thrombocythemia (ET), 446
in hepatosplenic lymphoma, 316
in juvenile myelomonocytic leukemia (jMML), 467
in NK-cell leukemia, 310
in prolymphocytic leukemia (PLL), 302
pyruvate kinase deficiency, 109, 109f–110f
refractory in myelodysplastic syndromes, 475–480, 475f–480f

Anemia (*cont.*)
sickle cell, 108, 108f
in small lymphocytic leukemia (SLL), 150
thalassemia, 108–109, 109f
Angiocentric lymphoma, 311
Angioendotheliomatosis, 358
Angioimmunoblastic lymphoma with dysproteinemia (AILD), 312, 497
Angioimmunoblastic T-cell lymphoma (AILT), 312–315, 312f–315f
Angioma, 61, 61f
Angiotropic lymphoma, 358f–360f
Anisocytosis, in erythroid leukemia, 407
Anisokaryosis
in lymphoplasmacytic lymphoma (LPL), 208f
in mast cell tumors, 457, 458f–459f
in myeloma, 203
in plasmacytoma, 201, 203
Anthrax, 36, 37f
Anti-CD20
for lymphoplasmacytic lymphoma (LPL), 214
for mantle cell lymphoma (MCL), 238
Anticytokeratin, 43
Antigen presenting cells (APCs)
dendritic cell proliferations, 22, 505–506, 515
MHC restriction, 80–81
T-cell activation, 505–506
APL. *See* Acute promyelocytic leukemia (APL)
Apoptosis
B-cell, 23
in diffuse large B-cell lymphoma (DLBCL), 240
in myeloma, 206
in thymus, 79, 80, 81, 85–86, 85f
Arsenic
dyserythropoiesis from, 486, 486f
myelodysplastic changes from, 115
Asplenia, 62
ATRA. *See* alltrans-retinoic acid (ATRA)
Atypical Burkitt's lymphoma, 140
Atypical chronic myeloid leukemia (aCML), 461
Atypical lymphoproliferative disorders (ALPDs), 119
Auer rods, 371, 478, 480, 481
Autoimmune hyperplasia of the thymus gland, 88–90, 88f–90f
Autoimmune polyendocrinopathy, 80
Autoimmune regulator, 80

B

B5 fixative, 117, 138, 494
Bacterial infection, lymphadenitis due to, 36–38, 36f–38f
B-ALL. *See* B-cell acute lymphoblastic leukemia (B-ALL)
Basophil leukemia, 454–456, 455f–456f
Basophils
in chronic eosinophilic leukemia, 439f
in chronic idiopathic myelofibrosis, 450–451
in chronic myeloid leukemia, 426, 426f, 428, 430
in chronic neutrophilic leukemia, 435
in polycythemic vera, 441f
BASP, 213
B cell
activation, 23
function, 23–24
immunodeficiency, 81
proliferation
in myasthenia gravis, 88–90
thymic inflammation, 91
RS (Reed-Sternberg) cells, 491
splenic, 51
thymic, 79, 79f
B-cell acute lymphoblastic leukemia (B-ALL)
cell of origin, 135–136
clinical presentation and features, 124–125, 125f–127f
definition, 124
diagnostic criteria, 136
differential diagnosis, 136
epidemiology, 124
evaluation of treated animals, 136
immunologic features, 134–135
incidence, 124
pathologic features
blood, 128, 128f–130f
bone marrow, 130–131, 131f–132f
liver, 134, 135f
lymph node, 131, 133–134, 133f–134f
spleen, 134, 134f
staging, 136
transformation and progression, 136
treatment and survival, 136
B-cell chronic lymphocytic leukemia (B-CLL), 142–160
cell of origin, 157
clinical presentation and features, 142–143
cytogenic and molecular features, 156–157
definition, 142
diagnostic criteria, 157
differential diagnosis, 157
epidemiology, 142
evaluation of treated animal, 160
immunologic features, 155–156
incidence, 142
pathologic features, 143–155, 143f–156f
blood, 143–149, 143f–149f
bone marrow, 143f–144f, 149–150, 150f–151f
lymph node, 152, 152f
other organs, 155, 156f
spleen, 152–153, 154f–155f, 155
staging, 157
transformation and progression, 157–158, 158f–160f, 160
treatment and survival, 160
B-cell lymphoblastic lymphoma (B-LBL)
cell of origin, 135–136
clinical presentation and features, 125, 127
definition, 124
diagnostic criteria, 136
differential diagnosis, 136
pathologic features
lymph node, 131, 133–134, 133f, 134f
spleen, 134
staging, 136

B-cell neoplasms
B-cell chronic lymphocytic leukemia (B-CLL)/small lymphocytic lymphoma (SLL), 142–160
cell of origin, 157
clinical presentation and features, 142–143
cytogenic and molecular features, 156–157
definition, 142
diagnostic criteria, 157
differential diagnosis, 157
epidemiology, 142
evaluation of treated animal, 160
immunologic features, 155–156
incidence, 142
pathologic features, 143–155, 143f–156f
staging, 157
transformation and progression, 157–158, 158f–160f, 160
treatment and survival, 160
diffuse large B-cell lymphoma (DLBCL), 238–258
cell of origin, 255
clinical presentation and features, 239
cytogenetic and molecular features, 255
definition, 238
diagnostic criteria, 256, 256f–257f
differential diagnosis, 257, 257f
epidemiology, 238–239
evaluation of the treated animal, 258
immunologic features, 254–255
pathologic features, 239–254, 240f–256f
transformation and progression, 257–258
treatment and survival, 258
follicular lymphoma (FL), 215–226
cell of origin, 225
clinical presentation and features, 215
cytogenetic and molecular features, 224–225
definition, 215
diagnostic criteria, 225
differential diagnosis, 225
epidemiology and incidence, 215
evaluation of the treated animal, 225–226
immunologic features, 224
pathologic features, 215–224, 217f–224f
staging, 225
transformation and progression, 225
treatment and survival, 226
hairy cell leukemia, 164, 165f–166f
lymphoplasmacytic lymphoma (LPL), 207–214
cell of origin, 213
clinical presentation and features, 207
cytogenetic and molecular features, 213
definition, 207
diagnostic criteria, 213–214
differential diagnosis, 214
epidemiology and incidence, 207
evaluation of the treated animal, 214
immunologic features, 212
pathologic features, 207–212, 208f–213f
staging, 214
transformation and progression, 214
treatment and survival, 214
lymphoproliferative diseases, 119–124
acute lymphoblastic leukemia (ALL) L1 type, 120, 120f, 121
acute lymphoblastic leukemia (ALL) L2 type, 120, 121, 121f
acute lymphoblastic leukemia (ALL) L3 type, 120–121, 121f–122f
classification algorithms, 122t, 123t
definition, 119
FAB (French-American-British) classification system, 120
leukemia and lymphoma presentations, 119
MALT (mucosal associated lymphoid tissue) lymphoma, 168, 171, 177, 178f, 180, 182, 182f–183f, 185, 187f, 188
mantle cell lymphoma (MCL), 164, 166f–167f, 227–238
cell of origin, 236
clinical presentation and features, 227–230
cytogenetic and molecular features, 235–236
definition, 227
diagnostic criteria, 236
differential diagnosis, 236, 237f
epidemiology and incidence, 227
evaluation of the treated animal, 237
immunologic features, 230–234, 230f–235f, 234–235, 236f
pathologic features, 230–234, 230f–235f
staging, 236–237
transformation and progression, 237
treatment and survival, 237–238
marginal zone lymphoma (MZL), 164, 167f, 168–188, 168f–188f
cell of origin, 181–182
clinical presentation and features, 169–170
cytogenetic and molecular feature, 180–181
definition, 168
diagnostic criteria, 183–184
differential diagnosis, 184–185
epidemiology and incidence, 168–169
evaluation of the treated animal, 187–188
immunologic features, 178, 180
pathologic features, 170–178, 171f–181f
staging, 185–186
transformation and progression, 187
treatment and survival, 188
mature (peripheral neoplasms), 142–272
plasmacytoma and melanoma, 189–206
cell of origin, 202
clinical presentation and features, 192, 192f–198f, 197–198
cytogenetic and molecular features, 202
definition, 189–191
diagnostic criteria, 202–204
differential diagnosis, 204
epidemiology and incidence, 191–192
evaluation of the treated animal, 206
immunologic features, 202
pathologic features, 198–202
staging, 205–206

B-cell neoplasms (*cont.*)
transformation and progression, 206
treatment and survival, 206
precursor B-cell neoplasms, 124–141
B-cell acute lymphoblastic leukemia (B-ALL) and B-cell lymphoblastic lymphoma (B-LBL), 124–136
cell of origin, 135–136
clinical presentation and features, 124–127, 125f–127f
definition, 124
diagnostic criteria, 136
differential diagnosis, 136
epidemiology, 124
evaluation of treated animal, 136
immunologic features, 134–135
incidence, 124
pathological features, 128–134, 128f–135f
staging, 136
transformation and progression, 136
treatment and survival, 136
Burkitt's-like lymphoma, 140–141
differential diagnosis, 141
overview, 140
pathologic feature, 140–141, 140f–141f
Burkitt's lymphoma (BKL), 137–140
atypical, 140–141
clinical presentation and features, 138
definition, 137–138
pathologic features, 138–140, 138f–139f
prolymphocytic leukemia (PLL), 155f, 156, 157–158, 158f–159f
cell of origins, 164
clinical presentation and features, 161
cytogenetic and molecular features, 164
definition, 161
diagnostic criteria, 164
differential diagnosis, 164
epidemiology and incidence, 161
immunologic features, 163
pathologic features, 162–163
blood, 162, 162f
bone marrow, 162, 162f–163f
lymph nodes, 162–163, 163f
other organs, 163
spleen, 163, 164f
staging, 164, 168
transformation and progression, 168
treatment and survival, 168
REAL classification, 6t
T-cell rich large B-cell lymphoma (TCRBCL)/lymphomatoid granulomatosis (LYG), 260–272
cell of origin, 271
clinical presentation and features, 262–263, 262f
cytogenetic and molecular features, 271
definition, 260–261
diagnostic criteria, 271
differential diagnosis, 272
epidemiology and incidence, 261–262
evaluation of the treated animal, 272
immunologic features, 270–271, 271f
pathologic features, 263–269, 263f–270f
staging, 272
transformation and progression, 272
treatment and survival, 272
Bcl-2 protein/gene, 23, 140, 206, 224–225, 258, 271, 287
Bcl-6 protein, 23, 140
BCR-ABL fusion gene, 425, 426, 428
Bence-Jones proteinuria, 199
B2 integrin, 515
Beta$_2$-microglobulin, 205
Bilroth, T., 3
Binet system, 157
Birds, hematopoiesis in, 100
BKL. *See* Burkitt's lymphoma (BKL)
BLA36, 135f, 270
Black rhinoceros, congenital anemia in, 105–106, 105f–106f, 486, 487f
Blastic NK-cell lymphoma, 310–311
Blastomycosis, 38
Blood
acute lymphoblastic leukemia (ALL)
B-cell (B-ALL), 128, 128f–130f
T-cell (T-ALL), 275–277, 276f–277f
acute myeloid leukemia (AML)
M0 (minimally differentiated) and M1 (without maturation), 374–375, 374f–375f
M2 (AML with maturation), 383–384, 383f–384f
M6B (pure erythroid leukemia), 406–407, 406f–408f
cat
acute lymphoblastic leukemia (ALL), 121f, 129f, 276f
acute myeloid leukemia (AML), 369f, 370f–371f, 374f–375f
chronic lymphocytic leukemia (CLL), 130f, 144f, 145f, 288f
chronic myelogenous leukemia of eosinophil type, 437f–438f
chronic myeloid leukemia, 430f–432f
erythroleukemia, 402f–403f
hypereosinophilic syndrome (HES), 438f
pure erythroid leukemia (erythremic myelosis), 406f–408f
cattle
acute lymphoblastic leukemia (ALL) L3 type, 122f, 125f, 126f
acute monoblastic leukemia, 396f
erythroid leukemia, 407f, 408f
prolymphocytic leukemia (PLL), 162f
small lymphocytic lymphoma, 149f
chronic lymphocytic leukemia (CLL), 143–149, 143f–149f, 287–288, 288f, 291f
chronic myeloid leukemia (CML), 430, 430f–432f, 432
cord blood, 99
diffuse large B-cell lymphoma (DLBCL), 239
dog
acute lymphoblastic leukemia (ALL), 276f–277f
acute lymphoblastic leukemia (ALL), L1 type, 120f, 128f, 130f
acute lymphoblastic leukemia (ALL), L2 type, 121f
acute lymphoblastic leukemia (ALL), L3 type, 129f

Blood (*cont.*)
acute monoblastic leukemia, 396f–397f, 397f
acute monocytic leukemia, 399f
acute myeloid leukemia (AML) M2, 383f–384f
chronic lymphocytic leukemia (CLL), 143f, 145f, 151f, 288f, 291f
chronic lymphocytic leukemia (CLL), LGL type, 306f
chronic myeloid leukemia of basophil type, 455f
chronic myelomonocytic leukemia (CMML), 463f–464f
essential thrombocythemia (ET), 444f–446f
megakaryoblastic leukemia, 412f–413f
myelofibrosis, 450f
myeloma, 199f
polycythemic vera (PV), 441f
postsplenectomy, 55f, 57f
prolymphocytic leukemia (PLL), 303f
small lymphocytic lymphoma, 146f
follicular lymphoma (FL), 215–216
horse
acute lymphoblastic leukemia (ALL) L3 type, 127f
Sézary syndrome, 332f
human
acute lymphoblastic leukemia (ALL), 120f
aggressive NK-cell leukemia, 309f
beta thalassemia, 109f
chronic lymphocytic leukemia (CLL), 159f
chronic myeloid leukemia (CML), 426f–428f
follicular lymphoma, 215f, 217f
hairy cell leukemia, 165f
prolymphocytic leukemia (PLL), 158f, 162f
Sézary syndrome, 338f
spherocytosis, hereditary, 109f
lymphoplasmacytic lymphoma (LPL), 207–208
mantle cell lymphoma (MCL), 230
marginal zone lymphoma (MZL), 170–171
melanoma, 198, 199f
plasmacytoma, 198
polycythemia vera (PV), 441–442, 441f
prolymphocytic leukemia (PLL), 162, 162f
pure erythroid leukemia, 406–407, 406f–408f
rat
large granulocytic leukemia, 308f
small lymphocytic lymphoma (SLL), 145–146, 145f–149f
T-cell rich large B-cell lymphoma (TCRLBCL), 263
Blood islands, yolk sac, 99
BLV. *See* Bovine leukemia virus (BLV)
BMS-354825, 425
Bone marrow
acute lymphoblastic leukemia (ALL), 120f, 121f, 123f, 127f–129f, 130–131, 131f–132f, 136, 277–278, 277f–278f
acute megakaryoblastic leukemia, 412–414, 413f–415f
acute monoblastic leukemia, 395, 396–398, 397f
acute monocytic leukemia, 399–400, 400f
acute myeloid leukemia (AML)
M0/M1, 375–377, 376f–377f, 381f
M2, 384–385, 384f–386f, 388f
acute myelomonocytic leukemia M4, 391–393, 392f–395f
acute panmyelosis, 417–418, 417f–418f
acute promyelocytic leukemia M3, 389–390, 390f–391f
aggressive NK-cell leukemia, 309f, 310
aplastic, 101, 101f–102f, 116
basophil leukemia, 455–456, 455f–456f
Burkitt's lymphoma, 138
cat
acute lymphoblastic leukemia (ALL), 131f, 132f, 354f
acute myeloid leukemia (AML)
M0, 369f
M0/M1, 376f, 381f
M3, 390f–391f
type III myeloblasts, 370f
type II myeloblasts, 369f–370f
acute myelomonocytic leukemia, 392f, 393f–395f
anemia of chronic disease, 151f
aplastic, 102f
chronic lymphocytic leukemia (CLL), 151f, 290f
chronic myeloid leukemia of eosinophil type, 438f–439f
erythroid leukemia, 408f–409f
erythroleukemia, 403f–404f
follicular lymphoma (FL), 224f
hypereosinophilic syndrome (HES), 439f
lymphoplasmacytic lymphoma (LPL), 209f–210f
promyelocytic leukemia, 371f
refractory anemia with excess blasts, 478f–480f
refractory cytopenia, 482f–483f
cattle
acute lymphoblastic leukemia (ALL), 122f, 132f
acute monocytic leukemia, 398f
erythroid leukemia, 409f–410f
cell types, number of, 105
chronic idiopathic myelofibrosis, 449, 450–454, 450f–452f
chronic lymphocytic leukemia (CLL), 143f–144f, 149–150, 150f–151f, 159f, 288–289, 290f
chronic myeloid leukemia, 426f–427f, 433, 433f, 435, 435f–436f
degenerative diseases
nutritional diseases, 114–115, 115f
toxic and drug-induced changes, 115–116
developmental diseases, 105–114, 105f–111f
Chédiak Higashi anomaly, 110–112, 111f
congenital, 105–106, 105f–106f
black rhinoceros congenital anemia, 105–106, 105f–106f
Diamond Blank-fan anemia, 105
Fanconi anemia, 106
Reticular Dysgenesis, 105
cyclic hematopoiesis, 106–107, 107f
hemoglobinopathies, 108–109, 109f–110f
hereditary anemias, 108–109, 109f–110f
leukocyte adhesion deficiency (LAD), 112–113
lysosomal storage diseases, 113–114
Maroteaux-Lamy Syndrome, 114
mucopolysaccharidoses (MPS), 113, 114
Niemann-Picck disease (NPD), 114
Pelger-Huët anomaly, 110
differential cell counts, 104
diffuse large B-cell lymphoma (DLBCL), 239–240, 240f, 257f

Bone marrow (*cont.*)
dog
acute lymphoblastic leukemia (ALL), 128f, 132f, 277f–278f
acute monocytic leukemia, 400f
acute myeloid leukemia (AML), 371f–372f, 376f–377f, 384f–386f, 388f
acute myelomonocytic leukemia, 372f–373f
anaplastic large cell lymphoma, 257f
aplastic, 101f
chronic lymphocytic leukemia (CLL), 144f, 150f–151f, 290f
chronic myeloid leukemia, 433, 433f
of basophil type, 455f–456f
chronic myelomonocytic leukemia (CMML), 464f, 465f
diffuse large B-cell lymphoma (DLBCL), 240f
erythroid hyperplasia due to immune mediated hemolytic anemia, 103f
essential thrombocythemia (ET), 446f
grey collie syndrome, 107f
LGL (large granular lymphocytic) neoplasia, 308f
marginal zone lymphoma, 172f
megakaryoblastic leukemia, 413f–415f
myelodysplasia, 484f–486f
myelofibrosis, 452f
myeloid hyperplasia associated with pyometra, 104f
myeloma, 190f–191f, 197f–198f
refractory anemia
with excess blasts, 480f
of myelodysplastic syndrome, 475f–476f
small lymphocytic leukemia (SLL), 146f
embryology, 98–102, 98f–102f
erythroid leukemia, 407–409, 408f–410f
erythroleukemia, 402–404, 403f–404f
essential thrombocythemia (ET), 443, 443f–444f, 445–446, 446f
failure, 119
follicular lymphoma (FL), 216–217, 217f–218f, 224f
function, 103–105, 103f–104f
gross anatomy, 99–100
hairy cell leukemia, 165f
horse
acute lymphoblastic leukemia (ALL), 127f, 131f
biopsy, 117
human
acute lymphoblastic leukemia (ALL), 121f–122f, 129f–130f, 276f
acute panmyelosis with myelofibrosis, 417F–418F
aggressive NK-cell leukemia, 309f
arsenic poisoning, 486f
chronic idiopathic myelofibrosis, 450f–451f
chronic lymphocytic leukemia (CLL), 159f
chronic myeloid leukemia (CML), 427f
essential thrombocytopenia, 433f–434f
follicular lymphoma, 217f, 218f
hairy cell leukemia, 165f
myeloma, 191f
precursor cell leukemia lymphoma, 283
precursor T-cell leukemia, 276f
prolymphocytic leukemia (PLL), 158f, 162f–163f
sideroblastic anemia, 477f
lymphoplasmacytic lymphoma (LPL), 208, 209f
macaque
hematopoiesis in, 101f
starvation, 115
mantle cell lymphoma (MCL), 230
marginal zone lymphoma, 171, 172f
microanatomy, 100–101
mouse
chronic myeloid leukemia, 435f–436f
development, 98, 98f
myelodysplasia, 487f
myelofibrosis, 419f
myeloma, 190f–191f, 197f–198f, 198–199
prolymphocytic leukemia (PLL), 158f, 162, 162f–163f
small lymphocytic lymphoma (SLL), 149, 150
T-cell rich large B-cell lymphoma (TCRLBCL), 263
Bone marrow biopsy
for Hodgkin's lymphoma, 499
preparation, 117
technical aspects, 117
Bone marrow transplants, 99
Bovine leukemia virus (BLV), 135, 346–347, 349–350
Bovine virus diarrhea (BVD), 34, 35f, 85f
Bracken fern, bone marrow effects, 116
Brain
angiotropic T-cell lymphoma, 359f
intravascular B-cell lymphoma, 247f–248f
plasmablastic lymphoma, 247f
British National Lymphoma Investigation Classification, 260
Burkitt's-like lymphoma, 140–141
differential diagnosis, 141
overview, 140
pathologic feature, 140–141, 140f–141f
Burkitt's lymphoma (BKL), 137–140
atypical, 140–141
clinical presentation and features, 138
definition, 137–138
lymphoblastic lymphoma distinguished from, 284–285
pathologic features, 138–140, 138f–139f
Butler, J., 4
Butyl acetate esterase, 465, 506
BVD. *See* Bovine virus diarrhea (BVD)

C

CAE. *See* Chloroacetate esterase (CAE)
Calmodulin, 449
Caloric restriction, 84
Canine cutaneous histiocytoma (CCH), 507–510, 507f–510f
Canine distemper virus, 97
Canine granulocytopathy syndrome, 113
Carcinoma, splenic metastatic, 76–77
Carpenter, Jim, 322
Carter, R. F., 248
Caseous lymphadenitis, 38
Castleman lymphadenopathy, 33–34, 34f, 63

Cat
acute lymphoblastic leukemia (ALL)
B-cell (B-ALL), 124, 128, 129f, 131, 131f, 132f, 135
T-cell (T-ALL), 275–276, 276f
acute myeloid leukemia (AML)
M0 (AML minimally differentiated) and M1 (AML without maturation), 374, 374f–381f
M2 (AML with maturation), 383
M3 (acute promyelocytic leukemia), 389, 390f–391f
M4 (acute myelomonocytic leukemia), 392, 392f–395f
M6A (erythroleukemia), 401–402, 402f–406f
M6B (pure erythroid leukemia), 402, 406, 406f–411f
M7 (acute megakaryoblastic leukemia), 412
type III myeloblasts, 370f–371f
adult T-cell lymphoma/leukemia, 346–348, 348f–349f, 353f–354f
anaplastic large cell lymphoma, 340f, 341
angioimmunoblastic T-cell lymphoma (AILT), 314
basophil leukemia, 454
blood
acute lymphoblastic leukemia (ALL), 121f, 129f, 276f
acute myeloid leukemia, 369f
acute myeloid leukemia (AML), 370f–371f, 374f–375f
chronic lymphocytic leukemia (CLL), 130f, 144f, 145f, 288f
chronic myelogenous leukemia of eosinophil type, 437f–438f
chronic myeloid leukemia, 430f–432f
erythroleukemia, 402f–403f
hypereosinophilic syndrome (HES), 438f
pure erythroid leukemia (erythremic myelosis), 406f–408f
bone marrow
acute lymphoblastic leukemia (ALL), 131f, 132f, 354f
acute myeloid leukemia (AML)
M0, 369f
M0/M1, 376f, 381f
M3, 390f–391f
type III myeloblasts, 370f
type II myeloblasts, 369f–370f
acute myelomonocytic leukemia, 392f, 393f–395f
anemia of chronic disease, 151f
aplastic, 102f
chronic lymphocytic leukemia (CLL), 151f, 290f
chronic myeloid leukemia of eosinophil type, 438f–439f
erythroid leukemia, 408f–409f
erythroleukemia, 403f–404f
follicular lymphoma (FL), 224f
hypereosinophilic syndrome (HES), 439f
lymphoplasmacytic lymphoma (LPL), 209f–210f
promyelocytic leukemia, 371f
refractory anemia with excess blasts, 478f–480f
refractory cytopenia, 482f–483f
bone marrow biopsy, 117
cervical cyst, 81–82f
Chédiak Higashi trait, 111f
chronic eosinophilic leukemia (CEL), 436–438, 437f–439f
chronic idiopathic myelofibrosis, 449, 452
chronic lymphocytic leukemia (CLL), 130f, 142, 144, 144f–145f, 151f–152f, 152, 156f, 287–288, 288f, 290f
chronic myeloid leukemia, 430, 430f–432f, 432
chronic myelomonocytic leukemia (CMML), 462
cryptococcosis, 39f
diffuse large B-cell lymphoma (DLBCL), 238–239, 246, 248, 250–251, 253f–257f, 254–255
duodenum, epitheliotropic infiltration, 322f
enteropathy-type T-cell lymphoma, 319, 320f–323f
essential thrombocythemia (ET), 443
feline immunodeficiency virus (FIV), 91, 93
feline leukemia virus (FeLV), 69, 124, 346, 347, 401–402, 436, 437, 452
feline panleukopenia virus, 86, 87f
follicular lymphoma (FL), 215, 220f, 222f, 224f
granulocytic sarcoma, 419, 420f–423f
hemoglobin "C," 109
hemophagocytic histiocytic sarcoma (HHS), 518, 519
hepatosplenic lymphoma, 316f–317f
histiocytic sarcoma, 506
hypereosinophilic syndrome (HES), 436–438, 438f–439f
ileum
granulocytic sarcoma (GS), 421f
lymphoma, 168f–169f
intestinal adenocarcinoma, 44f
intravascular large T-cell lymphoma, 356f
jejunum
granulocytic sarcoma (GS), 422f–423f
kidney
large cell lymphoma, 255f
large granular lymphocytic lymphoma, 305f
lymphoplasmacytic lymphoma (LPL), 213f
large granulated lymphocytic (LGL) neoplasia, 304–305, 305f, 307
liver
acute lymphoblastic leukemia (ALL) L1, 156f
acute myeloid leukemia (AML) (M0/M1), 380f
chronic lymphocytic leukemia (CLL), 145f, 156f, 288f, 293f
erythroid leukemia, 410f
erythroleukemia, 405f–406f
granulocytic sarcoma (GS), 422f
large cell lymphoma, 254f–255f, 353f
lymphoma, 348f
lymphoplasmacytic lymphoma (LPL), 213f
mantle cell lymphoma (MCL), 235f
lung
granulocytic sarcoma (GS), 420f–421f
pneumonia due to pancytopenia of refractory anemia, 480f
lymph node
acute myeloid leukemia (AML), 19f, 377f–378f
anaplastic large cell lymphoma, 256f–257f, 340
atrophy, 11f
capsule and peripheral sinus, 11f
chronic lymphocytic leukemia (CLL), 152f, 291f
cryptococcosis, 39f
diffuse large B-cell lymphoma (DLBCL), 253f

Cat (*cont.*)
erythroleukemia, 406f
follicular hyperplasia, 18f, 31f, 32f
follicular lymphoma (FL), 220f, 222f
follicular polarity, 14f
granulocytic sarcoma (GS), 421f–422f
intestinal adenocarcinoma, 44f–45f
large granular lymphocytic lymphoma, 305f
lymphoblastic lymphoma, 353f
mammary adenocarcinoma, 44f
mantle cell cuff, 15f
panleukopenia virus infection, 35f–36f
paracortex, 12f, 31f, 32f
sclerosis, 12f
T-cell rich large B-cell lymphoma (TCRLBCL), 264f–265f, 268f, 271f, 494f
lymph node biopsy, 24–25, 27
lymphoblastic lymphoma (LBL), 275, 283
lymphoplasmacytic lymphoma (LPL), 207, 209f–210f, 213f
mammary adenocarcinoma, 44f
mantle cell lymphoma (MCL), 227, 231, 235f
marginal zone lymphoma (MZL), 168f–169f, 173, 175f, 176, 177f, 180f–181f
mast cell tumor (MCT), 456, 457f
melanoma, 192f, 198, 202, 206
mycosis fungoides, 331f, 332, 333f, 334f
ocular lymphoma, 349f
oral cavity
plasmacytoma, 201f–202f
panleukopenia virus infection, 35, 35f–36f, 101, 102f
plasmacytoma, 192, 192f, 195f–196f, 200–201, 201f–202f, 202
pleural fluid
thymic lymphoma, 348f
polycythemic vera (PV), 441
prolymphocytic leukemia (PLL), 161
refractory anemia, 475, 478f–480f
skin
cutaneous T-cell lymphoma, 335f
epitheliotropic T-cell lymphoma, 334
lymphoma with a collar lesion, 356f
mast cell tumor, 457f
mycosis fungoides (MF), 331f, 333f, 334f
plasmacytoma, 195f
T-cell rich large B-cell lymphoma (TCRLBCL), 269f–270f
vaccination sarcoma, 356f
small intestine
enteric epitheliotropic infiltration, 322f
intermediate-type lymphoma, 181f
small lymphocytic lymphoma (SLL), 142
spinal column
lymphoma, 349f
spleen
acute myeloid leukemia (AML) (M0/M1), 378f–379f
benign reactive, 175f
chronic lymphocytic leukemia (CLL), 291f–292f
chronic myelogenous leukemia, 379f
diffuse large B-cell lymphoma (DLBCL), 253f–254f
erythroid leukemia, 410f–411f
erythroleukemia, 405f
hepatosplenic lymphoma, 316f–317f
immune hemolytic anemia, 175f
mantle cell lymphoma (MCL), 235f
marginal zone lymphoma (MZL), 177f, 180f
metastatic mast cell tumor, 77f
plasmacytoma, 196f
structure, 50
vascular system, 48
splenic function, 55–56
T-cell rich large B-cell lymphoma (TCRLBCL), 261–262, 263, 264f–265f, 268, 268f–271f, 271–272, 491, 492, 493, 494, 494f
thymus
acute myeloid leukemia (AML) (M0/M1), 380f
involution, 86, 87f, 93
lymphoma, 348f
thymic remnant, 81f, 82f
T-zone lymphoma (TZL), 294, 300f–301f, 301
Cattle
abomasum
lymphoma, 351f
acute monoblastic leukemia, 396f
acute monocytic leukemia, 398f
adult T-cell lymphoma/leukemia, 346–350, 349f–353f
anthrax, 36, 37f
B-cell acute lymphoblastic leukemia (B-ALL), 124–125, 125f–126f, 128, 131, 132f
blood
acute lymphoblastic leukemia (ALL), 122f, 125f, 126f
acute monoblastic leukemia, 396f
erythroid leukemia, 407f, 408f
prolymphocytic leukemia (PLL), 162f
small lymphocytic lymphoma, 149f
bone marrow
acute lymphoblastic leukemia (ALL), 122f, 132f
acute monocytic leukemia, 398f
erythroid leukemia, 409f–410f
bone marrow biopsy, 117
bovine leukemia virus (BLV), 135, 346–347, 349–350
bovine virus diarrhea (BVD), 34, 35f, 85f
Bracken fern toxicity, 116
Burkitt's-like lymphoma, 140–141
in Chédiak Higashi anomaly, 111f
chronic lymphocytic leukemia (CLL), 142, 154f
chronic myelomonocytic leukemia (CMML), 462
diffuse large B-cell lymphoma (DLBCL), 238–239, 250, 254
epizootic bovine abortion (EBA), 96, 96f–97f
erythroid leukemia, 402, 407f–410f, 408f–410f
follicular lymphoma (FL), 215, 216
granulocytic sarcoma (GS), 419, 423
heart
lymphoma, 350f–351f
Johne's disease, 37
in leukocyte adhesion deficiency, 112–113
leukopheresis, effect of, 103–104
lymph node
anthrax, 37f
atrophy, 19f

Cattle (*cont.*)
bovine viral diarrhea, 35f
lymphoma, 352f–353f
salmonellosis, 36f–37f
small cell lymphocytic lymphoma, 149f–150f, 352f
lymphoplasmacytic lymphoma (LPL), 207
mycosis fungoides, 332, 334–337, 335f–336f
myelodysplastic syndromes, 473
neutrophil/lymphocyte (N:L) level, 104
porphyria, 486
prolymphocytic leukemia (PLL), 161, 162f, 302
retrobulbar lymphoma, 349f
salmonellosis, 36f, 68, 70f
sciatic nerve
lymphoma, 350f
skin
mycosis fungoides (MF), 336f
small intestine
lymphoma, 351f
small lymphocytic lymphoma (SLL), 142, 149f–150f, 352f
spinal canal
lymphoma, 350f
spleen
chronic lymphocytic leukemia (CLL), 154f
function, 56
salmonella septicemia, 70f
structure, 49f
torsion, 66
T-cell rich large B-cell lymphoma (TCRLBCL), 262
theileriosis, 36
thymus
bovine viral diarrhea (BVD), 85f
epizootic bovine abortion, 96f–97f
Toxoplasma, 36
tuberculosis, 37–38
uterus
lymphoma, 351f
CCH (canine cutaneous histiocytoma), 507–510, 507f–510f
CCND1 gene, 235
CD1, 506, 510, 515
CD1^{+}, 508, 514
CD1^{-}, 505
CD1a, in chronic lymphocytic leukemia (CLL), 156
CD1c, in chronic lymphocytic leukemia (CLL), 156
CD2
aggressive NK-cell lymphoma, 311
CD3, 52, 79, 508
adult T-cell lymphoma/leukemia, 347
aggressive NK-cell lymphoma, 311, 311f
anaplastic large cell lymphoma, 341, 342–343, 342f, 343f
angiotropic T-cell lymphoma, 360f
follicular lymphoma (FL), 219f
lymphoblastic lymphoma, 275, 283
lymphomatoid granulomatosis (LYG), 261, 261f
mycosis fungoides (MF), 334, 334f, 337, 337f
NK-cell leukemia, 309
peripheral T-cell lymphoma of large cell type, 364f
prolymphocytic leukemia (PLL), 303
subcutaneous panniculitis-like T-cell lymphoma, 327
subcutaneous panniculitis-like T-cell lymphoma (SPTCL), 329f, 330f
T-cell acute lymphoblastic leukemia, 275
T-cell rich large B-cell lymphoma (TCRLBCL), 270, 270f–271f
CD4, 23, 79, 508, 510
adult T-cell lymphoma/leukemia, 347
differentiation, 80–81
feline immunodeficiency virus infection, 91
lymphoblastic lymphoma, 283
maturation of helper T-cells, 81
simian immunodeficiency virus infection, 93
CD8, 22, 508
differentiation, 80–81
lymphoblastic lymphoma, 283
mycosis fungoides, 332
subcutaneous panniculitis-like T-cell lymphoma, 329
CD10, 140
CD11, in leukocyte adhesion deficiency, 112–113
CD11a, 23
CD11b, 506
CD11b^{+}, 505, 514
CD11c, 506, 510, 515
CD11c^{+}, 508, 514
CD11c^{-}, 505
CD11d, 317, 515
CD14, 506
CD14^{+}, 505
CD15, 492
CD18, 30f, 510, 514, 515
acute myeloid leukemia (AML), 381f
cutaneous histiocytosis, 512f, 513f
hemophagocytic histiocytic sarcoma (HHS), 521
histiocytic sarcoma, 515f, 516f, 518f
intravascular large T-cell lymphoma, 356
leukocyte adhesion deficiency, 112–113
CD19, in human marginal zone lymphoma, 180
CD20, 136
B-ALL, 124
Burkitt's-like lymphoma, 140, 141
diffuse large B-cell lymphoma (DLBCL), 241f, 245, 246f, 254
follicular lymphoma (FL), 224
lymphoblastic lymphoma, 283
mantle cell lymphoma (MCL), 234, 236f
marginal zone lymphomas, 178
mycosis fungoides (MF), 334, 337
plasmablastic lymphoma, 204
RS cells, 492
T-cell rich large B-cell lymphoma (TCRLBCL), 270–271
CD21, in chronic lymphocytic leukemia (CLL), 156
CD23, 23
CD25^{+}, in adult T-cell lymphoma/leukemia, 347
CD29, 23
CD30, 518
anaplastic large cell lymphoma, 339, 340, 341
lymphomatoid papulosis (LYP), 345
RS cells, 492

CD31, 43, 54, 61, 72, 73f, 452
CD34, 480, 505
  acute myeloid leukemia (AML), 380
  myelodysplastic syndromes, 476
CD40, 23, 492
CD45
  acute myeloid leukemia (AML), 381f
  RS cells, 492
CD49, in acute myeloid leukemia (AML), 381f
CD56, marker for NK-cells in humans, 310, 311
CD61, 451f
CD68, 506, 518
CD71, 23
CD73⁻, in adult T-cell lymphoma/leukemia, 347
CD79, 16f, 59f, 132f, 135, 136
  B-ALL, 124
  Burkitt's-like lymphoma, 140, 141
  chronic lymphocytic leukemia (CLL), 144f, 156
  diffuse large B-cell lymphoma, 245, 246f, 251f, 254
  follicular lymphoma (FL), 218f, 219f, 224
  intravascular large T-cell lymphoma, 356f
  lymphomatoid granulomatosis (LYG), 261, 261f
  mantle cell lymphoma (MCL), 234, 236
  marginal zone lymphomas, 178, 178f
  mycosis fungoides (MF), 334, 335f, 337, 337f
  myeloma, 202
  prolymphocytic leukemia (PLL), 163
  T-cell rich large B-cell lymphoma (TCRLBCL), 270, 271f
CD86, 23
CD90, 508, 510, 514, 515
CEL (chronic eosinophilic leukemia), 436–440, 437f–439f
Celiac disease, 319
Centroblasts, 23
Centrocytes, 23
Centrocytic lymphoma, 227
C-fos, 347
Chédiak Higashi anomaly, 110–112, 111f
Chlorambucil
  for follicular lymphoma (FL), 226
  for myeloma, 206
Chlorinated hydrocarbons, thymic toxicity and, 84
Chloroacetate esterase (CAE), 372, 373f, 465
  acute myelomonocytic leukemia, 393, 394f–395f
  acute promyelocytic leukemia, 390
  basophil leukemia, 455–456
  granulocytic sarcoma, 423
  mast cell tumors, 456–457
Chloroma, 419
CHOP
  for diffuse large B-cell lymphoma (DLBCL), 258
  for T-cell rich large B-cell lymphoma (TCRLBCL), 272
Chromogranin, 43
Chronic eosinophilic leukemia (CEL), 436–440, 437f–439f
Chronic idiopathic myelofibrosis (CIMF), 449–454, 450f–453f
Chronic lymphocytic leukemia (CLL), 287–294
  B-cell (B-CLL), 142–160
    cell of origin, 157
    clinical presentation and features, 142–143
    cytogenic and molecular features, 156–157
    definition, 142
    diagnostic criteria, 157
    differential diagnosis, 157
    epidemiology, 142
    evaluation of treated animal, 160
    immunologic features, 155–156
    incidence, 142
    pathologic features, 143–155, 143f–156f
      blood, 143–149, 143f–149f
      bone marrow, 143f–144f, 149–150, 150f–151f
      lymph node, 152, 152f
      other organs, 155, 156f
      spleen, 152–153, 154f–155f, 155
    staging, 157
    transformation and progression, 157–158, 158f–160f, 160
    treatment and survival, 160
  clinical presentation and features, 287
  definition, 287
  differential diagnosis, 292–293
  epidemiology and features, 287
  lymphocyte-rich classic Hodgkin's lymphoma compared, 494
  pathologic features, 287–292
    blood, 287–288, 288f, 291f
    bone marrow, 288–289, 290f
    liver, 288f, 291–292, 293f–294f
    lymph node, 289–290, 289f–291f
    spleen, 290–291, 291f–292f
  treatment and survival, 293
  T-zone lymphoma distinguished from, 300
Chronic lymphoid leukemia
  neoplastic cell colonization of bone marrow, 101
Chronic myeloid leukemia (CML), 425–434
  animal, 429–434, 430f–433f
    clinical presentation, 430
    pathologic features, 430, 430f–433f, 432–434
      blood, 430, 430f–432f, 432
      bone marrow, 433, 433f
      lymph node, 433
      other organs, 434
      spleen, 433
  atypical (aCML), 461
  human, 425–428, 426f–428f
  overview, 425
Chronic myelomonocytic leukemia (CMML), 462–466, 463f–466f
Chronic myeloproliferative diseases, 425–459
  basophil leukemia, 454–456, 455f–456f
  chronic eosinophilic leukemia (CEL), 436–440, 437f–439f
  chronic idiopathic myelofibrosis (CIMF), 449–454, 450f–453f
  chronic myeloid leukemia (CML), 425–434
    animal, 429–434, 430f–433f
      clinical presentation, 430
      pathologic features, 430, 430f–433f, 432–434
    human, 425–428, 426f–428f
    overview, 425
  chronic neutrophilic leukemia, 434–435, 434f–436f
  essential thrombocythemia (ET), 443–448, 443f–448f
  hypereosinophilic syndrome (HES), 436–440, 437f–439f

Chronic myeloproliferative diseases (*cont.*)
mast cell tumor (MCT), 456–457, 457f–459f
polycythemia vera (PV), 440–442, 441f
blood, 441–442, 441f
overview, 440–441
Chronic neutrophilic leukemia, 434–435, 434f–436f
CID (combined immunodeficiency), 27
CIMF (chronic idiopathic myelofibrosis), 449–454, 450f–453f
Circulating granulocyte pool, 103–104
CLA^+ (cutaneous lymphocyte-associated $antigen^+$), 505
Cladaribine, for lymphoplasmacytic lymphoma (LPL), 214
Classification
of cell types in the peripheral blood, 120
systems for hematopoietic neoplasms, 3–7
American Registry of Pathology, 3
basis of, 3
chronology of lymphoid tumor descriptions, 3
Gall and Mallory, 4
Jackson and Parker, 4
Kiel Classification, 4–5
Lukes and Butler, 4
Lukes and Collins, 4–5
Rappaport, 4
REAL (REAL-WHO), 5–6, 6t
Robb-Smith, 3–4
Working Formulation (WF), 5
CLL. *See* Chronic lymphocytic leukemia (CLL)
CLTCL-ALS (clathrin heavy polypeptide-like) gene fusion, 340
CML. *See* Chronic myeloid leukemia (CML)
CMML (chronic myelomonocytic leukemia), 462–466, 463f–466f
C-myc, 137
Coccidioides, 38
Collagen, 449, 452f
Collar lesions, 355, 356f
Collins, R., 4–5
Combined immunodeficiency (CID), 27
Common variable immunodeficiency, 27
Conditioning, 68
Congenital diseases of bone marrow, 105–106, 105f–106f
Cord blood, 99
Corticosteroids, for systemic histiocytosis, 515
Corynebacterium pseudotuberculosis, 38
CPB-associated factor, 347
CREB, 347
Crohn's disease, 318
Cryptococcosis, 38, 39f
CTCL (cutaneous T-cell lymphoma), 236
Cutaneous histiocytoma, 506, 507–510, 507f–510f
Cutaneous histiocytosis (cutaneous reactive histiocytosis), 506, 510–512, 511f–513f, 514
Cutaneous lymphocyte-associated $antigen^+$ (CLA^+), 505
Cutaneous T-cell lymphoma (CTCL), 236
Cyclic hematopoiesis, 106–107, 107f
Cyclic hydrocarbons, myelodysplastic changes from, 115
Cyclin D1 protein, 227, 236, 238
Cyclophosphamide
for follicular lymphoma (FL), 226
for myeloma, 206
Cyclosporin A, for systemic histiocytosis, 515
Cytarabine
for acute myelomonocytic leukemia, 392
for myelodysplastic syndromes, 488
Cyticercus sp., 70
Cytokeratin, 43–44, 43f–46f, 82f, 89, 90
Cytopenia, refractory with multilineage dysplasia, 478, 481–482, 481f–482f
Cytotoxic T-cells, maturation of, 81

D
Dacie technique, 117
Deep cortical units, 12, 12f, 13f, 28f
Degenerative diseases
bone marrow, 114–116, 115f
lymph node, 28–29, 29f
spleen, 63–66, 63f–66f
thymus gland, 84–87, 84f–87f
Dendritic cells
as antigen presenting cells, 505–506
development of, 22
lytic activity, 22
migration, 22–23
proliferations, 505–506, 510
RS (Reed-Sternberg) cells, 491
splenic, 53
Developmental diseases
bone marrow, 105–114, 105f–111f
lymph node, 27–28
spleen, 62, 62f–63f
thymus, 81–83, 81f–83f
Dexamethasone, for myeloma, 206
Dexter culture, 100
Diagnostic cytopathology, 26
Diamond Black-fan anemia, 105
Diffuse large B-cell lymphoma (DLBCL), 238–258
cell of origin, 255
clinical presentation and features, 239
cytogenetic and molecular features, 255
definition, 238
diagnostic criteria, 256, 256f–257f
differential diagnosis, 257, 257f
epidemiology, 238–239
evaluation of the treated animal, 258
immunologic features, 254–255
pathologic features, 239–254, 240f–256f
blood, 239
bone marrow, 239–240, 240f, 257f
lymph node, 240, 240f–246f, 245–251, 253f, 256f–257f
other organs, 253–254, 254f–256f
spleen, 251–253, 251f–254f
transformation and progression, 257–258
treatment and survival, 258
variants
anaplastic large cell lymphoma (ALCL-B), 256, 256f–257f, 257
intravascular, 246–248, 247f–248f
mediastinal, 248–250, 248f–250f

Diffuse large B-cell lymphoma (DLBCL) (*cont.*)
plasmablastic, 244–246, 244f–247f
primary effusion, 250–251, 250f
Diffuse large cell lymphomas (DLCL), BCL-6 protein and, 23
Diffuse large T-cell lymphoma, 29f
Diffuse mixed Hodgkin's lymphoma, 491
Dioxin, thymic toxicity and, 84
Disseminated histiocytic sarcoma, 30f
Distemper hepatitis vaccination, 13
DLBCL. *See* Diffuse large B-cell lymphoma (DLBCL)
DLCL (diffuse large cell lymphomas), BCL-6 protein and, 23
Doehle bodies, 402f, 407, 431f, 432
Dog
acute lymphoblastic leukemia (ALL), 275–277, 276f–278f, 284
aggressive NK-cell lymphoma, 310, 310f–311f
anaplastic large cell lymphoma, 341–342, 341f–343f
angioimmunoblastic T-cell lymphoma (AILT), 312, 312f–315f
basophil leukemia, 454, 455f–456f
B-cell acute lymphoblastic leukemia (B-ALL), 128, 129f, 130–131, 132f, 135
B-cell lymphoblastic lymphoma (B-LBL), 124, 125, 133f, 134f
blood
acute lymphoblastic leukemia (ALL), 276f–277f
L1 type, 120f, 128f, 130f
L2 type, 121f
L3 type, 129f
acute monoblastic leukemia, 396f–397f, 397f
acute monocytic leukemia, 399f
acute myeloid leukemia (AML) M2, 383f–384f
chronic lymphocytic leukemia (CLL), 143f, 145f, 151f, 288f, 291f
LGL type, 306f
chronic myeloid leukemia of basophil type, 455f
chronic myelomonocytic leukemia (CMML), 463f–464f
essential thrombocythemia (ET), 444f–446f
megakaryoblastic leukemia, 412f–413f
myelofibrosis, 450f
myeloma, 199f
polycythemic vera (PV), 441f
postsplenectomy, 55f, 57f
prolymphocytic leukemia (PLL), 303f
small lymphocytic lymphoma, 146f
bone marrow
acute lymphoblastic leukemia (ALL), 128f, 132f, 277f–278f
acute monocytic leukemia, 400f
acute myeloid leukemia (AML), 371f–372f, 376f–377f, 384f–386f, 388f
acute myelomonocytic leukemia, 372f–373f
anaplastic large cell lymphoma, 257f
aplastic, 101f
chronic lymphocytic leukemia (CLL), 144f, 150f–151f, 290f
chronic myeloid leukemia, 433, 433f
of basophil type, 455f–456f
chronic myelomonocytic leukemia (CMML), 464f, 465f
diffuse large B-cell lymphoma (DLBCL), 240f
erythroid hyperplasia due to immune mediated hemolytic anemia, 103f
essential thrombocythemia (ET), 446f
grey collie syndrome, 107f
LGL (large granular lymphocytic) neoplasia, 308f
marginal zone lymphoma, 172f
megakaryoblastic leukemia, 413f–415f
myelodysplasia, 484f–486f
myelofibrosis, 452f
myeloid hyperplasia associated with pyometra, 104f
myeloma, 190f–191f, 197f–198f
refractory anemia
with excess blasts, 480f
of myelodysplastic syndrome, 475f–476f
small lymphocytic leukemia (SLL), 146f
bone marrow biopsy, 117
brain
angiotropic T-cell lymphoma, 359f
intravascular B-cell lymphoma, 247f–248f
plasmablastic lymphoma, 247f
Burkitt's-like lymphoma, 140f–141f, 141
cerebrospinal fluid
effusion lymphoma, 250
chronic idiopathic myelofibrosis, 449f, 450f, 452, 452f
chronic lymphocytic leukemia (CLL), 142–144, 143f–145f, 150f–151f, 154f, 287–288, 288f, 290f
chronic myeloid leukemia, 430, 433f
chronic myelomonocytic leukemia (CMML), 462–466, 463f–466f
cutaneous histiocytosis, 506, 510–512, 511f–513f, 514
cyclic hematopoiesis, 104, 106–107, 107f
diffuse large B-cell lymphoma (DLBCL), 238–239, 240f–244f, 246, 246f–252f, 248–251, 255f–257f
duodenum
epitheliotropic T-cell lymphoma, 319f–321f, 323f–326f
enteropathy-type T-cell lymphoma, 319, 319f–321f, 323f–326f
essential thrombocythemia (ET), 443–445, 444f–446f
follicular lymphoma (FL), 215, 218f–221f, 224
gastric adenocarcinoma, 41f
gastric epitheliotropic inflammatory bowel disease, 323f
gastric plasmacytoma, 193f–194f
glucosylceramidase deficiency, 64
hemoglobin "C," 109, 110f
hemophagocytic histiocytic sarcoma (HHS), 506, 518, 519, 519f–521f, 521
hepatosplenic lymphoma, 316–317, 317f–318f
histiocytic sarcoma, 42f, 516f–518f, 517–519
hypereosinophilic syndrome (HES), 436, 439–440
intravascular large T-cell lymphoma, 357f–360f, 358
jejunum
enteric epitheliotropic infiltration, 320f–321f, 323f
juvenile myelomonocytic leukemia (jMML), 467–468, 467g–471g, 471
in leukocyte adhesion deficiency, 112–113
leukopheresis, effect of, 103–104
LGL (large granular lymphocytic) neoplasia, 304, 305–307, 306f–308f

Dog (*cont.*)
liver
acute monocytic leukemia, 400f
acute myeloid leukemia (AML) M2, 387f
aggressive T-cell lymphoma, 310f–311f
enteric T-cell lymphoma, 325f
hepatosplenic lymphoma, 318f
juvenile CMML, 468f–469f, 469f
LGL (large granular lymphocytic) neoplasia, 307f
lymphoblastic lymphoma, 283f
megakaryoblastic leukemia, 415f
lung
angiotropic lymphoma, 358f
lymphomatoid granulomatosis (LYG), 260f–261f
megakaryoblastic leukemia, 416f
myeloproliferative disease resembling juvenile CMML, 468f
lymph node
afferent lymphatics, 10f
anaplastic large cell lymphoma, 256f
angioimmunoblastic T-cell lymphoma (AILT), 312f–314f
B-cell lymphoblastic lymphoma (B-LBL), 133f, 134f
benign medullary cord plasma cell hyperplasia, 189f
Burkitt's-like lymphoma, 140f–141f
Burkitt's-type lymphoma, 139f–140f
Castlemanlike proliferation, 34f
diffuse large B-cell lymphoma (DLBCL), 20f–21f, 29f, 240f–244f
diffuse small cell lymphoma intermediate type (DSLI), 147f
efferent lymphatics, 10f
enteric T-cell lymphoma, 326f
fading follicular hyperplasia, 32f
follicular architecture, 12f
follicular hyperplasia, 13f, 21f, 33f
follicular hypoplasia, 83f
follicular involution, 15f
follicular lymphoma (FL), 218f–221f
gastric adenocarcinoma, 41f
histiocytic sarcoma, 30f, 42f, 357f
hyperplasia, diffuse, 31f
immunoblastic lymphoma, 160f
lollipop vascular lesion, 34f
lymphoblastic lymphoma, 278f–281f
lymphoid proliferation, 11f
lymphoma, 358f
lymphoplasmacytic lymphoma (LPL), 209f, 211f
mantle cell lymphoma (MCL), 230f
marginal zone hyperplasia, 16f
marginal zone lymphoma, 17f–18f, 167f, 171f–174f, 181f
medullary structure, 11f
paracortex, 10f, 31f, 32f, 33f
paracortical hyperplasia, 13f
peripheral T-cell lymphoma, mixed cell type, 363f
plasmablastic lymphoma, 244f, 246f
plasmacytoma, 197f, 200f
prolymphocytic leukemia (PLL), 303f–304f
pulmonary adenocarcinoma, 43f–44f
sclerosis, 21f
small cell lymphocytic leukemia (SLL), 20f, 145f–147f
small lymphocytic leukemia (SLL), 153f
sternal node in hemorrhagic pleural effusion, 46f
systemic anaplastic large cell lymphoma of T-cell type, 342f–343f
T-zone lymphoma (TZL), 15f–16f, 184f–185f, 237f, 295f–300f
lymph node biopsy, 24–25, 27
lymphoblastic lymphoma (LBL), 275, 278f–281f, 283–284
lymphomatoid granulomatosis (LYG), 260–261, 260f–261f
lymphoplasmacytic lymphoma (LPL), 207, 209f, 211f–212f
mantle cell lymphoma (MCL), 55f, 227, 227f–228f, 229–231, 230f–234f, 236f–237f
marginal zone hyperplasia of the spleen, 52
marginal zone lymphoma (MZL), 168–170, 169f–176f, 170, 173, 179f–181f, 183f–184f, 186f–188f, 188
mast cell tumor (MCT), 456, 458f–459f
mediastinal mass
diffuse large B-cell lymphoma, 249f–250f
melanoma, 191–192, 191f, 197–199, 197f–199f, 202, 203, 206
meninges
angiotropic T-cell lymphoma, 359f–360f
myasthenia gravis (MG), 88–90
mycosis fungoides, 331f–332f, 334f, 335–337, 336f–337f
myeloid AML (acute myeloid leukemia)
granulocytic sarcoma, 419, 423
M0 (AML minimally differentiated) and M1 (AML without maturation), 374, 376f–377f
M2 (AML with maturation), 383, 383f–388f
M3 (acute promyelocytic leukemia), 389
M4 (acute myelomonocytic leukemia), 392
M5A (acute monoblastic leukemia), 396f–398f
M5B (acute monocytic leukemia), 399, 399f–400f
M7 (acute megakaryoblastic leukemia), 412, 412f–416f
myelolipoma, 71f, 72f
nasal turbinates
angiotropic T-cell lymphoma, 358f–359f
Neospora, 36
neutrophil/lymphocyte (N:L) level, 104
Niemann-Pick disease, 114
oral cavity
plasmacytoma, 192f
pararectal plasmacytoma, 194f–195f
peripheral T-cell lymphoma NOS, 361–363, 361f–364f
plasmacytoma, 189f–190f, 191–192, 192f–197f, 200, 200f–201f, 202, 205
pleural effusion, 46f
polycythemic vera (PV), 441, 441f
prolymphocytic leukemia (PLL), 161, 302, 302f–304f
pulmonary adenocarcinoma, 43f
pyometra, 68, 70f
pyruvate kinase deficiency, 109, 109f–110f
refractory anemia, 475, 475f–476f
salivary gland
MALT lymphoma, 178f, 187f

Dog (*cont.*)
skin
anaplastic large cell lymphoma, 341f–342f
cutaneous anaplastic large cell lymphoma of T-cell type, 341f
cutaneous histiocytoma, 506, 507–510, 507f–510f
cutaneous histiocytosis, 511f–513f
cutaneous T-cell lymphoma, 361f–362f
epitheliotropic T-cell lymphoma, 334f, 337
mast cell tumor, 205f, 458f–459f
mycosis fungoides (MF), 331f
pagetoid reticulosis (PR), 331f–332f, 336f–337f
peripheral T-cell lymphoma, large cell type, 363f–364f
plasmacytoma, 189f–190f
subcutaneous panniculitis-like T-cell lymphoma, 327f–330f
systemic aggressive T-cell lymphoma, 361f
T-cell rich large B-cell lymphoma (TCRLBCL), 270f
small intestine
myeloproliferative disease, 470f–471f
small lymphocytic lymphoma (SLL), 142, 145f–148f, 153f–155f
spinal cord
intravascular B-cell lymphoma, 247f
spleen
acute monoblastic leukemia, 398f
acute myeloid leukemia (AML) M2, 386f–387f
atrophy, 67f
benign reactive, 174f–175f
chronic dermatitis, 64f
chronic idiopathic thrombocytopenic purpura, 64f
chronic immune stimulation, 71f
chronic lymphocytic leukemia (CLL), 154f
congestion, 53f
diffuse large B-cell lymphoma, 251f–252f
fading follicular hyperplasia, 175f
fibrohistiocytic nodule, 58f, 72f, 187f–188f
focal nodular lymphoid hyperplasia, 60f
follicular hyperplasia, 71f
function, 55, 55f–57f
hemangiosarcoma, 57
hemophagocytic histiocytic sarcoma (HHS), 519f–521f
hemosiderosis, 65f
hepatosplenic lymphoma, 306f–307f, 317f
histiocytic sarcoma, 63f
hyperplasia, 67f–72f
immune thrombocytopenic purpura, 68f
juvenile CMML, 469f–470f
lymphoplasmacytic lymphoma (LPL), 211f–212f
macrophages, 56f
mantle cell lymphoma (MCL), 55f, 147f–148f, 148f, 166f–167f, 185f–186f, 201f, 227f–228f, 231f–234f, 236f
marginal zone hyperplasia, 75f
marginal zone lymphoma (MZL), 59f, 66f, 169f–171f, 179f–180f
mass with age, 48
megakaryoblastic leukemia, 415f
metastatic histiocytic sarcoma, 76f
metastatic osteosarcoma, 76f, 77f
myelolipomas, 60f, 65f, 69f, 71f, 72f
nodular lymphoid proliferation, 74f
periarteriolar lymphoid sheath, 67f–70f
plasmacytoma, 196f, 200f–201f
pyometra, 70f
sclerosis, 73f
septic shock, 69f–70f
small lymphocytic leukemia (SLL), 154f–155f
structure, 49f, 50, 51f–54f
torsion, 66
vascular system, 48
splenomegaly, 65
splenosis, 62f
subcutaneous mass
mixed cell type peripheral T-cell lymphoma, 362f
systemic histiocytosis, 514f–515f
T-cell rich large B-cell lymphoma (TCRLBCL), 263f–264f
subcutaneous panniculitis-like T-cell lymphoma, 327–329, 327f–330f
systemic histiocytosis, 506, 514, 514f–515f
T-cell rich large B-cell lymphoma (TCRLBCL), 262, 263f–264f, 268, 270f
thymus
B-cell nodule, 79f
hypoplasia, 82f–83f
idiopathic hemorrhagic infarction, 85f
thymoma, 89f–90f
tonsil
diffuse large cell lymphoma, 255f–256f
T-zone lymphoma (TZL), 294–295, 295f–300f, 299, 301
Downs syndrome, 427
Doxorubicin
for diffuse large B-cell lymphoma (DLBCL), 258
for myeloma, 206
for T-cell rich large B-cell lymphoma (TCRLBCL), 272
Drug-induced changes in bone marrow, 115–116
Dysplasia
spleen, 70, 72–75, 72f–75f

E

EBA (epizootic bovine abortion), 96, 96f–97f
EBV. *See* Epstein-Barr virus (EBV)
EBV-encoded nuclear RNA (EBER), 311
E-cadherin, 40, 508, 515
EHS (ergthrophogocytic histiocytic sarcoma), 42
EIA (equine infectious anemia), 32, 69, 115
Ellipsoids, 48
Elliptocytosis, 109, 109f
EMA (epithelial membrane antigen), 43
Embryology
bone marrow, 98–102, 98f–102f
lymph node, 9
spleen, 47–48, 47f
thymus, 78–79, 78f–79f
EMH. *See* Extramedullary hematopoiesis (EMH)
Emmel, V.E., 108
Emperipolesis, 427f, 443, 444f
Enteropathy-type T-cell lymphoma (ETCL), 318–326, 319f–326f

Eosinophilic granuloma, 436, 440
Eosinophils
  chronic eosinophilic leukemia (CEL), 436–440, 437f–439f
  in chronic idiopathic myelofibrosis, 450
  in chronic myeloid leukemia, 426, 426f, 428, 432
  hypereosinophilic syndrome (HES), 436–440, 438f–439f
  pulmonary infiltrates with eosinophilia (PIE), 440
Epistaxis, 125, 142
Epithelial membrane antigen (EMA), 43
Epitheliotropic lymphoma, 507, 508f
Epizootic bovine abortion (EBA), 96, 96f–97f
Epo (erythropoietin), 442, 476
Epstein-Barr virus (EBV), 137–138, 260, 309, 310, 311, 347
Equine herpesvirus type 1, 63, 85–86, 86f
Equine infectious anemia (EIA), 32, 69, 115
Equine viral rhinopneumonitis (EVR) virus, 9
Ergthrophagocytic histiocytic sarcoma (EHS), 42
ERV (equine viral rhinopneumonitis) virus, 9
Erythremic myelosis, 401, 406–411
Erythroblasts, 402
Erythrocytosis, in polycythemic vera (PV), 440–442, 441f
Erythroid leukemia, pure (M6B), 406–411
  blood, 406–407, 406f–408f
  bone marrow, 407–409, 408f–410f
  classification, 401–402
  definition, 402
  epidemiology and incidence, 402
  liver, 409–410, 410f
  spleen, 410, 410f–411f
Erythroid leukemia (erythremic myelosis), 368
Erythroid system
  in chronic myelomonocytic leukemia (CMML), 464, 465f–466f
  in juvenile myelomonocytic leukemia (jMML), 467
  in myelodysplastic syndromes, 473, 475–480, 475f–480f, 486
Erythroleukemia, 371
Erythroleukemia (M6A)
  classification, 401–402
  clinical presentation and feature, 402
  definition, 402
  epidemiology and incidence, 402
  pathologic features, 402–406, 402f–406f
Erythrophagocytosis, in hepatosplenic T-cell lymphoma, 316
Erythropoiesis, development of, 98. *See also* Hematopoiesis
Erythropoietin (epo)
  erythrocytosis, 442
  for refractory anemia, 476
Essential thrombocythemia (ET), 443–448, 443f–448f
Esterases, 27, 42, 518, 521. *See also specific esterases*
ETCL (enteropathy-type T-cell lymphoma), 318–326, 319f–326f
ET (essential thrombocythemia), 443–448, 443f–448f
Extramedullary granulocytic sarcoma in association with AML, 384
Extramedullary hematopoiesis (EMH), 449
  in acute myeloid leukemia (AML) (M0/M1), 377–379, 378f, 380f
  in acute myeloid leukemia (AML) M2, 386
  in chronic lymphocytic leukemia (CLL), 291
  in medullary cords of lymph node, 18–19
  splenic, 67f, 68, 68f, 69f
Extramedullary plasmacytoma, 189

F
FAB (French-American-British) system, 120
Fabry's disease, 113
Factor VIII, 61, 480
Fading follicular hyperplasia (FFH), 171, 175f
Faggot cells, 389
Familial hemophagocytic lymphohistiocytosis, 522
Fanconi anemia, 106
Fascin, 492
Feline immunodeficiency virus (FIV), 91
Feline leukemia virus (FeLV), 69, 124, 346, 347, 401–402, 436, 437, 452
Feline panleukopenia virus, 86, 87f
Ferritin, 65
Ferry, J.A., 3
FFH (fading follicular hyperplasia), 171, 175f
Fibrohistiocytic nodule, 57, 58f, 70, 72f, 73, 74f, 185–186, 187f–188f, 200
Fine needle aspiration
  histiocytic sarcoma, 42f
  lymph node, 25
  of splenic lesions, 59
5q-syndrome, 473
Fixation
  blood marrow biopsy, 117
  for lymph node biopsy, 25–26
  splenic biopsy, 60–61
Flow cytometry, 27
Flower cells, 347
Fludarabine, for lymphoplasmacytic lymphoma (LPL), 214
Fluorescent in situ hybridization (FISH), 135
Folic acid deficiency, 486
Follicular hyalinosis, 32, 33f, 223, 231, 252, 378, 379f, 404
Follicular hyperplasia
  lymph node, 12f, 13, 13f, 15f, 18f, 21f, 24, 30–34, 31f–34f, 87f, 93f
  spleen, 71f, 94f
  thymus, 89f
Follicular hypoplasia, lymph node, 83f
Follicular involution, 15, 15f, 70
Follicular lymphoma (FL), 215–226
  cell of origin, 225
  clinical presentation and features, 215
  cytogenetic and molecular features, 224–225
  definition, 215
  diagnostic criteria, 225
  differential diagnosis, 225
  diffuse large B-cell lymphoma (DLBCL) distinguished from, 257
  epidemiology and incidence, 215
  evaluation of the treated animal, 225–226
  immunologic features, 224
  pathologic features, 215–224, 217f–224f

Follicular lymphoma (FL) (*cont.*)
blood, 215–216
bone marrow, 216–217, 217f–218f, 224f
lymph node, 216f–223f, 217–222
other organs, 224
spleen, 222–224, 222f–223f
staging, 225
transformation and progression, 225
treatment and survival, 226
Follicular lymphomas
BCL-6 protein and, 23
chromosomal rearrangement, 23
infrequent recognition of, 25
Follicular polarity, 13, 14f
Formalin, 25–26, 60f
French-American-British (FAB) system, 120, 367
Friend F-MuLV, 401–402
Friend leukemia virus, 442
Fungal infection, lymphadenitis due to, 38, 39f

G
Gall, E.A., 4
Gamma scintillation scanning, 41–42
Gamna-Gandy bodies, 65
Gangliosidoses, 64
Gastric adenocarcinoma, 41f
Gastric plasmacytoma, 193f–194f
Gastritis, 182
Gastritis MALT lymphoma, 182, 182f–183f
Gaucher's disease, 113
G-CSF, 100, 107, 476
Germinal centers
lymph node
development of, 23
involution, 24
polarity of, 13, 14f
structure, normal and benign reactive, 11–17, 11f–17f
spleen, 48–52, 51f–52f, 54, 69, 70f, 74
thymus, 88–90, 89f–90f, 91, 91f–92f, 93
Gleevec, 425
Globoid cell leukodystrophy, 64
Glomerulopathy, 202
Glucosylceramidase deficiency (Gaucher's disease), 64
Glycogen storage diseases, 113
Glycosaminoglycans, 113, 114
Goat
caseous lymphadenitis, 38
Johne's disease, 37, 38f
myelofiborsis, 417–418, 419f
splenic torsion, 66
Goldschmidt, M.H., 457
Graft *versus* host disease, 99
Granulocyte macrophage-colony stimulating factor (GM-CSF), 22, 100
induction of histiocytic and dendritic cell proliferations, 505
lack of response to, 107
for myelodysplastic syndromes, 486–487
Granulocytic sarcoma, 419–423, 420f–423f, 440
Granulomatous lymphadenitis, 37
Grenz zone, 201
Grey collie syndrome, 106–107, 107f

H
Hairy cell leukemia, 164, 165f–166f, 171
Half-body irradiation, 99
Hallmark cells, 240, 339
Ham test, 106
Harbor seal, lymph node atrophy in, 19f
Harris, N.L., 3
Hassall's corpuscles, 78, 79, 83f, 87, 89, 93, 94f
Helicobacter spp., 182
Hematopoiesis
in birds, 100
development of, 98–99
extramedullary, 449
in acute myeloid leukemia (AML) (M0/M1), 377–379, 378f, 380f
in acute myeloid leukemia (AML) M2, 386
in chronic lymphocytic leukemia (CLL), 291
in medullary cords of lymph node, 18–19
splenic, 67f, 68, 68f, 69f
homeostatic, 104
ineffective, 462
location of, 98, 99–100
proliferating cell pool and maturation pool ratio, 104
splenic, 47, 54, 67f, 68, 68f, 69f
Hematopoietic stem cells (HSC)
in cord blood, 99
lineage committed, 99
long term (LT), 99
origin of, 98–99
short term (ST), 99
spleen colony technique, 101–102, 102f
transplantation, 105
Hemobartonella, 402
Hemochromatosis, 106
Hemoglobin
hemoglobin "C," 109, 110f
hemoglobin F (fetal), 467
sickle cell, 108
in thalassemia, 108–109
Hemoglobinopathies, 108–109, 109f–110f
Hemolytic anemia, in black rhinoceros, 105–106, 105f–106f
Hemophagocytic histiocytic sarcoma (HHS), 506, 517–519, 519f–521f, 521
Hemorrhage, thymic, 84
Hemosiderin
in acute myeloid leukemia (AML), 376f–377f, 379, 386f, 387f
in bone marrow, 101
in congenital hemolytic anemia, 105, 105f–106f
in diffuse large B-cell lymphoma (DLBCL), 252, 253f
equine infectious anemia (EIA), 115
in erythroid leukemia, 404, 405
in follicular lymphoma (FL), 216
in hemophagocytic histiocytic sarcoma (HHS), 519, 520f, 521f
spleen, 54, 54f, 56, 56f–57f, 65, 65f, 66f, 69f, 72, 73f

HEMPAS test, 106
Hepatomegaly
in acute megakaryoblastic leukemia, 412
in acute monoblastic leukemia M5A, 396
in acute monocytic leukemia, 399
in acute myeloid leukemia (AML) M2, 383
in acute myelomonocytic leukemia, 392
in chronic idiopathic myelofibrosis, 449–450
in chronic lymphocytic leukemia (CLL), 142, 287
in essential thrombocythemia (ET), 443
in hepatosplenic lymphoma, 316
in LGL (large granular lymphocytic) neoplasia, 306
in lymphoblastic lymphoma, 275
in MDS/MPD, 461, 465
in NK-cell leukemia, 310
in polycythemic vera (PV), 442
Hepatosplenic γδ T-cell lymphoma, 316
Hepatosplenic T-cell lymphoma (HSTL), 316–318, 316f–318f
Hepatosplenomegaly
in acute megakaryoblastic leukemia, 412
in acute monoblastic leukemia M5A, 396
in acute monocytic leukemia, 399
in acute myeloid leukemia (AML) M2, 383
in acute myelomonocytic leukemia, 392
in LGL (large granular lymphocytic) neoplasia, 306
in lymphoblastic lymphoma, 275
in NK-cell leukemia, 310
Herrick, J.B., 108
HES (hypereosinophilic syndrome), 436–440, 438f–439f
HHS (hemophagocytic histiocytic sarcoma), 506, 517–519, 519f–521f, 521
High endothelial venules (HEVs), 23, 31, 31f–33f
Histiocyte, 506
Histiocytic sarcoma, 30f, 42f, 76f, 357f, 506, 517–519, 519f–521f, 521
Histiocytoses, 505–522
cell proliferations, histiocytic and dendritic, 505–506
neoplasms
cutaneous histiocytoma, 506, 507–510, 507f–510f
cutaneous histiocytosis, 506, 510–512, 511f–513f
hemophagocytic histiocytic sarcoma, 506, 517–519, 519f–521f, 521
histiocytic sarcoma, 506, 515–517, 516f–518f
human disorders, 521–522, 522f
infection associated hemophagocytic syndrome (IAHS), 522
sinus histiocytosis with massive lymphadenopathy (SHML), 521–522, 522f
systemic histiocytosis, 506, 514–515, 514f–515f
Histiocytosis X, 510, 511f
Histopathology of lymph node metastases, 42–45, 42f–46f
Histoplasma, 38
HIV, bone marrow dysplastic changes in, 486
HLA haplotype, 99
Hodgkin's lymphoma (HL), 491–501
in animals, 499, 500f–501f
cat type of TCRBCL compared, 265–267, 265f–268f
classification, 3–4, 6, 491
general pathology
lymphocyte depletion, 497–498, 497f–498f
lymphocyte predominance type, 492–493, 492f–493f
lymphocyte-rich classic type, 493–494, 494f
mixed cellularity type, 496–497, 497f
nodular sclerosis type, 494–495, 495f–496f
Hodgkin's-like lymphoma in animals, 499, 500f–501f
name of disease, 491
REAL classification, 6t
regional pathology and staging, 498–499
RS (Reed-Sternberg) cell
morphology, 491–492
phenotypic characteristics, 492
sarcomatous type, 492
T-cell rich large B-cell lymphoma in animals compared, 491, 492, 493, 494f
types
lymphocyte depletion, 265, 267f
lymphocyte predominance, 265–266, 267, 267f–268f
lymphocyte-rich, 267
mixed cellularity, 265, 266f
nodular sclerosis, 265–266, 265f–266f, 266–267, 267, 267f–268f, 494–495, 495f–496f
Hog cholera, 35, 93, 96
Horse
acute myelomonocytic leukemia, 392
B-cell acute lymphoblastic leukemia (B-ALL), 125, 126f–128f, 128, 131, 131f, 135
blood
acute lymphoblastic leukemia (ALL) L3 type, 127f
Sézary syndrome, 332f
bone marrow
acute lymphoblastic leukemia (ALL), 127f, 131f
biopsy, 117
Bracken fern toxicity, 116
chronic lymphocytic leukemia (CLL), 142, 289f, 292f–294f
diffuse large B-cell lymphoma (DLBCL), 239, 244f–246f, 251, 252, 252f–253f
enteropathy-type T-cell lymphoma, 319
equine herpesvirus type I, 63, 85–86, 86f
equine infectious anemia (EIA), 115
follicular lymphoma (FL), 215
immunodeficiency diseases, 27
isoimmune hemolytic anemia, 56
large granulated lymphocytic (LGL) neoplasia, 304, 308
liver
chronic lymphocytic leukemia (CLL), 293f–294f
lung
plasmablastic lymphoma, 245f, 246f
lymph node
chronic lymphocytic leukemia (CLL), 289f
lymphoplasmacytic lymphoma (LPL), 211f
plasmablastic lymphoma, 204f–205f, 244f–246f
lymphoplasmacytic lymphoma (LPL), 207, 208f, 211f
mantle cell lymphoma (MCL), 227
mycosis fungoides, 332, 332f–333f
myelodysplastic syndromes, 473
oral mucosa
Sézary syndrome, 333f

Horse (*cont.*)
skin
T-cell rich large B-cell lymphoma (TCRLBCL), 262f
small intestine
lymphoplasmacytic lymphoma (LPL), 208f
small lymphocytic lymphoma (SLL), 142, 155f
spleen
diffuse large B-cell lymphoma (DLBCL), 252f–253f
follicular hyperplasia, 87f
function, 56
small lymphocytic leukemia (SLL), 154f
T-cell rich large B-cell lymphoma (TCRLBCL), 261–262, 262f, 264, 268–272, 491
thymus
EHV-induced involution, 86f
thymic atrophy, acute lymphoblastic leukemia (ALL) L3, 135f
thymic involution, 85–86, 86f
Howell-Jolly body, 55, 55f, 57f, 66, 407f
HSC. *See* Hematopoietic stem cells (HSC)
HSTL (hepatosplenic T-cell lymphoma), 316–318, 316f–318f
HTLV-1 (human T-cell leukemia virus), 346–347
Human
blood
acute lymphoblastic leukemia (ALL), 120f
aggressive NK-cell leukemia, 309f
beta thalassemia, 109f
chronic lymphocytic leukemia (CLL), 159f
chronic myeloid leukemia (CML), 426f–428f
follicular lymphoma, 215f, 217f
hairy cell leukemia, 165f
prolymphocytic leukemia (PLL), 158f, 162f
Sézary syndrome, 338f
spherocytosis, hereditary, 109f
bone marrow
acute lymphoblastic leukemia (ALL), 121f–122f, 129f–130f, 276f
acute panmyelosis with myelofibrosis, 417F–418F
aggressive NK-cell leukemia, 309f
arsenic poisoning, 486f
chronic idiopathic myelofibrosis, 450f–451f
chronic lymphocytic leukemia (CLL), 159f
chronic myeloid leukemia (CML), 427f
essential thrombocytopenia, 433f–434f
follicular lymphoma, 217f, 218f
hairy cell leukemia, 165f
myeloma, 191f
precursor cell leukemia lymphoma, 283
precursor T-cell leukemia, 276f
prolymphocytic leukemia (PLL), 158f, 162f–163f
sideroblastic anemia, 477f
breast biopsy
Burkitt's lymphoma, 139f
colon
mantle cell lymphoma, 229f–230f
liver
Hodgkin's lymphoma, nodular sclerosis type, 496f
lymph node
anaplastic large cell lymphoma, 343f–344f
angioimmunoblastic T-cell lymphoma (AILT), 315f
Burkitt's lymphoma, 138f–139f, 284f–285f
chronic idiopathic myelofibrosis, 453f
chronic lymphocytic leukemia (CLL), 152f, 289f–290f
diffuse large B-cell lymphoma, 243f
follicular lymphoma, 216f–217f, 220f–221f, 223f
gastric MALT lymphoma, 182f–183f
hairy cell leukemia, 166f
Hodgkin's lymphoma
lymphocyte depletion type, 267f, 497f–498f
lymphocyte predominance type, 267f–268f, 492f–493f
mixed cellularity type, 266f, 496f–497f
nodular sclerosis type, 265–266f, 495f
immunoblastic lymphoma, 160f
Langerhans cell histiocytosis, 511f
lymphoplasmocytic lymphoma, 207f
mantle cell lymphoma, 229f
marginal zone lymphoma, 182f
mycosis fungoides, 338f
peripheral T-cell lymphoma, 300f
plasmacytoma, 196f
prolymphocytic leukemia (PLL), 158f–1599, 163f
sinus histiocytosis, 522f
mediastinal mass
acute lymphoblastic leukemia (ALL), 129f–130f
large B-cell lymphoma, 248f–249f
lymphoblastic lymphoma, 281f
skin
lymphomatoid papulosis (LYP), 345f
mycosis fungoides, 338f
spleen
diffuse large B-cell lymphoma (DLBCL), 254f
follicular lymphoma, 222f–223f
hairy cell leukemia, 165f
hepatosplenic lymphoma, 306f
mantle cell lymphoma, 228f–229f
mycosis fungoides, 339f
prolymphocytic leukemia (PLL), 155f, 164f
Human herpesvirus-8, 119, 191
Human T-cell leukemia virus (HTLV-1), 346–347
Hydatid cestodes, 70
Hypercalcemia, in T-cell LBL, 285
Hypereosinophilic syndrome (HES), 436–440, 438f–439f
Hyperglobulinemia, in myeloma, 203–204
Hyperplasia
lymph node, 92f
spleen, 67–70, 67f–72f, 91f, 92f, 94f, 95f
thymus, autoimmune, 88–90, 88f–90f
Hypersplenism, 67–68
Hypotensive shock, 66
Hypotrichosis, 82

I

IAHS (infection associated hemophagocytic syndrome), 522
ICAMs. *See* Intercellular cytoplasmic adhesion molecules (ICAMs)
IgA, 23
in follicular lymphoma (FL), 224
in myeloma, 202, 203

IgD, in mantle cell lymphoma (MCL), 234
IgG, 23
  in follicular lymphoma (FL), 224
  in mantle cell lymphoma (MCL), 234
  in myeloma, 202, 203
IgH, 135
IgM, 23
  in follicular lymphoma (FL), 224
  in mantle cell lymphoma (MCL), 234
Ikaros, 22
IL-2, 347
IL-3, 100
IL-3α receptors (IL-3Rα), 505
IL-4
  induction of histiocytic and dendritic cell proliferations, 505
IL-6, 100, 191, 347
IL-6 Syndrome, 119
Imatinib, 425
Immunodeficiency, 27–28
  classification of congenital, 82–83
  thymus developmental diseases, 81–83
Immunoglobulin. *See also specific immunoglobulin classes*
  gene rearrangement
    in chronic lymphocytic leukemia (CLL), 157
    in RS cells, 491
  isotype class switch, 23
  VDJ rearrangement, 23
Immunohistochemistry
  cross-reactivity, 43
  for cytokeratin, 43–44, 43f–46f
  for mast cell tumors, 457
  of metastatic tumor, 43–45, 43f–46f
  splenic, 61
Indian file node arrangement, 279
Indolent lymphomas, 25
Infarction
  hemorrhagic, 227, 228f, 379
  liver, 379
  lymph node, 29, 29f, 30f, 35, 36
  spleen, 61, 65, 71f
  thymic, 84–85, 85f
Infection associated hemophagocytic syndrome (IAHS), 522
Inflammation
  dendritic cell migration and, 22
  of thymus gland due to infectious agents, 91–97, 91f–97f
Inflammatory myofibroblastic tumor, 73
Inflammatory pseudotumor
  lymph node, 29, 41
  spleen, 73, 73f
Insertional mutagenesis, 401
In situ hybridization, 27
Integrin receptors, 40
Intercellular cytoplasmic adhesion molecules (ICAMs), 9, 79, 119, 239, 290, 508, 514
Interferon, 238, 505
International Prognostic Index (IPI), 258
Interoperative cytology, 43
Intestinal adenocarcinoma, 44f
Intestine. *See specific locations*
Intraoperative cytologic examination, 26–27
Intravascular large T-cell lymphoma, 355–356, 356f–360f, 358–359
Intravascular variant of large B-cell lymphoma, 246–248, 247f–248f
Involution
  lymph node, 15f, 24
  spleen, 51
  thymic, 84, 85–86, 91, 93f, 96
Iron deficiency, 116
Irradiation, half-body, 99
Isoimmune hemolytic anemia, 56

J
Jackson, H., Jr., 4
Jamshidi needle, 117
Jamshidi procedure, 375
Johne's disease, 37, 38f
Juvenile myelomonocytic leukemia (jMML), 467–468, 468f–471f, 471, 486

K
Kaposi sarcoma, 191
Ki-1, 240, 339
Kidney
  in diffuse large B-cell lymphoma (DLBCL), 253, 255f
  in T-cell rich large B-cell lymphoma (TCRLBCL), 269
Kiel Classification, 4–5, 260, 294
Kisseberth, William, 168
KIT, 457
Knowles, Daniel, 3
Koch's Blue Bodies, 36
Kociba, Gary, 168
Kwashiorkor, 115

L
Lactate dehydrogenase, 225
Lacunar cells, 492, 493, 494, 495, 495f
Lambda light chain, 201, 201f, 204, 235
Langerhans cells
  dendritic cell proliferations, 505–506
  histiocytosis, 29, 30f, 508, 510, 511f
LAP (leukopheresis), 103–104
Large granulated lymphocytic (LGL) neoplasms, 304–308, 305f–308f
Laser capture microscope, 491
LBL. *See* Lymphoblastic lymphoma (LBL)
LcK, 347
Lead, myelodysplastic changes from, 115
Leflunomide, for systemic histiocytosis, 515
Leishmaniasis, 38, 199, 204
Lennert, Karl, 4
Lennert's lymphoma, 496, 497
Leukemia. *See also specific types*
  coining of term, 425
  definition, 119
  lymphoma distinguished from, 119
  splenic hypofunction in, 55

Leukointegrin, 305
Leukopheresis (LAP), 103–104
LGL (large granulated lymphocytic) neoplasms, 304–308, 305f–308f
L&H type of RS cells, 493, 493f, 499
Lineage promiscuity, 284
Lithium, 107
Littoral cell angioma, 61
Liver
  acute lymphoblastic leukemia (ALL), 134, 135f
  acute megakaryoblastic leukemia, 415, 415f
  acute monocytic leukemia, 400f
  acute myeloid leukemia (AML)
    M0/M1, 379, 380f
    M2, 386, 387f
  aggressive T-cell lymphoma, 310f–311f
  basophil leukemia, 455
  cat
    acute lymphoblastic leukemia (ALL) L1, 156f
    acute myeloid leukemia (AML) (M0/M1), 380f
    chronic lymphocytic leukemia (CLL), 145f, 156f, 288f, 293f
    erythroid leukemia, 410f
    erythroleukemia, 405f–406f
    granulocytic sarcoma (GS), 422f
    large cell lymphoma, 254f–255f, 353f
    lymphoma, 348f
    lymphoplasmacytic lymphoma (LPL), 213f
    mantle cell lymphoma (MCL), 235f
  chronic idiopathic myelofibrosis, 449–450, 452
  chronic lymphocytic leukemia (CLL), 145f, 155, 156f, 288f, 291–292, 293f–294f
  chronic myeloid leukemia, 434, 434f–435f, 435
  diffuse large B-cell lymphoma (DLBCL), 253–254, 254f–255f
  dog
    acute monocytic leukemia, 400f
    acute myeloid leukemia (AML) M2, 387f
    aggressive T-cell lymphoma, 310f–311f
    enteric T-cell lymphoma, 325f
    hepatosplenic lymphoma, 318f
    juvenile CMML, 468f–469f, 469f
    LGL (large granular lymphocytic) neoplasia, 307f
    lymphoblastic lymphoma, 283f
    megakaryoblastic leukemia, 415f
  enteric T-cell lymphoma, 325f
  erythroid leukemia, 409–410, 410f
  erythroleukemia, 404–405, 405f–406f
  essential thrombocythemia (ET), 447, 447f
  granulocytic sarcoma (GS), 421, 422f
  hepatomegaly
    in acute megakaryoblastic leukemia, 412
    in acute monoblastic leukemia M5A, 396
    in acute monocytic leukemia, 399
    in acute myeloid leukemia (AML) M2, 383
    in acute myelomonocytic leukemia, 392
    in chronic idiopathic myelofibrosis, 449–450
    in chronic lymphocytic leukemia (CLL), 142, 287
    in essential thrombocythemia (ET), 443
    in hepatosplenic lymphoma, 316
    in LGL (large granular lymphocytic) neoplasia, 306
    in lymphoblastic lymphoma, 275
    in MDS/MPD, 461, 465
    in NK-cell leukemia, 310
    in polycythemic vera (PV), 442
  hepatosplenic lymphoma, 316–318, 317f
  Hodgkin's lymphoma in, 499
  horse, chronic lymphocytic leukemia (CLL) in, 293f–294f
  human, Hodgkin's lymphoma in, 496f
  large cell lymphoma, 353f
  lymphoblastic lymphoma (LBL), 282, 283f
  lymphoplasmacytic lymphoma (LPL), 212, 213f
  mantle cell lymphoma (MCL), 234, 235f
  mouse
    acute lymphoblastic leukemia (ALL), 135f
    chronic myeloid leukemia, 434f–435f
    essential thrombocythemia (ET), 447f
    neonatal, 98f
  pig, erythropoiesis in, 47–48, 53
  prolymphocytic leukemia (PLL), 163
  small lymphocytic lymphoma (SLL), 155
  in T-cell rich large B-cell lymphoma (TCRLBCL), 269
Loefflers syndrome, 440
Lollipop vascular lesion, 34, 34f
Longevity, calorie restriction and, 84
Long terminal repeat (LTR) region, 347
LPL. *See* Lymphoplasmacytic lymphoma (LPL)
Lukes, R., 4–5
Lung
  cat
    granulocytic sarcoma (GS), 420f–421f
    pneumonia due to pancytopenia of refractory anemia, 480f
  dog
    angiotropic lymphoma, 358f
    lymphomatoid granulomatosis (LYG), 260f–261f
    megakaryoblastic leukemia, 416f
    myeloproliferative disease resembling juvenile CMML, 468f
  Hodgkin's lymphoma in, 499
  horse
    plasmablastic lymphoma, 245f, 246f
LYG (lymphomatoid granulomatosis), 240
Lymphadenopathy, 29
Lymph node
  acute myeloid leukemia (AML) (M0/M1), 377–378, 377f–378f
  acute myeloid leukemia (AML) M2, 386, 387f–388f
  anaplastic large cell lymphoma, 340f, 342f–344f
  angioimmunoblastic T-cell lymphoma (AILT), 312f–315f
  atrophy, 11f, 95f
  B-cell lymphoblastic lymphoma (B-LBL), 131, 133–134, 133f
  Burkitt's-like lymphoma, 140–141, 140f–141f
  Burkitt's lymphoma, 138–140, 138f–140f, 284f–285f
  cat
    acute myeloid leukemia (AML), 19f, 377f–378f
    anaplastic large cell lymphoma, 256f–257f, 340

Lymph node (*cont.*)
atrophy, 11f
capsule and peripheral sinus, 11f
chronic lymphocytic leukemia (CLL), 152f, 291f
cryptococcosis, 39f
diffuse large B-cell lymphoma (DLBCL), 253f
erythroleukemia, 406f
follicular hyperplasia, 18f, 31f, 32f
follicular lymphoma (FL), 220f, 222f
follicular polarity, 14f
granulocytic sarcoma (GS), 421f–422f
intestinal adenocarcinoma, 44f–45f
large granular lymphocytic lymphoma, 305f
lymphoblastic lymphoma, 353f
mammary adenocarcinoma, 44f
mantle cell cuff, 15f
panleukopenia virus infection, 35f–36f
paracortex, 12f, 31f, 32f
sclerosis, 12f
T-cell rich large B-cell lymphoma (TCRLBCL), 264f–265f, 268f, 271f, 494f
cattle
anthrax, 37f
atrophy, 19f
bovine viral diarrhea, 35f
lymphoma, 352f–353f
salmonellosis, 36f–37f
small cell lymphocytic lymphoma, 149f–150f, 352f
chronic idiopathic myelofibrosis, 453f
chronic lymphocytic leukemia (CLL), 152, 152f, 289–290, 289f–291f
chronic myeloid leukemia, 433
degenerative diseases, 28–29, 28f, 29f
developmental diseases, 27–28
diffuse large B-cell lymphoma (DLBCL), 240, 240f–246f, 245–251, 253f, 256f–257f
dog
afferent lymphatics, 10f
anaplastic large cell lymphoma, 256f
angioimmunoblastic T-cell lymphoma (AILT), 312f–314f
B-cell lymphoblastic lymphoma (B-LBL), 133f, 134f
benign medullary cord plasma cell hyperplasia, 189f
Burkitt's-like lymphoma, 140f–141f
Burkitt's-type lymphoma, 139f–140f
Castlemanlike proliferation, 34f
diffuse large B-cell lymphoma (DLBCL), 20f–21f, 29f, 240f–244f
diffuse small cell lymphoma intermediate type (DSLI), 147f
efferent lymphatics, 10f
enteric T-cell lymphoma, 326f
fading follicular hyperplasia, 32f
follicular architecture, 12f
follicular hyperplasia, 13f, 21f, 33f
follicular hypoplasia, 83f
follicular involution, 15f
follicular lymphoma (FL), 218f–221f
gastric adenocarcinoma, 41f
histiocytic sarcoma, 30f, 42f, 357f
hyperplasia, diffuse, 31f
immunoblastic lymphoma, 160f
lollipop vascular lesion, 34f
lymphoblastic lymphoma, 278f–281f
lymphoid proliferation, 11f
lymphoma, 358f
lymphoplasmacytic lymphoma (LPL), 209f, 211f
mantle cell lymphoma (MCL), 230f
marginal zone hyperplasia, 16f
marginal zone lymphoma, 17f–18f, 167f, 171f–174f, 181f
medullary structure, 11f
paracortex, 10f, 31f, 32f, 33f
paracortical hyperplasia, 13f
peripheral T-cell lymphoma, mixed cell type, 363f
plasmablastic lymphoma, 244f, 246f
plasmacytoma, 197f, 200f
prolymphocytic leukemia (PLL), 303f–304f
pulmonary adenocarcinoma, 43f–44f
sclerosis, 21f
small cell lymphocytic leukemia (SLL), 20f, 145f–147f
small lymphocytic leukemia (SLL), 153f
sternal node in hemorrhagic pleural effusion, 46f
systemic anaplastic large cell lymphoma of T-cell type, 342f–343f
T-zone lymphoma (TZL), 15f–16f, 184f–185f, 237f, 295f–300f
embryology, 9
in erythroleukemia, 405, 406f
follicular involution, 15f
follicular lymphoma (FL), 216f–223f, 217–222
function, 22–24
granulocytic sarcoma (GS), 421, 421f–422f
hairy cell leukemia, 166f
histiocytic sarcoma, 357f
Hodgkin's lymphoma
lymphocyte predominance type, 267f–268f
mixed cellularity type, 266f
nodular sclerosis type, 265f–266f
staging, 499
horse
chronic lymphocytic leukemia (CLL), 289f
lymphoplasmacytic lymphoma (LPL), 211f
plasmablastic lymphoma, 204f–205f, 244f–246f
human
anaplastic large cell lymphoma, 343f–344f
angioimmunoblastic T-cell lymphoma (AILT), 315f
Burkitt's lymphoma, 138f–139f, 284f–285f
chronic idiopathic myelofibrosis, 453f
chronic lymphocytic leukemia (CLL), 152f, 289f–290f
diffuse large B-cell lymphoma, 243f
follicular lymphoma, 216f–217f, 220f–221f, 223f
gastric MALT lymphoma, 182f–183f
hairy cell leukemia, 166f
Hodgkin's lymphoma
lymphocyte depletion type, 267f, 497f–498f
lymphocyte predominance type, 267f–268f, 492f–493f
mixed cellularity type, 266f, 496f–497f
nodular sclerosis type, 265–266f, 495f

Lymph node (*cont.*)
immunoblastic lymphoma, 160f
Langerhans cell histiocytosis, 511f
lymphoplasmocytic lymphoma, 207f
mantle cell lymphoma, 229f
marginal zone lymphoma, 182f
mycosis fungoides, 338f
peripheral T-cell lymphoma, 300f
plasmacytoma, 196f
prolymphocytic leukemia (PLL), 158f–1599, 163f
sinus histiocytosis, 522f
hyperplastic changes, 29–34
diffuse reactive hyperplasia, 30, 31f
follicular hyperplasia, 30–34, 31f–34f
immunoblastic lymphoma, 160f
large cell lymphoma, 354f
lymphadenitis
bacterial infection, 36–38, 36f–38f
fungal infection, 38, 39f
viral and protozoal infections, 34–36, 35f–36f
lymphoblastic lymphoma (LBL), 278–281, 278f–282f, 353f
lymphoplasmacytic lymphoma (LPL), 207f, 208–211, 209f–211f
mantle cell lymphoma (MCL), 167f, 229f–230f, 230–231, 237f
marginal zone lymphoma (MZL), 171–173, 171f–174f, 181f–184f, 183f–184f
metastatic neoplasm
histopathology, 42–45, 42f–46f
mechanisms of metastasis, 40
sentinel node detection, 41–42
mouse
acute lymphoblastic leukemia, 281f–282f
diffuse large B-cell lymphoma (DLBCL), 243f
essential thrombocythemia (ET), 448f
MuLV infection, 92f
plasmablastic lymphoma, 245f
tingible body, 221f
myeloma, 199
peripheral T-cell lymphoma, mixed cell type, 363f
plasmablastic lymphoma, 204f–205f
plasmacytoma, 196f–197f, 199, 200f
prolymphocytic leukemia (PLL), 158f–159f, 162–163, 163f, 303
rat
hyperplasia, 13f
paracortical hyperplasia, 28f
sinus histiocytosis, 522, 522f
small lymphocytic lymphoma (SLL), 145f–147f, 149f–150f, 152, 152f–153f
structure, normal and benign reactive, 9–21
afferent lymphatics, 9–10, 10f
calf, 19f
capsule, 10–11, 10f, 11f
cat, 11f–12f, 14f–15f, 18f–19f
cortex, 10f, 11–17, 11f–17f
dog, 10f–13f, 15, 15f–18f, 20f–21f
efferent lymphatics, 9–10, 10f, 12
germinal centers, 11–17, 11f–17f
harbor seal, 19f
hyperplasia, 11f, 12f, 13, 13f, 15–18, 15f, 16f, 18f, 21f
lymphoid atrophy, 11f
mantle cells, 14–15, 15f, 16f
medulla, 11f, 17–19, 18f–21f, 21
medullary sinus, 11f, 12, 19, 19f, 20f, 21, 21f
paracortex, 10f, 12f, 13f
peripheral sinus, 11f, 14
pig, 10, 10f
rat, 12, 13f
T-cell rich large B-cell lymphoma (TCRLBCL), 263–267, 263f–268f
T-zone lymphoma (TZL), 184f–185f, 294–297, 295f–301f
Lymph node biopsy
choice of node for, 24–25
diagnostic cytopathology, 26
fine needle aspiration, 25
FISH, 27
flow cytometry, 27
intraoperative procedures, 26–27
misdiagnosis, causes of, 24
sampling process, 25–26, 25f
transport media, 26
Tru-cut, 25
Lymphoblastic lymphoma (LBL)
B-cell (B-LBL)
cell of origin, 135–136
clinical presentation and features, 125, 127
definition, 124
diagnostic criteria, 136
differential diagnosis, 136
pathologic features
lymph node, 131, 133–134, 133f, 134f
spleen, 134
staging, 136
Burkitt's lymphoma distinguished from, 141
T-cell (T-LBL)
cell of origin, 284
clinical presentation and features, 275
cytogenetic and molecular features, 283–284
definition, 275
diagnostic criteria, 284–285
differential diagnosis, 284–285, 284f–285f
epidemiology and features, 275
evaluation of the treated animal, 285
immunologic features, 283
pathologic features, 275–283
lymph node, 278–281, 278f–282f
other organs, 282–283, 283f
spleen, 282
staging, 285
transformation and progression, 285
treatment and survival, 285
Lymphoid structure of the spleen, 50–53, 50f–53f
Lymphoma. *See also specific types*
definition, 119
intermediate cell type, 227
leukemia distinguished from, 119
Lymphomatoid granulomatosis (LYG), 240, 260–261, 260f–261f

Lymphomatoid papulosis, 345, 345f
Lymphomatous polyposis, 228
Lymphoplasmacytic enteritis, 318
Lymphoplasmacytic lymphoma (LPL), 207–214
  cell of origin, 213
  clinical presentation and features, 207
  cytogenetic and molecular features, 213
  definition, 207
  diagnostic criteria, 213–214
  differential diagnosis, 214
  epidemiology and incidence, 207
  evaluation of the treated animal, 214
  immunologic features, 212
  pathologic features, 207–212, 208f–213f
    blood, 207–208
    bone marrow, 208, 209f
    lymph node, 207f, 208–211, 209f–211f
    other organs, 212
    spleen, 211–212, 211f–212f
  staging, 214
  transformation and progression, 214
  treatment and survival, 214
Lymphoproliferative diseases, 119–124
  acute lymphoblastic leukemia (ALL)
    L1 type, 120, 120f, 121
    L2 type, 120, 121, 121f
    L3 type, 120–121, 121f–122f
  classification algorithms, 122t, 123t
  definition, 119
  FAB (French-American-British) classification system, 120
  leukemia and lymphoma presentations, 119
Lysosomal storage diseases, 64, 113–114
Lysosomes
  in Chédiak Higashi anomaly, 110
  dendritic, 22
Lysozyme, 72, 73f, 506
LYVE-1 receptors, 9

M
M6A (erytholeukemia), 401–406
Macaque
  adrenal gland
    diffuse large B-cell lymphoma (DLBCL), 243f
  bone marrow
    hematopoiesis in, 101f
    starvation, 115
  simian immunodeficiency virus, 91–92, 93f–96f
  spleen, follicular hyalinosis, 64f
  thymus, 91–92, 93f–96f
MacEwen, E.G., 456
Macrophage colony-stimulating factor (M-CSF), 505
Macrophages
  hemosiderin, 56f, 65, 65f, 66f, 69f, 73f, 101, 106f, 252, 376f–377f
  in mantle cell lymphoma (MCL), 230
  in Niemann-Pick disease, 114
  proliferation, 506
  pseudo-Gaucher cells, 428
  splenic, 53–54
  thymic, 79
  tingible body, 221, 230, 407
Macroschizonts, 36
Mahaffey, E.T., 455
Major Histocompatibility Complex. *See* MHC
Malignant catarrhal fever (MCF), 35
Malignant fibrous histiocytoma, 73
Malignant histiocytosis, 517
Malignant myelosclerosis, 454
Mallory, T.B., 4
Malnutrition, 114–115
MALT (mucosal associated lymphoid tissue lymphoma), 119, 168, 171, 177, 178f, 180, 182, 182f–183f, 185, 187f, 188
Mammary adenocarcinoma, 44f
Mantle cell cuffs, in follicular hyperplasia, 31–32, 31f–32f
Mantle cell hyperplasia (MCH), 74, 74f
Mantle cell lymphoma (MCL), 146, 147f–148f, 164, 166f–167f, 227–238
  cell of origin, 236
  clinical presentation and features, 227–230
  cytogenetic and molecular features, 235–236
  definition, 227
  diagnostic criteria, 236
  differential diagnosis, 236, 237f
  epidemiology and incidence, 227
  evaluation of the treated animal, 237
  immunologic features, 230–234, 230f–235f, 234–235, 236f
  marginal zone lymphoma distinguished from, 185, 185f–186f
  pathologic features, 230–234, 230f–235f
    blood, 230
    bone marrow, 230
    lymph nodes, 229f–230f, 230–231, 237f
    other organs, 234
    spleen, 227f–229f, 231–234, 231f–236f
  spleen, 55f, 58, 200, 201f, 227f–229f, 231–234, 231f–236f
  staging, 236–237
  transformation and progression, 237
  treatment and survival, 237–238
Mantle cells
  lymph node, 14–15, 15f, 16f, 23–24
  spleen, 52f, 53, 69–70, 71f
Marasmus, 114, 115
Marginal zone cells
  benign, 24
  description, 15–17
  hyperplasia, 15–17, 16f
  as memory cells, 24
  spleen, 50–53, 52f
Marginal zone hyperplasia (MZH), 15–17, 16f
  lymph node, 93f
  spleen, 67f, 68f, 69–70, 70f, 71f, 74, 75f, 94f
Marginal zone lymphoma (MZL), 17f–18f, 164, 167f, 168–188, 168f–188f
  cell of origin, 181–182
  clinical presentation and features, 169–170
  cytogenetic and molecular feature, 180–181

Marginal zone lymphoma (MZL) *(cont.)*
definition, 168
diagnostic criteria, 183–184
differential diagnosis, 184–185
diffuse large B-cell lymphoma (DLBCL) distinguished from, 257
epidemiology and incidence, 168–169
evaluation of the treated animal, 187–188
immunologic features, 178, 180
marginal zone hyperplasia compared, 16–17
pathologic features, 170–178, 171f–181f
blood, 170–171
bone marrow, 171, 172f
lymph node, 171–173, 171f–174f, 181f–184f
other organs, 177–178
salivary gland, 177, 178f
spleen, 169f–171f, 173–174, 174f–177f, 176–177, 179f–180f, 186f–187f
spleen, 52, 58, 74–75, 169f–171f, 173–174, 174f–177f, 176–177, 179f–180f, 186f–187f
staging, 185–186
transformation and progression, 187
treatment and survival, 188
Marginal zone neoplasia, 24
Marmoset, 449
Maroteaux-Lamy Syndrome, 114
Marrow granulocyte reserves (MGR), 103–104
Mast cell tumor (MCT), 77f, 204, 205f, 456–457, 457f–459f
Mastitis, lymph node changes in, 11
Mature (peripheral) nodal T-cell (T-zone) lymphoma. *See* T-zone lymphoma (TZL)
MCF (malignant catarrhal fever), 35
MCH (mantle cell hyperplasia), 74, 74f
MCL. *See* Mantle cell lymphoma (MCL)
M-CSF (macrophage colony-stimulating factor), 505
MCT. *See* Mast cell tumor (MCT)
Mediastinal large B-cell variant of large B-cell lymphomas, 248–250, 248f–250f
Medullary cord atrophy, 19f
Medullary cord plasma cell hyperplasia, 18f
Medullary sinus structure, normal and benign reactive, 11f, 12, 19, 19f, 20f, 21, 21f
Megakaryocytes, 19f
acute megakaryoblastic leukemia M7, 412–416, 412f–416f
in acute myeloid leukemia (AML) (M0/M1), 376f, 377–378, 378f, 379
in acute panmyelosis with myelofibrosis, 417–418, 418f
in chronic idiopathic myelofibrosis, 449, 450, 450f, 453–454
in chronic lymphocytic leukemia (CLL), 144
in chronic myeloid leukemia, 427f, 428, 433
dwarf, 412
in erythroid leukemia, 407, 410
in essential thrombocythemia (ET), 443, 443f–444f, 445, 446f–448f, 447
in lymphoplasmacytic lymphoma (LPL), 208
micromegakaryocytes, 412, 450, 452, 461, 481
in myelodysplastic syndromes, 473, 475f, 480, 484
spleen, 68, 68f
Melan A, 43
Melanoma
amelanotic, 204
cell of origin, 202
clinical presentation and features, 192, 197–198, 197f–198f
cytogenetic and molecular features, 202
definition, 189, 190–191
diagnostic criteria, 203–204
differential diagnosis, 204, 205f
epidemiology and incidence, 191–192
evaluation of the treated animal, 206
immunologic features, 202
pathologic features
blood, 198, 199f
bone marrow, 190f–191f, 197f–198f, 198–199
lymph node, 199
staging, 205–206
transformation and progression, 206
treatment and survival, 206
Melphalan, for myeloma, 206
Memory cells, marginal zone cells as, 24
Mercury, myelodysplastic changes from, 115
Metamyelocytes
in acute myeloid leukemia (AML) M2, 383–384, 384f–385f, 387f
in acute promyelocytic leukemia (APL), 389
in chronic myeloid leukemia, 426, 426f, 427, 431f, 433, 433f
in chronic myelomonocytic leukemia (CMML), 463, 464f, 465, 465f
in erythroleukemia, 404
in essential thrombocythemia (ET), 445
Metarubricyte
in chronic myeloid leukemia, 428f
in erythroid leukemia, 407, 407f
Metastatic neoplasms
lymph nodes, 40–45
histopathology, 42–45, 42f–46f
sentinel node detection, 41–42
mechanisms of metastasis, 40
organ specificity, 40
splenic, 76–77, 77f
MG (myasthenia gravis), 79, 88–90
MGR (marrow granulocyte reserves), 103–104
MHC
class II, 505–506, 508, 510, 514, 515
graft *versus* host disease, 99
polymorphism, 80
restriction, 80–81
Micromegakaryocytes, 412, 450, 452, 461, 481
Mixed cellularity HL, 496–497, 497f
MMM (myeloid metaplasia with myelofibrosis), 434
Moesin-ALK fusion gene, 340
Monoclonal gammopathy of undetermined significance (MGUS), 191
Monocytes
acute monoblastic leukemia M5A, 395–399, 396f–398f
acute monocytic leukemia M5B, 399–400, 399f–400f
acute myelomonocytic leukemia M4, 391–393, 392f–395f

Monocytes (*cont.*)
chronic myeloid leukemia, 427, 430, 431f, 432
chronic myelomonocytic leukemia (CMML), 462–466, 463f–465f
juvenile myelomonocytic leukemia (jMML), 467–468, 468f–471f, 471
Monocytoid B-cells, 168
Monostotic lesion, 199
Mott-type plasma cells, 56f
Mouse
bone marrow
chronic myeloid leukemia, 435f–436f
development, 98, 98f
myelodysplasia, 487f
Chédiak Higashi anomaly, 111f
essential thrombocythemia (ET), 447, 447f
liver
acute lymphoblastic leukemia (ALL), 135f
chronic myeloid leukemia, 434f–435f
essential thrombocythemia (ET), 447f
neonatal, 98f
lymph node
acute lymphoblastic leukemia, 281f–282f
diffuse large B-cell lymphoma (DLBCL), 243f
essential thrombocythemia (ET), 448f
MuLV infection, 92f
plasmablastic lymphoma, 245f
tingible body, 221f
lymphoma
diffuse mixed cell type, 269f
murine leukemia virus (MuLV) infection, 91, 91f–93f
small intestine
chronic myeloid leukemia, 436f
spleen
acute lymphoblastic leukemia, 282f
anaplastic plasmacytoma, 199f
chronic myeloid leukemia, 435f
essential thrombocythemia (ET), 447f
hematopoiesis, 47
murine leukemia virus (MuLV), 91f–92f
myelodysplasia, 488f
neonatal, 99f
structure, 47f
tingible body, 223f
spleen colony technique, 101–102, 102f
thymus
atrophy, 93f
hyperplasia, 88, 88f
MuLV infection, 93f
structure, 78f
MPO. *See* Myeloperoxidase (MPO)
MPS (mucopolysaccharidoses), 113, 114
Mucolipidoses, 113
Mucopolysaccharidoses (MPS), 113, 114
Mucosal associated lymphoid tissue (MALT) lymphoma, 119, 168, 171, 177, 178f, 180, 182, 182f–183f, 185, 187f, 188
Multicentric Castleman's Disease, 119
Multiple myeloma, 190
Murine leukemia virus (MuLV), 91, 91f–93f
Myasthenia gravis (MG), 79, 88–90
Mycoplasma haemocanis, 48, 66
Mycosis fungoides (MF), 135, 331–337, 331f–339f
Mycotoxins, bone marrow effects on, 116
Myelocyte bulge, 426, 426f, 428
Myelodysplastic/myeloproliferative diseases (MDS/MPD), 461–471
atypical chronic myeloid leukemia (aCML), 461
chronic myelomonocytic leukemia (CMML), 462–466, 463f–466f
classification, 461, 467
juvenile myelomonocytic leukemia (jMML), 467–468, 468f–471f, 471
MDS conditions compared, 461
overview, 461
Myelodysplastic syndromes, 473–488
differential diagnosis, 486–487, 487f–488f
genetic abnormalities associated with, 484–485
management, 488
overview, 473–474
prognosis, 487–488
refractory anemia
with excess blasts (RAEB), 477–480, 478f–480f
with ringed sideroblasts (RARS), 477, 477f
without ringed sideroblasts (RA), 475–476, 475f–476f
refractory cytopenia with multilineage dysplasia, 478, 481–482, 481f–482f
unclassified cases, 483–486, 484f–486f
Myelofibrosis, with acute panmyelosis, 417–418, 417f–419f
Myelogene, 425
Myeloid:erythroid (M:E) ratios, in chronic eosinophilic leukemia (CEL), 437
Myeloid metaplasia with myelofibrosis (MMM), 434, 449
Myelokathexis, 462
Myelolipoma, 68, 69f, 71f, 227, 227f
Myeloma
kidney, 202
phenotypic escape, 206
Myeloperoxidase (MPO), 27
acute monocytic leukemia, 400
acute myeloid leukemia (AML), 372, 372f, 374, 380, 381, 385, 387
acute myelomonocytic leukemia, 392
acute promyelocytic leukemia, 390
granulocytic sarcoma, 423
Myelophthisic thrombocytopenia, 125
Myelopoiesis, development of, 98. *See also* Hematopoiesis
MZH. *See* Marginal zone hyperplasia (MZH)
MZL. *See* Marginal zone lymphoma (MZL)

N

Naming systems for hematopoietic neoplasms, 3–7
N-butyl acetate esterase, for acute monocytic leukemia M5A, 398f
Necrosis factor kB, 238
Neospora, 36
Neumann, 425
Neurovisceral storage disease, 64

Neutrophil/lymphocyte (N:L) level, 104
Neutrophils
in Chédiak Higashi anomaly, 111, 111f
in chronic myeloid leukemia, 426, 426f, 427, 428f, 430, 431f, 432, 432f, 433, 433f
in chronic myelomonocytic leukemia (CMML), 463–464, 465–466
in chronic neutrophilic leukemia, 434–435, 434f–436f
in juvenile myelomonocytic leukemia (jMML), 467
in myelodysplastic syndromes, 473
neutropenia
congenital, 106
cyclic, 106
inflammation-associated, 103
neutrophilia, inflammation-associated, 103
in polycythemic vera (PV), 441f
splenic, 53
Niemann-Pick disease (NPD), 114
NK-cell neoplasms
aggressive NK-cell leukemia, 309–310, 309f
blastic NK-cell lymphoma, 310–311, 310f, 311f
NK-cells, 41
activation, 99
deficiency, 82
Nodular lymphocyte predominance Hodgkin's lymphoma (NLPHL), 491, 492–493, 492f–493f
Nonspecific esterase (NSE) reaction, 372, 392, 393, 394f
NPD (Niemann-Pick disease), 114
NPM (nucleophosmin) gene, 339–340
NSE. *See* Nonspecific esterase (NSE) reaction
Nuclear factor (NF)-κB, 347
Nu gene, 28
Nutritional diseases of bone marrow, 114–115, 115f

O

Organomegaly, in MDS/MPD, 461, 465
Organ specificity of metastases, 40
Ornithodorus coriaceous, 96
Osteosarcoma, splenic metastatic, 76f, 77f

P

P181NK4c, 347
Pagetoid reticulosis (PR), 331, 331f–332f, 336f–337f
PALS. *See* Periarteriolar lymphoid sheath (PALS)
Panleukopenia virus infection, 35, 35f–36f, 101, 102f
Panmyelosis, acute, 417–418, 417f–419f
Pappenheimer bodies, 477
Paracortex, lymph node, 10f, 12f, 13f
Paracortical hyperplasia, 12f, 13f
Paraneoplastic production of parathormone type products, 285
Pararectal plasmacytoma, 194f–195f
Parker, F. Jr., 4
PAS (periodic Schiff stain), 38, 39f, 414, 480
Pauling, Linus, 108
Pautrier's microabscess, 331
PAX5 gene, 213
PBB, thymic toxicity and, 84
PCB, thymic toxicity and, 84
PCR (polymerase chain reaction), for B-cell acute lymphoblastic leukemia (B-ALL) detection, 136
Pearl disease, 38
Pelger-Huët anomaly, 110, 461, 484
Perforin, 329
Periarteriolar lymphoid sheath (PALS), 50, 51f, 52, 53f, 64f, 67f–70f, 70, 71f, 90, 95f, 97, 223f, 290–291, 291f, 378, 378f, 410
Periodic Schiff stain (PAS), 38, 39f, 414, 480
Periodontal disease, lymph node changes in, 11
Peripheral sinus, lymph node, 9, 11f, 14
Peripheral T-cell lymphoma, not otherwise specified (PTCL, NOS), 298, 360–364, 361f–364f
Phenylaminopyrimidine, 425
Phthisis, 143f, 199, 263, 376, 377, 389, 403, 413, 451, 451f
PIE (pulmonary infiltrates with eosinophilia), 440
Pig
acute myeloid leukemia (AML), 374
African swine fever, 35
Bracken fern toxicity, 116
diffuse large B-cell lymphoma, 251
enteropathy-type T-cell lymphoma, 319
erythropoiesis in liver, 47–48, 53
hog cholera, 35, 93, 96
lymph node structure, 10f
pseudorabies virus, 69
T-cell rich large B-cell lymphoma (TCRLBCL), 262
Pinkus, G.S., 361
Plasmablastic lymphoma, plasmacytoma distinguished from, 204, 204f–205f
Plasmablastic variant of DLBCL, 244–246, 244f–247f
Plasma cell hyperplasia, 18f
Plasmacytoma, 189–206
anaplastic, 203
cell of origin, 202
clinical presentation and features, 192, 192f–198f, 197–198
cutaneous, 457
cytogenetic and molecular features, 202
definition, 189–191
diagnostic criteria, 202–204
differential diagnosis, 204
epidemiology and incidence, 191–192
evaluation of the treated animal, 206
immunologic features, 202
pathologic features, 198–202
blood, 198
bone marrow, 198–199
lymph node, 196f–197f, 199, 200f
other organs, 201
spleen, 196f, 200–201, 200f–201f
staging, 205–206
transformation and progression, 206
treatment and survival, 206
Platelet-derived collagenase inhibitors, 449
Platelet-derived growth factor, 449
Platelets. *See also* Thrombocytopenia
in chronic idiopathic myelofibrosis, 449
in essential thrombocythemia (ET), 443–445, 447–448
Pleural effusion, 45, 46f

PLL. *See* Prolymphocytic leukemia (PLL)
PML (promyelocytic leukemia) gene, 389
Polioencephalomalacia, 116
Polycythemia vera
  blood, 441–442, 441f
  overview, 440–441
Polymerase chain reaction (PCR), for B-cell acute lymphoblastic leukemia (B-ALL) detection, 136
Polystotic lesion, 199
Popcorn type RS cells, 492, 493, 493f, 499
Popliteal lymph node, biopsy of, 24–25
Porphyria, 486
PR. *See* Pagetoid reticulosis (PR)
Preleukemic syndrome, 462
Prescapular lymph node, biopsy of, 24–25
Primary effusion lymphoma variant of DLBCL, 250–251, 250f
Primary foci, 23
Programmed cell death, B-cell, 23. *See also* Apoptosis
Proliferation centers, 150, 287
Prolymphocytic leukemia (PLL), 155f, 156, 157–158, 158f–159f
  cell of origins, 164
  clinical presentation and features, 161
  cytogenetic and molecular features, 164
  definition, 161
  diagnostic criteria, 164
  differential diagnosis, 164
  epidemiology and incidence, 161
  immunologic features, 163
  pathologic features, 162–163
    blood, 162, 162f
    bone marrow, 162, 162f–163f
    lymph nodes, 162–163, 163f
    other organs, 163
    spleen, 163, 164f
  staging, 164, 168
  T-cell, 302–304, 303f–304f
  transformation and progression, 168
  treatment and survival, 168
Promyelocytes
  in acute myeloid leukemia (AML) M2, 383–384, 384f, 387
  in acute promyelocytic leukemia (APL), 389–390, 391f–392f
  in basophil leukemia, 455–456
  in chronic myeloid leukemia, 428, 428f, 430, 431f, 432f, 433
  in eosinophilic leukemia, 439f
Proteasome inhibitor, for mantle cell lymphoma (MCL), 238
Proteinuira, 199
Prox-1 gene, 9
Pseudo-Gaucher cells, 428
Pseudo-Pelger-Huët, 466, 473
Pseudorabies virus, 69
Pulmonary adenocarcinoma, 43f
Pulmonary hypertrophic osteopathy, 451
Pulmonary infiltrates with eosinophilia (PIE), 440
Puppy strangles, 83f
Pure erythroid leukemia (M6B), 406–411
  blood, 406–407, 406f–408f
  bone marrow, 407–409, 408f–410f
  classification, 401–402
  definition, 402
  epidemiology and incidence, 402
  liver, 409–410, 410f
  spleen, 410, 410f–411f
Purine analogs
  for lymphoplasmacytic lymphoma (LPL), 214
  for mantle cell lymphoma (MCL), 238
Pyometra, canine, 68, 70f
Pyruvate kinase deficiency, 109, 109f–110f

R

Rabbit, small lymphocytic leukemia (SLL) in, 152f–153f
RAEB (refractory anemia with excess blasts), 477–480, 478f–480f
Rai system, 157
Rappaport, Henry, 4, 134
RARA retinoic acid receptor-alpha gene, 389
RARS (refractory anemia with ringed sideroblasts), 477, 477f
RAS gene, 467
Rat
  blood
    large granulocytic leukemia, 308f
  bone marrow structure, 100f
  lymph node
    hyperplasia, 13f
    paracortical hyperplasia, 28f
  spleen
    splenic hematopoiesis, 47
    structure, 48f, 50, 51f
  thymus, 84f–85f
REAL/WHO classification system, 5–6, 6t
  leukemia/lymphoma distinction, 119119
  T-cell rich large B-cell lymphoma (TCRLBCL), 260
Refractory anemia
  with excess blasts (RAEB), 477–480, 478f–480f
  with ringed sideroblasts (RARS), 477, 477f
  with severe dysplasia, 481
  without ringed sideroblasts (RA), 475–476, 475f–476f
Refractory cytopenia with multilineage dysplasia, 478, 481–482, 481f–482f
Rennin, 53
Reticular dysgenesis, 105
Reticular type RS cell, 497–498
Reticulin, 222, 263f, 417, 426, 433, 451, 452, 452f, 479
Reticuloendothelial system (RES), 119
Revised European American Classification of Lymphoid Neoplasms (REAL). *See* REAL/WHO classification system
Rhabdomyosarcoma, 136
Ribozyme, 108
Rinderpest, 35
Ringed sideroblasts, 473, 477, 477f
Rituximab
  for lymphoplasmacytic lymphoma (LPL), 214
  for T-cell rich large B-cell lymphoma (TCRLBCL), 272
Robb-Smith, A.H.T., 3
Rosetting pattern, 492
RS (Reed-Sternberg) cell

RS (Reed-Sternberg) cell (*cont.*)
as hallmark of Hodgkin's lymphoma, 491
harvesting with laser capture microscope, 491
in Hodgkin's-like lymphoma in animals, 499, 500f
immunoglobulin gene rearrangements, 491
morphology, 491–492
phenotypic characteristics, 492
types
classic, 265
diagnostic, 492, 499
lacunar, 265, 266, 492, 493, 494, 495, 495f
L&H or popcorn, 265–266, 267, 492, 493, 493f, 499
reticular, 497–498
Rubricytes
in chronic myeloid leukemia, 428f
in chronic myelomonocytic leukemia (CMML), 464, 465f–466f
in erythroid leukemia, 402–404, 406–410
in myelodysplastic syndromes, 473, 475–477, 475f–480f
ringed sideroblasts, 473, 477, 477f
Russell bodies, 56f

S
Said, J.W., 361
Salivary gland, MALT lymphoma of, 177, 178f, 187f
Salmonellosis, 36, 36f, 68, 70f
Sarcoma, granulocytic, 419–423, 420f–423f
Sarcosporidiosis, 36
Schalm, Oscar, 104
SCID (severe combined immunodeficiency), 28, 81–83
Sclerosis
lymph node, 12f
nodular sclerosis of Hodgkin's lymphoma (HL), 265–266, 265f–266f, 266–267, 267, 267f–268f, 494–495, 495f–496f
spleen, 73f
Seal, lymph node atrophy in, 19f
Secondary immune response, 23
Secondary lymphoid chemokine (SLC), 9
Sentinel node detection of metastatic cancer, 41–42
Septicemia, 70f
Septic shock, 69f
Serum response factor, 347
Severe combined immunodeficiency (SCID), 28, 81–83
Sézary syndrome, 135, 331–337, 332f–333f, 338f
SFFV (spleen focus forming virus), 401
Sheathed capillaries, 48
Sheep
Bracken fern toxicity, 116
caseous lymphadenitis, 38
glucosylceramidase deficiency, 64
Johne's disease, 37
malnutrition, 114, 115
splenic function, 56
splenic torsion, 66
Sherman, I.J., 108
Sickle cell anemia, 108, 108f
Sideroblasts, ringed, 473, 477, 477f
Siderotic nodules, 65
Simian immunodeficiency virus (SIV), 91–92, 93f–96f, 486
Sinus histiocytosis with massive lymphadenopathy (SHML), 521–522, 522f
Sinus vascular transformation, 29
Skunk, Hodgkin's-like lymphoma in, 499, 500f–501f
SLC (secondary lymphoid chemokine), 9
SLL. *See* Small lymphocytic lymphoma (SLL)
Small intestine
chronic myeloid leukemia, 435, 436f
enteric epitheliotropic infiltration, 322f
lymphoma, 351f
lymphoplasmacytic lymphoma (LPL), 208f
myeloproliferative disease, 470f–471f
Small lymphocytic lymphoma (SLL), 142–160
cell of origin, 157
clinical presentation and features, 142–143
cytogenetic and molecular features, 156–157
definition, 142
diagnostic criteria, 157
differential diagnosis, 157
epidemiology, 142
evaluation of treated animal, 160
immunologic features, 155–156
incidence, 142
mantle cell lymphoma (MCL), 146, 147f–148f
pathologic features
blood, 145–146, 145f–149f
bone marrow, 149, 150
lymph node, 145f–147f, 152, 152f, 153f
other organs, 155
spleen, 152–153, 154f–155f
staging, 157
treatment and survival, 160
T-zone lymphoma distinguished from, 300–302
Small non-cleaved cell, 136
Small non-cleaved cell lymphomas, 140
Solitary osseous plasmacytoma, 189
Spherocytosis, hereditary, 109f
Sphingolipidoses, 113
Spleen
accessory, 62
acute lymphoblastic leukemia (ALL), 134, 134f, 282, 282f
acute megakaryoblastic leukemia, 415–416, 415f–416f
acute monoblastic leukemia, 397, 398f
acute myeloid leukemia (AML)
M0/M1, 378–379, 378f–379f
M2, 385–386, 386f–387f
basophil leukemia, 455
biopsy, 57–61
clinical presentation, 57
fine needle aspiration, 59
lesions, 57–59, 58f–61f
sample processing, 59–61
cat
acute myeloid leukemia (AML) (M0/M1), 378f–379f
benign reactive, 175f
chronic lymphocytic leukemia (CLL), 291f–292f
chronic myelogenous leukemia, 379f
diffuse large B-cell lymphoma (DLBCL), 253f–254f
erythroid leukemia, 410f–411f

Spleen (*cont.*)
erythroleukemia, 405f
hepatosplenic lymphoma, 316f–317f
immune hemolytic anemia, 175f
mantle cell lymphoma (MCL), 235f
marginal zone lymphoma (MZL), 177f, 180f
metastatic mast cell tumor, 77f
plasmacytoma, 196f
structure, 50
vascular system, 48
cattle
chronic lymphocytic leukemia (CLL), 154f
function, 56
salmonella septicemia, 70f
structure, 49f
torsion, 66
chronic idiopathic myelofibrosis, 449–450, 452
chronic lymphocytic leukemia (CLL), 152–153, 154f–155f, 155, 290–291, 291f–292f
chronic myeloid leukemia, 433, 435, 435f
degenerative diseases, 63–66, 63f–66f
developmental diseases, 62, 62f–63f
diffuse large B-cell lymphoma (DLBCL), 251–253, 251f–254f
dog
acute monoblastic leukemia, 398f
acute myeloid leukemia (AML) M2, 386f–387f
atrophy, 67f
benign reactive, 174f–175f
chronic dermatitis, 64f
chronic idiopathic thrombocytopenic purpura, 64f
chronic immune stimulation, 71f
chronic lymphocytic leukemia (CLL), 154f
congestion, 53f
diffuse large B-cell lymphoma, 251f–252f
fading follicular hyperplasia, 175f
fibrohistiocytic nodule, 58f, 72f, 187f–188f
focal nodular lymphoid hyperplasia, 60f
follicular hyperplasia, 71f
function, 55, 55f–57f
hemangiosarcoma, 57
hemophagocytic histiocytic sarcoma (HHS), 519f–521f
hemosiderosis, 65f
hepatosplenic lymphoma, 306f–307f, 317f
histiocytic sarcoma, 63f
hyperplasia, 67f–72f
immune thrombocytopenic purpura, 68f
juvenile CMML, 469f–470f
lymphoplasmacytic lymphoma (LPL), 211f–212f
macrophages, 56f
mantle cell lymphoma (MCL), 55f, 147f–148f, 148f, 166f–167f, 185f–186f, 201f, 227f–228f, 231f–234f, 236f
marginal zone hyperplasia, 75f
marginal zone lymphoma (MZL), 59f, 66f, 169f–171f, 179f–180f
mass with age, 48
megakaryoblastic leukemia, 415f
metastatic histiocytic sarcoma, 76f
metastatic osteosarcoma, 76f, 77f
myelolipomas, 60f, 65f, 69f, 71f, 72f
nodular lymphoid proliferation, 74f
periarteriolar lymphiod sheath, 67f–70f
plasmacytoma, 196f, 200f–201f
pyometra, 70f
sclerosis, 73f
septic shock, 69f–70f
small lymphocytic leukemia (SLL), 154f–155f
structure, 49f, 50, 51f–54f
torsion, 66
vascular system, 48
dysplastic changes, 70, 72–75, 72f–75f
embryology, 47–48, 47f
erythroid leukemia, 410, 410f–411f
erythroleukemia, 404, 405f
essential thrombocythemia (ET), 447, 447f
fibrohistiocytic nodule, 187f–188f, 200
follicular hyperplasia, 94f
follicular lymphoma (FL), 222–224, 222f–223f
function, 54–57, 55f–57f
hairy cell leukemia, 165f–166f
hepatosplenic lymphoma, 316–318, 316f–317f
Hodgkin's lymphoma in, 499
horse
diffuse large B-cell lymphoma (DLBCL), 252f–253f
follicular hyperplasia, 87f
function, 56
small lymphocytic leukemia (SLL), 154f
human
diffuse large B-cell lymphoma, 254f
diffuse large B-cell lymphoma (DLBCL), 254f
follicular lymphoma, 222f–223f
hairy cell leukemia, 165f
hepatosplenic lymphoma, 306f
mantle cell lymphoma, 228f–229f
mycosis fungoides, 339f
prolymphocytic leukemia (PLL), 155f, 164f
hyperplasia, 67–70, 67f–72f
lymphoblastic lymphoma (LBL), 134, 282
lymphoplasmacytic lymphoma (LPL), 211–212, 211f–212f
macaque, follicular hyalinosis, 64f
mantle cell lymphoma (MCL), 166f–167f, 185f–186f, 201f, 227f–229f, 231–234, 231f–236f
marginal zone lymphoma (MZL), 168–171, 169f–171f, 173–174, 174f–177f, 176–177, 179f–180f, 186f–187f
metastatic neoplasms, 76–77, 77f
mouse
acute lymphoblastic leukemia, 282f
anaplastic plasmacytoma, 199f
chronic myeloid leukemia, 435f
essential thrombocythemia (ET), 447f
hematopoiesis, 47
murine leukemia virus (MuLV), 91f–92f
myelodysplasia, 488f
neonatal, 99f
structure, 47f
tingible body, 223f

Spleen (*cont.*)
plasmacytoma, 196f, 200–201, 200f–201f
prolymphocytic leukemia (PLL), 155f, 163, 164f
rat
splenic hematopoiesis, 47
structure, 48f, 50, 51f
small lymphocytic lymphoma (SLL), 148f, 152–153, 154f–155f
structure
lymphoid, 50–53, 50f–53f
sinus, 53–54
vascular, 48–49, 48f–49f
T-cell rich large B-cell lymphoma (TCRLBCL), 268, 269f
torsion, 66
trauma, 66
Spleen colony technique, 101–102, 102f
Spleen focus forming virus (SFFV), 401
Splenectomy, 54, 55f, 60, 60f, 66
Splenomegaly, 67
in acute lymphoblastic leukemia (ALL), 134, 134f
in acute megakaryoblastic leukemia, 412
in acute monoblastic leukemia M5A, 396
in acute monocytic leukemia, 399
in acute myeloid leukemia (AML) M2, 383
in acute myelomonocytic leukemia, 392
in acute panmyelosis, 417
in chronic idiopathic myelofibrosis, 449–450
in chronic lymphocytic leukemia (CLL), 142, 287
in chronic myeloid leukemia, 428, 430
in erythroid leukemia, 402, 410
in essential thrombocythemia (ET), 443
in hemophagocytic histiocytic sarcoma (HHS), 519
in hepatosplenic lymphoma, 316
in LGL (large granular lymphocytic) neoplasia, 306
in lymphoblastic lymphoma, 275
in mantle cell lymphoma (MCL), 237
in MDS/MPD, 461, 465–466, 467
in myelodysplastic syndromes, 484, 485
in Niemann-Pick disease, 114
in NK-cell leukemia, 310
in polycythemic vera (PV), 442
in prolymphocytic leukemia (PLL), 302
Splenosis, 62, 62f–63f
SPTCL (subcutaneous panniculitis-like T-cell lymphoma), 327–329, 327f–330f
Squaring-off artifact of formalin fixation, 284, 285f
ST1571, 425
Stachybotrys alternans, 116
Staging
B-cell acute lymphoblastic leukemia (B-ALL), 136
B-cell chronic lymphocytic leukemia (B-CLL), 157
B-cell lymphoblastic lymphoma (B-LBL), 136
chronic lymphocytic leukemia (CLL), 157
follicular lymphoma (FL), 225
Hodgkin's lymphoma, 498–499
lymphoblastic lymphoma, 136, 285
lymphoplasmacytic lymphoma (LPL), 214
mantle cell lymphoma (MCL), 236–237
marginal zone lymphoma (MZL), 185–186
melanoma, 205–206
plasmacytoma, 205–206
prolymphocytic leukemia (PLL), 164, 168
small lymphocytic lymphoma (SLL), 157
T-cell acute lymphoblastic leukemia, 285
T-cell rich large B-cell lymphoma (TCRLBCL), 272
Stem cells
in chronic idiopathic myelofibrosis, 449
congenitally defective, 105–106, 105f–106f
differentiation, lithium effect on, 107
differentiation and maturation in bone marrow, 103
hematopoietic (HSC)
in cord blood, 99
lineage committed, 99
long term (LT), 99
origin of, 98–99
short term (ST), 99
spleen colony technique, 101–102, 102f
transplantation, 105
polycythemic vera (PV), 440, 442
spleen colony technique, 101–102, 102f
stimulation, recombinant drugs for, 488
Steroid therapy, effect on thymus, 85
Subcutaneous panniculitis-like T-cell lymphoma (SPTCL), 327–329, 327f–330f
Submandibular lymph node, biopsy of, 24–25
Sudan Black-B (SBB), 27, 42
acute monocytic leukemia, 400
acute myeloid leukemia (AML), 372, 372f, 374, 380, 381, 387, 388f
acute myelomonocytic leukemia, 392
acute promyelocytic leukemia, 390
histiocytic sarcoma, 521
Surface immunoglobulin (sIg), 135–136
Synaptophysin, 43
Systemic histiocytosis (systemic reactive histiocytosis), 506, 514–515, 514f–515f

T

T1A-1$^+$, 329
T-ALL. *See* T-cell acute lymphoblastic leukemia (T-ALL)
Tax factor, 347
Tay-Sachs disease, 113
T cell
dendritic cell effect on, 22
differentiation, 80–81
immunodeficiency, 81
maturation, 80–81
selection, 80
splenic, 50–53
thymus, entry into, 79
T-cell acute lymphoblastic leukemia (T-ALL)
cell of origin, 284
clinical presentation and features, 275
cytogenetic and molecular features, 283–284
definition, 275
diagnostic criteria, 284–285
epidemiology and features, 275
evaluation of the treated animal, 285
immunologic features, 283

T-cell acute lymphoblastic leukemia (T-ALL) (*cont.*)
pathologic features, 275–283
blood, 275–277, 276f–277f
bone marrow, 277–278, 277f–278f
other organs, 282
spleen, 282, 282f
staging, 285
transformation and progression, 285
treatment and survival, 285
T-cell granular lymphocytic leukemia/lymphoma, 304–308, 305f–308f
T-cell neoplasms
adult T-cell lymphoma/leukemia, 346–350, 348f–354f
anaplastic large cell lymphoma (ALCL)
description, 339–341
primary cutaneous ALCL of T-cell type, 341, 341f–342f
primary systemic ALCL of T-cell type, 342–343, 342f–343f
chronic lymphocytic leukemia (CLL), 287–294
clinical presentation and features, 287
definition, 287
differential diagnosis, 292–293
epidemiology and features, 287
pathologic features, 287–292
blood, 287–288, 288f, 291f
bone marrow, 288–289, 290f
liver, 288f, 291–292, 293f–294f
lymph node, 289–290, 289f–291f
spleen, 290–291, 291f–292f
treatment and survival, 293
intravascular large T-cell lymphoma, 355–356, 356f–360f, 358–359
lymphomatoid papulosis (LYP), 345, 345f
mature nodal and extranodal T-cell lymphoma
angioimmunoblastic T-cell lymphoma (AILT), 312–315, 312f–315f
enteropathy-type T-cell lymphoma (ETCL), 318–326, 319f–326f
hepatosplenic T-cell lymphoma (HSTL), 316–318, 316f–318f
subcutaneous panniculitis-like T-cell lymphoma (SPTCL), 327–329, 327f–330f
mature (peripheral) neoplasms, 287–364
mycosis fungoides (MF)/Sézary syndrome, 331–337, 331f–339f
peripheral T-cell lymphoma (PTCL), not otherwise specified (NOS), 360–364, 361f–364f
precursor T-cell neoplasms (T-ALL and LBL)
cell of origin, 284
clinical presentation and features, 275
cytogenetic and molecular features, 283–284
definition, 275
diagnostic criteria, 284–285
differential diagnosis, 284–285, 284f–285f
epidemiology and features, 275
evaluation of the treated animal, 285
immunologic features, 283
pathologic features, 275–283
blood, 275–277, 276f–277f
bone marrow, 277–278, 277f–278f
lymph node, 278–281, 278f–282f
other organs, 282–283, 283f
spleen, 282, 282f
staging, 285
transformation and progression, 285
treatment and survival, 285
REAL classification, 6t
T-cell granular lymphocytic leukemia/lymphoma, 304–308, 305f–308f
T-cell prolymphocytic leukemia (PLL), 302–304, 303f–304f
T-zone lymphoma (TZL), 294–302
clinical presentation and features, 295
definition, 294
differential diagnosis, 300–302
epidemiology and features, 295
immunologic features, 297–298
pathologic features, 295–297, 295f–301f
transformation and progression, 299–300
treatment and survival, 302
T-cell receptor (TCR), 79
gene rearrangement, 157, 284
in precursor T-cell neoplasma, 283–284
in prolymphocytic leukemia (PLL), 304
in small lymphocytic leukemia (SLL), 157
T-cell rich large B-cell lymphoma (TCRLBCL), 240, 260–272, 491, 492, 493, 494, 494f
cell of origin, 271
clinical presentation and features, 262–263, 262f
cytogenetic and molecular features, 271
definition, 260
diagnostic criteria, 271
differential diagnosis, 272
epidemiology and incidence, 261–262
evaluation of the treated animal, 272
immunologic features, 270–271, 271f
pathologic features
blood, 263
bone marrow, 263
lymph node, 263–267, 263f–268f
other organs, 268–269, 269f–270f
spleen, 268, 269f
staging, 272
transformation and progression, 272
treatment and survival, 272
TCR/CD3 complex, 81
TCRLBCL. *See* T-cell rich large B-cell lymphoma (TCRLBCL)
TdT (terminal deoxynucleotidyl transferase, CD99), 284
Technium^{99m}, 41
Tetrahymena thermophila, 108
TGF beta, 449
Thalassemia, 108–109, 109f
Theileriasis (East Coast Fever), 36
Thiaminase, bone marrow effects, 116
Thrombocytopenia
in acute lymphoblastic leukemia (ALL), 277
in acute megakaryoblastic leukemia, 412
in acute monoblastic leukemia M5A, 396

Thrombocytopenia (*cont.*)
in acute myeloid leukemia (AML) M2, 383, 384
in acute myelomonocytic leukemia, 392
in acute promyelocytic leukemia (APL), 389
in chronic lymphocytic leukemia (CLL), 287
in chronic myeloid leukemia, 428, 430
in erythroid leukemia, 402
in hepatosplenic lymphoma, 316
in NK-cell leukemia, 310
underestimates of, 374
Thrombocytopenia, essential, 443–448, 443f–448f
Thrombopoietin (TPO), 449
Thy-1, 508, 510, 514
Thymoma, 88, 89f–90f
Thymus
acute myeloid leukemia (AML) (M0/M1), 379, 380f
autoimmune hyperplasia, 88–90, 88f–90f
cat
acute myeloid leukemia (AML) (M0/M1), 380f
involution, 86, 87f, 93
lymphoma, 348f
thymic remnant, 81f, 82f
cattle
bovine viral diarrhea (BVD), 85f
epizootic bovine abortion, 96f–97f
degenerative diseases, 84–87, 84f–87f
developmental diseases, 81–83, 81f–83f
dog
B-cell nodule, 79f
hypoplasia, 82f–83f
idiopathic hemorrhagic infarction, 85f
thymoma, 89f–90f
embryology, 78–79, 78f–79f
function, 80–81
horse
EHV-induced involution, 86f
thymic atrophy, acute lymphoblastic leukemia (ALL) L3, 135f
thymic involution, 85–86, 86f
inflammation, infectious, 91–97, 91f–97f
canine distemper virus, 97
epizootic bovine abortion (EBA), 96, 96f–97f
feline immunodeficiency virus (FIV), 91
hog cholera, 93, 96
murine leukemia virus (MuLV), 91, 91f–93f
simian immunodeficiency virus (SIV), 91–92, 93f–96f
involution, 84, 85–86, 91, 93f, 96
lymphoma, 348f
macaque, 91–92, 93f–96f
mouse
atrophy, 93f
hyperplasia, 88, 88f
MuLV infection, 93f
structure, 78f
rat, 84f–85f
thymic remnant, 78f, 81, 81f, 82f
Tide marks, 278
Tingible body macrophages, 221, 230
Titan antigen, 88
TNF-α (tumor necrosis factor α), 505
Topotecan, for myelodysplastic syndromes, 488
Torsion, splenic, 66
Toxic effects on bone marrow, 115–116
Toxoplasmosis, 36
TPM3 nonmuscle tropomyosin, 340
TPO (thrombopoietin), 449
Transactivation, 347
Transport media, 26
Tru-cut biopsy, 25
Trypanosomiasis, bovine, 32, 49, 69
Tryptase, 457
Tuberculosis, 37
Tumor necrosis factor α (TNF-α), 505
Tyrosine kinase
Bcr-Abl, 425
signaling system, 81
T-zone lymphoma (TZL), 15f, 294–302
clinical presentation and features, 295
definition, 294
differential diagnosis, 300–302
epidemiology and features, 295
immunologic features, 297–298
mantle cell lymphoma (MCL) compared, 230, 236, 237f
marginal zone lymphoma distinguished from, 184–185, 184f–185f
pathologic features, 295–297, 295f–301f
transformation and progression, 299–300
treatment and survival, 302

U
Ulcerative colitis, 319
Ultrasound examination of a splenic mass lesion, 57, 59

V
Vaccination site sarcoma, 356f
Vascular system
spleen, 48–49, 48f–49f
thymus, 78
VEGF-D, 40
VEGF induction, 41
VEGFR-3 receptors, 9
Vimentin, 201, 492
Vincristine, for myeloma, 206
Viral associated hemophagocytic syndrome, 522
Viral infections, lymphadenitis from, 34–36, 35f–36f
Virchow, Rudolf, 3, 425
Vitamin B_{12} deficiency, 116, 486
Vitronectin, 40

W
Waldenstrom macroglobulinemia, 156, 180, 208
WHO classification system. *See also* REAL/WHO classification system
acute myeloid leukemia, 367, 368t
anaplastic large cell lymphoma (ALCL), 339
Hodgkin's lymphoma, 491, 495
MDS/MPD diseases, 461, 467
plasmacytoma and multiple myeloma, 189
tingible body, 221

Woringer-Kolopp disease, 336. *See also* Pagetoid reticulosis (PR)
Working Formulation (WF), 5, 260

X
Xid gene, 28

Y
Yolk sac blood islands, 99

Z
Zebra bodies, 114
Zenker's, 117, 494
Zinc chloride, 26
Zinc deficiency, 84H